VOLUME 27 / NUMBER 21
NOVEMBER 8, 1989
ACC. NOS. N89-26807 TO N89-27631

STAR

AN ABSTRACT JOURNAL

Scientific and Technical Aerospace Reports

PRODUCED BY THE
SCIENTIFIC AND TECHNICAL
INFORMATION
DIVISION

NASA

NATIONAL AERONAUTICS AND SPACE ADMINISTRATION

WHAT YOU CAN DO FOR *STAR*

All users of this abstract service are urged to forward reports to be considered for announcement in *STAR*. This will aid NASA in its efforts to provide the fullest possible coverage of all scientific and technical publications that might support aeronautics and space research and development. If you have prepared relevant reports (other than those that you will transmit to NASA, DoD, or DOE through the usual contract- or grant-reporting channels), please send them for consideration to the NASA Scientific and Technical Information Facility, P.O. Box 8757, BWI Airport, Maryland 21240.

Reprints of journal articles, book chapters, and conference papers are also welcome. These will be considered for announcement in *STAR's* companion journal, *International Aerospace Abstracts*.

You may specify a particular source to be included in a report announcement if you wish; otherwise the report will be placed on public sale at the National Technical Information Service. Copyrighted publications will be announced but not distributed or sold.

PURCHASE OF *STAR*

The semimonthly issues are available to registered users on annual subscription for $99.00 from the NASA Scientific and Technical Information Facility, ATTN: Registration Services, P.O. Box 8757, BWI Airport, MD 21240. *STAR* is publically available on annual subscription for $99.00 from the Superintendent of Documents, U.S. Government Printing Office, Washington, DC 20402.

PUBLISHED BY:

UNITED STATES GOVERNMENT
NATIONAL AERONAUTICS AND SPACE ADMINISTRATION
SCIENTIFIC AND TECHNICAL INFORMATION DIVISION
Scientific and Technical Aerospace Reports, Volume 27, is prepared by the NASA Scientific and Technical Information Facility operated for the National Aeronautics and Space Administration by RMS Associates.

The Administrator of the National Aeronautics and Space Administration has determined that the publication of this periodical is necessary in the transaction of the public business required by law of this Agency. Use of funds for printing this periodical has been approved by the Director of the Office of Management and Budget through March 22, 1990.

US ISSN 0036-8741

INTRODUCTION

Scientific and Technical Aerospace Reports (STAR) is a major component of a comprehensive National Aeronautics and Space Administration information system covering aeronautics, space, and supporting disciplines. *STAR* is issued on the 8th and 23rd of each month and announces current publications of the following types:

- NASA, NASA contractor, and NASA grantee reports
- Reports issued by other U.S. Government Agencies, domestic and foreign institutions, universities, and private firms
- Translations in report form
- NASA-owned patents and patent applications
- Other U.S. Government Agency and foreign patents and patent applications
- Domestic and foreign dissertations and theses

Journal, book, and conference literature, cover-to-cover journal translations, and certain foreign dissertations are announced in a companion journal, *International Aerospace Abstracts (IAA),* available on subscription from the American Institute of Aeronautics and Astronautics, Technical Information Service, 555 West 57th Street, 12th Floor, New York, New York 10019.

SUBJECT SCOPE

Subject scope of *STAR,* and *IAA* includes all aspects of aeronautics and space research and development, supporting basic and applied research, and applications. Aerospace aspects of earth resources, energy development, conservation, oceanography, environmental protection, urban transportation, and other topics of high national priority are also covered.

OTHER NASA PUBLICATIONS

Other NASA publications and information services are described in the publication, *The NASA Scientific and Technical Information System ... and How to Use It,* available without charge from the NASA Scientific and Technical Information Facility, P.O. Box 8757, BWI Airport, Maryland 21240.

HOW TO USE *STAR* SUBJECT CATEGORIES

STAR is categorized by 10 major subject divisions divided into 76 specific subject categories and one general category/division. The major subject divisions are listed in the Table of Contents, together with a note for each that defines its scope and provides any cross-references. For example:

AERONAUTICS

Includes aeronautics (general); aerodynamics; air transportation and safety; aircraft communications and navigation; aircraft design, testing and performance; aircraft instrumentation; aircraft propulsion and power; aircraft stability and control; and research and support facilities (air).

For related information see also *Astronautics.*

Each major division is further divided into as many as nine specific categories, which are identified by category numbers.

Abstracts in *STAR* are grouped by specific category, the categories appearing in sequential order. Category breaks in the abstract section are identified by the category number and title, and a scope note. Cross-references to other categories are provided as appropriate. For example:

02 AERODYNAMICS

Includes aerodynamics of bodies, combinations, wings, rotors, and control surfaces; and internal flow in ducts and turbomachinery.

For related information see also *34 Fluid Mechanics and Heat Transfer.*

CROSS-REFERENCES

Individual *STAR* abstracts are not ordinarily cross-referenced, except for certain conference reports or book translations that have had separate abstracts written for their component papers or chapters. Citations and abstracts of the components follow immediately after those of the parent document. When the subject content of a component differs sufficiently from the general content of the parent, a cross-reference citation also is printed at the end of the category to which it normally would have been assigned if it were independent.

DOCUMENTS ON MICROFICHE

Documents on microfiche[1] are designated by a pound sign (#) following the accession number. The pound sign is used without regard to the source or quality of the microfiche.

AVAILABILITIES

One or more sources from which a document announced in *STAR* is available to the public is given in each citation. The most commonly indicated sources and their acronyms or abbreviations are listed below. If the publication is available from a source other than those listed, the publisher and his address will be displayed on the availability line or in combination with the corporate source line.

Avail: NTIS. Sold by the National Technical Information Service. Prices for hard copy (HC) and microfiche (MF) are indicated by a price code following the letters HC or MF in the *STAR* citation. Current values for the price codes are given in the tables on page vii.

Initially distributed microfiche under the NTIS SRIM (Selected Research in Microfiche) is available at greatly reduced unit prices. For this service and for information concerning subscription to NASA printed reports, consult the NTIS Subscription Section, Springfield, Va. 22161.

NOTE ON ORDERING DOCUMENTS: When ordering NASA publications (those followed by the * symbol), use the N accession number. NASA patent applications (only the specifications are offered) should be ordered by the US-Patent-Appl-SN number. Non-NASA publications (no asterisk) should be ordered by the AD, PB, or other *report number* shown on the last line of the citation, not by the N accession number. It is also advisable to cite the title and other bibliographic identification.

Avail: SOD (or GPO). Sold by the Superintendent of Documents, U.S. Government Printing Office, in hard copy. The current price and order number are given following the availability line. (NTIS will fill microfiche requests, as indicated above, for those documents identified by a # symbol.)

(1) A microfiche is a transparent sheet of film, 105 by 148 mm in size, containing as many as 60 to 98 pages of information reduced to micro images (not to exceed 26:1 reduction).

Avail: BLL (formerly NLL): British Library Lending Division, Boston Spa, Wetherby, Yorkshire, England. Photocopies available from this organization at the price shown. (If none is given, inquiry should be addressed to the BLL.)

Avail: DOE Depository Libraries. Organizations in U.S. cities and abroad that maintain collections of Department of Energy reports, usually in microfiche form, are listed in *Energy Research Abstracts*. Services available from the DOE and its depositories are described in a booklet, *DOE Technical Information Center - Its Functions and Services* (TID-4660), which may be obtained without charge from the DOE Technical Information Center.

Avail: ESDU. Pricing information on specific data, computer programs, and details on ESDU topic categories can be obtained from ESDU International Ltd. Requesters in North America should use the Virginia address while all other requesters should use the London address, both of which are on page vi.

Avail: Fachinformationszentrum, Karlsruhe. Sold by the Fachinformationszentrum Energie, Physik, Mathematik GMBH, Eggenstein Leopoldshafen, Federal Republic of Germany, at the price shown in deutschmarks (DM).

Avail: HMSO. Publications of Her Majesty's Stationery Office are sold in the U.S. by Pendragon House, Inc. (PHI), Redwood City, California. The U.S. price (including a service and mailing charge) is given, or a conversion table may be obtained from PHI.

Avail: NASA Public Document Rooms. Documents so indicated may be examined at or purchased from the National Aeronautics and Space Administration, Public Documents Room (Room 126), 600 Independence Ave., S.W., Washington, D.C. 20546, or public document rooms located at each of the NASA research centers, the NASA Space Technology Laboratories, and the NASA Pasadena Office at the Jet Propulsion Laboratory.

Avail: Univ. Microfilms. Documents so indicated are dissertations selected from *Dissertation Abstracts* and are sold by University Microfilms as xerographic copy (HC) and microfilm. All requests should cite the author and the Order Number as they appear in the citation.

Avail: US Patent and Trademark Office. Sold by Commissioner of Patents and Trademarks, U.S. Patent and Trademark Office, at the standard price of $1.50 each, postage free. (See discussion of NASA patents and patent applications below.)

Avail: (US Sales Only). These foreign documents are available to users within the United States from the National Technical Information Service (NTIS). They are available to users outside the United States through the International Nuclear Information Service (INIS) representative in their country, or by applying directly to the issuing organization.

Avail: USGS. Originals of many reports from the U.S. Geological Survey, which may contain color illustrations, or otherwise may not have the quality of illustrations preserved in the microfiche or facsimile reproduction, may be examined by the public at the libraries of the USGS field offices whose addresses are listed in this Introduction. The libraries may be queried concerning the availability of specific documents and the possible utilization of local copying services, such as color reproduction.

Avail: Issuing Activity, or Corporate Author, or no indication of availability. Inquiries as to the availability of these documents should be addressed to the organization shown in the citation as the corporate author of the document.

NASA PATENTS AND PATENT APPLICATIONS

Patents and patent applications owned by NASA are announced in *STAR* under appropriate subject categories and are referenced in the *STAR* indexes. In the Report/Accession Number Index, patents are indexed by the NASA Case Number (which appears in lieu of the report number in other indexes), the U.S. Patent Number, the U.S. Patent Application Serial Number, and the U.S. Patent Class. Patent applications for which patents have not yet been issued are indexed by the NASA Case Number and the U.S. Patent Application Serial Number.

NASA *patent application specifications* are sold in paper copy by the National Technical Information Service at price code A02. Microfiche are sold at price code A01. The US-Patent-Appl-SN- number should be used in ordering either paper copy or microfiche from NTIS. Printed copies of *patents* (which are not microfiched) are available for purchase at $1.50 per copy from:

Commissioner of Patents and Trademarks
U.S. Patent and Trademark Office
Washington, D.C. 20231

When ordering patents, the U.S. Patent Number should be used, and payment must be remitted in advance, preferably by money order or check payable to the Commissioner of Patents and Trademarks. Prepaid purchase coupons for ordering are also available from the Patent and Trademark Office. The patents and patent applications announced in *STAR* are owned by NASA and are available for royalty-free licensing. Requests for licensing terms and further information should be addressed to:

Associate General Counsel for Intellectual Property/Code GP
National Aeronautics and Space Administration
Washington, D.C. 20546

ELIGIBILITY AND REGISTRATION FOR NASA INFORMATION PRODUCTS AND SERVICES

A variety of services is available to organizations of the following types that have registered with NASA to receive specific services or products:

1. NASA offices, research centers, contractors, subcontractors, grantees, and consultants;
2. Other U.S. Government agencies and their contractors;
3. Libraries in the United States that have arrangements with NASA to maintain collections of NASA documents for public reference;
4. Other organizations in the United States having a need for NASA documents in work related to aeronautics and space research;
5. Organizations abroad that have established reciprocal document exchange arrangements with NASA.

Only the central service points or central points of document acquisition and control within qualified organizations are eligible to register for NASA products and services. Domestic organizations that may be eligible to receive various classes of NASA publications and services should address their requests for registration or for further information to:

NASA Scientific and Technical Information Facility
ATTN: Registration Services
Post Office Box 8757
BWI Airport, Maryland 21240

Organizations abroad should direct requests to Manager, International STI Activities, NTT, NASA Headquarters, Washington, D.C. 20546.

AVAILABILITY OF *STAR* ABSTRACTS ON MICROFICHE

Microfiche of the abstract sections of this issue and other issues of *STAR* are available on annual subscription from NTIS as PB89-911300, Attn: Subscriptions, 5285 Port Royal Road, Springfield, Virginia 22161. Annual subscription rates are $70.00 North America; $140.00 foreign. Abstract sections for previous years retroactive to 1964 are available at the current rates. Microfiche for individual *STAR* issue abstract sections are not available.

PUBLIC COLLECTIONS OF NASA DOCUMENTS

DOMESTIC: NASA and NASA-sponsored documents and a large number of aerospace publications are available to the public for reference purposes at the library maintained by the American Institute of Aeronautics and Astronautics, Technical Information Service, 555 West 57th Street, 12th Floor, New York, New York 10019

EUROPEAN: An extensive collection of NASA and NASA-sponsored publications is maintained by the British Library Lending Division, Boston Spa, Wetherby, Yorkshire, England for public access. The British Library Lending Division also has available many of the non-NASA publications cited in *STAR*. European requesters may purchase facsimile copy or microfiche of NASA and NASA-sponsored documents, those identified by both the symbols # and * from ESA - Information Retrieval Service European Space Agency, 8-10 rue Mario-Nikis, 75738 Paris CEDEX 15, France.

FEDERAL DEPOSITORY LIBRARY PROGRAM

In order to provide the general public with greater access to U.S. Government publications, Congress established the Federal Depository Library Program under the Government Printing Office (GPO), with 50 regional depositories responsible for permanent retention of material, inter-library loan, and reference services. At least one copy of nearly every NASA and NASA-sponsored publication, either in printed or microfiche format, is received and retained by the 50 regional depositories. A list of the regional GPO libraries, arranged alphabetically by state, appears on the inside back cover. These libraries are *not* sales outlets. A local library can contact a Regional Depository to help locate specific reports, or direct contact may be made by an individual.

ADDRESSES OF ORGANIZATIONS

American Institute of Aeronautics and Astronautics
Technical Information Service
555 West 57th Street, 12th Floor
New York, New York 10019

British Library Lending Division,
Boston Spa, Wetherby, Yorkshire,
England

Commissioner of Patents and Trademarks
U.S. Patent and Trademark Office
Washington, D.C. 20231

Department of Energy
Technical Information Center
P.O. Box 62
Oak Ridge, Tennessee 37830

ESA-Information Retrieval Service
ESRIN
Via Galileo Galilei
00044 Frascati (Rome) Italy

ESDU International
P.O. Box 1633
Manassas, Virginia 22110

ESDU International, Ltd.
251-259 Regent Street
London, W1R 7AD, England

Fachinformationszentrum Energie, Physik, Mathematik GMBH
7514 Eggenstein Leopoldshafen
Federal Republic of Germany

Her Majesty's Stationery Office
P.O. Box 569, S.E. 1
London, England

NASA Scientific and Technical Information Facility
P.O. Box 8757
B.W.I. Airport, Maryland 21240

National Aeronautics and Space Administration
Scientific and Technical Information Division (NTT)
Washington, D.C. 20546

National Technical Information Service
5285 Port Royal Road
Springfield, Virginia 22161

Pendragon House, Inc.
899 Broadway Avenue
Redwood City, California 94063

Superintendent of Documents
U.S. Government Printing Office
Washington, D.C. 20402

University Microfilms
A Xerox Company
300 North Zeeb Road
Ann Arbor, Michigan 48106

University Microfilms, Ltd.
Tylers Green
London, England

U.S. Geological Survey Library
National Center - MS 950
12201 Sunrise Valley Drive
Reston, Virginia 22092

U.S. Geological Survey Library
2255 North Gemini Drive
Flagstaff, Arizona 86001

U.S. Geological Survey
345 Middlefield Road
Menlo Park, California 94025

U.S. Geological Survey Library
Box 25046
Denver Federal Center, MS914
Denver, Colorado 80225

NTIS PRICE SCHEDULES

(Effective January 1, 1989)

Schedule A
STANDARD PRICE DOCUMENTS AND MICROFICHE

PRICE CODE	NORTH AMERICAN PRICE	FOREIGN PRICE
A01	$ 6.95	$13.90
A02	10.95	21.90
A03	13.95	27.90
A04-A05	15.95	31.90
A06-A09	21.95	43.90
A10-A13	28.95	57.90
A14-A17	36.95	73.90
A18-A21	42.95	85.90
A22-A25	49.95	99.90
A99	*	*
NO1	55.00	70.00
NO2	55.00	80.00

Schedule E
EXCEPTION PRICE DOCUMENTS AND MICROFICHE

PRICE CODE	NORTH AMERICAN PRICE	FOREIGN PRICE
E01	$ 9.00	18.00
E02	11.50	23.00
E03	13.00	26.00
E04	15.50	31.00
E05	17.50	35.00
E06	20.50	41.00
E07	23.00	46.00
E08	25.50	51.00
E09	28.00	56.00
E10	31.00	62.00
E11	33.50	67.00
E12	36.50	73.00
E13	39.00	78.00
E14	42.50	85.00
E15	46.00	92.00
E16	50.50	101.00
E17	54.50	109.00
E18	59.00	118.00
E19	65.50	131.00
E20	76.00	152.00
E99	*	*

*Contact NTIS for price quote.

IMPORTANT NOTICE

NTIS Shipping and Handling Charges

U.S., Canada, Mexico — ADD $3.00 per TOTAL ORDER

All Other Countries — ADD $4.00 per TOTAL ORDER

Exceptions — Does NOT apply to:

ORDERS REQUESTING NTIS RUSH HANDLING

ORDERS FOR SUBSCRIPTION OR STANDING ORDER PRODUCTS *ONLY*

NOTE: Each additional delivery address on an order requires a separate shipping and handling charge.

VOLUME 27 NUMBER 21 / NOVEMBER 8, 1989

TABLE OF CONTENTS

AERONAUTICS

Includes aeronautics (general); aerodynamics; air transportation and safety; aircraft communications and navigation; aircraft design, testing and performance; aircraft instrumentation; aircraft propulsion and power; aircraft stability and control; and research and support facilities (air).

For related information see also *Astronautics.*

01 AERONAUTICS (GENERAL) 2957

02 AERODYNAMICS 2957

Includes aerodynamics of bodies, combinations, wings, rotors, and control surfaces; and internal flow in ducts and turbomachinery.

For related information see also *34 Fluid Mechanics and Heat Transfer*

03 AIR TRANSPORTATION AND SAFETY 2960

Includes passenger and cargo air transport operations; and aircraft accidents.

For related information see also *16 Space Transportation* and *85 Urban Technology and Transportation.*

04 AIRCRAFT COMMUNICATIONS AND NAVIGATION 2961

Includes digital and voice communication with aircraft; air navigation systems (satellite and ground based); and air traffic control.

For related information see also *17 Space Communications, Spacecraft Communications, Command and Tracking* and *32 Communications and Radar.*

05 AIRCRAFT DESIGN, TESTING AND PERFORMANCE 2961

Includes aircraft simulation technology.

For related information see also *18 Spacecraft Design, Testing and Performance* and *39 Structural Mechanics.* For land transportation vehicles see *85 Urban Technology and Transportation.*

06 AIRCRAFT INSTRUMENTATION 2963

Includes cockpit and cabin display devices; and flight instruments.

For related information see also *19 Spacecraft Instrumentation* and *35 Instrumentation and Photography.*

07 AIRCRAFT PROPULSION AND POWER 2964

Includes prime propulsion systems and systems components, e.g., gas turbine engines and compressors; and onboard auxiliary power plants for aircraft.

For related information see also *20 Spacecraft Propulsion and Power, 28 Propellants and Fuels,* and *44 Energy Production and Conversion.*

08 AIRCRAFT STABILITY AND CONTROL 2965

Includes aircraft handling qualities; piloting; flight controls; and autopilots.

For related information see also *05 Aircraft Design, Testing and Performance.*

09 RESEARCH AND SUPPORT FACILITIES (AIR) 2967

Includes airports, hangars and runways; aircraft repair and overhaul facilities; wind tunnels; shock tubes; and aircraft engine test stands.

For related information see also *14 Ground Support Systems and Facilities (Space).*

ASTRONAUTICS

Includes astronautics (general); astrodynamics; ground support systems and facilities (space); launch vehicles and space vehicles; space transportation; space communications, spacecraft communications, command and tracking; spacecraft design, testing and performance; spacecraft instrumentation; and spacecraft propulsion and power.

For related information see also *Aeronautics*

12 ASTRONAUTICS (GENERAL) 2968

For extraterrestrial exploration see *91 Lunar and Planetary Exploration.*

13 ASTRODYNAMICS 2968

Includes powered and free-flight trajectories; and orbital and launching dynamics.

14 GROUND SUPPORT SYSTEMS AND FACILITIES (SPACE) N.A.

Includes launch complexes, research and production facilities; ground support equipment, e.g., mobile transporters; and simulators.

For related information see also *09 Research and Support Facilities (Air).*

15 LAUNCH VEHICLES AND SPACE VEHICLES 2969

Includes boosters; operating problems of launch/space vehicle systems; and reusable vehicles.

For related information see also *20 Spacecraft Propulsion and Power.*

16 SPACE TRANSPORTATION 2969

Includes passenger and cargo space transportation, e.g., shuttle operations; and space rescue techniques.

For related information see also *03 Air Transportation and Safety* and *18 Spacecraft Design, Testing and Performance.* For space suits see *54 Man/System Technology and Life Support.*

17 SPACE COMMUNICATIONS, SPACECRAFT COMMUNICATIONS, COMMAND AND TRACKING 2969

Includes telemetry; space communications networks; astronavigation and guidance; and radio blackout.

For related information see also *04 Aircraft Communications and Navigation* and *32 Communications and Radar.*

18 SPACECRAFT DESIGN, TESTING AND PERFORMANCE **2970**

Includes satellites; space platforms; space stations; spacecraft systems and components such as thermal and environmental controls; and attitude controls.

For life support systems see *54 Man/System Technology and Life Support.* For related information see also *05 Aircraft Design, Testing and Performance, 39 Structural Mechanics,* and *16 Space Transportation.*

19 SPACECRAFT INSTRUMENTATION **N.A.**

For related information see also *06 Aircraft Instrumentation* and *35 Instrumentation and Photography.*

20 SPACECRAFT PROPULSION AND POWER **2971**

Includes main propulsion systems and components, e.g. rocket engines; and spacecraft auxiliary power sources.

For related information see also *07 Aircraft Propulsion and Power, 28 Propellants and Fuels, 44 Energy Production and Conversion,* and *15 Launch Vehicles and Space Vehicles.*

CHEMISTRY AND MATERIALS

Includes chemistry and materials (general); composite materials; inorganic and physical chemistry; metallic materials; nonmetallic materials; propellants and fuels; and materials processing.

23 CHEMISTRY AND MATERIALS (GENERAL) **N.A.**

24 COMPOSITE MATERIALS **2974**

Includes physical, chemical, and mechanical properties of laminates and other composite materials.

For ceramic materials see *27 Nonmetallic Materials.*

25 INORGANIC AND PHYSICAL CHEMISTRY **2977**

Includes chemical analysis, e.g., chromatography; combustion theory; electrochemistry; and photochemistry.

For related information see also *77 Thermodynamics and Statistical Physics.*

26 METALLIC MATERIALS **2982**

Includes physical, chemical, and mechanical properties of metals, e.g., corrosion; and metallurgy.

27 NONMETALLIC MATERIALS **2988**

Includes physical, chemical, and mechanical properties of plastics, elastomers, lubricants, polymers, textiles, adhesives, and ceramic materials.

For composite materials see *24 Composite Materials.*

28 PROPELLANTS AND FUELS **2994**

Includes rocket propellants, igniters and oxidizers; their storage and handling procedures; and aircraft fuels.

For related information see also *07 Aircraft Propulsion and Power, 20 Spacecraft Propulsion and Power,* and *44 Energy Production and Conversion.*

29 MATERIALS PROCESSING **2995**

Includes space-based development of products and processes for commercial application.

For biological materials see *55 Space Biology.*

ENGINEERING

Includes engineering (general); communications and radar; electronics and electrical engineering; fluid mechanics and heat transfer; instrumentation and photography; lasers and masers; mechanical engineering; quality assurance and reliability; and structural mechanics.

For related information see also *Physics.*

31 ENGINEERING (GENERAL) **2996**

Includes vacuum technology; control engineering; display engineering; cryogenics; and fire prevention.

32 COMMUNICATIONS AND RADAR **2997**

Includes radar; land and global communications; communications theory; and optical communications.

For related information see also *04 Aircraft Communications and Navigation* and *17 Space Communications, Spacecraft Communications, Command and Tracking.* For search and rescue see *03 Air Transportation and Safety,* and *16 Space Transportation.*

33 ELECTRONICS AND ELECTRICAL ENGINEERING **3001**

Includes test equipment and maintainability; components, e.g., tunnel diodes and transistors; microminiaturization; and integrated circuitry.

For related information see also *60 Computer Operations and Hardware* and *76 Solid-State Physics.*

34 FLUID MECHANICS AND HEAT TRANSFER **3005**

Includes boundary layers; hydrodynamics; fluidics; mass transfer and ablation cooling.

For related information see also *02 Aerodynamics* and *77 Thermodynamics and Statistical Physics.*

35 INSTRUMENTATION AND PHOTOGRAPHY **3012**

Includes remote sensors; measuring instruments and gages; detectors; cameras and photographic supplies; and holography.

For aerial photography see *43 Earth Resources and Remote Sensing.* For related information see also *06 Aircraft Instrumentation* and *19 Spacecraft Instrumentation.*

36 LASERS AND MASERS **3015**

Includes parametric amplifiers.

For related information see also *76 Solid-State Physics.*

37 MECHANICAL ENGINEERING **3018**

Includes auxiliary systems (nonpower); machine elements and processes; and mechanical equipment.

38 QUALITY ASSURANCE AND RELIABILITY **3022**

Includes product sampling procedures and techniques; and quality control.

39 STRUCTURAL MECHANICS **3022**

Includes structural element design and weight analysis; fatigue; and thermal stress.

For applications see *05 Aircraft Design, Testing and Performance* and *18 Spacecraft Design, Testing and Performance.*

GEOSCIENCES

Includes geosciences (general); earth resources and remote sensing; energy production and conversion; environment pollution; geophysics; meteorology and climatology; and oceanography.

For related information see also *Space Sciences.*

42 GEOSCIENCES (GENERAL) **3026**

43 EARTH RESOURCES AND REMOTE SENSING **3026**

Includes remote sensing of earth resources by aircraft and spacecraft; photogrammetry; and aerial photography.

For instrumentation see *35 Instrumentation and Photography.*

44 ENERGY PRODUCTION AND CONVERSION **3028**

Includes specific energy conversion systems, e.g., fuel cells; global sources of energy; geophysical conversion; and windpower.

For related information see also *07 Aircraft Propulsion and Power, 20 Spacecraft Propulsion and Power,* and *28 Propellants and Fuels.*

45 ENVIRONMENT POLLUTION **3031**

Includes atmospheric, noise, thermal, and water pollution.

46 GEOPHYSICS **3034**

Includes aeronomy; upper and lower atmosphere studies; ionospheric and magnetospheric physics; and geomagnetism.

For space radiation see *93 Space Radiation.*

47 METEOROLOGY AND CLIMATOLOGY **3038**

Includes weather forecasting and modification.

48 OCEANOGRAPHY **3042**

Includes biological, dynamic, and physical oceanography; and marine resources.

For related information see also *43 Earth Resources and Remote Sensing.*

LIFE SCIENCES

Includes life sciences (general); aerospace medicine; behavioral sciences; man/system technology and life support; and space biology.

51 LIFE SCIENCES (GENERAL) **3042**

52 AEROSPACE MEDICINE **3043**

Includes physiological factors; biological effects of radiation; and effects of weightlessness on man and animals.

53 BEHAVIORAL SCIENCES **3044**

Includes psychological factors; individual and group behavior; crew training and evaluation; and psychiatric research.

54 MAN/SYSTEM TECHNOLOGY AND LIFE SUPPORT **3045**

Includes human engineering; biotechnology; and space suits and protective clothing.

For related information see also *16 Space Transportation.*

55 SPACE BIOLOGY **N.A.**

Includes exobiology; planetary biology; and extraterrestrial life.

MATHEMATICAL AND COMPUTER SCIENCES

Includes mathematical and computer sciences (general); computer operations and hardware; computer programming and software; computer systems; cybernetics; numerical analysis; statistics and probability; systems analysis; and theoretical mathematics.

59 MATHEMATICAL AND COMPUTER SCIENCES (GENERAL) **3046**

60 COMPUTER OPERATIONS AND HARDWARE **3047**

Includes hardware for computer graphics, firmware, and data processing.

For components see *33 Electronics and Electrical Engineering.*

61 COMPUTER PROGRAMMING AND SOFTWARE **3048**

Includes computer programs, routines, algorithms, and specific applications, e.g., CAD/CAM.

62 COMPUTER SYSTEMS **3056**

Includes computer networks and special application computer systems.

63 CYBERNETICS **3056**

Includes feedback and control theory, artificial intelligence, robotics and expert systems.

For related information see also *54 Man/System Technology and Life Support.*

64 NUMERICAL ANALYSIS **3057**

Includes iteration, difference equations, and numerical approximation.

65 STATISTICS AND PROBABILITY **3061**

Includes data sampling and smoothing; Monte Carlo method; and stochastic processes.

66 SYSTEMS ANALYSIS **3062**

Includes mathematical modeling; network analysis; and operations research.

67 THEORETICAL MATHEMATICS **N.A.**

Includes topology and number theory.

PHYSICS

Includes physics (general); acoustics; atomic and molecular physics; nuclear and high-energy physics; optics; plasma physics; solid-state physics; and thermodynamics and statistical physics.

For related information see also *Engineering.*

70 PHYSICS (GENERAL) **3062**

For precision time and time interval (PTTI) see *35 Instrumentation and Photography;* for geophysics, astrophysics or solar physics see *46 Geophysics, 90 Astrophysics,* or *92 Solar Physics.*

71 ACOUSTICS 3063
Includes sound generation, transmission, and attenuation.
For noise pollution see *45 Environment Pollution.*

72 ATOMIC AND MOLECULAR PHYSICS 3065
Includes atomic structure, electron properties, and molecular spectra.

73 NUCLEAR AND HIGH-ENERGY PHYSICS 3068
Includes elementary and nuclear particles; and reactor theory.
For space radiation see *93 Space Radiation.*

74 OPTICS 3069
Includes light phenomena and optical devices.
For lasers see *36 Lasers and Masers.*

75 PLASMA PHYSICS 3071
Includes magnetohydrodynamics and plasma fusion.
For ionospheric plasmas see *46 Geophysics.* For space plasmas see *90 Astrophysics.*

76 SOLID-STATE PHYSICS 3077
Includes superconductivity.
For related information see also *33 Electronics and Electrical Engineering* and *36 Lasers and Masers.*

77 THERMODYNAMICS AND STATISTICAL PHYSICS 3082
Includes quantum mechanics; theoretical physics; and Bose and Fermi statistics.
For related information see also *25 Inorganic and Physical Chemistry* and *34 Fluid Mechanics and Heat Transfer.*

SOCIAL SCIENCES

Includes social sciences (general); administration and management; documentation and information science; economics and cost analysis; law, political science, and space policy; and urban technology and transportation.

80 SOCIAL SCIENCES (GENERAL) N.A.
Includes educational matters.

81 ADMINISTRATION AND MANAGEMENT 3083
Includes management planning and research.

82 DOCUMENTATION AND INFORMATION SCIENCE 3084
Includes information management; information storage and retrieval technology; technical writing; graphic arts; and micrography.
For computer documentation see *61 Computer Programming and Software.*

83 ECONOMICS AND COST ANALYSIS N.A.
Includes cost effectiveness studies.

84 LAW, POLITICAL SCIENCE AND SPACE POLICY N.A.
Includes NASA appropriation hearings; aviation law; space law and policy; international law; international cooperation; and patent policy.

85 URBAN TECHNOLOGY AND TRANSPORTATION 3085
Includes applications of space technology to urban problems; technology transfer; technology assessment; and surface and mass transportation.
For related information see *03 Air Transportation and Safety, 16 Space Transportation,* and *44 Energy Production and Conversion.*

SPACE SCIENCES

Includes space sciences (general); astronomy; astrophysics; lunar and planetary exploration; solar physics; and space radiation.
For related information see also *Geosciences.*

88 SPACE SCIENCES (GENERAL) N.A.

89 ASTRONOMY 3086
Includes radio, gamma-ray, and infrared astronomy; and astrometry.

90 ASTROPHYSICS 3087
Includes cosmology; celestial mechanics; space plasmas; and interstellar and interplanetary gases and dust.
For related information see also *75 Plasma Physics.*

91 LUNAR AND PLANETARY EXPLORATION 3088
Includes planetology; and manned and unmanned flights.
For spacecraft design or space stations see *18 Spacecraft Design, Testing and Performance.*

92 SOLAR PHYSICS 3089
Includes solar activity, solar flares, solar radiation and sunspots.
For related information see *93 Space Radiation.*

93 SPACE RADIATION 3090
Includes cosmic radiation; and inner and outer earth's radiation belts.
For biological effects of radiation see *52 Aerospace Medicine.* For theory see *73 Nuclear and High-Energy Physics.*

GENERAL

Includes aeronautical, astronautical, and space science related histories, biographies, and pertinent reports too broad for categorization; histories or broad overviews of NASA programs.

99 GENERAL N.A.

Note: N.A. means that no abstracts were assigned to this category for this issue.

SUBJECT INDEX I-1
PERSONAL AUTHOR INDEX I-59
CORPORATE SOURCE INDEX I-67
CONTRACT NUMBER INDEX I-79
REPORT/ACCESSION NUMBER INDEX I-83

TYPICAL CITATION AND ABSTRACT

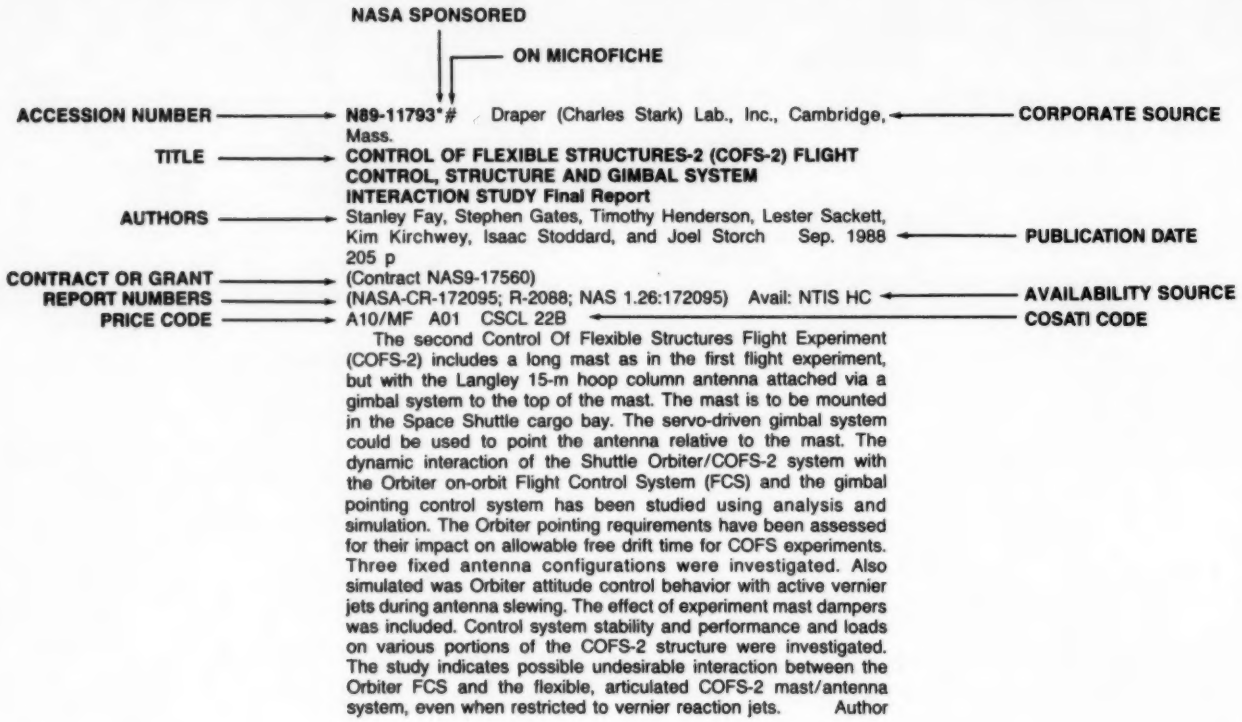
NASA SPONSORED
ON MICROFICHE
ACCESSION NUMBER
N89-11793*# Draper (Charles Stark) Lab., Inc., Cambridge, Mass.
CORPORATE SOURCE
TITLE
CONTROL OF FLEXIBLE STRUCTURES-2 (COFS-2) FLIGHT CONTROL, STRUCTURE AND GIMBAL SYSTEM INTERACTION STUDY Final Report
AUTHORS
Stanley Fay, Stephen Gates, Timothy Henderson, Lester Sackett, Kim Kirchwey, Isaac Stoddard, and Joel Storch Sep. 1988
PUBLICATION DATE
205 p
CONTRACT OR GRANT
(Contract NAS9-17560)
REPORT NUMBERS
(NASA-CR-172095; R-2088; NAS 1.26:172095) Avail: NTIS HC
AVAILABILITY SOURCE
PRICE CODE
A10/MF A01 CSCL 22B
COSATI CODE
The second Control Of Flexible Structures Flight Experiment (COFS-2) includes a long mast as in the first flight experiment, but with the Langley 15-m hoop column antenna attached via a gimbal system to the top of the mast. The mast is to be mounted in the Space Shuttle cargo bay. The servo-driven gimbal system could be used to point the antenna relative to the mast. The dynamic interaction of the Shuttle Orbiter/COFS-2 system with the Orbiter on-orbit Flight Control System (FCS) and the gimbal pointing control system has been studied using analysis and simulation. The Orbiter pointing requirements have been assessed for their impact on allowable free drift time for COFS experiments. Three fixed antenna configurations were investigated. Also simulated was Orbiter attitude control behavior with active vernier jets during antenna slewing. The effect of experiment mast dampers was included. Control system stability and performance and loads on various portions of the COFS-2 structure were investigated. The study indicates possible undesirable interaction between the Orbiter FCS and the flexible, articulated COFS-2 mast/antenna system, even when restricted to vernier reaction jets. Author

VOLUME 27 NUMBER 21 / NOVEMBER 8, 1989

Scientific and Technical Aerospace Reports

A Semimonthly Publication of the National Aeronautics and Space Administration

01 AERONAUTICS (GENERAL)

N89-26807# Air Force Systems Command, Wright-Patterson AFB, OH. Foreign Technology Div.
ACTA AERONAUTICA ET ASTRONAUTICA SINICA, VOLUME 8, NUMBER 12, DECEMBER 1987 (SELECTED ARTICLES)
15 Feb. 1989 71 p Transl. into ENGLISH from Hangkong Xuebao (Peoples Republic of China), v. 8, no. 12, Dec. 1987 p 8557-8562, 8585-8593, and 8601-8610
(AD-A206782; FTD-ID(RS)T-0942-88) Avail: NTIS HC A04/MF A01 CSCL 01/2

Aircraft take off and landing gear are studied in order to understand nose wheel shimmy and provide measures to prevent it. It also deals with an analysis of runway dynamics and other such similar areas as nose wheel operation. Semi-Prepared Airfield and Design of Double-Action Shock Absorber: Airfields, in wars of the future, most necessarily suffer damage. To satisfy the peculiar demands of using this type of airfield, the design concepts of double action or double gas chamber shock shock absorbers. Moreover, as concerns their static and dynamic characteristics as well as the main parameters in the principles for their selection, it makes a relatively detailed comparative analysis. The settlement on standards for the unevenness of airfield runways, is based on the concept of power spectra. It introduces basic methods for measuring random variables from the unevenness of airfield runways. It drafts curves for the power spectra of uneven runways and carries out a preliminary analysis of the dynamic effects in aircraft ground surface taxing. GRA

N89-26808*# National Aeronautics and Space Administration. Ames Research Center, Moffett Field, CA.
SENSOR DEVELOPMENT PROGRAMS AT NASA AMES RESEARCH CENTER
Y.-C. Cho Aug. 1989 8 p Presented at the International Society for Optical Engineering's 1989 Technical Symposia on Aerospace Sensing, Orlando, FL, 27-31 Mar. 1989
(NASA-TM-102217; A-89167; NAS 1.15:102217) Avail: NTIS HC A02/MF A01 CSCL 01B

Two sensor development programs being conducted at the Fluid Mechanics Laboratory, NASA Ames Research Center are described, one in progress and the other being initiated. The ongoing program involves digital image velocimetry for velocity field measurements of time-dependent flows. The new program involves advanced acoustic sensors for wind tunnel applications. Author

N89-26809# Naval Postgraduate School, Monterey, CA. Dept. of Administrative Sciences.
ESTIMATING AND EXPLAINING THE PRODUCTION COST OF HIGH-TECHNOLOGY SYSTEMS: THE CASE OF MILITARY AIRCRAFT
O. Douglas Moses 17 May 1989 85 p
(AD-A208391; NPS54-89-07) Avail: NTIS HC A05/MF A01 CSCL 01/3

This study tests relationships between measures of the state-of-the-art of technology and advances in technology with production cost. The analysis is conducted using a sample of military aircraft. Parametric cost estimating models are developed. Actual production costs are compared with estimated production costs predicted from the models to create measure of cost overruns and cost underruns. A set of factors that are associated with instances of cost over/underruns are identified. These factors reflect aspects of the aircraft program, the political and economic environment at the time of commencement of production on the aircraft program, and the financial condition of the prime contractor. GRA

02 AERODYNAMICS

Includes aerodynamics of bodies, combinations, wings, rotors, and control surfaces; and internal flow in ducts and turbomachinery.

For related information see also *34 Fluid Mechanics and Heat Transfer.*

N89-26810*# National Aeronautics and Space Administration. Langley Research Center, Hampton, VA.
WIND-TUNNEL INVESTIGATION OF AERODYNAMIC CHARACTERISTICS AND WING PRESSURE DISTRIBUTIONS OF AN AIRPLANE WITH VARIABLE-SWEEP WINGS MODIFIED FOR LAMINAR FLOW
James B. Hallissy and Pamela S. Phillips Washington Aug. 1989 222 p
(NASA-TM-4124; L-16493; NAS 1.15:4124) Avail: NTIS HC A10/MF A01 CSCL 01A

A wind tunnel test was conducted to evaluate the aerodynamic characteristics and wing pressure distributions of a variable wing sweep aircraft having wing panels that are modified to promote laminar flow. The modified wing section shapes were incorporated over most of the exposed outer wing panel span and were obtained by extending the leading edge and adding thickness to the existing wing upper surface forward of 60 percent chord. Two different wing configurations, one each for Mach numbers 0.7 and 0.8, were tested on the model simultaneously, with one wing configuration on the left side and the other on the right. The tests were conducted at Mach numbers 0.20 to 0.90 for wing sweep angles of 20, 25, 30, and 35 degrees. Longitudinal, lateral and directional aerodynamic characteristics of the modified and baseline configurations, and selected pressure distributions for the modified configurations, are presented in graphical form without analysis. A tabulation of the pressure data for the modified configuration is available as microfiche. Author

N89-26811*# National Aeronautics and Space Administration. Langley Research Center, Hampton, VA.
A PROCEDURE FOR COMPUTING SURFACE WAVE TRAJECTORIES ON AN INHOMOGENEOUS SURFACE
Raymond L. Barger Washington Aug. 1989 14 p
(NASA-TP-2929; L-16558; NAS 1.60:2929) Avail: NTIS HC A03/MF A01 CSCL 01A

Equations are derived for computing surface waves on smooth surfaces, including surfaces with a nonuniform wave speed. The prior literature dealt primarily with the theoretical development with little consideration given to computational methods, and examples were limited to waves on surfaces of simple analytic description, such as cones, spheres, and cylinders. The computational procedure presented is a relatively general method. Sample

calculations illustrate the procedure for a class of practical shapes of the type that include aerodynamic and hydrodynamic surfaces. Equations are also included for computing the spreading of rays into a surrounding medium that will support waves. Author

N89-26812# International Centre for Theoretical Physics, Trieste (Italy).
MHD FORCED AND FREE CONVECTION BOUNDARY LAYER FLOW NEAR THE LEADING EDGE
M. A. Hossain and M. Ahmed (Dacca Univ., Bangladesh) Jul. 1988 20 p Submitted for publication
(DE88-705974; IC-88/140) Avail: NTIS (US Sales Only) HC A03/MF A01

Magnetohydrodynamic forced and free convection flow of an electrically conducting viscous incompressible fluid past a vertical flat plate with uniform heat flux in the presence of a magnetic field acting normal to the plate that moves with the fluid has been studied near the leading edge of the plate. The coupled non-linear equations are solved by the method of superposition for the values of the Prandtl number ranges from 0.01 to 10.0. The velocity and the temperature profiles are presented graphically and the values of the wall shear-stress as well as the heat transfer rate are presented in tabular form showing the effect of the buoyancy force and the applied magnetic field. To show the accuracy of the present method some typical values are compared with the available one. DOE

N89-26813# Coleman Research Corp., Huntsville, AL.
EXPENDABLE AIR VEHICLES/HIGH ALTITUDE BALLOON TECHNOLOGY Final Report, 13 Jul. 1988 - 28 Feb. 1989
Robert L. Hawkins 28 Feb. 1989 100 p
(Contract DAAH01-88-C-0581; ARPA Order 5916)
(AD-A206972; CHR/89-1909) Avail: NTIS HC A05/MF A01 CSCL 01/3

Coleman Research Corporation demonstrates a capability to produce drift patterns for high-altitude zero-pressure and super-pressure balloons. A simplified balloon dynamics model and a highly detailed, statistical wind model are integrated into a proprietary flight simulation framework to enable the production of balloon drift patterns. The worldwide, time-dependent wind model in conjunction with the data-configurable balloon model allow the production and analysis of drift patterns for balloons launched from any point on the earth's surface at any time of year. Sample drift patterns are produced for a zero-pressure balloon floating at 70,000 feet for 24 hours and for a super-pressure balloon floating at 120,000 feet for one year. GRA

N89-26814# California Univ., Irvine. Dept. of Physics.
SUPERSONICS Final Report, Apr. 1985 - Jun. 1988
R. F. Wallis Mar. 1989 83 p
(Contract F33615-85-K-2501)
(AD-A207394; AFWAL-TR-88-2141) Avail: NTIS HC A05/MF A01 CSCL 20/12

The correlation between the infrared and Raman spectra of lithium borate glasses and their structure has been investigated. The results are consistent with the increasing incorporation of tetrahedrally coordinated boron into the boroxol rings with increasing Li2O content. The spectra reveal the onset of crystallization as the annealing temperature increases. The variation of the ionic conductivity with temperature and composition is shown to be well described by a weak electrolyte theory. The conductivity increases by an order of magnitude when the fractional content of Li2SO4 increases from 0.00 to 0.15. A tight binding method has been used to calculate the energy bands of InSe and the activation energy for motion of Li+ in the Van der Waals gap of InSe. The increase in resistance of a lithium borate glass sample when the Li+ ions are required to flow into the Van der Waals gaps of a contiguous InSe sample has been investigated. GRA

N89-26815*# Stewart (V. R.), Columbus, OH.
AN EXPERIMENTAL INVESTIGATION OF THE GROUND VORTEX CREATED BY A MOVING JET
V. R. Stewart Jul. 1989 124 p
(NASA Order L-29341-C)
(NASA-CR-181841; NAS 1.26:181841; VS-1-88) Avail: NTIS HC A06/MF A01 CSCL 01A

A 1 inch circular jet moving over a fixed ground board was studied in the NASA Langley Research Center Vortex Research Center. The jet passing over the ground board at a height of three nozzle diameters creates a ground vortex which was measured by a pattern of Endevco high response pressure transducers. The results are compared to existing data to determine the effect of the ground boundary eliminated by the moving jet. The penetration of the vortex both forward of and latterly to the impact point of the jet on the ground. The resulting ground vortex penetration forward of the impact point is reduced by approximately 30 percent and the lateral penetration is reduced by 50 percent over that experienced from a stationary jet over a stationary ground board with a free stream velocity. Author

N89-26816*# National Aeronautics and Space Administration. Ames Research Center, Moffett Field, CA.
EXPERIMENTAL PROGRAM FOR REAL GAS FLOW CODE VALIDATION AT NASA AMES RESEARCH CENTER
George S. Deiwert, Anthony W. Strawa, Surendra P. Sharma, and Chul Park Jul. 1989 19 p Presented at the AGARD Symposium on Validation of Computational Fluid Dynamics, Lisbon, Portugal, 2-5 May 1988 Previously announced as N89-18630
(NASA-TM-100093; A-88135; NAS 1.15:100093) Avail: NTIS HC A03/MF A01 CSCL 01A

The experimental program for validating real gas hypersonic flow codes at NASA Ames Rsearch Center is described. Ground-based test facilities used include ballistic ranges, shock tubes and shock tunnels, arc jet facilities and heated-air hypersonic wind tunnels. Also included are large-scale computer systems for kinetic theory simulations and benchmark code solutions. Flight tests consist of the Aeroassist Flight Experiment, the Space Shuttle, Project Fire 2, and planetary probes such as Galileo, Pioneer Venus, and PAET. Author

N89-26817# Advisory Group for Aerospace Research and Development, Neuilly-Sur-Seine (France). Fluid Dynamics Panel.
TECHNICAL STATUS REVIEW ON DRAG PREDICTION AND ANALYSIS FROM COMPUTATIONAL FLUID DYNAMICS: STATE OF THE ART
Jun. 1989 156 p In ENGLISH and FRENCH Review held in Lisbon, Portugal, 5 May 1988
(AGARD-AR-256; ISBN-92-835-0516-6) Copyright Avail: NTIS HC A08/MF A01

The papers presented at the AGARD Fluid Dynamics Panel Technical Status Review on, Drag Prediction and Analysis from Computational Fluid Dynamics: State of the Art, are contained. Speakers presented a state of the art review from their individual nation. The Program Chairman summarized the key conclusions from all the papers presented. It is recommended that the Fluid Dynamics Panel consider possibilities for further stimulation of progress in the field of CFD-based drag prediction and analysis. For individual titles, see N89-26818 through N89-26825.

N89-26818# Office National d'Etudes et de Recherches Aerospatiales, Paris (France). Aerodynamique Appliquee.
DRAG PREDICTION AND ANALYSIS FROM COMPUTATIONAL FLUID DYNAMICS, STATE-OF-THE-ART IN FRANCE **c34**
J. J. Thibert *In* AGARD, Technical Status Review on Drag Prediction and Analysis from Computational Fluid Dynamics: State of the Art Jun. 1989 11 p In FRENCH; ENGLISH summary Original language document was announced in IAA as A89-29239
(For primary document see N89-26817 21-02)
Copyright Avail: NTIS HC A08/MF A01

Various two-dimensional and three-dimensional inviscid-flow methods for drag component analysis are presented which are based on solving either the potential equation or the Euler equations. Comparison with experimental results demonstrates that coupled methods can predict drag to within a few percent. It is suggested that the pressure term should be replaced in the

two-dimensional case by the shock drag term and in the three-dimensional case by the sum of the induced drag and the shock drag. Author

N89-26819# Dornier-Werke G.m.b.H., Friedrichshafen (Germany, F.R.).
DRAG PREDICTION AND ANALYSIS FROM CFD STATE-OF-THE-ART IN GERMANY
Wolfgang Schmidt and Peter Sacher (Messerschmitt-Boelkow G.m.b.H., Munich, Germany, F.R.) *In* AGARD, Technical Status Review on Drag Prediction and Analysis from Computational Fluid Dynamics: State of the Art Jun. 1989 22 p (For primary document see N89-26817 21-02)
Copyright Avail: NTIS HC A08/MF A01

Consistent and accurate prediction of absolute drag for aircraft configurations is currently beyond reach computationally as well as experimentally using wind tunnel model testing. This is attributed to several elements ranging from lack of physical understanding up to limitations in numerical methods and scaling laws. To access drag by computational methods, drag components and the overall drag built-up have to be specified. For the individual drag component semi-empirical as well as theoretical estimates are discussed. Problems and limitations in drag estimates using computational fluid mechanics (CFD) are demonstrated for different types of flowfields. Within the scope of the present conference, our survey over the state-of-the-art in Germany will cover industrial aspects for commuter and transport aircraft, trainer, as well as fighter configurations, missiles, and space vehicles. Author

N89-26820# National Technical Univ., Athens (Greece). Lab. of Thermal Turbomachines.
SOME RESULTS ON FLOW CALCULATIONS INVOLVING DRAG PREDICTION
K. D. Papailiou *In* AGARD, Technical Status Review on Drag Prediction and Analysis from Computational Fluid Dynamics: State of the Art Jun. 1989 24 p (For primary document see N89-26817 21-02)
Copyright Avail: NTIS HC A08/MF A01

Different calculation methods were developed in the Thermal Turbomachinery Lab. of the Athens National Technical University concerning drag prediction. A Navier-Stokes solver, based on a fractional step method, was developed in order to solve viscous incompressible flow in ducts. A second Navier-Stokes solver was developed for transonic flow using, again, a fractional step method, but this time for quasi-three dimensional cascade flow. Integral methods were developed as well in order to predict secondary flows in compressors and shear layer development on blades. High speed laminar and turbulent flow is predicted, attached and separated. Viscous inviscid interaction techniques were developed for the stabilization of the separated flow calculation. Phenomena such as transitional flow, laminar separation bubbles and shock/shear layer interaction for turbulent flow are predicted with good accuracy. The general methods will be reviewed briefly and results will be presented. Author

N89-26821# Aeritalia S.p.A., Turin (Italy). Combat Aircraft Group.
STATE-OF-THE-ART OF AIRCRAFT DRAG PREDICTION IN ITALY BY MEANS OF THEORETICAL METHODS
G. Bucciantini and M. Borsi *In* AGARD, Technical Status Review on Drag Prediction and Analysis from Computational Fluid Dynamics: State of the Art Jun. 1989 12 p (For primary document see N89-26817 21-02)
Copyright Avail: NTIS HC A08/MF A01

The state-of-the-art in Italy on the aerodynamic drag prediction, based on theoretical methods, is presented and discussed. A brief description of the methods used is given, with examples of application for typical aircraft configurations. A survey of critical areas is provided, together with present research activities to improve the drag prediction capabilities and accuracy. Author

N89-26822# National Aerospace Lab., Amsterdam (Netherlands). Informatics Div.
AIRCRAFT DRAG PREDICTION FOR TRANSONIC POTENTIAL FLOW
J. vanderVooren *In* AGARD, Technical Status Review on Drag Prediction and Analysis from Computational Fluid Dynamics: State of the Art Jun. 1989 17 p Sponsored in part by Netherlands Agency for Aerospace Programs (NIVR) (For primary document see N89-26817 21-02)
Copyright Avail: NTIS HC A08/MF A01

The state-of-the-art on computational drag prediction and diagnostics in The Netherlands for transport aircraft in the transonic flight regime is described. Subsequently, a method is discussed that is currently being developed at NLR to calculate wave drag in transonic potential flow. The method is a generalization and extension of Garabedian's and McFadden's idea of determining wave drag by volume-integration of the artificial viscosity. The generalization involves the introduction of a reference artificial viscosity which provides a solid theoretical basis. At the same time this ensures that calculated wave drag is to a certain extent independent of the specific details of the artificial viscosity in different codes. The extension accounts for the fact that artificial viscosity does not smear out supersonic/subsonic shock waves completely, but leaves room for a truly discontinuous sonic/subsonic shock remainder that contributes substantially to the wave drag. A number of first results that illustrate the potential of the method are presented and discussed. Author

N89-26823# Royal Aircraft Establishment, Bedford (England).
CFD METHODS FOR DRAG PREDICTION AND ANALYSIS CURRENTLY IN USE IN UK
P. R. Ashill *In* AGARD, Technical Status Review on Drag Prediction and Analysis from Computational Fluid Dynamics: State of the Art Jun. 1989 19 p (For primary document see N89-26817 21-02)
Copyright Avail: NTIS HC A08/MF A01

Computational methods developed in UK for the prediction of the drag of aircraft components at subsonic and supersonic speeds are critically reviewed. In many cases, the flow modeling is found to be lacking in certain respects. Despite this, however, the review suggests that these methods have a useful function both in the early stages of aircraft design, when they may be used to study differences in the drag of various shapes, and later in support of wind-tunnel tests as a diagnostic tool and also to extrapolate the data to full scale. Author

N89-26824*# National Aeronautics and Space Administration. Ames Research Center, Moffett Field, CA. Applied Computational Fluids Branch.
COMPUTATIONAL FLUID DYNAMICS DRAG PREDICTION: RESULTS FROM THE VISCOUS TRANSONIC AIRFOIL WORKSHOP
Terry L. Holst *In* AGARD, Technical Status Review on Drag Prediction and Analysis from Computational Fluid Dynamics: State of the Art Jun. 1989 12 p Previously announced as N88-22009 (For primary document see N89-26817 21-02)
Copyright Avail: NTIS HC A08/MF A01 CSCL 01A

Results from the Viscous Transonic Airfoil Workshop held in January 1987, are compared with each other and with experimental data. Test cases used include attached and separated transonic flows for the NACA 0012 airfoil. A total of 23 sets of numerical results from 15 different author groups are included. The numerical methods used vary widely and include: 16 Navier-Stokes methods, 2 Euler/boundary-layer methods, and 5 potential/boundary-layer methods. The results indicate a high degree of sophistication among the numerical methods with generally good agreement between the various computed and experimental results for attached or moderately separated cases. The agreement for cases with larger separation is only fair and suggests additional work is required in this area. Author

N89-26825# Grumman Aerospace Corp., Bethpage, NY. Aircraft Systems Div.

CFD DRAG PREDICTION FOR AERODYNAMIC DESIGN

Charles W. Boppe *In* AGARD, Technical Status Review on Drag Prediction and Analysis from Computational Fluid Dynamics: State of the Art Jun. 1989 28 p (For primary document see N89-26817 21-02)

Copyright Avail: NTIS HC A08/MF A01

Consistent and accurate Computation Fluid Dynamics (CFD) prediction of absolute drag level for aircraft configurations is currently beyond reach. This is attributed to several elements characterizing state-of-the-art computer algorithms and hardware. With considerable research focused on the 2-D airfoil analysis problem, an exercise is conducted to quantify the implications for 3-D wings. Recent highlights in the U.S.A. which have advanced drag prediction capabilities or improved understanding of the problem are described. Examples are taken from the areas of computational physics, viscous airfoil simulation, component analysis, hypersonics, and conceptual design/configuration optimization. Primary attention is concentrated on aircraft but helicopter, missile, and automobile cases are also included. A near term solution to the CFD drag prediction problem can not be identified. Instead, means based on CFD's strengths are discussed which make computational methods valuable for drag reduction/prediction during aerodynamic design processes. Author

N89-26826*# Old Dominion Univ., Norfolk, VA. Dept. of Mechanical Engineering and Mechanics.

NUMERICAL STUDY OF THREE-DIMENSIONAL SEPARATION AND FLOW CONTROL AT A WING/BODY JUNCTION Progress Report, period ended 30 Apr. 1989

Robert L. Ash and Balakrishnan Lakshmanan Aug. 1989 214 p

(Grant NAG1-530)

(NASA-CR-185819; NAS 1.26:185819) Avail: NTIS HC A10/MF A01 CSCL 01A

The problem of three-dimensional separation and flow control at a wing/body junction has been investigated numerically using a three-dimensional Navier-Stokes code. The numerical code employs an algebraic grid generation technique for generating the grid for unmodified junction and an elliptic grid generation technique for filleted fin junction. The results for laminar flow past a blunt fin/flat plate junction demonstrate that after grid refinement, the computations agree with experiment and reveal a strong dependency of the number of vortices at the junction on Mach number and Reynolds number. The numerical results for pressure distribution, particle paths and limiting streamlines for turbulent flow past a swept fin show a decrease in the peak pressure and in the extent of the separated flow region compared to the laminar case. The results for a filleted juncture indicate that the streamline patterns lose much of their vortical character with proper filleting. Fillets with a radius of three and one-half times the fin leading edge diameter or two times the incoming boundary layer thickness, significantly weaken the usual necklace interaction vortex for the Mach number and Reynolds number considered in the present study. Author

N89-26827# Technische Univ., Delft (Netherlands).

A NONLINEAR MULTIGRID METHOD FOR THREE-DIMENSIONAL TRANSONIC POTENTIAL FLOW Ph.D. Thesis

A. J. vanderWees 1988 163 p Sponsored by the Netherlands Agency for Aerospace Programs, Delft

(ETN-89-94802) Avail: NTIS HC A08/MF A01

The application of the nonlinear multigrid method to three-dimensional transonic potential flow is discussed. The flow is described by the full potential equation, which is discretized using a finite volume method. The smoothing algorithm in the multigrid method is a combination of Incomplete Lower Upper decomposition and Strongly Implicit Procedure. In general this algorithm is a faster smoothing algorithm than the often used successive line relaxation, while it is also more robust, because it is uniformly stable in the supersonic regions of the flow. The influence of computational grid properties, such as grid aspect ratio and grid skewness, on the multigrid convergence speed is investigated theoretically and experimentally. The usefulness of the method for practical applications is demonstrated for the transonic flow about the DFVLR-F4 and ONERA-M6 wing. ESA

03 AIR TRANSPORTATION AND SAFETY

Includes passenger and cargo air transport operations; and aircraft accidents.

For related information see also *16 Space Transportation* and *85 Urban Technology and Transportation.*

N89-26828# Naval Air Development Center, Warminster, PA. Air Vehicle and Crew Systems Technology Dept.

AIRCRAFT COLOR DISPLAYS: CHROMATICITY AND LUMINANCE REQUIREMENTS Final Report, Oct. 1987 - Sep. 1988

William A. Breitmaier 23 Aug. 1988 31 p

(AD-A206786; NADC-88105-60) Avail: NTIS HC A03/MF A01 CSCL 23/2

Color coding of aircraft display information, when used properly, can decrease the pilot's workload in performing certain visual tasks. In order to be effective, the luminance levels and chromaticity coordinates (with limits) need to be specified. This report provides human factors design guidelines for developing color display criteria. The issues addressed include luminance contrast, color differences, sunlight ambient illumination, and chromaticity recommendations. GRA

N89-26829# Textron Bell Helicopter, Fort Worth, TX.

OH-58 ENERGY ATTENUATING CREW SEAT FEASIBILITY STUDY Final Report, 28 Sep. 1987 - 27 Sep. 1988

Roy G. Fox 1 Nov. 1988 74 p

(Contract DAMD17-87-C-7032; DA Proj. 3E1-62777-A-878)

(AD-A207506; BHTI-699-099-286) Avail: NTIS HC A04/MF A01 CSCL 01/3

Special energy attenuating seats are used to provide a controlled deceleration over a vertical stroking distance to keep aircraft crash loads within human tolerance. Present energy attenuating crew seats use this approach of translating the entire seat vertically. This requires an area clear of equipment and structure between the seat and the fuselage floor. Installation of an energy attenuating seat in the OH-58 could provide reduced spinal loading in some crashes. However, the OH-58 crew seat is integral with the aircraft structure with no room for an energy attenuating seat which gave rise to the belief that a stroking energy attenuating seat was not technically feasible. An innovative approach was needed to provide such seats with a minimum of OH-58 structural modification. A pivoting seat pan design was conceived and feasibility study was performed for the U.S. Army to provide this preliminary design, fabricate test seats, and modify a dynamic test fuselage and a flyable aircraft. Dynamic testing was performed to prove the feasibility of the pivoting seat pan energy attenuating crew seat approach. This report discusses the approach which can provide energy attenuating crew seats to be installed in an OH-58, while providing a concept which could potentially provide similar solutions for other aircraft. GRA

N89-26830# Federal Aviation Administration, Washington, DC. Office of Aviation Medicine.

INJURIES TO SEAT OCCUPANTS OF LIGHT AIRPLANES

Eugene J. Colangelo and Julie C. Russell Feb. 1989 37 p

(AD-A207579; DOT/FAA/AM-89/3) Avail: NTIS HC A03/MF A01 CSCL 01/3

A series of 55 light-airplane accidents was examined in an effort to demonstrate the role of seats in the genesis of injury in seat occupants. Good engineering design of airplane seats is an important related issue which is not treated in this study. Case selection attempted to include only those events in which significant

but not extreme accelerations occurred. Ten of the fifty-five cases involved joint failure of seats and restraint systems. The majority of the observations were provided by aviation medical examiners who were typically very highly motivated practitioners of medicine with special interests and accomplishments in aviation. The other cases were reported by FAA accident investigators. No reliable marker of energy level was found in the data collected to control the finding that large accelerations tend to injure people and damage seats as well as most other structures regardless of the other interrelationships that might be involved. GRA

04 AIRCRAFT COMMUNICATIONS AND NAVIGATION

Includes digital and voice communication with aircraft; air navigation systems (satellite and ground based); and air traffic control.

For related information see also *17 Space Communications, Spacecraft Communications, Command and Tracking* and *Communications and Radar.*

N89-26831# Federal Aviation Administration, Atlantic City, NJ. Technical Center.

LORAN C COVERAGE IN ALASKA AFTER DUAL RATING PORT CLARENCE

Robert H. Erikson Jun. 1988 40 p

(Contract FAA-T0702-N)

(AD-A196032; DOT/FAA/CT-TN88/22) Avail: NTIS HC A03/MF A01

An analysis by the Federal Aviation Administration predicted Loran C coverage could be expanded throughout the interior of Alaska by modification of an existing Loran C transmitter. The modification would include adding Loran C station Port Clarence as a secondary on the Gulf of Alaska chain (7960) by dual rating the station. A flight test probe conducted in the summer of 1987 into the interior of Alaska to determine the extent of usable signals after dual rating Loran C station Port Clarence is described. Flight measurements indicated a largely increased operational area located in the middle to southern interior of Alaska. Author

N89-26832*# Federal Aviation Administration, Atlantic City, NJ.

ILS/MLS COLLOCATION TESTS AT MIAMI/TAMIAMI, FLORIDA AIRPORT

John Townsend Jun. 1989 23 p

(NASA Order T-0604-L)

(NASA-CR-185715; NAS 1.26:185715; DOT/FAA/CT-TN89/38)

Avail: NTIS HC A03/MF A01 CSCL 17G

A series of tests were performed by the Federal Aviation Administration (FAA) Technical Center at the Miami/Tamiami, Florida, Airport to verify the guidance material contained in the proposed amendments to Attachment G to Part 1 of the International Civil Aviation Organization (ICAO) Annex 10. A mock-up of the Technical Center's Test Bed Microwave Landing System (MLS) was collocated with the category 1 instrument landing system (ILS) on runway 9R. Several engineering flight tests were flown with ILS data collected and analyzed. These results were later verified by actually installing the MLS test bed at one of the locations used for the mockup tests. The results indicate that the proposed guidelines are adequate as published, but several items should be considered when implementing these guidelines. These items are presented as recommendations. Author

N89-26833# Federal Aviation Administration, Atlantic City, NJ.

AN OPERATIONAL DEMONSTRATION AND FLIGHT TEST OF THE MICROWAVE LANDING SYSTEM (MLS) AT THE MIAMI/TAMIAMI, FLORIDA AIRPORT Technical Report, Apr. 1989

Vincent L. Bencivenga and Robert H. Pursel Jul. 1989 37 p

(DOT/FAA/CT-TN89/37) Avail: NTIS HC A03/MF A01

At the request of the Microwave Landing System (MLS) Program Office, the Federal Aviation Administration (FAA) Technical Center conducted an operational demonstration and flight test of the MLS at Miami/Tamiami, Florida Airport. The demonstration/flight test was conducted in conjunction with an MLS seminar jointly sponsored by U.S. Department of Transportation, FAA, and Transport Canada Aviation Group. The Technical Center's MLS test bed, consisting of a 1.5 deg beamwidth elevation station and a 2 deg beamwidth azimuth station, was transported to, and temporarily installed at the Miami/Tamiami Airport on runway 9R, collocated with the commissioned instrument landing system (ILS). Additionally, an E-Systems preproduction model precision distance measuring equipment (DME/P) transponder was also installed adjacent to the runway 9R localizer equipment shelter. On March 29, 1989, seven 1-hour demonstration and data collection flights were flown for over 60 aviation, industry, and U.S. and international Government attendees. By careful siting of the MLS on runway 9R, proportional MLS signal coverage was also obtained in the approach regions of runways 9L and 13. By utilizing an FAA Technical Center designed and fabricated MLS area navigation (RNAV) computer on board the demonstration aircraft, precision approaches were flown not only to runway 9R, but also to runways 9L and 13. This demonstrated the tremendous flexibility and operational capability of MLS. The MLS signal-in-space on runway 9R met Category 2 ILS tolerances. No degradation of the ILS performance due to the MLS collocation was detected during this demonstration. Author

N89-26834# University of Southern California, Los Angeles. Inst. for Robotics and Intelligent Systems.

RESEARCH IN KNOWLEDGE-BASED VISION TECHNIQUES FOR THE AUTONOMOUS LAND VEHICLE PROGRAM Annual Technical Report No. 3, 1 Jun. 1987 - 31 May 1988

R. Nevatia, ed., K. Price, ed., W. Franzen, S. Gazit, G. Medioni, I. Paolin, and S. Peng Dec. 1988 87 p Prepared in cooperation with Defense Advanced Research Projects Agency, Arlington, VA; and Army Engineer Topographic Labs., Fort Belvoir, VA

(Contract DACA76-85-C-0009)

(AD-A208546; IRIS-248; ETL-0522) Avail: NTIS HC A05/MF A01 CSCL 12/9

This report describes our research in motion analysis and estimation techniques. This research is of particular relevance to the DARPA Autonomous Land Vehicle (ALV) program, but should also be of other general utility. Our basic approach for detecting and tracking motion is to extract and match features, such as lines and regions, from a sequence and to generate emotion estimates from these. We present one report on matching edge elements in connected line segments (contours) in a sequence of views. This work assumes relatively small motions between views. We also present a report on an alternative representation for motion and a technique to use occlusion in spatio-temporal analysis. We also present results from a basic integrated system that combines feature extraction, matching and motion estimation. GRA

05 AIRCRAFT DESIGN, TESTING AND PERFORMANCE

Includes aircraft simulation technology.

For related information see also *18 Spacecraft Design, Testing and Performance* and *39 Structural Mechanics.* For land transportation vehicles see *85 Urban Technology and Transportation.*

N89-26835# National Aerospace Lab., Tokyo (Japan). STOL Aircraft Project Group.

THE CONCEPTIONAL DESIGN STUDY OF USB POWERED LIFT AIRCRAFTS IN FY 1986

Jan. 1988 57 p In JAPANESE; ENGLISH summary

(NAL-TR-958; ISSN-0389-4010) Avail: NTIS HC A04/MF A01

The possibility of applications to various types of transports of the overwhelming high lift capability inherent in the USB powered lift concept was investigated with the use of a computer aided design (CAD) program. Emphasis is placed on the application of USB technology to regional transports of both land based and amphibian types, because of their relatively high probability of

realization relating to the 4th national comprehensive development plan. In addition to the CAD study, some relevant subjects such as examination of the predicted demand for regional air transportation, an evaluation of the engine cross shafting concept, an estimation of aerodynamic derivatives due to side-slip motion, consideration of common aircraft structure for both land based and amphibian type aircraft, and a survey of advanced navigation systems were also studied. Author

N89-26836 Department of the Air Force, Washington, DC.
HOSE REEL MONITOR FOR INFLIGHT REFUELING SYSTEM Patent
Tsutomu Yamamoto, inventor (to AF) 10 Jan. 1989 6 p Filed 14 Jan. 1988
(AD-D014054; US-Patent-4,796,838; US-Patent-Appl-SN-144885; US-Patent-Class-244-135) Avail: US Patent and Trademark Office CSCL 13/7

A bank of comparators is used to control a logic circuit which indicates proper system operation when measured hydraulic reel motor control pressures are within normal limits for the current airspeed after hose deployment. Also, before such deployment, simulated test signals are applied to the comparators to ensure proper operation of the comparators and logic circuitry. GRA

N89-26837 Department of the Air Force, Washington, DC.
COMBINATION BOUNDARY LAYER CONTROL SYSTEM FOR HIGH ALTITUDE AIRCRAFT Patent
George D. Brewer, inventor (to AF) and David P. Marshall, inventor (to AF) 28 Feb. 1989 5 p Filed 12 Aug. 1987
(AD-D014075; US-Patent-4,807,831; US-Patent-Appl-SN-084341; US-Patent-Class-244-117) Avail: US Patent and Trademark Office CSCL 13/7

This patent comprises a combination boundary layer control system that uses both suction and cryogenic wall cooling to reduce aircraft drag. The invention is particulary useful in circumstances where liquid hydrogen or other cryogenic fuels are used to operate the aircraft. In the preferred embodiment, a network of D-tube ducts are provided that are fluidly connected to a cryogenic fluid source. These cryogenic fluid ducts are selectively fed cryogenic fluid to reduce aircraft surface temperature and promote adhesion of boundary layer air to the aircraft. An air duct system is also provided to apply suction to the aircraft surface in order to remove the boundary layer at low altitude. The suction is applied by means of a multitude of minute holes in the aircraft skin which are fluidly connected to the air duct system. GRA

N89-26838# General Dynamics Corp., Fort Worth, TX.
ADVANCED DURABILITY ANALYSIS. VOLUME 2: ANALYTICAL PREDICTIONS, TEST RESULTS AND ANALYTICAL CORRELATIONS Final Report, Oct. 1984 - Feb. 1989
S. D. Manning and J. N. Yang (United Analysis, Inc., Vienna, VA.) 27 Feb. 1989 286 p
(Contract F33615-84-C-3208)
(AD-A207215; AFWAL-TR-86-3017-Vol-2) Avail: NTIS HC A13/MF A01 CSCL 01/3

Advanced durability analysis design tools have been developed for metallic aircraft structures. These tools can be used to evaluate durability design requirements for functional impairments due to: (1) excessive cracking, and (2) fuel leakage ligament breakage. The methodology accounts for the initial fatigue quality variation of structural details, the crack growth accumulation for a population of structural details under specified design conditions and structural properties. Step by step procedures are provided. This volume is limited to the analytical methods, technical aspects, concepts and philosophy for the durability analysis of metallic aircraft structures. The methodology reflects a probabilistic approach, a fracture mechanics philosophy and both deterministic and stochastic crack growth methods. It can be used to predict the probability of crack exceedance at any service time and/or the cumulative distribution of the time to reach any crack size. The methodology applies to the small crack size range associated with excessive cracking (e.g., less than 0.05') and to large through-the-thickness cracks (e.g., 0.5' to 0.75') associated with fuel leakage/ligament breakage. GRA

N89-26839# Army Aviation Engineering Flight Activity, Edwards AFB, CA.
AIRWORTHINESS AND FLIGHT CHARACTERISTICS EVALUATION OF THE EH-60A (QUICK FIX) HELICOPTER Final Report, 25 Nov. 1987 - 18 May 1988
David B. Cripps, Donald L. Underwood, David A. Downey, George M. Yamakawa, Charles Q. Crowell, and Joseph A. Lyle Oct. 1988 98 p
(AD-A207417; USAAEFA-87-07) Avail: NTIS HC A05/MF A01 CSCL 01/3

The U.S. Army Aviation Engineering Flight Activity conducted a limited Airworthiness and Flight Characteristics test of the EH-60A (Quick Fix) helicopter. During the test program, 49 flights were conducted for a total of 63.5 hours, of which 47.1 were productive. Initially the EH-60A was modified to the utility configuration where 22.3 productive hours were flown airspeed calibration, level flight performance, and vibration characteristics. All tests were performed at a Quick Fix mission center of gravity of approximately 361.9 fuselage station for both the utility and Quick Fix configuration. The Quick Fix configuration resulted in a 5.2 square feet increase in equivalent flat plate area which results in a 5 percent degradation in specific range at the recommended cruise airspeed, a 2 percent increase in fuel flow at the maximum endurance airspeed, and a 4 knot degradation in maximum level flight airspeed at sea level standard day conditions and mission gross weight (17,200 pound). The handling qualities of the Quick Fix configured EH-60A were essentially unchanged from the standard UH-60A helicopter. The clearance between the main rotor blades and direction finding dipole antennas during nose down slope landings was adequate. The absence of lower console lighting for the communication and navigation equipment was identified as a deficiency. GRA

N89-26840# Army Aviation Engineering Flight Activity, Edwards AFB, CA.
PRELIMINARY AIRWORTHINESS EVALUATION OF THE UH-60A EXTERNAL FUEL SYSTEM Final Report, 21 May - 20 May 1988
Michael K. Herbst, Michael A. Gleason, Paul Losier, and Reginald C. Murrell Dec. 1988 114 p
(AD-A207570; USAAEFA-87-04) Avail: NTIS HC A06/MF A01 CSCL 01/3

Testing was conducted to determine the effects of the installation of the External Fuel System (EFS) on the performance and handling qualities of the UH-60A helicopter. A total of 27 productive flight hours were flown at Edwards Air Force Base, California between 21 March and 20 May 1988. The evaluation did not reveal any problems that should preclude airworthiness qualification. The installation of the EFS with two 230-gallon tanks caused an increase in power required to hover in ground effect (10-foot wheel height) and out of ground effect of approximately 5 percent and 6 percent, respectively. The change in equivalent flat plate area in the EFS configuration with two 230-gallon tanks varied from 6.2 to 12.4 square feet when compared to the UH-60A in the normal utility configuration. The drag of the UH-60A in the EFS configuration with two 230-gallon tanks is significantly increased when the cargo doors and gunner windows are open. Three shortcomings and two Prime Item Development Specification noncompliances were identified during the handling qualities evaluation of the UH-60A in the EFS configuration. Two of the shortcomings have been noted during previous evaluations of the UH-60A in the normal utility configuration. Handling qualities were not significantly different than those of the UH-60A in the normal utility configuration. GRA

N89-26841*# McDonnell-Douglas Corp., Long Beach, CA.
FEASIBILITY AND BENEFITS OF LAMINAR FLOW CONTROL ON SUPERSONIC CRUISE AIRPLANES
A. G. Powell, S. Agrawal, and T. R. Lacey Jul. 1989 121 p Prepared in cooperation with McDonnell Aircraft Co.,

Saint Louis, MO
(Contract NAS1-18037)
(NASA-CR-181817; NAS 1.26:181817) Avail: NTIS HC A06/MF A01 CSCL 01C

An evaluation was made of the applicability and benefits of laminar flow control (LFC) technology to supersonic cruise airplanes. Ancillary objectives were to identify the technical issues critical to supersonic LFC application, and to determine how those issues can be addressed through flight and wind-tunnel testing. Vehicle types studied include a Mach 2.2 supersonic transport configuration, a Mach 4.0 transport, and two Mach 2-class fighter concepts. Laminar flow control methodologies developed for subsonic and transonic wing laminarization were extended and applied. No intractible aerodynamic problems were found in applying LFC to airplanes of the Mach 2 class, even ones of large size. Improvements of 12 to 17 percent in lift-drag ratios were found. Several key technical issues, such as contamination avoidance and excresence criteria were identified. Recommendations are made for their resolution. A need for an inverse supersonic wing design methodology is indicated. Author

N89-26842*# Douglas Aircraft Co., Inc., Long Beach, CA.
COMPOSITE TRANSPORT WING TECHNOLOGY DEVELOPMENT
Ram C. Madan Feb. 1988 92 p
(Contract NAS1-17970)
(NASA-CR-178409; NAS 1.26:178409) Avail: NTIS HC A05/MF A01 CSCL 01C

The design, fabrication, testing, and analysis of stiffened wing cover panels to assess damage tolerance criteria are discussed. The damage tolerance improvements were demonstrated in a test program using full-sized cover panel subcomponents. The panels utilized a hard skin concept with identical laminates of 44-percent 0-degree, 44-percent plus or minus 45-degree, and 12-percent 90-degree plies in the skins and stiffeners. The panel skins were impacted at midbay between the stiffeners, directly over the stiffener, and over the stiffener flange edge. The stiffener blades were impacted laterally. Impact energy levels of 100 ft-lb and 200 ft-lb were used. NASTRAN finite-element analyses were performed to simulate the nonvisible damage that was detected in the panels by nondestructive inspection. A closed-form solution for generalized loading was developed to evaluate the peel stresses in the bonded structure. Two-dimensional delamination growth analysis was developed using the principle of minimum potential energy in terms of closed-form solution for critical strain. An analysis was conducted to determine the residual compressive stress in the panels after impact damage, and the analytical predictions were verified by compression testing of the damaged panels. Author

N89-26843*# Army Aerostructures Directorate, Hampton, VA.
SCALING EFFECTS IN THE STATIC LARGE DEFLECTION RESPONSE OF GRAPHITE-EPOXY COMPOSITE BEAMS
Karen E. Jackson and Edwin L. Fasanella (Planning Research Corp., Hampton, VA.) Jun. 1989 15 p Presented at the AHS National Technical Specialists' Meeting on Advanced Rotorcraft Structures, Williamsburg, VA, 25-27 Oct. 1988 Previously announced in IAA as A89-29466
(NASA-TM-101619; NAS 1.15:101619; AVSCOM-TM-89-B-006) Avail: NTIS HC A03/MF A01 CSCL 01C

Scaling effects in the large deflection response of graphite-epoxy composite beams was investigated. Eight different scale model beams ranging from 1/6 to full-scale were subjected to an eccentric axial compressive load to promote large bending deformations and failures. Beams having laminate stacking sequences including unidirectional, angle ply, cross ply, and quasi-isotropic were tested to examine a wide variety of composite response and failure modes. The model beams were loaded under scaled test conditions until catastrophic failure. Data acquired included load, end displacement, and strain measurements, and qualitative failure measurements. The experimental data is compared to a large rotation beam analysis and a finite element model analysis. Results from the tests indicate that the beam response becomes nonlinear. Failure modes are consistent between scale models within a laminate family, however, a significant scale effect is observed in strength of the scaled beams. Author

N89-26844*# National Aeronautics and Space Administration. Ames Research Center, Moffett Field, CA.
METHOD FOR EXPERIMENTAL DETERMINATION OF FLUTTER SPEED BY PARAMETER IDENTIFICATION
E. Nissim (Technion - Israel Inst. of Tech., Haifa.) and Glenn B. Gilyard Washington Jun. 1989 44 p Previously announced in IAA as A89-30801
(NASA-TP-2923; H-1510; NAS 1.60:2923) Avail: NTIS HC A03/MF A01 CSCL 01C

A method for flight flutter testing is proposed which enables one to determine the flutter dynamic pressure from flights flown far below the flutter dynamic pressure. The method is based on the identification of the coefficients of the equations of motion at low dynamic pressures, followed by the solution of these equations to compute the flutter dynamic pressure. The initial results of simulated data reported in the present work indicate that the method can accurately predict the flutter dynamic pressure, as described. If no insurmountable difficulties arise in the implementation of this method, it may significantly improve the procedures for flight flutter testing. Author

06 AIRCRAFT INSTRUMENTATION

Includes cockpit and cabin display devices; and flight instruments.

For related information see also *19 Spacecraft Instrumentation* and *35 Instrumentation and Photography.*

N89-26845 Department of the Navy, Washington, DC.
COMPUTER-OPTIMAL STATE FEEDBACK CONTROLLER FOR ALL-ATTITUDE GIMBAL SYSTEM Patent
George L. Lauro, inventor (to Navy) 7 Mar. 1989 11 p Filed 2 Apr. 1987
(AD-D013972; US-Patent-4,811,233; US-Patent-Appl-SN-036225) Avail: US Patent and Trademark Office CSCL 17/7

An improved cost-optimal state feedback control system is disclosed for stabilizing the inertial reference platform in all-attitude inertial guidance systems which uses the region control concept. It reduces the computational requirements of cost-minimizing state feedback to within the capacity of aerospace vehicle on board control processors. The control system iterates the feedback compensation process so as to reduce the R-gyro error to essentially a zero value and to prevent the gimbal assembly from entering a gimbal lock orientation. GRA

N89-26846# Aeronautical Systems Div., Wright-Patterson AFB, OH.
F-15E EADI (ELECTRONIC ATTITUDE DIRECTOR INDICATOR) EVALUATION: A COMPARISON OF THREE FORMATS Final Report, Apr. - May 1988
R. K. Burns and P. B. Lovering (Midwest Research Inst., Dayton, OH.) Jun. 1988 74 p
(AD-A206809; ASD-TR-88-5030) Avail: NTIS HC A04/MF A01 CSCL 01/3

The primary task for any pilot is to maintain attitude awareness and spatial orientation throughout all phases of flight. Even the slightest hesitation or attitude interpretation error during the all intensive low altitude, high speed night mission could rapidly become a catastrophic error. The attitude display must provide an unambiguous presentation of aircraft attitude in a manner which allows the pilot to respond immediately without thinking which way is the shortest path to wings level flight. The present study compared the baseline F-15E electronic attitude display to two other displays: the F-15E display with sky pointer arrows and a 180-degree field-of-view-dimensional display with sky pointer arrows. The results indicated significantly faster decision times for the baseline F-15E display (1.03 seconds) and F-15E display with arrows (1.00 seconds) relative to the three-dimensional display

(1.18 seconds). This difference was present only for the 55-degree nose high attitude conditions. Nose low attitudes were significantly different in decision time. Correct responses using the F-15E display with arrows (90 percent) were significantly higher than the baseline F-15E display (76 percent) for nose low attitudes. GRA

07 AIRCRAFT PROPULSION AND POWER

Includes prime propulsion systems and systems components, e.g., gas turbine engines and compressors; and onboard auxilliary power plants for aircraft.

For related information see also *20 Spacecraft Propulsion and Power, 28 Propellants and Fuels,* and *44 Energy Production and Conversion.*

N89-26847 Department of the Air Force, Washington, DC.
NOZZLE FLAP HINGE JOINT Patent
William M. Madden, inventor (to AF), Claude R. Stogner, inventor (to AF), and Charles E. Spaeth, inventor (to AF) 12 Jul. 1988 4 p Filed 24 Feb. 1987
(AD-D014002; US-Patent-4,756,053; US-Patent-Appl-SN-018118; US-Patent-Class-162-23) Avail: US Patent and Trademark Office CSCL 13/5

This patent relates to a hinge joint for a nozzle flap for a gas turbine engine exhaust nozzle. First and second flaps are joined at a hinge joint formed by a hollow hinge pin passing through alternating lug extensions of the first and second flaps. A plurality of flow openings in the hollow hinge pin are provided for establishing fluid communication between the interior of the first flap and the interior of the second flap. GRA

N89-26848 Department of the Air Force, Washington, DC.
BACK-UP CONTROL SYSTEM FOR F101 ENGINE AND ITS DERIVATIVES Patent
Walter D. Hutto, Jr., inventor (to AF) and William W. Stockton, inventor (to AF) 3 Jan. 1989 13 p Filed 14 May 1987
(AD-D014051; US-Patent-4,794,755; US-Patent-Appl-SN-049351; US-Patent-Class-60-39-281) Avail: US Patent and Trademark Office CSCL 01/4

A back-up control system is implemented in a single engine aircraft to provide inactivation of a faulty primary system and engagement of secondary system, and thereby provide a means of maintaining controllable flight sustaining thrust. The aircraft's hydromechanical main engine control and its companion pressure and temperature sensors can develop faults which can result in the inability of the engine to deliver flight sustaining thrust. The electronic control contains logic functions which indicate failure of the main engine control when all of the following exists for a minimum of three seconds: (1) the power lever is at a position requesting a level of dry thrust which exceeds a predetermined threshold; (2) core engine speed is below that required to deliver the predetermined level of dry thrust; (3) core engine speed is not increasing; and (4) turbine temperature is beneath the maximum allowable limit. The backup system is used in conjunction with a three position cockpit switch having normal, on and standby position. In the normal position the back-up system is off and must be manually activated by switching to the on position. In the standby position, the backup system is automatically activated when the necessary conditions occur. GRA

N89-26849 Department of the Air Force, Washington, DC.
VARIABLE NOZZLE AREA TURBINE VANE COOLING Patent
Edward S. Hsia, inventor (to AF), John H. Starkweather, inventor (to AF), and William K. Koffel, inventor (to AF) 17 Jan. 1989 13 p Filed 19 May 1986
(AD-D014071; US-Patent-4,798,515; US-Patent-Appl-SN-895016; US-Patent-Class-415-115) Avail: US Patent and Trademark Office CSCL 21/5

The cooling insert for a movable vane in a jet engine is divided into plural overlapping forward and aft segregated members, each member being coolant fed through separate vane trunnion areas and each insert is of successively decreasing cross-sectional area. Problems of locally inadequate vane cooling, coolant match point movement, and unequal coolant supply pressures are addressed by the disclosed apparatus. Reuse of the trunnion supplied impingement cooling air for additional cooling functions is also disclosed. GRA

N89-26850 Department of the Air Force, Washington, DC.
COMPRESSOR BLADE CLEARANCE MEASUREMENT SYSTEM Patent
Rosario N. Demers, inventor (to AF) 21 Feb. 1989 19 p Filed 11 Mar. 1987 Supersedes AD-D012777
(AD-D014073; US-Patent-4,806,848; US-Patent-Appl-SN-024490; US-Patent-Class-324-61) Avail: US Patent and Trademark Office CSCL 14/2

The system is used to measure the gap between the turbine engine compressor blade tip and the compressor case. The measurement is accomplished while the engine is running. This system has several features which minimize problems plaguing earlier systems. These include tuning stability and sensitivity drift. Both these problems are intensified by the environmental factors present on compressors, i.e., wide temperature fluctuations, vibrations, conductive contamination of probe tips and others. The circuitry in this new system provides phase lock feedback to control tuning and shunt calibration to measure sensitivity. The use of high frequency excitation lowers the probe tip impedance, thus minimizing the effects of contamination. The ability to control tuning and to calibrate has been demonstrated. GRA

N89-26851# Naval Air Propulsion Test Center, Trenton, NJ. Propulsion Engineering Dept.
STATISTICS ON AIRCRAFT GAS TURBINE ENGINE ROTOR FAILURES THAT OCCURRED IN US COMMERCIAL AVIATION DURING 1983 Final Report
R. A. Delucia and J. T. Salvino Mar. 1989 23 p
(Contract DOT-FA71NAA-P98)
(AD-A207592; NAPC-PE-184; DOT/FAA/CT-89/5) Avail: NTIS HC A03/MF A01 CSCL 21/5

This report presents statistics relating to gas turbine engine rotor failures which occurred during 1983 in commercial aviation service use. One-hundred and seventy-two failures occurred in 1983. Rotor fragments were generated in 96 of the failures and, of these, 9 were uncontained. The predominant failures involved blade fragments, 95.4 percent of which were contained. Five disk failures occurred and four were uncontained. Fifty-nine percent of the 172 failures occurred during the takeoff and climb stages of flight. This service data analysis is prepared on a calendar year basis and published yearly. The data support flight safety analyses, proposed regulatory actions, certification standards, and cost benefit analyses. GRA

N89-26852 Department of the Air Force, Washington, DC.
AFTERBURNER FLAMEHOLDER CONSTRUCTION Patent
Donald W. Eldredge, inventor (to AF) and Billy R. Milam, inventor (to AF) 28 Mar. 1989 4 p Filed 25 Jun. 1987
(AD-D014116; US-Patent-4,815,283; US-Patent-Appl-SN-066154; US-Patent-Class-602-610) Avail: US Patent and Trademark Office CSCL 21/5

A flameholder for a gas turbine engine includes a retainer plate on the igniter holder boss which protrudes from the flameholder gutter and extends through a clearance hole in the outer shroud. The retainer plate permits thermally induced growth of the parts but does not allow the fuel spray and air flow gap near the igniter to increase significantly, thus assuredly maintaining a sufficiently rich fuel/air mixture to promote ignition. GRA

N89-26853 Department of the Air Force, Washington, DC.
NOZZLE FLANGE ATTACHMENT AND SEALING ARRANGEMENT Patent
Harold R. Hansel, inventor (to AF) and Vincent M. Drerup, inventor (to AF) 28 Mar. 1989 5 p Filed 13 Nov. 1987
(AD-D014123; US-Patent-4,815,933; US-Patent-Appl-SN-122153;

US-Patent-Class-415-189) Avail: US Patent and Trademark Office CSCL 21/5

The invention comprises a boltless turbine nozzle and nozzle support assembly that includes a turbine nozzle mounting flange seated in a nozzle seat forming a part of the nozzle support. Pins are used for affixing the nozzle support seat and baffles are providing for maintaining the pins in their desired locations. A retaining ring is preferably used to retain the baffles adjacent to the pins. A pressure actuated pliable seal is affixed to the turbine nozzle adjacent to the nozzle seat in order to provide an air seal across the completed assembly. GRA

N89-26854# Advisory Group for Aerospace Research and Development, Neuilly-Sur-Seine (France).
MEASUREMENT UNCERTAINTY WITHIN THE UNIFORM ENGINE TEST PROGRAMME
J. P. K. Vleghert, ed. (National Aerospace Lab., Amsterdam, Netherlands) May 1989 77 p
(AGARD-AG-307; ISBN-92-835-0508-5) Copyright Avail: NTIS HC A05/MF A01

This AGARDograph is an outcome of the Propulsion and Energetics Panel Working Group 15 on, Uniform Engine Testing Programme (AGARD AR 248). During the performance of this Group it appeared that the results of some test runs were somewhat scattered, without an obvious explanation. The Group, therefore, formed a sub-Group with the task of carefully assessing the uncertainties of the measured data in order to find out whether the scattering was within the expected uncertainty or whether an explanation must be found. Since the results of the efforts of the sub-Group have some importance beyond the Working Group 15 tests, it was decided to report them in the form of an AGARDograph. In Chapter 5 the different uncertainties are estimated. The discussion on the uncertainties appears in Chapter 6 and in the following Chapter 7, ten conclusions are drawn from the efforts. This AGARDograph was prepared at the request of the Propulsion and Energetics Panel of AGARD. Author

N89-26855# Sandia National Labs., Albuquerque, NM. Advanced Technology Div.
AUTONOMOUS LAND NAVIGATION: A DEMONSTRATION OF RETROTRAVERSE
P. R. Klarer 1989 8 p Presented at the 16th AUVS Annual Technical Symposium and Exhibit, Washington, DC, 17 Jul. 1989
(Contract DE-AC04-76DP-00789)
(DE89-011881; SAND-89-0393C; CONF-890783-1) Avail: NTIS HC A02/MF A01

This paper describes a hardware and software system developed to perform autonomous navigation of a land vehicle in a structured environment. The vehicle used for development and testing of the system was the Jeep Cherokee Mobile Robotics Testbed Vehicle developed at Sandia National Laboratories in Albuquerque. Since obstacle detection/avoidance has not yet been incorporated into the system, a structured environment is postulated that presumes the paths to be traversed are obstacle-free. The system performs path planning and execution (following) based on maps constructed using the vehicle's navigation system and onboard map-maker. The system configuration allows a map to be generated and stored during teleoperation of the vehicle, which may then be inverted and autonomously followed to perform retrotraverse back to the path start point. The system software, hardware, and performance data are discussed. DOE

N89-26856# Astron Research and Engineering, Sunnyvale, CA.
DEMONSTRATION OF OBLIQUE DETONATION WAVE FOR HYPERSONIC PROPULSION Final Technical Report, 1 Aug. 1988 - 31 Jan. 1989
Takashi Nakamura, Michael J. Schuh, Donald S. Randall, Thomas J. Dahm, and David T. Pratt 30 Mar. 1989 118 p
(Contract F49620-88-C-0130)
(AD-A208268; ASTRON-7151-001; AFOSR-89-0659TR) Avail: NTIS HC A06/MF A01 CSCL 21/5

The Oblique Detonation Wave Engine (ODWE) offers a number of advantages over the Supersonic Combustor Ramjet (SCRAMJET) for hypersonic aeropropulsion. The objective of this program is to obtain data on the stability of the Oblique Detonation Wave (ODW) and to assess the applicability of the ODW to hypersonic propulsion. The program consists of the basic study of the ODW phenomenon and the design study of the test facility (Phase 1), and an indepth experimental study of the ODW in a ram cannon-type combustion tube with a hypervelocity projectile launched into the tube by a two-stage light-gas gun (Phase 2). This Phase 1 report summarizes the results pertaining to the stability of the ODW and the experimental facility designs. It is concluded that ODW will be initiated and sustained in the test facility configuration and that the tests will generate data concerning key issues for the application of the ODW to hypersonic propulsion. GRA

08 AIRCRAFT STABILITY AND CONTROL

Includes aircraft handling qualities; piloting; flight controls; and autopilots.

For related information see also *05 Aircraft Design, Testing and Performance.*

N89-26857 Department of the Air Force, Washington, DC.
CONTROL SURFACE DUAL REDUNDANT SERVOMECHANISM Patent
Clete M. Boldrin, inventor (to AF), Richard D. McCorkle, inventor (to AF), Jimmy W. Rice, inventor (to AF), and James J. Rustik, inventor (to AF) 31 Jan. 1989 6 p Filed 11 Dec. 1984
(AD-D014058; US-Patent-4,800,798; US-Patent-Appl-SN-680674)
Avail: US Patent and Trademark Office CSCL 09/1

A dual redundant servomechanism for moving aircraft control surfaces is disclosed. The servomechanism is of the type whose input commands, from the pilot of the aircraft, are transmitted electrically. Force fight, which is associated with such dual servomechanisms when they are connected to a common aircraft control surface, is minimized. This is accomplished by providing the control system for each servomechanism with input signals which are electrically summed. Each control system includes electrical transducers which provide a signal indicative of actuator position and the pressure associated with the hydraulic motor used in each servomechanism. GRA

N89-26858 Department of the Air Force, Washington, DC.
BRAIN O2 RESERVE LIMITER FOR HIGH PERFORMANCE AIRCRAFT Patent
Robert E. VanPatten, inventor (to AF) 18 Apr. 1989 6 p Filed 7 Apr. 1987 Supersedes AD-D012902
(AD-D014137; US-Patent-4,821,982; US-Patent-Appl-SN-035425; US-Patent-Class-244-76R) Avail: US Patent and Trademark Office CSCL 01/4

A method for controlling an aircraft to prevent high G-caused pilot unconsciousness is disclosed. Data defining a state space of acceleration, rate of change of acceleration and duration of acceleration at maximum acceleration within which an aircraft may be operated without causing pilot unconsciousness is provided to an aircraft intelligent flight control system. The flight control system continuously monitors the past and present state of the aircraft and compares to the surface boundaries of the defined safe state space. Whenever the aircraft exceeds those boundaries, the flight control system intervenes to unload the aircraft to within those boundaries. Additional data and measurements may be added to define an n-dimensional state space. Another embodiment unloads the aircraft to a baseline acceleration. A simplified embodiment is described which compares current acceleration to a preselected value of acceleration. If the current acceleration exceeds the preselected value, the previous acceleration onset rate is compared to a preselected acceleration onset rate. If it exceeds the preselected onset rate, the duration of time the current and immediately past acceleration has exceeded the preselected value of acceleration is determined. If that value is greater than a

preselected duration, the flight control system commands the aircraft ot perform an unloading maneuver to reduce the G loading on the aircraft to a preselected baseline acceleration. GRA

N89-26859*# Princeton Univ., NJ. Dept. of Mechanical and Aerospace Engineering.
DESIGN OF AN ACTIVE HELICOPTER CONTROL EXPERIMENT AT THE PRINCETON ROTORCRAFT DYNAMICS LABORATORY Interim Report, Jan. 1988 - May 1989
Andrew M. Marraffa and R. M. McKillip, Jr. May 1989 106 p
(Grant NAG2-415)
(NASA-CR-185490; NAS 1.26:185490) Avail: NTIS HC A06/MF A01 CSCL 01C

In an effort to develop an active control technique for reducing helicopter vibrations stemming from the main rotor system, a helicopter model was designed and tested at the Princeton Rotorcraft Dynamics Laboratory (PRDL). A description of this facility, including its latest data acquisition upgrade, are given. The design procedures for the test model and its Froude scaled rotor system are also discussed. The approach for performing active control is based on the idea that rotor states can be identified by instrumenting the rotor blades. Using this knowledge, Individual Blade Control (IBC) or Higher Harmonic Control (HHC) pitch input commands may be used to impact on rotor dynamics in such a way as to reduce rotor vibrations. Discussed here is an instrumentation configuration utilizing miniature accelerometers to measure and estimate first and second out-of-plane bending mode positions and velocities. To verify this technique, the model was tested, and resulting data were used to estimate rotor states as well as flap and bending coefficients, procedures for which are discussed. Overall results show that a cost- and time-effective method for building a useful test model for future active control experiments was developed. With some fine-tuning or slight adjustments in sensor configuration, prospects for obtaining good state estimates look promising. Author

N89-26860*# Systems Technology, Inc., Hawthorne, CA.
DESIGN CONSIDERATIONS OF MANIPULATOR AND FEEL SYSTEM CHARACTERISTICS IN ROLL TRACKING Final Report
Donald E. Johnston and Bimal L. Aponso Washington Feb. 1988 240 p
(Contract NAS2-12221)
(NASA-CR-4111; H-1438; NAS 1.26:4111) Avail: NTIS HC A11/MF A01 CSCL 01C

A fixed-base simulation was performed to identify and quantify interactions between the pilot's hand/arm neuromuscular subsystem and such control system features of typical modern fighter aircraft roll rate command mechanizations as: (1) force versus displacement sensing side-stick type manipulator, (2) feel force/displacement gradient, (3) feel system versus command prefilter dynamic lag, and (4) flight control system effective time delay. The experiment encompassed some 48 manipulator/filter/aircraft configurations. Displacement side-stick experiment results are given and compared with the previous force sidestick experiment results. Attention is focused on control bandwidth, excitement (peaking) of the neuromuscular mode, feel force/displacement gradient effects, time delay effects, etc. Section 5 is devoted to experiments with a center-stick in which force versus displacement sensing, feel system lag, and command prefilter lag influences on tracking performance and pilot preference are investigated. Author

N89-26861*# National Aeronautics and Space Administration. Langley Research Center, Hampton, VA.
AERODYNAMIC PARAMETERS OF AN ADVANCED FIGHTER AIRCRAFT ESTIMATED FROM FLIGHT DATA. PRELIMINARY RESULTS
Vladislav Klein, Keven P. Breneman, and Thomas P. Ratvasky (Joint Inst. for Advancement of Flight Sciences, Hampton, VA.) Jul. 1989 59 p
(NASA-TM-101631; NAS 1.15:101631) Avail: NTIS HC A04/MF A01 CSCL 01C

Preliminary estimates of aerodynamic parameters of an advanced fighter aircraft were obtained from flight data of different values of the angle of attack from 8 to 54 deg. The data were analyzed by a stepwise regression with the ordinary least squares technique. The estimated stability and control derivatives are plotted against the angle of attack and compared with wind tunnel measurement and previous flight results. Also included is the data compatibility check of measured data. The effect of various input forms on the estimates is demonstrated in two examples using simulated data. Author

N89-26862# Messerschmitt-Boelkow-Blohm G.m.b.H., Bremen (Germany, F.R.). Unternehmensbereich Transportflugzeuge.
ELECTRICAL PRIMARY FLIGHT CONTROL SYSTEM (FLY BY WIRE). FLIGHT CONTROL SYSTEMS OF NEW TECHNOLOGY Final Report, Dec. 1987
U. B. Carl Jun. 1988 202 p In GERMAN; ENGLISH summary
Original contains color illustrations
(Contract BMFT-LFL-8360-7)
(MBB-UT-122/88; ETN-89-94615) Avail: NTIS HC A10/MF A01

Results of a predevelopment program for Fly by Wire (FBW) flight control systems in civil aircraft are presented. The concept is based on requirements for certification of safety-critical functions, capacity of the computer systems to implement active control function (gust load alleviation, variable camber wing control etc) and a cockpit standard with mini-stick and digital display and operation systems. The experimental system consists of a quad-redundant, fault-tolerant multicomputer system and a quadruplex Actuator Electronic Unit (AEU) providing the redundancy management and force synchronization of parallel-active electrohydraulic servoactuators. The computer-interlane communication is by fiber optics. By A300/310 flight simulator-investigations the control laws with command and flight envelope protections are validated. The experimental system was tested in a rig with aircraft-simulation in the loop. The control and redundancy management-concept for the AEU's and parallel-redundant actuator configurations are verified by test results. ESA

N89-26863# Naval Postgraduate School, Monterey, CA.
FEASIBILITY STUDY FOR ENHANCED LATERAL CONTROL OF THE P-3C AIRCRAFT M.S. Thesis
Kimberly K. Smith Mar. 1989 118 p
(AD-A208461) Avail: NTIS HC A06/MF A01 CSCL 01/4

New mission requirements dictate the need to improve the P-3's defensive maneuvering capabilities. Research was conducted to find viable methods of increasing the current roll response of the P-3. First, a flight simulator was used to determine an initial target roll response. Next, a computer code was used to evaluate the aerodynamic effect of varying the size and deflection of the aileron. These results, along with the flight simulator tests, were used to analyze the requirements to reach the target response. Several ways to achieve this goal are discussed. It was found that by increasing the aileron deflection from + or - 20 deg to + or - 25 deg and increasing the aileron chord by 50 percent, a 58 percent increase in Ci (total rolling moment coefficient) could be realized. This does not reach the goal of a 100 percent increase in Ci, but, it does yield a large increase in lateral control response. An increase in aileron size and deflection along with some of the other suggested modifications would certainly approach the desired goal. GRA

09 RESEARCH AND SUPPORT FACILITIES (AIR)

Includes airports, hangars and runways; aircraft repair and overhaul facilities; wind tunnels; shock tubes; and aircraft engine test stands.

For related information see also *14 Ground Support Systems and Facilities (Space).*

N89-26864# Concrete Technology Information Analysis Center, Vicksburg, MS.

EVALUATION OF BARRIER CABLE IMPACT PAD MATERIALS Final Report, Sep. 1983 - Sep. 1984

Tony B. Husbands and Dennis L. Bean Apr. 1989 93 p

(AD-A207554; CTIAC-84; WES/TR/SL-87-33; WES/TR/SL-89-5) Avail: NTIS HC A05/MF A01 CSCL 01/4

The U.S. Air Force uses an aircraft arresting system on many of their runways for emergency stopping of aircraft. It consists of a 1- or 1-1/4-inch steel cable stretched across the runway connected to a braking mechanism. When aircraft tires impact the cable, considerable damage occurs to concrete and other materials placed underneath the cable. Materials previously used were not performing satisfactorily for various reasons. A survey was made in 1980 for the Air Force Engineering and Services Center (AFESC) to locate materials for evaluation. Five of these were selected for detailed testing. The materials were tested for gel times, peak exotherms, bond strength, abrasion resistivity, ultraviolet degradation, resiliency, hardness, abrasion-impact resistance, effect of curing temperature, and proportioning errors. The materials which showed most promise were field tested at Homestead and Tyndall Air Force Bases. GRA

N89-26865*# Princeton Univ., NJ. Dept. of Mechanical and Aerospace Engineering.

HIGH-SPEED DATA ACQUISITION FOR THE PRINCETON UNIVERSITY DYNAMIC MODEL TRACK Interim Report, Jan. 1987 - Jan. 1988

Michael G. Demko and R. M. McKillip, Jr. Jan. 1988 42 p

(Grant NAG2-415)

(NASA-CR-185491; NAS 1.26:185491) Avail: NTIS HC A03/MF A01 CSCL 14B

Real time analysis of data can reduce the time involved in exploring dynamic systems. The failure of the data acquisition system at the Princeton Dynamic Model Track prompted its replacement with a real time data acquisition system. Data can be obtained from an experiment and analyzed during and immediately following a data run. The new system employs high speed analog to digital conversion and a small computer to collect data. Sampling rates of 1000 hertz over 44 channels (44,000 words/sec) are obtainable. The data can be accessed as it enters the computer's environment where it may be displayed or stored for later processing. The system was tested on a helicopter rotor steep descent experiment. The data collected compares with previous data from a similar experiment. Author

N89-26866*# Stanford Univ., CA. Dept. of Aeronautics and Astronautics.

DESIGN AND CALIBRATION OF THE MIXING LAYER AND WIND TUNNEL

James H. Bell and Rabindra D. Mehta May 1989 36 p

(Contract NCC2-55)

(NASA-CR-185472; NAS 1.26:185472; JIAA-TR-89) Avail: NTIS HC A03/MF A01 CSCL 01E

A detailed account of the design, assembly and calibration of a wind tunnel specifically designed for free-shear layer research is contained. The construction of this new facility was motivated by a strong interest in the study of plane mixing layers with varying initial and operating conditions. The Mixing Layer Wind tunnel is located in the Fluid Mechanics Laboratory at NASA Ames Research Center. The tunnel consists of two separate legs which are driven independently by centrifugal blowers connected to variable speed motors. The blower/motor combinations are sized such that one is smaller than the other, giving maximum flow speeds of about 20 and 40 m/s, respectively. The blower speeds can either be set manually or via the Microvax II computer. The two streams are allowed to merge in the test section at the sharp trailing edge of a slowly tapering splitter plate. The test section is 36 cm in the cross-stream direction, 91 cm in the spanwise direction and 366 cm in length. One test section side-wall is slotted for probe access and adjustable so that the streamwise pressure gradient may be controlled. The wind tunnel is also equipped with a computer controlled, three-dimensional traversing system which is used to investigate the flow fields with pressure and hot-wire instrumentation. The wind tunnel calibration results show that the mean flow in the test section is uniform to within plus or minus 0.25 pct and the flow angularity is less than 0.25 deg. The total streamwise free-stream turbulence intensity level is approximately 0.15 pct. Currently the wind tunnel is being used in experiments designed to study the three-dimensional structure of plane mixing layers and wakes. Author

N89-26867# Wisconsin Univ., Madison. Applied Superconductivity Center.

DESIGN AND OPERATION OF A HORIZONTAL LIQUID HELIUM FLOW FACILITY

S. W. VanSciver and J. G. Wiesend, II 1988 6 p Presented at the 12th International Cryogenic Engineering Conference and Exhibition, Southampton, United Kingdom, 12-15 Jul. 1988

(Contract DE-AC02-86ER-40306)

(DE89-013482; CONF-880736-6) Avail: NTIS HC A02/MF A01

The University of Wisconsin horizontal liquid helium flow facility (LHFF) consists of a five meter long 20 cm ID horizontal dewar connected to two end boxes. Several heat exchanger inserts have been built to allow variable temperature operation of 1.6 K less than or equal to T less than or equal to 4.2 K. A centrifugal pump is installed at one end of the facility permitting experiments in forced flow liquid helium up to 100 gm/s. The horizontal design allows experimentation on long straight test sections which may be used either to study fundamental properties of heat and mass transfer in helium or prototype cryogenic components under realistic conditions. A detailed description of the design and operating experience of the LHFF is presented. DOE

N89-26868# Federal Aviation Administration, Atlantic City, NJ.

EVALUATION OF AN UPDATED DESIGN OF AN INTERNALLY LIGHTED WIND CONE

Eric S. Katz Aug. 1989 14 p

(DOT/FAA/CT-TN89/45) Avail: NTIS HC A03/MF A01

An updated version of an 18-inch internally lighted wind cone was evaluated. The original model was evaluated at the Federal Aviation Administration (FAA) Technical Center. The results of that evaluation, as detailed in Technical Note DOT/FAA/CT-TN85/4 (February 1985), revealed that the original model of the internally lighted wind cone did not provide adequate wind direction and speed information under low velocity (10 knots or less) wind conditions. The new model was installed in close proximity to the standard externally lighted wind cone at the Atlantic City International Airport, N.J., to permit a comparative evaluation by FAA and general aviation pilots. Results of the testing, accomplished during taxi and flight operations under wind conditions of 10 knots or less, revealed that the updated model still does not provide adequate wind direction and speed information. Participating pilots preferred the standard externally lighted wind cone. Author

N89-26869*# Vigyan Research Associates, Inc., Hampton, VA.

THE NASA LANGLEY RESEARCH CENTER 0.3-METER TRANSONIC CRYOGENIC TUNNEL T-P/Re-M CONTROLLER MANUAL

S. Balakrishna and W. Allen Kilgore Jul. 1989 41 p

(Contract NAS1-17919)

(NASA-CR-181868; NAS 1.26:181868) Avail: NTIS HC A03/MF A01 CSCL 14B

A new microcomputer based controller for the 0.3-m Transonic Cryogenic Tunnel (TCT) has been commissioned in 1988 and has reliably operated for more than a year. The tunnel stagnation

pressure, gas stagnation temperature, tunnel wall structural temperature and flow Mach number are precisely controlled by the new controller in a stable manner. The tunnel control hardware, software, and the flow chart to assist in calibration of the sensors, actuators, and the controller real time functions are described. The software installation details are also presented. The report serves as the maintenance and trouble shooting manual for the 0.3-m TCT controller. Author

N89-26870# Aktiebolaget Rollab, Stockholm (Sweden).
ON INTERNAL BENDING-BEAM STRAIN-GAGE WIND TUNNEL BALANCES
Knut Fristedt Jan. 1989 99 p
(RR-070; ETN-89-94940) Avail: NTIS HC A05/MF A01

The relative load-carrying capacity of three types of internal balances was compared using information in the literature. The bending-beam balance is superior, when D is less than 35 mm. The capacity of task-balances is equal at larger diameters and the two-shell balance is a competitor, when D is greater than 50 mm. A strength computation model of the bending-beam balance of the Rollab type based on simple engineering theories is presented. The strength of available types of high alloy steels is discussed as well as the expected relations between mechanical stresses and electrical signals. It is shown during the calculation of the 30 mm balance, that the angle deflection of the sting at maximum load is very large, and that it is very beneficial to have access to a sting material with higher modulus of elasticity than steel. The influence of the numerical value of the diameter on the load carrying capacity at constant stress of the current type of balance is discussed, and task and two-shell balances are compared. A mathematical model of 2nd degree, which combines the force system loading the balance with the balance signals is described. This model can be used during calibration and wind-tunnel testing. ESA

N89-26871# Ballistic Research Labs., Aberdeen Proving Ground, MD.
A MULTIDRIVER SHOCK TUBE MODEL OF A LARGE BLAST SIMULATOR Final Report
Edmund J. Gion May 1989 41 p
(AD-A208324; BRL-MR-3757) Avail: NTIS HC A03/MF A01 CSCL 20/4

The construction of the BRL Multidriver Shock Tube (MD-ST) Model is documented. The facility is a 1:22 model of the Large Blast Simulator at the Centre d'Etude de Gramat, France, except for a lengthened driven tube to permit observation of the full waveform development without interference from the open-end, reflected rarefaction wave (since the Rarefaction Wave Eliminator was not modeled). It is designed with a good safety factor to withstand driver pressures to 24,000 kPa (3,500 psi). Initial tests to greater than 22,100 kPa (3,200 psi) have been performed, and results are compared to other available data. Additionally, the double diaphragm technique, described, was used to attain the highest shock pressures. GRA

N89-26872# Naval Postgraduate School, Monterey, CA.
AN INVESTIGATION INTO THE USE OF AN EXISTING SHOCK TUBE AS A DRIVER FOR A HYPERSONIC SHOCK TUNNEL M.S. Thesis
Michael H. Sherman Mar. 1989 152 p
(AD-A208483) Avail: NTIS HC A08/MF A01 CSCL 01/1

This thesis describes experiments carried out using an existing tube alone, and with the tube connected to two-dimensional wedge nozzle. The range of maximum duration of steady reflected pressure from 3.5 to 5 milliseconds was achieved through tailored operation for incident shock strengths of 3.4 and 2.0, using pure Helium and a 70 percent Helium/30 percent Nitrogen mixture as the driver gas respectfully. Spark and continuous light shadowgraph techniques were attempted using an optical window at the Mach 4.3 location. Results demonstrated that the short duration flow phenomena in a shock tunnel can be recorded successfully using existing equipment. Calculations showed that the addition of a Mach 10 nozzle and 15 cu m (6' diameter x 15' long) dump chamber would provide a useful hypersonic facility for instruction and research. GRA

12 ASTRONAUTICS (GENERAL)

For extraterrestrial exploration see *91 Lunar and Planetary Exploration.*

N89-26873*# National Aeronautics and Space Administration, Washington, DC.
THE BEST WE CAN BE
1989 28 p
(NASA-TM-101781; NAS 1.15:101781) Avail: NTIS HC A03/MF A01; SOD HC $2.00 as 033-000-01037-1 CSCL 22A

A brief history of the U.S. manned space program is presented covering the early Mercury and Gemini missions, the Apollo lunar missions, the Skylab project, and the Space Shuttle missions. The role of the Space Station in future manned missions is also discussed. Descriptions of government centers and major contractors supporting the Space Shuttle program are given. M.G.

N89-26874# Deutsche Forschungsgemeinschaft, Bonn (Germany, F.R.).
SPACE RESEARCH IN THE FEDERAL REPUBLIC OF GERMANY (FRG), 1986 AND 1987
1988 56 p
(ETN-89-94427) Avail: NTIS HC A04/MF A01

Space astronomy and solar physics; solar system; solar wind, magnetospheres, and energetic particules; atmospheres and ionospheres; Earth observations; materials science; life sciences; and rocket launches are discussed. ESA

13 ASTRODYNAMICS

Includes powered and free-flight trajectories; and orbital and launching dynamics.

N89-26875# Instituto de Pesquisas Espaciais, Itajuba (Brazil).
FORMULATION OF NUMERICAL ORBIT PROPAGATION AND TIME ERROR CORRECTION
Sebastiao Cicero PinheiroGomes and Helio KoitiKuga Dec. 1988 8 p Presented at the 39th Congress of the International Astronautical Federation, Bangalore, India, 8-15 Oct. 1988
(INPE-4774-PRE/1443) Avail: NTIS HC A02/MF A01

Several forms of numerical orbit propagation are reviewed. Basically, they consist of formulating in different fashions the differential equations which represent the dynamics of orbital motion. Such formulations (time transformation, stabilization, regularization) are developed within a fictitious time frame which varies nonlinearly with the physical time. Thus, the physical time becomes a generalized coordinate of the system which should be obtained numerically and, as a consequence, with a certain inevitable numerical error. The nature of this time error is analyzed and a simple correction is proposed here, together with computer simulation results. Author

14 GROUND SUPPORT SYSTEMS AND FACILITIES (SPACE)

Includes launch complexes, research and production facilities; ground support equipment, e.g., mobile transporters; and simulators.

For related information see also *09 Research and Support Facilities (Air).*

No abstracts in this category.

15 LAUNCH VEHICLES AND SPACE VEHICLES

Includes boosters; operating problems of launch/space vehicle systems; and reusable vehicles.

For related information see also *20 Spacecraft Propulsion and Power.*

N89-26876*# National Aeronautics and Space Administration. Lewis Research Center, Cleveland, OH.
NASA'S CHEMICAL TRANSFER PROPULSION PROGRAM FOR PATHFINDER
Ned P. Hannum, Frank D. Berkopec, and Robert L. Zurawski 1989 18 p Presented at the 25th Joint Propulsion Conference, Monterey, CA, 10-12 Jul. 1989; cosponsored by the AIAA, ASME, SAE, and ASEE
(NASA-TM-102298; E-4976; NAS 1.15:102298; AIAA-89-2298) Avail: NTIS HC A03/MF A01 CSCL 22B

Pathfinder is a research and technology project, with specific deliverables, initiated by the National Aeronautics and Space Administration (NASA) which will strengthen the technology base of the United States civil space program in preparation for future space exploration missions. Pathfinder begins in Fiscal Year 1989, and is to advance a collection of critical technologies for these missions and ensure technology readiness for future national decisions regarding exploration of the solar system. The four major thrusts of Pathfinder are: surface exploration, in-space operations, humans-in-space, and space transfer. The space transfer thrust will provide the critical technologies needed for transportation to, and return from, the Moon, Mars, and other planets in the solar system, as well as for reliable and cost-effective Earth-orbit operations. A key element of this thrust is the Chemical Transfer Propulsion program which will provide the propulsion technology for high performance, liquid oxygen/liquid hydrogen expander cycle engines which may be operated and maintained in space. Described here are the program overview including the goals and objectives, management, technical plan, and technology transfer for the Chemical Transfer Propulsion element of Pathfinder. Author

16 SPACE TRANSPORTATION

Includes passenger and cargo space transportation, e.g., shuttle operations; and space rescue techniques.

For related information see also *03 Air Transportation and Safety* and *18 Spacecraft Design, Testing and Performance.* For space suits see *54 Man/System Technology and Life Support.*

N89-26877*# National Aeronautics and Space Administration. Lewis Research Center, Cleveland, OH.
SATELLITE RELOCATION BY TETHER DEPLOYMENT
Geoffrey A. Landis and Frank J. Hrach Apr. 1989 16 p
(NASA-TM-101992; E-4696; NAS 1.15:101992) Avail: NTIS HC A03/MF A01 CSCL 22B

Several new uses of satellite tethers are discussed, including: (1) using tether extension to reposition a satellite in orbit without fuel expenditure by extending a mass on the end of a tether; (2) using a tether for energy storage to power the satellite during eclipse; and (3) using a tether for eccentricity pumping to correct perturbations in the orbit and as a means of adding energy to the orbit for boosting and orbital transfer. Author

N89-26878*# National Aeronautics and Space Administration. Langley Research Center, Hampton, VA.
TWO-STAGE REUSABLE LAUNCH SYSTEM UTILIZING A WINGED CORE VEHICLE AND GLIDEBACK BOOSTERS
Ian O. MacConochie, James A. Martin, James S. Wood, and Miles O. Duquette (Joint Inst. for Advancement of Flight Sciences, Washington, DC.) Jul. 1989 21 p
(NASA-TM-101513; NAS 1.15:101513) Avail: NTIS HC A03/MF A01 CSCL 22B

A near-term technology launch system is described in which Space Shuttle main engines are used on a manned orbiter and also on twin strap-on unmanned boosters. The orbiter has a circular body and clipped delta wings. The twin strap-on boosters have a circular body and deployable oblique wings for a glideback recovery. The dry and gross weights of the system, capable of delivering 70klb of cargo to orbit, are compared with a similar system with hydrocarbon-fueled boosters and with the current Shuttle. Author

17 SPACE COMM., SPACECRAFT COMM., COMMAND & TRACKING

Includes telemetry; space communications networks; astronavigation and guidance; and radio blackout.

For related information see also *04 Aircraft Communications and Navigation* and *32 Communications and Radar.*

N89-26879*# Multipoint Communications Corp., Sunnyvale, CA.
PROGRAMMABLE RATE MODEM UTILIZING DIGITAL SIGNAL PROCESSING TECHNIQUES Final Report
George K. Bunya and Robert L. Wallace Jul. 1989 110 p
(Contract NAS3-25336)
(NASA-CR-185124; NAS 1.26:185124) Avail: NTIS HC A06/MF A01 CSCL 17B

The engineering development study to follow was written to address the need for a Programmable Rate Digital Satellite Modem capable of supporting both burst and continuous transmission modes with either binary phase shift keying (BPSK) or quadrature phase shift keying (QPSK) modulation. The preferred implementation technique is an all digital one which utilizes as much digital signal processing (DSP) as possible. Here design tradeoffs in each portion of the modulator and demodulator subsystem are outlined, and viable circuit approaches which are easily repeatable, have low implementation losses and have low production costs are identified. The research involved for this study was divided into nine technical papers, each addressing a significant region of concern in a variable rate modem design. Trivial portions and basic support logic designs surrounding the nine major modem blocks were omitted. In brief, the nine topic areas were: (1) Transmit Data Filtering; (2) Transmit Clock Generation; (3) Carrier Synthesizer; (4) Receive AGC; (5) Receive Data Filtering; (6) RF Oscillator Phase Noise; (7) Receive Carrier Selectivity; (8) Carrier Recovery; and (9) Timing Recovery. Author

N89-26880*# Harris Corp., Melbourne, FL.
ADVANCED MODULATION TECHNOLOGY DEVELOPMENT FOR EARTH STATION DEMODULATOR APPLICATIONS Final Report
R. C. Davis, J. V. Wernlund, J. A. Gann, J. F. Roesch, T. Wright, and R. D. Crowley Jul. 1989 282 p
(Contract NAS3-24681)
(NASA-CR-185126; NAS 1.26:185126) Avail: NTIS HC A13/MF A01 CSCL 09F

The purpose of this contract was to develop a high rate (200 Mbps), bandwidth efficient, modulation format using low cost hardware, in 1990's technology. The modulation format chosen is 16-ary continuous phase frequency shift keying (CPFSK). The implementation of the modulation format uses a unique combination of a limiter/discriminator followed by an accumulator to determine transmitted phase. An important feature of the modulation scheme is the way coding is applied to efficiently gain back the performance lost by the close spacing of the phase points. Author

18 SPACECRAFT DESIGN, TESTING AND PERFORMANCE

Includes satellites; space platforms; space stations; spacecraft systems and components such as thermal and environmental controls; and attitude controls.

For life support systems see *54 Man/System Technology and Life Support.* For related information see also *05 Aircraft Design, Testing and Performance, 39 Structural Mechanics,* and *16 Space Transportation.*

N89-26881# Office of Technology Assessment, Washington, DC.
BIG DUMB BOOSTERS: A LOW-COST SPACE TRANSPORTATION OPTION. AN OTA (OFFICE OF TECHNOLOGY AND ASSESSMENT) BACKGROUND PAPER
Feb. 1989 35 p
(PB89-155196) Avail: NTIS HC A03/MF A01 CSCL 22B

A launch vehicle concept commonly known as the Big Dumb Booster, a concept that derives from efforts first made in the 1960s to minimize costs of space launch systems is described and examined. Some launch system analysts believe that the use of this concept, when applied to existing technology, could markedly reduce space transportation costs. Other analysts disagree. Low-cost space transportation is one of the keys to more effective exploration and exploitation of outer space. If space transportation costs were much lower, government agencies and firms with good ideas for using the space environment might be more willing to risk their investment capital. In this area of increased budget stringency, the high cost of space transportation has prompted analysts to examine a wide variety of ideas to reduce these costs. GRA

N89-26882 Department of the Air Force, Washington, DC.
LOW LOSS RADAR WINDOW FOR REENTRY VEHICLE Patent
Thomas M. Place, Jr., inventor (to AF) 22 Nov. 1988 6 p Filed 10 Sep. 1987
(AD-D014045; US-Patent-4,786,548; US-Patent-Appl-SN-095062) Avail: US Patent and Trademark Office CSCL 17/9

A radar window for a reentry vehicle where the window is made of a composite material of boron nitride, silica, and boron nitride yarn is described. Silica in the range of 2 to 18 percent is the preferred range in the composite material and the boron nitride matrix ranges from 5 to 15 percent. GRA

N89-26883# Optimization, Inc., Blacksburg, VA.
CONTROL OF FLEXIBLE STRUCTURES Final Report, 1 Mar. 1986 - 30 Sep. 1988
John A. Burns, Eugene M. Cliff, H. J. Kelley, F. H. Lutze, and R. E. Miller Apr. 1989 151 p
(Contract F04611-86-C-0008)
(AD-A207520; K511-3; AL-TR-89-001) Avail: NTIS HC A08/MF A01 CSCL 13/13

This report summarizes the work done under contract FO 4611-86-C-0008. The principal goals were to develop state-space models and computational algorithms for control of beam and plate type structures, and, more generally, to increase the understanding of the basic problems associated with this development. The state-space approach is based on a distributed parameter model of the structure that includes the fundamental equations without modal truncation. The approach is to use basic physical principles to write down the governing partial differential equations, construct a state-space model from these governing equations, formulate the optimal control problem in terms of the state-space model, develop a convergent approximation scheme and conduct numerical experiments to test the method. GRA

N89-26884# Instituto de Pesquisas Espaciais, Sao Jose dos Campos (Brazil).
STUDY OF JITTER ON THE ATTITUDE MOTION OF A SPIN STABILIZED SATELLITE WITH TWO FLEXIBLE SOLAR PANELS [ESTUDO DO JITTER NA ATITUDE DE UM SATELITE ARTIFICIAL COM PAINEIS FLEXIVEIS ESTABILIZADOS FOR ROTACAO DUAL]
Ijar MilagredaFonseca Dec. 1988 9 p In PORTUGUESE; ENGLISH summary Presented at the 7th Brazilian Conference on automation, Sao Jose dos Campos, Brazil, 15-19 Aug.
(INPE-4744-PRE/1418) Avail: NTIS HC A02/MF A01

The jitter on the attitude motion of a spin stabilized satellite with two flexible solar panels is studied. The panels vibration displacements are discretized by the assumed modes method to obtain a model described by ordinary differential equations only. The Lagrangian formulation was used to derive the equations of motion. These equations were integrated numerically and the results, presented in graphical form, show the effects of the rotor misalignment and of the flexibility of the solar panels on the attitude motion. The results also show that the Jitter specification for the satellite under study is satisfied. Author

N89-26885*# Teledyne Brown Engineering, Huntsville, AL.
ADVANCED SOLAR OBSERVATORY (ASO) ACCOMMODATIONS REQUIREMENTS STUDY Final Report
May 1989 330 p
(Contract NAS8-37128)
(NASA-CR-183718; NAS 1.26:183718; SP89-MSFC-3225) Avail: NTIS HC A15/MF A01 CSCL 22B

Results of an accommodations analysis for the Advanced Solar Observatory on Space Station Freedom are reported. Concepts for the High Resolution Telescope Cluster, Pinhole/Occulter Facility, and High Energy Cluster were developed which can be accommodated on Space Station Freedom. It is shown that workable accommodations concepts are possible. Areas of emphasis for the next stage of engineering development are identified. Author

N89-26886# Instituto de Pesquisas Espaciais, Sao Jose dos Campos (Brazil). Dept. de Controle e Guiagem.
SATELLITE ATTITUDE CONTROL ANALYSIS AND DESIGN USING LINEARIZING TRANSFORMATIONS
Antonio Felix Martin Neto Dec. 1988 7 p Presented at the 7th Congresso Brasileiro de Automatica, Sao Jose dos Campos, Brazil Submitted for publication
(INPE-4772-PRE/1441) Avail: NTIS HC A02/MF A01

The problem of maneuvering a satellite relative to a desired noninertial reference is examined by using linearizing transformations and the concept of relative quaternion. The rigid body attitude equations are transformed into an equivalent linear form which considers the fact that the control purpose is to align the satellite with a moving reference frame (e.g., and Earth resource satellite). The equations so obtained are used to design control strategies for stabilizing the satellite attitude by linear techniques. This approach is more useful for algorithm design for on-board processors than the technique using inertial quaternion since the laws obtained are a function of the noninertial sensor outputs (sun sensors, earth sensors, etc.) and of the inertial sensor (gyroscopes) outputs. Author

N89-26887*# National Aeronautics and Space Administration. Lewis Research Center, Cleveland, OH.
PHOTOVOLTAIC MODULE ON-ORBIT ASSEMBLY FOR SPACE STATION FREEDOM
Thomas Sours, R. Lovely, and D. Clark 1989 10 p Presented at the 24th Intersociety Energy Conversion Engineering Conference, Washington, DC, 6-11 Aug. 1989; cosponsored by the IEEE, AIAA, ANS, ASME, SAE, ACS, and AIChE
(NASA-TM-102297; E-4973; NAS 1.15:102297) Avail: NTIS HC A02/MF A01 CSCL 22B

One of the elements of the Space Station Freedom power system is the Photovoltaic (PV) module. These modules will be assembled on-orbit during the assembly phase of the program.

These modules will be assembled either from the shuttle orbiter or from the Mobile Servicing Center (MSC). The different types of assembly operations that will be used to assemble PV Modules are described. Author

N89-26888*# National Aeronautics and Space Administration. Langley Research Center, Hampton, VA.
ALTERNATE SPACE STATION FREEDOM CONFIGURATION CONSIDERATIONS TO ACCOMMODATE SOLAR DYNAMIC POWER
L. J. DeRyder, J. N. Cruz, M. L. Heck, B. P. Robertson, and P. A. Troutman 28 May 1989 35 p
(NASA-TM-101603; NAS 1.15:101603) Avail: NTIS HC A03/MF A01 CSCL 22B

The results of a technical audit of the Space Station Freedom Program conducted by the Program Director was announced in early 1989 and included a proposal to use solar dynamic power generation systems to provide primary electrical energy for orbital flight operations rather than photovoltaic solar array systems. To generate the current program baseline power of 75 kW, two or more solar concentrators approximately 50 feet in diameter would be required to replace four pairs of solar arrays whose rectangular blanket size is approximately 200 feet by 30 feet. The photovoltaic power system concept uses solar arrays to generate electricity that is stored in nickel-hydrogen batteries. The proposed concept uses the solar concentrator dishes to reflect and focus the Sun's energy to heat helium-xenon gas to drive electricity generating turbines. The purpose here is to consider the station configuration issues for incorporation of solar dynamic power system components. Key flight dynamic configuration geometry issues are addressed and an assembly sequence scenario is developed. Author

N89-26889# Centre National d'Etudes Spatiales, Toulouse (France). Div. Techniques Vehicules.
SPOT 1-2-3 PYROTECHNICS SYSTEM: DEFINITION REPO RT [PROJETS SPOTS 1, 2 ET 3. SYSTEME PYROTECHNIQUE. DOSSIER DE SYNTHESE DE DEFINITION]
Jean-Pierre Bouloumie 2 Mar. 1989 67 p In FRENCH Original contains color illustrations
(CNES-CT/DRT/TVE/IL-89-035; ETN-89-94808) AVAIL: NTIS HC A04/MF A01

Information on platform and payload pyrotechnical systems of Spot projects 1, 2, and 3 is presented. The technical specifications and definition sheets are summarized to describe the systems. The description includes separation of Ariane launcher, antenna S2 deployment, deblocking optical instruments, deployment of solar panels, and deblocking of the solar generator drive. ESA

N89-26890# Messerschmitt-Boelkow-Blohm G.m.b.H., Bremen (Germany, F.R.).
COLUMBUS LOGISTICS PROGRAM
Mike C. Attwood 1988 11 p Previously announced in IAA as A89-18314
(MBB-UO-0039/88-Pub; ETN-89-94617) Avail: NTIS HC A03/MF A01

The overall logistics scenario which reflects the design configurations and operational concepts as derived from the Columbus phase B activities and results of considerations of coherence with other European space elements, (e.g., Hermes), is described. The required resupply infrastructure, covering the range from provisions for off-line repair of units at a manufacturer's site via ground/orbit transport to on-orbit storage, until utilization in a servicing activity, are identified. ESA

N89-26891# Messerschmitt-Boelkow-Blohm G.m.b.H., Ottobrunn (Germany, F.R.). Space Communications and Propulsion Systems Div.
MODELING OF LIQUID SLOSHING EFFECTS IN MULTI BODY SYSTEMS
K. Ebert 1988 7 p
(MBB-UK-0024/88-Pub; ETN-89-94618) Avail: NTIS HC A02/MF A01

Two modeling methods for the sloshing dynamics of liquids in partially filled tanks in a spinning spacecraft, the homogeneous vortex flow approximation and the boundary layer model, are presented. A modeling method used to implement liquid sloshing effects into the simulation program DISCOS for multibody systems is described. The computer programs for the analysis of sloshing effects and the extended simulation program DISCOSL were applied to the INTELSAT 6 spacecraft. ESA

N89-26892# Naval Postgraduate School, Monterey, CA.
SPIN STABILIZATION OF THE ORION SATELLITE USING A THRUSTER ATTITUDE CONTROL SYSTEM WITH OPTIMAL CONTROL CONSIDERATIONS M.S. Thesis
Janet L. Cunningham Mar. 1989 48 p
(AD-A208484) Avail: NTIS HC A03/MF A01 CSCL 22/1

The controlled system is the ORION satellite spinning about its single axis of symmetry. Hydrazine thrusters are used as the control and are modeled by ideal, constant magnitude step functions. The system is normalized and driven from non-zero initial angular velocities of the two axes other than the spin axis to the final condition zero. The control profiles required to do this are determined based on a desired controller duty cycle. Adaption of the duty cycle changes the ratio of the time the thrusters are on (fuel use) and total time to completion of the evolution. A comparison between a single axis and a dual axis controller is presented. Simulation programs for the normalized system using a single axis controller simulation program, with each controller having a duty cycle of no more than 50 percent are developed. Operation of the system is optimized using a system cost function. An equation relating the controller duty cycle of the dual system to the fuel/time trade-off parameter of the system cost function is required. A nonlinear feedback control algorithm (function of attitude angle rates) is developed from iterations of the simulation, and a priori knowledge of the form of the control from optimal control theory. This numerical solution will allow system designers to incorporate a closed form state feedback control for minimum fuel/time strategies using the ORION satellite's onboard software. GRA

19 SPACECRAFT INSTRUMENTATION

For related information see also *06 Aircraft Instrumentation* and *35 Instrumentation and Photography.*

No abstracts in this category.

20 SPACECRAFT PROPULSION AND POWER

Includes main propulsion systems and components, e.g., rocket engines; and spacecraft auxilliary power sources.

For related information see also *07 Aircraft Propulsion and Power, 28 Propellants and Fuels, 44 Energy Production and Conversion,* and *15 Launch Vehicles and Space Vehicles.*

N89-26893# National Aerospace Lab., Tokyo (Japan).
LH SUB 2/LO SUB 2 ROCKET ENGINE WITH SOLAR ENERGY
Takeshi Kanda, Yoshio Wakamatsu, and Akio Kanmuri Aug. 1988 16 p In JAPANESE; ENGLISH summary
(NAL-TR-992; ISSN-0389-4010) Avail: NTIS HC A03/MF A01

Solar energy is already used in the form of electric power generated by solar cells in satellites. And a solar thermal propulsion system, a kind of gas jet engine, was studied. Large expansion area ratio engines were studied to achieve high specific impulse, Isp. If external energy is added to an engine, Isp can be better than the theoretical Isp based on tank level enthalpy. Solar energy was used as the additional energy supplied to a rocket engine.

The LH2/LO2 expander cycle engine with a solar heat exchanger was studied. This engine has two merits. One is the increase of Isp, which allows a greater payload to be carried by a rocket with the solar heat exchanger than by a normal rocket. The other merit is a cycle pressure level decrease. The Isp increase is realized for every engine and for every propellant, if additional energy is available. Author

N89-26894*# Lockheed Missiles and Space Co., Huntsville, AL. Engineering Center.
SPACE SHUTTLE MAIN ENGINE STRUCTURAL ANALYSIS AND DATA REDUCTION/EVALUATION. VOLUME 7: HIGH PRESSURE FUEL TURBO-PUMP THIRD STAGE IMPELLER ANALYSIS Final Report
Kirby V. Pool Apr. 1989 226 p Original contains color illustrations
(Contract NAS8-37282)
(NASA-CR-183670; NAS 1.26:183670; LMSC-HEC-TR-F268584-Vol-7) Avail: NTIS HC A11/MF A01 CSCL 21H

This volume summarizes the analysis used to assess the structural life of the Space Shuttle Main Engine (SSME) High Pressure Fuel Turbo-Pump (HPFTP) Third Stage Impeller. This analysis was performed in three phases, all using the DIAL finite element code. The first phase was a static stress analysis to determine the mean (non-varying) stress and static margin of safety for the part. The loads involved were steady state pressure and centrifugal force due to spinning. The second phase of the analysis was a modal survey to determine the vibrational modes and natural frequencies of the impeller. The third phase was a dynamic response analysis to determine the alternating component of the stress due to time varying pressure impulses at the outlet (diffuser) side of the impeller. The results of the three phases of the analysis show that the Third Stage Impeller operates very near the upper limits of its capability at full power level (FPL) loading. The static loading alone creates stresses in some areas of the shroud which exceed the yield point of the material. Additional cyclic loading due to the dynamic force could lead to a significant reduction in the life of this part. The cyclic stresses determined in the dynamic response phase of this study are based on an assumption regarding the magnitude of the forcing function. K.C.D.

N89-26895*# National Aeronautics and Space Administration, Washington, DC.
THE NASA LOW THRUST PROPULSION PROGRAM
James R. Stone and Gary L. Bennett Jul. 1989 31 p Presented at the 25th Joint Propulsion Conference, Monterey, CA, 10-12 Jul. 1989; sponsored in part by AIAA, ASME, SAE, and ASEE
(NASA-TM-102065; E-4822; NAS 1.15:102065; AIAA-89-2492) Avail: NTIS HC A03/MF A01 CSCL 10B

The NASA OAST Propulsion, Power, and Energy Division supports a low thrust propulsion program aimed at providing high performance options for a broad range of near-term and far-term mission and vehicles. Low thrust propulsion has a major impact on the mission performance of essentially all spacecraft and vehicles. On-orbit lifetimes, payloads, and trip times are significantly impacted by low thrust propulsion performance and integration features for Earth-to-orbit (ETO) vehicles, Earth-orbit and planetary spacecraft, and large platforms in Earth orbit. Major emphases are on low thrust chemical propulsion, both storables and hydrogen/oxygen; low-power (auxiliary) electric arcjects and resistojets; and high-power (primary) electric propulsion, including ion, magnetoplasmadynamic (MPD), and electrodeless concepts. The major recent accomplishments of the program are presented and their impacts discussed. Author

N89-26896*# Sverdrup Technology, Inc., Bay Saint Louis, MS.
SPACE SHUTTLE MAIN ENGINE RADIO FREQUENCY EMISSIONS Final Report, May - Sep. 1988
A. W. Rester, E. L. Valenti, and L. R. Smith Nov. 1988 23 p
(NASA-CR-184707; NAS 1.26:184707) Avail: NTIS HC A03/MF A01 CSCL 21H

Several approaches to develop a diagnostics system for monitoring the operational health of the Space Shuttle Main Engine (SSME) are being evaluated. The ultimate goal is providing protection for the SSME as well as improving ground and flight test techniques. One scenario with some potential is measuring radio frequency (RF) emissions (if present) in the exhaust plume and correlating the data to engine health. An RF emissions detection system was therefore designed, the equipment leased, and the components integrated and checked out to conduct a quick-look investigation of RF emissions in the SSME exhaust plume. The system was installed on the A-1 Test Stand at Stennis Space Center, MS, and data were successfully acquired during SSME firings from May 3 to September 15, 1988. The experiments indicated that emitted radiation in the RF (20 to 470 MHz) spectrum definitely exists in the SSME exhaust plume, and is of such magnitude that it can be distinguished during the firing from background noise. Although additional efforts are necessary to assess the merit of this approach as a health monitoring technique, the potential is significant, and additional studies are recommended. Author

N89-26897 Department of the Air Force, Washington, DC.
CONTEMPORARY COMPOSITE POLAR BOSS Patent
Hugh M. Reynolds, inventor (to AF) and Curt M. Kawabata, inventor (to AF) 28 Feb. 1989 9 p Filed 16 Oct. 1987
(AD-D014074; US-Patent-4,807,531; US-Patent-Appl-SN-109557; US-Patent-Class-102-347) Avail: US Patent and Trademark Office CSCL 21/8

Composite polar bosses applied in rocket motor cases have very desirable characteristics. The lead time for a boss can be reduced from 6 to 12 months to 2 to 3 months. Weight savings for the boss are about 20 to 40 pct. A composite polar boss which attaches closures to solid fueled rocket motor cases is disclosed. This polar boss is a carbonized fabrication which sits within a circumferential indentation within the motor case, and has a threaded inner circumference which permits the closure to be attached thereto. The materials of the boss are selected to permit a service temperature of 350 F. GRA

N89-26898# Aerospace Corp., El Segundo, CA. Aerophysics Lab.
HYBRID ELECTRIC CHEMICAL PROPULSION
James E. Pollard and Ronald B. Cohen 1 Apr. 1989 27 p
(Contract F04701-85-C-0086)
(AD-A207584; TR-0086(6930-03)-1; SD-TR-89-24) Avail: NTIS HC A03/MF A01 CSCL 21/8

A spacecraft propulsion concept that uses a combination of electrical energy and chemical energy for thrust is explored using thermodynamic modeling calculations. The essence of this concept consists of adding a carefully chosen amount of O2 or F2 oxidizer to the propellant flow of a conventional H2 electrothermal thruster. A general method is given for selecting the fuel - an oxidizer ratio so as to optimize the thruster performance for any set of mission constraints. GRA

N89-26899*# Rockwell International Corp., Canoga Park, CA. Rocketdyne Div.
OTVE COMBUSTOR WALL CONDITION MONITORING Final Report, Nov. 1986 - Sep. 1988
Brian Szemenyei, Robert S. Nelson, and S. Barkhoudarian Aug. 1989 38 p Presented at the 24th AIAA/ASME/SAE/ASEE Joint Propulsion Conference on Improved Maintainability of Space-Based Reuseable Rocket Engines, Boston, MA, Jul. 1988
(Contract NAS3-23773)
(NASA-CR-182275; NAS 1.26:182275; RI/RD89-212) Avail: NTIS HC A03/MF A01 CSCL 21H

Conventional ultrasonics, eddy current, and electromagnetic acoustic transduction (EMAT) technologies were evaluated to determine their capability of measuring wall thickness/wear of individual cooling channels in test specimens simulating conditions in the throat region of an OTVE combustion chamber liner. Quantitative results are presented for the eddy current technology, which was shown to measure up to the optimum 20-mil wall thickness with near single channel resolution. Additional results

demonstrate the capability of the conventional ultrasonics and EMAT technologies to detect a thinning or cracked wall. Recommendations for additional eddy current and EMAT development tests are presented. Author

N89-26900*# SECA, Inc., Huntsville, AL.
INVESTIGATION OF THE TRANSIENT FUEL PREBURNER MANIFOLD AND COMBUSTOR Final Report
Ten-See Wang, Yen-Sen Chen, and Richard C. Farmer Jun. 1989 89 p
(Contract NAS8-37461)
(NASA-CR-183715; NAS 1.26:183715; SECA-89-10) Avail: NTIS HC A05/MF A01 CSCL 21H

A computational fluid dynamics (CFD) model with finite rate reactions, FDNS, was developed to study the start transient of the Space Shuttle Main Engine (SSME) fuel preburner (FPB). FDNS is a time accurate, pressure based CFD code. An upwind scheme was employed for spatial discretization. The upwind scheme was based on second and fourth order central differencing with adaptive artificial dissipation. A state of the art two-equation k-epsilon (T) turbulence model was employed for the turbulence calculation. A Pade' Rational Solution (PARASOL) chemistry algorithm was coupled with the point implicit procedure. FDNS was benchmarked with three well documented experiments: a confined swirling coaxial jet, a non-reactive ramjet dump combustor, and a reactive ramjet dump combustor. Excellent comparisons were obtained for the benchmark cases. The code was then used to study the start transient of an axisymmetric SSME fuel preburner. Predicted transient operation of the preburner agrees well with experiment. Furthermore, it was also found that an appreciable amount of unburned oxygen entered the turbine stages. GRA

N89-26901*# Morton Thiokol, Brigham City, UT. Aerospace Group.
FIELD JOINT PROTECTION SYSTEM RAIN QUALIFICATION TEST REPORT Final Report
M. Cook 11 May 1989 41 p
(Contract NAS8-30490)
(NASA-CR-183702; NAS 1.26:183702; TWR-18076; WBS-4B102-10-03; ECS-SS1323) Avail: NTIS HC A03/MF A01 CSCL 21H

This report documents the procedures, performance, and results obtained from the Field Joint Protection System (FJPS) rain test. This test was performed to validate that the flight configuration FJPS prevents the accumulation of moisture in the redesigned solid rocket motor (RSRM) field joints when subjected to simulated prelaunch natural rain environments. The FJPS test article was exposed to rain simulation for approximately 50 minutes. During the test, water entered through the open upper end of the systems tunnel and was funneled down between the tunnel and case. A sealant void at the moisture seal butt splice allowed this water to flow underneath the FJPS. The most likely cause of voids was improper bondline preparation, particularly on the moisture seal surface. In total, water penetrated underneath approximately 60 percent of the FJPS circumference. Because the test article was substantially different from flight configuration (no systems tunnel closeout), results of this test will not affect current flight motors. Due to the omission of systems tunnel covers and systems tunnel floor plate closeout, the test assembly was not representative of flight hardware and resulted in a gross overtest. It is therefore recommended that the test be declared void. It is also recommended that the test be repeated with a complete closeout of the systems tunnel, sealed systems tunnel ends, and improved adhesive bondline preparation. Author

N89-26902*# National Aeronautics and Space Administration. Goddard Space Flight Center, Greenbelt, MD.
FLOW FIELDS OF LOW PRESSURE VENT EXHAUSTS
John J. Scialdone Washington Jul. 1989 15 p
(NASA-TM-100738; NAS 1.15:100738; Rept-89B00151) Avail: NTIS HC A03/MF A01 CSCL 21H

The flow field produced by low pressure gas vents are described based on experimental data obtained from tests in a large vacuum chamber. The gas density, pressure, and flux at any location in the flow field are calculated based on the vent plume description and the knowledge of the flow rate and velocity of the venting gas. The same parameters and the column densities along a specified line of sight traversing the plume are also obtained and shown by a computer-generated graphical representation. The fields obtained with a radially scanning Pitot probe within the exhausting gas are described by a power of the cosine function, the mass rate and the distance from the exit port. The field measurements were made for gas at pressures ranging from 2 to 50 torr venting from pipe fittings with diameters of 3/16 inch to 1-1/2 inches I.D. (4.76 mm to 38.1 mm). The N(2) mass flow rates ranged from 2E-4 to 3.7E-1 g/s. Author

N89-26903*# Cummings (Robert L.), Litchfield, OH.
PERFORMANCE ESTIMATES FOR THE SPACE STATION POWER SYSTEM BRAYTON CYCLE COMPRESSOR AND TURBINE Final Report
Robert L. Cummings Aug. 1989 35 p
(NASA Order C-22187-M)
(NASA-CR-182263; E-4657; NAS 1.26:182263) Avail: NTIS HC A03/MF A01 CSCL 21H

The methods which have been used by the NASA Lewis Research Center for predicting Brayton Cycle compressor and turbine performance for different gases and flow rates are described. These methods were developed by NASA Lewis during the early days of Brayton cycle component development and they can now be applied to the task of predicting the performance of the Closed Brayton Cycle (CBC) Space Station Freedom power system. Computer programs are given for performing these calculations and data from previous NASA Lewis Brayton Compressor and Turbine tests is used to make accurate estimates of the compressor and turbine performance for the CBC power system. Results of these calculations are also given. In general, calculations confirm that the CBC Brayton Cycle contractor has made realistic compressor and turbine performance estimates. Author

N89-26904*# National Aeronautics and Space Administration. Lewis Research Center, Cleveland, OH.
DEVELOPMENT OF A HIGH POWER MICROWAVE THRUSTER, WITH A MAGNETIC NOZZLE, FOR SPACE APPLICATIONS
John L. Power and Randall A. Chapman 1989 26 p Presented at the 24th Microwave Power Symposium, Stanford, CT, 21-23 Aug. 1989; sponsored by the International Microwave Power Inst.
(NASA-TM-102321; E-5017; NAS 1.15:102321) Avail: NTIS HC A03/MF A01 CSCL 21H

This paper describes the current development of a high-power microwave electrothermal thruster (MET) concept at the NASA Lewis Research Center. Such a thruster would be employed in space for applications such as orbit raining, orbit maneuvering, station change, and possibly trans-lunar or trans-planetary propulsion of spacecraft. The MET concept employs low frequency continuous wave (CW) microwave power to create and continuously pump energy into a flowing propellant gas at relative high pressure via a plasma discharge. The propellant is heated to very high bulk temperatures while passing through the plasma discharge region and then is expanded through a throat-nozzle assembly to produce thrust, as in a conventional rocket engine. Apparatus, which is described, is being assembled at NASA Lewis to test the MET concept to CW power levels of 30 kW at a frequency of 915 MHz. The microwave energy is applied in a resonant cavity applicator and is absorbed by a plasma discharge in the flowing propellant. The ignited plasma acts as a lossy load, and with optimal tuning, energy absorption efficiencies over 95 percent (based on the applied microwave power) are expected. Nitrogen, helium, and hydrogen will be tested as propellants in the MET, at discharge chamber pressures to 10 atm. Author

N89-26905* Rockwell International Corp., Canoga Park, CA. Rocketdyne Div.
SPACE STATION HYDROGEN/OXYGEN THRUSTER TECHNOLOGY Final Report
G. L. Briley and R. S. Iacabucci Nov. 1988 111 p
(Contract NAS3-25142)
(NASA-CR-182280; NAS 1.26:182280; RI/RD88-256) Avail: Issuing Activity CSCL 21H

The effort expended by the Rocketdyne Division of Rockwell International in fulfilling the requirements of the Space Station Freedom Hydrogen/Oxygen Thruster Technology program is discussed. Included are the basis and the rationale for the design of the thruster, injector, and nozzle; the test results; and the lessons learned, together with conclusions and recommendations for the development of the Space Station Freedom thrusters. Author

N89-26906*# National Aeronautics and Space Administration. Lewis Research Center, Cleveland, OH.
ELECTRIC PROPULSION OPTIONS FOR 10 kW CLASS EARTH SPACE MISSIONS
M. J. Patterson and Francis M. Curran May 1989 29 p Presented at the JANNAF Propulsion Meeting, Cleveland, OH, 23-25 May 1989
(NASA-TM-102337; E-5046; NAS 1.15:102337) Avail: NTIS HC A03/MF A01 CSCL 21C

Five and 10 kW ion and arcjet propulsion system options for a near-term space demonstration experiment have been evaluated. Analyses were conducted to determine first-order propulsion system performance and system component mass estimates. Overall mission performance of the electric propulsion systems was quantified in terms of the maximum thrusting time, total impulse, and velocity increment capability available when integrated onto a generic spacecraft under fixed mission model assumptions. Maximum available thrusting times for the ion-propelled spacecraft options, launched on a DELTA II 6920 vehicle, range from approximately 8,600 hours for a 4-engine 10 kW system to more than 29,600 hours for a single-engine 5 kW system. Maximum total impulse values and maximum delta-v's range from 1.2x10(7) to 2.1x10(7) N-s, and 3550 to 6200 m/s, respectively. Maximum available thrusting times for the arcjet propelled spacecraft launched on the DELTA II 6920 vehicle range from approximately 528 hours for the 6-engine 10 kW hydrazine system to 2328 hours for the single-engine 5 kW system. Maximum total impulse values and maximum delta-v's range from 2.2x10(6) to 3.6x10(6) N-s, and approximately 662 to 1072 m/s, respectively. Author

23 CHEMISTRY AND MATERIALS (GENERAL)

No abstracts in this category.

24 COMPOSITE MATERIALS

Includes physical, chemical, and mechanical properties of laminates and other composite materials.
For ceramic materials see *27 Nonmetallic Materials*.

N89-26907 Department of the Air Force, Washington, DC.
METHOD TO PRODUCE METAL MATRIX COMPOSITE ARTICLES FROM RICH METASTABLE-BETA TITANIUM ALLOYS Patent
Daniel Eylon, inventor (to AF) and Francis H. Froes, inventor (to AF) 7 Mar. 1989 5 p Filed 26 Nov. 1986 Supersedes AD-D012674
(AD-D014064; US-Patent-4,809,903; US-Patent-Appl-SN-935363; US-Patent-Class-228-194) Avail: US Patent and Trademark Office CSCL 11/6

A method for fabricating an improved titanium alloy composite consisting of a least one high strength/high stiffness filament or fiber embedded in an alpha-beta titanium alloy matrix which comprises the steps of providing a rapidly-solidified foil made of a rich metastable beta titanium alloy, fabricating a preform consisting of alternating layers of the rapidly-solidified foil and the filamentary material, and applying heat and pressure to consolidate the preform, wherein consolidation is carried out at a temperature below the beta-transus temperature of the alloy. GRA

N89-26908 Department of the Air Force, Washington, DC.
METHOD TO PRODUCE METAL MATRIX COMPOSITE ARTICLES FROM LEAN METASTABLE BETA TITANIUM ALLOYS Patent
Daniel Eylon, inventor (to AF) and Francis H. Froes, inventor (to AF) 28 Feb. 1989 5 p Filed 26 Nov. 1986 Supersedes AD-D012673
(AD-D014065; US-Patent-4,807,798; US-Patent-Appl-SN-935362; US-Patent-Class-288-190) Avail: US Patent and Trademark Office CSCL 11/4

A method for fabricating an improved titanium alloy composite consisting of at least one high strength/high stiffness filament or fiber embedded in an alpha-beta titanium alloy matrix which comprises the steps of providing a rapidly-solidified foil made of a lean metastable beta titanium alloy, fabricating a preform consisting of alternating layers of the rapidly-solidified foil and the filamentary material, and applying heat and pressure to consolidate the preform, wherein consolidation is carried out at a temperature below the beta-transus temperature of the alloy. GRA

N89-26909# Army Lab. Command, Watertown, MA. Material Technology Lab.
EXAMINATION OF THE TENSILE STRENGTH OF GRAPHITE FIBERS Final Report
Elizabeth C. Goeke and Shun-Chin Chou Feb. 1989 72 p
(AD-A207277; MTL-TR-89-16) Avail: NTIS HC A04/MF A01 CSCL 11/2

The Single Fiber Graphite Tester was developed to measure the failure load and fiber diameter of graphite fibers. Data have been taken on a number of commercially available fibers with the tester. These data have been examined in order to understand the dispersion in these properties and the correlation between them. GRA

N89-26910# Foster-Miller Associates, Inc., Waltham, MA.
INTERFACE MODIFIED GLASS FIBER/THERMOPLASTIC MATRIX COMPOSITES Progress Report, 1 Oct. 1988 - 1 Mar. 1989
Robert F. Kovar and Richard W. Lusignea 1 Mar. 1989 14 p
(Contract N00014-88-C-0725)
(AD-A207308; NAV-0125-FM-8945-182; CDRL-0001AB) Avail: NTIS HC A03/MF A01 CSCL 11/4

This Phase 1 SBIR program is applying a proprietary interface-modification process to improve the interaction between glass fibers and thermoplastic resin composite matrices. In our accomplishments thus far, we have selected PEEK as the thermoplastic matrix resin and chosen three candidate interface-modifier resins. Fiber wetting experiments will determine which of these candidates is best suited for use on the program. A glass fiber tow spreader that effectively separates the tow into a narrow ribbon of fibers was constructed. Extraction experiments have demonstrated that the oil-based, PEEK compatible sizing can be effectively removed from glass fibers without damage by extraction with an appropriate solvent. Equipment was constructed for winding separated glass tow onto a large diameter drum, then processing the separated tow to remove the present sizing and coat with interface-modifier resin solution while the fibers remain in place upon the drum. Coated fibers will also be staged-dried and heat-treated in place, forming interface-modified glass fibers that have been protected from abrasive damage during the entire interface-modification process. GRA

N89-26911 Department of the Air Force, Washington, DC.
METHOD TO PRODUCE TITANIUM METAL MATRIX COMPOSITES WITH IMPROVED FRACTURE AND CREEP RESISTANCE Patent
Daniel Eylon, inventor (to AF) and Francis H. Froes, inventor (to AF) 18 Apr. 1989 4 p Filed 1 Feb. 1988
(AD-D014111; US-Patent-4,822,432; US-Patent-Appl-SN-150677) Avail: US Patent and Trademark Office CSCL 11/4

A method for improving the microstructure of consolidated titanium alloy metal matrix composites which comprises the steps of: (1) heating the composite to a temperature in the range of 800 to 2000 F, the temperature being below the temperature at which interfacial reactions occur between the metal matrix and the fiber, and diffusing hydrogen into the composite to achieve a hydrogen level of about 0.50 to 1.50 weight percent; (2) altering the temperature of the composite to a transformation temperature at or near the temperature of transformation of (HCP) alpha in the hydrogenated composite to (BCC) beta; (3) cooling the composite to room temperature; (4) heating the thus-cooled composite to a temperature below the transformation temperature, and diffusing hydrogen out from the composite; and (5) cooling the composite to room temperature. GRA

N89-26912*# National Aeronautics and Space Administration. Lewis Research Center, Cleveland, OH.
TAILORING OF COMPOSITE LINKS FOR OPTIMAL DAMPED ELASTO-DYNAMIC PERFORMANCE
D. A. Saravanos and C. C. Chamis 1989 30 p Prepared for presentation at the Design Automation Conference, Montreal, Quebec, 17-20 Sep. 1989; sponsored by ASME
(NASA-TM-102094; E-4875; NAS 1.15:102094) Avail: NTIS HC A03/MF A01 CSCL 11D

A method is developed for the optimal design of composite links based on dynamic performance criteria directly related to structural modal damping and dynamic stiffness. An integrated mechanics theory correlates structural composite damping to the parameters of basic composite material systems, laminate parameters, link shape, and modal deformations. The inclusion of modal properties allows the selective minimization of vibrations associated with specific modes. Ply angles and fiber volumes are tailored to obtain optimal combinations of damping and stiffness. Applications to simple composite links indicate wide margins for trade-offs and illustrate the importance of various design variables to the optimal design. Author

N89-26913# Argonne National Lab., IL.
EROSION OF Al AND Al/SiC
W. Wu, K. C. Goretta, P. K. Rohatgi, S. Mostovoy (Illinois Inst. of Tech., Chicago.), and J. L. Routbort Feb. 1989 12 p Presented at the Industry-University Advanced Materials Conference, Denver, CO, 6-9 Mar. 1989
(Contract W-31-109-eng-38)
(DE89-013623; CONF-890306-4) Avail: NTIS HC A03/MF A01

Aluminum-matrix composites are being developed for a variety of applications. In some of the applications, the composites may be subjected to erosion by solid particles. Previous studies of erosion of metal-matrix composites have shown that erosion rates are generally higher for the composites than for the unreinforced matrix. Increased erosion has been ascribed to the low ductility inherent in the composite materials. The effect of reduced ductility is especially strong for whisker-reinforced composites. This work was undertaken to investigate systematically solid-particle erosion of a common composite: cast 2014 Al containing particulate SiC. To further elucidate the mechanisms for erosion and the materials parameters affecting erosion rate, the alloys were examined in the as-received and heat-treated conditions. DOE

N89-26914# National Inst. of Standards and Technology, Gaithersburg, MD. Polymers Div.
COMPOSITES DATABASES FOR THE 1990'S
Darrell H. Reneker, John M. Crissman, and Donald L. Hunston Feb. 1989 62 p
(PB89-180376; NISTIR-88/4016) Avail: NTIS HC A04/MF A01 CSCL 11D

A draft standard is given for identification of polymer matrix composite materials and for reporting test results. The draft standard is based on a comprehensive description of the flow of data through the polymer matrix composites community. Two essentially different kinds of data bases are required, one oriented toward a particular group of data users, and one designed to make the collection of all kinds of data straightforward. An interactive dictionary to serve as a tool in the development of the best names is described. Relationships of the draft standard to various groups concerned with composites are noted. Author

N89-26915# California Univ., Davis. Dept. of Chemical Engineering.
PROCESSING OF CONTINUOUS FIBER COMPOSITES Final Report
Brian G. Higgins, Robert L. Powell, and You-Lo Hsieh Feb. 1989 32 p
(Contract W-7405-eng-48)
(DE89-012608; UCRL-21206) Avail: NTIS HC A03/MF A01

This report covers the first year progress in the four main areas of this project. The goals of this project are: the characterization of single carbon fibers by wetting studies and SEM; the kinetics of impregnation into carbon fiber bundles tows (axial and normal); the factors affecting void formation in carbon fiber composites; and process simulations and optimization. DOE

N89-26916# Oak Ridge National Lab., TN.
STATISTICS OF FRACTURE IN TWO GRADES OF ISOTROPIC GRAPHITE
C. R. Kennedy and Suzanne Montgomery 1989 3 p Presented at the 19th Biennial Conference on Carbon, University Park, PA, 25 Jun. 1989
(Contract DE-AC05-84OR-21400)
(DE89-013703; CONF-890627-1) Avail: NTIS HC A02/MF A01

A test program to determine the flexure strength of graphite grades 2020 and IG-11 has been accomplished. Within three billets of each grade, bend samples were taken from three different orientations in three separate positions. The test data were statistically evaluated using one-way and two-way analyses of variance. Using Bartlett's test, homogeneity of variance for strength was clearly a tenable hypothesis of the 27 separate populations for both graphite grades. DOE

N89-26917*# Planning Research Corp., Hampton, VA. Aerospace Technologies Div.
ON PROCESSING DEVELOPMENT FOR FABRICATION OF FIBER REINFORCED COMPOSITE, PART 2
Tan-Hung Hou, Gene J. W. Hou, and Jeen S. Sheen (Old Dominion Univ., Norfolk, VA.) Jul. 1989 56 p Presented at the AIAA/ASME/ASCE/AHS 28th Structures, Structural Dynamics and Materials Conference, Monterey, CA, 6-8 Apr. 1987 Submitted for publication
(Contract NAS1-18000; NAG1-561)
(NASA-CR-181866; NAS 1.26:181866; AIAA-87-0751-CP) Avail: NTIS HC A04/MF A01 CSCL 11D

Fiber-reinforced composite laminates are used in many aerospace and automobile applications. The magnitudes and durations of the cure temperature and the cure pressure applied during the curing process have significant consequences for the performance of the finished product. The objective of this study is to exploit the potential of applying the optimization technique to the cure cycle design. Using the compression molding of a filled polyester sheet molding compound (SMC) as an example, a unified Computer Aided Design (CAD) methodology, consisting of three uncoupled modules, (i.e., optimization, analysis and sensitivity calculations), is developed to systematically generate optimal cure cycle designs. Various optimization formulations for the cure cycle design are investigated. The uniformities in the distributions of the temperature and the degree with those resulting from conventional isothermal processing conditions with pre-warmed platens.

Recommendations with regards to further research in the computerization of the cure cycle design are also addressed.
Author

N89-26918*# National Aeronautics and Space Administration. Goddard Space Flight Center, Greenbelt, MD.
FRACTURE TOUGHNESS OF SiC/Al METAL MATRIX COMPOSITE
Yury Flom, B. H. Parker, and H. P. Chu Washington Aug. 1989 18 p Presented at the 21st International SAMPE Technical Conference, Atlantic City, NJ, 26-28 Sep. 1989
(NASA-TM-100745; NAS 1.15:100745; Rept-89B00215) Avail: NTIS HC A03/MF A01 CSCL 11D

An experimental study was conducted to evaluate fracture toughness of SiC/Al metal matrix composite (MMC). The material was a 12.7 mm thick extrusion of 6061-T6 aluminum alloy with 40 v/o SiC particulates. Specimen configuration and test procedure conformed to ASTM E399 Standard for compact specimens. It was found that special procedures were necessary to obtain fatigue cracks of controlled lengths in the preparation of precracked specimens for the MMC material. Fatigue loading with both minimum and maximum loads in compression was used to start the precrack. The initial precracking would stop by self-arrest. Afterwards, the precrack could be safely extended to the desired length by additional cyclic tensile loading. Test results met practically all the E399 criteria for the calculation of plane strain fracture toughness of the material. A valid K sub IC value of the SiC/Al composite was established as K sub IC = 8.9 MPa square root of m. The threshold stress intensity under which crack would cease to grow in the material was estimated as delta K sub th = 2MPa square root of m for R = 0.09 using the fatigue precracking data. Fractographic examinations show that failure occurred by the micromechanism involved with plastic deformation although the specimens broke by brittle fracture. The effect of precracking by cyclic loading in compression on fracture toughness is included in the discussion.
Author

N89-26919*# National Aeronautics and Space Administration. Lewis Research Center, Cleveland, OH.
UNIFIED MICROMECHANICS OF DAMPING FOR UNIDIRECTIONAL FIBER REINFORCED COMPOSITES
D. A. Saravanos and C. C. Chamis Aug. 1989 28 p Submitted for publication
(NASA-TM-102107; E-4874; NAS 1.15:102107) Avail: NTIS HC A03/MF A01 CSCL 11D

An integrated micromechanics methodology for the prediction of damping capacity in fiber-reinforced polymer matrix unidirectional composites has been developed. Explicit micromechanics equations based on hysteretic damping are presented relating the on-axis damping capacities to the fiber and matrix properties and volume fraction. The damping capacities of unidirectional composites subjected to off-axis loading are synthesized from thermal effect on the damping performance of unidirectional composites due to temperature and moisture variations is also modeled. The damping contributions from interfacial friction between broken fibers and matrix are incorporated. Finally, the temperature rise in continuously vibrating composite plies is estimated. Application examples illustrate the significance of various parameters on the damping performance of unidirectional and off-axis fiber reinforced composites.
Author

N89-26920# Sandia National Labs., Livermore, CA. Component Research Div.
DEVELOPMENT OF A THIN WALL GRAPHITE/POLYIMIDE COMPOSITE PRESSURE VESSEL WITH A LARGE ASPECT RATIO
C. A. LaJeunesse, K. V. Trinh, J. J. Bartel, and J. R. Spingarn Oct. 1988 26 p Presented at the Joint ASME/JSME Pressure Vessel and Piping Conference, Honolulu, HI, 23-27 Jul. 1989
(Contract DE-AC04-76DR-00789)
(DE89-002536; SAND-88-8934; CONF-890721-1) Avail: NTIS HC A03/MF A01

A graphite/polyimide composite pressure vessel has been developed to contain corrosive gas mixtures up to 400 psig and 300 F. The goal of this research project was to develop a lightweight, thin-walled, composite pressure vessel with an l/d aspect ratio of 42 capable of containing hydrogen fluoride and chlorine trifluoride. The vessel was to have a crown radius approaching infinity, a desired knuckle radius approaching zero, and a desired wall thickness of 0.023 in. In this paper the problems encountered and the iterative solutions in addition to the design, analysis, and fabrication of the vessel are presented.
DOE

N89-26921# Sandia National Labs., Albuquerque, NM.
MOLECULAR SIEVE FILMS FROM ZEOLITED-SILICA MICROCOMPOSITES
T. Bein, K. Brown (New Mexico Univ., Albuquerque.), and C. J. Brinker 1989 10 p Presented at the 8th International Zeolite Conference, Amsterdam, Netherlands, 10 Jul. 1989
(Contract DE-AC04-76DP-00789; NSF DMR-87-06167)
(DE89-009831; SAND-89-0664C; CONF-890705-2) Avail: NTIS HC A02/MF A01

Inorganic thin films with molecular sieving properties have been formed by embedding microcrystals of zeolite Y and chabazite in a glassy silica matrix. The silica matrix was derived from sols prepared from tetraethylorthosilicate hydrolyzed under either acidic or basic conditions in alcoholic solution. Dip-coating, deposition of suspensions, or coating of zeolite dispersions with the glassy silica matrix were used to create the zeolite-silica films. The access of different probe molecules into the zeolitic part of the thin film was examined with in situ Fourier transform infrared radiation (FTIR) techniques and temperature-programmed-desorption studies. With all combinations of deposition techniques and silica matrices, the resulting films showed the molecular sieving properties of the parent zeolite.
DOE

N89-26922# Sandia National Labs., Livermore, CA. Structural Mechanics Div.
NONLINEAR DYNAMIC RESPONSE OF PRESSURIZED COMPOSITE BOTTLES SUBJECTED TO SHOCK LOADING
K. V. Trinh and L. I. Weingarten Mar. 1989 28 p Presented at the Joint ASME/JSME Pressure Vessel and Piping Conference, Honolulu, HI, 23-27 Jul. 1989
(Contract DE-AC04-76DR-00789)
(DE89-010553; SAND-88-8935; CONF-890721-26) Avail: NTIS HC A03/MF A01

A combined experimental and analytical program has been developed to examine the structural dynamic response of pressurized composite bottles subjected to spatially localized loadings. These bottles were constructed from graphite/epoxy, Kevlar/epoxy and fiberglass/epoxy. Some bottles also contained mock solid propellant. The impulsive, exponentially decaying shock loads were applied using blast tube techniques. Dynamic response analyses of the bottles were performed using the finite element code ABAQUS. A damage model was developed to account for material degradations due to the progressive failures of the composite material. The report presents the comparisons between results obtained from experiments and analytical methods.
DOE

N89-26923# Los Alamos National Lab., NM.
SiC-MoSi COMPOSITES
David H. Carter, John J. Petrovic, Richard E. Honnell, and W. Scott Gibbs Jun. 1989 13 p
(Contract W-7405-eng-36)
(DE89-013656; LA-11577-MS) Avail: NTIS HC A03/MF A01

Previous studies have shown that SiC whisker-reinforced MoSi sub 2 is an excellent candidate material for structural use at elevated temperatures. The yield strength at 1400 C was doubled with the addition of Los Alamos VLS SiC whiskers, and increased by a factor of five with the addition of VS SiC whiskers, despite a non-optimal distribution of the reinforcement resulting from dry blending fabrication procedures. A more optimal wet processing technique, providing a much more uniform distribution of the whisker reinforcement will be discussed. Activities directed at alloying MoSi sub 2 with other silicides to improve the mechanical properties of the matrix material will also be described.
DOE

N89-26924*# National Aeronautics and Space Administration. Lewis Research Center, Cleveland, OH.
METAL MATRIX COMPOSITE MICROMECHANICS: IN-SITU BEHAVIOR INFLUENCE ON COMPOSITE PROPERTIES
P. L. N. Murthy, D. A. Hopkins, and C. C. Chamis Jul. 1989 21 p Presented at the 3rd Joint Mechanics Conference, San Diego, CA, 9-12 Jul. 1989; sponsored in part by ASCE and ASME
(NASA-TM-102302; E-4982; NAS 1.15:102302) Avail: NTIS HC A03/MF A01 CSCL 11D

Recent efforts in computational mechanics methods for simulating the nonlinear behavior of metal matrix composites have culminated in the implementation of the Metal Matrix Composite Analyzer (METCAN) computer code. In METCAN material nonlinearity is treated at the constituent (fiber, matrix, and interphase) level where the current material model describes a time-temperature-stress dependency of the constituent properties in a material behavior space. The composite properties are synthesized from the constituent instantaneous properties by virtue of composite micromechanics and macromechanics models. The behavior of metal matrix composites depends on fabrication process variables, in situ fiber and matrix properties, bonding between the fiber and matrix, and/or the properties of an interphase between the fiber and matrix. Specifically, the influence of in situ matrix strength and the interphase degradation on the unidirectional composite stress-strain behavior is examined. These types of studies provide insight into micromechanical behavior that may be helpful in resolving discrepancies between experimentally observed composite behavior and predicted response. Author

N89-26925# Army Materials Technology Lab., Watertown, MA.
STATISTICAL STRENGTH COMPARISON OF METAL-MATRIX AND POLYMERIC-MATRIX COMPOSITES
Edward M. Wu (Naval Postgraduate School, Monterey, CA.) and Shun-Chin Chou Apr. 1989 26 p Repr. from Special Technical Publication (Philadelphia, PA), 1988
(AD-A208316; MTL-TR-89-30) Avail: NTIS HC A03/MF A01 CSCL 11/4

The reliability of a composite structure depends on the materials strength variability. Unidirectional composites fail sequentially initiating from the very weakest fiber sites with matrix binder providing local redundancy by transferring load to neighboring fibers until cumulation and clustering of these sites lead to severe stress concentration and ultimate structure failure. As a consequence, the variability of the metal matrix structure is traceable to the strength variability of the constituent fiber, the metal matrix coating process, and the composite wire consolidation process. This report focuses on the partitioning of the first two sources of variability, identification and modeling of the dominant parameters, together with experimental measurement on a current graphite-aluminum composite. The statistical strength of several graphite spools are measured by testing single filament specimens at the beginning and at the end of the spools, thereby characterizing the statistical parameters associated with the aluminum wire, produced from continuous liquid infiltration process are tested in tension. The metal matrix composite statistical strengths from different spools are compared with the respective statistical strength of the parent fiber. The results suggest that, given proper interpretation, single filament fiber strength is a sensitive parameter for quality assurance of metal matrix composites. GRA

25 INORGANIC AND PHYSICAL CHEMISTRY

Includes chemical analysis, e.g., chromatography; combustion theory; electrochemistry; and photochemistry.

For related information see also *77 Thermodynamics and Statistical Physics.*.

N89-26926# Lawrence Livermore National Lab., CA.
DETONABILITY OF HYDROCARBON FUELS IN AIR
H. D. Beeson, R. D. McClenagan, F. J. Benz, W. J. Pitz, C. K. Westbrook, and J. H. S. Lee (McGill Univ., Montreal, Quebec) 1 Mar. 1989 29 p Presented at the 12th International Colloquium of the Dynamics of Explosions and Reactive Systems, Ann Arbor, MI, 23-28 Jul. 1988
(Contract W-7405-eng-48)
(DE89-008801; UCRL-100490; CONF-8807160-1) Avail: NTIS HC A03/MF A01

Liquid hydrocarbon fuels are used extensively in propulsion systems, and explosion hazards associated with fuel vapors mixed with air must be assessed. In this paper, the detonation of gas phase mixtures of n-hexane and the commercial fuel, JP-4, with oxidizers varying from pure oxygen to air, were studied both experimentally and theoretically via kinetic modeling. Experiments were carried out in a detonation tube 150 mm in diameter and 1.75 m long. Detonation velocities and cell sizes (lambda) were measured as a function of stoichiometry and diluent concentration. The theoretical model calculates the induction length (lambda) of a one-dimensional Zeldovich-von Neumann-Doring (ZND) detonation using the detailed kinetics for the reaction of the hydrocarbon fuel used. The theoretical prediction for the cell size of n-hexane is found to agree well with the experimental data. Because n-hexane is the principal component of JP-4, this fuel would be expected to behave similarly to n-hexane. This similarity is confirmed experimentally. Critical energy and critical tube diameter are compared for a relative measure of the detonability of the heavy hydrocarbon fuels studied, and it appears from kinetic modeling that the detonation sensitivity increases slightly with increasing carbon number; however, this trend cannot be distinguished experimentally with the error in cell size measurement. DOE

N89-26927# Illinois Univ., Urbana. Dept. of Chemistry.
FLUIDS, GELS AND GLASSES UNDER EXTREME CONDITIONS OF PRESSURE AND TEMPERATURE Final Report, 1 Oct. 1985 - 31 Oct. 1988
Jiri Jonas 17 Feb. 1989 17 p
(Grant AF-AFOSR-0345-85; AF Proj. 2303)
(AD-A205292; AFOSR-89-0263TR) Avail: NTIS HC A03/MF A01 CSCL 07/2

The NMR and Raman techniques were used to investigate the hydrolysis and condensation mechanism in B2O3-SiO2; Al2O3-SiO2; and Na2O-Al2O3-SiO2 systems. The solid state NMR techniques were employed together with BET methods to follow the thermal treatment of the gels. In addition to the NMR and Raman techniques, the SANS method was employed to study the effects of fluoride anion catalyst on the sol-gel process involving TMOS. High pressure NMR studies of the dynamic structure of the highly viscous liquids focused on three projects: (1) The self-diffusion behavior, and the applicability of hydrodynamic equations at the molecular level for a model lubricant - 2-ethylhexylbenzoate; (2) the effect of the dipole moment on the hydrodynamic behavior of highly polar fluids; and (3) the effect of molecular flexibility on the relationship between molecular properties and shear viscosity at extreme conditions of pressure. GRA

N89-26928# National Inst. of Standards and Technology, Gaithersburg, MD. Surface Science Div.
TECHNICAL ACTIVITIES 1988, SURFACE SCIENCE DIVISION
C. J. Powell, ed. Jan. 1989 142 p
(PB89-161889; NISTIR-89/4025) Avail: NTIS HC A07/MF A01 CSCL 07D

Technical activities of the NIST Surface Science Division during Fiscal Years 1987 and 1988 are summarized. These activities include surface-standards work, experimental and theoretical research in surface science, the development of improved measurement methods, and applications to important scientific and national problems. A listing is given of publications, talks, professional committee participation, and professional interactions by the Division staff. GRA

N89-26929# Pennsylvania State Univ., University Park. Dept. of Mechanical Engineering.
MIXING AND COMBUSTION OF PULSED GAS JETS Annual Report, Jul. 1987 - Jun. 1988
S. R. Turns, C. L. Merkle, J. A. Lovett, and A. Hosangadi Sep. 1988 123 p
(Contract GRI-5086-260-1308)
(PB89-155550; PSU-ME-R-0053-87/88; GRI-88/0297) Avail: NTIS HC A06/MF A01 CSCL 21B

The objective of the research is to experimentally and analytically characterize the detailed structure of pulsed gas-air diffusion flames to provide an understanding of the enhanced mixing that can occur in such flames. Studying pulsed jets is a particularly attractive means to understand the role that jet structure plays in mixing and combustion. Pulsed jet flames also provide an excellent means to study the influence of mixing on the formation and destruction of flame generated pollutants. Several types of measurements were performed on pulsed propane jet diffusion flames, where the pulse source was either a piston driver or a loudspeaker. These measurements include NO/NOx emission indices, flame length and width measurements using still photography, detailed planar flow visualization using light scattering techniques, and axial phase-averaged velocity distributions using Laser Doppler Velocimeter (LDV). Data were acquired for an extensive test matrix in which both a range of frequencies and pulse amplitudes were covered. Results showed that pulsing could either enhance mixing or hinder it. This effect was primarily controlled by pulse frequency, while pulse amplitude controlled the magnitude of the effect. GRA

N89-26930# Brigham Young Univ., Provo, UT. Dept. of Chemistry.
SUPERCRITICAL FLUID CHROMATOGRAPHY OF POLAR ORGANIC COMPOUNDS IN COMBUSTION PARTICULATES Final Report
Milton L. Lee 16 Sep. 1988 77 p Sponsored by Coordinating Research Council, Inc., Atlanta, GA
(PB89-152441; CRC-APRAC-CAPE-30-81-07A) Avail: NTIS HC A05/MF A01 CSCL 07D

A thermionic detector was evaluated for capillary supercritical fluid chromatography (SFC) of polar nitro-containing polycyclic aromatic compounds (nitro-PAC). Three modes of operation were studied. The best performance was obtained using a nitro-selective mode of detection. A number of nitro-PAC were successfully chromatographed using density programming at 101 C. Capillary column gas chromatography-mass spectrometry was used with state-of-the-art injection techniques and inert columns to analyze diesel exhaust particulate extracts. Polar normal phase HPLC fractions of a heavy-duty diesel exhaust particulate, a National Bureau of Standards (NBS) Standard Reference Material (SRM) 1650, were analyzed by capillary column GC coupled to high resolution mass spectrometry using electron impact (EI) and negative ion chemical ionization (NICI). A total of 80 polycyclic aromatic compounds, belonging to many different chemical classes, were identified. Among them, phenazine and phthalic anhydride were positively identified for the first time in diesel exhaust particulates. In addition, cyclic imides and their alkylated derivatives were tentatively identified for the first time, according to their electron impact mass spectra and exact mass measurements. Other novel polar chemical classes of PAC were evidence by NICI MS using a direct insertion probe. GRA

N89-26931 Department of the Air Force, Washington, DC.
AUTOMATIC OXYGEN MEASURING SYSTEM Patent
Arthur A. Krawetz, inventor (to AF) and Theodore Tovrog, inventor (to AF) 19 Jul. 1988 30 p Filed 27 Feb. 1985
(AD-D014003; US-Patent-4,758,408; US-Patent-Appl-SN-705950; US-Patent-Class-422-92) Avail: US Patent and Trademark Office CSCL 11/8

This invention relates generally to an automated measuring system for determining gas contents of fluids, and, in particular, relates to a system for determining the inherent oxidation stability of base oils and lubricants over a temperature range and for a period of time. A great variety of standardized tests were developed over the years in an attempt to simulate in the laboratory the conditions of oxidation to which lubricants are exposed during the course of their operative life. Described is an automatic oxygen absorption measuring system having a controllable source of pressurized oxygen, a controllable venting device, and a device for indicating incremental gas volume changes connected through a controlled gas reservoir to an oxygen circulating testing section where oxygen is passed through a liquid sample at a fixed temperature. Upon the liberation of other gases than oxygen or absorption of oxygen, the gas pressure changes a liquid fluid level in the device for indicating incremental gas changes. An electronic circuit causes the venting or inputting of gas until an equilibrium pressure is obtained. Each change is noted on a recording device. The device for indicating incremental gas volume changes has two glass bulbs attached in line with a manometer filled with electrically conductive liquid fluid. Four electrical contacts placed about the bulbs indicate the level of the liquid fluid. GRA

N89-26932# Illinois Univ., Urbana-Champaign. Dept. of Chemistry.
SYNTHESIS AND CHARACTERIZATION OF GROUP 4 ORGANOMETAL OXIDE COMPLEXES Ph.D. Thesis
Laura Mae Babcock 1988 168 p
(Contract DE-AC02-76ER-01198)
(DE89-010944; DOE/ER-01198/T34) Avail: NTIS HC A08/MF A01

The organometallic substituted Keggin polyoxoanions ((eta(sup 5)-CH5(CH3)5) MPW11O39), M = Ti(1), Zr(2), or HF(3), were prepared by reaction of (eta (sup5)-C5(CH3)5) MCl3 with the lacunary Keggin heteropolyanion alpha-H3 PW11O39 (eta-CH4-H9)N-4(4). Infrared data indicated that complexes 2 and 3 have a normal Keggin structure however complex 1 has a distorted structure. Based-assisted hydrolysis of (eta(sup 5)-C4(CH3)5) MCl3, M = Zr or Hf in THF solution gave (eta(sup 5)-C5(CH3)5) MCl3O(OH)3Cl, M = Zr(4) or Hf(5), and(eta(sup5)-C5(CH3)5) MCl3O(OH)4, M = Zr(6) or Hf(7). The crystal structure of 6, determined by Dr. Victor Day at Crystalytics Company in Lincoln, NB, revealed a trimer of metals capped on one side by an oxygen atom and on the other side by a hydroxyl ligand with the three edges bridged by hydroxyl ligands. The hydrolysis of (eta(sup 5)-CH(CH3)5) TiCl)3 resulted in the formation of a six membered titanium oxygen ring ((eta(sup 5)-C5(CH3)5) TiClO)3. Hydrolysis in the presence of base has produced a tetrameric ligand stabilized titanoxane complex, ((eta(sup 5)-C5(CH3)5) TiC)O6. DOE

N89-26933# Lehigh Univ., Bethlehem, PA. Materials Research Center.
NANOSTRUCTURE AND DEFECT CHEMISTRY OF RELAXOR FERRO ELECTRICS Interim Report No. 4, 1 Aug. 1986 - 31 Jul. 1988
Martin P. Harmer and Donald M. Smyth 31 Jul. 1988 144 p
(Contract N00014-82-K-0190)
(AD-A207217) Avail: NTIS HC A07/MF A01 CSCL 07/2

The microstructure, microchemistry, and dielectric properties of relaxor ferroelectrics and structurally related compounds are described. The emphasis was on the use of transmission electron microscopy to correlate changes in the composition and processing conditions with changes in microstructure and properties. The report is in three parts that dealt with cation-ordering and microchemical domains in Pb(Sc1/2Ta1/2)3 (PST); undoped and La/Na-doped Pb(Mg1/3Nb2/3)3 (PMN) and Ba(Zn1/3Nb2/3) 3 (BZN), micro-polar domains in normal ferroelectrics (BaTiO3) and relaxor ferroelectrics (PMN:PT and PZN=:PT); and the effect of a pyrochlore second phase on the dielectric properties of PMN. GRA

N89-26934# Clarkson Univ., Potsdam, NY. Dept. of Chemistry.
CATALYTIC REDUCTION OF CARBON DIOXIDE BY METAL CENTERS Final Report No. 6, 1 Aug. 1984 - 28 Feb. 1989
Lauri Vaska 20 Apr. 1989 5 p

(Contract N00014-84-K-0658)
(AD-A207227) Avail: NTIS HC A02/MF A01 CSCL 07/3

The results of the work carried out under this contract include the following significant discoveries: (1) we have demonstrated the first homogeneous catalytic hydrogenation/reduction of carbon dioxide to the methyl group (-CH3, C2-) in the presence of several transition metal complexes (in previous work, the reduction has terminated at the C2+level), (2) another catalytic system was found to reduce CO2 to elemental carbon via formamide intermediation, (3) a platinum cluster complex has been discovered which catalyzes the CO2 reduction reversibly under ambient conditions, both unusual in homogeneous catalysis by metal complexes. The same Pt compound is the most active homogeneous catalyst for CO2 hydrogenation reported to data. GRA

N89-26935# Cornell Univ., Ithaca, NY. Dept. of Chemistry.
ADSORPTION AND COADSORPTION OF CO AND NO ON THE Rh(100) SURFACE: A THEORETICAL ANALYSIS
Dragan Lj. Vuckovic, Susan A. Jansen, and Roald Hoffmann 14 Apr. 1989 67 p
(Contract N00014-82-K-0576)
(AD-A207323; TR-41) Avail: NTIS HC A04/MF A01 CSCL 07/4

The adsorption of carbon monoxide, nitricoxide and their coadsorption on the Rh (100) surface are discussed in terms of extended Huckel/tight binding calculations. Experimentally, it is not easy to resolve the linear and bent forms of NO and for this reason our calculations serve to examine not only the proposed adsorption geometries but also as means to investigate the NO dissociation mechanism. This dissociation is believed to be the fundamental step in the CO/NO reaction. The adsorption site and geometry are discussed for several NO chemisorptions. In addition, a discussion of the CO/NO reaction for the proposed adsorption of NO is presented. From this analysis, it is clear that predissociation of NO into atomic components can lead to recombination producing the desired reaction products, carbon dioxide and diatomic nitrogen. Furthermore, the co-adsorbate interactions can lead directly to the desired products. GRA

N89-26936# Aarhus Univ. (Denmark). Dept. of Chemistry.
OXYGEN TRANSFER TO ETHYLENE CATALYZED BY THE Ag(110) SURFACE
Karl Anker Jorgensen and Roald Hoffmann (Cornell Univ., Ithaca, NY.) Apr. 1989 42 p
(Contract N00014-82-K-0576)
(AD-A207325; TR-43) Avail: NTIS HC A03/MF A01 CSCL 07/2

The silver surface catalyzed epoxidation of ethylene using molecular oxygen as an oxygen donor been studied using extended Huckel calculations. Five types of absorbed molecular oxygen on an Ag(110) surface have been considered, an end-on adsorption on top of silver, a peroxidic adsorbed molecular oxygen, both on a silver atom on the surface or bound to one in the second layer, and finally molecular oxygen bridging between two silver atoms in the (110) and the (001) direction. For atomic adsorbed oxygen four types of geometries have been considered: two adsorption geometries on top of a silver atom, one on the surface and one in the second layer, and two bridging positions, one between two silver atoms in the (110) direction and the other in the (001) direction. The calculations indicate that the most probable adsorption sites for molecular oxygen are end-on or bridging between two silver atoms in the (110) or (001) directions; for atomically absorbed oxygen the adsorption on top of a silver atom on the surface, or bridging between two silver atoms in the (110) direction, are favored. GRA

N89-26937# Boeing Advanced Systems Co., Seattle, WA. Propulsion Technology.
HOT SURFACE IGNITION TESTS OF AIRCRAFT FLUIDS Final Report, May 1987 - May 1988
A. M. Johnson, A. J. Roth, and N. Albert Moussa (Blazetech Corp., Winchester, MA.) Nov. 1988 239 p
(Contract F33615-84-C-2431)
(AD-A207372; AFWAL-TR-88-2101) Avail: NTIS HC A11/MF A01 CSCL 01/3

Five fluids commonly found in aircraft engine components, JP-4 and JP-8 fuels, Mil-H-5606 and Mil-H-83282 hydraulic fluids and Mil-L-7808 lubricating oil, were tested in the Aircraft Engine Nacelle Fire Test simulator (AENFTS) to define their Minimum Hot Surface Ignition Temperature (MHSIT's) when introduced as a spray or stream onto a hot engine bleed duct. The test employed a simple, uncluttered test section and a realistically simulated portion of the F-16 engine compartment. MHSIT's for all but Mil-H-83282 were consistently found to be higher than the fluids autoignition temperature. GRA

N89-26938# State Univ. of New York, Buffalo. Dept. of Chemistry.
SURFACE PLASMON STUDY OF MONOLAYER-BILAYER TRANSITION IN POLY-4-BCMU AND POLY-3-BCMU POLYDIACETYLENE LANGMUIR-BLODGETT FILMS
X. Huang, R. Burzynski, and P. N. Prasad 1989 7 p Submitted for publication
(Contract F49620-87-C-0042; NSF DMR-84-03987)
(AD-A207404; AFOSR-89-0471TR) Avail: NTIS HC A02/MF A01 CSCL 07/4

Surface plasmon wave spectroscopy was successfully used to study the monolayer-bilayer transition in poly-4-BCMU and poly-3-BCMU polydiacetylene Langmuir-Blodgett films. The linear refractive index and the thickness were obtained for the monolayer yellow and bilayer red forms of poly-4-BCMU. Surface plasmon coupling using resonance enhancement was found to sufficiently enhance the Raman scattering, so Raman spectra of the monolayer films could be obtained with a relatively small laser intensity of a few milliwatts. The differences in the c(doubles bond)c and c(triple bond)c vibrational stretching frequencies of the monolayer yellow and the bilayer films were observed arising from the difference in the effective conjugation of the two forms. GRA

N89-26939# Risoe National Lab., Roskilde (Denmark).
ANALYSIS OF LOW-PRESSURE GAS-PHASE PYROLYTIC REACTIONS BY MASS SPECTROMETRIC TECHNIQUES
Lars Carlsen Jan. 1989 246 p
(AD-A207457; RISOE-R-545) Avail: NTIS HC A11/MF A01 CSCL 07/3

The present report highlights applications of mass spectrometric techniques in the analysis of low-pressure pyrolytic reactions, based on work carried out at the Chemistry Department, Riso National Laboratory. The Riso contributions to this field of research started in 1979. The major part of the work summarized in the present report has previously been published in the below mentioned 18 papers. Reprints of these papers are included in this report as appendices 1 through 18. For a more detailed description of the technique, and especially the applications the appendices 1 through 7 and 8 through 18, respectively, should be consulted. GRA

N89-26940# International Business Machines Corp., San Jose, CA.
OPTICAL DETECTION AND SPECTROSCOPY OF SINGLE MOLECULES IN A SOLID
W. E. Moerner and L. Kador 23 Mar. 1989 19 p Submitted for publication
(Contract N00014-84-C-0708)
(AD-A207594; TR-17) Avail: NTIS HC A03/MF A01 CSCL 07/4

Using two different double modulation techniques, we have observed the optical absorption spectrum of single dopant molecules of pentacene in a p-terphenyl host crystal at liquid helium temperatures. To achieve this, frequency-modulation spectroscopy was combined either with Stark or ultrasonic modulation to remove interfering background signals from residual amplitude modulation, and the number of molecules in resonance was reduced to one by operating in the wings of the inhomogeneous line. Triplet bottleneck saturation appears in the single-molecule regime. GRA

N89-26941# Argonne National Lab., IL. Mathematics and Computer Science Div.
NUMERICAL COMPUTATION OF BIFURCATION PHENOMENA AND PATTERN FORMATION IN COMBUSTION
A. Bayliss, B. J. Matkowsky (Northwestern Univ., Evanston, IL.), and M. Minkoff 1989 20 p Presented at the 3rd International Conference on Numerical Combustion, Antibes, France, 23 May 1989
(Contracts W-31-109-eng-38; DE-FG02-87ER-25027; NSF DMS-87-01543)
(DE89-013628; CONF-8905105-2) Avail: NTIS HC A03

We develop and employ a new numerical method to study problems in both gaseous and solid fuel (condensed phase) combustion. The numerical method is an extension of the adaptive pseudo-spectral method previously introduced, in that two dimensional, non-product coordinate transformations are introduced so as to efficiently compute fronts which have a strong transverse variation. DOE

N89-26942# National Inst. of Standards and Technology, Gaithersburg, MD. Center for Atomic, Molecular and Optical Physics.
TECHNICAL ACTIVITIES 1986-1988, MOLECULAR SPECTROSCOPY DIV.
A. Weber Mar. 1989 136 p
(PB89-175418; NISTIR-89/4051) Avail: NTIS HC A07/MF A01 CSCL 07D

The report summarizes the technical activities of the National Institute of Standards and Technology (NIST) Molecular Spectroscopy Division for the Fiscal Year 1987 and 1988. The activities span experimental and theoretical research in high resolution molecular spectroscopy, quantum chemistry, and laser photo-chemistry, and include the development of frequency standards, critically evaluated spectral data applications of spectroscopy to important scientific and technological problems, and the advancement of spectroscopy measurement methods and techniques. A listing is given of publications and talks by the Division staff. Author

N89-26943# Sandia National Labs., Albuquerque, NM. Combustion Research Facility.
LEAN-BURN GAS ENGINE IGNITION PROCESSES Annual Report, Nov. 1987 - Nov. 1988
Matthew J. Hall Dec. 1988 47 p
(Contract GRI-5086-260-1458)
(PB89-181119; GRI-89/0007) Avail: NTIS HC A03/MF A01 CSCL 21B

The objective of this research was to investigate the effect of engine flow field characteristics on cycle-to-cycle variation in a methane fueled engine. The rate of early flame development was correlated with the turbulence characteristics, mean flow, and cylinder pressure history. Drastically different flow field characteristics were achieved in the engine through the use of a prechamber having a variable inlet orifice diameter. Three combustion chamber geometries were examined: main chamber combustion without a prechamber, a prechamber with a 9 mm entrance orifice, and a prechamber with a 27 mm entrance orifice. Velocities were measured in the region of the spark using laser velocimetry. The engine had a compression ratio of 5.1, was operated at speeds of 300, 600, and 1200 rpm. The equivalence ratios were 0.7 and 0.8. A newly developed fiber optic spark plug probe was used to measure early flame development. It was found that the early flame development rate increased with increasing turbulence intensity. Under most operating conditions, a strong correlation was found between how quickly the flame grew to a diameter of 1 cm and cycle-to-cycle variation of cylinder pressure. GRA

N89-26944# Adiabatics, Inc., Columbus, IN.
FEASIBILITY DEMONSTRATION OF THE THERMAL IGNITION COMBUSTION SYSTEM (TICS) FOR HIGH PRESSURE NATURAL GAS INJECTED ENGINE
R. M. Kalwani, D. McNulty, P. Badgley, and R. Kamo Feb. 1989 73 p
(Contract GRI-5084-223-1048)
(PB89-178792; AI-84-15-1; GRI-89/0056) Avail: NTIS HC A04/MF A01 CSCL 21B

The objective of the program was the feasibility demonstration of the Thermal Ignition Combustion System (TICS) concept for the ignition and combustion of high pressure injected natural gas. TICS concept relies on the ignition of fuel by high temperature combustion chamber walls without external ignition sources like spark plug, glow plug or pilot diesel fuel. The program was successful in achieving ignition and combustion of natural gas in a single cylinder diesel engine with the TICS concept. An electronically controlled gas injector, designed and fabricated in the program, was used to inject natural gas at 13.8 to 20.7 MPa (2000 to 3000 psig) pressure in the TICS chamber. Cold starting of the test engine was achieved by external heating of the chamber for a few minutes. Natural gas ignition and combustion was then sustained by the high temperature TICS chamber. The test engine was operated from idle to full load and from 600 to 1400 rpm engine speed range. Author

N89-26945# California Univ., Berkeley. Dept. of Mechanical Engineering.
FIRE PROPAGATION IN CONCURRENT FLOWS Final Report, 1 Aug. 1987 - 31 Jul. 1988
A. C. Fernandez-Pello Aug. 1988 42 p
(Grant NIST-60NANB7D0737)
(PB89-188577; NIST/GCR-89/560) Avail: NTIS HC A03/MF A01 CSCL 21B

The research tasks completed during the reporting period include an experimental study of the effect on the spread of flames of the turbulence intensity of an opposed air flow, and a theoretical analysis of the concurrent spread of flames over thin fuels. Both studies are important contributions in the study of the flame spread process. The results of the experimental study show that the flame spread process is significantly affected by the flow turbulence intensity for flames spreading over both thin and thick fuels. The results of the theoretical analysis, which are in good agreement with previous experimental measurements, give detailed information about the flame structure and mechanisms of flame spread. GRA

N89-26946# Yale Univ., New Haven, CT. Dept. of Chemical Engineering.
CATALYTIC COMBUSTION OF METHANE Annual Report, 15 May 1987 - 15 May 1988
L. D. Pfefferle and M. D. Smooke Mar. 1989 85 p
(Contract GRI-5086-260-1249)
(PB89-188874; GRI-88/0284) Avail: NTIS HC A05/MF A01 CSCL 21B

Catalytically stabilized combustion represents an extremely promising but underexploited technology. Catalytic combustors can be designed to combine the high reaction rates of thermal combustors with the low NOx and soot levels of conventional catalytic oxidation reactors. This research focuses on examining the basic chemical and transport mechanisms from a fundamental point of view with the objective of determining how these mechanisms affect design considerations. Findings with respect to the effect of a platinum catalyst on the concentration of oxidizing radicals (O, OH) in a combustion boundary layer and the relation of this effect to gas phase ignition criteria are reported. The authors also report results from the reacting boundary layer model for combustion of hydrogen over reactive and nonreactive surfaces. Thermal diffusion, complex chemistry in the gas phase, surface oxidation of hydrogen and surface production of OH were considered. Author

N89-26947# Pittsburgh Univ., PA. Dept. of Chemistry.
STUDIES OF THE FUNDAMENTAL NATURE OF CATALYTIC ACIDITY, SITES AND INTERMEDIATES Progress Report
1989 5 p
(Contract DE-FG02-87ER-13774)

(DE89-012946; DOE/ER-13774/T1) Avail: NTIS HC A02/MF A01

Advances in the understanding of the acidic and catalytic properties of H-zeolites have been achieved from several kinds of experiments. These included: (1) MASNMR studies of adsorbed alcohols, (2) optical spectroscopy of Hammett indicators, (3) studies of the kinetics and mechanisms of the catalytic decomposition of isobutane and neopentane, (4) site poisoning experiments using NH sub 3, and (5) preparation and characterization of dealuminated zeolites by Si (29) and Al (27) MASNMR, ^{1}H-NMR, X-ray diffraction and physical adsorption. DOE

N89-26948# Oak Ridge National Lab., TN. Chemical Technology Div.

GAS SEPARATIONS USING INORGANIC MEMBRANES

B. Z. Egan, S. P. N. Singh, D. E. Fain, G. J. Kidd, G. E. Roettger, and D. E. White (Oak Ridge Gaseous Diffusion Plant, TN.) 1989 10 p Presented at the Gasification and Gas Stream Cleanup Systems, Morgantown, WV, 27-29 Jun. 1989 Submitted for publication

(Contract DE-AC05-84OR-21400)

(DE89-013010; CONF-890666-1) Avail: NTIS HC A02/MF A01

The research and development program consists of developing, fabricating, and testing inorganic membrane separation systems for the recovery of H sub 2 and the separation of coal gasification gases. Major parts of the program include: (1) assessment of the status of R and D activity related to gas separations using inorganic membranes; (2) identification and selection of candidate membrane materials, based on the chemistry of the separation environment and the availability and cost of the materials; (3) fabrication and characterization of candidate membranes using specialized techniques available at the Oak Ridge Gaseous Diffusion Plant; and (4) evaluation of the separations capability of the fabricated membranes in terms of permeabilities and fluxes of gases. This quarter, literature searches of several data bases were completed to compile information on the status of R and D on inorganic membranes for gas separations. A commercially available tubular alumina membrane was evaluated in terms of mean pore size, pore size distribution, and gas permeabilities of nitrogen, helium, and carbon dioxide. Several tubular alumina membranes were fabricated and characterized by pore size distribution measurements. The design of a test apparatus for measuring the gas permeabilities of membranes at high temperatures and pressures was completed. DOE

N89-26949# Sandia National Labs., Albuquerque, NM.

MICROPYROLYZER DESIGN FOR INFRARED SPECTROSCOPY APPLICATIONS

D. S. Blair and M. C. Oborny May 1989 15 p

(Contract DE-AC04-76DP-00789)

(DE89-013329; SAND-89-0842) Avail: NTIS HC A03/MF A01

Traditionally, pyrolysis combined with infrared (IR) detection of the decomposition products for the analysis of small (less than 1 mg) samples has been limited due to the size and geometry of commercially available pyrolysis chambers. To reduce the sample size requirements for pyrolysis-IR, a system has been designed and built that allows various microgram sized polymer samples to be examined. The design incorporates a commercial pyrolysis system with a small chamber built from readily available parts. Minimal modifications of these components are required to build the system. The micropyrolyzer has been used to successfully identify various filled epoxy samples, such as three Epon 828 samples: 0.46 mg of alumina filled; 0.15 mg of mica filled; and 0.28 mg of glass microballoon (GMB) filled. DOE

N89-26950# California Univ., Berkeley. Lawrence Berkeley Lab. Center for X-Ray Optics.

A PRELIMINARY REPORT ON X-RAY PHOTOABSORPTION COEFFICIENTS AND ATOMIC SCATTERING FACTORS FOR 92 ELEMENTS IN THE 10-10,000 eV REGION

B. L. Henke, J. C. Davis, E. M. Gullikson, and R. C. C. Perera Nov. 1988 322 p

(Contract DE-AC03-76SF-00098)

(DE89-013392; LBL-26259) Avail: NTIS HC A14/MF A01

Based on currently available photoabsorption measurements and recent theoretical calculations by Doolen and Liberman, a revised best-fit determination of the photoabsorption cross sections is presented here for the elements Z = 1 to Z = 92 in the 10 to 10,000 eV range. The photoabsorption data used include those described in the Lockheed and DOE listings of research abstracts for the past ten years and those which have been recently added to the comprehensive NBS Measured Data Base. The best-fit curves are compared with both the compilation of measurements and the calculations by Doolen and Liberman. Using the photoabsorption curves, the atomic scattering factors have been calculated for the energy range 50 to 10,000 eV and are also presented. DOE

N89-26951# City Coll. of the City Univ. of New York, NY. Dept. of Physics.

THERMODYNAMICS AND HIGH TEMPERATURE CHEMISTRY OF THE CHEMICAL VAPOR DEPOSITION OF DIAMOND FILMS

M. Sommer and F. W. Smith 1989 20 p Presented at the 6th International Conference on High Temperatures: Chemistry of Inorganic Materials, Gaithersburg, MD, 3 Apr. 1989

(Contract DE-FG02-87ER-45317)

(DE89-013574; CONF-890435-3) Avail: NTIS HC A03/MF A01

The chemical vapor deposition of carbon films is analyzed using the thermodynamic quasiequilibrium model and a phase diagram for the carbon-hydrogen system is obtained. When the enhanced etching of graphite by hydrogen is included in the model, a region in the phase diagram where diamond is the only stable solid phase of carbon is predicted, consistent with the experimental results. Details of the model and additional comparisons with experiment are presented. DOE

N89-26952# Argonne National Lab., IL.

THE ROLE OF X-RAY ABSORPTION SPECTROSCOPY IN ELECTRONIC STRUCTURE STUDIES

E. Ercon Alp May 1989 12 p Presented at the Workshop on Applications of Synchrotron Radiation in Chemical Research, Argonne, IL, 3-4 Oct. 1988

(Contract W-31-109-eng-38)

(DE89-014677; CONF-8810117-2) Avail: NTIS HC A03/MF A01

The usefulness of X-ray absorption spectroscopy in studies of electronic structure in materials is discussed. DOE

N89-26953# Argonne National Lab., IL. Intense Pulsed Neutron Source and Materials Science Div.

MOMENTUM DISTRIBUTIONS IN LIQUID HELIUM

P. E. Sokol (Pennsylvania State Univ., University Park.), T. R. Sosnick, and W. M. Snow 1988 19 p Presented at the Workshop on Momentum Distributions, Argonne, IL, 24 Oct. 1988

(Contract W-31-109-eng-38)

(DE89-014679; CONF-8810118-9) Avail: NTIS HC A03/MF A01

The appearance of the superfluid phase, with its unique macroscopic properties, and the success of the two-fluid model in describing the transport properties are intimately linked to the Bose statistics obeyed by He-4 atoms. The most direct signature of the Bose condensate is in the single particle momentum distribution n(p). In the normal liquid the momentum distribution has a broad Gaussian shape, as predicted for classical systems, with a width determined by the quantum zero point motion. In the superfluid phase a new feature appears, the Bose condensate. The condensate appears as a delta-function singularity in n(p) with an intensity proportional to n(0), the condensate fraction. There has been extensive experimental work attempting to verify the existence of the condensate. Hohenberg and Platzman originally suggested that inelastic neutron scattering at high momentum transfer Q, where the Impulse Approximation (IA) can be used to directly relate the observed scattering to n(p), could provide a means of directly observing the condensate. In this review we will concentrate on recent experimental studies that utilize the large flux of high

energy neutrons available at spallation neutron sources. These sources, which have become available only recently, have made it possible to make detailed measurements at large enough momentum transfers that the conditions for the Impulse Approximation are approximately satisfied. While deviations from the IA are still present at these higher Q's, they are more amenable to theoretical treatment and detailed predictions are available. Thus, even though no distinct condensate peak is observed, for the first time excellent agreement with the theoretical predictions for n(p) can be obtained. DOE

N89-26954# IIT Research Inst., Bartlesville, OK. National Inst. for Petroleum and Energy Research.
THERMODYNAMIC EQUILIBRIA IN THE BIPHENYL/HYDROGEN SYSTEM (THE POWER AND LIMITATIONS OF GROUP ADDITIVITY ESTIMATIONS)
W. V. Steele and R. D. Chirico Jul. 1989 32 p
(Contracts DE-FC22-83FE-60149; DE-FG05-87ER-13758)
(DE89-000754; NIPER-403) Avail: NTIS HC A03/MF A01

Calculated equilibria in the biphenyl/phenylcyclohexane/bicyclohexane/hydrogen system are presented and compared with experimental values reported in the literature. Gibbs energies of formation were estimated for phenylcyclohexane and bicyclohexane using group-additivities. The results were combined with values for biphenyl obtained from experimental thermodynamics to calculate the equilibria in the system. Under thermodynamic equilibrium conditions the maximum concentration of phenylcyclohexane obtainable is approx. 60 mole per cent. As the temperature is increased this maximum concentration can only be obtained by a corresponding increase in hydrogen pressure. In a given temperature regime, too high a hydrogen pressure will facilitate the formation of the fully saturated compound, bicyclohexane, and too low a hydrogen pressure the formation of biphenyl. Equilibrium conditions for the generation of hydroaromatics were defined. Hydrogen transfer from a donor molecule (here tetralin) to an aromatic acceptor (here biphenyl) is favored by low temperature and a large excess of the donor over the acceptor. It is concluded that an order of magnitude improvement in the additivity methodology (increase in the accuracy and precision of the group-contribution term parameters) is required to enable meaningful calculation of the conditions under which thermodynamic equilibria exist in the hydrogenation of multi-ring aromatic systems. DOE

N89-26955# Sandia National Labs., Albuquerque, NM.
DETONATION OF UNCONFINED LARGE SCALE FUEL SPRAY-AIR CLOUDS
W. B. Benedick, J. H. S. Lee, and R. Knystautas (McGill Univ., Montreal, Quebec) 1989 22 p Presented at the 12th International Colloquium on the Dynamics of Explosions and Reactive Systems, Ann Arbor, MI, 23 Jul. 1989
(Contract DE-AC04-76DP-00789)
(DE89-006510; SAND-89-0090C; CONF-890739-1) Avail: NTIS HC A03/MF A01

Unconfined heterogeneous two-phase detonations in liquid droplet-air mixtures are investigated. The liquid fuel is placed in a V-shaped channel and is dispersed into the atmosphere to form a cloud by an explosive detonating cord laid along the bottom vertex of the channel. An aerosol cloud 7 m high by about 1.5 m averaged width can be generated in this way with a typical mass ratio of fuel to explosive charge of 150. In the present study the length of channel used is typically 10 m giving a detonable fuel-air cloud of about 100 cu m. The propylene-oxide driver and the test fuel are disseminated simultaneously. Detonation in the propylene-oxide section is initiated by the sheet explosive and the detonation then transmits from this driver section into the rest of the cloud formed from the test fuel. For insensitive fuels requiring a larger cloud dimension, two parallel fuel troughs spaced 1.2 m apart are used. It is found that propylene-oxide and nitrated hydrocarbon fuels detonate quite readily. For the case of propylene-oxide, significant vaporization of the aerosol is observed prior to initiation so that detonation is essentially in the gas phase. DOE

N89-26956# Kentucky Univ., Lexington. Dept. of Chemistry.
LASER SPECTROSCOPY AND DYNAMICS OF COMBUSTION INTERMEDIATES Annual Progress Report No. 3, 1 Jun. 1986 - 31 May 1989
Dennis J. Clouthier Oct. 1988 10 p
(Contract DE-FG05-86ER-13544)
(DE89-014498; DOE/ER-13544/T2) Avail: NTIS HC A02/MF A01

The research originally proposed under this grant concerned the study of the spectroscopy and excited state dynamics of a number of transient sulfur-containing molecules and free radicals. It was suggested that the identification and study of sulfur species which are analogs of important oxygen-containing combustion intermediates would be important to our understanding of reactive intermediates. The specific systems chosen for study were thioformaldehyde (H sub 2 CS), thioketene (H sub 2 CCS), disulfur monoxide (S sub 2 O), and the free radical HCCS, C sub 2 S and HCS. Since most of the species had not been previously studied by laser techniques and some of them were completely unknown, much effort has been devoted to determining methods for producing and observing them. We have been successful in a number of studies and have developed a new technique called pyrolysis jet spectroscopy which promises to be widely applicable. A detailed description of progress in each area is given. DOE

N89-26957# Institut Franco-Allemand de Recherches, Saint-Louis (France).
DYNAMIC MEASUREMENTS IN COMBUSTIBLE AND DETONABLE AEROSOLS
Michel Samirant, Guenter Smeets, Christian Baras, Henri Royer, and Louis-Remy Oudin 1988 43 p Previously announced in IAA as A89-45218
(ISL-PU-306/88; ETN-89-94859) Avail: NTIS HC A03/MF A01

Methods used for determining the principal parameters of rapid fuel air aerosol dispersions and of their reactions, i.e., combustion and detonation, are presented. In a shock tube or in the free atmosphere, the velocity of the dispersed fuel, the breaking of the droplets, their size distribution and their velocities are measured. The investigation of the thermal variations due to the fuel evaporation allows the composition of the two-phase mixture air-combustible gas-fuel to be obtained. ESA

N89-26958# North Carolina Univ., Chapel Hill. Dept. of Chemistry.
MAGNETIC AND ELECTRICAL PROPERTIES OF SANDWICH-LIKE LANTHANIDE PHTHALOCYANINES
Juan Padilla and William E. Hatfield 8 May 1989 10 p Submitted for publication
(Contract N00014-89-J-1734)
(AD-A208411; TR-34) Avail: NTIS HC A02/MF A01 CSCL 07/2

Rare earth phthalocyanine sandwich compounds and their iodine analogues have been synthesized. Single crystals were obtained by electrochemical means, and magnetic susceptibility measurements on the polycrystalline samples follow the Curie Weiss law. Room temperature and 77 K EPR spectra at X band for undoped lutetium phthalocyanine indicate the presence of a free radical phthalocyanine unit. Doped complexes also show a narrow signal with a g value of 2.00. GRA

26 METALLIC MATERIALS

Includes physical, chemical, and mechanical properties of metals, e.g., corrosion; and metallurgy.

N89-26959 Department of the Air Force, Washington, DC.
DISPERSION STRENGTHENED ALUMINUM-BASE ALLOY Patent
Yashwant R. Mahajan, inventor (to AF), Susan D. Kirchoff, inventor (to AF), and Francis H. Froes, inventor (to AF) 29 Nov. 1988 9 p Filed 30 Apr. 1987

(AD-D014044; US-Patent-4,787,943; US-Patent-Appl-SN-045970) Avail: US Patent and Trademark Office CSCL 11/6

An aluminum alloy containing about 2 to 6 weight percent titanium, about 3 to 11 weight percent of a rare earth of the Lanthanide Series and up to about 3 weight percent of a least one Group VIII metal, balance aluminum, is disclosed. The alloy is preferably prepared by rapid solidification in powder, particulate or ribbon form, and is subsequently compacted under controlled conditions. GRA

N89-26960 Department of the Air Force, Washington, DC.
METHOD FOR MAKING AN INTEGRAL TITANIUM ALLOY ARTICLE HAVING AT LEAST TWO DISTINCT MICROSTRUCTURAL REGIONS Patent
Daniel Eylon, inventor (to AF) and Francis H. Froes, inventor (to AF) 28 Feb. 1989 7 p Filed 6 May 1988
(AD-D014066; US-Patent-4,808,249; US-Patent-Appl-SN-198800; US-Patent-Class-148-133) Avail: US Patent and Trademark Office CSCL 11/6

A method for producing an integral titanium alloy article having at least two regions, each region having a distinct microstructure is provided. The method comprises heat treating one or more selected region(s) of the article at a temperature greater than the beta-transus temperature of the region(s), while simultaneously heat treating the remaining region(s) of the article at a temperature below the beta-transus temperature of the remaining region(s). GRA

N89-26961 Department of the Air Force, Washington, DC.
METHOD FOR REFINING MICROSTRUCTURES OF BLENDED ELEMENTAL TITANIUM POWDER COMPACTS Patent
Daniel Eylon, inventor (to AF) and Francis H. Froes, inventor (to AF) 28 Feb. 1989 6 p Filed 4 Dec. 1987
(AD-D014067; US-Patent-4,808,250; US-Patent-Appl-SN-128840; US-Patent-Class-148-20.3) Avail: US Patent and Trademark Office CSCL 11/6

This invention relates to the processing of titanium articles fabricated by powder metallurgy to improve the microstructure of such articles. In general terms, powder metallurgy involves production, processing and consolidation of fine particles to produce a solid article. The small, homogeneous powder particles result in a uniform microstructure in the final product. If the final product is made net-shape by application of hot isostatic pressing (HIP), a lack of texture can result, thus giving equal properties in all directions. In accordance with the present invention there is provided a process for improving the microstructure of a blended elemental titanium article made by powder metallurgy which comprises, in combination, the steps of hydrogenating the compacted article at a temperature of about 780 to 1020 C to a hydrogen level of about 0.50 to 1.50 weight percent, cooling the thus-hydrogenated article to room temperature at a controlled rate, heating the thus-cooled, hydrogenated article to a temperature of about 650 to 750 C. and applying a vacuum to dehydrogenate the article, and cooling the thus-hydrogenated article to room temperature at a controlled rate. GRA

N89-26962# Fairchild Republic Div., Farmingdale, NY.
SUPERPLASTIC FORMING OF ALUMINUM, TASK C Final Report, Mar. 1986 - Jan. 1988
Theodore Renshaw Mar. 1989 100 p
(Contract F33615-83-C-3208)
(AD-A207282; WRDC-TR-89-3027) Avail: NTIS HC A05/MF A01 CSCL 01/3

This report covers the work under Task C of Contract F33615-83-C-3208. An SPF based A-10 nose landing gear door was designed using Supral 220 alloy. The part count for the basic door was reduced to 4 components as compared to 52 for the conventional construction method. The superplastic pan comprising the stiffening structure of the door was assembled to the external skin using the ultrasonic weldbonding process. Test results show that the two doors are approximately equivalent in strength. Economic analysis indicates that the SPF door is less than half the cost of the conventional door for production quantities larger than 100. GRA

N89-26963# Washington Univ., Seattle. Dept. of Mechanical Engineering.
HRR FIELD IN AN ALUMINUM SEN SPECIMEN
Mahyar Dadkhah (Rockwell International Science Center, Thousand Oaks, CA.) and Albert S. Kobayashi Apr. 1989 19 p
(Contract N00014-89-J-1276)
(AD-A207578; UWA/DME/TR-89/63) Avail: NTIS HC A03/MF A01 CSCL 11/6

Moire interferometry was used to record simultaneously the vertical and horizontal displacements associated with stable crack growth in single edge notched, 2024-0 aluminum specimens. For a small stable crack growth of 1.5 mm, the vertical displacement showed the dominance of the HRR field but the horizontal displacement deviated from the HRR field at the early stage of loading. GRA

N89-26964# Army Lab. Command, Watertown, MA. Material Technology Lab.
THE RECRYSTALLIZATION AND RESPHEROIDIZATION OF TUNGSTEN GRAINS IN A TUNGSTEN-HEAVY ALLOY Final Report
Robert J. Dowding Apr. 1989 23 p
(AD-A207647; MTL-TR-89-31) Avail: NTIS HC A03/MF A01 CSCL 11/6

Refinement of the microstructure of tungsten-heavy alloys, specifically 90 W-7 Ni-3 Fe, was achieved through heavy cold working followed by a heat treatment that recrystallized and respheroidized the tungsten grains. Hydrostatic extrusion of the alloy to reductions of area of 83 and 96 percent followed by isothermal annealing gives fine, spherical tungsten grains imbedded within the nickel-iron matrix. The finest grain size achieved was 15 microns for the 96 percent extrusion when subjected to an anneal at 1300 C for 2 hours. The apparent activation energy for the process was found to be 530 kJ/mole. This value indicates that volume diffusion is significant in respheroidizing the grains. GRA

N89-26965 Department of the Air Force, Washington, DC.
METHOD FOR DEVELOPING ULTRAFINE MICROSTRUCTURES IN TITANIUM ALLOY CASTINGS Patent
Daniel Eylon, inventor (to AF), Francis H. Froes, inventor (to AF), and Charles F. Yolton, inventor (to AF) 11 Apr. 1989 5 p Filed 4 Dec. 1987
(AD-D014115; US-Patent-4,820,360; US-Patent-Appl-SN-128839) Avail: US Patent and Trademark Office CSCL 11/6

A method is disclosed for improving the microstructure of cast titanium alloy articles. it is comprised of the following steps: hydrogenating the cast article at a temperature near or above the titanium-hydrogen eutectoid of 815 C (of about 780 to 1020 C) to a hydrogen level of about 0.50 to 1.50 weight percent, cooling the thus-hydrogenated article to room temperature at a controlled rate, heating the thus-cooled, hydrogenated article to a temperature of about 650 to 750 C applying a vacuum to dehydrogenate the article, and cooling the thus-dehydrogenated article at a controlled rate. GRA

N89-26966# Sandia National Labs., Albuquerque, NM.
THE SOLIDIFICATION METALLURGY OF ALLOY 718 AND OTHER Nb-CONTAINING SUPERALLOYS
M. J. Cieslak, G. A. Knorovsky, T. J. Headley, and A. D. Romig, Jr. 1989 22 p Presented at the International Symposium on Alloy 718 Metallurgy and Applications, Pittsburgh, PA, 12 Jun. 1989
(Contract DE-AC04-76DP-00789)
(DE89-008196; SAND-89-0264C; CONF-890646-1) Avail: NTIS HC A03/MF A01

The solidification behavior of Alloy 718 and other Nb-bearing austenitic superalloys has been examined using an integrated analytical approach. All alloys of this type begin solidification with the formation of Nb-lean austenitic dendrites. Interdendritic

eutectic-type solidification constituents involving MC-type carbides and a Nb-rich Laves phase occur in these alloys. The gamma/Laves eutectic constituent terminates solidification in these alloys. Nb is the dominant element in the evolution of solidification microstructure with C and Si affecting the amounts of gamma/MC and gamma/Laves constituent observed. Simple solidification models predict reasonably well the amount of eutectic constituent observed. DOE

N89-26967# Oak Ridge National Lab., TN.
DEGRADATION OF Fe-25Cr, Fe-25Cr-20Ni AND Fe-25Cr-6Al ALLOYS IN H2/H2O/H2S ENVIRONMENTS AT 700 C
K. Vedula and G. M. Michal (Case Western Reserve Univ., Cleveland, OH.) 1 Mar. 1989 26 p
(Contract DE-AC05-84OR-21400)
(DE89-011873; ORNL/Sub-86-95900/01) Avail: NTIS HC A03

Fe-25 wt pct Cr, Fe-25 wt pct Cr-20 wt pct Ni and Fe-25 wt pct Cr-6 wt pct Al alloys have been exposed to H sub 2/H sub 2 O/H sub 2 S/Ar gas mixtures at 700 C. The mechanisms of formation and degradation of oxide scales on these alloys have been investigated using electron microscopy and surface analytical techniques. The Fe-25Cr-6Al alloy is attacked the least as a result of the formation of a Al sub 2 O sub 3 layer in the scale, whereas the Fe-25Cr-20Ni alloy is attacked the most, through rapid formation of Fe and Ni sulfides. The Fe-25Cr alloy, forms a Cr sub 2 O sub 3 scale containing CrS sub 1.17 precipitates, and other phases which eventually lead to scale breakdown. DOE

N89-26968# California Univ., Berkeley. Lawrence Berkeley Lab. Center for Advanced Materials.
OBSERVATIONS ON THE MECHANISMS OF FATIGUE IN EUTECTIC Pb-Sn SOLDER JOINTS
D. Tribula, D. Grivas, D. R. Frear, and J. W. Morris, Jr. Aug. 1988 22 p Presented at the ASME Winter Annual Meeting, Chicago, IL, 28 Nov. 1988 Prepared in cooperation with California Univ., Berkeley
(Contract DE-AC03-76SF-00098)
(DE89-000553; LBL-25831; CONF-881120-10) Avail: NTIS HC A03/MF A01

Near-eutectic Pb-Sn solders are widely used for joints in electrical devices. These are liable to failure by thermal fatigue during operation of the device. Since the thermal fatigue load is often in shear, the mechanisms of thermal fatigue in shear are of particular interest. Recent research has shown that the thermal fatigue of eutectic solders in shear is preceded by the formation of bands of coarsened material in the eutectic microstructure, which concentrate the deformation and cause the nucleation of fatigue cracks. Such coarsened bands are also observed in isothermal fatigue and unidirectional creep in shear. Since creep experiments are relatively simple to conduct and analyze, these have been used to study the formation and growth of coarsened bands. The mechanism includes three steps: the formation of inhomogeneous shear bands, the onset of recrystallization in the shear band to create a planar region of coarsened material, and the propagation of the coarsened band by progressive recrystallization at its tip. The results are applied to thermal fatigue and some of their implications are discussed. DOE

N89-26969# Oak Ridge National Lab., TN. Metals and Ceramics Div.
EVALUATION OF MECHANICAL PROPERTIES OF TiN FILMS BY ULTRA-LOW LOAD INDENTATION
Michael E. OHern, Robert H. Parrish (Vanderbilt Univ., Nashville, TN.), and Warren C. Oliver 1989 14 p Presented at the 16th International Conference on Metallurgical Coatings and Equipment Exhibit, San Diego, CA, 17 Apr. 1989
(Contract DE-AC05-84OR-21400)
(DE89-009618; CONF-890468-2) Avail: NTIS HC A03/MF A01

The mechanical properties of titanium nitride films of varying composition deposited on stainless steel substrates were studied using an indentation technique with a mechanical properties microprobe which allows measurement of film properties without contribution from the substrate material. A polishing technique was developed that gave consistent indentation measurements on films with initially rough surfaces. The elastic modulus increases linearly with increasing nitrogen content in the N:Ti range of 0.5 to 1.05, while the hardness of the film depends on other factors. Possible factors contributing to the hardness of the films are discussed. DOE

N89-26970# Brookhaven National Lab., Upton, NY. Dept. of Nuclear Energy.
EFFECTS OF HIGH THERMAL AND HIGH FAST FLUENCES ON THE MECHANICAL PROPERTIES OF TYPE 6061 ALUMINUM IN THE HFBR
John R. Weeks, Carl J. Czajkowski, and Paul R. Tichler 1988 25 p Presented at the 14th International Symposium on Effects of Radiation on Materials, Andover, MA, 27 Jun. 1988
(Contract DE-AC02-76CH-00016)
(DE89-012636; BNL-42692; CONF-880613-32) Avail: NTIS HC A03/MF A01

The High Flux Beam Reactor (HFBR) at Brookhaven National Laboratory (BNL) is an epithermal, externally moderated (by D2O) facility designed to produce neutron beams for research. Type 6061 T-6 aluminum was used for the beam tubes, pressure vessel, fuel cladding, and most other components in the high flux area. The HFBR has operated since 1965. The epithermal, external moderation of the HFBR means that materials irradiated in different areas of the facility receive widely different flux spectra. Thus, specimens from a control rod drive follower tube (CRDF) have received 1.5 x 10(22) n/sq cm (E is greater than 0.1 MeV) and 3.2 x 10(23) n/sq cm thermal fluence, while those from a vertical thimble flow shroud received 1.9 x 10(23) n/sq cm (E is greater than 0.1 MeV) and 1.0 x 10(23) n/sq cm thermal. These numbers correspond to fast to thermal fluence ratios ranging from 0.05 to 1.9. Irradiations are occurring at approximately 333 K. The data indicate that the increase in tensile strength and decrease in ductility result primarily from the thermal fluence, i.e., the transmutation of aluminum to silicon. These effects appear to be saturating at fluences above approximately 1.8 x 10(23) n/sq cm thermal at values of 90,000 psi (6700 Kg/sq mm) and 9 percent, respectively. The specimens receiving the highest fluence ratios appear to have less increase in tensile strength and less decrease in ductility than specimens with a lower fast to thermal fluence ratio and the same thermal fluence, suggesting a possible beneficial effect of the high energy neutrons in preventing formation of silicon crystallites. DOE

N89-26971# California Univ., Berkeley. Lawrence Berkeley Lab. Center for Advanced Materials.
CRYOGENIC TENSILE PROPERTIES OF AA 2090 WELDMENTS
A. J. Sunwoo and J. W. Morris, Jr. Mar. 1989 15 p Presented at the 5th International Aluminum-Lithium Conference, Williamsburg, VA, 28-31 Mar. 1989 Prepared in cooperation with California Univ., Berkeley
(Contract DE-AC03-76SF-00098)
(DE89-012979; LBL-26651; CONF-8903109-4) Avail: NTIS HC A03/MF A01

The influence of base metal temper and filter metal additions on the cryogenic properties Al-Li 2090 weldments are studied. The results show that as the strength of the base metal increases, strength mismatch increases and the joint efficiency decreases. Inhomogeneous deformation is confined to the fusion zone and the strain localization results in premature failure in the weldment. As the temperature decreases, T3 base metal weldments show better properties than T8 base metal weldments. The influence of filler metal additions on the weldment properties shows that the strength is limited without post-weld aging, but the increase in elongation is significant. At 77 K, a 6 Cu addition to 2090 yields the best UTS and elongation combination of the filler metals studied. Mg addition leads to embrittlement at 77 K. DOE

N89-26972# California Univ., Berkeley. Lawrence Berkeley Lab. Center for Advanced Materials.
MICROSTRUCTURAL EVOLUTION OF Al-Li AND Al-Li-Cu-Mg ALLOYS
S. Miyasato and G. Thomas Mar. 1989 12 p Presented at the 5th International Aluminum-Lithium Conference, Williamsburg, VA, 28-31 Mar. 1989
(Contract DE-AC03-76SF-00098)
(DE89-012981; LBL-26168; CONF-8903109-5) Avail: NTIS HC A03/MF A01

Since subsequent microstructures and properties depend upon initial decomposition processes, the early developments in a binary Al-Li and quaternary Al-Li-Cu-Mg alloy were observed by high resolution transmission electron microscopy. Interpretation of high resolution images involved appropriate image simulations. The as-quenched microstructure was found to consist of small ordered domains which were unaffected by the presence of Cu and Mg alloying additions, BETA (Al sub 3 Zr) dispersoids and grain boundaries, and are thus interpreted as forming by spinodal decomposition. The ordered domains, approximately 4 nm in diameter, were often observed in antiphase with each other and were separated by regions of disordered matrix. No discrete delta (Al sub 3 Li) particles were observed for natural aging times between 24 hours and 3 weeks. DOE

N89-26973# Oak Ridge National Lab., TN.
ANALYSIS OF MICROSTRUCTURAL DEVELOPMENT IN SINGLE CRYSTAL WELDS
M. Rappaz, S. A. David, J. M. Vitek, and L. A. Boatner 1989 6 p Presented at the 2nd International Conference on Trends in Welding Research, Gatlinburg, TN, 15 May 1989
(Contract DE-AC05-84OR-21400)
(DE89-013537; CONF-8905118-10) Avail: NTIS HC A02/MF A01

A detailed analysis of the dendritic microstructure produced in autogenously welded single crystals Fe-15Ni-15Cr has been performed in order to investigate the relationship between growth crystallography and solidification behavior. From a geometrical analysis relating the dendrite growth velocities to the weld velocity, it has been shown that, at a given point of the melt pool surface, selection of the preferred dendrite trunk growth direction occurs according to a minimum velocity (i.e., minimum undercooling) criterion. Knowing the growth rate of the selected dendrite orientation, the dendrite tip radius and the dendrite trunk spacing have been computed using recent theories of rapid solidification of ternary systems. The predicted dendrite growth orientation and spacing have been successfully compared to experimental observations made on electron beam and laser welds, thus clearly demonstrating the effect of crystallography on the microstructural development during weld pool solidification. DOE

N89-26974# Oak Ridge National Lab., TN.
THE EFFECT OF AGING AT 343 DEG C ON TYPE 308 STAINLESS STEEL WELDS
D. J. Alexander, K. B. Alexander, and Randy K. Nanstad 1989 5 p Presented at the 2nd International Conference on Trends in Welding Research, Gatlinburg, TN, 15 May 1989
(Contract DE-AC05-84OR-21400)
(DE89-013545; CONF-8905118-12) Avail: NTIS HC A02/MF A01

Three nominally 25 mm (1 in.) thick shielded metal-arc welds were prepared from 304L base plate with 308 filler material, to obtain three different ferrite levels (4, 8, and 12 pct). Portions of these welds were then aged at 343 C for 3000, 10000, and 20000 hours. Charpy V-notch and tensile specimens were taken from the welds. The tensile results were similar for all the specimens and showed little effect of aging on either the yield or ultimate tensile strengths. The Charpy impact properties of the higher ferrite content materials were significantly degraded by these agings, with larger decreases in the impact energy with increased aging time. The microstructures of the welds were examined by metallography and transmission electron microscopy, and the fracture surfaces were examined by scanning electron microscopy. The changes in the mechanical properties and the fractography are discussed in light of the observed changes in the microstructure. DOE

N89-26975# Rockwell International Corp., Golden, CO.
EFFECT OF OXIDATION, SANDBLASTING AND PICKLING ON WELDABILITY
Jouko Leinonen Jun. 1989 24 p Transl. into ENGLISH of Report 28, (1981) Oulu Univ., Finland
(Contract DE-AC04-76DP-03533)
(DE89-013795; RFP-Trans-499; OU-Rept-28; ISBN-951-42-0965-6) Avail: NTIS HC A03/MF A01

Studies of the weldability problem of austenitic steels have led to new methods for improving weldability. Majetic and Yeo have patented a method on which the weldable surface is oxidized by annealing, or on it is spread a thin layer of certain oxides. The welding speed increases up to 350 percent due to the oxide layer. The weldability problems also disappear when a method invented by Moisio and Leinonen is used. In this case, small amounts of oxygen, carbon dioxide, or steam are added into the customary TIG shielding gases. A third way to improve the weldability is to sandblast the surface to be welded. If the weldability of steel is poor, it is often advisable to use the methods mentioned. The purpose of this study is to clarify the effects of oxidation, sandblasting, and pickling on penetration. The matter is particularly studied by welding tests performed under laboratory conditions. DOE

N89-26976*# National Aeronautics and Space Administration. Marshall Space Flight Center, Huntsville, AL.
STRESS CORROSION STUDY OF PH13-8Mo STAINLESS STEEL USING THE SLOW STRAIN RATE TECHNIQUE
Pablo D. Torres Washington Jul. 1989 32 p
(NASA-TP-2934; NAS 1.60:2934) Avail: NTIS HC A03/MF A01 CSCL 11F

The need for a fast and reliable method to study stress corrosion in metals has caused increased interest in the Slow Strain Rate Technique (SSRT) during the last few decades. PH13-8MoH950 and H1000 round tensile specimens were studied by this method. Percent reduction-in-area, time-to-failure, elongation at fracture, and fracture energy were used to express the loss in ductility, which has been used to indicate susceptibility to stress corrosion cracking (SCC). Results from a 3.5 percent salt solution (corrosive medium) were compared to those in air (inert medium). A tendency to early failure was found when testing in the vicinity of 1.0 x 10(-6) mm/mm/sec in the 3.5 percent salt solution. PH13-8Mo H1000 was found to be less likely to suffer SCC than PH13-8Mo H950. This program showed that the SSRT is promising for the SCC characterization of metals and results can be obtained in much shorter times (18 hr for PH steels) than those required using conventional techniques. Author

N89-26977# National Inst. of Standards and Technology, Boulder, CO. Fracture and Deformation Div.
FRACTURE BEHAVIOR OF A PRESSURE VESSEL STEEL IN THE DUCTILE-TO-BRITTLE TRANSITION REGION
Juergen Heerens (GKSS-Forschungszentrum Geesthacht, Germany, F.R.) and D. T. Read Dec. 1988 44 p
(PB89-189195; NISTIR-88/3099) Avail: NTIS HC A03/MF A01 CSCL 11F

The reasons for the scatter of fracture toughness in the ductile-to-brittle transition region, as well as the mechanisms leading to cleavage fracture, were investigated for a quenched and tempered pressure vessel steel, DIN 20 MnMoNi 55. The fracture surfaces indicate that cleavage fracture starts at one small area in the ligament, the cleavage initiation site. Cleavage initiation occurs ahead of the crack tip at the location of the maximum normal stresses. Fractography and metallography show four different types of initiation sites. The mechanisms which may trigger cleavage fracture at these initiation sites are discussed. The results indicate that the scatter of fracture toughness is due to the scatter in the distance between the cleavage initiation site and the fatigue crack tip. GRA

N89-26978# Oak Ridge National Lab., TN. Engineering Technology Div.

RATE-SENSITIVITY AND SHORT TERM RELAXATION BEHAVIOR OF AISI TYPE 304 STAINLESS STEEL AT ROOM TEMPERATURE AND AT 650 C; INFLUENCE OF PRIOR AGING

Marina B. Ruggles and Erhard Krempl (Rensselaer Polytechnic Inst., Troy, NY.) 1989 25 p Presented at the Joint ASME/JSME Pressure Vessel and Piping Conference, Honolulu, HI, 23-27 Jul. 1989

(Contract DE-AC05-84OR-21400)

(DE89-007823; CONF-890721-9) Avail: NTIS HC A03/MF A01

The strain rate sensitivity and short term relaxation behavior of Type 304 Stainless Steel were investigated in the uniaxial strain rate jump tests with intermittent periods of relaxation at room temperature and at 650 C. At room temperature material exhibited conventional strain rate sensitivity and no strain rate history effect. The high-temperature experimental results revealed a complex and dramatically different material behavior. At 650 C the pattern of strain rate sensitivity was not set as soon as the plastic flow was fully established, but continued to evolve with the further straining in the plastic range. Test results indicate that at 650 C the material may exhibit a strain rate history effect. Both at room temperature and at 650 C the relaxation behavior was independent of the stress and/or strain level at the beginning of the relaxation, but depended nonlinearly on the strain rate preceding the relaxation test. Prior aging had no significant influence on the rate-dependent material response. The irregular material behavior at 650 C is attributed to dynamic strain aging as indicated by serrated stress-strain curves (the Portevin-LeChatelier effect). DOE

N89-26979# Oak Ridge National Lab., TN. Metals and Ceramics Div.

LOSS OF GRAIN BOUNDARY SEGREGANT DURING ION MILLING

E. A. Kenik 1989 7 p Presented at the Microbeam Analysis Society Meeting, Asheville, NC, 16 Jul. 1989

(Contract DE-AC05-84OR-21400)

(DE89-007835; CONF-890748-3) Avail: NTIS HC A02/MF A01

Bismuth segregates to grain boundaries in copper at intermediate temperatures (400 to 800 C). Currently, X-ray microanalysis is being used to measure the degree of equilibrium segregation as a function of boundary character. As part of that study, transmission electron microscopy specimens were prepared by several techniques in order to select that method which produced optimum specimens. Electropolishing produced specimens of marginal quality because of preferential grain boundary attack. On the other hand, ion-milling produced good, thin specimens with little or no boundary attack. However, X-ray microanalysis on specimens ion-milled at room temperature indicated no bismuth segregation, whereas analysis on electropolished specimens indicated bismuth segregation. A loss of bismuth from the ion-milled specimens was proposed to result from the high vapor pressure of bismuth at slightly elevated temperatures. The use of a liquid nitrogen cold stage during ion-milling minimizes the loss of bismuth. It is likely that beam heating during ion-milling is a contributing factor in this process and must be controlled. DOE

N89-26980# Oak Ridge National Lab., TN. Metals and Ceramics Div.

AN EXPERIMENTAL STUDY OF THE EFFECT OF STAINLESS STEEL CLADDING ON THE STRUCTURAL INTEGRITY OF FLAWED STEEL PLATES IN BENDING

S. K. Iskander, Randy K. Nanstad, G. C. Robinson, and C. B. Oland 1989 17 p Presented at the Joint ASME/JSME Pressure Vessel and Piping Conference, Honolulu, HI, 23-27 Jul. 1989

(Contract DE-AC05-84OR-21400)

(DE89-008735; CONF-890721-11) Avail: NTIS HC A03/MF A01

A small crack near the inner surface of clad nuclear reactor pressure vessels is an important consideration in the safety assessment of the structural integrity of the vessel. Experimental results from tests on large clad and unclad plate specimens with surface flaws have shown that: (1) a tough surface layer composed of cladding and/or a heat-affected zone has arrested running flaws in clad plates under conditions where unclad plates have ruptured, and (2) the residual load-bearing capacity of clad plates with large subclad flaws significantly exceeded that of an unclad plate. The fracture surfaces of unclad plates suggest that the flaw evolves through alternately tunneling then breaking to the surface. In the case of clad plates, it is hypothesized that the tough, strong surface layer inhibits the tunneled flaw from propagating to the surface. DOE

N89-26981# Sandia National Labs., Albuquerque, NM.

QUANTITATIVE THIN FILM X-RAY MICROANALYSIS OF Nb MODIFIED Ti3Al

A. D. Romig, Jr., T. J. Headley, M. J. Carr, and M. J. Cieslak 1989 9 p Presented at the Microbeam Analysis Society Meeting, Asheville, NC, 16 Jul. 1989

(Contract DE-AC04-76DP-00789)

(DE89-009946; SAND-89-0683C; CONF-890748-7) Avail: NTIS HC A02/MF A01

Advanced titanium-aluminum intermetallic alloys (often simply called titanium aluminides) have certain properties which make them potentially attractive as advanced aerospace alloys. In order to utilize these alloys in engineering applications, it is necessary to process the alloys in a variety of ways including casting, hot forming and welding. All of these processes modify the microstructure of the alloy, which in turn directly influences the properties. The key to optimizing the alloy's properties is to control the microstructure by careful control of the processing parameters. Control for the microstructure requires a thorough understanding of the evolution of the microstructure, including elemental partitioning between the various phases which form in the alloy. Analytical electron microscopy (AEM) is an ideal way to characterize the microstructures on a fine spatial scale. Such high spatial resolution microanalysis is required to understand the microstructural evolution in these alloys. In this case, the alloy is a Nb modified Ti sub 3 Al, and the partitioning behavior of interest is between a variety of ternary phases which are produced as a function of alloy cooling rate from a single homogeneous high temperature beta phase. The Nb is added to the alloy to enhance its performance, primarily through an improvement in ductility. In this work, the details of the procedure for quantitative analysis of these alloys are presented. DOE

N89-26982# Oak Ridge National Lab., TN. Metals and Ceramics Div.

RELAXATION RESPONSE OF A533B STEEL FROM 25 TO 600 C

R. W. Swindeman and E. Bolling 1989 8 p Presented at the Joint ASME/JSME Pressure Vessel and Piping Conference, Honolulu, HI, 23-27 Jul. 1989

(Contract DE-AC05-84OR-21400)

(DE89-010179; CONF-890721-22) Avail: NTIS HC A02

Relaxation tests were performed on A533B steel over the range 25 to 600 C in order to examine the general features of time-dependent deformation. It was found that the relaxation strength increased with the flow stress at low temperatures and was relatively independent of history at high temperatures. In the temperature range 400 to 600 C the inelastic strain rates calculated from the relaxation rates followed stress dependencies that were consistent with expectations based on a model proposed by Hart and coworkers for matrix deformation. DOE

N89-26983# Los Alamos National Lab., NM.

POLYCRYSTAL PLASTICITY AS APPLIED TO THE PROBLEM OF IN-PLANE ANISOTROPY IN ROLLED CUBIC METALS

Anthony D. Rollett, Michael G. Stout, and U. Fred Kocks 1989 5 p Presented at the Plasticity '89: International Symposium on Plasticity, Ton, Japan, 31 Jul. - 4 Aug. 1989

(Contract W-7405-eng-36)

(DE89-011181; LA-UR-89-1241; CONF-890772-1) Avail: NTIS HC A02/MF A01

A fundamental property of cubic metals is that slip occurs on close-packed planes in close-packed directions, which for the f.c.c. case results in 12 set of (111) planes/group of zone axes (100) slip systems. This crystallographic restriction on the plastic behavior causes significant crystallographic preferred orientation (texture), hence anisotropy, to develop once a large strain has been imposed. Moreover, whereas annealing can generally reset the flow stress and ductility, it does not generally randomize the texture: therefore most metallic materials have some degree of texture and consequent anisotropy. The problem of earing in deep drawing can be simply related to the variation of r-value with angle from the rolling direction, i.e., the in-plane anisotropy of the sheet. The r-value can be calculated from a given texture with the use of a polycrystal plasticity model. The Los Alamos polycrystal plasticity (LApp) code is based on the Bishop-Hill single crystal yield surface (SCYS) but with a mildly strain-rate sensitive modification where the stress exponent is of order 30. This modification of the SCYS removes the ambiguity of slip system selection inherent in the Bishop-Hill formulation and permits other phenomena to be treated such as latent hardening and pencil glide. DOE

N89-26984# California Univ., Berkeley.
HISTORY OF THE APPLICATION OF THE GENERALIZED LEWIS ACID-BASE THEORY TO METALS
L. Brewer Nov. 1988 6 p Presented at the World Material Congress, Chicago, IL, 24 Sep. 1988 Prepared in cooperation with California Univ., Be rkeley. Lawrence Berkeley Lab.
(Contract DE-AC03-76SF-00098)
(DE89-012992; LBL-26942; CONF-8809360-1) Avail: NTIS HC A02/MF A01

The history of experiences with intermetallics has been found useful by students seeking my advice on which directions in science they should be emphasizing. In response to their question, I point to a mobile in my office consisting of seven hands pointing in different directions. Science comes up with so many unexpected developments that one's education should have a broad enough base to allow one to branch out in any direction to take advantage of unexpected opportunities. My historical presentation will be a personal account that I hope will serve as a guide to students. There have been many unexpected abrupt changes in my research. DOE

N89-26985# Argonne National Lab., IL. Materials and Components Technology Div.
CROSS-SECTIONAL TEM (TRANSMISSION ELECTRON MICROSCOPY) STUDIES OF Cr FILMS DEPOSITED BY ION-ASSISTED DEPOSITION AND PHYSICAL VAPOR DEPOSITION
C. C. Cheng, R. A. Erck, and G. R. Fenske 1989 19 p Presented at the 16th International Conference on Metallurgical Coatings and Equipment Exhibit, San Diego, CA, 17-21 Apr. 1989
(Contract W-31-109-eng-38)
(DE89-014643; CONF-890468-11) Avail: NTIS HC A03/MF A01

A series of Cr films were deposited by physical vapor deposition and ion-assisted deposition as a function of the incident ion energy and the ion/atom arrival-rate ratio, R. Cross section transmission electron microscopy was used to study the microstructure of the substrate/film interface and film surface regions of these Cr films. High-energy ion bombardment (greater than 300 eV) was found to enhance the adhesion of the deposited film owing to the formation of an intermixing layer at the interface region. Hardness data suggest that high ion energy and low ion/atom arrival-rate ratios produce films with relatively high hardness because few pores and many defects are present. DOE

N89-26986# Northwestern Univ., Evanston, IL. Dept. of Physics and Astronomy.
LOCAL DENSITY THEORY OF HEATS OF FORMATION AND SHORT-RANGE ORDER PARAMETERS IN SUBSTITUTIONALLY DISORDERED ALLOYS Final Technical Report
A. J. Freeman and A. Gonis 1988 15 p
(Contract DE-FG02-84ER-45080)
(DE89-014696; DOE/ER-45080/T3) Avail: NTIS HC A03/MF A01

Since previous Progress Reports presented results obtained in several other areas of our research, we highlight some results here of our investigations of the energetics of alloy phase diagrams. These have been carried out along both a theoretical and computational front. The theoretical studies were necessitated by the need to apply Green function methods, or the Korringa-Kohn-Rostoker (KKR) formalism, to a diverse number of cases such as isolated impurities, substitutional or interstitial, in pure elemental solids and in substitutionally disordered alloys, and to the treatment of lattice relaxation around impurities. Our computational endeavors were directed toward developing computer programs based on theoretical advances and toward refining existing codes. In the following we describe briefly the results we have obtained thus far along theoretical and computational lines. DOE

N89-26987# EG and G Mound Applied Technologies, Miamisburg, OH.
AN AUGER SPUTTER PROFILING STUDY OF NITROGEN AND OXYGEN ION IMPLANTATION IN TWO TITANIUM ALLOYS
B. D. Barton, L. E. Pope, and T. N. Wittberg (Dayton Univ., OH.) 1989 33 p Presented at the 11th Symposium on Applied Surface Analysis, Cleveland, OH, 31 May 1989
(Contract DE-AC04-88DP-43495)
(DE89-014734; MLM-3951(OP); CONF-8905167-1) Avail: NTIS HC A03/MF A01

Samples of two titanium alloys, Ti-6Al-4V and Ti-15V-3Cr-3Sn-3Al, were ion implanted with a combination of nitrogen (N+) and oxygen (O+). For each alloy, implantation parameters were chosen to give implanted nitrogen concentrations of approximately 10 or 50 atomic percent, from a depth of 100 nanometers to a depth of 400 nanometers. In all but one case, dual energy (200 keV and 90 keV) implantations of nitrogen were used to give a relatively uniform nitrogen concentration to a depth of 300 nanometers. In each case, oxygen was implanted at 35 keV, following the nitrogen implantation, to give an oxygen-enriched region near the surface. The implanted samples were then examined by Auger electron spectroscopy (AES) combined with argon ion sputtering. In order to determine the stoichiometry of the nitrogen implanted regions, it was necessary to determine the N(KVV) contribution to the overlapping N(KVV) and Ti(LMM) Auger transitions. It was also necessary to correct for the ion-bombardment-induced compositional changes which have been described in an earlier study titanium nitride thin films. The corrected Auger electron spectroscopy (AES) depth profiles were in good agreement with theoretical predictions. DOE

N89-26988# Pittsburgh Univ., PA. Dept. of Materials Science and Engineering.
BREAKDOWN MECHANISMS OF Al2O3, Cr2O3 AND SiO2 SCALES IN H2/H2O/H2S ENVIRONMENTS, VOLUME 1 Final Report
Gil M. Kim and Gerald H. Meier 31 Jan. 1989 81 p Prepared for ORNL, TN
(Contract DE-AC05-84OR-21400)
(DE89-014789; ORNL/Sub-83-43346/02-Vol-1) Avail: NTIS HC A05/MF A01

The breakdown mechanisms of preformed oxide scales, Cr2O3, Al2O3 and SiO2, have been studied at low oxygen and high sulfur potentials in the temperature range 550 C to 950 C. For Cr2O3 on Ni-30Cr, sulfur penetration occurs through thin areas in the Cr2O3 scale. The first sulfides to form on Fe-25Cr and Co-30Cr were observed at the scale/gas interface as the result of Fe or

Co transport through the Cr2O3 scale. Alumina scales on Fe-18Cr-6Al-1Hf were broken down by crack formation. Addition of Hf to the alloy improved scale adherence and extended the time to breakdown. Additions of Ti to Fe-18Cr-6Al provided improved scale adherence without introducing continuous paths through the oxide scales. These scales were even more resistant than those on the Hf-containing alloys when exposed in high sulfur potential atmospheres. These results also extended to long term cyclic sulfidation/oxidation experiments and simulated syngas exposures. Pure alumina scales were never formed on Ni-18Cr-6Al and Co-18Cr-6Al alloys and the NiCrAl alloy underwent catastrophic corrosion in most sulfidation/oxidation exposures. For SiO2 on Ni-20Si, although porosity can form at the scale/gas interface due to the high vapor pressures of SiS and SiO, the formation of a thin layer of vitreous silica and good scale adherence provide better resistance to sulfur penetration than do Cr2O3 and Al2O3. The SiO2 scales formed on Fe-20Si and Co-20Si were not as protective as those formed on Ni-20Si. DOE

N89-26989*# National Aeronautics and Space Administration. Lewis Research Center, Cleveland, OH.
FATIGUE CRACK GROWTH STUDY OF SCS6/Ti-15-3 COMPOSITE
Peter Kantzos and Jack Telesman Aug. 1989 20 p
(NASA-TM-102332; E-5041; NAS 1.15:102332) Avail: NTIS HC A03/MF A01 CSCL 11F

A study was performed to determine the fatigue crack growth (FCG) behavior and the associated fatigue damage processes in a (0)(8) and (90)(8) oriented SCS(6)/Ti-15-3 composite. Companion testing (CT) was also done on identically processed Ti-15-3 unreinforced material. The active fatigue crack growth failure processes were very similar for both composite orientations tested. For both orientations, fatigue crack growth was along the fiber direction. It was found that the composite constituent most susceptible to fatigue damage was the interface region and in particular the carbon coating surrounding the fiber. The failure of the interface region lead to crack initiation and also strongly influenced the FCG behavior in this composite. The failure of the interface region was apparently driven by normal stresses perpendicular to the fiber direction. The FCG rates were considerably higher for the (90)(8) oriented CT specimens in comparison to the unreinforced material. This is consistent with the scenario in which the interface has lower fatigue resistance than the matrix, causing lower composite fatigue resistance. The FCG rates of the (0)(8) composite could not be directly compared to the (90)(8) composite but were shown to increase with an increase in the crack length. Author

N89-26990# Naval Postgraduate School, Monterey, CA.
EFFECT OF HEATING RATE TO TEST TEMPERATURE ON SUPERPLASTIC RESPONSE IN AN Al-8 PERCENT Mg-1 PERCENT Li-0.2 PERCENT Zr ALLOY M.S. Thesis
Duncan OMara Mar. 1989 151 p
(AD-A208462) Avail: NTIS HC A08/MF A01 CSCL 11/6

The effect of heating rate to tension test temperature on superplastic response in an Al-8 percent Mg-1 percent Li-0.2 percent Zr alloy was studied. A thermomechanical process (TMP) was used that involved warm rolling with controlled reheating between rolling passes. During the TMP, microstructural evolution was controlled by a continuous reaction (CRX). Superplastic response was studied using five heating rates, ranging from 7.1X10-3 C/s to 2.4 x 10+1 C/s, following TMP. Heating rates greater than 10 C/s resulted in a discontinuous reaction (DRX) with a likely coarsening of grain size. Conversely, high ductilities and enhancement of superplasticity resulted from slower heating rates (1 deg C/s) that facilitated recovery and CRX in a microstructure already highly refined by CRX during the TMP. GRA

N89-26991# Naval Postgraduate School, Monterey, CA.
A MICROSTRUCTURAL INVESTIGATION OF THE SHEAR DISTORTIONS AND ENERGETICS OF MOTIONS OBSERVED IN AN AGED HIGH DAMPING 53Cu-45Mn-2Al ALLOY M.S. Thesis
David M. Farkas Mar. 1989 113 p
(AD-A208467) Avail: NTIS HC A06/MF A01 CSCL 11/6

The shear distortions developed upon aging of a 53Cu-45Mn-2Al alloy were studied using transmission electron microscope image extinctions and diffraction spot streak analysis. It was determined that a lattice distortion of (110) planes, in (111) directions developed in the alloy as aging progressed. This matured (111) shear induces a distinct V-shaped contrast which displays dynamic motion under the electron-beam irradiation of TEM examination. Video imaging techniques were applied to this activity, termed flickering, to investigate the energetics of the underlying crystalline lattice motion. The real-time behavior at the flicker sites suggests that the underlying mechanism which produces the dynamic contrast change is a gradual crystallographic transition, typical of a second-order phase transition. GRA

N89-26992# Naval Postgraduate School, Monterey, CA.
THERMOMECHANICAL PROCESSING OF ALUMINUM ALLOY 2090 FOR SUPERPLASTICITY M.S. Thesis
Mohammad B. Choudhry Mar. 1989 85 p
(AD-A208764) Avail: NTIS HC A05/MF A01 CSCL 11/6

The effect of processing variables on the microstructural development and superplasticity of aluminum alloy 2090, a high strength Aluminum-Copper-Lithium-Zirconium alloy of reduced density in comparison to other Al-based materials, was investigated. Following previous research, warm rolling was conducted to strains, up to 3.36 and it was found that increasing the strain to values greater than 2.6 offered no improvement in subsequent superplastic response. Increased rolling speeds likewise did not enhance ductibility above a maximum value of approximately 240 percent. Microstructural examination revealed a refined, homogeneous microstructure consisting of T2 particles distributed in an alloy matrix. These particles reside in triple junctions in a recovered microstructure. GRA

27 NONMETALLIC MATERIALS

Includes physical, chemical, and mechanical properties of plastics, elastomers, lubricants, polymers, textiles, adhesives, and ceramic materials.

For composite materials see *24 Composite Materials.*

N89-26993# National Inst. of Standards and Technology, Gaithersburg, MD. Polymers Div.
INSTITUTE FOR MATERIALS SCIENCE AND ENGINEERING, POLYMERS: TECHNICAL ACTIVITIES 1988 Annual Report, 1 Oct. 1987 - 30 Sep. 1988
Leslie E. Smith and Brunu M. Fanconi Nov. 1988 120 p
(PB89-166094; NISTIR-88/3842) Avail: NTIS HC A06/MF A01 CSCL 11B

The Technical Activities of the Polymers Division for FY-88 are reviewed. Included are descriptions of the 6 tasks of the Division, project reports, publications, and other technical activities. Author

N89-26994# National Bureau of Standards, Gaithersburg, MD. Ceramics Div.
STRUCTURAL RELIABILITY AND DAMAGE TOLERANCE OF CERAMIC COMPOSITES FOR HIGH-TEMPERATURE APPLICATIONS Semiannual Progress Report, period ending 30 Sep. 1987
E. R. Fuller, Jr., T. W. Coyle, and R. F. Krause, Jr. Feb. 1988 27 p Sponsored by DOE, Oak Ridge, TN
(PB89-156350; NBSIR-88/3710) Avail: NTIS HC A03/MF A01 CSCL 11C

The achievement of higher efficiency heat engines and heat recovery systems requires the availability of high-temperature,

high-performance structural materials. Structural ceramics, and more recently, ceramic matrix composites have received particular attention for these applications due to their high strength and resistance to corrosion and thermal shock. Even with these positive attributes, improved reliability and extended lifetime under service conditions are necessary for structural ceramics to gain industrial acceptance. The problems with these materials are mechanical and chemical in nature and are enhanced by the fact that they are subjected to high temperatures, reactive environments and extreme thermal gradients. With an objective of improved performance for heat engine/heat recovery applications, the NBS program on structural ceramics and ceramic composites addresses these problems through the determination of critical factors that influence mechanical and microstructural behavior. Interfacial and microstructural properties of Nicalon fiber-reinforced SiC composites are discussed. Matrix crack-fiber interactions are characterized. Creep and creep rupture behavior are also presented. GRA

N89-26995# National Inst. of Standards and Technology, Gaithersburg, MD. Ceramics Div.
STRUCTURAL RELIABILITY AND DAMAGE TOLERANCE OF CERAMIC COMPOSITES FOR HIGH-TEMPERATURE APPLICATIONS Semiannual Progress Report, period ending 31 Mar. 1988
E. R. Fuller, T. W. Coyle, T. R. Palamides, and R. F. Krause Aug. 1988 18 p Sponsored by DOE, Oak Ridge, TN
(PB89-156368; NISTIR-88/3817) Avail: NTIS HC A03/MF A01 CSCL 11B

The achievement of higher efficiency heat engines and heat recovery systems requires the availability of high-temperature, high-performance structural materials. Structural ceramics, and more recently, ceramic matrix composites have received particular attention for these applications due to their high strength, and resistance to corrosion and thermal shock. Even with these positive attributes, improved reliability and extended lifetime under service conditions are necessary for structural ceramics to gain industrial acceptance. The problems with these materials are mechanical and chemical in nature and are enhanced by the fact that they are subjected to high temperatures, reactive environments and extreme thermal gradients. With an objective of improved performance for heat engine/heat recovery applications, the NBS program on structural ceramics and ceramic composites addresses these problems through the determination of critical factors that influence mechanical and microstructural behavior. Mechanical behavior of fiber/matrix interfaces is measured using an indentation technique on a Nicalon fiber, glass ceramic composite. Matrix crack-fiber interactions are characterized. A double cleavage drilled compression configuration is used to study the influence of multiple fiber arrays on the toughening increment resulting from individual fibers. The influence of fiber coating and coating thickness on the toughening increment is also examined. Creep and creep rupture behavior of SiC whisker-reinforced alumina ceramics is reported. GRA

N89-26996# National Inst. of Standards and Technology, Gaithersburg, MD. Ceramics Div.
TOUGHENING MECHANISMS IN CERAMIC COMPOSITES Semiannual Interim Progress Report, period ending 30 Sep. 1988
E. R. Fuller, R. F. Krause, M. D. Vaudin, and T. R. Palamides Feb. 1989 24 p Sponsored by DOE, Oak Ridge, TN
(PB89-162606; NISTIR-88/4018) Avail: NTIS HC A03/MF A01 CSCL 11B

A fracture mechanics specimen known as the double-cleavage drilled-compression (DCDC) specimen has been used to study crack-fiber interactions and toughening increments in a model composite system of SiC monofilaments in a borosilicate glass matrix. The toughening increments were measured from changes in applied stress intensity factor as a function of crack length and number of monofilament fibers. Both the fiber-matrix debond strength and the interfacial frictional shear resistance, which influence these toughening increments, were measured independently by a single fiber pull-out test and were correlated with the toughness increases measured by the DCDC specimen. A ceramic composite material that has received much attention because of its increased toughness and creep resistance compared with alumina is aluminum oxide reinforced with silicon carbide whiskers. In the study, the creep and creep rupture behavior of a 25 wt pct SiC whisker-reinforced alumina ceramic with 4.9 pct porosity were measured at temperature between 100 C and 1300 C and at applied stresses between 55 and 306 MPa, although the applied stresses at each temperature varied over a much narrower range. Creep strains were determined from loading-point displacement measurements in four-point flexure. Author

N89-26997# Coors Porcelain Co., Golden, CO.
COMPACT CERAMIC HEAT EXCHANGERS Final Report, Feb. 1983 - Jun. 1988
Lawrence E. Coubrough, Charles J. Dobos, and Richard N. Kleiner Jun. 1988 131 p
(Contract GRI-5082-232-0696)
(PB89-173603; GRI-88/0172) Avail: NTIS HC A07/MF A01 CSCL 11C

The objective of the project was to develop and field test a durable compact ceramic heat exchanger for improved process efficiency in industrial gas-fired furnace. A unique aluminum titanate ceramic material and crossflow recuperator design was developed and analyzed in laboratory testing in 1983 and 1984. Testing of the recuperator performance and system benefits began in the heat treating industry on three separate direct fired furnace installations. Over five years of trouble-free operation has produced operating cost reductions of 30 to 45 percent and productivity improvements up to 16 percent. In 1985 testing on a box forge furnace at temperatures up to 2250 F has provided 30 percent fuel cost savings. In 1987, application of this technology is being extended to radiant tube systems through design and laboratory testing of counterflow radiant tube recuperator packages. GRA

N89-26998# Dayton Univ., OH. Research Inst.
COMPRESSIVE PROPERTIES OF HIGH PERFORMANCE POLYMERIC FIBERS Interim Report, Apr. - Dec. 1988
Scott A. Fawaz, Anthony N. Palazotto, and Chyi-Shan Wang Mar. 1989 102 p
(Contract F33615-87-C-5241)
(AD-A207271; AFWAL-TR-88-4262) Avail: NTIS HC A06/MF A01 CSCL 07/6

In directing the research effort for improving the compressive properties of rigid-rod polymeric composite fibers, a reliable testing technique for determining compressive properties is needed. The technique developed used the Tecam Micro-Tensile Testing Machine, MTM-8 and allowed direct tension and compression testing of composite fibers of extremely short gage length. The measured data was analyzed for corrections in machine compliance and possible errors in gage length misreading, fiber slippage, glue deformation, fiber misalignment, and nonuniform stress distribution. A non polymeric fiber was tested to determine if any fiber material dependence existed. GRA

N89-26999# Lehigh Univ., Bethlehem, PA. Dept. of Physics.
THEORY OF AGGREGATE DEFECTS IN SILICON Final Technical Report, 1 Jun. 1985 - 28 Feb. 1989
Gary G. DeLeo and W. B. Fowler 1989 6 p
(Contract N00014-85-K-0460)
(AD-A207273) Avail: NTIS HC A02/MF A01 CSCL 09/1

The research summarized in this final technical report was supported under ONR contract N00014-85-K-0460 during the period 1 June 1985 to 28 February 1989. Included are: (1) a brief (two page) summary of contract-period research accomplishments, and (2) an appendix listing publications and presented papers. Reprints of published papers are appended to selected copies of this report; otherwise, they are available upon request. During the contract period, our efforts were focussed on point defects in silicon which exhibit large structural departures (relaxations) from the high-symmetry geometry, and defects which combine to form defect aggregates. The primary goals were to understand on an

atomic scale the electronic characteristics of selected defects and defect reactions and, in so doing, reveal physical phenomena basic to defect systems. GRA

N89-27000# George Mason Univ., Fairfax, VA.
ANALYSIS AND EVALUATION OF TECHNICAL DATA ON THE PHOTOCHROMIC AND NON-LINEAR OPTICAL PROPERTIES OF MATERIALS Quarterly Technical Report No. 1
Robert F. Cozzens 1 Mar. 1989 21 p
(Contract DAAB07-89-C-F404; ARPA Order 6631)
(AD-A207275) Avail: NTIS HC A03/MF A01 CSCL 07/3

The overall goal of this relatively small contractural effort is to provide technical assistance to Dr. Frank Pattern (DARPA) in evaluating data on materials, especially polymers, that may be useful in the development of optical limiters for the protection of eyes and electrooptic sensors from exposure to damaging levels of laser radiation. A major task is to assist in the development of a predictive capability in assessing the viability of various protective approaches and to determine the theoretical limitations which may exist in the use of organic materials as optical switches and limiters. A search of the literature has been initiated in an attempt to gather into one table the magnitude of the nonlinear optical properties of various organic materials as a function of molecular structure. The search includes research activities supported by the Federal Government as well as the open literature. GRA

N89-27001*# National Aeronautics and Space Administration. Langley Research Center, Hampton, VA.
FLEXIBLE BACKBONE AROMATIC POLYIMIDE ADHESIVES
Donald J. Progar and Terry L. St.Clair Jul. 1988 31 p
(NASA-TM-100631; NAS 1.15:100631) Avail: NTIS HC A03/MF A01 CSCL 11C

Continuing research at Langley Research Center on the synthesis and development of new inexpensive flexible aromatic polyimides as adhesives has resulted in a material identified as LARC-F-SO2 with similarities to polyimidesulfone, PISO2, and other flexible backbone polyimides recently reported by Progar and St. Clair. Also prepared and evaluated was an endcapped version of PISO2. These two polymers were compared with LARC-TPI and LARC-STPI, polyimides research in our laboratory and reported in the literature. The adhesive evaluation, primarily based on lap shear strength (LSS) tests at RT, 177 C and 204 C, involved preparing adhesive tapes, conducting bonding studies and exposing lap shear specimens to 204 C air for up to 1000 hrs and to a 72-hour water boil. The type of adhesive failure as well as the Tg was determined for the fractured specimens. The results indicate that LARC-TPI provides the highest LSSs. LARC-F-SO2, LARC-TPI and LARC-STPI all retain their strengths after thermal exposure for 1000 hrs and PISO2 retains greater than 80 percent of its control strengths. After a 72-hr water boil exposure, most of the four adhesive systems showed reduced strengths for all test temperatures although still retaining a high percentage of their original strength (greater than 60 percent) except for one case. The predominant failure type was cohesive with no significant change in the Tgs. Author

N89-27002# Argonne National Lab., IL. Energy and Environmental Systems Div.
FUTURE APPLICATIONS OF ENGINE CERAMICS: FACTORS INFLUENCING MARKET OPPORTUNITIES, TIMING, AND GROWTH
Robert P. Larsen 1989 5 p Presented at the Ceramtec '89, Dearborn, MI, 30 Jan. 1989
(Contract W-31-109-eng-38)
(DE89-012426; CONF-890108-1) Avail: NTIS HC A02/MF A01

Since 1986, the Center for Transportation Research (CTR) at Argonne National Laboratory has conducted market-based research focusing on the use of ceramics in heat engines for transportation applications. The purpose of my presentation is to share some of the insights we have gained over the past several years and some of the techniques we have found useful in making projections for engine ceramics. For these studies, which are funded by the U.S. Department of Energy, we developed a modeling technique that is useful in examining different scenarios for the timing and growth of the market for engine ceramics. I want to make you aware of these models and how to interpret them and use their results and other information from our research for decisions in your organizations. The data used in developing the models were gathered in a comprehensive worldwide Delphi survey designed to determine when ceramic engine components and ceramic intensive engines would become available in the United States. Information was also gathered on the rate of market growth for engine ceramics, incentives and barriers to their use, and the status of international competition for the worldwide engine ceramics market. DOE

N89-27003# Argonne National Lab., IL. Materials and Components Technology Div.
DEVELOPMENT OF MAGNETIC RESONANCE IMAGING TECHNOLOGY FOR IMAGING BINDER DISTRIBUTION IN CERAMICS
W. A. Ellingson, P. S. Wong, J. L. Ackerman, H. C. Yeh, and J. P. Pollinger (Allied-Signal Aerospace Co., Torrance, CA.) Dec. 1988 15 p Presented at the 26th Automotive Technology Development Contractors' Coordination Meeting, Dearborn, MI, 24-27 Oct. 1988
(Contract W-31-109-eng-38)
(DE89-013185; CONF-8810290-2) Avail: NTIS HC A03/MF A01

Nuclear Magnetic Resonance (NMR) Technology is being developed as a method to characterize the distribution of organic binder/plasticizers in injection molded ceramics. Garrett Ceramic Component Divisions GN-10 Si3N4 is the material being studied. Binder loadings studied varied from 2 to 20 wt percent. NMR spectroscopy data showed that NMR signals correlate to binder content. However, imaging data show that there is a peak value at 15.5 wt percent. NMR relaxation phenomenon, e.g., T2, does not vary with magnetic field strength, but does vary with temperature. For the present text setup, i.e., a 2T system with 3G/cm gradient, there is a limit of about 1-mm in spatial resolution. Higher gradients and changes in data acquisition techniques will significantly improve this limit. DOE

N89-27004# Pennsylvania State Univ., University Park. Center for Advanced Materials.
CORROSION OF CERAMIC MATERIALS WORKSHOP HELD NOVEMBER 12-13, 1987, PENNSYLVANIA STATE UNIVERSITY, UNIVERSITY PARK, PENNSYLVANIA
B. K. Kennedy, ed. Sep. 1988 482 p Proceedings of workshop held in University Park, PA, 12-13 Nov. 1987
(Contract GRI-5084-238-1302)
(PB89-175343; CAM-8809; GRI-88/0356) Avail: NTIS HC A21/MF A01 CSCL 11C

The Center for Advanced Materials held a workshop on the in-service corrosion and degradation of ceramic materials. The status of experimental and theoretical work on the corrosion of ceramics in energy systems was assessed, directions for future research were suggested, and appropriate formats for compiling and disseminating corrosion information were recommended. Copies of the technical presentation materials are included. GRA

N89-27005# National Inst. of Standards and Technology, Gaithersburg, MD. Ceramics Div.
ADVANCED CERAMICS: A CRITICAL ASSESSMENT OF WEAR AND LUBRICATION Topical Report, Jun. - Oct. 1986
R. G. Munro and S. M. Hsu Jan. 1989 109 p Sponsored in part by Pennsylvania State Univ., University Park
(Contract GRI-5084-238-1302)
(PB89-188569; NISTIR-88/3722; GRI-88/0290; CAM-8901)
Avail: NTIS HC A06/MF A01 CSCL 11C

A critical assessment of the state of the art of the tribology of ceramics is made. To identify the critical technical barriers confronting the utilization of advanced gas-fired engines, data were gathered specifically on the tribology of materials for gas-fired engine applications. Site visits and discussions with a number of

contractors in industry were conducted as the first step in identifying critical issues. Then, an extensive review of the technical literature was made to determine what information was available to resolve those issues, and, more importantly, what critical information was not yet available. These data were used to examine the issues for each of the principal engine types (rotary, reciprocating, and turbine). Materials property data for ceramics were then reviewed in the context of the operating environments and conditions for these engines. Thermal, mechanical, and tribological properties were examined, along with the important considerations for lubricating ceramics in engine applications. The analysis of these data considered the impact and relative merits of using various advanced materials and resulted in recommendations for research activities that could have a significant impact on the development of gas-fired prime movers. Author

N89-27006# Oak Ridge National Lab., TN.
FRACTOGRAPHIC STUDY OF A SILICON NITRIDE CERAMIC
M. K. Ferber and V. J. Tennery 1989 9 p Presented at the First European Ceramic Society Conference (ECerS-1), Maastricht, Netherlands, 19 Jun. 1989
(Contract DE-AC05-84OR-21400)
(DE89-013012; CONF-890653-1) Avail: NTIS HC A02/MF A01

A commercially available Si sub 3 N sub 4 ceramic was fractured in four-point flexure at room temperature as part of a round robin study involving 13 laboratories in the United States, Federal Republic of Germany, and Sweden. A minimum of 60 samples were fractured by each participant. For each specimen set tested, approximately 15 samples representing the five highest strength bars, the five lowest strength bars, and five bars nearest the mean of the strength distribution were chosen for fractographic examination. The nature, location, and size of the defects responsible for failure were determined. The resulting information was used to examine the applicability of strength-flaw size relationships. DOE

N89-27007# National Inst. of Standards and Technology, Gaithersburg, MD. Ceramics Div.
MECHANICAL PROPERTY ENHANCEMENT IN CERAMIC MATRIX COMPOSITES Interim Report, 1 Jan. 1988 - 31 Dec. 1988
S. W. Freiman, D. C. Cranmer, E. R. Fuller, Jr., W. Haller, M. J. Koczak, M. Barsoum, T. R. Palamides, and U. V. Deshmukh (Drexel Univ., Philadelphia, PA.) Apr. 1989 80 p
(Contract N00014-86-F-0096)
(PB89-189138; NISTIR-89/4073) Avail: NTIS HC A05/MF A01 CSCL 11B

The fiber-matrix interfacial properties of several glass and ceramic matrix composites were determined using two indentation techniques and a single fiber pull-out technique. An instrumented indenter was developed to improve the acquisition and analysis of the data. The effects of thermal expansion mismatch were determined from three model composite systems containing large SiC monofilaments using the single fiber pull-out test. An indentation push-out test was successfully used to determine the debond strength of a borosilicate matrix/SiC monofilament/carbon core material. A comparison of the various techniques for determining the fiber-matrix interfacial properties was conducted. GRA

N89-27008# Oak Ridge National Lab., TN.
STRUCTURAL CERAMICS IN THE ADVANCED MATERIALS WORLD
Douglas F. Craig 1989 12 p Presented at the Evolution of Advanced Materials, Milan, Italy, 31 May - 2 Jun. 1989
(Contract DE-AC05-84OR-21400)
(DE89-013046; CONF-890541-1) Avail: NTIS HC A03/MF A01

In the last sixty years, significant changes have occurred which have made ceramics attractive for a variety of complex and sophisticated applications. As higher values of strength and fracture toughness have been achieved, these advanced ceramics are being used or considered in high temperature, load bearing applications. The status of these ceramics is reviewed, with emphasis on methods to increase toughness. DOE

N89-27009# Sandia National Labs., Albuquerque, NM. Metallurgical Process Div.
A METHOD OF REMOVING OXIDES FROM THE SURFACE OF Fe-Ni-Co ALLOY PARTICLES BY CHEMICAL ETCHING
W. Graham Yelton Apr. 1989 23 p
(Contract DE-AC04-76DP-00789)
(DE89-014597; SAND-87-1249) Avail: NTIS HC A03/MF A01

The addition of metal particles to bulk glass has been shown to increase fracture strength and toughness. Composites containing well-bonded particles exhibit the largest increases in these properties. This report discusses a study in which a method was developed to alter the surfaces of Fe-Ni-Co particles so that improved particle/glass matrix bonding resulted. In this method, as received Fe-Ni-Co particles were intentionally oxidized to create surface and grain boundary oxides. The surface and grain boundary oxides were then preferentially removed from the surfaces of iron-nickel-cobalt alloy particles by chemical etching. After removal of the surface oxides, coral-like structures remained on the surfaces of the metal particles and furnished good mechanical bonding sites to the glass matrix. The progression of this study involved completion of three designed experiments. In the first experiment, an etching process was identified by controlling etching solution temperature and hold time. Data from the first study were then incorporated into the design of a second experiment which examined solution temperature heating rate and hold time at 60 C. Finally, the best conditions of the previous studies were selected to investigate the effects of the agitation rate of the etching solution on the particle yield. Combining the best conditions from each study yielded the most efficient method of removing oxides, in which a solution of 120 ml/l H3PO4 and 50 ml/l HCl was heated at 1 C/min to 60 C, held at 60 C, and then moderately agitated for 30 min. DOE

N89-27010 National Physical Lab., Teddington (England). Div. of Materials Applications.
DYNAMIC MECHANICAL INVESTIGATIONS OF LLDPE/PC BLENDS
B. E. Read Apr. 1989 23 p
(NPL-DMA(A)-177; ISSN-0143-7313; ETN-89-94965) Copyright Avail: National Physical Laboratory, Teddington, Middlesex, TW11 OLW, United Kingdom

Tensile storage moduli (E') and loss factors were determined as a function of temperature at a frequency of 1 Hz for blends of linear low-density polyethylene (LLDPE) and polycarbonate (PC). Moduli obtained from dynamic tensile tests required length corrections up to 10 percent for clamping errors. Corrections of 22 percent for shear deformation and 30 percent for clamping effects were required to the E' values obtained from dynamic flexural tests on short, thick specimens. Loss peaks for the blends were located at temperatures close to those observed for the constituent homopolymers, as expected for immiscible two-phase systems. Anisotropic two-phase structures, consistent with morphological studies, were also reflected in the values of a reinforcement parameter derived from an analysis of the E' data in terms of theories for composite materials. ESA

N89-27011# Harvard Univ., Cambridge, MA. Dept. of Chemistry.
THE STRUCTURE AND REACTIVITY OF ALKYLSILOXANE MONOLAYERS FORMED BY REACTION OF ALKYLTRICHLOROSILANES ON SILICON SUBSTRATES Interim Technical Report No. 17
Stephen R. Wasserman, Yu-Tai Tao, and George M. Whitesides May 1989 120 p Submitted for publication
(Contract N00014-85-K-0898; NR Proj. 356-856)
(AD-A208267; TR-17) Avail: NTIS HC A06/MF A01 CSCL 07/4

Long-chain alkyltrichlorosilanes, Cl3Si(CH2)nX, adsorb from solution onto silicon-silicon dioxide (Si/SiO2) substrates and form ordered alkylsiloxane monolayer films. These films were characterized by wettability, ellipsometry, and X-ray photoelectron spectroscopy (XPS). Except for very short chains (n = 0,1,2), the wetting of these monolayers was approximately independent of

chain length. The presence of small amounts of water was necessary for the formation of these films. The alkylsiloxane monolayers were stable in common organic solvents, water, and acid, but were destroyed by prolonged exposure to base. Simple reactions on vinyl-terminated monolayers generated alcohol-, carboxylic acid-, and bromine-terminated films whose contact angles were lower than the starting monolayers, but whose lengths were largely unchanged. Measurements of the contact angle of acid-terminated interfaces as a function of pH indicated that ionization of the surface-immobilized acids required stronger base than does ionization of soluble carboxylic acids. Monolayers containing mixtures of methyl- and carboxyl-functionalities exhibited wetting properties that mirrored the composition of the interface. GRA

N89-27012# Rensselaer Polytechnic Inst., Troy, NY. Dept. of Chemistry.
CHEMICAL VAPOR DEPOSITION OF SILICON CARBIDE USING A NOVEL ORGANOMETALLIC PRECURSOR
Wei Lee, Leonard V. Interrante, Corrina Czekaj, John Hudson, and Klaus Lenz 15 May 1989 9 p
(Contract N00014-85-K-0632)
(AD-A208273; RPI/DC-TR-5) Avail: NTIS HC A02/MF A01 CSCL 07/3

Dense silicon carbide films have been prepared by low pressure chemical vapor deposition (LPCVD) using a volatile, heterocyclic, carbosilane precursor. At deposition temperatures between 700 and 800 C, polycrystalline, stoichiometric SiC films have been deposited on single crystal silicon and fused silica substrates. Optical microscopy and SEM analyses indicated formation of a transparent yellow film with a uniform, featureless surface and good adherence to the Si(111) substrate. The results of preliminary studies of the nature of the gaseous by-products of the CVD processes and ultrahigh vacuum physisorption and decomposition of the precursor on Si(100) substrates are discussed. GRA

N89-27013# Pittsburgh Univ., PA. Dept. of Materials Science and Engineering.
SYNTHESIS, CHARACTERIZATION AND PHYSICAL PROPERTIES OF POLYPHOSPHAZENES Final Report
J. H. Magill 1989 15 p
(Contract N00014-85-K-0358)
(AD-A208296) Avail: NTIS HC A03/MF A01 CSCL 07/6

This report summarizes work carried out on the subject of synthesis, characterization and physical properties of polyphosphazenes. The investigation was comprised of three parts namely: (1) synthesis of polyphosphazenes, (2) characterization, and (3) investigation of physical properties. GRA

N89-27014# Case Western Reserve Univ., Cleveland, OH. Dept. of Chemistry.
SYNTHESIS AND STRUCTURAL CHARACTERIZATION OF Pt-Si DIMERS WITH UNUSUALLY SHORT CROSS-RING SILICON-SILICON INTERACTIONS Technical Report No. 1
Eugene A. Zarate, Claire A. Tessier-Youngs, and Wiley J. Youngs 5 May 1989 5 p Repr. from Journal of the American Chemical Society, 1988
(Contract N00014-86-K-0640)
(AD-A208310) Avail: NTIS HC A02/MF A01 CSCL 07/3

Polysilanes have use in applications where photosensitivity is required and as precursors to beta-SiC. Polysilanes are usually prepared from dichloroorganosilanes and sodium at approx. 100 C. Several reports of transition metal catalyzed formation of polysilanes from R2SiH2 and RSiH3 have appeared in which product distributions have been the main focus. Herein we report the synthesis and structural characterization of a series of platinum-silyl dimers with unusually short cross-ring Si-Si distances. These dimers are catalysts or catalyst precursors in silane oligomerization reactions. GRA

N89-27015# Massachusetts Inst. of Tech., Cambridge. Dept. of Chemistry.
NON-POLYMERIC BINDERS FOR CERAMIC POWDERS: UTILIZATION OF NEUTRAL AND IONIC SPECIES DERIVED FROM DECABORANE(14)
William S. Rees, Jr. and Dietmar Seyferth 13 May 1989 19 p
(Contract N00014-82-K-0322)
(AD-A208338; TR-30) Avail: NTIS HC A03/MF A01 CSCL 07/2

The pyrolytic conversion of bis-Lewis base adducts of decaborane(14), L.B sub 10 H sub 12.L (L= neutral monophosphine) and phosphonium salts of the (B sub 10 H sug 10)2- anion (e.g., (Ph sub 4 P sub (+)2, etc.), to ceramic materials was studied. All species examined served as binders for a variety of non-oxide refractory ceramic powders (e.g., B sub 4 C, BN, BP, B sub 13 P sub 2, SiC, Si sub 3 N sub 4, B, C, AlN). GRA

N89-27016# Harvard Univ., Cambridge, MA. Dept. of Chemistry.
THE STRUCTURE OF SELF-ASSEMBLED MONOLAYERS OF ALKYLSILOXANES ON SILICON: A COMPARISON OF RESULTS FROM ELLIPSOMETRY AND LOW-ANGLE X-RAY REFLECTIVITY Interim Report
Stephen R. Wasserman, George M. Whitesides, I. M. Tidswell, B. M. Ocko, Peter S. Pershan, and J. D. Axe (Brookhaven National Lab., Upton, NY.) May 1989 91 p Prepared for DARPA, Arlington, VA; and Dept. of Navy, Arlington, VA Submitted for publication
(Contract N00014-85-K-0898)
(AD-A208341; TR-15) Avail: NTIS HC A05/MF A01 CSCL 07/3

The thicknesses of alkylsiloxane monolayers on silicon-silicon dioxide substrates were measured using ellipsometry and low angle X-ray reflection. Thicknesses measured by the two methods differ by 2.2 A (rms) for alkyl chains of 10 to 18 carbon atoms have a maximum difference of 4.2 A. Ellipsometry systematically yields a larger thickness. This discrepancy may result from differences between the two techniques in their sensitivity to the structure of the interface between silicon dioxide and the alkylsiloxane monolayer. The X-ray reflectivity measurements provide evidence that these organic monolayers do not build up as island structures and demonstrate that the approximate area projected by each alkyl group in the plane of the monolayer is approx. 20 + or - 4 A2. GRA

N89-27017# Rensselaer Polytechnic Inst., Troy, NY. Dept. of Chemistry.
BLENDS OF POLY(ENAMINONITRILES)
J. A. Moore and Ji-Heung Kim Jun. 1989 10 p Submitted for publication
(Contract N00014-85-K-0632)
(AD-A208441; TR-16) Avail: NTIS HC A02/MF A01 CSCL 07/6

Poly(enaminonitriles) contain structural elements which have sufficient hydrogen bonding capability that these polymers can form compatible blends by solution casting with polymers such as poly ethylene oxide, partially miscible, poly ethyl oxazoline and poly 4-vinyl pyridine miscible over the whole concentration range. The properties of these membranes are described and their potential use as separation membranes is considered. GRA

N89-27018# University of Southern Mississippi, Hattiesburg. Dept. of Polymer Science.
PHOTODEGRADATION OF POLYIMIDES 2. THERMAL PROPERTY CHANGES OF POLYIMIDES BASED ON A PERFLUORINATED DIANHYDRIDE Technical Report, No. 2, 1 Jun. 1988 - 31 May 1989
C. E. Hoyle and E. T. Anzures 31 May 1989 22 p Submitted for publication
(Contract N00014-89-J-1028)
(AD-A208447) Avail: NTIS HC A02/MF A01 CSCL 07/6

Polyimides based on a perfluorinated dianhydride decrease in thermal and thermal oxidative stability upon photolysis with an

unfiltered medium pressure mercury lamp source. Additionally, the glass transition of photolyzed of polyimides containing the perfluorinated moiety is lowered with increasing photolysis time. By contrast, pyromellitic dianhydride polymers are relatively thermally stable even after prolonged photolysis under similar conditions. GRA

N89-27019# University of Southern Mississippi, Hattiesburg. Dept. of Polymer Science.
NATURAL ABUNDANCE 15N CP/MAS NMR OF SOLID POLYAMIDES: A SENSITIVE TECHNIQUE FOR EXAMINING CRYSTALLINE COMPOSITION AND CONFORMATION IN THE SOLID STATE Technical Report, 1 Jun. 1988 - 31 May 1989
Douglas G. Powell, Allison M. Sikes, and Lon J. Mathias 31 May 1989 28 p Submitted for publication
(Contract N00014-89-J-1225)
(AD-A208563; TR-24) Avail: NTIS HC A03/MF A01 CSCL 07/6

High resolution solid state 15N NMR of several AB and AA-BB polyamides were obtained at the nitrogen natural abundance level. Resonances at 84 and 89 ppm (relative to solid glycine) clearly delineate alpha and gamma crystal forms, respectively. In addition, intermediate resonances are seen which have not been identified by X-ray or IR. These resonances are thought to belong to rigid noncrystalline or amorphous regions in these semicrystalline polymer samples. Amorphous nylons have also been examined using this technique and found to have a broad envelope of resonances indicative of random conformations of amide groups. The origin of the chemical shift difference is rationalized in terms of chain conformation about the plane of the amide group. Semi-empirical MO calculations of model amides show electron density variations which correlate with the shielding and deshielding of the nitrogen atom consistent with this interpretation. Based on these results, 15N solid state NMR is found to be a sensitive technique for examining local conformations in solid polyamides. GRA

N89-27020# Missouri Univ., Rolla. Dept. of Chemistry.
DYNAMICS OF SURFACE BOUND POLYMERS AND COUPLING AGENTS Interim Report, 1 Nov. 1987 - 15 Jul. 1988
Frank D. Blum, Robert B. Funchess, and Wiriya Meesiri 15 Jul. 1988 18 p
(Contract N00014-88-K-0109)
(AD-A208747; UMR-FDB-5) Avail: NTIS HC A03/MF A01 CSCL 07/6

A review of recent work on the dynamics of polymers and coupling agents on solid surfaces is made. The primary results show how molecular motion of polymers affects the carbon 13 NMR cross polarization magic angle spinning spectra. For poly (isopropyl acrylate) it is found that one can actually obtain better spectra from surface bound materials. The synthesis of deuterated amino-propylsilane is also described and the effect of water on the deuterium NMR spectrum shown. GRA

N89-27021# Massachusetts Inst. of Tech., Cambridge. Dept. of Materials Science and Engineering.
SYNTHESIS AND OPTICAL PROPERTIES OF A NEW CLASS OF POLYAMIDES CONTAINING REACTIVE DIACETYLENE GROUPS Technical Report No. 3, Jun. 1988 - Jun. 1989
H. W. Beckham and M. F. Rubner 31 May 1989 39 p
(Contract N00014-88-K-0144)
(AD-A208752) Avail: NTIS HC A03/MF A01 CSCL 07/6

New polyamides containing reactive diacetylene groups in their repeat structures were synthesized from a diacetylene diacid chloride and two different diamines using interfacial polymerization techniques. Thermal analysis and carbon 13 NMR spectroscopy were used to estimate the extent of conversion of the diacetylene groups to polydiacetylene network chains upon exposure to electron beam radiation in the solid state. The diacetylene groups contained in a polyamide based on an aliphatic diamine were found to be more reactable than those incorporated in a polyamide based on an aromatic diamine. The cross-polymerized polyamide-diacetylenes were found to exhibit reversible thermochromic behavior during temperature cycling which occurs with complete retention of hydrogen bonds and without any hysteresis effects. The thermochromic reversibility of these materials was attributed to the strongly hydrogen bonded chain segments pendent to the newly formed polydiacetylene chains. GRA

N89-27022# Massachusetts Inst. of Tech., Cambridge. Dept. of Materials Science and Engineering.
THERMAL AND MECHANICAL PROPERTIES OF POLYURETHANE-DIACETYLENE SEGMENTED COPOLYMERS. PART 1: MOLECULAR WEIGHT AND ANNEALING EFFECTS Technical Report No. 1, Jun. 1988 - Jun. 1989
Renu N. Agrawal and M. F. Rubner 31 May 1989 48 p
(Contract N00014-88-K-0144)
(AD-A208753) Avail: NTIS HC A03/MF A01 CSCL 07/6

The thermal transitions and mechanical properties of a number of segmented polyurethanes containing diacetylene groups within their hard segments were evaluated. The ultimate tensile properties of these materials were found to be strongly dependent on their overall molecular weight and thermal history. In all cases, increased molecular weight resulted in improved mechanical properties. Annealing treatments were also found to dramatically improve the mechanical properties of these elastomers. Thermal analysis revealed that annealing increased the cohesive forces of the hard domains thereby increasing their mechanical integrity. The effect that annealing had on the mechanical behavior was found to be highly dependent on the particular mechanisms of deformation active in these segmented copolymers. Two distinctly different modes of deformation were observed in the polyurethane-diacetylene elastomers. GRA

N89-27023# Massachusetts Inst. of Tech., Cambridge. Dept. of Materials Science and Engineering.
THERMAL AND MECHANICAL PROPERTIES OF POLYURETHANE-DIACETYLENE SEGMENTED COPOLYMERS. PART 2: EFFECTS OF DIACETYLENE CROSS-POLYMERIZATION Technical Report No. 2, Jun. 1988 - Jun. 1989
Renu N. Agrawal and M. F. Rubner 31 May 1989 36 p
(Contract N00014-88-K-0144)
(AD-A208754) Avail: NTIS HC A03/MF A01 CSCL 07/6

Selective crosslinking of the hard domains of segmented polyurethanes via the radiation induced solid state reaction of diacetylene groups was utilized to ascertain the influence of hard domain cohesion and rigidity on the mechanical properties of these materials. The rigidity and mechanical integrity of the hard segment domains was found to play an extremely important role in determining their mechanical behavior. The specific influence exerted by the hard domains was found to be strongly dependent on molecular weight, the level and type of hard segment ordering, and the microstructure of the material. In all cases, the effect of diacetylene cross-polymerizations was to increase the modulus and decrease the ultimate tensile strain. The ultimate tensile strength was found to initially increase, reach a maximum, and eventually decrease upon exposure to high energy electrons. Disruption and reorganization of the hard domain system at high stress levels was verified as an important strengthening mechanism in segmented polyurethanes. GRA

28 PROPELLANTS AND FUELS

Includes rocket propellants, igniters, and oxidizers; their storage and handling procedures; and aircraft fuels.

For related information see also *07 Aircraft Propulsion and Power, 20 Spacecraft Propulsion and Power,* and *44 Energy Production and Conversion.*

N89-27024# Army Missile Command, Redstone Arsenal, AL. Research Directorate.
SELECTIVE NITRATIONS: LASER-INDUCED NITRATIONS Technical Report, period ending Jun. 1988
A. E. Stanley and S. E. Godbey Jan. 1989 45 p
(AD-A207406; AD-E951322; AMSMI/TR-RD-RE-88-6) Avail: NTIS HC A03/MF A01 CSCL 07/5

The Army uses nitrated compounds as explosives and propellants. There is a special need for propellants with the chemical composition necessary to burn exactly with a minimum of side products which create smoke, but with high energy production. An important part of this process is the ability to selectively nitrate materials. Laser-induced chemistry possesses the potential to drive some reactions in an efficient and selective manner. Laser-induced chemistry may be useful in driving nitration reactions toward specific products. Reported herein are the results of several successful attempts to laser-induce the reaction of nitrogen dioxide with hydrocarbons of 3, 4 and 5 carbons. Specifically, the tunable continuous wave infrared laser was used to drive the reaction between nitrogen dioxide, and propane, n-butane, isobutane, and n-pentane. The major products of the reactions were secondary (tertiary in the isobutane reaction) nitro-hydro carbons, of the same chain length as the reacting hydrocarbon. Some short chain nitrated compounds were also identified. The yield of acting hydrocarbon. Some short chain nitrated compounds were also identified. The yield of 2-nitro-butane observed in the nitration of butane is approximately 20 percent based on the depletion of nitrogen dioxide. Author (GRA)

N89-27025# Army Missile Command, Redstone Arsenal, AL. Systems Simulation and Development Directorate.
APPLICATION OF CRYSTAL LATTICE DISINTEGRATION CRITERIA TO COMPUTE MINIMUM SHOCK INDUCED REACTIVE CONDITIONS IN SOLID EXPLOSIVES AND INERT MATERIALS Final Technical Report, Aug. 1987 - Aug. 1988
James P. Billingsley and Carl L. Adams Mar. 1989 34 p
(AD-A207557; AD-E951334; AMSMI/TR-RD-SS-88-10) Avail: NTIS HC A03/MF A01 CSCL 19/1

A threshold particle velocity criteria for the beginning of crystal lattice breakup and disintegration has been applied to shocked explosives and an inert material. In shocked explosives, reactions leading to detonation occur above a certain threshold magnitude. The computed crystal lattice breakup shock pressures compare rather well with observed experimental threshold shock pressures for six high explosives. The six explosives are: Comp-B3, Comp-B, TNT, PBX-9404, Tetryl, and H-6. In addition, the crystal lattice breakup criteria provides an explanation for the observed lowering of the detonation threshold shock pressure as the explosives are made more porous or less dense. Finally, the shock pressures, at which output from thermocouples embedded in shocked materials (PBX-9404 and Plexiglass) increases dramatically, compare favorably with predictions based on crystal lattice disintegration criteria. Consequently, it is tentatively concluded that crystal lattice breakup, or self-sustained phonon fission, is responsible for the initiation of detonation in shocked explosives and enhanced thermocouple output in shocked materials. Several recommendations for future work are given. GHA

N89-27026 Department of the Air Force, Washington, DC.
PROCESS FOR ASSESSING THE EFFECT OF PROPELLANT STRAIN ON PROPELLANT BURN RATE Patent
Gary N. Bonadies, inventor (to AF), Mark OClair, inventor (to AF), and David W. Parry, inventor (to AF) 28 Mar. 1989 4 p Filed 13 Oct. 1987
(AD-D014119; US-Patent-4,815,315; US-Patent-Appl-SN-107184; US-Patent-Class-73-35) Avail: US Patent and Trademark Office CSCL 21/9

The present invention describes a process for relating burn rate in a sample propellant to a strain field imposed therein by bending the sample propellant by a determined amount. The propellant is cast upon an initially flat plate having a single pair of fixed parallel walls. The plate is bent parallel to the walls before the test burn. Measurement of thickness of the propellant before the burn and after the burn are related to the strain placed in the propellant by the bending. All measurements occur when the plate is flat. GRA

N89-27027# Lawrence Livermore National Lab., CA.
THIN PULSE SHOCK INITIATION CHARACTERIZATION OF EXTRUSION-CAST EXPLOSIVES: REVISION
George Bloom, Ronald Lee, and William VonHolle 1989 10 p Presented at the 3rd International Symposium on Behavior of Media under High Dynamic Pressures, La Grande Motte, France, 5-9 Jun. 1989 Revised
(Contract W-7405-eng-48)
(DE89-008029; UCRL-98864-Rev; CONF-890661-6-Rev) Avail: NTIS HC A02/MF A01

An electric gun was used to measure detonation thresholds of two voidless HMX-based extrusion-cast explosives (ECX) for various pulse widths and flyer diameters. Thin-pulse shock-initiation thresholds were measured using a 56 microF, 40-kV capacitor bank to explode aluminum foils that drive polyester (Mylar) or polycarbonate (Lexan) flyers of various thicknesses and diameters. The results were compared with those for the HMX-based PBX-9404, which contains 2 percent voids. For various pulse widths the ECXs are less sensitive, particularly for longer pulse lengths. The ECXs are less sensitive for larger flyer diameters and the same sensitivity for the smallest diameter flyers. DOE

N89-27028# Delaware Univ., Newark. Dept. of Chemical Engineering.
MODIFIERS IN RHODIUM CATALYSTS FOR CARBON MONOXIDE HYDROGENATION: STRUCTURE-ACTIVITY RELATIONSHIPS Ph.D. Thesis
Nazeer Ahmed Bhore May 1989 424 p
(Contract DE-FG22-84PC-70780)
(DE89-013802; DOE/PC-70780/T10) Avail: NTIS HC A18/MF A01

This report is aimed at identifying interesting modified rhodium systems and elucidating structure-activity relationships in these systems with the overall goal of understanding the scientific issues in the catalytic conversion of syngas to oxygenates. Specific additives (sodium and molybdenum) are selected based on the scoping experiments. The effect of the additives on supported rhodium catalysts is then investigated. Throughout the investigation, experiments and analysis were performed on real systems instead of ideal systems. DOE

N89-27029# Oak Ridge National Lab., TN.
EXPLOSIVES DETECTION WITH AN ION TRAP MASS SPECTROMETER
Scott A. McLuckey, Gary L. Glish, and Barry C. Grant 1989 18 p Presented at the 3rd International Symposium on Analysis and Detection of Explosives, Mannheim, (Federal Republic of Germany), 10 Jul. 1989
(Contract DE-AC05-84OR-21400)
(DE89-012510; CONF-890769-2) Avail: NTIS HC A03

The combination of atmospheric sampling glow discharge ionization with mass spectrometry/mass spectrometry provides a powerful approach to the detection of trace quantities of explosives in air. The ion source is operated in such a way as to make it relatively immune to ionization interferences. False alarms are minimized by mass spectrometry/mass spectrometry, which has orders of magnitude greater informing power than other analyzers used in explosives detection. The ion trap mass spectrometer is a promising new device for mass spectrometry/mass spectrometry. A glow discharge ion source has been coupled to an ion trap. Even in its early stage of development it has proved superior to

devices that employ more conventional approaches to mass spectrometry/mass spectrometry. Improvements in ion injection into the ion trap, however, are desirable (and are likely). DOE

N89-27030# Sandia National Labs., Albuquerque, NM.
TECHNIQUES FOR THE DETECTION OF EXPLOSIVES
1989 5 p Presented at the 3rd International Symposium on Analysis and Detection of Explosives, Mannheim, Federal (Republic of Germany), 10 Jul. 1989
(Contract DE-AC04-76DP-00789)
(DE89-012570; SAND-89-0677C; CONF-890769-3) Avail: NTIS HC A02/MF A01

Novel methods/techniques for the detection of explosives are briefly described. The methods include vapor detection, preconcentrators, chemiluminescence detectors and microwave detectors. DOE

N89-27031# Sandia National Labs., Albuquerque, NM. Explosive Projects and Diagnostic Div.
CHARACTERIZATION OF MORTON-THIOKOL BOOSTER-ROCKET PROPELLANT TP-H1207C AND ITS SIMULANT H-19
L. J. Weirick and D. W. Dugan May 1989 48 p
(Contract DE-AC04-76DP-00789)
(DE89-013347; SAND-88-0930) Avail: NTIS HC A03/MF A01

A series of experiments on a propellant and its simulant have recently been completed on a light-gas gun. The intent of this work is to characterize the shock sensitivity of booster-rocket propellants and their simulants. The initial objectives are to obtain Hugoniot data, to investigate the pressure threshold at which a reaction occurs, and to measure spall damage at various impact velocities. The Hugoniot data obtained for the propellant fits the Hugoniot curve provided by the manufacturer of the propellant extremely well. The Hugoniot curve developed for the simulant was found to match that of the propellant very well. The density, initial bulk sound velocity, and empirical parameter S values for the composite propellant, TP-H1207C, are 1.84 g/cu cm, 2.3 mm/ms, and 2.16, respectively; for its simulant, H-19, they are 1.89 g/cu cm, 2.25 mm/ms, and 1.5, respectively. The ignition threshold pressure of the TP-H1207C was found to be in the range of 40 kbar. Violent reactions were observed at impact pressures of 50 kbar. The propellant exhibited spall strengths around 0.25 kbar, with its simulant being somewhat weaker, 0.18 kbar. DOE

N89-27032# Pennsylvania State Univ., University Park. Coll. of Earth and Mineral Sciences.
THERMAL STABILITY OF JET FUEL Quarterly Report No. 2, Jan. - Mar. 1989
Semih Eser, Janice Perison, Ronald M. Copenhaver, and Harold H. Schobert 1989 71 p
(Contract DE-AC22-88PC-88827)
(DE89-013516; DOE/PC-88827/T2) Avail: NTIS HC A04/MF A01

Six model compounds have been heat treated in nitrogen and air atmospheres at temperatures between 250 and 450 C for 1 to 4 hours. The treatments were carried out in microautoclave reactors according to the procedure outlined in the previous reports. The thermal treatments in air were carried out under 100 psig cold air pressure at 350 and 400 C. Some observations on the appearance of the reaction products are described. The reaction products from the thermal treatments in nitrogen have been analyzed by gas chromatography-mass spectroscopy (GC-MS). The results of these analyses are discussed. The NMR analysis of the reaction products from the treatments in air will be presented in the next report. DOE

N89-27033# California Univ., Berkeley. Dept. of Chemistry.
PRIMARY DISSOCIATION PROCESSES OF ENERGETIC COMPOUNDS Final Report, 22 Nov. 1981 - 21 Nov. 1988
Yuan T. Lee 21 Nov. 1988 29 p
(Contract N00014-83-K-0069)
(AD-A208312) Avail: NTIS HC A03/MF A01 CSCL 14/2

During the last contract period, we have successfully constructed a very sophisticated and highly sensitive molecular beam apparatus for the investigation of primary thermal and photon induced dissociation processes of polyatomic molecules under isolate conditions. This machine incorporates many new ideas and has been shown to be the best molecular beam apparatus for this purpose in the world. It has enabled us to carry out a series of investigations which are relevant to the decomposition of energetic compounds. The understanding of the dynamics of concerted unimolecular decomposition, the determination of the energetics of important radical species and the elucidation of the primary dissociation mechanisms of various nitro and nitramine compounds are three areas in which we have made important contributions. GRA

29 MATERIALS PROCESSING

Includes space-based development of products and processes for commercial applications.
For biological materials see *55 Space Biology*.

N89-27034*# National Academy of Sciences - National Research Council, Washington, DC. Commission on Engineering and Technical Systems.
INDUSTRIAL APPLICATIONS OF THE MICROGRAVITY ENVIRONMENT
1988 64 p
(Contract NASw-4154)
(NASA-CR-181516; NAS 1.26:181516; PB89-170559) Avail: NTIS HC A04/MF A01 CSCL 22A

Opportunities for commercialization of the microgravity environment will depend upon the success of basic research projects performed in space. Significant demands for manufacturing opportunities are unlikely in the near term. The microgravity environment is to be considered primarily as a tool for research and secondarily as a manufacturing site. This research tool is unique, valuable, and presently available to U.S. investigators only through resources provided by NASA. The United States has an obligation to facilitate corporate research, maintain a flexible international policy, foster use of and assure access to a wide variety of facilities, and develop a posture of national and international leadership in and stewardship of research and materials processing in the microgravity environment. The National Research Council's Committee on Industrial Applications of the Microgravity Environment recommends six actions that strengthen this posture, including the formation of an authoritative organization to oversee the implementation of a program of microgravity research and its industrial applications. GRA

N89-27035# Aerospatiale Aquitaine, Saint-Medard en Jalles (France). Div. Systemes Strategiques et Spatiaux.
LARGE PROTEIN CRYSTALLIZATION FACILITY, PHASE A. EXECUTIVE SUMMARY Final Report
Paris, France ESA 15 Feb. 1988 39 p
(Contract ESA-7004/86/F/FL(SC))
(AQ-ES-175/88; ESA-CR(P)-2714; ETN-89-94451) Copyright Avail: NTIS HC A03/MF A01

A multiuser spacelab experimental facility able to automatically grow large single protein crystals is proposed. A specific drawer processes 20 samples with dialysis techniques: concentration is individually controlled and the temperature regulated by group of five samples. Another drawer processes 24 samples with free interface technique with fixed concentration and with an individual control of the temperature. The last drawer also processes 24 samples with vapor phase techniques with fixed concentration and with an individual control of the temperature. A total of 68 samples can be processed with 3 different techniques in a temperature range of 4 to 20 C. During growth each sample is individually observed, using an individual CCD camera and associated imaging lenses and illumination. A dry and inert atmosphere is maintained inside the facility. The adequate accommodation of samples against mechanical and thermal disturbances is ensured all the mission

long. The generated heat is dissipated in air-loop and cooling liquid-loops. The facility converts unregulated Spacelab dc voltage into regulated one. A set of housekeeping data and video pictures are generated, displayed to the crew, and stored. These datas and pictures can be optionally downlinked. The facility also optionally accepts and executes telecommands (for parameters updating, selection of pictures, reconfiguration). ESA

31 ENGINEERING (GENERAL)

Includes vacuum technology; control engineering; display engineering; cryogenics; and fire prevention.

N89-27036# Wisconsin Univ., Madison.
LIQUID HELIUM FLUID DYNAMICS STUDIES
S. W. VanSciver 1989 7 p
(Contract DE-AC02-86ER-40306)
(DE89-013124; DOE/ER-40306/1) Avail: NTIS HC A02/MF A01

The main focus of the first three year period of this research program was to set up our liquid helium flow facility and begin experiments on the flow of liquid helium within this system. The first task of our experimental program involved the set up and check out of the Liquid Helium Flow Facility (LHFF). This facility is the centerpost of our fluid dynamics experiments. The LHFF is designed to allow a variety of experiments which test important helium fluid dynamics behavior on a scale close to that involved in large scale applications. To achieve this goal, we chose a horizontal dewar configuration with a cold bore access on either end. A nominal length of five meters was selected with a sufficiently large inner diameter to allow insertion of various tubing configurations, flow metering devices and heat exchangers. Further, to minimize consumption of liquid helium, the dewar design includes two actively cooled shields, one cooled by LN sub 2 to 77 K and one at 4.5 K maintained by a closed cycle helium refrigerator. Helium flow is to be provided by a cold centrifugal pump. DOE

N89-27037# Oak Ridge National Lab., TN. Energy Div.
REFRIGERATOR-FREEZER ENERGY TESTING WITH ALTERNATIVE REFRIGERANTS
E. A. Vineyard, J. R. Sand, and W. A. Miller 1989 14 p Presented at the ASHRAE Annual Meeting, Vancouver, Canada, 24-28 Jun. 1989
(Contract DE-AC05-84OR-21400)
(DE89-013543; CONF-890609-4) Avail: NTIS HC A03/MF A01

As a result of the Montreal Protocol that limits the production of ozone-depleting refrigerants, manufacturers are searching for alternatives to replace the R12 that is presently used in residential refrigerator-freezers. Before an alternative can be selected, several issues must be resolved. Among these are energy impacts, system compatibility, cost, and availability. In an effort to determine the energy impacts of some of the alternatives, energy consumption tests were performed in accordance with section 8 of the Association of Home Appliance Manufacturers (AHAM) standard for household refrigerators and household freezers. The results are presented for an 18 cubic foot (0.51 cubic meter), top-mount refrigerator-freezer with a static condenser using the following refrigerants: R12, R500, R12/Dimethyl-ether (DME), R22/R142b, and R134a. Conclusions from the AHAM test are that R500 and R12 /DME have a reduced energy consumption relative to R12 when replaced in the test unit with no modifications to the refrigeration system. Run times were slightly lower than R12 for both refrigerants indicating a higher capacity. While the R134a and R22/R142b results were less promising, changes to the refrigeration system, such as a different capillary tube or compressor, may improve performance. DOE

N89-27038*# National Aeronautics and Space Administration. Lewis Research Center, Cleveland, OH.
MEASUREMENTS OF COMPLEX PERMITTIVITY OF MICROWAVE SUBSTRATES IN THE 20 TO 300 K TEMPERATURE RANGE FROM 26.5 TO 40.0 GHz
Felix A. Miranda, William L. Gordon (Case Western Reserve Univ., Cleveland, OH.), Vernon O. Heinen, Ben T. Ebihara, and Kul B. Bhasin Jul. 1989 10 p Presented at the Cryogenic Engineering Conference, Los Angeles, CA, 24-28 Jul. 1989; sponsored in part by California Univ., Los Angeles
(NASA-TM-102123; E-4903; NAS 1.15:102123) Avail: NTIS HC A02/MF A01 CSCL 13B

A knowledge of the dielectric properties of microwave substrates at low temperatures is useful in the design of superconducting microwave circuits. Results are reported for a study of the complex permittivity of sapphire (Al2O3), magnesium oxide (MgO), silicon oxide (SiO2), lanthanum aluminate (LaAlO3), and zirconium oxide (ZrO2), in the 20 to 300 Kelvin temperature range, at frequencies from 26.5 to 40.0 GHz. The values of the real and imaginary parts of the complex permittivity were obtained from the scattering parameters, which were measured using a HP-8510 automatic network analyzer. For these measurements, the samples were mounted on the cold head of a helium gas closed cycle refrigerator, in a specially designed vacuum chamber. An arrangement of wave guides, with mica windows, was used to connect the cooling system to the network analyzer. A decrease in the value of the real part of the complex permittivity of these substrates, with decreasing temperature, was observed. For MgO and Al2O3, the decrease from room temperature to 20 K was of 7 and 15 percent, respectively. For LaAlO3, it decreased by 14 percent, for ZrO2 by 15 percent, and for SiO2 by 2 percent, in the above mentioned temperature range. Author

N89-27039*# National Aeronautics and Space Administration. Marshall Space Flight Center, Huntsville, AL.
A NEW STATE RECONSTRUCTOR FOR DIGITAL CONTROLS SYSTEMS USING WEIGHTED-AVERAGE MEASUREMENTS
Michael E. Polites Washington Aug. 1989 17 p
(NASA-TP-2936; M-615; NAS 1.60:2936) Avail: NTIS HC A03/MF A01 CSCL 09B

A state reconstructor is presented for a linear continuous-time plant driven by a zero-order-hold. It takes a continuous-time output vector from the plant and convolutes it with a weighting-function matrix whose elements are time dependent. This result is integrated over T second intervals to generate weighted-averaged measurements, every T seconds, that are used in the state reconstruction process. If the plant is noise-free and can be modeled precisely, the output of this state reconstructor exactly equals the true state of the plant and accomplishes this without knowledge of the plant's initial state. If noise or modeling errors are a problem, it can be catenated with a state observer or a Kalman filter for a synergistic effect. Author

N89-27040# National Inst. of Standards and Technology, Gaithersburg, MD.
QUALITY IN AUTOMATION PROJECT FOR FY 88 Progress Report
C. D. Lovett Apr. 1989 108 p Prepared in cooperation with Dept. of the Navy, Washington, DC; and DOE, Washington, DC
(PB89-193296; NISTIR-89/4045) Avail: NTIS HC A06/MF A01 CSCL 13B

A quality control architecture that uses real-time sensing, deterministic metrology methods, machine tool characterization, process-intermittent gauging, and process certification to control the machining process with the objective of reducing the reliance on traditional post-process inspections methods and moving toward greater reliance on in-process verification is discussed. The Quality In Automation project is developing a computer-based system that includes real-time sensors, a quality database, quality monitors, quality controllers, an inspection station, and a communication network which allows data to flow among components of the quality system. The quality architecture includes control loops such as post-processing characterization, pre-processing characterization, process intermittent gauging, and real-time sensing. The sensors for temperature, force and ultrasonic may result in a command signal to the machine tool controller to alter its pre-programmed positions, to change its manipulative variables (speed and feed),

and to modify the NC code. The corrective action will depend on the time varying nature of the errors and the predictions derived from the analysis models. Author

N89-27041# Massachusetts Inst. of Tech., Cambridge. Sea Grant Coll. Program.
AUTONOMOUS UNDERWATER SYSTEMS FOR SURVEY OPERATIONS
Norman Doelling, ed. and Elizabeth T. Gowell, ed. 3 Jun. 1987 89 p Sponsored by Naval Surface Weapons Center, White Oaks, MD
(Grant NOAA-NA86AA-D-SG089)
(PB89-187397; MITSG-89-4) Avail: NTIS HC A05/MF A01 CSCL 13B

An autonomous underwater vehicle (AUV) that can be released at sea, find a harbor, perform a task, and return to a designated location is highly desirable. The military applications of such a system are obvious. Mine clearing and mine laying come to mind. Other applications could include oceanographic surveys, mineral exploration, fish population studies, and underwater equipment repair. In 1987, the Naval Surface Weapons Center (NSWC) posed the development of such a vehicle as a research problem, and asked the NOAA Office of Sea Grant to recommend several Sea Grant Institutions with expertise in AUVs to investigate. MIT Sea Grant was invited to submit a proposal and was one of three Sea Grant Programs awarded a one-year grant by NSWC. The study developed a vehicle concept and outlined a plan of research necessary for its development. The findings of the MIT research team are summarized here. GRA

N89-27042# Rome Univ. (Italy). Dipartimento di Fisica.
PRODUCTION OF PURE OZONE BY MEANS OF ELECTRIC DISCHARGES FOR MEASURING ABSORPTION COEFFICIENTS [PRODUZIONE DI OZONO PURO CON OZONIZZATORE A SCARICA ELETTRICA PER MISURE DEI COEFFICIENTI D'ASSORBIMENTO]
Marco Cacciani and Alcide diSarra 16 May 1988 17 p In ITALIAN
(Nota-Interna-913; ETN-89-94732) Avail: NTIS HC A03/MF A01

Ozone production methods and the main chemical reaction on which the methods are based are studied. The procedures discussed include electrical discharges at room temperature and at cryogenic temperatures. Photochemical reactions at 185 to 254 nm wavelength and 140 to 170 nm wavelength, electrolysis, and thermal decomposition. The prototype described works at oxygen pressures between 900 and 130 Torr and 77 K. The ozone produced in liquid phase is very pure. The stability is low, with risks of explosion. ESA

32 COMMUNICATIONS AND RADAR

Includes radar; land and global communications; communications theory; and optical communications.

For related information see also *04 Aircraft Communications and Navigation* and *17 Space Communications, Spacecraft Communications, Command and Tracking.* For search and rescue see *03 Air Transportation and Safety,* and *16 Space Transportation.*

N89-27043# National Bureau of Standards, Boulder, CO. Center for Electronics and Electrical Engineering.
DEVELOPMENT OF NEAR-FIELD TEST PROCEDURES FOR COMMUNICATION SATELLITE ANTENNAS, PHASE 1, PART 2
Allen C. Newell Aug. 1988 83 p
(PB89-156152; NBSIR-87/3081-Pt-2) Avail: NTIS HC A05/MF A01 CSCL 20N

The purpose is to define and further develop the capabilities of near-field antenna test techniques, specifically for the requirements associated with the development and verification testing of reconfigurable, multibeam, frequency reuse, commercial satellite antennas. The focus is on the planar near-field measurement method and covers the determination of sampling criteria and scan limits, development of diagnostic and design assist methods, development of beam alignment techniques, development of swept-frequency equivalent tests, and specification of hardware requirements for the measurement system. The basis for the choice of the best measurement technique was established with the planar near-field measurement method receiving the best score for the directive antennas considered. GRA

N89-27044# Helsinki Univ. of Technology, Espoo (Finland). Electromagnetics Lab.
THE 14TH CONVENTION ON RADIO SCIENCE, FINNISH NATIONAL COMMITTEE OF URSI HELD IN OTANIEMI (FINLAND) ON OCTOBER 17-18, 1988: ABSTRACTS OF PAPERS
Ismo V. Lindell, ed. and Ari H. Sihvola, ed. Sep. 1988 95 p Convention held in Otaniemi, Finland, 17-18 Oct. 1988
(PB89-145767; Rept-32; ISBN-951-754-628-0) Avail: NTIS HC A05/MF A01 CSCL 17B

The present 14th Convention on Radio Science is one of the traditional reviews of progress made in Finland in the broad realm of Radio Science. Topics chosen with the number of papers submitted are the following: (1) Electromagnetics - 18 papers; (2) Metrology - 12 papers; (3) Space engineering - 11 papers; and (4) Integrated circuits - 39 papers. Together with two invited papers, the total number of submitted papers amounts to 82. In contrast to recent years, the present convention is not purely national, since contributions from the neighboring countries were included. GRA

N89-27045# Helsinki Univ. of Technology, Espoo (Finland). Electromagnetics Lab.
COMPLEX VECTORS AND DYADICS FOR ELECTROMAGNETISTS
Ismo V. Lindell Nov. 1988 55 p
(PB89-146443; ISSN-0784-848X; ISBN-951-754-706-4; Rept-36)
Avail: NTIS HC A04/MF A01 CSCL 20N

An exposition of complex vector and dyadic algebra applicable to electromagnetic field analysis is presented The material given in chapter 1 on complex vectors was essentially published in the International Journal on Electrical Engineering Education, vol. 20, 1983. The material in chapter 2 on dyadic algebra is based on the report no. S126/1981 in the series Helsinki University of Technology, Radio Laboratory Reports. Because the report is now out of print and the interest seems to continue, the present report was created while waiting for the above-mentioned book to realize itself, which may still take some time. GRA

N89-27046 Department of the Air Force, Washington, DC.
DUAL FREQUENCY MICROSTRIP ANTENNA Patent
Yuen T. Lo, inventor (to AF) and Boa F. Wang, inventor (to AF) 13 Sep. 1988 13 p Filed 30 Aug. 1985 Supersedes N86-25715 (24 - 16, p 2582)
(AD-D014019; US-Patent-4,771,291; US-Patent-Appl-SN-771529)
Avail: US Patent and Trademark Office CSCL 09/1

A single element patch microstrip antenna for dual frequency operation is disclosed. By placing shorting pins at appropriate locations in the patch, the ratio of two band frequencies can be varied from 3 to 1.8. By also introducing slots in the patch, the ratio can be reduced from 3 to less than 1.3. A second embodiment of the antenna uses a c-shaped slot to obtain an even smaller ratio of two band frequencies. GRA

N89-27047# Computer Technology Associates, Inc., McLean, VA.
EVALUATION OF LOW DATA RATE VOICE CODECS FOR AIR TRAFFIC CONTROL APPLICATIONS Technical Report, Apr. 1988 - May 1989
Joseph Child, Robert Cleve, and Mark Grable Jun. 1989 47 p
(Contract DTFA-03-86-C-00018)
(DOT/FAA/CT-TN89/13) Avail: NTIS HC A03/MF A01

The test objectives, methodologies, and results of prequalification testing and evaluation of various 4.8 and 2.4 kilo

bit per second (kbps) compression rate voice coder/decoders (CODECS) that are being considered for the use in supporting the Federal Aviation Administration's (FAA's) satellite communications technology demonstration program are discussed. The principal objectives of this program are to evaluate the performance of these CODECS for potential air traffic applications and to develop CODEC testing procedures tailored to the specific needs of air traffic control (ATC) communications. A description is given of the relative performance and ranking of the CODECS tested. This information has led to the selection of a quantity of 4.8 and 2.4 kbps CODECS for more comprehensive testing under simulated background noise and satellite channel noise conditions in the CODEC Test Bed Facility. Author

N89-27048 Department of the Air Force, Washington, DC.
WINDOW GENERATOR Patent
William K. Johnson, inventor (to AF) and Roger A. May, inventor (to AF) 21 Mar. 1989 10 p Filed 21 Oct. 1987
(AD-D014068; US-Patent-4,814,884; US-Patent-Appl-SN-110918; US-Patent-Class-358-183) Avail: US Patent and Trademark Office CSCL 17/11

The present invention relates generally to video target recognition systems and more specifically to a window generator which receives a field of video data and applies an identification code to rectangular subregions to identify distinct target areas within a given background area. The present invention comprises a window generator which provides a 6 bit target identification number for up to 63 target areas and one background area in a frame of serially scanned data. The window generator receives a field of video data from an image data source. This video data consists of digitized frames of serially scanned data similar to a conventional television screen image, which is divided horizontally in pixels, and vertically in lines. The window generator permits any given frame to be subdivided into specific rectangular subregions, which may be located anywhere on the video picture. By allowing statistics to be collected on the individual subregions (or target areas) the window generator permits local processing of video data within the specified target areas as opposed to processing of video data over the entire video field. One embodiment of the window generator is composed of: a microprocessor, a random access memory (RAM), a comparator, a line memory, two counters, an OR gate, a frame initialization circuit, and a buffer. These elements function as described below. GRA

N89-27049# Michigan Univ., Ann Arbor. Radiation Lab.
SYNTHESIS OF RESISTIVE TAPERS TO CONTROL SCATTERING PATTERNS OF STRIPS Final Technical Report, Jul. - Sep. 1987
Randy L. Haupt and Valdis V. Liepa Sep. 1988 173 p
(Contract F30602-81-C-0206)
(AD-A207211; RADC-TR-88-198) Avail: NTIS HC A08/MF A01 CSCL 17/9

This document outlines a technique for synthesizing a resistive taper that generates desired bistatic scattering and backscattering patterns from a strip. Antenna synthesis techniques relate the scattered field to the induced surface current density to get low sidelobes and nulls in the scattering patterns. Either physical optics or an integral equation approach relates the surface current density to the resistive taper. Numerical methods are used to analyze the errors in measuring a resistive taper on a sheet with the four point probe. The impact of the manufacturing and resistivity measurement errors on the low sidelobe scattering patterns is examined. Finally, experimental bistatic scattering patterns of a tapered resistive sheet and a metal plate are compared with theoretical predictions. GRA

N89-27050# North Carolina Univ., Chapel Hill. Dept. of Statistics.
SOME RESULTS ON NONGAUSSIAN SIGNAL DETECTION
C. R. Baker, Michael R. Frey, and A. F. Gualtierotti (Lausanne Univ., Switzerland) Mar. 1989 12 p
(Contracts N00014-86-K-0039; N00014-89-J-1175)
(AD-A207255; AD-E801886; LISS-31) Avail: NTIS HC A03/MF A01 CSCL 12/3

Recent results on detection of random nonGaussian signals in additive Gaussian noise are discussed. A discrete-time approximation to a likelihood ratio detection algorithm is discussed, and preliminary results are presented for a computational evaluation of the performance for this approximation. GRA

N89-27051# North Carolina Univ., Chapel Hill. Dept. of Statistics.
INFORMATION CAPACITY OF ADDITIVE GAUSSIAN CHANNELS WITH JAMMING
C. R. Baker and I. F. Chao (Soochow Univ., Taipei, Taiwan) Mar. 1989 11 p Presented at the Conference on Information and Systems Sciences, Baltimore, MD, 21-23 Mar. 1989 Submitted for publication
(Contract N00014-86-K-0039; NSF NCR-87-13726)
(AD-A207256; AD-E801886; LISS-32) Avail: NTIS HC A03/MF A01 CSCL 17/4

Information capacity is determined for the matched Gaussian channel when jamming is added to the ambient noise. The problem is modeled as a zero-sum two-person game, with mutual information as the payoff function. The saddle value, a saddle point, and an optimum jammer strategy are given for both the finite-dimensional and the infinite-dimensional channel. GRA

N89-27052# Kansas Univ. Center for Research, Inc., Lawrence.
MODEL-BASED PARAMETER ESTIMATION IN ELECTROMAGNETIC COMPUTER MODELING Final Report
Kenneth R. Demarest Apr. 1989 15 p
(Contract N00014-86-K-0326)
(AD-A207399; RSL-TR-7360-5) Avail: NTIS HC A03/MF A01 CSCL 20/3

Modeling in Computational Electromagnetics (CEM) can be a numerically demanding exercise. There are essentially two factors that contribute to this situation. One is the need to describe the propagation of the electromagnetic field via the Maxwell curl equations, Green's function, mode expansions, or ray and geometrical optics. It is in this part of the problem that a source-field relationship is quantitatively developed. The other is the subsequent need to invert the source-field relationship to proceed from prescribed existing fields and known sources to the induced sources that result and the fields they consequently produce. A moment-method solution, based on an integral equation formulation, embodies both of these factors. There are basically two paths by which the computer times involved in CEM applications might be reduced. One would be the development of alternate formulations that reduce the time required for either of the activities listed above, or that eliminate the need for it completely. The geometrical theory of diffraction is one example of this path. The other would be the development of more efficient numerical approaches for implementing the moment-method model. Under this contract we have investigated several means of reducing the computation time involved in the applications of integral equation, moment-method modeling. GRA

N89-27053# General Atomics Technologies Corp., San Diego, CA.
DISPERSED AND PERIODIC MICROSTRUCTURES FOR MAGNETIC AND INFRARED ABSORBERS Final Report
J. L. Kaae and D. W. Duggan Mar. 1989 37 p
(Contract N00014-88-C-0165)
(AD-A207428; GA-C19612) Avail: NTIS HC A03/MF A01 CSCL 07/2

This is the final report on a study of the electromagnetic characteristics of model materials having a finely divided ferromagnetic phase in a nonmetallic matrix. The overall objective of the work was to achieve a theoretical understanding of the physics of microwave and infrared absorption in these materials, but because of lack of funds only fabrication and microstructure and electromagnetic characterization of one material combination made by one process was completed, although a theoretical

framework for analytical modeling of the materials was laid out. The process used to fabricate model specimens that were studied was chemical vapor co-deposition, and the material combination studied was a dispersion of cobalt particles in carbon. GRA

N89-27054# Army Missile Command, Redstone Arsenal, AL. Research Directorate.
EVALUATION OF AN OPTICAL CORRELATOR AND MATCHED FILTER MAKER Final Technical Report
John L. Stensby and Charles R. Christensen 28 Feb. 1989 28 p
(AD-A207556; AD-E951331; AMSMI/TR-RD-RE-89-4) Avail: NTIS HC A03/MF A01 CSCL 09/5

Experimental work with a compact, coherent, real-time optical correlator and a matched filter maker system is described. The system was designed and built by the technical staff of The Environmental Research Institute of Michigan. Attributes of the correlator included small size, the ability to correlate an input image with multiple references, and operation over a wide range of input light levels. The input scene enters the correlator by a system of lenses while the matched filters are prerecorded on a photographic plate that is inserted into the correlator. The correlator contains a miniature CCD television camera upon which the correlations are projected. The output of the camera is a standard composite video signal which can be displayed on a simple monitor. A match between the input scene and one of the stored filters is indicated by the appearance of a bright correlation spot on the output monitor. GRA

N89-27055# Instituto de Pesquisas Espaciais, Sao Jose dos Campos (Brazil).
PERFORMANCE COMPARISON AMONG SEVERAL FILTERS FOR THE REDUCTON OF SPECKLE NOISE IN RADAR IMAGERY [COMPARACAO DO DESEMPENHO ENTRE VARIOS FILTROS PARA A REDUCAO DO RUIDO SPECKLE EM IMAGENS DE RADAR]
Silvia Shizue Ii and Gerald Jean Francis Banon Dec. 1988 7 p In PORTUGUESE; ENGLISH summary Presented at the 5th Brazilian Symposium of Remote Sensing, Natal, R. S., 11-15 Oct. 1988
(INPE-4768-PRE/1437) Avail: NTIS HC A02/MF A01

Synthetic aperture radar images have become an increasing popular remote sensing data, because of its climatic independent acquisition characteristics. Unfortunately, they are disturbed by a so called speckle noise, which gives them a granular aspect. In the past, several methods were prepared to improve the visual quality of such images. Lee and Frost's filters for speckle reduction are presented, and their performance are discussed through a visual comparison of resulting images obtained from a original SAR-580 image. Author

N89-27056# Oak Ridge National Lab., TN.
AN EXPERT SYSTEM FOR CORRELATION OF RADAR AND PASSIVE SENSOR SIGNALS
Laird C. Williams and Rudy J. Gamberini (Grumman Aerospace Corp., Bethpage, NY.) 1989 4 p Presented at the Data Fusion Symposium, Baltimore, MD, 14 May 1989
(Contract DE-AC05-84OR-21400)
(DE89-011575; CONF-8905135-1) Avail: NTIS HC A02/MF A01

A system is described for automating the correlation task by combining high speed hardware with symbolic pattern-matching software to perform correlation of active and passive signals in real time. The first section describes the hardware and software used to implement the inference engine so that correlations can be performed in real time. The second section describes the expert system, with emphasis on the heuristics used to code the correlator efficiently. The final section describes the simulation environment under which the system is operated, current efforts, and plans for further development. DOE

N89-27057# Lawrence Livermore National Lab., CA.
RADIATION FROM WAVES GUIDED BY NONUNIFORM ACTIVE SURFACES
R. J. King Apr. 1989 6 p Presented at the IEEE/AP-S International Symposium, San Jose, CA, 26-30 Jun. 1989
(Contract W-7405-eng-48)
(DE89-012286; UCRL-100883; CONF-890660-7) Avail: NTIS HC A02/MF A01

The concept of electronically manipulating the complex wave numbers of waves launched along guiding surfaces is intriguing and appropriate for this special session on new trends. The fact that technology for designing and constructing nonuniform and active wave-guiding surfaces is not yet developed has precluded wide knowledge or acceptance of these concepts. Nevertheless, the concepts are still unique and worthy of re-examination within the realm of feasible but undeveloped ideas. DOE

N89-27058# National Telecommunications and Information Administration, Boulder, CO. Inst. for Telecommunication Sciences.
MILLIMETER-WAVE PROPAGATION CHARACTERISTICS AND CHANNEL PERFORMANCE FOR URBAN-SUBURBAN ENVIRONMENTS
Edmond Violette, Richard Espeland, and Kenneth C. Allen Dec. 1988 181 p
(PB89-180251; NTIA-88-239) Avail: NTIS HC A09/MF A01 CSCL 20N

Measurements were performed in an urban-suburban environment with narrow and wideband RF probes, which included millimeter wave frequencies, in order to study propagation characteristics for street level paths. The performance of the RF channels was evaluated in these environments for both line-of-sight and non-line-of sight paths and compares a model developed for line-of-sight paths to measurements taken in Denver, CO. GRA

N89-27059# Sandia National Labs., Albuquerque, NM. Dept. of Electrical and Computer Engineering.
A FINITE ELEMENT METHOD FOR SOLVING ELECTROMAGNETIC SCATTERING PROBLEMS
Andreas C. Cangellaris and Robert Lee 1989 4 p Presented at the Institute of Electrical and Electronics Engineers (IEEE) Antennas Propagation Society (AP-S) International Symposium, San Jose, CA, 26 Jun. 1989 Prepared in cooperation with Arizona Univ., Tucson
(Contract DE-AC04-76DP-00789)
(DE89-013496; SAND-89-7082C; CONF-890660-8) Avail: NTIS HC A02/MF A01

One of the major issues associated with using the finite element method in opening regions is the problem of truncating the computational mesh. There have been numerous techniques which have been developed in the past several years. Hybrid finite element methods were first introduced by Silvester and Hsieh and McDonald and Wexler. They used a surface integral equation involving the appropriate Green's function that satisfies Sommerfeld's radiation condition at infinity to account for the truncation at the boundary. Mei developed an innovative method called the unimoment method that utilizes finite-element solutions inside a sphere containing the scatterer and eigenfunction expansions in the exterior of the sphere to compute the fields everywhere. Since then, several modifications and/or extensions of the aforementioned methods have appeared. In this paper, we present a new finite element formulation of the electromagnetic scattering problem. This new formulation could be thought of as a generalization of the unimoment method. Although our preliminary results are for two-dimensional problems, the method can be extended to three-dimensional geometries. DOE

N89-27060*# National Aeronautics and Space Administration. Langley Research Center, Hampton, VA.
SOLUTIONS OF DIFFERENTIAL EQUATIONS WITH REGULAR COEFFICIENTS BY THE METHODS OF RICHMOND AND RUNGE-KUTTA

C. R. Cockrell Aug. 1989 20 p
(NASA-TM-101609; NAS 1.15:101609) Avail: NTIS HC A03/MF A01 CSCL 20N

Numerical solutions of the differential equation which describe the electric field within an inhomogeneous layer of permittivity, upon which a perpendicularly-polarized plane wave is incident, are considered. Richmond's method and the Runge-Kutta method are compared for linear and exponential profiles of permittivities. These two approximate solutions are also compared with the exact solutions. Author

N89-27061# Instituto de Pesquisas Espaciais, Sao Jose dos Campos (Brazil).
DETECTION, ACQUISITION AND SIGNAL DEMODULATION IN A COMMUNICATION SYSTEM WITH RANDOM ACCESS M.S. Thesis - Technical Inst. of Aeronautics [DETECAO, AQUISICAO E DEMODULACAO DE SINAIS EM UM SISTEMA DE COMUNICACAO COMACESSO ALEATORIO]
Luiz Carlos PacolaSobrinho Dec. 1988 134 p In PORTUGUESE; ENGLISH summary
(INPE-4779-RPE/581) Avail: NTIS HC A07/MF A01

The development of a signal processor for the Data Collecting System of the first Brazilian Complete Space Mission is presented. The signals from the data collecting platforms are random both in time and frequency, and are spread over a band of 24 kHz. The search and detection of these signals is presented. The optimum detector as well as the adapted practical solution are described. Once they are detected, the signals are demodulated and the platform data are recovered. Author

N89-27062*# Hawaii Univ., Honolulu. Dept. of Electrical Engineering.
BANDWIDTH EFFICIENT CODING FOR ERROR CONTROL Final Technical Report
Shu Lin 1 Aug. 1989 38 p
(Grant NAG5-931)
(NASA-CR-185836; NASA-89-001; NAS 1.26:185836) Avail: NTIS HC A03/MF A01 CSCL 17B

One of the dramatic developments in bandwidth-efficient communications over the past few years is the introduction and rapid applications of combined coding and bandwidth efficient modulation, known as coded modulation, for error control. Using coded modulation, reliable data transmission can be attained without compromising bandwidth efficiency. Presented here are the basic concepts of coded modulation. Two simple examples are used to demonstrate how significant coding gains can be achieved without bandwidth expansion. Author

N89-27063*# National Aeronautics and Space Administration. Langley Research Center, Hampton, VA.
CWG: A FORTRAN PROGRAM FOR MUTUAL COUPLING IN A PLANAR ARRAY OF CIRCULAR WAVEGUIDE-FED APERTURES
M. C. Bailey Jun. 1989 46 p
(NASA-TM-101614; NAS 1.15:101614) Avail: NTIS HC A03/MF A01 CSCL 17I

A FORTRAN program which calculates the mutual coupling between circular apertures in a conductive plane is documented. The program is quite general in that the apertures do not have to be the same sizes, nor do they have to be polarized in the same direction. In addition, several waveguide modes (TE and/or TM) may be specified in the apertures and the mutual coupling between all combinations of apertures and modes will be calculated. The program also allows multiple layers of homogeneous dielectrics to be placed over the aperture array. Outside the layered region, one can specify either a homogeneous half-space, or a perfect reflecting surface. Author

N89-27064*# Ohio State Univ., Columbus. ElectroScience Lab.
RADAR CROSS SECTION STUDIES/COMPACT RANGE RESEARCH
W. D. Burnside, A. K. Dominek, I. J. Gupta, E. H. Newman, P. H. Pathak, and L. Peters, Jr. Mar. 1989 84 p
(Grant NsG-1613)
(NASA-CR-185848; NAS 1.26:185848; OSU-719493-7) Avail: NTIS HC A05/MF A01 CSCL 17I

Achievements in advancing the state-of-the-art in the measurement, control, and analysis of electromagnetic scattering from general aerodynamic targets are summarized. The major topics associated with this study include: (1) electromagnetic scattering analysis; (2) indoor scattering measurement systems; (3) RCS control; (4) waveform processing techniques; (5) material scattering and design studies; (6) design and evaluation of standard targets; and (7) antenna studies. Progress in each of these areas is reported and related publications are listed. M.G.

N89-27065# FUBA Hans Kolbe und Co., Bad Salzdetfurth (Germany, F.R.).
DEVELOPMENT OF A DFS (DEUTSCHE FERNMELDESATELLIT) RECEPTION CONVERTER [ENTWICKLUNG EINES DFS-EMPFANGS-KONVERTERS]
Joerg Hehlgans, Peter Kallmeyer, Martin Koch, Juergen Goehler, Heino Schroedl, Horst Denneng, Wolfgang Grethe, Heinrich Dierks, Eberhard Torunsky, and Bernd Anger et al Oct. 1988 60 p In GERMAN
(Contract BMFT-01-YH-86-138)
(ETN-89-94629) Avail: NTIS HC A04/MF A01

The German satellite communication system Kopernikus is described. Converter thick layer solid state technology in the range of 12 GHz is developed. Main components characteristics are: primary focus antenna with high system storage, converter amplifier 50 dB, system noise temperature 330 K to 3.2 dB, transparent signal transmission for a satellite middle frequency of 950 to 1700 MHz. ESA

N89-27066# Naval Postgraduate School, Monterey, CA.
ON CAPTURE EFFECT OF FM DEMODULATORS M.S. Thesis
Park S. Sang Mar. 1989 46 p
(AD-A208479) Avail: NTIS HC A03/MF A01 CSCL 25/2

The reception of FM carriers is characterized by a capture effect whereby the message of the dominant carrier is recovered when two or more FM carriers are present. This research uses a computer to form a type of average of the instantaneous frequency of the receiver input. The results establish that averaging (smoothing or lowpass filtering) of the instantaneous frequency reveals the capture effect. The effect on capture of bandwidth and amplitude ratio for the case of two carriers is revealed. The results show that capture can occur when two carriers are separated by as little as 0.17 dB in amplitude. GRA

N89-27067# Environmental Research Inst. of Michigan, Ann Arbor. Radar Science Lab.
ALASKA COLLECTION SAR (SYNTHETIC APERTURE RADAR) DATA SUMMARY Summary Report
D. H. Gineris, R. A. Shuchman, J. D. Lyden, A. S. Milman, and E. S. Kasischke Jan. 1989 55 p
(Contract N00014-87-C-0726)
(AD-A208530; ERIM-202-800-1-T) Avail: NTIS HC A04/MF A01 CSCL 17/9

Four synthetic aperture radar (SAR) data collection flights were made over Alaska and the surrounding waters in March of 1988, to obtain SAR images of sea ice and forested areas. The P-3 SAR, that operates at C-, L-, and X-bands, was used. 85 passes were collected over four days. The flights produced imagery of use to oceanographic, glaciological, geological, and botanical studies, This report describes the extent, location, and characteristics of the SAR data collected in this experiment. GRA

N89-27068# Naval Postgraduate School, Monterey, CA.
DEVELOPMENT OF A SYSTEM MODEL AND LEAST MEAN SQUARE (LMS) FILTER FOR THE NAVAL POSTGRADUATE SCHOOL (NPS) INFRARED SEARCH AND TARGET DESIGNATION SYSTEM (IRSTD) M.S. Thesis
Michael L. Gribaudo Mar. 1989 107 p
(AD-A208536) Avail: NTIS HC A06/MF A01 CSCL 17/5

A system model and a least mean square (LMS) filter for the Naval Postgraduate School (NPS) Infrared Search and Target Designation (IRSTD) system were developed. The system model was developed and run on the NPS IBM 3033/4381 mainframe computer network. The model simulated the effects of the optics and electronic processing equipment of the IRSTD system, and produced output data representative of the detector outputs of the system. The outputs of the IRSTD model were used to develop a digital filter based on the principle of least mean square optimization between an actual IRSTD detector output and a power series expansion representing a detector output containing both background clutter and a model target signal. It was determined that the raised cosine function served as the best model for IRSTD point and near-point targets, (0.1 mrad by 0.1 mrad to 1.5 mrad by 1.5 mrad), and a set of trial LMS filters were generated based on this model. After filtering both simulated and real data, consisting of simulated and real target signals embedded in simulated and real backgrounds, it was determined that an LMS filter generated from a raised cosine with a half-amplitude width of 0.9 mrad was optimal for point and near-point targets. GRA

33 ELECTRONICS AND ELECTRICAL ENGINEERING

Includes test equipment and maintainability; components, e.g., tunnel diodes and transistors; microminiaturization; and integrated circuitry.

For related information see also *60 Computer Operations and Hardware* and *76 Solid-State Physics.*

N89-27069# Danish Space Research Inst., Lyngby.
THE SHORT-CIRCUITED FLUXGATE OUTPUT CURRENT
F. Primdahl, J. R. Petersen, C. Olin, and K. Harbo Andersen Apr. 1988 24 p
(ISSN-0109-6605) Avail: NTIS HC A03/MF A01

The alternative coupling of short-circuiting a fluxgate sensor secondary coil by connecting it to the inverting input of a current amplifier is shown to have significant advantages over the more conventional unloaded or second harmonic tuned voltage coupling. The short-circuit output current impulses are independent of changes in the excitation level, and sensor performance is not degraded by cable and coil stray capacitances or by resistive loads from the feed-back circuit. The current impulse amplitude is proportional to the average-to-minimum secondary self-induction ratio minus 1, and to a virtual current in the secondary coil corresponding to the external magnetic field. Author

N89-27070 Department of the Air Force, Washington, DC.
MINIATURE HIGH VOLTAGE SOLID STATE RELAY Patent
Stanley D. Battle, inventor (to Air Force) 28 Jun. 1988 6 p Filed 23 Nov. 1986
(AD-D013979; US-Patent-4,754,176; US-Patent-Appl-SN-818922) Avail: US Patent and Trademark Office CSCL 09/1

High voltage is connected and disconnected in less than a microsecond from a high voltage power supply to a radar transmitter using a solid state relay. The solid state relay supplies this high voltage using multiple power MOSFETs, which are serially-connected between the source and the load. The gate of each power MOSFET is simultaneously triggered by trigger circuits which, in turn, are activated and coupled by a single turn transformer. The transformer is driven by a pair of field effect transistors, which are activated by a pair of open collector comparators. The open collector comparators only activate when they receive a signal indicating that the radar transmitter should transmit a waveform. GRA

N89-27071# Illinois Univ., Urbana-Champaign. Coordinated Science Lab.
RECONFIGURATION STRATEGIES IN VLSI (VERY LARGE SCALE INTEGRATION) ARRAYS AND TREES M.S. Thesis
Krishna P. Belkhale Dec. 1988 45 p
(Contract SRC-87-DP-109; NSF MID-87-14646)
(PB89-165468; CSG-93; UILU-ENG-88-2260) Avail: NTIS HC A03/MF A01 CSCL 09C

Reconfiguration strategies in VLSI processor arrays were advocated in the recent literature as a means of achieving higher production yield and higher reliability. New reconfiguration techniques are presented for rectangular arrays and trees that are generalizations of the Diogenes approach. The reconfiguration techniques present two schemes for reconfiguring rectangular arrays and a scheme for reconfiguring trees. For the analysis of the different schemes presented, it is assumed that a processor has a square layout. The first scheme for reconfiguring an NxN rectangular array uses r additional rows and c additional columns. The scheme guarantees reconfiguration as long as there are at most c columns that have more than r faulty processors. The second scheme uses S spare processors. Here k is a parameter of the design. It guarantees reconfiguration as long as there are enough spare processors, and in any window of N processors in a particular linearization there are at most k faulty processors. The scheme for reconfiguring a tree can tolerate as many faults as the number of spare processors S. Generalizations of the above scheme for trees, that improve on the number of switches an edge has to traverse, are also presented. GRA

N89-27072 Department of the Air Force, Washington, DC.
LOW NOISE CRYSTAL CONTROLLED OSCILLATOR Patent
Michael M. Driscoll, inventor (to AF) 10 Jan. 1989 5 p Filed 22 May 1987
(AD-D014070; US-Patent-4,797,639; US-Patent-Appl-SN-057461; US-Patent-Class-331-158) Avail: US Patent and Trademark Office CSCL 09/1

A low noise crystal controlled oscillator utilizes a single low impedance modular amplifier in conjunction with matching low impedance fixed element subcircuits to achieve predictable and repeatable frequency stability. A low component count enhances circuit reliability. GRA

N89-27073# Magnavox Government and Industrial Electronics Co., Mahwah, NJ. Electro-Optical Systems.
MM AND T FOR LINEAR RESONANT COOLER, VOLUME 2 Final Report, Oct. 1984 - Sep. 1986
R. Narayan and J. Silvestro 2 Feb. 1989 111 p
(Contract DAAK20-84-C-0440)
(AD-A207236; EOSR-1608-Vol-2) Avail: NTIS HC A06/MF A01 CSCL 13/1

The topics addressed include: SM-D-5005843 0.25 Watt Linear Resonant Cooler Assembly Drawing and Parts List; Acceptance/Performance Test; Acoustic Noise Test Data and Plots; Baseline and Post Temperature Shock; Low Temperature and Post Low Temperatures; High Temperature and Post High Temperatures; Post Mechanical Shock; Post Vibration; EMI; Reliability; and Failure Reports. GRA

N89-27074# Massachusetts Inst. of Tech., Cambridge. Research Lab. of Electronics.
THEORETICAL ANALYSIS OF MICROWAVE AND MILLIMETER WAVE INTEGRATED CIRCUITS BASED ON MAGNETIC FILMS Semiannual Report, 1 Oct. 1988 - 31 Mar. 1989
Jin Au Kong 31 Mar. 1989 87 p
(Contract N00014-89-J-1019)
(AD-A207508) Avail: NTIS HC A05/MF A01 CSCL 09/1

The complex resonant frequencies of the open structure of a microstrip antenna consisting of two circular microstrip disks in a three layer stacked configuration have been rigorously calculated as a function of the layered parameters and the ratio of the radii of the two disks. Using a dyadic Green's function formulation for horizontally stratified media and the vector Hankel transform, the mixed boundary value problem is reduced to a set of coupled vector integral equations. A rigorous dyadic Green's function formulation in the spectral domain is used to study the dispersion characteristics of signal strip lines in the presence of metallic crossing strips. A set of coupled vector integral equations for the current distribution on the conductors is derived. Galerkin's method

is then applied to derive the matrix eigenvalue equation for the propagation constant. A new method for analyzing frequency-dependent transmission line systems with nonlinear terminations is presented. The generalized scattering matrix foundation is used as the foundation for the time domain iteration scheme. Compared to the admittance matrix approach proposed in a previous paper, it has the advantage of shorter impulse response which leads to smaller computer memory requirement and faster computation time. Examples of a microstrip line loaded with nonlinear elements are given to illustrate the efficiency of this method. GRA

N89-27075# Air Force Inst. of Tech., Wright-Patterson AFB, OH. School of Engineering.
AN EXPERT SYSTEM IN C FOR COMPUTER-AIDED DIGITAL CIRCUIT DESIGN M.S. Thesis
Jorge S. Santos Jun. 1989 92 p
(AD-A207518; AFIT/GCS/ENG/89J-1) Avail: NTIS HC A05/MF A01 CSCL 20/3

This thesis effort documents the design, development, implementation, and test of an expert system which decomposes digital circuits into subproblems in order to detect wiring errors, which consist of improperly connected gates, missing connections, and violation of fanout or race conditions. Information needed to connect chips together is viewed as knowledge base information for the expert system. Information such type as number of pins, value of each pin (input, output, power, ground, clock), fanout for a particular type of chip are retrieved from a central database where they are represented. Implementation was done in the C programming language, which although is not design specially for dealing with problems in the Artificial Intelligence (AI) field could be used with success. An integration with a graphics package and a central database was achieved. Tests conducted with the system running in a personal computer Zenith 248 and compatible microcomputers under the Disk Operational System (DOS) version 3.2 proved the portability and efficiency of the expert system. A user's manual is included for the operation of the InterConnect Expert System (ICE). GRA

N89-27076# Kaman Sciences Corp., Colorado Springs, CO.
MICROWAVE HARDENING TECHNOLOGY DEVELOPMENT PROGRAM Final Report, 22 Sep. 1987 - 31 Oct. 1988
D. Robert Smith, Christopher C. Smith, and Katy DAmico 20 Dec. 1988 24 p Prepared for Booz-Allen and Hamilton, Inc., New York, NY
(Contract DAAL02-86-D-0042)
(AD-A207535; HDL-CR-88-042-1) Avail: NTIS HC A03/MF A01 CSCL 09/1

This report summarizes efforts in the following areas: (1) A series of microwave direct injection tests to determine burnout thresholds and upset effects for fiber-optic system components including light emitting diodes (LEDs) and PIN photodiodes. (2) An examination of the small signal and high power limiting effects of varistor paint material applied to a co-planar waveguide transmission line when injected with microwave pulses, as well as the impact of the paint upon the normal transmission characteristics of the line such as characteristic impedance and loss. If more detailed information is needed on the results of these efforts, two other unpublished reports on the fiber-optics components direct injection tests and the varistor paint limiter study can be requested. GRA

N89-27077# Lawrence Livermore National Lab., CA. Beam Research Program.
PROCEEDINGS OF THE SWITCHED POWER WORKSHOP: POWER SUPPLY WORKING GROUP
H. Haseroth, D. Hopkins, H. Ikezi, H. C. Kirbie, E. Lincke, and M. Wilson 14 Apr. 1989 8 p Workshop held at Shelter Island, NY, 16 Oct. 1988 Island, NY, 16 Oct. 1988
(Contract W-7405-eng-48)
(DE89-012293; UCRL-100911; CONF-8810135-4) Avail: NTIS HC A02/MF A01

The power supply working group was assigned the problem of pulse charging the 3-MeV gun. The gun is a radial line structure that has two charging configurations: a single ring charged to 500 kV or nine rings charged from 100 to 200 kV. In either configuration, the pulsed source must rapidly charge the structure's ring(s) before breakdown can begin. The issues encountered in charging the structure can be divided into two categories. First, the charging system must be well matched to the gun structure. Proper impedance matching will avoid reflections and limit the fault current if the ring should spark. Second, several systems can achieve the wide range of charge voltages necessary. Some are better suited to high voltages, while others are better at low voltages. The following paragraphs will address the impedance matching issues and review three choices for pulse generators. A system for each type of source is described along with a very rough cost estimate. DOE

N89-27078# National Inst. of Standards and Technology, Gaithersburg, MD. Center for Electronics and Electrical Engineering.
EMERGING TECHNOLOGIES IN ELECTRONICS AND THEIR MEASUREMENT NEEDS
Mar. 1989 79 p
(PB89-189245; NISTIR-89/4057) Avail: NTIS HC A05/MF A01 CSCL 09C

Emerging technologies are identified in electronics that the Center for Electronics and Electrical Engineering (CEEE) believes will require increased measurement support from CEEE in coming years. The emerging technologies described here are new to the marketplace or are experiencing major technological advances. The document is designed to stimulate feedback that CEEE needs to refine its plans for developing measurement capability to support emerging electronic technologies that are important to the national interest. GRA

N89-27079# Sandia National Labs., Albuquerque, NM.
THERMOELECTRIC TERMINOLOGY IN METROLOGY AND STANDARDS
R. P. Reed 1989 19 p Presented at the National Conference of Standards Laboratories (NCSL) Annual Conference and Symposium, Denver, CO, 9-13 Jul. 1989
(Contract DE-AC04-76DP-00789)
(DE89-011512; SAND-88-3408C; CONF-890773-1) Avail: NTIS HC A03/MF A01

In metrology and standards, thermoelectricity is most often associated with thermometry. Therefore, this paper emphasizes thermoelectricity in thermometry and it focuses on the Seebeck effect. Yet, the thermoelectric terminology applies generally to all the diverse areas in which Seebeck, Peltier, and Thomson thermoelectric effects are encountered. The literature of thermoelectricity is cluttered with false notions and inapt terminology. This paper attempts to discriminate between authentic and spurious views of thermoelectricity as they relate to thermometry. As inappropriate models and nomenclature can degrade the quality of thermometry in practice, the goals of this paper are: (1) to illustrate the commonplace contradictions between some present day thermoelectric definitions and terminology, (2) to present a consistent rational basis for thermoelectric terminology, (3) to offer a general, physically realistic, and internally consistent set of definitions of the field of applied thermoelectricity, and (4) to describe practical consequences of inappropriate terminology. DOE

N89-27080# Sandia National Labs., Albuquerque, NM.
PHOTOCONDUCTIVE SEMICONDUCTOR SWITCH (PCSS) RECOVERY
F. J. Zutavern, G. M. Loubriel, B. B. McKenzie, W. M. OMalley, R. A. Hamil, L. P. Schanwald, and H. P. Hijalmarson 1989 24 p Presented at the 7th Institute of Electrical and Electronics Engineers Pulsed Power Conference, Monterey, CA, 12 Jun. 1989
(Contract DE-AC04-76DP-00789)
(DE89-012657; SAND-88-3356C; CONF-890665-2) Avail: NTIS HC A03/MF A01

Attempts to use photoconductive semiconductors as high-power

(10 to 100 kV, 0.1 to 2 kA) toggling switches with recovery times of 5 to 100 ns have stimulated the exploration of their recovery mechanisms. We have observed that optically triggered GaAs switches exhibit lock-on, i.e., when triggered, they do not recover as long as they are holding more than 4 to 8 kV/cm. Experiments are being performed to determine the minimum recovery time of these switches after lock-on, by immediately reducing fields or currents. As an alternative to GaAs, Si is a semiconductor that does not exhibit lock-on. It has a very long recovery time that can be shortened with highly concentrated gold doping. Device models that predict behavior of PCSS and experiments on the recovery of GaAs and Au:Si switches are presented. DOE

N89-27081# Stanford Univ., CA. Dept. of Materials Science and Engineering.
NEW BATTERY MATERIALS Final Report
Robert A. Huggins Mar. 1989 27 p
(Contract DE-AC03-76SF-00098)
(DE89-012845; LBL-26923) Avail: NTIS HC A03/MF A01

This program is aimed at the study of materials and phenomena related to advanced battery systems, special attention being given to secondary systems which might be useful for vehicular propulsion or utility load levelling. In particular, the objectives of this program are to understand and evaluate the important structural, thermodynamic and kinetic parameters related to the use of materials as electrolyte or electrode components in high performance secondary battery systems. What follows is a report of our activities in some research areas. These include: the study of negative electrode materials for use in reversible sodium-based systems; the study of novel electrolyte systems for use in reversible sodium-based batteries; and the use of atmospheric pressure chemical vapor deposition for the preparation of thin film battery components. These will now be considered in turn. Several publications have resulted from this work, and are listed in the Appendix. DOE

N89-27082# Sandia National Labs., Albuquerque, NM.
CLOSING PHOTOCONDUCTIVE SEMICONDUCTOR SWITCHES
G. M. Loubriel, F. J. Zutavern, H. P. Hjalmarson, and M. W. OMalley 1989 13 p Presented at the 7th Institute of Electrical and Electronics Engineers Pulsed Power Conference, Monterey, CA, 12 Jun. 1989
(Contract DE-AC04-76DP-00789)
(DE89-013073; SAND-88-3399C; CONF-890665-10) Avail: NTIS HC A03/MF A01

One of the most important limitations of Photoconductive Semiconductor Switches (PCSS) for pulsed power applications is the high laser powers required to activate the switches. In this paper, we discuss recent developments on two different aspects of GaAs PCSS that result in reductions in laser power by a factor of nearly 1000. The advantages of using GaAs over Si are many. First of all, the resistivity of GaAs can be orders of magnitude higher than that of the highest resistivity Si material, thus allowing GaAs switches to withstand dc voltages without thermal runaway. Secondly, GaAs has a higher carrier mobility than Si and, thus, is more efficient (per carrier). Finally, GaAs switches can have naturally fast (ns) opening times at room temperature and low fields, microsecond opening times at liquid nitrogen temperature of 77 K, or, on demand, closing and opening at high fields and room temperature by a mechanism called lock-on. DOE

N89-27083# California Univ., Berkeley. Lawrence Berkeley Lab.
PROPOSED THIN FILM ELECTRONICS FOR A-Si:H PIXEL DETECTOR
V. Perez-Mendez, G. Cho, I. Fujieda, S. N. Kaplan, S. Qureshi, and R. A. Street (Xerox Palo Alto Research Center, CA.) Apr. 1989 29 p
(Contract DE-AC03-76SF-00098)
(DE89-013410; LBL-26254) Avail: NTIS HC A03/MF A01

We describe a proposed 2-D PIXEL detector and its electronic circuit. The dimensions of each PIXEL are 300 times 300 sq microns. Signal-to-noise ratio is in excess of 8 when connected to an a-Si:H TFT with gm = 3, and 10 when a polysilicon PMOSFET with gm = 50 is used. For both cases we assume an RC-CR shaping time of 1 microsecond. The signal amplification and readout circuit will be placed under the detector and can consist of 5 or 6 FETs and some passive elements. DOE

N89-27084# Lawrence Livermore National Lab., CA.
COMPUTER CODE PREDICTION OF PICOSECOND VOLTAGE SWITCHING AND TEM WAVE GENERATION IN AIR GAS AVALANCHE SWITCHES
D. J. Mayhall, J. H. Yee, and F. Villa (Stanford Linear Accelerator Center, CA.) 1 Jun. 1989 6 p Presented at the 7th Inst. of Electrical and Electronics Engineers Pulsed Power Conference, Monterey, CA, 11-14 Jun. 1989
(Contract W-7405-eng-48)
(DE89-013778; UCRL-100122; CONF-890665-15) Avail: NTIS HC A02/MF A01

The realization of efficient, reliable picosecond closing switches will make possible high gradient (1 to 3 GeV) linacs with pulsed accelerating electrode structures. Recently a promising candidate for picosecond, high voltage switching, the gas avalanche switch, has been proposed. The medium in this switch is high pressure (10 to 800 atm) gas. An avalanche discharge is initiated between pulse-charged high voltage electrodes by multiphoton ionization from a picosecond order laser pulse. The laser-initiated electrons avalanche toward the anode, causing the applied voltage to collapse in picoseconds, long before the hot current channel formation of a conventional spark gap. Several versions of the gas avalanche switch may be conceived. A parallel plate capacitor version consists of a high pressure gas confined between two parallel metal plates. An analysis of the formation or voltage delay and voltage collapse times for this geometry has been done by Villa and Cassell by numerical integration of a zero-dimensional (OD) electric circuit equation, which includes a resistively limited charge feed. This analysis predicts voltage collapse times of the order of several picoseconds for N sub 2 and air and 1 psec or less for Ar. DOE

N89-27085# Instituto de Pesquisas Espaciais, Sao Paulo (Brazil). Dept. de Processamento de Imagens.
AN EXPERT SYSTEM FOR FAULT DIAGNOSIS IN DIGITAL CIRCUITS
Laercio Massaru Namikawa and Flavio Roberto Dias Velasco Dec. 1988 13 p In PORTUGESE Presented at the 5th Brazilian Symposium on Artificial Intelligence, Natal, RN, 7-11 Nov. 1988
(INPE-4743-PRE/1417) Avail: NTIS HC A03/MF A01

The system SEDIG for fault diagnosis in digital circuits is presented. SEDIG, written in the OPS-5 language, is a rule based system which separates the knowledge concerning circuits from the returning diagnostic knowledge applicable to a large range of digital circuits. The structure of the system and its application for visualization of imagery are presented. Author

N89-27086# Iowa Univ., Iowa City. Dept. of Chemistry.
SYNTHESIS OF NOVEL FLUORINATED PHOSPHONIC AND PHOSPHINIC ACID ELECTROLYTES FOR PHOSPHORIC ACID FUEL CELLS Final Report, May 1985 - Dec. 1988
Donald J. Burton Feb. 1989 30 p
(Contract GRI-5084-260-1081)
(PB89-194120; GRI-89/0061) Avail: NTIS HC A03/MF A01
CSCL 09C

New methodology was developed for the preparation of difluoromethylene phosponate deriviatives, perfluorinated bis-phosphonates, and mixed phosphonate-sulfonates. The phosphonates were converted to the respective difluoromethylene phosphonic acids, perfluorinated bis-phosphonic acids, and a mixed fluorinated phosphonic-sulfonic acid. The acids were evaluated as a fuel cell electrolyte. The mono phosphonic acids wetted the Teflon electrode and were found to be unsuitable electrolyte candidates. The bis-phosphonic acids and the mixed phosphonic-sulfonic acid did not wet the Teflon electrode, dissolved more oxygen than phosphonic acid, exhibited excellent thermal

stability, and were found to warrant additional study as fuel cell electrolytes. GRA

N89-27087# National Inst. of Standards and Technology, Gaithersburg, MD. National Engineering Lab.
CENTER FOR ELECTRONICS AND ELECTRICAL ENGINEERING TECHNICAL PROGRESS BULLETIN COVERING CENTER PROGRAMS, OCTOBER TO DECEMBER 1988 WITH 1989 CEEE EVENTS CALENDER Quarterly Report
E. Jane Walters, comp. May 1989 44 p
(PB89-193270; NISTIR-89/4076) Avail: NTIS HC A03/MF A01 CSCL 09C

The report is the twenty-fifth issue of a quarterly publication providing information on the technical work of the National Institute of Standards and Technology (NIST) (formerly The National Bureau of Standards) Center for Electronics and Electrical Engineering. The issue of the CEEE Technical Progress Bulletin covers the fourth quarter of calendar year 1988. Abstracts are provided by technical area for both published papers and papers approved by NIST for publication. Author

N89-27088# Sandia National Labs., Albuquerque, NM.
DUAL-TRANSISTOR METHOD TO DETERMINE DELTA V SUB ot AND DELTA V SUB it FOR MOS DEVICES
D. M. Fleetwood, J. R. Schwank, and F. W. Sexton 1989 5 p Presented at the 26th Annual Conference on Nuclear and Space Radiation Effects, Marco Island, FL, 24 Jul. 1989
(Contract DE-AC04-76DP-00789)
(DE89-006725; SAND-89-0218C; CONF-890723-1) Avail: NTIS HC A02/MF A01

It is shown how standard Vth and mobility measurements made on otherwise identical n- and p-channel transistors can be combined to accurately estimate radiation-induced V sub ot and V sub it. Applications of the method are described. DOE

N89-27089# Sandia National Labs., Albuquerque, NM.
TOTAL-DOSE HARDNESS ASSURANCE FOR SPACE APPLICATIONS OF COMMERCIAL CMOS DEVICES
D. M. Fleetwood, P. S. Winokur, and R. L. Pease (Mission Research Corp., Albuquerque, NM.) 1989 5 p Presented at the 26th Annual Conference on Nuclear and Space Radiation Effects, Marco Island, FL, 24 Jul. 1989
(Contract DE-AC04-76DP-00789)
(DE89-006765; SAND-89-0181C; CONF-890723-2) Avail: NTIS HC A02/MF A01

Lot acceptance tests are evaluated for nonhardened CMOS devices for low total-dose space applications. Examples are presented for cases in which gate- or field-oxide leakage dominates device response. DOE

N89-27090# Los Alamos National Lab., NM.
RADIATION EVALUATION OF SEVERAL COMPLEX VERY LARGE SCALE INTEGRATION CIRCUITS
S. A. Spraggins, S. B. Roeske, J. S. Browning (Sandia National Labs., Albuquerque, NM.), and D. B. Holtkamp 1989 5 p Presented at the 26th Annual Conference on Nuclear and Space Radiation Effects, Marco Island, FL, 24-28 Jul. 1989
(Contract W-7405-eng-36)
(DE89-007985; LA-UR-89-490; CONF-890723-4) Avail: NTIS HC A02/MF A01

The results are presented of an evaluation of the radiation tolerance for natural space environments of several complex microprocessors, coprocessors and associated peripheral components; as well as an analog to digital converter and a power MOSFET. DOE

N89-27091# Oak Ridge National Lab., TN.
THE EFFECTS OF STEEP-FRONT, SHORT-DURATION IMPULSES ON POWER DISTRIBUTION COMPONENTS
David B. Miller, Andre E. Lux, Stanislaw Grzybowski (Mississippi State Univ., Mississippi State.), and Paul R. Barnes Jul. 1989 6 p Presented at the IEEE Summer Power Meeting, Long Beach, CA, 10-14 Jul. 1989
(Contract DE-AC05-84OR-21400)
(DE89-012338; CONF-890781-2) Avail: NTIS HC A02

A line type pulser has been developed to test the effects of steep-front, short duration (SFSD) pulses on distribution components. Risetime is 50 to 100 ns, and pulse duration is on the order of 300 ns. Terminators often shattered or punctured rather than flashing over. Insulator flashover voltage is approximately 1.5 times critical flashover (CFO) voltage for standard lightning impulses. Arresters exhibit an inductive character, with SFSD peak voltage at 10 kA approximately 4 to 5 times the 8 times 20 microsecond 10 kA discharge voltage. Polyethylene insulated cable has a characteristic degradation in which failure voltage decreases with number of SFSD pulses. DOE

N89-27092# Argonne National Lab., IL. Chemical Technology Div.
DEVELOPMENT OF COMPRESSED MULTIFOIL INSULATION FOR HIGH-TEMPERATURE BATTERIES AND OTHER APPLICATIONS
A. A. Chilenskas, R. F. Malecha, A. F. Tummillo, F. J. Meyer, and J. R. Missig (Meyer Tool and Mfg. Co., Inc., Oak Lawn, IL.) Feb. 1989 14 p
(Contract W-31-109-eng-38)
(DE89-012877; ANL-89/4) Avail: NTIS HC A03/MF A01

The Li-alloy/FeS battery operates a greater than 450 C and thus requires an insulated jacket for thermal management. The use of compressed multifoil confined in a light-weight, stainless steel, double-walled jacket at a pressure of less than 100 micrometers Hg was tested as an insulating medium for a 36-V, 8-kWh Li-alloy/FeS battery. Two battery jackets measuring approximately 48 x 28 x 85 cm were fabricated and tested in this program. Test results were encouraging. Product development and marketing are planned by Meyer Tool and Manufacturing, Inc. DOE

N89-27093# Sandia National Labs., Albuquerque, NM.
IMPROVED CORE INSULATION SCHEMES FOR MULTI-TERAWATT MAGNETIC SWITCHES
H. C. Harjes, G. A. Mann, E. L. Neau, and F. A. Morgan 1989 5 p Presented at the 7th Institute of Electrical and Electronics Engineers Pulsed Power Conference, Monterey, CA, 12 Jun. 1989
(Contract DE-AC04-76DP-00789)
(DE89-013814; SAND-89-0091C; CONF-890665-21) Avail: NTIS HC A02/MF A01

The operation of multi-terawatt magnetic switches was successfully demonstrated in the Comet 2 pulsed power module in 1984. Those switches, however, had short lifetimes (less than 100 shots) due to inter-lamina dielectric breakdowns at electric-field levels far lower than expected. Since then, experiments have been conducted to gain an understanding of this problem. We found that the breakdowns occurred at low electric-field levels, because the thin dielectric film (Mylar) was abrasively degraded by the relatively rough surface of the magnetic tape (Metglas) during the core winding process. This problem can be solved by modifying the Metglas surface before winding. A factor of 2 improvement in breakdown level, from 0.8 MV/cm to 1.6 MV/cm, has been demonstrated on the MSTF module (a Marx driven, 500 kV, 2 ohm, 50 ns PFN) in 18 in. OD switches wound with Electrodag coated Metglas (nominal coating thickness of approx. 6 microns). Even better performance has been achieved in smaller scale tests with an electrophoretically applied plastic-coated Metglas. A description of these experiments and a discussion of the results will be presented. DOE

N89-27094 Max-Planck-Inst. fuer Plasmaphysik, Garching (Germany, F.R.).
LOW-NOISE CABLE FOR DIAGNOSTICS, CONTROL AND INSTRUMENTATION OF THE ASDEX TOKAMAK FUSION EXPERIMENT
Joachim Gernhardt Nov. 1988 69 p
(IPP-III/67; ETN-89-94573) Copyright Avail:

Fachinformationszentrum Karlsruhe, 7514
Eggenstein-Leopoldshafen 2, Fed. Republic of Germany

Cabling considerations for the ASDEX tokamak are discussed. The relatively large stray field compared with that of an iron transformer and the cable length of over 30 m from the experiment to the control room, make the magnetically induced and capacitively coupled noise signal in the cable relatively high. As a result of neutral injection and lower hybrid ion cyclotron and Alfven wave heating, strong E-fields are produced and noise is coupled into the cables. These magnetic and electric field gradients during the plasma shot vary with time and location. It is shown how these noise signals can be reduced without reducing the broadcast frequency of the signal. Electromagnetic compatibility and interference are discussed. ESA

N89-27095# Technische Univ., Delft (Netherlands).
ON TRANSFORMER MODELING. A PHYSICALLY BASED THREE-PHASE TRANSFORMER MODEL FOR THE STUDY OF LOW FREQUENCY PHENOMENA IN ELECTRICAL POWER SYSTEMS Ph.D. Thesis
Harold Edwin Dijk 1988 205 p
(ETN-89-94801) Avail: NTIS HC A10/MF A01

Starting from the elementary Maxwell's equations, it is shown which assumptions and simplifications are required to arrive at what can be seen as a physically based network description of the transformer. As a result of this analysis, the link between the T-network and the Pi-network, both describing the single-phase transformer, is revealed. From a modeling point of view, the T-network results from the assumption that the total flux can be divided in main flux and leakage fluxes, while the Pi-network results from an integral flux approach. It is shown that these two approaches are mathematically related via the star-delta transformation. As a consequence, these two transformer descriptions, of which the T-network is most popular, yield the same behavior in the hypothetical case of the transformer being a linear device. It is shown that the three-phase transformer can perfectly and also more realistically be described when the integral flux approach is used. ESA

N89-27096# Syracuse Univ., NY. Dept. of Computer and Information Sciences.
FAULT TOLERANT VLSI (VERY LARGE-SCALE INTEGRATION) DESIGN USING ERROR CORRECTING CODES Final Technical Report, Mar. 1987 - Mar. 1988
C. R. Hartmann, P. K. Lala, A. M. Ali, S. Ganguly, and G. S. Visweswaran Feb. 1989 67 p
(Contract F30602-81-C-0169; AF Proj. 2338)
(AD-A208337; RADC-TR-88-321) Avail: NTIS HC A04/MF A01 CSCL 09/1

Very Large-Scale Integration (VLSI) provides the opportunity to design fault tolerant, self-checking circuits with on-chip, concurrent error correction. This study determines the applicability of a variety of error-detecting, error-correcting codes (EDAC) in high speed digital data processors and buses. In considering both microcircuit faults and bus faults, some of the codes examined are: Berger, repetition, parity, residue, and Modified Reflected Binary codes. The report describes the improvement in fault tolerance obtained as a result of implementing these EDAC schemes and the associated penalties in circuit area. GRA

N89-27097# Army Lab. Command, Fort Monmouth, NJ. Electronics Technology and Devices Lab.
POLARIZATION MATRICES OF LITHIUM TANTALATE Technical Report, Jan. 1988 - Jan. 1989
Arthur Ballato Apr. 1989 27 p
(DA Proj. 1L1-62705-H-94)
(AD-A208349; SLCET-TR-89-2) Avail: NTIS HC A03/MF A01 CSCL 07/2

In analytical treatments of piezoelectric acoustic transducers, signal processors, and resonators, the electromechanical transduction mechanism is most often expressed in terms of the elements of the piezoelectric (e) or (d) matrices. Molecular interpretations of piezoelectricity, and especially electro-optical applications, usually involve polarization as the preferred variable, and consequently the alternative (a) and (b) matrices are of interest. The elements of these latter sets are calculated for lithium tantalate from measured elastopiezodielectric constants taken from the literature. GRA

N89-27098# Massachusetts Inst. of Tech., Cambridge. Microsystems Research Center.
EASILY TESTABLE PLA-BASED FINITE STATE MACHINES
Srinivas Devadas, Hi-Keung Tony Ma, and A. Richard Newton (California Univ., Berkeley.) Mar. 1989 9 p Submitted for publication
(Contract N00014-87-K-0825)
(AD-A208371; VLSI-Memo-89-514) Avail: NTIS HC A02/MF A01 CSCL 09/1

This paper outlines a synthesis procedure, which beginning from a State Transition Graph description of a sequential machine, produces an optimized easily testable Programmable Logic Array (PLA) based logic implementation. Previous approaches to synthesizing easily testable sequential machines have concentrated on the stuck-at fault mode. For PLAs, and extended fault model called the crosspoint fault model is used. This paper, proposes a procedure of constrained state assignment and logic optimization which guarantees testability for all combinationally irredundant crosspoint faults in a PLA-based finite state machine. No direct access to the flip-flops is required. The test sequences to detect these faults can be obtained using combinational test generation techniques alone. This procedure thus represents an alternative to a Scan Design methodology. We present results which illustrate the efficacy of this procedure--the area/performance penalties in return for easy testability are small. GRA

N89-27099# Naval Postgraduate School, Monterey, CA.
IMPLEMENTATION OF A DESIGN FOR TESTABILITY STRATEGY USING THE GENESIL SILICON COMPILER M.S. Thesis
John C. Davidson Mar. 1989 122 p
(AD-A208458) Avail: NTIS HC A06/MF A01 CSCL 09/1

Design for Testability (DFT) is receiving major emphasis in the very large scale integration design field due to increasing circuit complexity. The utility of the silicon compiler and its value to a system designer without extensive VLSI design experience is discussed. Two major techniques for DFT, Scanpath Design and Built-in Test Design, are implemented using the Genesil silicon compiler. The basic building block, the shiftable test latch, is described in random logic block form and parallel datapath form. Linear feedback shift registers used as random vector generators and signature analyzers are used in the Built-in Test design. An Automatic Test Generation program is used to provide a measure of fault coverage for the two DFT techniques. The appendix is a brief tutorial illustrating the use of the Genesil system's shiftable test latch in its different configurations. GRA

34 FLUID MECHANICS AND HEAT TRANSFER

Includes boundary layers; hydrodynamics; fluidics; mass transfer; and ablation cooling.

For related information see also *02 Aerodynamics* and *77 Thermodynamics and Statistical Physics.*

N89-27100# Maryland Univ., College Park. Dept. of Mechanical Engineering.
TRANSIENT COOLING OF A HOT SURFACE BY DROPLETS EVAPORATION Final Report
M. diMarzo, F. Kavoosi, and M. Klassen Nov. 1988 65 p
(Grant NIST-70NANB5H0525)
(PB89-161897; NIST/GCR-89/559; Rept-88-3) Avail: NTIS HC A04/MF A01 CSCL 20D

The formulation of a model for the prediction of the cooling induced by an evaporating droplet impinging a semi-infinite solid

is described. The thermal interactions during the evaporation of a liquid droplet deposited on a low conductivity semi-infinite solid are complex because the evaporative process is coupled to the solid intense local cooling. Numerical techniques based on finite difference methods have failed to provide meaningful results. This is due to the sharp temperature gradients in the proximity of the droplet edge which cause instabilities in the solution for reasonable time steps due to the explicit coupling of the liquid-vapor regions. An integral method was proposed in order to overcome difficulties. The methodology and its application to this specific problem is described. GRA

N89-27101 Department of the Air Force, Washington, DC.
SYSTEM FOR BOUNDARY LAYER CONTROL THROUGH PULSED HEATING OF A STRIP HEATER Patent
Milton E. Franke, inventor (to AF) and Lawrence Kudelka, inventor (to AF) 22 Nov. 1988 5 p Filed 29 Jan. 1988
(AD-D013999; US-Patent-4,786,020; US-Patent-Appl-SN-149814; US-Patent-Class-244-204) Avail: US Patent and Trademark Office CSCL 20/4

A system is described for controlling the transition of laminar/turbulent flow at a surface which comprises a thin narrow strip heater disposed adjacent the surface and extending substantially transversely of the flow of the air stream thereacross, the heater being resiliently held in tension on or in closely spaced relationship to the surface, and a power source operatively connected to the heater for applying pulsed voltage of preselected amplitude and frequency to the heater. GRA

N89-27102# Selskapet for Industriell og Teknisk Forskning, Trondheim (Norway). Div. of Fluid Dynamics.
THE 1ST SCANDINAVIAN CONFERENCE ON VISCOUS AND T URBULENT FLOW IN HYDRAULIC MACHINERY
Kurt Alming and J. Vassenden, ed. 29 Sep. 1988 171 p Conference held in Trondheim, Norway, 28-29 Apr. 1987; sponsored by Nordisk Industrifond
(NI Proj. P87035)
(PB89-161327; STF67-A88031; ISBN-82-595-5290-6) Avail: NTIS HC A08/MF A01 CSCL 20D

Eight papers are presented which related to modeling, computation and measurement of viscous and turbulent flow with reference to fans, pumps, and hydraulic turbines. Examples of grid generation and flow analysis are given for different geometrical shapes. Author

N89-27103*# National Aeronautics and Space Administration. Lewis Research Center, Cleveland, OH.
HIGH SPEED CORNER AND GAP-SEAL COMPUTATIONS USING AN LU-SGS SCHEME
William J. Coirier 1989 16 p Presented at the 25th Joint Propulsion Conference, Monterey, CA, 10-12 Jul. 1989; cosponsored by the AIAA, ASME, SAE, and ASEE
(NASA-TM-102138; E-4936; NAS 1.15:102138; AIAA-89-2669) Avail: NTIS HC A03/MF A01 CSCL 20D

The hybrid Lower-Upper Symmetric Gauss-Seidel (LU-SGS) algorithm was added to a widely used series of 2D/3D Euler/Navier-Stokes solvers and was demonstrated for a particular class of high-speed flows. A limited study was conducted to compare the hybrid LU-SGS for approximate Newton iteration and diagonalized Beam-Warming (DBW) schemes on a work and convergence history basis. The hybrid LU-SGS algorithm is more efficient and easier to implement than the DBW scheme originally present in the code for the cases considered. The code was validated for the hypersonic flow through two mutually perpendicular flat plates and then used to investigate the flow field in and around a simplified scramjet module gap seal configuration. Due to the similarities, the gap seal flow was compared to hypersonic corner flow at the same freestream conditions and Reynolds number. Author

N89-27104# Advisory Group for Aerospace Research and Development, Neuilly-Sur-Seine (France). Fluid Dynamics Panel.
VALIDATION OF COMPUTATIONAL FLUID DYNAMICS
P. W. Sacher, R. G. Bradley, Jr., ed., and W. Schmidt, ed. (Dornier-Werke G.m.b.H., Immenstaad, Germany, F.R.) May 1989 26 p Presented at the AGARD Fluid Dynamics Panel Symposium, Lisbon, Portugal, 2-5 May 1988
(AGARD-AR-257; ISBN-92-835-0504-2) Copyright Avail: NTIS HC A03/MF A01

The Fluid Dynamics Panel AGARD Symposium entitled Validation of Computational Fluid Dynamics is reviewed and evaluated. The purpose of the Symposium was to assess the state of the art of Validation of Computer Codes and to ensure that the mathematical and numerical schemes employed in the codes correctly model the critical physics of the flow field under consideration. The evaluator addresses each of the papers presented separately and makes general comments on the seven major topic sessions. In addition, a Poster Session is reviewed in detail. It is evident that the new possibilities of CFD provide efficient tools for Analysis and Design in the Aeronautical Industry, but it is also evident that in spite of the existence of a number of excellent experimental databases, there is still a need for efforts in validating the computer programs both by experiment as well as by numerical exercises. Author

N89-27105# Bielefeld Univ. (Germany, F.R.).
GLOBAL FLOWS WITH INVARIANT (GIBBS) MEASURES FOR EULER AND NAVIER-STOKES TWO-DIMENSIONAL FLUIDS
Sergio Albeverio and Ana-Bela Cruzeiro (Centro de Documentacao Cientifica e Tecnica, Lisbon, Portugal) Feb. 1988 22 p Submitted for publication
(BIBOS-310/88; SFB-Preprint-10; ETN-89-94403) Avail: NTIS HC A03/MF A01

We construct a family of probability spaces (Omega, F, P gamma), gamma is greater than 0 associated with the Euler equation for a two-dimensional inviscid incompressible fluid which carries a pointwise flow Phi t (time evolution) leaving P gamma globally invariant. Phi t is obtained as limit of Galerkin approximations associated with Euler equations. P gamma is also an invariant measure for a stochastic process associated with Navier-Stokes equation with viscosity gamma, stochastically perturbed by a white noise force. ESA

N89-27106 Department of the Air Force, Washington, DC.
SURFACE COOLING SYSTEM Patent
Anthony M. Zimmerman, inventor (to AF) 31 Jan. 1989 4 p Filed 24 Dec. 1986
(AD-D014057; US-Patent-4,800,718; US-Patent-Appl-SN-946541; US-Patent-Class-60-264) Avail: US Patent and Trademark Office CSCL 13/1

This patent discloses a cooling system for providing a layer of relatively cool gas adjacent the surface of a duct carrying a flow of relatively hot gas. It includes an elongated louver nozzle, an elongated plenum and one or more crosswise dividers for separating the plenum and nozzle into a plurality of individual segments having sized supply orifices disposed therein. GRA

N89-27107# Nielsen Engineering and Research, Inc., Mountain View, CA.
NUMERICAL SIMULATION OF A TURBULENT FLOW THROUGH A SHOCK WAVE Final Technical Report, 1 Feb. 1987 - 31 Jan. 1989
David Nixon, Gary D. Kuhn, and Mohammad Farshchi 21 Apr. 1989 94 p
(Contract N00014-87-C-0483)
(AD-A207581; NEAR-TR-402) Avail: NTIS HC A05/MF A01 CSCL 20/4

This report describes the results of research into the interactions between shock waves and turbulent flows using numerical simulations. The research was conducted at transonic speeds with a normal shock wave and two dimensional turbulence, making use of existing knowledge and computational methods for developing insight to the shock/turbulence interaction. The results indicate that the shock has a significant effect on the turbulence. The shock produces a jump in the turbulence statistics, with a long relaxation distance to return to unshocked values. The

turbulence kinetic energy is increased by as much as 30 percent by the shock. The density-velocity correlation becomes important during the shock jump and is greatly increased over the case without a shock. On the other hand, the pressure-velocity correlation is not so important. The shock speed and ripple were found to be important factors in determining the turbulence downstream of a shock wave. Shock speed and ripple correlations are the same size as other important turbulence correlations. The work must be extended to higher Mach numbers and three-dimensional turbulence, with oblique shocks and shear flows. The shock ripple may be more important for oblique shocks because of the larger v component. GRA

N89-27108# Manchester Univ. (England). Dept. of Engineering.
A MODEL FOR TRANSITION BY ATTACHMENT-LINE CONTAMINATION AND AN EXAMINATION OF CROSS-FLOW INSTABILITY IN 3-D BOUNDARY LAYERS
I. R. Stewart and D. I. A. Poll 1988 160 p Sponsored by the Ministry of Defence, London, United Kingdom
(AERO-Rept-8804; ETN-89-94955) Avail: NTIS HC A08/MF A01

A model for predicting the development of intermittent turbulence in a boundary layer flow downstream of a large 2-D circular trip on an attachment-line was produced. It gives good predictions of intermittency at any point in the flow. Stability calculations were performed for the Falkner-Skan-Cooke family of boundary layers using linear stability theory. A relationship for the minimum critical Reynolds number and the height of the inflection point in the profile is identified. This correlation gives good agreement with the stability characteristics for boundary layer profiles typical of those occurring on suction wings. A discrepancy in previous empirical relations between skin friction and Reynolds number in fully developed turbulent flow on an attachment-line is discovered. To investigate this an experiment was undertaken using Preston tubes and a Pitot tube with the Clauser Chart method. An accurate correlation of skin friction on an attachment-line was determined from the experimental data. Small diameter Preston tubes underestimate skin friction on an attachment-line to the order of 10 percent which is not inconsistent with a reduction of the effective measurement height, possibly due to vortex shedding in the divergent flow at the mouth of the tube. ESA

N89-27109# Joint Inst. for Nuclear Research, Dubna (USSR).
TRANSIENT HEAT TRANSFER INTO SUPERFLUID HELIUM UNDER CONFINED CONDITIONS
Yu. P. Filippov, V. M. Miklyaev, and I. A. Sergeev 1988 6 p Presented at the 12th International Cryogenic Engineering Conference, Southampton, United Kingdom, 12-15 Jul. 1988
(DE88-706312; JINR-E-8-88-361) Avail: NTIS (US Sales Only) HC A02/MF A01

Transient thermal processes at solid-Hell interface at input of step pulse of heat load was investigated. Particular attention is given to the study of influence of geometry of experimental specimen upon the heat transfer dynamics. Abrupt breakdown of highly efficient transfer modes caused by the developmet of superfluid turbulence under confined condition is revealed, and accompanying temperature shift is registered. Some characteristic parameters are selected, their dependence on experimental conditions is established. DOE

N89-27110# Lawrence Livermore National Lab., CA. Center for Compressible Turbulence.
NUMERICAL STUDIES OF SHOCK WAVE STRUCTURE SENSITIVITY TO INTERACTIONS WITH TURBULENT FIELDS
Alfred C. Buckingham Apr. 1989 12 p Presented at the 6th International Conference on Numerical Methods in Laminar and Turbulent Flows, Swansea, United Kingdom, 11-15 Jul. 1989 Submitted for publication
(Contract W-7405-eng-48)
(DE89-012288; UCRL-100203; CONF-890752-3) Avail: NTIS HC A03/MF A01

This paper concerns the observed random changes to velocity, density, temperature, and pressure distributions induced in shock waves when weak shocks interact with relatively intense turbulence. Here numerical procedures are applied in order to examine this interaction process and to simulate its influence on turbulence. This interaction may be used as a diagnostic for ascertaining the distribution of interaction energy between competitive acoustic, entropy and vortical modes. Numerical procedures used here are supplements to physical experiments for tracking the dynamical mechanisms which may control the evolution of shock-turbulence interaction. The results are intended to provide assistance in the development and refinement of compressible turbulent closure models. They are obtained from use of a mixed Eulerian-Lagrangian semicontinuous rezoning finite difference method, a hybrid Euler/Lagrange pseudospectral method, and a Monte-Carlo random-choice procedure. The latter effectively magnifies the shock front region through use of finite range shock-transition integrals generating simulated interactive transition profiles. DOE

N89-27111*# Iowa State Univ. of Science and Technology, Ames. Heat Tranfer Lab.
A DUAL POTENTIAL FORMULATION OF THE NAVIER-STOKES EQUATIONS Final Report
S. G. Gegg, R. H. Pletcher, and J. L. Steger Aug. 1989 221 p
(Contract NCA2-174)
(NASA-CR-185098; NAS 1.26:185098; HTL-51; CFD-21; ISU-ERI-Ames-90030) Avail: NTIS HC A10/MF A01 CSCL 20D

A dual potential formulation for numerically solving the Navier-Stokes equations is developed and presented. The velocity field is decomposed using a scalar and vector potential. Vorticity and dilatation are used as the dependent variables in the momentum equations. Test cases in two dimensions verify the capability to solve flows using approximations from potential flow to full Navier-Stokes simulations. A three-dimensional incompressible flow formulation is also described. An interesting feature of this approach to solving the Navier-Stokes equations is the decomposition of the velocity field into a rotational part (vector potential) and an irrotational part (scalar potential). The Helmholtz decomposition theorem allows this splitting of the velocity field. This approach has had only limited use since it increases the number of dependent variables in the solution. However, it has often been used for incompressible flows where the solution scheme is known to be fast and accurate. This research extends the usage of this method to fully compressible Navier-Stokes simulations by using the dilatation variable along with vorticity. A time-accurate, iterative algorithm is used for the uncoupled solution of the governing equations. Several levels of flow approximation are available within the framework of this method. Potential flow, Euler and full Navier-Stokes solutions are possible using the dual potential formulation. Solution efficiency can be enhanced in a straightforward way. For some flows, the vorticity and/or dilatation may be negligible in certain regions (e.g., far from a viscous boundary in an external flow). It is possible to drop the calculation of these variables then and optimize the solution speed. Also, efficient Poisson solvers are available for the potentials. The relative merits of non-primitive variables versus primitive variables for solution of the Navier-Stokes equations are also discussed.
Author

N89-27112*# Institute for Computer Applications in Science and Engineering, Hampton, VA.
INVISCID SPATIAL STABILITY OF A COMPRESSIBLE MIXING LAYER. PART 3: EFFECT OF THERMODYNAMICS Final Report
T. L. Jackson and C. E. Grosch (Old Dominion Univ., Norfolk, VA.) Jun. 1989 47 p Submitted for publication
(Contract NAS1-18605)
(NASA-CR-181855; NAS 1.26:181855; ICASE-89-32-Pt-3) Avail: NTIS HC A03/MF A01 CSCL 20D

The results of a comprehensive comparative study of the inviscid spatial stability of a parallel compressible mixing layer using various models for the mean flow are reported. The models are: (1) the hyperbolic tangent profile for the mean speed and the Crocco relation for the mean temperature, with the Chapman

viscosity-temperature relation and a Prandtl number of one; (2) the Lock profile for the mean speed and the Crocco relation for the mean temperature, with the Chapman viscosity-temperature relation and a Prandtl number of one; and (3) the similarity solution for the coupled velocity and temperature equations using the Sutherland viscosity temperature relation and arbitrary but constant Prandtl number. The purpose was to determine the sensitivity of the stability characteristics of the compressible mixing layer to the assumed thermodynamic properties of the fluid. It is shown that the quantative features of the stability characteristics are quite similiar for all models but that there are quantitative differences resulting from the difference in the thermodynamic models. In particular, it is shown that the stability characteristics are sensitive to the value of the Prandtl number. Author

N89-27113*# Institute for Computer Applications in Science and Engineering, Hampton, VA.

ABSOLUTE/CONVECTIVE INSTABILITIES AND THE CONVECTIVE MACH NUMBER IN A COMPRESSIBLE MIXING LAYER Final Report

T. L. Jackson and C. E. Grosch (Old Dominion Univ., Norfolk, VA.) Jun. 1989 24 p

(Contract NAS1-18605)

(NASA-CR-181861; NAS 1.26:181861; ICASE-89-38) Avail: NTIS HC A03/MF A01 CSCL 20D

Two aspects of the stability of a compressible mixing layer: Absolute/Convective instability and the convective Mach number were considered. It was shown that, for Mach numbers less than one, the compressible mixing layer is convectively unstable unless there is an appreciable amount of backflow. Also presented was a rigorous derivation of a convective Mach number based on linear stability theory for the flow of a multi-species gas in a mixing layer. The result is compared with the heuristic definitions of others and to selected experimental results. Author

N89-27114*# National Aeronautics and Space Administration. Lewis Research Center, Cleveland, OH.

STABILITY OF A RIGID ROTOR SUPPORTED ON OIL-FILM JOURNAL BEARINGS UNDER DYNAMIC LOAD

B. C. Majumdar and D. E. Brewe (Army Aviation Systems Command, Cleveland, OH.) 1987 13 p Presented at the National Seminar on Bearings, Madras, India, 17-18 Sep. 1987

(NASA-TM-102309; E-3727; NAS 1.15:102309; AVSCOM-TR-87-C-26) Avail: NTIS HC A03/MF A01 CSCL 20D

Most published work relating to dynamically loaded journal bearings are directed to determining the minimum film thickness from the predicted journal trajectories. These do not give any information about the subsynchronous whirl stability of journal bearing systems since they do not consider the equations of motion. It is, however, necessary to know whether the bearing system operation is stable or not under such an operating condition. The stability characteristics of the system are analyzed. A linearized perturbation theory about the equilibrium point can predict the threshold of stability; however it does not indicate postwhirl orbit detail. The linearized method may indicate that a bearing is unstable for a given operating condition whereas the nonlinear analysis may indicate that it forms a stable limit cycle. For this reason, a nonlinear transient analysis of a rigid rotor supported on oil journal bearings under: (1) a unidirectional constant load, (2) a unidirectional periodic load, and (3) variable rotating load are performed. The hydrodynamic forces are calculated after solving the time-dependent Reynolds equation by a finite difference method with a successive overrelaxation scheme. Using these forces, equations of motion are solved by the fourth-order Runge-Kutta method to predict the transient behavior of the rotor. With the aid of a high-speed digital computer and graphics, the journal trajectories are obtained for several different operating conditions. Author

N89-27115*# National Aeronautics and Space Administration. Lewis Research Center, Cleveland, OH.

CALCULATION OF TURBULENCE-DRIVEN SECONDARY MOTION IN DUCTS WITH ARBITRARY CROSS SECTION

A. O. Demuren (Lagos Univ., Nigeria) Jul. 1989 23 p

(NASA Order C-99066-G)

(NASA-TM-102142; ICOMP-89-16; E-4941; NAS 1.15:102142) Avail: NTIS HC A03/MF A01 CSCL 20D

Calculation methods for turbulent duct flows are generalized for ducts with arbitrary cross-sections. The irregular physical geometry is transformed into a regular one in computational space, and the flow equations are solved with a finite-volume numerical procedure. The turbulent stresses are calculated with an algebraic stress model derived by simplifying model transport equations for the individual Reynolds stresses. Two variants of such a model are considered. These procedures enable the prediction of both the turbulence-driven secondary flow and the anisotropy of the Reynolds stresses, in contrast to some of the earlier calculation methods. Model predictions are compared to experimental data for developed flow in triangular duct, trapezoidal duct and a rod-bundle geometry. The correct trends are predicted, and the quantitative agreement is mostly fair. The simpler variant of the algebraic stress model procured better agreement with the measured data. GRA

N89-27116*# National Aeronautics and Space Administration. Ames Research Center, Moffett Field, CA.

A REVIEW OF HIGH-SPEED, CONVECTIVE, HEAT-TRANSFER COMPUTATION METHODS

Michael E. Tauber Washington Jul. 1989 38 p

(NASA-TP-2914; A-89042; NAS 1.60:2914) Avail: NTIS HC A03/MF A01 CSCL 20D

The objective of this report is to provide useful engineering formulations and to instill a modest degree of physical understanding of the phenomena governing convective aerodynamic heating at high flight speeds. Some physical insight is not only essential to the application of the information presented here, but also to the effective use of computer codes which may be available to the reader. A discussion is given of cold-wall, laminar boundary layer heating. A brief presentation of the complex boundary layer transition phenomenon follows. Next, cold-wall turbulent boundary layer heating is discussed. This topic is followed by a brief coverage of separated flow-region and shock-interaction heating. A review of heat protection methods follows, including the influence of mass addition on laminar and turbulent boundary layers. Also discussed are a discussion of finite-difference computer codes and a comparison of some results from these codes. An extensive list of references is also provided from sources such as the various AIAA journals and NASA reports which are available in the open literature. Author

N89-27117*# National Aeronautics and Space Administration. Ames Research Center, Moffett Field, CA.

HYPERVELOCITY ATMOSPHERIC FLIGHT: REAL GAS FLOW FIELDS

John T. Howe Jun. 1989 224 p

(NASA-TM-101055; A-89011; NAS 1.15:101055) Avail: NTIS HC A10/MF A01 CSCL 20D

Flight in the atmosphere is examined from the viewpoint of including real gas phenomena in the flow field about a vehicle flying at hypervelocity. That is to say, the flow field is subject not only to compressible phenomena, but is dominated by energetic phenomena. There are several significant features of such a flow field. Spatially, its composition can vary by both chemical and elemental species. The equations which describe the flow field include equations of state and mass, species, elemental, and electric charge continuity; momentum; and energy equations. These are nonlinear, coupled, partial differential equations that have been reduced to a relatively compact set of equations in a self-consistent manner (which allows mass addition at the surface at a rate comparable to the free-stream mass flux). The equations and their inputs allow for transport of these quantities relative to the mass-average behavior of the flow field. Thus transport of mass

by chemical, thermal, pressure, and forced diffusion; transport of momentum by viscosity; and transport of energy by conduction, chemical considerations, viscosity, and radiative transfer are included. The last of these complicate the set of equations by making the energy equations a partial integrodifferential equation. Each phenomenon is considered and represented mathematically by one or more developments. The coefficients which pertain are both thermodynamically and chemically dependent. Solutions of the equations are presented and discussed in considerable detail, with emphasis on severe energetic flow fields. Hypervelocity flight in low-density environments where gaseous reactions proceed at finite rates chemical nonequilibrium is considered, and some illustrations are presented. Finally, flight where the flow field may be out of equilibrium, both chemically and thermodynamically, is presented briefly. Author

N89-27118*# Ohio State Univ., Columbus. Dept. of Aeronautical and Astronautical Engineering.

INTERACTION BETWEEN TOLLMIEN-SCHLICHTING WAVES AND FREE-STREAM DISTURBANCES IN BOUNDARY-LAYER FLOWS

R. J. Bodonyi Aug. 1989 53 p
(Grant NAG3-743)
(NASA-CR-185847; NAS 1.26:185847) Avail: NTIS HC A04/MF A01 CSCL 20D

A numerical study of the generation of Tollmien-Schlichting (T-S) waves due to the interaction between a small freestream disturbance and a small localized variation of the surface geometry has been carried out using finite difference methods. The nonlinear steady flow is of the viscous-inviscid interactive type while the unsteady disturbed flow is assumed to be governed by the Navier-Stokes equations linearized about this flow. Numerical solutions illustrate the growth or decay of the T-S waves generated by the interaction between the freestream disturbance and the surface distortion, depending on the value of the scaled Strouhal number. An important result of this receptivity problem is the numerical determination of the amplitude of the Tollmien-Schlichting waves. Author

N89-27119# Sandia National Labs., Albuquerque, NM. Fluid Mechanics and Heat Transfer Div.

NUMERICAL SOLUTION OF THE NAVIER-STOKES EQUATIONS FOR THREE-DIMENSIONAL INCOMPRESSIBLE FLOWS WITH OPEN BOUNDARIES

J. A. Schutt 1989 11 p Presented at the 6th International Conference on Numerical Methods in Laminar and Turbulent Flows, Swansea, England, 11 Jul. 1989
(Contract DE-AC04-76DP-00789)
(DE89-009333; SAND-89-0046C; CONF-890752-1) Avail: NTIS HC A03/MF A01

Numerical modeling of the transient, nonisothermal, three-dimensional, incompressible Navier-Stokes equations imposes extreme demands on computational resources. For incompressible flow the Navier-Stokes equations form a coupled parabolic-elliptic set, with the elliptic nature caused by the incompressibility constraint. The elliptic nature of the incompressibility constraint forces some portion of the solution algorithm to be implicit, with the attendant computational costs. In addition, in regions of the computational domain where advective effects overwhelm viscous effects, the Navier-Stokes equations exhibit behavior which is similar to the hyperbolic nature of the Euler (inviscid) equations. In such regions many numerical methods which are suitable for parabolic equations will be dispersive, causing oscillations to appear in the solution. If accurate long-time solutions are required, dispersion must be avoided, as well as excessive numerical diffusion, which can result from attempts to control dispersion. The numerical algorithm presented here attempts to address these issues. DOE

N89-27120# Sandia National Labs., Albuquerque, NM.

FINITE CONTROL VOLUME MODELING OF LAMINAR AND TURBULENT FLOW OF AIR IN AN ENCLOSURE

R. E. Hogan and C. F. Kettleborough (Texas A&M Univ., College Station.) 1989 11 p Presented at the 6th International Conference on Numerical Methods in Laminar and Turbulent Flows, Swansea, England, 11 Jul. 1989
(Contract DE-AC04-76DP-00789)
(DE89-009334; SAND-89-0780C; CONF-890752-2) Avail: NTIS HC A03/MF A01

The finite control volume method (FCVM) was successfully used to calculate both laminar and turbulent buoyancy driven flow of air in a square enclosure for Ra = 10(3) to 10(8). For laminar flow, comparisons of the computed solution with both experimental data and other numerical solutions are in excellent agreement. Comparisons of selected velocities and average Nusselt numbers with a benchmark solution presented by deVahl Davis are consistently within 4 percent. For turbulent flow, the agreement with another numerical solution is generally good, considering the large difference in the number of nodes employed. The agreement with extrapolated experimental correlations for the average Nusselt number was acceptable. DOE

N89-27121*# National Aeronautics and Space Administration. Lewis Research Center, Cleveland, OH.

ARCJET CATHODE PHENOMENA

Francis M. Curran, Thomas W. Haag, and John F. Raquet (Air Force Academy, CO.) May 1989 17 p Presented at the JANNAF Propulsion Meeting, Cleveland, OH, 23-25 May 1989
(NASA-TM-102099; E-4841; NAS 1.15:102099) Avail: NTIS HC A03/MF A01 CSCL 20D

Cathode tips made from a number of different materials were tested in a modular arcjet thruster in order to examine cathode phenomena. Periodic disassembly and examination, along with the data collected during testing, indicated that all of the tungsten-based materials behaved similarly despite the fact that in one of these samples the percentage of thorium oxide was doubled and another was 25 percent rhenium. The mass loss rate from a 2 percent thoriated rhenium cathode was found to be an order of magnitude greater than that observed using 2 percent thoriated tungsten. Detailed analysis of one of these cathode tips showed that the molten crater contained pure tungsten to a depth of about 150 microns. Problems with thermal stress cracking were encountered in the testing of a hafnium carbide tip. Post test analysis showed that the active area of the tip had chemically reacted with the propellant. A 100 hour continuous test was run at about 1 kW. Post test analysis revealed no dendrite formation, such as observed in a 30 kW arcjet lifetest, near the cathode crater. The cathodes from both this test and a previously run 1000 hour cycled test displayed nearly identical arc craters. Data and calculations indicate that the mass losses observed in testing can be explained by evaporation. Author

N89-27122# Max-Planck-Institut fuer Stroemungsforschung, Goettingen (Germany, F.R.).

GENERATION OF UNDERWATER SOUND PULSES, CAVITATION AND SHEAR WAVES WITH HYDRAULIC HAMMER [ERZEUGUNG VON WASSERSCHALLIMPULSEN, KAVITATION UND SCHERWELLEN MIT EINEM HYDRAULISCHEN HAMMER]

G. E. A. Meier, A. Laake, and M. Rein Apr. 1988 200 p In GERMAN
(MPIS-8/1988; ISSN-0436-1199; ETN-89-94385) Avail: NTIS HC A09/MF A01; Max-Planck Inst. fuer Stroemungsforschung, Boettinger Strasse 6-8, 3400 Goettingen, Fed. Republic of Germany, DM 40

A hydrodynamic acoustic generator with shear waves source for seismic sea bottom profiling was developed. The principle of inversed water hammer is applied for the production of high energy pressure pulses. The mechanism of acoustic cavitation in water hammer is detailed. Homogeneous mixing of gas bubbles and fluid is numericaly modeled. Bubble dynamics is described by relations between bubble radius, pressure, nucleation, amplitude of expansion waves, and relaxation effects. A shear wave generator using inversed water hammer effects and sea water as working medium is described. ESA

N89-27123# Office National d'Etudes et de Recherches Aerospatiales, Paris (France). Direction de l'Aerodynamique.
STUDY OF SUBGRID MODELS IN INCOMPRESSIBLE TURBULENT FLOW, HOMOGENEOUS OR INHOMOGENEOUS Final Report [ETUDE DE MODELES DE SOUS-MAILLE EN TURBULENCE INCOMPRESSIBLE, HOMOGENE OU INHOMOGENE]
C. Teissedre Oct. 1988 42 p In FRENCH
(ONERA-RSF-17/3619-AY-110-A; ETN-89-94809) Avail: NTIS HC A03/MF A01

A data base of simulated homogeneous incompressible turbulent fields in anisotropic situations is made from direct simulations. Filters are permitted to adjust and validate different models of subgrids. A first extension of the over-dissipative model to inhomogeneous flow on flat channels is proposed. The spectral information required for each model evaluation allows adjustment of the dissipation in homogeneous planes as a function of the distance to the wall. ESA

N89-27124# Institut de Mecanique des Fluides de Lille (France). Groupe Mecanique des Fluides Fondamentale.
STUDY OF A TURBULENT BOUNDARY LAYER BY LASER PLANE VISUALIZATION [ETUDE D'UNE COUCHE LIMITE TURBULENTE PAR VISUALISATION PAR PLAN LASER]
M. Stanislas, M. C. Hoyez, and J. Pruvost 1 Dec. 1988 116 p In FRENCH
(Contracts DRET-86-003/05; DRET-87-003/05)
(IMFL-88/33; ETN-89-94810) Avail: NTIS HC A06/MF A01

Flow visualization was implemented with a laser light plane longitudinal to the flow in wind tunnel experiments. The experimental setup was complemented by wall friction sensors and hot film transducers. The influence of large eddy breakup devices was also tested. The visualization results are in accord with those obtained by FALCO. When manipulating the boundary layer, the results confirm the screen effect played by the wake on the fluid penetration in the inside part of the boundary layer. ESA

N89-27125# Institut de Mecanique des Fluides de Lille (France).
BASE WAKES FROM TWO DIMENSIONAL JETS IN SUBSONIC FLOW WITH INJECTION [SILLAGES DE CULOT BIDIMENSIONNEL EN SUBSONIQUE AVEC INJECTION]
O. Rodriguez, J. M. Desse, and C. Ducruet 25 Apr. 1986 96 p In FRENCH
(Contract DRET-84-003)
(IMFL-86/20; IMFL-4107; ETN-89-94811) Avail: NTIS HC A05/MF A01

The perturbation induced by the injection of momentum in the wake of a two-dimensional jet and the coupling between the jet and the wake close to the obstacle were studied. Transonic wind tunnel experiments were carried out. The experimental devices included ultrafast visualization, and average and unsteady pressure transducers. The results show the large influence of the unsteady characteristics of a two-dimensional jet entering the atmosphere through a narrow slot. ESA

N89-27126# Office National d'Etudes et de Recherches Aerospatiales, Paris (France).
SOLUTION OF COMPRESSIBLE TIME-DEPENDENT NAVIER-STOKES EQUATIONS BY CHEBYCHEV SPECTRAL METHODS Ph.D. Thesis - Paris VI Univ.
Patrice Loisel 1987 60 p In FRENCH; ENGLISH summary
(ONERA-NT-1987-1; ISSN-0078-3781; ETN-89-94813) Avail: NTIS HC A04/MF A01

Navier-Stokes equations for two and three dimensional time dependent compressible flows where high gradient zones are presented are solved numerically. Different treatment of these zones are proposed according to these gradients corresponding to physical discontinuities or to boundary layers. A hybrid spectral finite difference method is proposed for flow far from walls. For confined boundary layer flows, a spectral method based on the use of predictor-corrector schemes is presented. Results for simple geometry cases are given. ESA

N89-27127# Max-Planck-Institut fuer Stroemungsforschung, Goettingen (Germany, F.R.).
CONSTRUCTION OF DIFFERENTIAL EQUATIONS FROM EXPERIMENTAL DATA OF KARMAN VORTEX STREETS
E. Roesch, H. Eckelmann, and A. Huebler (Illinois Univ., Urbana.) Jun. 1988 56 p
(MPIS-11/1988; ISSN-0436-1199; ETN-89-94568) Avail: NTIS HC A04/MF A01; Max-Planck Inst. fuer Stroemungsforschung, Boettinger Strasse 6-8, 3400 Goettingen, Fed. Rep. of Germany DM 19

The construction of a differential equation from the experimental data of a Karman vortex street shows that the dynamics of the vortex street for Re less than or = 150, measured with a hot wire probe at a distance a less than d from the cylinder axis can be described by a differential equation system. The differential equation of the van der Pol oscillator form is a special case. Both systems can be described by a second order differential equation and third order polynomial. Thus the model of the van der Pol oscillator can be confirmed within the limits mentioned. For the Karman vortex street, though, all the terms are necessary whereas the van der Pol oscillator in this simple form consists of only three terms. The method of construction of a differential equation has several advantages compared to the Fourier transformation. The basic idea of transformations of a measured time series is to find a precise description of the data with a few parameters. If a time series is periodic a Fourier transformation is very useful, since the basic frequency together with its Fourier amplitude and the Fourier amplitudes for higher harmonics provides a description of the data with a few quantities. ESA

N89-27128# Rome Univ. (Italy). Dipartimento di Fisica.
STATISTICS OF AN INTEGRABLE DISCRETE SINE GORDON SYSTEM
S. DeLillo (Perugia Univ., Italy) and D. Levi 2 Nov. 1988 4 p Submitted for publication
(Preprint-638; ETN-89-94718) Avail: NTIS HC A02/MF A01

The soliton free energy density is obtained for a discrete completely integrable Sine Gordon system in the framework of the ideal gas approach. The results show that this gas of phonon kink and antikinks behaves as an ideal gas of noninteracting aspects. ESA

N89-27129# Technical Research Centre of Finland, Espoo. Lab. of Heating and Ventilating.
MEASUREMENT OF THE BENDING WAVE POWER FLOW BY THE STRUCTURAL INTENSITY TECHNIQUE
Jukka Linjama and Tapio Lahti Feb. 1989 58 p
(VTT-583; ISBN-951-38-3351-8; ISSN-0358-5077; ETN-89-94922) Copyright Avail: NTIS HC A04/MF A01; Technical Research Center of Finland, Vuorimiehentie 5, SF-02150 Espoo, Finland, 62 Finnish marks

Literature on the theory of bending waves and power flow, measurement of the structural intensity, and its applications to machinery and buildings is reviewed. Based on intensity measurement equations, a set of frequency domain expressions is derived for bending wave intensity measurements in a beam. A practical procedure for the general 4-transducer method is developed, using the sequential 1-transducer frequency response technique. Expressions for the determination of the force- and moment-related power components separately are derived. In laboratory experiments the power carried by bending waves was measured in a simple beam, and the developed configurations were tested and compared. The frequency response approach to detect the total power flow is shown to work well. The estimation of the force- and moment-related power components, both in the near and the far field, was also demonstrated. ESA

N89-27130# Aeronautical Research Inst. of Sweden, Stockholm. Aerodynamics Dept.
THE BEHAVIOR OF FLUX DIFFERENCE SPLITTING SCHEMES NEAR SLOWLY MOVING SHOCK WAVES
Thomas W. Roberts Dec. 1988 25 p Submitted for publication
(Contract STU(F)-87-00415P)
(FFA-TN-1988-58; ETN-89-94945) Avail: NTIS HC A03/MF A01

The behavior of shock capturing schemes which compute the numerical flux from a solution of Riemann's problem was investigated. The schemes of Godunov, Roe, and Osher are examined for a one dimensional model problem consisting of a nearly stationary shock. Both scalar results and systems of equations are examined. It is found that for slow shocks there is a significant error generated when solving systems of equations, while the scalar results are well behaved. This error consists of a long wavelength noise in the downstream running wave families that is not effectively damped by the dissipation of the scheme. The source of this error is shown, and the implications for the performance of these schemes are considered. This error may contribute to the reported slow convergence to steady state. ESA

N89-27131# Wichita State Univ., KS. Dept. of Mathematics and Statistics.
IDEAL JET FLOW IN TWO DIMENSIONS Final Report, 30 Sep. 1986 - 31 Jan. 1989
A. Elcrat 31 Jan. 1989 3 p
(Grant AF-AFOSR-0276-86; AF Proj. 2304)
(AD-A208275; AFOSR-89-0411TR) Avail: NTIS HC A02/MF A01 CSCL 20/4

This research has been concerned with two dimensional flows of an ideal fluid with concentrated regions of vorticity. The methods used involve ideas connected with conformal mapping and variational principles. GRA

N89-27132# Massachusetts Inst. of Tech., Cambridge. Acoustics and Vibration Lab.
MEASUREMENT OF WALL SHEAR AND WALL PRESSURE DOWNSTREAM OF A HONEYCOMB BOUNDARY LAYER MANIPULATOR
James Christian Moller and Patrick Leehey Apr. 1989 75 p
(Contract N00014-86-K-0183)
(AD-A208297; A/V-97457-3) Avail: NTIS HC A04/MF A01 CSCL 20/4

A boundary layer manipulator in the shape of a honeycomb placed in a turbulent boundary layer has been shown experimentally to reduce local wall shear downstream by as much as 38 pct and wall pressure by 36 pct. The zone of measureable shear and pressure reduction extends for at least 300 pre-manipulator displacement thicknesses downstream. Pressure spectra of the manipulated flow scales better with inner-outer variables than does the unmanipulated flow. Convective pressure speeds are reduced by as much as approximately 30 pct for Strouhal numbers above 0.3. Below Strouhal numbers = 0.3 convective phase speeds are not noticeably changed. This indicates pressure disturbances for Strouhal numbers less than 0.3 may originate from the inner portion of the boundary layer since the manipulator scales are far larger than the viscous sublayer. Coherence appears to be reduced in the streamwise direction and increased in the spanwise direction. All tests were done in the same facility as in Blake using the same microphones and wall insert. Unlike his work and similar to the work of other more recent investigations peaks were found in plots of coherence vs. phase in the vicinity of Strouhal numbers approx. = 0.3. GRA

N89-27133# Chemical Research and Development Center, Aberdeen Proving Ground, MD.
DESIGN AND CHARACTERIZATION OF LARGE-DROP GENERATORS FOR VISCOUS, NEWTONIAN, AND NON-NEWTONIAN LIQUIDS Technical Report, Apr. 1986 - Dec. 1987
Richard L. Pitter, Thomas E. Hoffer, Craig R. Allan, Hugh R. Carlon, and Arthur K. Stuempfle Mar. 1989 29 p Prepared in cooperation with Nevada Univ., Reno
(AD-A208330; CRDEC-TR-050) Avail: NTIS HC A03/MF A01 CSCL 07/3

Work performed by contractor personnel in conjunction with CRDEC Engineering Center (CRDEC) scientists is described. To evaluate protective clothing and the effects of chemical aerosols dispersed over a battlefield, a physical testing facility capable of simulating the behavior of falling drops is needed. In such a facility, the effects of drop size, surface interactions, long-term evaporation, and similar phenomena can be studied. This report describes two drop generators developed at the Desert Research Institute (DRI) and one drop generator developed at CRDEC. The first generator uses a drop injection of impulse technique and is appropriate for a wide variety of drop sizes using Newtonian liquids of various viscosities. The drop ejection technique has been improved in this work. The second generator uses a unique, two-step process. A microfilm is formed across a horizontal loop, and the test liquid is extruded onto the microfilm surface. The liquid drop is released into freefall by a short burst of solvent directed at the loop, causing the microfilm to disintegrate. GRA

N89-27134# McDonnell-Douglas Research Labs., Saint Louis, MO. Flight Sciences Dept.
THE STRUCTURE OF NORMAL-SHOCK/TURBULENT-BOUNDARY-LAYER INTERACTIONS MODIFIED BY MASS REMOVAL Final Technical Report, 1 Jun. 1986 - 31 Dec. 1988
M. Sajben, M. J. Morris, J. C. Kroutil, and T. J. Bogar 28 Feb. 1989 55 p
(Contract F49620-86-C-0063; AF Proj. 2307)
(AD-A208402; MDC-QA026; AFOSR-89-0650TR) Avail: NTIS HC A04/MF A01 CSCL 20/4

The effect of mass removal on nominally two-dimensional, normal-shock/turbulent-boundary-layer interactions was investigated experimentally. The flowfield had a freestream approach Mach number of 1.49 and a Reynolds number based on boundary layer momentum thickness of 14,600. Distributed mass removal was imposed over a length of approximately 40 initial displacement thicknesses, the entire bleed zone being located immediately upstream of the shock. Detailed velocity field information was obtained for two flows, using a two component laser Doppler velocimeter system. The two time mean velocity components and the three Reynolds stress components were determined. Measurements were extended over both supersonic and subsonic regions. Surface pressure information was also obtained. The removed mass flow, averaged over the length of the bleed zone, was 2.5 percent and 8 percent of the freestream mass flow, for the two cases investigated. The data indicates that the mass removal initiates an oblique expansion wave at the leading edge of the bleed zone, increasing the Mach number of the normal shock. The expansion wave intersects the shock, initiating a weak shear layer in the subsonic flow. The boundary layer thickness remains approximately constant over the bleed zone. GRA

N89-27135# Massachusetts Univ., Amherst. Dept. of Chemical Engineering.
LAGRANGIAN TURBULENCE NEAR WALLS: STRUCTURES AND MIXING IN ADMISSIBLE MODEL FLOWS Final Report, 1 Sep. 1987 - 31 Dec. 1988
J. M. Ottino 9 May 1989 7 p
(Grant AF-AFOSR-0385-87; AF Proj. 2307)
(AD-A208466; AFOSR-89-0733TR) Avail: NTIS HC A02/MF A01 CSCL 20/4

The general objective of work during this period was to bridge the gap between modern ideas from dynamical systems and chaos and more traditional approaches to turbulence. In order to reach this objective we conducted theoretical and computational work on two systems: a perturbed Kelvin cat eyes flow, and prototype solutions of the Navier-Stokes equations near solid walls. The main results obtained are two-fold: production flows capable of producing complex distributions of vorticity, and constructed flow

fields, based on solutions of the Navier Stokes equations, which are capable of displaying both Eulerian and Lagrangian turbulence. GRA

N89-26818# Office National d'Etudes et de Recherches Aerospatiales, Paris (France). Aerodynamique Appliquee.
DRAG PREDICTION AND ANALYSIS FROM COMPUTATIONAL FLUID DYNAMICS, STATE-OF-THE-ART IN FRANCE
J. J. Thibert *In* AGARD, Technical Status Review on Drag Prediction and Analysis from Computational Fluid Dynamics: State of the Art Jun. 1989 11 p In FRENCH; ENGLISH summary Original language document was announced in IAA as A89-29239 (For primary document see N89-26817 21-02)
Copyright Avail: NTIS HC A08/MF A01

35 INSTRUMENTATION AND PHOTOGRAPHY

Includes remote sensors; measuring instruments and gages; detectors; cameras and photographic supplies; and holography.

For aerial photography see *43 Earth Resources and Remote Sensing.* For related information see also *06 Aircraft Instrumentation,* and *19 Spacecraft Instrumentation.*

N89-27136# Science Applications International Corp., McLean, VA.
JTECH (JAPANESE TECHNOLOGY EVALUATION PROGRAM) PANEL REPORT ON ADVANCED SENSORS IN JAPAN
G. L. Miller, H. Guckel, E. Haller, T. Kanade, W. Ko, and V. Radeka Jan. 1989 293 p Sponsored by NSF, Washington, DC; DARPA, Arlington, VA and Department of Commerce, Washington, DC
(PB89-158760) Avail: NTIS HC A13/MF A01 CSCL 14B

The document provides the results of a detailed evaluation of the current state of Japanese sensor development. The analysis was performed by a panel of technical experts drawn from U.S industry and academia. It covers not only specific technical work, but also covers issues of organization, trends, funding, and methods of organizing work and setting priorities. The topics covered include: Tutorial introduction to sensors, machine vision (charge coupled device (CCD) sensors, vision processing systems, active 3-D range sensors, Research Institution on Machine Vision); sensors for electromagnetic radiation (far infrared, near infrared, visible light, X-rays, gamma-rays); sensors for factory automation and robotics; micromechanical and superconducting sensors; gas sensors; ion sensors; ion selective field effect transistors (ISFET); and biosensors. Also included is an extensive listing of Japanese sensor manufacturers. GRA

N89-27137# National Inst. of Standards and Technology, Gaithersburg, MD. Precision Engineering Div.
AN APPROACH TO ACCURATE X-RAY MASK MEASUREMENTS IN A SCANNING ELECTRON MICROSCOPE
Michael T. Postek, Robert D. Larrabee, and William J. Keery Jan. 1989 14 p
(Contract N00173-88-WR-80360)
(PB89-172555; NISTIR-89/4047) Avail: NTIS HC A03/MF A01 CSCL 14B

The concept and some preliminary experimental data is presented on a new method for measuring critical dimensions on masks used for X-ray lithography. The method uses a scanning electron microscope (SEM) in a transmitted-scanning electron microscope (TSEM) imaging mode and can achieve nanometer precision. Use of this technique in conjunction with measurement algorithms derived from electron beam interaction modeling may ultimately enable measurements of these masks to be made to nanometer accuracy. GRA

N89-27138 Department of the Navy, Washington, DC.
METHOD FOR CALIBRATING A HEAT FLUX GAUGE Patent
Alan H. Epstein, inventor (to Navy), Gerald R. Guenette, inventor (to Navy), and Robert J. Norton, inventor (to Navy) 14 Mar. 1989 16 p Filed 19 Oct. 1987
(AD-D013974; US-Patent-4,812,050; US-Patent-Appl-SN-111846; US-Patent-Class-374-1) Avail: US Patent and Trademark Office CSCL 20/13

A double-sided, high-frequency response heat flux gauge for use on metal turbine blading consists of a metal film (1500A) resistance thermometer sputtered on both sides of a thin (25 micro) polyimide sheet. The temperature difference across the polyimide is a direct measure of the heat flux at low frequencies, while a quasi one-dimensional analysis is used to infer the high-frequency heat flux from the upper surface history. A new method of calibrating the heat flux gauge utilizes a light source applied to a plurality of fluids covering the surface of the gauge, measuring the temporal output of the gauge and utilizing derived calibration formula. The object of the invention was the development of heat transfer gauge technology which would permit simultaneous measurement of both the steady state and time resolved heat flux distribution about the rotor blades in the MIT Blowdown Turbine facility. GRA

N89-27139 Department of the Air Force, Washington, DC.
SOLID STATE GAS PRESSURE SENSOR Patent
James Halvis, inventor (to AF), Nathan Bluzer, inventor (to AF), and Robert Shiskowski, inventor (to AF) 14 Mar. 1989 5 p Filed 14 May 1987 Supersedes AD-D013187
(AD-D014105; US-Patent-4,812,801; US-Patent-Appl-SN-049363; US-Patent-Class-338-4) Avail: NTIS HC A02/MF A01 CSCL 07/2

A solid state gas pressure sensor has a resistor of polysilicon deposited upon a dielectric substrate which electrically isolates and thermally prevents heat transfer to other devices thereon. A constant voltage is applied to the resistor. Depending upon the gas pressure over the sensor, a given current will be output once temperature equilibrium is established. A change in the gas pressure changes the output current of the resistor. The output current indicative of pressure is temperature corrected. GRA

N89-27140# Utah Univ., Salt Lake City. Microwave Device and Physical Electronics Lab.
DEVELOPMENT OF THEORETICAL AND NUMERICAL TECHNIQUES FOR ACHIEVING STABILITY IN GYROTRON TRAVELING-WAVE AMPLIFIERS Final Report, Sep. 1985 - Jun. 1988
Jeff E. Arrington Feb. 1989 239 p
(Contract F30602-84-C-0153)
(AD-A207451; UTEC-MD-88-072; RADC-TR-88-298) Avail: NTIS HC A11/MF A01 CSCL 09/1

The gyrotron traveling-wave amplifier is investigated with the purpose of developing the necessary analytical and numerical tools to allow analysis of proposed device based solutions to problems that currently limit the usefulness of the device. These solutions involve a fuller development of a scheme to increase the oscillation start current by use of spatially located, frequency selective loss mechanisms. The second problem considered is the narrow bandwidth of the cyclotron resonance maser interaction. A reverse injection scheme is discussed. It is found that the available analytical techniques are severely limited in their ability to analyze and simulate the proposed solutions, therefore indicating the development of the new tools discussed in this report. GRA

N89-27141# Aerospace Corp., El Segundo, CA. Aerophysics Lab.
ELECTRON-IMPACT IONIZATION TIME-OF-FLIGHT MASS SPECTROMETER FOR MOLECULAR BEAMS
James E. Pollard and Ronald B. Cohen 15 Apr. 1989 26 p
(Contract F04701-85-C-0086)
(AD-A207585; TR-0086(6908)-1; SD-TR-89-25) Avail: NTIS HC A03/MF A01 CSCL 07/4

A method is described for performing electron impact ionization time of flight mass spectrometry in a molecular beam apparatus. The method is a convenient way to optimize the performance of pulsed or continuous nozzle sources and can be used in conjunction with laser excitation. Mass spectra are produced either as analog

waveforms or in a high repetition rate ion counting mode. The device can also be operated as a fast ionization gauge for time resolved detection of pulsed beams. GRA

N89-27142 Department of the Air Force, Washington, DC.
INTERFEROMETRIC LOAD SENSOR AND STRAIN GAGE Patent
William P. Dixon, inventor (to AF) 28 Mar. 1989 8 p Filed 3 Jul. 1986 Supersedes AD-D012509
(AD-D014122; US-Patent-4,815,855; US-Patent-Appl-SN-882059; US-Patent-Class-356-358) Avail: US Patent and Trademark Office CSCL 20/11

The invention comprises an interferometric load sensor, or force balance which utilizes the etalons to form a reflective cavity. A fringe pattern is formed in cavity by light from laser source. One of the etalons is mounted to a section that is sensitive to the application of a force. Flexing of the cantilever due to application of force on the section changes the air gap wedge angle between the etalons and thereby shifts the fringe the field formed in cavity. The shift in the fringe field is observed by light detectors. GRA

N89-27143# Midwest Research Inst., Golden, CO. Solar Energy Research Inst.
DEVELOPMENT OF A SECOND-GENERATION, VIDEO-BASED LUMINANCE MAPPER FOR DAYLIGHTING RESEARCH
N. L. Weaver, C. L. Robbins, K. C. Hunter, and T. W. Cannon Nov. 1988 13 p Presented at the 2nd International Daylighting Conference: Architecture and Natural Light, Long Beach, CA, 4-7 Nov. 1986
(Contract DE-AC02-83CH-10093)
(DE89-000850; SERI/TP-254-3049; CONF-861109-9) Avail: NTIS HC A03/MF A01

Quantitative mapping of sky or room luminance distributions is a technically challenging endeavor. Several approaches have been developed based on using photometric or photographic techniques. Video-based imaging photometry has the demonstrated capability to generate luminance distribution data for both the sky dome and interior spaces. This paper discusses a new microcomputer/solid-state camera-based system with expanded graphic and high-speed data manipulation capabilities. The focus of the paper is a discussion of preliminary calibration specifications for the system and applications. DOE

N89-27144# Sandia National Labs., Albuquerque, NM.
STANDARDIZED PIEZOELECTRIC POLYMER (PVDF) GAUGE FOR DETONATOR RESPONSE MEASUREMENT
L. M. Moore, R. A. Graham, R. P. Reed, L. M. Lee, F. Bauer, and T. W. Warren (Mason and Hanger-Silas Mason Co., Inc., Amarillo, TX.) 1989 12 p Presented at the International Conference of the GTPS, La Grande Motte, France, 5 Jun. 1989
(Contract DE-AC04-76DP-00789)
(DE89-010437; SAND-88-2098C; CONF-8906118-1) Avail: NTIS HC A03/MF A01

Time-resolved measurements of pressure profiles from the detonation of explosive devices have proven to be essential for the detailed study of device performance. At present such measurements are routinely carried out with laser velocity interferometer (VISAR) systems, electromagnetic particle velocity gauges or piezoresistant (Manganin) gauges. One of the most promising new gauges to appear in recent years is the piezoelectric polymer gauge (PVDF) which has been standardized for general use based on the materials processing techniques developed by Bauer. The special problems presented by small size piezoelectric polymer gauges and nonplanar impacts are studied over a range of impact conditions. The response of 1 mm by 1 mm active area PVDF gauges under precisely controlled compressed-gas gun impacts shows highly reproducible results to pressures of 20 GPa. For the PVDF gauge which is placed within 12 microns of the impact surface and under approximately planar loading with small detonator flyer plates, PVDF gauge signals appear to be reduced by about 15 percent compared to the compressed-gas gun loading response. For highly nonplanar flyer impacts the PVDF signals are reduced by about 35 percent. In all stress environments, high quality, time-resolved current pulses are observed. DOE

N89-27145# Lawrence Livermore National Lab., CA.
SENSORS FOR IN SITU MONITORING OF ELASTIC PROPERTIES
D. Olness 11 Apr. 1989 11 p
(Contract W-7405-eng-48)
(DE89-012795; UCRL-53924) Avail: NTIS HC A03/MF A01

Preliminary experiments have been carried out to examine an invention for in situ monitoring of elasticity. The elasticity monitor consists of a piezoelectric material placed in contact with an elastomer to form an oscillating system. Monitoring the resonant frequency, amplitude, or Q value of this system provides a measure of elasticity of the elastomer. The experiments are described and their results and implications discussed. DOE

N89-27146# Quaid-i-Azam Univ., Islamabad (Pakistan). Dept. of Physics.
APPLICATIONS OF HOLOGRAPHY TO PATTERN RECOGNITION AND OPTICAL MEMORIES Thesis
Shakil-Ur Rehman 1988 92 p
(PB89-174668) Avail: NTIS HC A05/MF A01 CSCL 20F

Holography and its applications to optical associative memories, pattern recognition and three dimensional imaging are discussed. An optical holographic analogue of Hopfield's neural network model is also presented. Using Fourier transform holograms, limited shift invariant associative memories have been fabricated. A pattern recognition scheme is modified and is implemented optically using a simple and different way of achieving thresholding in the correlation domain. Author

N89-27147# Environmental Protection Agency, Research Triangle Park, NC. Atmospheric Research and Exposure Assessment Lab.
EVALUATION OF A FTIR (FOURIER TRANSFORM INFRARED SPECTROMETER) MOBILE SOURCE MEASUREMENT SYSTEM Status Report
John E. Sigsby, Jr., Alex McArver, and Richard Snow (Northrop Services, Inc., Research Triangle Park, NC.) Apr. 1989 45 p
(Contract EPA-68-02-4443)
(PB89-180822; EPA/600/3-89/036) Avail: NTIS HC A03/MF A01 CSCL 14B

An initial evaluation was made of a prototype Fourier transform infrared spectrometer on its ability to measure mobile source emissions. This prototype represents the commercialization of research technology developed by the Ford Motor Co. The system utilizes a Mattson Instruments Co. interferometer coupled to a Masscomp computer. The required software is still incomplete. This has resulted in the inability to correct errors or optimize results. Unreliability of both hardware and software is a major shortcoming of the system. When operating properly, the system measures carbon dioxide, nitric oxide, and formaldehyde accurately, both when compared to bag analysis and on direct point-by-point comparisons with real-time data. Completion of the evaluation awaits the final software translations and improvements in reliability. GRA

N89-27148# California Univ., Berkeley. Lawrence Berkeley Lab. Center for X-Ray Optics.
THEORY OF X-RAY HOLOGRAPHY INCLUDING PHASE AND AMPLITUDE CONTRAST AND FINITE TRANSFER FUNCTIONS
M. R. Howells Jan. 1989 14 p
(Contract DE-AC03-76SF-00098)
(DE89-012835; LBL-26953) Avail: NTIS HC A03/MF A01

We present the theory in broadly the same way as for visible holography, specializing to the Gabor, in-line case with plane-wave illumination, but allowing phase and amplitude contrast and a fairly general transfer function. Much of this theory is treated by a number of earlier authors but none with the particular choice of issues that we wish to address. These are those mentioned plus numerical reconstruction from a digitized hologram and of course application

to the soft X-ray spectral range. For simplicity and clarity, we consider first an amplitude and phase object consisting of a single, on-axis pixel and an ideal, perfect transfer function. DOE

N89-27149# California Univ., Berkeley. Lawrence Berkeley Lab. Center for X-Ray Optics.
X-RAY HOLOGRAPHY: A HISTORY
Chris Jacobsen Apr. 1989 15 p Presented at the Conference on X-ray Microscopy in Biology and Medicine, Tochigi, Japan, 25-27 Aug. 1988 Submitted for publication
(Contract DE-AC03-76SF-00098)
(DE89-012983; LBL-27040; CONF-8808233-1) Avail: NTIS HC A03/MF A01

X-ray holographic microscopy has recently reached a milestone in its development by producing images of biological specimens at sub-micron resolution. However, X-ray holography is by no means a new subject, and it is the purpose of this article to review the history of experimental activity in this field (theoretical activities will also be mentioned). DOE

N89-27150# Lawrence Livermore National Lab., CA.
AN INSTANTANEOUS CCN (CLOUD CONDENSATION NUCLEUS) SPECTROMETER
J. G. Hudson (Desert Research Inst., Reno, NV.) May 1989 42 p
(Contract W-7405-eng-48)
(DE89-014807; UCRL-21154) Avail: NTIS HC A03/MF A01

A thermal gradient diffusion cloud chamber with a supersaturation field which increases along the path of the flow of sample is used as a cloud condensation nucleus (CCN) spectrometer. The CCN spectrum is derived from the final droplet distribution which has been determined to be related to the nucleus critical supersaturation based on routine calibration procedures using laboratory-produced monodisperse salt particles. The instrument is compared against a previously reported CCN counter on natural laboratory produced aerosol and against an absolute CN counter on the monodisperse aerosol. Preliminary results of atmospheric measurements are given. This device produces a CCN spectrum over the entire useful range of interest for cloud physics (0.01 to 1 percent supersaturation). More than 40 channels of resolution over this range are simultaneously provided. Data can be collected on a continuous basis for integration times as short as 2 seconds. The instrument has obtained data from four different airborne platforms, as well as from a mobile surface platform. The large number of channels allows the CCN spectrum to be displayed differentially instead of the usual cumulative display which is traditionally used in cloud physics. DOE

N89-27151*# National Aeronautics and Space Administration. Langley Research Center, Hampton, VA.
THERMAL ENCLOSURES FOR ELECTRONICALLY SCANNED PRESSURE MODULES OPERATING IN CRYOGENIC ENVIRONMENTS
Michael Mitchell and Bradley S. Sealey Aug. 1989 16 p
(NASA-TM-101635; NAS 1.15:101635) Avail: NTIS HC A03/MF A01 CSCL 14B

Specific guidelines to design, construct, and test ESP thermal enclosures for applications at cryogenic temperatures are given. The enclosures maintain the ESP modules at a constant temperature (10 C plus or minus 1 C) to minimize thermal zero and sensitivity shifts, to minimize the frequency of expensive on-line calibrations, and to avoid adverse effects on tunnel and model boundary layers. The enclosures are constructed of a rigid closed-cell foam and are capable of withstanding the stagnation pressures to 932kPa (135 psia) without reduction in thermal insulation properties. This construction procedure has been used to construct several thermal packages which have been successfully used in National Transonic Facility. Author

N89-27152*# Miletus Associates, Inc., Albuquerque, NM.
FILM ANNOTATION SYSTEM FOR A SPACE EXPERIMENT
W. R. Browne and S. S. Johnson Jul. 1989 124 p
(Contract NAS3-25055)
(NASA-CR-185114; NAS 1.26:185114) Avail: NTIS HC A06/MF A01 CSCL 14E

This microprocessor system was designed to control and annotate a Nikon 35 mm camera for the purpose of obtaining photographs and data at predefined time intervals. The single STD BUSS interface card was designed in such a way as to allow it to be used in either a stand alone application with minimum features or installed in a STD BUSS computer allowing for maximum features. This control system also allows the exposure of twenty eight alpha/numeric characters across the bottom of each photograph. The data contains such information as camera identification, frame count, user defined text, and time to .01 second. Author

N89-27153# Babcock and Wilcox Co., Alliance, OH. Research and Development Div.
FUNDAMENTAL STUDIES OF THE CAVITY FLOWMETER Final Report, Oct. 1986 - Dec. 1988
Raymond K. Kim 15 Apr. 1989 78 p
(Contract GRI-5086-260-1296)
(PB89-188825; RDD:88:4744-24-01:01; GRI-89/0064) Avail: NTIS HC A05/MF A01 CSCL 14B

Self-sustaining fluid dynamic oscillations, known as cavity oscillations, have been known to cause undesirable noise, vibration and structural damage. The objective of the R and D program is to establish the feasibility of designing a new type of volumetric, gas flowmeter based on the cavity oscillation as the operating principle. Experiments were conducted with a 3-inch and a 4-inch cavity flowmeter during 1987 and 1988 covering the Reynolds number range from 5 x 10(4) to 7 x 10(6) and pressures up to 800 psig. The test data show that for cavities of certain geometry the frequency of cavity oscillation is a linear function of gas velocity and is independent of pressure and temperature. Accordingly, the data acquired in the program strongly support the conclusion that practical cavity flowmeters with digital outputs and without any moving parts can be built for natural gas pipelines operating at high pressures. A field demonstration of a prototype at a natural gas metering station is recommended as a means to bridge the gap between the R and D program and the eventual commercialization of the product. Author

N89-27154# Sandia National Labs., Albuquerque, NM.
NOVEL APPLICATIONS OF THE FIELD ION MICROSCOPE AND ATOM-PROBE
G. L. Kellogg 1989 24 p Presented at the Microbeam Analysis Society Meeting, Asheville, NC, 16 Jul. 1989
(Contract DE-AC04-76DP-00789)
(DE89-008684; SAND-89-0589C; CONF-890748-4) Avail: NTIS HC A03/MF A01

Introduced in 1951 and 1966 respectively, the field ion microscope and atom-probe mass spectrometer can hardly be considered new or emerging microprobes. Over the years, the ability to use these instruments to examine the structure and composition of various materials at the atomic level has been well established. However, recent advances in more conventional microanalytical techniques, particularly progress toward a higher degree of spatial resolution, has created renewed interest in all techniques capable of analysis on a very fine scale. Also, there has been an increased emphasis over the past several years in the application of the field ion microscope and atom-probe to problems of greater general interest in surface and materials science. It is therefore not totally inappropriate to discuss the field ion microscope and atom-probe within the context of emerging microprobes. The intent of this paper is to familiarize the reader with the techniques of field ion microscopy and atom-probe mass spectroscopy and describe several recent applications which demonstrate some of their unique attributes. DOE

N89-27155*# Brookhaven National Lab., Upton, NY. Dept. of Applied Science.
X-RAY MICROSCOPY USING SYNCHROTRON RADIATION
K. W. Jones, B. M. Gordon, A. L. Hanson, J. G. Pounds, M. L.

Rivers, George Schidlovsky, J. V. Smith, Per Spanne, and S. R. Sutton (Chicago Univ., IL.) 1989 18 p Presented at the 24th Microbeam Analysis Society Meeting, Asheville, NC, 16-21 Jul. 1989
(Contract NAG9-109; DE-AC02-76CH-00016; NIH-P41RR01838; NSF EAR-86-18346)
(NASA-CR-184800; NAS 1.26:184800; DE89-010569; BNL-42582; CONF-890748-9) Avail: NTIS HC A03/MF A01 CSCL 14B

The system for X-ray microscopy now being developed at the X-26 beam line of the Brookhaven National Synchrotron Light Source (NSLS) is described here. Examples of the use of X-ray microscopy for trace element geochemistry, biology and medicine, and materials investigations are given to emphasize the scientific applications of the technique. Future directions for the improvement and further development of the X-26 microscope and of the X-ray microscopy field in general are discussed. DOE

N89-27156# Oak Ridge National Lab., TN. Metals and Ceramics Div.
STRUCTURAL INTEGRITY EVALUATION BASED ON AN INNOVATIVE FIELD INDENTATION MICROPROBE
Fahmy M. Haggag, Randy K. Nanstad, and D. N. Braski 1989 8 p Presented at the Joint ASME/JSME Pressure Vessel and Piping Conference, Honolulu, HI, 23-27 Jul. 1989
(Contract DE-AC05-84OR-21400)
(DE89-010840; CONF-890721-25) Avail: NTIS HC A02/MF A01

A brief description is given for a field indentation microprobe (FIM) apparatus which was developed to evaluate, nondestructively in situ, the integrity of metallic structures. The FIM consists of an automated ball indentation (ABI) unit for determining the mechanical properties (yield strength, flow properties, fracture toughness, etc.) and a nondestructive evaluation (NDE) unit (consisting of ultrasonic transducers and a video camera) for determining the physical properties such as crack size, material pile-up around indentation, and residual stress presence and orientation. The laboratory version used here performs only ABI testing. Results of the laboratory version of the FIM tests on unirradiated and irradiated A212 grade B pressure vessel steel are discussed in this paper. Excellent agreement was obtained between yield strength and flow properties (true-stress/true-plastic-strain curve) measured by the ABI tests and those of uniaxial tensile tests. DOE

N89-27157# Technische Univ., Munich (Germany, F.R.). Lehrstuhl fuer Elektrische Messtechnik.
INFRARED TEMPERATURE MEASUREMENT WITH SELF REGULATING EMISSION RATIO Ph.D. Thesis [INFRAROT-TEMPERATURMESSUNG MIT SELBSTTAETIGER BERUECKSICHTIGUNG DES EMISSIONSGRADS]
V. Tank 1987 167 p In GERMAN
(ETN-89-94654) Avail: NTIS HC A08/MF A01

A temperature measuring procedure without contact, based on infrared radiation pyrometers is described. A self-regulating emission ratio multispectral pyrometer able to register three parameters related to the spectral composition of a non-black object: object temperature, emission ratio, and object environmental temperature was developed. Self-calibrating factors depending on wavelength via computer program simulation are described. Commercial infrared detector components are investigated for their adaptability to requirements. ESA

N89-27158# Rome Univ. (Italy). Dipartimento di Fisica.
TESTS OF LOW RESISTIVITY ELECTRODELESS STREAMER TUBES
F. Ferrarotto and B. Stella 27 Oct. 1988 31 p
(Nota-Interna-922; ETN-89-94741) Avail: NTIS HC A03/MF A01

As an option for the tail catcher of the hadronic calorimeter and the muon chambers of the H1 detector at HERA, a solution with plastic streamer tubes with low resistivity varnish to overcome the difficulties originating from the nonuniformity of the normally used high resistivity varnish of graphite is discussed. In order to allow for top and bottom inductive readout, only the side walls were painted with 1 to 2 K Ohm/surface resistivity. A set of these bottomless and coverless low resistivity streamer tubes, after laboratory tests, were arranged in chambers with longitudinal and transverse strip digital readout or pad analog readout and tested at the CERN SpS with high energy pion beams in strict correlation with usual high resistivity coverless streamer tubes to compare their performances under experimental conditions. The results are satisfactory for tracking and calorimetric purposes. ESA

N89-27159# Rome Univ. (Italy). Dipartimento di Fisica.
THE DIAGONAL STRIP SYSTEM IN THE MACRO EXPERIMENT [IL SISTEMA DI STRIP DIAGONALI DELL'ESPERIMENTO MACRO]
M. DeVicenzi, P. Lipari, G. Martellotti, and G. Pellizzoni 18 Nov. 1988 18 p In ITALIAN Original contains color illustrations
(Nota-Interna-924; ETN-89-94743) Avail: NTIS HC A03/MF A01

The Macro scintillation counter modular system with streamer tubes and track-etch detectors is presented, and the characteristics, manufacturing, and assembling of its pick-up strips are described. The strips are composed of thin conducting plates 31 mm long, spaced 2.6 mm apart, and bonded on a 1 mm polyvinyl chloride (PVC) ribbon with a grounded metal surface on the other side of the ribbon. The manufacturing is done by bonding the aluminum elements on the PVC ribbon. ESA

36 LASERS AND MASERS

Includes parametric amplifiers.
For related information see also *76 Solid-State Physics*.

N89-27160 Department of the Navy, Washington, DC.
LASER DYES DERIVED FROM BIMANES Patent
Theodore G. Pavlopoulos, inventor (to Navy) and Joseph H. Boyer, inventor (to Navy) 17 Jan. 1989 5 p Filed 20 Nov. 1987
(AD-D013994; US-Patent-4,799,230; US-Patent-Appl-SN-125646; US-Patent-Class-372-53) Avail: US Patent and Trademark Office CSCL 09/3

A new class of laser dyes has a lasing compound syn (R1,R2) bimanes that shows efficient laser action under flashlamp excitation. In the laser action spectral region there is little or no triplet-triplet absorption so that laser efficiencies in the range of 1 to 3 percent can be provided. Good solubility in many solvents (especially water) good photochemical stability and simplicity of preparation are inherent in this new lasing media. GRA

N89-27161# Iowa State Univ. of Science and Technology, Ames.
PARTIAL SUPPORT OF THE 3RD INTERNATIONAL LASER SCIENCE CONFERENCE HELD IN ATLANTIC CITY, NEW JERSEY ON 1-4 NOVEMBER 1987 Final Report, 15 Jul. 1987 - 14 Jul. 1988
William C. Stwalley Dec. 1988 3 p Conference held in Atlantic City, NJ, 1-4 Nov. 1987
(Grant AF-AFOSR-0319-87; AF Proj. 2301)
(AD-A206812; AFOSR-89-0413TR) Avail: NTIS HC A02/MF A01 CSCL 09/3

The annual International Laser Science Conferences have been established to survey the core laser science areas including lasers and their properties, spectroscopy, laser-induced processes, and a selection of laser applications. This meeting is a Topical Conference of the American Physical Society (APS) and is also the annual meeting of the APS Topical Group on Laser Science. Earlier ILS Conferences were held in Dallas in 1985 (ILS-I) and in Seattle in 1986 (ILS-II). ILS-III was held in Atlantic City, New Jersey, November 1-4, 1987, with the co-sponsorship of the Optical Society of America. GRA

N89-27162# Science Research Corp., Somerville, MA.
COMPACT, LIGHTWEIGHT CO2 LASERS FOR SDIO APPLICATIONS Final Report, 30 Sep. 1988 - 31 Mar. 1989
Jonah Jacob 11 Apr. 1989 108 p

(Contract N00014-88-C-0727)
(AD-A207052; SRL-07-F-1989) Avail: NTIS HC A06/MF A01 CSCL 09/3

During the past decade, substantial investments were made in the development of gas discharge pumped CO2 lasers for military and civilian applications. Compact, lightweight CO2 lasers for airborne and spaced based radar applications directed toward target ranging, imaging, and discrimination are discussed. These CO2 laser systems are being developed under the SDIO Lowkater Program, in the Airborne Laser Experiment (ALE) Program by the Army/SDC and in Lincoln Laboratory's space based CO2 laser radar research and development program. The three major components of a CO2 laser radar are the laser head and flow loop, the pulsed power system and the optics and beam control system. A self-sustained discharge concept that should result in the stable and efficient extraction of large specific energies (50 J/liter atmosphere) for pulse lengths as long as 100 micro s is discussed. GRA

N89-27163 Department of the Air Force, Washington, DC.
VARIABLE AREA MANIFOLDS FOR RING MIRROR HEAT EXCHANGERS Patent
Albert Eng, inventor (to AF) and Donald R. Senterfitt, inventor (to AF) 10 May 1988 6 p Filed 14 Oct. 1986
(AD-D014050; US-Patent-4,743,104; US-Patent-Appl-SN-917933; US-Patent-Class-350-610) Avail: US Patent and Trademark Office CSCL 09/3

A laser ring mirror assembly is disclosed which supports and cools an annular ring mirror of a high powered laser with a cooling manifold which has a coolant flow design which is intended to reduce thermal distortions of the ring mirror by minimizing azimuthal variations in temperature around its circumference. The cooling manifold has complementary pairs of cooling passages each of which conduct coolant in opposite flow directions. The manifold also houses adjusters which vary the depth between the annular ring mirror and each cooling, and which vary the flow area of the cooling passage to produce a control over the cooling characteristics of the cooling manifold. GRA

N89-27164 Department of the Air Force, Washington, DC.
HIGH ENERGY LASER TARGET PLATE Patent
Charles R. LaMar, inventor (to AF) 10 Jan. 1989 5 p Filed 28 May 1987
(AD-D014053; US-Patent-4,797,555; US-Patent-Appl-SN-055092; US-Patent-Class-250-336.1) Avail: US Patent and Trademark Office CSCL 14/2

This patent discloses an apparatus for determining the intensity profile of a high energy laser beam. A target plate having a temperature sensitive paint on the rear surface thereof has its front surface irradiated by the laser beam under analysis. A high speed camera records the isothermal lines formed when the temperature sensitive paint changes from its solid phase to its liquid phase. Iso-intensity lines are then calculated from the recorded isothermal lines. GRA

N89-27165# Thermo Electron Technologies Corp., San Diego, CA.
TRANSVERSE PUMPING WITH DIODE LASERS
E. B. Treacy 6 Jan. 1989 86 p
(Contract N00014-87-C-2412)
(AD-A207261; TTC-1529-R) Avail: NTIS HC A05/MF A01 CSCL 09/3

The transverse pumping of a cylindrical laser rod such as YAG by a set of diode laser arrays equally spaced in angle around the rod has been analyzed using both geometrical and wave optics. Between the pump sources and the laser rod there may be an arbitrary number of concentric media, transparent to the pump light; and in addition modification of the diode laser radiation patterns will require other optical components. The analysis accommodates both of these complications, even when the optics in front of the diodes do not image point sources to points. It is sufficient to be able to describe the intensity and ray directions in finite apertures concentric with the rod. One result of the cylindrical geometry is the formation of caustics which have infinite intensity in the geometrical optics approximation; and it is necessary to develop a wave optics theory to predict the intensity in the neighborhood of the caustic edge of the illuminated region inside the laser rod. The wave theory first uses the geometrical optics method to calculate the amplitude and phase just inside the rod's surface, which serves then as an aperture distribution function describing the source of Huygens wavelets in the computation of a diffraction integral. GRA

N89-27166# Autonomous Technologies, Orlando, FL.
DEEP SPACE LADAR, PHASE 1 Final Report, Oct. 1988 - Mar. 1989
Randy W. Frey, Greg Rawlins, Neil Zepkin, and John Bohlin 27 Mar. 1989 119 p
(Contract DASG60-88-C-0076)
(AD-A207454) Avail: NTIS HC A06/MF A01 CSCL 17/5

A pseudo-ranging laser radar (PRLADAR) concept is proposed to provide extended range capability to tracking LADAR systems meeting the long-range requirements of SDI mission scenarios such as the SIE midcourse program. The project will investigate the payoff of several transmitter modulation techniques and a feasibility demonstration using a breadboard implementation of a new receiver concept called the Phase Multiplexed Correlator (PMC) will be accomplished. The PRLADAR concept has specific application to spaceborne LADAR tracking missions where increased CNR/SNR performance gained by the proposed technique may reduce the laser power and/or optical aperture requirement for a given mission. The reduction in power/aperture has similar cost reduction advantages in commercial ranging applications. A successful Phase 1 program will lay the groundwork for a quick reaction upgrade to the AMOS/LASE system in support of near term SIE measurement objectives. GRA

N89-27167# California Inst. of Tech., Pasadena.
HIGH POWER SEMICONDUCTOR LASER SOURCES Final Report
Amnon Yariv 1989 93 p
(Contract N00014-85-K-0211)
(AD-A207569) Avail: NTIS HC A05/MF A01 CSCL 20/12

The main purpose of the research was to design and fabricate a surface emitting semiconductor laser based on multi quantum well amplification. During the contract period we have succeeded in improvement of the basic quantum well active medium so as to result in maximum gain for a given inversion density and have analyzed the fabrication of GaAs/GaAlAs multilayer dielectric reflectors for providing the optical feedback to the surface emitting semiconductor laser. We have also made significant progress in the development of diffusion techniques to provide the p and n regions adjacent to the active region for carrier injection. With continued effort and support we should stand a fair chance of realizing an operating surface emitting semiconductor laser. GRA

N89-27168# Department of the Air Force, Washington, DC.
STATIC PERIODIC FIELD DEVICE FOR FREE ELECTRON LASER Patent Application
Brian S. Ahern, inventor (to AF) 6 Dec. 1988 13 p
(AD-D014125; US-Patent-Appl-SN-280607) Avail: NTIS HC A03/MF A01 CSCL 09/3

A static periodic field device for a free electron laser has a plurality of holes there through to allow the interaction of electrons flowing there through to interact with either an electric or a magnetic fields as desired. The device is composed of a plurality of conducting layers separated by insulating layers and appropriately connected to provide either an electric or a magnetic field therein. The separation of the conducting layers determines the radiated energy wavelength. GRA

N89-27169# California Univ., Berkeley. Lawrence Berkeley Lab. Accelerator and Fusion Research Div.
ELEMENTS OF A REALISTIC 17 GHz FEL/TBA DESIGN
D. B. Hopkins, K. Halbach, E. H. Hoyer, A. M. Sessler, and E. J.

Sternbach Jan. 1989 14 p Presented at the Advanced Accelerator Concepts Workshop, Lake Arrowhead, CA, 9-13 Jan. 1989
(Contract DE-AC03-76SF-00098)
(DE89-013427; LBL-27059; CONF-890197-9) Avail: NTIS HC A03/MF A01

Recently, renewed interest in a free electron laser (FEL) version of a two-beam accelerator (TBA) has prompted a study of practical system and structure designs for achieving the specified physics goals. This paper presents elements of a realistic design for an FEL/TBA suitable for a 1 TeV, 17 GHz linear collider. DOE

N89-27170# California Univ., Berkeley. Lawrence Berkeley Lab. Materials and Chemical Sciences Div.
REPORT OF THE WORKSHOP ON SCIENTIFIC OPPORTUNITIES FOR INFRARED FREE-ELECTRON LASERS, VOLUME 1
Feb. 1989 40 p Workshop held in Berkeley, CA, 31 Oct. - 1 Nov. 1988 Prepared in cooperation with BNL, Upton, NY
(Contracts DE-AC03-76SF-00098; DE-AC02-76CH-00016)
(DE89-012836; LBL-26783-Vol-1; CONF-8810126-Vol-1) Avail: NTIS HC A03/MF A01

With the characteristics of very broad wavelength coverage, high average and peak power, and variable time structure, the free-electron laser (FEL) shows great promise of having a major impact in many areas of science and technology - an impact similar to those of the ultrahigh vacuum system, the computer, and the conventional laser. As a technology, the FEL has reached an advanced development stage. There are several FELs in operation and several more in the design stage. However, as a tool for scientific research and applications it is still very much in its infancy. Now is an appropriate time to define the FELs that are needed to perform the science that should and can be done, particularly with the characteristics that are unique to FELs. A workshop co-sponsored by Lawrence Berkeley Laboratory and Brookhaven National Laboratory was held on October 31 to November 1, 1988 with this goal in mind. The workshop focused on the infrared region where there is a scarcity of intense sources and where the FEL technology is most mature. The purposes of the workshop were: to review the performance of existing infrared FELs; to identify the significant scientific experiments that could be done, as well as those that are being done, with these FELs; and to define the FEL characteristics that are required to realize these possibilities and how they can be achieved. DOE

N89-27171# Los Alamos National Lab., NM.
RECENT EXPERIMENTS WITH THE FREE-ELECTRON LASER AT LOS ALAMOS
Donald W. Feldman and Roger W. Warren 1989 4 p Presented at the 13th Particle Accelerator Conference, Chicago, IL, 20-23 Mar. 1989
(Contract W-7405-eng-36)
(DE89-013469; LA-UR-89-1838; CONF-890335-183) Avail: NTIS HC A02/MF A01

Improvements in the operational characteristics of the Los Alamos free-electron laser have produced experimental results in reasonable agreement with theory and simulation. The results of these experiments will be described. DOE

N89-27172# Lawrence Livermore National Lab., CA.
PASSIVE OPTICAL LOSSES IN LASER GLASS
J. A. Caird, F. P. Milanovich, N. D. Nielsen, H. T. Powell, J. E. Marion, A. J. Pertica, and J. N. Roe 11 May 1989 21 p Presented at the Conference on Lasers and Electro Optics, Baltimore, MD, 24-29 Apr. 1989
(Contract W-7405-eng-48)
(DE89-013784; UCRL-100012; CONF-890423-10) Avail: NTIS HC A03/MF A01

Background absorption, scattering, and stress-birefringence loss measurements are reported for phosphate laser glass amplifier media used in fusion and high average power laser systems. Typical background absorption and stress birefringence losses were found to be comparable, and on the order of 10 (-3) cm (-1). Scattering losses, on the other hand, were typically found to be more than an order of magnitude smaller. The results indicate that improvements in the cost/performance ratio can be achieved by reducing background absorption of birefringence, and possibly also through the use of cheaper polishing techniques. DOE

N89-27173# Maryland Univ., College Park. Lab. for Plasma Research.
FREE ELECTRON LASERS WITH SMALL PERIOD WIGGLERS Progress Report, 15 Sep. 1988 - 14 Sep. 1989
T. M. Antonsen, Jr., J. H. Booske, W. W. Destler, V. L. Granatstein, I. D. Mayergoyz, and E. Ott May 1989 57 p
(Contract DE-FG05-87ER-52147)
(DE89-014715; DOE/ER-52147/2) Avail: NTIS HC A04/MF A01

Progress of research on a short period wiggler (SPW) free electron laser (FEL) with a sheet electron beam is reviewed. Most of the recent work has concentrated on addressing thermal engineering issued in the device. This particular emphasis was particularly stimulated by an evaluation by Panel XXI for the Magnetic Fusion Advisory Committee which stated that there are serious thermal management engineering uncertainties in the electron gun, the microwave cavity, and the wiggler that will need to be addressed for CW operation. In the panel's judgment, these thermal problems are likely to be insurmountable for fusion applications. In fact, recent experimental and theoretical results challenge this judgment. For example, our most recent conceptual designs involve small-to-negligible RF losses in the cavity walls. In addition, we have convincingly established that for electron beams of quality achievable with thermionic Pierce guns, body currents should be negligible to nonexistent, thus ensuring a thermally stable cavity. These discoveries, as well as other research progress, are reviewed in detail in the following report. Plans are described for a pulsed (100 ns) proof-of-principle lasing experiment to be conducted during the remainder of this fiscal year. In addition, we present a revised statement of work and budget for the follow-on year of the current grant. These proposed tasks will address the remaining risk issues for an ERCH source based on the SPW sheet-beam FEL. Upon the completion of those tasks, sufficient information will exist to confidently assess the feasibility of the proposed concept. DOE

N89-27174# CD Metrology, Inc., Germantown, MD.
NARROW-ANGLE LASER SCANNING MICROSCOPE SYSTEM FOR LINEWIDTH MEASUREMENTS ON WAFERS
Diane Nyyssonen (National Inst. of Standards and Technology, Gaithersburg, MD.) Apr. 1989 111 p
(PB89-189344; NISTIR-88/3808) Avail: NTIS HC A06/MF A01 CSCL 20E

The integrated-circuit industry in its push to finer and finer line geometries approaching submicrometer dimensions has created a need for ever more accurate and precise feature-size measurements to establish tighter control of fabrication processes. In conjunction with the NBS Semiconductor Linewidth Metrology Program, a unique narrow-angle laser measurement system was developed. The report describes the theory, optical design, and operation of the system and includes computer software useful for characterizing the pertinent optical parameters and images for patterned thin layers. For thick layers, the physics is more complex and only elements of the theory are included. For more detail the reader is referred to several related reports listed in the references. Author

N89-27175# California Univ., Berkeley. Lawrence Berkeley Lab. Accelerator and Fusion Research Div.
PROSPECTS FOR THE FEL (FREE ELECTRON LASER)
Andrew M. Sessler Apr. 1989 20 p Presented at the CERN Accelerator School, Chester, UK, 6 Apr. 1989
(Contract DE-AC03-76SF-00098)
(DE89-012998; LBL-27034; CONF-8904228-1) Avail: NTIS HC A03/MF A01

The future for FELs depends upon the very large number of applications which is envisioned for them. These grow out of the

FEL extensive range of wavelengths, tunability, and high power capability. High power requires demonstration of optical guiding. Tunability has already been demonstrated. And the effort to extend the range of wavelengths is ever ongoing. The future will also bring more work on gas-loaded FELs, on electromagnetic wigglers, and on harmonic generation. Observation of various new effects, a few of which will be described, are yet to be seen. Finally, a list of various FEL projects around the world will be given. DOE

N89-27176# Institut Franco-Allemand de Recherches, Saint-Louis (France).
BATTERY-DRIVEN MINIATURE LDA SYSTEM WITH SEMICONDUCTOR LASER DIODE
S. Damp 7 Jun. 1988 11 p Presented at the 4th International Symposium on Application of Laser Anemometry to Fluid Mechanics, Lisbon, Portugal, 11-14 Jul. 1988 Previously announced in IAA as A89-33366
(ISL-CO-214/88; ETN-89-94852) Avail: NTIS HC A03/MF A01

A one-component miniature system with dimensions of 11 by 4 by 4 cubic centimeters for laser-Doppler anemometry (LDA) is described. As power supply a 12V battery or any other source with the capability to drive a current up to 200mA can be used. The system contains the whole electronics to drive the used laser diode is a safe way. The electronics to amplify and buffer the LDA-signal which is received by a PIN-diode is included. The output of the system can directly fit a filterbank for example. Possible applications in rough environments are mentioned. Measurements show the reliability of the system. ESA

N89-27177# Defense Intelligence Agency, Washington, DC. Directorate for Scientific and Technical Intelligence.
BIBLIOGRAPHY OF SOVIET LASER DEVELOPMENTS, NO. 92, NOVEMBER - DECEMBER 1987
22 Dec. 1988 153 p
(AD-A207794; DIA-DST-2700Z-006-88) Avail: NTIS HC A08/MF A01 CSCL 09/3

This bibliography has been compiled under an interagency agreement as a continuing effort to document current Soviet-bloc developments in the quantum electronics field. It includes all significant laser-related articles received by the Agency in that interval. The bulk of the entries come from the approximately 30 periodicals which are known to publish the most significant findings in Soviet laser technology. Citations from the Soviet reference journals (journals of abstracts) are also included. Laser items from the popular or semipopular press are generally omitted. Citation topics include: solid state lasers, liquid lasers, gas lasers, chemical lasers, laser components, nonlinear optics, and laser applications. GRA

37 MECHANICAL ENGINEERING

Includes auxiliary systems (nonpower); machine elements and processes; and mechanical equipment.

N89-27178# Northern Research and Engineering Corp., Woburn, MA.
HIGH PERFORMANCE INTERCOOLED AND RECUPERATED GAS TURBINE Topical Report, Sep. 1986 - Oct. 1988
James E. Staudt Oct. 1988 206 p
(Contract GRI-5086-233-1436)
(PB89-152284; NREC-1626; GRI-88/0274) Avail: NTIS HC A10/MF A01 CSCL 13I

A preliminary design for a Dresser-Rand DC990 industrial gas turbine engine modified for intercooling and recuperation (ICR) is presented. The DC990 was selected because its configuration is amenable to intercooling and because it is in the power range of interest. Based upon preliminary estimates, engine power output will increase from 6000 bhp to 8400 bhp at design point. Design point specific fuel consumption will be reduced 26 percent to a heat rate of 6300 BTU/bhp-hr. Moreover, the DC990 ICR engine maintains a high thermal efficiency during part-load operation. These performance improvements are achievable using proven, low-risk technology. The resulting combination of low fuel consumption and low maintenance costs makes the DC990 ICR gas turbine engine an attractive engine package for several applications. GRA

N89-27179 Department of the Air Force, Washington, DC.
SELF-LOCKING OUTER AIR SEAL WITH FULL BACKSIDE COOLING Patent
George Liang, inventor (to Air Force) 21 Jun. 1988 6 p Filed 12 May 1986 Supersedes N87-12880 (25 - 4, p 494)
(AD-D013975; US-Patent-4,752,184; US-Patent-Appl-SN-861908)
Avail: US Patent and Trademark Office CSCL 21/5

An air seal assembly for a gas turbine engine comprising a full ring cover plate and seal segment attached to impingement boxes is described. The impingement boxes have counter mounted hooks that interlock with a turbine flange and cover plate to secure the seal assembly. Holes in the impingement boxes direct cooling air to the entire backside of seal. Seals are mounted to the impingement boxes by pedestals that are positioned to enhance seal flexibility since axial edges are unrestrained. GRA

N89-27180 Department of the Air Force, Washington, DC.
VANE PLATFORM SEALING AND RETENTION MEANS Patent
George A. Bonner, inventor (to AF) and James E. Fisher, inventor (to AF) 7 Jun. 1988 6 p Filed 12 May 1986 Supersedes N87-12881 (25 - 04, p 494)
(AD-D013980; US-Patent-4,749,333; US-Patent-Appl-SN-861905)
Avail: US Patent and Trademark Office CSCL 21/5

An improved vane platform feather seal is disclosed for use in turbine engines. This feather seal contains a flat, thin feather seal, which is attached by adhesive to ease assembly to an L-shaped retainer plate to result in a combined thickness of 0.032 inches. This new seal may be used to replace the inner vane platform seals which are currently used in F-100 turbine engines, which have a history of not bending easily to conform to seal slots. The new seal provides improved platform sealing without loss of platform retention in the event of vane burn through. GRA

N89-27181# University of Central Florida, Orlando. Dept. of Mechanical Engineering and Aerospace Sciences.
DYNAMIC ANALYSIS OF FLEXIBLE MECHANISMS BY A COMBINED TRANSFER MATRIX FINITE ELEMENT METHOD Final Report
Levent Kitis 8 Dec. 1988 98 p
(Grant NSF MEA-84-21249)
(PB89-160865; NSF/ENG-88026) Avail: NTIS HC A05/MF A01 CSCL 13I

Transfer matrices are used in the dynamic analysis of planar elastic mechanisms. Mechanism motion is discretized by dividing the motion into a finite number of intervals over which the mechanism is considered to be an instantaneous structure with constant geometry. Transfer matrix methods are then used to calculate the natural frequencies and corresponding mode shapes of the instantaneous structure. A transfer matrix relating the continuous, non-zero components of the state vector across a pin joint is developed. An elastic four bar mechanism and a crank slider mechanism with a rigid crank and elastic connecting rod are analyzed using lumped mass models. Results of the four bar mechanism analysis show good correlation with results obtained by others using finite element methods. GRA

N89-27182# National Inst. of Standards and Technology, Gaithersburg, MD. National Engineering Lab.
INTERACTIONS BETWEEN THE NATIONAL INSTITUTE OF STANDARDS AND TECHNOLOGY AND THE AMERICAN SOCIETY OF MECHANICAL ENGINEERS Report, 1982 - 1989
Gail K. Ehrlich Feb. 1989 32 p
(PB89-172563; NISTIR-89/4038) Avail: NTIS HC A03/MF A01 CSCL 13B

Examples of interactions between the National Institute of Standards and Technology (NIST) and the American Society of Mechanical Engineers (ASME) over the past several years are highlighted. It is meant to be representative, not all-inclusive. The

interactions are organized by discipline in the following categories: conferences, committee memberships and contribution to standards, editors, publications which are designed to disseminate NIST's most recent technical advances and to learn of the technical challenges facing engineers in industry. GRA

N89-27183# Westinghouse Electric Corp., Orlando, FL. Power Systems Div.
ADVANCED COAL-FUELED GAS TURBINE SYSTEMS, VOLUME 2 Annual Technical Progress Report
Jul. 1988 80 p
(Contract DE-AC21-86MC-23167)
(DE89-000954; DOE/MC-23167/2678-Vol-2) Avail: NTIS HC A05/MF A01

The objective of this contract is to establish the technology required for subsequent commercial development and application by the private sector of utility-size direct coal-fueled gas turbines. Emissions from these units are to meet or be lower than EPA's New Source Performance Standards (NSPS) for coal-fired steam generators. This report is submitted in two volumes. The narrative supporting figures and tables are contained in Volume 1. Thirty-six (36) drawings which were used in the design and manufacture of the subscale slagging combustor, hot gas particulate and alkali probe, and modifications and/or additions to the Haverhill test site are placed in this report. DOE

N89-27184# Battelle Columbus Labs., OH.
GAS ENGINE HEAT PUMP SYSTEM AND COMPONENT EFFICIENCY AND RELIABILITY IMPROVEMENT, PHASE 2 Report, Sep. 1986 - Jan. 1989
Frank E. Jakob and V. Brown Jan. 1989 67 p
(Contract GRI-5084-242-1118)
(PB89-173645; N4577-2501; GRI-88/0331) Avail: NTIS HC A04/MF A01 CSCL 13I

The Gas Research Institute is directing several research projects to develop gas-fired heat pumps for residential and light commercial use. The project work described identifies and evaluates potential improvements in the cycle and key components of these heat pumps and provides short- and long-term inputs for the heat pump product development efforts. Principal results of Phase 2 studies under the project are: compressors for commercialized gas engine heat pumps (GEHPs), auxilliary heat recommendations for GEHPs, rotary engine test data, duty cycle test stands, and heat pump design specifications. GRA

N89-27185 Department of the Air Force, Washington, DC.
BEARINGS FABRICATED FROM RAPIDLY SOLIDIFIED POWDER AND METHOD Patent
Colin M. Adam, inventor (to AF) 28 Feb. 1989 11 p Filed 24 Nov. 1987
(AD-D014072; US-Patent-4,808,226; US-Patent-Appl-SN-124805)
Avail: US Patent and Trademark Office CSCL 11/6

A process of fabricating steel stock for bearing components from highly alloyed steel powders supersaturated in carbon up to 0.5 weight percent in ferrite and up to 1.0 weight percent in austenite type combinations is disclosed. Rapid solidification of an atomized molten composition yields a metal powder with a diameter ranging between 75 and 105 microns. The metal powder is then compressed and heated to a low forging temperature between 1,600 and 1,800 F to yield the steel stock. GRA

N89-27186 Department of the Air Force, Washington, DC.
ANTI-ROTATION GUIDE BUSHING Patent
George Booner, inventor (to AF), Milo R. Rodriguez, inventor (to AF), and Douglas L. Kisling, inventor (to AF) 28 Feb. 1989 5 p Filed 3 Jul. 1986 Supersedes AD-D012510
(AD-D014079; US-Patent-Appl-SN-881741;
US-Patent-Class-415-160) Avail: US Patent and Trademark Office CSCL 20/11

A variable guide vane bushing assembly which features means that prevents bushing rotation is disclosed. A bushing comprises flats on its outer sleeve, the flats interlock with race track shaped holes on a tab-lock washer. The tab-lock washer spans two or more adjacent vane stems and thus is not susceptible to rotation. A retainer and the vane arm assemble on top of the tab-lock washer complete the assembly. GRA

N89-27187 Department of the Air Force, Washington, DC.
ELECTROMAGNETIC PULSE ROTARY SEAL Patent
Clarence W. Neher, inventor (to AF) 28 Feb. 1989 4 p Filed 6 Jul. 1987 Supersedes AD-D013423
(AD-D014080; US-Patent-4,807,891; US-Patent-Appl-SN-069999;
US-Patent-Class-277-80) Avail: US Patent and Trademark Office CSCL 09/7

A rotary seal for protection against electromagnetic interference and electromagnetic pulses is disclosed. An electrically conductive resilient bellows surrounds a shaft extending through an opening in an enclosure. The bellows is attached at one end to the shaft and biased against the enclosure at the other end. The attachment of the bellows to the shaft includes a static electromagnetic seal. GRA

N89-27188 Department of the Air Force, Washington, DC.
DUAL LOAD PATH PIN CLEVIS JOINT Patent
Alison M. Arnold, inventor (to AF) and Ronald G. Reed, inventor (to AF) 28 Feb. 1989 7 p Filed 22 May 1987
(AD-D014081; US-Patent-4,808,023; US-Patent-Appl-SN-058004;
US-Patent-Class-403-157) Avail: US Patent and Trademark Office CSCL 13/5

A dual load path connector for pivotally joining a movable member to a structural member, is described which comprises a pair of spaced apart lugs attached to a first of the members, each of the lugs including an outwardly projecting boss, a clevis disposed between the lugs and attached to the first member, a pivot pin, received by the lugs and clevis, which may support a self-aligning bearing between the ends of the clevis, and a connecting link assembly including a first connecting link pivotally supported at a first end on the pin and connected at the other end to the second member, and a pair of second connecting links pivotally supported at respective first ends on the bosses and at the second ends to the second member, the first load bearing path between the structural and movable members, and the second connecting links, bosses and lugs providing a second load bearing path. GRA

N89-27189 Department of the Air Force, Washington, DC.
BIMETALLIC AIR SEAL FOR EXHAUST NOZZLES Patent
Joseph Holowach, inventor (to AF) and George D. Lee, inventor (to AF) 21 Mar. 1989 7 p Filed 10 Dec. 1986
(AD-D014106; US-Patent-4,813,608; US-Patent-Appl-SN-939999;
US-Patent-Class-239-265.37) Avail: NTIS HC A02/MF A01
CSCL 11/6

A bimetallic leaf seal for forming an air seal between adjacent structures is disclosed. The bimetallic seal comprises two metallic layers having different coefficients of thermal expansion. The seal moves in a preferred direction upon the application of heat to form an air seal upon the application of heat. GRA

N89-27190 Department of the Air Force, Washington, DC.
SIX DEGREES OF FREEDOM MICROMANIPULATOR Patent
Gad Shelef, inventor (to AF) 11 Apr. 1989 11 p Filed 17 Nov. 1987
(AD-D014113; US-Patent-4,819,496; US-Patent-Appl-SN-121493)
Avail: US Patent and Trademark Office CSCL 12/9

A six degree of freedom micromanipulator is disclosed which may be interposed between the fingers and the remainder of a robotic arm's structure for increasing the accuracy with which an arm's fingers may be positioned independently of the accuracy achievable through motions originating at or near the arm's shoulder. Included in the structure are a base plate and yokes; drive rods and trunnions; drive rod ends; and a manipulator plate and yokes. Motor driven push-pull assemblies may be used in place of the elongated drive rods and their associated trunnions to electrically control the position of the manipulator plate. GRA

N89-27191 Department of the Air Force, Washington, DC.
ANTENNA SHAFT POSITIONING DEVICE Patent
Gary N. Bonadies, inventor (to AF), Mark OClair, inventor (to AF), and David W. Parry, inventor (to AF) 28 Mar. 1989 7 p Filed 24 Oct. 1986
(AD-D014120; US-Patent-4,815,339; US-Patent-Appl-SN-922642) Avail: US Patent and Trademark Office CSCL 09/1

An apparatus is presented for stopping a rotating antenna shaft at a distinct position intermediate two end stop positions. The paddle on the rotating shaft cooperates with intermediate stop assembly to arrest bi-directional shaft rotation at an intermediate point when such stopping is desired, the intermediate stop assembly being activated by springs and deactivated by action of solenoids. GRA

N89-27192 Department of the Navy, Washington, DC.
LOW FREQUENCY STRUCTUREBORNE VIBRATION ISOLATION MOUNT Patent
Valentino N. Fazi, Jr., inventor (to Navy), Ronald G. Murdock, inventor (to Navy), Ernest O. Hancock, inventor (to Navy), and John W. McGready, inventor (to Navy) 11 Apr. 1989 8 p Filed 22 Dec. 1987
(AD-D014133; US-Patent-4,819,503; US-Patent-Appl-SN-137558; US-Patent-Class-74-573) Avail: US Patent and Trademark Office CSCL 13/9

A low frequency structureborne vibration isolation mount includes an annular disk pad of vibration damping material which is sandwiched and bonded between two similar light but rugged annular disks. The annular disk pad and the two annular disks have equal number of matching and corresponding holes along the circumferences thereof. The sizes of the holes are so chosen that one of the annular disks can be secured to the moving piece of equipment and isolated from everything else and the other annular disk can be secured to the stationary piece of equipment. The vibrations of the moving piece of equipment are thus isolated from everything else. GRA

N89-27193# Illinois Univ., Chicago. Dept. of Civil Engineering/Mechanics and Metallurgy.
ELECTROCHEMICAL TRANSPORT OF MANGANESE BETWEEN THE FLUX AND THE WELD METAL IN SUBMERGED ARC WELDING
J. E. Indacochea, M. Blander (Argonne National Lab., IL.), and A. Polar 1989 7 p Presented at the 2nd International Conference on Trends in Welding Research, Gatlinburg, TN, 14-18 May 1989
(Contract W-31-109-eng-38)
(DE89-012419; CONF-8905118-9) Avail: NTIS HC A02/MF A01

Submerged arc welds were made using a SiO sub 2 CaO CaF sub 2 MnO flux containing 20 w/o MnO, 15 w/o CaF sub 2, and SiO sub 2 to CaO , ratios that varied from 5.5 to 1.17; the slags formed from this flux system show good detachability and the welds produced have good bead morphology. The effect of dilution was eliminated by drawing the filler metal from the same material as the base plate. The welding parameters were the same for all welds and two polarities were used. The stability of the arc was also monitored and found to be stable, but more so for the reverse polarity welds. Chemical analyses were performed on flux, slag, and weld samples. The manganese content in the weld metal increases for all the fluxes, with the increases being larger the smaller the silica to calcium oxide ratio. This behavior can be explained by thermodynamically driven kinetic factors since, in this composition range, the activity of the manganese oxide increases with a decrease in the SiO sub 2/CaO ratio. When the SiO sub 2/CaO ratio is smaller than about 2.25, the manganese content in the welds made with reverse polarity is higher than those made with straight polarity. This difference in the manganese level is explained in terms of an electrochemical mechanism. DOE

N89-27194# Illinois Univ., Chicago. Dept. of Civil Engineering, Mechanics and Metallurgy.
ELECTROCHEMICAL REACTIONS IN SUBMERGED ARC WELDING WITH SiO2-CaO-CaF2 FLUXES WITH HIGH AND LOW SILICA CONTENTS
J. E. Indacochea, M. Blander (Argonne National Lab., IL.), and A. Polar 1989 6 p Presented at the 2nd International Conference on Trends in Welding Research, Gatlinburg, TN, 14-18 May 1989
(Contract W-31-109-eng-38)
(DE89-012421; CONF-8905118-8) Avail: NTIS HC A02/MF A01

The role of electrochemical reactions was examined in submerged arc welding with different flux compositions based on high and low silica levels (40 w/o and 20 w/o, respectively) in the SiO2-CaO-CaF2 system. The welds were bead-on-plate, using d.c. reverse and straight polarities. Weld samples were removed for oxygen analysis and a number of electrode tips were collected for every weld sample by interrupting the arc after a fixed time into the weld operation; oxygen levels in these tips were determined. Optical microscopy was also performed on electrode tips to observe the inclusion population. The oxygen levels in the weld metal and electrode tip do not change significantly as the polarity is changed with the high silica fluxes. For the low silica fluxes, on the other hand, there are differences in the oxygen levels in the wire tips and weld metals as the polarity is changed. These results are consistent with an electrochemical mechanism and with preferential mechanical entrainment of flux in straight polarity. DOE

N89-27195# Argonne National Lab., IL. Materials and Components Technology Div.
ATTRACTIVE LEVITATION FOR HIGH-SPEED GROUND TRANSPORT WITH LARGE GUIDEWAY CLEARANCE AND ALTERNATING-GRADIENT STABILIZATION
John R. Hull 1989 17 p Presented at the INTERMAG: International Magnetics Conference, Washington, DC, 28-31 Mar. 1989 Submitted for publication
(Contract W-31-109-eng-38)
(DE89-013640; CONF-890309-1) Avail: NTIS HC A03/MF A01

This paper describes an attractive levitation concept that results in large guideway clearance and low magnetic drag and requires no feedback for stability. Dynamic stability is achieved by establishing alternating gradients of force, in which the spatial dependence of the attractive force between superconducting coils on the vehicle and iron rails in the guideway is altered by periodic changes in the rail configuration. For a vehicle velocity of 500 km/h, the appropriate lengths for each configuration are in the range of 5 to 40 m, and the guideway clearance is in the range of 50 to 100 mm, depending on the details of the rail and vehicle magnet design. DOE

N89-27196# Science Applications International Corp., McLean, VA.
RISK ASSESSMENT OF COMPRESSED NATURAL GAS-FUELED VEHICLE OPERATIONS, PHASE 1 Topical Report, Dec. 1987 - Nov. 1988
David M. Friedman and Laura C. Zuber Feb. 1989 192 p
(Contract GRI-5087-254-1621)
(PB89-188841; GRI-89/0037) Avail: NTIS HC A09/MF A01 CSCL 13F

The Gas Research Institute has embarked on a technology and safety oriented program with the objective of developing a cost-effective, advanced natural gas engine, a compression station, and storage systems that will capitalize on the economic and environmental benefits of using natural gas in vehicular applications. As the first step in a two phase project, a program was initiated to develop a remotely accessible and publicly available, international data base of natural gas vehicle (NGV) safety information. Its purpose is to improve GRI's ability to conduct detailed, quantitative risk assessments of NGVs and NGV systems. In addition to bibliographic reference, scientific data are currently available in a computerized, menu-driven data base management system (DBMS). Data reflect current, domestic, and international

knowledge of NGV safety, fire, and injury statistics, refueling station equipment design, and applicable codes and standards. Additional data required for a probabilistic risk assessment include topics such as vehicle component failure modes, strength of materials, natural gas physical properties, and general transportation safety statistics. Author

N89-27197# Adiabatics, Inc., Columbus, IN.
COMBUSTION CHARACTERISTICS OF DRY COAL-POWDER-FUELED ADIABATIC DIESEL ENGINE Final Report
R. M. Kakwani and R. Kamo Jan. 1989 92 p
(Contract DE-AC21-86MC-23258)
(DE89-000978; DOE/MC-23258/2693) Avail: NTIS HC A05/MF A01

This report describes the progress and findings of a research program aimed at investigating the combustion characteristics of dry coal powder fueled diesel engine. During this program, significant achievements were made in overcoming many problems facing the coal-powder-fueled engine. The Thermal Ignition Combustion System (TICS) concept was used to enhance the combustion of coal powder fuel. The major coal-fueled engine test results and accomplishments are as follows: design, fabrication and engine testing of improved coal feed system for fumigation of coal powder to the intake air; design, fabrication and engine testing of the TICS chamber made from a superalloy material (Hastelloy X); design, fabrication and engine testing of wear resistant chrome oxide ceramic coated piston rings and cylinder liner; lubrication system was improved to separate coal particles from the contaminated lubricating oil; control of the ignition timing of fumigated coal powder by utilizing exhaust gas recirculation (EGR) and variable TICS chamber temperature; coal-fueled engine testing was conducted in two configurations: dual fuel (with diesel pilot) and 100 pct coal-fueled engine without diesel pilot or heated intake air; cold starting of the 100 pct coal-powder-fueled engine with a glow plug; and coal-fueled-engine was operated from 800 to 1800 rpm speed and idle to full load engine conditions. DOE

N89-27198# Oak Ridge National Lab., TN. Center for Engineering Systems Advanced Research.
RESEARCH IN AUTONOMOUS ROBOTICS AT ORNL USING HERMIES-3
C. R. Weisbin, B. L. Burks, J. R. Einstein, R. R. Feezell, W. W. Manges, and D. H. Thompson 1989 20 p Presented at the Joint ASME/JSME Pressure Vessel and Piping Conference, Honolulu, HI, 23-27 Jul. 1989
(Contract DE-AC05-84OR-21400)
(DE89-004933; CONF-890721-5) Avail: NTIS HC A03/MF A01

HERMIES-3 is an autonomous robot comprised of a seven degree-of-freedom (DOF) manipulator designed for human scale tasks, a laser range finder, a sonar array, an omnidirectional wheel-driven chassis, multiple cameras, and a dual computer system containing a 16-node hypercube expandable to 128 nodes. The current experimental program involves performance of human-scale tasks (e.g., valve manipulation, use of tools), integration of a dexterous manipulator and platform motion in geometrically complex environments, and effective use of multiple cooperating robots (HERMIES-2B and HERMIES-3). The environment in which the robots operate has been designed to include multiple valves, pipes, meters, obstacles on the floor, valves occluded from view, and multiple paths of differing navigation complexity. The ongoing research program supports the development of autonomous capability for HERMIES-2B and 3 to perform complex navigation and manipulation under time constraints, while dealing with imprecise sensory information. DOE

N89-27199# Sandia National Labs., Albuquerque, NM.
MICROMECHANICAL CHARACTERIZATION OF NEAR-SURFACE LAYERS
Roy J. Bourcier 1989 21 p Presented at the Microbeam Analysis Society Meeting, Asheville, NC, 16 Jul. 1989
(Contract DE-AC04-76DP-00789)
(DE89-008710; SAND-89-0490C; CONF-890748-6) Avail: NTIS HC A03/MF A01

This paper reviews several techniques available to the experimenter to characterize the mechanical properties of near surface layers of engineering materials. The test methods examined are: micro-tensile testing, bulge testing, ultra-low load indentation testing, and microfabricated test structures. The applicability of these techniques as well as their advantages and difficulties are examined. Special emphasis is given to recent developments in ultra-low load indentation testing and microfabricated test structures. DOE

N89-27200# Sandia National Labs., Albuquerque, NM.
MECHANISMS THAT CONTROL THE GEOMETRY OF PULSED Nd:YAG LASER WELDS
J. L. Jellison, A. J. Russo, H. C. Peebles, and R. L. Williamson 1988 24 p Presented at the JOWOG 22D Joining Subgroup, Aldermasten, United Kingdom, 4 Oct. 1988
(Contract DE-AC04-76DP-00789)
(DE89-014490; SAND-88-0973C; CONF-8810176-5) Avail: NTIS HC A03/MF A01

A two-dimensional conduction laser welding code developed by Russo overpredicted the geometry of pulsed welds for welding parameters typically used in production. At low heat fluxes, however, there was good agreement between the experimental results and the welding code. The limitations of the code appear to result from ignoring some of the important physics of the laser welding processes. Subsequent experimental process research and further efforts have concentrated on beam-plume interactions and weld pool convection. A key experiment that has been used in testing the physical models is one where the role of a surface active element in controlling the geometry of austenitic stainless steels welds was evaluated. This experiment involved a significant range of heat fluxes and addressed the role of the laser plume. In this paper, both experimental and theoretical studies of the laser plume are discussed. Furthermore, the role of surface tension-driven convection (Marangoni flow) is explored. The results of this research are used to explain the geometry of austenitic stainless steel welds from the above experiment. DOE

N89-27201# Army Lab. Command, Watertown, MA. Material Technology Lab.
AUTOMATED IMMERSION TESTING ROBOTIC SYSTEM: HARDWARE AND SOFTWARE DESIGN Final Report
Suzanne G. Dunn Apr. 1989 64 p
(AD-A208755; MTL-TR-89-36) Avail: NTIS HC A04/MF A01
CSCL 11/4

Hardware and software development of a fully automated robotic work cell to determine the water sorption-diffusion properties of plastics and organic matrix composite materials and to handle all data acquisition is described. Immersion testing involves measuring weight changes of specimens as a function of the time they are immersed in water at a particular temperature. This test method is labor intensive and tedious, involving repetitive operations such as transferring liquids and specimens, blotting and weighing specimens, and recording data. Immersion studies can take years to complete and generate enormous amounts of data which must be recorded and evaluated. Through automation, immersion testing is no longer limited to an 8-hour work schedule, labor costs have been reduced, productivity has been increased tenfold, and the reliability, precision, and accuracy of the test have been improved. GRA

38 QUALITY ASSURANCE AND RELIABILITY

Includes product sampling procedures and techniques; and quality control.

N89-27202# Wallace and Co., Fairborn, OH.
COST OF QUALITY EVALUATION METHODOLOGIES HANDBOOK Final Report
William J. Grunewald, Donovan C. Wikstrom, Robert Simon, and William Cance 28 Jul. 1988 233 p
(Contract F33657-86-D-0094)
(AD-A206935) Avail: NTIS HC A11/MF A01 CSCL 05/1

The purpose of the handbook is to function as an aid to the understanding of the concept of cost of quality and its value as a management tool. Individuals who are not a part of a quality assurance organization must recognize that there are activities which go on in their area of interest that are indeed part of the total cost of quality for an organization. This handbook is designed to be used by people involved with proposal evaluation, fact finding, should cost, quality audits, contractor operation reviews, source selection, pre-award surveys, or any review effort in which visibility into what the government is paying for quality would be useful. All disciplines are involved in these types of reviews and all disciplines have a share in the cost of quality. The quality representative involved in a particular review would be the focal point for overall cost of quality evaluation results. But each of the other team members must find the cost of quality in their specific area, evaluate the cost, and make input to the quality representative for consolidation. The handbook is designed to enable each participant team member to accomplish that task in support of the overall cost of quality effort. GRA

N89-27203# Sandia National Labs., Albuquerque, NM. Statistics, Computing and Human Factors Div.
SYSTEM-BASED COMPONENT TEST PLANS AND OPERATING CHARACTERISTICS: INTRODUCTION AND OVERVIEW
Robert G. Easterling, Floyd W. Spencer, Kathleen V. Diegert, and Mainak Mazumdar (Pittsburgh Univ., PA.) May 1989 20 p
(Contract DE-AC04-76DP-00789)
(DE89-012255; SAND-88-0173) Avail: NTIS HC A03/MF A01

Component test plans are often designed by allocating system reliability among the system's components, then choosing individual component plans suitable for demonstrating achievement of each component's reliability goal. This approach does not consider how much information relative to the system reliability goal is provided by the ensemble of component tests. We propose and develop the notion of system reliability O.C. curves, based on the component tests, and illustrate their use in designing or evaluating an overall test program. By specifying O.C. values (akin to producer's and consumer's risks), optimum, system-oriented component test plans can be derived. These ideas are illustrated in this paper for a series system and for a simple series-parallel system, with binomial data. These and other system configurations and data structures will be considered in more detail in later reports. DOE

N89-27204*# Rockwell International Corp., Canoga Park, CA. Rocketdyne Div.
OTVE TURBOPUMP CONDITION MONITORING, TASK E.5 Final Report, Oct. 1988 - Sep. 1989
Paul T. Coleman and J. J. Collins Aug. 1989 27 p
(Contract NAS3-23773)
(NASA-CR-182274; NAS 1.26:182274; RI/RD89-214-Task-E.5)
Avail: NTIS HC A03/MF A01 CSCL 14D

Recent work has been carried out on development of isotope wear analysis and optical and eddy current technologies to provide bearing wear measurements and real time monitoring of shaft speed, shaft axial displacement and shaft orbit of the Orbit Transfer Vehicle hydrostatic bearing tester. Results show shaft axial displacement can be optically measured (at the same time as shaft orbital motion and speed) to within 0.3 mils by two fiberoptic deflectometers. Evaluation of eddy current probes showed that, in addition to measuring shaft orbital motion, they can be used to measure shaft speed without having to machine grooves on the shaft surface as is the usual practice for turbomachinery. The interim results of this condition monitoring effort are presented. Author

N89-27205# Sandia National Labs., Albuquerque, NM.
THE 1/f NOISE: A NONDESTRUCTIVE TECHNIQUE TO PREDICT MOS RADIATION HARDNESS
John H. Scofield, T. P. Doerr (Oberlin Coll., OH.), and D. M. Fleetwood 1989 5 p Presented at the 26th Annual Conference on Nuclear and Space Radiation Effects, Marco Island, FL, 24 Jul. 1989
(Contract DE-AC04-76DP-00789)
(DE89-007419; SAND-89-0379C; CONF-890723-3) Avail: NTIS HC A02/MF A01

We find a strong correlation between the preirradiation 1/f noise of metal oxide semiconductor (MOS) transistors and their radiation hardness. This suggests that current fluctuations may provide a useful, nondestructive probe of defects in MOS devices. DOE

N89-27206# Sandia National Labs., Albuquerque, NM.
MATERIALS ANALYSIS WITH NUCLEAR MICROPROBES: SUPERCONDUCTORS AND BURIED CONDUCTORS
J. C. Barbour and B. L. Doyle 1989 12 p Presented at the Microbeam Analysis Society Meeting, Asheville, NC, 16 Jul. 1989
(Contract DE-AC04-76DP-00789)
(DE89-008580; SAND-89-0633C; CONF-890748-5) Avail: NTIS HC A03/MF A01

Nuclear microprobe analysis (NMA) is a unique form of microbeam analysis in that it combines high lateral resolution with the high depth resolution techniques of conventional ion beam analysis (IBA) to nondestructively determine sample composition in three dimensions. By using depth sensitive IBA techniques (e.g., Rutherford Backscattering Spectrometry (RBS), Enhanced Backscattering Spectrometry (EBS) or Elastic Recoil Detection (ERD)), NMA finds its greatest utility in analyses requiring the following information: (1) 1 to 100 ppM sensitivity, (2) nondestructive three-dimensional depth profiling, and (3) quantitative light element analysis (e.g., the first two rows of the periodic table). This paper demonstrates the continuing evolution of NMA capabilities through two examples. First, the unique capabilities afforded NMA are shown in a simple yet accurate method to measure both oxygen and metal atom concentrations in Y-Ba-Cu-O alloys with micro-area ion beam analysis. Second, a NMA of buried tungsten lines in a silicon wafer demonstrates the complementary nature of information determined by NMA and scanning electron microscopy (SEM). DOE

39 STRUCTURAL MECHANICS

Includes structural element design and weight analysis; fatigue; and thermal stress.

For applications see *05 Aircraft Design, Testing and Performance* and *18 Spacecraft Design, Testing and Performance.*

N89-27207# Sydney Univ. (Australia). School of Civil and Mining Engineering.
INELASTIC BUCKLING OF CHANNEL COLUMNS IN THE DISTORTIONAL MODE
S. C. W. Lau and G. J. Hancock Aug. 1988 48 p
(PB89-156053; R-578) Avail: NTIS HC A03/MF A01 CSCL 20K

Thin-walled channel sections may buckle in a distortional mode when subjected to compression. A variety of cold-formed channel columns were tested recently to study distortional buckling in the inelastic range. A comparison of a theoretical method for predicting the inelastic distortion buckling strengths of thin-walled columns with the column tests is described. The method is based on a spline finite strip buckling analysis which takes into account the nonlinear stress-strain behavior of the steel making up the test

sections, and the fixed-ended test conditions. The inelastic buckling analysis is found to produce accurate estimates of the test failure loads and failure modes. GRA

N89-27208 Department of the Air Force, Washington, DC.
WIDEBAND ELECTROMAGNETIC DAMPING OF VIBRATING STRUCTURES Patent
Robert L. Forward, inventor (to AF) and William S. Griffin, inventor (to AF) 3 Jan. 1989 5 p Filed 14 May 1987
(AD-D014069; US-Patent-4,795,123; US-Patent-Appl-SN-049358; US-Patent-Class-248-550) Avail: US Patent and Trademark Office CSCL 20/11

The damping of vibrations in a mechanical structure is accomplished while minimizing the impact on the design and operation of the structure through the use of a plurality of attachable vibration damping elements. Each vibration damping element contains: an accelerometer, an integrator, mixer, power amplifier, and a force actuator. The accelerometer measures the motion of the vibration in the structure at its attachment point and produces an acceleration measurement signal. The integrator integrates the acceleration measurement signal to produce a velocity measurement signal. The mixer produces a composite motion signal by mixing the acceleration measurement signal with the velocity measurement signal. The power amplifier adjusts the phase and amplitude of the composite motion signal to drive the force actuator to damp the sensed vibration along one dimension at the attachment point of the force actuator. By placing three vibration damping element at right angles to each other at a location on the structure, three-dimensional vibration damping is obtained at that point. GRA

N89-27209# Oak Ridge National Lab., TN. Applied Technology Div.
MEASURED DAMPING AND MODULUS OF COMPOSITE CYLINDERS
J. B. Andriulli 1989 64 p Presented at the Damping '89, Palm Beach, FL, 8 Feb. 1989
(Contract DE-AC05-84OR-21400)
(DE89-010369; CONF-890277-1) Avail: NTIS HC A04/MF A01

Damping and moduli are measured on graphite and glass fiber/thermoset, thermoplastic, and metal matrix composite cylinders. Measurements are made by the impact-hammer modal-test method with the specimen suspended in the near free-free boundary condition. The axial and in-plane shear moduli are determined from the free-free axial and torsional vibration modes of the cylinder. Damping-loss factors for each of the associated modes are determined from the frequency-response function by the half-power point method or may also be determined by other curve-fitting methods. The effects on damping are presented for a number of different fiber/resin composites and for different layups of the same fiber/resin material. Cylinders are unique specimen configurations that permit simplified measurements of both the axial and in-plane shear (torsional) material properties from the same sample. The impact-hammer modal-test method provides a quick, inexpensive, small deformation, nondestructive estimate of the moduli and damping for the as-fabricated cylinders. After tests are completed, the cylinder can subsequently be used for its intended purpose. Details of the test method and procedure are described. DOE

N89-27210# Oak Ridge National Lab., TN. Engineering Technology Div.
HIGH-TEMPERATURE FLAW ASSESSMENT PROCEDURE: A STATE-OF-THE-ART SURVEY
Marina B. Ruggles and Y. Takahashi (Central Research Inst. of Electric Power Industry, Tokyo, Japan) May 1989 70 p
(Contract DE-AC05-84OR-21400; EPRI Proj. 2658-21)
(DE89-012740; ORNL-6546) Avail: NTIS HC A04/MF A01

High-temperature crack growth under cyclic, static, and combined loading is received with an emphasis on fracture mechanics aspects. Experimental studies of the effects of loading history, microstructure, temperature, and environment on crack growth behavior are described and interpreted. The experimental evidence is used to examine crack growth parameters and theoretical models for fatigue, creep, and creep-fatigue crack propagation at elevated temperatures. The limitations of both elastic and elastic-plastic fracture mechanics for high-temperature subcritical crack growth are assessed. Existing techniques for modeling critical crack growth/ligament instability failure are also presented. Related topics of defect modeling and engineering flaw assessment procedures, nondestructive evaluation methods, and probabilistic failure analysis are briefly discussed. DOE

N89-27211# Oak Ridge National Lab., TN. Metals and Ceramics Div.
THE USE OF FIELD INDENTATION MICROPROBE IN MEASURING MECHANICAL PROPERTIES OF WELDS
Fahmy M. Haggag, H. Wong, D. J. Alexander, and Randy K. Nanstad 1989 7 p Presented at the 2nd International Conference on Trends in Welding Research, Gatlinburg, TN, 15 May 1989
(Contract DE-AC05-84OR-21400)
(DE89-013548; CONF-8905118-11) Avail: NTIS HC A02/MF A01

A field indentation microprobe (FIM) was conceived for evaluating the structural integrity of metallic components (including base metal, welds, and heat-affected zones) in situ in a nondestructive manner. The FIM consists of an automated ball indentation (ABI) unit for determining the mechanical properties (yield strength, flow properties, estimates of fracture toughness, etc.) and a nondestructive evaluation (NDE) unit (consisting of ultrasonic transducers and a video camera) for determining the physical properties such as crack size, material pileup around indentation, and residual stress presence and orientation. The laboratory version used in this work performs only ABI testing. ABI tests were performed on stainless steel base metal (type 316L), heat-affected zone, and welds (type 308). Excellent agreement was obtained between yield strength and flow properties (true-stress/true-plastic-strain curve) measured by the ABI tests and those from uniaxial tensile tests conducted on 308 stainless steel welds, thermally aged at 343 C for different times, and on the base material. DOE

N89-27212*# National Aeronautics and Space Administration. Langley Research Center, Hampton, VA.
STRUCTURAL ANALYSIS OF A THERMAL INSULATION RETAINER ASSEMBLY
William H. Greene and Carl E. Gray, Jr. Jul. 1989 27 p Original contains color illustrations
(NASA-TM-101580; NAS 1.15:101580) Avail: NTIS HC A03/MF A01 CSCL 20K

In January 1989 an accident occurred in the National Transonic Facility wind tunnel at NASA Langley Research Center that was believed to be caused by the failure of a thermal insulation retainer. A structural analysis of this retainer assembly was performed in order to understand the possible failure mechanisms. Two loading conditions are important and were considered in the analysis. The first is the centrifugal force due to the fact that this retainer is located on the fan drive shaft. The second loading is a differential temperature between the retainer assembly and the underlying shaft. Geometrically nonlinear analysis is required to predict the stiffness of this component and to account for varying contact regions between various components in the assembly. High, local stresses develop in the band part of the assembly near discontinuities under both the centrifugal and thermal loadings. The presence of an aluminum ring during a portion of the part's operating life was found to increase the stresses in other regions of the band. Under the centrifugal load, high bending stresses develop near the intersection of the band with joints in the assembly. These high bending stresses are believed to be the most likely cause for failure of the assembly. Author

N89-27213*# National Aeronautics and Space Administration. Ames Research Center, Moffett Field, CA.
A THREE-NODE C DEG ELEMENT FOR ANALYSIS OF LAMINATED COMPOSITE SANDWICH SHELLS

C. Wayne Martin, S. F. Lung, and K. K. Gupta Jun. 1989 16 p (NASA-TM-4125; H-1479; NAS 1.15:4125) Avail: NTIS HC A03/MF A01 CSCL 20K

A three-node flat shell element with C deg rotation fields has been developed for analysis of arbitrary composite shells. The element may consist of any number of orthotropic layers, each layer having different material properties and angular orientation. The formulation includes coupling between bending and extension, which is essential for analysis of unsymmetric laminates. Shearing deflections are included, since laminated and sandwich construction frequently results in shear stiffness much smaller than bending stiffness. Formulation of the element is straightforward, and calculation of its stiffness matrix is simple and fast. Convergence of solutions with mesh refinement is uniform for both thin and thick shells and is insensitive to element shape, although not as rapid as some other elements that lack one or more capabilities of the newly developed element. An experimental verification of the shall element is reported in the appendix. Author

N89-27214*# National Aeronautics and Space Administration. Marshall Space Flight Center, Huntsville, AL.

WELD STRESSES BEYOND ELASTIC LIMIT: MATERIALS DISCONTINUITY

V. Verderaime Washington Aug. 1989 28 p (NASA-TP-2935; NAS 1.60:2935) Avail: NTIS HC A03/MF A01 CSCL 20L

When welded structures depend on properties beyond the elastic limit to qualify their ultimate safety factor, and weld-parent materials abruptly change at the interface, then stress discontinuity is inevitable. The stress concentration is mildly sensitive to material relative strain hardening and acutely sensitive to applied stress fields. Peak stresses occur on the weld surface, at the interface, and dissipate within a 0.01-inch band. When the stress is intense, the weld will always fracture at the interface. The analysis incorporates a classical mechanics model to more sharply define stress spikes within the bandwidth, and suggests a relative material index and Poisson's ratio related to strain hardening. Implications are discussed which are applicable to industries of high performance structures. Author

N89-27215*# National Aeronautics and Space Administration. Langley Research Center, Hampton, VA.

STABILITY AND DYNAMIC ANALYSIS OF A SLENDER COLUMN WITH CURVED LONGITUDINAL STIFFENERS

Mark S. Lake Aug. 1989 67 p (NASA-TM-101636; NAS 1.15:101636) Avail: NTIS HC A04/MF A01 CSCL 20K

The results of a stability design study are presented for a slender column with curved longitudinal stiffeners for large space structure applications. Linear stability analyses are performed using a link-plate representation of the stiffeners to determine stiffener local buckling stresses. Results from a set of parametric analyses are used to determine an approximate explicit expression for stiffener local buckling in terms of its geometric parameters. This expression along with other equations governing column stability and mass are assembled into a determinate system describing minimum mass stiffened column design. An iterative solution is determined to solve this system and a computer program incorporating this routine is presented. Example design problems are presented which verify the solution accuracy and illustrate the implementation of the solution routine. Also, observations are made which lead to a greatly simplified first iteration design equation relating the percent increase in column mass to the percent increase in column buckling load. From this, generalizations are drawn as to the mass savings offered by the stiffened column concept. Finally, the percent increase in fundamental column vibration frequency due to the addition of deployable stiffeners is studied. Author

N89-27216# Sydney Univ. (Australia). School of Civil and Mining Engineering.

STRENGTH TESTS AND DESIGN METHODS FOR COLD-FORMED CHANNEL COLUMNS UNDERGOING DISTORTIONAL BUCKLING

S. C. W. Lau and G. J. Hancock Aug. 1988 127 p Sponsored by Civil Engineering Graduate's Association (PB89-183958; R-579) Avail: NTIS HC A07/MF A01 CSCL 20K

The columns of industrial steel storage rack structures are generally cold-formed open sections manufactured either by roll-forming or brake-pressing. The commonly used sections are thin-walled lipped channels whose width and depth are approximately equal. Depending on the length of the columns and the restraints provided by pallet beams and bracing, these types of sections may fall in a mode of local, distortional or flexural-torsional buckling. The results of compression tests of thin-walled channel section columns formed by brake-pressing are described. Detailed measurements of the stress-strain characteristics of the material forming the sections are also described. Design methods to account for the inelastic behavior in the distortional mode of buckling are proposed and compared with the test results. GRA

N89-27217# Los Alamos National Lab., NM.

DYNAMIC PLASTIC BUCKLING OF SPHERICAL SHELLS DURING COLLAPSE

Thomas A. Duffey 1989 22 p Presented at the Joint ASME/JSME Pressure Vessel and Piping Conference, Honolulu, HI, 23-27 Jul. 1989 (Contract W-7405-eng-36) (DE89-006543; LA-UR-89-5; CONF-890721-8) Avail: NTIS HC A03/MF A01

Conditions are established that lead to the growth of initial displacement imperfections (buckling) of complete spherical shells during significant inward motion. This study is limited to axisymmetric buckling modes only. Shell thickening during inward motion is taken into account, and its effect is found to be important for the stability and maximum growth of a given initial imperfection mode. Upper and lower bounds on the initial, uniform impulsive velocity loading are found (in terms of spherical shell geometry and material parameters) such that growth of buckling remains less than a prescribed multiplier when initial inward velocity lies outside the bounded region. DOE

N89-27218# Oak Ridge National Lab., TN.

EVALUATION OF WELDMENT CREEP AND FATIGUE STRENGTH-REDUCTION FACTORS FOR ELEVATED-TEMPERATURE DESIGN

J. M. Corum 1989 30 p Presented at the Joint ASME/JSME Pressure Vessel and Piping Conference, Honolulu, HI, 23-27 Jul. 1989 (Contract DE-AC05-84OR-21400) (DE89-008242; CONF-890721-12) Avail: NTIS HC A03/MF A01

New explicit weldment strength criteria in the form of creep and fatigue strength-reduction factors were recently introduced into the American Society of Mechanical Engineers Code Case N-47, which governs the design of elevated-temperature nuclear plants components in the United States. This paper provides some of the background and logic for these factors and their use, and it describes the results of a series of long-term, confirmatory, creep-rupture and fatigue tests of simple welded structures. The structures (welded plates and tubes) were made of 316 stainless steel base metal and 16-8-2 weld filler metal. Overall, the results provide further substantiation of the validity of the strength-reduction factor approach for ensuring adequate life in elevated-temperature nuclear component weldments. DOE

N89-27219# Sandia National Labs., Albuquerque, NM. Experimental Mechanics Dept.

STRAIN TO FAILURE OF PRESSURIZED THICK WALL CYLINDERS

Thomas G. Priddy and Dennis P. Roach 1989 20 p Presented at the Joint ASME/JSME Pressure Vessel and Piping Conference, Honolulu, HI, 23-27 Jul. 1989
(Contract DE-AC04-76DP-00789)
(DE89-009969; SAND-89-0343C; CONF-890721-20) Avail: NTIS HC A03/MF A01

The determination of the fully plastic response and pressure limit of a highly pressurized vessel is of considerable importance in design. The plastic-strain response during and following autofrettage operations, in comparison with the limiting strain condition, is of special interest. This paper presents the results of an analysis method for thick wall, high pressure cylinders where the effective plastic strain distribution through the thickness is the material response variable of primary interest. The limiting value of this effective plastic strain depends on the level of tensile-stress triaxiality which also varies through the thickness. This strain-to-failure criterion is used to predict the complete pressure versus strain response and the maximum pressure for test cylinders. A simple model of effective-stress versus effective plastic strain is employed. This model is quantified by data taken from uniaxial, tension, true-stress-strain curves and from the fracture zone of the tensile specimen. A sample calculation is included and, in a companion paper, a series of burst tubes having properties ranging from brittle to ductile are compared with this analytical method. DOE

N89-27220# Oak Ridge National Lab., TN. Metals and Ceramics Div.
ESTIMATING FRACTURE TOUGHNESS USING TENSION OR BALL INDENTATION TESTS AND A MODIFIED CRITICAL STRAIN MODEL
Fahmy M. Haggag and Randy K. Nanstad 1989 7 p Presented at the Joint ASME/JSME Pressure Vessel and Piping Conference, Honolulu, HI, 23-27 Jul. 1989
(Contract DE-AC05-84OR-21400)
(DE89-010324; CONF-890721-24) Avail: NTIS HC A02

A simple technique is described for estimating the fracture toughness by coupling the measured flow properties (either from a uniaxial tensile test or from a new automated ball indentation test) with a modified but empirically correlated critical fracture strain model. This technique is currently limited to ductile fracture applications. The modified model was used in combination with either tensile or ball indentation data to estimate fracture toughness of A515 grade 70 carbon steel and A533 grade B class 1 pressure vessel steel, respectively. The difference between fracture toughness predictions and measured values, using a computerized single-specimen unloading compliance technique in accordance with ASTM E-813, was less than 11 percent. DOE

N89-27221# Westinghouse Hanford Co., Richland, WA.
CREEP-FATIGUE ASSESSMENT METHODS USING ELASTIC ANALYSIS RESULTS AND ADJUSTMENTS
L. K. Severud Mar. 1989 10 p Presented at the Joint ASME/JSME Pressure Vessel and Piping Conference, Honolulu, HI, 23-27 Jul. 1989
(Contract DE-AC06-87RL-10930)
(DE89-011858; WHC-SA-0536; CONF-890721-30) Avail: NTIS HC A02/MF A01

The design of mechanical components that operate in elevated temperature environments where creep effects are significant usually requires creep-fatigue assessments. The ASME Code Case N-47 contains rules for these assessments based on both inelastic and elastic stress analysis. Although an inelastic stress analysis generally more accurately predicts effects from creep and plasticity, an elastic analysis is often preferred since it is much simpler and less costly. New creep-fatigue rules for use with elastic analysis results have recently been proposed to enhance the rules' accuracy and usefulness. This paper describes such new methods and rules for creep-fatigue assessments. Ingredients of the new methods include elastic follow up, ratcheting, multiaxiality, plasticity, creep, and relaxation considerations and associated adjustment factors. The basis for the adjustments and a comparison of results to those obtained using inelastic analysis are provided. The new methods will provide a wide range of practical application of elastic creep-fatigue rules than permitted by previous code methods in design of components for elevated temperature service. DOE

N89-27222# Lawrence Livermore National Lab., CA. Methods Development Group.
DYNA3D USER'S MANUAL: (NONLINEAR DYNAMIC ANALYSIS OF STRUCTURES IN THREE DIMENSIONS), REVISION 5
John O. Hallquist and Robert G. Whirley May 1989 206 p Revised
(Contract W-7405-eng-48)
(DE89-014304; UCID-19592-Rev-5) Avail: NTIS HC A10/MF A01

This report provides an updated user's manual for DYNA3D, an explicit three-dimensional finite element code for analyzing the large deformation response of inelastic solids and structures. A contact-impact algorithm permits gaps and sliding along material interfaces with friction. Using a specialization of this algorithm, such interfaces can be rigidly tied to admit variable zoning without the need of transition regions. Spatial discretization is achieved by the use of 8-node solid elements, 2-node beam elements, 4-node shell elements, 8-node solid shell elements, and rigid bodies. The equations-of-motion are integrated in time by the central difference method. The 1989 version of DYNA3D contains thirty material models and ten equations of state to cover a wide range of material behavior. DOE

N89-27223*# National Aeronautics and Space Administration. Lewis Research Center, Cleveland, OH.
OPTIMUM INTERFACE PROPERTIES FOR METAL MATRIX COMPOSITES
Louis J. Ghosn (Sverdrup Technology, Inc., Cleveland, OH.) and Bradley A. Lerch Aug. 1989 21 p
(NASA-TM-102295; E-4964; NAS 1.15:102295) Avail: NTIS HC A03/MF A01 CSCL 20K

Due to the thermal expansion coefficient mismatch (CTE) between the fiber and the matrix, high residual sresses exist in metal matrix composite systems upon cool down from processing temperature to room temperature. An interface material can be placed between the fiber and the matrix to reduce the high tensile residual stresses in the matrix. A computer program was written to minimize the residual stress in the matrix subject to the interface material properties. The decision variables are the interface modulus, thickness and thermal expansion coefficient. The properties of the interface material are optimized such that the average distortion energy in the matrix and the interface is minimized. As a result, the only active variable is the thermal expansion coefficient. The optimum modulus of the interface is always the minimum allowable value and the interface thickness is always the maximum allowable value, independent of the fiber/matrix system. The optimum interface thermal expansion coefficient is always between the values of the fiber and the matrix. Using this analysis, a survey of materials was conducted for use as fiber coatings in some specific composite systems. Author

N89-27224# Rome Univ. (Italy). Dipartimento of Fisica.
ON THE MULTIPLICITY AND SYMMETRIES OF THE BIFURCATION BRANCHING POINT IN THE SQUARE CLAMPED PLATE
Arturo Marcello Allega 15 Jun. 1988 20 p Submitted for publication Prepared in cooperation with Istituto Nazionale di Fisica Nucleare, Rome, Italy
(Preprint-604; ETN-89-94693) Avail: NTIS HC A03/MF A01

The symmetries of the eigenfunctions corresponding to the first eigenvalue in a square clamped plate are considered by the Weinstein method for intermediate problems. It is shown how this powerful method can be useful in studying a class of bifurcation problems whose prototype is the elastic plate. Knowledge of the eigenfunction symmetries provides a straighforward way to demonstrate the simple multiplicity of the principal bifurcation point by Weyl's lemma. ESA

N89-27225# Virginia Polytechnic Inst. and State Univ., Blacksburg. Dept. of Engineering Science and Mechanics.
RESIDUAL STRESS CHANGES IN FATIGUE. VOLUME 1: RESIDUAL STRESS MEASUREMENTS BY X-RAY DIFFRACTION IN NOTCHED TEST SPECIMENS Interim Report, Oct. 1985 - Sep. 1987
N. E. Dowling and D. O. Dunn 1 Mar. 1989 88 p
(Contract N62269-85-C-0256)
(AD-A208345; NADC-88141-60-Vol-1) Avail: NTIS HC A05/MF A01 CSCL 01/3

An experimental setup is described for performing stress measurements on notched test specimens under load using a TEC series 1600 X-ray diffraction system. Excellent results are being obtained for Ti6Al4V material, but measurements on 7475-t651 Al are complicated by a texturing problem. Also, some unusual effects are observed during plastic deformation which are not yet understood. The performance of the X-ray diffraction system is found to be quite good in general, but some minor problems are noted. GRA

N89-27226# Virginia Polytechnic Inst. and State Univ., Blacksburg. Dept. of Engineering Science and Mechanics.
RESIDUAL STRESS CHANGES IN FATIGUE. VOLUME 2: A SIMULATION MODEL FOR STRESS MEASUREMENTS IN NOTCHED TEST SPECIMENS BY X-RAY DIFFRACTION Interim Report, Oct. 1985 - Dec. 1987
K. Ranganathan 1 Mar. 1989 111 p
(Contract N62269-85-C-0256; RR02303)
(AD-A208346; NADC-88141-60-Vol-2) Avail: NTIS HC A06/MF A01 CSCL 01/3

The state of stress developed during fatigue testing of notched specimens was modeled analytically. From this model, the X-ray response to the stress state of the specimen was determined with an aim of measuring the X-ray effects that result from residual stresses. This model was also used to estimate the error in stress measurements caused by a stress gradient. The error in the measured stresses caused by the varying radius of curvature of the test specimen was also studied. It was concluded that the stress distribution model for an infinite specimen can be extended to a specimen of finite geometry with an error of approximately 3 percent; that precision in positioning the X-ray beam on the specimen is very important; and that residual stress measurements are feasible along the edge of the specimen. GRA

N89-27227# Computational Mechanics Co., Austin, TX.
COMPUTATIONAL METHODS FOR NONLINEAR DYNAMIC PROBLEMS IN SOLID AND STRUCTURAL MECHANICS: PROGRESS IN THE THEORY AND MODELING OF FRICTION AND IN THE CONTROL OF DYNAMICAL SYSTEMS WITH FRICTIONAL FORCES Final Technical Report, 1 Nov. 1988 - 28 Feb. 1989
J. T. Oden, W. W. Tworzydlo, and J. A. Martins 31 Mar. 1989 405 p
(Contract F49620-86-C-0051; AF Proj. 2302)
(AD-A208763; TR-89-05; AFOSR-89-0627TR) Avail: NTIS HC A18/MF A01 CSCL 20/11

This final report summarizes work on a three-year project devoted to dynamic friction and on control of systems with frictional forces. Detailed theoretical and numerical studies of static and dynamic friction and various phenomena of dynamic friction (stick-slip motion, self-excited oscillations, frictional damping, etc.) are described. Included in the report is also a study of methods of statistical homogenization, devised to develop new micro-mechanics-based models of contact and friction. The question of optimal control with distributed dynamical systems of viscoelastic bodies with frictional forces is also described. A final component of this study focuses on the mathematical and numerical analysis of elastohydrodynamic lubrication problems and is included in the final chapter. The studies presented in this report provide both a theoretical and numerical basis for modeling contact and friction. These models are shown to produce results in very good qualitative and quantitative agreement with experimental results. GRA

42 GEOSCIENCES (GENERAL)

N89-27228# Lawrence Livermore National Lab., CA.
EARTH SCIENCES Annual Report, 1987
L. W. Younker, ed., M. L. Donohue, ed., and S. J. Peterson, ed. Dec. 1988 80 p
(Contract W-7405-eng-48)
(DE89-013344; UCRL-53615-87) Avail: NTIS HC A05/MF A01

The Earth Sciences Department at Lawrence Livermore National Laboratory conducts work in support of the Laboratory's energy, defense, and research programs. The Department is organized into ten groups. Five of these -- Nuclear Waste Management, Fossil Energy, Containment, Verification, and Research -- represent major programmatic activities within the Department. Five others -- Experimental Geophysics, Geomechanics, Geology/Geological Engineering, Geochemistry, and Seismology/Applied Geophysics -- are major disciplinary areas that support these and other laboratory programs. This report summarizes work carried out in 1987 by each group and contains a bibliography of their 1987 publications. DOE

43 EARTH RESOURCES AND REMOTE SENSING

Includes remote sensing of earth resources by aircraft and spacecraft; photogrammetry; and aerial photography.

For instrumentation see *35 Instrumentation and Photography.*

N89-27229*# National Aeronautics and Space Administration. Goddard Space Flight Center, Greenbelt, MD.
ALTIMETRIC SYSTEM: EARTH OBSERVING SYSTEM. VOLUME 2H: PANEL REPORT
Robert A. Bindschadler, George Born, Robert R. P. Chase, Lee-Lueng Fu, Peter Mouginis-Mark, Chester Parsons, and Byron Tapley 1987 75 p Original contains color illustrations
(NASA-TM-89722; NAS 1.15:89722) Avail: NTIS HC A04/MF A01 CSCL 12B

A rationale and recommendations for planning, implementing, and operating an altimetric system aboard the Earth observing system (Eos) spacecraft is provided. In keeping with the recommendations of the Eos Science and Mission Requirements Working Group, a complete altimetric system is defined that is capable of perpetuating the data set to be derived from TOPEX/Poseidon, enabling key scientific questions to be addressed. Since the scientific utility and technical maturity of spaceborne radar altimeters is well documented, the discussion is limited to highlighting those Eos-specific considerations that materially impact upon radar altimetric measurements. Author

N89-27230# Egan Group, Washington, DC.
STUDY FOR ADVANCED CIVIL EARTH REMOTE SENSING SYSTEM: FOCUSED FINANCE STUDY. VOLUME 1: EXECUTIVE SUMMARY
12 Aug. 1988 10 p
(Contract MANE-8-00003)
(PB89-163224; NOAA-NESDIS-89/03-Vol-1) Avail: NTIS HC A02/MF A01 CSCL 08B

The Egan Group was asked to study the issues and prospects for private sector financing of commercial remote sensing ventures. The report is one of three studies to evaluate options for an advanced civil earth remote sensing system to follow the recently funded LANDSAT 6 system. The executive summary presents an overview of the study scope and approach, enabling technologies, financing environment, risks, conclusions, and recommended actions which are discussed in detail in the Final Report. GRA

N89-27231# KRS Remote Sensing, Landover, MD.
STUDY FOR AN ADVANCED CIVIL EARTH REMOTE SENSING SYSTEM. VOLUME 1: EXECUTIVE SUMMARY

Aug. 1988 47 p
(Contract MANE-8-00001)
(PB89-163257; NOAA-NERDIS-89/05-Vol-1) Avail: NTIS HC A03/MF A01; also available in set of 3 reports HC E99 as PB89-163240 CSCL 08B

Presented here are the results of a comprehensive study of options for an Advanced Civil Earth Remote Sensing System (ACERSS) to follow LANDSAT 6. The study approach followed three basic steps: projection of worldwide market demand for raw data and value added information products; identification of technical and implementation options for satisfying this demand; and determination of the commercial viability of these options. Author

N89-27232# KRS Remote Sensing, Landover, MD.
STUDY FOR AN ADVANCED CIVIL EARTH REMOTE SENSING SYSTEM. VOLUME 2: MARKET AND FINANCIAL ASSESSMENT Final Report
Aug. 1988 470 p
(Contract MANE-8-00001)
(PB89-163265; NOAA-NESDIS-89/06-Vol-2) Avail: NTIS HC A20/MF A01; also available in set of 3 reports HC E99 as PB89-163240 CSCL 08B

The results of a comprehensive study of options for an Advanced Civil Earth Remote Sensing System (ACERSS) to follow LANDSAT 6 are given. The study approach followed three basic steps: projection of worldwide market demand for raw data and value added information products; identification of technical and implementation options for satisfying this demand; and determination of the commercial viability of these options. Here, market profiles for remote sensing data are given. Author

N89-27233# Earth Satellite Corp., Chevy Chase, MD.
AN ASSESSMENT OF INFORMATION DEMANDS FOR REMOTE SENSING AND GEOGRAPHIC INFORMATION SYSTEM TECHNOLOGIES Final Report
William G. Brooner, Paul M. Maughan, and David A. Thibault Feb. 1988 145 p
(Contract AID/PDC-1406-I-00-7070-00)
(PB89-159313; AID-PN-AAZ-554) Avail: NTIS HC A07/MF A01 CSCL 08B

In the Fall of 1987, a research assessment of the potential benefits to the Third World of new applications of remote sensing and geographic based information systems (GIS) technologies was completed. Presented here are the findings, conclusions, and recommendations of that assessment. The principal need in the developing countries is for information which will support the production of food and fiber. Information on current food and fiber production, and near-term forecasts, is essential if nations are to avoid the impact of catastrophic shortages. There is an increasing recognition by Third World countries that critical biological resources are threatened by uncontrolled development and that the long-term consequences of the process may irreversibly impact both the local and world environment. Effective development planning requires basic maps of the physical environment, including planimetric base maps, current and potential land use, demography, current and planned infrastructure. Author

N89-27234# Naval Ocean Research and Development Activity, Bay Saint Louis, MS.
GEOSAT ALTIMETER SEA-ICE MAPPING
Jeffrey D. Hawkins and Matthew Lybanon Apr. 1989 12 p Previously announced in IAA as A89-34267 Submitted for publication
(AD-A207391; NORDA-JA-321-061-88) Avail: NTIS HC A03/MF A01 CSCL 08/12

The 12 March 1985 GEOSAT launch enable satellite oceanographers to continue the earlier sea-ice monitoring shown to be feasible with the GEOS-3 and SEASAT altimeters (1). The large difference in return signals from a 13.5 GHz pulse over water versus over sea-ice permits the generation of an ice index that responds abruptly to sea-ice edges. Sample Arctic and Antarctic operational sea-ice index plots are shown, depicting the current effort within the Remote Sensing Branch at the Naval Ocean Research and Development Activity (NORDA). This NORDA program provides graphical ice-index displays along GEOSAT nadir tracks to the Navy/National Oceanic and Atmospheric Administration (NOAA) Joint Ice Center (JIC) for assimilation into their sea-ice database. The altimeter's all-weather capability has been an important addition to the JIC data bases, since cloud cover can drastically curtail visible and infrared viewing, and passive microwave data has coarser resolution. Ongoing research efforts are aimed at extracting additional sea-ice parameters from the altimeter waveform, which contain information on the reflecting surface. Possibilities include discrimination between water, land, ice, combination water/ice, and water/land, as well as distinguishing various ice concentrations and possibly ice types. Coincident airborne passive microwave and synthetic aperture radar (SAR) data have been collected to test several methods which appear to be promising. GRA

N89-27235*# Ohio State Univ., Columbus. Dept. of Civil Engineering.
A CENTER FOR COMMERCIAL DEVELOPMENT OF SPACE: REAL-TIME SATELLITE MAPPING. REMOTE SENSING-BASED AGRICULTURAL INFORMATION EXPERT SYSTEM
Fabian C. Hadipriono, Carlos F. Diaz, and Earl S. Merritt (Earth Satellite Corp., Chevy Chase, MD.) Aug. 1989 170 p
(Grant NAGw-973)
(NASA-CR-185473; NAS 1.26:185473) Avail: NTIS HC A08/MF A01 CSCL 08B

The research project results in a powerful yet user friendly CROPCAST expert system for use by a client to determine the crop yield production of a certain crop field. The study is based on the facts that heuristic assessment and decision making in agriculture are significant and dominate much of agribusiness. Transfer of the expert knowledge concerning remote sensing based crop yield production into a specific expert system is the key program in this study. A knowledge base consisting of a root frame, CROP-YIELD-FORECAST, and four subframes, namely, SATELLITE, PLANT-PHYSIOLOGY, GROUND, and MODEL were developed to accomodate the production rules obtained from the domain expert. The expert system shell Personal Consultant Plus version 4.0. was used for this purpose. An external geographic program was integrated to the system. This project is the first part of a completely built expert system. The study reveals that much effort was given to the development of the rules. Such effort is inevitable if workable, efficient, and accurate rules are desired. Furthermore, abundant help statements and graphics were included. Internal and external display routines add to the visual capability of the system. The work results in a useful tool for the client for making decisions on crop yield production. Author

N89-27236# Instituto de Pesquisas Espaciais, Sao Jose dos Campos (Brazil). Dept. de Processamento de Imagens.
SP-ATUS: AN EXPERT SYSTEM FOR SPECIFICATIONS OF SATELLITE IMAGERY [SP-ATUS: UM SISTEMA ESPECIALISTA EM ESPECIFICACAO DE IMAGENS DE SATELLITE]
Edson Luiz FrancaSenne (Universidade Estadual de Paulista, Guaratingueta, Brazil), Antonio Miguel VieiraMonteiro, Leonardo SantAnnaBins, Antonio FranciscoJunior, and Flavio Roberto DiasVelasco Dec. 1988 13 p In PORTUGESE Presented at the 5th Symposium on Artificial Intelligence, Natal, RN, 7-11 Nov. 1988
(INPE-4754-PRE/1426) Avail: NTIS HC A03/MF A01

Satellite imagery constitutes an extremely powerful tool of relatively low cost for the solution of various problems in the efficient use of Earth resources. The repetitivity, various spectral bands, and other characteristics make the images obtained by orbital platforms an attractive instrument in innumerable applications. Although it has existed since 1975, today's methodologies increase the use of these images in various areas of application: atmospheric analysis, forestry, agriculture, geology, and cartography. Even though lack of technical knowledge concerning this tool hampers its dissemination, the use of imagery

is augmented year by year. An expert system prototype is described which is capable of specifying such satellite products employed for the solution of a remote sensing problem, in other words, which spectral band scale, presentation, and data were most adequate for the problem in question. A programming language was selected for implementation in the prototype OPS-5. Author

N89-27237# Washington State Univ., Pullman. Dept. of Geology.
COMPARISON OF SPECTRAL DATA GATHERED FROM A LABORATORY SPECTROMETER AND TM IMAGES WITH AND WITHOUT SHADOW CORRECTION
Richard L. Thiessen and Jay R. Eliason 1989 5 p Presented at the 12th International Geoscience and Remote Sensing Symposium, Vancouver, British Columbia, 10-14 Jul. 1989
(Contract DE-FG06-87ER-13796)
(DE89-010877; DOE/ER-13796/3; CONF-890768-1) Avail: NTIS HC A02

Spectral reflectance data from field samples were determined with a laboratory spectrometer (Beckman DK-2A). The spectral curves obtained with the spectrometer were correlated with the histograms determined from the images. The tightly defined histograms from the shadow corrected TM provided the best correlation with the rock data. Several units, including the Rainier Mesa Member of the Timber Mountain Tuff, showed multiple spectral patterns on both images and rock spectra. This difference was evaluated versus geochemistry, hematitic alteration, devitrification, pumice content, and degree of welding. DOE

N89-27238# Washington State Univ., Pullman.
QUANTITATIVE THREE-DIMENSIONAL STRUCTURAL TECHNIQUES
Richard L. Thiessen, Jay R. Eliason, and Harlan P. Foote (Department of Energy, Richland, WA.) 1989 58 p Presented at the 28th International Geologic Congress, Washington, DC, 9-19 Jul. 1989
(Contract DE-FG06-87ER-13796)
(DE89-010879; DOE/ER-13796/6; CONF-890784) Avail: NTIS HC A04/MF A01

Quantitative three-dimensional structural analysis using computer-based techniques will be presented and demonstrated. These analyses will demonstrate the use of remote sensing, seismic, geophysical, and field data sets to develop three-dimensional digital structural and lithologic models. The course will include both lectures on the digital analysis techniques and demonstrations of the analyses on an interactive workstation. DOE

N89-27239# Los Alamos National Lab., NM.
MODELING OF THE ANGULAR REFLECTANCE OF AN ARTIFICIAL PLANT CANOPY NEAR THE RETROREFLECTION PEAK IN THE OPTICAL REGIME
Christoph C. Borel, B. J. Powers, and S. A. W. Gerstl Apr. 1989 4 p Presented at the International Geoscience and Remote Sensing Symposium, Vancouver, Canada, 10-14 Jul. 1989
(Contract W-7405-eng-36)
(DE89-011174; LA-UR-89-1305; CONF-890768-3) Avail: NTIS HC A02

The narrow intensity peak in the reverse solar direction, also called the canopy hot spot or Heiligenschein, is studied using an artificial canopy. Polar Fourier analysis is proposed to classify asymmetric peaks for various canopy architectures. DOE

44 ENERGY PRODUCTION AND CONVERSION

Includes specific energy conversion systems, e.g., fuel cells; global sources of energy; geophysical conversion; and windpower.

For related information see also *07 Aircraft Propulsion and Power, 20 Spacecraft Propulsion and Power,* and *28 Propellants and Fuels.*

N89-27240# Sandia National Labs., Albuquerque, NM.
DRILLING OPERATIONS PLAN FOR THE MAGMA ENERGY EXPLORATORY WELL
John T. Finger, Bill J. Livesay, and Don Ash (Livesay, Inc., San Diego, CA.) 1989 3 p Presented at the 7th US DOE for the Geothermal Marketplace: Geothermal Program Review, San Francisco, CA, 21 Mar. 1989
(Contract DE-AC04-76DP-00789)
(DE89-010037; SAND-89-0440C; CONF-890352-4) Avail: NTIS HC A02

This paper is a summary of the proposed drilling plan for the first phase (to 2500 feet depth) of the Magma Energy Exploratory Well. The drilling program comprises four phases, spaced approximately one year apart, which culminate in a large-diameter well to a total depth near 20,000 feet. Included here are descriptions of the well design, predictions of potential drilling problems, a list of restrictions imposed by regulatory agencies, an outline of Sandia's management structure, and an explanation of how the magma energy technology will benefit from this drilling. DOE

N89-27241# Rensselaer Polytechnic Inst., Troy, NY.
VERIFICATION ANALYSIS OF THE TOROIDAL ACCELERATOR ROTOR PLATFORM WIND ENERGY CONVERSION SYSTEM
Robert E. Duffy Sep. 1988 271 p
(PB89-162069; NYSERDA-88-5; Rept-431-ET-RER-82) Avail: NTIS HC A12/MF A01 CSCL 10A

A unique wind energy system, the Toroidal Accelerator Rotor Platform (TARP) is studied. The TARP system places the rotors in pairs on either side of a torus-shaped platform, so that the wind is forced to flow into the rotors. As the wind is forced around the form, it picks up velocity and turns the rotors faster, generating more power. By concentrating the wind's power, the TARP system can be constructed in modules using 10 foot diameter rotor blades. Mounted on a track suspension system, the rotors are able to yaw with the wind to take advantage of breezes from any direction. The basic TARP design was tested and modified in a wind tunnel. The system was then analyzed for its integration into a farm silo and as a multistacked wind power needle. It was determined that the TARP technology would be feasible for application involving sites with high wind velocities, including some sites in New York State. GRA

N89-27242# Photon Energy, Inc., El Paso, TX.
HIGH-EFFICIENCY, LARGE-AREA CdTe PANELS Annual Report, Jun. 1987 - Jun. 1988
S. P. Albright, V. P. Singh, and B. Ackerman Apr. 1989 43 p Prepared for Midwest Research Inst., Golden, CO
(Contract DE-AC02-83CH-10093)
(DE89-000891; SERI/STR-211-3450) Avail: NTIS HC A03

This technical progress report on large-area CdTe solar panels cover work accomplished from June 1987 to May 1988. The highest-efficiency devices produced during this period measured 10.6 percent efficient on a 0.302-cm(2) cell. On 11-7/8 in. by 12 in. panels, the highest output obtained was 5.3 W over 847 cm(2), or 7.0 percent active-area efficiency. The aperture-area efficiency is presently about 12 percent lower, or 6.3 percent efficiency, because of interconnection losses. A 4-ft(2) panel was also produced. Resistivities of less than 100 ohm-cm have been observed consistently in phosphorus- or copper-doped CdTe. Surface analysis is presented for various CdTe treatments. Devices were characterized and analyzed using electron-beam-induced current, capacitance, spectral response, and I-V curves at various

temperatures. A model for junction transport is presented. An encapsulation system is described, and lifetime test results are presented. DOE

N89-27243# Florida Univ., Gainesville. Dept. of Electrical Engineering.
FREQUENCY-DOMAIN TRANSIENT ANALYSIS OF SILICON SOLAR CELLS
Russel E. Haney, Arnost Neugroschel, Konstantino Misiakos, and Fredrik A. Lindholm Mar. 1989 132 p Sponsored by Sandia National Labs.
(Contract DE-AC04-76DP-00789)
(DE89-010555; SAND-88-7039) Avail: NTIS HC A07/MF A01

A new technique, Frequency-Domain Transient Analysis (FDTA), has been proposed as a method for determining the transport parameters in a semiconducting material. It relies upon the performance of two separate experiments in order to characterize the particular device under test, one for uniformly absorbed light (h(nu) is approximately E sub g) and one for strongly absorbed light (h(nu) is much greater than E sub g.) The time-domain responses of the two forms of excitation are measured and transferred to a computer where they are then Fourier transformed. In the frequency domain, the experimental spectra may be related to analytic expressions, which are a function of minority carrier diffusivity. By optimizing the agreement between experimental and analytic spectra, predictions of the parameter values are made. In this study, the FDTA technique is applied to the characterization of base transport parameters in silicon solar cells, primarily those with back-surface field configurations. Evidence is presented which implies that the common assumption of the equality of majority and minority carrier diffusivity in comparably doped samples may often be invalid. DOE

N89-27244# Sandia National Labs., Albuquerque, NM.
DYNAMIC SIMULATION OF A MOLTEN-SALT SOLAR RECEIVER
Gregory J. Kolb, Douglas Neary, Michael R. Ringham, and Terry L. Greenlee Mar. 1989 90 p Prepared in cooperation with ESSCOR Corp., Solana Beach, CA
(Contract DE-AC04-76DP-00789)
(DE89-010556; SAND-88-2895) Avail: NTIS HC A05/MF A01

A dynamic simulation model of the solar subsystem of a molten-salt-in-tube central receiver power plant was constructed. It consists of 132 ordinary differential equations and is programmed in the system simulation language. The model was validated with experimental data obtained at the Central Receiver Test Facility and was shown to accurately predict actual receiver performance. It can be used to perform the following types of studies: (1) optimization of control algorithms for salt-in-tube receiver plants; (2) analysis of system performance during transient conditions; (3) response of the system following component failures; and (4) optimization of power production. The model is user friendly, includes several real-time graphic displays, and runs in real time on a personal computer. DOE

N89-27245# Polar Products, Torrance, CA.
SUN SYNCHRONOUS SOLAR REFRIGERATION Final Report
1989 43 p
(Contract DE-FG01-85CE-15219)
(DE89-011375; DOE/CE-15219/T4) Avail: NTIS HC A03/MF A01

The primary goal of this project was to prototype a complete Sun Synchronous Solar Powered Refrigerator. The key element to the technology is the development of the hermetic motor compressor assembly. The prototype was to be developed to either the stage where Polar Products could receive additional venture capital or to the point whereby Polar could use their own capital to manufacture the systems. Our goal was to construct a prototype which would be the next step to a proven and market ready product. To demonstrate the technology under laboratory conditions was a very minimal goal. DOE

N89-27246# Minnesota Univ., Minneapolis. Dept. of Mechanical Engineering.
HIGH TEMPERATURE SOLAR ELECTROTHERMAL PROCESSING Final Report, Jul. 1982 - Mar. 1989
Edward A. Fletcher 18 Apr. 1989 8 p
(Contract N00014-82-K-0523)
(AD-A207555; AD-E951331) Avail: NTIS HC A02/MF A01 CSCL 07/4

Chemical transformation at a given temperature and pressure requires a total energy input, Delta H of the chemical reaction. The minimum amount of energy which must be supplied as (electrical) work is Delta G of the reaction. The rest may be supplied as process heat or as work. Since Delta H of most chemical reactions is relatively independent of temperature, and Delta G decreases with temperature, there is an energy advantage in conducting electrolytic separations at high temperatures. At sufficiently high temperatures all of the necessary energy may be solar process heat, replacing all of the electrical energy input, as we have experimentally observed. We conducted analytical and experimental studies high temperature electrolysis in a highly concentrating solar furnace as well as in an electric furnace. We sought and found suitable materials for the construction of electrodes and cells and appropriate reactions which will acquire technological significance, designed and built receivers for sunlight and reactors which can interface with them, acquired operating experience with them, and conducted electrochemical and thermochemical measurements. GRA

N89-27247# Tel-Aviv Univ. (Israel). Authority for Research and Industrial Development Ltd.
ADVANCED CALCIUM-THIONYL CHLORIDE HIGH-POWER BATTERY Final Report, 23 Dec. 1987 - 22 Dec. 1988
Emanuel Peled 8 Feb. 1989 91 p
(Contract DAJA45-88-C-0012)
(AD-A207612; R/D-5899-CH-01) Avail: NTIS HC A05/MF A01 CSCL 10/3

Recently TAU has made a breakthrough in the development of two advanced Calcium Thionyl chloride systems which have much better storage properties than the state-of-art Ca-SOCl2 cell. This has been done by replacing the CaX2(X=AaCl4) electrolyte by SrX2 (type A), or BaX2 type B. The project's goals are to gain a better understanding fo the electrochemistry of the advanced systems and to establish their safety and performance. This report contains four chapters. The calorimetric study of Ca/Sr(AlCl4)-2-SOCl2 + 7 percent (v/v)SO2 C-size cells during constant-temperature discharge is reported in chapter 1. Fresh and stored (70 C for four weeks) cells were discharged inside a dedicated home-made calorimeter on two loads. There was no significant difference between fresh and stored cells with respect to heat generation during discharge. There was no loss in capacity during four weeks of storage at 70 C. Chapter 2 presents a calorimetric study of the baseline cell Ca/Ca(AlCl4)2-SOCl2 + 7 percent (V/V)SO2. Chapter 3 presents the performance, safety and storage properties of Ca/CaX2 and CA/SrX2 cells. Chapter 4 presents a summary of the results regarding the properties of MX2-SO2-TC solutions (M=Ca,Sr,Ba) including Raman spectra, viscosity and conductivity data. We explain the effect of SO2 and temperature on the conductivity and conduction mechanism. GRA

N89-27248# Midwest Research Inst., Golden, CO.
OCEAN ENERGY PROGRAM SUMMARY. VOLUME 2: RESEARCH SUMMARIES, FISCAL YEAR 1988
D. Bharathan Apr. 1989 39 p
(Contract DE-AC02-83CH-10093)
(DE89-000859; DOE/CH-10093/44) Avail: NTIS HC A03/MF A01

The Ocean Energy Program Summary for Fiscal Year 1988 is a two-volume reference set describing the technological advances and future research and development (R and D) direction of the Ocean Energy Program. This volume consists mainly of a compilation of detailed descriptions of the various R and D activities performed by the national laboratories and their subcontractors

from industry, academia, and nonprofit research institutions. It also contains a bibliography of the various publications produced under the program in recent years. DOE

N89-27249# Midwest Research Inst., Golden, CO. Solar Energy Research Inst.
YAW DYNAMICS OF HORIZONTAL AXIS WIND TURBINES Annual Report No. 2
A. Hansen and C. Xudong (Utah Univ., Salt Lake City.) Mar. 1989 200 p
(Contract DE-AC02-83CH-10093)
(DE89-000888; SERI/STR-217-3476) Avail: NTIS HC A09/MF A01

Numerous problems associated with yaw exist on free-yaw and yaw-driven wind turbines. Yaw-driven machines experience failures in the yaw drive mechanism due to excessive loads, while free-yaw machines experience high yaw rates and yaw misalignment problems. This report describes validation of a model for prediction of wind turbine yaw behavior. The model accounts for the coupled yaw and blade flapping motion of wind machines. The results from the model are compared to results from other analysis methods and to test data. Wind tunnel tests of a rigid-hub, two-bladed rotor, as well as full scale field test data from a rigid-hub, three-bladed turbine are used as the comparison cases in this report. The model predictions show good qualitative agreement with test data, but the magnitudes of predicted yaw moments are in error for some comparison cases. Future work will involve a more in-depth comparison of model results to comprehensive machine test data. Refinements will be made to the analytical model in order to improve correlations between theory and experiment. DOE

N89-27250# Giner, Inc., Waltham, MA.
DEVELOPMENT OF TERNARY ALLOY CATHODE CATALYSTS FOR PHOSPHORIC ACID FUEL CELLS Final Report
Nov. 1988 91 p
(Contract DE-AC21-82MC-24261)
(DE89-000926; DOE/MC-24261/2672) Avail: NTIS HC A05/MF A01

The overall objective of the program was the identification development and incorporation of high activity platinum ternary alloys on corrosion resistant supports, for use in advanced phosphoric acid fuel cells. Two high activity ternary alloys, Pr-Cr-Ce and Pt-Ni-Co, both supported on Vulcan XC-72, were identified during the course of the program. The Pr-Ni-Co system was selected for optimization, including preparation and evaluation on corrosion resistant supports such as 2700 C heat-treated Vulcan XC-72 and 2700 C heat-treated Black Pearls 2000. A series of tests identified optimum metal ratios, heat-treatment temperatures and heat-treatment atmospheres for the Pr-Ni-Co system. During characterization testing, it was discovered that approximately 50 percent of the nickel and cobalt present in the starting material could be removed, subsequent to alloy formation, without degrading performance. Extremely stable full cell performance was observed for the Pt-Ni-Co system during a 10,000 hour atmosphere pressure life test. Several theories are proposed to explain the enhancement in activity due to alloy formation. Recommendations are made for future research in this area. DOE

N89-27251# Sandia National Labs., Albuquerque, NM.
PROCEEDINGS OF THE ANNUAL SOLAR THERMAL TECHNOLOGY RESEARCH AND DEVELOPMENT CONFERENCE
W. A. Couch, ed. Feb. 1989 282 p Conference held in Arlington, VA, 8-9 Mar. 1989
(Contract DE-AC04-76DP-00789)
(DE89-010538; SAND-89-0463; CONF-8903117-Vugraphs) Avail: NTIS HC A13/MF A01

The Annual Solar Thermal Technology Research and Development Conference is being held at the Holiday Inn Crowne Plaza in Arlington, Virgina, March 8 and 9, 1989. This year the conference is meeting in conjunction with SOLTECH '89. SOLTECH '89 is a jointly sponsored meeting of the Solar Energy Industries Association, Interstate Solar Coordination Council, Sandia National Laboratories and the Solar Energy Research Institute. This report contains the agenda, extended abstracts and most significant visual aids used by the speakers during the Solar Thermal Technology research and development sessions. The program is divided into three sessions: Solar Electric Technology, Non-Electric Research and Development and Applications, and Concentrators. DOE

N89-27252# Midwest Research Inst., Golden, CO. Solar Energy Research Inst.
THE IMPACT OF SOLAR RADIATION RESOURCES ON THE SITING OF SOLAR THERMAL POWER PLANTS
E. L. Maxwell and M. D. Rymes Dec. 1988 81 p
(Contract DE-AC02-83CH-10093)
(DE89-000839; SERI/TR-215-3323) Avail: NTIS HC A05/MF A01

This report describes results of an effort to study the impact of solar radiation resources and enhance the use of solar radiation data for siting solar thermal power plants. This was a follow-on to an initial development of a siting methodology by the same authors. The work was done on a limited budget and does not constitute an actual power plant siting. Rather, these results demonstrate a methodology that incorporates various means for improving solar resource information and its use in identifying the best locations for power plants. These reports represent the first step in a technology transfer process that may lead to industrial applications of the methods described. The solar radiation characteristics must be analyzed further before accurate site selections and system designs can be made. DOE

N89-27253# Midwest Research Inst., Golden, CO. Solar Energy Research Inst.
WIND POWER: TODAY'S ENERGY OPTION
Apr. 1989 19 p
(Contract DE-AC02-83CH-10093)
(DE89-000876; SERI/SP-220-3486) Avail: NTIS HC A03/MF A01

This report is an overview of the current state of wind power programs. In addition to technical briefs, the report contains program management summaries and future goals of the wind power industry. DOE

N89-27254# California Univ., Berkeley. Lawrence Berkeley Lab. Materials and Chemical Sciences Div.
ELECTROCHEMICAL EVALUATION OF NEW FLUOROSULFONIC AND FLUOROPHOSPHONIC ACIDS AS FUEL CELL ELECTROLYTES Annual Report, 1 Jan. - 31 Dec. 1988
M. H. Saffarian and P. N. Ross Dec. 1988 69 p
(Contracts DE-AC03-76SF-00098; GRI-5086-260-1229)
(DE89-012840; LBL-27025; GRI-89/0060) Avail: NTIS HC A04/MF A01

The objective of this research program is to evaluate a series of new fluorosulfonic and fluorophosphonic acid as alternative fuel cell electrolytes having superior performance than phosphoric acid. Phosphoric acid, the electrolyte currently in use in acid H sub 2 O sub 2 fuel cells, suffers from several limitations. It is desirable to identify new electrolytes that have electrochemical and physical properties superior to those of phosphoric acid such as faster kinetics for oxygen reduction, higher oxygen solubility and lower anion adsorption on the platinum catalyst. Moreover, they should possess high ionic conductivities, low vapor pressures, electrochemical and thermal stabilities and low contact angles with Teflon, characteristics of phosphoric acid. DOE

N89-27255# California Univ., Berkeley. Lawrence Berkeley Lab. Materials and Chemical Sciences Div.
ELECTROCHEMICAL EVALUATION OF NEW FLUOROSULFONIC AND FLUOROPHOSPHONIC ACIDS AS FUEL CELL ELECTROLYTES Annual Report, Apr. 1987 - Apr. 1988
M. H. Saffarian and P. N. Ross Jun. 1988 56 p

(Contract DE-AC03-76SF-00098)
(DE89-013391; LBL-25492; GRI-88/0160) Avail: NTIS HC A04/MF A01

Phosphoric acid, the electrolyte currently in use in acid H sub 2 O sub 2 fuel cells, suffers from several limitations. It is desirable to identify new electrodes that have electrochemical and physical properties superior to those of phosphoric acid as faster kinetics for oxygen reduction, higher oxygen solubility and lower anion absorption on the platinum catalyst. Moreover, they should possess high ionic conductivities, low vapor pressures, electrochemical and thermal stabilities and low contact angles with Teflon, characteristics of phosphoric acid. A number of new fluorosulfonic and fluorophosphonic acids have been evaluated as candidates for fuel cell electrolytes. Oxygen reduction data on smooth platinum electrodes indicate that the addition of the new electrolytes to 85 pct phosphoric acid increases the oxygen solubility in the mixture. Solubility of (CF sub 3 SO sub 2) sub 2 CH sub 2 in water is quite good. Aqueous solutions of monosulfonic acids with a terminal SF sub 5 group such as SF sub 5 CHFCF sub 2 SO sub 3 H, are highly soluble in water and show high ionic conductivities, especially at elevated temperatures. The performance of the oxygen cathode of the fuel cell in 85 pct phosphoric acid containing 1.3 pct (HSO sub 3 (CF sub 2) sub 2) sub 2 O is superior to that of pure phosphoric acid. DOE

N89-27256*# University of South Florida, Tampa.
THERMAL EVALUATION OF ADVANCED SOLAR DYNAMIC HEAT RECEIVER PERFORMANCE Final Report, Jan - Dec. 1988
Roger A. Crane Mar. 1989 131 p
(Grant NAG3-851)
(NASA-CR-185117; NAS 1.26:185117) Avail: NTIS HC A07/MF A01 CSCL 10A

The thermal performance of a variety of concepts for thermal energy storage as applied to solar dynamic applications is discussed. It is recognized that designs providing large thermal gradients or large temperature swings during orbit are susceptible to early mechanical failure. Concepts incorporating heat pipe technology may encounter operational limitations over sufficiently large ranges. By reviewing the thermal performance of basic designs, the relative merits of the basic concepts are compared. In addition the effect of thermal enhancement and metal utilization as applied to each design provides a partial characterization of the performance improvements to be achieved by developing these technologies. Author

45 ENVIRONMENT POLLUTION

Includes atmospheric, noise, thermal, and water pollution.

N89-27257*# National Oceanic and Atmospheric Administration, Boulder, CO. Wave Propagation Lab.
OBSERVATIONS OF ATMOSPHERIC EMISSION AND ATTENUATION AT 20.6, 31.65 AND 90 GHz BY A GROUND-BASED RADIOMETER
E. R. Westwater, J. B. Snider, and M. Falls Nov. 1988 22 p
Sponsored by JPL, Pasadena, CA
(NASA-CR-185719; NAS 1.26:185719; PB89-152466; NOAA-TM-ERL-WPL-156) Avail: NTIS HC A03/MF A01 CSCL 13B

During 1987 and 1988, ground-based zenith-viewing observations of atmospheric thermal emission were made at frequencies of 20.6, 31.65, and 90.0 GHz. At the locations of the experiments-San Nicolas Island, California, and Denver, Colorado-radiosonde observations of temperature and humidity were also available. The data, after conversion to attenuation by use of the mean radiating temperature approximation, were processed to derive attenuation statistics. Both clear and cloudy attenuation characteristics are examined and compared with results from most recent theories. The predictability and interdependence of the three separate channels are also examined. It is found that attenuation for any two channels can predict that of the third to within 25 percent. GRA

N89-27258# Environmental Protection Agency, Research Triangle Park, NC. Environmental Criteria and Assessment Office.
CONCENTRATIONS AND PATTERNS OF PHOTOCHEMICAL OXIDANTS IN THE UNITED STATES
B. E. Tilton and S. A. Meeks Jan. 1989 22 p
(PB89-136683; ECAO-R-0223; EPA/600/D-88/239) Avail: NTIS HC A03/MF A01 CSCL 13B

The report describes ozone and peroxyacetyl nitrate (PAN) levels at urban sites in the U.S., and ozone levels at selected nonurban sites. Sample diurnal curves for ozone at suburban and nonurban sites are presented. Highest concentrations of both oxidants occur in California, where the second-highest 1-hr concentration of ozone in 1983 was 0.37 ppm, and the highest PAN concentration reported in this decade was 0.047 ppm, in 1980. At selected nonurban sites, maximum 1-hr ozone levels for 1978 to 1981 were about half the second-highest 1-hr ozone levels at urban sites in those years. Examples presented of temporal patterns of ozone show distinct seasonality at suburban versus nonurban sites, and point out potential implications for exposures to ozone of populations, vegetation, and other receptors. Data on co-occurrences of ozone with nitrogen dioxide or sulfur dioxide indicate relatively few such events at levels of potential concern for vegetation and public health. GRA

N89-27259# Environmental Protection Agency, Research Triangle Park, NC. Atmospheric Research and Exposure Assessment Lab.
REGIONAL OZONE MODELING IN THE NORTHEASTERN US: SELECTION OF METEOROLOGICAL EPISODES Report, Mar. - Oct. 1988
Dennis C. Doll, Thomas E. Pierce, and Norman C. Possiel Jan. 1989 8 p
(PB89-136691; EPA/600/D-88/273) Avail: NTIS HC A02/MF A01 CSCL 13B

In 1987 a study was initiated of the photochemical smog problem along the Northeast U.S. Corridor. The study, Regional Ozone Modeling for Northeast Transport (ROMNET), has three major components: (1) to identify emission control strategies; (2) to assemble emission inventories suitable for regional ozone modeling; and (3) to model the control strategies with appropriate meteorological and emissions data. One important prerequisite for the third component is to select three meteorological episodes that reflect typical transport patterns associated with high ozone levels. These flow regimes were along-corridor flow, recirculation, and westerly flow into the corridor. Author

N89-27260# Environmental Protection Agency, Research Triangle Park, NC. Atmospheric Research and Exposure Assessment Lab.
COMPARISON OF MODELLED AND MEASURED TRACER GAS CONCENTRATIONS DURING THE ACROSS NORTH AMERICA TRACER EXPERIMENT (ANATEX)
T. L. Clark, R. D. Cohn, S. K. Seilkop, R. R. Draxler, and J. L. Heffter (National Oceanic and Atmospheric Administration, Washington, DC.) Jan. 1989 17 p
(PB89-136709; EPA/600/D-88/274) Avail: NTIS HC A03/MF A01 CSCL 13B

The 24-hour surface concentrations of several perfluorocarbon tracer gases measured during the 1987 Across North America Tracer Experiment (ANATEX) provided a unique continental-scale data set with which to evaluate long-range transport and diffusion models. One such model, a multilayer Lagrangian model, was evaluated in the ANATEX Model Evaluation Study (AMES) by comparing distributions and time series of calculated and measured tracer concentrations at bands of sampling sites nearly equidistant from one of the two tracer release sites and by computing spatial differences in the concentration-weighted centroids of 20, 24-hour tracer footprints or composite plumes. The results for this model indicated that it overemphasized the effects of the stronger

upper-level winds. In spite of the bias in transport speed, the distributions of the calculated and measured concentrations were quite similar. GRA

N89-27261# Environmental Protection Agency, Las Vegas, NV. Environmental Monitoring Systems Lab.
GEO-EAS (GEOSTATISTICAL ENVIRONMENTAL ASSESSMENT SOFTWARE) USER'S GUIDE
Evan J. Englund and Allen R. Sparks (Computer Sciences Corp., Las Vegas, NV.) Sep. 1988 182 p
(Contract EPA-68-01-7325)
(PB89-151252; EPA/600/4-88/033A; EPA/SW/DK-89/019A)
Avail: NTIS HC A09/MF A01 CSCL 13B

The installation and use of the Geo-EAS (Geostatistical Environmental Assessment Software) software package on an IBM-PC compatible computer system are described. A detailed example is provided showing how to use the software to conduct a geostatistical analysis of a data set. Thirteen Geo-EAS programs are documented. The principal functions of the package are the production of 2-dimensional grids and contour maps of interpolated (kriged) estimates from sample data. Other functions include data preparation, data maps, univariate statistics, scatter plots/linear regression, and variogram computation and model fitting. Extensive use of screen graphics such as maps, histograms, scatter plots and variograms help the user search for patterns, correlations, and problems in a data set. Data maps, contour maps, and scatter plots can be plotted on an HP compatible pen plotter. Individual programs can be run independently; the statistics and graphics routines may prove useful even when a full geostatistical study is not appropriate. GRA

N89-27262# New Mexico Inst. of Mining and Technology, Socorro. Dept. of Chemistry.
ASSESSING THE SENSITIVITY OF HIGH ALTITUDE NEW MEXICAN WILDERNESS LAKES TO ACIDIC PRECIPITATION AND TRACE METAL CONTAMINATION
Thomas R. Lynch, Carl J. Popp, Gerald Z. Jacobi, and James Robertson (New Mexico State Bureau of Mines and Mineral Resources, Socorro.) Oct. 1988 189 p
(Grant DI-14-08-0001-G-1505)
(PB89-148456) Avail: NTIS HC A09/MF A01 CSCL 13B

Seventeen high mountain lakes in northern New Mexico were sampled to determine their present biological and chemical condition. Sediment cores were collected at each of the lakes to determine trace metal concentrations, diatom assemblages, and mineralogies as a function of depth. Two of the cores were agedated using Pb-210 chronology. Eight of the lakes exhibited low alkalinities and, therefore, low capacities for neutralization. Atmospheric deposition appears to be contributing acid and trace metals associated with anthropogenic sources to some of the lakes. Trace metal accumulations in the upper layers of Santa Fe Lake began about 60 years ago and about 10 years ago in Truchas Lake. An acid pulse (pH 5.7) associated with snow melt was documented in Santa Fe Lake, and corresponded with an observed decrease of Daphnia sp. populations. Sediment diatom assemblages in cores from Santa Fe Lake and Truchas Lake appear to be shifting to more acid tolerant species than in the past. GRA

N89-27263# Katholieke Universiteit, Nijmegen (Netherlands).
THE PHOTOACOUSTIC EFFECT, REFINED AND APPLIED TO BIOLOGICAL PROBLEMS Ph.D. Thesis
Fransiscus Johannes Harren 1988 107 p
(PB89-153597) Avail: NTIS HC A06/MF A01 CSCL 13B

The photoacoustic effect is used to determine the presence of trace gases in air. The method is improved to an extreme sensitivity threshold, so that the ethylene production of flowers and plants can be measured with high accuracy. GRA

N89-27264# Alliance Technologies Corp., Chapel Hill, NC.
PROCEDURES FOR THE PREPARATION OF EMISSION INVENTORIES FOR PRECURSORS OF OZONE, VOLUME 1, THIRD EDITION
Sharon L. Kersteter Dec. 1988 246 p
(Contract EPA-68-02-4396)
(PB89-154209; EPA/450/4-88/021-Vol-1) Avail: NTIS HC A11/MF A01 CSCL 13B

Procedures are described for compiling emission inventories of precursors of ozone (volatile organic compounds, nitrogen oxides and carbon monoxide) for use in less data-intensive models such as the Empirical Kinetic Modeling Approach (EKMA). Such inventories are required for submission of ozone State Implementation Plans (SIPs) for those areas acquired to revise their plans after December 31, 1987. The basic inventory elements - planning, data collection, emission inventory estimates, reporting - are discussed. Various examples are included to aid the agency in the understanding and use of the document. Author

N89-27265# Environmental Protection Agency, Annapolis, MD.
CHESAPEAKE BAY NONPOINT SOURCE PROGRAMS
Jan. 1988 129 p
(PB89-152037) Avail: NTIS HC A07/MF A01 CSCL 13B

Described here are the current programs to ameliorate nonpoint sources of pollution to the Chesapeake Bay which have been developed by the four jurisdictions in cooperation with other agencies, the achievements to date in terms of pollutant removal, and recommendations for future directions of the Bay Program over the next several years. Author

N89-27266# Environmental Protection Agency, Washington, DC.
ANALYTICAL PROCEDURES FOR ENVIRONMENTAL QUALITY CONTROL, VOLUME 1
Lawrence K. Wang, ed. and Mu Hao Sung Wang, ed. (New York State Dept. of Environmental Conservation, Albany.) 15 Jan. 1989 279 p Prepared in cooperation with Stevens Inst. of Tech., Hoboken, NJ; Rensselaer Polytechnic Inst., Troy, NY; and National Cheng Kung Univ., Tainan, Taiwan
(PB89-158604; LIR/1-89/331-Vol-1) Avail: NTIS HC A13/MF A01 CSCL 13B

The report covers fourteen important documents. Topics include: analysis of trihalomethanes in drinking water; methods for the determination of organic compounds in finished drinking water and raw source water; direct measurement of volatile organic compounds in breathing-zone air, drinking water, breath, blood, and urine; techniques to determine a company's ability to conduct a quality stack test; laboratory evaluation of level one organic analysis procedures; application of methods for analysis of polychorinated biphenyls (PCB), organochlorine pesticides and phthalate esters contained in landfill leachates; method development for determination of polychlorinated hydrocarbons in municipal sludge; application and determination of organic polymers; and a test method for analyzing anionic or cationic surfactants in industrial water. GRA

N89-27267# Oak Ridge National Lab., TN. Environmental Sciences Div.
FATE AND EFFECTS OF PAHS IN THE TERRESTRIAL ENVIRONMENT: AN OVERVIEW
Nelson T. Edwards 1989 16 p Presented at the 82nd Annual Air and Waste Management Association Meeting and Exhibition, Anaheim, CA, 25 Jun. 1989
(Contract DE-AC05-84OR-21400)
(DE89-010319; CONF-890692-5) Avail: NTIS HC A03/MF A01

A recent review of polycyclic aromatic hydrocarbons (PAHs) in the terrestrial environment pointed to the need for more information and a better understanding of factors controlling the fate of PAHs. With ever increasing energy demands by a growing world population, the amount of PAHs released from energy-producing technologies becomes potentially greater. When PAHs are released into the atmosphere in the vapor phase, most are adsorbed to particles (e.g., fly ash). They are also found in solid and liquid wastes from various energy technologies. PAHs that adsorb to particles in the atmosphere may be carried kilometers from the source before being deposited on vegetation and soil. The well-known PAHs such as benzo(a)pyrene (BaP) are innocuous by themselves, but can be biologically activated by enzymes to

form epoxides that are carcinogenic and mutagenic. This report summarizes our knowledge about PAHs in the terrestrial environment with emphasis on their fate and effects on vegetation. DOE

N89-27268# Oak Ridge National Lab., TN.
CRITERIA FOR SELECTING A CO2/CLIMATE CHANGE REGION OF STUDY
Jae Edmonds, Robert Cushman, William Easterling, Thomas Malone, Norman Rosenberg, Michael Scott, and Gerold Stokes 1989 15 p Presented at the 82nd Annual Air and Waste Management Association Meeting and Exhibition, Anaheim, CA, 25 Jun. 1989
(Contracts DE-AC05-84OR-21400; DE-AC06-76RL-01830)
(DE89-011233; CONF-890692-6) Avail: NTIS HC A03

One of the most important research issues active today is the greenhouse issue. Progress has been made in exploring the relationship between human activities and the accumulation of CO2 and other radiatively important gases in the atmosphere. While significant research remains in refining our understanding of the timing of possible CO2/climate change, the examination of the nature and magnitude of consequences of CO1/climate change remains in a relatively early stage of development. While the accumulation of greenhouse gases in the atmosphere may be a global problem, the consequences of CO1/climate change will be experienced regionally. It is therefore critical that methods be developed to address the regional examination of CO2/climate change. An analytical framework is described and a cookie cutter technique is utilized to deal with multiple resource sectors in selecting a Region of Study. The result leads to the selection of the four midwestern states of Kansas, Nebraska, Iowa, and Missouri. The role of information systems, uncertainty analysis, and knowledge transfer is discussed. DOE

N89-27269# Oak Ridge Gaseous Diffusion Plant, TN.
A COMPUTER PROGRAM FOR SIMULATING THE ATMOSPHERIC DISPERSION OF UF6 AND OTHER REACTIVE GASES HAVING POSITIVE, NEUTRAL, OR NEGATIVE BUOYANCY
S. G. Bloom, R. A. Just, and W. R. Williams Mar. 1989 234 p
(Contract DE-AC05-84OT-21400)
(DE89-012734; K/D-5694) Avail: NTIS HC A11/MF A01

This report describes a mathematical model which was developed to simulate the atmospheric dispersion of chemically reactive gases that may be neutrally buoyant, positively buoyant, or negatively buoyant with respect to the ambient air. Emphasis is on materials used at uranium enrichment facilities, particularly uranium hexafluoride and its hydrolysis products. The report discusses the mathematical principles of the model, the chemical and physical properties used in the model, the computer program which was developed to perform the calculations, and the iterative techniques used in the model. Descriptions of the computer program are given as appendices. DOE

N89-27270# Pechan (E. H.) and Associates, Inc., Durham, NC.
HISTORIC EMISSIONS OF VOC (VOLATILE ORGANIC COMPOUNDS) AND NOx IN THE UNITED STATES FROM 1900 TO 1985
Gerhard Gschwandtner and J. David Mobley (Environmental Protection Agency, Research Triangle Park, NC.) 1989 9 p
(Contract EPA-68-02-4271)
(PB89-173223; EPA/600/D-89/012) Avail: NTIS HC A02/MF A01 CSCL 13B

Historic emissions of volatile organic compounds (VOCs) and nitrogen oxides (NOx) in the U.S. from 1900 to 1985 are discussed. Total VOC emissions have increased over the study period with peaks around 1930 and 1970. In 1900, transportation sources contributed 2 percent of the total emissions. By 1960, these sources contributed nearly 50 percent of the total VOC emissions. Also, the percentage contribution of industrial processes increased from about 3 percent in 1900 to 26 percent in 1960 and 39 percent in 1980. External fuel combustion was a major category from 1900 to 1940, but the percentage contribution has decreased since then. Similarly, the contribution by miscellaneous other sources has also decreased with time. The percentage contribution of solid waste disposal appears to have remained nearly constant over time. NOx emissions have increased nearly steadily since 1900, while SO2 emissions have gradually increased from 1900 to 1980 with considerable changes during certain shorter periods of time. VOCs have also increased, but the rate of increase appears to be less than that of NOx and more than SO2, at least on the national level. Author

N89-27271# Department of Energy, Washington, DC. Office of Basic Energy Sciences.
ATMOSPHERIC CARBON DIOXIDE AND THE GREENHOUSE EFFECT
M. W. Firestine, ed. May 1989 36 p
(DE89-012869; DOE/ER-0411) Avail: NTIS HC A03/MF A01

This document contains a non-technical review of the problems associated with atmospheric carbon dioxide and the resulting greenhouse effect. DOE

N89-27272# Lawrence Livermore National Lab., CA. Atmospheric and Geophysical Sciences Div.
INTRODUCTION TO BACKGROUND MATERIALS FOR WORKSHOP NO. 1: GLOBAL CLIMATE CHANGE AND ITS EFFECTS ON CALIFORNIA
John B. Knox Mar. 1989 12 p
(Contract W-7405-eng-48)
(DE89-013381; UCID-21631) Avail: NTIS HC A03/MF A01

In the fall of 1988, the University of California organized a new public service initiative on global climate change in response to inquiries and requests from members of Congress and the Department of Energy. This new system-wide initiative involves all of the University of California campuses and the University's three national laboratories at Berkeley, Los Alamos, and Livermore. Our goal in organizing this new Greenhouse Initiative is to focus the multidisciplinary resources of the UC campuses and the team-oriented research capabilities of the laboratories on the prospect of global warming and its plausible associated effects on the planet and its nations, on what may be the most challenging global environmental issue facing the world in the 1990's and beyond. With the consultation of many people, we have organized a series of three workshops all scheduled to occur by November 1989, to assure that our findings will be available in a timely fashion to the national dialogue on global warming and the national studies in progress. We briefly summarize the scope of these three workshops. DOE

N89-27273# Lawrence Livermore National Lab., CA.
PREVENTING DEPLETION OF STRATOSPHERIC OZONE: IMPLICATIONS ON FUTURE AIRCRAFT EMISSIONS, REVISION 1
Douglas E. Kinnison and Donald J. Wuebbles May 1989 15 p Presented at the 82nd Annual Air and Waste Management Association Meeting and Exhibition, Anaheim, CA, 25-30 Jun. 1989
(Contract W-7405-eng-48)
(DE89-013779; UCRL-99926-Rev-1; CONF-890692-4-Rev-1)
Avail: NTIS HC A03/MF A01

There is much renewed interest in the development of faster aircraft for intercontinental passenger flights. Such aircraft would likely spend a large fraction of their flight time in the stratosphere, at altitudes as high as 35 km. It is important, in order to prevent the problems with the proposed supersonic-transport that occurred in the early 1970's, that the aircraft industry work together with the atmospheric science community to insure that future aircraft emissions will not deplete stratospheric ozone. In this study, we have used our two-dimensional model of the troposphere and stratosphere to examine the sensitivity of stratospheric ozone to such emissions. Initial results indicate, for commercial fleets as large as proposed for the original SST and depending on the odd-nitrogen emissions per engine, that substantial decreases in stratospheric ozone could result. The decrease in ozone is sensitive

to the altitude and latitude in the emissions. Effects on ozone, for the same emission rate, tend to be larger as altitude increases, until a maximum effect is reached near 30 km. DOE

N89-27274# California Univ., Berkeley. Lawrence Berkeley Lab.
PROCEEDINGS OF THE ENERGY EFFICIENCY AND STRUCTURAL CHANGE: IMPLICATIONS FOR THE GREENHOUSE PROBLEM WORKSHOP
S. Meyers, ed. Aug. 1988 81 p Workshop held in Oakland, CA, 1 May 1988
(Contract DE-AC03-76SF-00098)
(DE89-012852; LBL-25716; CONF-8805294-Summ) Avail: NTIS HC A05/MF A01

The Workshop on Energy Efficiency and Structural Change: Implications for the Greenhouse Problem, was part of a major study of global change and options for mitigating such change being conducted by the U.S. Environmental Protection Agency (EPA). It was one of four workshops sponsored by EPA on various topics important to analysis of the greenhouse problem. The purpose of this workshop, which was organized and co-sponsored by Lawrence Berkeley Laboratory, was to provide a forum for experts from a variety of backgrounds to share information and ideas about the long-run prospects for energy efficiency and the effect on energy demand of structural economic and demographic changes. The information presented and discussed at the workshop is being used by the EPA in refining scenarios of long-range energy consumption and the climatic implications of different levels of energy use, and in its examination of the impact of policy options that might be available to the global community to limit emissions of atmospheric gases that contribute to global climate change. DOE

N89-27275# Argonne National Lab., IL.
FIELD STUDIES FOR DETERMINING THE CHARACTERISTICS AND DYNAMICS OF LOCAL CIRCULATIONS
Paul Gudiksen, William E. Clements, Rayford P. Hosker, Jr., C. David Whiteman, William D. Neff, Richard L. Coulter, and G. Eugene Start (National Oceanic and Atmospheric Administration, Boulder, CO.) 1989 39 p Presented at the 2nd International Workshop on Real-Time Computing of the Environmental Consequences of an Accidental Release to the Atmosphere from Nuclear Installations, Leuembourg, Netherlands, 16 May 1989
(Contract W-31-109-eng-38)
(DE89-013639; CONF-8905148-1) Avail: NTIS HC A03/MF A01

The U.S. Department of Energy sponsored Atmospheric Studies in Complex Terrain (ASCOT) program is designed to improve our understanding of the physical processes that govern pollutant dispersion in areas of complex terrain and to develop the technology needed to predict the air quality impact of pollutants released into terrain dominated flows. The focus of the program has been on the study of the characteristics of locally generated valley circulations with the primary emphasis being on evaluating the life-cycle of nocturnal cold air slope and valley flows. This phenomenon was selected on the basis of its importance for transporting pollutants from energy related facilities to population centers that are generally situated within valleys. The program's field studies component, which is closely integrated with the modeling activities, provides the data needed to evaluate the characteristics and dynamics of locally generated valley circulations. The Geysers geothermal area in northern California, situated within the coastal-mountain range, was chosen as the initial field studies area. Three series of major field experiments were performed in this area during the period from 1979 to 1981. DOE

N89-27276# Lawrence Livermore National Lab., CA.
GLOBAL ENVIRONMENTAL EFFECTS OF IMPACT-GENERATED AEROSOLS: RESULTS FROM A GENERAL CIRCULATION MODEL, REVISION 1
Curt Covey, Steven J. Ghan, John J. Walton, and Paul R. Weissman (Jet Propulsion Lab., California Inst. of Tech., Pasadena.) Jun. 1989 22 p Presented at the Global Catastrophes Conference, Snowbird, UT, 20 Oct. 1988 Revised
(Contract W-7405-eng-48)
(DE89-014179; UCRL-98894-Rev-1; CONF-8810341-2-Rev-1)
Avail: NTIS HC A03/MF A01

Interception of sunlight by the high altitude worldwide dust cloud generated by impact of a large asteroid or comet would lead to substantial land surface cooling, according to our three-dimensional atmospheric general circulation model (GCM). This result is qualitatively similar to conclusions drawn from an earlier study that employed a one-dimensional atmospheric model, but in the GCM simulation the heat capacity of the oceans substantially mitigates land surface cooling, an effect that one-dimensional models cannot quantify. On the other hand, the low heat capacity of the GCM's land surface allows temperatures to drop more rapidly in the initial stage of cooling than in the one-dimensional model study. These two differences between three-dimensional and one-dimensional model simulations were noted previously in studies of nuclear winter; GCM-simulated climatic changes in the Alvarez-inspired scenario of asteroid/comet winter, however, are more severe than in nuclear winter because the assumed aerosol amount is large enough to intercept all sunlight falling on earth. Impacts of smaller objects could also lead to dramatic, though less severe, climatic changes, according to our GCM. Our conclusion is that it is difficult to imagine an asteroid or comet impact leading to anything approaching complete global freezing, but quite reasonable to assume that impacts at the Alvarez level, or even smaller, dramatically alter the climate in at least a patchy sense. DOE

N89-27277# Direction des Recherches, Etudes et Techniques, Paris (France). Groupe Mecanique et Physique des Fluides.
STUDY OF DISPERSION AND PENETRATION OF TRACER AND POLLUTANTS IN POROUS MEDIA AND FRACTURED ROCKS Final Report [ETUDE DE LA DISPERSION ET LA PENETRATION DE TRACEURS ET DE POLLUANTS DANS LES MILIEUX POREUX ET LES ROCHES FRACTUREES]
1988 147 p In FRENCH
(Contract DRET-85-172)
(ETN-89-94806) Avail: NTIS HC A07/MF A01

The prediction of macroscopic parameter variations such as permeability and conductivity is discussed. The space distribution of the parameters, and the characterization of the heterogeneity of laboratory specimens or those on the ground with the help of measurements of tracer dispersion is considered. Numerical simulation procedures, two dimensional models, and experimental dispersion tests are described. ESA

46 GEOPHYSICS

Includes aeronomy; upper and lower atmosphere studies; ionospheric and magnetospheric physics; and geomagnetism.

For space radiation see *93 Space Radiation.*

N89-27278# Geological Survey, Reston, VA.
MAFIC AND ULTRAMAFIC XENOLITHS FROM VOLCANIC ROCKS OF THE WESTERN UNITED STATES
H. G. Wilshire, C. E. Meyer, J. K. Nakata, L. C. Calk, J. W. Shervais, J. E. Nielson, and E. C. Schwarzman 1988 180 p
(PB89-124127; PP-1443; LC-88-600047) Avail: NTIS HC A09/MF A01 CSCL 08G

Mafic and ultramafic xenoliths in the Western United States are present in volcanic rocks ranging from lamprophyric to dacitic in composition and are found in every major tectonic province from the Coast Ranges in California to the Great Plains. Xenoliths from 68 localities are described here. Xenoliths in volcanic rocks in the Western United States are placed here in eight main groups: (1) accidental inclusions of crustal sedimentary, igneous, and metamorphic rocks; (2) gabbroids; (3) metagabbroids; (4) spinel peridotite, pyroxenite, and phlogopite-rich rocks of the Cr-diopside group; (5) spinel peridotite, pyroxenite, and amphibole-, and

mica-rich rocks of the Al-augite group; (6) spinel peridotite and pyroxenite of the bottle-green pyroxene group; (7) spinel peridotite and pyroxenite of the feldspathic ultramafic group; and (8) peridotite and pyroxenite of the garnetiferous ultramafic group. Relative abundances of groups 2 through 8 vary from locality to locality, but in general peridotite of group 4 is dominant, and all other types, including pyroxenites of group 4, are very subordinate in abundance. Author

N89-27279*# National Aeronautics and Space Administration. Goddard Space Flight Center, Greenbelt, MD.
GEODETIC MEASUREMENT OF DEFORMATION IN CALIFORNIA Ph.D. Thesis - Massachusetts Inst. of Technology
Jeanne Sauber Apr. 1989 213 p
(Grants NAG5-814; NAG5-459; NGT-50103)
(NASA-TM-100732; Rept-89B00124; NAS 1.15:100732) Avail: NTIS HC A10/MF A01 CSCL 08G

The very long baseline interferometry (VLBI) measurements made in the western U.S. since 1979 as part of the NASA Crustal Dynamics Project provide discrete samples of the temporal and spatial deformation field. The interpretation of the VLBI-derived rates of deformation requires an examination of geologic information and more densely sampled ground-based geodetic data. In the first two of three related studies, triangulation and trilateration data measured on two regional networks, one in the central Mojave Desert and one in the Coast Ranges east of the San Andreas fault, have been processed. At the spatial scales spanned by these local geodetic networks, auxiliary geologic and geophysical data have been utilized to examine the relation between measured incremental strain and the accommodation of strain seen in local geological structures, strain release in earthquakes, and principal stress directions inferred from in situ measurements. In a third study, the geocentric position vectors from a set of 77 VLBI experiments beginning in October 1982 have been used to estimate the tangential rate of change of station positions in the western U.S. in a North-America-Fixed reference frame. Author

N89-27280# National Oceanic and Atmospheric Administration, Boulder, CO. Air Resources Lab.
TRACE GASES IN AND OVER THE WEST PACIFIC AND EAST INDIAN OCEANS DURING THE EL NINO-SOUTHERN OSCILLATION EVENT OF 1987: A REPORT OF GMCC (GEOPHYSICAL MONITORING FOR CLIMATIC CHANGE) DATA COLLECTED ON THE SECOND SOVIET-AMERICAN GAS AND AEROSOL EXPERIMENT (SAGA 2)
James H. Butler, James W. Elkins, Christina M. Brunson, Keith B. Egan, Thayne M. Thompson, Thomas J. Conway, and Brad D. Hall Dec. 1988 117 p
(PB89-159685; NOAA-DR-ERL-ARL-16) Avail: NTIS HC A06/MF A01 CSCL 04A

Five trace gases in the surface water and atmosphere of the West Pacific and East Indian Oceans were measured by automated gas chromatography from May through July 1987. The data included more than 1000 measurements each of N2O, F11 and F12 in the surface water and in the atmosphere, and about 2000 measurements each of CH4 and CO2 in the surface water and atmospheric boundary layer of the West Pacific. In addition, over 600 measurements of dissolved N2O were obtained from hydrocasts made along the entire 45,000 km cruise track. Data from this cruise are presented here in graphic and tabular form, along with detailed discussions of the methods used in analyzing the samples and reducing the data, and a brief summary of the results and their significance. Also included are results from laboratory tests of a new, automated headspace technique for dissolved N2O and laboratory tests of the Weiss equilibrator. Data from the equilibrator tests were used to develop a mathematical model of its performance. GRA

N89-27281*# Jet Propulsion Lab., California Inst. of Tech., Pasadena.
ATMOSPHERIC PROPAGATION ISSUES RELEVANT TO OPTICAL COMMUNICATIONS
James H. Churnside (National Oceanic and Atmospheric Administration, Boulder, CO.) and Kamran Shaik Jan. 1989 57 p
(NASA-CR-185718; NAS 1.26:185718; PB89-159701; NOAA-TM-ERL-WPL-159) Avail: NTIS HC A04/MF A01 CSCL 04A

Atmospheric propagation issues relevant to space-to-ground optical communications for near-earth applications are studied. Propagation effects, current optical communication activities, potential applications, and communication techniques are surveyed. It is concluded that a direct-detection space-to-ground link using redundant receiver sites and temporal encoding is likely to be employed to transmit earth-sensing satellite data to the ground some time in the future. Low-level, long-term studies of link availability, fading statistics, and turbulence climatology are recommended to support this type of application. GRA

N89-27282# Kansas State Univ., Manhattan. Engineering Experiment Station.
COMPUTATIONAL TECHNIQUES IN GAMMA-RAY SKYSHINE ANALYSIS M.S. Thesis
Darin L. George Dec. 1988 242 p
(Contract DE-AC05-76OR-00033)
(DE89-010156; DOE/OR-00033/T417; Rept-204) Avail: NTIS HC A11/MF A01

Two computer codes were developed to analyze gamma-ray skyshine, the scattering of gamma photons by air molecules. A review of previous gamma-ray skyshine studies discusses several Monte Carlo codes, programs using a single-scatter model, and the MicroSkyshine program for microcomputers. A benchmark gamma-ray skyshine experiment performed at Kansas State University is also described. A single-scatter numerical model was presented which traces photons from the source to their first scatter, then applies a buildup factor along a direct path from the scattering point to a detector. The FORTRAN code SKY, developed with this model before the present study, was modified to use Gauss quadrature, recent photon attenuation data and a more accurate buildup approximation. The resulting code, SILOGP, computes response from a point photon source on the axis of a silo, with and without concrete shielding over the opening. Another program, WALLGP, was developed using the same model to compute response from a point gamma source behind a perfectly absorbing wall, with and without shielding overhead. DOE

N89-27283# Radiomana, Paris (France).
INVESTIGATIONS ON LOCAL SEISMIC PHASES AND EVALUATION OF BODY WAVES MAGNITUDE Scientific Report No. 1, 15 Jul. 1987 - 14 Jul. 1988
Stephane Gaffet, Bernard Massinon, Pierre Mechler, and Florence Riviere 14 Sep. 1988 22 p
(Grant AF-AFOSR-0331-87; DARPA Order 5299; AF Proj. 7A10)
(AD-A206633; AFGL-TR-88-0334) Avail: NTIS HC A03/MF A01 CSCL 08/11

For near events, synthetics seismograms are computed using BOUCHON's method, for various heterogeneous structures. A special emphasis is put on topographic irregularities. This work was presented in the poster session at the 10th annual DARPA/AFGL SEISMIC RESEARCH SYMPOSIUM (2 to 5 May 1988). The programs used for this work are now implemented on our new SUN 3/280 system. For teleseisms, the main effort was first to obtain attenuation models between Eastern Kazakh and several regions in France. The application of those results to source functions for a series of events recorded in France is currently being done. A first by-product from this study was a re-evaluation of the magnitude of all events and a determination of stations corrections. GRA

N89-27284# California Univ., Santa Cruz. Dept. of Physics.
APPLICATION OF THE THEORY OF WAVE PROPAGATION THROUGH RANDOM MEDIA TO PHASE AND AMPLITUDE FLUCTUATIONS OF SEISMIC P-WAVES Final Report, 18 Feb. - 30 Sep. 1988
Stanley M. Flatte 18 Oct. 1988 39 p
(Contract F19628-88-K-0014)
(AD-A207207; AFGL-TR-88-0315) Avail: NTIS HC A03/MF A01 CSCL 08/11

Statistical descriptions of variations in P-wave velocity in the earth are related to observations in phase, travel-time, and amplitude fluctuations of seismic-wave signals received at teleseismic distances. A number of results have been obtained, including a model for variations down to 250 km under the NOSAR array in Norway, and for variations at a number of locations at the core-mantle boundary. Our final report consists of a list of articles published or submitted during the contact period, a short description of our objectives, a list of conferences attended, and copies of two reprints that give the essential technical content of our recent progress. GRA

N89-27285# Army Cold Regions Research and Engineering Lab., Hanover, NH.
INVESTIGATIONS OF DIELECTRIC PROPERTIES OF SOME FROZEN MATERIALS USING CROSS-BOREHOLE RADIOWAVE PULSE TRANSMISSIONS
Steven A. Arcone and Allan J. Delaney Mar. 1989 26 p
(AD-A207302; CRREL-89-4) Avail: NTIS HC A03/MF A01 CSCL 08/10

Pulsed radiowaves have been transmitted between boreholes at specially prepared sites in central Alaska to determine physical properties of the intervening material. The boreholes were drilled 12 to 25 m deep in both ice-rich silt and frozen alluvium materials commonly found in the Alaskan interior. The pulse spectra were centered near 100 MHz and were analyzed to obtain the ground dielectric constant epsilon and the attenuation rate beta, which were then correlated with material type, water content and temperature. The ice-rich silt, which had volumetric ice contents between 47 and 70 percent, gave epsilon values between 4 and 7 and beta values between 2 and 4 dB/m, thus limiting the use of our commercial equipment to borehole spacings of less than 20 m. For this material, epsilon correlated well with volumetric ice content but not with temperature. In a deep section (25m), dielectric contrasts were seen between ice-rich silt, massive ice and frozen gravel. GRA

N89-27286# Naval Research Lab., Washington, DC.
COLLISIONLESS TEARING INSTABILITY OF A BI-MAXWELLIAN NEUTRAL SHEET WITH EXACT PARTICLE ORBITS Interim Report
G. R. Burkhart (Science Applications International Corp., McLean, VA.) and James Chen 27 Mar. 1989 56 p
(AD-A207310; NRL-MR-6405) Avail: NTIS HC A04/MF A01 CSCL 20/9

The tearing instability of a neutral sheet may be important to reconnection in the magnetosphere and elsewhere. The use of a bi-Maxwellian Harris equilibrium is broadly applicable to the physical environment and allows a continuous variation from isotropic situations. The integro-differential equation describing the linear tearing instability in the bi-Maxwellian neutral sheet is solved without approximating the particle orbits. Results of this calculation are presented. Comparison between the exact solution and the 3-region approximation motivates the piecewise-straight-line approximation, a simplification which allows faster solution of the integro-differential equation, yet retains the important features of the exact solution. GRA

N89-27287# Aerospace Corp., El Segundo, CA. Space Sciences Lab.
THE SPACE PARTICLE ENVIRONMENT
Alfred L. Vampola 28 Mar. 1989 32 p Previously announced as N89-23548
(Contract F04701-85-C-0086)
(AD-A207547; TR-0088(3940-05)-8; SD-TR-89-30) Avail: NTIS HC A03/MF A01 CSCL 04/1

This report is a tutorial covering the energetic charged particle environment in the earth's magnetosphere. It provides an overview of trapped particle morphology, the geometry of the trapping regions, the radiation environmental models, the current status of these models, and future modelling requirements. GRA

N89-27288*# Japan Meteorological Agency, Tokyo.
IMPLEMENTING THE SIMPLE BIOSPHERE MODEL (SiB) IN A GENERAL CIRCULATION MODEL: METHODOLOGIES AND RESULTS
N. Sato, P. J. Sellers, D. A. Randall, E. K. Schneider, J. Shukla, J. L. Kinter, III, Y.-T. Hou, and E. Albertazzi (Maryland Univ., College Park.) Aug. 1989 81 p
(Grants NAGw-492; NAGw-557)
(NASA-CR-185509; NAS 1.26:185509) Avail: NTIS HC A05/MF A01 CSCL 04A

The Simple Biosphere MOdel (SiB) of Sellers et al., (1986) was designed to simulate the interactions between the Earth's land surface and the atmosphere by treating the vegetation explicitly and relistically, thereby incorporating biophysical controls on the exchanges of radiation, momentum, sensible and latent heat between the two systems. The steps taken to implement SiB in a modified version of the National Meteorological Center's spectral GCM are described. The coupled model (SiB-GCM) was used with a conventional hydrological model (Ctl-GCM) to produce summer and winter simulations. The same GCM was used with a conventional hydrological model (Ctl-GCM) to produce comparable 'control' summer and winter variations. It was found that SiB-GCM produced a more realistic partitioning of energy at the land surface than Ctl-GCM. Generally, SiB-GCM produced more sensible heat flux and less latent heat flux over vegetated land than did Ctl-GCM and this resulted in the development of a much deeper daytime planetary boundary and reduced precipitation rates over the continents in SiB-GCM. In the summer simulation, the 200 mb jet stream and the wind speed at 850 mb were slightly weakened in the SiB-GCM relative to the Ctl-GCM results and equivalent analyses from observations. Author

N89-27289*# National Aeronautics and Space Administration. Goddard Space Flight Center, Greenbelt, MD.
ATTITUDE ANGLE EFFECTS ON NIMBUS-7 SCANNING MULTICHANNEL MICROWAVE RADIOMETER RADIANCES AND GEOPHYSICAL PARAMETER RETRIEVALS
Daniel S. MacMillan (ST Systems Corp., Lanham, MD.) and Daesoo Han Washington Aug. 1989 51 p
(Contract NAS5-29386)
(NASA-TM-4132; NAS 1.15:4132; Rept-89B00237) Avail: NTIS HC A04/MF A01 CSCL 08E

The attitude of the Nimbus-7 spacecraft has varied significantly over its lifetime. A summary of the orbital and long-term behavior of the attitude angles and the effects of attitude variations on Scanning Multichannel Microwave Radiometer (SMMR) brightness temperatures is presented. One of the principal effects of these variations is to change the incident angle at which the SMMR views the Earth's surface. The brightness temperatures depend upon the incident angle sensitivities of both the ocean surface emissivity and the atmospheric path length. Ocean surface emissivity is quite sensitive to incident angle variation near the SMMR incident angle, which is about 50 degrees. This sensitivity was estimated theoretically for a smooth ocean surface and no atmosphere. A 1-degree increase in the angle of incidence produces a 2.9 C increase in the retrieved sea surface temperature and a 5.7 m/sec decrease in retrieved sea surface wind speed. An incident angle correction is applied to the SMMR radiances before using them in the geophysical parameter retrieval algorithms. The corrected retrieval data is compared with data obtained without applying the correction. Author

N89-27290# Los Alamos National Lab., NM.
COMPUTER SIMULATIONS OF EXPLOSIVE VOLCANIC ERUPTIONS
Kenneth H. Wohletz and Greg A. Valentine 1989 40 p Presented at the 28th International Geological Congress, Washington, DC, 9-19 Jul. 1989
(Contract W-7405-eng-36)
(DE89-014024; LA-UR-89-1928; CONF-890702-3) Avail: NTIS HC A03/MF A01

We have adapted computer codes that provide such solutions to study explosive volcanic phenomena. These fully nonlinear conservation equations are cast in two-dimensional cylindrical coordinates, which with closure equations comprise 16 equations with 16 unknown variables. Solutions for several hundred seconds of simulated eruption time require two to three hours of a Cray-1 computer time. Over 100 simulations have been run to simulate the physics of highly unsteady blasts, sustained and steady Plinian eruptions, fountaining, column eruptions, and multiphase flow of magma in lithospheric conduits. The unsteady-flow calculations show resemblance to shock-tube physics with propagation of shock waves into the atmosphere and rarefaction waves down the volcanic conduit. Steady-flow eruption simulations demonstrate the importance of supersonic flow and overpressure of erupted jets of tephra and gases in determining whether the jet will buoyantly rise or collapse back to the earth as a fountain. Flow conditions within conduits rising through the lithosphere determine eruptive conditions of overpressure, velocity, bulk density, and vent size. Such conditions within conduit systems are thought to be linked to low-frequency, sustained seismicity known as volcanic tremor. These calculations demonstrate the validity of some analytical eruption calculations under limited conditions. DOE

N89-27291# Rome Univ. (Italy). Dipartimento di Fisica.
ABSORPTION CROSS-SECTION OF OZONE IN THE 590 TO 610 nm REGION AT DIFFERENT TEMPERATURES
A. Amoruso, Marco Cacciani, Alcide diSarra, and G. Fiocco 12 Dec. 1988 25 p Sponsored in part by the Programma Nazionale Ricerche, Antartide, Italy and Piano Spaziale Nazionale, Rome, Italy
(Nota-Interna-928; ETN-89-94747) Avail: NTIS HC A03/MF A01

The ozone absorption cross section in the 590 to 610 nm spectral range, a portion of the Chappuis bands, was measured at different temperatures. The values can be used in particular to invert atmospheric O3 data acquired by SAGE 2. The independence of the absorption coefficient on the temperature in this spectral region is confirmed, within experimental errors, at least at 230 and 299 K. ESA

N89-27292# Danish Meteorological Inst., Copenhagen. Div. of Geophysics.
DISTRIBUTION OF AURORAL ARCS DURING QUIET GEOMAGNETIC CONDITIONS
K. Lassen and C. Danielsen 1987 30 p
(DMI-Geophys-Papers-R-78; ISBN-87-7478-285-1; ETN-89-94924) Avail: NTIS HC A03/MF A01

Auroral arcs observed from the Greenland all-sky camera network during quiet intervals (AE less than 50 nT) were ordered in corrected geomagnetic latitude/time mass plots for different values of AE. With decreasing AE the pattern of oval-aligned arcs dissolves, so that for AE less than 20 nT practically all arcs belong to the so-called polar cap pattern of discrete arcs. It is demonstrated that this pattern is limited toward equator by the trapping boundary of energetic electrons which is regarded as the boundary between open and closed field lines. Toward the pole the pattern is limited by the polar precipitation boundary of electrons of average energy lower that 500 eV, although cross-polar cap arcs do occur isolated from the electron precipitation belt, especially during very low activity. Thus, the polar cap arc pattern appears to consist essentially of discrete arcs embedded in the inner low-energy electron precipitation belt. The oval arc pattern, which is more prominent for AE greater than 30 nT, is situated on the equatorial side of the trapping boundary. It forms part of the classical auroral oval, and the arcs are embedded in the outer higher-energy part of the auroral electron precipitation belt. ESA

N89-27293# Danish Meteorological Inst., Copenhagen. Div. of Geophysics.
BRORFELDE GEOMAGNETIC OBSERVATORY: MAGNETIC RESULTS, 1986 Annual Report
1987 41 p
(ISBN-87-7478-287-8; ETN-89-94925) Avail: NTIS HC A03/MF A01

The results of the standard observations carried out at the magnetic laboratory during 1986 are presented. The measurements show hourly means of horizontal and vertical intensity and hourly means of magnetic declination. Diurnal extreme values and mean diurnal inequalities are also given. ESA

N89-27294# Air Force Inst. of Tech., Wright-Patterson AFB, OH.
AN OBJECTIVE COMPARISON OF VERTICAL MOTIONS FROM THE KINEMATIC METHOD AND THREE FORMS OF THE OMEGA EQUATION M.S. Thesis
Gerald E. Hevrdeys 1988 97 p
(AD-A208451; AFIT/CI/CIA-88-202) Avail: NTIS HC A05/MF A01 CSCL 04/1

Subjective and objective comparisons were performed on large scale vertical motions from the kinematic method, the traditional omega equation, Trenberth's form of the omega equation, and the Q vector approach. Vertical motions from these routines were qualitatively compared to flow patterns and cloud/precipitation regions associated with a developing midlatitude springtime cyclone during the period 17 to 19 March 1986. Objective comparisons were also accomplished using a scoring scheme which rated each method. Results showed that kinematic motions were far superior to those from any of the three omega equation techniques. However, when the various omega equation output was compared with each other, they were found to be very similar. The Q vector method yielded slightly better scores for the entire 48 h period, but none of the three methods was clearly superior at the individual times. Because of the closeness of results, the omega equation routines were judged according to their ease of use and computation. From this analysis, the Q vector algorithm was chosen as the best of the three methods. GRA

N89-27295# Air Force Inst. of Tech., Wright-Patterson AFB, OH.
AN INVESTIGATION INTO THE GRAVITY CURRENT ASPECTS OF A COLD AIR OUTBREAK USING VARIATIONAL ANALYSIS TECHNIQUES M.S. Thesis
Stephen B. Allen 1988 92 p
(AD-A208464; AFIT/CI/CIA-88-214) Avail: NTIS HC A05/MF A01 CSCL 04/1

During the time period of January 27th through January 28th, 1986, the central and southeastern U.S. experienced a cold air outbreak. Surface temperatures dropped 30 degrees in a matter of hours in central Florida with dramatic drops in dewpoint as well. A method is developed using variational calculus to decompose observed gridded radiosonde data from this period into component fields. Three variational filters are used iteratively to extract the desired components of the observed data. These components are then used in concert with quasi-geostrophic theory to examine the similarities between this cold air outbreak, the gust front associated with an active thunderstorm, and a gravity current. Sensitivity studies of this method with respect to weight factors are shown. Results indicate some of the interactions between synoptic and sub-synoptic forcing in the development and maintenance of such a system. GRA

47 METEOROLOGY AND CLIMATOLOGY

Includes weather forecasting and modification.

N89-27296# International Centre for Theoretical Physics, Trieste (Italy).
ANALYSIS OF THE WIND DATA AND ESTIMATION OF THE RESULTANT AIR CONCENTRATION RATES
Shze Jer Hu, Hiroshi Katagiri, and Hideo Kobayashi (Japan Atomic Energy Research Inst., Tokai.) Sep. 1988 27 p Submitted for publication
(DE88-705980; IC-88/294) Avail: NTIS (US Sales Only) HC A03/MF A01

Statistical analyses and comparisons of the meteorological wind data obtained by the propeller and supersonic anemometers for the year of 1987 in the Japan Atomic Energy Research Institute, Tokai, were performed. For wind speeds less than 1 m/s, the propeller readings are generally 0.5 m/s less than those of the supersonic readings. The resultant average air concentration and ground level exposure rates due to the radioactive releases for the normal operation of a nuclear plant are over-estimated when calculated using the propeller wind data. As supersonic anemometer can give accurate wind speed to as low as 0.01 m/s, it should be used to measure the low wind speed. The difference in the average air concentrations and exposure rates calculated using the two different sets of wind data, is due to the influence of low wind speeds at calm. If the number at calm is large, actual low wind speeds and wind directions should be used in the statistical analysis of atmospheric dispersion to give a more accurate and realistic estimation of the air concentrations and exposure rates due to the normal operation of a nuclear plant. DOE

N89-27297# National Severe Storms Forecast Center, Kansas City, MO.
VERIFICATION OF SEVERE LOCAL STORM FORECASTS ISSUED BY THE NATIONAL SEVERE STORMS FORECAST CENTER, 1987 Final Technical Report
Dec. 1988 16 p
(PB89-159719; NOAA-TM-NWS-NSSFC-21) Avail: NTIS HC A03/MF A01 CSCL 04B

The Severe Local Storms (SELS) Unit of the national Severe Storms Forecast Center routinely issues convective outlooks and severe local storm watches to delineate areas that are favorable for development of severe local storms. The report summarizes verification of those forecasts that were issued during 1987. High percentages of tornado-related fatalities (89 percent) and injuries (92 percent) occurred within valid severe local storm watches. GRA

N89-27298# National Oceanic and Atmospheric Administration, Boulder, CO. Wave Propagation Lab.
DUAL-CHANNEL MICROWAVE RADIOMETER FOR AIRBORNE METEOROLOGICAL APPLICATIONS
L. S. Fedor, M. D. Jacobson, A. J. Bedard, Jr., E. R. Westwater, D. C. Hogg, and R. T. Nishiyama (Colorado Univ., Boulder.) Dec. 1988 35 p
(PB89-159693; NOAA-TM-ERL-WPL-157) Avail: NTIS HC A03/MF A01 CSCL 04B

Cloud liquid and water vapor are important parameters in meteorological processes. The memorandum presents the design of a dual-channel microwave radiometer to be installed on a NOAA research aircraft in order to measure these parameters. The discussion includes the utility of the instrument in a variety of research programs including cloud physics, severe storms, cloud climatology, and satellite sensor validation. Author

N89-27299# Environmental Protection Agency, Research Triangle Park, NC. Atmospheric Research and Exposure Assessment Lab.
CLIMATOLOGY OF TEMPERATURE AND PRECIPITATION VARIABILITY IN THE UNITED STATES Final Report
Brian K. Eder, Lawrence E. Truppi, and Peter L. Finkelstein Mar. 1989 47 p
(PB89-165930; EPA/600/3-89/025) Avail: NTIS HC A03/MF A01 CSCL 04B

The seasonal and annual variance and standardized range for temperature and the seasonal and annual coefficient of variation and normalized standardized range for precipitation, are examined on a climatic division level for the contiguous United States for the period 1895 to 1985. Examination of the temperature variance reveals a continentality phenomenon in which the largest variances occur in the upper midwest section of the country, while the smallest variances are generally found in coastal regions along the west coast, the Gulf coast and southeastern states. Examination of the coefficient of variation for precipitation depicts a propensity for the largest seasonal and annual variation to occur over the southwestern states from Texas to California. GRA

N89-27300# National Oceanic and Atmospheric Administration, Boulder, CO. Wave Propagation Lab.
PROCEDURAL GUIDE FOR THE RETRIEVAL OF DROPSIZE DISTRIBUTIONS IN WATER CLOUDS FROM GROUND-BASED CLEAR-AIR-SENSING DOPPLER RADAR OBSERVATIONS
R. G. Strauch and E. E. Gossard (Colorado Univ., Boulder.) Jul. 1988 49 p
(PB89-152474) Avail: NTIS HC A03/MF A01 CSCL 04B

The advent of Doppler clear-air radars for wind-height profiling opens the way for their use in a variety of other applications. Knowledge of the clear-air Doppler spectrum from a zenith-pointing radar together with the measured water droplet Doppler vertical velocity spectrum is used to calculate spectra of drop number density through clouds of droplets having substantial fall velocity. The method is extended and procedures are described that allow spectral lines and details to be extracted from the radar data. Spectra measured with a 915 MHz, wind-profiling radar are used as examples and compared with the spectra that would have been obtained if the clear-air information were ignored. From the number density vs. dropsize distribution, the corresponding liquid water distribution can be calculated. Failure to take into account turbulence in the medium can result in large errors in number density and liquid water especially in the neighborhood of spectral lines and large gradients. The advantages and limitations of a radar remote sensing drop spectrometer are described. GRA

N89-27301# Instituto de Pesquisas Espaciais, Sao Jose dos Campos (Brazil).
AMAZON FOREST WIND AND TEMPERATURE PROFILES
Y. Viswanadham, Vicente dePaulaSilvaFilho, Antonio Ocimar Manzi, and Leonardo Deane deAbreuSa Oct. 1988 11 p Presented at the 3rd Scientific Assembly of the International Association of Hydrological Sciences of the International Union of Geodesy and Geophysics, Baltimore, MD, 10-19 May 1989
(INPE-4724-PRE/1401) Avail: NTIS HC A03/MF A01

The micrometeorological research program for the Amazonian Forest has provided data on wind and temperature profile structure under lapse to extreme inversion conditions. Significant variations in the determinations of surface roughness (z sub o) and zero plane displacement (d) from quasi-neutral wind profiles are noted. Differences in the shear stress (tau) are largely dependent on the selected z sub 0 and d. The Deacon numbers for wind (beta sub u) and potential temperature (beta sub theta) were computed, to investigate in detail the curvatures of these profiles. A relation between beta's and Richardson gradient number (Ri) is obtained. The empirical relationship between the beta's and Ri seems to become erratic for strong inversion conditions. The ratio K sub H/K sub M is greater than unity for all stabilities and slowly decreases for large values of Ri. It is shown that it is possible to compare the results of observed data wind theoretical models. Author

N89-27302*# National Aeronautics and Space Administration. Goddard Space Flight Center, Greenbelt, MD.
THE 1989 AIRBORNE ARCTIC STRATOSPHERIC EXPEDITION NIMBUS-7 TOMS DATA ATLAS
Arlin J. Krueger, Lanning M. Penn, David E. Larko, Scott D. Doiron,

and Patricia T. Guimaraes (ST Systems Corp., Vienna, VA.) Washington Jul. 1989 154 p
(Contract NAS5-29373)
(NASA-RP-1227; Rept-89B00188; NAS 1.61:1227) Avail: NTIS HC A08/MF A01 CSCL 04B

Over the past several years, world scientific attention was focused on the rapid and unanticipated decrease in the abundance of ozone over Antarctica during the Austral spring. A major aircraft campaign was conducted from December 1988 to February 1989 in response to the recently published Ozone Trends Panel Report which found that the largest decreases in Arctic ozone occurred during January to February at latitudes near the edge of the Arctic vortex. This atlas provides a complete set of TOMS ozone measurements over Europe and the North Atlantic for the duration of the experiment. These were the orbital TOMS measurements provided to the experimenters in near-real-time. In addition, a set of Northern Hemisphere TOMS ozone measurements for the period December 26, 1988 to March 20, 1989 is presented. A comparison of January and February 1989 mean ozone values to prior years is also presented. Author

N89-27303# Naval Oceanography Command Center/Joint Typhoon Warning Center, FPO San Francisco, CA.
TROPICAL CYCLONE REPORT, 1988 Annual Report
Robert J. Plante and Daniel J. McMorrow 1988 227 p
(AD-A207206) Avail: NTIS HC A11/MF A01 CSCL 04/2

This report summarizes Tropical cyclone activity in the western North Pacific Ocean; Bay of Bengal; Arabian Sea; Western South Pacific and South Indian Oceans; A best track is provided for each significant tropical cyclone. A brief narrative is given for all typhoons and selected tropical cyclones in the western North Pacific and North Indian Oceans. All reconnaissance data used to construct the best tracks are provided, upon request, on floppy diskettes. Forecast verification data and statistics for the joint typhoon warning center are submitted. GRA

N89-27304# Naval Research Lab., Washington, DC. Atmospheric Physics Branch.
NAVY TETHERED BALLOON MEASUREMENTS MADE DURING THE FIRE MARINE STRATOCU IFO (INTENSIVE FIELD OPERATION)
Jeffrey E. James, H. Gerber, S. G. Gathman, Mike Smith, and Ian Consterdine (Manchester Univ., England) 3 Apr. 1989 127 p
(AD-A207312; NRL-MR-6445) Avail: NTIS HC A07/MF A01 CSCL 04/2

For a ten-day period beginning 15 July 1987, tethered balloon measurements were made of turbulence, aerosol, cloud particles, and meteorology at San Nicolas Island, CA during the FIRE marine strato-cumulus Intensive Field Operation (IFO). The primary interest of the Naval Research Laboratory during this experiment was to obtain a data set which could be used for testing the predictions of the Navy Oceanic Vertical Aerosol Model (NOVAM) which describes the atmosphere's optical/infrared properties in terms of easily obtained meteorological data. Two new instruments, flown aboard the balloon, were a saturation hygrometer, which measures 95 percent less than RH less than 150 percent with an accuracy of 0.05 near 100 percent RH, and a forward scatter meter which gives in situ measurements of liquid water content at more than 10 Hz. As a result of this experiment a unique and greatly improved look at the microphysics of the clear and cloud topped boundary layer can be taken. In this report the quality of the data obtained is discussed and some preliminary results are given. Algorithms for the instrumentation flown aboard the balloon are given and profiles of some of the measurements are shown. GRA

N89-27305# Risoe National Lab., Roskilde (Denmark).
AERIAL SMOKE PLUME OBSERVATIONS AND SURFACE LAYER TURBULENCE MEASUREMENTS. PART 1: PROJECT WIND. PHASE 4: DISPERSION STUDY Final Report, Sep. 1987 - Feb. 1988
Torben Mikkelsen, A. Hansen, R. M. Eckman, and S. Thykier-Nielsen Jan. 1989 129 p
(Contract DAJA45-87-M-0475; DA Proj. 1L1-61102-BH-57)
(AD-A207370; RISOE-M-2718-Pt-1; R/D-5898-EN-01-Pt-1; ISBN-87-550-1431-3; ISSN-0418-6435) Avail: NTIS HC A07/MF A01 CSCL 04/2

The present data report is based on direct turbulence and diffusion measurements performed by Risoe National Laboratory during the AMADEUS smoke tests of Project Wind, Phase 4, which took place as a cooperative research-oriented field effort between the U.S. Army Atmospheric Sciences Laboratory (ASL) and the U.S. Dept. of Agriculture Forest Service (USDAFS) in the Meadow Brook Valley near Red Bluff, California, between 23 September and 7 October 1987. In particular, Risoe National Laboratory performed: (1) direct measurements of the surface layer scaling parameters such as heat flux, shear stress, turbulence, and stability measurements at two characteristic locations in the Meadow Brook Valley floor; and (2) concurrently obtained documentation of the plume and puff spread based on aerial photography. The present report provides time series plots of the 10-min averaged covariance matrix of u, v, w, and T from the two sonics together with prints of photos taken of smoke/puff plumes from an aircraft in a form suitable for subsequent model simulation of individual dispersion scenarios. GRA

N89-27306# Naval Environmental Prediction Research Facility, Monterey, CA.
THE INTERNATIONAL TOVS (TIROS OPERATIONAL VERTICAL SOUNDER) PROCESSING PACKAGE: AN EVALUATION Final Report, Jun. - Oct. 1988
Charles R. Sampson Apr. 1989 25 p Previously announced as N89-23548
(AD-A207548; NEPRF-TR-89-05) Avail: NTIS HC A03/MF A01 CSCL 04/2

Satellite soundings of temperature, pressure and moisture are important sources of data over remote ocean areas where data voids exist and Navy vessels frequently are deployed. This study evaluates the International TOVS (Tiros Operational Vertical Sounder) Processing Package (ITPP) -retrieved temperature and moisture profiles over the eastern United States and Canada during winter 1986, by comparing them with collocated satellite profiles retrieved by a statistical method. Biases and root mean standard deviations (RMSD) between satellite profiles and collocated radiosonde profiles are determined for both the ITPP and Smith and Woolf methods. Layer mean temperature biases for ITPP data are within 1 K of radiosonde data. Layer mean temperature RMSDs for ITPP profiles are between 1 and 5 K with a minimum at the 500/400 mb layer of 1.37 K. ITPP layer mean temperatures better approximate radiosonde profiles in the layers between 500 mb and 200 mb than those of the Smith and Woolf scheme. ITPP precipitable water profiles exhibit a moist bias when compared with radiosonde moisture profiles. RMSDs for ITPP precipitable water are between 3 and 5 mm. ITPP-retrieved profiles have increased vertical and horizontal moisture resolution when compared with statistically-retrieved profiles. GRA

N89-27307# Army Missile Command, Redstone Arsenal, AL. Research Directorate.
LOW RELATIVE HUMIDITY IN THE ATMOSPHERE Final Technical Report, 2 Jan. - 1 Oct. 1988
Dorathy A. Stewart Jan. 1989 56 p
(AD-A207558; AD-E951328; AMSMI/TR-RD-RE-89-3) Avail: NTIS HC A04/MF A01 CSCL 04/2

Relative humidities below 3 percent are rare and last less than 24 hours. The limitation on the duration of extreme relative humidities exists because of the diurnal cycle. The lowest relative humidities are associated with high temperatures. When air temperature decreases after sunset, the relative humidity increases because there is not a comparable decrease of water vapor content. On a day with a minimum relative humidity of 3 percent, the maximum in the diurnal cycle should be about 8 percent. When ambient relative humidity is 3 percent, the relative humidity in a hot storage container may be only 1 percent. The maximum in the diurnal cycle in the container should then be about 7 percent. The most extensive areas of low relative humidity are in northern Africa and southwestern Asia. Typical afternoon minima are in the

range 10 to 20 percent over a major portion of these deserts in spring and summer. In small areas the average afternoon minimum in the driest months is slightly less than 10 percent. In some parts of the world, very rapid changes of relative humidity occur in certain weather situations. At coastal stations with well-developed sea breezes, relative humidities may increase from 10 percent to 80 percent in one or two hours. In the lee of mountain ranges, abrupt decreases of a comparable magnitude can occur with chinook (foehn) winds. GRA

N89-27308# Lawrence Livermore National Lab., CA.
LIGHTNING: UNDERSTANDING IT AND PROTECTING SYSTEMS FROM ITS EFFECTS
R. T. Hasbrouck 10 Apr. 1989 45 p Presented at the 35th International Instrumentation Symposium, Orlando, FL, 30 May 1989
(Contract W-7405-eng-48)
(DE89-012796; UCRL-53925; CONF-890589-2) Avail: NTIS HC A03/MF A01

This tutorial will raise the reader's level of lightning consciousness by providing an overview of the atmospheric electrification process and by discussing the development and characteristics of a lightning discharge. Next, techniques and instrumentation for lightning threat warning, detection and tracking will be presented. Finally, the principles of protection will be discussed, along with several methods for testing that protection. DOE

N89-27309# National Center for Atmospheric Research, Boulder, CO.
EVOLUTION AND STRUCTURE OF THE BOW ECHO/MICROBURST EVENTS Ph.D. Thesis
Wen-Chau Lee 1989 294 p Prepared in cooperation with California Univ., Los Angeles
(Grant NSF ATM-87-09659)
(PB89-174767; NCAR/CT-117) Avail: NTIS HC A13/MF A01 CSCL 04B

The evolution and structure of several bow echo/microburst events are investigated. Multiple Doppler radar analysis is performed for the primary case of 14 July 1982 during the Joint Airport Weather Study (JAWS) experiment while single Doppler radar analysis is performed in 4 other bow echo/microburst events. Three dimensional wind fields, pressure and buoyance fields, vorticity budget and trajectories are computed for the 14 July 1982 case. Rawinsonde data, damage survey, satellite imagery and cloud photogrammetry are also incorporated in the study. The microburst and bow echo are well known as a potential hazard to aviation safety. When an aircraft penetrates a descending microburst or bow echo, its performance is seriously affected. The aviation hazards are the reason for the study. Author

N89-27310# National Weather Service, Washington, DC. Climate Analysis Center.
PROCEEDINGS OF THE 13TH ANNUAL CLIMATE DIAGNOSTICS WORKSHOP HELD AT CAMBRIDGE, MASSACHUSETTS ON OCTOBER 31 - NOVEMBER 4, 1988
Mar. 1989 525 p Workshop held in Cambridge, MA, 31 Oct. - 4 Nov. 1988
(PB89-178115) Avail: NTIS HC A22/MF A01 CSCL 04B

The proceedings provide the following topics: analysis of recent climate anomalies; large scale diagnostics; interannual variability; climate trends; regional climate studies; large scale model diagnostics; and coupled ocean atmosphere models. GRA

N89-27311# Florida Agricultural and Mechanical Univ., Tallahassee. Coll. of Engineering Science.
METEOROLOGICAL DATABASE AND SYNTHESIS FOR THE GULF OF MEXICO Final Report
Jerry Ford, Robert Wayland, Evans Waddell, and Bob Hamilton (Evans-Hamilton, Inc., Seattle, WA.) Dec. 1988 333 p
(Contract DI-14-12-0001-30191)
(PB89-178222; MMS/GM-88/0064) Avail: NTIS HC A15/MF A01 CSCL 04B

The meteorological summary consists of a compilation of data from a number of sources and a statistical description by month, season, and year of the pertinent meteorological variables affecting oceanographic operations in the Gulf of Mexico region. The primary data sets utilized in the study are as follows: National Weather Service (NWS) coastal station data; National Data Buoy Center (NDBC) moored-buoy and marine platform network; NDBC Coastal Marine Automated Network (CMAN) stations; a segment of the Ocean Currents Measurement Program (OCMP) data; National Hurricane Center 101-year storm track data (HURDAT); and the University of Virginia cyclone data set. The coastal data covers the period 1970 to 1986, while the buoy data exists for only 1976 to 1986. The CMAN data set spans the period 1985 to 1987, depending upon which station is considered. The hurricane and cyclone climatologies are for 101 and 100 years, respectively. In addition, a ship-based sea surface temperature (SST) climatology is analyzed by 1 deg quadrangles for the period 1854 to 1973. The analyses included in the report should provide useful information on the variability of meteorological conditions in the Gulf of Mexico. The primary results emphasize the difference between winter and summer means and variances, particularly for the central and northwestern Gulf of Mexico. Author

N89-27312# National Weather Service, Fort Worth, TX.
INTENSE HEAT CHECKLIST BASED ON THE 1980 HEAT WAVE
Kenneth W. Falk and Stanley C. Christmas Mar. 1989 22 p
(PB89-181200; NOAA-TM-NWS-SR-124) Avail: NTIS HC A03/MF A01 CSCL 04B

The heat wave of 1980, one of the worst in modern history in both magnitude and duration in Texas, was responsible for at least 60 deaths in the state, and nearly 1300 deaths nationwide. A discussion of a climatological normal summer for North Texas is presented, followed by some statistics of the summer of 1980. The mean circulation for each month (June through September) of the heat wave of 1980 is presented. Suggested papers for additional information are given. Next, the surface and upper air features of the 1980 heat wave are discussed in an attempt to find synoptic scale features which may be used in forecasting extremely hot days (105 F or greater). Finally, a checklist is included to aid forecasters in predicting summer maximum temperatures. GRA

N89-27313# Washington Univ., Seattle. Cloud and Aerosol Research Group.
CLOUD AND PRECIPITATION SCAVENGING PROCESS IN THE SOUTH COAST AIR BASIN
Dean A. Hegg and Peter V. Hobbs 8 Nov. 1988 149 p Sponsored by California State Air Resources Board, Sacramento
(PB89-181788; ARB-R-89/386) Avail: NTIS HC A07/MF A01 CSCL 04B

Results are presented on airborne aerometric measurements of particles and trace gases during the Southern California Air Quality Study (SCAQS). Nine flights were made on six of the SCAQS study days during June and July 1987. Samples were collected at four sites per flight for measurement of sulfur dioxide, nitric acid, peroxyacetyl nitrate (PAN), ammonia, fine particle (ionic species, metals, and elemental and organic carbon), carbonyl, and non-methane hydrocarbon concentrations. Analysis of the samples were performed by other SCAQS contractors. In addition, ancillary meteorological, and continuous ozone, nitrous oxide, nitrogen dioxide, sulfur dioxide and light scattering measurements were obtained. Cloud samples were also collected when present. Measured atmospheric particle size distributions are also presented. GRA

N89-27314*# National Aeronautics and Space Administration. Goddard Space Flight Center, Greenbelt, MD.
A GRAPHICS PACKAGE FOR METEOROLOGICAL DATA, VERSION 1.5
Shrinivas Moorthi, Max Suarez, Bill Phillips, Jae-Kyung Schemm (Centel Federal Services Corp., Washington, DC.), and Siegfried Schubert Washington Aug. 1989 42 p

(Contract NAS5-30506)
(NASA-TM-100742; Rept-89B00216; NAS 1.15:100742) Avail: NTIS HC A03/MF A01 CSCL 04B

A plotting package has been developed to simplify the task of plotting meteorological data. The calling sequences and examples of high level yet flexible routines which allow contouring, vectors and shading of cylindrical, polar, orthographic and Mollweide (egg) projections are given. Routines are also included for contouring pressure-latitude and pressure-longitude fields with linear or log scales in pressure (interpolation to fixed grid interval is done automatically). Also included is a fairly general line plotting routine. The present version (1.5) produces plots on WMS laser printers and uses graphics primitives from WOLFPLOT. Author

N89-27315# Instituto de Pesquisas Espaciais, Itajuba (Brazil).
TROPICAL CIRCULATION AND THE ASSOCIATED PRECIPITATION ANOMALIES IN TWO YEARS OF CONTRAST [CIRCULACOES TROPICAIS E AS ASSOCIADAS ANOMALIAS DE PRECIPITACOES EM DOIS ANOS DE CONTRASTE]
Mary Toshie Kayano Oct. 1988 8 p In PORTUGESE
(INPE-4715-PRE/1395) Avail: NTIS HC A02/MF A01

Severe droughts observed during 1983 over a large range of tropical continental areas were associated with the 1982 to 1983 El Nino Event. In contrast, during 1984 above average precipitation was observed over these areas. The tropical circulation for the two years of contrast are examined. The intensity and position of ascending and descending movements are consistent with the precipitation anomalies. The concept theories concerning the induced tropical circulation for the heat source, accepted currently, can be applied to explain some of the deserved characteristics. Author

N89-27316*# National Aeronautics and Space Administration. Marshall Space Flight Center, Huntsville, AL.
ATMOSPHERIC ENVIRONMENT FOR SPACE SHUTTLE (STS-27) LAUNCH
G. L. Jasper, D. L. Johnson, and G. W. Batts (Computer Sciences Corp., Huntsville, AL.) Jul. 1989 44 p
(NASA-TM-100370; NAS 1.15:100370) Avail: NTIS HC A03/MF A01 CSCL 04B

Selected articles on atmospheric conditions observed near Space Shuttle STS-27 launch time on December 2, 1988, at Kennedy Space Center, Florida are summarized. STS-27 carried a Department of Defense payload and the flight azimuth in this report will be denoted by reference flight azimuth, since the actual flight azimuth is not known. Values of ambient pressure, temperature, moisture, ground winds, visual observations (cloud), and winds aloft are included. The sequence of pre-launch Jimsphere-measured vertical wind profiles is given. The final atmospheric tape, which consists of wind and thermodynamic parameters versus altitude, for STS-27 vehicle ascent was constructed. The STS-27 ascent atmospheric data tape was constructed by Marshall Space Flight Center's Earth Science and Applications Division to provide an internally consistent data set for use in post-flight performance assessments. Author

N89-27317# California Inst. of Tech., Pasadena. Environmental Engineering Science.
FOG, CLOUD, AND DEW CHEMISTRY Final Report
Michael R. Hoffmann 28 Feb. 1989 496 p Sponsored in part by Coordinating Research Council
(Contract ARB-A4-075-32)
(PB89-187314; ARB-R-89/390) Avail: NTIS HC A21/MF A01 CSCL 04B

The spatial and temporal variations of fog/cloud chemistry were determined in the San Joaquin Valley, in the Los Angeles Basin and in the Santa Barbara Channel area using automated fog- and cloudwater collectors that were designed and constructed for the project. A significant correlation was observed between the average nighttime cloud- and fogwater loadings of H+ and NO3-and the maximum levels of O3-Higher aldehydes, a series of dicarbonyls, and a variety of sulfonic acid salts formed by reaction of S(IV) and aldehydes were quantitatively determined in the droplet phase. GRA

N89-27318# National Oceanic and Atmospheric Administration, Las Vegas, NV. Weather Service Nuclear Support Office.
WEATHER PREDICTIONS AND SURFACE RADIATION ESTIMATES FOR PROJECT BUGGY 1
May 1989 79 p
(Contract DE-AI08-87NV-10566)
(DE89-014687; NVO-332; PNE-328) Avail: NTIS HC A05/MF A01

This report documents the activities of the Air Resources Laboratory-Las Vegas (ARL-LV) in support of Project BUGGY 1. The participation of ARL-LV in the Safety Program is stressed, but the full scope of objectives and functions is covered. A description is given of observational facilities used to provide weather services. Weather predictions and fallout estimates issued for the project, as well as procedures and techniques, are discussed. A comparison of predicted and observed weather and fallout is made. The results of these activities will serve as a basis for planning and participating in future projects. DOE

N89-27319# Office National d'Etudes et de Recherches Aerospatiales, Paris (France).
AIRBORNE MEASUREMENTS OF THE ELECTRIC FIELD AND THE CHARGE PRECIPITATION PARTICLES IN CONVECTIVE CLOUDS: LOWER POSITIVE CHARGE CENTERS Ph.D. Thesis - Clermont-Ferrand Univ. 2
Pascal Gondot 1988 120 p In FRENCH; ENGLISH summary
(ONERA-NT-1988-1; ISSN-0078-3781; ETN-89-94814) Avail: NTIS HC A06/MF A01

A comparative analysis of two different meteorological situations is presented: in the first the clouds were stopped below the minus 20 C level and most of the precipitating particles were positively charged, and in the second there were classical thunderclouds reaching the tropopause and observed at nearly the same levels as the majority of precipitations carrying strongly negative charges. It is concluded that the sign of the charge of precipitation particles is related to the altitude of the cloud top which implies a given temperature for the level of formation of precipitations. A detailed case study shows the association of positive charge centers with large particle charges and also with largest ice particle location. The observations corroborate experimental results on collisions between graupels and ice crystals with supercooled water. ESA

N89-27320# Battelle Memorial Inst., Research Triangle Park, NC.
DEVELOPMENT OF LOW-LEVEL TURBULENCE (LLT) FORECASTING METHODOLOGIES Final Report
Peter F. Lester and Mark W. Burton Dec. 1988 63 p Prepared in cooperation with San Jose State Univ., CA
(Contract DAAL03-86-D-0001)
(AD-A208457; ARO-TCN-87-597) Avail: NTIS HC A04/MF A01 CSCL 04/2

The improvement of low-level turbulence (LLT) forecasting was investigated. The literature review documents the current forecast problem as one of scale, that is, large-scale data are used to predict a small-scale phenomena. Although the current forecast procedures are objective at the level of the weather Central, the methods are simplistic and there is a high degree of subjectivity when the forecast is adapted to the local area. It was determined that significant improvements in forecasts can be made in the near future by improving local observations, communications, and developing compute based objective forecasting techniques. Finally, the LLT problem at Fort Irwin is documented and objective procedures are developed to improve LLT forecasts. GRA

N89-27321# Naval Postgraduate School, Monterey, CA.
SYNOPTIC FORCING OF EAST ASIAN COLD SURGES M.S. Thesis
Randy J. Lefevre Mar. 1989 121 p
(AD-A208765) Avail: NTIS HC A06/MF A01 CSCL 04/2

A linearized, global spectral model with eight levels was used

to determine whether the nonlinear interaction between a planetary-scale wave (wavenumber four) and a rapidly growing synoptic-scale wave (wavenumber seven) could produce a northeasterly wind, characteristic of East Asian cold surges. The amplitude of the synoptic-scale wave, or generic cyclone, was produced by a nonlinear Eady model of the atmosphere that included friction. The resulting nonlinear forcing was applied to either the first law of thermodynamics, the vorticity equation, or both. The thermal forcing did not produce a significant cold surge response. The vorticity forcing produced a respectable cold surge within 48 hours. The results of this study indicate that planetary-synoptic wave interaction is a possible method for initiating East Asian cold surges. GRA

48 OCEANOGRAPHY

Includes biological, dynamic, and physical oceanography; and marine resources.

For related information see also *43 Earth Resources and Remote Sensing.*

N89-27322# National Oceanic and Atmospheric Administration, Miami, FL. Oceanographic and Meteorological Lab.
JOINT CGS-AOML (CHARTING AND GEODETIC SERVICE-ATLANTIC OCEANOGRAPHIC AND METEOROLOGICAL LABORATORY) ACOUSTICAL BOTTOM ECHO-FORMATION RESEARCH. 2: FIELD EXPERIMENT RESULTS AND RECOMMENDATIONS FOR ECHO-SOUNDER DESIGN
Thomas L. Clarke, John R. Proni, and Lloyd C. Huff Jul. 1988 127 p
(PB89-152417; NOAA-TM-ERL-AOML-67) Avail: NTIS HC A07/MF A01 CSCL 08C

Field experiments were conducted to test and verify a mathematical model that was developed to assess the effects of bottom roughness and material properties on bottom echo shape. The experiments were conducted in lower Chesapeake Bay. A high resolution bottom profiler was used to measure bottom roughness profiles for input to the model. An extension to the model was developed that considers bottom surface scattering as arising from a number of statistically independent patches within the transducer beam. The algorithm developed for removing ship motion from the observations suggests a new echo-sounder detector circuit based on an energy threshold. This circuit could be easily implemented with modern digital signal processing circuits, and it might be suitable for retro-fitting to existing echosounders. GRA

N89-27323# Coastal Engineering Research Center, Vicksburg, MS.
PACIFIC COAST HINDCAST PHASE 3 NORTH WAVE INFORMATION Final Report
Robert E. Jensen, Jon M. Hubertz, and Jane B. Payne Mar. 1989 608 p
(AD-A207189; CERC-WIS-17) Avail: NTIS HC A99/MF A01 CSCL 08/3

Twenty years of hindcast significant height, peak period, and mean direction wave information is summarized for 134 Pacific locations in four data products: (1) percent occurrence tables; (2) wave rose diagrams; (3) mean and largest significant height and 20-year statistics tables; and (4) return period tables. Brief descriptions and examples for each data product are provided. GRA

N89-27324# Borgman (Leon E.), Inc., Laramie, WY.
BRIEF INSTRUCTIONS FOR SIMBAT, A COMPUTER PACKAGE FOR UNCONDITIONAL AND CONDITIONAL SIMULATION OF OCEAN WAVE KINEMATICS Final Report, Jul. 1986 - May 1988
Leon E. Borgman Mar. 1989 47 p Sponsored in part by Naval Civil Engineering Lab., Port Hueneme, CA and Mineral Management Service, Reston, VA
(AD-A207627; NCEL-CR-89.007) Avail: NTIS HC A03/MF A01 CSCL 12/3

SIMBAT is a FORTRAN subroutine for computer simulation of ocean wave kinematics. Given an estimate of directional wave spectrum, the program calculates kinematics in the irregular wave field. The calculations can be conditioned on a particular kinematic or surface elevation time series. Brief instructions for use of SIMBAT are given. Sample runs are included in the appendix. GRA

N89-27325# Delaware Univ., Newark. Dept. of Mathematical Sciences.
PROPAGATING SOLUTIONS AND FAR-FIELD PATTERNS FOR ACOUSTIC HARMONIC WAVES IN A FINITE DEPTH OCEAN
Yongzhi Xu Feb. 1989 28 p
(Grant NA86AA-D-SG040)
(PB89-180715; DEL-SG-07-89) Avail: NTIS HC A03/MF A01 CSCL 08C

In the theoretical study of the sound field produced by a source in an ocean, to detect the sound field the source must be close. In the future, the effects of the distributed sources of sound must be assessed, that is, the shapes of the sound sources must be considered. The direct propagation problem and the inverse scattering problem are discussed. A representation is obtained in terms of single and double layer potentials for the solutions, an existence theorem established, and furthermore, a representation was found for the far field pattern. Based on these results, it can characterize the far-field pattern and discuss the inverse scattering problem. GRA

N89-27326# Mitre Corp., McLean, VA. JASON Program Office.
SPECTRA OF SURFACE WAVES
K. Watson 22 Mar. 1989 36 p
(AD-A208482; JSR-88-130) Avail: NTIS HC A03/MF A01 CSCL 08/3

This document represents notes, collected by the author over the past decade which describe surface wave spectra. There are some references that others may find useful. The first section gives some conventional definitions to provide a common notation. Generation of surface waves is discussed next. Lastly, some models that are used to describe equilibrium spectra are presented. GRA

51 LIFE SCIENCES (GENERAL)

N89-27327# Rome Univ. (Italy). Dipartimento di Fisica.
CATEGORIZATION IN NEURAL NETWORKS AND PROSOPAGNOSIA
M. A. Virasoro 28 Jun. 1988 11 p Submitted for publication
(Preprint-608; ETN-89-94696) Avail: NTIS HC A03/MF A01

It is argued that prosopagnosia, a syndrome characterized by a generalized difficulty to visually recognize individual patterns among those that are similar to it and that therefore can be said to belong to the same catagory, may be an important clue for understanding the categorization process in the brain. In this direction neural network performance under random destruction of synapses is analyzed. It is found that in almost every network that stores correlated patterns, the coding of the discriminating details between individuals inside a class is more sensitive to noise or to random destruction than the coding that distinguishes classes. It follows that a process of death and/or deterioration at an intermediate level of intensity, even if it acts randomly on the network may lead to a malfunctioning of the network that resembles prosopagnosia. ESA

N89-27328# Rome Univ. (Italy). Dipartimento di Fisica.
THE EFFECT OF SYNAPSES DESTRUCTION ON CATEGORIZATION BY NEURAL NETWORKS
M. A. Virasoro 28 Jun. 1988 10 p Submitted for publication
(Preprint-609; ETN-89-94697) Avail: NTIS HC A02/MF A01

The probability measure on neural network interactions introduced by Gardner (1988) is used to analyze the effect of a random destruction of synapses in a network that stores ultrametric patterns. At an intermediate level of destruction the retrieval of the pattern is impaired particularly in those items that permit the distinction among exemplars in a class. ESA

N89-27329# Chicago Univ., IL. Dept. of Medicine.
DEVELOPMENT OF ADVANCED METHODS BASED ON STABLE ISOTOPE TECHNOLOGY FOR STUDIES OF EXERCISE IN HEAT Report, 28 Sep. 1987 - 31 Mar. 1989
Morteza Janghorbani 15 Apr. 1989 19 p
(Contract DAMD17-87-C-7235; DA Proj. 3M1-61102-AS-15)
(AD-A208758) Avail: NTIS HC A03/MF A01 CSCL 06/10

Stable isotope methods were developed for precise and accurate measurement of isotopes of bromine, magnesium, and potassium in tissues. The methods were applied to the measurement of extracellular fluid volume using the swine model, and to exchangeable pool sizes of magnesium and potassium using the rat model. It was shown that the bromine method could be combined with the stable isotope methodology for the measurement of total body water to investigate body water compartments. It was shown that the bromine method could be used to investigate changes in exchangeable body magnesium in the rat by dietary manipulation. GRA

52 AEROSPACE MEDICINE

Includes physiological factors; biological effects of radiation; and effects of weightlessness on man and animals.

N89-27330# Advisory Group for Aerospace Research and Development, Neuilly-Sur-Seine (France). Aerospace Medical Panel.
SHORT COURSE ON CARDIOPULMONARY ASPECTS OF AEROSPACE MEDICINE
G. W. Gray, ed. (Defence and Civil Inst. of Environmental Medicine, Toronto, Ontario) May 1989 81 p
(AGARD-R-758-Add; ISBN-92-835-0497-6) Copyright Avail: NTIS HC A05/MF A01

AGARD Report 758, Short Course on Cardiopulmonary Aspects of Aerospace Medicine, presented the lecture material and case history information from a Short Course by the Aerospace Medical Panel during Spring 1987. This Addendum presents the discussions which took place throughout the duration of the Short Course. Author

N89-27331# Letterman Army Inst. of Research, San Francisco, CA.
MERIDIAN VARIATIONS IN SPECTRAL DARK ADAPTATION Report, 14 Feb. - 14 Mar 1989
O. Joseph Calabrese and Harry Zwick Mar. 1989 27 p
(AD-A207248; AD-E801886; LAIR-372) Avail: NTIS HC A03/MF A01 CSCL 06/4

Spectral dark adaptation as a function of retinal meridian and of eccentricity was investigated by testing the absolute threshold dark adaptation curves for eight human volunteers at two retinal meridians. The horizontal and vertical meridians. The horizontal and vertical meridians separately and together at eccentricities of 2 degrees and 16 degrees from a fixation point were studied. A microprocessor-operated dark adaptometer was used, and analysis of variance was performed on the data. The study indicated that meridian differences in the dark-adapted retina exist and that the horizontal meridian is more sensitive than the vertical meridian when the retina is tested at 16 degrees with medium wavelength light. This may indicate meridian differences in photoreceptor distribution. GRA

N89-27332# Army Research Inst. of Environmental Medicine, Natick, MA.
ALTITUDE SYMPTOMATOLOGY AND MOOD STATES DURING A CLIMB TO 3630 m
Barbara S. Hale, Terry M. Rauch, and Richard Foutch Apr. 1989 18 p
(AD-A208261; USARIEM-M41-89) Avail: NTIS HC A03/MF A01 CSCL 06/10

Ascents to altitude above 3050 m have been shown to cause adverse changes in symptoms and moods. It is thought that the severity of these changes not only depends on the altitude and rate of climb, but also on the length of stay and the effort expended to reach the desired altitude. In order to better understand how these factors influence symptom and mood changes during a climb, this study systematically assessed symptoms and moods during an ascent to 3630 m. Seven symptom factors and two mood factors were found to be adversely affected over time by the changes in altitude. More specifically, the subjects experienced more respiratory acute mountain sickness (AMS), exertion stress, and muscular discomfort and they were also colder, less alert, less vigorous, and more fatigued at higher elevations. These changes occurred primarily at 3630 m and most also occurred at 3080 m. The changes were always different from the values on the second day at 2225 m and they sometimes differed from the values on the first day at 2225 or 2530 m. Therefore, this study demonstrated that a climb to 3630 m produces adverse changes in symptomatology and mood states and that factors other than just level of altitude can affect these parameters. GRA

N89-27333# Army Research Inst. of Environmental Medicine, Natick, MA.
ANNUAL HISTORICAL REPORT - AMEDD ACTIVITIES
1988 108 p
(AD-A208301; RCS-MED-41(R4)) Avail: NTIS HC A06/MF A01 CSCL 06/10

The Mission of the U.S. Army Research Institute of Environmental Medicine is to conduct research on the effects of temperature, altitude, work and nutrition on the health and performance of the individual soldier and combat crews operating Army systems. It assesses decrements to soldier or combat crew performance caused by the synergy of environmental extremes protective measures. It conducts research on the biomedical processes limiting physical performance to determine physical fitness requirements and seek solutions to medical problems related to physical training and exercise. It defines the complex interaction of environmental/operational stress and Army systems and develops, evaluates and assists in the implementation of strategies designed to protect the soldier and enhance performance. In coordination with the Natick Research, Development and Engineering Center (Natick) and through liaison with other Federal agencies, USARIEM conducts research to develop the technology base required to evaluate feeding strategies for operation rations and supplements to minimize soldier performance decrements under sustained combat conditions and discharge the Army Surgeon General's responsibilities as DOD executive agent for nutrition. Assists Natick in the development of personal clothing and equipment. GRA

N89-27334# Army Research Inst. of Environmental Medicine, Natick, MA.
THERMOREGULATORY RESPONSES IN THE COLD-EFFECT OF AN EXTENDED COLD WEATHER CLOTHING SYSTEM (ECWCS)
Richard R. Gonzalez, Thomas L. Endrusick, and William L. Santee Apr. 1989 35 p Presented at the 15th Commonwealth Defence Conference on Operational Clothing and Combat Equipment, Canada, 1989
(DA Proj. 3E1-62787-A-878)
(AD-A208314; USARIEM-M42-89) Avail: NTIS HC A03/MF A01 CSCL 06/19

The human thermoregulatory responses of wearing a new cold-weather system (ECWCS) at rest or during exercise is addressed. The ECWCS (insulation = 3.6 clo; weight = 10.1 kg) encompasses skin-tight polypropylene underwear, polyester/cotton fatigues; polyester-insulated liners, balaclava, vapor-barrier boots, and polytetrafluorethylene (PTFE)-lined outer garments. Six fit males each rested and did treadmill exercise while wearing different

handwear with the ECWCS; the handwear included: a light duty glove heavy duty glove, or an Arctic mitten. A maximal 120 min cold challenge for each soldier was designated (based on physiological safety measures) as a maximal endurance time (ET,min). A multiple correlation analysis demonstrated that ET could be predicted adequately by finger temperature, absolute metabolism, rectal and 10-site skin temperatures. Effect of sweating during exercise reduced the effective thermal insulation of the ensemble thereby lowering the ET's for each handwear item. The Arctic mitten rendered the highest ETs during rest or exercise. The ECWCS should tender adequate endurance times in cold-dry ambients provided that ventilation and removal of extra layers is allowed as an easy option during heavy exercise so that thermal insulation is not excessively decreased by body moisture. GRA

N89-27335# Army Research Inst. of Environmental Medicine, Natick, MA.

CONSIDERATIONS FOR REPLACEMENT BEVERAGES: FLUID-ELECTROLYTE BALANCE AND HEAT ILLNESS Report, period ending Feb. 1989

Lawrence E. Armstrong 28 Feb. 1989 18 p
(AD-A208342; USARIEM-M32-89) Avail: NTIS HC A03/MF A01 CSCL 06/8

This article emphasizes the specific need (or lack of need) for carbohydrate-electrolyte solutions, which soldiers experience during duty in hot environments. Because this article focuses on fluids and electrolytes, it is helpful to reiterate the following aspects of their reports: (1) Gatorade was used in dilute form, at 2/3 (Alltz) and 1/4 (Donovan) strength, (2) meals were sacrificed so that the mission could be accomplished, and (3) a rigorous hydration program virtually eliminated heat illness at a time when the other U.S. personnel experienced significant casualties. Carbohydrate-electrolyte replacement fluids may be necessary in some, but not all, military field situations. The greatest need for carbohydrate-electrolyte replacement fluids will be experienced by soldiers who: (1) lose more than 8 L of sweat per day; (2) are not heat acclimatized (e.g., during the initial 8 days of field living); (3) are performing a prolonged, continuous exercise bout (greater than 60 min); (4) skip meals, have meals interrupted, or encounter anorexia due to a hot environment; (5) experience a caloric deficit greater than 1000 Kcal/day; or (6) are ill with diarrheal disease. The fluid-electrolyte needs of soldiers will be specific to the intensity, frequency and duration of the exercise involved, as well as the environmental stress encountered. GRA

N89-27336# Army Research Inst. of Environmental Medicine, Natick, MA. Exercise Physiology Div.

ENDOGENOUS HORMONAL AND GROWTH FACTOR RESPONSES TO HEAVY RESISTANCE EXERCISE PROTOCOLS

William J. Kraemer, Louis Marchitelli, Dini McCurry, Robert Mello, Joseph E. Dziados, Everett A. Harman, Peter N. Frykman, Scott E. Gordon, and Steven J. Fleck 20 Mar. 1989 29 p Submitted for publication Prepared in cooperation with Connecticut Univ., Storrs; and US Olympic Committee, Colorado Springs, CO
(AD-A208375) Avail: NTIS HC A03/MF A01 CSCL 06/10

To examine endogenous anabolic hormone and growth factor responses to various heavy resistance exercise protocols (HREPs), nine male subjects performed each of six randomly assigned HREPs which consisted of identically ordered exercises carefully designed to control for load (5RM vs 10RM), rest period length (1 min vs 3 min) and total work (J) effects. Serum human growth hormone (hGH), tesosterone (T), somatomedin-C (SM-C), serum glucose and whole blood lactate (HLa) concentrations were determined pre-exercise, mid-exercise and at 0, 5, 15, 20, 60, 90, and 120 min post-exercise. All HREPs produced significant increases in serum T concentrations although the magnitude and frequency above resting values varied across HREPs. The highest hGH concentrations were observed consequent to high total work, 1 min rest periods and 10RM load. All HREPs did not produce increases in serum hGH. The pattern of SM-C increases varied among HREPs and did not follow hGH changes. These data suggest that the release patterns and the magnitude of increases are functions of the type of HREPs utilized. Thus, all HREPs may not effect muscle and connective tissue growth in the same manner due to differences in hormonal and growth factor responses. GRA

N89-27337# Army Research Inst. of Environmental Medicine, Natick, MA.

EFFECTIVENESS AND ACCEPTABILITY OF NUTRIENT SOLUTIONS IN ENHANCING FLUID INTAKE IN THE HEAT Final Report, Jun. - Nov. 1988

Madeleine S. Rose, Patrica C. Szlyk, Ralph P. Francesconi, Laurie S. Lester, Lawrence E. Armstrong, William Matthew, Armand V. Cardello, Richard D. Popper, Ingrid Sils, and Glenn Thomas et al 18 Nov. 1988 252 p
(AD-A208428; USARIEM-T-10/89) Avail: NTIS HC A12/MF A01 CSCL 06/8

Two colored, flavored, 2.5 percent carbohydrate-electrolyte solutions (Armyade and NBC Nutrient solution) with varying level of magnesium, potassium, and phosphorus were tested for ad libitum consumption and acceptability during 8 days of work in a hot environment. Sixty-one male and female soldiers were divided into 4 test groups. A Control group drank water while the remaining three groups were given one of the following test beverages: NBC Nutrient solution, Armyade, or a colored flavored water (placebo). All four groups were allowed to consume other fluids such as plain water, soda, juice, etc. Acceptability in terms of hedonic ratings and consumption rate was determined. There were no group difference in terms of energy intake. Urine specific gravity and electrolytes, body weight, and fluid intake were monitored twice daily to assess hydration status. Drinking NBC and Armyade solutions appeared to be safe under the conditions studied. The ability to measure heat stress levels across a large area would provide valuable information for optimizing soldier performance. The close correlation between field and satellite-derived WBGT readings during the field trial indicates significant potential for the use of satellite remote sensing technology to accurately assess WBGT in training/operational environments. GRA

53 BEHAVIORAL SCIENCES

Includes psychological factors; individual and group behavior; crew training and evaluation; and psychiatric research.

N89-27338# Advisory Group for Aerospace Research and Development, Neuilly-Sur-Seine (France). Aerospace Medical Panel.

HUMAN PERFORMANCE ASSESSMENT METHODS

May 1989 70 p Prepared for a Lecture Series, Downsview, Ontario, 5-6 Jun. 1989; Soesterberg, Netherlands, 12-13 Jun. 1989; and Rome (Italy), 15-16 Jun. 1989
(AGARD-AG-308; ISBN-92-835-0510-7) Copyright Avail: NTIS HC A04/MF A01

The results are presented of the second phase of AGARD Aerospace Medical Panel Working Group 12 on Human Performance Assessment Methods. The major goal of WG 12 was to develop the Standardized Tests for Research on Environmental Stressors or STRES Battery, satisfying conventional psychometric criteria such as reliability, validity and sensitivity for which an extensive data base may now be compiled among the NATO nations. The protocol for the 7 selected tests is presented. AGARDograph 308 also serves as the Lecture Series Notes for AGARD Aerospace Medical Panel Lecture Series 163, Human Performance Assessment Methods. Author

N89-27339# National Inst. for Occupational Safety and Health, Morgantown, WV. Div. of Industrial Engineering.

A MODEL OF HUMAN REACTION TIME TO DANGEROUS ROBOT ARM MOVEMENTS

Martin G. Helander, Mark H. Karwan (State Univ. of New York at Buffalo, Amherst.), and John Etherton 1989 7 p
(PB89-186522) Avail: NTIS HC A02/MF A01 CSCL 05I

A model was presented of human reaction time and emergency behavior in the presence of a hazard caused by the use of a robot. The total reaction time was the sum of three elements: perception, decision making and motor response. The perceptual system must detect that the robot is moving and recognize this movement as potentially dangerous. The decision making involves whether to push the emergency stop on the teach pendant. The moving hand to the emergency stop would be accomplished by commands from the motor processor. Each of these elements was modeled using concepts such as perceptual discriminability and single detection theory. Finally the results of an experiment were presented where the relationships of the customer and the contractor, their characteristics, individual instruments for the configuration and securing of relationships and appropriate forms of contract are examined. The organizational/legal structure of collaboration, the planning of the fulfillment of the work tasks and the configuration of firms' information and control mechanisms in the project-related technology transfer with their interconnections and partners are discussed. GRA

N89-27340# Army Research Inst. of Environmental Medicine, Natick, MA.
PSYCHOLOGICAL ATTRIBUTES, COPING STRATEGIES AND OTHER FACTORS ASSOCIATED WITH ULTRAMARATHON PERFORMANCE
W. J. Tharion, A. L. Terry, D. J. McMenemy, T. M. Rauch, B. L. Shukitt, E. Gallego, and L. Gowenlock Jan. 1989 106 p
(DA Proj. 3A1-61101-A-91C)
(AD-A208300; USARIEM-T-8/89) Avail: NTIS HC A06/MF A01 CSCL 05/8

Mood states, symptomatology, coping strategies and training characteristics associated with running an ultramarathon were examined to explain racing performance and assess psychological health state. A total of 117 subjects were surveyed in 2 races (50-mile and 100-mile). Mood states and symptomatology were examined via a time-series approach with subjects queried pre, post, 1 week post, 1 month post, and 3 months postrun. Tension was found to be significantly greater prerun when compared to other administrations. Vigor was found to be significantly lower immediately postrun compared to the other administrations, whereas fatigue was found to be greater immediately postrun. Confusion was greater immediately postrun but had returned to prerace levels by 1 month postrun. Casualties were less fatigued and more depressed immediately postrun than were survivors. Additionally, survivors were found to be in better physical condition than casualties. The survivors weighed less, had been running for a longer period of time, ran more miles per week and ran at a faster training pace. Coping strategies were found to have an effect on performance. It appears that individuals who partition the race into segments fare better than those who do not. Finally, age, expected finish time and training pace are the best predictors for one's finish time in a 50-mile ultramarathon. GRA

54 MAN/SYSTEM TECHNOLOGY AND LIFE SUPPORT

Includes human engineering; biotechnology; and space suits and protective clothing.

For related information see also *16 Space Transportation.*

N89-27341# Technology, Inc., San Antonio, TX. Life Sciences Div.
RESEARCH AND DEVELOPMENT OF ANTI-G LIFE SUPPORT SYSTEMS. PART 4: ENGINEERING TEST AND EVALUATION OF SIX ANTI-G VALVES Final Report, 1 Apr. 1981 - 31 Jul. 1985
Larry J. Meeker (School of Aerospace Medicine, Brooks AFB, TX.), Arnold G. Krueger, Paul E. Love, Emily M. Gause, and Robert W. Krutz Aug. 1988 118 p
(Contract F33615-81-C-0600)
(AD-A206996; USAFSAM-TR-86-36-Pt-4) Avail: NTIS HC A06/MF A01 CSCL 23/5

Six anti-G valves (i.e., valves designed to rapidly deliver output pressures proportional to + Gz forces acting upon valve control elements) were evaluated for performance under conditions simulating the spectrum of Gz-onset conditions likely to be encountered by pilots of current U.S. Air Force high-performance aircraft. This Engineering Test and Evaluation Task was conducted on-site at Brooks Air Force Base, Texas, using the School of Aerospace Medicine (USAFSAM) human centrifuge facility. One objective was validation of uniform testing procedures for evaluation of anti-G valves under controlled conditions of: acceleration, source pressure, valve angles, and simulated anti-G suit volumes. A second objective was measurement of actual dynamic performance of the standard ALAR High-flow Ready-pressure; ALAR High-flow; Garrett Electronic/Pneumatic; Hymatic VAG-110-022; and AAMRL Electropneumatic (Bang Bang). The battery of test conditions employed was divided into three phases: Phase 1 - Maximum Flow Capacity Testing; Phase 2 - Dynamic Response Testing; and Phase 3 - Complex Dynamic Response Testing. Results of testing under all conditions are presented for each valve and the performance characteristics of all six valves are compared. GRA

N89-27342# Analytics, Inc., Willow Grove, PA.
HUMAN OPERATOR SIMULATOR (HOS) 4 PROGRAMMER'S GUIDE Final Report, 1987 - 1988
Regina Harris, Jonathan Kaplan, Christopher Bare, Helene Lavecchia, and Lorna Ross Jan. 1989 186 p
(Contract F33615-86-C-0019)
(AD-A207241; ARI-RP-89-06) Avail: NTIS HC A09/MF A01 CSCL 23/2

This report is a guide to maintaining and updating the source code for the Human Operator Simulator (HOS) 4, which was developed to aid in the design and evaluation of interfaces between operators or maintainers and weapon system hardware and software. HOS 4 creates simulations of manned systems on an IBM-AT PC or compatible. It does this by using micromodels of basic human processes to produce both system and human performance estimates. HOS 4 also includes a mechanism to aid in the creation of new micromodels. GRA

N89-27343# Foersvarets Forskingsanstalt, Stockholm (Sweden). Dept. of Human Studies.
FULL COVERAGE ANTI-G-SUIT AND BALANCED PRESSURE BREATHING
Ulf Balldin, Gunnar Dahlbaeck, and Lars-Erik Larsson Feb. 1989 24 p
(PB89-174635; FOA-C-50065-5.1; ISSN-0347-7665) Avail: NTIS HC A03/MF A01 CSCL 05H

A full coverage anti-G-suit (FCAGS) was compared to a normal anti-G-suit (NAGS) in 9 fighter pilots. The G-tolerance was tested during gradual and rapid onset runs up to 9 G and during simulated aerial combat maneuvers in a human centrifuge. In 35 percent of the tests the subjects succeeded in reaching 9 G without straining maneuvers with FCAGS in comparison to only 12 percent with NAGS, and succeeded in staying there for 5 s in 18 percent and 0 percent of the tests, respectively. With rapid onset runs with straining maneuvers, 2 cases of G-induced loss of consciousness (GLOC) occurred with NAGS. The FCAGS was similarly tested up to 9 G in 9 subjects with and without balanced positive pressure breathing (BPPB). No GLOC occurred. Without straining maneuvers the subjects succeeded in reaching 9 G in 94 percent of the tests with BPPB in comparison to only 59 percent without BPPB and in staying at 9 G for 10 s in 82 percent and 18 percent of the tests, respectively. FCAGS gives substantial G-protection, especially when combined with BPPB. GRA

N89-27344*# National Academy of Sciences - National Research Council, Washington, DC. Committee on Human Factors.
ERGONOMIC MODELS OF ANTHROPOMETRY, HUMAN BIOMECHANICS AND OPERATOR-EQUIPMENT INTERFACES
Karl H. E. Kroemer, ed., Stover H. Snook, ed., Susan K. Meadows, ed., and Stanley Deutsch, ed. 1988 114 p Proceedings of a

Workshop held in Washington, DC, 17-18 Jun. 1985 Sponsored in part by AFOSR, Washington, DC; Army Research Inst. for the Behavioral and Social Sciences, Arlington, VA; NASA, Washington, DC and NSF, Washington, DC
(Contract N00014-85-G-0093)
(NASA-CR-185720; NAS 1.26:185720; PB89-175491) Avail: NTIS HC A06/MF A01 CSCL 06P

The Committee on Human Factors was established in October 1980 by the Commission on Behavioral and Social Sciences and Education of the National Research Council. The committee is sponsored by the Office of Naval Research, the Air Force Office of Scientific Research, the Army Research Institute for the Behavioral and Social Sciences, the National Aeronautics and Space Administration, and the National Science Foundation. The workshop discussed the following: anthropometric models; biomechanical models; human-machine interface models; and research recommendations. A 17-page bibliography is included.
Author

N89-27345# National Academy of Sciences - National Research Council, Washington, DC. Committee on Toxicology.
SUBMARINE AIR QUALITY: MONITORING THE AIR IN SUBMARINES. HEALTH EFFECTS IN DIVERS OF BREATHING SUBMARINE AIR UNDER HYPERBARIC CONDITIONS Final Report
Dec. 1988 160 p
(Contract DAMD17-86-C-6151)
(PB89-174213) Avail: NTIS HC A08/MF A01 CSCL 05H

The report is an assessment of the quality of the air in the enclosed environment of a nuclear submarine. Part 1 is a review of the analytic techniques used in monitoring submarine contaminants, a study of possible alternate monitoring methods, and recommendations on which compounds would be most useful to monitor. Part 2 is a review of the possible health effects in divers of breathing commonly encountered airborne contaminants at pressures of up to 6 atmospheres, considering possible interactions of substances encountered as mixtures. Recommendations include the curtailment of smoking, the possible elimination of deep-fat fryers, the use of nontoxic paints, an increased monitoring capability, the establishment of toxic categories for chemicals, a review of the methods of instruction of personnel regarding air control equipment, and increased communication with the British Royal Navy regarding the monitoring of air contaminants. Recommendations for divers' air include the monitoring of CO2 and particulates with their removal if necessary, and the study of animals or humans exposed to elevated levels of CO2. Also recommended is physiological research on the interaction of cold, extreme exercise, and breathing compressed gases.
Author

N89-27346*# California Univ., Davis. Plant Growth Lab.
EFFICIENCY OF N USE BY WHEAT AS A FUNCTION OF INFLUX AND EFFLUX OF NO SUB 3
R. C. Huffaker, M. Aslam, and M. R. Ward Jul. 1989 25 p
(Contract NCC2-99)
(NASA-CR-177534; NAS 1.26:177534) Avail: NTIS HC A03/MF A01 CSCL 06K

Since N assimilation is one of the most costly functions of a plant, its efflux before assimilation results in a serious energy cost and loss in efficiency which could decrease yields. Efficient crop production is critical to the Controlled Ecological Life-Support System (CELSS). The objective is to determine the extent of efflux of the N species NO3(-), NH4(+), NO2(-), and urea after uptake, and possible means of regulation. It was found that NO3(-) efflux became serious as its substrate level increased. Efflux/Influx (E/I) of 3NO3(-) was greater in darkness (35 pct) than in light (14 pct) and the ratio greatly increased with increased substrate NO3(-), (up to 45 pct at 10 mM). It seems advantageous to use the lowest possible nutrient concentration of NO3(-). The feasibility of using ClO3(-) as a trapping agent (competitive inhibitor of NO3(-) uptake) for effluxed NO3(-) was assessed and its toxicity determined.
Author

N89-27347# Army Research Inst. of Environmental Medicine, Natick, MA. Exercise Physiology Div.
THE EFFECTS OF ARMS AND COUNTERMOVEMENT ON VERTICAL JUMPING Scientific Paper
Everett A. Harman, Michael T. Rosenstein, Peter N. Frykman, and Richard Rosenstein 28 Apr. 1989 29 p
(AD-A208298) Avail: NTIS HC A03/MF A01 CSCL 06/10

Countermovement (C) and arm-swing (A) characterize most jumping. For determination of their effects and interaction, 18 males jumped for maximal height from a force platform four ways: C,A; C, no A; no C, A; no C, no A. For all jumps, vertical velocity peaked 0.03 sec before, and dropped 6 to 7 percent by takeoff. Peak positive power averaged over 3,000 W, and occurred about 0.07 s before takeoff, shortly after maximum vertical ground reaction force (VGRF) and just before peak vertical velocity. Both C and A significantly (p less than 0.05) improved jump height, but A's effect was greater, enhancing both height of the total body center of mass (TBCM) at takeoff and post-takeoff TBCM rise. C only affected the latter. Use of A resulted in less unweighting and slower descent of the TBCM during C, higher TBCM position at the bottom of C, higher peak VGRF, higher peak positive power, and lower negative power. C increased pretakeoff jump duration by 71 to 76 percent, increased average positive power, and resulted in large positive and negative impulses. Correlation of peak power with post-takeoff jump height was 0.88. Body weight and post-takeoff jump height effectively predicted peak power ($r=0.94$). The results lend insight into which jumping techniques are most appropriate for given sports situations.
GRA

55 SPACE BIOLOGY

Includes exobiology; planetary biology; and extraterrestrial life.

No abstracts in this category.

59 MATHEMATICAL AND COMPUTER SCIENCES (GENERAL)

N89-27348*# Institute for Computer Applications in Science and Engineering, Hampton, VA.
[SUMMARY OF RESEARCH CONDUCTED AT THE INSTITUTE FOR COMPUTER APPLICATIONS IN SCIENCE AND ENGINEERING IN APPLIED MATHEMATICS, NUMERICAL ANALYSIS AND COMPUTER SCIENCE] Semiannual Report, 1 Oct. 1988 - 31 Mar. 1989
Jun. 1989 44 p
(Contracts NAS1-18605; NAS1-18107)
(NASA-CR-181858; NAS 1.26:181858) Avail: NTIS HC A03/MF A01 CSCL 12A

Research conducted at the Institute for Computer Applications in Science and Engineering in applied mathematics, numerical analysis, and computer science during the period October 1, 1988 through March 31, 1989 is summarized.
Author

N89-27349*# Institute for Computer Applications in Science and Engineering, Hampton, VA.
DATA TRAFFIC REDUCTION SCHEMES FOR CHOLESKY FACTORIZATION ON ASYNCHRONOUS MULTIPROCESSOR SYSTEMS Final Report
Vijay K. Naik and Merrell L. Patrick (Duke Univ., Durham, NC.) Jun. 1989 32 p Submitted for publication
(Contracts NAS1-18107; NAS1-18605; AF-AFOSR-0117-88)
(NASA-CR-181863; ICASE-89-40; NAS 1.26:181863) Avail: NTIS HC A03/MF A01 CSCL 12A

Communication requirements of Cholesky factorization of dense

and sparse symmetric, positive definite matrices are analyzed. The communication requirement is characterized by the data traffic generated on multiprocessor systems with local and shared memory. Lower bound proofs are given to show that when the load is uniformly distributed the data traffic associated with factoring an n x n dense matrix using n to the alpha power (alpha less than or equal 2) processors is omega(n to the 2 + alpha/2 power). For n x n sparse matrices representing a square root of n x square root of n regular grid graph the data traffic is shown to be omega(n to the 1 + alpha/2 power), alpha less than or equal 1. Partitioning schemes that are variations of block assignment scheme are described and it is shown that the data traffic generated by these schemes are asymptotically optimal. The schemes allow efficient use of up to O(n to the 2nd power) processors in the dense case and up to O(n) processors in the sparse case before the total data traffic reaches the maximum value of O(n to the 3rd power) and O(n to the 3/2 power), respectively. It is shown that the block based partitioning schemes allow a better utilization of the data accessed from shared memory and thus reduce the data traffic than those based on column-wise wrap around assignment schemes. Author

60 COMPUTER OPERATIONS AND HARDWARE

Includes hardware for computer graphics, firmware, and data processing.

For components see *33 Electronics and Electrical Engineering.*

N89-27350# Edgerton, Germeshausen and Grier, Inc., Idaho Falls, ID.
ELECTRONIC INFORMATION DELIVERY AT THE JOB SITE
Donald L. Schurman and J. Peter Kincaid (Army Research Inst. for the Behavioral and Social Sciences, Orlando, FL.) 1988 5 p Presented at the IEEE International Conference on System Man and Cybernetics, Beijing, China, 1 Aug. 1988
(Contract DE-AC07-76ID-01570)
(DE89-009726; EGG-M-20887; CONF-8808208-1) Avail: NTIS HC A03/MF A01

The United States Department of Defense is actively investigating the usefulness of presenting procedural information for operation and maintenance of equipment on small, often hand-held, computers. The basic concept that is being explored is: the presentation of information that is necessary to job performance by means of computers rather than by means of text and drawings printed on paper. The Idaho National Engineering Laboratory (INEL) assisted the U.S. Army Research Institute for the Behavioral and Social Sciences (ARI) in performing a test and evaluation of a prototype device that was an instantiation of the electronic information delivery concept. The prototype device is called the Personal Electronic Aid to Maintenance (PEAM). The device was tested as a substitute for technical manuals when being used by U.S. Army mechanics in the repair of the fire control system of the M1 Abrams tank. This test and evaluation of the PEAM prototype revealed several general problems for the electronic delivery of information in terms of the human-computer interaction involved. It became clear, for example, that formatting and graphical standards that apply to paper manuals will not apply to electronically presented procedures. Another problem that appeared was the problem of losing one's place in a troubleshooting or other branching procedure. These and other problems are presented and suggestions are made for resolution of some, but not all, of these problems. DOE

N89-27351# Computational Logic, Inc., Austin, TX.
A PARALLEL VERSION OF THE BOYER-MOORE PROVER
Matt Kaufmann and Matt Wilding Feb. 1989 43 p
(Contract N00014-88-C-0454)
(AD-A207190; TR-39) Avail: NTIS HC A03/MF A01 CSCL 12/5

The idea of this system is to use idle processors to increase the speed of NQTHM. There were many design considerations, including: no shared file system; easy to kill jobs on a given host; easy to prevent job assignment on a given host; robust; and nicer user interface. The system will be used to process an NQTHM event list in parallel, with a given granularity. Given a granularity of n, then the first job will process the first n PROVE-LEMMAs. Each subsequent job will process n PROVE-LEMMAs. Since an arbitrary subsequence of PROVE-LEMMAs may require a previous definition, each will process all previous definitions. A subsequence of PROVE-LEMMAs may also require PROVE-LEMMAs from a previous subsequences, treating each PROVE-LEMMA as an ADD-AXIOM. This system allows the user to run a job on multiple machines in parallel. The issue of machine use has been discussed at Computational Logic and a preliminary policy adopted. It is the policy at Computational Logic to allow users to run parallel jobs using the dispatcher. Spawned jobs are to be run at the default (nice) priority level, and it is OK for any user to kick spawned parallel jobs off the local machine if he wishes (without feeling bad about it). GRA

N89-27352# Stanford Univ., CA. Computer Systems Lab.
MEMORY-REFERENCE CHARACTERISTICS OF MULTIPROCESSOR APPLICATIONS UNDER MACH
Anant Agarwal and Anoop Gupta 1988 11 p
(Contract MDA903-83-C-0335)
(AD-A207318) Avail: NTIS HC A03/MF A01 CSCL 12/5

Shared-memory multiprocessors have received wide attention in recent times as a means of achieving high-performance cost-effectively. Their viability requires a thorough understanding of the memory access patterns of parallel processing applications and operating systems. This paper reports on the memory reference behavior of several parallel applications running under the MACH operating system on a shared memory multiprocessor. The data used for this study is derived from multiprocessor address traces obtained from an extended ATUM address tracing scheme implemented on a 4-CPU DEC VAX 8350. The applications include parallel OPS5, logic simulation and a VSLI wire routing program. GRA

N89-27353# Stanford Univ., CA. Dept. of Computer Science.
PARALLEL IMPLEMENTATION OF OPS5 ON THE ENCORE MULTIPROCESSOR: RESULTS AND ANALYSIS
Anoop Gupta, Milind Tambe, Dirk Kalp, Charles Forgy, and Allen Newell (Carnegie-Mellon Univ., Pittsburgh, PA.) 1988 24 p
(Contract N00014-87-K-0828; ARPA Order 4864)
(AD-A207320) Avail: NTIS HC A03/MF A01 CSCL 12/5

Until now, most results reported for parallelism in production systems (rule-based systems) have been simulation results - very few real parallel implementations exist. In this paper, we present results from our parallel implementation of OPS5 on the Encore multiprocessor. The implementation exploits very-fine-grained parallelism to achieve significant speed-ups. For one of the applications, we achieve 12.4 fold speed-up using 13 processes. Our implementation is also distinct from other parallel implementations in that we parallelize a highly optimized C-based implementation of OPS5. Running on uniprocessor, our C-based implementation is 10 to 20 times faster than the standard lisp implementation distributed by Carnegie Mellon University. In addition to presenting the performance numbers, the paper discusses the details of the parallel implementation - the data structures used, the amount of contention observed for shared data structures, and the techniques used to reduce such contention. GRA

N89-27354# Massachusetts Inst. of Tech., Cambridge. Lab. for Computer Science.
IMPLEMENTATION INDICES (1975-1979), VOLUME 1
Gregory Michael Papadopoulos Dec. 1988 158 p
(Contract N00014-84-K-0099)
(AD-A207609; MIT/LCS/TR-432-Vol-1) Avail: NTIS HC A08/MF A01 CSCL 12/6

General purpose multiprocessors have largely failed to meet expectations for programmability and performance. We blame the

lack of usable parallel programming languages and systems on the underlying processor architecture. Machines built out of conventional sequential processors simply do not support the synchronization demands of parallel execution, so the programmer focuses upon the dangerous and arduous task of discovering a minimum set of synchronization points without introducing nondeterminism. We argue that processors must be fundamentally changed to execute a parallel machine language, in which parallel activities are coordinated as efficiently as instructions are scheduled. GRA

N89-27355# Fermi National Accelerator Lab., Batavia, IL.
ACP/R3000 PROCESSORS IN DATA ACQUISITION SYSTEMS
J. Deppe, H. Areti, R. Atac, J. Biel, A. Cook, M. Edel, M. Fischler, I. Gaines, D. Husby, and M. Isely et al Feb. 1989 4 p Presented at the 6th Conference on Real-Time Computer Applications in Nuclear, Particle and Plasma Physics, Williamsburg, VA, 16-19 May 1989
(Contract DE-AC02-76CH-03000)
(DE89-014811; FNAL/C-89/118; CONF-890545-3) Avail: NTIS HC A02/MF A01

We describe the advanced computer program ACP/R3000 processor based data acquisition systems for high energy physics. This VME bus compatible processor board, with a computational power equivalent to 15 VAX 11/780s or better, contains 8 Mb of memory for event buffering and has a high speed secondary bus that allows data gathering from front end electronics. DOE

N89-27356# National Inst. of Standards and Technology, Gaithersburg, MD. Advanced Systems Div.
HYBRID STRUCTURES FOR SIMPLE COMPUTER PERFORMANCE ESTIMATES
Gordon E. Lyon Mar. 1989 25 p
(Contracts DE-AI05-87ER-25046; ITA-87-PAY-226-B; ARPA Order 5520)
(PB89-189161; NISTIR-89/4063) Avail: NTIS HC A03/MF A01 CSCL 09B

Even the coarsest performance estimators for a modern computer must account for architectural dependencies and variabilities. For example, average execution rate is rather sensitive to the match between machine and application workload. Computing can be viewed as computational components that are loaded by demands of an application, or alternately, as an application workload partitioned by system components. Models based upon these simple perspectives help organize simple performance measurements. Several examples demonstrate strengths of a straight-forward and flexible partitioning scheme based upon tree graphs. Quite explicit, the graphs promote a more critical view of measurements and support multiple interpretations. Author

N89-27357# Sandia National Labs., Albuquerque, NM. Integrated Circuits Design Dept.
A RADIATION-HARDENED 16/32-BIT MICROPROCESSOR
K. J. Hass, R. K. Treece, and A. E. Giddings 1989 5 p Presented at the 26th Annual Conference on Nuclear and Space Radiation Effects, Marco Island, FL, 24 Jul. 1989
(Contract DE-AC04-76DP-00789)
(DE89-008111; SAND-89-0334C; CONF-890723-5) Avail: NTIS HC A02/MF A01

A radiation-hardened 16/32-bit microprocessor has been fabricated and tested. Our initial evaluation has demonstrated that it is functional after a total gamma dose of 5Mrad(Si) and is immune to single event upset (SEU) from Krypton ions. DOE

N89-27358# Lawrence Livermore National Lab., CA.
CRAY-TO-SUN PROTOTYPE
Joe Requa 26 Apr. 1989 8 p Presented at the Cray User's Group Conference, Los Angeles, CA, 24 Apr. 1989
(Contract W-7405-eng-48)
(DE89-013087; UCRL-101034; CONF-8904210-6) Avail: NTIS HC A02/MF A01

The Cray-to-Sun prototype is an experiment in providing an in-the-office graphics tool using the LINCS architecture developed at LLNL. It represents one of the first attempts at developing a true distributed application utilizing the number-crunching power of the Cray and the interactive and graphics capabilities of the Sun workstation. DOE

N89-27359# Brown Univ., Providence, RI.
OFFLINE COMPUTING FARMS
D. Cutts, J. Hoftun, and R. Partridge 26 Jan. 1989 4 p
(Contract DE-AC02-76ER-03130)
(DE89-013958; DOE/ER-03130/48C) Avail: NTIS HC A02/MF A01

The D/null/ experiment will require substantial offline computing resources to perform production analysis, data reduction, and Monte Carlo event generation. Given the significant head start obtained by CDF, it is imperative that D/null/ have a fully functional offline computing environment ready at detector turn on to allow fast hardware and software shakedown and quick analysis of the data. The ability to get physics results out quickly is especially important to the graduate students, postdocs, and junior faculty who need to be able to present physics talks for future jobs/tenure. For these reasons, it is believed that D/null/ must begin planning its offline computing environment now, paying particular attention to the issue of software compatibility which has plagued CDF. In particular, proper evaluation of system cost should give at least equal weight to software development, management, and operational demands on the collaboration. It is believed the best solution to the D/null/ offline computing needs is the development of computing farms utilizing DEC VAX computers. This note describes a model for such farms that can be realized with today's technology. DOE

N89-27360# Rome Univ. (Italy). Dipartimento di Fisica.
ON-LINE COMPUTER UTILIZATION TO UNDERSTAND SOME PHYSICAL PROCESSES (EXAMPLE: PENDULUM MOTION) [L'ELABORATORE IN LINEA PER CAPIRE ALCUNI PROCEDIMENTI DELLA FISICA (L'ESEMPIO DEL MOTO DEL PERDOLO)]
G. Cortini, L. Danusso, P. Festa, and F. Scalzo 9 Dec. 1988 13 p In ITALIAN
(Nota-Interna-927; ETN-89-94746) Avail: NTIS HC A03/MF A01

Didactic methods for physics are discussed. A procedure based on the use of a microprocessor to simulate measuring physical phenomena is presented. The validity limits of mathematical models and the experimental errors are explained better by this method. The program includes instructions for the teacher. ESA

61 COMPUTER PROGRAMMING AND SOFTWARE

Includes computer programs, routines, alogorithms, and specific applications, e.g., CAD/CAM.

N89-27361*# Systems and Processes Engineering Corp., Austin, TX.
DFT ALGORITHMS FOR BIT-SERIAL GaAs ARRAY PROCESSOR ARCHITECTURES Final Report
Gary B. McMillan 19 Aug. 1988 78 p
(Contract NAS5-30291)
(NASA-CR-183436; NAS 1.26:183436) Avail: NTIS HC A05/MF A01 CSCL 09B

Systems and Processes Engineering Corporation (SPEC) has developed an innovative array processor architecture for computing Fourier transforms and other commonly used signal processing algorithms. This architecture is designed to extract the highest possible array performance from state-of-the-art GaAs technology. SPEC's architectural design includes a high performance RISC processor implemented in GaAs, along with a Floating Point Coprocessor and a unique Array Communications Coprocessor, also implemented in GaAs technology. Together, these data

processors represent the latest in technology, both from an architectural and implementation viewpoint. SPEC has examined numerous algorithms and parallel processing architectures to determine the optimum array processor architecture. SPEC has developed an array processor architecture with integral communications ability to provide maximum node connectivity. The Array Communications Coprocessor embeds communications operations directly in the core of the processor architecture. A Floating Point Coprocessor architecture has been defined that utilizes Bit-Serial arithmetic units, operating at very high frequency, to perform floating point operations. These Bit-Serial devices reduce the device integration level and complexity to a level compatible with state-of-the-art GaAs device technology. Author

N89-27362*# Institute for Computer Applications in Science and Engineering, Hampton, VA.
PROGRAMMING PARALLEL ARCHITECTURES: THE BLAZE FAMILY OF LANGUAGES Final Report
Piyush Mehrotra (Purdue Univ., West Lafayette, IN.) Mar. 1988 21 p Presented at the 3rd Conference on Parallel Processing for Scientific Computing
(Contract NAS1-18107)
(NASA-CR-185826; NAS 1.26:185826; ICASE-88-21) Avail: NTIS HC A03/MF A01 CSCL 09B

Programming multiprocessor architectures is a critical research issue. An overview is given of the various approaches to programming these architectures that are currently being explored. It is argued that two of these approaches, interactive programming environments and functional parallel languages, are particularly attractive since they remove much of the burden of exploiting parallel architectures from the user. Also described is recent work by the author in the design of parallel languages. Research on languages for both shared and nonshared memory multiprocessors is described, as well as the relations of this work to other current language research projects. Author

N89-27363# Du Pont de Nemours (E. I.) and Co., Aiken, SC.
AN ALGORITHM FOR SYMBOLIC DIMENSIONAL ANALYSIS
C. S. Loehle 1989 20 p
(Contract DE-AC09-76SR-00001)
(DE89-010409; DP-MS-88-240) Avail: NTIS HC A03/MF A01

An algorithm is described for symbolically manipulating equations to perform dimensional analysis. DOE

N89-27364*# University of Southern California, Marina del Rey. Information Sciences Inst.
EXPLANATION IN EXPERT SYSTEMS: A SURVEY
Johanna D. Moore (California Univ., Los Angeles.) and William R. Swartout Dec. 1988 58 p
(Contract NCC2-520)
(NASA-CR-185335; NAS 1.26:185335; ISI/RR-88-228) Avail: NTIS HC A04/MF A01 CSCL 09B

In order to be considered useful and acceptable, expert systems must be able to explain their knowledge of the domain and the reasoning process they employ to produce results and recommendations. Despite the fact that the need for explanation is widely recognized, current expert systems have only limited explanatory capabilities. Early approaches to explanation in expert systems are reviewed and their limitations discussed. Improvements to the explanation capabilities based on enriched knowledge bases of expert systems are presented. Further improvements in explanation requiring better generation techniques is stressed. Related work in the field of natural language generation suggests techniques that are useful to the task of explanation in expert systems; however, even those techniques will not provide all of the capabilities required for the task of carrying on a dialog with the user. Finally, the approach to explanation is described, which provides the facilities necessary to carry on an interactive dialog with the user. Author

N89-27365# Illinois Univ., Urbana-Champaign. Coordinated Science Lab.
HEURISTIC ALGORITHMS FOR STABILITY TESTING POLYTOPES OF MATRICES M.S. Thesis
Karen Lorraine Otto Jul. 1988 59 p
(Grant NSF ECS-87-09265)
(PB89-160840; UILU-ENG-88-2239; DC-106) Avail: NTIS HC A04/MF A01 CSCL 09B

The problem of robust stability for linear feedback systems is examined. Modeling uncertainty arises from a variety of sources, including linearization of nonlinear systems, inaccurately identified parameter values, neglected dynamics, and parameter drift. The robust stability problem addresses the issue of ensuring that stability of a feedback system is maintained in the presence of this modeling uncertainty. Two heuristic approaches to the robust stability problem of stability testing polytopes of matrices are provided: (1) the polytope-covering algorithm, which uses a Lyapunov-theoretic approach to iteratively remove closed balls of stable matrices from omega and terminates either when omega is exhausted or when an unstable matrix is found in omega; and (2) the annealing algorithm which uses simulated annealing to search for the least stable matrix in the set omega. Examples illustrate that the annealing algorithm may prove to be a valuable tool in solving the robust stability problem. GRA

N89-27366# Instituto de Pesquisas Espaciais, Sao Jose dos Campos (Brazil).
NATURAL LANGUAGE PROCESSING [PROCESSAMENTO DE LINGUAGEM NATURAL]
Carlos AlbertodeOliveira Dec. 1987 114 p In PORTUGUESE; ENGLISH summary
(INPE-4449-TDL/314) Avail: NTIS HC A06/MF A01

A synthesis of the state of art of Natural Language (NL) is presented. Some relevant models are pointed out for NL descriptors, interpreters and generators, and their respective development tools. Current trends for database NL interfaces, NL as a programming language and text knowledge systems are commented for solving real world NL interface problems, such as error correcting, robotics, automatic translation, text generation, etc. For the models and tools discussed, some NL interface systems are outlined. Author

N89-27367# Instituto de Pesquisas Espaciais, Sao Jose dos Campos (Brazil).
SATELLITE IMAGE PROCESSING USING SYMBOLIC STRUCTURES OF REDUCED VISION CONDITIONS M.S. Thesis [PROCESSAMENTO DE IMAGENS DE SATELITE USANDO ESTRUTURAS SIMBOLICAS DO BAIXO NIVEL DA VISAO]
Antonio Miguel VieiraMonteiro Aug. 1988 110 p In PORTUGUESE; ENGLISH summary
(INPE-4638-TDL/337) Avail: NTIS HC A06/MF A01

In automatic satellite image processing, tasks such as segmentations of the image into meaningful objects and even classification have been commonly performed using as input the raw satellite image (except for restoration and other cosmetic operations). In many cases the results obtained have not been very good, especially when compared with the performance of (human) photointerpreters in the same tasks. The increase in spatial resolution of recent satellites has added to the problem rather than improved it. Proposed here is the adoption of current models of human visual perception as the paradigm to organize processing systems for satellite images. In particular it is proposed that the Primal Sketch, as defined by David Marr, be the starting point of the processing instead of the raw image. Some experiments using the Primal Sketch to perform segmentation of satellite imagery are shown, and the applicability of the method is discussed. Author

N89-27368# California Univ., San Diego, La Jolla.
HIGH EFFICIENCY PATTERN RECOGNITION Final Technical Report, Mar. 1985 - Feb. 1987
S. H. Lee and S. Feynman Jan. 1989 10 p

(Contract F19628-85-K-0039)
(AD-A207210; RADC-TR-88-285) Avail: NTIS HC A02/MF A01 CSCL 20/5

This contract had two main goals: the improvement and comparison of optical pattern recognition filter algorithms and the improvement of the optical or Horner efficiency in order to allow smaller lower powered lasers for pattern recognition systems. The first goals was achieved by studying and comparing the performance results of three generic classes of filters: the Fukunaga-Koontz, the Hotelling, and the Foley-Sammon filter. All of these are of the classical statistical feature extraction type. In addition the effect of white noise on the recognition of a 2 class problem employing the LSLMT algorithm was evaluated. The second goal was apparently not achieved, as the simulated optical efficiency and classification reliability remained about the same as the full phase and amplitude filters. This may have been due to non-standard definition of Horner efficiency used by the contractor, and the fact that a limited database was used. GRA

N89-27369# Rome Air Development Center, Griffiss AFB, NY.
SOFTWARE DEFICIENCY ISSUES CONFRONTING THE UTILIZATION OF NON-VON NEUMANN ARCHITECTURES
Report, Jan. - Jun. 1988
Paul M. Engelhart Jan. 1989 103 p
(AD-A207268; RADC-TR-88-319) Avail: NTIS HC A06/MF A01 CSCL 12/5

Work is summarized for the current state-of-the-art in software engineering issues confronting the effective implementation of non-sequential architecture-based computers. Since these architects do not conform to the model of the von Neumann machine, the Non-von Neumann computers. It is apparent that utilization of Non-von Neumann computer systems is necessary to many of today's as well as the future's computational requirements. Advances in computer architecture technology, VLSI technology, and interconnection network topologies, to name but a few, have led to a multitude of relatively inexpensive but very powerful high performance processors. The development and utilization of Non-von Neumann systems requires a strong knowledge of the development and utilization of Non-von Neumann systems requires a strong knowledge of the underlying hardware and software structures. However, the largest problem in utilizing Non-von Neumann computers is not in the hardware, but in the software where software engineering remains oriented towards conventional von Neumann methodologies. Since these machines are highly concurrent in nature, a deep-rooted understanding is necessary to determine exactly what software engineering tools and techniques are necessary for their exploitation. GRA

N89-27370# Stanford Univ., CA. Computer Systems Lab.
HARDWARE C - A LANGUAGE FOR HARDWARE DESIGN
David C. Ku and Giovanni DeMicheli Aug. 1988 45 p
(Contract N00014-87-K-0828)
(AD-A207317; CSL-TR-88-362) Avail: NTIS HC A03/MF A01 CSCL 12/5

High-level synthesis is the transformation from a behavioral level specification of hardware to a register transfer level description, which may be mapped to a VLSI implementation. The success of high-level synthesis systems is heavily dependent on how effectively the behavioral language captures the ideas of the designer in a simple and understandable way. This paper describes Hardware C, a hardware description language that is based on the C programming language, extended with notions of concurrent processes, message passing, explicit instantiation of procedures, and templates. The language is used by the HERCULES High-Level Synthesis System. GRA

N89-27371# Stanford Univ., CA. Center for Integrated Systems.
THE HERMOD BEHAVIORAL SYNTHESIS SYSTEM
Masayasu Odani, Sun Y. Hwang, Tom Blank, and Tom Rokicki 8 Jun. 1988 34 p
(Contract N00014-87-K-0828)
(AD-A207319) Avail: NTIS HC A03/MF A01 CSCL 12/7

Silicon compilation is the process of automatically mapping an abstract design representation to a physical structure. Depending upon the input language, silicon compilers are classified into behavioral compilers (or behavioral synthesizers) and structural compliers. A behavioral synthesizer translates a behavioral synthesizer translates a behavioral description into a structure, creating structural designs consisting of functional blocks and their interconnection. In a behavioral synthesis system, the design is specified by a functional relationship between input and output ports described in hardware description language. The behavior of output ports is specified in terms of input ports internal state. The output from a behavioral synthesizer contains hardware modules (data paths) required to implement the given behavioral specification, and their scheduling (control). GRA

N89-27372# Carnegie-Mellon Univ., Pittsburgh, PA.
COMPETITIVE MANAGEMENT OF DISTRIBUTED SHARED MEMORY
David L. Black, Anoop Gupta, and Wolf-Dietrich Weber (Stanford Univ., CA.) 1988 8 p
(Contract N00014-87-K-0828)
(AD-A207322) Avail: NTIS HC A02/MF A01 CSCL 12/5

This paper presents and analyzes algorithms for managing the distributed shared memory present in non-uniform memory access multiprocessors and related systems. The competitive properties of these algorithms guarantee that their performance is within a small constant factor of optimal even though they make no use of any information about memory reference patterns. Both hardware and software implementation concerns are covered. A case study of the Mach operating systems indicates that integration of these algorithms into operating systems does not pose major problems. On the other hand, hardware support is required to obtain the full functionality of the algorithms. We also sketch possible algorithm extensions to additional hardware architectures and software programming models. GRA

N89-27373# Stanford Univ., CA. Systems Optimization Lab.
ON THE FEASIBILITY OF A GENERALIZED LINEAR PROGRAM
Hui Hu Mar. 1989 10 p
(Contract N00014-89-J-1659; NSF DMS-88-00589)
(AD-A207402; SU-SOL-TR-89-1) Avail: NTIS HC A02/MF A01 CSCL 12/4

The first algorithm for solving generalized linear programs was given by Dantzig. His algorithm assumes that a basic feasible solution of the generalized program to be solved exists and is given. If the initial basic feasible solution is non-degenerate, then his algorithm is guaranteed to converge. The purpose of this paper is to show how to find an initial basic feasible (possibly degenerate) solution of a generalized linear program by applying the same algorithm to a phase-one problem without requiring that the initial basic feasible solution to the latter be non-degenerate. GRA

N89-27374# Stanford Univ., CA. Systems Optimization Lab.
SEMI-INFINITE PROGRAMMING
Hui Hu Mar. 1989 66 p
(Contract N00014-89-J-1659; NSF DMS-88-00589)
(AD-A207403; SU-SOL-TR-89-2) Avail: NTIS HC A04/MF A01 CSCL 12/4

Semi-infinite programming, that allows for either infinitely many constraints or infinitely many variables but not both, is a natural extension of ordinary mathematical programming. There are many practical as well as theoretical problems in which the constraints depend on time or space and thus can be formulated as semi-infinite programs. The main results include: (1) An algorithm for solving a matrix rescaling problem formulated as a semi-infinite linear program; (2) An algorithm for solving a matrix estimation problem equivalent to a semi-infinite quadratic program; (3) A one-phase algorithm for solving a large class of semi-infinite linear programming problems; and (4) Applications of the above algorithm to convex programming. GRA

N89-27375# Carnegie-Mellon Univ., Pittsburgh, PA. Software Engineering Inst.
KERNEL USER'S MANUAL VERSION 1.0 Final Report
Judy Bamberger, Tim Coddington, Robert Firth, Daniel Klein, David Stinchcomb, and Roger VanScoy Feb. 1989 267 p
(Contract F19628-85-C-0003)
(AD-A207414; CMU/SEI-89-UG-1; ESD-TR-89-15) Avail: NTIS HC A12/MF A01 CSCL 12/7

This manual describes the models underlying the Kernel and its concept of operations, presents the primitives available to the application program, and provides a number of abstractions that may readily be built on top of Kernel primitives. The Kernel is a body of code that implements real-time facilities which can be invoked by applications written in Ada for execution on a distributed target. The requirements for the Kernel, both behavior and performance, are provided in the Kernel Facilities Definition, and its design will be provided in the forthcoming Kernel Architecture Model. The Kernel was built at the Software Engineering Institute by the Distributed Ada Real-Time Kernel (DARK) Project. Ada is now being mandated for a large number of DOD development projects as the sole programming language to be used for developing software. Many of these projects are trying to build distributed real-time systems. Many project managers and contractors are anxious to support this effort, to reap the advantages of Ada, and to use the newer techniques of software engineering that Ada can support. This tradition, however has not always been smooth; some serious problems have been encountered. GRA

N89-27376# Analytic Sciences Corp., Arlington, VA.
SDS SOFTWARE MEASUREMENT REQUIREMENTS Technical Report, 5 Dec. 1988 - 6 Apr. 1989
6 Apr. 1989 98 p Prepared in cooperation with SPARTA, Inc., Huntsville, AL and Teledyne Brown Engineering, Huntsville, AL
(Contract SDIO84-88-C-0018)
(AD-A207449; TASC-TR-9033-1) Avail: NTIS HC A05/MF A01 CSCL 12/5

This report addresses the criteria for evaluation of SDS software and measurement requirements by identifying the standards and attributes required for SDS software product sand the software development process. The identification of measurement requirements for SDS software was performed in three phases. The first phase was a review of standards and development process relevant to SDS, as they pertained to software metrics. The second phase was a detailed examination of SDS software characteristics, definition of software domains, and quality and productivity measurement requirements. The third phase integrated the measurement requirements identified previously into a methodology for the application of software metrics. GRA

N89-27377# Pittsburgh Univ., PA. Inst. for Computational Mathematics and Applications.
ON A COMPUTATIONAL METHOD FOR THE SECOND FUNDAMENTAL TENSOR AND ITS APPLICATION TO BIFURCATION PROBLEMS
Werner C. Rheinboldt and Patrick J. Rabier Feb. 1989 25 p
(Contract N00014-80-C-9455; NSF DCR-83-09926)
(AD-A207517; ICMA-89-131) Avail: NTIS HC A03/MF A01 CSCL 12/2

An algorithm is presented for the computation of the second fundamental tensor V of a Riemannian sub-manifold M of R superscript n. From V the Riemann curvature tensor of M is easily obtained. Moreover, V has a close relation to the second derivative of certain functionals on M which, in turn, provides a powerful new tool for the computational determination of multiple bifurcation directions. Frequently, in applications, the manifold M is defined implicitly as the zero set of a submersion F on R superscript n. In this case, the principal cost of algorithm for computing V (p) at a given point p an element of M involves only the decomposition of the Jacobian DF (p) of F at p and the projection of d(d+1) neighboring points onto M by means of a local iterative process using DF(p). Several numerical examples are given which show the efficiency and dependability of the method. GRA

N89-27378# Army Missile Command, Redstone Arsenal, AL. Research Directorate.
LOGNORMAL DISTRIBUTION MAXIMUM-LIKELIHOOD PARAMETER ESTIMATION ALGORITHMS Final Technical Report, Jun. 1988 - Jan. 1989
H. P. Dudel, C. E. Hall, Jr., and S. H. Lehnigk 1 Mar. 1989 43 p
(AD-A207586; AD-E951337; AMSMI/TR-RD-RE-89-1) Avail: NTIS HC A03/MF A01 CSCL 12/3

Microcomputer-based algorithms for lognormal distribution parameter estimation are presented. A program diskette will be made available upon request. For given data, the parameters (three or two) are estimated: (1) by means of the moments, and (2) by means of the maximum-likelihood principle. Maximum-likelihood estimation is done in two different ways: (1) by means of the derivative equations which result from the logarithmic likelihood function, and (2) by means of direct optimization of the logarithmic likelihood function itself. Moment estimates are used as starting values for the optimization process. GRA

N89-27379# Washington State Univ., Pullman.
RAPIDLY CONVERGENT ALGORITHMS FOR NONSMOOTH OPTIMIZATION Final Scientific Report, 15 Jul. 1983 - 14 Jun. 1988
Robert Mifflin 15 Dec. 1988 7 p
(Grant AF-AFOSR-0210-83; AF Proj. 2304)
(AD-A207629; AFOSR-89-0592TR) Avail: NTIS HC A02/MF A01 CSCL 12/4

The research supported by this grant has continued the development of efficient methods for solving optimization problems involving implicitly defined functions that are not everywhere differentiable. Research on a rapidly convergent algorithm for the constrained single variable case where generalized derivatives are known has been completed. Significant process has been made in extending this work to the n-variable case via the definition of better than linear convergence. Safeguarding techniques have been developed which ensure first order convergence on problems with semismooth functions, but do not prevent better than linear convergence on piecewise second order smooth functions. For the constrained case a scale-free automatic penalty technique has been devised. A new stable method for solving certain quadratic programming problems has been developed which includes a technique for resolving degeneracy. GRA

N89-27380# Instituto de Pesquisas Espaciais, Sao Paulo (Brazil).
CLASSIFICATION BY MAXIMUM LIKELIHOOD METHOD OF THE MASSIVELY PARALLEL ENVIRONMENT
Celso Luiz Mendes Dec. 1988 8 p In PORTUGUESE; ENGLISH summary Presented at the 5th Brazilian Symposium on Remote Sensing, Natal, RN, 11-15 Oct. 1988
(INPE-4765-PRE/1434) Avail: NTIS HC A02/MF A01

The theoretical basis for the problem of image classification by the maximum likelyhood method, is introduced according to statistical properties. It follows with some options, in terms of algorithms for implementing that operation. The development of a parallel system to perform that procedure in an efficient way is suggested, as opposed to the conventional serial approach. After describing an available parallel processor (Gapp), a massively parallel architecture currently being developed at INPE/DPI is presented, with an array of 48 x 48 processing elements and the main control in a general purpose microcomputer. The work is concluded with some comments related to the expected speed of this system. Author

N89-27381# Instituto de Pesquisas Espaciais, Sao Jose dos Campos (Brazil).
ABSTRACT DATA TYPES IN COMPUTER GRAPHICS AND IMAGE PROCESSING [TIPOS ABSTRATOS DE DADOS EM COMPUTACAO GRAFICA E PROCESSAMENTO DE IMAGENS]
Gilberto CamaraNeto, Joao Ricardo deFreitasOliveira, Fernando Ytaka Yamaguchi, Flavio Roberto DiasVelasco, and Ricardo Cartaxo ModestodeSouza Dec. 1988 14 p In PORTUGUESE;

ENGLISH summary Presented at the 2nd Brazilian Symposium on Software Engineering, Canela, RS, 27-28 Oct. 1988
(INPE-4745-PRE/1419) Avail: NTIS HC A03/MF A01

The use of abstract data types on software development is presented for applications in the areas of Computer Graphics and Image Processing. An analysis of the general characteristics of software development in this area is made, and some examples given. A project methodology for these areas is also proposed, using abstract data types. Finally, a design example on the development of a GKS standard using data abstractions is given. Author

N89-27382# Instituto de Pesquisas Espaciais, Sao Jose dos Campos (Brazil).
AUTOMATIC TREATMENT OF NATURAL LANGUAGE IN PROCESSES IN THE ACQUISTION OF KNOWLEDGE [O TRATAMENTO AUTOMATICO DE LINGUAGEM NATURAL EM PROCESSOS DE AQUISICAO DE CONHECIMENTO]
Carlos AlbertodeOliveira Nov. 1988 16 p In PORTUGUESE; ENGLISH summary Presented at the 5th Brazilian Symposium on Artificial Intelligence, Natal, RN, 7-11 Nov. 1988
(INPE-4737-PRE/1412) Avail: NTIS HC A03/MF A01

An approach for natural language processing based on textual knowledge is presented. In this way, any natural language interface must consult users' linguistic knowledge through a dynamic interactive process, in order to build the particular linguistic universe of an application domain. Author

N89-27383# Los Alamos National Lab., NM. Center for Nonlinear Studies.
THE DYNAMICAL BEHAVIOR OF CLASSIFIER SYSTEMS
Stephanie Forrest and John H. Miller 10 Feb. 1989 18 p Presented at the 3rd International Conference on Genetic Algorithms, Washington, DC, 4-7 Jun. 1989
(Contract W-7405-eng-36)
(DE89-009407; LA-UR-89-760; CONF-890693-1) Avail: NTIS HC A03/MF A01

Classifier systems are quite complicated, in terms of both their components and behavior. This complexity is understandable given the wide spectrum of activity they are intended to model. Unfortunately, the complexity of these systems also makes it difficult to understand them analytically. Previous analysis has focused on specific components of the classifier system, for example, the genetic algorithm or the bucket brigade. The lack of a unified theory has led users of these systems to rely on ad hoc methods for choosing representations and parameter settings. Recent results (Riolo, 1988) indicate that classifier systems can be very sensitive to particular encodings and parameter choices. In this paper, we propose a methodology for studying the interactions among various components of the classifier system architecture. DOE

N89-27384# Oak Ridge National Lab., TN. Mathematical Sciences Section.
A THEORETICAL INVESTIGATION OF A PARALLEL GENETIC ALGORITHM
Chrisila C. Pettey (Vanderbilt Univ., Nashville, TN.) and Michael R. Leuze 1989 13 p Presented at the 3rd International Conference on Genetic Algorithms, Washington, DC, 4 Jun. 1989
(Contract DE-AC05-84OR-21400)
(DE89-012508; CONF-890693-2) Avail: NTIS HC A03/MF A01

In the past few years the limitations of uniprocessor computing systems and the increasing availability of multiprocessors have led to investigations of parallel genetic algorithms. One algorithm in particular, called PGA, consists of a set of communicating sequential genetic algorithms. This paper includes an investigation of the theoretical allocation of trials to schemata by PGA's in general and by a particular PGA (which performs communication in a uniformly random manner) along with an experimental validation of an assumption made in the theoretical investigation. DOE

N89-27385# Instituto de Pesquisas Espaciais, Sao Paulo (Brazil). Dept. de Processamento de Imagens.
IMPLEMENTATION OF AN ORDER FILTER AND ITS APPLICATIONS IN RADAR IMAGERY (SAR)
Sueli Pissarra Castellari and Luciano Vieira Dutra Dec. 1988 11 p In PORTUGUESE; ENGLISH summary Presented at the 5th Brazilian Symposium on Remote Sensing, Natal, RN, 11-15 Oct. 1988
(INPE-4749-PRE/1422) Avail: NTIS HC A03/MF A01

The development of an order statistics filter, which selects the kth element in a sorted list of pixels derived from a pixel neighborhood is described. It is possible to combine this filter in two ways: by a weighted means of pixel values or by a weighted means of log pixel values followed by a exponentiation operation (homomorphic combination). The order filter has application in feature extraction, mathematical morphology and noise reduction. In particular, for radar images, the homomorphic combination has a suitable application due to the multiplicative nature of the speckle noise of these images. In this work the results of speckle noise reduction are presented with recursive and non-recursive median filtering (a particular case of order filter), using a SAR580 image. Also, we present a method for border detection in radar images using recursive filtering followed by a linear combination of filter outputs. Author

N89-27386# Lawrence Livermore National Lab., CA. Computing and Mathematics Research Div.
MONOTONE PIECEWISE CUBIC DATA FITTING
Frederick N. Fritsch Jul. 1988 10 p Presented at the 2nd Shrivenham International Conference on Algorithms for Approximation, Shrivenham, United Kingdom, 12-15 Jul. 1988
(Contract W-7405-eng-48)
(DE89-006742; UCRL-98149; CONF-890742-1) Avail: NTIS HC A02

PCHLS, an algorithm for least squares fitting of a monotone piecewise cubic function to data is described. It extends the piecewise cubic Hermite interpolation package PCHIP to situations in which the data are noisy or are adequately represented by far fewer cubic pieces than data points. DOE

N89-27387# Stanford Univ., CA. Systems Optimization Lab.
AN EFFICIENT EXACT ALGORITHM FOR THE LEAST SQUARES IMAGE REGISTRATION PROBLEMS
Karel Zikan May 1989 16 p
(Contract DE-FG03-87ER-25028)
(DE89-013116; SU-SOL-89-5) Avail: NTIS HC A03/MF A01

Image registration involves estimating how one set of n-dimensional points is rotated, scaled, and translates into a second set of n-dimensional points. In practice, n is usually 2 or 3. We give an exact algorithm to solve the least-squares formulation of the two-dimensional registration problem. The algorithm, which is based on parametric linear programming, can be viewed as a refinement of the $O(k^3)$ approximation method proposed by Zikan and Silberburg. The approach can be extended to handle registration of images of different cardinalities. DOE

N89-27388# Los Alamos National Lab., NM. Computing and Communications Div.
XCL: A FAMILY OF PROGRAMMING LANQUAGE-BASED SHELL S
Mark A. Roschke 1989 5 p Presented at the Cray User's Group Conference, Los Angeles, CA, 24-28 Apr. 1989
(Contract W-7405-eng-36)
(DE89-013442; LA-UR-89-1693; CONF-8904210-5) Avail: NTIS HC A02/MF A01

As the three major UNIX shells have emerged, they have shown little inclination to include syntax and semantics from existing programming languages. The first of these shells, sh, contains only a small amount of C-like syntax. Csh provides some C language expression syntax, but includes very little other C syntax. The newest of these shells, ksh, also includes some C-like expression syntax, although they contain some significantly un-C-like syntax in such areas as relational and logical operators.

Several much less widely used shells have been written that much more closely resemble particular programming languages. However, each of these shells have the disadvantage of not being based upon a widely used programming language. In addition, interactive commands tend to be difficult to enter because they must frequently be entered using normal programming language constructs such as function calls. Thus, the vast majority of programmers of today's UNIX shells must deal with a shell interface that is not based upon any familiar programming language. This paper describes some of the features of the xcl family of shells. Each of these shells is based closely upon an existing programming language and provides the user with a familiar and highly programmable shell interface. DOE

N89-27389# National Inst. of Standards and Technology, Gaithersburg, MD. Advanced Systems Div.
SMALL COMPUTER SYSTEM INTERFACE (SCSI) COMMAND SYSTEM: SOFTWARE SUPPORT FOR CONTROL OF SMALL COMPUTER SYSTEM INTERFACE DEVICES
John Gorczyca Jan. 1989 125 p
(PB89-151815; NISTIR-89/4023) Avail: NTIS HC A06/MF A01 CSCL 09B

The Small Computer System Interface (SCSI) Command System was created for the control of SCSI host adapter. The Command Interfacing Function permits all SCSI standard and manufacturer commands to be sent to external devices. The system allows two levels of user programming. The upper and lower levels offer the ability to utilize libraries of commands, and the ability to edit system parameters and commands directly by using the system's variables. Programming for the system is done in the C language. Also included with the documentation are references, which provide additional information. GRA

N89-27390*# Institute for Computer Applications in Science and Engineering, Hampton, VA.
INDIRECT ADDRESSING AND LOAD BALANCING FOR FASTER SOLUTION TO MANDELBROT SET ON SIMD ARCHITECTURES Final Report
Sherryl Tomboulian (MasPar Computer Corp., Santa Clara, CA.) May 1989 11 p
(Contract NAS1-18605)
(NASA-CR-181847; NAS 1.26:181847; ICASE-89-33) Avail: NTIS HC A03/MF A01 CSCL 09B

SIMD computers with local indirect addressing allow programs to have queues and buffers, making certain kinds of problems much more efficient. Examined here are a class of problems characterized by computations on data points where the computation is identical, but the convergence rate is data dependent. Normally, in this situation, the algorithm time is governed by the maximum number of iterations required by each point. Using indirect addressing allows a processor to proceed to the next data point when it is done, reducing the overall number of iterations required to approach the mean convergence rate when a sufficiently large problem set is solved. Load balancing techniques can be applied for additional performance improvement. Simulations of this technique applied to solving Mandelbrot Sets indicate significant performance gains. Author

N89-27391# Instituto de Pesquisas Espaciais, Itajuba (Brazil).
AN APPLE-2 COMPATIBLE PROGRAM TO DRAW MAPS CONTAINING OCEANOGRAPHIC STATION POSITIONS BUOY TRAJECTORIES AND THE COASTAL MARGINS OF THE ANTARCTIC PENINSULA AND NEARBY ISLANDS
Merritt R. Stevenson and Ronald BussdeSouza Apr. 1989 49 p
(Proj. MEDICA-9571)
(INPE-4805-RPE/588) Avail: NTIS HC A03/MF A01

Continued progress in Project MEDICA (Measurements of the Antarctic Current) in the Brazilian Antarctic Program (PROANTAR) indicated the need to develop a computer program for the graphical presentation of the Antarctic Peninsula. The program was developed for the project's System for Acquisition/Processing of Oceanographic Data (SADOC). The program (PL. ANTARTICA) was written for an APPLE-2+ microcomputer and uses approximately 44 kilobytes of computer memory. The coastal margins of the Antarctic Peninsula and nearby islands were digitized from nautical maps and form a data base within the program. The program has zoom and translational capability, that is the user specified the desired scale amplification and the geographic centerpoint of the modified mercator map. After the user specifies these two parameters, the computer: (1) draws and scales the margins of the map; (2) draws the outline of the relevant parts of the Peninsula and islands within the map's margins; (3) plots oceanographic station positions if desired; (4) draws trajectories of one or more drifting buoys if desired; (5) plots any other positions desired; and (6) draws one of three symbols (+, x, delta) at any of the station and trajectory positions if desired. Figures are used to illustrate some of the graphical options. Author

N89-27392# Instituto de Pesquisas Espaciais, Sao Paulo (Brazil). Dept. de Processamento de Imagens.
APPLICATIONS OF NUMERICAL MODELS FOR ELEVATION AND INTEGRATION WITH DIGITAL IMAGES
Carlos Alberto Felgueiras and Guaraci Jose Erthal Dec. 1988 8 p In PORTUGUESE; ENGLISH summary Presented at the 5th Brazilian Symposium on Remote Sensing, Natal, RN, 11-15 Oct. 1988
(INPE-4776-PRE/1445) Avail: NTIS HC A02/MF A01

The main aims are: to show the definition, creation and use concepts of Digital Elevation Models (DEM's); and to describe and analyze the DEM applications and their integration with digital images. Author

N89-27393*# Titan Systems, Inc., La Jolla, CA.
RULE-BASED AIR COMBAT SIMULATION Final Report
G. H. Burgin and L. B. Sidor Washington Sep. 1988 138 p
(Contract NAS2-11990)
(NASA-CR-4160; H-1501; NAS 1.26:4160) Avail: NTIS HC A07/MF A01 CSCL 09B

An improved version of the Adaptive Maneuvering Logic (AML) program for air-combat maneuvering is discussed. The modifications and improvements incorporated into the AML program are documented. Author

N89-27394# Oak Ridge National Lab., TN.
A VIRTUAL ZERO-TIME, MONOLITHIC SYSTOLIC SORTING ARRAY
C. L. Britton, M. N. Ericson, and D. W. Bouldin (Tennessee Univ., Knoxville.) 1989 12 p Presented at the VLSI Education Conference and Exposition, Santa Clara, CA, 19 Jul. 1989
(Contract DE-AC05-84OR-21400)
(DE89-007515; CONF-890744-2) Avail: NTIS HC A03/MF A01

A virtual zero-time monolithic sorting chip is described. The chip has a systolic array architecture and implements the sinking sort algorithm. The basic functional module of the systolic array is detailed and development techniques employed. Functional simulation and results are presented. Lessons learned and educational significance of the development of this chip at a university are discussed. DOE

N89-27395# Sandia National Labs., Albuquerque, NM. Geotechnical Research Div.
ASR4: A COMPUTER CODE FOR FITTING AND PROCESSING 4-GAGE ANELASTIC STRAIN RECOVERY DATA
N. R. Warpinski May 1989 55 p
(Contract DE-AC04-76DP-00789)
(DE89-012239; SAND-89-0484) Avail: NTIS HC A04/MF A01

A computer code for analyzing four-gage Anelastic Strain Recovery (ASR) data has been modified for use on a personal computer. This code fits the viscoelastic model of Warpinski and Teufel to measured ASR data, calculates the stress orientation directly, and computes stress magnitudes if sufficient input data are available. The code also calculates the stress orientation using strain-rosette equations, and it calculates stress magnitudes using Blanton's approach, assuming sufficient input data are available. The program is written in FORTRAN, compiled with

Ryan-McFarland Version 2.4. Graphics use PLOT88 software by Plotworks, Inc., but the graphics software must be obtained by the user because of licensing restrictions. A version without graphics can also be run. This code is available through the National Energy Software Center (NESC), operated by Argonne National Laboratory. DOE

N89-27396# Oak Ridge National Lab., TN. Engineering Technology Div.
ORMONTE: AN UNCERTAINTY ANALYSIS CODE FOR USE WITH USER-DEVELOPED SYSTEMS MODELS ON MAINFRAME OR PERSONAL COMPUTERS. A USER'S GUIDE
K. A. Williams and C. R. Hudson, II May 1989 190 p
(Contract DE-AC05-84OR-21400)
(DE89-013730; ORNL/TM-10714) Avail: NTIS HC A09/MF A01

Documentation is provided for a general purpose uncertainty analysis code entitled ORMONTE. The code is intended to be linked with FORTRAN-77 models designed by the user. ORMONTE is capable of performing sequential single-variable sensitivity studies (SVSS), elasticity analyses, and multivariable sensitivity studies (MVSS) by acting as a driver on the user's model. The MVSS function utilizes the Monte Carlo simulation method of probabilistic analysis. The model accessed by the ORMONTE driver code and the names and characteristics of the modeler's uncertain variables are provided by the user. ORMONTE is essentially a bookkeeping code which keeps track of inputs and outputs defined by the user, samples the user-defined uncertainty distributions, repeatedly runs the user's model, and produces statistical data and output probability histograms for the output variables of interest to the user. ORMONTE has been utilized extensively by the USDOE and its Oak Ridge contractors, Martin Marietta Energy Systems Inc., and its predecessor, Union Carbide Corp.; Nuclear Division, for the economic evaluation of large-scale energy projects for which computer models have been constructed for performance and cost projection purposes. DOE

N89-27397# Oak Ridge National Lab., TN. Engineering Physics and Mathematics Div.
A SYMBOLIC GENERATOR OF STATE EQUATIONS FOR MODELING OF DYNAMIC SYSTEMS BASED ON THE ELECTRICAL NETWORK ANALOG PARADIGM
Eduardo V. Depiante Mar. 1989 38 p
(Contract DE-AC05-84OR-21400)
(DE89-013763; ORNL/TM-10979) Avail: NTIS HC A03/MF A01

The capability of automatically generating state equations for a given system is a desirable component of an integrated environment for system control and simulation studies. A step towards the development of this capability is described in the following sections. Section 2 presents the statement of the problem to be solved. Since the solution approach involves the use of circuit analogs, topology concepts are required; these are presented in Section 3. The governing network equations and different network formulations are given in Section 4. The problem of systematically formulating the state equations is the topic of Section 5. A program (SEQS) developed to automatically generate the state equations is described in Section 6 and its application is illustrated in Section 7. Section 8 contains the conclusions. Appendix A gives a listing of the SEQS program and Appendix B gives a sample input file for the SEQS program. DOE

N89-27398# Sandia National Labs., Albuquerque, NM. Photovoltaic Cell Research Div.
ELLIPSE USER'S MANUAL AND PROGRAM REFERENCE
Herbert L. Tardy Mar. 1989 129 p
(Contract DE-AC04-76DP-00789)
(DE89-014575; SAND-89-0008) Avail: NTIS HC A07/MF A01

A new program, ELLIPSE, for the analysis of ellipsometric data is described. The program is interactive and includes on-line help, performs explicit error analysis for single angle-of-incidence measurements, allows the input of four-zone null data, and performs least-squares analysis of multiple angle-of-incidence data. Solutions for the transparent-film-on-substrate model are obtained using decoupled equations for film thickness and index. No initial guess is required for thickness, and the algorithm is insensitive to the initial guess for film index. This document combines the user's manual and program description for ELLIPSE, and includes several examples of its use. DOE

N89-27399# Argonne National Lab., IL.
PORTABLE PARALLEL PROGRAMMING IN A FORTRAN ENVIRONMENT
Edward N. May 1989 16 p Presented at the Conference on Computing in High Energy Physics, Oxford, United Kingdom, 10-14 Apr. 1989
(Contract W-31-109-eng-38)
(DE89-014670; ANL-HEP-CP-89-50; CONF-890415-3) Avail: NTIS HC A03/MF A01

Experience using the Argonne-developed PARMACs macro package to implement a portable parallel programming environment is described. FORTRAN programs with intrinsic parallelism of coarse and medium granularity are easily converted to parallel programs which are portable among a number of commercially available parallel processors in the class of shared-memory bus-based and local-memory network based MIMD processors. The parallelism is implemented using standard UNIX(TM) tools and a small number of easily understood synchronization concepts (monitors and message-passing techniques) to construct and coordinate multiple cooperating processes on one or many processors. Benchmark results are presented for parallel computers such as the Alliant FX/8, the Encore MultiMax, the Sequent Balance, the Intel iPSC/2 Hypercube and a network of Sun 3 workstations. These parallel machines are typical MIMD types with from 8 to 30 processors, each rated at from 1 to 10 MIPS processing power. The demonstration code used for this work is a Monte Carlo simulation of the response to photons of a nearly realistic lead, iron and plastic electromagnetic and hadronic calorimeter, using the EGS4 code system. DOE

N89-27400# Fermi National Accelerator Lab., Batavia, IL. Theoretical Physics Group.
MACHINES FOR LATTICE GAUGE THEORY
Paul B. Mackenzie May 1989 15 p Presented at the Conference on Computing in High Energy Physics, Oxford, United Kingdom, 10-14 Aug. 1989
(Contract DE-AC02-76CH-03000)
(DE89-014815; FNAL/C-89/125-T; CONF-890415-5) Avail: NTIS HC A03/MF A01

The most promising approach to the solution of the theory of strong interactions is large scale numerical simulation using the techniques of lattice gauge theory. At the present time, computing requirements for convincing calculations of the properties of hadrons exceed the capabilities of even the most powerful commercial supercomputers. This has led to the development of massively parallel computers dedicated to lattice gauge theory. This talk will discuss the computing requirements behind these machines, and general features of the components and architectures of the half dozen major projects now in existence. DOE

N89-27401# Universiteit Twente, Enschede (Netherlands). Dept. of Computer Science.
PROCESSOR CONTROL PATH SYNTHESIS: LITERATURE SURVEY AND PRELIMINARY ANALYSIS
A. J. W. M. tenBerg 26 Oct. 1988 49 p
(MEMO-INF-88-46; ISBN-90-365-0216-0; ETN-89-94764) Avail: NTIS HC A03/MF A01

The literature related to control path synthesis is surveyed in order to get an idea about the state of the art and of the unaddressed problems at this moment. ESA

N89-27402# Universiteit Twente, Enschede (Netherlands). Dept. of Computer Science.
AUTOMATIC GENERATION OF FORTRAN-CODED JACOBIANS AND HESSIANS

P. vandenHeuvel, J. A. vanHulzen, and V. V. Goldman Nov. 1988 17 p Supercedes MEMO-INF-87-4 Submitted for publication
(MEMO-INF-88-47; MEMO-INF-87-4; ETN-89-94765) Avail: NTIS HC A03/MF A01

A package for automatically generating efficient FORTRAN code for calculating Jacobians and Hessians is presented. It is used in combination with Gentran, a code generation and translation package for translating LISP code into FORTRAN and for template processing. ESA

N89-27403# Universiteit Twente, Enschede (Netherlands). Dept. of Computer Science.
AN OVERVIEW OF SOME METHODS FOR THE HIGH-LEVEL SPECIFICATION OF SYNCHRONIZATION
J. J. Luursema Nov. 1988 23 p
(MEMO-INF-88-50; ISBN-90-365-0223-3; ETN-89-94768) Avail: NTIS HC A03/MF A01

Approaches developed for experimental languages and parallelism or synchronization notations are presented. The synchronized actions are treated as abstract objects and can be assimilated to the operations offered by a resource, or the commands for a command shell. Synchronization includes subjects like mutual exclusion, parallelism and sequencing. Languages discussed include path expressions, process algebra methods, temporal logic based methods, and finite automata based methods. ESA

N89-27404# Virginia Polytechnic Inst. and State Univ., Blacksburg. Interdisciplinary Center for Applied Mathematics.
MODELING AND COMPUTATIONAL ALGORITHMS FOR PARAMETER ESTIMATION AND OPTIMAL CONTROL OF AEROELASTIC SYSTEMS AND LARGE FLEXIBLE STRUCTURES Final Report, 30 Sep. 1985 - 30 Sep. 1988
John A. Burns and Eugene M. Cliff 15 Feb. 1989 14 p
(Grant AF-AFOSR-0287-85; AF Proj. 2304)
(AD-A208274; AFOSR-89-0600TR) Avail: NTIS HC A03/MF A01 CSCL 20/4

The basic goal of this project is the study of computational algorithms for control design of partial functional differential equations that model structural and fluid dynamic systems. We investigated several aspects of the development of computational algorithms for identification and control of distributed parameter systems. We also spent considerable effort on specific applications involving elastic, aeroelastic and viscoelastic systems. Progress was made on many of these problems. However, in this report we shall concentrate on the major accomplishments. GRA

N89-27405# Georgia Inst. of Tech., Atlanta.
FAULT TOLERANT SOFTWARE TECHNOLOGY FOR DISTRIBUTED COMPUTER SYSTEMS Final Technical Report, Feb. 1986 - Feb. 1988
Richard J. LeBlanc Mar. 1989 74 p
(Contract F30602-86-C-0032; AF Proj. 5581)
(AD-A208329; RADC-TR-88-296) Avail: NTIS HC A04/MF A01 CSCL 12/5

Work performed by the CLOUDS project at Georgia Institute of Technology to address the methodologies for fault tolerant software design and implementation in an object-oriented distributed operating system is summarized. The major research results are contained in two companion guide book reports resulting from this effort entitled, Action Based Programming for Embedded Systems and Programming Techniques for Resilience and Availability. The information in this report provides an overview of the major aspects of the system and identifies the major issues which are considered in detail in the guidebooks. GRA

N89-27406# Naval Postgraduate School, Monterey, CA.
A LANGUAGE TRANSLATOR FOR A COMPUTER AIDED RAPID PROTOTYPING SYSTEM Annual Report, Sep. 1987 - Aug. 1988 M.S. Thesis
Charlie Robert Moffitt, II Sep. 1988 119 p
(AD-A208358; NPS52-88-021) Avail: NTIS HC A06/MF A01 CSCL 12/5

While the cost of computing hardware has decreased steadily, the cost of software design, development and, maintenance has increased. One approach to reduce the cost of software development is rapid prototyping. Further, it has been proposed to combine the design strategy of rapid prototyping with a computer aided software prototyping system. Such a system would allow the software designer to employ a software base of reusable program modules. It would assist in prototyping and would automate a large part of the development effort. An important component of the automation would be a language translator facility. This translator would allow the designer to develop a software prototype in a high level specification language which would be simple and convenient to use and would translate the specification statements into an executable software language. This thesis demonstrates the feasibility of using a language translator by developing a prototype translator for a computer aided software prototyping system. The translator is written in Attribute Grammar (AG) language and translates software specifications stated in the Prototype System Description Language (PSDL) into computer executable code in the Ada language. GRA

N89-27407# Naval Postgraduate School, Monterey, CA.
A DYNAMIC SCHEDULER FOR A COMPUTER AIDED PROTOTYPING SYSTEM Annual Report, Sep. 1987 - Aug. 1988 M.S. Thesis
Susan L. Eaton Sep. 1988 61 p
(AD-A208389; NPS52-88-019) Avail: NTIS HC A04/MF A01 CSCL 12/5

Current software development methodologies have proven to be ineffective for meeting the rising demand for fast production of reliable software for hard real-time computer systems. A computer-aided, rapid prototyping system (CAPS) based on a Prototype System Description Language (PSDL) and a set of software tools including an Execution Support System (ESS), has been proposed by other research and provides a promising and cost effective alternative to the traditional development life cycle of these systems. This study proposes a four function design for the dynamic scheduler of the CAPS ESS. This design includes a method for invoking processed for the ESS static scheduler and translator, a scheduling algorithm for the scheduling of the prototype's non-time critical processes, and a method for error and interrupt handling during prototype execution. GRA

N89-27408# Air Force Inst. of Tech., Wright-Patterson AFB, OH.
SOFTWARE MANAGEMENT INDICATORS: MANAGING THE RISK OF PROJECT MANAGEMENT M.S. Thesis
Court C. Allen 1989 78 p
(AD-A208443; AFIT/CI/CIA-88-216) Avail: NTIS HC A05/MF A01 CSCL 05/1

Managing software projects continues to be a high risk activity. Projects often end up out of control and result in cost and time overruns. Projects could be better managed if managers were forewarned that a project may be out of control before it is actually out of control. With advance notice of changing risk factors, project managers can take appropriate action to bring the project back on track and reduce project management risk's impact. To create this early warning system, an effort to develop a suite of software management indicators has been evolving. Software management indicators are equivalent that predict project development process quality or health. This will allow managers to manage risk associated with software development efforts. Software management indicators will be discussed and explained. Since much of this work has been done by government contractors in the United States, the focus will be to explain the use of methods developed in this environment. Exploration of experiences with these indicators will be shared. Qualitative research done by querying promoters and users of these techniques will explain what software management indicators are, why they should be used, when they are appropriate, and implementation hurdles that need to be cleared. GRA

N89-27409# Air Force Flight Dynamics Lab., Wright-Patterson AFB, OH.
A COMPOUND SCALING ALGORITHM FOR MATHEMATICAL OPTIMIZATION Final Report, Nov. 1988 - Feb. 1989
Vipperla B. Venkayya and Victoria A. Tischler Feb. 1989 53 p
(AD-A208446; WRDC-TR-89-3040) Avail: NTIS HC A04/MF A01 CSCL 12/1

A compound scaling algorithm is derived from a single scaling algorithm for use with general mathematical optimization problems. Compound scaling is necessary when the constraints are nonlinear and the variables do not all belong to the active set. Compound scaling in conjunction with the optimality criteria method has practical applications in large scaled multidisciplinary design. It will extend the scope of the optimality criteria method to handle problems with thousands of variables and constraints. The development of simple scaling is included as a basis for the development of the compound scaling algorithm. Five problems were selected to demonstrate the effectiveness of the simple and compound scaling algorithms. GRA

N89-27410# Naval Postgraduate School, Monterey, CA.
ALGORITHMS FOR COMPUTER AIDED DESIGN OF DIGITAL FILTERS M.S. Thesis
Thomas H. Rich Dec. 1988 53 p
(AD-A208485) Avail: NTIS HC A04/MF A01 CSCL 12/5

The algorithms necessary for the computer aided design of digital filters from lowpass prototypes has been developed and compared, then implemented in a computer program to aid in the instruction of digital filter design. The procedure for the design of lowpass, highpass, bandpass, and bandstop digital filters from lowpass prototypes is well established, and is based on transforming the prototype frequency response to meet desired characteristics. This transformation can be accomplished in either the analog (s) domain or the digital (z) domain. Therefore, the two classical design techniques, analog-digital and digital-digital design, are based on doing the frequency response transformations in their respective analog or digital domains. Since the theory for the standard filter types (Butterworth, Chebyshev, and elliptic) is developed in the analog or (s) domain, the two methods for designing digital filters differ basically in the sequence of the design steps. In the analog-digital method the analog prototype is transformed and then digitized, while in the digital-digital method the analog prototype is digitized and then transformed. GRA

62 COMPUTER SYSTEMS

Includes computer networks and special application computer systems.

N89-27411# Stanford Univ., CA. Dept. of Computer Science.
SUITABILITY OF MESSAGE PASSING COMPUTERS FOR IMPLEMENTING PRODUCTION SYSTEMS
Anoop Gupta and Milind Tambe (Carnegie-Mellon Univ., Pittsburgh, PA.) 1988 6 p
(Contract N00014-87-K-0828; ARPA Order 4976)
(AD-A207321) Avail: NTIS HC A02/MF A01 CSCL 12/5

Two important parallel architecture types are the shared-memory architectures and the message-passing architectures. In the past researchers working on the parallel implementations of production systems have focussed either on shared-memory multiprocessors or on special purpose architectures. Message-passing computers have not been studied. The main reasons have been the large message-passing latency (as large as a few milliseconds) and high message reception overheads (several hundred microseconds) exhibited by the first generation message-passing computers. These overheads are too large for the parallel implementation of production systems, where it is necessary to exploit parallelism at a very fine granularity to obtain significant speed-up (subtasks execute about 100 machine instructions). GRA

N89-27412# Technische Hogeschool, Delft (Netherlands). Dept. of Mathematics and Informatics Computer Science.
PERFORMANCE ANALYSIS OF DATA-DRIVEN NETWORKS
Geert Jan Olsder 1988 25 p
(PB89-170906; Rept-88-84) Copyright Avail: NTIS HC A03/MF A01 CSCL 09B

A method is presented which calculates the performance or throughput rate of wavefront array processors. The processing times of the individual processing elements are assumed to depend on the input data. The underlying mathematics is the theory of stochastic discrete event dynamic systems. GRA

N89-27413*# Draper (Charles Stark) Lab., Inc., Cambridge, MA.
ADVANCED INFORMATION PROCESSING SYSTEM: INPUT/OUTPUT SYSTEM SERVICES
Tom Masotto and Linda Alger Aug. 1989 186 p
(Contract NAS1-18565)
(NASA-CR-181874; NAS 1.26:181874) Avail: NTIS HC A09/MF A01 CSCL 09B

The functional requirements and detailed specifications for the Input/Output (I/O) Systems Services of the Advanced Information Processing System (AIPS) are discussed. The introductory section is provided to outline the overall architecture and functional requirements of the AIPS system. Section 1.1 gives a brief overview of the AIPS architecture as well as a detailed description of the AIPS fault tolerant network architecture, while section 1.2 provides an introduction to the AIPS systems software. Sections 2 and 3 describe the functional requirements and design and detailed specifications of the I/O User Interface and Communications Management modules of the I/O System Services, respectively. Section 4 illustrates the use of the I/O System Services, while Section 5 concludes with a summary of results and suggestions for future work in this area. Author

N89-27414# Universiteit Twente, Enschede (Netherlands). Dept. of Computer Science.
AUTOMATIC CODE VECTORIZATION OF ARITHEMETIC EXPRESSIONS BY BOTTOM-UP STRUCTURE RECOGNITION
V. V. Goldman and J. A. vanHulzen Nov. 1988 14 p Presented at the CAP '88 1st International Workshop on Computer Algebra and Parallelism, Grenoble, France, 29 Jun. - 1 Jul. 1989
(MEMO-INF-88-48; ETN-89-94766) Avail: NTIS HC A03/MF A01

A bottom-up structure for vectorizing or parallelizing scalar code typically generated by computer algebra processing is proposed. An example is worked out, and issues are discussed including the fact that vectorized code will not necessarily speed up the computation due to start-up overheads associated with small vectors. ESA

63 CYBERNETICS

Includes feedback and control theory, artificial intelligence, robotics and expert systems.

For related information see also *54 Man/System Technology and Life Support.*

N89-27415# Oak Ridge National Lab., TN. Center for Engineering Systems Advanced Research.
AUTONOMOUS DISCOVERY AND LEARNING BY A MOBILE ROBOT IN UNSTRUCTURED ENVIRONMENTS
Francois G. Pin, Gerard deSaussure, Philip F. Spelt, D. L. Barnett, S. M. Killough (Martin Marietta Energy Systems, Inc., Oak Ridge, TN.), and C. R. Weisbin 1988 15 p Presented at the International Conference on Robotics and Automation, Scottsdale, AZ, 14-19 May 1989
(Contract DE-AC05-84OR-21400)
(DE89-001525; CONF-890522-2) Avail: NTIS HC A03/MF A01

This paper presents recent research activities at the Center for Engineering Systems Advanced Research (CESAR) in the area of autonomous discovery and learning of emergency and maintenance tasks in unstructured environments by a mobile robot.

The methodologies for learning basic operating principles of control devices, and for using the acquired knowledge to solve new problems with conditions not encountered before are presented. The algorithms necessary for the robot to discover problem-solving sequences of actions, through experimentation with the environment, in the two cases of immediate feedback and delayed feedback are described. The inferencing schemes allowing the robot to classify the information acquired from a reduced set of examples and to generalize its knowledge to a much wider problem-solving domain are also provided. A demonstration of the successful implementation of the algorithms on our HERMIES-IIB autonomous robot is then presented. DOE

N89-27416*# Integrated Systems, Inc., Palo Alto, CA.
AIRCRAFT FLIGHT TEST TRAJECTORY CONTROL Final Report
P. K. A. Menon and R. A. Walker Washington Sep. 1988 198 p
(Contract NAS2-11877)
(NASA-CR-4161; H-1497; NAS 1.26:4161) Avail: NTIS HC A09/MF A01 CSCL 09B

Two control law design techniques are compared and the performance of the resulting controllers evaluated. The design requirement is for a flight test trajectory controller (FTTC) capable of closed-loop, outer-loop control of an F-15 aircraft performing high-quality research flight test maneuvers. The maneuver modeling, linearization, and design methodologies utilized in this research, are detailed. The results of applying these FTTCs to a nonlinear F-15 simulation are presented. Author

N89-27417# Syracuse Univ., NY.
NORTHEAST ARTIFICIAL INTELLIGENCE CONSORTIUM: VOLUME 2, PART A: THE VERSATILE MAINTENANCE EXPERT SYSTEM (VMES) RESEARCH PROJECT Annual Report, Dec. 1986 - Dec. 1987
Stuart C. Shapiro and Sargur N. Srihari Mar. 1989 85 p
(Contract F30602-85-C-0008)
(AD-A208344; RADC-TR-88-324-Vol-2-Pt-A) Avail: NTIS HC A05/MF A01 CSCL 12/7

The Northeast Artificial Intelligence Consortium (NAIC) whose purpose is to conduct pertinent research in artificial intelligence and to perform activities ancillary to this research is discussed. This report describes progress that was made in the third year of the Consortium on the Versatile Maintenance Expert System research task. Technical areas addressed include device representation, modelling of connections, and interactions between logical and physical models. Investigation of analog components and differing levels of diagnosis was also initiated. Research on the Versatile Maintenance Expert System (VMES) project is concerned with issues in the development of a system that could diagnose faults in an electronic circuit and interact with a maintenance technician. During 1987 our research on this project had two distinct but overlapping phases: consolidation of work done during the previous two years and developing new directions of research. GRA

N89-27418# Northeast Artificial Intelligence Consortium, Syracuse, NY.
NORTHEAST ARTIFICIAL INTELLIGENCE CONSORTIUM ANNUAL REPORT 1987. VOLUME 2, PART B: DISCUSSING, USING, AND RECOGNIZING PLANS Interim Report, Dec. 1986 - Dec. 1987
Stuart C. Shapiro and Beverly Woolf (Massachusetts Univ., Amherst.) Mar. 1989 224 p
(Contract F30602-85-C-0008; AF Proj. 5581)
(AD-A208378; RADC-TR-88-324-Vol-2-Pt-B) Avail: NTIS HC A10/MF A01 CSCL 12/9

The Northeast Artificial Intelligence Consortium (NAIC) was created to conduct pertinent research in artificial intelligence and to perform activities ancillary to this research. This report describes progress that has been made in the third year of the existence of the NAIC on the technical research tasks undertaken at the member universities. The topics covered in general are: versatile expert system for equipment maintenance, distributed AI for communications system control, automatic photo interpretation, time-oriented problem solving, speech understanding systems, knowledge base maintenance, hardware architectures for very large systems, knowledge-based reasoning and planning, and a knowledge acquisition, assistance, and explanation system. The specific topic for this volume is the development of a natural language interacting system with the ability to discuss, use, and recognize plans. This project requires the investigation of a knowledge representation design compatible with the intensional knowledge representation theory previously developed by Dr. Stuart Shapiro et al. GRA

N89-27419# Northeast Artificial Intelligence Consortium, Syracuse, NY.
NORTHEAST ARTIFICIAL INTELLIGENCE CONSORTIUM ANNUAL REPORT 1987. VOLUME 3: DISTRIBUTED ARTIFICIAL INTELLIGENCE FOR COMMUNICATIONS NETWORK MANAGEMENT Interim Report, Dec. 1986 - Dec. 1987
Robert A. Meyer and Susan E. Conry (Clarkson Univ., Potsdam, NY.) Mar. 1989 109 p
(Contract F30602-85-C-0008; AF Proj. 2155)
(AD-A208379; RADC-TR-88-324-Vol-3) Avail: NTIS HC A06/MF A01 CSCL 12/9

The Northeast Artificial Intelligence Consortium (NAIC) was created to conduct pertinent research in artificial intelligence and to perform activities ancillary to this research. This report describes progress that has been made in the third year of the existence of the NAIC on the technical research tasks undertaken at the member universities. The topics covered in general are: versatile expert system for equipment maintenance, distributed AI for communications system control, automatic photo interpretation, time-oriented problem solving, speech understanding systems, knowledge base maintenance, hardware architectures for very large systems, knowledge-based reasoning and planning, and a knowledge acquisition, assistance, and explanation system. The specific topic for this volume is the use of knowledge-based systems for communications network management and control via an architecture for a diversely distributed multi-agency system. The work described in this volume has focused in three areas: distributed planning, distributed knowledge base management, and an environment for the development of distributed systems. GRA

64 NUMERICAL ANALYSIS

Includes iteration, difference equations, and numerical approximation.

N89-27420*# Institute for Computer Applications in Science and Engineering, Hampton, VA.
MULTIGRID METHOD FOR STABILITY PROBLEMS Final Report
Shlomo Taasan (Weizmann Inst. of Science, Rehovoth, Israel) Sep. 1988 18 p Submitted for publication
(Contracts NAS1-18107; NAS1-18605; AF-AFOSR-0127-86)
(NASA-CR-185825; NAS 1.26:185825; ICASE-88-50) Avail: NTIS HC A03/MF A01 CSCL 12A

The problem of calculating the stability of steady state solutions of differential equations is treated. Leading eigenvalues (i.e., having maximal real part) of large matrices that arise from discretization are to be calculated. An efficient multigrid method for solving these problems is presented. The method begins by obtaining an initial approximation for the dominant subspace on a coarse level using a damped Jacobi relaxation. This proceeds until enough accuracy for the dominant subspace has been obtained. The resulting grid functions are then used as an initial approximation for appropriate eigenvalue problems. These problems are being solved first on coarse levels, followed by refinement until a desired accuracy for the eigenvalues has been achieved. The method employs local relaxation on all levels together with a global change on the

coarsest level only, which is designed to separate the different eigenfunctions as well as to update their corresponding eigenvalues. Coarsening is done using the FAS formulation in a non-standard way in which the right hand side of the coarse grid equations involves unknown parameters to be solved for on the coarse grid. This in particular leads to a new multigrid method for calculating the eigenvalues of symmetric problems. Numerical experiments with a model problem demonstrate the effectiveness of the method proposed. Using an FMG algorithm a solution to the level of discretization errors is obtained in just a few work units (less than 10), where a work unit is the work involved in one Jacobi relization on the finest level. Author

N89-27421# International Centre for Theoretical Physics, Trieste (Italy).
USE OF THE FOX DERIVATIVES IN THE SOLUTION OF THE WORD PROBLEM FOR GROUPS
Subrata Majumdar (Rajahahi Univ., Bangladesh) Sep. 1988 6 p Submitted for publication
(DE88-705978; IC-88/242) Avail: NTIS (US Sales Only) HC A02/MF A01

Applying Fox's free partial derivative, the word problem of a finitely presented group has been reduced to the problem of finding an algorithm for determining the existence of a root of a system of linear equations over the integral group ring. The solubility of the word problem for torsion-free one-relator groups and torsion-free polycyclic-by-finite groups has been deduced. DOE

N89-27422# Keuring van Electrotechnische Materialen N.V., Arnhem (Netherlands). Dept. of Performance Testing and Reliability Analysis of Production Installations.
ANALYSIS OF HUMAN-ERROR SEQUENCES WITH FAULT TREES
G. Heslinga 1988 88 p
(PB89-147631; ISSN-0167-8590; ISBN-90-353-0070-X) Avail: NTIS HC A05/MF A01 CSCL 12A

It was investigated whether the event-tree technique, which is frequently used to analyze technical failures, can also be used for the analysis of human errors. The study was limited to errors that can occur during performance of procedural actions and to their possible consequences. The event-tree technique was modified for the purpose and is referred to as the Technique for Human-Error-Sequence Identification and Signification (THESIS). It appeared that the THESIS event trees raise problems if applied to human performance instead of technical systems. The influence of these problems on the applicability of THESIS was assessed by means of mathematical analyses, field studies and laboratory experiments. The main conclusion is that, with certain limitations, event trees can be used to predict sequences of human errors if procedural actions are performed. The limitations are related to the nature of the process that has to be controlled, the existence of several procedures to achieve the same goal and the knowledge of all kinds of data, such as dependence between human errors, human-error probabilities and recovery-attempt probabilities. Author

N89-27423# Stanford Univ., CA. Information Systems Lab.
LINEARIZATION OF NONLINEAR SYSTEMS Final Technical Report, 1 Dec. 1985 - 30 Nov. 1988
Stephen P. Boyd 7 Jan. 1989 7 p
(Contract N00014-86-K-0112)
(AD-A206073) Avail: NTIS HC A02/MF A01 CSCL 12/2

A detailed study of the the problem of low crest-factor signals was made based on the techniques used in harmonic probing of nonlinear systems. Particularly interesting here is the numerical evidence suggesting that the phases used originally exceed the performance achievable with the Shapiro-Rudin phases, which can be proved to yield bounded crest factor for multitone signals containing an arbitrarily large number of tones. The crest factor problem relates two norms, L-sq and L at infinity, of a signal; comparing the gains of an operator with respect to two norms is much harder. A new computational method for the design of linear controllers was developed. A new method of computational stability analysis of systems is derived. Many system stability and robustness problems can be reduced to the question of when there is a quadratic Lyapunov function of a certain structure which establishes stability of x-dot = Ax for some appropriate A. The existence of such Lyapunov function can be determined by solving a non-differentiable convex program. GRA

N89-27424# Army Research Office, Research Triangle Park, NC.
TRANSACTIONS OF THE 6TH ARMY CONFERENCE ON APPLIED MATHEMATICS AND COMPUTING HELD IN BOULDER, COLORADO ON 31 MAY - 3 JUNE 1988
Feb. 1989 1171 p Conference held in Boulder, CO, 31 May - 3 Jun. 1988
(AD-A207252; AD-E801886; ARO-89-1) Avail: NTIS HC A08/MF A04 CSCL 20/4

This year the planned program of the conference consisted of three parts, namely: seven one hour invited addresses; thirty-two half hour solicited talks covering the following topics: Computational Solid and Structural Mechanics, Reactive and Compressible Flows, Symbolic Computing and Applications, and Parallel Computing; and thirty-two contributed papers. Most of the latter were presented by Army scientists and covered topics directly related to problems they face in their laboratories. During the course of the conference, these Army scientists had an opportunity to discuss problems with nationally known scientists. Topics addressed include: Nonlinear Elasto-Plastic Finite Element Analysis of the Thin Shell of Revolution; Aspects of Edge Constraints in Shear-Deformable Plate and Shell Elements; Anomalous Waves in Shock Wave-Fluid Interface Interactions; Mathematical Modeling of Sound Propagation in the Atmosphere Using the Parabolic Approximation; Time-Dependent Shear Flow of a Non-Newtonian Fluid; and On the Positive Roots of an Equation Involving a Bessel Function. GRA

N89-27425# Florida Univ., Gainesville. Dept. of Computer and Information Sciences.
IMAGE ALGEBRA SYNTHESIS Final Report, Jan. - Dec. 1987
G. X. Ritter, Joseph N. Wilson, and Jennifer L. Davidson Mar. 1989 58 p
(Contract F08635-84-C-0295)
(AD-A207257; AD-E801886; AFATL-TR-88-155) Avail: NTIS HC A04/MF A01 CSCL 12/9

This report provides a through review and mathematical analysis of the alternative Image Algebra parallel research effort conducted by the Singer-Kearfott Corporation. The analysis shows a comparison and the contrasting features of this effort and the Image Algebra developed by the University of Florida. The rationale for the strengths and weaknesses of the respective algebras are documented and a proposed synthesis of the two efforts is presented. GRA

N89-27426# Naval Ship Research and Development Center, Bethesda, MD. Propulsion and Auxiliary Systems Dept.
DIFFERENTIAL FORMS OF EULER'S TURBO-MACHINERY EQUATION Final Report, 1987 - 1988
Herman B. Urbach Apr. 1989 66 p
(AD-A207279; DTRC/TM-27-88-56) Avail: NTIS HC A04/MF A01 CSCL 20/11

Galilean transformations between the absolute and moving frame impose a crypto-steady state relation between time derivations of a thermodynamic function in the absolute frame and their gradients in the moving frame. These crypto steady relationships are inherently contained within the Navier-Stokes equations for the absolute and moving frames. The substantial total enthalpy derivative coupled with the substantial entropic energy derivative may be written solely in terms of the flow field of the moving frame. In the moving frame the relative total enthalpy, known as the rothalpy, yields a vanishing substantial derivative. Therefore, the substantial entropic energy derivative is uncoupled and explicit in the moving frames and may be used to obtain an uncoupled explicit substantial total enthalpy derivative. GRA

N89-27427# Maryland Univ., College Park. Inst. for Physical Science and Technology.
AN APPROACH FOR CONSTRUCTING FAMILIES OF HOMOGENIZED EQUATIONS FOR PERIODIC MEDIA. 1: AN INTEGRAL REPRESENTATION AND ITS CONSEQUENCES Final Report
R. C. Morgan and Ivo Babuska Feb. 1989 31 p
(Contract N00014-85-K-0169)
(AD-A207572; MD89-09-RCM-IB-1; TR89-09-1; BN-1094-1)
Avail: NTIS HC A03/MF A01 CSCL 12/1

An approach is presented which allows us to derive a family of homogenization approaches and assess the accuracy of any homogenization in the relation of given input data. The study of periodic media is one application of partial differential equations that have highly oscillatory, periodic coefficients. Essentially, the problem is to solve a elliptic differential equation. One of the main applications of this differential equation is in the field of composite materials. Here the aim is to replace the composite by homogeneous materials with the bulk material properties. GRA

N89-27428# Maryland Univ., College Park. Inst. for Physical Science and Technology.
AN APPROACH FOR CONSTRUCTING FAMILIES OF HOMOGENIZED EQUATIONS FOR PERIODIC MEDIA. 2: PROPERTIES OF THE KERNEL Final Report
R. C. Morgan and Ivo Babuska Feb. 1989 36 p
(Contract N00014-85-K-0169)
(AD-A207573; MD89-10-RCM-IB-2; TR89-10-2; BN-1095-2)
Avail: NTIS HC A03/MF A01 CSCL 12/1

The paper is the second in the series devoted to the study of constructions of families of homogenizations. In the first paper the properties of the kernel Phi were utilized. In this paper these properties are established. An integral representation of the solution to a differential equation is developed that models the equations that arise in the study of periodic media (e.g., composite materials). GRA

N89-27429# Maryland Univ., College Park. Inst. for Physical Science and Technology.
THE h-p VERSION OF THE FINITE ELEMENT METHOD PARABOLIC EQUATIONS. PART 2: THE h-p VERSION IN TIME Final Report
Ivo Babuska and Tadeusz Janik Feb. 1989 46 p
(Contract N00014-85-K-0169; NSF DMS-85-16191)
(AD-A207575; MD89-04-IB-TJ-Pt-2; TR89-04-Pt-2; BN-1093-Pt-2)
Avail: NTIS HC A03/MF A01 CSCL 12/1

The paper is the second in the series addressing the h-p version of the finite element method for parabolic equations. The present paper addresses the case where in both variables, (spatial and time) the h-p version is used. Error estimation is given and numerical computations are presented. In both cases we used the same p and q in all time intervals. The results show that the flexibility of the method, when properly employed, leads to the large increase of computational effectivity. Various adaptive approaches here will be very effective tools for such an optimal choice. GRA

N89-27430# Wisconsin Univ., Madison.
COMPUTATION AND THEORY IN NONLINEAR OPTIMIZATION Final Report, 15 Jan. - 14 Nov. 1988
Stephen M. Robinson 14 Nov. 1988 6 p
(Grant AF-AFOSR-0090-88)
(AD-A207610; AFOSR-89-0534TR) Avail: NTIS HC A02/MF A01 CSCL 12/4

Researchers have made substantial progress in the decomposition of large-scale nonlinear problems for accelerated convergence. A Newton method for nonsmooth equations has been developed and conditions for its convergence determined. The original proposal suggested work in the general area of large-scale optimization: in particular, methods for decomposition based on the so-called Bundle method, decomposition of large-scale nonlinear problems, including parameter optimization in networks of queues, and accelerating the convergence of bundle-type methods, including developing the theory base in areas such as implementable second-order models of functions to be optimized. A particular area of work suggested as a major topic of investigation was the development of a computationally implementable and efficient Newton-type algorithm for nonsmooth problems. GRA

N89-27431# Technische Univ., Delft (Netherlands). Faculty of Technical Mathematics and Informatics.
LOCAL MODE SMOOTHING ANALYSIS OF VARIOUS TWO-DIMENSIONAL INCOMPLETE FACTORIZATION ITERATIVE METHODS
M. Khalil 1988 19 p
(Rept-88-67; ISSN-0922-5641; ETN-89-94898) Copyright Avail: NTIS HC A03/MF A01

Local mode analysis on a finite domain with periodic boundary conditions is used to assess the smoothing efficiency of iterative methods based on incomplete factorizations. The analysis consists of an analytic and numerical study of a simple 2-D problem discretized by finite differences. This analysis is done for pointwise and blockwise incomplete factorizations. Results show how this analysis is helpful to obtain simple expressions for the smoothing factors and to introduce new smoothers. It gives also a good prediction of the multigrid convergence rate. ESA

N89-27432# Technische Univ., Delft (Netherlands). Faculty of Technical Mathematics and Informatics.
ROW-ORIENTED DIRECT SOLVING OF LINEAR ALGEBRAIC EQUATIONS. INVERSE PROJECTION METHOD
E. Dekker and L. Dekker 1988 21 p
(Rept-88-81; ISSN-0922-5641; ETN-89-94910) Copyright Avail: NTIS HC A03/MF A01

Serial and parallel algorithms are discussed, which were derived from a direct solution method for linear algebraic equations based on row-oriented matrix claculus: the inverse-projection method. In this method no elimination of unknowns is applied. The matrix equation is considered to be a set of inner product equations that are solved by means of orthogonalization techniques. This orthogonalization requires extensive inner product calculus. Pipelined as well as parallel processing can be applied, resulting in parallel algorithms with a large speed-up and which can easily and efficiently be implemented onto MIMD supercomputers provided with local memories and designed to perform both parallel and pipelined processing. An example of a structured sparse matrix is used to show that by taking the structural characteristics into account, inverse projection algorithms can be designed which take considerably less computing time than is necessary in the case of full matrices. ESA

N89-27433*# National Aeronautics and Space Administration. Ames Research Center, Moffett Field, CA.
A DIRECT PROCEDURE FOR INTERPOLATION ON A STRUCTURED CURVILINEAR TWO-DIMENSIONAL GRID
David W. Zingg and Maurice Yarrow (Sterling Software, Moffett field, CA.) Jul. 1989 12 p
(NASA-TM-102213; A-89210; NAS 1.15:102213) Avail: NTIS HC A03/MF A01 CSCL 12A

A direct procedure is presented for locally bicubic interpolation on a structured, curvilinear, two-dimensional grid. The physical (Cartesian) space is transformed to a computational space in which the grid is uniform and rectangular by a generalized curvilinear coordinate transformation. Required partial derivative information is obtained by finite differences in the computational space. The partial derivatives in physical space are determined by repeated application of the chain rule for partial differentiation. A bilinear transformation is used to analytically transform the individual quadrilateral cells in physical space into unit squares. The interpolation is performed within each unit square using a piecewise bicubic spline. Author

N89-27434*# California State Univ., Northridge.
EFFICIENT GRID GENERATION Final Report, 1 Aug. 1987 - 31 Jul. 1989
Rycichi Seki Jul. 1989 126 p

(Contract NCC2-515)
(NASA-CR-185034; NAS 1.26:185034) Avail: NTIS HC A07/MF A01 CSCL 12A

Because the governing equations in fluid dynamics contain partial differentials and are too difficult in most cases to solve analytically, these differentials are generally replaced by finite difference terms. These terms contain terms in the solution at nearby states. This procedure discretizes the field into a finite number of states. These states, when plotted, form a grid, or mesh, of points. It is at these states, or field points, that the solution is found. The optimum choice of states, the x, y, z coordinate values, minimizes error and computational time. But the process of finding these states is made more difficult by complex boundaries, and by the need to control step size differences between the states, that is, the need to control the spacing of field points. One solution technique uses a different set of state variables, which define a different coordinate system, to generate the grid more easily. A new method, developed by Dr. Joseph Steger, combines elliptic and hyperbolic partial differential equations into a r.apping function between the physical and computational coordinate systems. This system of equations offers more control than either equation provides alone. The Steger algorithm was modified in order to allow bodies with stronger concavities to be used, offering the possibility of generating a single grid about multiple bodies. Work was also done on identifying areas where grid breakdown occurs. Author

N89-27435# Sandia National Labs., Albuquerque, NM.
USING CONJOINT MESHING PRIMITIVES TO GENERATE QUADRILATERAL AND HEXAHEDRAL ELEMENTS IN IRREGULAR REGIONS
Michael B. Stephenson (Brigham Young Univ., Provo, UT.) and Ted D. Blacker Jan. 1989 33 p Presented at the ASME International Computers in Engineering Conference, Anaheim, CA, 30 Jul. 1989
(Contract DE-AC04-76DP-00789)
(DE89-005918; SAND-88-3089C; CONF-890741-1) Avail: NTIS HC A03/MF A01

The parameter-space mapping technique used in most finite element mesh generation programs requires that the geometry be subdivided into either rectangular areas in 2-D or rectilinear volumes in 3-D to produce, respectively, quadrilateral or hexahedral elements. Since subdivision occurs in parameter space, the edges bounding the areas and volumes need not be straight or parallel lines. Simple geometries may be subdivided easily while irregular features challenge the analyst. This paper presents the formulation and application of conjoint meshing primitives that assist the analyst in meshing in and around irregular features. The term conjoint is applied to these primitives because each is composed of several rectangular areas or rectilinear volumes. Interval assignments may vary from side to side, within a set of constraints, for each primitive. Thus, all of them are useful for transitions between other regular areas or volumes. In 2-D, the primitive areas are the triangle, pentagon, semi-circle, circle, and rectangular transition. These primitives are implemented in the Sandia meshing program FASTQ and are used in regular production work. They are also the basis for decomposition regions in the developing artificial intelligence Automated Meshing Knowledge System, AMEKS. DOE

N89-27436# Lawrence Livermore National Lab., CA.
A MACSYMA PACKAGE FOR THE GENERATION AND MANIPULATION OF CHEBYSHEV SERIES
Theodore H. Einwohner and Richard J. Fateman 19 Apr. 1989 14 p Presented at the International Symposium on Symbolic and Algebraic Computing, Portland, OR, 17-19 Jul. 1989
(Contract W-7405-eng-48)
(DE89-011404; UCRL-100959; CONF-890779-1) Avail: NTIS HC A03/MF A01

Techniques for a MACSYMA package for expanding an arbitrary univariate expression as a truncated series in Chebyshev polynomials and manipulating such expansions is described. A data structure is introduced to represent a truncated expansion in a set of orthogonal polynomials. The data structure contains the independent variable, the name of the orthogonal polynomial set, the number of terms retained, and a list of the expansion coefficients. Although we restrict attention here to the set of Chebyshev polynomials as the orthogonal set, extension to other orthogonal polynomials will be done later. A data structure for truncated power series is provided as an alternative. The principal function of the package converts a given expression into the aforementioned data structure. Special cases are the conversion of sums, products, the ratio, or the composition of truncated Chebyshev expansions. DOE

N89-27437# Illinois Univ., Urbana. Dept. of Computer Science.
ACCURACY INCREASE IN WAVEFORM GAUSS SEIDEL
F. Juang and C. W. Gear Jun. 1989 30 p
(Contract DE-FG02-87ER-25026)
(DE89-014812; DOE/ER-25026/29; UILU-ENG-89-1737; UIUCDCS-R-89-1518) Avail: NTIS HC A03/MF A01

The traditional approach for solving large dynamical systems is time consuming. Waveform relaxation, an iterative technique for solving systems of differential equations, can be used to reduce the processing time. It has been shown to converge superlinearly on finite intervals. In this paper, the order of accuracy of solutions generated by a relaxation approach, the waveform Gauss-Seidel method, is discussed. In this approach, a directed graph, called a dependency graph, is used to indicate the coupling relations among all components. The relation between the accuracy increase after each Gauss-Seidel iteration and the lengths of ascending chains (simple directed paths) in cycles in the dependency graph is discussed. It is proved that the cycle in the dependency graph which has the minimum ratio of its length to its number of ascending chains, determines the average accuracy increase. Effective use of the waveform Gauss-Seidel method depends on the ordering of the components. The result in this paper provides a basis for selecting the ordering. DOE

N89-27438# Illinois Univ., Urbana. Dept. of Computer Science.
SAFETY IN NUMBERS: THE BOUNDLESS ERRORS OF NUMERICAL COMPUTATION
Robert D. Skeel Jun. 1989 13 p
(Contract DE-FG02-87ER-25026)
(DE89-014813; DOE/ER-25026/30; NCG-89-3) Avail: NTIS HC A03/MF A01

Perhaps the greatest unresolved question in numerical computing is how to cope with the issue of uncertainty in the accuracy of computed numerical quantities. The problem is not so much the errors in the answers, but the lack of a correct error bound or a confidence interval. The problem arises because of the failure to keep track of known errors and because of unknown errors due to finite sampling techniques. Several approaches to this question are discussed, principally interval analysis and probabilistic techniques. Reasons for the neglect of the uncertainty issue are suggested, and the benefits of providing consistently correct answers are considered. DOE

N89-27439# Universiteit Twente, Enschede (Netherlands). Dept. of Computer Science.
A QUALITATIVE WAY OF SOLVING THE POLE BALANCING PROBLEM
A. Makarovic 4 Nov. 1988 37 p
(MEMO-INF-88-44; UT-KBS-88-03; ISBN-90-365-0220-9; ETN-89-94762) Avail: NTIS HC A03/MF A01

A method for designing a control rule for the pole-cart system is presented. Conventional techniques are used to model the system by a set of differential equations. The high complexity of the model is simplified by restructuring and approximating the equations. Ultimately a very simple model results. It is shown that designing a control rule for this model is an easy task. Even small changes in complexity may have a great influence on the search space of potential solutions. ESA

N89-27440# Universiteit Twente, Enschede (Netherlands). Dept. of Computer Science.
ATTRIBUTED TREE TRANSFORMATIONS WITH DELAYED AND SMART RE-EVALUATION
Henk Alblas Oct. 1988 17 p
(MEMO-INF-88-45; ETN-89-94763) Avail: NTIS HC A03/MF A01

Criteria which allow a delay in calling the re-evaluator used for the correct attribution of the tree in compiler optimizations are formulated. The criteria allow a strategy of repeatedly applying alternate attribute evaluation and tree transformation phases. The first is a tree walk in which all attribute instances receive their correct values. The second consists of a tree walk in which as many tree transformations are performed as possible. The transformation phase is never interrupted to carry out a re-evaluation. An optimized incremental multipass evaluator is presented. ESA

N89-27441# Rome Univ. (Italy). Dipartimento di Fisica.
THE BURGERS EQUATION ON THE SEMI-FINITE AND FINITE INTERVALS
F. Calogero and S. DeLillo (Salerno Univ., Italy) 31 May 1988 9 p Submitted for publication
(Preprint-602; ETN-89-94691) Avail: NTIS HC A02/MF A01

The initial/boundary value problem on the semiline and on a finite interval, for the Burgers equation ut=uxx+2uxu, are solved, i.e., reduced, by quadratures, to a linear integral equation of Volterra type in one independent variable. This can be itself solved by quadratures if the boundary data are time-independent. ESA

N89-27442# Rome Univ. (Italy). Dipartimento di Fisica.
UNIVERSALITY AND INTEGRABILITY OF THE NONLINEAR EVOLUTION PDES DESCRIBING N-WAVE INTERACTIONS
F. Calogero 7 Jul. 1988 36 p Submitted for publication
(Preprint-603; ETN-89-94692) Avail: NTIS HC A03/MF A01

The universality of the equations describing N-wave interactions is demonstrated by deriving them from a very large class of nonlinear evolution equations (essentially all those whose linea part is dispersive). Various forms of these equations are displayed. The fact that these universal nonlinear evolution equations are obtained by an appropriate asymptotic limit from such a large class of nonlinear evolution equations, suggests that they should be integrable, since for this it is sufficient that the large class from which they are obtainable contains just one integrable equation. This expectation is validated in several cases, by deriving the equations from known integrable equations. In this manner an explanation may be provided of the (already known) integrable nature of certain equations; and integrable equations may be obtained. Both S-integrable and C-integrable equations are discussed, namely both equations integrable via an appropriate spectral transform and solvable via an appropriate change of variables. The treatment is limited to equations in 1+1 dimensions. ESA

N89-27443# Rome Univ. (Italy). Dipartimento di Fisica.
NONLINEAR WAVE EQUATIONS SOLVABLE BY THE SPECTRAL TRANSFORM
A. Degasperis 30 Jan. 1989 91 p Presented at the International School of Physics E. Fermi Lectures on Nonlinear Topics in Ocean Physics, Varenna, Italy, 26 Jul. - 5 Aug. 1988 Submitted for publication
(Preprint-957; ETN-89-94730) Avail: NTIS HC A05/MF A01

The main mathematical tools which prove to be essential to the spectral analysis of (special classes of) solutions of nonlinear wave equations are introduced. The two basic ingredients of the spectral analysis are a linear differential equation containing a complex (spectral) parameter, and a linear Riemann-Hilbert boundary value problem or, more generally, a linear D-bar problem in the complex plane of this parameter. ESA

N89-27444 National Physical Lab., Teddington (England). Div. of Information Technology and Computing.
THE LEAST SQUARES SOLUTION OF LINEAR EQUATIONS WITH BLOCK-ANGULAR OBSERVATION MATRIX
M. G. Cox Apr. 1989 18 p Presented at the NPL Conference on Advances in Reliable Numerical Computation, Teddington, United Kingdom, 8-10 Jul. 1987
(NPL-DITC-139/89; ISSN-0262-5369; ETN-89-94964) Copyright Avail: National Physical Laboratory, Teddington, Middlesex, TW11 OLW, United Kingdom

The least-squares solution of a system of overdetermined linear equations whose observation matrix is block angular is considered. A structure-exploiting method of solution based on the use of orthogonal transformations is described. The algorithm requires considerably less storage space than other direct methods and, unlike otherwise competitive iterative techniques, permits accurate statistics (variances, covariances) associated with the solution to be provided. ESA

N89-27445# Stanford Univ., CA. Dept. of Statistics.
ON ESTIMATING THE DEPENDENCE BETWEEN TWO POINT PROCESSES
Hani Doss 4 May 1989 23 p
(Contract N00014-86-K-0156; NR Proj. 042-267)
(AD-A208311; SU-TR-417) Avail: NTIS HC A03/MF A01 CSCL 12/3

To assess the dependence structure in a stationary bivariate point process the second-order distribution (Ripley 1976, 1977) can be very useful. It is proven that the natural estimates of this distribution, based on a certain realization are asymptotically normal, and the author presents a method for constructing approximate confidence intervals for this distribution. GRA

65 STATISTICS AND PROBABILITY

Includes data sampling and smoothing; Monte Carlo method; and stochastic processes.

N89-27446# North Carolina Univ., Chapel Hill. Dept. of Statistics.
CAPACITY OF THE POISSON CHANNEL WITH TIME-VARYING NOISE INTENSITY AND JAMMING
Michael R. Frey May 1988 26 p
(Contracts N00014-86-K-0039; DAAL03-86-G-0022)
(AD-A207225; LISS-25) Avail: NTIS HC A03/MF A01 CSCL 17/4

The information capacity of the Poisson channel with jamming and nonrandom time varying noise intensity is obtained for a time-varying peak constraint on the encoder intensity. The optimal jamming signal is determined. Feedback is shown not to increase the channel capacity for the case of nonrandom noise intensity. Poisson channels with thinning are introduced. GRA

N89-27447# North Carolina Univ., Chapel Hill. Dept. of Statistics.
CAPACITY OF THE POISSON CHANNEL WITH RANDOM NOISE INTENSITY
Michael R. Frey Mar. 1989 19 p
(Contracts N00014-86-K-0039; N00014-89-J-1175)
(AD-A207226; LISS-33) Avail: NTIS HC A03/MF A01 CSCL 12/9

An upper bound B sub f is given for the information capacity of the Poisson channel with marginally stationary random noise intensity and causal feedback. The capacity is shown to converge to B sub f in the limit of longer and longer communication intervals for a class of random noise intensities including the case in which the noise intensity is nontime-varying. An upper bound B sub nf on the capacity is also established for the Poisson channel with marginally stationary noise and no feedback. In this case also, for a class of random noise intensities including nontime-varying noise intensity, B sub nf is found to be the capacity of the channel without feedback in the limit of longer and long communication

intervals. The fractional difference between B sub f and B sub nf is considered as a means to quantify the improvement afforded by feedback. Also, certain nonstandard encoder constraints are addressed and the importance of the encoder intensity peak constraint to the channel capacity problem is explored. GRA

N89-27448# Naval Postgraduate School, Monterey, CA.
CONSTANT ACCESS SYSTEMS: A GENERAL FRAMEWORK FOR GREEDY OPTIMIZATION ON STOCHASTIC NETWORKS
Michael P. Bailey Mar. 1989 39 p
(AD-A207525; NPS55-89-02) Avail: NTIS HC A03/MF A01 CSCL 12/3

We consider network optimization problems in which the weights of the edges are random variables. We develop conditions on the combinatorial structure of the problem which guarantee that the objective function value is a first passage time in an appropriately constructed Markov process. The arc weights must be exponentially distributed, the method of solution of the deterministic problem must be greedy in a general sense, and the accumulation of objective function value during the greedy procedure must occur at a constant rate. We call these structures constant access systems after the third property. Examples of constant access systems include the shortest path system, time until disconnection in a network of failing components, and some bottleneck optimization problems. For each system, we give the distribution of the objective function, the distribution of the solution of the problem, and the probability that a given arc is a member of the optimal solution. We also provide easily implementable formulae for the moments of these quantities. GRA

N89-27449# Rome Univ. (Italy). Dipartimento di Fisica.
DIFFERENTIAL STOCHASTIC EQUATIONS [EQUAZIONI DIFFERENZIALI STOCASTICHE]
Francesco Guerra 24 Oct. 1988 47 p In ITALIAN Submitted for publication
(Preprint-635; ETN-89-94715) Avail: NTIS NC A03/MF A01

Stochastic differential equations and their physical interpretation are explained. Deterministic evolutions subjected to stochastic perturbations are discussed. The applications to quantum mechanics, astrophysics, and in general dynamic systems are explained. Transformations under time inversion are discussed. The equations presented include Fokker-Plank, Ito-Girsanov and Feynman-Kac. ESA

N89-27450# Office National d'Etudes et de Recherches Aerospatiales, Paris (France).
SOLUTION OF DETERMINISTIC DIFFERENTIAL GAMES: THE APPROXIMATE STRATEGY METHOD
C. Marchal 1987 28 p In FRENCH; ENGLISH summary
(ONERA-NT-1987-6; ISSN-0078-3781; ETN-89-94812) Avail: NTIS HC A03/MF A01

Deterministic differential games are described and strategies are discussed. The interest of the appoximate strategy method is that it reduces the game to a succesion of ordinary problems of optimization and allows a systematic step by step improvement of the strategies. Two good opposing strategies give close upper and lower bounds of the value of the game. If the Hamiltonian of the game is either convex or concave with respect to the adjunct vector, the game is equivalent to a problem of optimization. ESA

N89-27451# Stanford Univ., CA. Dept. of Statistics.
SAMPLING BASED APPROACHES TO CALCULATING MARGINAL DENSITIES Technical Report No. 415
Alan E. Gelfand and Adrian F. M. Smith 11 Apr. 1989 26 p
(Contract N00014-86-K-0156; NR Proj. 042-267)
(AD-A208388; SU-TR-415) Avail: NTIS HC A03/MF A01 CSCL 12/3

Stochastic substitution, the Gibbs sampler and the sampling-importance-resampling algorithm can be viewed as three alternative sampling, or Monte Carlo, based approaches to the calculation of numerical estimates of marginal probability distributions. The three approaches will be reviewed, and compared and contrasted, in relation to various joint probability structures frequently encountered in applications. In particular, the relevance of the approaches to calculating Bayesian posterior densities for a variety of structured models will be discussed and illustrated. GRA

66 SYSTEMS ANALYSIS

Includes mathematical modeling; network analysis; and operations research.

N89-27452# Los Alamos National Lab., NM.
DIRECTED ENERGY WEAPONS/EN DASH/LASERS: GROUND- AND SPACE-BASED SYSTEMS
Gregory H. Canavan Jun. 1989 35 p
(Contract W-7405-eng-36)
(DE89-012804; LA-11557-MS) Avail: NTIS HC A03/MF A01

Directed energy weapons (DEWs) range and speed complement kinetic energy weapons (KEWs) lethality and offset their sensitivity to launch area and time. Lasers could be developed to the power and brightness required to offset the degradation of KEWs by advanced threats. This report reviews their scaling, discusses how they could extend the effectiveness of KEW systems, and estimates when they could enter the defenses. DOE

67 THEORETICAL MATHEMATICS

Includes topology and number theory.

No abstracts in this category.

70 PHYSICS (GENERAL)

For precision time and time interval (PTTI) see *35 Instrumentation and Photography;* for geophysics, astrophysics or solar physics see *46 Geophysics, 90 Astrophysics,* or *92 Solar Physics.*

N89-27453# Los Alamos National Lab., NM. Neutron Scattering Center.
MOMENTUM DISTRIBUTIONS: AN OVERVIEW
P. E. Sokol, R. N. Silver, and J. W. Clark (Washington Univ., Saint Louis, MO.) 1989 36 p Presented at the Workshop on Momentum Distributions, Argonne, IL, 24 Oct. 1988
(Contracts W-7405-eng-36; W-31-109-eng-38)
(DE89-012617; LA-UR-89-1604; CONF-8810118-7) Avail: NTIS HC A03/MF A01

There have been several excellent reviews of momentum-distribution research in particular subject areas of physics such as electronic systems and nuclear systems. However, it is the commonality of interests, difficulties, and prospects across all of physics, along with certain pivotal advances, which led to the organization of an interdisciplinary Workshop on Momentum Distributions held at Argonne National Laboratory on 24 and 26 October 1988. The purpose of this overview is to explain why scientists with such diverse backgrounds were brought together at this meeting, to introduce and discuss the common elements of momentum-distribution studies, and to establish a common language. We hope to facilitate an appreciation of the more specialized articles which follow in these proceedings. We begin by summarizing the general properties of momentum distributions. Differences and similarities of atomic, electronic, and nuclear many-body systems are examined, in terms of characteristic lengths and energies, relative importance of exchange, and the nature of the two-particle interactions. We continue with a brief commentary on the microscopic methods used to calculate n(p) from first principles. DOE

N89-27454# Lawrence Livermore National Lab., CA.
A TEST OF NEWTON'S LAW OF GRAVITY USING THE BREN TOWER, NEVADA
P. Kasameyer, J. Thomas, O. Fackler, M. Mugge, J. Kammeraad, M. Millett, B. Harris, and D. Felske 22 May 1989 16 p Presented at the 8th Moriond Workshop on Tests of Fundamental Laws in Physics, Savoie, France, 21-28 Jan. 1989
(Contracts W-7405-eng-48; DE-AC03-81ER-40050)
(DE89-013262; UCRL-101001; CONF-890199-5) Avail: NTIS HC A03/MF A01

Gravity values were predicted on a tower by upward continuing an extensive set of surface data in order to test the 1/r squared dependence of Newton's Law of Universal Gravitation. Gravity was measured at 12 heights up to 454 m on a tower at the Nevada Test Site, and at 91 locations on the surface of the earth within 2.5 kilometers of the tower. These data were combined with 60,000 surface gravity measurements within 300 kilometers of the tower and were used to predict the gravitational field on the tower via a solution of Laplace's equation. A discrepancy between the observed gravity values and the prediction could suggest a breakdown of Newtonian Gravity, but none were observed. Preliminary results are consistent with the Newtonian hypothesis to within 93 + or - 95 microgals at the top of the tower, a result which conflicts with the previously reported 500 microgal non-Newtonian signal seen at 562 meters above the earth. DOE

N89-27455# California Univ., Berkeley. Lawrence Berkeley Lab. Engineering Div.
CRYOGENIC TECHNIQUES FOR LARGE SUPERCONDUCTING MAGNETS IN SPACE
Michael A. Green Dec. 1988 26 p Presented at the Space Cryogenics Workshop, Frascati, Italy, 18 Jul. 1988
(Contract DE-AC03-76SF-00098)
(DE89-013431; LBL-25735; CONF-8807123-2) Avail: NTIS HC A03/MF A01

A large superconducting magnet is proposed for use in a particle astrophysics experiment, ASTROMAG, which is to be mounted on the United States Space Station. This experiment will have a two-coil superconducting magnet with coils which are 1.3 to 1.7 meters in diameter. The two-coil magnet will have zero net magnetic dipole moment. The field 15 meters from the magnet will approach earth's field in low earth orbit. The issue of high Tc superconductor will be discussed in the paper. The reasons for using conventional niobium-titanium superconductor cooled with superfluid helium will be presented. Since the purpose of the magnet is to do particle astrophysics, the superconducting coils must be located close to the charged particle detectors. The trade off between the particle physics possible and the cryogenic insulation around the coils is discussed. As a result, the ASTROMAG magnet coils will be operated outside of the superfluid helium storage tank. The fountain effect pumping system which will be used to cool the coil is described in the report. Two methods for extending the operating life of the superfluid helium dewar are discussed. These include: operation with a third shield cooled to 90 K with a sterling cycle cryocooler, and a hybrid cryogenic system where there are three hydrogen-cooled shields and cryostat support heat intercept points. DOE

N89-27456*# National Aeronautics and Space Administration. Goddard Space Flight Center, Greenbelt, MD.
GEODETIC PRECESSION OR DRAGGING OF INERTIAL FRAMES
Neil Ashby (Colorado Univ., Boulder.) and Bahman Shahid-Saless Aug. 1989 14 p
(NASA-TM-100744; Rept-89B00267; NAS 1.15:100744) Avail: NTIS HC A03/MF A01 CSCL 20C

In General Relativity, the Principle of General Covariance allows one to describe phenomena by means of any convenient choice of coordinate system. Here, it is shown that the geodetic precession of a gyroscope orbiting a spherically symmetric, nonrotating mass can be recast as a Lense-Thirring frame-dragging effect, in an appropriately chosen coordinate frame whose origin falls freely along with the gyroscope and whose spatial coordinate axes point in fixed directions. Author

N89-27457# National Bureau of Standards, Boulder, CO. Electromagnetic Technology Div.
GROUP INDEX AND TIME DELAY MEASUREMENTS OF A STANDARD REFERENCE FIBER
B. L. Danielson and C. D. Whittenberg Jul. 1988 20 p Sponsored by NWC
(PB89-189179; NBSIR-88/3091) Avail: NTIS HC A03/MF A01 CSCL 20C

Measurement techniques for establishing a standard reference fiber with well characterized group index and time or group delay are described. Evaluation of an interferometric method indicates that fiber group index can be determined with a total estimated uncertainty of about 0.03 percent in small samples. Group delay of the reference fiber was measured with an overall uncertainty less than 0.004 percent in a 7 km waveguide. The application of a standard reference fiber to calibration of the distance measurement accuracy of an optical time-domain reflectometer (OTDR) is discussed. Author

N89-27458# Swedish Inst. of Space Physics, Kiruna.
[ACTIVITIES REPORT IN SPACE ACTIVITIES] Annual Report, 1988
Lars Eliasson, ed. and Gunnar Holmgren, ed. 1989 66 p
(ISSN-0284-169X; ETN-89-94942) Avail: NTIS HC A04/MF A01

In situ hot plasma investigations, EISCAT research, radio remote sensing, plasma simulation, research on mechanical waves especially concerning infrasound and vibration, the Swedish Viking satellite, ionospheric modification, and sounding rocket programs are discussed. ESA

71 ACOUSTICS

Includes sound generation, transmission and attenuation. For noise pollution see *45 Environmental Pollution.*

N89-27459# Wyle Labs., Inc., Arlington, VA.
ROUTEMAP MODEL FOR PREDICTING NOISE EXPOSURE FROM AIRCRAFT OPERATIONS ON MILITARY TRAINING ROUTES Final Report, Jan. - Sep. 1988
Michael J. Lucas and Kenneth J. Plotkin Sep. 1988 95 p
(Contract F33615-85-C-0534; AF Proj. 7231)
(AD-A203849; WR-88-15; AAMRL-TR-88-060) Avail: NTIS HC A05/MF A01 CSCL 20/1

Low altitude, high speed training operations are routinely conducted along specially designated Military Training Routes (MTRs). The location of these routes is continually changed for a variety of reasons. Each new route requires an environmental assessment to determine the community noise impact. A computer program, ROUTEMAP, is described which calculates the noise level on the ground along an MTR corridor. Program ROUTEMAP is a menu-driven program that runs on any IBM PC or PC-compatible computer. ROUTEMAP requires MS DOS Version 2.0 or later, with at least one megabyte of available disk space, 640 K of random access memory, and an 8087/80287 math coprocessor. The model requires the Air Force planner to specify the nature of the flight activity for the segment of the route in question. The information needed for each aircraft type are the number of day and night operations during a month, and nominal values for the airspeed, engine power setting, and altitude. In addition, the user must input whether the activity is usually under visual or instrument flying rules and if there are single or multiple flight tracks within the route corridor. With this input data, the program computes the onset rate-adjusted monthly day-night average A-weighted sound level, L sub dnmr in dB for ground positions located within 13 miles of the route centerline. For comparison purposes, the program also computes the monthly average A-weighted noise exposure level without the penalty for

high onset rates and without the penalty for operations during the night. The program also computes the probability of being highly annoyed as a function of the L sub dnmr values. This information, along with the noise-compatible land-use guides normally associated with planning around airbases, can be used to interpret the noise resulting from military training route operations. Author

N89-27460# National Oceanic and Atmospheric Administration, Boulder, CO. Wave Propagation Lab.
EIGEN: A PROGRAM TO COMPUTE EIGENRAYS FROM HARPA (HAMILTONIAN ACOUSTIC RAY-TRACING PROGRAM FOR THE ATMOSPHERE)/HARPO (HAMILTONIAN ACOUSTIC RAY-TRACING PROGRAM FOR THE OCEAN) RAYSETS
A. M. Weickmann, J. P. Riley, T. M. Georges, and R. M. Jones Feb. 1989 97 p
(PB89-165781; NOAA-TM-ERL-WPL-160) Avail: NTIS HC A05/MF A01 CSCL 20A

EIGEN is a FORTRAN computer program that processes the rayset (machine-readable) output of the HARPA and HARPO acoustic ray-tracing programs. It interpolates in elevation angle to find the eigenrays that connect the source and a specified receiver. It also creates plots of range vs. elevation angle and range vs. travel time. GRA

N89-27461 Department of the Air Force, Washington, DC.
MULTICHANNEL PHASE NOISE MEASUREMENT SYSTEM Patent
Stephen P. Caldwell, inventor (to AF), James T. Haynes, inventor (to AF), and S. Buchalter, inventor (to AF) 31 May 1988 6 p Filed 21 Apr. 1986 Supersedes AD-D012372
(AD-D014056; US-Patent-4,748,399; US-Patent-Appl-SN-853827) Avail: US Patent and Trademark Office CSCL 12/9

A multichannel phase noise measuring system is disclosed which is capable of measuring the phase noise of two signal source operating between 100 MHz and 24 GHz. This system has two input channels and a mixer which produces a difference frequency between the signals received in the input channels. The difference frequency containing the phase noise is frequency multiplied and amplified to raise the phase noise level 12 dB. The multiplied and amplified difference signal is phase locked to a commercially available frequency synthesizer with inferior noise characteristics to the units being tested. By amplifying the phase noise of the original signals above the phase noise levels of the commercially available frequency synthesizer, they become measurable. GRA

N89-27462# Army Lab. Command, Fort Monmouth, NJ. Electronics Technology and Devices Lab.
POLARIZATION MATRICES OF LITHIUM NIOBATE Technical Report, Jan. 1988 - Jan. 1989
Arthur Ballato Apr. 1989 29 p
(AD-A207231; SLCET-TR-89-1) Avail: NTIS HC A03/MF A01 CSCL 09/1

In analytical treatments of piezoelectric-acoustic transducers, signal processors, and resonators, the electromechanical transduction mechanism is most often expressed in terms of the elements of the piezoelectric (e) or (d) matrices. Molecular interpretations of piezoelectricity, and especially electrooptical applications, usually involve polarization as the preferred variable, and consequently the alternative (a) and (b) matrices are of interest. The elements of these latter sets are calculated for lithium niobate from measured elastopiezodielectric constants taken from the literature. GRA

N89-27463# Army Lab. Command, Watertown, MA. Material Technology Lab.
CEPSTRAL METHOD FOR THE MEASUREMENT OF ULTRASONIC PULSE TRANSMISSION TIME VARIATIONS Final Report
Otto R. Gericke Apr. 1989 20 p
(AD-A207410; MTL-TR-89-25) Avail: NTIS HC A03/MF A01 CSCL 14/2

A precise method for determining relative changes or small differences in ultra-sonic pulse transmission times has been developed. The method uses multiple-echo signals obtained by injecting a pulsed, plane ultrasonic wave of the compressional mode into a sample with free, parallel surfaces. The ultrasonic transducer employed for this purpose acts as both transmitter and receiver. The received ultrasonic signals are subjected to two consecutive Fourier transformations to produce a cepstrum. The cepstral function derived from the multiple-echo signal exhibits characteristic maxima whose positions on the frequency abscissa, after calibration in units of time, represent multiples of the ultrasonic transmission time. Since minute variations of this time can be determined from a shift in the position of a cepstral maximum, the detection of very small changes or differences in sample thickness or ultrasonic propagation velocity becomes feasible. GRA

N89-27464# Dayton Univ., OH. Research Inst.
KC-135R RUMBLE INVESTIGATION Final Report, Oct. 1986 - Jan. 1988
Michael L. Drake and Dennis G. Davis 27 Feb. 1989 242 p
(Contract F33615-85-C-5040)
(AD-A207532; UDR-TR-88-04; AFWAL-TR-88-4260) Avail: NTIS HC A11/MF A01 CSCL 01/3

The KC-135R is a modified KC-135A which has had, among other things, the engines changed from the J-57 to the new F-108-CF-100 engines. Shortly after the KC-135R began SAC flight operations, a noise problem perceived as a rumbling sound in the cabin area was found in various aircraft; i.e., Rumble. The Air Force, the aircraft manufacturer and the engine manufacturer studied the problem briefly developing a better definition of the general problem. The forcing function was determined to be the F-108 engine; however, the precise source of the noise and vibration, and the transmission path from the engine to the cabin were unknown. GRA

N89-27465*# National Aeronautics and Space Administration. Langley Research Center, Hampton, VA.
REDUCTION OF BLADE-VORTEX INTERACTION NOISE USING HIGHER HARMONIC PITCH CONTROL
Thomas F. Brooks, Earl R. Booth, Jr., J. Ralph Jolly, Jr., William T. Yeager, Jr., and Matthew L. Wilbur (Army Aviation Systems Command, Hampton, VA.) Jul. 1989 20 p
(NASA-TM-101624; AVSCOM-TM-89-B-005; NAS 1.15:101624) Avail: NTIS HC A03/MF A01 CSCL 20A

An acoustics test using an aeroelastically scaled rotor was conducted to examine the effectiveness of higher harmonic blade pitch control for the reduction of impulsive blade-vortex interaction (BVI) noise. A four-bladed, 110 in. diameter, articulated rotor model was tested in a heavy gas (Freon-12) medium in Langley's Transonic Dynamics Tunnel. Noise and vibration measurements were made for a range of matched flight conditions, where prescribed (open-loop) higher harmonic pitch was superimposed on the normal (baseline) collective and cyclic trim pitch. For the inflow-microphone noise measurements, advantage was taken of the reverberance in the hard walled tunnel by using a sound power determination approach. Initial findings from on-line data processing for three of the test microphones are reported for a 4/rev (4P) collective pitch control for a range of input amplitudes and phases. By comparing these results to corresponding baseline (no control) conditions, significant noise reductions (4 to 5 dB) were found for low-speed descent conditions, where helicopter BVI noise is most intense. For other rotor flight conditions, the overall noise was found to increase. All cases show increased vibration levels. Author

N89-27466*# United Technologies Research Center, East Hartford, CT.
NOISE PRODUCED BY TURBULENT FLOW INTO A ROTOR: THEORY MANUAL FOR ATMOSPHERIC TURBULENCE PREDICTION AND MEAN FLOW AND TURBULENCE CONTRACTION PREDICTION Final Report
J. C. Simonich Jun. 1989 23 p

(Contract NAS1-17763)
(NASA-CR-181789; NAS 1.26:181789) Avail: NTIS HC A03/MF A01 CSCL 20A

Prediction of helicopter main rotor noise due to ingestion of atmospheric turbulence was analyzed. The analysis combines several different models that describe the fluid mechanics of the turbulence and the ingestion process. Two models, atmospheric turbulence, and mean flow and turbulence contraction were covered. The third model, covered in a separate report, describes the rotor acoustic mode. The method incorporates the atmospheric turbulence model and a rapid distortion turbulence contraction description to determine the statistics of the anisotropic turbulence at the rotor plane. The analytical basis for a module was provided which was incorporated in NASA's ROTONET helicopter noise prediction program. The mean flow and turbulence statistics associated with the atmospheric boundary layer were modeled including effects of atmospheric stability length, wind speed, and altitude. The turbulence distortion process is modeled as a deformation of vortex filaments (which represent the turbulence field) by a mean flow field due to the rotor inflow. Author

N89-27467*# National Aeronautics and Space Administration. Langley Research Center, Hampton, VA.
NOISE RADIATION CHARACTERISTICS OF THE WESTINGHOUSE WWG-0600 (600kW) WIND TURBINE GENERATOR
Kevin P. Shepherd and Harvey H. Hubbard (Planning Research Corp., Hampton, VA.) Jul. 1989 32 p Sponsored by Solar Energy Research Inst.
(NASA-TM-101576; NAS 1.15:101576) Avail: NTIS HC A03/MF A01 CSCL 20A

Acoustic data are presented from five different WWG-0600 machines for the wind speed range 6.7 to 13.4 m/s, for a power output range of 51 to 600 kW and for upwind, downwind and crosswind locations. Both broadband and narrowband data are presented and are compared with calculations and with similar data from other machines. Predicted broadband spectra are in good agreement with measurements at high power and underestimate them at low power. Discrete frequency rotational noise components are present in all measurements and are believed due to terrain induced wind gradients. Predictions are in general agreement with measurements upwind and downwind but underestimate them in the crosswind direction. Author

N89-27468*# United Technologies Research Center, East Hartford, CT.
EXPERIMENTAL ASSESSMENT OF HELICOPTER ROTOR TURBULENCE INGESTION NOISE IN HOVER Final Report
J. C. Simonich, R. H. Schlinker, and R. K. Amiet Jul. 1989 68 p
(Contract NAS1-17763)
(NASA-CR-181792; NAS 1.26:181792) Avail: NTIS HC A04/MF A01 CSCL 20A

An experiment was conducted to assess the accuracy of a theory for non-isotropic turbulence ingestion. In order to generate non-isotropic turbulence in a controlled environment, a scale model rotor in a closed chamber was used so that the turbulence generated by the rotor was reingested by the recirculating flow. Simultaneous measurements of turbulence inflow properties and far field acoustics were acquired. Measurements confirmed that the inflow turbulence was highly non-isotropic. The measured aerodynamic properties were used as inputs for the noise prediction procedure. The general agreement between the non-isotropic noise prediction procedure and the experiment was good, although the procedure generally overpredicts the quasi-tonal low to mid range frequencies and underpredicts the higher broadband signals. The predicted sound power level as a function of polar angle was in close agreement with measurements, except near the rotor plane, which is not modeled by the present analysis. It is determined that the most sensitive parameter influencing the predicted noise was the turbulence intensity. Author

N89-27469*# Rensselaer Polytechnic Inst., Troy, NY. Dept. of Mathematical Sciences.
LOW-FREQUENCY SOUND PROPAGATION MODELING OVER A LOCALLY-REACTING BOUNDARY USING THE PARABOLIC APPROXIMATION
J. S. Robertson, W. L. Siegman, and M. J. Jacobson 31 Aug. 1989 26 p
(Grant NAG1-929)
(NASA-CR-185864; NAS 1.26:185864; RPI-Math-175) Avail: NTIS HC A03/MF A01 CSCL 20A

There is substantial interest in the analytical and numerical modeling of low-frequency, long-range atmospheric acoustic propagation. Ray-based models, because of frequency limitations, do not always give an adequate prediction of quantities such as sound pressure or intensity levels. However, the parabolic approximation method, widely used in ocean acoustics, and often more accurate than ray models for lower frequencies of interest, can be applied to acoustic propagation in the atmosphere. Modifications of an existing implicit finite-difference implementation for computing solutions to the parabolic approximation are discussed. A locally-reacting boundary is used together with a one-parameter impedance model. Intensity calculations are performed for a number of flow resistivity values in both quiescent and windy atmospheres. Variations in the value of this parameter are shown to have substantial effects on the spatial variation of the acoustic signal. Author

72 ATOMIC AND MOLECULAR PHYSICS

Includes atomic structure, electron properties, and molecular spectra.

N89-27470# State Univ. of New York, Buffalo. Dept. of Chemistry.
NONRESONANT INTERACTION OF A THREE-LEVEL ATOM WITH CAVITY FIELDS. PART 4: ATOMIC DIPOLE MOMENT AND SQUEEZING EFFECTS Technical Report
Xiao-shen Li, D. L. Lin, Thomas F. George, and Zhen-dong Liu (Center of Theoretical Physics, Beijing, China) Apr. 1989 43 p Prepared in cooperation with Academia Sinica, Shanghai (Peoples Republic of China); and Jiangxi Normal Univ., Nanchang (Peoples Republic of China) Submitted for publication
(Contract N00014-86-K-0043)
(AD-A206788; UBUFFALO/DC/89/TR-97) Avail: NTIS HC A03/MF A01 CSCL 20/5

The behavior of the dipole moment of a three-level atom interacting with cavity fields of arbitrary de-tunings is investigated. The time evolution and squeezing conditions of the components and correlation function of the dipole moment are calculated for three cases: One-mode field and Xi type-atom initially in the upper state, two-mode field and a Lambda-type atom initially in the upper state, and two-mode field and a Lambda-type atom initially in one of the lower states. A number of interesting features are found and discussed. GRA

N89-27471# North Texas State Univ., Denton. Dept. of Physics.
TWO-PHOTON ABSORPTION CHARACTERIZATION OF HgCdTe Annual Interim Report, Aug. 1987 - Aug. 1988
David G. Seiler Jan. 1989 81 p
(Contract DAAB07-87-C-F094; DA Proj. 1L1-61102-A-31-B)
(AD-A207198) Avail: NTIS HC A05/MF A01 CSCL 20/3

Magneto-Optical measurements of Hg(1-x)Cd(X)Te alloys have provided a new means of studying impurities and defects in this important II-VI material. Two-photon magnetoabsorption (TMPA) was used to accurately determine the temperature dependence of the energy gap of various HgCdTe alloys, revealing behavior that deviates from currently accepted models. In addition, magneto-optical techniques were used to detect the presence of both shallow and deep impurities/defects and accurately determine their activation energies, thus providing information necessary for

understanding the electrical and optical properties of the material. GRA

N89-27472# Los Alamos National Lab., NM. Theoretical Div.
FINAL STATE EFFECTS IN LIQUID He4: AN EXPERIMENTAL TEST
P. E. Sokol, R. N. Silver, T. R. Sosnick, and W. M. Snow (Argonne National Lab., IL.) 1989 9 p Presented at the Workshop on Momentum Distributions, Argonne, IL, 24 Oct. 1988
(Contract W-7405-eng-36)
(DE89-012615; LA-UR-89-1607; CONF-8810118-8) Avail: NTIS HC A02/MF A01

Inelastic neutron scattering at high momentum transfers can provide direct information on the atomic momentum distribution n(p) when the Impulse Approximation (IA) is valid. In isotropic systems, the scattering in the IA is directly proportional to the longitudinal momentum distribution which is a function of a single scaling variable Y is identical with (M/Q)(omega - omega sub r), where M is the mass of the scatterer, Q is the momentum transfer, and omega sub r = Q squared/2M is the recoiled energy. However, the experimentally attainable Q's are not large enough to reach the IA limit. Deviations from the IA due to final state scattering by neighboring atoms, known as final state effects, will distort the observed scattering from the IA prediction. Thus, an understanding of deviations from the IA is essential to accurate determination of n(p). Liquid helium provides an excellent testing ground for studying FSE in a dense, strongly interacting system for two reasons. First, theoretical calculations of the momentum distributions are available in both the normal liquid, and superfluid phases. These calculations are believed to be quite accurate, since they agree well with several other measured properties of the liquid. In addition, n(p) in the superfluid exhibits a very sharp feature, the Bose condensate peak, which should be very sensitive to FSE. Comparison of the predicted scattering obtained from the theoretical n(p) using the IA to the experimentally observed scattering can be used to study deviations due to FSE. DOE

N89-27473# Illinois Inst. of Tech., Chicago. Dept. of Physics.
THEORETICAL STUDIES IN ELEMENTARY PARTICLE PHYSICS Progress Report, Mar. 1988 - Jan. 1989
John Clements Collins 1989 20 p
(Contract DE-FG02-85ER-40235)
(DE89-012701; DOE/ER-40235/T5) Avail: NTIS HC A03/MF A01

This report briefly discusses the following topics: factorization, fundamental perturbative quantum chromodynamics (QCD); polarization and hard scattering; small x; Drell-Yan phenomenology; cosmic ray physics; cosmic strings and proton decay; dynamical symmetry breaking and inflation; and QCD as a model for mesons. DOE

N89-27474# Argonne National Lab., IL. Materials Science Div.
HIGH-TEMPERATURE BEHAVIOR OF GRAIN BOUNDARIES FROM EMBEDDED ATOM METHOD MOLECULAR DYNAMICS SIMULATION
J. F. Lutsko, D. Wolf, and S. R. Phillpot Dec. 1988 8 p Presented at the Symposium on Atomic Scale Calculations in Materials Science, Boston, MA, 28 Nov. - 3 Dec. 1988
(Contract W-31-109-eng-38)
(DE89-013641; CONF-8811147-3) Avail: NTIS HC A02/MF A01

The behavior of a metallic grain boundary at high temperatures is studied using an embedded atom potential. A recently developed molecular dynamics code is used which allows the simulation of an isolated grain boundary at temperatures as high as the bulk melting point. The stability of the boundary below the melting point is studied and compared with earlier investigations which have suggested the existence of a premelting transition. It is found that the boundary migrates at high temperature but remains well defined up to the bulk melting point. In contrast to simulations of ideal crystals, it was not possible to superheat the grain boundary due to the nucleation of bulk melting at the boundary. DOE

N89-27475# California Univ., Berkeley. Lawrence Berkeley Lab. Accelerator and Fusion Research Div.
MULTIPLE-ELECTRON PROCESSES IN FAST ION-ATOM COLLISIONS
A. S. Schlachter Mar. 1989 29 p Presented at the Workshop on Highly Charged Ions: New Physics and Advanced Techniques, Berkeley, CA, 13-15 Mar. 1989 Submitted for publication
(Contract DE-AC03-76SF-00098)
(DE89-012982; LBL-26900; CONF-890387-6) Avail: NTIS HC A03/MF A01

Research in atomic physics at the Lawrence Berkeley Laboratory Super-HILAC and Bevalac accelerators on multiple-electron processes in fast ion-atom collisions is described. Experiments have studied various aspects of the charge-transfer, ionization, and excitation processes. Examples of processes in which electron correlation plays a role are resonant transfer and excitation and Auger-electron emission. Processes in which electron behavior can generally be described as uncorrelated include ionization and charge transfer in high-energy ion-atom collisions. A variety of experiments and results for energies from 1 MeV/u to 420 MeV/u are presented. DOE

N89-27476# Oak Ridge National Lab., TN. Engineering Physics and Mathematics Div.
SHIELD OPTIMIZATION PROGRAM. PART 1: EXECUTIVE SUMMARY
R. T. Santoro and T. A. Gabriel Jun. 1989 48 p
(Contract DE-AC05-84OR-21400)
(DE89-013335; ORNL/TM-11143-Pt-1) Avail: NTIS HC A03/MF A01

Detailed studies have been completed to estimate the radiation-induced damage in sensitive electronic components carried on a space-based interceptor weapons platform. The architecture of the interceptor was devised to be as realistic as possible. The analyses were completed for natural (Van Allen belt protons and electrons at an orbital altitude of 500 km) and man-made (nuclear weapons: neutrons, gamma-rays, X-rays, and pumped electron belts) radiation expected to be encountered by a SDI platform. Studies have also been completed to determine the hydrodynamic responses of beryllium mirror surfaces to mono-energetic X-rays (1 and 2 keV). This work included the effects of impurities which are introduced into the surface during machining. Finally, a comparison of the HULL and PUFF-TFT codes are presented which includes the thermo-mechanical response of an Al slab to 5 keV black body radiation. DOE

N89-27477*# Old Dominion Univ., Norfolk, VA. Dept. of Physics.
NUCLEAR FRAGMENTATION ENERGY AND MOMENTUM TRANSFER DISTRIBUTIONS IN RELATIVISTIC HEAVY-ION COLLISIONS Progress Report, period ended 30 Jun. 1989
Govind S. Khandelwal and Ferdous Khan Aug. 1989 152 p
(Contract NCC1-42)
(NASA-CR-185501; NAS 1.26:185501) Avail: NTIS HC A08/MF A01 CSCL 20H

An optical model description of energy and momentum transfer in relativistic heavy-ion collisions, based upon composite particle multiple scattering theory, is presented. Transverse and longitudinal momentum transfers to the projectile are shown to arise from the real and absorptive part of the optical potential, respectively. Comparisons of fragment momentum distribution observables with experiments are made and trends outlined based on our knowledge of the underlying nucleon-nucleon interaction. Corrections to the above calculations are discussed. Finally, use of the model as a tool for estimating collision impact parameters is indicated. Author

N89-27478# Los Alamos National Lab., NM.
PHYSICS WITH ETA MESONS
Lon-chang Liu 1989 16 p Presented at the Symposium on Pion-nucleon and Nucleon-nucleon Physics, Leningrad, USSR, 22 Apr. 1989

(Contract W-7405-eng-36)
(DE89-012582; LA-UR-89-1751; CONF-8904233-1) Avail: NTIS HC A03/MF A01

Since the advent of pion factories, an impressive amount of information about the nuclear dynamics of the delta (1232) pion-nucleon resonance has been obtained. The study of this isospin-3/2 resonance has greatly benefited from the fact that pi(-)n and pi(+) systems are pure I = 3/2 states, which couple only to the delta in the resonance region. Such isospin selectivity of the pion does not exist, however, for the I = 1/2 N* resonances because it is not possible to form a pure I = 1/2 state with a pion and a nucleon. Eta mesons have zero isospin. Consequently, the (eta)N systems are in a pure I = 1/2 state, and eta can be used to tag those N* resonances to which it strongly couples. We will briefly review the N interaction from the threshold region to c.m. energy square root of s is approximate or = to 1600 MeV. It is seen how improved (pi)N data can help the study of (eta)N interactions. What new information about the hadronic interaction that can be learned from the study of eta production in pp collisions is discussed. The behavior of eta meson in nuclei will be discussed. The interesting question of the quark structure of eta(549) and eta'(958) will also be discussed within the framework of a simple model. DOE

N89-27479# Lawrence Livermore National Lab., CA. Theoretical Atomic and Molecular Physics Group.
MOLECULES IN INTENSE LASER FIELDS
S. N. Dixit and V. McKoy (California Inst. of Tech., Pasadena.) May 1989 5 p Presented at the NATO Advanced Study Institute on Atoms in Strong Fields, Kos, Greece, 9-21 Oct. 1988 Submitted for publication
(Contract W-7405-eng-48)
(DE89-013807; UCRL-101134; CONF-8810376-1) Avail: NTIS HC A02/MF A01

In this paper, we will present some thoughts on the dynamics of interaction of molecules with intense laser fields. We will discuss the possible role of dissociation and autoionization in influencing the overall resonant enhanced multiphoton ionization (REMPI) dynamics. Our arguments are of a speculative and qualitative nature and the hope is to stimulate the reader in the complex issues related to the intense field molecule interaction. It is hoped that carefully controlled experiments and new developments in theoretical techniques will help unravel the underlying details of the REMPI dynamics. DOE

N89-27480 Max-Planck-Inst. fuer Plasmaphysik, Garching (Germany, F.R.).
INFLUENCE OF PARTICLE COLLISIONS ON THE CHARACTERISTICS OF H-LIKE ION EMISSION DUE TO CHARGE EXCHANGE REACTIONS WITH FAST ATOMS
A. A. Korotkov Jan. 1989 41 p
(IPP-III/142; ETN-89-94574) Copyright Avail: Fachinformationszentrum Karlsruhe, 7514 Eggenstein-Leopoldshafen 2, Fed. Republic of Germany

The effective emission cross-sections of CVI (3434 A, 5291 A, 7717 A), NVII (3887 A, 5669 A, 7926 A), OVIII (2976 A, 4341 A, 6068 A) lines in charge-exchange reactions of nuclei with hydrogen atoms are calculated. The ground state and the first excited state of hydrogen are considered. The calculation takes into account the mixing of nl-levels due to collisions with plasma deuterons and electrons and Stark 1-mixing in the Lorentz field (V bar X B bar). Calculation of the effective cross-sections with allowance for the atomic beam density distribution in the plasma allows the determination of the line intensities. The influence of the fine structure and Zeeman splitting on the 2976 A OVII line profile is considered. ESA

N89-27481# Max-Planck-Inst. fuer Physik und Astrophysik, Munich (Germany, F.R.). Inst. fuer Physik.
[ACTIVITIES OF THE WERNER-HEISENBERG INSTITUTE OF PHYSICS] Annual Report, 1988 [JAHRESBERICHT 1988]
Dec. 1988 157 p In GERMAN Original contains color illustrations
(ISSN-0173-6256; ETN-89-94607) Copyright Avail: NTIS HC A08/MF A01

Theoretical studies are devoted to elementary particle physics, renormalization of quantum field theories, methods of statistical mechanics, investigation of standard models, supersymmetry, strings, membranes, elementary particles in cosmology, neutrino detectors, nonrelativistic particle physics and quantum history. Experimental studies concern the production and transformation processes of elementary particles neutrino-nucleon interactions, electron-proton storage ring HERA, electronic equipment for CERN, ALEPH project, NA32, DELOS, and HEGRA experiments. ESA

N89-27482# Rome Univ. (Italy). Dipartimento di Fisica.
SOME CONSIDERATIONS ON THE BIRTH OF MOLECULAR PHYSICS IN THE FIRST HALF OF THE 19TH CENTURY [ALCUNE CONSIDERAZIONI SULLA NASCITA DELLA FISICA MOLECOLARE NELLA PRIMA META' DELL'OTTOCENTO]
M. Grilli and F. Sebastiani 30 Jun. 1988 21 p In ITALIAN
(Nota-Interna-917; ETN-89-94736) Avail: NTIS HC A03/MF A01

The history of the introduction of molecular concepts in physics is discussed, including Mosotti's analysis of intramolecular forces (1836), dielectric polarization, and double refraction. ESA

N89-27483# Rome Univ. (Italy). Dipartimento di Fisica.
PRECISION MEASUREMENTS WITHOUT POLARIZATION AT LEP
E. Longo 4 Aug. 1988 18 p Presented at the Workshop on Polarization, Geneva, Switzerland, 9-11 Nov. 1987 Submitted for publication
(Nota-Interna-921; ETN-89-94740) Avail: NTIS HC A03/MF A01

Many measurements, in particular precision tests of the Standard Model, will be based on energy scans, say a coarse one through the whole range of the machine, and a finer one across the resonance. An integrated luminosity of 50 p/b should safely lead to the limits set by the systematics. Similarly, 100 to 200 p/b on top of the Z(0) will fully probe the discovery potential of unpolarized LEP-1. These figures must be completely revised in the case of unexpected deviations from Standard Model predictions or (even more) in the case of new discoveries, for instance to the case where the top is in the LEP-1 range. Standard measurements at LEP-2 call for a substantially higher amount of integrated luminosity (order of 500 p/b), so that every effort should be invested in reaching for this phase the highest possible performances of the machine. ESA

N89-27484# Rome Univ. (Italy). Dipartimento di Fisica.
SEARCH FOR THE INCLUSIVE PRODUCTION OF J/psi IN e(+)e(-) COLLISIONS USING PLUTO DATA
F. Ferrarotto 27 Oct. 1988 15 p
(Nota-Interna-923; ETN-89-94742) Avail: NTIS HC A03/MF A01

Inclusive production of J/psi was searched for in e+ e- hadronic events collected by the PLUTO detector at the storage ring PETRA in a range of energies from 30 to 35 GeV. The data were analyzed identifying muons in multihadronic events and looking for the decay mode J/psi yields mu(+)mu(-). With no candidate found, the upper limit obtained for the total cross section is sigma (e+ e- yields J/psi + X) less than or = 12 pb (90 percent C.L.) using an integrated luminosity (integral of dL approx. = 42 p/b) at the average c.m. energy, square root of s = 34.4 GeV. Together with previous results, this rules out a model based on nonperturbative quantum chromodynamic (QCD) production mechanisms. ESA

N89-27485# Rome Univ. (Italy). Dipartimento di Fisica.
FIRST RESULTS FOR THE DELTA I = 1/2 AMPLITUDE IN K DECAYS, WITH QUENCHED LATTICE QCD AND WILSON FERMIONS
M. B. Gavela, L. Maiani, S. Petrarca, G. Martinelli, and O. Pene (Centre National de la Recherche Scientifique, Orsay, France)

1988 14 p Submitted for publication Sponsored in part by Italian Ministry of Education, Rome
(Preprint-599; ETN-89-94688) Avail: NTIS HC A03/MF A01

The results of a calculation of the Delta I = 1/2 K-pi and K-pipi amplitudes in quenched lattice QCD with Wilson fermions are presented. The results were obtained on a 20 x 10 sq x 40 lattice at beta = 6.0 for 3 values of the light quark masses and on a 16 cu x 48 lattice at Beta = 6.2 for 2 values of the light quark masses. Within large statistical and systematic uncertainties, results support the observed enhancement. The eye diagrams, from which penguin operators are generated at low scales, are the sources of the enhancement. The possible role played by octet-scalar particles in the quark mass range is discussed. ESA

N89-27486# Rome Univ. (Italy). Dipartemento di Fisica.
VERTEX DETECTORS AT e(+) e(-) B MESON FACTORIES
G. Gratta, A. S. Schwarz, and C. Zaccardelli (California Univ., Santa Cruz.) 16 May 1988 56 p Submitted for publication Sponsored by DOE, Washington, DC
(Nota-Interna-914; ETN-89-94733; SCIPP-88/04) Avail: NTIS HC A04/MF A01

The possible applications of high resolution vertex detectors at B meson factories based on e(+) e(-) collisions are discussed with special emphasis on the different possible kinematic regions (Upsilon (4S) resonance, boosted Upsilon (4S) resonance and e(+) e(-) continuum at 12 to 20 GeV). The observability of B(0) B(0) mixing as a function of the B meson decay length is used to define the minimal requirements on the precision of a vertex detector system. Implications on the design of the detector as well as of the collider are investigated and the technological feasibility of the required spatial resolution is discussed. ESA

N89-27487# Rome Univ. (Italy). Dipartimento di Fisica.
RELATIVISTIC CORRECTIONS TO PHOTON SCATTERING POLARIZABILITIES
M. DeSanctis 22 Jun. 1988 28 p Sponsored by the Italian Ministry of Public Education, Rome
(Nota-Interna-916; ETN-89-94735) Avail: NTIS HC A03/MF A01

Photon scattering polarizabilities including m(-2) relativistic corrections are studied. The significant cancellations obtained by extensive use of gauge conditions are emphasized. Low-energy theorems are derived for both elastic and inelastic parity non-changing transitions. ESA

N89-27488# Rome Univ. (Italy). Dipartimento di Fisica.
CORRELATION AND ANALYSIS BETWEEN THE KAMIOKA NEUTRINO DETECTOR DATA AND THE MARYLAND AND ROME GRAVITATIONAL ANTENNA DATA
E. Amaldi, P. Bonifazi, E. Coccia, S. Frasca, D. Gretz, G. V. Pallotino, G. Pizzella, P. Rapagnagni, F. Ricci, and J. Weber (Maryland Univ., College Park.) et al 5 Jul. 1988 26 p Sponsored by the Instituto Nazionale di Fisica Nucleare, Italy; CNR, Italy and NSF, Washington, DC
(Nota-Interna-918; ETN-89-94737) Avail: NTIS HC A03/MF A01

The data recorded by the gravitational wave and by the neutrino detectors were analyzed from 22 February 0 hr UT to 23 February 8 hr UT 1987. A correlation is found at the Mont Blanc time with features very similar to that already found using the Mont Blanc data if a time of 8 sec is added to the time recorded on the Kamiokande magnetic tape. This time difference is in agreement with the time difference between the IMB and Kamiokande signals. The probability that the above correlation be due to change is estimated to be of the order of a few percent. ESA

N89-27489# Rome Univ. (Italy). Dipartimento di Fisica.
COVARIANCE PROPERTIES OF THE MULTIQUARK HAMILTONIAN IN THE CONSTITUENT QUARK MODEL
M. DeSanctis, R. Mignani, and D. Prosperi 13 Jul. 1988 42 p Prepared in cooperation with Istituto Nazionale di Fisica Nucleare, Rome, Italy
(Nota-Interna-920; ETN-89-94739) Avail: NTIS HC A03/MF A01

The Poincare covariance of the Hamiltonian of a N-fermion system, in which the two-body interaction is produced by the exchange of a massless vector boson with a nonconstant form factor at vertices, is investigated. The relativistic separation of center-of-mass and internal-motion variables is performed by exploiting an approach developed by Krajcik and Foldy (1974). It is shown that, in order to ensure that the N-fermion Hamiltonian (expanded up to the order 1/cs) is the time-translation generator of the Poincare algebra, one requires a correct treatment of the form factor at the order considered, and, for non-commuting particle charges, the inclusion in the potential of three-body terms, whose expression is explicitly derived. Analysis of the effect of such terms is given for baryons and deuterium in the framework of the constituent quark model. ESA

N89-27490# Rome Univ. (Italy). Dipartimento di Fisica.
MULTIPARTICLE DYNAMICS AT THE Sp(-)p COLLIDER
Filippo Ceradini 20 Dec. 1988 21 p Presented at the Perugia Workshop on Multiparticle Dynamics, Italy, 21-28 Jun. 1988
(Nota-Interna-929; ETN-89-94748) Avail: NTIS HC A03/MF A01

Features of inelastic proton-antiproton collisions at the CERN SPS collider are studied with the UA1 detector using magnetic and calorimetric analysis. Results on charged particle multiplicities, on transverse and longitudinal momenta, and on transverse energy distributions at center of mass energies 0.2 to 0.9 TeV are presented. The same variables are used to study the multiparticle system (spectators) produced in events with jets of W bosons at root s = 0.63 TeV. ESA

N89-27491# Washington Univ., Seattle.
ANTIPROTON AND MILLIMETER WAVE RESEARCH Final Report, 30 Jul. 1986 - 29 Mar. 1988
Gerald Gabrielse 26 Jan. 1989 3 p
(Grant AF-AFOSR-0250-86; AF Proj. 2917)
(AD-A208363; AFOSR-89-0657TR) Avail: NTIS HC A02/MF A01 CSCL 20/8

The DOD Instrumentation Grant was used to purchase equipment for antiproton experiments and for the production of high frequency microwaves. The antiproton experiments are progressing very nicely. In particular, we have recently cooled antiprotons below 1 eV in energy. Before we started these experiments, the lowest energy antiprotons available had kinetic energies 5 million times higher. The purchased equipment was essential to the antiproton experiments and is being very heavily used. The final version of the millimeter microwave system is completed. It is working although there are still some problems remaining. GRA

73 NUCLEAR AND HIGH-ENERGY PHYSICS

Includes elementary and nuclear particles; and reactor theory.

For space radiation see *93 Space Radiation.*

N89-27492# Sandia National Labs., Albuquerque, NM.
A ONE-DIMENSIONAL SCINTILLATOR CAMERA FOR THE SATURN X-RAY SIMULATION ACCELERATOR
D. L. Fehl, J. R. Lee, R. J. Leeper, M. A. Hedemann, and W. A. Stygar 1989 28 p Presented at the Instrumentation for Nuclear Weapons Effects Testing Conference, Monterey, CA, 5 Jun. 1989
(Contract DE-AC04-76DP-00789)
(DE89-009327; SAND-89-0188C; CONF-890694-1) Avail: NTIS HC A03/MF A01

New X-ray diagnostics are needed to probe the efficiency of a modern pulsed-power, flash X-ray simulator. In this talk we shall examine some of the critical diagnostic issues which pertain to the SATURN facility located at Sandia National Laboratories. Two

new X-ray cameras have been developed for this simulator. A multiframe pinhole camera will be described in a companion talk at this conference. This talk focuses on a one-dimensional camera based on a fast scintillator array. I shall describe its construction, operation, and relative calibration. These cameras together have given us valuable insights into the workings of the SATURN X-ray source, and we shall examine in some detail the results from a SATURN experiment. DOE

N89-27493# Los Alamos National Lab., NM.
RECENT PROGRESS IN THE LOS ALAMOS KrF PROGRAM
T. E. McDonald, D. C. Cartwright, S. V. Coggeshall, C. A. Fenstermacher, J. F. Figueira, L. R. Foreman, P. D. Goldstone, D. E. Hanson, D. B. Harris, and A. A. Hauer et al 1988 8 p Presented at the 12th International Conference on Plasma Physics and Controlled Nuclear Fusion Research, Nice, France, 12-19 Oct. 1988
(Contract W-7405-eng-36)
(DE88-016235; LA-UR-88-2743; CONF-881015-7; IAEA-CN-50/B272) Avail: NTIS HC A02/MF A01

The goal of the Inertial Confinement Fusion Program (ICF) is to develop the ability to ignite and burn small masses of thermonuclear fuel. Although the present near-term objectives of the program are directed toward defense applications, ICF research continues to be carried out with a view to the longer term goal of commercial power production. The characteristics of a KrF laser make it an attractive candidate as an ICF driver. The KrF wavelength of 248 nm provides a target coupling that is very high at intensities of 10(14) w/sq cm. In addition, the KrF laser can be repetitively operated at frequencies appropriate for a power reactor and has an intrinsically high efficiency, which allows projections to the long-term goal of energy production. The ICF program at Los Alamos consists of driver development, target design and fabrication, and target experimentation. The major effort at present is the investigation and development of KrF technology to determine its applicability for use in a laboratory driver at Los Alamos. Such a driver would be used in defense related technology studies and in areas of scientific study such as highly ionized materials and high energy density physics. DOE

N89-27494# Los Alamos National Lab., NM.
SAFETY TESTING PROGRAM FOR THE GALILEO MISSION RADIOISOTOPE THERMOELECTRIC GENERATOR
Theresa A. Cull 1989 16 p Presented at the 9th International System Safety Conference, Long Beach, CA, 17 Jul. 1989
(Contract W-7405-eng-36)
(DE89-011192; LA-UR-89-1178; CONF-890780-1) Avail: NTIS HC A03/MF A01

The major design requirement for any space nuclear power system is to minimize the potential for interaction of the radioactive materials with Earth's population and environment. All previous space power systems were launched on expendable launch vehicles (ELVs), so the design emphasis for the General Purpose Heat Source (GPHS) was on surviving the most severe ELV accident environments (launch pad explosion and solid propellant fire) and on surviving accident environments resulting from spacecraft failure (reentry and land impact). DOE

N89-27495# Technische Univ., Delft (Netherlands).
ADVANCED ELECTRON BEAM EVAPORATION Ph.D. Thesis
Abraham Jacob Guilla Schellingerhout 1988 124 p Sponsored by Stichting voor Fundamenteel Onderzoek der Materie, Amsterdam, Netherlands
(ETN-89-94799) Avail: NTIS HC A06/MF A01

Rate control for electron gun evaporation; mass spectrometer controlled fabrication of Si/Ge superlattices; critical thickness for pseudomorphic growth of Si/Ge alloys and superlattices; fabrication of low-capacitance Josephson-junctions; oxygen concentration and microstructure of granular aluminum; strong electric field effect in granular aluminum; analysis of YBa2Cu3O(7-y) thin films on sapphire substrates made by electron beam evaporation; growth and characterization of a sinusoidally modulated Nb/V superlattice; critical modulation amplitude in monocrystalline Nb/V and Ta/V superlattices; and a strong voltage dependence of the conductivity in granular aluminum are discussed. ESA

N89-27496# Rome Univ. (Italy). Dipartimento di Fisica.
BEAM-GAS BACKGROUND REJECTION IN L3 FIRST LEVEL ENERGY TRANSFER
P. Baratti 11 Jul. 1988 28 p
(Nota-Interna-919; ETN-89-94738) Avail: NTIS HC A03/MF A01

The effect of beam-gas background on L3 experiment is evaluated, computing the rates on individual detectors, and the rejection performance of first level energy trigger. A simulation with Decay-Turtle and Sigel3 programs was done. It uses a complete description of the upward beam line until 640 m from the interaction point and the detailed geometry of L3 setup. Full detector response was considered to produce the trigger data. They were later analyzed with the code that simulates the trigger logic algorithms. ESA

74 OPTICS

Includes light phenomena; and optical devices.
For lasers see *36 Lasers and Masers.*

N89-27497 Department of the Air Force, Washington, DC.
FIBER OPTIC ROTARY SWITCHING DEVICE Patent
Stanley D. Battle, inventor (to Air Force) 28 Jun. 1988 6 p Filed 15 Jan. 1986 Supersedes N86-30499(24 - 21, p 3377)
(AD-D013978; US-Patent-4,753,501; US-Patent-Appl-SN-818922)
Avail: US Patent and Trademark Office CSCL 20/6

A fiber optic rotary switching device having a single optical fiber rotatable between a plurality of optical fibers is disclosed. The arrangement for rotating the single optical fiber is designed such that the single optical fiber flexes but does not twist with respect to an end thereof which is fixed to a light source (or, in the alternative to a light detector). As a result, the switching device switches light passing through the single optical fiber to a preselected one of the plurality of optical fibers while simultaneously preventing extraneous light from reaching the other optical fibers. GRA

N89-27498# Technische Univ., Eindhoven (Netherlands). Telecommunication Div.
OPTICAL COUPLERS FOR COHERENT OPTICAL PHASE DIVERSITY SYSTEMS
J. Siuzdak (Instytut Telekomunikacji PW, Warsaw, Poland) Mar. 1988 44 p
(EUT-88-E-190; ISBN-90-6144-190-0; ISSN-0167-9708; ETN-89-94778) Avail: NTIS HC A03/MF A01

Optical couplers, used in coherent optical phase diversity systems, are analyzed. On the basis of the coupled modes propagation theory, expressions for the output optical fields are obtained. The signal to noise ratio (SNR) at the output of a receiver using these couplers is computed. The variation of SNR with changes of the coupling coefficient is examined for various couplers. The influence of coupling losses is also investigated. The analysis favors two schemes: a three fiber coupler and a four fiber coupler. When the relative noise intensity (RIN) is substantial the four fiber device is best. Three fiber couplers are best when RIN is negligible. ESA

N89-27499 Department of the Air Force, Washington, DC.
OPTICAL MIRROR COATED WITH ORGANIC SUPERCONDUCTING MATERIAL Patent
John A. Lake, inventor (to AF) and William B. Heath, inventor (to AF) 16 Aug. 1988 4 p Filed 3 Nov. 1986
(AD-D014047; US-Patent-4,764,003; US-Patent-Appl-SN-925959)
Avail: US Patent and Trademark Office CSCL 11/3

An optical mirror has enhanced reflectivity and reduced thermal distortions when it is composed of a substrate coated with a reflective coating made of an organic superconducting material.

The substrate is best constructed of materials which have the most favorable thermal expansion and thermal conduction characteristics at temperatures near 0 K. such as: silicon, diamond, copper, and sapphire. The reflective coating is only a few microns thick and composed of organometallic compounds and is cooled to superconducting or cryogenic temperatures of less than 100 K. GRA

N89-27500# Carnegie-Mellon Univ., Pittsburgh, PA. Dept. of Electrical and Computer Engineering.
TIME-SEQUENTIAL OPTICAL DATA PROCESSING Annual Report, 1 Jan. 1988 - 31 Dec. 1989
David Casasent 1 Feb. 1989 78 p
(Contract N00014-86-K-0599)
(AD-A207514) Avail: NTIS HC A05/MF A01 CSCL 17/5

Our work has emphasized analog optical processing for three levels of multitarget tracking: target detection, track initiation and target tracking. New algorithms and new optical processing architectures have resulted, and initial quantitative results have been obtained for each phase of the work. A new acousto-optic implementation of our sub-pixel target detection algorithm was devised and tested. This involved a new algorithm and architecture that achieves image registration, interpolation and subtraction. This technique is thus suitable for general image registration applications also. A 2-D Hough transform optical processor is used for track initiation. It allows accumulation of target measurements until sufficient confidence has been established that a target track exists. It provides position and velocity estimates for each target and predictions of the next vector location of each target. A new threshold Hough transform provides improved performance and reduced false alarms in noise. Very impressive results from many multiple targets were obtained. This work is also suitable for general object feature extraction and product inspection applications. We devised a completely new realization of the Joint Probabilistic Data Association Algorithm for multitarget tracking and a most attractive new acousto-optic architecture to achieve this. Finally, a new analogy neural net algorithm and architecture was formulated. GRA

N89-27501# Army Lab. Command, Watertown, MA. Material Technology Lab.
THE QUANTITATIVE DEPENDENCE OF TRANSMISSIVITY ON FLEXURAL STRAIN FOR MULTIMODE OPTICAL FIBER Final Report
James A. Kidd, Jr. Feb. 1989 29 p
(AD-A207522; MTL-TR-89-14) Avail: NTIS HC A03/MF A01 CSCL 20/6

Four different multimode optical fibers were tested to obtain the following correlations: (1) signal power with bend radius, (2) strain with bend radius, and (3) signal power with strain. The data are presented numerically, graphically, and mathematically. Graded index multimode and step index multimode fibers are discussed. The mechanism for the attenuation of light in optical fiber as a result of macrobending is examined. Three of the tested fibers demonstrated a consistent relationship between flexural strain and light transmissivity and could potentially be inlaid with a curved composite material system for use as the principal component in a stress or strain transducer. GRA

N89-27502# Air Force Inst. of Tech., Wright-Patterson AFB, OH. School of Engineering.
MULTIPLE SENSOR FUSION FOR DETECTING TARGETS IN FLIR (FORWARD-LOOKING INFRARED) AND RANGE IMAGES Ph.D. Thesis
Michael C. Roggemann May 1989 142 p
(AD-A207577; AFIT/DS/ENP/89-1) Avail: NTIS HC A07/MF A01 CSCL 17/5

Automatic detection of tactical targets in corresponding sets of non-pixel registered forward-looking infrared (FLIR) sensor images and range sensor images was studied. A processing architecture was developed to address the problems associated with processing non-pixel registered imagery. The architecture used specialized sensor-dependent processing to segment the images, measure features, and analyze the single sensor feature data. The multiple sensor process of geometric registration, multiple sensor feature measurement, and multiple sensor target detection were then applied. Sensor-dependent segmentation processes passed a large fraction of the targets present in the imagery, along with a larger number of regions which did not correspond to any target. FLIR images were segmented based on pixel brightness. A new range image segmentation algorithm was developed which exploited the small-scale planarity of tactical vehicles. The post-segmentation target detection problem was that of partitioning segmented targets from segmented non-target regions. Feature information was processed to accomplish this task. The Bayesian minimum error criterion was adopted as the decision rule. When performance was optimized for all cases, the multiple sensor approaches were found to provide improved performance in all comparative performance measures. GRA

N89-27503# Department of the Navy, Washington, DC.
EFFICIENT DYNAMIC PHASEFRONT MODULATION SYSTEM FOR FREE-SPACE OPTICAL COMMUNICATIONS Patent Application
G. G. Gilbreath, inventor (to Navy) and F. E. Davidson, inventor (to Navy) 9 Sep. 1988 29 p
(AD-D014128; US-Patent-Appl-SN-242678) Avail: NTIS HC A03/MF A01 CSCL 25/5

An optical communications system is disclosed for correcting in real-time the wavefront distortions of a beam from a coherent optical transmitting source. The system includes a collimating lens and beam splitter for receiving distorted wavefront signal beam and splitting the beam into a pump beam and a weaker intensity signal beam. The system includes a detector and computer for measuring the beam distortion and specifying a compensatory wavefront. The weaker intensity signal beam is modified in a 2-D spatial light modulator according to a compensatory wavefront. A photo-refractive material is used to couple energy from the pump beam to the compensated wavefront signal beam thereby producing a corrected and intensity-enhanced communications beam. GRA

N89-27504*# National Aeronautics and Space Administration. Langley Research Center, Hampton, VA.
ROTATION OF IMAGES BY SCAN MIRRORS
Stephen J. Katzberg Jun. 1989 11 p
(NASA-TM-101628; NAS 1.15:101628) Avail: NTIS HC A03/MF A01 CSCL 20F

An analysis is presented of the effects of scan mirrors on scene orientation or rotation for image forming systems. Some simple vector relationships are presented, which when combined with the anticipated application conditions, make it possible to easily assess image orientation effects resulting from scan mirrors. Examples are cited to demonstrate the application of the analysis. K.C.D.

N89-27505# Sandia National Labs., Albuquerque, NM. Microsensor Research Div.
A FIBER OPTIC TEST SYSTEM FOR QUANTUM EFFICIENCY MEASUREMENTS
K. B. Pfeifer and M. W. Jenkins May 1989 24 p
(Contract DE-AC04-76DP-00789)
(DE89-012823; SAND-89-0593) Avail: NTIS HC A03/MF A01

A design for a photodetector quantum efficiency measurement test system is presented. The system hardware and control software are explained and the measurement theory is given. A brief discussion of the operation of the prototype is given. Finally, the article concludes with an example of a quantum efficiency measurement of a sample and a discussion of the errors involved in the measurement. DOE

N89-27506*# National Aeronautics and Space Administration. Lewis Research Center, Cleveland, OH.
DIAMONDLIKE CARBON PROTECTIVE COATINGS FOR OPTICAL WINDOWS
Diane M. Swec and Michael J. Mirtich 1989 16 p Presented at the 1989 Technical Symposia on Aerospace Sensing, Orlando,

FL, 27-31 Mar. 1989; sponsored by The International Society for Optical Engineering
(NASA-TM-102111; E-4881; NAS 1.15:102111) Avail: NTIS HC A03/MF A01 CSCL 20F

Diamondlike carbon (DLC) films were deposited on infrared transmitting optical windows and were evaluated as protective coatings for these windows exposed to particle and rain erosion. The DLC films were deposited on zinc selenide (ZnSe) and zinc sulfide (ZnS) by three different ion beam methods: (1) sputter deposition from a carbon target using an 8-cm argon ion source; (2) direct deposition by a 30-cm hollow cathode ion source with hydrocarbon gas in argon; and (3) dual beam direct deposition by the 30-cm hollow cathode ion source and an 8-cm argon ion source. In an attempt to improve the adherence of the DLC films on ZnSc and ZnS, ion beam cleaning, ion implantation with helium and neon ions, or sputter deposition of a thin, ion beam intermediate coating was employed prior to deposition of the DLC film. The protection that the DLC films afforded the windows from particle and rain erosion was evaluated, along with the hydrogen content, adherence, intrinsic stress, and infrared transmittance of the films. Because of the elevated stress levels in the ion beam sputtered DLC films and in those ion beam deposited with butane, films thicker than 0.1 micron and with good adherence on ZnS and ZnSe could not be generated. An intermediate coating of germanium successfully allowed the DLC films to remain adherent to the optical windows and caused only negligible reduction in the specular transmittance of the ZnS and ZnSe at 10 microns.
Author

N89-27507# National Bureau of Standards, Boulder, CO. Electromagnetic Technology Div.
SYSTEM FOR MEASURING OPTICAL WAVEGUIDE INTENSITY PROFILES
Lee E. Larson (Denison Univ., Granville, OH.), Donald R. Larson, and Robert J. Phelan, Jr. Aug. 1988 67 p
(PB89-188593; NBSIR-88/3092) Avail: NTIS HC A04/MF A01 CSCL 20A

A computer controlled system has been developed to measure the intensity profile of optical waveguides. Knowledge of the intensity profile provides an indication of the shape of the waveguide, and therefore the degree to which light can be coupled to the guide from an optical fiber. The report describes the construction and operation of the system.
Author

N89-27508# Argonne National Lab., IL. Materials Science Div.
MAGNETO-OPTICAL PROPERTIES OF ULTRATHIN FERROMAGNETIC FILMS
S. D. Bader, E. R. Moog, C. Liu, and J. Zak Apr. 1989 12 p Presented at the Spring Meeting of the Materials Research Society, Symposium on Magneto-Optic Data, San Diego, CA, 24-29 Apr. 1989
(Contract W-31-109-eng-38)
(DE89-014640; CONF-890426-20) Avail: NTIS HC A03/MF A01

The surface magneto-optic Kerr effect (SMOKE) has been used to explore the properties of ultrathin ferromagnetic films. The ultrathin regime corresponds to thicknesses less than the depth penetration of light and includes the monolayer range. The ultrathin regime possesses unique magneto-optic properties: the Kerr rotation and ellipticity, in general, behave differently than in the thick film limit. Measurements and simulation in the longitudinal geometry for bcc Fe on Au(100) provide a dramatic example of the metallic reflector enhancement effect due to the nonmagnetic Au underlayer. The rotation enhancement is accompanied by a high reflectivity, as opposed to being at the expense of the reflectivity. Measurements in both polar and longitudinal geometries for epitaxially-stabilized fcc Fe films grown on Cu(100) and Pd(100) indicate the presence of perpendicular surface anisotropy, which suggests new approaches to realizing vertical data-storage media.
DOE

N89-27509# Technische Univ., Delft (Netherlands).
INTEGRATED SILICON COLOR SENSORS Ph.D. Thesis
Reinoud Felix Wolffenbuttel 1988 114 p
(ETN-89-94800) Avail: NTIS HC A06/MF A01

The possibility of applying the wavelength dependence of the absorption coefficient in silicon for radiation in the visible part of the spectrum for color sensing was investigated. Evaluation of the parasitic wavelength dependences shows that color detectors in silicon with a well-defined, distinct, and reproducible response can be obtained by using an electrical control parameter in a single photodiode. Implementations of the basic color-sensing mechanism are evaluated. The applicability of this sensor in a high-density CCD color imager is restricted by the signal-to-noise ratio. The properties of the two different versions of the color indicator are also discussed. The measured responses are consistent with the results of the simulations. The ratio-type of color indicator has the best performance/complexity ratio.
ESA

N89-27510# Naval Research Lab., Washington, DC. Optical Techniques Branch.
FREQUENCY DIVISION MULTIPLEXING OF INTERFEROMETRIC SENSOR ARRAYS
A. Dandridge, A. B. Tveten, A. M. Yurek, A. D. Kersey, and E. C. McGarry (Sachs/Freeman Associates, Inc., Landover, MD.) 3 May 1989 32 p
(AD-A208448; NRL-MR-6457) Avail: NTIS HC A03/MF A01 CSCL 20/6

This report demonstrates the multiplexing of fiber optic interferometric sensors using a CW phase generated carrier technique. The technique employs modulated diode laser sources at different carrier frequencies, near balanced interferometers (approx. 4 cm path difference) and phase generated carrier demultiplexing demodulation. This approach leads to a simple all-passive sensor array which has intrinsically low crosstalk. The system is analyzed in terms of shot noise performance and crosstalk. An experimental all optical implementation of a four sensor array was demonstrated; both the single sensor and multisensor arrays were limited by the laser phase noise to a sensitivity of approx. 18 micro rad/(sq rt Hz). Crosstalk between individual channels was better than -60 dB. In the absence of laser phase/noise the demodulator/demultiplexer demonstrated approx. 2 microrad performance with both single sensor and four element array operation, and 4 microrad performance with 8 elements in operation.
GRA

75 PLASMA PHYSICS

Includes magnetohydrodynamics and plasma fusion.

For ionospheric plasmas see *46 Geophysics*. For space plasmas see *90 Astrophysics*.

N89-27511# Nagoya Univ. (Japan). Inst. of Plasma Physics.
LIMITER H-MODES IN THE JIPP T-IIU TOKAMAK
K. Toi, K. Adati, R. Akiyama, A. Ando, R. Ando, T. Aoki, D. G. Bi, J. Fujita, Y. Hamada, and S. Hidekuma (National Lab. for High Energy Physics, Tsukuba, Japan) et al Jan. 1989 15 p Presented at the 16th European Conference on Controlled Fusion and Plasma Physics, Venice, Italy, 13-17 Mar. 1989
(IPPJ-898; ISSN-0469-4732) Avail: NTIS HC A03/MF A01

The H-mode is observed in a circular cross-section plasma bounded by a limiter on the JIPP T-IIU tokamak. This H-mode is achieved in the smallest tokamak and also in the highest density regime up to 10(14) cm(-3). The rapid current ramp-down during the additional heating considerably reduces the threshold power to the transition.
Author

N89-27512# Commissariat a l'Energie Atomique, Saint-Paul-les-Durance (France).
TORE SUPRA GRAPHITE INNER FIRST WALL
P. Chappuis, R. Aymar, P. Deschamps, M. Gabriel, and C. Croessman (Sandia National Labs., Albuquerque, NM.) 1988 4 p Presented at the 15th Symposium on Fusion Technology, Utrecht, Netherlands, 19 Sep. 1988

(Contract DE-AC04-76DP-00789)
(DE89-009325; SAND-89-0670C; CONF-880929-11) Avail: NTIS HC A02/MF A01

TORE SUPRA is a fairly large tokamak and has an original goal to withstand a large power removal (25 MW) during a 30 seconds long pulse. One of the main energy removal systems is the inner first wall which was originally designed for the following aims: protect the inner side of the vacuum vessel from normal plasma operation (participates to the plasma power removal) and against disruptive events (plasma energy quench and current decay); act as a toroidal belt limiter during steady state operation and plasma start up; and protect the vacuum vessel from the shine through of the neutral beam injectors and act as a beam dump for short shots. In order to match those different goals the design choice was oriented towards an actively cooled graphite wall capable to sustain an 1 MW/m(2) continuous heat flux. This paper discusses this design concept further. DOE

N89-27513# Helsinki Univ. of Technology, Espoo (Finland). Dept. of Technical Physics.
DYNAMICS OF DOUBLE STIMULATED BRILLOUIN SCATTERING
T. J. H. Paettikangas and R. R. E. Salomaa 1988 34 p
(PB89-146369; TKK-F-A638; ISBN-951-754-704-8) Avail: NTIS HC A03/MF A01 CSCL 20I

The pump wave reflected from the overdense plasma may play an important role in the dynamics of stimulated Brillouin scattering. The particular case of Double Stimulated Brillouin Scattering (DSBS) suggested by Zozulya, Silin, and Tikhonchuk is studied in detail. In DSBS the incident pump wave and the reflected pump wave scatter from a common ion acoustic wave. Some steady state properties of DSBS are reviewed. The analysis of DSBS dynamics is based on a series of numerical experiments. At small pump intensities the system asymptotically approaches a true steady state. When the intensity is increased the solution turns into a regular pulse train with intensity dependent period. Connections between the pulses and soliton-like solutions of a damped sine-Gordon equation are discussed. GRA

N89-27514 Department of the Air Force, Washington, DC.
RADIO FREQUENCY PLASMA GENERATOR Patent
James P. OLoughlin, inventor (to Air Force) 20 Dec. 1988 9 p Filed 12 Jun. 1987
(AD-D013990; US-Patent-4,792,732; US-Patent-Appl-SN-060881)
Avail: US Patent and Trademark Office CSCL 20/9

A plasma generator is disclosed for exciting electrons in the plasma to a uniform energy level. In a preferred embodiment, two sets of mutually perpendicular electrodes surround a container of gas, with one set being driven through a ninety degree phase shifter to establish a circularly polarized field in the space within the container. Alternative means are disclosed for launching circularly polarized RF waves into the container of gas. A desired level of uniform electron energy is achieved by establishing the proper relationship between the frequency and magnitude of the applied circularly polarized field and the mean free path of the electrons in the plasma. GRA

N89-27515# Massachusetts Inst. of Tech., Cambridge. Plasma Fusion Center.
WAVES AND INSTABILITIES IN NONNEUTRAL PLASMAS
Ronald C. Davidson 1989 70 p Presented at the Nonneutral Plasma Physics, Washington, DC, 28 Mar. 1988
(Contract DE-FG02-88ER-40465)
(DE89-012403; DOE/ER-40465/T1; CONF-8803133-1) Avail: NTIS HC A04/MF A01

This paper presents a survey of the equilibrium, stability and collective oscillation properties of magnetically-confined nonneutral plasmas. Emphasis is placed on summarizing several of the technical advances that have occurred in both theory and experiment since the early 1970's. DOE

N89-27516# Sandia National Labs., Albuquerque, NM. Thermophysical Properties Div.
THERMOPHYSICAL PROPERTIES OF ADVANCED CARBON MATERIALS FOR TOKAMAK LIMITERS
E. P. Roth, R. D. Watson, M. Moss, and W. D. Drotning Apr. 1989 142 p
(Contract DE-AC04-76DP-00789)
(DE89-012799; SAND-88-2057) Avail: NTIS HC A07/MF A01

A plasma limiter is used to control the plasma size in Tokamak fusion research devices and serves as the primary area of plasma wall interaction. Contact with the plasma produces very high heat fluxes, typically 500 to 5000 W/sq cm for pulse lengths of 1 to 10 seconds. Wall temperatures can reach as high as 3000 K resulting in significant melting or wall erosion. Graphite and graphite composites have been chosen as the materials that best meet the requirements of this severe environment. Measurement of the thermophysical properties of these materials is critical to the modeling of the thermal response of the limiters during operation. The thermal diffusivities, thermal conductivities and thermal expansions of several candidate materials were measured. The categories of materials investigated in this study were pyrolytic graphite and annealed pyrolytic graphite; fine-grained graphites; anisotropic carbon/carbon fiber composites; two-directionally woven fibers with a graphitized pitch matrix; and carbon/carbon fiber composites with a four-directionally woven carbon fiber wave. The thermal conductivities of the carbon/carbon fiber composites were determined as a function of fiber orientation. Conductivities were measured using both the laser flash diffusivity technique and the thermal comparative method. The advantages and disadvantages of each of these methods are discussed and the data compared. DOE

N89-27517# Colorado Univ., Boulder. Dept. of Astrophysical, Planetary and Atmospheric Sciences.
APPLICATION OF MODERN MATHEMATICAL CONCEPTS TO PLASMA CONFINEMENT Progress Report
John R. Cary Jun. 1989 14 p
(Contract DE-FG02-85ER-53207)
(DE89-012952; DOE/ER-53207/4) Avail: NTIS HC A03/MF A01

Progress in four research areas has been achieved. A second-order symplectic integration algorithm has been developed and tested. Use of this algorithm allows integration of systems of Hamiltonian equations of motion to be carried out with much less computation. Vacuum field optimization techniques have been improved. One result of this work is a simple method for calculating magnetic island widths. Studies of alpha particle transport in toroidal confinement systems were initiated. This has been used as a test bed for studies of symplectic integrators. Quantum modifications of separatrix crossing theory were calculated. In addition the principal investigator is organizing a U.S.-Japan conference concerning the use of modern techniques for the study of plasma confinement. DOE

N89-27518# Texas Univ., Austin. Inst. for Fusion Studies.
EQUILIBRIUM OF A PLASMA IN THE FLUID- AND VLASOV-MAXWELL SYSTEMS
Swadesh M. Mahajan and Wann-Quan Li May 1989 11 p
(Contract DE-FG05-80ET-53088)
(DE89-013315; DOE/ET-53088/372; IFSR-372) Avail: NTIS HC A03/MF A01

It is shown that a recently constructed exact solution of the Vlasov equation describing a plasma with density and temperature gradients can be expressed in terms of the constants of motion. The distribution function is then used to illustrate the differences between a Vlasov and a one fluid description. In fluid theory, only the pressure profile is determined (unless one postulates an equation of state), while the Vlasov description leads to a separate determination of density (g) and temperature (psi) profiles. The equation of state, g = psi to the 3-2/beta power, comes out naturally in the latter case. DOE

N89-27519# National Academy of Sciences - National Research Council, Washington, DC. Committee on Magnetic Fusion in Energy Policy.

PACING THE US MAGNETIC FUSION PROGRAM

1989 157 p

(Contract DE-FG05-87ER-54034)

(DE89-012959; NRC-9012959) Avail: NTIS HC A08/MF A01

This study addresses the priority and pace of the nation's magnetic fusion research and development program in the context of long-term national energy policy. In particular, the committee interpreted its task as follows: to review the implications of long-term national energy policy for current research and development in magnetic fusion; to identify factors that should enter the further development of such policy to reduce risks associated with the future electricity supply system; to propose criteria applicable to research and develop in electric generation in reaching long-term energy policy goals; to apply these criteria to magnetic fusion and alternative electric generation technologies in order to develop recommendations on the priority pace of the magnetic fusion program; and to present its results in a final report. The most important goals of the U.S. Department of Energy's current Magnetic Fusion Energy Program Plan are to demonstrate the scientific and engineering feasibility of fusion. Demonstrating engineering feasibility will require the design, construction, and operation of an engineering test reactor, which the plan envisions financing through a combination of domestic and international funding. The committee believes that current domestic program funding levels are inadequate to meet even the near-term objectives of the plan. DOE

N89-27520# Oak Ridge National Lab., TN.

FAST WAVE CURRENT DRIVE MODELING FOR ITER AND PROSPECTS FOR A NEAR-TERM PROOF OF PRINCIPLE EXPERIMENT

D. B. Batchelor, E. F. Jaeger, M. D. Carter, and D. W. Swain 1989 5 p Presented at the 8th Topical Conference on Radio Frequency Power in Plasmas, Irvine, CA, 1 May 1989

(Contract DE-AC05-84OR-21400)

(DE89-013049; CONF-8905120-16) Avail: NTIS HC A02/MF A01

It is widely recognized that a key element in the development of an attractive tokamak reactor, and in the successful achievement of the mission of ITER is the development of an efficient steady state current drive technique. The two primary issues to be resolved are: An acceptable antenna design producing a k sub parallel spectrum with most power in the phase velocity range nu sub epsilon is less than nu sub phase is less than c and an efficient RF power that will be absorbed by electrons in the desired velocity range without unacceptable parasitic damping by fuel ions and alpha particles. To address these issues the Orion code is employed which gives a 3-D full-wave solution of the fast wave equations in tokamak geometry along with power absorption and current drive profiles. This 3-D code realistically models the launched antenna spectrum with radial focusing, includes toroidal eigenmode effects (multiple pass absorption) if present, and includes the effects of ion cyclotron harmonic and alpha particle damping. DOE

N89-27521# Lawrence Livermore National Lab., CA.

PULSED LOWER-HYBRID WAVE PENETRATION IN REACTOR PLASMAS

Ronald H. Cohen, Paul T. Bonoli, Miklos Porkolab (Massachusetts Inst. of Tech., Cambridge.), and Thomas D. Rognlien 1989 5 p Presented at the 8th Topical Conference on Radio Frequency Power in Plasmas, Irvine, CA, 1-3 May 1989

(Contract W-7405-eng-48)

(DE89-013260; UCRL-100574; CONF-8905120-13) Avail: NTIS HC A02/MF A01

Providing lower-hybrid power in short, intense (GW) pulses allows enhanced wave penetration in reactor-grade plasmas. We examine nonlinear absorption, ray propagation, and parametric instability of the intense pulses. We find that simultaneously achieving good penetration while avoiding parametric instabilities is possible, but imposes restrictions on the peak power density, pulse duration, and/or RF spot shape. In particular, power launched in narrow strips, elongated along the field direction, is desired. DOE

N89-27522# Lawrence Livermore National Lab., CA.

MODELING OF LH CURRENT DRIVE IN SELF-CONSISTENT ELONGATED TOKAMAK MHD EQUILIBRIA

D. T. Blackfield, R. S. Devoto, M. E. Fenstermacher, Paul T. Bonoli, Miklos Porkolab, and J. Yugo (Oak Ridge National Lab., TN.) May 1989 5 p Presented at the 8th Tropical Conference on Radio Frequency Power in Plasmas, Irvine, CA, 1-3 May 1989

(Contract W-7405-eng-48)

(DE89-013263; UCRL-100591; CONF-8905120-14) Avail: NTIS HC A02/MF A01

Calculations of non-inductive current drive typically were used with model MHD equilibria which are independently generated from an assumed toroidal current profile or from a fit to an experiment. Such a method can lead to serious errors since the driven current can dramatically alter the equilibrium and changes in the equilibrium B-fields can dramatically alter the current drive. The latter effect is quite pronounced in LH current drive where the ray trajectories are sensitive to the local values of the magnetic shear and the density gradient. In order to overcome these problems, a LH simulation code was modified to accommodate elongated plasmas with numerically generated equilibria. The new LH module was added to the ACCOME code which solves for current drive by neutral beams, electric fields, and bootstrap effects in a self-consistent 2-D equilibrium. The model is briefly described in the next section and then results of a study of LH current drive in ITER are presented. DOE

N89-27523# Sandia National Labs., Albuquerque, NM.

Z-PINCH EXPERIMENTS ON SATURN AT 30 TW

R. B. Spielman, R. J. Dukart, D. L. Hanson, B. A. Hammel, W. W. Hsing, M. K. Matzen, and J. L. Porter 1989 14 p Presented at the 2nd International Conference on High-Density Pinches, Laguna Beach, CA, 26 Apr. 1989

(Contract DE-AC04-76DP-00789)

(DE89-013497; SAND-89-0289C; CONF-8904107-3) Avail: NTIS HC A03/MF A01

We have recently completed the first gas-puff z-pinch on Saturn (32 TW, 1.4 MJ, 1.9 MV, 40-ns FWHM, and 0.11 ohm). These experiments used the most powerful driver to date for fast z-pinch experiments. Saturn, a 36 module accelerator, uses a double post-hole vacuum convolute to deliver the total machine current to the load. The 10-nH Saturn z-pinch diode is capable of delivering a peak current of 10.5 MA. We diagnosed the current using segmented Rogowski coils at the insulator, resistive shunts in the vacuum transmission lines, and B-dot loops and piezoelectric pressure gauges near the load. On most shots electrical losses in the vacuum convolute were minimal with nearly complete current delivery to the z-pinch load. We have conducted experiments with deuterium, neon, argon, krypton, and xenon gas puffs. A maximum total radiation yield of 505 + or - 25 kJ was obtained with xenon. The peak keV X-ray yields were 100 + or - 5 kJ for neon K-shell radiation, 30 + or - 4 kJ for krypton L-shell radiation, and 39 + or - 4 kJ for argon K-shell radiation. DOE

N89-27524# Missouri Univ., Rolla.

COLLISION PROCESSES OF INTEREST IN MFE PLASMA RESEARCH Progress Report

1989 3 p

(Contract DE-FG02-84ER-53175)

(DE89-013681; DOE/ER-53175/T1) Avail: NTIS HC A02/MF A01

Research on this grant is devoted to the calculation of heavy particle collision cross sections needed for diagnostics studies of magnetic fusion plasmas. This work requires the development and testing of new theoretical techniques, and the implementation of benchmarked methods to collisions pertinent to fusion reactors. On the last context, we have provided the cross sections for modeling the beam penetration in an ETR plasma, charge exchange

recombination values for impurity ion diagnostic studies, and those for assessing the feasibility of using a high efficiency plasma neutralizer for 0.5 to 1.0 MeV/u D(-) beams. We have also extended our theoretical understanding to H(+), He(++) and He collisions in order to be prepared for the modeling of helium and transport in the next generation of reactors. DOE

N89-27525# Argonne National Lab., IL. High Energy Physics Div.
EXPERIMENTAL MEASUREMENT OF NONLINEAR PLASMA WAKE-FIELDS
J. B. Rosenzweig, P. Schoessow, B. Cole, W. Gai, R. Konecny, J. Norem, and J. Simpson 1989 3 p Presented at the 13th Particle Accelerator Conference, Chicago, IL, 20 Mar. 1989
(Contract W-31-109-eng-38)
(DE89-014636; ANL-HEP-PR-89-45; CONF-890335-210) Avail: NTIS HC A02/MF A01

We report direct high resolution observation of nonlinear steepened plasma waves excited in the wake of an intense, self-pinched electron beam. Oscillators in both accelerating and deflecting fields are measured, and analyzed in the context of linear and nonlinear plasma wave theory. The degree of nonlinearity in the wake-fields is shown to be consistent with analytical predictions of the beam self-pinching. The impact of these results on plasma acceleration and focusing schemes is discussed. DOE

N89-27526# Lockheed Missiles and Space Co., Palo Alto, CA. Applied Physics Lab.
MEASUREMENT OF THE TIME-DEPENDENT DISTRIBUTION OF IONIZATION STATES IN AN ARGON PLASMA FROM A MACH-10 JET Final Report
P. C. Filbert, T. R. Fisher, D. Kohler, J. D. Perez, R. A. Walton, and G. Dahlbacka (Plasma Research Corp., Alameda, CA.) 28 Sep. 1988 56 p
(Contract DE-AC08-86NV-10571)
(DE89-014699; DOE/NV-10571/T2) Avail: NTIS HC A04/MF A01

Results from experiments designed to measure the time-dependent distribution of ionization states in an argon plasma produced by laser irradiation of a high-Mach-number gas jet are presented. The gas valve/nozzle target system was designed for nominal Mach-10 performance and produced a jet of neutral gas several centimeters long from a nozzle exit of 1.5 mm diameter. The jet was irradiated at a position having an approximate atomic density of 1 x 10(18)/cu cm by 500 J of 351-nm laser light with a pulse width of 600 ps at the NLUF's OMEGA laser facility. It was necessary to pre-ionize the gas in order to couple-in sufficient laser energy to produce a plasma. An argon plasma was then created that was dominated by charge states of Ar VIII through Ar XI. Comparison with a theoretical model which solved the time-dependent rate equations indicates that a plasma temperature of approximately 70 eV was achieved. A subsequent development effort carried out at the Lockheed Palo Alto Research Laboratory (LPARL) to improve the gas jet target system is also described. This work indicated that by increasing the pressure in the valve by a factor of 5 increased the coupling to the laser and produced significantly larger signals and higher plasma temperatures. DOE

N89-27527# Nagoya Univ. (Japan). Inst. of Plasma Physics.
IMPROVED CONFINEMENT REGIMES IN JIPP T-IIU
T. Watari, R. Kumazawa, K. Toi, Y. Hamada, A. Ando, Y. Oka, O. Kaneko, K. Kawahata, K. Adati, and R. Akiyama et al Apr. 1989 41 p
(IPPJ-909) Avail: NTIS HC A03/MF A01

The H-mode, an improved confinement regime, was observed recently in JIPP T-IIU high power heating experiments. It was obtained in a limiter configuration without any shaping of the plasma cross-section. This H-mode is not common because it is obtained with ICRF heating. The H-mode is also obtained in a combined heating with NBI and ICRF and it is found that the threshold power level is similar to that of averaged ICRF heating. The power threshold of the H-Mode is then studied for its dependence on various plasma parameters: It increases with plasma current, insensitive to plasma density, and optimized against toroidal field intensity. The power deposition profile of ICRF heating is analyzed using a ray-tracing code, and used to explain the observed B sub T dependence. A class of strange shorts observed in the same series of experiments is studied. The shorts appeared at a power level close to the H-mode threshold with a remarkable improvement of confinement. However, the shorts are different from the H-mode in the time evolution of the profiles. Author

N89-27528# Nagoya Univ. (Japan). Inst. of Plasma Physics.
STOCHASTICITY AND SYMMETRY OF THE STANDARD MAP
Y. H. Ichikawa, T. Kamimura, T. Hatori, and S. Y. Kim Apr. 1989 38 p
(IPPJ-910) Avail: NTIS HC A03/MF A01

The stochasticity and symmetry of the standard map were discussed to explore the generic aspect of the statistical properties inherent to the low dimensional classical Hamiltonian systems. The accelerator modes of the standard map give rise to anomalous enhancement of the stochastic diffusion. Systematic analysis of symmetry of the standard map is undertaken to investigate structure of the periodic orbits around the stable fixed point, and the method is applied to the Poincare-Birkhoff chains around the accelerator mode. The squeeze effect of the period-3 accelerator orbits is examined explicitly, in terms of the reduced accelerator mode map. Furthermore, it is shown that the period-3 accelerator orbits are born as intrinsic nonlinear multifurcation, differing from birth of the Poincare-Birkhoff chains with the higher periodicity q equal to or greater than 4. Author

N89-27529# Los Alamos National Lab., NM.
THE MAGNETIC TOPOLOGY OF THE PLASMOID FLUX ROPE IN A MHD SIMULATION OF MAGNETOTAIL RECONNECTION
J. Birn and M. Hesse 1989 17 p Presented at the Chapman Conference on the Physics of Magnetic Flux Ropes, Hamilton, Bermuda, 27-31 Mar. 1989
(Contract W-7405-eng-36)
(DE89-012621; LA-UR-89-1593; CONF-8903131-2) Avail: NTIS HC A03/MF A01

On the basis of a three-dimensional MHD simulation we discuss the magnetic topology of a plasmoid that forms by a localized reconnection process in a magnetotail configuration including a net dawn-dusk magnetic field component B sub yN. As a consequence of B sub yN ne 0 the plasmoid gets a helical flux rope structure rather than an isolated island or bubble structure. Initially all field lines of the plasmoid flux rope remain connected with the Earth, while at later times a gradually increasing number of flux tubes becomes separated, connecting to either the distant boundary or to the flank boundaries. In this stage topologically different flux tubes become tangled and wrapped around each other, consistent with predictions on the basis of ad hoc plasmoid models. DOE

N89-27530# Sandia National Labs., Albuquerque, NM.
ELECTROHYDRODYNAMICALLY DRIVEN, LARGE-AREA LIQUID METAL ION SOURCE FOR INERTIAL CONFINEMENT FUSION
Arian L. Pregenzer 1989 16 p Presented at the International Conference on Ion Sources, Berkeley, CA, 9 Jul. 1989
(Contract DE-AC04-76DP-00789)
(DE89-012665; SAND-89-1390C; CONF-890703-2) Avail: NTIS HC A03/MF A01

Analysis of the electrohydrodynamic (EHD) equations of motion of a planar liquid-lithium surface in the presence of a normal electric field suggest that liquid lithium may provide a large-area ion source for intense ion-beam diodes. Such sources are being developed for the Particle Beam Fusion Accelerator 2 at Sandia National Laboratories. In this paper, theoretical and experimental studies of the planar EHD ion source will be reviewed. When a planar liquid surface is subjected to an electric field of sufficient magnitude, EHD instabilities produce an array of cusps on the surface. The electric field enhancement at the apex of each cusp is sufficient to permit field evaporation of ions. The time delay between

application of the electric field and ion emission depends on the magnitude and rate of increase of the applied electric field, and on the initial amplitude of the surface perturbation. Above 10 MV/cm, theory indicates that field emission will occur on a nanosecond time scale and that the characteristic spacing of emitters will be less than one micrometer. At these fields, the source should have an intrinsic divergence of less than 6 mrad and the effects of space charge from neighboring emitters should not inhibit emission significantly. Experimental measurements of wavelength and cusp-formation-times for water and ethanol at electric fields near the critical field for instability have agreed well with theory. DOE

N89-27531# Sandia National Labs., Albuquerque, NM.
TWO-DIMENSIONAL EFFECTS IN HOLLOW CORE z-PINCHES
N. F. Roderick (New Mexico Univ., Albuquerque.) and T. W. Hussey 1989 15 p Presented at the 2nd International Conference on High-Density Pinches (ICHDP-2), Laguna Beach, CA, 26 Apr. 1989
(Contract DE-AC04-76DP-00789)
(DE89-014188; SAND-89-0443C; CONF-8904107-4) Avail: NTIS HC A03/MF A01

Analytic modeling and magnetohydrodynamic simulations have been conducted to investigate two-dimensional effects in imploding plasma shells. These effects include short wavelength disturbances caused by instabilities at the plasma magnetic field interface, long wavelength instabilities associated with plasma annulus formation, and perturbations resulting from the power flow to the plasma annulus. The numerical calculations were carried out using the two-dimensional single-fluid magnetohydrodynamic (MHD) code MACH2 for different plasma density profiles and electrode geometries. Results for short wavelength perturbations show that these phenomena behave in a manner consistent with analytic linear and heuristic nonlinear models. At stagnation they have a negligible effect on the uniformity during the initial coupling to the target, even for large initial perturbations. The disturbances manifest themselves primarily in a rippling of the back of the plasma shell with significant effects, even in this region, not occurring until late in the stagnation process. Long wavelength perturbations produced by a straight axial gas injection for gas puff implosions can lead to pronounced axial nonuniformity, zippering, at stagnation. Variations of the injection conditions and electrode geometry can produce more uniform stagnation. Changes in the mass profile, gas injection angle, and electrode shape can all be used to achieve significantly greater stagnation uniformity. Consistent calculations for an entire implosion process from a gas injection to stagnation including vacuum power flow indicate the degree of coupling of short wavelength, long wavelength and power flow perturbations. Comparison with experimental data show agreement between analytic, numerical and experimental results. DOE

N89-27532# Los Alamos National Lab., NM.
STUDY OF ATOMIC PHYSICS AND POPULATION INVERSIONS WITH PLASMA FOCUS
H. Oona, M. L. Hodgdon, D. G. Rickel, and B. L. Freeman 1989 7 p Presented at the 5th International Conference on Megagauss Magnetic Field Generation and Related Topics, Novosibirsk, USSR, 3-7 Jul. 1989
(Contract W-7405-eng-36)
(DE89-014282; LA-UR-89-2164; CONF-890710-14) Avail: NTIS HC A02/MF A01

The plasma focus can be used to generate high temperature and high density plasmas. Neon-like plasmas have previously been studied in Z-pinches and laser produced plasmas as sources for XUV and X-ray lasers. The plasma focus provides a simple and inexpensive source for studying atomic physics of highly ionized atoms. A detailed understanding of atomic physics at high temperatures, densities, and megagauss magnetic fields is necessary for possible X-ray laser designs. Methods that are generally used for obtaining population inversions include collisional ionization of the inner shells of multi-electron atoms and ions, photoexcitation, and electron collisional excitation of ions, collisional combination of ions, and atom-ion resonant charge exchange. We will discuss some possible experiments to help understand the atomic physics under the above condition. Some ideas and calculations will be given to show the feasibility of doing atomic physics relating to X-ray lasers with a plasma focus. DOE

N89-27533# Los Alamos National Lab., NM.
RADIATIVE COLLAPSE OF A BENNETT-RELAXED z-PINCH
Leaf Turner 1989 10 p Presented at the 2nd International Conference on High-Density Pinches (ICHDP-2), Laguna Beach, CA, 26-28 Apr. 1989
(Contract W-7405-eng-36)
(DE89-014290; LA-UR-89-2144; CONF-8904107-5) Avail: NTIS HC A02

The global evolution of a z-pinch has been studied with the assumption of a relaxed state consisting of ions and electrons, each in a rigidly drifting isothermal Maxwellian distribution. This speculative approach has the pragmatic feature of possessing phenomenologically useful global parameters such as drift velocity and temperature that vary in accordance with global physical quantities such as energy and entropy. The plasma gains energy from a time-dependent electric field by means of Poynting's vector. Coulomb collisions between electrons and ions are calculated with a Fokker-Planck treatment analogous to that used by Dreicer to calculate runaways. For a variety of initial conditions and time-independent applied electric fields, the pinch evolution always culminates in a time-independent (attractor) state whose current is the Pease-Braginskii current and whose final radius is proportional to (line density to the 3/4 power)/(electric field to the 1/2 power). Before the final state is attained, the pinch may bounce toward and away from a highly collapsed state. For the case of a Bennett pinch, the classical limit of the resistivity is attained when the line density is much greater than 4(eta)m(sub e)/e(2)mu(sub 0); i.e., 3.55 x 10(14) m(-1). DOE

N89-27534# Sandia National Labs., Albuquerque, NM.
TWO-DIMENSIONAL EFFECTS IN IMPLODING PLASMA LINERS
N. F. Roderick (New Mexico Univ., Albuquerque.) and T. W. Hussey 1989 12 p Presented at the 5th International Conference on Megagauss Magnetic Field Generation and Related Topics, Novosibirsk, USSR, 3 Jul. 1989
(Contract DE-AC04-76DP-00789)
(DE89-014482; SAND-88-3311C; CONF-890710-1) Avail: NTIS HC A03/MF A01

Analytic modeling and magnetohydrodynamic (MHD) simulations have been conducted to investigate two-dimensional effects in imploding plasma shells. These effects include short wavelength disturbances caused by instabilities at the plasma magnetic field interface, long wavelength instabilities associated with plasma annulus formation, and perturbations resulting from the power flow to the plasma annulus. The numerical calculations were carried out using the two-dimensional single-fluid MHD code MACH2 for different plasma density profiles and electrode geometries. Results for short wavelength perturbations show that these phenomena behave in a manner consistent with analytic linear and heuristic nonlinear models. At stagnation they have a negligible effect on the uniformity during the initial coupling to the target, even for large initial perturbations. The disturbances manifest themselves primarily in a rippling of the back of the plasma shell with significant effects, even in this region, not occurring until late in the stagnation process. Long wavelength perturbations produced by a straight axial gas injection for gas puff implosions can lead to pronounced axial nonuniformity, zippering, at stagnation. Variations of the injection conditions and electrode geometry can produce more uniform stagnation. Changes in the mass profile, gas injection angle, and electrode shape can all be used to achieve significantly greater stagnation uniformity. Consistent calculations for a entire implosion process form gas injection to stagnation including vacuum power flow indicate the degree of coupling of short wavelength, long wavelength and power flow perturbations. Comparison with experimental data show agreement between analytic, numerical and experimental results. DOE

N89-27535# Sandia National Labs., Albuquerque, NM.
MHD CALCULATIONS OF ANODE PLASMAS
T. W. Hussey, S. A. Slutz, and M. P. Desjarlais 1989 15 p Presented at the 7th Institute of Electrical and Electronics Engineers Pulsed Power Conference, Monterey, CA, 12 Jun. 1989
(Contract DE-AC04-76DP-00789)
(DE89-014485; SAND-89-0025C; CONF-890665-23) Avail: NTIS HC A03/MF A01

We have performed a series of idealized magnetohydrodynamic (MHD) calculations of the response of an anode plasma layer to the rising magnetic field in an applied-B ion diode. The purposes of this study were to consider Joule heating of the plasma layer, which could pose potential problems for lithium ion diodes, and the leakage of flux behind the ion-emitting surface, which is related to impedance collapse. We find that, as induced JxB forces move the plasma toward the wall, the entrained, initial field is compressed until it just equals the rising external field. Achieving such equilibrium decreases both Joule heating and flux leakage into the plasma. For relatively thin (approximately 1 mm) plasma layers at moderate densities (10 to the 16th power to 10 to the 17th power cm(-3)) we calculate that this equilibrium is achieved quite rapidly, leading to acceptably low levels of both flux penetration and Joule heating. DOE

N89-27536 Max-Planck-Inst. fuer Plasmaphysik, Garching (Germany, F.R.).
ON BOOTSTRAP CURRENTS IN TOROIDAL SYSTEMS
Horst Wobig Oct. 1988 55 p
(IPP-2/297; ETN-89-94571) Copyright Avail:
Fachinformationszentrum Karlsruhe, 7514
Eggenstein-Leopoldshafen 2, Fed. Republic of Germany

The diffusion driven current in tokamaks and stellarators is investigated. It can be shown that in stellarator configurations with symmetry - axisymmetry, helical symmetry, quasi-helical symmetry, bootstrap current and radial particle loss are proportional to each other. This relation follows directly from the momentum balance and the plasma viscosity given in Chew-Goldberger-Low formulation. This general relation, which is already known for tokamaks can be derived without solving the kinetic equation. If the symmetry of the configuration is destroyed, it is possible to minimize the bootstrap current by a suitable choice of the magnetic field geometry. The parallel and the perpendicular viscosities have to be calculated for the various regimes of collisionality starting from the kinetic equation. In a collision dominated plasma these effects are small. The viscous tensor of a collisional plasma given by Braginskii allows one to calculate these average viscous forces for an arbitrary stellarator geometry and a geometrical factor Cb can be defined which characterizes the dependence of the bootstrap current on the topology of the magnetic surface. Such a geometrical factor also exists in the plateau regime; in the long-mean-free-path regime the bootstrap current depends on the collisionality and the radial electric field and thus a factor Cb depending on the magnetic field alone cannot be defined. ESA

N89-27537 Max-Planck-Inst. fuer Plasmaphysik, Garching (Germany, F.R.).
A NEW VERSION OF THE FULL-WAVE ICRH CODE FISIC FOR PLASMAS WITH NONCIRCULAR FLUX SURFACES
T. Kruecken Dec. 1988 43 p
(IPP-5/25; ETN-89-94575) Copyright Avail:
Fachinformationszentrum Karlsruhe, 7514
Eggenstein-Leopoldshafen 2, Fed. Republic of Germany

A user manual for a new version of the FISIC code which is now applicable to arbitrary (toroidal) geometry is presented. It describes the input parameters and quantities of all subroutines and contains a list of all common blocks. ESA

N89-27538 Max-Planck-Inst. fuer Plasmaphysik, Garching (Germany, F.R.).
INTEGRAL CONSTITUTIVE RELATION FOR THE INVESTIGATION OF ION BERNSTEIN WAVES IN NON-HOMOGENEOUS PLASMAS
Marco Brambilla Jan. 1989 25 p
(IPP-5/27; ETN-89-94576) Copyright Avail:
Fachinformationszentrum Karlsruhe, 7514
Eggenstein-Leopoldshafen 2, Fed. Republic of Germany

By integrating the linearized Vlasov equation, an integral form of the constitutive relation (the relation between the HF electric field and the HF current) valid to all orders in the Larmor radius in axially magnetized inhomogeneous plasmas is derived. It has the form of a convolution integral in Fourier space, whose kernel can be expanded in Bessel functions, or put in a form analogous to the Gordeev integral form of the usual uniform plasma conductivity tensor, to which it reduces in the uniform plasma limit. Alternatively, it can be formulated as an integral equation in real space. Both formulations can be useful for the investigation of ion Bernstein waves near ion cyclotron resonances and near the lower hybrid resonance, where a WKB analysis alone is insufficient. ESA

N89-27539 Max-Planck-Inst. fuer Plasmaphysik, Garching (Germany, F.R.).
ON THE ECONOMIC PROSPECTS OF NUCLEAR FUSION WITH TOKAMAKS
D. Pfirsch and K. H. Schmitter Dec. 1987 56 p Revised
(IPP-6/271; ETN-89-94577) Copyright Avail:
Fachinformationszentrum Karlsruhe, 7514
Eggenstein-Leopoldshafen 2, Fed. Republic of Germany

A method of cost and construction energy estimation for tokamak fusion power stations conforming to the present stage of fusion development is described. The method is based on first-wall heat load constraints rather than Beta limitations, which, however, might eventually be the more critical of the two. It is used to discuss the economic efficiency of pure fusion, with particular reference to the European study entitled Environmental Impact and Economic Prospects of Nuclear Fusion (1986). It is shown that the claims made therein for the economic prospects of pure fusion with tokamaks, when discussed on the basis of the present-day technology, do not stand up to critical examination. A fusion-fission hybrid, however, could afford more positive prospects. Support for the stated method is derived when it is properly applied for cost estimation of advanced gas-cooled and Magnox reactors, the two examples presented by the European study to disprove it. ESA

N89-27540 Max-Planck-Inst. fuer Plasmaphysik, Garching (Germany, F.R.).
RADIO FREQUENCY PLASMA HEATING AND CURRENT DRIVE
E. Canobbio (Commission of the European Communities, Brussels, Belgium) and R. Croci Dec. 1988 70 p Submitted for publication
(IPP-6/278; ETN-89-94578) Copyright Avail:
Fachinformationszentrum Karlsruhe, 7514
Eggenstein-Leopoldshafen 2, Fed. Republic of Germany

The mechanisms underlying radiofrequency plasma heating and current drive in closed configurations are considered together with the theoretical tools describing them. The heating schemes of interest for thermonuclear devices span a wide range of frequencies from the Alfven wave resonance to the ion-cyclotron, lower hybrid, and electron-cyclotron resonances. Heating at frequencies below the Alfven wave resonance (magnetic pumping in its numerous versions), which is of limited thermonuclear relevance, is presented for its fundamental aspects - more than any other heating scheme it involves properties of particle motion in the large which are specific to the magnetic traps, in order to provide a broader and more integrated view of the whole subject. ESA

N89-27541 Max-Planck-Inst. fuer Plasmaphysik, Garching (Germany, F.R.).
DYNAMICS OF DECAYING TWO-DIMENSIONAL MAGNETOHYDRODYNAMIC TURBULENCE
Dieter Biskamp and Helmut Welter Dec. 1988 52 p
(IPP-6/279; ETN-89-94579) Copyright Avail:
Fachinformationszentrum Karlsruhe, 7514
Eggenstein-Leopoldshafen 2, Fed. Republic of Germany

High-resolution numerical studies of decaying two-dimensional magnetohydrodynamic turbulence using up to 768 sq modes in general periodic systems are reviewed. The evolution proceeds in a quasi-selfsimilar way with constant kinetic to magnetic energy ratio and constant micro- and macro-scale Reynolds numbers. The energy dissipation rate is independent of the values of the dissipation coefficients. The inertial-range energy spectra follow a Kolmogorov law, Ek = C epsilon sup 2/3 K sup (-5/3) with C = 3.7 + or - 0.3. Small-scale fluctuations are concentrated in the region of weak large-scale magnetic fields. The resulting strong intermittency is analogous to the behavior observed in two-dimensional hydrodynamic turbulence (J. Fluid Mech. (1988) 194, 333), with the magnetic field intensity taking the role vorticity plays in hydrodynamic systems. ESA

N89-27542# Swedish Inst. of Space Physics, Kiruna.
IONOSPHERIC PLASMA ESCAPE BY HIGH-ALTITUDE ELECTRIC FIELDS: MAGNETIC MOMENT PUMPING
Richard Lundin and Bengt Hultqvist Jan. 1989 39 p Submitted for publication Sponsored by the Swedish Board for Space Activities
(IRF-Preprint-111; ETN-89-94941) Avail: NTIS HC A03/MF A01

Viking results of the temperature and mass-composition of individual ion beams suggest that upward flowing ion beams can be generated by a magnetic moment pumping mechanism caused by low-frequency transverse electric field fluctuations, in addition to a field aligned quasi-electrostatic acceleration process. Magnetic moment pumping within transverse electric field gradients can be described as a conversion of electric drift velocity to cyclotron velocity by the inertial drift in a time-dependent electric field. This gives an equal cyclotron velocity gain for all plasma species irrespective of mass. Oxygen ions thus gain 16 times higher transverse energy as compared to protons. In addition to a transverse energy gain above the escape energy, a field aligned quasi-electrostatic acceleration is considered primarily responsible for the collimated upward flow of ions. The field aligned acceleration adds a constant parallel energy to escaping ionospheric ions. Thus, ion beams at high altitudes can be explained by a bimodal acceleration from both a transverse (equal velocity) and a parallel (equal energy) acceleration process. The Viking observations also show that the thermal energy of ion beams, and the ion beam width are mass dependent. The average O+/H+ temperature ratio is found to be 4.0 from the Viking observations. This is less than the factor of 16 anticipated from a coherent transverse electric field acceleration but greater than the factor of 1 (or even less than 1) expected from a turbulent acceleration process. ESA

76 SOLID-STATE PHYSICS

Includes superconductivity.

For related information, see also *33 Electronics and Electrical Engineering* and *36 Lasers and Masers.*

N89-27543# Los Alamos National Lab., NM. Materials Science and Technology Div.
WEAR AND FRICTION OF THIN FILM HIGH TEMPERATURE OXIDE SUPERCONDUCTORS
Michael Nastasi, Juha-Pekka Hirvonen, and Risto O. Toivanen (Helsinki Univ. of Technology, Espoo, Finland) 1989 14 p Presented at the 16th International Conference on Metallurgical Coatings and Equipment Exhibit, San Diego, CA, 17-21 Apr. 1989
(Contract W-7405-eng-36)
(DE89-009397; LA-UR-89-825; CONF-890468-1) Avail: NTIS HC A03/MF A01

The sliding properties of a Nd-Fe-B magnet were examined against a thin film YBa2Cu3O7 superconductor. Pin-on-disk experiments were performed at room temperature and in normal air using a 10 mm magnetic Nd-Fe-B ball loaded to 31.22 g and a sliding speed of approximately 0.57 cm/sec. Such condition produced a steady state friction coefficient of 1.1 + or - 0.3. Wear rate measurements indicated that Nd-Fe-B will wear YBa2Cu3O7 at a rate 1.3 x 10(-14) cu m/m and that the Nd-Fe-B/YBa2Cu3O7 sliding system possess a wear coefficient of 4.2 x 10(-14)cu m/Nm. These unusually high values appear to be the result of both abrasive and adhesive wear. Adhesion between the sliding surfaces is most probably enhanced by the oxygen reactivity of the pin material and the high oxygen content in the superconductor. DOE

N89-27544# International Centre for Theoretical Physics, Trieste (Italy).
MODEL FOR HOT ELECTRON PHENOMENA: THEORY AND GENERAL RESULTS
J. L. Carrillo and M. A. Rodriquez (Universidad Autonoma de Puebla, Mexico) Oct. 1988 37 p Submitted for publication
(DE88-705986; IC-88/336) Avail: NTIS (US Sales Only) HC A03/MF A01

We propose a model for the description of the hot electron phenomena in semiconductors. Based on this model we are able to reproduce accurately the main characteristics observed in experiments of electric field transport, optical absorption, steady state photoluminescence and relaxation process. Our theory does not contain free nor adjustable parameters, it is very fast computerwise, and incorporates the main collision mechanisms including screening and phonon heating effects. Our description is based on a set of nonlinear rate equations in which the interactions are represented by coupling coefficients or effective frequencies. We calculate three coefficients from the characteristic constants and the band structure of the material. DOE

N89-27545 Department of the Air Force, Washington, DC.
HYBRID SINGLE CRYSTAL OPTIC FIBERS BY EMBEDDING Patent
Stephen C. Rand, inventor (to AF) and Ricardo C. Pastor, inventor (to AF) 15 Nov. 1988 4 p Filed 6 Nov. 1985 Supersedes N86-26204 (24 - 16, p 2667)
(AD-D013986; US-Patent-4,784,716; US-Patent-Appl-SN-795572; US-Patent-Class-156-621) Avail: US Patent and Trademark Office CSCL 20/6

A process of fabricating a hybrid single crystal fiber having nonlinear optical properties such as frequency doubling is presented. Said process includes applying a force to a fiber core resting upon a bulk nonlinear crystal such as LiIO3 in a saturated solution of LiIO3 in water. After the core is embedded a sufficient distance into the crystal the force is removed. This invention relates generally to glass fiber optics, and particularly, relates to a process of fabricating fibers useful in nonlinear optics applications. The instant invention set forth a process of fabricating hybrid single crystal optical fibers having nonlinear optical properties therein and thereby overcome the problems set forth hereinabove. This process is distinct from the well known process of regelation. In the process of this invention, a fiber core is placed in direct contact with a bulk nonlinear crystal having an essentially flat surface thereon. The fiber core and bulk nonlinear crystal are immersed in a saturated solution where the equilibrium solid phase has the same composition as the bulk nonlinear crystal. GRA

N89-27546# Argonne National Lab., IL. Materials Science Div.
DIFFUSION IN HIGH-T SUB c SUPERCONDUCTORS
S. J. Rothman and J. L. Routbort Mar. 1989 21 p Presented at the NATO Advanced Study Institute on Diffusion in Materials, Aussois, France, 12 Mar. 1989
(Contract W-31-109-eng-38)
(DE89-009792; CONF-8903102-2) Avail: NTIS HC A03/MF A01

The tracer diffusion of oxygen was measured in the high T(sub c) superconductors La(2-x)Sr(x)CuO4 (x = 0.1, 0.15, 0.2) and in YBa2Cu3O(7 - delta), using secondary ion mass spectrometry (SIMS) to obtain the depth profiles. The diffusion coefficients in La(2-x)Sr(x)CuO4 decrease with increasing x, a result that is explained on the basis of a simple defect model, which also provides an explanation for the peak in the plot of T(sub c) vs x. The depth profiles for YBa2Cu3O(7 - delta) require two volume diffusion terms for a good fit, and this is explained in terms of the

anisotropy of diffusion in this structure. The results are compared to values in the literature, and analyzed in terms of the theories of Bakker et al., Tu et al., and Ronay and Nordlander. DOE

N89-27547# Technische Univ., Eindhoven (Netherlands). Solid State Div.
MAGNETIC MULTILAYERS Ph.D. Thesis
Henricus Johannes Ge Draaisma 1988 170 p Prepared in cooperation with Philips Gloeilampenfabrieken N.V., Eindhoven, Netherlands
(ETN-89-94294) Avail: NTIS HC A08/MF A01

Multilayers were prepared by vacuum deposition and characterized. A Pd/Co multilayer was examined using X-ray diffraction, computer simulations, spectroscopy and transmission electron microscopy. Magnetic measurements are presented. It is shown that the magnetic properties of multilayer thin films, especially magnetic anisotropy, can be understood and modified by the influence of the interfaces between the different materials. ESA

N89-27548# Geochemical Services, Inc., Torrance, CA.
DEPTH PROFILES AND BULK ANALYSIS OF SEMICONDUCTOR MATERIALS USING ICP MASS SPECTROSCOPY WITH ELECTROTHERMAL ATOMIZATION Final Technical Report, Jul. 1986 - Mar. 1987
William Faulkner, William Henderson, and Michael Rogers Oct. 1988 92 p
(Contract F19628-86-C-0122)
(AD-A206974; RADC-TR-88-218) Avail: NTIS HC A05/MF A01 CSCL 07/4

The purpose of the contract was to build the equipment necessary to show technical feasibility of a Demand Modulated Electrothermal Atomization System. This system was thought to have advantages over current technology as follows: (1) Prevents excessive analyte concentrations in the plasma giving the analyst control over matrix suppression effects. (2) Allows the analyst to control atomization rates and avoid buildup of deposits in the throat of the sample cone opening. (3) Allows the analyst to work in the optimum counting range for isotropic ratio work regardless of concentration variations. (4) Allows the data to be taken over the temperature dimension, thus resolving isobaric interferences as well as improving the signal to noise ratio resulting in improved detection limits across the entire mass range. GRA

N89-27549# Frequency Electronics, Inc., Mitchel AFB, NY.
DESIGN, DEVELOPMENT AND EVALUATION OF A DOUBLY ROTATED AK-CUT QUARTZ CRYSTAL Final Technical Report, Feb. 1984 - Oct. 1986
B. Goldfrank Nov. 1988 63 p
(Contract F19628-84-C-0074)
(AD-A207209; RADC-TR-88-263) Avail: NTIS HC A04/MF A01 CSCL 07/2

The work accomplished in designing, developing and evaluating a doubly rotated AK-cut quartz crystal is described. Standard production processes were used to fabricate AK-cut crystals with 0 = 36.48oo = 26.000 or 0 = 35.000 and 0 = 25.000. Frequency versus temperature characteristics room temperature mode spectra and G sensitivity data were the main sources of data for evaluation. Crystals were fabricated at low frequencies and through subsequent lapping and polishing operations the frequencies were increased to determine a range of useful frequencies. Comparisons made of B mode to C mode coupling and separation. GRA

N89-27550# State Univ. of New York, Buffalo. Dept. of Electrical and Computer Engineering.
MeV IMPLANTATION STUDIES IN LPE-GROWN GaAs AND InP Final Report, 1 Oct. 1987 - 31 Mar. 1989
Y. S. Park 31 Mar. 1989 80 p
(Contract N00014-87-K-0799)
(AD-A207220) Avail: NTIS HC A05/MF A01 CSCL 07/2

Research was conducted on growth and evaluation of high quality Gallium Arsenide layer using Liquid Phase Epitaxy (LPE) and on MeV ion implantation processings of Molecular Beam Epitaxy (MBE) grown GaInaS layers on GaAs and LPE-grown GaAs layers on GaAs. By a growth method i.e., isoelectronic doping of LPE GaAs layers with indium, high structural and electrical quality layers were successfully grown. In the as-grown indium-doped LPE GaAs layers, the etch pit density, rocking curve FWHM, and the ideality factor of a Schottky diode have improved significantly, showing an optimal In doping density of 2.4 x 10 to the 19th. The effects of MeV ion bombardment in a strained but partially relaxed GaInAs epitaxial layer on GaAs were systematically investigated. Depending on the state of initial relaxation, film thickness, and incident ion beam current, the lattice strain changed differently with the increasing ion beam dose. GRA

N89-27551# Technische Univ., Delft (Netherlands).
ARTIFICIAL SUPERLATTICES Ph.D. Thesis
Roland Henri Marie vandeLeur 1988 191 p
(ETN-89-94889) Avail: NTIS HC A09/MF A01

Metallic superlattices and semiconductor Si/Ge superlattices are discussed. The origin of the modulation as well as the effect of this modulation on the diffraction pattern is considered. Because in real superlattices several nonperiodic distortions of the ideal structure influence the diffraction pattern, distortions which are likely to occur in metallic superlattices are examined. The fabrication method and the growth of metallic superlattices are treated. It is shown that there exists a maximum strain for monocrystalline growth of sinusoidally modulated Nb/V and Ta/V superlattices which sets an upper limit to the modulation amplitude. Superlattices, such as Si/Ge, of a very good crystalline quality can be used to determine the performances of the deposition control during the growth of these structures. The growth of dislocation-free Si/Ge superlattices is outlined. A model that describes the relation between the thickness of Si/Ge films grown on a Si substrate and the substrate imposed strain in these lattice mismatched films is presented. The fabrication of Y1Ba2Cu3O7-y thin films is described. ESA

N89-27552# Lawrence Livermore National Lab., CA.
A HYDRID 3 Gs/s, 6-BIT DIGITAL TO ANALOG CONVERTER
Gordon J. Priatko, Barry L. Thompson, and Jeffrey A. Kaskey Apr. 1989 17 p Presented at the UGIM Symposium, West Borough, MA, 12-14 Jun. 1989
(Contract W-7405-eng-48)
(DE89-012302; UCRL-100861; CONF-8906127-1) Avail: NTIS HC A03/MF A01

A hybrid GaAs 3 Gigasample per second (Gs/s) digital to analog converter (DAC) is presented. Five-hit 1-Gs/s operation and peak operating speeds of 3 Gs/s are demonstrated. DC differential and integral linearity are shown to be consistent with 6-bit operation. Sub-500-ps settling times are demonstrated at operating speeds of 1 to 3 Gs/s. The device has ECL level differential inputs and is capable of producing a 1-V output when driven into 50 omega. The hybrid DAC is implemented with thin film resistors and commercially available GaAs MESFETs. Power dissipation is approximately 1.5 W. DOE

N89-27553# Argonne National Lab., IL. Materials Science Div.
STUDY OF NANOPHASE TiO2 GRAIN BOUNDARIES BY RAMAN SPECTROSCOPY
C. A. Melendres, A. Narayanasamy (Madras Univ., India), V. A. Maroni, and R. W. Siegel 1989 6 p Presented at the Spring Meeting of the Materials Research Society, San Diego, CA, 24 Apr. 1989
(Contract W-31-109-eng-38)
(DE89-012416; CONF-890426-12) Avail: NTIS HC A02/MF A01

Raman spectra have been recorded for as-consolidated nanophase TiO2 samples with differing grain sizes and on samples annealed in air at a variety of temperatures up to 1273 K. The nanophase samples with the smallest grain size, about 12 nm average diameter, could have 15 to 30 percent of their atoms in grain boundaries; nevertheless, the strong Raman-active lines representative of the rutile structure were found to dominate all of the observed spectra, independent of grain size and annealing

treatment. These lines were quite broad in the as-consolidated nanophase samples, equally in 12 nm and 100 nm grain-size compacts, but sharpened considerably upon annealing at elevated temperatures. The Raman data give no indication of grain-boundary structures in nanophase TiO2 that are significantly different from those in conventional polycrystals. However, defect structures within the grains, which anneal out at elevated temperatures, are evidenced by changes in the Raman spectra. DOE

N89-27554# North Carolina State Univ., Raleigh. Dept. of Materials Science and Engineering.
THE STUDY OF STRUCTURE-PROCESSING-PROPERTY RELATIONS IN COPPER OXIDE-BASED HIGH T SUB c SUPERCONDUCTORS Progress Report, 1 Jul. 1988 - 1 Mar. 1989
Angus I. Kingon, Carl C. Koch, and David G. Haase 27 Feb. 1989 3 p
(Contract DE-FG05-88ER-45359)
(DE89-012764; DOE/ER-45359/1) Avail: NTIS HC A02/MF A01

This report is a brief summary of research from July 1, 1988 to March 1, 1989. Microstructure-property relations have been examined in a series of polycrystalline ceramic YBa sub 2 Cu sub 3 O sub 7 sigma samples. DOE

N89-27555# Argonne National Lab., IL. Materials Science Div.
COMPOSITION OF SUPERCONDUCTING La2CuO4+DELTA: A SUPERCONDUCTOR DOPED BY EXCESS OXYGEN DEFECTS
B. Dabrowski, D. G. Hinks, J. D. Jorgensen, and D. R. Richards 1989 9 p Presented at the Spring Meeting, Symposium on High Temperature Superconductors, San Diego, CA, 24-29 Apr. 1989; sponsored by the Materials and Research Society
(Contract W-31-109-eng-38)
(DE89-013299; CONF-890426-11) Avail: NTIS HC A02/MF A01

We have studied mixed-phase samples of bulk La(z)CuO4 using neutron powder diffraction, thermogravimetric analysis and resistivity measurements. Samples fired at 950 C and slowly cooled form in the K2NiF4 structure with CuO impurities for z less than 2 and La2O3 impurities for z greater than 2. Neither La-vacancies nor stacking defects were found. The bulk resistivity of the samples show semiconducting behavior which is shorted at 38 K by small amounts of superconducting material. The superconductivity is due to the presence of an oxygen-rich phase with stoichiometry La2CuO4.08. The occurrence of superconductivity in pure La2CuO4.08 with the same T(c) as observed in the doped La1.85Sr(0.15)CuO4 indicates that the excess oxygen provides the same level of doping as metal-ion substitution. DOE

N89-27556# California Univ., Berkeley. Lawrence Berkeley Lab. Engineering Div.
A METHOD FOR GENERATING THE J SUB c, B, T SURFACE FOR NIOBIUM-ALLOY SUPERCONDUCTORS
Michael A. Green Mar. 1989 14 p Presented at the TMS Symposium on High Temperature Superconductors, Las Vegas, NV, 27 Feb. - 3 Mar. 1989
(Contract DE-AC03-76SF-00098)
(DE89-012977; LBL-27064; CONF-8902100-2) Avail: NTIS HC A03/MF A01

This report shows how the J sub c, B, T surface can be created for various niobium-alloy superconductors using a reduced critical state model. Using this method, one can calculate the J sub c of the superconductor over a range of B and T given the J sub c at 4.2 K over a limited range of B. The calculated value of J sub c agrees favorably with measured values over a range of temperatures from 1.5 to 7.0 K and a range of inductions from 0.1 to B sub c2 . This method has been applied to various niobium-titanium-alloys, niobium-zirconium and niobium-tantalum-titanium. The paper compares calculated values of J sub c with measured values of J sub c for niobium-alloy superconductors manufactured since 1965. As an illustration, a computer generated J sub c, B, T surface is presented for some of the superconductors. DOE

N89-27557# Lawrence Livermore National Lab., CA.
PHOTOELECTRONIC PROPERTIES OF LOW TEMPERATURE GaAs GROWN ON SILICON AND GaAs SUBSTRATES BY MBE
Raymond P. Mariella, Jeffrey D. Morse, Roger Aines, and Charles E. Hunt (California Univ., Davis.) 25 Apr. 1989 6 p Presented at the Spring Meeting of the Materials Research Society, San Diego, CA, 24-28 Apr. 1989
(Contract W-7405-eng-48)
(DE89-013148; UCRL-99832; CONF-890426-17) Avail: NTIS HC A02/MF A01

The characteristics of GaAs layers grown by molecular beam epitaxy (MBE) at growth temperatures from 200 C to 400 C have been evaluated by photoconductivity experiments in order to understand the photoelectronic properties of this material. Low temperature (LT) growth of GaAs on both silicon and GaAs substrates has been investigated in an attempt to better understand the nature defects which are created in epitaxial layers grown under these conditions. Results from experiments on both annealed and unannealed LT samples indicate that the electronic transport properties of the epilayers can be controlled by selecting the appropriate growth conditions. DOE

N89-27558# California Univ., Berkeley. Lawrence Berkeley Lab. Superconductivity Research Center for Thin-Film Applications.
SPUTTERING OF HIGH-TEMPERATURE SUPERCONDUCTORS: A BIBLIOGRAPHY
Paul Berdahl and Richard B. Buckius Aug. 1988 29 p
(Contract DE-AC03-76SF-00098)
(DE89-013374; LBL-25722) Avail: NTIS HC A03/MF A01

The literature on the sputtering of high-temperature superconducting cuprate thin films is presented. Much of the work is on YBa sub 2 Cu sub 3 O sub 7 and the related compounds with Y replaced by a +3 valence lanthanide. However, work on (La sub 1-x) sub 2 CuO sub 4 is included, as are the few available papers on films based on the Bi-Sr-Ca-Cu-O and Tl-Ca-Ba-Cu-O material systems. A listing of authors by institution shows which laboratories are currently most active in this field. DOE

N89-27559# California Univ., Berkeley. Lawrence Berkeley Lab. Engineering Div.
PASSIVE SUPERCONDUCTOR: A VIABLE METHOD OF CONTROLLING MAGNETIZATION MULTIPOLES IN THE SSC DIPOLE
Michael A. Green Feb. 1989 16 p Presented at the International Industrial Symposium on the Super Collider, New Orleans, LA, 8 Feb. 1989
(Contract DE-AC03-76SF-00098)
(DE89-013432; LBL-27062; CONF-890270-16) Avail: NTIS HC A03/MF A01

At injection, the magnetization of the superconductor produces the dominant field error in the Superconducting Super Collider (SSC) dipole magnets. The field generated by magnetization currents in the superconductor is rich in higher symmetric multipoles (normal sextupole, normal decapole, and so on). Pieces of passive superconductor properly located within the bore of the dipole magnet can cancel the higher multipoles generated by the SSC dipole coils. The multipoles generated by the passive superconductor (predominantly sextupole and decapole) are controlled by the angular and radial location of the superconductor, the volume of superconductor, and the size of the superconducting filaments within the passive conductor. This paper will present the tolerances on each of these factors. The paper will show that multipole correction using passive superconductor is in general immune to the effects of temperature and magnetization decay due to flux creep, provided that dipole superconductor and the passive correction superconductor are properly specified. When combined with a lumped correction system, the passive superconductor can be a viable alternative to continuous correction coils within the SSC dipoles. DOE

N89-27560# Los Alamos National Lab., NM.
HIGH-FREQUENCY CAVITY APPLICATIONS AND MEASUREMENTS OF HIGH-TEMPERATURE SUPERCONDUCTORS
D. W. Cooke and E. R. Gray 1989 18 p Presented at the Workshop on High Temperature Superconductivity, Huntsville, AL, 23-25 May 1989
(Contract W-7405-eng-36)
(DE89-013467; LA-UR-89-1852; CONF-8905133-2) Avail: NTIS HC A03/MF A01

A potentially important application of high-temperature superconductors will be high-frequency accelerating cavities. Currently these materials are not competitive with Nb at liquid helium temperature or with Cu at room temperature. However, available data on high-quality single crystals suggest that the relatively poor RF properties (high surface resistance and low surface magnetic field) of bulk and film specimens are due to materials properties that can be eliminated by improved processing techniques. Recent progress in the fabrication of thin films, for example, demonstrates that this is indeed the case. DOE

N89-27561# Sandia National Labs., Albuquerque, NM.
THIN FILM PREPARATION AND SINGLE FILM DEVICE FABRICATION IN THE Tl-Ca-Ba-Cu-O HTS SYSTEM
D. S. Ginley, J. F. Kwak, E. L. Venturini, B. Morosin, R. J. Baughman, J. S. Martins, J. E. Nordman, J. B. Beyer, and G. K. G. Hohenwarter 1989 4 p Presented at the International Superconductivity Electronics Conference, Tokyo, Japan, 12 Jun. 1989
(Contract DE-AC04-76DP-00789)
(DE89-013560; SAND-89-1300C; CONF-890663-1) Avail: NTIS HC A02/MF A01

Superconducting polycrystalline thin films in the Tl-Ca-Bu-Cu-O system have been prepared by electron beam evaporation followed by appropriate sintering and annealing. Transition temperatures to 110 K and critical current densities to 600,000 A/sq cm have been attained in oxygen annealed films. However, with only 16 minutes of air sintering and no oxygen anneal, oriented films have been obtained with T sub c's to 107 K and J sub c's to 450,000 A/sq cm. Single film devices utilizing a parallel array of weak links and a coplanar control line have been fabricated from the films. Oscillators as well as AM and FM modulators operating between 3 and 6 GHz have been demonstrated using this device concept. DOE

N89-27562# Argonne National Lab., IL.
RECENT IMPROVEMENTS IN BULK PROPERTIES OF CERAMIC SUPERCONDUCTORS
R. B. Poeppel, U. Balachandran, I. Bloom, S. E. Dorris, J. T. Dusek, K. C. Goretta, M. T. Lanagan, H. J. Leu, V. A. Maroni, and J. J. Picciola et al Jan. 1989 14 p Presented at the International Symposium on High Tc Superconducting Oxides: Processing and Related Properties, Las Vegas, NV, 27 Feb. - 3 Mar. 1989
(Contract W-31-109-eng-38)
(DE89-013626; CONF-890216-2) Avail: NTIS HC A03/MF A01

Ceramic superconductors are being considered for uses ranging from large-scale applications such as the generation, transmission, and storage of electricity to small-scale applications such as electronic circuitry. These applications require that the electrical, mechanical, and chemical properties of superconductors meet certain specifications. The properties of superconductors are strongly influenced by each step of the processing procedure, which includes powder processing to form the superconductor powder, shape forming to produce bulk superconductors in convenient shapes, and finally an appropriate heat treatment to yield good superconducting properties. In this paper, the processing procedures for Y-Ba-Cu-O, Bi-Sr-Ca-Cu-O, Tl-Ca-Ba-Cu-O will be reviewed. Improvements in the processing procedures, and the resulting improvements in the mechanical and electrical properties, will be discussed. In addition, several fabrication techniques will be described which have produced bulk conductors having critical current densities approaching those of thin films. DOE

N89-27563# Argonne National Lab., IL. Materials and Components Technology Div.
STUDY OF THE MICROSTRUCTURE OF SILVER FILMS DEPOSITED BY ION ASSISTED DEPOSITION ONTO ALUMINUM OXIDE SUBSTRATES
R. A. Erck and G. R. Fenske 1989 18 p Presented at the 16th International Conference on Metallurgical Coatings and Equipment Exhibit, San Diego, CA, 17-21 Apr. 1989
(Contract W-31-109-eng-38)
(DE89-014665; CONF-890468-9) Avail: NTIS HC A03/MF A01

Ion-assisted deposition (IAD) can be used to modify the microstructure, density, or other properties of thin films. To understand the effects of ion bombardment on film growth, we studied the film morphology and hardness of evaporated Ag films that had been bombarded by Ar ions during deposition. Cross sections of deposited films were examined by scanning electron microscopy, and film hardness was measured with a diamond indenter. Substantial increases in film porosity and surface roughness were seen in the 1000-eV Ar-ion-bombarded specimens, compared to vapor-deposited specimens or to specimens bombarded with 300 or 150-eV ions. The IAD films generally had hardness values greater than that of evaporated films. Low hardness values were obtained for a porous 1000-eV IAD film; these are attributed to the presence of compressible pores. No Ar was detected in the films. DOE

N89-27564# Los Alamos National Lab., NM.
THE RESPONSE OF SINGLE CRYSTAL AND POLYCRYSTAL NICKEL TO QUASISTATIC AND SHOCK DEFORMATION
P. S. Follansbee and G. T. Gray, III 1989 5 p Presented at the Plasticity '89: International Symposium on Plasticity, Ton, Japan, 31 Jul. - 4 Aug. 1989
(Contract W-7405-eng-36)
(DE89-011168; LA-UR-89-1423; CONF-890772-2) Avail: NTIS HC A02/MF A01

Stress-strain measurements and TEM observations in shock-deformed nickel single and polycrystalline samples are reported. When the stress measurements are normalized by the appropriate Taylor factor, the shock induced strain hardening is shown to be similar in all materials studied. DOE

N89-27565# Los Alamos National Lab., NM.
ANOMALOUS TEMPERATURE DEPENDENCE OF Cu NMR LINE WIDTH AND MAGNETIZATION IN YBa2Cu3O(7-DELTA)
Masashi Takigawa, Chris P. Hammel, Robert H. Heffner, Zachary Fisk, Joe D. Thompson, and Martin Maley 1989 3 p Presented at the International Conference on Materials and Mechanisms of Superconductivity - High-Temperature Superconductors, Stanford, CA, 24-28 Jul. 1989
(Contract W-7405-eng-36)
(DE89-014291; LA-UR-89-2142; CONF-890718-4) Avail: NTIS HC A02

We report an anomalous temperature dependence of the magnetization and the NMR line width at the planar Cu(2) and oxygen sites in the mixed state of aligned YBa2Cu3O(7-delta) powder at relatively high field (greater than or equal to 30 kOe), where hysteresis of the magnetization due to flux pinning is not important. Both the magnetization and the NMR line width at all sites show a steep increase at low temperature. We found a much larger line width at Cu(2) sites than at oxygen sites when the magnetic field is applied perpendicular to the c-axis, indicating a very microscopic local field modulation. DOE

N89-27566# Los Alamos National Lab., NM.
O-17 NMR STUDY OF YBa2Cu3O(7-DELTA)
Masashi Takigawa, Chris P. Hammel, Robert H. Heffner, Zachary Fisk, Kevin C. Ott, and Joe D. Thompson 1989 5 p Presented at the International Conference on Materials and Mechanisms of Superconductivity - High-Temperature Superconductors, Stanford, CA, 24-28 Jul. 1989
(Contract W-7405-eng-36)
(DE89-014292; LA-UR-89-2141; CONF-890718-3) Avail: NTIS HC A02

We present our O-17 NMR experimental results in a magnetically aligned powder sample of YBa2Cu3O(7-delta) (T(c) = 93 K). The sign of the anisotropic Knight Shift shows that the spin density resides mainly on the p(sigma) orbitals at the planar O(2,3) and bridging O(4) sites. About 30 percent of the total spin susceptibility is attributed to the oxygen 2p(sigma) states. The Knight Shift at the O(2,3) sites decreases more rapidly than that at the chain O(1) sites, indicating a larger gap in the planes. The nuclear relaxation rate at the O(2,3) sites shows linear-T (Korringa) behavior above T(c), in contrast to the much weaker temperature dependence at the planar Cu(2) sites. However, these two rates show identical temperature dependence below about 110 K, indicating that an important change in the spin dynamics takes place above T(c). DOE

N89-27567# Los Alamos National Lab., NM.
NUCLEAR RELAXATION RATES AT COPPER AND OXYGEN SITES IN YBa2Cu3O7
Chris P. Hammel, Masashi Takigawa, Robert H. Heffner, Zachary Fisk, and Kevin C. Ott 1989 3 p Presented at the International Conference on Materials and Mechanisms of Superconductivity - High-Temperature Superconductors, Stanford, CA, 24-28 Jul. 1989
(Contract W-7405-eng-36)
(DE89-014308; LA-UR-89-2059; CONF-890718-5) Avail: NTIS HC A02/MF A01

We report NMR measurements of the nuclear relaxation rate at all copper and oxygen sites in magnetically aligned powder samples of YBa2Cu3O7. There is no peak in the oxygen relaxation rate below T(c) at any oxygen site supporting the possibility that d-wave pairs are formed in the superconducting state. Comparison of the oxygen and copper rates in the planes reveals a characteristic temperature greater than T(c). DOE

N89-27568# Argonne National Lab., IL. Materials Science Div.
EVIDENCE FOR PHONON-MEDIATED COUPLING IN SUPERCONDUCTING Ba SUB 0.6 K SUB 0.4 BiO3
D. G. Hinks, B. Dabrowski, D. R. Richards, J. D. Jorgensen, Shiyou Pei, and J. F. Zasadzinski (Illinois Inst. of Tech., Chicago.) 1989 12 p Presented at the Spring Meeting of the Materials Research Society, San Diego, CA, 24-28 Apr. 1989
(Contract W-31-109-eng-38)
(DE89-014642; CONF-890426-21) Avail: NTIS HC A03/MF A01

Superconducting Ba sub 0.6 K sub 0.4 BiO3, with a T sub c of 30K, shows a large O-18 isotope effect which indicates that phonons are involved in the pairing mechanism. Infrared reflectivity measurements indicate a value for the superconducting gap consistent with moderate coupling (2 delta kT sub c = 3.5 + or - 0.5). A mediating energy for pairing of about 40 MeV would be required to obtain a T sub c of 30K. Strong coupling of electrons by optical phonons (which are present in this material with energies up to 80 MeV) could account for the observed transition temperature. Recent tunneling spectroscopy shows the presence of strongly coupled optical phonons in the 40 to 70 MeV region, indicating that superconductivity in this material may be phonon mediated. DOE

N89-27569# Rome Univ. (Italy). Dipartimento di Fisica.
DETERMINATION OF THE KINETIC PARAMETERS OF THE THERMOLUMINESCENT CaF2 (Tm) CRYSTAL [DETERMINAZIONE DEI PARAMETRI CINETICI DEL CRISTALLO TERMOLUMINESCENTE CAF2 (TM)]
P. Bernardini, C. Bini, M. Crisafulli, D. Moraldi, and S. Orlando 6 Jun. 1988 21 p In ITALIAN
(Nota-Interna-915; ETN-89-94734) Avail: NTIS HC A03/MF A01

The kinetic parameters are determined following different procedures, based on the thermoluminescent light emission characteristics curve. The methods include the initial gradient method, the numerical fitting of the glow curve, and the peak shape method. The results obtained by the different methods are relatively close. Results for three peaks are detailed. ESA

N89-27570 Technische Univ., Delft (Netherlands). Lab. for Process Equipment.
CRYSTALLIZATION OF PARAXYLENE WITH SCRAPED SURFACE HEAT EXCHANGERS Thesis
R. deGoede Sep. 1988 184 p Sponsored by Esso Nederland B.V.
(WTHD-189; ISBN-90-370-0018-5; ETN-89-94803) Copyright Avail: Technische Univ. Delft, Faculteit der Werktuigbouwkunde en Maritieme Techniek, Leeghwaterstraat 44, 2628 CA Delft, Netherlands

Crystallization of paraxylene with a scraped surface heat exchanger process was studied in order to obtain useful tools to increase the purity of the final product and to reach a more efficient way of processing. The mechanisms leading to contamination of the product can be divided into two classes: (1) incorporation of impurities in the crystal body; and (2) attachment of impurities to the crystal surface. Class (1) mechanisms involve the formation of solid solutions because of thermodynamic and/or kinetic reasons. Class (2) mainly involves incomplete solid-liquid separation. Therefore, the specific surface area strongly determines the contribution of the second mechanism. Hence, control of the crystal size distribution is required in order to optimize the product quality for a given combination of crystallization and purification steps. The underlying crystallization process is inefficient in the sense that incrustation at the wall of the scraped surface heat exchangers severely disturbs heat transfer. The presence of a solid layer introduces an additional resistance against heat transfer. Therefore, a lower coolant temperature is required than without incrustation. ESA

N89-27571# Poitiers Univ. (France). Lab. de Metallurgie Physique.
ATOMIC SIMULATION OF CRYSTALLINE DEFECTS IN ORDERED STRUCTURES Final Report [SIMULATION ATOMIQUE DE DEFAUTS CRISTALLINS DANS LES STRUCTURES ORDONNEES]
P. Beauchamp and P. Veyssiere 1988 12 p In FRENCH
(Contract ERS-86/1468/DRET/DS/SR)
(ETN-89-94807) Avail: NTIS HC A03/MF A01

The plastic properties of ordered alloys are studied, and particularly the behavior of Ni3Al elastic limit and yield properties near 800 C. The state and energy of a crystal antiphase wall as a function of temperature and composition is calculated. Correlation functions are found and energy minimization is done by the joint gradient method. The results are not available. ESA

N89-27572# Maryland Univ., College Park. Dept. of Chemistry and Biochemistry.
MACROMOLECULAR CALCULATIONS FOR THE XTAL SYSTEM OF CRYSTALLOGRAPHIC PROGRAMS Annual Report, 1 Jun. 1988 - 31 May 1989
James M. Stewart 1 Jun. 1989 12 p
(Contract N00014-88-K-0323)
(AD-A208272) Avail: NTIS HC A03/MF A01 CSCL 06/1

During the last year effort has been concentrated on the adaption of the constrained refinement programs, i.e., PROTIN and PROLSQ to the XTAL system of crystallographic programs. The checking and documentation of programs for maximum entropy density calculations has been completed (programs MERUN, MEDENS, MEFFIT). Two new programs for modifying and manipulating electron density functions, CONVOL and FOGNU have been coded and documented. The generation of a test deck of idealized macromolecular data has been undertaken. GRA

N89-27573# Wisconsin Univ., Madison. Dept. of Chemistry.
NEW STRATEGIES FOR DISPLAY DEVICES BASED ON 2-6 MATERIALS
Elizabeth R. Leubker, Harvey Kalweit (Minnesota Mining and Mfg. Co., Saint Paul.), and Arthur B. Ellis 12 May 1989 9 p
(Contract N00014-85-K-0631)
(AD-A208288; UWIS/DC/TR-89/2) Avail: NTIS HC A02/MF A01 CSCL 07/2

Vapor phase diffusion and ion implantation provide versatile

synthetic techniques for preparing spatially inhomogeneous n-CdSxSe1-x samples. The color coded nature of photoluminescence and electroluminescence from these materials and the susceptibility of the emission to perturbation by electric fields gives rise to novel electro-optical effects: the spectral distribution can be altered by applied potential and can serve as the basis for patterned, multicolored emissive displays through the use of chemical and photoelectrochemical etching techniques. GRA

N89-27574# General Electric Co., Schenectady, NY. Research and Development.
DEVELOPMENT OF ELEMENTS OF A HIGH Tc SUPERCONDUCTING CABLE Report, 1 Dec. 1988 - 31 Mar. 1989
Kenneth W. Lay 31 Mar. 1989 7 p
(Contract N00014-88-C-0681)
(AD-A208370) Avail: NTIS HC A02/MF A01 CSCL 20/3

The goal of the program is the development of materials and processes for the fabrication of a composite superconductor element made of a superconducting coating on a supporting fiber. The composite will also include a barrier layer between the fiber and the superconductor and a protective layer on the surface. GRA

N89-27575# University of Southern Mississippi, Hattiesburg. Dept. of Polymer Science.
NITROGEN 15 T1 MEASUREMENTS OF SEMICRYSTALLINE NYLON 6 Technical Report No. 22, 1 Jun. 1988 - 31 May 1989
Douglas G. Powell and Lon J. Mathias 31 May 1989 12 p
(Contract N00014-89-J-1225)
(AD-A208481) Avail: NTIS HC A03/MF A01 CSCL 07/3

The solid state 15N NMR characterization of nylon 6 is reported. Nylon 6 (20 percent 15N enriched) was prepared by anionic polymerization of isotopically enriched caprolactam. The samples were prepared by three different treatments: quenched from the melt, slowly cooled and annealed, and artificially plasticized with excess caprolactam. CP/MAS spectra of the 15N enriched samples showed a single sharp peak (alpha crystal form) at 84.2ppm (relative to glycine) and a broader resonance at 87.2 ppm. Relaxation experiments were conducted to determine the spin lattice relaxation time T1N for each sample at 300K. The crystalline resonance was found to have T1N's of 125-416s, consistent with a rigid, crystalline component. The downfield peak (87.2 ppm) had two measurable T1N's: a short component with T1 of 1-3s and a second component with a longer T1 of 19-29s. GRA

N89-27576# Massachusetts Inst. of Tech., Cambridge. Center for Materials Science and Engineering.
SUPERCONDUCTIVITY AND MAGNETISM IN LAYERED MATERIALS Final Report, 15 Oct. 1987 - 14 Oct. 1988
M. S. Dresselhaus and G. Dresselhaus 16 May 1989 13 p
(Grant AF-AFOSR-0021-88; AF Proj. 2306)
(AD-A208487; AFOSR-89-0719TR) Avail: NTIS HC A02/MF A01 CSCL 20/3

During the one year period of this grant October 15, 1987 to October 14, 1988, efforts on the Program Superconductivity and Magnetism in Layered Materials were largely focused on introduction of our new program in high temperature superconductivity. We also completed studies of magnetic and superconducting graphite intercalation compounds. GRA

N89-27577# University of Southern Mississippi, Hattiesburg. Dept. of Polymer Science.
THE 15N NMR POWDER SPECTRA OF SEMICRYSTALLINE NYLON 6 Technical Report No. 23, 1 Jun. 1988 - 31 May 1989
Douglas G. Powell and Lon J. Mathias 31 May 1989 12 p
Submitted for publication
(Contract N00014-89-J-1225)
(AD-A208502) Avail: NTIS HC A02/MF A01 CSCL 07/3

The solid state 15N NMR chemical shift anisotropy (CSA) spectra of nylon 6 is reported. Nylon 6 (20 percent 15N enriched) was prepared by anionic polymerization of isotopically enriched caprolactam. The samples observed were prepared by extraction with methanol to remove unreacted caprolactam, then either annealed to promote crystallization or artificially plasticized by immersion in molten caprolactam. The anisotropic linewidth was approximately 200 ppm, intermediate between the range reported for sp2 and sp3 hybridized nitrogens and consistent with the partial double-bond character of the carbon-nitrogen bond in amides. GRA

77 THERMODYNAMICS AND STATISTICAL PHYSICS

Includes quantum mechanics; theoretical physics; and Bose and Fermi statistics.

For related information see also *25 Inorganic and Physical Chemistry* and *34 Fluid Mechanics and Heat Transfer.*

N89-27578# Nationaal Inst. voor Kernfysica en Hoge Energiefysica, Amsterdam (Netherlands).
THE sl (1/1;R)-COHOMOLOGIES IN BRST-GUPTA-BLEULER QUANTIZATION
Z. Hasiewicz, J. Kowalski-Glikman, J. Lukierski (Wroclaw Univ., Poland), and J. W. vanHolten Sep. 1988 8 p Sponsored in part by Stichting voor Fundamentel Onderzoek der Materie, Amsterdam, Netherlands
(NIKHEF-H/88-17; ETN-89-94256) Avail: NTIS HC A02/MF A01

For any theory with holomorphic first-class constraints, the real sl (1/1;R)-cohomology operator, the cohomology classes of which coincide with physical states defined by complex BRST-operators in Gupta-Bleuler quantization scheme, are constructed. ESA

N89-27579# State Univ. of New York, Buffalo. Dept. of Chemistry.
DYNAMICS OF AN M-LEVEL ATOM INTERACTING WITH GRAVITY FIELDS. 1: EFFECTS OF THE LEVEL NUMBER ON QUANTUM COLLAPSE AND REVIVAL
Xiao-shen Li, D. L. Lin, Thomas F. George, and Fu-li Li Apr. 1989 31 p
(Contract N00014-86-K-0043)
(AD-A207278; UBUFFALO/DC/89/TR-99-1) Avail: NTIS HC A03/MF A01 CSCL 20/10

A quantum mechanical theory is developed to treat the inter action of a multilevel atom with cavity fields of arbitrary detuning. The Hilbert space spanned by the energy eigenvectors is divided into subspaces specified by eigenvalues of the total excitation number, which is a constant of motion. Since the total Hamiltonian does not connect states in different subspaces, it can be diagonalized in each subspace independently. The time evolutions of the level occupation probabilities and the mean photon number are investigated numerically, and their variations with the atomic level number and the initial photon number are discussed. Their relation with the field squeezing is also discussed. GRA

N89-27580# Joint Inst. for Nuclear Research, Dubna (USSR). Lab. of Theoretical Physics.
QUANTUM AND THERMODYNAMIC FLUCTUATIONS IN THE DEGENERATE SCHEMATIC MODEL OF THE FINITE TEMPERATURE RANDOM PHASE APPROXIMATION
Dinh Nguyen Dang 1988 7 p
(DE88-706310; JINR-E-4-88-40) Avail: NTIS (US Sales Only) HC A02/MF A01

The system of equations of the finite temperature random phase approximation in frames of the degenerate schematic model is solved. The calculations are performed for the dipole state in the N=58 nucleon scheme. It is shown that the particle number fluctuations increase the dipole state energy whereas the thermodynamic ones wash out the discontinuity on the curve of the energy dependence on the temperature at the critical point of the phase transition from superfluid to normal state. DOE

N89-27581# Rome Univ. (Italy). Dipartimento di Fisica.
NOTE ON MULTILOOP CALCULATIONS FOR SUPERSTRINGS IN THE NSR FORMALISM
A. Yu. Morozov (Academy of Sciences, USSR, Moscow) and A. M. Perelomov 24 May 1988 12 p Submitted for publication
(Preprint-601; ETN-89-94690) Avail: NTIS HC A03/MF A01

A rather simple and attractive prescription for multiloop calculations is discussed. It consists of specification of metric, super-Beltrami differentials and the sum over spin structures in terms of the same odd characteristic e. At the end of calculations, summation over e is performed in order to restore modular invariance. For a special choice of regularization the contributions of matter supercurrents to cosmological constant vanish at least for p less than 5. ESA

N89-27582# Rome Univ. (Italy). Dipartimento di Fisica.
STOCHASTIC MECHANICS [MECCANICA STOCASTICA]
Francesco Guerra 24 Oct. 1988 26 p In ITALIAN Submitted for publication
(Preprint-634; ETN-89-94714) Avail: NTIS HC A03/MF A01

Stochastic mechanics is explained. The relation to quantum mechanics is described. It is shown that the stochastic variational principle for systems controlled in configuration space by a choice of Lagrange coordinates leads to a continuity equation and to a Hamilton-Jacobi-Madelung programming equation for a given Hamiltonian. ESA

N89-27583# Rome Univ. (Italy). Dipartimento di Fisica.
EFFECTIVE ACTION FOR QUANTUM GRAVITY IN TWO DIMENSIONS
K. Yoshida 11 May 1988 15 p Submitted for publication
Sponsored in part by Italian Ministry of Education, Rome
(Preprint-600; ETN-89-94689) Avail: NTIS HC A03/MF A01

The generating functional of the correlation functions of the stress energy tensor in conformal field theory is derived and shown to be equal to the effective action for two-dimensional induced gravity in the light cone gauge given by Polyakov (1987). Seeking the condition for consistent quantatization of such an action, one arrives at a chiral SU(2)xSU(2) current algebra. The corresponding Kac-Moody algebra has the central charge given by k=(C-26)/6. ESA

N89-27584# Rome Univ. (Italy). Dipartimento di Fisica.
ON THE INTEGRABILITY OF THE ERNST EQUATION
Donato Bini and Valeria Ferrari 16 Jun. 1988 7 p Submitted for publication
(Preprint-606; ETN-89-94694) Avail: NTIS HC A02/MF A01

A method of integration of the Ernst equation is proposed. A class of exact solutions allowing a conservation law is found. ESA

N89-27585# Rome Univ. (Italy). Dipartimento di Fisica.
KNOT THEORY AND QUANTUM GRAVITY
Carlo Rovelli and Lee Smolin (Yale Univ., New Haven, CT.) 17 Jun. 1987 11 p Previously announced in IAA as A88-53533 Submitted for publication
(Preprint-607; ETN-89-94695) Avail: NTIS HC A03/MF A01

Quantum general relativity is defined in terms of functionals of sets of loops in 3-space. In this representation exact solutions of the quantum constraints may be obtained. This result is related to the simplication of the constraints in Ashtekar's formalism. The general solution of the diffeomorphisms constraint and a large class of solutions of the full set of constraints are given in closed form. These are classified by the knot and link classes of the spatial 3-manifold. ESA

N89-27586# Rome Univ. (Italy).
BAE MEANSUREMENT SCHEMES AND OPTIMAL SENSITIVITY FOR GENERALIZED PARAMETRIC DEVICES
R. Onofio 15 Nov. 1988 13 p Presented at the International Workshop on Gravitational Wave Signal Analysis and Processing, Amalfi, Italy, 1-5 Jul. 1988 Submitted for publication
(Preprint-641; ETN-89-94719) Avail: NTIS HC A03/MF A01

Back Action Evasion stragegies of measurement are introduced. A technique for the treatment of the parametric transducers is discussed. A perturbative approach is used in the computation of the equation of the motion of a parametric transducer under resonance forcing terms. The concept of optimal pumping spectrum and the general framework in which this concept can be fully developed are outlined. It is shown that the stroboscopic measurement scheme may be considered as a by-product of the search for an optimal pumping spectrum having an infinite number of pumps. ESA

N89-27587# Rome Univ. (Italy). Dipartimento di Fisica.
ON THE PRODUCTION AND DETECTION OF GRAVITATIONAL WAVES FROM ARTIFICIAL SOURCES
Giordano DiambriniPalazzi 20 Apr. 1988 16 p
(Nota-Interna-912; ETN-89-94731) Avail: NTIS HC A03/MF A01

It is shown that it is conceivable to build sources on Earth to produce fluxes of continuous and monochromatic gravity waves of the order of 0.001 to 0.00001 erg/s/sq cm. The obtainable frequencies are in the range 10 to the 15 to 8th power Hz, corresponding to wavelengths from 1 micron to several meters. The fluxes estimated are not far from the fluxes expected from the supernova explosions inside the bandwidth of a bar detector of the Weber type and are of the same order or higher than those expected from periodic astrophysics sources like the Crab pulsar. It is also shown that for a certain range of frequencies detectors exist with sufficient sensitivity to detect the signal. ESA

80 SOCIAL SCIENCES (GENERAL)

Includes educational matters.

No abstracts in this category.

81 ADMINISTRATION AND MANAGEMENT

Includes management planning and research.

N89-27588# Tilburg Univ. (Netherlands). Dept. of Economics.
ESTIMATION OF THE RELATIONSHIP BETWEEN PROJECT ATTRIBUTES AND THE IMPLEMENTATION OF ENGINEERING TOOLS
K. A. Bubshait and W. J. Selen 1988 29 p
(PB89-149470; FEW-350) Avail: NTIS HC A03/MF A01 CSCL 05A

The study elaborates on earlier work by Bu-Bshait in identifying which project characteristics significantly intensify the need for a more elaborate use of project management techniques for various project types. A regression model is developed to estimate the number of project management techniques used, based upon a set of project characteristics. As such, the study provides further insight in the understanding of the missing link between project attributes and the implementation of engineering management tools. Author

82 DOCUMENTATION AND INFORMATION SCIENCE

Includes information management; information storage and retrieval technology; technical writing; graphic arts; and micrography.

For computer documentation see *61 Computer Programming and Software.*

N89-27589# National Oceanic and Atmospheric Administration, Boulder, CO. Environmental Research Lab.
ENVIRONMENTAL RESEARCH LABORATORIES PUBLICATION ABSTRACTS, FY 1988
Oct. 1988 214 p
(PB89-152656) Avail: NTIS HC A10/MF A01 CSCL 05B

All known Environmental Research Laboratories (ERL) articles published in journals for FY-1988 and those reports published within the official series of the Laboratories, as well as conference proceedings and other reports are included. Also included are publications by ERL-University cooperative institutes and by contractors funded by ERL. They include: investigation of ocean processes and their interactions with the atmosphere; studies of the ocean environment as it is affected by waste disposal and development of energy and food resources; fundamental studies of the upper atmosphere and space environments; atmosphere and ocean research on weather and climate change; research on severe local storms, hurricanes, and tsunamis; studies of cloud processes; research on the environmental effects of regional and global pollution; and development of equipment, instruments, systems, and facilities for these programs. Author

N89-27590# Economic Systems Analysis, Inc., Oak Ridge, TN.
TECHNOLOGY MASTER LIST DATA BASE MANAGEMENT SYSTEM, USER'S MANUAL
Jeanne Yates Rimpo and Marlene J. Owens Sep. 1988 111 p
(Contract GRI-5088-450-1667)
(PB89-177802; GRI-88/0249) Avail: NTIS HC A06/MF A01 CSCL 05B

In order to track the movement of Gas Research Institute (GRI) projects from the drawing-board concept to commercialized product, GRI developed a Master List of these technologies and research applications. An interactive data base management program (titled WIN) was developed to permit manipulation and updating of the Master List data base. The user's manual provides information on using this data base management program, including record management (adding, editing, deleting, and moving records), report generation (selecting, sorting, and printing), and data base maintenance. The system is designed to be used with the dBase III Plus software on IBM or compatible personal computers. Author

N89-27591# Lawrence Livermore National Lab., CA.
TECHNICAL ABSTRACTS, 1988
Marie Kotowski, ed. 1 May 1989 71 p
(Contract W-7405-eng-48)
(DE89-012811; UCID-21646) Avail: NTIS HC A04/MF A01

This document is a compilation of the abstracts from unclassified documents published by Mechanical Engineering at Lawrence Livermore National Laboratory (LLNL) during the calendar year 1988. Many abstracts summarize work completed and published in report form. These are UCRL-90,000 and 100,000 series documents, which include the full text of articles to be published in journals and of papers to be presented at meetings, and UCID reports, which are informal documents. Not all UCIDs contain abstracts: short summaries were generated when abstracts were not included. Technical Abstracts also provides brief descriptions of those documents assigned to the MISC (miscellaneous) category. These are generally viewgraphs or photographs presented at meetings. The abstracts cover the broad range of technologies within Mechanical Engineering and are grouped by the principal author's division. An eighth category is devoted to abstracts presented at the CUBE symposium sponsored jointly by LLNL, Los Alamos National Laboratory, and Sandia Laboratories. Within these areas, abstracts are listed numerically. An author index and title index are provided at the back of the book for cross referencing. DOE

N89-27592# Argonne National Lab., IL. Energy and Environmental Systems Div.
USER GUIDE FOR THE DATA ANALYSIS, RETRIEVAL, AND TABULATION SYSTEM (DARTS): A MAINFRAME COMPUTER CODE FOR GENERATING CROSS-TABULATION REPORTS
John L. Anderson Dec. 1988 39 p
(Contract W-31-109-eng-38)
(DE89-012930; ANL/EES-TM-371) Avail: NTIS HC A03/MF A01

A computer system known as the Data Analysis, Retrieval, and Tabulation System (DARTS) was developed by the Energy and Environmental Systems Division at Argonne National Laboratory to generate tables of descriptive statistics derived from analyses of housing and energy data sources. Through a simple input command, the user can request the preparation of a hierarchical table based on any combination of several hundred of the most commonly analyzed variables. The system was written in the Statistical Analysis System (SAS) language and designed for use on a large-scale IBM mainframe computer. DOE

N89-27593# Sandia National Labs., Albuquerque, NM. Geo-Science Analysis Div.
DEVELOPING A GEOLOGIC AND ENGINEERING PROPERTIES DATA BASE WITH INGRES
Margaret L. Krebs-Jespersen 1989 26 p Presented at the INGRES User Association Meeting, New Orleans, LA, 23 Apr. 1989
(Contract DE-AC04-76DP-00789)
(DE89-013520; SAND-89-0838C; CONF-8904194-3) Avail: NTIS HC A03/MF A01

The design of a data base for storing diverse geological and site engineering properties data from various sources using the INGRES data base management system has required: (1) designing tables for data that are similar but have very different test conditions to be reported; (2) determining what data is necessary to ensure that all records are unique; (3) changing, as necessary, the design of data base tables to accommodate the needs of new data submittals; (4) defining limits to comments and descriptions of test conditions to be stored in the data base; (5) solving problems caused by the limitations of the available field types in INGRES; and (6) designing a tracking system for data submissions to satisfy Project quality assurance requirements. The resulting relational data base design is simple, flexible, and capable of accommodating changes in requirements for data storage and user needs. The INGRES Report Writer utility has proven to be a powerful tool for generating reports because the Report Writer code is easily revised as table structure changes. Separate data storage tables can be joined for report production, and output can be customized for each user. DOE

N89-27594# National Inst. of Standards and Technology, Gaithersburg, MD.
NIST (NATIONAL INSTITUTE OF STANDARDS AND TECHNOLOGY) RESEARCH REPORTS, MARCH 1989
1989 36 p
(PB89-189310; NIST/SP-761) Avail: NTIS HC A03/MF A01 CSCL 05B

A number of articles are contained which discuss the following subjects: Research update; Light: The wave of the future; New centers to aid industry; Commercialization of technology: Whose job; NIST 1990 budget proposed; Quest for quality; Too hot to handle, but not to measure; the beauty of time; and Cold neutron facility. GRA

N89-27595# Federal Communications Commission, Washington, DC. Computer Applications Div.
COMMON CARRIER EARTH STATION DATABASE DOCUMENTATION

1988 275 p
(PB89-186050; FCC/DF/MT-89/005A) Avail: NTIS HC A12/MF A01 CSCL 05B

The documentation contains the Common Carrier Earth Station Application File information used by the Common Carrier Bureau in processing applications for licenses and permits. Each application is made up of 15 records containing such information as the status of the station, identification information, technical information, frequency information and any special provisions. Author

N89-27596# Oak Ridge Gaseous Diffusion Plant, TN.
ISSUES AND APPROACHES FOR ELECTRONIC DOCUMENT APPROVAL AND TRANSMITTAL USING DIGITAL SIGNATURES AND TEXT AUTHENTICATION
K. D. Streetman, A. J. Klein, J. L. Hardee, and M. E. Boling 10 Feb. 1989 65 p
(Contract DE-AC05-84OT-21400)
(DE89-013102; K/DSRD-96) Avail: NTIS HC A04/MF A01

This study identifies approaches to digital signature and text authentication (DS and TA) concerns for DOE-wide applications. Recommendations were derived from among the optional approaches identifiable from the literature and from known systems implementing digital signatures and text authenication. The primary issue is the adequacy of safeguards to assure signature and text authenticity. DOE

N89-27597# Sandia National Labs., Albuquerque, NM. Organic Materials Div.
MANAGEMENT INFORMATION DATABASE SYSTEM
Nancy L. Leishman May 1989 34 p
(Contract DE-AC04-76DP-00789)
(DE89-014595; SAND-88-3439) Avail: NTIS HC A03/MF A01

This is a description of a computerized database tool for use by operational management. The Management Information Database System was created to more efficiently maintain the information needed by managers for time and material cost accounting and resource scheduling. Reports produced reflect the current status of assignments and balances of F-orders. DOE

N89-27598# Rutgers - The State Univ., New Brunswick, NJ. Center for Expert Systems Research.
EMPIRICAL ANALYSIS AND REFINEMENT OF EXPERT SYSTEM KNOWLEDGE BASES Quarterly Report
Sholom M. Weiss and Casimir A. Kulikowski 31 May 1989 12 p
(Contract N00014-87-K-0398)
(AD-A208294) Avail: NTIS HC A03/MF A01 CSCL 12/7

Knowledge base refinement is the modification of an existing expert system knowledge base with the goals of localizing specific weaknesses in a knowledge base and improving an expert system's performance. Systems that automate some aspects of knowledge base refinement can have a significant impact on the related problems of knowledge base acquisition, maintenance, verification, and learning from experience. The SEEK system was the first expert system framework to integrate large-scale performance information into all phases of knowledge base development and to provide automatic information about rule refinement. A recently developed successor system, SEEK2 Ginsberg, Weiss, and Politakis 88 significantly expands the scope of the original system in terms of generality and automated capabilities. The investigators expect to make significant progress in automating empirical expert system techniques for knowledge acquisition, knowledge base refinement, maintenance, and verification. The investigators will demonstrate a rule refinement system in an application of the diagnosis of complex equipment failure: computer network troubleshooting. GRA

N89-27599# California Univ., Marina del Rey. Information Sciences Inst.
RESEARCH IN KNOWLEDGE DELIVERY Final Technical Report, 1 Nov. 1986 - 30 Sep. 1988
Eduard H. Hovy and William C. Mann 28 Mar. 1989 26 p
(Contract F49620-87-C-0005; AF Proj. 2304)
(AD-A208327; AFOSR-89-0609TR) Avail: NTIS HC A03/MF A01 CSCL 05/7

The research and development toward the goal of automatically planning and generating fluent multisentence paragraphs of English text is summarized. The work consisted of three principal components, namely knowledge representation, grammar development, and text structuring. With respect to knowledge representation, a powerful technique of linking the generator with arbitrary applications was developed by using a very general underlying taxonomy of entities in the world and various specific domain-related taxonomies. As part of grammar development, the invertibility of the grammar in use by the project was investigated, with the eventual goal of developing a combined bidirectional parsing-generation system using the same grammar net-work. Finally, a text structure planner was developed and the whole system was successfully used to generate paragraphs in three different application domains. GRA

83 ECONOMICS AND COST ANALYSIS

Includes cost effectiveness studies.

No abstracts in this category.

84 LAW, POLITICAL SCIENCE AND SPACE POLICY

Includes NASA appropriation hearings; aviation law; space law and policy; international law; international cooperation; and patent policy.

No abstracts in this category.

85 URBAN TECHNOLOGY AND TRANSPORTATION

Includes applications of space technology to urban problems; technology transfer; technology assessment; and surface and mass transportation.

For related information see also *03 Air Transportation and Safety, 16 Space Transportation,* and *44 Energy Production and Conversion.*

N89-27600# National Academy of Sciences - National Research Council, Washington, DC.
SCIENCE AND TECHNOLOGY ADVICE IN THE WHITE HOUSE: RECOMMENDATIONS FOR PRESIDENT-ELECT GEORGE BUSH
1988 20 p
(PB89-169817) Avail: NTIS HC A03/MF A01 CSCL 05D

The role and qualifications of the science and technology adviser from the perspective of pressures upon and opportunities available to the Bush Administration are discussed. Like the office itself, the following analysis and recommendations serve no purpose unless they serve the interests of the President of the United States. Author

N89-27601# Rensselaer Polytechnic Inst., Troy, NY. Center for Architectural Research.
NEW FRONTIER: ENVIRONMENTS FOR INNOVATION
Walter M. Kroner, ed. 1988 389 p Proceedings of the International Symposium on Advanced Comfort Systems for the Work-Environment, Rensselaerville, NY, 1-3 May 1988

(Grant NSF MSM-86-13483)
(PB89-151054; LC-89-060510) Copyright Avail: NTIS HC A17/MF A01 CSCL 05D

The collection of 37 papers addresses the sick building syndrome, the changes due to the introduction of computers in the workplace, low productivity in the work environment, electronically enhanced building systems, shifts in usage patterns, building diagnostics, energy efficiency, and whole building performance. GRA

N89-27602# National Inst. of Standards and Technology, Gaithersburg, MD. National Engineering Lab.
NATIONAL ENGINEERING LABORATORY'S 1989 REPORT TO THE NATIONAL RESEARCH COUNCIL'S BOARD ON ASSESSMENT OF NIST (NATIONAL INSTITUTE OF STANDARDS AND TECHNOLOGY) PROGRAMS Report, Apr. 1988 - Apr. 1989
Gail K. Ehrlich, ed. Mar. 1989 45 p
(PB89-189294; NISTIR-89/4060) Avail: NTIS HC A03/MF A01 CSCL 05A

An overview is given of the National Engineering Laboratory (NEL). Described is the climate that influences NEL's work, program and budget trends, and the external interactions with industry, academia, and trade and professional organizations. Descriptions of NEL's program activities with accompanying lists of recent accomplishments, trends, and significant budget changes are also included. The programs described are Electronic and Electrical Measurements, Manufacturing Research and Standards, Building Research, Fire Research, Chemical Engineering Metrology, Mathematical Sciences, Computing Support, Energy Related Inventions, and Law Enforcement Standards. The impact of the recently enacted Omnibus Trade and Competitiveness Act of 1988 is discussed. Author

N89-27603# Office of Technology Assessment, Washington, DC.
REPORT TO THE CONGRESS Annual Report, Fiscal Year 1988
Mar. 1989 137 p
(PB89-195408; OTA-A-411) Avail: NTIS HC A07/MF A01 CSCL 05A

(Public Law 92-484) to provide the Congress with the new effective means for securing competent, unbiased information concerning the physical, biological, economic, social and political effects of technological applications. The activities of OTA for the calendar year 1988 are summarized. Included are discussions of its organization and operation, summaries of assessments completed during 1986, descriptions of work in progress, and a list of staff members, advisors, and panel members. A copy of the Technology Assessment Act of 1972 is also included. GRA

N89-27604# Institute of Gas Technology, Chicago, IL.
DEDICATED LOW-PRESSURE NATURAL GAS-FUELED VEHICLE BASELINE ASSESSMENT. TASK 3 TOPICAL REPORT ON LIGHT-DUTY VEHICLES Topical Report, Jan. 1987 - Jan. 1989
R. T. Biederman, J. A. Arnold, and C. F. Blazek Jan. 1989 118 p
(Contract GRI-5086-530-1365; IGT Proj. 32001-03)
(PB89-195820; GRI-89/0122) Avail: NTIS HC A06/MF A01 CSCL 13F

The study defines a dedicated natural gas-fueled vehicle system that best incorporates all the features of the low-pressure natural gas storage system being developed. Cost sensitivity analyses are presented for 250, 100, and 25 vehicle fleets. These analyses are useful in assessing the feasibility of individual fleet applications under a variety of possible scenarios. These scenarios are approached using ranges to describe the critical parameters involved in the analysis, such as vehicle cost premium, fuel cost differential, annual mileage, O and M costs, and capital costs. GRA

88 SPACE SCIENCES (GENERAL)

No abstracts in this category.

89 ASTRONOMY

Includes radio, gamma-ray, and infrared astronomy, and astrometry.

N89-27605# Onsala Space Observatory (Sweden).
THE SWEDISH-ESO SUBMILLIMETER TELESCOPE (SEST)
R. S. Booth, G. Delgado, M. Hagstroem, L. E. B. Johansson, D. C. Murphy, M. Olberg, N. D. Whyborn, A. Greve (Domaine Univ., Saint Martin d'Heres, France), B. Hansson, and C. O. Lindstroem et al 1988 24 p Submitted for publication
(PB89-154892; Rept-88/31) Avail: NTIS HC A03/MF A01 CSCL 03A

The Swedish-ESO Submillimeter Telescope (SEST) is a 15 m telescope, which can operate at wavelengths down to 0.8 mm, built on the European Southern Observatory (ESO) site of La Silla, in the Chilean Andes, at an altitude of 2300 m. It is the only large submillimeter telescope in the Southern Hemisphere. The main technical features of the telescope and observing system, and the results of the commissioning tests by the team in Chile are described. The telescope reflector surface has been set within 65 micrometers vms of the ideal paraboloid, and the aperture efficiency at 100 GHz is about 60 percent. GRA

N89-27606# Michigan Univ., Ann Arbor. Physics Lab.
OBSERVING PRIMEVAL GALAXIES AND DARK MATTER WITH LAIRTS Final Report, 1 Feb. 1985 - 31 Aug. 1988
Dennis J. Hegyi 5 Dec. 1988 7 p
(Grant AF-AFOSR-0120-85; AF Proj. 2311)
(AD-A208286; AFOSR-89-0575TR) Avail: NTIS HC A02/MF A01 CSCL 03/1

Observations of the extragalactic background light have been made at three wavelengths using our charge coupled device (CCD) system with a large angular field of view on the McGraw-Hill 1.3 m telescope. Data has been obtained at high galactic latitudes to reduce complications resulting from foreground stars and galaxies and from infrared cirrus. Exposures from overlapping fields were obtained to check the internal consistency of the data. Also, a grid of scattering profiles was obtained in which a star was imaged at many different positions on and off the CCD to take account of scattering contributions. Because the fields contained so many foreground stars and galaxies, it was necessary to develop an automated technique using a matched filter to pick out these objects and to then subtract them from the data. This has been accomplished for fields consisting of one-quarter of a CCD field. Our data analysis has yielded an amplitude for the power spectrum which is about 2.5 times larger than calculated using a model with no galaxy luminosity evolution. Recently, Tyson has shown some clear evidence for galaxy luminosity evolution which while not quantitative, qualitatively explains our data. Other work during this funding period has been on the nature of dark matter, speckle inteferametric resolution of the binary star system Mu Cassioppeiae, and a measurement of the temperature of the cosmic background radiation at 2.64 mm. GRA

90 ASTROPHYSICS

Includes cosmology; celestial mechanics; space plasmas; and interstellar and interplanetary gases and dust.

For related information see also *75 Plasma Physics.*

N89-27607# National Oceanic and Atmospheric Administration, Boulder, CO. Space Environment Lab.

SPACE ENVIRONMENT LABORATORY Annual Report, FY 1988, 1 Oct. 1987 - 30 Sep. 1988

Jan. 1989 50 p

(PB89-159602) Avail: NTIS HC A03/MF A01 CSCL 03B

Topics covered include: space environment data collection services; solar flare forecasting and analysis; geomagnetic services development; research (ionospheric radio, sudden ionospheric disturbances, atmospheric ionospheric magnetospheric interactions, magnetospheric physics, interplanetary physics, solar physics, and solar X-ray physics); and development (space environment data system, operational satellite instrumentation, workstation and expert systems, object oriented programming, wide-area networking, and interplanetary scintillation observations). A listing of personnel, publications and talks is also presented. K.C.D.

N89-27608*# Fermi National Accelerator Lab., Batavia, IL.

COSMIC EVOLUTION OF NON-TOPOLOGICAL SOLITONS, PAPER 1

Joshua A. Frieman, Angela V. Olinto, Marcelo Gleiser, and Charles Alcock (Lawrence Livermore National Lab., CA.) May 1989 37 p

(Contract NAGw-1340; W-7405-eng-48; NSF PHY-82-17853) (NASA-CR-185353; NAS 1.26:185353; FERMILAB-Pub-89/128-A-Paper-1; NSF-ITP-89-87-Paper-1) Avail: NTIS HC A03/MF A01 CSCL 03B

Nontopological solitons are stable field configurations which may be formed in a primordial phase transition. Their cosmic evolution is studied, and the possibility that such objects could contribute significantly to the energy density of the Universe is examined. As the Universe cools, initially all but the largest lumps evaporate into free particles; those which survive may subsequently enter a brief accretion phase before they freeze out at a final size. Although the minimum critical charges which survive depend on particle masses and couplings, researchers develop an analysis which applies to a wide class of models. In most cases, solitons of moderate size survive the evaporation process only if there is a significant charge asymmetry or if they form at a temperature well below their binding energy per charge. Author

N89-27609# Instituto de Pesquisas Espaciais, Sao Jose dos Campos (Brazil).

TEMPORAL VARIABILITY OF WATER MASERS IN THE SOUTHERN HEMISPHERE M.S. Thesis [VARIABILIDADE TEMPORAL DOS MASERS DE AGUA NO HEMISFERIO SUL]

Bruno SestokasFilho Aug. 1988 130 p In PORTUGUESE; ENGLISH summary

(INPE-4646-TDL/338) Avail: NTIS HC A07/MF A01

A brief review is presented of radiation maser molecules, their observational characteristics and their importance to astrophysics. The molecular rotational spectra was analyzed and the basic equations of the maser theory was developed. In the water vapor maser monitoring program associated with regions of star formation at the Itapetinga Radio Observatory (ROI), the sources Orion A, G331.5-0.1 and GGD25 (NGC6334) was observed almost monthly from December 1980 to December 1986. The temporal variability of the intensity obtained from these masers had time scales 10(6) to 10(7) s providing rigid constraints to the possible pumping mechanisms. As a result of this monitoring program, several conclusions can be obtained depending of the evolutionary state and the dynamics of the sources. Author

N89-27610# Quaid-i-Azam Univ., Islamabad (Pakistan). Dept. of Mathematics.

BLACK HOLES IN CLOSED UNIVERSES

Asghar Qadir Aug. 1988 35 p Presented at the 5th Marcel Grossman Meeting, Perth, Australia, 8-13 Aug. 1988 Submitted for publication Prepared in cooperation with International Centre for Theoretical Physics, Trieste, Italy

(PB89-170039; QAUM-88/36) Avail: NTIS HC A03/MF A01 CSCL 03B

Black holes are usually defined in the context of asymptotically flat spacetimes. In order to demonstrate that the black hole and big crunch singularities are essentially part and parcel of the same singularity, cut-and-paste methods were used to construct models in which the black hole was embedded in a closed cosmology. The variation of the properties of the model with initial conditions is investigated. The problem, that there is no longer an observer at infinity (as a ready reference to define the black hole), is overcome by using a foliation of constant mean extrinsic curvature to define the preferred observer at every point. GRA

N89-27611# Quaid-i-Azam Univ., Islamabad (Pakistan). Dept. of Mathematics.

RELATIVISTIC EXPLANATION OF THE INCLINATION OF PLANETARY ORBITS

Asghar Qadir and H. A. Rizvi Aug. 1988 25 p

(PB89-170005; QAUM-88/35) Avail: NTIS HC A03/MF A01 CSCL 03B

While the planetary orbits are nearly in the same plane, they are in sufficiently different planes that either the inclination has to be taken as an initial condition or there has to be some driving mechanism. This mechanism must either take the planets out of their common plane or bring them towards the common plane. It was suggested that the General Relativistic force due to solar rotation, acting over sufficiently long times might provide the former mechanism. Using the pseudo-Newtonian formalism to express relativity in terms of forces, it is shown that the inclination could not be an initial condition. A generally accepted model of the early stages of the formation of the solar system is used to follow up the suggestion more concretely. GRA

N89-27612*# National Aeronautics and Space Administration. Goddard Space Flight Center, Greenbelt, MD.

COMMENTARY ON INTERSTELLAR MATTER ASSOCIATED WITH 18 OPEN CLUSTERS

David Leisawitz Washington Sep. 1989 20 p Sponsored by National Research Council

(Grants R033-87; NSF AST-81-6403; NSF AST-83-12332) (NASA-RP-1229; Rept-89B00238; NAS 1.61:1229) Avail: NTIS HC A03/MF A01 CSCL 03B

Information supplementary to that contained in Section 4 of an article entitled, A CO Survey of Regions Around 34 Open Clusters, (Leisawitz, Bash, and Thaddeus) published in the Astrophysical Journal Supplement Series, Volume 70, Number 4, August 1989 is summarized. The information presented here, which describes the interstellar environments of young clusters and some cluster physical characteristics, comes from observations published in the astronomical literature and the author's carbon monoxide (CO) emission line survey, and may help clarify our understanding of the interaction of massive stars with the interstellar medium. Author

N89-27613# Onsala Space Observatory (Sweden).

THE MOLECULAR CLOUD CONTENT OF EARLY TYPE GALAXIES. 1: DETECTIONS AND GLOBAL PROPERTIES

Tommy Wiklind and Christian Henkel (Max-Planck-Inst. fuer Radioastronomie, Bonn, Germany, F.R.) 1989 25 p Submitted for publication

(PB89-184949; Rept-89/01) Avail: NTIS HC A03/MF A01 CSCL 03B

An observing program was started to detect and map the molecular gas in elliptical and lenticular galaxies using the CO(1-0) and (2-1) emission lines as tracers of the gas. The galaxies they have observed to date constitute a sample selected through their far-IR properties and the presence of dust only. Remarkably enough, the detection rate was very high, approaching 100 percent if one excludes those with upper limits too large to be significant when compared with the levels of the detected ones. The

observations are presented and the global properties of the molecular content of early type galaxies compared with a sample of spiral galaxies compiled from the literature. GRA

N89-27614# Fermi National Accelerator Lab., Batavia, IL.
THE COSMOLOGICAL CONSTANT PROBLEM
A. D. Dolgov (Institute for Theoretical and Experimental Physics, Moscow, USSR) May 1989 14 p Presented at the 24th Rencontres de Moriond: Electroweak Interactions and Unified Theories, Les Arcs, France, 5-12 Mar. 1989
(Contract DE-AC02-76CH-03000)
(DE89-013150; FNAL/C-89/112-A; CONF-8903132-2) Avail: NTIS HC A03/MF A01

A review of the cosmological term problem is presented. Baby universe model and the compensating field model are discussed. The importance of more accurate data on the Hubble constant and the Universe age is stressed. DOE

N89-27615# Ceskoslovenska Akademie Ved, Ondrejov. Astronomicky Ustav.
DYNAMICS OF THE SOLAR SYSTEM: PROCEEDINGS, VOLUME 3
Milos Sidlichovsky, ed. 1987 211 p Proceedings of the 10th European Regional Astronomy Meeting of the IAU, Prague, Czechoslovakia, 24-29 Aug. 1987
(DE89-609828; INIS-mf-11400-Vol-3; CONF-8708269-Vol-3; Publ-68-Vol-3) Avail: NTIS HC A10/MF A01

The conference proceedings contains a total of 31 papers of which 7 were not incoporated in INIS. The mathematical methods of calculating the movements of the planets, their satellites and asteroids in the solar system, and the mathematical modeling of the past development of the solar system are discussed. Great attention is also devoted to resonance in the solar system and to the study of many celestial bodies. Four papers are devoted to planetary rings and three to modern astrometry. DOE

N89-27616# Ceskoslovenska Akademie Ved, Ondrejov. Astronomicky Ustav.
EVOLUTION OF GALAXIES. PROCEEDINGS, VOLUME 4
Jan Palous, ed. 1987 479 p Proceedings of the 10th European Regional Astronomy Meeting of the IAU, Prague, Czechoslovakia, 24-29 Aug. 1987
(DE89-609850; INIS-mf-11401-Vol-4; CONF-8708269-Vol-4; Publ-69-Vol-4) Avail: NTIS (US Sales Only) HC A21/MF A01

The proceedings contain 87 papers divided into 8 chapters. The chapter Bipolar outflows and star formations contains papers on optical and infrared observations of young bipolar outflow objects and the theory thereof, and observations of cometary nebulae. The chapter Masers and early stellar evolution discusses molecular masers and star forming regions. The following chapter contains papers on initial mass function and star formation rates in galaxies. The chapter Clusters and star formation contains data on OB associations and open star clusters, their development, and observations, CO and H sub 2 in the galaxy, the four vector model of radio emission and an atlas of the wavelength dependence of ultraviolet extinction in the Galaxy. The most voluminous is the chapter Evolution of galaxies. It contains papers on the theories of the physical and chemocynamic development of galaxies of different types, rotation research and rotation velocities of galaxies and their arms, and mathematical and laboratory models of morphological development. Chapter seven contains papers dealing with active extragalactic objects, quasars, and active galactic nuclei. The last chapter discusses cosmological models, the theory of the inflationary universe, and presents an interpretation of the central void and X-ray background. DOE

N89-27617# Rome Univ. (Italy). Dipartimento di Fisica.
RESONANT HELICITY FLIP OF ELECTRON NEUTRINO DUE TO MAGNETIC MOMENT AND DYNAMICS OF SUPERNOVA
M. B. Voloshin May 1988 10 p Submitted for publication Prepared in cooperation with Academy of Sciences (USSR), Moscow
(Preprint-598; ETN-89-94687) Avail: NTIS HC A02/MF A01

It is argued that magnetic moment of electron neutrino mu=10 to the minus 11th power muB is most likely to induce adiabatic resonant (i.e., complete) helicity flip of neutrino in the layer of the supernova core with density 10 to the 12th power g/cc. Therefore such a value of mu does not lead to an inconsistency with the observed neutrino events from the supernova SN1987a. The process proposed gives rise to a rapid energy transfer from the inner core to the outer layers which can explain the mechanism of blowing of the supernova's envelope. ESA

91 LUNAR AND PLANETARY EXPLORATION

Includes planetology; and manned and unmanned flights.
For spacecraft design or space stations see *18 Spacecraft Design, Testing and Performance.*

N89-27618# Los Alamos National Lab., NM. Earth and Space Sciences Div.
CHARACTERIZATION OF LUNAR ILMENITE RESOURCES
Grant Heiken and David T. Vaniman 1989 30 p Presented at the Lunar Planetary Science Conference, Houston, TX, 12 Mar. 1989
(Contract W-7405-eng-36)
(DE89-013455; LA-UR-89-1793; CONF-8903111-3) Avail: NTIS HC A03/MF A01

Ilmenite will be an important lunar resource, to be used mainly for oxygen production but also as a source of iron. Ilmenite abundances in high-Ti basaltic lavas are higher (10 to 20 percent) than in high-Ti mare soils (mostly less than 10 percent). This factor alone may make crushed high-Ti basaltic lavas most attractive as a target for ilmenite extraction. Concentration of ilmenite from either a crushed basalt or regolith requires sizing to avoid polycrystalline fragments. In coarse-grained high-Ti basaltic lavas, about 60 to 80 percent of the ilmenite will consist of relatively clean single crystals if the rocks are crushed to a size of 0.2 mm. Fine-grained high-Ti basalts, with thin skeletal or hopper-shaped ilmenites, would produce essentially no free or clean ilmenite grains unless crushed to sizes of less than 0.15 mm, and only approximately 7 percent free ilmenite if crushed to sizes smaller than 0.05 mm. Data from the 2.8 m-thick regolith sampled by coring at the Apollo 17 site show that in even the most basalt-clast-rich and least mature stratigraphic intervals, free ilmenite grains make up less than 2 percent of the 0.02- to 0.2-mm size fraction and a mere 0.3 percent of the 0.2- to 2-mm size fraction. DOE

N89-27619*# National Aeronautics and Space Administration. Lewis Research Center, Cleveland, OH.
LUNAR PRODUCTION OF SOLAR CELLS
Geoffrey A. Landis and Maria Antonietta Perino (Aeritalia S.p.A., Turin, Italy) May 1989 18 p Presented at the 9th Biennial SSI/Princeton Conference on Space Manufacturing, Princeton, NJ, 10-13 May 1989; sponsored by the Space Studies Inst.
(NASA-TM-102102; E-4866; NAS 1.15:102102) Avail: NTIS HC A03/MF A01 CSCL 03B

The feasibility of manufacturing of solar cells on the moon for spacecraft applications is examined. Because of the much lower escape velocity, there is a great advantage in lunar manufacture of solar cells compared to Earth manufacture. Silicon is abundant on the moon, and new refining methods allow it to be reduced and purified without extensive reliance on materials unavailable on the moon. Silicon and amorphous silicon solar cells could be manufactured on the moon for use in space. Concepts for the production of a baseline amorphous silicon cell are discussed, and specific power levels are calculated for cells designed for both lunar and Earth manufacture. Author

N89-27620# Rome Univ. (Italy). Dipartimento di Fisica.
MERCURY'S MAGNETIC FIELD: IMPLICATIONS ON THE INNER COMPOSITION OF THE PLANET
M. Chiappini 30 Nov. 1988 18 p In ITALIAN; ENGLISH

summary
(Nota-Interna-926; ETN-89-94745) Avail: NTIS HC A03/MF A01

The data from Mariner 10 on Mercury is analyzed. The magnetic field intensity is several hundred nT. The comparison of properties for Earth and Mercury indicate that the field strength is more determined by rotation rate then any other property such as heat or size of the core. The mechanisms suggested are either a dynamo like the one in the Earth or a residual magnetization (or both).
ESA

92 SOLAR PHYSICS

Includes solar activity, solar flares, solar radiation and sunspots.

For related information see *93 Space Radiation.*

N89-27621# Helsinki Univ. of Technology, Kylmaelae (Finland). Metsaehovi Radio Research Station.
SOLAR MICROWAVE RADIATION MAPS MEASURED AT METSAEHOVI RADIO RESEARCH STATION IN 1982 - 1983
Seppo Urpo, Silja Pohjolainen, and Harri Teraesranta 1988 97 p
(PB89-154876; SER-A-3; ISSN-0783-8751; ISBN-951-754-677-7) Avail: NTIS HC A05/MF A01 CSCL 03B

The Metsaehovi Radio Research Station operates a 14 m diameter radio telescope. Annually the telescope has been reserved for solar measurements for 4 to 10 weeks, typically during summer months. Measurements include maps of the whole or part of the Sun, tracking of active regions and solar oscillation monitoring. Most of the solar maps have been measured using receivers operating at 22.2 GHz or at 36.8 GHz. The sensitivity of receivers is good enough for 0.2 sfu resolution. In the temperature scale the resolution is better than 100 K and it is limited by the changes of the atmospheric attenuation. The purpose of the report is to publish at least one map for each of the days when measurements were performed. For some of these days there exist several measured maps. The volume contains selected maps measured in 1982 and 1983. A list of all measured maps during this period is included. GRA

N89-27622# Naval Research Lab., Washington, DC.
EQUILIBRIUM OF SOLAR CORONAL ARCADES Interim Report
John M. Finn (Science Applications International Corp., McLean, VA.) and James Chen 27 Mar. 1989 70 p Prepared in cooperation with Maryland Univ., College Park
(AD-A207311; NRL-MR-6402) Avail: NTIS HC A04/MF A01 CSCL 03/2

Properties of two-dimensional straight (symmetric in z) magnetic arcade equilibria in the solar corona are studied within the framework of magnetohydrodynamics. Sequences of MHD equilibria are obtained by solving the Grad-Shafranov equation with the footprint displacement and the entropy prescribed. It is shown that no multiple solutions, or bifurcations, result. This is to be contrasted with the approach of prescribing the axial magnetic field Bz(psi) or pressure p(psi), in which bifurcations do occur. The physical conditions for which the footprint displacement or entropy, as opposed to Bz or p, must be specified are discussed. It is argued that these conditions are more likely to occur in the corona than those conditions under which Bz and p may be prescribed. The lack of bifurcations indicates that equilibrium will not be lost as the footprint displacement or entropy is increased. The limiting configurations for infinite footprint displacement and infinite entropy are also discussed. It is shown that although the current density does become somewhat peaked, the total current in the peak region decreases as the system is sheared (or heated). In fact, the current in this peak region contains a rapidly decreasing fraction of the total current so that the limiting configuration is not one in which the current is concentrated into a current sheet.
GRA

N89-27623*# National Aeronautics and Space Administration. Lewis Research Center, Cleveland, OH.
SOLAR RADIATION ON MARS
Joseph Appelbaum and Dennis J. Flood Aug. 1989 33 p Prepared in cooperation with Tel-Aviv Univ. (Isra el)
(NASA-TM-102299; E-4865; NAS 1.15:102299) Avail: NTIS HC A03/MF A01 CSCL 03B

Detailed information on solar radiation characteristics on Mars are necessary for effective design of future planned solar energy systems operating on the surface of Mars. Presented here is a procedure and solar radiation related data from which the diurnally, hourly and daily variation of the global, direct beam and diffuse insolation on Mars are calculated. The radiation data are based on measured optical depth of the Martian atmosphere derived from images taken of the sun with a special diode on the Viking cameras; and computation based on multiple wavelength and multiple scattering of the solar radiation. Author

N89-27624# National Geophysical Data Center, Boulder, CO.
SOLAR-GEOPHYSICAL DATA NUMBER 535, PART 1. DATA FOR FEBRUARY, JANUARY 1989, AND LATE DATA Prompt Reports, March 1989
Helen E. Coffey, ed. Mar. 1989 143 p
(PB89-185987; SGD-535-Pt-1; LC-79-640375; ISSN-0038-0911) Avail: NTIS HC A07/MF A01 CSCL 03B

Solar-geophysical information is presented in tabular and graphic form. Categories include detailed index for 1988 and 1989; data for February 1989 (advance and world-wide IUWDS alert periods, solar activity indices, solar flares, solar radio emission, Stanford mean solar magnetic field); data for January 1989 (solar active regions, sudden ionospheric disturbances, solar radio spectral observations, cosmic ray measurements by neutron monitor, geomagnetic indices, radio propagation indices); and late data (solar active regions -- H-alpha synoptic charts 1806 to 1808 (September-November 1988), cosmic ray measurements by neutron monitor -- Thule, December 1988, geomagnetic indices -- sudden commencements/solar flare effects December 1988). GRA

N89-27625# National Geophysical Data Center, Boulder, CO.
SOLAR-GEOPHYSICAL DATA NUMBER 535, PART 2. DATA FOR SEPTEMBER 1988, AND MISCELLANEOUS Comprehensive Reports, March 1989
Helen E. Coffey, ed. Mar. 1989 77 p
(PB89-185995; SGD-535-Pt-2; LC-79-640375; ISSN-0038-0911) Avail: NTIS HC A05/MF A01 CSCL 03B

Solar-geophysical information is presented in tabular and graphic form. Categories include a detailed index for 1988 and 1989; data for September 1988 (solar flares, solar radio bursts at fixed frequencies, solar X-ray radiation from GOES satellite, mass ejections from the sun, active prominences and filaments); and miscellaneous data (interplanetary solar wind data, IMP-8, February-November 1988. GRA

N89-27626# Bern Univ. (Switzerland). Div. of Solar Observations.
BERNE SOLAR OBSERVATIONS FOR JANUARY-DECEMBER 1988
1989 84 p
(Rept-54; ETN-89-94926) Avail: NTIS HC A05/MF A01

The results of the standard measurements carried out at the solar observatory are presented. The measurements show start, maximum, duration, peak flux, and circular polarization at peak as percentage, of outstanding events. ESA

93 SPACE RADIATION

Includes cosmic radiation; and inner and outer earth's radiation belts.

For biological effects of radiation see *52 Aerospace Medicine*. For theory see *73 Nuclear and High-Energy Physics*.

N89-27627# Sandia National Labs., Albuquerque, NM.
DETECTION OF VERY HIGH ENERGY GAMMA-RAYS FROM THE CRAB NEBULA
C. Akerlof, J. DiMarco, H. Levy, D. Meyer, P. Radusewicz, R. Tschirhart, Z. Yama, and C. MacCallum 28 Apr. 1989 9 p Presented at the Gamma Ray Observatory Science Workshop, Greenbelt, MD, 10-12 Apr. 1989 Prepared in cooperation with Michigan Univ., Ann Arbor
(Contracts DE-AC04-76DP-00789; DE-AC02-76ER-01112)
(DE89-011840; SAND-89-1234C; UM-HE-89-11; CONF-8904216-1) Avail: NTIS HC A02/MF A01

During the period October 1988 through December 1988, a search was made for very high energy gamma rays from the direction of the Crab nebula using the atmospheric Cerenkov technique. The detector consisted of seven-fold arrays of photomultiplier tubes at the focii of two 11-meter diameter solar concentrators situated in Albuquerque, New Mexico. A dc signal was detected from the Crab nebula with a statistical significance of 5.8 sigma after the application of various cuts designed to suppress the background of hadronic showers. A search for a pulsed component failed to identify a significant signal in phase with the radio pulse from the Crab pulsar. These results, with a threshold energy of 200 GeV, are in substantial agreement with high energy results recently reported by the Mt. Hopkins group. DOE

N89-27628# Los Alamos National Lab., NM. Space Astronomy and Astrophysics Group.
SPECTRA OF CRAB-LIKE PULSARS: A GRO PERSPECTIVE
Cheng Ho 1989 9 p Presented at the Gamma Ray Observatory Science Workshop, Greenbelt, MD, 10-13 Apr. 1989
(Contract W-31-109-eng-38)
(DE89-013461; LA-UR-89-1760; CONF-8904216-2) Avail: NTIS HC A02/MF A01

A single-parameter model has been constructed to calculate the continuum spectrum of energetic pulsed radiation resulting from the formation of a Crab-type charge depletion region (gap) in the outer magnetosphere of rapidly spinning pulsars (Ho 1989). We discuss the characteristics of the theoretical predictions for the Crab pulsar and the specific features expected in the energy bands of the Gamma-Ray Observatory (GRO). These features include a possible spectral dip in the 0.3 to 30 MeV range, a change in polarization behavior below and above the dip, if polarization can be discerned, and most importantly, an exponential roll-over in the energy range necessary to detect the exponential roll-over. This model predicts that the 50 ms pulsar in the Large Magellanic Cloud (PSR0540-693) will be marginally detectable by GRO with a nominal two-week integration. Furthermore, we discuss the spectrum and detectability of a pulsar with 0.5 ms period and a surface magnetic field of 10(9) G. Such a pulsar may exist in SN 1987A. Since the 50 ms pulsar and SN 1987A are within the same field of view of GRO, it will be of great importance to take an extra long integration of this region to search for gamma-ray emission from these sources. DOE

N89-27629*# Stanford Univ., CA. Center for Space Science and Astrophysics.
STATISTICAL STUDY OF THE CORRELATION OF HARD X-RAY AND TYPE 3 RADIO BURSTS IN SOLAR FLARES
Russell J. Hamilton and Vahe Petrosian May 1989 39 p Submitted for publication
(Grants NsG-7092; NSF ATM-87-05084)
(NASA-CR-185833; NAS 1.26:185833; CSSA-ASTRO-89-03)
Avail: NTIS HC A03/MF A01 CSCL 03B

A large number of hard X-ray events which were recorded by the Hard X-Ray Burst Spectrometer (HXRBS) on the Solar Maximum Mission (SMM) during the maximum of the 21st solar cycle (circa 1980) are analyzed in order to study their statistical correlation with type 3 bursts. The earlier finding by Kane (1981) are confirmed qualitatively that flares with stronger hard X-ray emission, especially those with harder spectra, are more likely to produce a type 3 burst. The observed distribution of hard X-ray and type 3 events and their correlations are shown to be satisfactorily described by a bivariate distribution consistent with the assumption of statistical linear dependence of X-ray and radio burst intensities. From this analysis it was determined that the distribution of the ratio of X-ray intensity (in counts/s) to type 3 intensity (in solar flux units) which has a wide range and a typical value for this ratio of about 10. The implications of the results for impulsive phase models are discussed. Author

N89-27630# Lawrence Livermore National Lab., CA. Physics Dept.
USE OF THE EGRET (ENERGETIC GAMMA-RAY EXPERIMENT TELESCOPE) IN STUDIES OF THE ORIGIN OF THE COSMIC RADIATION
Charles D. Dermer 19 May 1989 9 p Presented at the Gamma Ray Observatory Science Workshop, Greenbelt, MD, 10-12 Apr. 1989
(Contract W-7405-eng-48)
(DE89-013785; UCRL-101129; CONF-8904216-4) Avail: NTIS HC A02/MF A01

The Energetic Gamma-Ray Telescope (EGRET) onboard the Gamma Ray Observatory will provide the first detailed map of the galaxy showing both intensity and spectral variations at greater than 20 MeV gamma-ray energies. Possible reasons for gamma-ray spectral variations are considered under the hypothesis that point sources of cosmic rays exist. We show how the spectrum and intensity of cosmic rays in the vicinity of such objects can depend on propagation effects, injection conditions and model geometry in a number of special cases. DOE

N89-27631# Rome Univ. (Italy). Dipartimento di Fisica.
A METHOD TO CALIBRATE THE LIGHT RESPONSE OF A HIGH RESOLUTION ELECTROMAGNETIC CALORIMETER WITH COSMIC RAYS
B. Borgia, M. Diemoz, and S. Morganti 22 Nov. 1988 17 p
(Nota-Interna-925; ETN-89-94744) Avail: NTIS HC A03/MF A01

In the framework of calibrating and monitoring the energy response of a high resolution electromagnetic calorimeter the different role played by electrons and muons is discussed. A set of relations between the signal amplitudes measured in cosmic ray events and the physical quantities entering in the energy determination is derived. The absolute light yield of the detector can be monitored by the ionization loss of muons of known momentum or by the average ionization of muons with the cosmic ray energy distribution. A method to determine this average ionization in a precise way, using noninteracting pions of known momentum is given. A system to correct the calibration constants for the effect of the variation of the optical properties of each detector element is outlined. It is stressed that precise knowledge of the ionization loss is crucial. This consideration led the L3 collaboration to measure the Bi4Ge3O12 (BGO) ionization loss and verify the agreement with theoretical formulas at the percent level. ESA

99 GENERAL

No abstracts in this category.

Typical Subject Index Listing

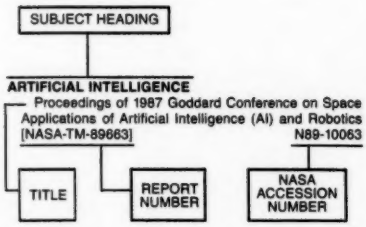

The subject heading is a key to the subject content of the document. Titles, report numbers, and accession numbers of pertinent documents are provided under each subject heading. When the title is insufficiently descriptive of the document content, a title extension has been added, separated from the title by three hyphens. The report number helps to indicate the type of document cited (e.g., NASA report, NASA translation, NASA contractor report). The NASA accession number is the number by which the document abstracts are arranged in this journal and by which the document is sold or requested. The titles, with title extensions if present, are arranged under each subject heading in ascending accession number order. The subject headings have been selected from the latest revision of the *NASA Thesaurus* (NASA SP-7064).

A

ABRASION RESISTANCE
Evaluation of barrier cable impact pad materials
[AD-A207554] N89-26864

ABSORBENTS
Molecular sieve films from zeolited-silica microcomposites
[DE89-009831] N89-26921

ABSORPTION CROSS SECTIONS
Production of pure ozone by means of electric discharges for measuring absorption coefficients
[NOTA-INTERNA-913] N89-27042

ABSORPTION SPECTROSCOPY
Optical detection and spectroscopy of single molecules in a solid
[AD-A207594] N89-26940
The role of X-ray absorption spectroscopy in electronic structure studies
[DE89-014677] N89-26952

ABSORPTIVITY
Production of pure ozone by means of electric discharges for measuring absorption coefficients
[NOTA-INTERNA-913] N89-27042

ABSTRACTS
Center for Electronics and Electrical Engineering Technical Progress Bulletin covering center programs, October to December 1988 with 1989 CEEE events calender
[PB89-193270] N89-27087
Environmental Research Laboratories publication abstracts, FY 1988
[PB89-152656] N89-27589
Technical Abstracts, 1988
[DE89-012811] N89-27591

ACCELERATION (PHYSICS)
Injuries to seat occupants of light airplanes
[AD-A207579] N89-26830

ACCELERATION STRESSES (PHYSIOLOGY)
Full coverage anti-G-suit and balanced pressure breathing
[PB89-174635] N89-27343

ACCELERATION TOLERANCE
Brain o2 reserve limiter for high performance aircraft
[AD-D014137] N89-26858

ACCELERATORS
A one-dimensional scintillator camera for the SATURN X-ray simulation accelerator
[DE89-009327] N89-27492

ACCELEROMETERS
Wideband electromagnetic damping of vibrating structures
[AD-D014069] N89-27208

ACCIDENTS
Structural analysis of a thermal insulation retainer assembly
[NASA-TM-101580] N89-27212
Safety testing program for the Galileo mission radioisotope thermoelectric generator
[DE89-011192] N89-27494

ACCURACY
Accuracy increase in waveform Gauss Seidel
[DE89-014812] N89-27437
Safety in numbers: The boundless errors of numerical computation
[DE89-014813] N89-27438

ACETYLENE
Surface plasmon study of monolayer-bilayer transition in poly-4-BCMU and poly-3-BCMU polydiacetylene Langmuir-Blodgett films
[AD-A207404] N89-26938
Synthesis and optical properties of a new class of polyamides containing reactive diacetylene groups
[AD-A208752] N89-27021
Thermal and mechanical properties of polyurethane-diacetylene segmented copolymers. Part 1: Molecular weight and annealing effects
[AD-A208753] N89-27022
Thermal and mechanical properties of polyurethane-diacetylene segmented copolymers. Part 2: Effects of diacetylene cross-polymerization
[AD-A208754] N89-27023

ACID BASE EQUILIBRIUM
History of the application of the generalized Lewis acid-base theory to metals
[DE89-012992] N89-26984

ACID RAIN
Assessing the sensitivity of high altitude New Mexican wilderness lakes to acidic precipitation and trace metal contamination
[PB89-148456] N89-27262

ACIDITY
Studies of the fundamental nature of catalytic acidity, sites and intermediates
[DE89-012946] N89-26947

ACOUSTIC MEASUREMENT
Sensor development programs at NASA Ames Research Center
[NASA-TM-102217] N89-26808
Measurement of the bending wave power flow by the structural intensity technique
[VTT-583] N89-27129

ACOUSTIC STREAMING
Measurement of the bending wave power flow by the structural intensity technique
[VTT-583] N89-27129

ACOUSTICS
EIGEN: A program to compute eigenrays from HARPA (Hamiltonian Acoustic Ray-Tracing Program for the Atmosphere)/HARPO (Hamiltonian Acoustic Ray-Tracing Program for the Ocean) raysets
[PB89-165781] N89-27460
Reduction of blade-vortex interaction noise using higher harmonic pitch control
[NASA-TM-101624] N89-27485

ACOUSTO-OPTICS
Polarization matrices of lithium niobate
[AD-A207231] N89-27462
Time-sequential optical data processing
[AD-A207514] N89-27500

ACRYLATES
Dynamics of surface bound polymers and coupling agents
[AD-A208747] N89-27020

ACTIVATION
Antenna shaft positioning device
[AD-D014120] N89-27191

ACTIVE CONTROL
Design of an active helicopter control experiment at the Princeton Rotorcraft Dynamics Laboratory
[NASA-CR-185490] N89-26859
Control of flexible structures
[AD-A207520] N89-26883

ACTUATORS
The NASA Langley Research Center 0.3-meter transonic cryogenic tunnel T-P/Re-M controller manual
[NASA-CR-181868] N89-26869

ADA (PROGRAMMING LANGUAGE)
Kernel user's manual version 1.0
[AD-A207414] N89-27375

ADDITIVES
Cryogenic tensile properties of AA 2090 weldments
[DE89-012979] N89-26971
Modifiers in rhodium catalysts for carbon monoxide hydrogenation: Structure-activity relationships
[DE89-013802] N89-27028

ADHESION
Flexible backbone aromatic polyimide adhesives
[NASA-TM-100631] N89-27001

ADHESION TESTS
Flexible backbone aromatic polyimide adhesives
[NASA-TM-100631] N89-27001

ADHESIVE BONDING
Flexible backbone aromatic polyimide adhesives
[NASA-TM-100631] N89-27001

ADHESIVES
Flexible backbone aromatic polyimide adhesives
[NASA-TM-100631] N89-27001

ADIABATIC CONDITIONS
Combustion characteristics of dry coal-powder-fueled adiabatic diesel engine
[DE89-000978] N89-27197

ADSORPTION
Molecular sieve films from zeolited-silica microcomposites
[DE89-009831] N89-26921
Adsorption and coadsorption of CO and NO on the Rh(100) surface: A theoretical analysis
[AD-A207323] N89-26935
Oxygen transfer to ethylene catalyzed by the Ag(110) surface
[AD-A207325] N89-26936
The structure and reactivity of alkylsiloxane monolayers formed by reaction of alkyltrichlorosilanes on silicon substrates
[AD-A208267] N89-27011

ADVANCED VERY HIGH RESOLUTION RADIOMETER
GEOSAT altimeter sea-ice mapping
[AD-A207391] N89-27234

AERIAL PHOTOGRAPHY
Alaska collection SAR (Synthetic Aperture Radar) data summary
[AD-A208530] N89-27067

AERODYNAMIC CHARACTERISTICS
A procedure for computing surface wave trajectories on an inhomogeneous surface
[NASA-TP-2929] N89-26811
An experimental investigation of the ground vortex created by a moving jet
[NASA-CR-181841] N89-26815
Airworthiness and flight characteristics evaluation of the EH-60A (Quick Fix) helicopter
[AD-A207417] N89-26839
Aerodynamic parameters of an advanced fighter aircraft estimated from flight data. Preliminary results
[NASA-TM-101631] N89-26861

AERODYNAMIC CONFIGURATIONS
Experimental program for real gas flow code validation at NASA Ames Research Center
[NASA-TM-100093] N89-26816

The conceptional design study of USB powered lift aircrafts in FY 1986
[NAL-TR-958] N89-26835
Feasibility and benefits of laminar flow control on supersonic cruise airplanes
[NASA-CR-181817] N89-26841
AERODYNAMIC DRAG
Technical Status Review on Drag Prediction and Analysis from Computational Fluid Dynamics: State of the Art
[AGARD-AR-256] N89-26817
Drag prediction and analysis from computational fluid dynamics, state-of-the-art in France N89-26818
Drag prediction and analysis from CFD state-of-the-art in Germany N89-26819
Some results on flow calculations involving drag prediction N89-26820
State-of-the-art of aircraft drag prediction in Italy by means of theoretical methods N89-26821
Aircraft drag prediction for transonic potential flow N89-26822
CFD methods for drag prediction and analysis currently in use in UK N89-26823
Computational fluid dynamics drag prediction: Results from the Viscous Transonic Airfoil Workshop N89-26824
CFD drag prediction for aerodynamic design N89-26825
Combination boundary layer control system for high altitude aircraft
[AD-D014075] N89-26837
AERODYNAMIC FORCES
Feasibility study for enhanced lateral control of the P-3C aircraft
[AD-A208461] N89-26863
AERODYNAMIC HEATING
A review of high-speed, convective, heat-transfer computation methods
[NASA-TP-2914] N89-27116
Hypervelocity atmospheric flight: Real gas flow fields
[NASA-TM-101055] N89-27117
AERODYNAMICS
Numerical study of three-dimensional separation and flow control at a wing/body junction
[NASA-CR-185819] N89-26826
Wind power: Today's energy option
[DE89-000876] N89-27253
AEROELASTICITY
Method for experimental determination of flutter speed by parameter identification
[NASA-TP-2923] N89-26844
ASR4: A computer code for fitting and processing 4-gage anelastic strain recovery data
[DE89-012239] N89-27395
Modeling and computational algorithms for parameter estimation and optimal control of aeroelastic systems and large flexible structures
[AD-A208274] N89-27404
AEROSOLS
Detonation of unconfined large scale fuel spray-air clouds
[DE89-006510] N89-26955
Dynamic measurements in combustible and detonable aerosols
[ISL-PU-306/88] N89-26957
Design and characterization of large-drop generators for viscous, Newtonian, and non-Newtonian liquids
[AD-A208330] N89-27133
An instantaneous CCN (Cloud Condensation Nucleus) spectrometer
[DE89-014807] N89-27150
Global environmental effects of impact-generated aerosols: Results from a general circulation model, revision 1
[DE89-014179] N89-27276
Trace gases in and over the West Pacific and East Indian Oceans during the El Nino-southern oscillation event of 1987: A report of GMCC (Geophysical Monitoring for Climatic Change) data collected on the second Soviet-American Gas and Aerosol Experiment (SAGA 2)
[PB89-159685] N89-27280
Navy tethered balloon measurements made during the Fire marine stratocu IFO (Intensive Field Operation)
[AD-A207312] N89-27304
AEROSPACE ENGINEERING
The 14th Convention on Radio Science, Finnish National Committee of URSI held in Otaniemi (Finland) on October 17-18, 1988: Abstracts of papers
[PB89-145767] N89-27044
AEROSPACE ENVIRONMENTS
The space particle environment
[AD-A207547] N89-27287
Space Environment Laboratory
[PB89-159602] N89-27607
AEROSPACE MEDICINE
Injuries to seat occupants of light airplanes
[AD-A207579] N89-26830
Short course on cardiopulmonary aspects of aerospace medicine
[AGARD-R-758-ADD] N89-27330
AEROSPACE SYSTEMS
SDS software measurement requirements
[AD-A207449] N89-27376
AEROSPACE VEHICLES
Cost-optimal state feedback controller for all-attitude gimbal system
[AD-D013972] N89-26845
AFTERBURNING
Afterburner flameholder construction
[AD-D014116] N89-26852
AGING (MATERIALS)
Rate-sensitivity and short term relaxation behavior of AISI Type 304 stainless steel at room temperature and at 650 C; influence of prior aging
[DE89-007823] N89-26978
AGING (METALLURGY)
The effect of aging at 343 deg C on type 308 stainless steel welds
[DE89-013545] N89-26974
Stress corrosion study of PH13-8Mo stainless steel using the Slow Strain Rate Technique
[NASA-TP-2934] N89-26976
Rate-sensitivity and short term relaxation behavior of AISI Type 304 stainless steel at room temperature and at 650 C; influence of prior aging
[DE89-007823] N89-26978
AGRICULTURE
An assessment of information demands for remote sensing and Geographic Information System technologies
[PB89-159313] N89-27233
A center for commercial development of space: Real-time satellite mapping. Remote sensing-based agricultural information expert system
[NASA-CR-185473] N89-27235
The photoacoustic effect, refined and applied to biological problems
[PB89-153597] N89-27263
AIR CONDITIONING EQUIPMENT
Surface cooling system
[AD-D014057] N89-27106
AIR COOLING
Surface cooling system
[AD-D014057] N89-27106
AIR CURRENTS
Finite control volume modeling of laminar and turbulent flow of air in an enclosure
[DE89-009334] N89-27120
AIR FLOW
Fire propagation in concurrent flows
[PB89-188577] N89-26945
Finite control volume modeling of laminar and turbulent flow of air in an enclosure
[DE89-009334] N89-27120
Synoptic forcing of East Asian cold surges
[AD-A208765] N89-27321
AIR LAND INTERACTIONS
Implementing the Simple Biosphere Model (SiB) in a general circulation model: Methodologies and results
[NASA-CR-185509] N89-27288
AIR POLLUTION
Concentrations and patterns of photochemical oxidants in the United States
[PB89-136683] N89-27258
Procedures for the preparation of emission inventories for precursors of ozone, volume 1, third edition
[PB89-154209] N89-27264
Historic emissions of VOC (Volatile Organic Compounds) and NOx in the United States from 1900 to 1985
[PB89-173223] N89-27270
Proceedings of the Energy Efficiency and Structural Change: Implications for the Greenhouse Problem Workshop
[DE89-012852] N89-27274
Field studies for determining the characteristics and dynamics of local circulations
[DE89-013639] N89-27275
Trace gases in and over the West Pacific and East Indian Oceans during the El Nino-southern oscillation event of 1987: A report of GMCC (Geophysical Monitoring for Climatic Change) data collected on the second Soviet-American Gas and Aerosol Experiment (SAGA 2)
[PB89-159685] N89-27280
Cloud and precipitation scavenging process in the South Coast Air Basin
[PB89-181788] N89-27313
AIR QUALITY
Concentrations and patterns of photochemical oxidants in the United States
[PB89-136683] N89-27258
Cloud and precipitation scavenging process in the South Coast Air Basin
[PB89-181788] N89-27313
Submarine air quality: Monitoring the air in submarines. Health effects in divers of breathing submarine air under hyperbaric conditions
[PB89-174213] N89-27345
AIR SAMPLING
Concentrations and patterns of photochemical oxidants in the United States
[PB89-136683] N89-27258
Comparison of modelled and measured tracer gas concentrations during the Across North America Tracer Experiment (ANATEX)
[PB89-136709] N89-27260
Cloud and precipitation scavenging process in the South Coast Air Basin
[PB89-181788] N89-27313
AIR TO AIR REFUELING
Hose reel monitor for inflight refueling system
[AD-D014054] N89-26836
AIR TRAFFIC CONTROL
Evaluation of low data rate voice CODECS for air traffic control applications
[DOT/FAA/CT-TN89/13] N89-27047
AIR WATER INTERACTIONS
Proceedings of the 13th Annual Climate Diagnostics Workshop held at Cambridge, Massachusetts on October 31 - November 4, 1988
[PB89-178115] N89-27310
AIRBORNE EQUIPMENT
Dual-channel microwave radiometer for airborne meteorological applications
[PB89-159683] N89-27298
AIRCRAFT ACCIDENTS
OH-58 energy attenuating crew seat feasibility study
[AD-A207506] N89-26829
Injuries to seat occupants of light airplanes
[AD-A207579] N89-26830
AIRCRAFT CONFIGURATIONS
Wind-tunnel investigation of aerodynamic characteristics and wing pressure distributions of an airplane with variable-sweep wings modified for laminar flow
[NASA-TM-4124] N89-26810
Numerical study of three-dimensional separation and flow control at a wing/body junction
[NASA-CR-185819] N89-26826
AIRCRAFT CONTROL
Back-up control system for f101 engine and its derivatives
[AD-D014051] N89-26848
Control surface dual redundant servomechanism
[AD-D014058] N89-26857
Electrical primary flight control system (fly by wire). Flight control systems of new technology
[MBB-UT-122/88] N89-26862
Feasibility study for enhanced lateral control of the P-3C aircraft
[AD-A208461] N89-26863
Research and development of anti-G life support systems. Part 4: Engineering test and evaluation of six anti-G valves
[AD-A206996] N89-27341
AIRCRAFT DESIGN
Technical Status Review on Drag Prediction and Analysis from Computational Fluid Dynamics: State of the Art
[AGARD-AR-256] N89-26817
State-of-the-art of aircraft drag prediction in Italy by means of theoretical methods N89-26821
CFD methods for drag prediction and analysis currently in use in UK N89-26823
CFD drag prediction for aerodynamic design N89-26825
The conceptional design study of USB powered lift aircrafts in FY 1986
[NAL-TR-958] N89-26835
AIRCRAFT ENGINES
Statistics on aircraft gas turbine engine rotor failures that occurred in US commercial aviation during 1983
[AD-A207592] N89-26851
AIRCRAFT EQUIPMENT
OH-58 energy attenuating crew seat feasibility study
[AD-A207506] N89-26829
AIRCRAFT INSTRUMENTS
Aircraft color displays: Chromaticity and luminance requirements
[AD-A206786] N89-26828
F-15E EADI (Electronic Attitude Director Indicator) evaluation: A comparison of three formats
[AD-A206809] N89-26846
Aerodynamic parameters of an advanced fighter aircraft estimated from flight data. Preliminary results
[NASA-TM-101631] N89-26861

AIRCRAFT MANEUVERS
Brain o2 reserve limiter for high performance aircraft
[AD-D014137] N89-26858
Aerodynamic parameters of an advanced fighter aircraft estimated from flight data. Preliminary results
[NASA-TM-101631] N89-26861
Rule-based air combat simulation
[NASA-CR-4160] N89-27393
AIRCRAFT NOISE
ROUTEMAP model for predicting noise exposure from aircraft operations on Military Training Routes
[AD-A203849] N89-27459
AIRCRAFT PILOTS
Short course on cardiopulmonary aspects of aerospace medicine
[AGARD-R-758-ADD] N89-27330
AIRCRAFT RELIABILITY
Airworthiness and flight characteristics evaluation of the EH-60A (Quick Fix) helicopter
[AD-A207417] N89-26839
Preliminary airworthiness evaluation of the UH-60A external fuel system
[AD-A207570] N89-26840
AIRCRAFT STRUCTURES
Superplastic forming of aluminum, task C
[AD-A207282] N89-26962
AIRCRAFT TIRES
Evaluation of barrier cable impact pad materials
[AD-A207554] N89-26864
AIRFOIL PROFILES
Computational fluid dynamics drag prediction: Results from the Viscous Transonic Airfoil Workshop
N89-26824
AIRFOILS
Technical Status Review on Drag Prediction and Analysis from Computational Fluid Dynamics: State of the Art
[AGARD-AR-256] N89-26817
Drag prediction and analysis from CFD state-of-the-art in Germany N89-26819
AIRFRAMES
Advanced durability analysis. Volume 2: Analytical predictions, test results and analytical correlations
[AD-A207215] N89-26838
Residual stress changes in fatigue. Volume 2: A simulation model for stress measurements in notched test specimens by X-ray diffraction
[AD-A208346] N89-27226
AIRGLOW
Observations of atmospheric emission and attenuation at 20.6, 31.65 and 90 GHz by a ground-based radiometer
[NASA-CR-185719] N89-27257
AIRPORTS
ILS/MLS collocation tests at Miami/Tamiami, Florida Airport
[NASA-CR-185715] N89-26832
An operational demonstration and flight test of the Microwave Landing System (MLS) at the Miami/Tamiami, Florida Airport
[DOT/FAA/CT-TN89/37] N89-26833
ALASKA
Alaska collection SAR (Synthetic Aperture Radar) data summary
[AD-A208530] N89-27067
ALGEBRA
Complex vectors and dyadics for electromagnetists
[PB89-146443] N89-27045
Automatic code vectorization of arithemetic expressions by bottom-up structure recognition
[MEMO-INF-88-48] N89-27414
Image algebra synthesis
[AD-A207257] N89-27425
ALGORITHMS
Control of flexible structures
[AD-A207520] N89-26883
High speed corner and gap-seal computations using an LU-SGS scheme
[NASA-TM-102138] N89-27103
Validation of computational fluid dynamics
[AGARD-AR-257] N89-27104
Navy tethered balloon measurements made during the Fire marine stratocu IFO (Intensive Field Operation)
[AD-A207312] N89-27304
DFT algorithms for bit-serial GaAs array processor architectures
[NASA-CR-183436] N89-27361
An algorithm for symbolic dimensional analysis
[DE89-010409] N89-27363
Heuristic algorithms for stability testing polytopes of matrices
[PB89-160840] N89-27365
High efficiency pattern recognition
[AD-A207210] N89-27368
Competitive management of distributed shared memory
[AD-A207322] N89-27372
On the feasibility of a generalized linear program
[AD-A207402] N89-27373
Lognormal distribution maximum-likelihood parameter estimation algorithms
[AD-A207586] N89-27378
Rapidly convergent algorithms for nonsmooth optimization
[AD-A207629] N89-27379
A theoretical investigation of a parallel genetic algorithm
[DE89-012508] N89-27384
Monotone piecewise cubic data fitting
[DE89-006742] N89-27386
An efficient exact algorithm for the least squares image registration problems
[DE89-013116] N89-27387
A virtual zero-time, monolithic systolic sorting array
[DE89-007515] N89-27394
ORMONTE: An uncertainty analysis code for use with user-developed systems models on mainframe or personal computers. A user's guide
[DE89-013730] N89-27396
Modeling and computational algorithms for parameter estimation and optimal control of aeroelastic systems and large flexible structures
[AD-A208274] N89-27404
A dynamic scheduler for a computer aided prototyping system
[AD-A208389] N89-27407
A compound scaling algorithm for mathematical optimization
[AD-A208446] N89-27409
Algorithms for computer aided design of digital filters
[AD-A208485] N89-27410
Image algebra synthesis
[AD-A207257] N89-27425
Row-oriented direct solving of linear algebraic equations. Inverse projection method
[REPT-88-81] N89-27432
A MACSYMA package for the generation and manipulation of Chebyshev series
[DE89-011404] N89-27436
Sampling based approaches to calculating marginal densities
[AD-A208388] N89-27451
Time-sequential optical data processing
[AD-A207514] N89-27500
Application of modern mathematical concepts to plasma confinement
[DE89-012952] N89-27517
ALKALINE BATTERIES
Supersonics
[AD-A207394] N89-26814
ALKYL COMPOUNDS
The structure and reactivity of alkylsiloxane monolayers formed by reaction of alkyltrichlorosilanes on silicon substrates
[AD-A208267] N89-27011
The structure of self-assembled monolayers of alkylsiloxanes on silicon: A comparison of results from ellipsometry and low-angle X-ray reflectivity
[AD-A208341] N89-27016
ALPHA PARTICLES
Application of modern mathematical concepts to plasma confinement
[DE89-012952] N89-27517
ALTITUDE SICKNESS
Altitude symptomatology and mood states during a climb to 3830 m
[AD-A208261] N89-27332
ALUMINUM
Erosion of Al and Al/SiC
[DE89-013623] N89-26913
HRR field in an aluminum SEN specimen
[AD-A207578] N89-26963
Effects of high thermal and high fast fluences on the mechanical properties of type 6061 aluminum in the HFBR
[DE89-012636] N89-26970
ALUMINUM ALLOYS
Fracture toughness of SiC/Al metal matrix composite
[NASA-TM-100745] N89-26918
Dispersion strengthened aluminum-base alloy
[AD-D014044] N89-26959
Superplastic forming of aluminum, task C
[AD-A207282] N89-26962
Microstructural evolution of Al-Li and Al-Li-Cu-Mg alloys
[DE89-012981] N89-26972
Quantitative thin film X-ray microanalysis of Nb modified Ti3Al
[DE89-009946] N89-26981
Thermomechanical processing of aluminum alloy 2090 for superplasticity
[AD-A208764] N89-26992
Residual stress changes in fatigue. Volume 1: Residual stress measurements by X-ray diffraction in notched test specimens
[AD-A208345] N89-27225
Residual stress changes in fatigue. Volume 2: A simulation model for stress measurements in notched test specimens by X-ray diffraction
[AD-A208346] N89-27226
ALUMINUM COMPOUNDS
Compact ceramic heat exchangers
[PB89-173603] N89-26997
ALUMINUM GALLIUM ARSENIDES
High power semiconductor laser sources
[AD-A207569] N89-27167
ALUMINUM OXIDES
Gas separations using inorganic membranes
[DE89-013010] N89-26948
Breakdown mechanisms of Al2O3, Cr2O3 and SiO2 scales in H2/H2O/H2S environments, volume 1
[DE89-014789] N89-26988
Toughening mechanisms in ceramic composites
[PB89-162606] N89-26996
Study of the microstructure of silver films deposited by ion assisted deposition onto aluminum oxide substrates
[DE89-014665] N89-27563
AMAZON REGION (SOUTH AMERICA)
Amazon Forest wind and temperature profiles
[INPE-4724-PRE/1401] N89-27301
AMMONIA
Studies of the fundamental nature of catalytic acidity, sites and intermediates
[DE89-012946] N89-26947
AMPLIFIERS
The short-circuited fluxgate output current
[ISSN-0109-6605] N89-27069
Proposed thin film electronics for a-Si:H PIXEL detector
[DE89-013410] N89-27083
Passive optical losses in laser glass
[DE89-013784] N89-27172
AMPLITUDE MODULATION
Optical detection and spectroscopy of single molecules in a solid
[AD-A207594] N89-26940
AMPLITUDES
High efficiency pattern recognition
[AD-A207210] N89-27368
ANALOG TO DIGITAL CONVERTERS
High-speed data acquisition for the Princeton University Dynamic Model Track
[NASA-CR-185491] N89-26865
Algorithms for computer aided design of digital filters
[AD-A208485] N89-27410
ANALYSIS (MATHEMATICS)
Computation and theory in nonlinear optimization
[AD-A207610] N89-27430
Note on multiloop calculations for superstrings in the NSR formalism
[PREPRINT-601] N89-27581
ANALYTIC FUNCTIONS
The sl (1/1;R)-cohomologies in BRST-Gupta-Bleuler quantization
[NIKHEF-H/88-17] N89-27578
ANALYTICAL CHEMISTRY
Analytical procedures for environmental quality control, volume 1
[PB89-158604] N89-27266
ANALYZERS
Implementation of a design for testability strategy using the Genesil silicon compiler
[AD-A208458] N89-27099
ANGLES (GEOMETRY)
ELLIPSE user's manual and program reference
[DE89-014575] N89-27398
ANISOTROPY
Polycrystal plasticity as applied to the problem of in-plane anisotropy in rolled cubic metals
[DE89-011181] N89-26983
ANNEALING
Supersonics
[AD-A207394] N89-26814
The recrystallization and respheroidization of tungsten grains in a tungsten-heavy alloy
[AD-A207647] N89-26964
Thermal and mechanical properties of polyurethane-diacetylene segmented copolymers. Part 1: Molecular weight and annealing effects
[AD-A208753] N89-27022
Study of nanophase TiO2 grain boundaries by Raman spectroscopy
[DE89-012416] N89-27553

Photoelectronic properties of low temperature GaAs grown on silicon and GaAs substrates by MBE
[DE89-013148] N89-27557
ANNIHILATION REACTIONS
Search for the inclusive production of J/psi in e(+)e(-) collisions using PLUTO data
[NOTA-INTERNA-923] N89-27484
Multiparticle dynamics at the Sp(-)p collider
[NOTA-INTERNA-929] N89-27490
ANODES
Computer code prediction of picosecond voltage switching and TEM wave generation in air gas avalanche switches
[DE89-013778] N89-27084
MHD calculations of anode plasmas
[DE89-014485] N89-27535
ANOMALIES
Proceedings of the 13th Annual Climate Diagnostics Workshop held at Cambridge, Massachusetts on October 31 - November 4, 1988
[PB89-178115] N89-27310
Tropical circulation and the associated precipitation anomalies in two years of contrast
[INPE-4715-PRE/1395] N89-27315
Transactions of the 6th Army Conference on Applied Mathematics and Computing held in Boulder, Colorado on 31 May - 3 June 1988
[AD-A207252] N89-27424
Stochasticity and symmetry of the standard map
[IPPJ-910] N89-27528
ANOMALOUS TEMPERATURE ZONES
Anomalous temperature dependence of Cu NMR line width and magnetization in YBa2Cu3O(7-delta)
[DE89-014291] N89-27565
ANTARCTIC REGIONS
An Apple-2 compatible program to draw maps containing oceanographic station positions buoy trajectories and the coastal margins of the Antarctic Peninsula and nearby islands
[INPE-4805-RPE/588] N89-27391
ANTENNA ARRAYS
CWG: A FORTRAN program for mutual coupling in a planar array of circular waveguide-fed apertures
[NASA-TM-101614] N89-27063
ANTENNA DESIGN
Development of near-field test procedures for communication satellite antennas, phase 1, part 2
[PB89-156152] N89-27043
Antenna shaft positioning device
[AD-D014120] N89-27191
Fast wave current drive modeling for ITER and prospects for a near-term proof of principle experiment
[DE89-013049] N89-27520
ANTENNA RADIATION PATTERNS
Development of near-field test procedures for communication satellite antennas, phase 1, part 2
[PB89-156152] N89-27043
ANTENNAS
Synthesis of resistive tapers to control scattering patterns of strips
[AD-A207211] N89-27049
Development of a DFS (Deutsche Fernmeldesatellit) reception converter
[ETN-89-94629] N89-27065
Center for Electronics and Electrical Engineering Technical Progress Bulletin covering center programs, October to December 1988 with 1989 CEEE events calender
[PB89-193270] N89-27087
Antenna shaft positioning device
[AD-D014120] N89-27191
ANTHROPOMETRY
Ergonomic Models of Anthropometry, Human Biomechanics and Operator-Equipment Interfaces
[NASA-CR-185720] N89-27344
ANTIGRAVITY
Research and development of anti-G life support systems. Part 4: Engineering test and evaluation of six anti-G valves
[AD-A206996] N89-27341
Full coverage anti-G-suit and balanced pressure breathing
[PB89-174635] N89-27343
ANTIPROTONS
Multiparticle dynamics at the Sp(-)p collider
[NOTA-INTERNA-929] N89-27490
Antiproton and millimeter wave research
[AD-A206363] N89-27491
APERTURES
CWG: A FORTRAN program for mutual coupling in a planar array of circular waveguide-fed apertures
[NASA-TM-101614] N89-27063
APPLICATIONS PROGRAMS (COMPUTERS)
GEO-EAS (Geostatistical Environmental Assessment Software) user's guide
[PB89-151252] N89-27261
ELLIPSE user's manual and program reference
[DE89-014575] N89-27398
ARC JET ENGINES
The NASA low thrust propulsion program
[NASA-TM-102065] N89-26895
Electric propulsion options for 10 kW class earth space missions
[NASA-TM-102337] N89-26906
Arcjet cathode phenomena
[NASA-TM-102099] N89-27121
ARC WELDING
Electrochemical transport of manganese between the flux and the weld metal in submerged arc welding
[DE89-012419] N89-27193
Electrochemical reactions in submerged arc welding with SiO2-CaO-CaF2 fluxes with high and low silica contents
[DE89-012421] N89-27194
ARCHITECTURE (COMPUTERS)
Autonomous land navigation: A demonstration of retrotraverse
[DE89-011681] N89-26855
Quality in automation project for FY 88
[PB89-193296] N89-27040
An expert system for correlation of radar and passive sensor signals
[DE89-011575] N89-27056
Research in autonomous robotics at ORNL using HERMIES-3
[DE89-004933] N89-27198
System-based component test plans and operating characteristics: Introduction and overview
[DE89-012255] N89-27203
DYNA3D user's manual: (Nonlinear Dynamic Analysis of Structures in Three Dimensions), revision 5
[DE89-014304] N89-27222
Implementation indices (1975-1979), volume 1
[AD-A207609] N89-27354
ACP/R3000 processors in data acquisition systems
[DE89-014811] N89-27355
Hybrid structures for simple computer performance estimates
[PB89-189161] N89-27356
Cray-to-sun prototype
[DE89-013087] N89-27358
Offline computing farms
[DE89-013958] N89-27359
DFT algorithms for bit-serial GaAs array processor architectures
[NASA-CR-183436] N89-27361
Programming parallel architectures: The BLAZE family of languages
[NASA-CR-185826] N89-27362
Software deficiency issues confronting the utilization of non-Von Neumann architectures
[AD-A207268] N89-27369
Competitive management of distributed shared memory
[AD-A207322] N89-27372
Kernel user's manual version 1.0
[AD-A207414] N89-27375
The dynamical behavior of classifier systems
[DE89-009407] N89-27383
XCL: A family of programming language-based shell s
[DE89-013442] N89-27388
Indirect addressing and load balancing for faster solution to Mandelbrot Set on SIMD architectures
[NASA-CR-181847] N89-27390
A virtual zero-time, monolithic systolic sorting array
[DE89-007515] N89-27394
ORMONTE: An uncertainty analysis code for use with user-developed systems models on mainframe or personal computers. A user's guide
[DE89-013730] N89-27396
Portable parallel programming in a FORTRAN environment
[DE89-014670] N89-27399
Machines for lattice gauge theory
[DE89-014815] N89-27400
Suitability of message passing computers for implementing production systems
[AD-A207321] N89-27411
Advanced information processing system: Input/output system services
[NASA-CR-181874] N89-27413
Northeast Artificial Intelligence Consortium annual report 1987. Volume 2, part b: Discussing, using, and recognizing plans
[AD-A208378] N89-27418
Northeast Artificial Intelligence Consortium annual report 1987. Volume 3: Distributed artificial intelligence for communications network management
[AD-A208379] N89-27419
Using conjoint meshing primitives to generate quadrilateral and hexahedral elements in irregular regions
[DE89-005918] N89-27435
Safety in numbers: The boundless errors of numerical computation
[DE89-014813] N89-27438
Issues and approaches for electronic document approval and transmittal using digital signatures and text authentication
[DE89-013102] N89-27596
ARCTIC REGIONS
The 1989 Airborne Arctic Stratospheric Expedition Nimbus-7 TOMS data atlas
[NASA-RP-1227] N89-27302
ARGON
Degradation of Fe-25Cr, Fe-25Cr-20Ni and Fe-25Cr-6Al alloys in H2/H2O/H2S environments at 700 C
[DE89-011873] N89-26967
Z-pinch experiments on Saturn at 30 TW
[DE89-013497] N89-27523
Measurement of the time-dependent distribution of ionization states in an argon plasma from a Mach-10 jet
[DE89-014699] N89-27526
ARGON PLASMA
Measurement of the time-dependent distribution of ionization states in an argon plasma from a Mach-10 jet
[DE89-014699] N89-27526
ARM (ANATOMY)
Design considerations of manipulator and feel system characteristics in roll tracking
[NASA-CR-4111] N89-26860
ARMED FORCES (UNITED STATES)
Annual historical report - AMEDD activities
[AD-A208301] N89-27333
ARRAYS
Reconfiguration strategies in VLSI (Very Large Scale Integration) arrays and trees
[PB89-165468] N89-27071
ARTIFICIAL INTELLIGENCE
Research in knowledge-based vision techniques for the autonomous land vehicle program
[AD-A208546] N89-26834
SP-ATUS: An expert system for specifications of satellite imagery
[INPE-4754-PRE/1426] N89-27236
Natural language processing
[INPE-4449-TDL/314] N89-27366
Automatic treatment of natural language in processes in the acquistion of knowledge
[INPE-4737-PRE/1412] N89-27382
An efficient exact algorithm for the least squares image registration problems
[DE89-013116] N89-27387
Autonomous discovery and learning by a mobile robot in unstructured environments
[DE89-001525] N89-27415
Northeast Artificial Intelligence Consortium annual report 1987. Volume 2, part b: Discussing, using, and recognizing plans
[AD-A208378] N89-27418
Northeast Artificial Intelligence Consortium annual report 1987. Volume 3: Distributed artificial intelligence for communications network management
[AD-A208379] N89-27419
Research in knowledge delivery
[AD-A208327] N89-27599
ASIA
Synoptic forcing of East Asian cold surges
[AD-A208765] N89-27321
ASPECT RATIO
Development of a thin wall graphite/polyimide composite pressure vessel with a large aspect ratio
[DE89-002536] N89-26920
ASSESSMENTS
Risk assessment of compressed natural gas-fueled vehicle operations, phase 1
[PB89-188841] N89-27196
ASSOCIATIVE PROCESSING (COMPUTERS)
Implementation indices (1975-1979), volume 1
[AD-A207609] N89-27354
ASTEROIDS
Global environmental effects of impact-generated aerosols: Results from a general circulation model, revision 1
[DE89-014179] N89-27276
ASTRODYNAMICS
Resonant helicity flip of electron neutrino due to magnetic moment and dynamics of supernova
[PREPRINT-598] N89-27617
ASTROMETRY
Dynamics of the solar system: Proceedings, volume 3
[DE89-609828] N89-27615
ASTRONOMICAL MODELS
Black holes in closed universes
[PB89-170039] N89-27610
The cosmological constant problem
[DE89-013150] N89-27614
Evolution of Galaxies. Proceedings, volume 4
[DE89-609850] N89-27616

Statistical study of the correlation of hard X-ray and type 3 radio bursts in solar flares
[NASA-CR-185833] N89-27629

ASTRONOMICAL OBSERVATORIES
The Swedish-ESO Submillimeter Telescope (SEST)
[PB89-154892] N89-27605

ASTRONOMY
Dynamics of the solar system: Proceedings, volume 3
[DE89-609828] N89-27615

ASTROPHYSICS
Evolution of Galaxies. Proceedings, volume 4
[DE89-609850] N89-27616

ATMOSPHERIC ATTENUATION
Observations of atmospheric emission and attenuation at 20.6, 31.65 and 90 GHz by a ground-based radiometer
[NASA-CR-185719] N89-27257
Atmospheric propagation issues relevant to optical communications
[NASA-CR-185718] N89-27281

ATMOSPHERIC BOUNDARY LAYER
Trace gases in and over the West Pacific and East Indian Oceans during the El Nino-southern oscillation event of 1987: A report of GMCC (Geophysical Monitoring for Climatic Change) data collected on the second Soviet-American Gas and Aerosol Experiment (SAGA 2)
[PB89-159685] N89-27280

ATMOSPHERIC CHEMISTRY
A computer program for simulating the atmospheric dispersion of UF6 and other reactive gases having positive, neutral, or negative buoyancy
[DE89-012734] N89-27269
Atmospheric carbon dioxide and the greenhouse effect
[DE89-012869] N89-27271
Preventing depletion of stratospheric ozone: Implications on future aircraft emissions, revision 1
[DE89-013779] N89-27273
Fog, cloud, and dew chemistry
[PB89-187314] N89-27317

ATMOSPHERIC CIRCULATION
Regional ozone modeling in the northeastern US: Selection of meteorological episodes
[PB89-136691] N89-27259
Field studies for determining the characteristics and dynamics of local circulations
[DE89-013639] N89-27275
Global environmental effects of impact-generated aerosols: Results from a general circulation model, revision 1
[DE89-014179] N89-27276
An objective comparison of vertical motions from the kinematic method and three forms of the omega equation
[AD-A208451] N89-27294
Intense heat checklist based on the 1980 heat wave
[PB89-181200] N89-27312
Tropical circulation and the associated precipitation anomalies in two years of contrast
[INPE-4715-PRE/1395] N89-27315

ATMOSPHERIC COMPOSITION
Regional ozone modeling in the northeastern US: Selection of meteorological episodes
[PB89-136691] N89-27259
Procedures for the preparation of emission inventories for precursors of ozone, volume 1, third edition
[PB89-154209] N89-27264
Criteria for selecting a CO2/climate change region of study
[DE89-011233] N89-27268
A computer program for simulating the atmospheric dispersion of UF6 and other reactive gases having positive, neutral, or negative buoyancy
[DE89-012734] N89-27269
Historic emissions of VOC (Volatile Organic Compounds) and NOx in the United States from 1900 to 1985
[PB89-173223] N89-27270
Analysis of the wind data and estimation of the resultant air concentration rates
[DE88-705980] N89-27296
Cloud and precipitation scavenging process in the South Coast Air Basin
[PB89-181788] N89-27313

ATMOSPHERIC ELECTRICITY
Airborne measurements of the electric field and the charge precipitation particles in convective clouds: Lower positive charge centers
[ONERA-NT-1988-1] N89-27319

ATMOSPHERIC GENERAL CIRCULATION MODELS
Implementing the Simple Biosphere Model (SiB) in a general circulation model: Methodologies and results
[NASA-CR-185509] N89-27288

ATMOSPHERIC MODELS
Regional ozone modeling in the northeastern US: Selection of meteorological episodes
[PB89-136691] N89-27259
Comparison of modelled and measured tracer gas concentrations during the Across North America Tracer Experiment (ANATEX)
[PB89-136709] N89-27260
Global environmental effects of impact-generated aerosols: Results from a general circulation model, revision 1
[DE89-014179] N89-27276
An objective comparison of vertical motions from the kinematic method and three forms of the omega equation
[AD-A208451] N89-27294
An investigation into the gravity current aspects of a cold air outbreak using variational analysis techniques
[AD-A208464] N89-27295
Navy tethered balloon measurements made during the Fire marine stratocu IFO (Intensive Field Operation)
[AD-A207312] N89-27304
Proceedings of the 13th Annual Climate Diagnostics Workshop held at Cambridge, Massachusetts on October 31 - November 4, 1988
[PB89-178115] N89-27310
Synoptic forcing of East Asian cold surges
[AD-A208765] N89-27321

ATMOSPHERIC MOISTURE
Low relative humidity in the atmosphere
[AD-A207558] N89-27307

ATMOSPHERIC PHYSICS
Space research in the Federal Republic of Germany (FRG), 1986 and 1987
[ETN-89-94427] N89-26874
Navy tethered balloon measurements made during the Fire marine stratocu IFO (Intensive Field Operation)
[AD-A207312] N89-27304
Space Environment Laboratory
[PB89-159602] N89-27607

ATMOSPHERIC SOUNDING
The international TOVS (Tiros Operational Vertical Sounder) processing package: An evaluation
[AD-A207548] N89-27306

ATMOSPHERIC TEMPERATURE
An investigation into the gravity current aspects of a cold air outbreak using variational analysis techniques
[AD-A208464] N89-27295
The international TOVS (Tiros Operational Vertical Sounder) processing package: An evaluation
[AD-A207548] N89-27306

ATMOSPHERIC TURBULENCE
Noise produced by turbulent flow into a rotor: Theory manual for atmospheric turbulence prediction and mean flow and turbulence contraction prediction
[NASA-CR-181789] N89-27466

ATOMIC COLLISIONS
Multiple-electron processes in fast ion-atom collisions
[DE89-012982] N89-27475
Nuclear fragmentation energy and momentum transfer distributions in relativistic heavy-ion collisions
[NASA-CR-185501] N89-27477

ATOMIC ENERGY LEVELS
Dynamics of an M-level atom interacting with gravity fields. 1: Effects of the level number on quantum collapse and revival
[AD-A207278] N89-27579

ATOMIC PHYSICS
Nonresonant interaction of a three-level atom with cavity fields. Part 4: Atomic dipole moment and squeezing effects
[AD-A206788] N89-27470
Multiple-electron processes in fast ion-atom collisions
[DE89-012982] N89-27475
Study of atomic physics and population inversions with plasma focus
[DE89-014282] N89-27532

ATOMIC SPECTRA
Nonresonant interaction of a three-level atom with cavity fields. Part 4: Atomic dipole moment and squeezing effects
[AD-A206788] N89-27470

ATOMIC STRUCTURE
The role of X-ray absorption spectroscopy in electronic structure studies
[DE89-014677] N89-26952

ATOMIC THEORY
Nonresonant interaction of a three-level atom with cavity fields. Part 4: Atomic dipole moment and squeezing effects
[AD-A206788] N89-27470

ATOMIZING
Depth profiles and bulk analysis of semiconductor materials using ICP mass spectroscopy with electrothermal atomization
[AD-A206974] N89-27548

ATOMS
Dynamics of an M-level atom interacting with gravity fields. 1: Effects of the level number on quantum collapse and revival
[AD-A207278] N89-27579

ATTENUATION
Investigations on local seismic phases and evaluation of body waves magnitude
[AD-A206833] N89-27283

ATTITUDE (INCLINATION)
Cost-optimal state feedback controller for all-attitude gimbal system
[AD-D013972] N89-26845
F-15E EADI (Electronic Attitude Director Indicator) evaluation: A comparison of three formats
[AD-A206809] N89-26846

ATTITUDE CONTROL
F-15E EADI (Electronic Attitude Director Indicator) evaluation: A comparison of three formats
[AD-A206809] N89-26846
Feasibility study for enhanced lateral control of the P-3C aircraft
[AD-A208461] N89-26863
Study of jitter on the attitude motion of a spin stabilized satellite with two flexible solar panels
[INPE-4744-PRE/1418] N89-26884
Altimetric system: Earth observing system. Volume 2h: Panel report
[NASA-TM-89722] N89-27229
Rule-based air combat simulation
[NASA-CR-4160] N89-27393

ATTITUDE INDICATORS
F-15E EADI (Electronic Attitude Director Indicator) evaluation: A comparison of three formats
[AD-A206809] N89-26846

AUGER SPECTROSCOPY
An Auger sputter profiling study of nitrogen and oxygen ion implantation in two titanium alloys
[DE89-014734] N89-26987

AURORAL ARCS
Distribution of auroral arcs during quiet geomagnetic conditions
[DMI-GEOPHYS-PAPERS-R-78] N89-27292

AUSTENITIC STAINLESS STEELS
Rate-sensitivity and short term relaxation behavior of AISI Type 304 stainless steel at room temperature and at 650 C; influence of prior aging
[DE89-007823] N89-26978
Bearings fabricated from rapidly solidified powder and method
[AD-D014072] N89-27185
Mechanisms that control the geometry of pulsed Nd:YAG laser welds
[DE89-014490] N89-27200

AUTOCORRELATION
An expert system for correlation of radar and passive sensor signals
[DE89-011575] N89-27056

AUTOIONIZATION
Molecules in intense laser fields
[DE89-013807] N89-27479

AUTOMATIC CONTROL
The NASA Langley Research Center 0.3-meter transonic cryogenic tunnel T-P/Re-M controller manual
[NASA-CR-181868] N89-26869
Automatic oxygen measuring system
[AD-D014003] N89-26931
Quality in automation project for FY 88
[PB89-193296] N89-27040
Automated immersion testing robotic system: Hardware and software design
[AD-A208755] N89-27201
Computational methods for nonlinear dynamic problems in solid and structural mechanics: Progress in the theory and modeling of friction and in the control of dynamical systems with frictional forces
[AD-A208763] N89-27227
Satellite image processing using symbolic structures of reduced vision conditions
[INPE-4638-TDL/337] N89-27367
System for measuring optical waveguide intensity profiles
[PB89-188593] N89-27507

AUTOMATIC FLIGHT CONTROL
Electrical primary flight control system (fly by wire). Flight control systems of new technology
[MBB-UT-122/88] N89-26862

AUTOMATIC PILOTS
Aircraft flight test trajectory control
[NASA-CR-4161] N89-27416

AUTOMOBILE ENGINES
Future applications of engine ceramics: Factors influencing market opportunities, timing, and growth
[DE89-012426] N89-27002

AUTOMOBILE FUELS
Dedicated low-pressure natural gas-fueled vehicle baseline assessment. Task 3 topical report on light-duty vehicles
[PB89-195820] N89-27604
AUTOMOBILES
Autonomous land navigation: A demonstration of retrotraverse
[DE89-011881] N89-26855
Future applications of engine ceramics: Factors influencing market opportunities, timing, and growth
[DE89-012426] N89-27002
AUTONOMOUS NAVIGATION
Autonomous land navigation: A demonstration of retrotraverse
[DE89-011881] N89-26855
AUTONOMY
Research in autonomous robotics at ORNL using HERMIES-3
[DE89-004933] N89-27196
Autonomous discovery and learning by a mobile robot in unstructured environments
[DE89-001525] N89-27415
AUXILIARY PROPULSION
Hybrid electric chemical propulsion
[AD-A207584] N89-26898
AVALANCHES
Computer code prediction of picosecond voltage switching and TEM wave generation in air gas avalanche switches
[DE89-013778] N89-27084
AVIONICS
Advanced information processing system: Input/output system services
[NASA-CR-181874] N89-27413

B

BACKSCATTERING
Synthesis of resistive tapers to control scattering patterns of strips
[AD-A207211] N89-27049
Materials analysis with nuclear microprobes: Superconductors and buried conductors
[DE89-008580] N89-27206
BACKUPS
Back-up control system for f101 engine and its derivatives
[AD-D014051] N89-26848
BAND STRUCTURE OF SOLIDS
Model for hot electron phenomena: Theory and general results
[DE88-705986] N89-27544
BANDSTOP FILTERS
Algorithms for computer aided design of digital filters
[AD-A208485] N89-27410
BANDWIDTH
Bandwidth efficient coding for error control
[NASA-CR-185836] N89-27062
BARIUM COMPOUNDS
Anomalous temperature dependence of Cu NMR line width and magnetization in YBa2Cu3O(7-delta)
[DE89-014291] N89-27565
BARIUM OXIDES
O-17 NMR study of YBa2Cu3O(7-delta)
[DE89-014292] N89-27566
Nuclear relaxation rates at copper and oxygen sites in YBa2Cu3O7
[DE89-014308] N89-27567
BARRIER LAYERS
Development of elements of a high Tc superconducting cable
[AD-A208370] N89-27574
BCS THEORY
Quantum and thermodynamic fluctuations in the degenerate schematic model of the finite temperature random phase approximation
[DE88-706310] N89-27580
BEAM INTERACTIONS
Beam-gas background rejection in L3 first level energy transfer
[NOTA-INTERNA-919] N89-27496
BEAM SPLITTERS
Efficient dynamic phasefront modulation system for free-space optical communications
[AD-D014128] N89-27503
BEARINGS
OTVE turbopump condition monitoring, task E.5
[NASA-CR-182274] N89-27204
BEHAVIOR
The HERMOD behavioral synthesis system
[AD-A207319] N89-27371
BELLOWS
Electromagnetic pulse rotary seal
[AD-D014080] N89-27187
BEND TESTS
Statistics of fracture in two grades of isotropic graphite
[DE89-013703] N89-26916
BENDING
Structural analysis of a thermal insulation retainer assembly
[NASA-TM-101580] N89-27212
BENDING THEORY
Measurement of the bending wave power flow by the structural intensity technique
[VTT-583] N89-27129
BESSEL FUNCTIONS
Transactions of the 6th Army Conference on Applied Mathematics and Computing held in Boulder, Colorado on 31 May - 3 June 1988
[AD-A207252] N89-27424
BEVERAGES
Considerations for replacement beverages: Fluid-electrolyte balance and heat illness
[AD-A208342] N89-27335
BIBLIOGRAPHIES
Center for Electronics and Electrical Engineering Technical Progress Bulletin covering center programs, October to December 1988 with 1989 CEEE events calender
[PB89-193270] N89-27087
Bibliography of Soviet laser developments, No. 92, November - December 1987
[AD-A207794] N89-27177
Ocean Energy Program summary. Volume 2: Research summaries, fiscal year 1988
[DE89-000859] N89-27248
Environmental Research Laboratories publication abstracts, FY 1988
[PB89-152656] N89-27589
Technical Abstracts, 1988
[DE89-012811] N89-27591
BIMETALS
Bimetallic air seal for exhaust nozzles
[AD-D014106] N89-27189
BINARY STARS
Observing primeval galaxies and dark matter with LAIRTS --- Large Aperture Infra-Red Telescope System
[AD-A208286] N89-27606
BINDERS (MATERIALS)
Development of magnetic resonance imaging technology for imaging binder distribution in ceramics
[DE89-013185] N89-27003
Non-polymeric binders for ceramic powders: Utilization of neutral and ionic species derived from decaborane(14)
[AD-A208338] N89-27015
BIOCHEMISTRY
Development of advanced methods based on stable isotope technology for studies of exercise in heat
[AD-A208758] N89-27329
BIOINSTRUMENTATION
JTECH (Japanese Technology Evaluation Program) panel report on advanced sensors in Japan
[PB89-158760] N89-27136
BIOSPHERE
Implementing the Simple Biosphere Model (SiB) in a general circulation model: Methodologies and results
[NASA-CR-185509] N89-27288
BISMUTH
Loss of grain boundary segregant during ion milling
[DE89-007835] N89-26979
BIT ERROR RATE
Advanced modulation technology development for earth station demodulator applications
[NASA-CR-185126] N89-26880
BIVARIATE ANALYSIS
On estimating the dependence between two point processes
[AD-A208311] N89-27445
BLACK HOLES (ASTRONOMY)
Black holes in closed universes
[PB89-170039] N89-27610
BLACKOUT (PHYSIOLOGY)
Brain o2 reserve limiter for high performance aircraft
[AD-D014137] N89-26858
BLADE-VORTEX INTERACTION
Reduction of blade-vortex interaction noise using higher harmonic pitch control
[NASA-TM-101624] N89-27465
BODY-WING CONFIGURATIONS
CFD methods for drag prediction and analysis currently in use in UK N89-26823
BONDING
A method of removing oxides from the surface of Fe-Ni-Co alloy particles by chemical etching
[DE89-014597] N89-27009
The diagonal strip system in the Macro experiment
[NOTA-INTERNA-924] N89-27159
NIST (National Institute of Standards and Technology) research reports, March 1989
[PB89-189310] N89-27594
BORANES
Non-polymeric binders for ceramic powders: Utilization of neutral and ionic species derived from decaborane(14)
[AD-A208338] N89-27015
BORATES
Supersonics
[AD-A207394] N89-26814
BOREHOLES
Investigations of dielectric properties of some frozen materials using cross-borehole radiowave pulse transmissions
[AD-A207302] N89-27285
BOROSILICATE GLASS
Toughening mechanisms in ceramic composites
[PB89-162606] N89-26996
BOSONS
Precision measurements without polarization at LEP --- LEP storage ring
[NOTA-INTERNA-921] N89-27483
BOTANY
The photoacoustic effect, refined and applied to biological problems
[PB89-153597] N89-27263
BOTTLES
Nonlinear dynamic response of pressurized composite bottles subjected to shock loading
[DE89-010553] N89-26922
BOUNDARY LAYER CONTROL
Combination boundary layer control system for high altitude aircraft
[AD-D014075] N89-26837
Feasibility and benefits of laminar flow control on supersonic cruise airplanes
[NASA-CR-181817] N89-26841
System for boundary layer control through pulsed heating of a strip heater
[AD-D013999] N89-27101
BOUNDARY LAYER FLOW
MHD forced and free convection boundary layer flow near the leading edge
[DE88-705974] N89-26812
Interaction between Tollmien-Schlichting waves and free-stream disturbances in boundary-layer flows
[NASA-CR-185847] N89-27118
BOUNDARY LAYER SEPARATION
A model for transition by attachment-line contamination and an examination of cross-flow instability in 3-D boundary layers
[AERO-REPT-8804] N89-27108
Interaction between Tollmien-Schlichting waves and free-stream disturbances in boundary-layer flows
[NASA-CR-185847] N89-27118
BOUNDARY LAYER STABILITY
Feasibility and benefits of laminar flow control on supersonic cruise airplanes
[NASA-CR-181817] N89-26841
A model for transition by attachment-line contamination and an examination of cross-flow instability in 3-D boundary layers
[AERO-REPT-8804] N89-27108
BOUNDARY LAYERS
Combination boundary layer control system for high altitude aircraft
[AD-D014075] N89-26837
The structure of Normal-Shock/Turbulent-Boundary-Layer interactions modified by mass removal
[AD-A208402] N89-27134
BOUNDARY VALUE PROBLEMS
The Burgers equation on the semi-finite and finite intervals
[PREPRINT-602] N89-27441
BOXES (CONTAINERS)
Self-locking outer air seal with full backside cooling
[AD-D013975] N89-27179
BRAIN
Brain o2 reserve limiter for high performance aircraft
[AD-D014137] N89-26858
BRANCHING (MATHEMATICS)
On the multiplicity and symmetries of the bifurcation branching point in the square clamped plate
[PREPRINT-604] N89-27224
BRAYTON CYCLE
Performance estimates for the Space Station power system Brayton Cycle compressor and turbine
[NASA-CR-182263] N89-26903
Thermal evaluation of advanced solar dynamic heat receiver performance
[NASA-CR-185117] N89-27256

BRIGHTNESS TEMPERATURE
Attitude angle effects on Nimbus-7 Scanning Multichannel Microwave Radiometer radiances and geophysical parameter retrievals
[NASA-TM-4132] N89-27289
BRILLOUIN EFFECT
Dynamics of double stimulated Brillouin scattering
[PB89-146369] N89-27513
BRITTLENESS
Fracture toughness of SiC/Al metal matrix composite
[NASA-TM-100745] N89-26918
Fracture behavior of a pressure vessel steel in the ductile-to-brittle transition region
[PB89-189195] N89-26977
BROKEN SYMMETRY
Theoretical studies in elementary particle physics
[DE89-012701] N89-27473
BROMINE ISOTOPES
Development of advanced methods based on stable isotope technology for studies of exercise in heat
[AD-A208758] N89-27329
BUBBLES
Generation of underwater sound pulses, cavitation and shear waves with hydraulic hammer
[MPIS-8/1988] N89-27122
BUCKLING
Inelastic buckling of channel columns in the distortional mode
[PB89-156053] N89-27207
Strength tests and design methods for cold-formed channel columns undergoing distortional buckling
[PB89-183958] N89-27216
Dynamic plastic buckling of spherical shells during collapse
[DE89-006543] N89-27217
BUDGETS
Emerging technologies in electronics and their measurement needs
[PB89-189245] N89-27078
BUILDINGS
Development of a second-generation, video-based luminance mapper for daylighting research
[DE89-000850] N89-27143
New Frontier: Environments for Innovation --- sick building syndrome
[PB89-151054] N89-27601
BUOYS
Tropical cyclone report, 1988
[AD-A207206] N89-27303
An Apple-2 compatible program to draw maps containing oceanographic station positions buoy trajectories and the coastal margins of the Antarctic Peninsula and nearby islands
[INPE-4805-RPE/588] N89-27391
BURGER EQUATION
The Burgers equation on the semi-finite and finite intervals
[PREPRINT-602] N89-27441
BURNING RATE
Process for assessing the effect of propellant strain on propellant burn rate
[AD-D014119] N89-27026
BUSHINGS
Anti-rotation guide bushing
[AD-D014079] N89-27186
BUTT JOINTS
Field joint protection system rain qualification test report
[NASA-CR-183702] N89-26901

C

C (PROGRAMMING LANGUAGE)
Hardware C - A language for hardware design
[AD-A207317] N89-27370
C-135 AIRCRAFT
KC-135R rumble investigation
[AD-A207532] N89-27464
CABLES (ROPES)
Evaluation of barrier cable impact pad materials
[AD-A207554] N89-26864
CADMIUM ALLOYS
New strategies for display devices based on 2-6 materials
[AD-A208288] N89-27573
CADMIUM TELLURIDES
High-efficiency, large-area CdTe panels
[DE89-000891] N89-27242
CALCIUM FLUORIDES
Electrochemical reactions in submerged arc welding with SiO2-CaO-CaF2 fluxes with high and low silica contents
[DE89-012421] N89-27194
Determination of the kinetic parameters of the thermoluminescent CaF2 (Tm) crystal
[NOTA-INTERNA-915] N89-27569
CALCIUM OXIDES
Electrochemical reactions in submerged arc welding with SiO2-CaO-CaF2 fluxes with high and low silica contents
[DE89-012421] N89-27194
CALIBRATING
Compressor blade clearance measurement system
[AD-D014073] N89-26850
Method for calibrating a heat flux gauge
[AD-D013974] N89-27138
Group index and time delay measurements of a standard reference fiber
[PB89-189179] N89-27457
A method to calibrate the light response of a high resolution electromagnetic calorimeter with cosmic rays
[NOTA-INTERNA-925] N89-27631
CALIFORNIA
Introduction to background materials for Workshop No. 1: Global climate change and its effects on California
[DE89-013381] N89-27272
Geodetic measurement of deformation in California
[NASA-TM-100732] N89-27279
Fog, cloud, and dew chemistry
[PB89-187314] N89-27317
CALORIMETERS
Tests of low resistivity electrodeless streamer tubes
[NOTA-INTERNA-922] N89-27158
Passive optical losses in laser glass
[DE89-013784] N89-27172
A method to calibrate the light response of a high resolution electromagnetic calorimeter with cosmic rays
[NOTA-INTERNA-925] N89-27631
CAMERAS
Development of a second-generation, video-based luminance mapper for daylighting research
[DE89-000850] N89-27143
CANOPIES (VEGETATION)
Modeling of the angular reflectance of an artificial plant canopy near the retroreflection peak in the optical regime
[DE89-011174] N89-27239
CAPACITORS
Computer code prediction of picosecond voltage switching and TEM wave generation in air gas avalanche switches
[DE89-013778] N89-27084
Improved core insulation schemes for multi-terawatt magnetic switches
[DE89-013814] N89-27093
CAPILLARY WAVES
Spectra of surface waves
[AD-A208482] N89-27326
CAPTURE EFFECT
On capture effect of FM demodulators
[AD-A208479] N89-27066
CARBIDES
The solidification metallurgy of Alloy 718 and other Nb-containing superalloys
[DE89-008196] N89-26966
CARBOHYDRATES
Considerations for replacement beverages: Fluid-electrolyte balance and heat illness
[AD-A208342] N89-27335
CARBON
Thermodynamics and high temperature chemistry of the chemical vapor deposition of diamond films
[DE89-013574] N89-26951
Diamondlike carbon protective coatings for optical windows
[NASA-TM-102111] N89-27506
CARBON DIOXIDE
Catalytic reduction of carbon dioxide by metal centers
[AD-A207227] N89-26934
Adsorption and coadsorption of CO and NO on the Rh(100) surface: A theoretical analysis
[AD-A207323] N89-26935
Criteria for selecting a CO2/climate change region of study
[DE89-011233] N89-27268
Atmospheric carbon dioxide and the greenhouse effect
[DE89-012869] N89-27271
Commentary on interstellar matter associated with 18 open clusters
[NASA-RP-1229] N89-27612
CARBON DIOXIDE CONCENTRATION
Criteria for selecting a CO2/climate change region of study
[DE89-011233] N89-27268
Atmospheric carbon dioxide and the greenhouse effect
[DE89-012869] N89-27271
CARBON DIOXIDE LASERS
Compact, lightweight CO2 lasers for SDIO applications
[AD-A207052] N89-27162
The photoacoustic effect, refined and applied to biological problems
[PB89-153597] N89-27263
CARBON FIBERS
Examination of the tensile strength of graphite fibers
[AD-A207277] N89-26909
Processing of continuous fiber composites
[DE89-012608] N89-26915
CARBON MONOXIDE
Adsorption and coadsorption of CO and NO on the Rh(100) surface: A theoretical analysis
[AD-A207323] N89-26935
Modifiers in rhodium catalysts for carbon monoxide hydrogenation: Structure-activity relationships
[DE89-013802] N89-27028
Procedures for the preparation of emission inventories for precursors of ozone, volume 1, third edition
[PB89-154209] N89-27264
CARBON STEELS
Estimating fracture toughness using tension or ball indentation tests and a modified critical strain model
[DE89-010324] N89-27220
CARBON-CARBON COMPOSITES
Thermophysical properties of advanced carbon materials for Tokamak limiters
[DE89-012799] N89-27516
CARBONACEOUS MATERIALS
Dispersed and periodic microstructures for magnetic and infrared absorbers
[AD-A207428] N89-27053
CARBORANE
Non-polymeric binders for ceramic powders: Utilization of neutral and ionic species derived from decaborane(14)
[AD-A208338] N89-27015
CARDIOVASCULAR SYSTEM
Short course on cardiopulmonary aspects of aerospace medicine
[AGARD-R-758-ADD] N89-27330
CARRIER DENSITY (SOLID STATE)
Model for hot electron phenomena: Theory and general results
[DE88-705986] N89-27544
CARRIER FREQUENCIES
Frequency division multiplexing of interferometric sensor arrays
[AD-A208448] N89-27510
CARRIER TRANSPORT (SOLID STATE)
Model for hot electron phenomena: Theory and general results
[DE88-705986] N89-27544
CARTS
A qualitative way of solving the pole balancing problem
[MEMO-INF-88-44] N89-27439
CASSEGRAIN OPTICS
The Swedish-ESO Submillimeter Telescope (SEST)
[PB89-154892] N89-27605
CAST ALLOYS
Method for developing ultrafine microstructures in titanium alloy castings
[AD-D014115] N89-26965
CASTING
The solidification metallurgy of Alloy 718 and other Nb-containing superalloys
[DE89-008196] N89-26966
CASTINGS
Method for developing ultrafine microstructures in titanium alloy castings
[AD-D014115] N89-26965
CATALYSIS
Catalytic reduction of carbon dioxide by metal centers
[AD-A207227] N89-26934
Oxygen transfer to ethylene catalyzed by the Ag(110) surface
[AD-A207325] N89-26936
Catalytic combustion of methane
[PB89-188874] N89-26946
Studies of the fundamental nature of catalytic acidity, sites and intermediates
[DE89-012946] N89-26947
CATALYSTS
Fluids, gels and glasses under extreme conditions of pressure and temperature
[AD-A205292] N89-26927
Catalytic reduction of carbon dioxide by metal centers
[AD-A207227] N89-26934
Catalytic combustion of methane
[PB89-188874] N89-26946
Synthesis and structural characterization of Pt-Si dimers with unusually short cross-ring silicon-silicon interactions
[AD-A208310] N89-27014
Modifiers in rhodium catalysts for carbon monoxide hydrogenation: Structure-activity relationships
[DE89-013802] N89-27028

Development of ternary alloy cathode catalysts for phosphoric acid fuel cells
[DE89-000926] N89-27250

CATHODES
Arcjet cathode phenomena
[NASA-TM-102099] N89-27121
Electrochemical evaluation of new fluorosulfonic and fluorophosphonic acids as fuel cell electrolytes
[DE89-013391] N89-27255

CATIONS
Diffusion in high-T sub c superconductors
[DE89-009792] N89-27546

CAUCHY PROBLEM
The behavior of flux difference splitting schemes near slowly moving shock waves
[FFA-TN-1988-58] N89-27130

CAUSTICS (OPTICS)
Transverse pumping with diode lasers
[AD-A207261] N89-27165

CAVITATION FLOW
Generation of underwater sound pulses, cavitation and shear waves with hydraulic hammer
[MPIS-6/1986] N89-27122

CAVITIES
Nonresonant interaction of a three-level atom with cavity fields. Part 4: Atomic dipole moment and squeezing effects
[AD-A206788] N89-27470
High-frequency cavity applications and measurements of high-temperature superconductors
[DE89-013467] N89-27560

CAVITY RESONATORS
Free electron lasers with small period wigglers
[DE89-014715] N89-27173

CELL CATHODES
Development of ternary alloy cathode catalysts for phosphoric acid fuel cells
[DE89-000926] N89-27250

CENTRAL PROCESSING UNITS
Reconfiguration strategies in VLSI (Very Large Scale Integration) arrays and trees
[PB89-165468] N89-27071
Implementation indices (1975-1979), volume 1
[AD-A207609] N89-27354
ACP/R3000 processors in data acquisition systems
[DE89-014811] N89-27355
DFT algorithms for bit-serial GaAs array processor architectures
[NASA-CR-183436] N89-27361
Performance analysis of data-driven networks
[PB89-170906] N89-27412

CENTRIFUGAL PUMPS
Space Shuttle Main Engine structural analysis and data reduction/evaluation. Volume 7: High pressure fuel turbo-pump third stage impeller analysis
[NASA-CR-183670] N89-26894

CEPSTRAL ANALYSIS
Capstral method for the measurement of ultrasonic pulse transmission time variations
[AD-A207410] N89-27463

CERAMIC MATRIX COMPOSITES
Structural reliability and damage tolerance of ceramic composites for high-temperature applications
[PB89-156350] N89-26994
Structural reliability and damage tolerance of ceramic composites for high-temperature applications
[PB89-156368] N89-26995
Toughening mechanisms in ceramic composites
[PB89-162606] N89-26996
Mechanical property enhancement in ceramic matrix composites
[PB89-189138] N89-27007

CERAMICS
Compact ceramic heat exchangers
[PB89-173603] N89-26997
Future applications of engine ceramics: Factors influencing market opportunities, timing, and growth
[DE89-012426] N89-27002
Development of magnetic resonance imaging technology for imaging binder distribution in ceramics
[DE89-013165] N89-27003
Corrosion of Ceramic Materials Workshop held November 12-13, 1987, Pennsylvania State University, University Park, Pennsylvania
[PB89-175343] N89-27004
Advanced ceramics: A critical assessment of wear and lubrication
[PB89-188569] N89-27005
Fractographic study of a silicon nitride ceramic
[DE89-013012] N89-27006
Structural ceramics in the advanced materials world
[DE89-013046] N89-27008
Non-polymeric binders for ceramic powders: Utilization of neutral and ionic species derived from decaborane(14)
[AD-A208338] N89-27015
The study of structure-processing-property relations in copper oxide-based high T sub c superconductors
[DE89-012764] N89-27554
Recent improvements in bulk properties of ceramic superconductors
[DE89-013626] N89-27562

CERENKOV COUNTERS
Detection of very high energy gamma-rays from the Crab nebula
[DE89-011840] N89-27627

CHANNEL CAPACITY
Information capacity of additive Gaussian channels with jamming
[AD-A207256] N89-27051
Capacity of the Poisson channel with time-varying noise intensity and jamming
[AD-A207225] N89-27446
Capacity of the poisson channel with random noise intensity
[AD-A207226] N89-27447

CHANNEL NOISE
Information capacity of additive Gaussian channels with jamming
[AD-A207256] N89-27051
Capacity of the Poisson channel with time-varying noise intensity and jamming
[AD-A207225] N89-27446
Capacity of the poisson channel with random noise intensity
[AD-A207226] N89-27447
Multichannel phase noise measurement system
[AD-D014056] N89-27461

CHANNELS (DATA TRANSMISSION)
Bandwidth efficient coding for error control
[NASA-CR-185836] N89-27062

CHAOS
Lagrangian turbulence near walls: Structures and mixing in admissible model flows
[AD-A208466] N89-27135

CHARACTERIZATION
Institute for Materials Science and Engineering, Polymers: Technical activities 1988
[PB89-166094] N89-26993
Micromechanical characterization of near-surface layers
[DE89-008710] N89-27199

CHARGE COUPLED DEVICES
JTECH (Japanese Technology Evaluation Program) panel report on advanced sensors in Japan
[PB89-158760] N89-27136
Observing primeval galaxies and dark matter with LAIRTS — Large Aperture Infra-Red Telescope System
[AD-A208286] N89-27606

CHARM (PARTICLE PHYSICS)
Search for the inclusive production of J/psi in e(+)e(-) collisions using PLUTO data
[NOTA-INTERNA-923] N89-27484

CHEBYSHEV APPROXIMATION
Solution of compressible time-dependent Navier-Stokes equations by Chebychev spectral methods
[ONERA-NT-1987-1] N89-27126
A MACSYMA package for the generation and manipulation of Chebyshev series
[DE89-011404] N89-27436

CHEMICAL ANALYSIS
Supersonics
[AD-A207394] N89-26814
Analysis of low-pressure gas-phase pyrolytic reactions by mass spectrometric techniques
[AD-A207457] N89-26939
Synthesis, characterization and physical properties of polyphosphazenes
[AD-A208296] N89-27013
Analytical procedures for environmental quality control, volume 1
[PB89-158604] N89-27266

CHEMICAL BONDS
Adsorption and coadsorption of CO and NO on the Rh(100) surface: A theoretical analysis
[AD-A207323] N89-26935

CHEMICAL ENERGY
Hybrid electric chemical propulsion
[AD-A207584] N89-26898
High temperature solar electrothermal processing
[AD-A207555] N89-27246

CHEMICAL ENGINEERING
National Engineering Laboratory's 1989 report to the National Research Council's Board on Assessment of NIST (National Institute of Standards and Technology) programs
[PB89-189294] N89-27602

CHEMICAL FUELS
Hybrid electric chemical propulsion
[AD-A207584] N89-26898

CHEMICAL LASERS
Bibliography of Soviet laser developments, No. 92, November - December 1987
[AD-A207794] N89-27177

CHEMICAL PROPERTIES
A computer program for simulating the atmospheric dispersion of UF6 and other reactive gases having positive, neutral, or negative buoyancy
[DE89-012734] N89-27269

CHEMICAL PROPULSION
NASA's Chemical Transfer Propulsion Program for Pathfinder
[NASA-TM-102298] N89-26876
The NASA low thrust propulsion program
[NASA-TM-102065] N89-26895

CHEMICAL REACTIONS
Technical activities 1988, Surface Science Division
[PB89-161889] N89-26928
Adsorption and coadsorption of CO and NO on the Rh(100) surface: A theoretical analysis
[AD-A207323] N89-26935
Electrochemical transport of manganese between the flux and the weld metal in submerged arc welding
[DE89-012419] N89-27193
Electrochemical reactions in submerged arc welding with SiO2-CaO-CaF2 fluxes with high and low silica contents
[DE89-012421] N89-27194
High temperature solar electrothermal processing
[AD-A207555] N89-27246
Fog, cloud, and dew chemistry
[PB89-187314] N89-27317

CHEMISORPTION
Studies of the fundamental nature of catalytic acidity, sites and intermediates
[DE89-012946] N89-26947

CHESAPEAKE BAY (US)
Chesapeake Bay nonpoint source programs
[PB89-152037] N89-27265
Joint CGS-AOML (Charting and Geodetic Service-Atlantic Oceanographic and Meteorological Laboratory) acoustical bottom echo-formation research. 2: Field experiment results and recommendations for echo-sounder design
[PB89-152417] N89-27322

CHIPS (ELECTRONICS)
Fault tolerant VLSI (Very Large-Scale Integration) design using error correcting codes
[AD-A208337] N89-27096
A virtual zero-time, monolithic systolic sorting array
[DE89-007515] N89-27394

CHIRAL DYNAMICS
Effective action for quantum gravity in two dimensions
[PREPRINT-600] N89-27583

CHOLESKY FACTORIZATION
Data traffic reduction schemes for Cholesky factorization on asynchronous multiprocessor systems
[NASA-CR-181863] N89-27349
The least squares solution of linear equations with block-angular observation matrix
[NPL-DITC-139/89] N89-27444

CHROMIUM
Cross-sectional TEM (Transmission Electron Microscopy) studies of Cr films deposited by ion-assisted deposition and physical vapor deposition
[DE89-014643] N89-26985

CHROMIUM ALLOYS
Degradation of Fe-25Cr, Fe-25Cr-20Ni and Fe-25Cr-6Al alloys in H2/H2O/H2S environments at 700 C
[DE89-011873] N89-26967
Breakdown mechanisms of Al2O3, Cr2O3 and SiO2 scales in H2/H2O/H2S environments, volume 1
[DE89-014789] N89-26988

CHROMIUM OXIDES
Breakdown mechanisms of Al2O3, Cr2O3 and SiO2 scales in H2/H2O/H2S environments, volume 1
[DE89-014789] N89-26988

CIRCUITS
Easily testable PLA-based finite state machines
[AD-A208371] N89-27098
The 1/f noise: A nondestructive technique to predict MOS radiation hardness
[DE89-007419] N89-27205
Lightning: Understanding it and protecting systems from its effects
[DE89-012796] N89-27308

CIRCULAR CYLINDERS
Measured damping and modulus of composite cylinders
[DE89-010369] N89-27209
Fate and effects of PAHs in the terrestrial environment: An overview
[DE89-010319] N89-27267

CIRCULAR POLARIZATION
Radio frequency plasma generator
[AD-D013890] N89-27514

CIRCULAR WAVEGUIDES
CWG: A FORTRAN program for mutual coupling in a planar array of circular waveguide-fed apertures
[NASA-TM-101614] N89-27063
CITIES
Millimeter-wave propagation characteristics and channel performance for urban-suburban environments
[PB89-180251] N89-27058
CIVIL AVIATION
Electrical primary flight control system (fly by wire). Flight control systems of new technology
[MBB-UT-122/88] N89-26862
CLADDING
An experimental study of the effect of stainless steel cladding on the structural integrity of flawed steel plates in bending
[DE89-008735] N89-26980
CLAMPS
Structural analysis of a thermal insulation retainer assembly
[NASA-TM-101580] N89-27212
CLASSIFICATIONS
Classification by maximum likelihood method of the massively parallel environment
[INPE-4765-PRE/1434] N89-27380
CLASSIFIERS
The dynamical behavior of classifier systems
[DE89-009407] N89-27383
CLEAR AIR TURBULENCE
Procedural guide for the retrieval of dropsize distributions in water clouds from ground-based clear-air-sensing Doppler radar observations
[PB89-152474] N89-27300
CLEARANCES
Compressor blade clearance measurement system
[AD-D014073] N89-26850
CLIMATE
Criteria for selecting a CO2/climate change region of study
[DE89-011233] N89-27268
Introduction to background materials for Workshop No. 1: Global climate change and its effects on California
[DE89-013381] N89-27272
Proceedings of the 13th Annual Climate Diagnostics Workshop held at Cambridge, Massachusetts on October 31 - November 4, 1988
[PB89-178115] N89-27310
Annual historical report - AMEDD activities
[AD-A208301] N89-27333
CLIMATE CHANGE
Proceedings of the Energy Efficiency and Structural Change: Implications for the Greenhouse Problem Workshop
[DE89-012852] N89-27274
Amazon Forest wind and temperature profiles
[INPE-4724-PRE/1401] N89-27301
CLIMATOLOGY
Introduction to background materials for Workshop No. 1: Global climate change and its effects on California
[DE89-013381] N89-27272
Climatology of temperature and precipitation variability in the United States
[PB89-165930] N89-27299
Tropical cyclone report, 1988
[AD-A207206] N89-27303
Proceedings of the 13th Annual Climate Diagnostics Workshop held at Cambridge, Massachusetts on October 31 - November 4, 1988
[PB89-178115] N89-27310
Meteorological database and synthesis for the Gulf of Mexico
[PB89-178222] N89-27311
Environmental Research Laboratories publication abstracts, FY 1988
[PB89-152656] N89-27589
CLOSED ECOLOGICAL SYSTEMS
Efficiency of N use by wheat as a function of influx and efflux of NO sub 3
[NASA-CR-177534] N89-27346
CLOUD CHAMBERS
An instantaneous CCN (Cloud Condensation Nucleus) spectrometer
[DE89-014807] N89-27150
CLOUD PHYSICS
An instantaneous CCN (Cloud Condensation Nucleus) spectrometer
[DE89-014807] N89-27150
Dual-channel microwave radiometer for airborne meteorological applications
[PB89-159693] N89-27298
Procedural guide for the retrieval of dropsize distributions in water clouds from ground-based clear-air-sensing Doppler radar observations
[PB89-152474] N89-27300
Airborne measurements of the electric field and the charge precipitation particles in convective clouds: Lower positive charge centers
[ONERA-NT-1988-1] N89-27319
CLOUDS
Fog, cloud, and dew chemistry
[PB89-187314] N89-27317
CLOUDS (METEOROLOGY)
Dual-channel microwave radiometer for airborne meteorological applications
[PB89-159693] N89-27298
Cloud and precipitation scavenging process in the South Coast Air Basin
[PB89-181788] N89-27313
CLUTTER
Development of a system model and Least Mean Square (LMS) filter for the Naval Postgraduate School (NPS) Infrared Search and Target Designation System (IRSTD)
[AD-A208536] N89-27068
CMOS
Total-dose hardness assurance for space applications of commercial CMOS devices
[DE89-006765] N89-27089
COAL
Combustion characteristics of dry coal-powder-fueled adiabatic diesel engine
[DE89-000978] N89-27197
COAL GASIFICATION
Gas separations using inorganic membranes
[DE89-013010] N89-26948
COASTS
Alaska collection SAR (Synthetic Aperture Radar) data summary
[AD-A208530] N89-27067
Pacific Coast hindcast phase 3 north wave information
[AD-A207189] N89-27323
COATINGS
Optimum interface properties for metal matrix composites
[NASA-TM-102295] N89-27223
Optical mirror coated with organic superconducting material
[AD-D014047] N89-27499
COAXIAL CABLES
Development of elements of a high Tc superconducting cable
[AD-A208370] N89-27574
COBALT
Dispersed and periodic microstructures for magnetic and infrared absorbers
[AD-A207428] N89-27053
CODERS
Evaluation of low data rate voice CODECS for air traffic control applications
[DOT/FAA/CT-TN89/13] N89-27047
Capacity of the Poisson channel with time-varying noise intensity and jamming
[AD-A207225] N89-27446
CODING
Advanced modulation technology development for earth station demodulator applications
[NASA-CR-185126] N89-26880
Bandwidth efficient coding for error control
[NASA-CR-185836] N89-27062
COHESION
Thermal and mechanical properties of polyurethane-diacetylene segmented copolymers. Part 2: Effects of diacetylene cross-polymerization
[AD-A208754] N89-27023
COILS
The short-circuited fluxgate output current
[ISSN-0109-6605] N89-27069
COLD FRONTS
An investigation into the gravity current aspects of a cold air outbreak using variational analysis techniques
[AD-A208464] N89-27295
COLD WEATHER TESTS
Thermoregulatory responses in the cold-effect of an Extended Cold Weather Clothing System (ECWCS)
[AD-A208314] N89-27334
COLD WORKING
The recrystallization and respheroidization of tungsten grains in a tungsten-heavy alloy
[AD-A207647] N89-26964
Strength tests and design methods for cold-formed channel columns undergoing distortional buckling
[PB89-183958] N89-27216
COLLAPSE
Dynamic plastic buckling of spherical shells during collapse
[DE89-006543] N89-27217
Dynamics of an M-level atom interacting with gravity fields. 1: Effects of the level number on quantum collapse and revival
[AD-A207278] N89-27579
COLLIMATORS
Efficient dynamic phasefront modulation system for free-space optical communications
[AD-D014128] N89-27503
COLLOCATION
ILS/MLS collocation tests at Miami/Tamiami, Florida Airport
[NASA-CR-185715] N89-26832
An operational demonstration and flight test of the Microwave Landing System (MLS) at the Miami/Tamiami, Florida Airport
[DOT/FAA/CT-TN89/37] N89-26833
COLOR CODING
Aircraft color displays: Chromaticity and luminance requirements
[AD-A206786] N89-26828
COLOR VISION
Integrated silicon color sensors
[ETN-89-94800] N89-27509
COLUMBUS SPACE STATION
Columbus Logistics Program
[MBB-UO-0039/88-PUB] N89-26890
COLUMNS
Inelastic buckling of channel columns in the distortional mode
[PB89-156053] N89-27207
Stability and dynamic analysis of a slender column with curved longitudinal stiffeners
[NASA-TM-101636] N89-27215
Strength tests and design methods for cold-formed channel columns undergoing distortional buckling
[PB89-183958] N89-27216
COMBAT
Annual historical report - AMEDD activities
[AD-A208301] N89-27333
Rule-based air combat simulation
[NASA-CR-4160] N89-27393
COMBUSTIBLE FLOW
Mixing and combustion of pulsed gas jets
[PB89-155550] N89-26929
COMBUSTION
Measurement uncertainty within the Uniform Engine Test Programme
[AGARD-AG-307] N89-26854
Mixing and combustion of pulsed gas jets
[PB89-155550] N89-26929
Laser spectroscopy and dynamics of combustion intermediates
[DE89-014498] N89-26956
COMBUSTION CHAMBERS
OTVE combustor wall condition monitoring
[NASA-CR-182275] N89-26899
Lean-burn gas engine ignition processes
[PB89-181119] N89-26943
Feasibility demonstration of the Thermal Ignition Combustion System (TICS) for high pressure natural gas injected engine
[PB89-178792] N89-26944
COMBUSTION PHYSICS
Feasibility demonstration of the Thermal Ignition Combustion System (TICS) for high pressure natural gas injected engine
[PB89-178792] N89-26944
Catalytic combustion of methane
[PB89-188874] N89-26946
COMBUSTION PRODUCTS
Atmospheric carbon dioxide and the greenhouse effect
[DE89-012869] N89-27271
COMETS
Global environmental effects of impact-generated aerosols: Results from a general circulation model, revision 1
[DE89-014179] N89-27276
COMMERCE
NIST (National Institute of Standards and Technology) research reports, March 1989
[PB89-189310] N89-27594
COMMERCIAL AIRCRAFT
Statistics on aircraft gas turbine engine rotor failures that occurred in US commercial aviation during 1983
[AD-A207592] N89-26851
COMMONALITY
Two-stage reusable launch system utilizing a winged core vehicle and glideback boosters
[NASA-TM-101513] N89-26878
COMMUNICATION EQUIPMENT
Development of a DFS (Deutsche Fernmeldesatellit) reception converter
[ETN-89-94629] N89-27065
COMMUNICATION SATELLITES
Development of near-field test procedures for communication satellite antennas, phase 1, part 2
[PB89-156152] N89-27043
Common carrier earth station database documentation
[PB89-186050] N89-27595

COMPACTING
Method for refining microstructures of blended elemental titanium powder compacts
[AD-D014067] N89-26961
COMPARATORS
Hose reel monitor for inflight refueling system
[AD-D014054] N89-26836
COMPILERS
Implementation of a design for testability strategy using the Genesil silicon compiler
[AD-A208458] N89-27099
Software deficiency issues confronting the utilization of non-Von Neumann architectures
[AD-A207268] N89-27369
The HERMOD behavioral synthesis system
[AD-A207319] N89-27371
Attributed tree transformations with delayed and smart re-evaluation
[MEMO-INF-88-45] N89-27440
COMPONENT RELIABILITY
Gas engine heat pump system and component efficiency and reliability improvement, phase 2
[PB89-173645] N89-27184
COMPONENTS
System-based component test plans and operating characteristics: Introduction and overview
[DE89-012255] N89-27203
COMPOSITE MATERIALS
Low loss radar window for reentry vehicle
[AD-D014045] N89-26882
Interface modified glass fiber/thermoplastic matrix composites
[AD-A207308] N89-26910
Processing of continuous fiber composites
[DE89-012608] N89-26915
Development of a thin wall graphite/polyimide composite pressure vessel with a large aspect ratio
[DE89-002536] N89-26920
Nonlinear dynamic response of pressurized composite bottles subjected to shock loading
[DE89-010553] N89-26922
Fatigue crack growth study of SCS6/Ti-15-3 composite
[NASA-TM-102332] N89-26989
A method of removing oxides from the surface of Fe-Ni-Co alloy particles by chemical etching
[DE89-014597] N89-27009
An approach for constructing families of homogenized equations for periodic media. 1: An integral representation and its consequences
[AD-A207572] N89-27427
An approach for constructing families of homogenized equations for periodic media. 2: Properties of the kernel
[AD-A207573] N89-27428
COMPOSITE PROPELLANTS
Characterization of Morton-Thiokol booster-rocket propellant TP-H1207C and its simulant H-19
[DE89-013347] N89-27031
COMPOSITE STRUCTURES
Measured damping and modulus of composite cylinders
[DE89-010369] N89-27209
Fate and effects of PAHs in the terrestrial environment: An overview
[DE89-010319] N89-27267
COMPRESSIBLE BOUNDARY LAYER
Inviscid spatial stability of a compressible mixing layer. Part 3: Effect of thermodynamics
[NASA-CR-181855] N89-27112
COMPRESSIBLE FLOW
A dual potential formulation of the Navier-Stokes equations
[NASA-CR-185098] N89-27111
Inviscid spatial stability of a compressible mixing layer. Part 3: Effect of thermodynamics
[NASA-CR-181855] N89-27112
Absolute/convective instabilities and the convective Mach number in a compressible mixing layer
[NASA-CR-181861] N89-27113
Transactions of the 6th Army Conference on Applied Mathematics and Computing held in Boulder, Colorado on 31 May - 3 June 1988
[AD-A207252] N89-27424
COMPRESSION TESTS
Composite transport wing technology development
[NASA-CR-178409] N89-26842
Scaling effects in the static large deflection response of graphite-epoxy composite beams
[NASA-TM-101619] N89-26843
Strength tests and design methods for cold-formed channel columns undergoing distortional buckling
[PB89-183958] N89-27216
COMPRESSIVE STRENGTH
Compressive properties of high performance polymeric fibers
[AD-A207271] N89-26998
COMPRESSOR BLADES
Compressor blade clearance measurement system
[AD-D014073] N89-26850
COMPRESSORS
Performance estimates for the Space Station power system Brayton Cycle compressor and turbine
[NASA-CR-182263] N89-26903
Sun synchronous solar refrigeration
[DE89-011375] N89-27245
COMPUTATION
A review of high-speed, convective, heat-transfer computation methods
[NASA-TP-2914] N89-27116
On a computational method for the second fundamental tensor and its application to bifurcation problems
[AD-A207517] N89-27377
Computation and theory in nonlinear optimization
[AD-A207610] N89-27430
COMPUTATIONAL FLUID DYNAMICS
A procedure for computing surface wave trajectories on an inhomogeneous surface
[NASA-TP-2929] N89-26811
Experimental program for real gas flow code validation at NASA Ames Research Center
[NASA-TM-100093] N89-26816
Technical Status Review on Drag Prediction and Analysis from Computational Fluid Dynamics: State of the Art
[AGARD-AR-256] N89-26817
Drag prediction and analysis from computational fluid dynamics, state-of-the-art in France N89-26818
Drag prediction and analysis from CFD state-of-the-art in Germany N89-26819
Some results on flow calculations involving drag prediction N89-26820
State-of-the-art of aircraft drag prediction in Italy by means of theoretical methods N89-26821
Aircraft drag prediction for transonic potential flow N89-26822
CFD methods for drag prediction and analysis currently in use in UK N89-26823
Computational fluid dynamics drag prediction: Results from the Viscous Transonic Airfoil Workshop N89-26824
CFD drag prediction for aerodynamic design N89-26825
Investigation of the transient fuel preburner manifold and combustor
[NASA-CR-183715] N89-26900
The 1st Scandinavian Conference on Viscous and T urbulent Flow in Hydraulic Machinery
[PB89-161327] N89-27102
Validation of computational fluid dynamics
[AGARD-AR-257] N89-27104
A dual potential formulation of the Navier-Stokes equations
[NASA-CR-185098] N89-27111
Stability of a rigid rotor supported on oil-film journal bearings under dynamic load
[NASA-TM-102309] N89-27114
Calculation of turbulence-driven secondary motion in ducts with arbitrary cross section
[NASA-TM-102142] N89-27115
Study of subgrid models in incompressible turbulent flow, homogeneous or inhomogeneous
[ONERA-RSF-17/3619-AY-110-A] N89-27123
Solution of compressible time-dependent Navier-Stokes equations by Chebychev spectral methods
[ONERA-NT-1987-1] N89-27126
Summary of research conducted at the Institute for Computer Applications in Science and Engineering in applied mathematics, numerical analysis and computer science
[NASA-CR-181858] N89-27348
Offline computing farms
[DE89-013958] N89-27359
Multigrid method for stability problems
[NASA-CR-185825] N89-27420
Efficient grid generation
[NASA-CR-185034] N89-27434
COMPUTATIONAL GRIDS
A nonlinear multigrid method for three-dimensional transonic potential flow
[ETN-89-94802] N89-26827
Study of subgrid models in incompressible turbulent flow, homogeneous or inhomogeneous
[ONERA-RSF-17/3619-AY-110-A] N89-27123
Summary of research conducted at the Institute for Computer Applications in Science and Engineering in applied mathematics, numerical analysis and computer science
[NASA-CR-181858] N89-27348
Multigrid method for stability problems
[NASA-CR-185825] N89-27420
A direct procedure for interpolation on a structured curvilinear two-dimensional grid
[NASA-TM-102213] N89-27433
Efficient grid generation
[NASA-CR-185034] N89-27434
Using conjoint meshing primitives to generate quadrilateral and hexahedral elements in irregular regions
[DE89-005918] N89-27435
COMPUTER AIDED DESIGN
The conceptional design study of USB powered lift aircrafts in FY 1986
[NAL-TR-958] N89-26835
Tailoring of composite links for optimal damped elasto-dynamic performance
[NASA-TM-102094] N89-26912
On processing development for fabrication of fiber reinforced composite, part 2
[NASA-CR-181866] N89-26917
An expert system in C for computer-aided digital circuit design
[AD-A207518] N89-27075
Implementation of a design for testability strategy using the Genesil silicon compiler
[AD-A208458] N89-27099
A language translator for a computer aided rapid prototyping system
[AD-A208358] N89-27406
A dynamic scheduler for a computer aided prototyping system
[AD-A208389] N89-27407
Algorithms for computer aided design of digital filters
[AD-A208485] N89-27410
COMPUTER AIDED MANUFACTURING
Quality in automation project for FY 88
[PB89-193296] N89-27040
COMPUTER ASSISTED INSTRUCTION
On-line computer utilization to understand some physical processes (example: Pendulum motion)
[NOTA-INTERNA-927] N89-27360
COMPUTER GRAPHICS
A graphics package for meteorological data, version 1.5
[NASA-TM-100742] N89-27314
Cray-to-sun prototype
[DE89-013087] N89-27358
Abstract data types in computer graphics and image processing
[INPE-4745-PRE/1419] N89-27381
Using conjoint meshing primitives to generate quadrilateral and hexahedral elements in irregular regions
[DE89-005918] N89-27435
COMPUTER INFORMATION SECURITY
Issues and approaches for electronic document approval and transmittal using digital signatures and text authentication
[DE89-013102] N89-27596
COMPUTER NETWORKS
An expert system in C for computer-aided digital circuit design
[AD-A207518] N89-27075
The dynamical behavior of classifier systems
[DE89-009407] N89-27383
Performance analysis of data-driven networks
[PB89-170906] N89-27412
Advanced information processing system: Input/output system services
[NASA-CR-181874] N89-27413
Northeast Artificial Intelligence Consortium annual report 1987. Volume 2, part b: Discussing, using, and recognizing plans
[AD-A208378] N89-27418
Northeast Artificial Intelligence Consortium annual report 1987. Volume 3: Distributed artificial intelligence for communications network management
[AD-A208379] N89-27419
Issues and approaches for electronic document approval and transmittal using digital signatures and text authentication
[DE89-013102] N89-27596
Empirical analysis and refinement of expert system knowledge bases
[AD-A208294] N89-27598
COMPUTER PROGRAMMING
Human Operator Simulator (HOS) 4 programmer's guide
[AD-A207241] N89-27342
Summary of research conducted at the Institute for Computer Applications in Science and Engineering in applied mathematics, numerical analysis and computer science
[NASA-CR-181858] N89-27348
Programming parallel architectures: The BLAZE family of languages
[NASA-CR-185826] N89-27362

Software deficiency issues confronting the utilization of non-Von Neumann architectures
[AD-A207268] N89-27369
Hardware C - A language for hardware design
[AD-A207317] N89-27370
Competitive management of distributed shared memory
[AD-A207322] N89-27372
SDS software measurement requirements
[AD-A207449] N89-27376
Small Computer System Interface (SCSI) command system: Software support for control of small computer system interface devices
[PB89-151815] N89-27389
ORMONTE: An uncertainty analysis code for use with user-developed systems models on mainframe or personal computers. A user's guide
[DE89-013730] N89-27396
Automatic generation of FORTRAN-coded Jacobians and Hessians
[MEMO-INF-88-47] N89-27402
An overview of some methods for the high-level specification of synchronization
[MEMO-INF-88-50] N89-27403
Fault tolerant software technology for distributed computer systems
[AD-A208329] N89-27405
A language translator for a computer aided rapid prototyping system
[AD-A208358] N89-27406
Automatic code vectorization of arithemetic expressions by bottom-up structure recognition
[MEMO-INF-88-48] N89-27414
Northeast artificial intelligence consortium: Volume 2, part A: The Versatile Maintenance Expert System (VMES) research project
[AD-A208344] N89-27417
Attributed tree transformations with delayed and smart re-evaluation
[MEMO-INF-88-45] N89-27440

COMPUTER PROGRAMS

Experimental program for real gas flow code validation at NASA Ames Research Center
[NASA-TM-100093] N89-26816
Feasibility study for enhanced lateral control of the P-3C aircraft
[AD-A208461] N89-26863
The NASA Langley Research Center 0.3-meter transonic cryogenic tunnel T-P/Re-M controller manual
[NASA-CR-181868] N89-26869
Metal matrix composite micromechanics: In-situ behavior influence on composite properties
[NASA-TM-102302] N89-26924
CWG: A FORTRAN program for mutual coupling in a planar array of circular waveguide-fed apertures
[NASA-TM-101614] N89-27063
Computer code prediction of picosecond voltage switching and TEM wave generation in air gas avalanche switches
[DE89-013778] N89-27084
Fault tolerant VLSI (Very Large-Scale Integration) design using error correcting codes
[AD-A208337] N89-27096
Validation of computational fluid dynamics
[AGARD-AR-257] N89-27104
Film annotation system for a space experiment
[NASA-CR-185114] N89-27152
A three-node C deg element for analysis of laminated composite sandwich shells
[NASA-TM-4125] N89-27213
Stability and dynamic analysis of a slender column with curved longitudinal stiffeners
[NASA-TM-101636] N89-27215
Quantitative three-dimensional structural techniques
[DE89-010879] N89-27238
A computer program for simulating the atmospheric dispersion of UF6 and other reactive gases having positive, neutral, or negative buoyancy
[DE89-012734] N89-27269
Development of Low-Level Turbulence (LLT) forecasting methodologies
[AD-A208457] N89-27320
Brief instructions for SIMBAT, a computer package for unconditional and conditional simulation of ocean wave kinematics
[AD-A207627] N89-27324
Parallel implementation of OPS5 on the encore multiprocessor: Results and analysis
[AD-A207320] N89-27353
Competitive management of distributed shared memory
[AD-A207322] N89-27372
SDS software measurement requirements
[AD-A207449] N89-27376
Rule-based air combat simulation
[NASA-CR-4160] N89-27393
ASR4: A computer code for fitting and processing 4-gage anelastic strain recovery data
[DE89-012239] N89-27395
A language translator for a computer aided rapid prototyping system
[AD-A208358] N89-27406
A dynamic scheduler for a computer aided prototyping system
[AD-A208389] N89-27407
Software management indicators: Managing the risk of project management
[AD-A208443] N89-27408
ROUTEMAP model for predicting noise exposure from aircraft operations on Military Training Routes
[AD-A203849] N89-27459
EIGEN: A program to compute eigenrays from HARPA (Hamiltonian Acoustic Ray-Tracing Program for the Atmosphere)/HARPO (Hamiltonian Acoustic Ray-Tracing Program for the Ocean) raysets
[PB89-165781] N89-27460
Fast wave current drive modeling for ITER and prospects for a near-term proof of principle experiment
[DE89-013049] N89-27520
Macromolecular calculations for the XTAL system of crystallographic programs
[AD-A208272] N89-27572

COMPUTER STORAGE DEVICES

Window generator
[AD-D014068] N89-27048
Memory-reference characteristics of multiprocessor applications under MACH
[AD-A207318] N89-27352
Competitive management of distributed shared memory
[AD-A207322] N89-27372
Suitability of message passing computers for implementing production systems
[AD-A207321] N89-27411

COMPUTER SYSTEMS DESIGN

Northeast artificial intelligence consortium: Volume 2, part A: The Versatile Maintenance Expert System (VMES) research project
[AD-A208344] N89-27417

COMPUTER SYSTEMS PERFORMANCE

Categorization in neural networks and prosopagnosia
[PREPRINT-608] N89-27327
Hybrid structures for simple computer performance estimates
[PB89-189161] N89-27356

COMPUTER TECHNIQUES

Automated immersion testing robotic system: Hardware and software design
[AD-A208755] N89-27201
Summary of research conducted at the Institute for Computer Applications in Science and Engineering in applied mathematics, numerical analysis and computer science
[NASA-CR-181858] N89-27348
SDS software measurement requirements
[AD-A207449] N89-27376
Lognormal distribution maximum-likelihood parameter estimation algorithms
[AD-A207586] N89-27378
A language translator for a computer aided rapid prototyping system
[AD-A208358] N89-27406

COMPUTER VISION

JTECH (Japanese Technology Evaluation Program) panel report on advanced sensors in Japan
[PB89-158760] N89-27136
Satellite image processing using symbolic structures of reduced vision conditions
[INPE-4638-TDL/337] N89-27367
An efficient exact algorithm for the least squares image registration problems
[DE89-013116] N89-27387
Integrated silicon color sensors
[ETN-89-94800] N89-27509

COMPUTERIZED SIMULATION

Experimental program for real gas flow code validation at NASA Ames Research Center
[NASA-TM-100093] N89-26816
Formulation of numerical orbit propagation and time error correction
[INPE-4774-PRE/1443] N89-26875
Spin stabilization of the ORION satellite using a thruster attitude control system with optimal control considerations
[AD-A208484] N89-26892
Flow fields of low pressure vent exhausts
[NASA-TM-100738] N89-26902
Model-based parameter estimation in electromagnetic computer modeling
[AD-A207399] N89-27052
An expert system for correlation of radar and passive sensor signals
[DE89-011575] N89-27056
DYNA3D user's manual: (Nonlinear Dynamic Analysis of Structures in Three Dimensions), revision 5
[DE89-014304] N89-27222
Residual stress changes in fatigue. Volume 1: Residual stress measurements by X-ray diffraction in notched test specimens
[AD-A208345] N89-27225
Modeling of the angular reflectance of an artificial plant canopy near the retroreflection peak in the optical regime
[DE89-011174] N89-27239
Dynamic simulation of a molten-salt solar receiver
[DE89-010556] N89-27244
A computer program for simulating the atmospheric dispersion of UF6 and other reactive gases having positive, neutral, or negative buoyancy
[DE89-012734] N89-27269
Computational techniques in gamma-ray Skyshine analysis
[DE89-010156] N89-27282
Investigations on local seismic phases and evaluation of body waves magnitude
[AD-A206633] N89-27283
Computer simulations of explosive volcanic eruptions
[DE89-014024] N89-27290
Verification of severe local storm forecasts issued by the National Severe Storms Forecast Center, 1987
[PB89-159719] N89-27297
Brief instructions for SIMBAT, a computer package for unconditional and conditional simulation of ocean wave kinematics
[AD-A207627] N89-27324
Human Operator Simulator (HOS) 4 programmer's guide
[AD-A207241] N89-27342
Rule-based air combat simulation
[NASA-CR-4160] N89-27393
A symbolic generator of state equations for modeling of dynamic systems based on the electrical network analog paradigm
[DE89-013763] N89-27397
Machines for lattice gauge theory
[DE89-014815] N89-27400
Using conjoint meshing primitives to generate quadrilateral and hexahedral elements in irregular regions
[DE89-005918] N89-27435
High-temperature behavior of grain boundaries from embedded atom method molecular dynamics simulation
[DE89-013641] N89-27474
Atomic simulation of crystalline defects in ordered structures
[ETN-89-94807] N89-27571

CONCENTRATORS

Alternate space station freedom configuration considerations to accommodate solar dynamic power
[NASA-TM-101603] N89-26888
Thermal evaluation of advanced solar dynamic heat receiver performance
[NASA-CR-185117] N89-27256

CONCRETES

Evaluation of barrier cable impact pad materials
[AD-A207554] N89-26864

CONDENSATION NUCLEI

An instantaneous CCN (Cloud Condensation Nucleus) spectrometer
[DE89-014807] N89-27150

CONES

Experimental program for real gas flow code validation at NASA Ames Research Center
[NASA-TM-100093] N89-26816
Evaluation of an updated design of an internally lighted wind cone
[DOT/FAA/CT-TN89/45] N89-26868

CONES (VOLCANOES)

Computer simulations of explosive volcanic eruptions
[DE89-014024] N89-27290

CONFERENCES

Technical Status Review on Drag Prediction and Analysis from Computational Fluid Dynamics: State of the Art
[AGARD-AR-256] N89-26817
Corrosion of Ceramic Materials Workshop held November 12-13, 1987, Pennsylvania State University, University Park, Pennsylvania
[PB89-175343] N89-27004
The 14th Convention on Radio Science, Finnish National Committee of URSI held in Otaniemi (Finland) on October 17-18, 1988: Abstracts of papers
[PB89-145767] N89-27044
The 1st Scandinavian Conference on Viscous and T urbulent Flow in Hydraulic Machinery
[PB89-161327] N89-27102

Partial support of the 3rd International Laser Science Conference held in Atlantic City, New Jersey on 1-4 November 1987
[AD-A206612] N89-27161

Report of the Workshop on Scientific Opportunities for Infrared Free-Electron Lasers, volume 1
[DE89-012836] N89-27170

Interactions between the National Institute of Standards and Technology and the American Society of Mechanical Engineers
[PB89-172563] N89-27182

Proceedings of the Annual Solar Thermal Technology Research and Development Conference
[DE89-010536] N89-27251

Investigations on local seismic phases and evaluation of body waves magnitude
[AD-A206633] N89-27283

Proceedings of the 13th Annual Climate Diagnostics Workshop held at Cambridge, Massachusetts on October 31 - November 4, 1988
[PB89-176115] N89-27310

Ergonomic Models of Anthropometry, Human Biomechanics and Operator-Equipment Interfaces
[NASA-CR-185720] N89-27344

Transactions of the 6th Army Conference on Applied Mathematics and Computing held in Boulder, Colorado on 31 May - 3 June 1988
[AD-A207252] N89-27424

New Frontier: Environments for Innovation --- sick building syndrome
[PB89-151054] N89-27601

CONFINEMENT

Transient heat transfer into superfluid helium under confined conditions
[DE88-706312] N89-27109

CONFORMAL MAPPING

Ideal jet flow in two dimensions
[AD-A208275] N89-27131

CONGRESSIONAL REPORTS

Report to the Congress --- Fiscal Year 1988
[PB89-195408] N89-27603

CONSTRAINTS

Injuries to seat occupants of light airplanes
[AD-A207579] N89-26830

CONSTRUCTION

Superplastic forming of aluminum, task C
[AD-A207282] N89-26962

CONTAINMENT

Earth sciences
[DE89-013344] N89-27228

CONTAMINANTS

Analytical procedures for environmental quality control, volume 1
[PB89-158604] N89-27286

Submarine air quality: Monitoring the air in submarines. Health effects in divers of breathing submarine air under hyperbaric conditions
[PB89-174213] N89-27345

CONTAMINATION

Flow fields of low pressure vent exhausts
[NASA-TM-100738] N89-26902

CONTINUOUS WAVE LASERS

Selective nitrations: Laser-induced nitrations
[AD-A207406] N89-27024

CONTOURS

GEO-EAS (Geostatistical Environmental Assessment Software) user's guide
[PB89-151252] N89-27261

A graphics package for meteorological data, version 1.5
[NASA-TM-100742] N89-27314

CONTRACT MANAGEMENT

Cost of quality evaluation methodologies handbook
[AD-A206935] N89-27202

Software management indicators: Managing the risk of project management
[AD-A208443] N89-27408

CONTRACTORS

Cost of quality evaluation methodologies handbook
[AD-A206935] N89-27202

CONTROL STABILITY

Automatic oxygen measuring system
[AD-D014003] N89-26931

Heuristic algorithms for stability testing polytopes of matrices
[PB89-160840] N89-27365

CONTROL STICKS

Design considerations of manipulator and feel system characteristics in roll tracking
[NASA-CR-4111] N89-26860

CONTROL SURFACES

Control surface dual redundant servomechanism
[AD-D014058] N89-26857

CONTROL SYSTEMS DESIGN

Back-up control system for f101 engine and its derivatives
[AD-D014051] N89-26848

Design of an active helicopter control experiment at the Princeton Rotorcraft Dynamics Laboratory
[NASA-CR-185490] N89-26859

Design considerations of manipulator and feel system characteristics in roll tracking
[NASA-CR-4111] N89-26860

A new state reconstructor for digital controls systems using weighted-average measurements
[NASA-TP-2936] N89-27039

Small Computer System Interface (SCSI) command system: Software support for control of small computer system interface devices
[PB89-151815] N89-27389

Processor control path synthesis: Literature survey and preliminary analysis
[MEMO-INF-88-46] N89-27401

A qualitative way of solving the pole balancing problem
[MEMO-INF-88-44] N89-27439

Reduction of blade-vortex interaction noise using higher harmonic pitch control
[NASA-TM-101624] N89-27465

CONTROL THEORY

Spin stabilization of the ORION satellite using a thruster attitude control system with optimal control considerations
[AD-A206484] N89-26892

Aircraft flight test trajectory control
[NASA-CR-4161] N89-27416

CONTROLLED ATMOSPHERES

Submarine air quality: Monitoring the air in submarines. Health effects in divers of breathing submarine air under hyperbaric conditions
[PB89-174213] N89-27345

CONTROLLED FUSION

On the economic prospects of nuclear fusion with tokamaks
[IPP-6/271] N89-27539

CONTROLLERS

Design considerations of manipulator and feel system characteristics in roll tracking
[NASA-CR-4111] N89-26860

The NASA Langley Research Center 0.3-meter transonic cryogenic tunnel T-P/Re-M controller manual
[NASA-CR-181868] N89-26869

Aircraft flight test trajectory control
[NASA-CR-4161] N89-27416

CONVECTION

Absolute/convective instabilities and the convective Mach number in a compressible mixing layer
[NASA-CR-181861] N89-27113

CONVECTIVE HEAT TRANSFER

A review of high-speed, convective, heat-transfer computation methods
[NASA-TP-2914] N89-27116

CONVERGENCE

Rapidly convergent algorithms for nonsmooth optimization
[AD-A207629] N89-27379

CONVOLUTION INTEGRALS

Integral constitutive relation for the investigation of ion Bernstein waves in non-homogeneous plasmas
[IPP-5/27] N89-27538

COOLING

Variable nozzle area turbine vane cooling
[AD-D014071] N89-26849

Variable area manifolds for ring mirror heat exchangers
[AD-D014050] N89-27163

High performance intercooled and recuperated gas turbine
[PB89-152284] N89-27178

Self-locking outer air seal with full backside cooling
[AD-D013975] N89-27179

Optimum interface properties for metal matrix composites
[NASA-TM-102295] N89-27223

COOLING SYSTEMS

Surface cooling system
[AD-D014057] N89-27106

COORDINATE TRANSFORMATIONS

A direct procedure for interpolation on a structured curvilinear two-dimensional grid
[NASA-TM-102213] N89-27433

COPOLYMERS

Thermal and mechanical properties of polyurethane-diacetylene segmented copolymers. Part 1: Molecular weight and annealing effects
[AD-A208753] N89-27022

Thermal and mechanical properties of polyurethane-diacetylene segmented copolymers. Part 2: Effects of diacetylene cross-polymerization
[AD-A208754] N89-27023

COPPER

Loss of grain boundary segregant during ion milling
[DE89-007835] N89-26979

Polycrystal plasticity as applied to the problem of in-plane anisotropy in rolled cubic metals
[DE89-011181] N89-26983

Anomalous temperature dependence of Cu NMR line width and magnetization in YBa2Cu3O(7-delta)
[DE89-014291] N89-27565

Nuclear relaxation rates at copper and oxygen sites in YBa2Cu3O7
[DE89-014308] N89-27567

COPPER ALLOYS

Microstructural evolution of Al-Li and Al-Li-Cu-Mg alloys
[DE89-012981] N89-26972

COPPER OXIDES

The study of structure-processing-property relations in copper oxide-based high T sub c superconductors
[DE89-012764] N89-27554

Composition of superconducting La2CuO4+delta: A superconductor doped by excess oxygen defects
[DE89-013299] N89-27555

O-17 NMR study of YBa2Cu3O(7-delta)
[DE89-014292] N89-27566

Nuclear relaxation rates at copper and oxygen sites in YBa2Cu3O7
[DE89-014308] N89-27567

CORIOLIS EFFECT

An investigation into the gravity current aspects of a cold air outbreak using variational analysis techniques
[AD-A208464] N89-27295

CORRELATORS

Evaluation of an optical correlator and matched filter maker
[AD-A207556] N89-27054

CORROSION

Degradation of Fe-25Cr, Fe-25Cr-20Ni and Fe-25Cr-6Al alloys in H2/H2O/H2S environments at 700 C
[DE89-011873] N89-26967

COSMIC RAYS

Theoretical studies in elementary particle physics
[DE89-012701] N89-27473

Use of the EGRET (Energetic Gamma-Ray Experiment Telescope) in studies of the origin of the cosmic radiation
[DE89-013785] N89-27630

A method to calibrate the light response of a high resolution electromagnetic calorimeter with cosmic rays
[NOTA-INTERNA-925] N89-27631

COSMOLOGY

Cosmic evolution of non-topological solitons, paper 1
[NASA-CR-185353] N89-27608

Black holes in closed universes
[PB89-170039] N89-27610

The cosmological constant problem
[DE89-013150] N89-27614

Evolution of Galaxies. Proceedings, volume 4
[DE89-609850] N89-27616

COST ANALYSIS

Estimating and explaining the production cost of high-technology systems: The case of military aircraft
[AD-A208391] N89-26809

Cost of quality evaluation methodologies handbook
[AD-A206935] N89-27202

Study for advanced civil earth remote sensing system: Focused finance study. Volume 1: Executive summary
[PB89-163224] N89-27230

Dedicated low-pressure natural gas-fueled vehicle baseline assessment. Task 3 topical report on light-duty vehicles
[PB89-195820] N89-27604

COST ESTIMATES

Estimating and explaining the production cost of high-technology systems: The case of military aircraft
[AD-A208391] N89-26809

COSTS

Software management indicators: Managing the risk of project management
[AD-A208443] N89-27408

COULOMB COLLISIONS

Radiative collapse of a Bennett-relaxed z-pinch
[DE89-014290] N89-27533

COUPLING

Surface plasmon study of monolayer-bilayer transition in poly-4-BCMU and poly-3-BCMU polydiacetylene Langmuir-Blodgett films
[AD-A207404] N89-26938

The short-circuited fluxgate output current
[ISSN-0109-6605] N89-27069

COUPLINGS
CWG: A FORTRAN program for mutual coupling in a planar array of circular waveguide-fed apertures
[NASA-TM-101614] N89-27063
COVARIANCE
Covariance properties of the multiquark Hamiltonian in the constituent quark model
[NOTA-INTERNA-920] N89-27489
CRAB NEBULA
Detection of very high energy gamma-rays from the Crab nebula
[DE89-011840] N89-27627
CRACK PROPAGATION
Advanced durability analysis. Volume 2: Analytical predictions, test results and analytical correlations
[AD-A207215] N89-26838
HRR field in an aluminum SEN specimen
[AD-A207578] N89-26963
An experimental study of the effect of stainless steel cladding on the structural integrity of flawed steel plates in bending
[DE89-008735] N89-26980
Fatigue crack growth study of SCS6/Ti-15-3 composite
[NASA-TM-102332] N89-26989
High-temperature flaw assessment procedure: A state-of-the-art survey
[DE89-012740] N89-27210
CRACKING (CHEMICAL ENGINEERING)
Catalytic reduction of carbon dioxide by metal centers
[AD-A207227] N89-26934
CRACKING (FRACTURING)
Advanced durability analysis. Volume 2: Analytical predictions, test results and analytical correlations
[AD-A207215] N89-26838
HRR field in an aluminum SEN specimen
[AD-A207578] N89-26963
NIST (National Institute of Standards and Technology) research reports, March 1989
[PB89-189310] N89-27594
CRACKS
An experimental study of the effect of stainless steel cladding on the structural integrity of flawed steel plates in bending
[DE89-008735] N89-26980
Toughening mechanisms in ceramic composites
[PB89-162606] N89-26996
Arcjet cathode phenomena
[NASA-TM-102099] N89-27121
High-temperature flaw assessment procedure: A state-of-the-art survey
[DE89-012740] N89-27210
CRASHES
OH-58 energy attenuating crew seat feasibility study
[AD-A207506] N89-26829
CRASHWORTHINESS
OH-58 energy attenuating crew seat feasibility study
[AD-A207506] N89-26829
CRAY COMPUTERS
Cray-to-sun prototype
[DE89-013087] N89-27358
CREEP ANALYSIS
Structural reliability and damage tolerance of ceramic composites for high-temperature applications
[PB89-156350] N89-26994
Structural reliability and damage tolerance of ceramic composites for high-temperature applications
[PB89-156368] N89-26995
CREEP PROPERTIES
Observations on the mechanisms of fatigue in eutectic Pb-Sn solder joints
[DE89-000553] N89-26968
High-temperature flaw assessment procedure: A state-of-the-art survey
[DE89-012740] N89-27210
Creep-fatigue assessment methods using elastic analysis results and adjustments
[DE89-011858] N89-27221
CREEP STRENGTH
Method to produce titanium metal matrix composites with improved fracture and creep resistance
[AD-D014111] N89-26911
CREWS
Annual historical report - AMEDD activities
[AD-A208301] N89-27333
CRITICAL TEMPERATURE
Quantum and thermodynamic fluctuations in the degenerate schematic model of the finite temperature random phase approximation
[DE88-706310] N89-27580
CROP GROWTH
Efficiency of N use by wheat as a function of influx and efflux of NO sub 3
[NASA-CR-177534] N89-27346
CROP VIGOR
A center for commercial development of space: Real-time satellite mapping. Remote sensing-based agricultural information expert system
[NASA-CR-185473] N89-27235
CROSS FLOW
A model for transition by attachment-line contamination and an examination of cross-flow instability in 3-D boundary layers
[AERO-REPT-8804] N89-27108
CROSS POLARIZATION
Dynamics of surface bound polymers and coupling agents
[AD-A208747] N89-27020
CROSSLINKING
Synthesis and structural characterization of Pt-Si dimers with unusually short cross-ring silicon-silicon interactions
[AD-A208310] N89-27014
CRYOGENIC COOLING
Combination boundary layer control system for high altitude aircraft
[AD-D014075] N89-26837
CRYOGENIC EQUIPMENT
Design and operation of a horizontal liquid helium flow facility
[DE89-013482] N89-26867
CRYOGENIC FLUID STORAGE
Design and operation of a horizontal liquid helium flow facility
[DE89-013482] N89-26867
CRYOGENIC FLUIDS
Combination boundary layer control system for high altitude aircraft
[AD-D014075] N89-26837
CRYOGENIC MAGNETS
Cryogenic techniques for large superconducting magnets in space
[DE89-013431] N89-27455
CRYOGENIC WIND TUNNELS
The NASA Langley Research Center 0.3-meter transonic cryogenic tunnel T-P/Re-M controller manual
[NASA-CR-181868] N89-26869
CRYOGENICS
Design and operation of a horizontal liquid helium flow facility
[DE89-013482] N89-26867
Cryogenic tensile properties of AA 2090 weldments
[DE89-012979] N89-26971
Liquid helium fluid dynamics studies
[DE89-013124] N89-27036
Production of pure ozone by means of electric discharges for measuring absorption coefficients
[NOTA-INTERNA-913] N89-27042
Thermal enclosures for electronically scanned pressure modules operating in cryogenic environments
[NASA-TM-101635] N89-27151
Cryogenic techniques for large superconducting magnets in space
[DE89-013431] N89-27455
Optical mirror coated with organic superconducting material
[AD-D014047] N89-27499
CRYOSTATS
Cryogenic techniques for large superconducting magnets in space
[DE89-013431] N89-27455
CRYSTAL DEFECTS
Local density theory of heats of formation and short-range order parameters in substitutionally disordered alloys
[DE89-014696] N89-26986
Atomic simulation of crystalline defects in ordered structures
[ETN-89-94807] N89-27571
CRYSTAL DISLOCATIONS
Artificial superlattices
[ETN-89-94889] N89-27551
The response of single crystal and polycrystal nickel to quasistatic and shock deformation
[DE89-011168] N89-27564
CRYSTAL GROWTH
Thermodynamics and high temperature chemistry of the chemical vapor deposition of diamond films
[DE89-013574] N89-26951
Large protein crystallization facility, phase A. Executive summary
[AQ-ES-175/88] N89-27035
Artificial superlattices
[ETN-89-94889] N89-27551
Crystallization of paraxylene with scraped surface heat exchangers
[WTHD-189] N89-27570
CRYSTAL LATTICES
A microstructural investigation of the shear distortions and energetics of motions observed in an aged high damping 53Cu-45Mn-2Al alloy
[AD-A208467] N89-26991
Application of crystal lattice disintegration criteria to compute minimum shock induced reactive conditions in solid explosives and inert materials
[AD-A207557] N89-27025
Nitrogen 15 T1 measurements of semicrystalline nylon 6
[AD-A208481] N89-27575
CRYSTAL OPTICS
Hybrid single crystal optic fibers by embedding
[AD-D013986] N89-27545
CRYSTAL OSCILLATORS
Low noise crystal controlled oscillator
[AD-D014070] N89-27072
CRYSTAL STRUCTURE
Analysis of microstructural development in single crystal welds
[DE89-013537] N89-26973
Polycrystal plasticity as applied to the problem of in-plane anisotropy in rolled cubic metals
[DE89-011181] N89-26983
Natural abundance 15N CP/MAS NMR of solid polyamides: A sensitive technique for examining crystalline composition and conformation in the solid state
[AD-A208563] N89-27019
High-temperature behavior of grain boundaries from embedded atom method molecular dynamics simulation
[DE89-013641] N89-27474
Artificial superlattices
[ETN-89-94889] N89-27551
CRYSTALLIZATION
Supersonics
[AD-A207394] N89-26814
Crystallization of paraxylene with scraped surface heat exchangers
[WTHD-189] N89-27570
The 15N NMR powder spectra of semicrystalline nylon 6
[AD-A208502] N89-27577
CRYSTALLOGRAPHY
Atomic simulation of crystalline defects in ordered structures
[ETN-89-94807] N89-27571
Macromolecular calculations for the XTAL system of crystallographic programs
[AD-A208272] N89-27572
CRYSTALS
Macromolecular calculations for the XTAL system of crystallographic programs
[AD-A208272] N89-27572
Nitrogen 15 T1 measurements of semicrystalline nylon 6
[AD-A208481] N89-27575
A method to calibrate the light response of a high resolution electromagnetic calorimeter with cosmic rays
[NOTA-INTERNA-925] N89-27631
CUBES (MATHEMATICS)
Polycrystal plasticity as applied to the problem of in-plane anisotropy in rolled cubic metals
[DE89-011181] N89-26983
CURING
On processing development for fabrication of fiber reinforced composite, part 2
[NASA-CR-181866] N89-26917
CURRENT DENSITY
A method for generating the J sub c, B, T surface for niobium-alloy superconductors
[DE89-012977] N89-27556
Equilibrium of solar coronal arcades
[AD-A207311] N89-27622
CUTTING
Design, development and evaluation of a doubly rotated AK-cut quartz crystal
[AD-A207209] N89-27549
CYCLOHEXANE
Thermodynamic equilibria in the biphenyl/hydrogen system (the power and limitations of group additivity estimations)
[DE89-000754] N89-26954
CYCLONES
Tropical cyclone report, 1988
[AD-A207206] N89-27303
Synoptic forcing of East Asian cold surges
[AD-A208765] N89-27321
CYCLOTRON RESONANCE DEVICES
Development of theoretical and numerical techniques for achieving stability in gyrotron traveling-wave amplifiers
[AD-A207451] N89-27140

D

DAMAGE
Nonlinear dynamic response of pressurized composite bottles subjected to shock loading
[DE89-010553] N89-26922
Analysis and evaluation of technical data on the photochromic and non-linear optical properties of materials
[AD-A207275] N89-27000
Lightning: Understanding it and protecting systems from its effects
[DE89-012796] N89-27308

DAMPING
Measured damping and modulus of composite cylinders
[DE89-010369] N89-27209
Fate and effects of PAHs in the terrestrial environment: An overview
[DE89-010319] N89-27267

DARK ADAPTATION
Meridian variations in spectral dark adaptation
[AD-A207248] N89-27331

DARK MATTER
Observing primeval galaxies and dark matter with LAIRTS — Large Aperture Infra-Red Telescope System
[AD-A208286] N89-27606

DATA ACQUISITION
High-speed data acquisition for the Princeton University Dynamic Model Track
[NASA-CR-185491] N89-26865
Composites databases for the 1990's
[PB89-180376] N89-26914
Automated immersion testing robotic system: Hardware and software design
[AD-A206755] N89-27201
The 1989 Airborne Arctic Stratospheric Expedition Nimbus-7 TOMS data atlas
[NASA-RP-1227] N89-27302
Navy tethered balloon measurements made during the Fire marine stratocu IFO (Intensive Field Operation)
[AD-A207312] N89-27304
ACP/R3000 processors in data acquisition systems
[DE89-014811] N89-27355
Automatic treatment of natural language in processes in the acquistion of knowledge
[INPE-4737-PRE/1412] N89-27382

DATA BASE MANAGEMENT SYSTEMS
Risk assessment of compressed natural gas-fueled vehicle operations, phase 1
[PB89-188841] N89-27196
Technology Master List data base management system, user's manual
[PB89-177802] N89-27590
Developing a geologic and engineering properties data base with INGRES
[DE89-013520] N89-27593
Management Information Database System
[DE89-014595] N89-27597

DATA BASES
Composites databases for the 1990's
[PB89-180376] N89-26914
Study of subgrid models in incompressible turbulent flow, homogeneous or inhomogeneous
[ONERA-RSF-17/3619-AY-110-A] N89-27123
Meteorological database and synthesis for the Gulf of Mexico
[PB89-178222] N89-27311
Parallel implementation of OPS5 on the encore multiprocessor: Results and analysis
[AD-A207320] N89-27353
Technology Master List data base management system, user's manual
[PB89-177802] N89-27590
User guide for the Data Analysis, Retrieval, and Tabulation System (DARTS): A mainframe computer code for generating cross-tabulation reports
[DE89-012930] N89-27592
Developing a geologic and engineering properties data base with INGRES
[DE89-013520] N89-27593
Common carrier earth station database documentation
[PB89-186050] N89-27595
Management Information Database System
[DE89-014595] N89-27597
Empirical analysis and refinement of expert system knowledge bases
[AD-A206294] N89-27598

DATA LINKS
Capacity of the poisson channel with random noise intensity
[AD-A207226] N89-27447

DATA MANAGEMENT
GEO-EAS (Geostatistical Environmental Assessment Software) user's guide
[PB89-151252] N89-27261

DATA PROCESSING
Natural language processing
[INPE-4449-TDL/314] N89-27366
Hardware C - A language for hardware design
[AD-A207317] N89-27370
Indirect addressing and load balancing for faster solution to Mandelbrot Set on SIMD architectures
[NASA-CR-181847] N89-27390
A virtual zero-time, monolithic systolic sorting array
[DE89-007515] N89-27394
Advanced information processing system: Input/output system services
[NASA-CR-181874] N89-27413
Correlation and analysis between the Kamioka neutrino detector data and the Maryland and Rome gravitational antenna data
[NOTA-INTERNA-916] N89-27488
A hydrid 3 Gs/s, 6-bit digital to analog converter
[DE89-012302] N89-27552

DATA REDUCTION
Space Shuttle Main Engine structural analysis and data reduction/evaluation. Volume 7: High pressure fuel turbo-pump third stage impeller analysis
[NASA-CR-183670] N89-26894
Data traffic reduction schemes for Cholesky factorization on asynchronous multiprocessor systems
[NASA-CR-181863] N89-27349
Offline computing farms
[DE89-013958] N89-27359

DATA SMOOTHING
Local mode smoothing analysis of various two-dimensional incomplete factorization iterative methods
[REPT-88-67] N89-27431

DATA STRUCTURES
A MACSYMA package for the generation and manipulation of Chebyshev series
[DE89-011404] N89-27436

DATA SYSTEMS
ACP/R3000 processors in data acquisition systems
[DE89-014811] N89-27355

DATA TRANSMISSION
Bandwidth efficient coding for error control
[NASA-CR-185836] N89-27062

DAYTIME
Development of a second-generation, video-based luminance mapper for daylighting research
[DE89-000850] N89-27143

DECISION MAKING
Rule-based air combat simulation
[NASA-CR-4160] N89-27393

DECODERS
Evaluation of low data rate voice CODECS for air traffic control applications
[DOT/FAA/CT-TN89/13] N89-27047

DECOMPOSITION
Studies of the fundamental nature of catalytic acidity, sites and intermediates
[DE89-012946] N89-26947
Primary dissociation processes of energetic compounds
[AD-A208312] N89-27033

DEEP SPACE
Deep space LADAR, phase 1
[AD-A207454] N89-27166

DEFECTS
Nanostructure and defect chemistry of relaxor ferro electrics
[AD-A207217] N89-26933
Arcjet cathode phenomena
[NASA-TM-102099] N89-27121
High-temperature flaw assessment procedure: A state-of-the-art survey
[DE89-012740] N89-27210

DEFENSE PROGRAM
Directed energy weapons/en dash/lasers: Ground- and space-based systems
[DE89-012804] N89-27452

DEFLECTION
Scaling effects in the static large deflection response of graphite-epoxy composite beams
[NASA-TM-101619] N89-26843

DEFORMATION
Relaxation response of A533B steel from 25 to 600 C
[DE89-010179] N89-26982
DYNA3D user's manual: (Nonlinear Dynamic Analysis of Structures in Three Dimensions), revision 5
[DE89-014304] N89-27222
Geodetic measurement of deformation in California
[NASA-TM-100732] N89-27279
The response of single crystal and polycrystal nickel to quasistatic and shock deformation
[DE89-011168] N89-27564

DEGRADATION
Erosion of Al and Al/SiC
[DE89-013623] N89-26913
Degradation of Fe-25Cr, Fe-25Cr-20Ni and Fe-25Cr-6Al alloys in H2/H2O/H2S environments at 700 C
[DE89-011873] N89-26967
Breakdown mechanisms of Al2O3, Cr2O3 and SiO2 scales in H2/H2O/H2S environments, volume 1
[DE89-014789] N89-26988

DEGREES OF FREEDOM
Six degrees of freedom micromanipulator
[AD-D014113] N89-27190

DEHYDRATION
Considerations for replacement beverages: Fluid-electrolyte balance and heat illness
[AD-A208342] N89-27335

DEMODULATION
Programmable rate modem utilizing digital signal processing techniques
[NASA-CR-185124] N89-26879
Detection, acquisition and signal demodulation in a communication system with random access
[INPE-4779-RPE/581] N89-27061

DEMODULATORS
Advanced modulation technology development for earth station demodulator applications
[NASA-CR-185126] N89-26880
On capture effect of FM demodulators
[AD-A206479] N89-27066

DEPLETION
Preventing depletion of stratospheric ozone: Implications on future aircraft emissions, revision 1
[DE89-013779] N89-27273

DEPLOYMENT
Hose reel monitor for inflight refueling system
[AD-D014054] N89-26836
Satellite relocation by tether deployment
[NASA-TM-101992] N89-26877

DEPOSITION
Diamondlike carbon protective coatings for optical windows
[NASA-TM-102111] N89-27506
Study of the microstructure of silver films deposited by ion assisted deposition onto aluminum oxide substrates
[DE89-014665] N89-27563

DEPTH
Depth profiles and bulk analysis of semiconductor materials using ICP mass spectroscopy with electrothermal atomization
[AD-A206974] N89-27548

DESIGN ANALYSIS
CFD drag prediction for aerodynamic design
N89-26825
Design considerations of manipulator and feel system characteristics in roll tracking
[NASA-CR-4111] N89-26860
Evaluation of an updated design of an internally lighted wind cone
[DOT/FAA/CT-TN89/45] N89-26868
Satellite attitude control analysis and design using linearizing transformations
[INPE-4772-PRE/1441] N89-26886
Elements of a realistic 17 GHz FEL/TBA design
[DE89-013427] N89-27169
Narrow-angle laser scanning microscope system for linewidth measurements on wafers
[PB89-189344] N89-27174
Thermal evaluation of advanced solar dynamic heat receiver performance
[NASA-CR-185117] N89-27256
Processor control path synthesis: Literature survey and preliminary analysis
[MEMO-INF-88-46] N89-27401

DETECTION
Optical detection and spectroscopy of single molecules in a solid
[AD-A207594] N89-26940
Explosives detection with an ion trap mass spectrometer
[DE89-012510] N89-27029
Techniques for the detection of explosives
[DE89-012570] N89-27030
Some results on nonGaussian signal detection
[AD-A207255] N89-27050
Proposed thin film electronics for a-Si:H PIXEL detector
[DE89-013410] N89-27083
Lightning: Understanding it and protecting systems from its effects
[DE89-012796] N89-27308
Frequency division multiplexing of interferometric sensor arrays
[AD-A208448] N89-27510

On the production and detection of gravitational waves from artificial sources
[NOTA-INTERNA-912] N89-27587
Spectra of crab-like pulsars: A GRO perspective
[DE89-013461] N89-27628

DETECTORS
Explosives detection with an ion trap mass spectrometer
[DE89-012510] N89-27029

DETONABLE GAS MIXTURES
Detonability of hydrocarbon fuels in air
[DE89-008801] N89-26926
Dynamic measurements in combustible and detonable aerosols
[ISL-PU-306/88] N89-26957

DETONATION
Detonability of hydrocarbon fuels in air
[DE89-008801] N89-26926
Detonation of unconfined large scale fuel spray-air clouds
[DE89-006510] N89-26955
Application of crystal lattice disintegration criteria to compute minimum shock induced reactive conditions in solid explosives and inert materials
[AD-A207557] N89-27025
Thin pulse shock initiation characterization of extrusion-cast explosives: Revision
[DE89-008029] N89-27027

DETONATION WAVES
Demonstration of oblique detonation wave for hypersonic propulsion
[AD-A208268] N89-26856

DETONATORS
Standardized piezoelectric polymer (PVDF) gauge for detonator response measurement
[DE89-010437] N89-27144

DEUTERIUM
Dynamics of surface bound polymers and coupling agents
[AD-A208747] N89-27020
Z-pinch experiments on Saturn at 30 TW
[DE89-013497] N89-27523

DEVELOPING NATIONS
An assessment of information demands for remote sensing and Geographic Information System technologies
[PB89-159313] N89-27233

DEW
Fog, cloud, and dew chemistry
[PB89-187314] N89-27317

DEW POINT
An investigation into the gravity current aspects of a cold air outbreak using variational analysis techniques
[AD-A208464] N89-27295

DIAMONDS
Thermodynamics and high temperature chemistry of the chemical vapor deposition of diamond films
[DE89-013574] N89-26951

DIAPHRAGMS (MECHANICS)
A multidriver shock tube model of a large blast simulator
[AD-A208324] N89-26871

DICTIONARIES
Composites databases for the 1990's
[PB89-180376] N89-26914

DIELECTRIC PROPERTIES
Nanostructure and defect chemistry of relaxor ferro electrics
[AD-A207217] N89-26933
Investigations of dielectric properties of some frozen materials using cross-borehole radiowave pulse transmissions
[AD-A207302] N89-27285

DIELECTRICS
Measurements of complex permittivity of microwave substrates in the 20 to 300 K temperature range from 26.5 to 40.0 GHz
[NASA-TM-102123] N89-27038
Solutions of differential equations with regular coefficients by the methods of Richmond and Runge-Kutta
[NASA-TM-101609] N89-27060
Solid state gas pressure sensor
[AD-D014105] N89-27139

DIESEL ENGINES
Feasibility demonstration of the Thermal Ignition Combustion System (TICS) for high pressure natural gas injected engine
[PB89-178792] N89-26944
Combustion characteristics of dry coal-powder-fueled adiabatic diesel engine
[DE89-000978] N89-27197

DIFFERENTIAL EQUATIONS
Solutions of differential equations with regular coefficients by the methods of Richmond and Runge-Kutta
[NASA-TM-101609] N89-27060
Accuracy increase in waveform Gauss Seidel
[DE89-014812] N89-27437
Differential stochastic equations
[PREPRINT-635] N89-27449

DIFFUSION
Loss of grain boundary segregant during ion milling
[DE89-007835] N89-26979
Finite control volume modeling of laminar and turbulent flow of air in an enclosure
[DE89-009334] N89-27120
Aerial smoke plume observations and surface layer turbulence measurements. Part 1: Project WIND. Phase 4: Dispersion study
[AD-A207370] N89-27305
Stochasticity and symmetry of the standard map
[IPPJ-910] N89-27528
Diffusion in high-T sub c superconductors
[DE89-009792] N89-27546

DIFFUSION FLAMES
Mixing and combustion of pulsed gas jets
[PB89-155550] N89-26929

DIGITAL COMPUTERS
Hybrid structures for simple computer performance estimates
[PB89-189161] N89-27356
Hardware C - A language for hardware design
[AD-A207317] N89-27370

DIGITAL DATA
Applications of numerical models for elevation and integration with digital images
[INPE-4776-PRE/1445] N89-27392

DIGITAL ELECTRONICS
An expert system in C for computer-aided digital circuit design
[AD-A207518] N89-27075
An expert system for fault diagnosis in digital circuits
[INPE-4743-PRE/1417] N89-27085

DIGITAL FILTERS
Development of a system model and Least Mean Square (LMS) filter for the Naval Postgraduate School (NPS) Infrared Search and Target Designation System (IRSTD)
[AD-A208536] N89-27068
Algorithms for computer aided design of digital filters
[AD-A208485] N89-27410

DIGITAL SYSTEMS
Window generator
[AD-D014068] N89-27048

DIGITAL TECHNIQUES
Programmable rate modem utilizing digital signal processing techniques
[NASA-CR-185124] N89-26879
A new state reconstructor for digital controls systems using weighted-average measurements
[NASA-TP-2936] N89-27039
Bandwidth efficient coding for error control
[NASA-CR-185836] N89-27062
Quantitative three-dimensional structural techniques
[DE89-010879] N89-27238
Joint CGS-AOML (Charting and Geodetic Service-Atlantic Oceanographic and Meteorological Laboratory) acoustical bottom echo-formation research. 2: Field experiment results and recommendations for echo-sounder design
[PB89-152417] N89-27322

DIGITAL TO ANALOG CONVERTERS
A hydrid 3 Gs/s, 6-bit digital to analog converter
[DE89-012302] N89-27552

DIMENSIONAL ANALYSIS
An algorithm for symbolic dimensional analysis
[DE89-010409] N89-27363

DIMERS
Synthesis and structural characterization of Pt-Si dimers with unusually short cross-ring silicon-silicon interactions
[AD-A208310] N89-27014

DIODES
Transverse pumping with diode lasers
[AD-A207261] N89-27165

DIOXIDES
Selective nitrations: Laser-induced nitrations
[AD-A207406] N89-27024

DIPOLE MOMENTS
Fluids, gels and glasses under extreme conditions of pressure and temperature
[AD-A205292] N89-26927
Nonresonant interaction of a three-level atom with cavity fields. Part 4: Atomic dipole moment and squeezing effects
[AD-A206788] N89-27470

DISEASES
Short course on cardiopulmonary aspects of aerospace medicine
[AGARD-R-758-ADD] N89-27330
Considerations for replacement beverages: Fluid-electrolyte balance and heat illness
[AD-A208342] N89-27335

DISINTEGRATION
Application of crystal lattice disintegration criteria to compute minimum shock induced reactive conditions in solid explosives and inert materials
[AD-A207557] N89-27025

DISPERSING
Dispersion strengthened aluminum-base alloy
[AD-D014044] N89-26959
Aerial smoke plume observations and surface layer turbulence measurements. Part 1: Project WIND. Phase 4: Dispersion study
[AD-A207370] N89-27305

DISPLACEMENT
HRR field in an aluminum SEN specimen
[AD-A207578] N89-26963
OTVE turbopump condition monitoring, task E.5
[NASA-CR-182274] N89-27204

DISPLAY DEVICES
Aircraft color displays: Chromaticity and luminance requirements
[AD-A206786] N89-26828
F-15E EADI (Electronic Attitude Director Indicator) evaluation: A comparison of three formats
[AD-A206809] N89-26846
New strategies for display devices based on 2-6 materials
[AD-A208288] N89-27573

DISSOCIATION
Primary dissociation processes of energetic compounds
[AD-A208312] N89-27033

DISTORTION
A microstructural investigation of the shear distortions and energetics of motions observed in an aged high damping 53Cu-45Mn-2Al alloy
[AD-A208467] N89-26991
Variable area manifolds for ring mirror heat exchangers
[AD-D014050] N89-27163
Inelastic buckling of channel columns in the distortional mode
[PB89-156053] N89-27207
Optical mirror coated with organic superconducting material
[AD-D014047] N89-27499

DISTRIBUTED PARAMETER SYSTEMS
Control of flexible structures
[AD-A207520] N89-26883
Modeling and computational algorithms for parameter estimation and optimal control of aeroelastic systems and large flexible structures
[AD-A208274] N89-27404

DISTRIBUTED PROCESSING
Fault tolerant software technology for distributed computer systems
[AD-A208329] N89-27405
Northeast Artificial Intelligence Consortium annual report 1987. Volume 3: Distributed artificial intelligence for communications network management
[AD-A208379] N89-27419

DISTRIBUTION (PROPERTY)
Competitive management of distributed shared memory
[AD-A207322] N89-27372

DIURNAL VARIATIONS
Concentrations and patterns of photochemical oxidants in the United States
[PB89-136683] N89-27258
Low relative humidity in the atmosphere
[AD-A207558] N89-27307

DIVING (UNDERWATER)
Submarine air quality: Monitoring the air in submarines. Health effects in divers of breathing submarine air under hyperbaric conditions
[PB89-174213] N89-27345

DOCUMENT STORAGE
A parallel version of the Boyer-Moore prover
[AD-A207190] N89-27351

DOCUMENTS
Interactions between the National Institute of Standards and Technology and the American Society of Mechanical Engineers
[PB89-172563] N89-27182

DOORS
Superplastic forming of aluminum, task C
[AD-A207282] N89-26962

DOPPLER RADAR
Procedural guide for the retrieval of dropsize distributions in water clouds from ground-based clear-air-sensing Doppler radar observations
[PB89-152474] N89-27300
DRAG
Experimental program for real gas flow code validation at NASA Ames Research Center
[NASA-TM-100093] N89-26816
DRAG REDUCTION
Drag prediction and analysis from CFD state-of-the-art in Germany N89-26819
Combination boundary layer control system for high altitude aircraft
[AD-D014075] N89-26837
DRIFT RATE
Expendable air vehicles/high altitude balloon technology
[AD-A206972] N89-26813
DRILLING
Drilling operations plan for the Magma Energy Exploratory Well
[DE89-010037] N89-27240
DROP SIZE
Design and characterization of large-drop generators for viscous, Newtonian, and non-Newtonian liquids
[AD-A208330] N89-27133
Procedural guide for the retrieval of dropsize distributions in water clouds from ground-based clear-air-sensing Doppler radar observations
[PB89-152474] N89-27300
DROPS (LIQUIDS)
Transient cooling of a hot surface by droplets evaporation
[PB89-161897] N89-27100
DUAL SPIN SPACECRAFT
Study of jitter on the attitude motion of a spin stabilized satellite with two flexible solar panels
[INPE-4744-PRE/1418] N89-26884
DUCTILITY
Effects of high thermal and high fast fluences on the mechanical properties of type 6061 aluminum in the HFBR
[DE89-012636] N89-26970
Fracture behavior of a pressure vessel steel in the ductile-to-brittle transition region
[PB89-189195] N89-26977
Quantitative thin film X-ray microanalysis of Nb modified Ti3Al
[DE89-009946] N89-26981
Effect of heating rate to test temperature on superplastic response in an Al-6 percent Mg-1 percent Li-0.2 percent Zr alloy
[AD-A206462] N89-26990
DUCTS
Calculation of turbulence-driven secondary motion in ducts with arbitrary cross section
[NASA-TM-102142] N89-27115
DUMP COMBUSTORS
Investigation of the transient fuel preburner manifold and combustor
[NASA-CR-183715] N89-26900
DURABILITY
Advanced durability analysis. Volume 2: Analytical predictions, test results and analytical correlations
[AD-A207215] N89-26838
DYES
Laser dyes derived from bimanes
[AD-D013994] N89-27160
DYNAMIC CHARACTERISTICS
Acta Aeronautica et Astronautica Sinica, Volume 8, Number 12, December 1987 (selected articles)
[AD-A206782] N89-26807
Lagrangian turbulence near walls: Structures and mixing in admissible model flows
[AD-A208466] N89-27135
Stability and dynamic analysis of a slender column with curved longitudinal stiffeners
[NASA-TM-101636] N89-27215
Yaw dynamics of horizontal axis wind turbines
[DE89-000888] N89-27249
Dynamics of an M-level atom interacting with gravity fields. 1: Effects of the level number on quantum collapse and revival
[AD-A207278] N89-27579
DYNAMIC CONTROL
Computational methods for nonlinear dynamic problems in solid and structural mechanics: Progress in the theory and modeling of friction and in the control of dynamical systems with frictional forces
[AD-A208763] N89-27227
DYNAMIC LOADS
Stability of a rigid rotor supported on oil-film journal bearings under dynamic load
[NASA-TM-102309] N89-27114
DYNAMIC MODELS
Fluids, gels and glasses under extreme conditions of pressure and temperature
[AD-A205292] N89-26927
Dynamic simulation of a molten-salt solar receiver
[DE89-010556] N89-27244
DYNAMIC PRESSURE
Method for experimental determination of flutter speed by parameter identification
[NASA-TP-2923] N89-26844
DYNAMIC RESPONSE
Acta Aeronautica et Astronautica Sinica, Volume 8, Number 12, December 1987 (selected articles)
[AD-A206782] N89-26807
Space Shuttle Main Engine structural analysis and data reduction/evaluation. Volume 7: High pressure fuel turbo-pump third stage impeller analysis
[NASA-CR-183670] N89-26894
Tailoring of composite links for optimal damped elasto-dynamic performance
[NASA-TM-102094] N89-26912
Nonlinear dynamic response of pressurized composite bottles subjected to shock loading
[DE89-010553] N89-26922
DYNAMIC STABILITY
Attractive levitation for high-speed ground transport with large guideway clearance and alternating-gradient stabilization
[DE89-013640] N89-27195
DYNAMIC STRUCTURAL ANALYSIS
Nonlinear dynamic response of pressurized composite bottles subjected to shock loading
[DE89-010553] N89-26922
Dynamic mechanical investigations of LLDPE/PC blends
[NPL-DMA(A)-177] N89-27010
Synthesis and structural characterization of Pt-Si dimers with unusually short cross-ring silicon-silicon interactions
[AD-A208310] N89-27014
Measurement of the bending wave power flow by the structural intensity technique
[VTT-583] N89-27129
Dynamic analysis of flexible mechanisms by a combined transfer matrix finite element method
[PB89-160865] N89-27181
DYNA3D user's manual: (Nonlinear Dynamic Analysis of Structures in Three Dimensions), revision 5
[DE89-014304] N89-27222
DYNAMIC TESTS
OH-58 energy attenuating crew seat feasibility study
[AD-A207506] N89-26829
DYNAMICAL SYSTEMS
Lagrangian turbulence near walls: Structures and mixing in admissible model flows
[AD-A208466] N89-27135
Computational methods for nonlinear dynamic problems in solid and structural mechanics: Progress in the theory and modeling of friction and in the control of dynamical systems with frictional forces
[AD-A208763] N89-27227
The dynamical behavior of classifier systems
[DE89-009407] N89-27383
A symbolic generator of state equations for modeling of dynamic systems based on the electrical network analog paradigm
[DE89-013763] N89-27397
Accuracy increase in waveform Gauss Seidel
[DE89-014812] N89-27437
DYNAMO THEORY
Mercury's magnetic field: Implications on the inner composition of the planet
[NOTA-INTERNA-926] N89-27620

E

EARTH ATMOSPHERE
A computer program for simulating the atmospheric dispersion of UF6 and other reactive gases having positive, neutral, or negative buoyancy
[DE89-012734] N89-27269
Computational techniques in gamma-ray Skyshine analysis
[DE89-010156] N89-27282
Navy tethered balloon measurements made during the Fire marine stratocu IFO (Intensive Field Operation)
[AD-A207312] N89-27304
EARTH CORE
Application of the theory of wave propagation through random media to phase and amplitude fluctuations of seismic P-waves
[AD-A207207] N89-27284
EARTH IONOSPHERE
Space Environment Laboratory
[PB89-159602] N89-27607
EARTH MAGNETOSPHERE
Space Environment Laboratory
[PB89-159602] N89-27607
EARTH MANTLE
Application of the theory of wave propagation through random media to phase and amplitude fluctuations of seismic P-waves
[AD-A207207] N89-27284
EARTH OBSERVATIONS (FROM SPACE)
Space research in the Federal Republic of Germany (FRG), 1986 and 1987
[ETN-89-94427] N89-26874
Study for an advanced civil earth remote sensing system. Volume 1: Executive summary
[PB89-163257] N89-27231
Study for an advanced civil earth remote sensing system. Volume 2: Market and financial assessment
[PB89-163265] N89-27232
Satellite image processing using symbolic structures of reduced vision conditions
[INPE-4638-TDL/337] N89-27367
EARTH OBSERVING SYSTEM (EOS)
Altimetric system: Earth observing system. Volume 2h: Panel report
[NASA-TM-89722] N89-27229
EARTH PLANETARY STRUCTURE
Investigations on local seismic phases and evaluation of body waves magnitude
[AD-A206633] N89-27283
EARTH SURFACE
Attitude angle effects on Nimbus-7 Scanning Multichannel Microwave Radiometer radiances and geophysical parameter retrievals
[NASA-TM-4132] N89-27289
EARTHQUAKES
Geodetic measurement of deformation in California
[NASA-TM-100732] N89-27279
ECHOES
Joint CGS-AOML (Charting and Geodetic Service-Atlantic Oceanographic and Meteorological Laboratory) acoustical bottom echo-formation research. 2: Field experiment results and recommendations for echo-sounder design
[PB89-152417] N89-27322
ECONOMIC ANALYSIS
Superplastic forming of aluminum, task C
[AD-A207282] N89-26962
Study for an advanced civil earth remote sensing system. Volume 1: Executive summary
[PB89-163257] N89-27231
Study for an advanced civil earth remote sensing system. Volume 2: Market and financial assessment
[PB89-163265] N89-27232
On the economic prospects of nuclear fusion with tokamaks
[IPP-6/271] N89-27539
EDGES
Research in knowledge-based vision techniques for the autonomous land vehicle program
[AD-A208546] N89-26834
HRR field in an aluminum SEN specimen
[AD-A207578] N89-26963
EDUCATION
On-line computer utilization to understand some physical processes (example: Pendulum motion)
[NOTA-INTERNA-927] N89-27360
EFFICIENCY
Efficiency of N use by wheat as a function of influx and efflux of NO sub 3
[NASA-CR-177534] N89-27346
EINSTEIN EQUATIONS
On the integrability of the Ernst equation
[PREPRINT-606] N89-27584
EL NINO
Tropical circulation and the associated precipitation anomalies in two years of contrast
[INPE-4715-PRE/1395] N89-27315
ELASTIC BODIES
Dynamic analysis of flexible mechanisms by a combined transfer matrix finite element method
[PB89-160865] N89-27181
ELASTIC BUCKLING
On the multiplicity and symmetries of the bifurcation branching point in the square clamped plate
[PREPRINT-604] N89-27224
ELASTIC PROPERTIES
Dynamic analysis of flexible mechanisms by a combined transfer matrix finite element method
[PB89-160865] N89-27181
Weld stresses beyond elastic limit: Materials discontinuity
[NASA-TP-2935] N89-27214
Creep-fatigue assessment methods using elastic analysis results and adjustments
[DE89-011858] N89-27221

ELASTODYNAMICS
Tailoring of composite links for optimal damped elasto-dynamic performance
[NASA-TM-102094] N89-26912
ELASTOMERS
Thermal and mechanical properties of polyurethane-diacetylene segmented copolymers. Part 1: Molecular weight and annealing effects
[AD-A208753] N89-27022
Sensors for in situ monitoring of elastic properties
[DE89-012795] N89-27145
ELECTRIC BATTERIES
New battery materials
[DE89-012845] N89-27081
Advanced calcium-thionyl chloride high-power battery
[AD-A207612] N89-27247
ELECTRIC CONNECTORS
Easily testable PLA-based finite state machines
[AD-A208371] N89-27098
ELECTRIC CURRENT
A symbolic generator of state equations for modeling of dynamic systems based on the electrical network analog paradigm
[DE89-013763] N89-27397
ELECTRIC DISCHARGES
Production of pure ozone by means of electric discharges for measuring absorption coefficients
[NOTA-INTERNA-913] N89-27042
Computer code prediction of picosecond voltage switching and TEM wave generation in air gas avalanche switches
[DE89-013778] N89-27084
ELECTRIC FIELDS
Solutions of differential equations with regular coefficients by the methods of Richmond and Runge-Kutta
[NASA-TM-101609] N89-27060
Improved core insulation schemes for multi-terawatt magnetic switches
[DE89-013814] N89-27093
Static periodic field device for free electron laser
[AD-D014125] N89-27168
Ionospheric plasma escape by high-altitude electric fields: Magnetic moment pumping
[IRF-PREPRINT-111] N89-27542
New strategies for display devices based on 2-6 materials
[AD-A208288] N89-27573
ELECTRIC MOTORS
Sun synchronous solar refrigeration
[DE89-011375] N89-27245
ELECTRIC NETWORKS
A symbolic generator of state equations for modeling of dynamic systems based on the electrical network analog paradigm
[DE89-013763] N89-27397
ELECTRIC POWER SUPPLIES
Photovoltaic module on-orbit assembly for Space Station Freedom
[NASA-TM-102297] N89-26887
ELECTRIC POWER TRANSMISSION
On transformer modeling. A physically based three-phase transformer model for the study of low frequency phenomena in electrical power systems
[ETN-89-94801] N89-27095
ELECTRIC PROPULSION
Hybrid electric chemical propulsion
[AD-A207584] N89-26898
Electric propulsion options for 10 kW class earth space missions
[NASA-TM-102337] N89-26906
ELECTRICAL ENGINEERING
Emerging technologies in electronics and their measurement needs
[PB89-189245] N89-27078
Center for Electronics and Electrical Engineering Technical Progress Bulletin covering center programs, October to December 1988 with 1989 CEEE events calender
[PB89-193270] N89-27087
ELECTRICAL GROUNDING
Lightning: Understanding it and protecting systems from its effects
[DE89-012796] N89-27308
ELECTRICAL INSULATION
Improved core insulation schemes for multi-terawatt magnetic switches
[DE89-013814] N89-27093
ELECTRICAL MEASUREMENT
National Engineering Laboratory's 1989 report to the National Research Council's Board on Assessment of NIST (National Institute of Standards and Technology) programs
[PB89-189294] N89-27602
ELECTRICAL PROPERTIES
Control surface dual redundant servomechanism
[AD-D014058] N89-26857
Magnetic and electrical properties of sandwich-like lanthanide phthalocyanines
[AD-A208411] N89-26958
Theory of aggregate defects in silicon
[AD-A207273] N89-26999
Six degrees of freedom micromanipulator
[AD-D014113] N89-27190
Two-photon absorption characterization of HgCdTe
[AD-A207198] N89-27471
MeV implantation studies in LPE-grown GaAs and InP
[AD-A207220] N89-27550
High-frequency cavity applications and measurements of high-temperature superconductors
[DE89-013467] N89-27560
Thin film preparation and single film device fabrication in the Tl-Ca-Ba-Cu-O HTS system
[DE89-013560] N89-27561
Recent improvements in bulk properties of ceramic superconductors
[DE89-013626] N89-27562
ELECTRICAL RESISTIVITY
Tests of low resistivity electrodeless streamer tubes
[NOTA-INTERNA-922] N89-27158
Advanced calcium-thionyl chloride high-power battery
[AD-A207612] N89-27247
ELECTRO-OPTICS
Analysis and evaluation of technical data on the photochromic and non-linear optical properties of materials
[AD-A207275] N89-27000
Polarization matrices of lithium niobate
[AD-A207231] N89-27462
Integrated silicon color sensors
[ETN-89-94800] N89-27509
New strategies for display devices based on 2-6 materials
[AD-A208288] N89-27573
ELECTROACOUSTIC WAVES
Measurement of the bending wave power flow by the structural intensity technique
[VTT-583] N89-27129
ELECTROCHEMISTRY
Surface plasmon study of monolayer-bilayer transition in poly-4-BCMU and poly-3-BCMU polydiacetylene Langmuir-Blodgett films
[AD-A207404] N89-26938
Electrochemical transport of manganese between the flux and the weld metal in submerged arc welding
[DE89-012419] N89-27193
Electrochemical reactions in submerged arc welding with SiO2-CaO-CaF2 fluxes with high and low silica contents
[DE89-012421] N89-27194
Advanced calcium-thionyl chloride high-power battery
[AD-A207612] N89-27247
Electrochemical evaluation of new fluorosulfonic and fluorophosphonic acids as fuel cell electrolytes
[DE89-012840] N89-27254
New strategies for display devices based on 2-6 materials
[AD-A208288] N89-27573
ELECTRODES
New battery materials
[DE89-012845] N89-27081
ELECTRODYNAMICS
Attractive levitation for high-speed ground transport with large guideway clearance and alternating-gradient stabilization
[DE89-013640] N89-27195
ELECTROHYDRODYNAMICS
Electrohydrodynamically driven, large-area liquid metal ion source for inertial confinement fusion
[DE89-012665] N89-27530
ELECTROLUMINESCENCE
New strategies for display devices based on 2-6 materials
[AD-A208288] N89-27573
ELECTROLYSIS
High temperature solar electrothermal processing
[AD-A207555] N89-27246
ELECTROLYTE METABOLISM
Considerations for replacement beverages: Fluid-electrolyte balance and heat illness
[AD-A208342] N89-27335
Effectiveness and acceptability of nutrient solutions in enhancing fluid intake in the heat
[AD-A208428] N89-27337
ELECTROLYTES
New battery materials
[DE89-012845] N89-27081
Synthesis of novel fluorinated phosphonic and phosphinic acid electrolytes for phosphoric acid fuel cells
[PB89-194120] N89-27086
ELECTROLYTIC CELLS
Advanced calcium-thionyl chloride high-power battery
[AD-A207612] N89-27247
Electrochemical evaluation of new fluorosulfonic and fluorophosphonic acids as fuel cell electrolytes
[DE89-012840] N89-27254
Electrochemical evaluation of new fluorosulfonic and fluorophosphonic acids as fuel cell electrolytes
[DE89-013391] N89-27255
ELECTROMAGNETIC ABSORPTION
Dispersed and periodic microstructures for magnetic and infrared absorbers
[AD-A207428] N89-27053
Two-photon absorption characterization of HgCdTe
[AD-A207198] N89-27471
ELECTROMAGNETIC ACCELERATION
Wideband electromagnetic damping of vibrating structures
[AD-D014069] N89-27208
ELECTROMAGNETIC COUPLING
Evidence for phonon-mediated coupling in superconducting Ba sub 0.6 K sub 0.4 BiO3
[DE89-014642] N89-27568
ELECTROMAGNETIC FIELDS
Model-based parameter estimation in electromagnetic computer modeling
[AD-A207399] N89-27052
A finite element method for solving electromagnetic scattering problems
[DE89-013496] N89-27059
ELECTROMAGNETIC INTERFERENCE
MM and T for linear resonant cooler, volume 2
[AD-A207236] N89-27073
Center for Electronics and Electrical Engineering Technical Progress Bulletin covering center programs, October to December 1988 with 1989 CEEE events calender
[PB89-193270] N89-27087
ELECTROMAGNETIC PROPERTIES
Dispersed and periodic microstructures for magnetic and infrared absorbers
[AD-A207428] N89-27053
ELECTROMAGNETIC PULSES
The effects of steep-front, short-duration impulses on power distribution components
[DE89-012336] N89-27091
ELECTROMAGNETIC RADIATION
Model-based parameter estimation in electromagnetic computer modeling
[AD-A207399] N89-27052
ELECTROMAGNETIC SCATTERING
A finite element method for solving electromagnetic scattering problems
[DE89-013496] N89-27059
ELECTROMAGNETIC SHIELDING
Electromagnetic pulse rotary seal
[AD-D014080] N89-27187
ELECTROMAGNETIC WAVE TRANSMISSION
Radiation from waves guided by nonuniform active surfaces
[DE89-012286] N89-27057
Atmospheric propagation issues relevant to optical communications
[NASA-CR-185718] N89-27281
ELECTROMAGNETISM
The 14th Convention on Radio Science, Finnish National Committee of URSI held in Otaniemi (Finland) on October 17-18, 1988: Abstracts of papers
[PB89-145767] N89-27044
Complex vectors and dyadics for electromagnetists
[PB89-146443] N89-27045
Electromagnetic pulse rotary seal
[AD-D014080] N89-27187
ELECTROMECHANICAL DEVICES
Polarization matrices of lithium niobate
[AD-A207231] N89-27462
ELECTRON BEAMS
Advanced electron beam evaporation
[ETN-89-94799] N89-27495
Experimental measurement of nonlinear plasma wake-fields
[DE89-014636] N89-27525
ELECTRON GAS
Computer code prediction of picosecond voltage switching and TEM wave generation in air gas avalanche switches
[DE89-013778] N89-27084
Momentum distributions: An overview
[DE89-012617] N89-27453
ELECTRON GUNS
Proceedings of the Switched Power Workshop: Power Supply Working Group
[DE89-012293] N89-27077

ELECTRON IMPACT
Electron-impact ionization time-of-flight mass spectrometer for molecular beams
[AD-A207585] N89-27141
ELECTRON MICROSCOPY
Cross-sectional TEM (Transmission Electron Microscopy) studies of Cr films deposited by ion-assisted deposition and physical vapor deposition
[DE89-014643] N89-26985
An approach to accurate X-ray mask measurements in a scanning electron microscope
[PB89-172555] N89-27137
ELECTRON PHONON INTERACTIONS
Evidence for phonon-mediated coupling in superconducting Ba sub 0.6 K sub 0.4 BiO3
[DE89-014642] N89-27568
ELECTRON SCATTERING
Search for the inclusive production of J/psi in e(+)e(-) collisions using PLUTO data
[NOTA-INTERNA-923] N89-27484
ELECTRON SPECTROSCOPY
An Auger sputter profiling study of nitrogen and oxygen ion implantation in two titanium alloys
[DE89-014734] N89-26987
ELECTRON TRANSFER
Multiple-electron processes in fast ion-atom collisions
[DE89-012982] N89-27475
ELECTRONIC CONTROL
Back-up control system for f101 engine and its derivatives
[AD-D014051] N89-26848
ELECTRONIC EQUIPMENT
Emerging technologies in electronics and their measurement needs
[PB89-189245] N89-27078
Thermal enclosures for electronically scanned pressure modules operating in cryogenic environments
[NASA-TM-101635] N89-27151
Electronic information delivery at the job site
[DE89-009726] N89-27350
Shield optimization program. Part 1: Executive summary
[DE89-013335] N89-27476
ELECTRONIC SPECTRA
Electron-impact ionization time-of-flight mass spectrometer for molecular beams
[AD-A207585] N89-27141
ELECTRONIC TRANSDUCERS
JTECH (Japanese Technology Evaluation Program) panel report on advanced sensors in Japan
[PB89-158760] N89-27136
ELEMENTARY PARTICLE INTERACTIONS
Activities of the Werner-Heisenberg Institute of Physics
[ISSN-0173-6256] N89-27481
ELEMENTARY PARTICLES
Activities of the Werner-Heisenberg Institute of Physics
[ISSN-0173-6256] N89-27481
ELEMENTS
A preliminary report on X-ray photoabsorption coefficients and atomic scattering factors for 92 elements in the 10-10,000 eV region
[DE89-013392] N89-26950
ELEVATION
Applications of numerical models for elevation and integration with digital images
[INPE-4776-PRE/1445] N89-27392
ELLIPSES
ELLIPSE user's manual and program reference
[DE89-014575] N89-27398
ELLIPSOMETERS
The structure of self-assembled monolayers of alkylsiloxanes on silicon: A comparison of results from ellipsometry and low-angle X-ray reflectivity
[AD-A208341] N89-27016
ELLIPTIC DIFFERENTIAL EQUATIONS
An approach for constructing families of homogenized equations for periodic media. 1: An integral representation and its consequences
[AD-A207572] N89-27427
EMBEDDED COMPUTER SYSTEMS
Fault tolerant software technology for distributed computer systems
[AD-A208329] N89-27405
A dynamic scheduler for a computer aided prototyping system
[AD-A208389] N89-27407
EMBEDDING
A language translator for a computer aided rapid prototyping system
[AD-A208358] N89-27406
Hybrid single crystal optic fibers by embedding
[AD-D013986] N89-27545
EMBRITTLEMENT
Cryogenic tensile properties of AA 2090 weldments
[DE89-012979] N89-26971
An experimental study of the effect of stainless steel cladding on the structural integrity of flawed steel plates in bending
[DE89-008735] N89-26980
The use of field indentation microprobe in measuring mechanical properties of welds
[DE89-013548] N89-27211
EMISSION SPECTRA
Comparison of spectral data gathered from a laboratory spectrometer and TM images with and without shadow correction
[DE89-010877] N89-27237
Commentary on interstellar matter associated with 18 open clusters
[NASA-RP-1229] N89-27612
ENCLOSURE
Finite control volume modeling of laminar and turbulent flow of air in an enclosure
[DE89-009334] N89-27120
ENCLOSURES
Thermal enclosures for electronically scanned pressure modules operating in cryogenic environments
[NASA-TM-101635] N89-27151
ENERGY ABSORPTION
OH-58 energy attenuating crew seat feasibility study
[AD-A207506] N89-26829
ENERGY CONSERVATION
Proceedings of the Energy Efficiency and Structural Change: Implications for the Greenhouse Problem Workshop
[DE89-012852] N89-27274
ENERGY CONSUMPTION
Refrigerator-freezer energy testing with alternative refrigerants
[DE89-013543] N89-27037
Proceedings of the Energy Efficiency and Structural Change: Implications for the Greenhouse Problem Workshop
[DE89-012852] N89-27274
ENERGY CONVERSION EFFICIENCY
Proceedings of the Energy Efficiency and Structural Change: Implications for the Greenhouse Problem Workshop
[DE89-012852] N89-27274
ENERGY DISSIPATION
Passive optical losses in laser glass
[DE89-013764] N89-27172
Dynamics of decaying two-dimensional magnetohydrodynamic turbulence
[IPP-6/279] N89-27541
ENERGY GAPS (SOLID STATE)
Two-photon absorption characterization of HgCdTe
[AD-A207198] N89-27471
ENERGY LEVELS
Injuries to seat occupants of light airplanes
[AD-A207579] N89-26830
Nuclear fragmentation energy and momentum transfer distributions in relativistic heavy-ion collisions
[NASA-CR-185501] N89-27477
Radio frequency plasma generator
[AD-D013990] N89-27514
Study of atomic physics and population inversions with plasma focus
[DE89-014282] N89-27532
ENERGY POLICY
Pacing the US magnetic fusion program
[DE89-012959] N89-27519
ENERGY TECHNOLOGY
Verification analysis of the Toroidal Accelerator Rotor Platform wind energy conversion system
[PB89-162069] N89-27241
Ocean Energy Program summary. Volume 2: Research summaries, fiscal year 1988
[DE89-000859] N89-27248
Wind power: Today's energy option
[DE89-000876] N89-27253
ENERGY TRANSFER
Differential forms of Euler's turbo-machinery equation
[AD-A207279] N89-27426
Beam-gas background rejection in L3 first level energy transfer
[NOTA-INTERNA-919] N89-27496
ENGINE DESIGN
Measurement uncertainty within the Uniform Engine Test Programme
[AGARD-AG-307] N89-26854
High performance intercooled and recuperated gas turbine
[PB89-152284] N89-27178
Self-locking outer air seal with full backside cooling
[AD-D013975] N89-27179
ENGINE FAILURE
Statistics on aircraft gas turbine engine rotor failures that occurred in US commercial aviation during 1983
[AD-A207592] N89-26851
ENGINE NOISE
KC-135R rumble investigation
[AD-A207532] N89-27464
ENGINE TESTS
Measurement uncertainty within the Uniform Engine Test Programme
[AGARD-AG-307] N89-26854
ENGINEERING DRAWINGS
Advanced coal-fueled gas turbine systems, volume 2
[DE89-000954] N89-27183
ENGINES
Risk assessment of compressed natural gas-fueled vehicle operations, phase 1
[PB89-188541] N89-27196
ENGLISH LANGUAGE
Research in knowledge delivery
[AD-A208327] N89-27599
ENTHALPY
Differential forms of Euler's turbo-machinery equation
[AD-A207279] N89-27426
ENTROPY
Equilibrium of solar coronal arcades
[AD-A207311] N89-27622
ENVIRONMENT EFFECTS
Assessing the sensitivity of high altitude New Mexican wilderness lakes to acidic precipitation and trace metal contamination
[PB89-148456] N89-27262
Global environmental effects of impact-generated aerosols: Results from a general circulation model, revision 1
[DE89-014179] N89-27276
ROUTEMAP model for predicting noise exposure from aircraft operations on Military Training Routes
[AD-A203849] N89-27459
ENVIRONMENT MANAGEMENT
GEO-EAS (Geostatistical Environmental Assessment Software) user's guide
[PB89-151252] N89-27261
ENVIRONMENT POLLUTION
Analytical procedures for environmental quality control, volume 1
[PB89-158604] N89-27266
ENVIRONMENT PROTECTION
Annual historical report - AMEDD activities
[AD-A208301] N89-27333
ENVIRONMENTAL CHEMISTRY
Assessing the sensitivity of high altitude New Mexican wilderness lakes to acidic precipitation and trace metal contamination
[PB89-148456] N89-27262
Analytical procedures for environmental quality control, volume 1
[PB89-158604] N89-27266
ENVIRONMENTAL ENGINEERING
New Frontier: Environments for Innovation --- sick building syndrome
[PB89-151054] N89-27601
ENVIRONMENTAL MONITORING
GEO-EAS (Geostatistical Environmental Assessment Software) user's guide
[PB89-151252] N89-27261
Analytical procedures for environmental quality control, volume 1
[PB89-158604] N89-27266
ENVIRONMENTAL TESTS
Automated immersion testing robotic system: Hardware and software design
[AD-A208755] N89-27201
EPOXIDATION
Oxygen transfer to ethylene catalyzed by the Ag(110) surface
[AD-A207325] N89-26936
EPOXY RESINS
Micropyrolyzer design for infrared spectroscopy applications
[DE89-013329] N89-26949
EQUATIONS OF MOTION
BAE measurement schemes and optimal sensitivity for generalized parametric devices
[PREPRINT-641] N89-27586
EQUATIONS OF STATE
A symbolic generator of state equations for modeling of dynamic systems based on the electrical network analog paradigm
[DE89-013763] N89-27397
EQUIPMENT SPECIFICATIONS
Design and calibration of the mixing layer and wind tunnel
[NASA-CR-185472] N89-26866
Film annotation system for a space experiment
[NASA-CR-185114] N89-27152

EROSION
Erosion of Al and Al/SiC
[DE89-013623] N89-26913
Diamondlike carbon protective coatings for optical windows
[NASA-TM-102111] N89-27506
ERROR ANALYSIS
Formulation of numerical orbit propagation and time error correction
[INPE-4774-PRE/1443] N89-26875
An expert system for fault diagnosis in digital circuits
[INPE-4743-PRE/1417] N89-27085
ERROR CORRECTING CODES
Bandwidth efficient coding for error control
[NASA-CR-185836] N89-27062
Fault tolerant VLSI (Very Large-Scale Integration) design using error correcting codes
[AD-A208337] N89-27096
ERROR DETECTION CODES
Fault tolerant VLSI (Very Large-Scale Integration) design using error correcting codes
[AD-A208337] N89-27096
ERRORS
Analysis of human-error sequences with fault trees
[PB89-147631] N89-27422
Safety in numbers: The boundless errors of numerical computation
[DE89-014813] N89-27438
ESTIMATES
Performance estimates for the Space Station power system Brayton Cycle compressor and turbine
[NASA-CR-182263] N89-26903
Hybrid structures for simple computer performance estimates
[PB89-189161] N89-27356
Estimation of the relationship between project attributes and the implementation of engineering tools
[PB89-149470] N89-27588
ESTIMATING
Estimating and explaining the production cost of high-technology systems: The case of military aircraft
[AD-A208391] N89-26809
Model-based parameter estimation in electromagnetic computer modeling
[AD-A207399] N89-27052
Estimating fracture toughness using tension or ball indentation tests and a modified critical strain model
[DE89-010324] N89-27220
Lognormal distribution maximum-likelihood parameter estimation algorithms
[AD-A207586] N89-27378
On estimating the dependence between two point processes
[AD-A208311] N89-27445
ETCHING
A method of removing oxides from the surface of Fe-Ni-Co alloy particles by chemical etching
[DE89-014597] N89-27009
New strategies for display devices based on 2-6 materials
[AD-A208288] N89-27573
ETHYLENE
Oxygen transfer to ethylene catalyzed by the Ag(110) surface
[AD-A207325] N89-26936
The photoacoustic effect, refined and applied to biological problems
[PB89-153597] N89-27263
ETHYLENE OXIDE
Blends of poly(enaminonitriles)
[AD-A208441] N89-27017
EULER EQUATIONS OF MOTION
High speed corner and gap-seal computations using an LU-SGS scheme
[NASA-TM-102138] N89-27103
Global flows with invariant (Gibbs) measures for Euler and Navier-Stokes two-dimensional fluids
[BIBOS-310/88] N89-27105
The behavior of flux difference splitting schemes near slowly moving shock waves
[FFA-TN-1988-58] N89-27130
EUROPEAN SPACE PROGRAMS
Columbus Logistics Program
[MBB-UO-0039/88-PUB] N89-26890
EUTECTICS
The solidification metallurgy of Alloy 718 and other Nb-containing superalloys
[DE89-008196] N89-26966
Observations on the mechanisms of fatigue in eutectic Pb-Sn solder joints
[DE89-000553] N89-26968
EVALUATION
Cost of quality evaluation methodologies handbook
[AD-A206935] N89-27202
EVAPORATION
Transient cooling of a hot surface by droplets evaporation
[PB89-161897] N89-27100
Design and characterization of large-drop generators for viscous, Newtonian, and non-Newtonian liquids
[AD-A208330] N89-27133
Advanced electron beam evaporation
[ETN-89-94799] N89-27495
Cosmic evolution of non-topological solitons, paper 1
[NASA-CR-185353] N89-27608
EVAPORATIVE COOLING
Transient cooling of a hot surface by droplets evaporation
[PB89-161897] N89-27100
EVOLUTION (DEVELOPMENT)
Evolution and structure of the bow echo/microburst events
[PB89-174767] N89-27309
Cosmic evolution of non-topological solitons, paper 1
[NASA-CR-185353] N89-27608
EXERCISE PHYSIOLOGY
Development of advanced methods based on stable isotope technology for studies of exercise in heat
[AD-A208758] N89-27329
The effects of arms and countermovement on vertical jumping
[AD-A208298] N89-27347
EXHAUST EMISSION
Space Shuttle Main Engine radio frequency emissions
[NASA-CR-184707] N89-26896
Historic emissions of VOC (Volatile Organic Compounds) and NOx in the United States from 1900 to 1985
[PB89-173223] N89-27270
EXHAUST NOZZLES
Nozzle flap hinge joint
[AD-D014002] N89-26847
Bimetallic air seal for exhaust nozzles
[AD-D014106] N89-27189
EXOBIOLOGY
Space research in the Federal Republic of Germany (FRG), 1986 and 1987
[ETN-89-94427] N89-26874
EXPERIMENT DESIGN
The diagonal strip system in the Macro experiment
[NOTA-INTERNA-924] N89-27159
Activities of the Werner-Heisenberg Institute of Physics
[ISSN-0173-6256] N89-27481
EXPERT SYSTEMS
An expert system for correlation of radar and passive sensor signals
[DE89-011575] N89-27056
An expert system in C for computer-aided digital circuit design
[AD-A207518] N89-27075
An expert system for fault diagnosis in digital circuits
[INPE-4743-PRE/1417] N89-27085
A center for commercial development of space: Real-time satellite mapping. Remote sensing-based agricultural information expert system
[NASA-CR-185473] N89-27235
SP-ATUS: An expert system for specifications of satellite imagery
[INPE-4754-PRE/1426] N89-27236
Development of Low-Level Turbulence (LLT) forecasting methodologies
[AD-A208457] N89-27320
Explanation in expert systems: A survey
[NASA-CR-185335] N89-27364
Automatic treatment of natural language in processes in the acquistion of knowledge
[INPE-4737-PRE/1412] N89-27382
Northeast artificial intelligence consortium: Volume 2, part A: The Versatile Maintenance Expert System (VMES) research project
[AD-A208344] N89-27417
Empirical analysis and refinement of expert system knowledge bases
[AD-A208294] N89-27598
EXPLOSIVES
Application of crystal lattice disintegration criteria to compute minimum shock induced reactive conditions in solid explosives and inert materials
[AD-A207557] N89-27025
Thin pulse shock initiation characterization of extrusion-cast explosives: Revision
[DE89-008029] N89-27027
Explosives detection with an ion trap mass spectrometer
[DE89-012510] N89-27029
Techniques for the detection of explosives
[DE89-012570] N89-27030
Standardized piezoelectric polymer (PVDF) gauge for detonator response measurement
[DE89-010437] N89-27144
EXTERNAL TANKS
Preliminary airworthiness evaluation of the UH-60A external fuel system
[AD-A207570] N89-26840
EXTRATERRESTRIAL RADIATION
Radiation evaluation of several complex very large scale integration circuits
[DE89-007985] N89-27090
Observing primeval galaxies and dark matter with LAIRTS — Large Aperture Infra-Red Telescope System
[AD-A208286] N89-27606
EXTRATERRESTRIAL RESOURCES
Characterization of lunar ilmenite resources
[DE89-013455] N89-27618
EYE PROTECTION
Analysis and evaluation of technical data on the photochromic and non-linear optical properties of materials
[AD-A207275] N89-27000

F

FABRICATION
Development of a thin wall graphite/polyimide composite pressure vessel with a large aspect ratio
[DE89-002536] N89-26920
SiC-MoSi composites
[DE89-013656] N89-26923
Method for making an integral titanium alloy article having at least two distinct microstructural regions
[AD-D014066] N89-26960
Bearings fabricated from rapidly solidified powder and method
[AD-D014072] N89-27185
Design, development and evaluation of a doubly rotated AK-cut quartz crystal
[AD-A207209] N89-27549
High-frequency cavity applications and measurements of high-temperature superconductors
[DE89-013467] N89-27560
Thin film preparation and single film device fabrication in the Tl-Ca-Ba-Cu-O HTS system
[DE89-013560] N89-27561
Recent improvements in bulk properties of ceramic superconductors
[DE89-013626] N89-27562
FACTORIZATION
Local mode smoothing analysis of various two-dimensional incomplete factorization iterative methods
[REPT-88-67] N89-27431
FAILURE
Strain to failure of pressurized thick wall cylinders
[DE89-009969] N89-27219
FAILURE ANALYSIS
Scaling effects in the static large deflection response of graphite-epoxy composite beams
[NASA-TM-101619] N89-26843
Flexible backbone aromatic polyimide adhesives
[NASA-TM-100631] N89-27001
MM and T for linear resonant cooler, volume 2
[AD-A207236] N89-27073
Inelastic buckling of channel columns in the distortional mode
[PB89-156053] N89-27207
FALLOUT
Weather predictions and surface radiation estimates for Project BUGGY 1
[DE89-014687] N89-27318
FAR FIELDS
Propagating solutions and far-field patterns for acoustic harmonic waves in a finite depth ocean
[PB89-180715] N89-27325
FATIGUE (BIOLOGY)
Psychological attributes, coping strategies and other factors associated with ultramarathon performance
[AD-A208300] N89-27340
FATIGUE (MATERIALS)
Fatigue crack growth study of SCS6/Ti-15-3 composite
[NASA-TM-102332] N89-26989
Structural reliability and damage tolerance of ceramic composites for high-temperature applications
[PB89-156350] N89-26994
Structural reliability and damage tolerance of ceramic composites for high-temperature applications
[PB89-156368] N89-26995
Creep-fatigue assessment methods using elastic analysis results and adjustments
[DE89-011858] N89-27221
FATIGUE LIFE
Residual stress changes in fatigue. Volume 1: Residual stress measurements by X-ray diffraction in notched test specimens
[AD-A208345] N89-27225

Residual stress changes in fatigue. Volume 2: A simulation model for stress measurements in notched test specimens by X-ray diffraction
[AD-A206346] N89-27226

FATIGUE TESTS
Residual stress changes in fatigue. Volume 2: A simulation model for stress measurements in notched test specimens by X-ray diffraction
[AD-A206346] N89-27226

FAULT TOLERANCE
Fault tolerant VLSI (Very Large-Scale Integration) design using error correcting codes
[AD-A206337] N89-27096
Fault tolerant software technology for distributed computer systems
[AD-A206329] N89-27405
Advanced information processing system: Input/output system services
[NASA-CR-181874] N89-27413

FAULT TREES
Analysis of human-error sequences with fault trees
[PB89-147631] N89-27422

FEASIBILITY ANALYSIS
Feasibility and benefits of laminar flow control on supersonic cruise airplanes
[NASA-CR-181817] N89-26841
Feasibility study for enhanced lateral control of the P-3C aircraft
[AD-A206461] N89-26863
Feasibility demonstration of the Thermal Ignition Combustion System (TICS) for high pressure natural gas injected engine
[PB89-178792] N89-26944

FEEDBACK CIRCUITS
Compressor blade clearance measurement system
[AD-D014073] N89-26850

FEEDBACK CONTROL
Cost-optimal state feedback controller for all-attitude gimbal system
[AD-D013972] N89-26845
Compressor blade clearance measurement system
[AD-D014073] N89-26850
Heuristic algorithms for stability testing polytopes of matrices
[PB89-160840] N89-27365
Autonomous discovery and learning by a mobile robot in unstructured environments
[DE89-001525] N89-27415

FERMIONS
First results for the delta I = 1/2 amplitude in K decays, with quenched lattice QCD and Wilson fermions
[PREPRINT-599] N89-27485

FERROELECTRICITY
Nanostructure and defect chemistry of relaxor ferro electrics
[AD-A207217] N89-26933

FERROMAGNETIC FILMS
Magneto-optical properties of ultrathin ferromagnetic films
[DE89-014640] N89-27508

FERROMAGNETIC MATERIALS
Dispersed and periodic microstructures for magnetic and infrared absorbers
[AD-A207428] N89-27053

FIBER COMPOSITES
Tailoring of composite links for optimal damped elasto-dynamic performance
[NASA-TM-102094] N89-26912
Processing of continuous fiber composites
[DE89-012608] N89-26915
On processing development for fabrication of fiber reinforced composite, part 2
[NASA-CR-181866] N89-26917
Unified micromechanics of damping for unidirectional fiber reinforced composites
[NASA-TM-102107] N89-26919

FIBER OPTICS
Sensor development programs at NASA Ames Research Center
[NASA-TM-102217] N89-26808
Microwave hardening technology development program
[AD-A207535] N89-27076
Fiber optic rotary switching device
[AD-D013978] N89-27497
Optical couplers for coherent optical phase diversity systems
[EUT-88-E-190] N89-27498
The quantitative dependence of transmissivity on flexural strain for multimode optical fiber
[AD-A207522] N89-27501
A fiber optic test system for quantum efficiency measurements
[DE89-012623] N89-27505
System for measuring optical waveguide intensity profiles
[PB89-186593] N89-27507
Frequency division multiplexing of interferometric sensor arrays
[AD-A206448] N89-27510

FIBER STRENGTH
Statistical strength comparison of metal-matrix and polymeric-matrix composites
[AD-A206316] N89-26925

FIBERS
Metal matrix composite micromechanics: In-situ behavior influence on composite properties
[NASA-TM-102302] N89-26924
Compressive properties of high performance polymeric fibers
[AD-A207271] N89-26998
Optimum interface properties for metal matrix composites
[NASA-TM-102295] N89-27223
Group index and time delay measurements of a standard reference fiber
[PB89-189179] N89-27457

FIELD EFFECT TRANSISTORS
Miniature high voltage solid state relay
[AD-D013979] N89-27070
Proposed thin film electronics for a-Si:H PIXEL detector
[DE89-013410] N89-27083
JTECH (Japanese Technology Evaluation Program) panel report on advanced sensors in Japan
[PB89-158760] N89-27136

FIELD THEORY (ALGEBRA)
Effective action for quantum gravity in two dimensions
[PREPRINT-600] N89-27583

FIELD THEORY (PHYSICS)
Activities of the Werner-Heisenberg Institute of Physics
[ISSN-0173-6256] N89-27481
Cosmic evolution of non-topological solitons, paper 1
[NASA-CR-185353] N89-27606

FIGHTER AIRCRAFT
Feasibility and benefits of laminar flow control on supersonic cruise airplanes
[NASA-CR-181817] N89-26841
Aerodynamic parameters of an advanced fighter aircraft estimated from flight data. Preliminary results
[NASA-TM-101631] N89-26861

FILE MAINTENANCE (COMPUTERS)
Northeast artificial intelligence consortium: Volume 2, part A: The Versatile Maintenance Expert System (VMES) research project
[AD-A206344] N89-27417

FILLERS
Micropyrolyzer design for infrared spectroscopy applications
[DE89-013329] N89-26949

FILM THICKNESS
ELLIPSE user's manual and program reference
[DE89-014575] N89-27398

FINANCE
Estimating and explaining the production cost of high-technology systems: The case of military aircraft
[AD-A206391] N89-26809
Study for advanced civil earth remote sensing system: Focused finance study. Volume 1: Executive summary
[PB89-163224] N89-27230

FINANCIAL MANAGEMENT
Study for advanced civil earth remote sensing system: Focused finance study. Volume 1: Executive summary
[PB89-163224] N89-27230

FINITE DIFFERENCE THEORY
Interaction between Tollmien-Schlichting waves and free-stream disturbances in boundary-layer flows
[NASA-CR-185847] N89-27118
A direct procedure for interpolation on a structured curvilinear two-dimensional grid
[NASA-TM-102213] N89-27433
Low-frequency sound propagation modeling over a locally-reacting boundary using the parabolic approximation
[NASA-CR-185864] N89-27469

FINITE ELEMENT METHOD
A finite element method for solving electromagnetic scattering problems
[DE89-013496] N89-27059
Dynamic analysis of flexible mechanisms by a combined transfer matrix finite element method
[PB89-160865] N89-27181
Structural analysis of a thermal insulation retainer assembly
[NASA-TM-101580] N89-27212
DYNA3D user's manual: (Nonlinear Dynamic Analysis of Structures in Three Dimensions), revision 5
[DE89-014304] N89-27222
The h-p version of the finite element method parabolic equations. Part 2: The h-p version in time
[AD-A207575] N89-27429

FINITE VOLUME METHOD
Calculation of turbulence-driven secondary motion in ducts with arbitrary cross section
[NASA-TM-102142] N89-27115

FITTING
Monotone piecewise cubic data fitting
[DE89-006742] N89-27386

FLAME HOLDERS
Afterburner flameholder construction
[AD-D014116] N89-26852

FLAME PROPAGATION
Numerical computation of bifurcation phenomena and pattern formation in combustion
[DE89-013628] N89-26941
Fire propagation in concurrent flows
[PB89-186577] N89-26945

FLAMMABLE GASES
Detonability of hydrocarbon fuels in air
[DE89-008601] N89-26926

FLANGES
Nozzle flange attachment and sealing arrangement
[AD-D014123] N89-26853

FLAT PLATES
Process for assessing the effect of propellant strain on propellant burn rate
[AD-D014119] N89-27026

FLEXIBILITY
Study of jitter on the attitude motion of a spin stabilized satellite with two flexible solar panels
[INPE-4744-PRE/1418] N89-26884
Statistics of fracture in two grades of isotropic graphite
[DE89-013703] N89-26916

FLEXIBLE BODIES
Control of flexible structures
[AD-A207520] N89-26883
Dynamic analysis of flexible mechanisms by a combined transfer matrix finite element method
[PB89-160865] N89-27181
Modeling and computational algorithms for parameter estimation and optimal control of aeroelastic systems and large flexible structures
[AD-A208274] N89-27404

FLIGHT CHARACTERISTICS
Airworthiness and flight characteristics evaluation of the EH-60A (Quick Fix) helicopter
[AD-A207417] N89-26839
Design considerations of manipulator and feel system characteristics in roll tracking
[NASA-CR-4111] N89-26860

FLIGHT CLOTHING
Full coverage anti-G-suit and balanced pressure breathing
[PB89-174635] N89-27343

FLIGHT CONTROL
Brain α2 reserve limiter for high performance aircraft
[AD-D014137] N89-26858
Design considerations of manipulator and feel system characteristics in roll tracking
[NASA-CR-4111] N89-26860
Aircraft flight test trajectory control
[NASA-CR-4161] N89-27416

FLIGHT CREWS
OH-58 energy attenuating crew seat feasibility study
[AD-A207506] N89-26829

FLIGHT ENVELOPES
Hypervelocity atmospheric flight: Real gas flow fields
[NASA-TM-101055] N89-27117

FLIGHT HAZARDS
Evolution and structure of the bow echo/microburst events
[PB89-174787] N89-27309

FLIGHT PATHS
Aircraft flight test trajectory control
[NASA-CR-4161] N89-27416

FLIGHT STABILITY TESTS
Airworthiness and flight characteristics evaluation of the EH-60A (Quick Fix) helicopter
[AD-A207417] N89-26839

FLIGHT TESTS
Loran C coverage in Alaska after dual rating Port Clarence
[AD-A196032] N89-26831
ILS/MLS collocation tests at Miami/Tamiami, Florida Airport
[NASA-CR-185715] N89-26832
Method for experimental determination of flutter speed by parameter identification
[NASA-TP-2923] N89-26844
Aerodynamic parameters of an advanced fighter aircraft estimated from flight data. Preliminary results
[NASA-TM-101631] N89-26861

FLIR DETECTORS
Multiple sensor fusion for detecting targets in FLIR (Forward-Looking Infrared) and range images
[AD-A207577] N89-27502
FLORIDA
ILS/MLS collocation tests at Miami/Tamiami, Florida Airport
[NASA-CR-185715] N89-26832
An operational demonstration and flight test of the Microwave Landing System (MLS) at the Miami/Tamiami, Florida Airport
[DOT/FAA/CT-TN89/37] N89-26833
An investigation into the gravity current aspects of a cold air outbreak using variational analysis techniques
[AD-A208464] N89-27295
FLOW DISTRIBUTION
Some results on flow calculations involving drag prediction N89-26820
Design and calibration of the mixing layer and wind tunnel
[NASA-CR-185472] N89-26866
Flow fields of low pressure vent exhausts
[NASA-TM-100738] N89-26902
Lean-burn gas engine ignition processes
[PB89-181119] N89-26943
Validation of computational fluid dynamics
[AGARD-AR-257] N89-27104
A model for transition by attachment-line contamination and an examination of cross-flow instability in 3-D boundary layers
[AERO-REPT-8804] N89-27108
Hypervelocity atmospheric flight: Real gas flow fields
[NASA-TM-101055] N89-27117
Measurement of wall shear and wall pressure downstream of a honeycomb boundary layer manipulator
[AD-A208297] N89-27132
The structure of Normal-Shock/Turbulent-Boundary-Layer interactions modified by mass removal
[AD-A208402] N89-27134
Lagrangian turbulence near walls: Structures and mixing in admissible model flows
[AD-A208466] N89-27135
An objective comparison of vertical motions from the kinematic method and three forms of the omega equation
[AD-A208451] N89-27294
Differential forms of Euler's turbo-machinery equation
[AD-A207279] N89-27426
FLOW EQUATIONS
Global flows with invariant (Gibbs) measures for Euler and Navier-Stokes two-dimensional fluids
[BIBOS-310/88] N89-27105
Transactions of the 6th Army Conference on Applied Mathematics and Computing held in Boulder, Colorado on 31 May - 3 June 1988
[AD-A207252] N89-27424
Dynamics of decaying two-dimensional magnetohydrodynamic turbulence
[IPP-6/279] N89-27541
FLOW MEASUREMENT
Sensor development programs at NASA Ames Research Center
[NASA-TM-102217] N89-26808
Dynamic measurements in combustible and detonable aerosols
[ISL-PU-306/88] N89-26957
Construction of differential equations from experimental data of Karman vortex streets
[MPIS-11/1988] N89-27127
FLOW STABILITY
Absolute/convective instabilities and the convective Mach number in a compressible mixing layer
[NASA-CR-181861] N89-27113
Multigrid method for stability problems
[NASA-CR-185825] N89-27420
FLOW THEORY
Numerical study of three-dimensional separation and flow control at a wing/body junction
[NASA-CR-185819] N89-26826
FLOW VELOCITY
A dual potential formulation of the Navier-Stokes equations
[NASA-CR-185098] N89-27111
FLOW VISUALIZATION
Study of a turbulent boundary layer by laser plane visualization
[IMFL-88/33] N89-27124
Base wakes from two dimensional jets in subsonic flow with injection
[IMFL-96/20] N89-27125
FLOWMETERS
Fundamental studies of the cavity flowmeter
[PB89-188825] N89-27153
FLUENCE
Effects of high thermal and high fast fluences on the mechanical properties of type 6061 aluminum in the HFBR
[DE89-012636] N89-26970
FLUID DYNAMICS
Liquid helium fluid dynamics studies
[DE89-013124] N89-27036
Interaction between Tollmien-Schlichting waves and free-stream disturbances in boundary-layer flows
[NASA-CR-185847] N89-27118
Finite control volume modeling of laminar and turbulent flow of air in an enclosure
[DE89-009334] N89-27120
Generation of underwater sound pulses, cavitation and shear waves with hydraulic hammer
[MPIS-8/1988] N89-27122
FLUID FLOW
Design and operation of a horizontal liquid helium flow facility
[DE89-013482] N89-26867
Liquid helium fluid dynamics studies
[DE89-013124] N89-27036
Variable area manifolds for ring mirror heat exchangers
[AD-D014050] N89-27163
FLUID MECHANICS
Liquid helium fluid dynamics studies
[DE89-013124] N89-27036
Summary of research conducted at the Institute for Computer Applications in Science and Engineering in applied mathematics, numerical analysis and computer science
[NASA-CR-181858] N89-27348
FLUID PRESSURE
Fluids, gels and glasses under extreme conditions of pressure and temperature
[AD-A205292] N89-26927
Automatic oxygen measuring system
[AD-D014003] N89-26931
FLUORESCENCE
Laser spectroscopy and dynamics of combustion intermediates
[DE89-014498] N89-26956
FLUORIDES
A computer program for simulating the atmospheric dispersion of UF6 and other reactive gases having positive, neutral, or negative buoyancy
[DE89-012734] N89-27269
FLUORINE COMPOUNDS
Electrochemical evaluation of new fluorosulfonic and fluorophosphonic acids as fuel cell electrolytes
[DE89-012840] N89-27254
Electrochemical evaluation of new fluorosulfonic and fluorophosphonic acids as fuel cell electrolytes
[DE89-013391] N89-27255
FLUOROCARBONS
Synthesis of novel fluorinated phosphonic and phosphinic acid electrolytes for phosphoric acid fuel cells
[PB89-194120] N89-27086
FLUTTER
Method for experimental determination of flutter speed by parameter identification
[NASA-TP-2923] N89-26844
FLUX VECTOR SPLITTING
The behavior of flux difference splitting schemes near slowly moving shock waves
[FFA-TN-1988-58] N89-27130
FLY BY WIRE CONTROL
Electrical primary flight control system (fly by wire). Flight control systems of new technology
[MBB-UT-122/88] N89-26862
FOG
Fog, cloud, and dew chemistry
[PB89-187314] N89-27317
FORCED CONVECTION
MHD forced and free convection boundary layer flow near the leading edge
[DE88-705974] N89-26812
FORECASTING
Field studies for determining the characteristics and dynamics of local circulations
[DE89-013639] N89-27275
FORESTS
Alaska collection SAR (Synthetic Aperture Radar) data summary
[AD-A208530] N89-27067
FORGING
Bearings fabricated from rapidly solidified powder and method
[AD-D014072] N89-27185
FORMALISM
Note on multiloop calculations for superstrings in the NSR formalism
[PREPRINT-601] N89-27581
FORMING TECHNIQUES
Superplastic forming of aluminum, task C
[AD-A207282] N89-26962
FORTRAN
CWG: A FORTRAN program for mutual coupling in a planar array of circular waveguide-fed apertures
[NASA-TM-101614] N89-27063
ASR4: A computer code for fitting and processing 4-gage anelastic strain recovery data
[DE89-012239] N89-27395
ELLIPSE user's manual and program reference
[DE89-014575] N89-27398
Portable parallel programming in a FORTRAN environment
[DE89-014670] N89-27399
Automatic generation of FORTRAN-coded Jacobians and Hessians
[MEMO-INF-88-47] N89-27402
FOSSIL FUELS
Earth sciences
[DE89-013344] N89-27228
FOURIER ANALYSIS
Modeling of the angular reflectance of an artificial plant canopy near the retroreflection peak in the optical regime
[DE89-011174] N89-27239
FOURIER TRANSFORMATION
Evaluation of a FTIR (Fourier Transform Infrared Spectrometer) mobile source measurement system
[PB89-180822] N89-27147
Frequency-domain transient analysis of silicon solar cells
[DE89-010555] N89-27243
DFT algorithms for bit-serial GaAs array processor architectures
[NASA-CR-183436] N89-27361
Nonlinear wave equations solvable by the spectral transform
[PREPRINT-957] N89-27443
FRACTOGRAPHY
Fractographic study of a silicon nitride ceramic
[DE89-013012] N89-27006
FRACTURE MECHANICS
Advanced durability analysis. Volume 2: Analytical predictions, test results and analytical correlations
[AD-A207215] N89-26838
Fracture toughness of SiC/Al metal matrix composite
[NASA-TM-100745] N89-26918
Unified micromechanics of damping for unidirectional fiber reinforced composites
[NASA-TM-102107] N89-26919
Fracture behavior of a pressure vessel steel in the ductile-to-brittle transition region
[PB89-189195] N89-26977
Fatigue crack growth study of SCS6/Ti-15-3 composite
[NASA-TM-102332] N89-26989
Toughening mechanisms in ceramic composites
[PB89-162606] N89-26996
High-temperature flaw assessment procedure: A state-of-the-art survey
[DE89-012740] N89-27210
Estimating fracture toughness using tension or ball indentation tests and a modified critical strain model
[DE89-010324] N89-27220
FRACTURE STRENGTH
Method to produce titanium metal matrix composites with improved fracture and creep resistance
[AD-D014111] N89-26911
Statistics of fracture in two grades of isotropic graphite
[DE89-013703] N89-26916
Fracture toughness of SiC/Al metal matrix composite
[NASA-TM-100745] N89-26918
Fracture behavior of a pressure vessel steel in the ductile-to-brittle transition region
[PB89-189195] N89-26977
Toughening mechanisms in ceramic composites
[PB89-162606] N89-26996
Fractographic study of a silicon nitride ceramic
[DE89-013012] N89-27006
Structural ceramics in the advanced materials world
[DE89-013046] N89-27008
Estimating fracture toughness using tension or ball indentation tests and a modified critical strain model
[DE89-010324] N89-27220
FRACTURES (MATERIALS)
Structural reliability and damage tolerance of ceramic composites for high-temperature applications
[PB89-156350] N89-26994
Structural reliability and damage tolerance of ceramic composites for high-temperature applications
[PB89-156368] N89-26995

FRACTURING
Statistics of fracture in two grades of isotropic graphite
[DE89-013703] N89-26916
Fracture toughness of SiC/Al metal matrix composite
[NASA-TM-100745] N89-26918
FRAGMENTATION
Nuclear fragmentation energy and momentum transfer distributions in relativistic heavy-ion collisions
[NASA-CR-185501] N89-27477
FRAMES
Geodetic precession or dragging of inertial frames
[NASA-TM-100744] N89-27456
FRAMING CAMERAS
Window generator
[AD-D014068] N89-27048
FREE CONVECTION
MHD forced and free convection boundary layer flow near the leading edge
[DE88-705974] N89-26812
FREE ELECTRON LASERS
Static periodic field device for free electron laser
[AD-D014125] N89-27168
Elements of a realistic 17 GHz FEL/TBA design
[DE89-013427] N89-27169
Report of the Workshop on Scientific Opportunities for Infrared Free-Electron Lasers, volume 1
[DE89-012836] N89-27170
Recent experiments with the free-electron laser at Los Alamos
[DE89-013469] N89-27171
Free electron lasers with small period wigglers
[DE89-014715] N89-27173
Prospects for the FEL (Free Electron Laser)
[DE89-012998] N89-27175
FREE FLOW
Interaction between Tollmien-Schlichting waves and free-stream disturbances in boundary-layer flows
[NASA-CR-185647] N89-27118
The structure of Normal-Shock/Turbulent-Boundary-Layer interactions modified by mass removal
[AD-A208402] N89-27134
FREQUENCIES
Common carrier earth station database documentation
[PB89-186050] N89-27595
FREQUENCY DIVISION MULTIPLEXING
Frequency division multiplexing of interferometric sensor arrays
[AD-A208448] N89-27510
FREQUENCY MODULATION
On capture effect of FM demodulators
[AD-A208479] N89-27066
FREQUENCY STABILITY
Low noise crystal controlled oscillator
[AD-D014070] N89-27072
FREQUENCY STANDARDS
Technical activities 1986-1988, Molecular Spectroscopy Div.
[PB89-175418] N89-26942
FREQUENCY SYNTHESIZERS
Multichannel phase noise measurement system
[AD-D014056] N89-27461
FRICTION
Computational methods for nonlinear dynamic problems in solid and structural mechanics: Progress in the theory and modeling of friction and in the control of dynamical systems with frictional forces
[AD-A208763] N89-27227
FRICTION FACTOR
Computational methods for nonlinear dynamic problems in solid and structural mechanics: Progress in the theory and modeling of friction and in the control of dynamical systems with frictional forces
[AD-A208763] N89-27227
FUEL CELLS
Synthesis of novel fluorinated phosphonic and phosphinic acid electrolytes for phosphoric acid fuel cells
[PB89-194120] N89-27088
Electrochemical evaluation of new fluorosulfonic and fluorophosphonic acids as fuel cell electrolytes
[DE89-013391] N89-27255
FUEL COMBUSTION
Numerical computation of bifurcation phenomena and pattern formation in combustion
[DE89-013628] N89-26941
Lean-burn gas engine ignition processes
[PB89-181119] N89-26943
Feasibility demonstration of the Thermal Ignition Combustion System (TICS) for high pressure natural gas injected engine
[PB89-178792] N89-26944
Catalytic combustion of methane
[PB89-186874] N89-26946
Dynamic measurements in combustible and detonable aerosols
[ISL-PU-306/88] N89-26957
Combustion characteristics of dry coal-powder-fueled adiabatic diesel engine
[DE89-000978] N89-27197
Historic emissions of VOC (Volatile Organic Compounds) and NOx in the United States from 1900 to 1985
[PB89-173223] N89-27270
FUEL FLOW
Mixing and combustion of pulsed gas jets
[PB89-155550] N89-26929
FUEL INJECTION
Feasibility demonstration of the Thermal Ignition Combustion System (TICS) for high pressure natural gas injected engine
[PB89-178792] N89-26944
FUEL SPRAYS
Afterburner flameholder construction
[AD-D014116] N89-26852
Detonation of unconfined large scale fuel spray-air clouds
[DE89-006510] N89-26955
FUEL SYSTEMS
Preliminary airworthiness evaluation of the UH-60A external fuel system
[AD-A207570] N89-26840
Combustion characteristics of dry coal-powder-fueled adiabatic diesel engine
[DE89-000978] N89-27197
FUEL TANKS
Preliminary airworthiness evaluation of the UH-60A external fuel system
[AD-A207570] N89-26840
FUNCTIONAL DESIGN SPECIFICATIONS
Advanced coal-fueled gas turbine systems, volume 2
[DE89-000954] N89-27183
FURNACES
Compact ceramic heat exchangers
[PB89-173603] N89-26997
FUSELAGES
Numerical study of three-dimensional separation and flow control at a wing/body junction
[NASA-CR-185819] N89-26826
FUSION
Multiple sensor fusion for detecting targets in FLIR (Forward-Looking Infrared) and range images
[AD-A207577] N89-27502

G

GALACTIC EVOLUTION
Observing primeval galaxies and dark matter with LAIRTS — Large Aperture Infra-Red Telescope System
[AD-A208286] N89-27606
Evolution of Galaxies. Proceedings, volume 4
[DE89-009850] N89-27616
GALAXIES
Observing primeval galaxies and dark matter with LAIRTS — Large Aperture Infra-Red Telescope System
[AD-A208286] N89-27606
Evolution of Galaxies. Proceedings, volume 4
[DE89-009850] N89-27616
Use of the EGRET (Energetic Gamma-Ray Experiment Telescope) in studies of the origin of the cosmic radiation
[DE89-013785] N89-27630
GALILEO PROJECT
Safety testing program for the Galileo mission radioisotope thermoelectric generator
[DE89-011192] N89-27494
GALLIUM ARSENIDE LASERS
High power semiconductor laser sources
[AD-A207569] N89-27167
GALLIUM ARSENIDES
Photoconductive semiconductor switch (PCSS) recovery
[DE89-012657] N89-27080
Closing photoconductive semiconductor switches
[DE89-013073] N89-27082
High power semiconductor laser sources
[AD-A207569] N89-27167
DFT algorithms for bit-serial GaAs array processor architectures
[NASA-CR-183436] N89-27361
Model for hot electron phenomena: Theory and general results
[DE88-705986] N89-27544
MeV implantation studies in LPE-grown GaAs and InP
[AD-A207220] N89-27550
A hydrid 3 Gs/s, 6-bit digital to analog converter
[DE89-012302] N89-27552
Photoelectronic properties of low temperature GaAs grown on silicon and GaAs substrates by MBE
[DE89-013148] N89-27557
GAME THEORY
Solution of deterministic differential games: The approximate strategy method
[ONERA-NT-1987-6] N89-27450
GAMMA RAY BURSTS
Detection of very high energy gamma-rays from the Crab nebula
[DE89-011840] N89-27627
GAMMA RAY OBSERVATORY
Spectra of crab-like pulsars: A GRO perspective
[DE89-013461] N89-27628
Use of the EGRET (Energetic Gamma-Ray Experiment Telescope) in studies of the origin of the cosmic radiation
[DE89-013785] N89-27630
GAMMA RAY SPECTROMETERS
Advanced Solar Observatory (ASO) accommodations requirements study
[NASA-CR-183718] N89-26885
GAMMA RAY TELESCOPES
Use of the EGRET (Energetic Gamma-Ray Experiment Telescope) in studies of the origin of the cosmic radiation
[DE89-013785] N89-27630
GAMMA RAYS
Computational techniques in gamma-ray Skyshine analysis
[DE89-010156] N89-27282
GAS CHROMATOGRAPHY
Supercritical fluid chromatography of polar organic compounds in combustion particulates
[PB89-152441] N89-26930
GAS DETECTORS
JTECH (Japanese Technology Evaluation Program) panel report on advanced sensors in Japan
[PB89-158760] N89-27136
GAS DYNAMICS
Statistics of an integrable discrete Sine Gordon system
[PREPRINT-638] N89-27128
GAS EXPLOSIONS
Detonability of hydrocarbon fuels in air
[DE89-008801] N89-26926
GAS FLOW
Experimental program for real gas flow code validation at NASA Ames Research Center
[NASA-TM-100093] N89-26816
Fundamental studies of the cavity flowmeter
[PB89-188825] N89-27153
GAS JETS
Mixing and combustion of pulsed gas jets
[PB89-155550] N89-26929
Measurement of the time-dependent distribution of ionization states in an argon plasma from a Mach-10 jet
[DE89-014699] N89-27526
GAS LASERS
Bibliography of Soviet laser developments, No. 92, November - December 1987
[AD-A207794] N89-27177
GAS PRESSURE
Solid state gas pressure sensor
[AD-D014105] N89-27139
GAS TRANSPORT
Comparison of modelled and measured tracer gas concentrations during the Across North America Tracer Experiment (ANATEX)
[PB89-136709] N89-27260
GAS TUNGSTEN ARC WELDING
Effect of oxidation, sandblasting and pickling on weldability
[DE89-013795] N89-26975
GAS TURBINE ENGINES
Statistics on aircraft gas turbine engine rotor failures that occurred in US commercial aviation during 1983
[AD-A207592] N89-26851
Measurement uncertainty within the Uniform Engine Test Programme
[AGARD-AG-307] N89-26854
High performance intercooled and recuperated gas turbine
[PB89-152284] N89-27178
GAS TURBINES
Nozzle flap hinge joint
[AD-D014002] N89-26847
Afterburner flameholder construction
[AD-D014116] N89-26852
Self-locking outer air seal with full backside cooling
[AD-D013975] N89-27179
Vane platform sealing and retention means
[AD-D013980] N89-27180
Advanced coal-fueled gas turbine systems, volume 2
[DE89-000954] N89-27183
GAS-SOLID INTERFACES
Transient cooling of a hot surface by droplets evaporation
[PB89-161897] N89-27100

GASEOUS DIFFUSION
Comparison of modelled and measured tracer gas concentrations during the Across North America Tracer Experiment (ANATEX)
[PB89-136709] N89-27260
GASEOUS FUELS
Numerical computation of bifurcation phenomena and pattern formation in combustion
[DE89-013628] N89-26941
GASES
The photoacoustic effect, refined and applied to biological problems
[PB89-153597] N89-27263
Trace gases in and over the West Pacific and East Indian Oceans during the El Nino-southern oscillation event of 1987: A report of GMCC (Geophysical Monitoring for Climatic Change) data collected on the second Soviet-American Gas and Aerosol Experiment (SAGA 2)
[PB89-159685] N89-27280
GATES (CIRCUITS)
The short-circuited fluxgate output current
[ISSN-0109-6605] N89-27069
GAUGE THEORY
Machines for lattice gauge theory
[DE89-014815] N89-27400
GAUSS EQUATION
High speed corner and gap-seal computations using an LU-SGS scheme
[NASA-TM-102138] N89-27103
GELS
Fluids, gels and glasses under extreme conditions of pressure and temperature
[AD-A205292] N89-26927
GENERATORS
Noise radiation characteristics of the Westinghouse WWG-0600 (600kW) wind turbine generator
[NASA-TM-101576] N89-27467
GEOCHEMISTRY
X-ray microscopy using synchrotron radiation
[NASA-CR-184800] N89-27155
Earth sciences
[DE89-013344] N89-27228
GEODETIC COORDINATES
Geodetic precession or dragging of inertial frames
[NASA-TM-100744] N89-27456
GEODETIC SURVEYS
Geodetic measurement of deformation in California
[NASA-TM-100732] N89-27279
GEOGRAPHIC INFORMATION SYSTEMS
An assessment of information demands for remote sensing and Geographic Information System technologies
[PB89-159313] N89-27233
Applications of numerical models for elevation and integration with digital images
[INPE-4776-PRE/1445] N89-27392
GEOLOGY
Earth sciences
[DE89-013344] N89-27228
Developing a geologic and engineering properties data base with INGRES
[DE89-013520] N89-27593
GEOMAGNETIC TAIL
The magnetic topology of the plasmoid flux rope in a MHD simulation of magnetotail reconnection
[DE89-012621] N89-27529
GEOMAGNETISM
Brorfeide Geomagnetic Observatory: Magnetic results, 1986
[ISBN-87-7478-287-8] N89-27293
GEOMETRICAL OPTICS
Transverse pumping with diode lasers
[AD-A207261] N89-27165
GEOMETRICAL THEORY OF DIFFRACTION
Transverse pumping with diode lasers
[AD-A207261] N89-27165
GEOMETRY
Mechanisms that control the geometry of pulsed Nd:YAG laser welds
[DE89-014490] N89-27200
Using conjoint meshing primitives to generate quadrilateral and hexahedral elements in irregular regions
[DE89-005918] N89-27435
GEOPHYSICAL OBSERVATORIES
Brorfeide Geomagnetic Observatory: Magnetic results, 1986
[ISBN-87-7478-287-8] N89-27293
GEOPHYSICS
Earth sciences
[DE89-013344] N89-27228
Attitude angle effects on Nimbus-7 Scanning Multichannel Microwave Radiometer radiances and geophysical parameter retrievals
[NASA-TM-4132] N89-27289
Solar-geophysical data number 535, part 1. Data for February, January 1989, and late data
[PB89-185987] N89-27624
Solar-geophysical data number 535, part 2. Data for September 1988, and miscellaneous
[PB89-185995] N89-27625
GEOSAT SATELLITES
GEOSAT altimeter sea-ice mapping
[AD-A207391] N89-27234
GEOTHERMAL RESOURCES
Drilling operations plan for the Magma Energy Exploratory Well
[DE89-010037] N89-27240
GEOTHERMAL TECHNOLOGY
Drilling operations plan for the Magma Energy Exploratory Well
[DE89-010037] N89-27240
GIMBALS
Cost-optimal state feedback controller for all-attitude gimbal system
[AD-D013972] N89-26845
GLASS
Supersonics
[AD-A207394] N89-26814
Fluids, gels and glasses under extreme conditions of pressure and temperature
[AD-A205292] N89-26927
A method of removing oxides from the surface of Fe-Ni-Co alloy particles by chemical etching
[DE89-014597] N89-27009
Passive optical losses in laser glass
[DE89-013784] N89-27172
GLASS COATINGS
Interface modified glass fiber/thermoplastic matrix composites
[AD-A207308] N89-26910
GLASS FIBERS
Interface modified glass fiber/thermoplastic matrix composites
[AD-A207308] N89-26910
Measured damping and modulus of composite cylinders
[DE89-010369] N89-27209
Fate and effects of PAHs in the terrestrial environment: An overview
[DE89-010319] N89-27267
Hybrid single crystal optic fibers by embedding
[AD-D013986] N89-27545
GLASS TRANSITION TEMPERATURE
Photodegradation of polyimides 2. Thermal property changes of polyimides based on a perfluorinated dianhydride
[AD-A208447] N89-27018
GNOMONIC PROJECTION
A graphics package for meteorological data, version 1.5
[NASA-TM-100742] N89-27314
GOVERNMENTS
Science and technology advice in the White House: Recommendations for President-Elect George Bush
[PB89-169817] N89-27600
GRAIN BOUNDARIES
Loss of grain boundary segregant during ion milling
[DE89-007835] N89-26979
High-temperature behavior of grain boundaries from embedded atom method molecular dynamics simulation
[DE89-013641] N89-27474
Study of nanophase TiO2 grain boundaries by Raman spectroscopy
[DE89-012416] N89-27553
The study of structure-processing-property relations in copper oxide-based high T sub c superconductors
[DE89-012764] N89-27554
GRAIN SIZE
The recrystallization and respheroidization of tungsten grains in a tungsten-heavy alloy
[AD-A207647] N89-26964
Study of nanophase TiO2 grain boundaries by Raman spectroscopy
[DE89-012416] N89-27553
GRAMMARS
Research in knowledge delivery
[AD-A208327] N89-27599
GRAPHITE
Examination of the tensile strength of graphite fibers
[AD-A207277] N89-26909
Statistics of fracture in two grades of isotropic graphite
[DE89-013703] N89-26916
Development of a thin wall graphite/polyimide composite pressure vessel with a large aspect ratio
[DE89-002536] N89-26920
Measured damping and modulus of composite cylinders
[DE89-010369] N89-27209
Fate and effects of PAHs in the terrestrial environment: An overview
[DE89-010319] N89-27267
TORE SUPRA graphite inner first wall --- tokamak devices
[DE89-009325] N89-27512
Thermophysical properties of advanced carbon materials for Tokamak limiters
[DE89-012799] N89-27516
GRAPHITE-EPOXY COMPOSITES
Scaling effects in the static large deflection response of graphite-epoxy composite beams
[NASA-TM-101619] N89-26843
GRAVITATION
A test of Newton's Law of Gravity using the BREN Tower, Nevada
[DE89-013262] N89-27454
GRAVITATION THEORY
An investigation into the gravity current aspects of a cold air outbreak using variational analysis techniques
[AD-A208464] N89-27295
Effective action for quantum gravity in two dimensions
[PREPRINT-600] N89-27583
On the integrability of the Ernst equation
[PREPRINT-606] N89-27584
Knot theory and quantum gravity
[PREPRINT-607] N89-27585
GRAVITATIONAL COLLAPSE
Radiative collapse of a Bennett-relaxed z-pinch
[DE89-014290] N89-27533
GRAVITATIONAL EFFECTS
Full coverage anti-G-suit and balanced pressure breathing
[PB89-174635] N89-27343
GRAVITATIONAL FIELDS
A test of Newton's Law of Gravity using the BREN Tower, Nevada
[DE89-013262] N89-27454
Dynamics of an M-level atom interacting with gravity fields. 1: Effects of the level number on quantum collapse and revival
[AD-A207278] N89-27579
The cosmological constant problem
[DE89-013150] N89-27614
GRAVITATIONAL PHYSIOLOGY
Full coverage anti-G-suit and balanced pressure breathing
[PB89-174635] N89-27343
GRAVITATIONAL WAVE ANTENNAS
Correlation and analysis between the Kamioka neutrino detector data and the Maryland and Rome gravitational antenna data
[NOTA-INTERNA-918] N89-27488
GRAVITATIONAL WAVES
On the production and detection of gravitational waves from artificial sources
[NOTA-INTERNA-912] N89-27587
GRAVITY WAVES
Spectra of surface waves
[AD-A208482] N89-27326
GREENHOUSE EFFECT
Criteria for selecting a CO2/climate change region of study
[DE89-011233] N89-27268
Atmospheric carbon dioxide and the greenhouse effect
[DE89-012869] N89-27271
Introduction to background materials for Workshop No. 1: Global climate change and its effects on California
[DE89-013381] N89-27272
Proceedings of the Energy Efficiency and Structural Change: Implications for the Greenhouse Problem Workshop
[DE89-012852] N89-27274
GRID GENERATION (MATHEMATICS)
Efficient grid generation
[NASA-CR-185034] N89-27434
GROUND STATIONS
Common carrier earth station database documentation
[PB89-186050] N89-27595
GROUP THEORY
Use of the Fox derivatives in the solution of the word problem for groups
[DE88-705978] N89-27421
GROWTH
Endogenous hormonal and growth factor responses to heavy resistance exercise protocols
[AD-A208375] N89-27336
GUIDE VANES
Vane platform sealing and retention means
[AD-D013980] N89-27180
Anti-rotation guide bushing
[AD-D014079] N89-27186

GULF OF ALASKA
Loran C coverage in Alaska after dual rating Port Clarence
[AD-A196032] N89-26831
GULF OF MEXICO
Meteorological database and synthesis for the Gulf of Mexico
[PB89-178222] N89-27311
GYROSCOPES
Geodetic precession or dragging of inertial frames
[NASA-TM-100744] N89-27456

H

HAMILTONIAN FUNCTIONS
EIGEN: A program to compute eigenrays from HARPA (Hamiltonian Acoustic Ray-Tracing Program for the Atmosphere)/HARPO (Hamiltonian Acoustic Ray-Tracing Program for the Ocean) raysets
[PB89-165781] N89-27460
Covariance properties of the multiquark Hamiltonian in the constituent quark model
[NOTA-INTERNA-920] N89-27489
HANDBOOKS
Cost of quality evaluation methodologies handbook
[AD-A206935] N89-27202
HARDNESS
Evaluation of mechanical properties of TiN films by ultra-low load indentation
[DE89-009618] N89-26969
HARTREE APPROXIMATION
Quantum and thermodynamic fluctuations in the degenerate schematic model of the finite temperature random phase approximation
[DE88-706310] N89-27580
HEALTH
Annual historical report - AMEDD activities
[AD-A208301] N89-27333
Submarine air quality: Monitoring the air in submarines. Health effects in divers of breathing submarine air under hyperbaric conditions
[PB89-174213] N89-27345
HEAT EXCHANGERS
Compact ceramic heat exchangers
[PB89-173603] N89-26997
Liquid helium fluid dynamics studies
[DE89-013124] N89-27036
Variable area manifolds for ring mirror heat exchangers
[AD-D014050] N89-27163
Crystallization of paraxylene with scraped surface heat exchangers
[WTHD-189] N89-27570
HEAT FLUX
Transient heat transfer into superfluid helium under confined conditions
[DE88-706312] N89-27109
Method for calibrating a heat flux gauge
[AD-D013974] N89-27138
HEAT OF FORMATION
Local density theory of heats of formation and short-range order parameters in substitutionally disordered alloys
[DE89-014696] N89-26986
HEAT PIPES
Thermal evaluation of advanced solar dynamic heat receiver performance
[NASA-CR-185117] N89-27256
HEAT PUMPS
Gas engine heat pump system and component efficiency and reliability improvement, phase 2
[PB89-173645] N89-27184
HEAT SOURCES
Safety testing program for the Galileo mission radioisotope thermoelectric generator
[DE89-011192] N89-27494
HEAT STORAGE
Dynamic simulation of a molten-salt solar receiver
[DE89-010556] N89-27244
HEAT TRANSFER
Compact ceramic heat exchangers
[PB89-173603] N89-26997
Liquid helium fluid dynamics studies
[DE89-013124] N89-27036
Development of compressed multifoil insulation for high-temperature batteries and other applications
[DE89-012877] N89-27092
Transient cooling of a hot surface by droplets evaporation
[PB89-161897] N89-27100
Method for calibrating a heat flux gauge
[AD-D013974] N89-27138
Solid state gas pressure sensor
[AD-D014105] N89-27139
HEAT TREATMENT
Method to produce metal matrix composite articles from rich metastable-beta titanium alloys
[AD-D014064] N89-26907
Method to produce metal matrix composite articles from lean metastable beta titanium alloys
[AD-D014065] N89-26908
Fluids, gels and glasses under extreme conditions of pressure and temperature
[AD-A205292] N89-26927
Method for making an integral titanium alloy article having at least two distinct microstructural regions
[AD-D014066] N89-26960
Thermomechanical processing of aluminum alloy 2090 for superplasticity
[AD-A206764] N89-26992
Compact ceramic heat exchangers
[PB89-173603] N89-26997
HEATERS
System for boundary layer control through pulsed heating of a strip heater
[AD-D013999] N89-27101
HEATING
Effect of heating rate to test temperature on superplastic response in an Al-6 percent Mg-1 percent Li-0.2 percent Zr alloy
[AD-A206462] N89-26990
HEAVY ICNS
Nuclear fragmentation energy and momentum transfer distributions in relativistic heavy-ion collisions
[NASA-CR-185501] N89-27477
HEIGHT
The effects of arms and countermovement on vertical jumping
[AD-A206298] N89-27347
HELICOPTER CONTROL
Design of an active helicopter control experiment at the Princeton Rotorcraft Dynamics Laboratory
[NASA-CR-185490] N89-26859
High-speed data acquisition for the Princeton University Dynamic Model Track
[NASA-CR-185491] N89-26865
HELICOPTER PERFORMANCE
Airworthiness and flight characteristics evaluation of the EH-60A (Quick Fix) helicopter
[AD-A207417] N89-26839
Preliminary airworthiness evaluation of the UH-60A external fuel system
[AD-A207570] N89-26840
HELICOPTERS
OH-58 energy attenuating crew seat feasibility study
[AD-A207506] N89-26829
Airworthiness and flight characteristics evaluation of the EH-60A (Quick Fix) helicopter
[AD-A207417] N89-26839
HELIUM ISOTOPES
Momentum distributions in liquid helium
[DE89-014679] N89-26953
Final state effects in liquid He4: An experimental test
[DE89-012615] N89-27472
HELIUM PLASMA
Collision processes of interest in MFE plasma research
[DE89-013681] N89-27524
HESSIAN MATRICES
Automatic generation of FORTRAN-coded Jacobians and Hessians
[MEMO-INF-88-47] N89-27402
HETEROJUNCTION DEVICES
High-efficiency, large-area CdTe panels
[DE89-000891] N89-27242
HEURISTIC METHODS
Heuristic algorithms for stability testing polytopes of matrices
[PB89-160840] N89-27365
HIGH ALTITUDE ENVIRONMENTS
Altitude symptomatology and mood states during a climb to 3630 m
[AD-A208261] N89-27332
HIGH FREQUENCIES
Antiproton and millimeter wave research
[AD-A208363] N89-27491
HIGH LEVEL LANGUAGES
An overview of some methods for the high-level specification of synchronization
[MEMO-INF-88-50] N89-27403
A language translator for a computer aided rapid prototyping system
[AD-A208358] N89-27406
HIGH POWER LASERS
High energy laser target plate
[AD-D014053] N89-27164
High power semiconductor laser sources
[AD-A207569] N89-27167
Prospects for the FEL (Free Electron Laser)
[DE89-012998] N89-27175
HIGH REYNOLDS NUMBER
Dynamics of decaying two-dimensional magnetohydrodynamic turbulence
[IPP-6/279] N89-27541
HIGH SPEED
Attractive levitation for high-speed ground transport with large guideway clearance and alternating-gradient stabilization
[DE89-013640] N89-27195
HIGH STRENGTH
Method to produce metal matrix composite articles from rich metastable-beta titanium alloys
[AD-D014064] N89-26907
Method to produce metal matrix composite articles from lean metastable beta titanium alloys
[AD-D014065] N89-26908
HIGH TEMPERATURE
Relaxation response of A533B steel from 25 to 600 C
[DE89-010179] N89-26982
Corrosion of Ceramic Materials Workshop held November 12-13, 1987, Pennsylvania State University, University Park, Pennsylvania
[PB89-175343] N89-27004
High-temperature flaw assessment procedure: A state-of-the-art survey
[DE89-012740] N89-27210
Intense heat checklist based on the 1980 heat wave
[PB89-181200] N89-27312
High-temperature behavior of grain boundaries from embedded atom method molecular dynamics simulation
[DE89-013641] N89-27474
HIGH TEMPERATURE ENVIRONMENTS
Structural reliability and damage tolerance of ceramic composites for high-temperature applications
[PB89-156350] N89-26994
Structural reliability and damage tolerance of ceramic composites for high-temperature applications
[PB89-156368] N89-26995
Evaluation of weldment creep and fatigue strength-reduction factors for elevated-temperature design
[DE89-006242] N89-27218
HIGH TEMPERATURE FLUIDS
Hot surface ignition tests of aircraft fluids
[AD-A207372] N89-26937
HIGH TEMPERATURE SUPERCONDUCTORS
Measurements of complex permittivity of microwave substrates in the 20 to 300 K temperature range from 26.5 to 40.0 GHz
[NASA-TM-102123] N89-27038
Wear and friction of thin film high temperature oxide superconductors
[DE89-009397] N89-27543
Diffusion in high-T sub c superconductors
[DE89-009792] N89-27546
Artificial superlattices
[ETN-89-94889] N89-27551
Sputtering of high-temperature superconductors: A bibliography
[DE89-013374] N89-27558
High-frequency cavity applications and measurements of high-temperature superconductors
[DE89-013467] N89-27560
Evidence for phonon-mediated coupling in superconducting Ba sub 0.6 K sub 0.4 BiO3
[DE89-014642] N89-27568
Development of elements of a high Tc superconducting cable
[AD-A208370] N89-27574
HIGH VOLTAGES
Miniature high voltage solid state relay
[AD-D013979] N89-27070
HILBERT SPACE
Dynamics of an M-level atom interacting with gravity fields. 1: Effects of the level number on quantum collapse and revival
[AD-A207278] N89-27579
HINGES
Nozzle flap hinge joint
[AD-D014002] N89-26847
HISTORIES
The best we can be
[NASA-TM-101781] N89-26873
Historic emissions of VOC (Volatile Organic Compounds) and NOx in the United States from 1900 to 1985
[PB89-173223] N89-27270
Some considerations on the birth of molecular physics in the first half of the 19th century
[NOTA-INTERNA-917] N89-27482
HOLOGRAPHY
Applications of holography to pattern recognition and optical memories
[PB89-174668] N89-27146
Theory of X-ray holography including phase and amplitude contrast and finite transfer functions
[DE89-012835] N89-27148

X-ray holography: A history
[DE89-012983] N89-27149

HOMOGENEITY
An approach for constructing families of homogenized equations for periodic media. 1: An integral representation and its consequences
[AD-A207572] N89-27427
An approach for constructing families of homogenized equations for periodic media. 2: Properties of the kernel
[AD-A207573] N89-27428

HOMOGENEOUS TURBULENCE
Study of subgrid models in incompressible turbulent flow, homogeneous or inhomogeneous
[ONERA-RSF-17/3619-AY-110-A] N89-27123

HOMOLOGY
The sl (1/1;R)-cohomologies in BRST-Gupta-Bleuler quantization
[NIKHEF-H/88-17] N89-27578

HONEYCOMB STRUCTURES
Measurement of wall shear and wall pressure downstream of a honeycomb boundary layer manipulator
[AD-A208297] N89-27132

HORIZONTAL ORIENTATION
Yaw dynamics of horizontal axis wind turbines
[DE89-000868] N89-27249

HORMONE METABOLISMS
Endogenous hormonal and growth factor responses to heavy resistance exercise protocols
[AD-A208375] N89-27336

HORMONES
Endogenous hormonal and growth factor responses to heavy resistance exercise protocols
[AD-A208375] N89-27336

HOSES
Hose reel monitor for inflight refueling system
[AD-D014054] N89-26836

HOT CORROSION
Corrosion of Ceramic Materials Workshop held November 12-13, 1987, Pennsylvania State University, University Park, Pennsylvania
[PB89-175343] N89-27004

HOT ELECTRONS
Model for hot electron phenomena: Theory and general results
[DE88-705986] N89-27544

HOT PRESSING
Method for refining microstructures of blended elemental titanium powder compacts
[AD-D014067] N89-26961

HOT SURFACES
Hot surface ignition tests of aircraft fluids
[AD-A207372] N89-26937
Transient cooling of a hot surface by droplets evaporation
[PB89-161897] N89-27100

HOVERING
Experimental assessment of helicopter rotor turbulence ingestion noise in hover
[NASA-CR-181792] N89-27468

HUBBLE CONSTANT
The cosmological constant problem
[DE89-013150] N89-27614

HUGONIOT EQUATION OF STATE
Characterization of Morton-Thiokol booster-rocket propellant TP-H1207C and its simulant H-19
[DE89-013347] N89-27031

HUMAN BEINGS
Meridian variations in spectral dark adaptation
[AD-A207248] N89-27331
The effects of arms and countermovement on vertical jumping
[AD-A208298] N89-27347

HUMAN FACTORS ENGINEERING
Aircraft color displays: Chromaticity and luminance requirements
[AD-A206786] N89-26828
Brain o2 reserve limiter for high performance aircraft
[AD-D014137] N89-26858
Annual historical report - AMEDD activities
[AD-A208301] N89-27333
Ergonomic Models of Anthropometry, Human Biomechanics and Operator-Equipment Interfaces
[NASA-CR-185720] N89-27344
New Frontier: Environments for Innovation --- sick building syndrome
[PB89-151054] N89-27601

HUMAN PERFORMANCE
Annual historical report - AMEDD activities
[AD-A206301] N89-27333
Effectiveness and acceptability of nutrient solutions in enhancing fluid intake in the heat
[AD-A208428] N89-27337
Human performance assessment methods
[AGARD-AG-308] N89-27338
Psychological attributes, coping strategies and other factors associated with ultramarathon performance
[AD-A208300] N89-27340
The effects of arms and countermovement on vertical jumping
[AD-A208298] N89-27347
Analysis of human-error sequences with fault trees
[PB89-147631] N89-27422
New Frontier: Environments for Innovation --- sick building syndrome
[PB89-151054] N89-27601

HUMAN REACTIONS
A model of human reaction time to dangerous robot arm movements
[PB89-186522] N89-27339

HUMAN TOLERANCES
Meridian variations in spectral dark adaptation
[AD-A207248] N89-27331

HUMIDITY
Low relative humidity in the atmosphere
[AD-A207558] N89-27307

HUMIDITY MEASUREMENT
Navy tethered balloon measurements made during the Fire marine stratocu IFO (Intensive Field Operation)
[AD-A207312] N89-27304

HURRICANES
Meteorological database and synthesis for the Gulf of Mexico
[PB89-178222] N89-27311

HYBRID PROPULSION
Hybrid electric chemical propulsion
[AD-A207584] N89-26898

HYDRAULIC EQUIPMENT
The 1st Scandinavian Conference on Viscous and T urbulent Flow in Hydraulic Machinery
[PB89-161327] N89-27102

HYDRAULIC FLUIDS
Hot surface ignition tests of aircraft fluids
[AD-A207372] N89-26937

HYDRAULIC SHOCK
Generation of underwater sound pulses, cavitation and shear waves with hydraulic hammer
[MPIS-8/1988] N89-27122

HYDROCARBON FUELS
Detonability of hydrocarbon fuels in air
[DE89-008801] N89-26926

HYDROCARBONS
Thermodynamics and high temperature chemistry of the chemical vapor deposition of diamond films
[DE89-013574] N89-26951

HYDRODYNAMIC EQUATIONS
Fluids, gels and glasses under extreme conditions of pressure and temperature
[AD-A205292] N89-26927

HYDRODYNAMICS
A procedure for computing surface wave trajectories on an inhomogeneous surface
[NASA-TP-2929] N89-26811
Computational methods for nonlinear dynamic problems in solid and structural mechanics: Progress in the theory and modeling of friction and in the control of dynamical systems with frictional forces
[AD-A208763] N89-27227

HYDROELASTICITY
Computational methods for nonlinear dynamic problems in solid and structural mechanics: Progress in the theory and modeling of friction and in the control of dynamical systems with frictional forces
[AD-A208763] N89-27227

HYDROFLUORIC ACID
Development of a thin wall graphite/polyimide composite pressure vessel with a large aspect ratio
[DE89-002536] N89-26920

HYDROGEN
Space station hydrogen/oxygen thruster technology
[NASA-CR-182280] N89-26905
Degradation of Fe-25Cr, Fe-25Cr-20Ni and Fe-25Cr-6Al alloys in H2/H2O/H2S environments at 700 C
[DE89-011873] N89-26967

HYDROGEN BONDS
Blends of poly(enaminonitriles)
[AD-A208441] N89-27017
Synthesis and optical properties of a new class of polyamides containing reactive diacetylene groups
[AD-A208752] N89-27021

HYDROGEN OXYGEN ENGINES
LH sub 2/LO sub 2 rocket engine with solar energy
[NAL-TR-992] N89-26893

HYDROGEN PLASMA
Collision processes of interest in MFE plasma research
[DE89-013681] N89-27524

HYDROGENATION
Thermodynamic equilibria in the biphenyl/hydrogen system (the power and limitations of group additivity estimations)
[DE89-000754] N89-26954
Modifiers in rhodium catalysts for carbon monoxide hydrogenation: Structure-activity relationships
[DE89-013802] N89-27028

HYDROLYSIS
Fluids, gels and glasses under extreme conditions of pressure and temperature
[AD-A205292] N89-26927
Synthesis and characterization of Group 4 organometal oxide complexes
[DE89-010944] N89-26932

HYPERBOLIC DIFFERENTIAL EQUATIONS
Efficient grid generation
[NASA-CR-185034] N89-27434

HYPERSONIC FLOW
Experimental program for real gas flow code validation at NASA Ames Research Center
[NASA-TM-100093] N89-26816
High speed corner and gap-seal computations using an LU-SGS scheme
[NASA-TM-102138] N89-27103

HYPERSONIC SHOCK
An investigation into the use of an existing shock tube as a driver for a hypersonic shock tunnel
[AD-A208483] N89-26872

HYPERSONIC WIND TUNNELS
An investigation into the use of an existing shock tube as a driver for a hypersonic shock tunnel
[AD-A208483] N89-26872

HYPERSONICS
An investigation into the use of an existing shock tube as a driver for a hypersonic shock tunnel
[AD-A208483] N89-26872

HYPERVELOCITY FLOW
Hypervelocity atmospheric flight: Real gas flow fields
[NASA-TM-101055] N89-27117

HYPERVELOCITY LAUNCHERS
Demonstration of oblique detonation wave for hypersonic propulsion
[AD-A208268] N89-26856

HYPERVELOCITY PROJECTILES
Demonstration of oblique detonation wave for hypersonic propulsion
[AD-A208268] N89-26856

HYSTERESIS
Synthesis and optical properties of a new class of polyamides containing reactive diacetylene groups
[AD-A208752] N89-27021

I

ICE
Investigations of dielectric properties of some frozen materials using cross-borehole radiowave pulse transmissions
[AD-A207302] N89-27285

ICE MAPPING
GEOSAT altimeter sea-ice mapping
[AD-A207391] N89-27234

IDEAL FLUIDS
Ideal jet flow in two dimensions
[AD-A208275] N89-27131

IDEAL GAS
Statistics of an integrable discrete Sine Gordon system
[PREPRINT-638] N89-27128

IGNITION
Afterburner flameholder construction
[AD-D014116] N89-26852
Hot surface ignition tests of aircraft fluids
[AD-A207372] N89-26937
Feasibility demonstration of the Thermal Ignition Combustion System (TICS) for high pressure natural gas injected engine
[PB89-178792] N89-26944

IGNITION SYSTEMS
Combustion characteristics of dry coal-powder-fueled adiabatic diesel engine
[DE89-000978] N89-27197

IGNITION TEMPERATURE
Hot surface ignition tests of aircraft fluids
[AD-A207372] N89-26937

ILMENITE
Characterization of lunar ilmenite resources
[DE89-013455] N89-27618

IMAGE ANALYSIS
Comparison of spectral data gathered from a laboratory spectrometer and TM images with and without shadow correction
[DE89-010877] N89-27237

IMAGE FILTERS
Implementation of an order filter and its applications in radar imagery (SAR)
[INPE-4749-PRE/1422] N89-27385
IMAGE PROCESSING
Window generator
[AD-D014068] N89-27048
Performance comparison among several filters for the reducton of speckle noise in radar imagery
[INPE-4768-PRE/1437] N89-27055
An expert system for fault diagnosis in digital circuits
[INPE-4743-PRE/1417] N89-27085
Development of a second-generation, video-based luminance mapper for daylighting research
[DE89-000850] N89-27143
Theory of X-ray holography including phase and amplitude contrast and finite transfer functions
[DE89-012635] N89-27148
SP-ATUS: An expert system for specifications of satellite imagery
[INPE-4754-PRE/1426] N89-27236
Modeling of the angular reflectance of an artificial plant canopy near the retroreflection peak in the optical regime
[DE89-011174] N89-27239
Satellite image processing using symbolic structures of reduced vision conditions
[INPE-4638-TDL/337] N89-27367
Classification by maximum likelihood method of the massively parallel environment
[INPE-4765-PRE/1434] N89-27380
Abstract data types in computer graphics and image processing
[INPE-4745-PRE/1419] N89-27381
implementation of an order filter and its applications in radar imagery (SAR)
[INPE-4749-PRE/1422] N89-27385
Applications of numerical models for elevation and integration with digital images
[INPE-4776-PRE/1445] N89-27392
image algebra synthesis
[AD-A207257] N89-27425
Multiple sensor fusion for detecting targets in FLIR (Forward-Looking Infrared) and range images
[AD-A207577] N89-27502
IMAGE ROTATION
Rotation of images by scan mirrors
[NASA-TM-101628] N89-27504
IMAGING TECHNIQUES
Development of magnetic resonance imaging technology for imaging binder distribution in ceramics
[DE89-013185] N89-27003
An approach to accurate X-ray mask measurements in a scanning electron microscope
[PB89-172555] N89-27137
Applications of holography to pattern recognition and optical memories
[PB89-174668] N89-27146
An efficient exact algorithm for the least squares image registration problems
[DE89-013116] N89-27387
Rotation of images by scan mirrors
[NASA-TM-101628] N89-27504
IMPACT ACCELERATION
Injuries to seat occupants of light airplanes
[AD-A207579] N89-26830
IMPACT DAMAGE
Injuries to seat occupants of light airplanes
[AD-A207579] N89-26830
Composite transport wing technology development
[NASA-CR-178409] N89-26842
IMPACT LOADS
Nonlinear dynamic response of pressurized composite bottles subjected to shock loading
[DE89-010553] N89-26922
Characterization of Morton-Thiokol booster-rocket propellant TP-H1207C and its simulant H-19
[DE89-013347] N89-27031
IMPACT RESISTANCE
Evaluation of barrier cable impact pad materials
[AD-A207554] N89-26864
IMPACT TESTS
Composite transport wing technology development
[NASA-CR-178409] N89-26842
Measured damping and modulus of composite cylinders
[DE89-010369] N89-27209
Fate and effects of PAHs in the terrestrial environment: An overview
[DE89-010319] N89-27267
Safety testing program for the Galileo mission radioisotope thermoelectric generator
[DE89-011192] N89-27494
IMPACT TOLERANCES
Evaluation of barrier cable impact pad materials
[AD-A207554] N89-26864
IMPEDANCE MATCHING
Proceedings of the Switched Power Workshop: Power Supply Working Group
[DE89-012293] N89-27077
IMPINGEMENT
Self-locking outer air seal with full backside cooling
[AD-D013975] N89-27179
IMPLOSIONS
Two-dimensional effects in hollow core z-pinches
[DE89-014188] N89-27531
Two-dimensional effects in imploding plasma liners
[DE89-014482] N89-27534
IMPREGNATING
Processing of continuous fiber composites
[DE89-012608] N89-26915
IMPULSES
The effects of steep-front, short-duration impulses on power distribution components
[DE89-012338] N89-27091
IMPURITIES
Optical detection and spectroscopy of single molecules in a solid
[AD-A207594] N89-26940
Local density theory of heats of formation and short-range order parameters in substitutionally disordered alloys
[DE89-014696] N89-26986
Crystallization of paraxylene with scraped surface heat exchangers
[WTHD-189] N89-27570
INCIDENCE
ELLIPSE user's manual and program reference
[DE89-014575] N89-27398
INCLINATION
Relativistic explanation of the inclination of planetary orbits
[PB89-170005] N89-27611
INCOMPRESSIBLE FLOW
MHD forced and free convection boundary layer flow near the leading edge
[DE88-705974] N89-26812
A dual potential formulation of the Navier-Stokes equations
[NASA-CR-185098] N89-27111
Numerical solution of the Navier-Stokes equations for three-dimensional incompressible flows with open boundaries
[DE89-009333] N89-27119
Study of subgrid models in incompressible turbulent flow, homogeneous or inhomogeneous
[ONERA-RSF-17/3619-AY-110-A] N89-27123
INDENTATION
The use of field indentation microprobe in measuring mechanical properties of welds
[DE89-013548] N89-27211
Estimating fracture toughness using tension or ball indentation tests and a modified critical strain model
[DE89-010324] N89-27220
INDIAN OCEAN
Trace gases in and over the West Pacific and East Indian Oceans during the El Nino-southern oscillation event of 1987: A report of GMCC (Geophysical Monitoring for Climatic Change) data collected on the second Soviet-American Gas and Aerosol Experiment (SAGA 2)
[PB89-159685] N89-27280
INDIUM PHOSPHIDES
MeV implantation studies in LPE-grown GaAs and InP
[AD-A207220] N89-27550
INDUCTION
The short-circuited fluxgate output current
[ISSN-0109-6605] N89-27069
INDUSTRIAL WASTES
Analytical procedures for environmental quality control, volume 1
[PB89-158604] N89-27266
INELASTIC COLLISIONS
Multiparticle dynamics at the Sp(-)p collider
[NOTA-INTERNA-929] N89-27490
INELASTIC SCATTERING
Final state effects in liquid He4: An experimental test
[DE89-012615] N89-27472
INELASTIC STRESS
Inelastic buckling of channel columns in the distortional mode
[PB89-156053] N89-27207
INERTIA
Geodetic precession or dragging of inertial frames
[NASA-TM-100744] N89-27458
INERTIAL CONFINEMENT FUSION
Recent progress in the Los Alamos KrF Program
[DE88-016235] N89-27493
Electrohydrodynamically driven, large-area liquid metal ion source for inertial confinement fusion
[DE89-012665] N89-27530
INERTIAL GUIDANCE
Cost-optimal state feedback controller for all-attitude gimbal system
[AD-D013972] N89-26845
INFORMATION DISSEMINATION
Study for an advanced civil earth remote sensing system. Volume 1: Executive summary
[PB89-163257] N89-27231
Study for an advanced civil earth remote sensing system. Volume 2: Market and financial assessment
[PB89-163265] N89-27232
INFORMATION MANAGEMENT
Electronic information delivery at the job site
[DE89-009726] N89-27350
Management Information Database System
[DE89-014595] N89-27597
INFORMATION PROCESSING (BIOLOGY)
Categorization in neural networks and prosopagnosia
[PREPRINT-608] N89-27327
The effect of synapses destruction on categorization by neural networks
[PREPRINT-609] N89-27328
INFORMATION RETRIEVAL
User guide for the Data Analysis, Retrieval, and Tabulation System (DARTS): A mainframe computer code for generating cross-tabulation reports
[DE89-012930] N89-27592
Empirical analysis and refinement of expert system knowledge bases
[AD-A208294] N89-27598
INFORMATION SYSTEMS
Altimetric system: Earth observing system. Volume 2h: Panel report
[NASA-TM-89722] N89-27229
Criteria for selecting a CO2/climate change region of study
[DE89-011233] N89-27268
Advanced information processing system: Input/output system services
[NASA-CR-181674] N89-27413
INFORMATION THEORY
Information capacity of additive Gaussian channels with jamming
[AD-A207256] N89-27051
INFRARED ABSORPTION
Infrared temperature measurement with self regulating emission ratio
[ETN-89-94654] N89-27157
INFRARED ASTRONOMY
Observing primeval galaxies and dark matter with LAIRTS — Large Aperture Infra-Red Telescope System
[AD-A208286] N89-27606
INFRARED IMAGERY
GEOSAT altimeter sea-ice mapping
[AD-A207391] N89-27234
Multiple sensor fusion for detecting targets in FLIR (Forward-Looking Infrared) and range images
[AD-A207577] N89-27502
INFRARED INSTRUMENTS
Development of a system model and Least Mean Square (LMS) filter for the Naval Postgraduate School (NPS) Infrared Search and Target Designation System (IRSTD)
[AD-A208536] N89-27068
INFRARED LASERS
Selective nitrations: Laser-induced nitrations
[AD-A207406] N89-27024
Report of the Workshop on Scientific Opportunities for Infrared Free-Electron Lasers, volume 1
[DE89-012836] N89-27170
INFRARED RADAR
Multiple sensor fusion for detecting targets in FLIR (Forward-Looking Infrared) and range images
[AD-A207577] N89-27502
INFRARED RADIATION
Dispersed and periodic microstructures for magnetic and infrared absorbers
[AD-A207428] N89-27053
Report of the Workshop on Scientific Opportunities for Infrared Free-Electron Lasers, volume 1
[DE89-012836] N89-27170
INFRARED SPECTRA
Molecular sieve films from zeolited-silica microcomposites
[DE89-009831] N89-26921
Infrared temperature measurement with self regulating emission ratio
[ETN-89-94654] N89-27157
INFRARED SPECTROMETERS
Evaluation of a FTIR (Fourier Transform Infrared Spectrometer) mobile source measurement system
[PB89-180822] N89-27147
INFRARED SPECTROSCOPY
Micropyrolyzer design for infrared spectroscopy applications
[DE89-013329] N89-26949

INGESTION
Noise produced by turbulent flow into a rotor: Theory manual for atmospheric turbulence prediction and mean flow and turbulence contraction prediction
[NASA-CR-181789] N89-27466
INHOMOGENEITY
A procedure for computing surface wave trajectories on an inhomogeneous surface
[NASA-TP-2929] N89-26811
INITIATION
Thin pulse shock initiation characterization of extrusion-cast explosives: Revision
[DE89-008029] N89-27027
INJECTION
Development of theoretical and numerical techniques for achieving stability in gyrotron traveling-wave amplifiers
[AD-A207451] N89-27140
INJECTION LASERS
High power semiconductor laser sources
[AD-A207569] N89-27167
INJURIES
Injuries to seat occupants of light airplanes
[AD-A207579] N89-26830
INPUT
Advanced information processing system: Input/output system services
[NASA-CR-181874] N89-27413
INSOLATION
Solar radiation on Mars
[NASA-TM-102299] N89-27623
INSPECTION
Quality in automation project for FY 88
[PB89-193296] N89-27040
INSTRUMENT LANDING SYSTEMS
ILS/MLS collocation tests at Miami/Tamiami, Florida Airport
[NASA-CR-185715] N89-26832
An operational demonstration and flight test of the Microwave Landing System (MLS) at the Miami/Tamiami, Florida Airport
[DOT/FAA/CT-TN89/37] N89-26833
INTEGRAL EQUATIONS
An approach for constructing families of homogenized equations for periodic media. 2: Properties of the kernel
[AD-A207573] N89-27428
INTEGRATED CIRCUITS
The 14th Convention on Radio Science, Finnish National Committee of URSI held in Otaniemi (Finland) on October 17-18, 1988: Abstracts of papers
[PB89-145767] N89-27044
Theoretical analysis of microwave and millimeter wave integrated circuits based on magnetic films
[AD-A207508] N89-27074
Narrow-angle laser scanning microscope system for linewidth measurements on wafers
[PB89-189344] N89-27174
A radiation-hardened 16/32-bit microprocessor
[DE89-008111] N89-27357
A virtual zero-time, monolithic systolic sorting array
[DE89-007515] N89-27394
A hydrid 3 Gs/s, 6-bit digital to analog converter
[DE89-012302] N89-27552
INTERACTIVE CONTROL
GEO-EAS (Geostatistical Environmental Assessment Software) user's guide
[PB89-151252] N89-27261
Northeast Artificial Intelligence Consortium annual report 1987. Volume 3: Distributed artificial intelligence for communications network management
[AD-A208379] N89-27419
INTERFACES
The NASA Langley Research Center 0.3-meter transonic cryogenic tunnel T-P/Re-M controller manual
[NASA-CR-181868] N89-26869
Interface modified glass fiber/thermoplastic matrix composites
[AD-A207308] N89-26910
Synthesis and optical properties of a new class of polyamides containing reactive diacetylene groups
[AD-A208752] N89-27021
Optimum interface properties for metal matrix composites
[NASA-TM-102295] N89-27223
Automatic treatment of natural language in processes in the acquisition of knowledge
[INPE-4737-PRE/1412] N89-27382
XCL: A family of programming lanquage-based shell s
[DE89-013442] N89-27388
INTERFEROMETRY
Interferometric load sensor and strain gage
[AD-D014122] N89-27142
Group index and time delay measurements of a standard reference fiber
[PB89-189179] N89-27457
INTERMETALLICS
History of the application of the generalized Lewis acid-base theory to metals
[DE89-012992] N89-26984
INTERNAL COMBUSTION ENGINES
Lean-burn gas engine ignition processes
[PB89-181119] N89-26943
INTERPOLATION
A direct procedure for interpolation on a structured curvilinear two-dimensional grid
[NASA-TM-102213] N89-27433
INTERSTELLAR MATTER
Commentary on interstellar matter associated with 18 open clusters
[NASA-RP-1229] N89-27612
The molecular cloud content of early type galaxies. 1: Detections and global properties
[PB89-184949] N89-27613
INVENTIONS
Nozzle flange attachment and sealing arrangement
[AD-D014123] N89-26853
Interferometric load sensor and strain gage
[AD-D014122] N89-27142
Low frequency structureborne vibration isolation mount
[AD-D014133] N89-27192
INVENTORIES
Regional ozone modeling in the northeastern US: Selection of meteorological episodes
[PB89-136691] N89-27259
Procedures for the preparation of emission inventories for precursors of ozone, volume 1, third edition
[PB89-154209] N89-27264
INVISCID FLOW
Inviscid spatial stability of a compressible mixing layer. Part 3: Effect of thermodynamics
[NASA-CR-181855] N89-27112
ION ATOM INTERACTIONS
Influence of particle collisions on the characteristics of H-like ion emission due to charge exchange reactions with fast atoms
[IPP-III/142] N89-27480
ION BEAMS
Loss of grain boundary segregant during ion milling
[DE89-007835] N89-26979
Materials analysis with nuclear microprobes: Superconductors and buried conductors
[DE89-008580] N89-27206
Study of the microstructure of silver films deposited by ion assisted deposition onto aluminum oxide substrates
[DE89-014665] N89-27563
ION CURRENTS
Supersonics
[AD-A207394] N89-26814
ION CYCLOTRON RADIATION
A new version of the full-wave ICRH code FISIC for plasmas with noncircular flux surfaces
[IPP-5/25] N89-27537
ION EMISSION
Influence of particle collisions on the characteristics of H-like ion emission due to charge exchange reactions with fast atoms
[IPP-III/142] N89-27480
ION IMPLANTATION
An Auger sputter profiling study of nitrogen and oxygen ion implantation in two titanium alloys
[DE89-014734] N89-26987
New strategies for display devices based on 2-6 materials
[AD-A208288] N89-27573
ION MICROSCOPES
Novel applications of the field ion microscope and atom-probe
[DE89-008684] N89-27154
ION SELECTIVE ELECTRODES
JTECH (Japanese Technology Evaluation Program) panel report on advanced sensors in Japan
[PB89-158760] N89-27136
ION SOURCES
Electrohydrodynamically driven, large-area liquid metal ion source for inertial confinement fusion
[DE89-012665] N89-27530
ION TRAPS (INSTRUMENTATION)
Explosives detection with an ion trap mass spectrometer
[DE89-012510] N89-27029
IONIZATION
Electron-impact ionization time-of-flight mass spectrometer for molecular beams
[AD-A207585] N89-27141
Measurement of the time-dependent distribution of ionization states in an argon plasma from a Mach-10 jet
[DE89-014699] N89-27526
A method to calibrate the light response of a high resolution electromagnetic calorimeter with cosmic rays
[NOTA-INTERNA-925] N89-27631
IONOSPHERIC SOUNDING
Ionospheric plasma escape by high-altitude electric fields: Magnetic moment pumping
[IRF-PREPRINT-111] N89-27542
IONS
Integral constitutive relation for the investigation of ion Bernstein waves in non-homogeneous plasmas
[IPP-5/27] N89-27538
IRON ALLOYS
The solidification metallurgy of Alloy 718 and other Nb-containing superalloys
[DE89-008196] N89-26966
Breakdown mechanisms of Al2O3, Cr2O3 and SiO2 scales in H2/H2O/H2S environments, volume 1
[DE89-014789] N89-26988
ISOPROPYL COMPOUNDS
Dynamics of surface bound polymers and coupling agents
[AD-A208747] N89-27020
ISOTOPIC SPIN
Physics with ETA mesons
[DE89-012582] N89-27478
ISOTROPIC MEDIA
Statistics of fracture in two grades of isotropic graphite
[DE89-013703] N89-26916
ISOTROPY
Statistics of fracture in two grades of isotropic graphite
[DE89-013703] N89-26916
ITERATION
Theoretical analysis of microwave and millimeter wave integrated circuits based on magnetic films
[AD-A207508] N89-27074
On a computational method for the second fundamental tensor and its application to bifurcation problems
[AD-A207517] N89-27377
Indirect addressing and load balancing for faster solution to Mandelbrot Set on SIMD architectures
[NASA-CR-181847] N89-27390
Accuracy increase in waveform Gauss Seidel
[DE89-014812] N89-27437
ITERATIVE SOLUTION
Local mode smoothing analysis of various two-dimensional incomplete factorization iterative methods
[REPT-88-67] N89-27431

J

JACOBI MATRIX METHOD
Automatic generation of FORTRAN-coded Jacobians and Hessians
[MEMO-INF-88-47] N89-27402
JAMMING
Information capacity of additive Gaussian channels with jamming
[AD-A207256] N89-27051
Capacity of the Poisson channel with time-varying noise intensity and jamming
[AD-A207225] N89-27446
JAPAN
JTECH (Japanese Technology Evaluation Program) panel report on advanced sensors in Japan
[PB89-158760] N89-27136
JET ENGINE FUELS
Hot surface ignition tests of aircraft fluids
[AD-A207372] N89-26937
Thermal stability of jet fuel
[DE89-013516] N89-27032
JET ENGINES
KC-135R rumble investigation
[AD-A207532] N89-27464
JET FLOW
An experimental investigation of the ground vortex created by a moving jet
[NASA-CR-181841] N89-26815
Base wakes from two dimensional jets in subsonic flow with injection
[IMFL-86/20] N89-27125
Ideal jet flow in two dimensions
[AD-A208275] N89-27131
JET VANES
Variable nozzle area turbine vane cooling
[AD-D014071] N89-26849
JOINTS (JUNCTIONS)
Nozzle flap hinge joint
[AD-D014002] N89-26847
Dual load path pin clevis joint
[AD-D014081] N89-27188
JOURNAL BEARINGS
Stability of a rigid rotor supported on oil-film journal bearings under dynamic load
[NASA-TM-102309] N89-27114

JP-4 JET FUEL
Detonability of hydrocarbon fuels in air
[DE89-008801] N89-26926

K

K-EPSILON TURBULENCE MODEL
Investigation of the transient fuel preburner manifold and combustor
[NASA-CR-183715] N89-26900
KARMAN VORTEX STREET
Construction of differential equations from experimental data of Karman vortex streets
[MPIS-11/1988] N89-27127
KERNEL FUNCTIONS
Kernel user's manual version 1.0
[AD-A207414] N89-27375
An approach for constructing families of homogenized equations for periodic media. 2: Properties of the kernel
[AD-A207573] N89-27428
KEVLAR (TRADEMARK)
Nonlinear dynamic response of pressurized composite bottles subjected to shock loading
[DE89-010553] N89-26922
Compressive properties of high performance polymeric fibers
[AD-A207271] N89-26998
KINEMATIC EQUATIONS
An objective comparison of vertical motions from the kinematic method and three forms of the omega equation
[AD-A208451] N89-27294
KINEMATICS
An objective comparison of vertical motions from the kinematic method and three forms of the omega equation
[AD-A208451] N89-27294
Brief instructions for SIMBAT, a computer package for unconditional and conditional simulation of ocean wave kinematics
[AD-A207627] N89-27324
KINETIC ENERGY
Directed energy weapons/en dash/lasers: Ground- and space-based systems
[DE89-012804] N89-27452
KINETICS
Studies of the fundamental nature of catalytic acidity, sites and intermediates
[DE89-012946] N89-26947
KNOWLEDGE BASES (ARTIFICIAL INTELLIGENCE)
Empirical analysis and refinement of expert system knowledge bases
[AD-A208294] N89-27598
KNOWLEDGE REPRESENTATION
Explanation in expert systems: A survey
[NASA-CR-185335] N89-27364
Northeast Artificial Intelligence Consortium annual report 1987. Volume 2, part b: Diecussing, using, and recognizing plans
[AD-A208378] N89-27418
Research in knowledge delivery
[AD-A208327] N89-27599
KOVAR (TRADEMARK)
A method of removing oxides from the surface of Fe-Ni-Co alloy particles by chemical etching
[DE89-014597] N89-27009
KRYPTON
Z-pinch experiments on Saturn at 30 TW
[DE89-013497] N89-27523
KRYPTON FLUORIDE LASERS
Recent progress in the Los Alamos KrF Program
[DE88-016235] N89-27493

L

LABORATORIES
National Engineering Laboratory's 1989 report to the National Research Council's Board on Assessment of NIST (National Institute of Standards and Technology) programs
[PB89-189294] N89-27602
LABORATORY EQUIPMENT
Large protein crystallization facility, phase A. Executive summary
[AQ-ES-175/88] N89-27035
LAGRANGE MULTIPLIERS
Lagrangian turbulence near walls: Structures and mixing in admissible model flows
[AD-A208466] N89-27135
LAKES
Assessing the sensitivity of high altitude New Mexican wilderness lakes to acidic precipitation and trace metal contamination
[PB89-148456] N89-27262
LAMINAR BOUNDARY LAYER
Feasibility and benefits of laminar flow control on supersonic cruise airplanes
[NASA-CR-181817] N89-26841
A review of high-speed, convective, heat-transfer computation methods
[NASA-TP-2914] N89-27116
LAMINAR FLOW
Wind-tunnel investigation of aerodynamic characteristics and wing pressure distributions of an airplane with variable-sweep wings modified for laminar flow
[NASA-TM-4124] N89-26810
Feasibility and benefits of laminar flow control on supersonic cruise airplanes
[NASA-CR-181817] N89-26841
Finite control volume modeling of laminar and turbulent flow of air in an enclosure
[DE89-009334] N89-27120
LAMINAR HEAT TRANSFER
Finite control volume modeling of laminar and turbulent flow of air in an enclosure
[DE89-009334] N89-27120
LAMINATES
Composite transport wing technology development
[NASA-CR-178409] N89-26842
Tailoring of composite links for optimal damped elasto-dynamic performance
[NASA-TM-102094] N89-26912
On processing development for fabrication of fiber reinforced composite, part 2
[NASA-CR-181866] N89-26917
A three-node C deg element for analysis of laminated composite sandwich shells
[NASA-TM-4125] N89-27213
Advanced electron beam evaporation
[ETN-89-94799] N89-27495
Magnetic multilayers
[ETN-89-94294] N89-27547
Superconductivity and magnetism in layered materials
[AD-A208487] N89-27576
LANDING MODULES
NASA's Chemical Transfer Propulsion Program for Pathfinder
[NASA-TM-102298] N89-26876
LANDSAT SATELLITES
Study for an advanced civil earth remote sensing system. Volume 1: Executive summary
[PB89-163257] N89-27231
Study for an advanced civil earth remote sensing system. Volume 2: Market and financial assessment
[PB89-163265] N89-27232
LANTHANUM OXIDES
Composition of superconducting La2CuO4 + delta: A superconductor doped by excess oxygen defects
[DE89-013299] N89-27555
LARGE SCALE INTEGRATION
Radiation evaluation of several complex very large scale integration circuits
[DE89-007985] N89-27090
LARGE SPACE STRUCTURES
Modeling and computational algorithms for parameter estimation and optimal control of aeroelastic systems and large flexible structures
[AD-A208274] N89-27404
LASER ANEMOMETERS
Study of a turbulent boundary layer by laser plane visualization
[IMFL-88/33] N89-27124
Battery-driven miniature LDA system with semiconductor laser diode
[ISL-CO-214/88] N89-27176
LASER APPLICATIONS
Selective nitrations: Laser-induced nitrations
[AD-A207406] N89-27024
Partial support of the 3rd International Laser Science Conference held in Atlantic City, New Jersey on 1-4 November 1987
[AD-A206812] N89-27161
Report of the Workshop on Scientific Opportunities for Infrared Free-Electron Lasers, volume 1
[DE89-012836] N89-27170
Prospects for the FEL (Free Electron Laser)
[DE89-012998] N89-27175
Bibliography of Soviet laser developments, No. 92, November - December 1987
[AD-A207794] N89-27177
LASER DOPPLER VELOCIMETERS
Battery-driven miniature LDA system with semiconductor laser diode
[ISL-CO-214/88] N89-27176
LASER FUSION
Recent progress in the Los Alamos KrF Program
[DE88-016235] N89-27493
LASER INTERFEROMETRY
Frequency division multiplexing of interferometric sensor arrays
[AD-A208448] N89-27510
LASER MATERIALS
Passive optical losses in laser glass
[DE89-013784] N89-27172
LASER MICROSCOPY
Narrow-angle laser scanning microscope system for linewidth measurements on wafers
[PB89-189344] N89-27174
LASER OUTPUTS
Analysis and evaluation of technical data on the photochromic and non-linear optical properties of materials
[AD-A207275] N89-27000
Compact, lightweight CO2 lasers for SDIO applications
[AD-A207052] N89-27162
High energy laser target plate
[AD-D014053] N89-27164
Transverse pumping with diode lasers
[AD-A207261] N89-27165
Deep space LADAR, phase 1
[AD-A207454] N89-27166
Free electron lasers with small period wigglers
[DE89-014715] N89-27173
Mechanisms that control the geometry of pulsed Nd:YAG laser welds
[DE89-014490] N89-27200
Molecules in intense laser fields
[DE89-013807] N89-27479
Z-pinch experiments on Saturn at 30 TW
[DE89-013497] N89-27523
LASER PLASMAS
Measurement of the time-dependent distribution of ionization states in an argon plasma from a Mach-10 jet
[DE89-014698] N89-27526
LASER PUMPING
Selective nitrations: Laser-induced nitrations
[AD-A207406] N89-27024
Transverse pumping with diode lasers
[AD-A207261] N89-27165
LASER SPECTROSCOPY
Optical detection and spectroscopy of single molecules in a solid
[AD-A207594] N89-26940
Laser spectroscopy and dynamics of combustion intermediates
[DE89-014498] N89-26956
LASER STABILITY
Laser dyes derived from bimanes
[AD-D013994] N89-27160
Compact, lightweight CO2 lasers for SDIO applications
[AD-A207052] N89-27162
LASER TARGET INTERACTIONS
High energy laser target plate
[AD-D014053] N89-27164
LASER WELDING
Mechanisms that control the geometry of pulsed Nd:YAG laser welds
[DE89-014490] N89-27200
LASERS
Closing photoconductive semiconductor switches
[DE89-013073] N89-27082
Computer code prediction of picosecond voltage switching and TEM wave generation in air gas avalanche switches
[DE89-013778] N89-27084
Center for Electronics and Electrical Engineering Technical Progress Bulletin covering center programs, October to December 1988 with 1989 CEEE events calender
[PB89-193270] N89-27087
Electron-impact ionization time-of-flight mass spectrometer for molecular beams
[AD-A207585] N89-27141
Partial support of the 3rd International Laser Science Conference held in Atlantic City, New Jersey on 1-4 November 1987
[AD-A206812] N89-27161
Passive optical losses in laser glass
[DE89-013784] N89-27172
Directed energy weapons/en dash/lasers: Ground- and space-based systems
[DE89-012804] N89-27452
LATERAL CONTROL
Feasibility study for enhanced lateral control of the P-3C aircraft
[AD-A208461] N89-26863
LATTICE VIBRATIONS
A microstructural investigation of the shear distortions and energetics of motions observed in an aged high damping 53Cu-45Mn-2Al alloy
[AD-A208467] N89-26991

LAUNCH VEHICLES
Two-stage reusable launch system utilizing a winged core vehicle and glideback boosters
[NASA-TM-101513] N89-26878
Big dumb boosters: A low-cost space transportation option. An OTA (Office of Technology and Assessment) background paper
[PB89-155196] N89-26881
LEADING EDGES
MHD forced and free convection boundary layer flow near the leading edge
[DE88-705974] N89-26812
The structure of Normal-Shock/Turbulent-Boundary-Layer interactions modified by mass removal
[AD-A208402] N89-27134
LEAKAGE
Total-dose hardness assurance for space applications of commercial CMOS devices
[DE89-006765] N89-27089
LEAST SQUARES METHOD
Development of a system model and Least Mean Square (LMS) filter for the Naval Postgraduate School (NPS) Infrared Search and Target Designation System (IRSTD)
[AD-A208536] N89-27068
An efficient exact algorithm for the least squares image registration problems
[DE89-013116] N89-27387
The least squares solution of linear equations with block-angular observation matrix
[NPL-DITC-139/89] N89-27444
LEVITATION
Attractive levitation for high-speed ground transport with large guideway clearance and alternating-gradient stabilization
[DE89-013640] N89-27195
LIAPUNOV FUNCTIONS
Linearization of nonlinear systems
[AD-A206073] N89-27423
LIFE SUPPORT SYSTEMS
Research and development of anti-G life support systems. Part 4: Engineering test and evaluation of six anti-G valves
[AD-A206996] N89-27341
LIFT
The conceptional design study of USB powered lift aircrafts in FY 1986
[NAL-TR-958] N89-26835
LIGANDS
Synthesis and characterization of Group 4 organometal oxide complexes
[DE89-010944] N89-26932
LIGHT (VISIBLE RADIATION)
Meridian variations in spectral dark adaptation
[AD-A207248] N89-27331
NIST (National Institute of Standards and Technology) research reports, March 1989
[PB89-189310] N89-27594
LIGHT AIRCRAFT
Injuries to seat occupants of light airplanes
[AD-A207579] N89-26830
LIGHT GAS GUNS
Characterization of Morton-Thiokol booster-rocket propellant TP-H1207C and its simulant H-19
[DE89-013347] N89-27031
LIGHT SCATTERING
Dynamics of double stimulated Brillouin scattering
[PB89-146369] N89-27513
LIGHT SOURCES
Evaluation of an updated design of an internally lighted wind cone
[DOT/FAA/CT-TN89/45] N89-26868
Fiber optic rotary switching device
[AD-D013978] N89-27497
LIGHT TRANSMISSION
The quantitative dependence of transmissivity on flexural strain for multimode optical fiber
[AD-A207522] N89-27501
LIGHTNING
The effects of steep-front, short-duration impulses on power distribution components
[DE89-012338] N89-27091
Lightning: Understanding it and protecting systems from its effects
[DE89-012796] N89-27308
LIGHTNING SUPPRESSION
The effects of steep-front, short-duration impulses on power distribution components
[DE89-012338] N89-27091
Lightning: Understanding it and protecting systems from its effects
[DE89-012796] N89-27308
LIMITERS (FUSION REACTORS)
Limiter H-modes in the JIPP T-IIU tokamak
[IPPJ-898] N89-27511
LINE SPECTRA
Influence of particle collisions on the characteristics of H-like ion emission due to charge exchange reactions with fast atoms
[IPP-III/142] N89-27480
The 15N NMR powder spectra of semicrystalline nylon 6
[AD-A208502] N89-27577
LINEAR ACCELERATORS
Proceedings of the Switched Power Workshop: Power Supply Working Group
[DE89-012293] N89-27077
Elements of a realistic 17 GHz FEL/TBA design
[DE89-013427] N89-27169
Beam-gas background rejection in L3 first level energy transfer
[NOTA-INTERNA-919] N89-27496
LINEAR EQUATIONS
Use of the Fox derivatives in the solution of the word problem for groups
[DE88-705978] N89-27421
The least squares solution of linear equations with block-angular obeservation matrix
[NPL-DITC-139/89] N89-27444
LINEAR INTEGRATED CIRCUITS
Implementation of a design for testability strategy using the Genesil silicon compiler
[AD-A208458] N89-27099
LINEAR PROGRAMMING
On the feasibility of a generalized linear program
[AD-A207402] N89-27373
Semi-infinite programming
[AD-A207403] N89-27374
An efficient exact algorithm for the least squares image registration problems
[DE89-013116] N89-27387
Portable parallel programming in a FORTRAN environment
[DE89-014670] N89-27399
LINEARIZATION
Satellite attitude control analysis and design using linearizing transformations
[INPE-4772-PRE/1441] N89-26886
Linearization of nonlinear systems
[AD-A206073] N89-27423
LINKAGES
Tailoring of composite links for optimal damped elasto-dynamic performance
[NASA-TM-102094] N89-26912
LIQUID HELIUM
Design and operation of a horizontal liquid helium flow facility
[DE89-013482] N89-26867
Optical detection and spectroscopy of single molecules in a solid
[AD-A207594] N89-26940
Momentum distributions in liquid helium
[DE89-014679] N89-26953
Liquid helium fluid dynamics studies
[DE89-013124] N89-27036
Final state effects in liquid He4: An experimental test
[DE89-012615] N89-27472
LIQUID HELIUM 2
Transient heat transfer into superfluid helium under confined conditions
[DE88-706312] N89-27109
LIQUID LASERS
Bibliography of Soviet laser developments, No. 92, November - December 1987
[AD-A207794] N89-27177
LIQUID METALS
MHD forced and free convection boundary layer flow near the leading edge
[DE88-705974] N89-26812
Electrohydrodynamically driven, large-area liquid metal ion source for inertial confinement fusion
[DE89-012665] N89-27530
LIQUID PHASE EPITAXY
MeV implantation studies in LPE-grown GaAs and InP
[AD-A207220] N89-27550
LIQUID PROPELLANT ROCKET ENGINES
NASA's Chemical Transfer Propulsion Program for Pathfinder
[NASA-TM-102298] N89-26876
LIQUID SLOSHING
Modeling of liquid sloshing effects in multi body systems
[MBB-UK-0024/88-PUB] N89-26891
LIQUID SURFACES
Design and characterization of large-drop generators for viscous, Newtonian, and non-Newtonian liquids
[AD-A208330] N89-27133
LIQUID-SOLID INTERFACES
Transient cooling of a hot surface by droplets evaporation
[PB89-161897] N89-27100
LIQUID-VAPOR INTERFACES
Transient cooling of a hot surface by droplets evaporation
[PB89-161897] N89-27100
LIQUIDS
Fluids, gels and glasses under extreme conditions of pressure and temperature
[AD-A205292] N89-26927
LISP (PROGRAMMING LANGUAGE)
Automatic generation of FORTRAN-coded Jacobians and Hessians
[MEMO-INF-88-47] N89-27402
LITHIUM
Supersonics
[AD-A207394] N89-26814
LITHIUM ALLOYS
Microstructural evolution of Al-Li and Al-Li-Cu-Mg alloys
[DE89-012981] N89-26972
LITHIUM COMPOUNDS
Polarization matrices of lithium tantalate
[AD-A208349] N89-27097
LITHIUM NIOBATES
Polarization matrices of lithium niobate
[AD-A207231] N89-27462
LITHIUM SULFUR BATTERIES
Development of compressed multifoil insulation for high-temperature batteries and other applications
[DE89-012877] N89-27092
LITHOGRAPHY
An approach to accurate X-ray mask measurements in a scanning electron microscope
[PB89-172555] N89-27137
LITHOLOGY
Quantitative three-dimensional structural techniques
[DE89-010879] N89-27238
LOAD TESTS
On internal bending-beam strain-gage wind tunnel balances
[RR-070] N89-26870
LOADS (FORCES)
Space Shuttle Main Engine structural analysis and data reduction/evaluation. Volume 7: High pressure fuel turbo-pump third stage impeller analysis
[NASA-CR-183670] N89-26894
Interferometric load sensor and strain gage
[AD-D014122] N89-27142
Dual load path pin clevis joint
[AD-D014081] N89-27188
Structural analysis of a thermal insulation retainer assembly
[NASA-TM-101580] N89-27212
LOGARITHMS
Lognormal distribution maximum-likelihood parameter estimation algorithms
[AD-A207586] N89-27378
LOGIC CIRCUITS
Back-up control system for f101 engine and its derivatives
[AD-D014051] N89-26848
An expert system in C for computer-aided digital circuit design
[AD-A207518] N89-27075
An expert system for fault diagnosis in digital circuits
[INPE-4743-PRE/1417] N89-27085
LOGIC DESIGN
Easily testable PLA-based finite state machines
[AD-A208371] N89-27098
LOOPS
Note on multiloop calculations for superstrings in the NSR formalism
[PREPRINT-601] N89-27581
LORAN C
Loran C coverage in Alaska after dual rating Port Clarence
[AD-A196032] N89-26831
LOSSES
Loss of grain boundary segregant during ion milling
[DE89-007835] N89-26979
LOW COST
Big dumb boosters: A low-cost space transportation option. An OTA (Office of Technology and Assessment) background paper
[PB89-155196] N89-26881
LOW FREQUENCIES
On transformer modeling. A physically based three-phase transformer model for the study of low frequency phenomena in electrical power systems
[ETN-89-94801] N89-27095
Low-frequency sound propagation modeling over a locally-reacting boundary using the parabolic approximation
[NASA-CR-185864] N89-27469

LOW LEVEL TURBULENCE
Development of Low-Level Turbulence (LLT) forecasting methodologies
[AD-A208457] N89-27320
LOW NOISE
Low noise crystal controlled oscillator
[AD-D014070] N89-27072
LOW PASS FILTERS
On capture effect of FM demodulators
[AD-A208479] N89-27066
Algorithms for computer aided design of digital filters
[AD-A208485] N89-27410
LOW PRESSURE
Analysis of low-pressure gas-phase pyrolytic reactions by mass spectrometric techniques
[AD-A207457] N89-26939
LOW TEMPERATURE
Cryogenic tensile properties of AA 2090 weldments
[DE89-012979] N89-26971
Bearings fabricated from rapidly solidified powder and method
[AD-D014072] N89-27185
Synoptic forcing of East Asian cold surges
[AD-A208765] N89-27321
LOW THRUST
The NASA low thrust propulsion program
[NASA-TM-102065] N89-26895
LUBRICATING OILS
Hot surface ignition tests of aircraft fluids
[AD-A207372] N89-26937
LUBRICATION
Advanced ceramics: A critical assessment of wear and lubrication
[PB89-188569] N89-27005
Computational methods for nonlinear dynamic problems in solid and structural mechanics: Progress in the theory and modeling of friction and in the control of dynamical systems with frictional forces
[AD-A208763] N89-27227
LUMINANCE
Aircraft color displays: Chromaticity and luminance requirements
[AD-A206786] N89-26828
Development of a second-generation, video-based luminance mapper for daylighting research
[DE89-000850] N89-27143
LUMINOUS INTENSITY
System for measuring optical waveguide intensity profiles
[PB89-188593] N89-27507
LUNAR BASES
Lunar production of solar cells
[NASA-TM-102102] N89-27619
LUNAR ROCKS
Characterization of lunar ilmenite resources
[DE89-013455] N89-27618
LUNGS
Short course on cardiopulmonary aspects of aerospace medicine
[AGARD-R-758-ADD] N89-27330
LUTETIUM
Magnetic and electrical properties of sandwich-like lanthanide phthalocyanines
[AD-A208411] N89-26958

M

MACH NUMBER
Absolute/convective instabilities and the convective Mach number in a compressible mixing layer
[NASA-CR-181861] N89-27113
MACHINE TOOLS
Quality in automation project for FY 88
[PB89-193296] N89-27040
MACHINING
Quality in automation project for FY 88
[PB89-193296] N89-27040
MAGMA
Drilling operations plan for the Magma Energy Exploratory Well
[DE89-010037] N89-27240
Computer simulations of explosive volcanic eruptions
[DE89-014024] N89-27290
MAGNESIUM ALLOYS
Microstructural evolution of Al-Li and Al-Li-Cu-Mg alloys
[DE89-012981] N89-26972
MAGNESIUM ISOTOPES
Development of advanced methods based on stable isotope technology for studies of exercise in heat
[AD-A208758] N89-27329
MAGNET COILS
Improved core insulation schemes for multi-terawatt magnetic switches
[DE89-013814] N89-27093
Cryogenic techniques for large superconducting magnets in space
[DE89-013431] N89-27455
MAGNETIC CONTROL
Passive superconductor: A viable method of controlling magnetization multipoles in the SSC dipole
[DE89-013432] N89-27559
MAGNETIC CORES
Improved core insulation schemes for multi-terawatt magnetic switches
[DE89-013814] N89-27093
MAGNETIC DIPOLES
Passive superconductor: A viable method of controlling magnetization multipoles in the SSC dipole
[DE89-013432] N89-27559
MAGNETIC FIELD RECONNECTION
The magnetic topology of the plasmoid flux rope in a MHD simulation of magnetotail reconnection
[DE89-012621] N89-27529
MAGNETIC FIELDS
A finite element method for solving electromagnetic scattering problems
[DE89-013496] N89-27059
Static periodic field device for free electron laser
[AD-D014125] N89-27168
Two-dimensional effects in imploding plasma liners
[DE89-014482] N89-27534
MHD calculations of anode plasmas
[DE89-014485] N89-27535
Solar-geophysical data number 535, part 1. Data for February, January 1989, and late data
[PB89-185987] N89-27624
MAGNETIC FILMS
Theoretical analysis of microwave and millimeter wave integrated circuits based on magnetic films
[AD-A207508] N89-27074
Magnetic multilayers
[ETN-89-94294] N89-27547
MAGNETIC FLUX
The magnetic topology of the plasmoid flux rope in a MHD simulation of magnetotail reconnection
[DE89-012621] N89-27529
Mercury's magnetic field: Implications on the inner composition of the planet
[NOTA-INTERNA-926] N89-27620
MAGNETIC LEVITATION VEHICLES
Attractive levitation for high-speed ground transport with large guideway clearance and alternating-gradient stabilization
[DE89-013640] N89-27195
MAGNETIC MATERIALS
Magnetic multilayers
[ETN-89-94294] N89-27547
MAGNETIC MEASUREMENT
Brorfelde Geomagnetic Observatory: Magnetic results, 1986
[ISBN-87-7478-287-8] N89-27293
MAGNETIC MOMENTS
Ionospheric plasma escape by high-altitude electric fields: Magnetic moment pumping
[IRF-PREPRINT-111] N89-27542
Resonant helicity flip of electron neutrino due to magnetic moment and dynamics of supernova
[PREPRINT-598] N89-27617
MAGNETIC PROPERTIES
Magnetic and electrical properties of sandwich-like lanthanide phthalocyanines
[AD-A208411] N89-26958
Magneto-optical properties of ultrathin ferromagnetic films
[DE89-014640] N89-27508
Superconductivity and magnetism in layered materials
[AD-A208487] N89-27576
MAGNETIC PUMPING
Ionospheric plasma escape by high-altitude electric fields: Magnetic moment pumping
[IRF-PREPRINT-111] N89-27542
MAGNETIZATION
Passive superconductor: A viable method of controlling magnetization multipoles in the SSC dipole
[DE89-013432] N89-27559
Anomalous temperature dependence of Cu NMR line width and magnetization in YBa2Cu3O(7-delta)
[DE89-014291] N89-27565
MAGNETO-OPTICS
Two-photon absorption characterization of HgCdTe
[AD-A207198] N89-27471
Magneto-optical properties of ultrathin ferromagnetic films
[DE89-014640] N89-27508
MAGNETOHYDRODYNAMIC FLOW
MHD forced and free convection boundary layer flow near the leading edge
[DE88-705974] N89-26812
MAGNETOHYDRODYNAMIC STABILITY
Collisionless tearing instability of a bi-Maxwellian neutral sheet with exact particle orbits
[AD-A207310] N89-27286
Electrohydrodynamically driven, large-area liquid metal ion source for inertial confinement fusion
[DE89-012665] N89-27530
MAGNETOHYDRODYNAMIC TURBULENCE
Dynamics of decaying two-dimensional magnetohydrodynamic turbulence
[IPP-6/279] N89-27541
MAGNETOHYDRODYNAMICS
MHD forced and free convection boundary layer flow near the leading edge
[DE88-705974] N89-26812
Modeling of LH current drive in self-consistent elongated tokamak MHD equilibria
[DE89-013263] N89-27522
The magnetic topology of the plasmoid flux rope in a MHD simulation of magnetotail reconnection
[DE89-012621] N89-27529
Two-dimensional effects in hollow core z-pinches
[DE89-014188] N89-27531
Two-dimensional effects in imploding plasma liners
[DE89-014482] N89-27534
MHD calculations of anode plasmas
[DE89-014485] N89-27535
Equilibrium of solar coronal arcades
[AD-A207311] N89-27622
MAGNETOSPHERIC INSTABILITY
Collisionless tearing instability of a bi-Maxwellian neutral sheet with exact particle orbits
[AD-A207310] N89-27286
MAGNITUDE
Investigations on local seismic phases and evaluation of body waves magnitude
[AD-A206633] N89-27283
MAINTENANCE
Electronic information delivery at the job site
[DE89-009726] N89-27350
MAN MACHINE SYSTEMS
Design considerations of manipulator and feel system characteristics in roll tracking
[NASA-CR-4111] N89-26860
Ergonomic Models of Anthropometry, Human Biomechanics and Operator-Equipment Interfaces
[NASA-CR-185720] N89-27344
MAN-COMPUTER INTERFACE
Northeast artificial intelligence consortium: Volume 2, part A: The Versatile Maintenance Expert System (VMES) research project
[AD-A208344] N89-27417
MANAGEMENT
Cost of quality evaluation methodologies handbook
[AD-A206935] N89-27202
MANAGEMENT INFORMATION SYSTEMS
Management Information Database System
[DE89-014595] N89-27597
MANAGEMENT PLANNING
Cost of quality evaluation methodologies handbook
[AD-A206935] N89-27202
MANEUVERS
Feasibility study for enhanced lateral control of the P-3C aircraft
[AD-A208461] N89-26863
MANGANESE OXIDES
Electrochemical transport of manganese between the flux and the weld metal in submerged arc welding
[DE89-012419] N89-27193
MANIFOLDS
Investigation of the transient fuel preburner manifold and combustor
[NASA-CR-183715] N89-26900
Variable area manifolds for ring mirror heat exchangers
[AD-D014050] N89-27163
MANIPULATORS
Design considerations of manipulator and feel system characteristics in roll tracking
[NASA-CR-4111] N89-26860
Six degrees of freedom micromanipulator
[AD-D014113] N89-27190
Research in autonomous robotics at ORNL using HERMIES-3
[DE89-004933] N89-27198
A model of human reaction time to dangerous robot arm movements
[PB89-186522] N89-27339
MANNED SPACE FLIGHT
The best we can be
[NASA-TM-101781] N89-26873
MANNED SPACECRAFT
NASA's Chemical Transfer Propulsion Program for Pathfinder
[NASA-TM-102298] N89-26876

MANUAL CONTROL
Back-up control system for f101 engine and its derivatives
[AD-D014051] N89-26848
MANUFACTURING
National Engineering Laboratory's 1989 report to the National Research Council's Board on Assessment of NIST (National Institute of Standards and Technology) programs
[PB89-189294] N89-27602
MANY BODY PROBLEM
Modeling of liquid sloshing effects in multi body systems
[MBB-UK-0024/88-PUB] N89-26891
Momentum distributions: An overview
[DE89-012617] N89-27453
MAPPING
Autonomous land navigation: A demonstration of retrotraverse
[DE89-011881] N89-26855
Development of a second-generation, video-based luminance mapper for daylighting research
[DE89-000850] N89-27143
A center for commercial development of space: Real-time satellite mapping. Remote sensing-based agricultural information expert system
[NASA-CR-185473] N89-27235
An Apple-2 compatible program to draw maps containing oceanographic station positions buoy trajectories and the coastal margins of the Antarctic Peninsula and nearby islands
[INPE-4805-RPE/588] N89-27391
Using conjoint meshing primitives to generate quadrilateral and hexahedral elements in irregular regions
[DE89-005918] N89-27435
Stochasticity and symmetry of the standard map
[IPPJ-910] N89-27528
The molecular cloud content of early type galaxies. 1: Detections and global properties
[PB89-184949] N89-27613
Use of the EGRET (Energetic Gamma-Ray Experiment Telescope) in studies of the origin of the cosmic radiation
[DE89-013785] N89-27630
MAPS
GEO-EAS (Geostatistical Environmental Assessment Software) user's guide
[PB89-151252] N89-27261
The 1989 Airborne Arctic Stratospheric Expedition Nimbus-7 TOMS data atlas
[NASA-RP-1227] N89-27302
A graphics package for meteorological data, version 1.5
[NASA-TM-100742] N89-27314
MARINE METEOROLOGY
The international TOVS (Tiros Operational Vertical Sounder) processing package: An evaluation
[AD-A207548] N89-27306
MARINER 10 SPACE PROBE
Mercury's magnetic field: Implications on the inner composition of the planet
[NOTA-INTERNA-926] N89-27620
MARKET RESEARCH
Study for advanced civil earth remote sensing system: Focused finance study. Volume 1: Executive summary
[PB89-163224] N89-27230
MARKETING
Future applications of engine ceramics: Factors influencing market opportunities, timing, and growth
[DE89-012426] N89-27002
Study for an advanced civil earth remote sensing system. Volume 2: Market and financial assessment
[PB89-163265] N89-27232
Sun synchronous solar refrigeration
[DE89-011375] N89-27245
MARKOV PROCESSES
Constant access systems: A general framework for greedy optimization on stochastic networks
[AD-A207525] N89-27448
MARS (PLANET)
Solar radiation on Mars
[NASA-TM-102299] N89-27623
MARS ATMOSPHERE
Solar radiation on Mars
[NASA-TM-102299] N89-27623
MARS SURFACE
Solar radiation on Mars
[NASA-TM-102299] N89-27623
MASERS
Development of theoretical and numerical techniques for achieving stability in gyrotron traveling-wave amplifiers
[AD-A207451] N89-27140
MASS DISTRIBUTION
The structure of Normal-Shock/Turbulent-Boundary-Layer interactions modified by mass removal
[AD-A208402] N89-27134
MASS FLOW
The structure of Normal-Shock/Turbulent-Boundary-Layer interactions modified by mass removal
[AD-A208402] N89-27134
MASS SPECTRA
Thermal stability of jet fuel
[DE89-013516] N89-27032
Electron-impact ionization time-of-flight mass spectrometer for molecular beams
[AD-A207585] N89-27141
Precision measurements without polarization at LEP --- LEP storage ring
[NOTA-INTERNA-921] N89-27483
MASS SPECTROMETERS
Explosives detection with an ion trap mass spectrometer
[DE89-012510] N89-27029
Novel applications of the field ion microscope and atom-probe
[DE89-009684] N89-27154
MASS SPECTROSCOPY
Analysis of low-pressure gas-phase pyrolytic reactions by mass spectrometric techniques
[AD-A207457] N89-26939
Electron-impact ionization time-of-flight mass spectrometer for molecular beams
[AD-A207585] N89-27141
Depth profiles and bulk analysis of semiconductor materials using ICP mass spectroscopy with electrothermal atomization
[AD-A206974] N89-27548
Nitrogen 15 T1 measurements of semicrystalline nylon 6
[AD-A208481] N89-27575
MASS TRANSFER
The structure of Normal-Shock/Turbulent-Boundary-Layer interactions modified by mass removal
[AD-A208402] N89-27134
MASSIVELY PARALLEL PROCESSORS
Classification by maximum likelihood method of the massively parallel environment
[INPE-4765-PRE/1434] N89-27380
MATCHED FILTERS
Evaluation of an optical correlator and matched filter maker
[AD-A207556] N89-27054
MATHEMATICAL MODELS
A procedure for computing surface wave trajectories on an inhomogeneous surface
[NASA-TP-2929] N89-26811
Expendable air vehicles/high altitude balloon technology
[AD-A206972] N89-26813
CFD methods for drag prediction and analysis currently in use in UK N89-26823
Aerodynamic parameters of an advanced fighter aircraft estimated from flight data. Preliminary results
[NASA-TM-101631] N89-26861
Control of flexible structures
[AD-A207520] N89-26883
Study of jitter on the attitude motion of a spin stabilized satellite with two flexible solar panels
[INPE-4744-PRE/1418] N89-26884
Investigation of the transient fuel preburner manifold and combustor
[NASA-CR-183715] N89-26900
Local density theory of heats of formation and short-range order parameters in substitutionally disordered alloys
[DE89-014696] N89-26986
Model-based parameter estimation in electromagnetic computer modeling
[AD-A207399] N89-27052
On transformer modeling. A physically based three-phase transformer model for the study of low frequency phenomena in electrical power systems
[ETN-89-94801] N89-27095
The 1st Scandinavian Conference on Viscous and T urbulent Flow in Hydraulic Machinery
[PB89-161327] N89-27102
Hypervelocity atmospheric flight: Real gas flow fields
[NASA-TM-101055] N89-27117
Numerical solution of the Navier-Stokes equations for three-dimensional incompressible flows with open boundaries
[DE89-009333] N89-27119
Strain to failure of pressurized thick wall cylinders
[DE89-009969] N89-27219
Estimating fracture toughness using tension or ball indentation tests and a modified critical strain model
[DE89-010324] N89-27220
Quantitative three-dimensional structural techniques
[DE89-010879] N89-27238
Comparison of modelled and measured tracer gas concentrations during the Across North America Tracer Experiment (ANATEX)
[PB89-136709] N89-27260
Joint CGS-AOML (Charting and Geodetic Service-Atlantic Oceanographic and Meteorological Laboratory) acoustical bottom echo-formation research. 2: Field experiment results and recommendations for echo-sounder design
[PB89-152417] N89-27322
Summary of research conducted at the Institute for Computer Applications in Science and Engineering in applied mathematics, numerical analysis and computer science
[NASA-CR-181858] N89-27348
Natural language processing
[INPE-4449-TDL/314] N89-27366
Applications of numerical models for elevation and integration with digital images
[INPE-4776-PRE/1445] N89-27392
Aircraft flight test trajectory control
[NASA-CR-4161] N89-27416
Transactions of the 6th Army Conference on Applied Mathematics and Computing held in Boulder, Colorado on 31 May - 3 June 1988
[AD-A207252] N89-27424
Solution of deterministic differential games: The approximate strategy method
[ONERA-NT-1987-6] N89-27450
ROUTEMAP model for predicting noise exposure from aircraft operations on Military Training Routes
[AD-A203849] N89-27459
Noise produced by turbulent flow into a rotor: Theory manual for atmospheric turbulence prediction and mean flow and turbulence contraction prediction
[NASA-CR-181789] N89-27466
Low-frequency sound propagation modeling over a locally-reacting boundary using the parabolic approximation
[NASA-CR-185864] N89-27469
Dynamics of double stimulated Brillouin scattering
[PB89-146369] N89-27513
Fast wave current drive modeling for ITER and prospects for a near-term proof of principle experiment
[DE89-013049] N89-27520
Modeling of LH current drive in self-consistent elongated tokamak MHD equilibria
[DE89-013263] N89-27522
Dynamics of the solar system: Proceedings, volume 3
[DE89-609828] N89-27615
MATHEMATICAL PROGRAMMING
Semi-infinite programming
[AD-A207403] N89-27374
Classification by maximum likelihood method of the massively parallel environment
[INPE-4765-PRE/1434] N89-27380
MATRICES (MATHEMATICS)
Heuristic algorithms for stability testing polytopes of matrices
[PB89-160840] N89-27365
Row-oriented direct solving of linear algebraic equations. Inverse projection method
[REPT-88-81] N89-27432
The least squares solution of linear equations with block-angular observation matrix
[NPL-DITC-139/89] N89-27444
Polarization matrices of lithium niobate
[AD-A207231] N89-27462
MATRIX MATERIALS
Low loss radar window for reentry vehicle
[AD-D014045] N89-26882
Method to produce titanium metal matrix composites with improved fracture and creep resistance
[AD-D014111] N89-26911
Tailoring of composite links for optimal damped elasto-dynamic performance
[NASA-TM-102094] N89-26912
Metal matrix composite micromechanics: In-situ behavior influence on composite properties
[NASA-TM-102302] N89-26924
Fatigue crack growth study of SCS6/Ti-15-3 composite
[NASA-TM-102332] N89-26989
A method of removing oxides from the surface of Fe-Ni-Co alloy particles by chemical etching
[DE89-014597] N89-27009
Automated immersion testing robotic system: Hardware and software design
[AD-A208755] N89-27201

Optimum interface properties for metal matrix composites
[NASA-TM-102295] N89-27223

MATRIX METHODS
Dynamic analysis of flexible mechanisms by a combined transfer matrix finite element method
[PB89-160865] N89-27181
On the multiplicity and symmetries of the bifurcation branching point in the square clamped plate
[PREPRINT-604] N89-27224

MAXIMUM ENTROPY METHOD
Macromolecular calculations for the XTAL system of crystallographic programs
[AD-A208272] N89-27572

MAXIMUM LIKELIHOOD ESTIMATES
Lognormal distribution maximum-likelihood parameter estimation algorithms
[AD-A207586] N89-27378
Classification by maximum likelihood method of the massively parallel environment
[INPE-4765-PRE/1434] N89-27380

MAXWELL EQUATION
Equilibrium of a plasma in the fluid- and Vlasov-Maxwell systems
[DE89-013315] N89-27518

MEAN SQUARE VALUES
Development of a system model and Least Mean Square (LMS) filter for the Naval Postgraduate School (NPS) Infrared Search and Target Designation System (IRSTD)
[AD-A208536] N89-27068

MEASURE AND INTEGRATION
On the integrability of the Ernst equation
[PREPRINT-606] N89-27584

MEASURING INSTRUMENTS
Standardized piezoelectric polymer (PVDF) gauge for detonator response measurement
[DE89-010437] N89-27144
Narrow-angle laser scanning microscope system for linewidth measurements on wafers
[PB89-189344] N89-27174

MECHANICAL ENGINEERING
Interactions between the National Institute of Standards and Technology and the American Society of Mechanical Engineers
[PB89-172563] N89-27182
Technical Abstracts, 1988
[DE89-012811] N89-27591

MECHANICAL PROPERTIES
SiC-MoSi composites
[DE89-013656] N89-26923
Metal matrix composite micromechanics: In-situ behavior influence on composite properties
[NASA-TM-102302] N89-26924
Effects of high thermal and high fast fluences on the mechanical properties of type 6061 aluminum in the HFBR
[DE89-012636] N89-26970
Mechanical property enhancement in ceramic matrix composites
[PB89-189138] N89-27007
Wideband electromagnetic damping of vibrating structures
[AD-D014069] N89-27208
The HERMOD behavioral synthesis system
[AD-A207319] N89-27371
ASR4: A computer code for fitting and processing 4-gage anelastic strain recovery data
[DE89-012239] N89-27395
MeV implantation studies in LPE-grown GaAs and InP
[AD-A207220] N89-27550
Recent improvements in bulk properties of ceramic superconductors
[DE89-013626] N89-27562

MEDICAL SERVICES
Annual historical report - AMEDD activities
[AD-A208301] N89-27333

MEMBRANES
Gas separations using inorganic membranes
[DE89-013010] N89-26948

MEMORY (COMPUTERS)
Applications of holography to pattern recognition and optical memories
[PB89-174668] N89-27146
Competitive management of distributed shared memory
[AD-A207322] N89-27372

MENTAL HEALTH
Psychological attributes, coping strategies and other factors associated with ultramarathon performance
[AD-A208300] N89-27340

MENTAL PERFORMANCE
Human performance assessment methods
[AGARD-AG-308] N89-27338

MERCURY (PLANET)
Mercury's magnetic field: Implications on the inner composition of the planet
[NOTA-INTERNA-926] N89-27620

MERCURY CADMIUM TELLURIDES
Two-photon absorption characterization of HgCdTe
[AD-A207198] N89-27471

MESONS
Theoretical studies in elementary particle physics
[DE89-012701] N89-27473
Physics with ETA mesons
[DE89-012582] N89-27478
Vertex detectors at e(+) e(-) B meson factories
[NOTA-INTERNA-914] N89-27486

MESSAGE PROCESSING
Suitability of message passing computers for implementing production systems
[AD-A207321] N89-27411

MESSAGES
Suitability of message passing computers for implementing production systems
[AD-A207321] N89-27411

METAL FATIGUE
Advanced durability analysis. Volume 2: Analytical predictions, test results and analytical correlations
[AD-A207215] N89-26838
Fracture toughness of SiC/Al metal matrix composite
[NASA-TM-100745] N89-26918
Evaluation of weldment creep and fatigue strength-reduction factors for elevated-temperature design
[DE89-008242] N89-27218

METAL FILMS
Method for calibrating a heat flux gauge
[AD-D013974] N89-27138
Study of the microstructure of silver films deposited by ion assisted deposition onto aluminum oxide substrates
[DE89-014665] N89-27563

METAL FINISHING
Effect of oxidation, sandblasting and pickling on weldability
[DE89-013795] N89-26975

METAL FOILS
Development of compressed multifoil insulation for high-temperature batteries and other applications
[DE89-012877] N89-27092

METAL IONS
Electrohydrodynamically driven, large-area liquid metal ion source for inertial confinement fusion
[DE89-012665] N89-27530

METAL MATRIX COMPOSITES
Method to produce metal matrix composite articles from rich metastable-beta titanium alloys
[AD-D014064] N89-26907
Method to produce metal matrix composite articles from lean metastable beta titanium alloys
[AD-D014065] N89-26908
Method to produce titanium metal matrix composites with improved fracture and creep resistance
[AD-D014111] N89-26911
Erosion of Al and Al/SiC
[DE89-013623] N89-26913
Fracture toughness of SiC/Al metal matrix composite
[NASA-TM-100745] N89-26918
Metal matrix composite micromechanics: In-situ behavior influence on composite properties
[NASA-TM-102302] N89-26924
Statistical strength comparison of metal-matrix and polymeric-matrix composites
[AD-A208316] N89-26925
Measured damping and modulus of composite cylinders
[DE89-010369] N89-27209
Optimum interface properties for metal matrix composites
[NASA-TM-102295] N89-27223
Fate and effects of PAHs in the terrestrial environment: An overview
[DE89-010319] N89-27267

METAL OXIDE SEMICONDUCTORS
Dual-transistor method to determine delta V sub ot and delta V sub it for MOS devices
[DE89-006725] N89-27088
The 1/f noise: A nondestructive technique to predict MOS radiation hardness
[DE89-007419] N89-27205

METAL PARTICLES
A method of removing oxides from the surface of Fe-Ni-Co alloy particles by chemical etching
[DE89-014597] N89-27009

METAL PLATES
An experimental study of the effect of stainless steel cladding on the structural integrity of flawed steel plates in bending
[DE89-008735] N89-26980

METAL POWDER
Bearings fabricated from rapidly solidified powder and method
[AD-D014072] N89-27185

METAL STRIPS
The diagonal strip system in the Macro experiment
[NOTA-INTERNA-924] N89-27159

METAL SURFACES
A method of removing oxides from the surface of Fe-Ni-Co alloy particles by chemical etching
[DE89-014597] N89-27009

METALS
Polycrystal plasticity as applied to the problem of in-plane anisotropy in rolled cubic metals
[DE89-011181] N89-26983
Structural integrity evaluation based on an innovative field indentation microprobe
[DE89-010840] N89-27156

METASTABLE STATE
Method to produce metal matrix composite articles from rich metastable-beta titanium alloys
[AD-D014064] N89-26907
Method to produce metal matrix composite articles from lean metastable beta titanium alloys
[AD-D014065] N89-26908

METEOROLOGICAL PARAMETERS
The international TOVS (Tiros Operational Vertical Sounder) processing package: An evaluation
[AD-A207548] N89-27306
A graphics package for meteorological data, version 1.5
[NASA-TM-100742] N89-27314

METEOROLOGICAL RADAR
Observations of atmospheric emission and attenuation at 20.6, 31.65 and 90 GHz by a ground-based radiometer
[NASA-CR-185719] N89-27257

METEOROLOGICAL SATELLITES
The international TOVS (Tiros Operational Vertical Sounder) processing package: An evaluation
[AD-A207548] N89-27306

METEOROLOGICAL SERVICES
Meteorological database and synthesis for the Gulf of Mexico
[PB89-178222] N89-27311

METEOROLOGY
Regional ozone modeling in the northeastern US: Selection of meteorological episodes
[PB89-136691] N89-27259
Dual-channel microwave radiometer for airborne meteorological applications
[PB89-159693] N89-27298
Low relative humidity in the atmosphere
[AD-A207558] N89-27307
Evolution and structure of the bow echo/microburst events
[PB89-174767] N89-27309
Meteorological database and synthesis for the Gulf of Mexico
[PB89-178222] N89-27311

METHANE
Lean-burn gas engine ignition processes
[PB89-181119] N89-26943
Catalytic combustion of methane
[PB89-188874] N89-26946

METHYL ALCOHOL
Studies of the fundamental nature of catalytic acidity, sites and intermediates
[DE89-012946] N89-26947

METHYL COMPOUNDS
Catalytic reduction of carbon dioxide by metal centers
[AD-A207227] N89-26934

METROLOGY
The 14th Convention on Radio Science, Finnish National Committee of URSI held in Otaniemi (Finland) on October 17-18, 1988: Abstracts of papers
[PB89-145767] N89-27044
Emerging technologies in electronics and their measurement needs
[PB89-189245] N89-27078
Thermoelectric terminology in metrology and standards
[DE89-011512] N89-27079
Narrow-angle laser scanning microscope system for linewidth measurements on wafers
[PB89-189344] N89-27174

MICROANALYSIS
Micropyrolyzer design for infrared spectroscopy applications
[DE89-013329] N89-26949
Quantitative thin film X-ray microanalysis of Nb modified Ti3Al
[DE89-009946] N89-26981
Novel applications of the field ion microscope and atom-probe
[DE89-008684] N89-27154

Structural integrity evaluation based on an innovative field indentation microprobe
[DE89-010840] N89-27156
Materials analysis with nuclear microprobes: Superconductors and buried conductors
[DE89-008580] N89-27206
The use of field indentation microprobe in measuring mechanical properties of welds
[DE89-013548] N89-27211

MICROBURSTS (METEOROLOGY)
Evolution and structure of the bow echo/microburst events
[PB89-174767] N89-27309

MICROCOMPUTERS
The NASA Langley Research Center 0.3-meter transonic cryogenic tunnel T-P/Re-M controller manual
[NASA-CR-181868] N89-26869
Development of a second-generation, video-based luminance mapper for daylighting research
[DE89-000850] N89-27143
Electronic information delivery at the job site
[DE89-009726] N89-27350
On-line computer utilization to understand some physical processes (example: Pendulum motion)
[NOTA-INTERNA-927] N89-27360
Lognormal distribution maximum-likelihood parameter estimation algorithms
[AD-A207586] N89-27378

MICROELECTRONICS
Emerging technologies in electronics and their measurement needs
[PB89-189245] N89-27078

MICROMECHANICS
Tailoring of composite links for optimal damped elasto-dynamic performance
[NASA-TM-102094] N89-26912
Metal matrix composite micromechanics: In-situ behavior influence on composite properties
[NASA-TM-102302] N89-26924
Micromechanical characterization of near-surface layers
[DE89-008710] N89-27199

MICROPROCESSORS
Radiation evaluation of several complex very large scale integration circuits
[DE89-007985] N89-27090
Film annotation system for a space experiment
[NASA-CR-185114] N89-27152
A radiation-hardened 16/32-bit microprocessor
[DE89-008111] N89-27357
Processor control path synthesis: Literature survey and preliminary analysis
[MEMO-INF-88-46] N89-27401

MICROSCOPY
X-ray holography: A history
[DE89-012983] N89-27149
X-ray microscopy using synchrotron radiation
[NASA-CR-184800] N89-27155

MICROSTRIP ANTENNAS
Dual frequency microstrip antenna
[AD-D014019] N89-27046
Theoretical analysis of microwave and millimeter wave integrated circuits based on magnetic films
[AD-A207508] N89-27074

MICROSTRIP TRANSMISSION LINES
Theoretical analysis of microwave and millimeter wave integrated circuits based on magnetic films
[AD-A207508] N89-27074

MICROSTRUCTURE
Method to produce titanium metal matrix composites with improved fracture and creep resistance
[AD-D014111] N89-26911
Erosion of Al and Al/SiC
[DE89-013623] N89-26913
Nanostructure and defect chemistry of relaxor ferro electrics
[AD-A207217] N89-26933
Method for making an integral titanium alloy article having at least two distinct microstructural regions
[AD-D014066] N89-26960
Method for refining microstructures of blended elemental titanium powder compacts
[AD-D014067] N89-26961
The recrystallization and respheroidization of tungsten grains in a tungsten-heavy alloy
[AD-A207647] N89-26964
Method for developing ultrafine microstructures in titanium alloy castings
[AD-D014115] N89-26965
The solidification metallurgy of Alloy 718 and other Nb-containing superalloys
[DE89-008196] N89-26966
Degradation of Fe-25Cr, Fe-25Cr-20Ni and Fe-25Cr-6Al alloys in H2/H2O/H2S environments at 700 C
[DE89-011873] N89-26967
Observations on the mechanisms of fatigue in eutectic Pb-Sn solder joints
[DE89-000553] N89-26968
Microstructural evolution of Al-Li and Al-Li-Cu-Mg alloys
[DE89-012981] N89-26972
Analysis of microstructural development in single crystal welds
[DE89-013537] N89-26973
The effect of aging at 343 deg C on type 308 stainless steel welds
[DE89-013545] N89-26974
Quantitative thin film X-ray microanalysis of Nb modified Ti3Al
[DE89-009946] N89-26981
Cross-sectional TEM (Transmission Electron Microscopy) studies of Cr films deposited by ion-assisted deposition and physical vapor deposition
[DE89-014643] N89-26985
Effect of heating rate to test temperature on superplastic response in an Al-6 percent Mg-1 percent Li-0.2 percent Zr alloy
[AD-A208462] N89-26990
A microstructural investigation of the shear distortions and energetics of motions observed in an aged high damping 53Cu-45Mn-2Al alloy
[AD-A208467] N89-26991
Thermomechanical processing of aluminum alloy 2090 for superplasticity
[AD-A208764] N89-26992
Fractographic study of a silicon nitride ceramic
[DE89-013012] N89-27006
Structural ceramics in the advanced materials world
[DE89-013046] N89-27008
Dynamic mechanical investigations of LLDPE/PC blends
[NPL-DMA(A)-177] N89-27010
Thermal and mechanical properties of polyurethane-diacetylene segmented copolymers. Part 2: Effects of diacetylene cross-polymerization
[AD-A208754] N89-27023
Dispersed and periodic microstructures for magnetic and infrared absorbers
[AD-A207428] N89-27053
High-temperature flaw assessment procedure: A state-of-the-art survey
[DE89-012740] N89-27210
The study of structure-processing-property relations in copper oxide-based high T sub c superconductors
[DE89-012764] N89-27554
Study of the microstructure of silver films deposited by ion assisted deposition onto aluminum oxide substrates
[DE89-014665] N89-27563

MICROWAVE ANTENNAS
Dual frequency microstrip antenna
[AD-D014019] N89-27046

MICROWAVE COUPLING
Theoretical analysis of microwave and millimeter wave integrated circuits based on magnetic films
[AD-A207508] N89-27074

MICROWAVE EQUIPMENT
Techniques for the detection of explosives
[DE89-012570] N89-27030

MICROWAVE IMAGERY
Solar microwave radiation maps measured at Metsaehovi Radio Research Station in 1982 - 1983
[PB89-154876] N89-27621

MICROWAVE LANDING SYSTEMS
ILS/MLS collocation tests at Miami/Tamiami, Florida Airport
[NASA-CR-185715] N89-26832
An operational demonstration and flight test of the Microwave Landing System (MLS) at the Miami/Tamiami, Florida Airport
[DOT/FAA/CT-TN89/37] N89-26833

MICROWAVE RADIOMETERS
Altimetric system: Earth observing system. Volume 2h: Panel report
[NASA-TM-89722] N89-27229
Attitude angle effects on Nimbus-7 Scanning Multichannel Microwave Radiometer radiances and geophysical parameter retrievals
[NASA-TM-4132] N89-27289
Dual-channel microwave radiometer for airborne meteorological applications
[PB89-159693] N89-27298

MICROWAVE SENSORS
GEOSAT altimeter sea-ice mapping
[AD-A207391] N89-27234

MICROWAVE SPECTRA
Theoretical analysis of microwave and millimeter wave integrated circuits based on magnetic films
[AD-A207508] N89-27074

MICROWAVES
Development of a high power microwave thruster, with a magnetic nozzle, for space applications
[NASA-TM-102321] N89-26904
Measurements of complex permittivity of microwave substrates in the 20 to 300 K temperature range from 26.5 to 40.0 GHz
[NASA-TM-102123] N89-27038
Dispersed and periodic microstructures for magnetic and infrared absorbers
[AD-A207428] N89-27053
Microwave hardening technology development program
[AD-A207535] N89-27076
Antiproton and millimeter wave research
[AD-A208363] N89-27491
Solar microwave radiation maps measured at Metsaehovi Radio Research Station in 1982 - 1983
[PB89-154876] N89-27621

MILITARY OPERATIONS
Annual historical report - AMEDD activities
[AD-A208301] N89-27333

MILITARY TECHNOLOGY
Compact, lightweight CO2 lasers for SDIO applications
[AD-A207052] N89-27162

MILLIMETER WAVES
Millimeter-wave propagation characteristics and channel performance for urban-suburban environments
[PB89-180251] N89-27058
Theoretical analysis of microwave and millimeter wave integrated circuits based on magnetic films
[AD-A207508] N89-27074
Antiproton and millimeter wave research
[AD-A208363] N89-27491

MILLING
Loss of grain boundary segregant during ion milling
[DE89-007835] N89-26979

MINIATURIZATION
Miniature high voltage solid state relay
[AD-D013979] N89-27070
Battery-driven miniature LDA system with semiconductor laser diode
[ISL-CO-214/88] N89-27176

MINORITIES
User guide for the Data Analysis, Retrieval, and Tabulation System (DARTS): A mainframe computer code for generating cross-tabulation reports
[DE89-012930] N89-27592

MIRRORS
Variable area manifolds for ring mirror heat exchangers
[AD-D014050] N89-27163
Optical mirror coated with organic superconducting material
[AD-D014047] N89-27499
Rotation of images by scan mirrors
[NASA-TM-101628] N89-27504

MISALIGNMENT
Mechanical property enhancement in ceramic matrix composites
[PB89-189138] N89-27007

MISSILE DEFENSE
SDS software measurement requirements
[AD-A207449] N89-27376
Directed energy weapons/en dash/lasers: Ground- and space-based systems
[DE89-012804] N89-27452
Shield optimization program. Part 1: Executive summary
[DE89-013335] N89-27476

MIXING
Mixing and combustion of pulsed gas jets
[PB89-155550] N89-26929
Inviscid spatial stability of a compressible mixing layer. Part 3: Effect of thermodynamics
[NASA-CR-181855] N89-27112

MIXING LAYERS (FLUIDS)
Design and calibration of the mixing layer and wind tunnel
[NASA-CR-185472] N89-26866
Absolute/convective instabilities and the convective Mach number in a compressible mixing layer
[NASA-CR-181861] N89-27113

MIXTURES
Blends of poly(enaminonitriles)
[AD-A208441] N89-27017

MODAL RESPONSE
Space Shuttle Main Engine structural analysis and data reduction/evaluation. Volume 7: High pressure fuel turbo-pump third stage impeller analysis
[NASA-CR-183670] N89-26894
Tailoring of composite links for optimal damped elasto-dynamic performance
[NASA-TM-102094] N89-26912

MODELS
Easily testable PLA-based finite state machines
[AD-A208371] N89-27098
MODEMS
Programmable rate modem utilizing digital signal processing techniques
[NASA-CR-185124] N89-26879
MODULATION
Advanced modulation technology development for earth station demodulator applications
[NASA-CR-185126] N89-26880
Bandwidth efficient coding for error control
[NASA-CR-185836] N89-27062
MODULES
Photovoltaic module on-orbit assembly for Space Station Freedom
[NASA-TM-102297] N89-26887
Low noise crystal controlled oscillator
[AD-D014070] N89-27072
MOISTURE
Field joint protection system rain qualification test report
[NASA-CR-183702] N89-26901
MOJAVE DESERT (CA)
Geodetic measurement of deformation in California
[NASA-TM-100732] N89-27279
MOLECULAR ABSORPTION
Molecular sieve films from zeolited-silica microcomposites
[DE89-009831] N89-26921
Optical detection and spectroscopy of single molecules in a solid
[AD-A207594] N89-26940
MOLECULAR BEAM EPITAXY
Photoelectronic properties of low temperature GaAs grown on silicon and GaAs substrates by MBE
[DE89-013148] N89-27557
MOLECULAR BEAMS
Primary dissociation processes of energetic compounds
[AD-A208312] N89-27033
Electron-impact ionization time-of-flight mass spectrometer for molecular beams
[AD-A207585] N89-27141
MOLECULAR CLOUDS
The molecular cloud content of early type galaxies. 1: Detections and global properties
[PB89-184949] N89-27613
MOLECULAR INTERACTIONS
Molecules in intense laser fields
[DE89-013807] N89-27479
Some considerations on the birth of molecular physics in the first half of the 19th century
[NOTA-INTERNA-917] N89-27482
MOLECULAR SPECTRA
Temporal variability of water masers in the Southern Hemisphere
[INPE-4646-TDL/338] N89-27609
MOLECULAR SPECTROSCOPY
Technical activities 1986-1988, Molecular Spectroscopy Div.
[PB89-175418] N89-26942
MOLECULAR STRUCTURE
Fluids, gels and glasses under extreme conditions of pressure and temperature
[AD-A205292] N89-26927
Synthesis and structural characterization of Pt-Si dimers with unusually short cross-ring silicon-silicon interactions
[AD-A208310] N89-27014
Thermal stability of jet fuel
[DE89-013516] N89-27032
MOLECULES
Optical detection and spectroscopy of single molecules in a solid
[AD-A207594] N89-26940
Primary dissociation processes of energetic compounds
[AD-A208312] N89-27033
High-temperature behavior of grain boundaries from embedded atom method molecular dynamics simulation
[DE89-013641] N89-27474
Macromolecular calculations for the XTAL system of crystallographic programs
[AD-A208272] N89-27572
MOLTEN SALTS
Dynamic simulation of a molten-salt solar receiver
[DE89-010556] N89-27244
MOLYBDENUM
SiC-MoSi composites
[DE89-013656] N89-26923
Modifiers in rhodium catalysts for carbon monoxide hydrogenation: Structure-activity relationships
[DE89-013802] N89-27028
MOMENTUM
Momentum distributions in liquid helium
[DE89-014679] N89-26953
MOMENTUM TRANSFER
Momentum distributions: An overview
[DE89-012617] N89-27453
MONITORS
Quality in automation project for FY 88
[PB89-193296] N89-27040
Sensors for in situ monitoring of elastic properties
[DE89-012795] N89-27145
OTVE turbopump condition monitoring, task E.5
[NASA-CR-182274] N89-27204
MONOCHROMATORS
A fiber optic test system for quantum efficiency measurements
[DE89-012823] N89-27505
MONTE CARLO METHOD
Offline computing farms
[DE89-013958] N89-27359
ORMONTE: An uncertainty analysis code for use with user-developed systems models on mainframe or personal computers. A user's guide
[DE89-013730] N89-27396
Portable parallel programming in a FORTRAN environment
[DE89-014670] N89-27399
Sampling based approaches to calculating marginal densities
[AD-A208388] N89-27451
MOODS
Altitude symptomatology and mood states during a climb to 3630 m
[AD-A208261] N89-27332
MOON
Characterization of lunar ilmenite resources
[DE89-013455] N89-27618
MORALE
New Frontier: Environments for Innovation --- sick building syndrome
[PB89-151054] N89-27601
MORPHOLOGY
Evaluation of mechanical properties of TiN films by ultra-low load indentation
[DE89-009618] N89-26969
Implementation of an order filter and its applications in radar imagery (SAR)
[INPE-4749-PRE/1422] N89-27385
MOTOR VEHICLES
Risk assessment of compressed natural gas-fueled vehicle operations, phase 1
[PB89-188841] N89-27196
Dedicated low-pressure natural gas-fueled vehicle baseline assessment. Task 3 topical report on light-duty vehicles
[PB89-195820] N89-27604
MULTILAYER INSULATION
Development of compressed multifoil insulation for high-temperature batteries and other applications
[DE89-012677] N89-27092
MULTIPLEXING
Deep space LADAR, phase 1
[AD-A207454] N89-27166
MULTIPROCESSING (COMPUTERS)
Data traffic reduction schemes for Cholesky factorization on asynchronous multiprocessor systems
[NASA-CR-181883] N89-27349
Memory-reference characteristics of multiprocessor applications under MACH
[AD-A207318] N89-27352
Parallel implementation of OPS5 on the encore multiprocessor: Results and analysis
[AD-A207320] N89-27353
Implementation indices (1975-1979), volume 1
[AD-A207609] N89-27354
Programming parallel architectures: The BLAZE family of languages
[NASA-CR-185826] N89-27362
Competitive management of distributed shared memory
[AD-A207322] N89-27372
A theoretical investigation of a parallel genetic algorithm
[DE89-012508] N89-27384
Advanced information processing system: Input/output system services
[NASA-CR-181874] N89-27413
MULTISENSOR APPLICATIONS
Multiple sensor fusion for detecting targets in FLIR (Forward-Looking Infrared) and range images
[AD-A207577] N89-27502
MULTISTATIC RADAR
Synthesis of resistive tapers to control scattering patterns of strips
[AD-A207211] N89-27049
MUONS
Search for the inclusive production of J/psi in e(+)e(-) collisions using PLUTO data
[NOTA-INTERNA-923] N89-27484
A method to calibrate the light response of a high resolution electromagnetic calorimeter with cosmic rays
[NOTA-INTERNA-925] N89-27631

N

NASA PROGRAMS
NASA's Chemical Transfer Propulsion Program for Pathfinder
[NASA-TM-102298] N89-26876
NASA SPACE PROGRAMS
The best we can be
[NASA-TM-101781] N89-26873
NATURAL GAS
Feasibility demonstration of the Thermal Ignition Combustion System (TICS) for high pressure natural gas injected engine
[PB89-178792] N89-26944
Fundamental studies of the cavity flowmeter
[PB89-188825] N89-27153
Risk assessment of compressed natural gas-fueled vehicle operations, phase 1
[PB89-188841] N89-27196
Dedicated low-pressure natural gas-fueled vehicle baseline assessment. Task 3 topical report on light-duty vehicles
[PB89-195820] N89-27604
NATURAL LANGUAGE (COMPUTERS)
Explanation in expert systems: A survey
[NASA-CR-185335] N89-27364
Natural language processing
[INPE-4449-TDL/314] N89-27366
Automatic treatment of natural language in processes in the acquistion of knowledge
[INPE-4737-PRE/1412] N89-27382
NAVIER-STOKES EQUATION
High speed corner and gap-seal computations using an LU-SGS scheme
[NASA-TM-102138] N89-27103
Global flows with invariant (Gibbs) measures for Euler and Navier-Stokes two-dimensional fluids
[BIBOS-310/88] N89-27105
A dual potential formulation of the Navier-Stokes equations
[NASA-CR-185098] N89-27111
Interaction between Tollmien-Schlichting waves and free-stream disturbances in boundary-layer flows
[NASA-CR-185847] N89-27118
Numerical solution of the Navier-Stokes equations for three-dimensional incompressible flows with open boundaries
[DE89-009333] N89-27119
Solution of compressible time-dependent Navier-Stokes equations by Chebychev spectral methods
[ONERA-NT-1987-1] N89-27126
Differential forms of Euler's turbo-machinery equation
[AD-A207279] N89-27426
NAVIGATION
Research in autonomous robotics at ORNL using HERMIES-3
[DE89-004933] N89-27198
NAVIGATION AIDS
Cost-optimal state feedback controller for all-attitude gimbal system
[AD-D013972] N89-26845
NEAR FIELDS
Development of near-field test procedures for communication satellite antennas, phase 1, part 2
[PB89-156152] N89-27043
NEODYMIUM LASERS
Mechanisms that control the geometry of pulsed Nd:YAG laser welds
[DE89-014490] N89-27200
NEON
Z-pinch experiments on Saturn at 30 TW
[DE89-013497] N89-27523
NETWORK ANALYSIS
A symbolic generator of state equations for modeling of dynamic systems based on the electrical network analog paradigm
[DE89-013763] N89-27397
Processor control path synthesis: Literature survey and preliminary analysis
[MEMO-INF-88-46] N89-27401
Constant access systems: A general framework for greedy optimization on stochastic networks
[AD-A207525] N89-27448
NETWORK CONTROL
Northeast Artificial Intelligence Consortium annual report 1987. Volume 2, part b: Discussing, using, and recognizing plans
[AD-A208378] N89-27418
NEURAL NETS
Categorization in neural networks and prosopagnosia
[PREPRINT-608] N89-27327

The effect of synapses destruction on categorization by neural networks
[PREPRINT-609] N89-27328

NEUROLOGY
Categorization in neural networks and prosopagnosia
[PREPRINT-608] N89-27327

NEUROPHYSIOLOGY
Design considerations of manipulator and feel system characteristics in roll tracking
[NASA-CR-4111] N89-26860

NEUTRAL PARTICLES
Collisionless tearing instability of a bi-Maxwellian neutral sheet with exact particle orbits
[AD-A207310] N89-27286

NEUTRAL SHEETS
Collisionless tearing instability of a bi-Maxwellian neutral sheet with exact particle orbits
[AD-A207310] N89-27286

NEUTRINOS
Correlation and analysis between the Kamioka neutrino detector data and the Maryland and Rome gravitational antenna data
[NOTA-INTERNA-918] N89-27488
Resonant helicity flip of electron neutrino due to magnetic moment and dynamics of supernova
[PREPRINT-598] N89-27617

NEUTRON DIFFRACTION
Momentum distributions: An overview
[DE89-012617] N89-27453
Final state effects in liquid He4: An experimental test
[DE89-012615] N89-27472
Evidence for phonon-mediated coupling in superconducting Ba sub 0.6 K sub 0.4 BiO3
[DE89-014642] N89-27568

NEUTRON IRRADIATION
Radiation evaluation of several complex very large scale integration circuits
[DE89-007985] N89-27090

NEUTRON SCATTERING
Momentum distributions in liquid helium
[DE89-014679] N89-26953

NEUTRON SPECTROMETERS
Advanced Solar Observatory (ASO) accommodations requirements study
[NASA-CR-183718] N89-26885

NEUTRONS
NIST (National Institute of Standards and Technology) research reports, March 1989
[PB89-189310] N89-27594

NEW MEXICO
Assessing the sensitivity of high altitude New Mexican wilderness lakes to acidic precipitation and trace metal contamination
[PB89-148456] N89-27262

NEWTONIAN FLUIDS
Design and characterization of large-drop generators for viscous, Newtonian, and non-Newtonian liquids
[AD-A208330] N89-27133

NICKEL
The response of single crystal and polycrystal nickel to quasistatic and shock deformation
[DE89-011168] N89-27564

NICKEL ALLOYS
The solidification metallurgy of Alloy 718 and other Nb-containing superalloys
[DE89-008196] N89-26966
Degradation of Fe-25Cr, Fe-25Cr-20Ni and Fe-25Cr-6Al alloys in H2/H2O/H2S environments at 700 C
[DE89-011873] N89-26967
Breakdown mechanisms of Al2O3, Cr2O3 and SiO2 scales in H2/H2O/H2S environments, volume 1
[DE89-014789] N89-26988

NIOBIUM ALLOYS
The solidification metallurgy of Alloy 718 and other Nb-containing superalloys
[DE89-008196] N89-26966
Quantitative thin film X-ray microanalysis of Nb modified Ti3Al
[DE89-009946] N89-26981
A method for generating the J sub c, B, T surface for niobium-alloy superconductors
[DE89-012977] N89-27556

NITRATION
Selective nitrations: Laser-induced nitrations
[AD-A207406] N89-27024

NITRILES
Blends of poly(enaminonitriles)
[AD-A208441] N89-27017

NITROGEN
Thermal stability of jet fuel
[DE89-013516] N89-27032

NITROGEN METABOLISM
Efficiency of N use by wheat as a function of influx and efflux of NO sub 3
[NASA-CR-177534] N89-27346

NITROGEN OXIDES
Adsorption and coadsorption of CO and NO on the Rh(100) surface: A theoretical analysis
[AD-A207323] N89-26935
Selective nitrations: Laser-induced nitrations
[AD-A207406] N89-27024
Procedures for the preparation of emission inventories for precursors of ozone, volume 1, third edition
[PB89-154209] N89-27264
Historic emissions of VOC (Volatile Organic Compounds) and NOx in the United States from 1900 to 1985
[PB89-173223] N89-27270
Efficiency of N use by wheat as a function of influx and efflux of NO sub 3
[NASA-CR-177534] N89-27346

NITROGEN POLYMERS
Natural abundance 15N CP/MAS NMR of solid polyamides: A sensitive technique for examining crystalline composition and conformation in the solid state
[AD-A208563] N89-27019

NITROGEN 15
Nitrogen 15 T1 measurements of semicrystalline nylon 6
[AD-A208481] N89-27575

NOISE (SOUND)
Information capacity of additive Gaussian channels with jamming
[AD-A207256] N89-27051

NOISE INTENSITY
Capacity of the Poisson channel with time-varying noise intensity and jamming
[AD-A207225] N89-27446
Capacity of the poisson channel with random noise intensity
[AD-A207226] N89-27447
Multichannel phase noise measurement system
[AD-D014056] N89-27461
KC-135R rumble investigation
[AD-A207532] N89-27464

NOISE MEASUREMENT
Multichannel phase noise measurement system
[AD-D014056] N89-27461
Noise radiation characteristics of the Westinghouse WWG-0600 (600kW) wind turbine generator
[NASA-TM-101576] N89-27467

NOISE POLLUTION
ROUTEMAP model for predicting noise exposure from aircraft operations on Military Training Routes
[AD-A203849] N89-27459

NOISE PREDICTION
ROUTEMAP model for predicting noise exposure from aircraft operations on Military Training Routes
[AD-A203849] N89-27459
Noise radiation characteristics of the Westinghouse WWG-0600 (600kW) wind turbine generator
[NASA-TM-101576] N89-27467

NOISE REDUCTION
Performance comparison among several filters for the reducton of speckle noise in radar imagery
[INPE-4768-PRE/1437] N89-27055
Implementation of an order filter and its applications in radar imagery (SAR)
[INPE-4749-PRE/1422] N89-27385
Reduction of blade-vortex interaction noise using higher harmonic pitch control
[NASA-TM-101624] N89-27465

NOMENCLATURES
Composites databases for the 1990's
[PB89-180376] N89-26914

NONDESTRUCTIVE TESTS
OTVE combustor wall condition monitoring
[NASA-CR-182275] N89-26899
Structural integrity evaluation based on an innovative field indentation microprobe
[DE89-010840] N89-27156
The 1/f noise: A nondestructive technique to predict MOS radiation hardness
[DE89-007419] N89-27205
Materials analysis with nuclear microprobes: Superconductors and buried conductors
[DE89-008580] N89-27206
Measured damping and modulus of composite cylinders
[DE89-010369] N89-27209
The use of field indentation microprobe in measuring mechanical properties of welds
[DE89-013548] N89-27211
Fate and effects of PAHs in the terrestrial environment: An overview
[DE89-010319] N89-27267
Cepstral method for the measurement of ultrasonic pulse transmission time variations
[AD-A207410] N89-27463

NONLINEAR EVOLUTION EQUATIONS
Universality and integrability of the nonlinear evolution PDEs describing N-wave interactions
[PREPRINT-603] N89-27442

NONLINEAR FEEDBACK
Spin stabilization of the ORION satellite using a thruster attitude control system with optimal control considerations
[AD-A208484] N89-26892

NONLINEAR OPTICS
Bibliography of Soviet laser developments, No. 92, November - December 1987
[AD-A207794] N89-27177
Hybrid single crystal optic fibers by embedding
[AD-D013986] N89-27545

NONLINEAR SYSTEMS
Computational methods for nonlinear dynamic problems in solid and structural mechanics: Progress in the theory and modeling of friction and in the control of dynamical systems with frictional forces
[AD-A208763] N89-27227
Linearization of nonlinear systems
[AD-A206073] N89-27423

NONLINEARITY
Nonlinear dynamic response of pressurized composite bottles subjected to shock loading
[DE89-010553] N89-26922
Metal matrix composite micromechanics: In-situ behavior influence on composite properties
[NASA-TM-102302] N89-26924
Analysis and evaluation of technical data on the photochromic and non-linear optical properties of materials
[AD-A207275] N89-27000
DYNA3D user's manual: (Nonlinear Dynamic Analysis of Structures in Three Dimensions), revision 5
[DE89-014304] N89-27222
Computation and theory in nonlinear optimization
[AD-A207610] N89-27430

NONNEWTONIAN FLUIDS
Design and characterization of large-drop generators for viscous, Newtonian, and non-Newtonian liquids
[AD-A208330] N89-27133

NOSE WHEELS
Acta Aeronautica et Astronautica Sinica, Volume 8, Number 12, December 1987 (selected articles)
[AD-A206782] N89-26807

NOZZLE DESIGN
Variable nozzle area turbine vane cooling
[AD-D014071] N89-26849
Nozzle flange attachment and sealing arrangement
[AD-D014123] N89-26853
Space station hydrogen/oxygen thruster technology
[NASA-CR-182280] N89-26905

NOZZLE FLOW
Nozzle flap hinge joint
[AD-D014002] N89-26847
An investigation into the use of an existing shock tube as a driver for a hypersonic shock tunnel
[AD-A208483] N89-26872

NUCLEAR EXPLOSIONS
Weather predictions and surface radiation estimates for Project BUGGY 1
[DE89-014687] N89-27318

NUCLEAR FUSION
Pacing the US magnetic fusion program
[DE89-012959] N89-27519
Radio frequency plasma heating and current drive
[IPP-6/278] N89-27540

NUCLEAR MAGNETIC RESONANCE
Development of magnetic resonance imaging technology for imaging binder distribution in ceramics
[DE89-013185] N89-27003
Natural abundance 15N CP/MAS NMR of solid polyamides: A sensitive technique for examining crystalline composition and conformation in the solid state
[AD-A208563] N89-27019
Dynamics of surface bound polymers and coupling agents
[AD-A208747] N89-27020
Anomalous temperature dependence of Cu NMR line width and magnetization in YBa2Cu3O(7-delta)
[DE89-014291] N89-27565
O-17 NMR study of YBa2Cu3O(7-delta)
[DE89-014292] N89-27566
Nuclear relaxation rates at copper and oxygen sites in YBa2Cu3O7
[DE89-014308] N89-27567
Nitrogen 15 T1 measurements of semicrystalline nylon 6
[AD-A208481] N89-27575
The 15N NMR powder spectra of semicrystalline nylon 6
[AD-A208502] N89-27577

NUCLEAR POWER PLANTS
Evaluation of weldment creep and fatigue strength-reduction factors for elevated-temperature design
[DE89-008242] N89-27218
On the economic prospects of nuclear fusion with tokamaks
[IPP-6/271] N89-27539
NUCLEAR RELAXATION
Nuclear relaxation rates at copper and oxygen sites in YBa2Cu3O7
[DE89-014308] N89-27567
NUCLEAR WARHEADS
Earth sciences
[DE89-013344] N89-27228
NUCLEAR WEAPONS
Shield optimization program. Part 1: Executive summary
[DE89-013335] N89-27476
NUCLEONS
Quantum and thermodynamic fluctuations in the degenerate schematic model of the finite temperature random phase approximation
[DE88-706310] N89-27580
NUMERICAL ANALYSIS
Numerical computation of bifurcation phenomena and pattern formation in combustion
[DE89-013628] N89-26941
Synthesis of resistive tapers to control scattering patterns of strips
[AD-A207211] N89-27049
Numerical simulation of a turbulent flow through a shock wave
[AD-A207581] N89-27107
Computational methods for nonlinear dynamic problems in solid and structural mechanics: Progress in the theory and modeling of friction and in the control of dynamical systems with frictional forces
[AD-A208763] N89-27227
Summary of research conducted at the Institute for Computer Applications in Science and Engineering in applied mathematics, numerical analysis and computer science
[NASA-CR-181858] N89-27348
The h-p version of the finite element method parabolic equations. Part 2: The h-p version in time
[AD-A207575] N89-27429
Safety in numbers: The boundless errors of numerical computation
[DE89-014813] N89-27438
NUMERICAL STABILITY
Development of theoretical and numerical techniques for achieving stability in gyrotron traveling-wave amplifiers
[AD-A207451] N89-27140
Linearization of nonlinear systems
[AD-A206073] N89-27423
NUTRITION
Effectiveness and acceptability of nutrient solutions in enhancing fluid intake in the heat
[AD-A208428] N89-27337
NUTRITIONAL REQUIREMENTS
Annual historical report - AMEDD activities
[AD-A208301] N89-27333
NYLON (TRADEMARK)
Nitrogen 15 T1 measurements of semicrystalline nylon 6
[AD-A208481] N89-27575
The 15N NMR powder spectra of semicrystalline nylon 6
[AD-A208502] N89-27577

O

OBLIQUE SHOCK WAVES
Demonstration of oblique detonation wave for hypersonic propulsion
[AD-A208268] N89-26856
OCCULTATION
Global environmental effects of impact-generated aerosols: Results from a general circulation model, revision 1
[DE89-014179] N89-27276
OCEAN BOTTOM
Joint CGS-AOML (Charting and Geodetic Service-Atlantic Oceanographic and Meteorological Laboratory) acoustical bottom echo-formation research. 2: Field experiment results and recommendations for echo-sounder design
[PB89-152417] N89-27322
OCEAN SURFACE
Spectra of surface waves
[AD-A208482] N89-27326
OCEAN THERMAL ENERGY CONVERSION
Ocean Energy Program summary. Volume 2: Research summaries, fiscal year 1988
[DE89-000859] N89-27248
OCEANOGRAPHIC PARAMETERS
Pacific Coast hindcast phase 3 north wave information
[AD-A207189] N89-27323
An Apple-2 compatible program to draw maps containing oceanographic station positions buoy trajectories and the coastal margins of the Antarctic Peninsula and nearby islands
[INPE-4805-RPE/566] N89-27391
OCEANOGRAPHY
Environmental Research Laboratories publication abstracts, FY 1988
[PB89-152656] N89-27589
ON-LINE SYSTEMS
On-line computer utilization to understand some physical processes (example: Pendulum motion)
[NOTA-INTERNA-927] N89-27360
ONBOARD DATA PROCESSING
Altimetric system: Earth observing system. Volume 2h: Panel report
[NASA-TM-89722] N89-27229
OPEN CLUSTERS
Commentary on interstellar matter associated with 18 open clusters
[NASA-RP-1229] N89-27612
OPENINGS
Low frequency structureborne vibration isolation mount
[AD-D014133] N89-27192
OPERATING SYSTEMS (COMPUTERS)
Memory-reference characteristics of multiprocessor applications under MACH
[AD-A207318] N89-27352
OPERATIONS RESEARCH
Software deficiency issues confronting the utilization of non-Von Neumann architectures
[AD-A207268] N89-27369
OPERATOR PERFORMANCE
Human Operator Simulator (HOS) 4 programmer's guide
[AD-A207241] N89-27342
OPERATORS (PERSONNEL)
Ergonomic Models of Anthropometry, Human Biomechanics and Operator-Equipment Interfaces
[NASA-CR-185720] N89-27344
OPTICAL COMMUNICATION
Development of a system model and Least Mean Square (LMS) filter for the Naval Postgraduate School (NPS) Infrared Search and Target Designation System (IRSTD)
[AD-A208536] N89-27068
Atmospheric propagation issues relevant to optical communications
[NASA-CR-185718] N89-27281
Efficient dynamic phasefront modulation system for free-space optical communications
[AD-D014128] N89-27503
OPTICAL COUPLING
Optical couplers for coherent optical phase diversity systems
[EUT-88-E-190] N89-27498
OPTICAL DATA PROCESSING
Time-sequential optical data processing
[AD-A207514] N89-27500
OPTICAL EQUIPMENT
An investigation into the use of an existing shock tube as a driver for a hypersonic shock tunnel
[AD-A208483] N89-26872
Analysis and evaluation of technical data on the photochromic and non-linear optical properties of materials
[AD-A207275] N89-27000
Diamondlike carbon protective coatings for optical windows
[NASA-TM-102111] N89-27506
OPTICAL FIBERS
The quantitative dependence of transmissivity on flexural strain for multimode optical fiber
[AD-A207522] N89-27501
OPTICAL MEASUREMENT
Optical detection and spectroscopy of single molecules in a solid
[AD-A207594] N89-26940
Synthesis of resistive tapers to control scattering patterns of strips
[AD-A207211] N89-27049
OPTICAL MEASURING INSTRUMENTS
JTECH (Japanese Technology Evaluation Program) panel report on advanced sensors in Japan
[PB89-158760] N89-27136
OPTICAL PROPERTIES
Analysis and evaluation of technical data on the photochromic and non-linear optical properties of materials
[AD-A207275] N89-27000
Synthesis and optical properties of a new class of polyamides containing reactive diacetylene groups
[AD-A208752] N89-27021
Passive optical losses in laser glass
[DE89-013784] N89-27172
High efficiency pattern recognition
[AD-A207210] N89-27368
Two-photon absorption characterization of HgCdTe
[AD-A207198] N89-27471
Magneto-optical properties of ultrathin ferromagnetic films
[DE89-014640] N89-27508
Hybrid single crystal optic fibers by embedding
[AD-D013986] N89-27545
OPTICAL RADAR
Deep space LADAR, phase 1
[AD-A207454] N89-27166
OPTICAL REFLECTION
Optical mirror coated with organic superconducting material
[AD-D014047] N89-27499
OPTICAL WAVEGUIDES
System for measuring optical waveguide intensity profiles
[PB89-188593] N89-27507
OPTIMAL CONTROL
Control of flexible structures
[AD-A207520] N89-26883
Spin stabilization of the ORION satellite using a thruster attitude control system with optimal control considerations
[AD-A208484] N89-26892
Modeling and computational algorithms for parameter estimation and optimal control of aeroelastic systems and large flexible structures
[AD-A208274] N89-27404
OPTIMIZATION
Tailoring of composite links for optimal damped elasto-dynamic performance
[NASA-TM-102094] N89-26912
On processing development for fabrication of fiber reinforced composite, part 2
[NASA-CR-181866] N89-26917
Easily testable PLA-based finite state machines
[AD-A208371] N89-27098
A compound scaling algorithm for mathematical optimization
[AD-A208446] N89-27409
Computation and theory in nonlinear optimization
[AD-A207610] N89-27430
Attributed tree transformations with delayed and smart re-evaluation
[MEMO-INF-88-45] N89-27440
Constant access systems: A general framework for greedy optimization on stochastic networks
[AD-A207525] N89-27448
ORBIT CALCULATION
Formulation of numerical orbit propagation and time error correction
[INPE-4774-PRE/1443] N89-26875
ORBIT TRANSFER VEHICLES
NASA's Chemical Transfer Propulsion Program for Pathfinder
[NASA-TM-102298] N89-26876
OTVE turbopump condition monitoring, task E.5
[NASA-CR-182274] N89-27204
ORBITAL ASSEMBLY
Photovoltaic module on-orbit assembly for Space Station Freedom
[NASA-TM-102297] N89-26887
ORBITAL MECHANICS
Formulation of numerical orbit propagation and time error correction
[INPE-4774-PRE/1443] N89-26875
Relativistic explanation of the inclination of planetary orbits
[PB89-170005] N89-27611
ORBITS
Collisionless tearing instability of a bi-Maxwellian neutral sheet with exact particle orbits
[AD-A207310] N89-27286
ORDER-DISORDER TRANSFORMATIONS
Local density theory of heats of formation and short-range order parameters in substitutionally disordered alloys
[DE89-014696] N89-26986
ORGANIC COMPOUNDS
Supercritical fluid chromatography of polar organic compounds in combustion particulates
[PB89-152441] N89-26930

Development of magnetic resonance imaging technology for imaging binder distribution in ceramics
[DE89-013185] N89-27003
Historic emissions of VOC (Volatile Organic Compounds) and NOx in the United States from 1900 to 1985
[PB89-173223] N89-27270

ORGANIC MATERIALS
Automated immersion testing robotic system: Hardware and software design
[AD-A208755] N89-27201
Optical mirror coated with organic superconducting material
[AD-D014047] N89-27499

ORGANIC SULFUR COMPOUNDS
Laser spectroscopy and dynamics of combustion intermediates
[DE89-014498] N89-26956

ORGANIZATIONS
National Engineering Laboratory's 1989 report to the National Research Council's Board on Assessment of NIST (National Institute of Standards and Technology) programs
[PB89-189294] N89-27602

ORGANOMETALLIC COMPOUNDS
Synthesis and characterization of Group 4 organometal oxide complexes
[DE89-010944] N89-26932
Chemical vapor deposition of silicon carbide using a novel organometallic precursor
[AD-A208273] N89-27012

OSCILLATION DAMPERS
Acta Aeronautica et Astronautica Sinica, Volume 8, Number 12, December 1987 (selected articles)
[AD-A206782] N89-26807
Computational methods for nonlinear dynamic problems in solid and structural mechanics: Progress in the theory and modeling of friction and in the control of dynamical systems with frictional forces
[AD-A208763] N89-27227

OSCILLATIONS
Fundamental studies of the cavity flowmeter
[PB89-188825] N89-27153

OSCILLATORS
Thin film preparation and single film device fabrication in the Tl-Ca-Ba-Cu-O HTS system
[DE89-013560] N89-27561

OUTPUT
Advanced information processing system: Input/output system services
[NASA-CR-181874] N89-27413

OXIDATION
Effect of oxidation, sandblasting and pickling on weldability
[DE89-013795] N89-26975
Corrosion of Ceramic Materials Workshop held November 12-13, 1987, Pennsylvania State University, University Park, Pennsylvania
[PB89-175343] N89-27004

OXIDE FILMS
Breakdown mechanisms of Al2O3, Cr2O3 and SiO2 scales in H2/H2O/H2S environments, volume 1
[DE89-014789] N89-26988
A method of removing oxides from the surface of Fe-Ni-Co alloy particles by chemical etching
[DE89-014597] N89-27009

OXIDES
Synthesis and characterization of Group 4 organometal oxide complexes
[DE89-010944] N89-26932
Total-dose hardness assurance for space applications of commercial CMOS devices
[DE89-006765] N89-27089

OXYGEN
Space station hydrogen/oxygen thruster technology
[NASA-CR-182280] N89-26905
Oxygen transfer to ethylene catalyzed by the Ag(110) surface
[AD-A207325] N89-26936
Composition of superconducting La2CuO4 + delta: A superconductor doped by excess oxygen defects
[DE89-013299] N89-27555
Anomalous temperature dependence of Cu NMR line width and magnetization in YBa2Cu3O(7-delta)
[DE89-014291] N89-27565
Nuclear relaxation rates at copper and oxygen sites in YBa2Cu3O7
[DE89-014308] N89-27567

OXYGEN ATOMS
Oxygen transfer to ethylene catalyzed by the Ag(110) surface
[AD-A207325] N89-26936

OXYGEN SUPPLY EQUIPMENT
Automatic oxygen measuring system
[AD-D014003] N89-26931

OXYGEN 17
O-17 NMR study of YBa2Cu3O(7-delta)
[DE89-014292] N89-27566

OZONE
Production of pure ozone by means of electric discharges for measuring absorption coefficients
[NOTA-INTERNA-913] N89-27042
Concentrations and patterns of photochemical oxidants in the United States
[PB89-136683] N89-27258
Procedures for the preparation of emission inventories for precursors of ozone, volume 1, third edition
[PB89-154209] N89-27264
Preventing depletion of stratospheric ozone: Implications on future aircraft emissions, revision 1
[DE89-013779] N89-27273

OZONOMETRY
Absorption cross-section of ozone in the 590 to 610 nm region at different temperatures
[NOTA-INTERNA-928] N89-27291

OZONOSPHERE
Absorption cross-section of ozone in the 590 to 610 nm region at different temperatures
[NOTA-INTERNA-928] N89-27291

P

P-I-N JUNCTIONS
Battery-driven miniature LDA system with semiconductor laser diode
[ISL-CO-214/88] N89-27176

P-3 AIRCRAFT
Feasibility study for enhanced lateral control of the P-3C aircraft
[AD-A208461] N89-26863

PACIFIC OCEAN
Trace gases in and over the West Pacific and East Indian Oceans during the El Nino-southern oscillation event of 1987: A report of GMCC (Geophysical Monitoring for Climatic Change) data collected on the second Soviet-American Gas and Aerosol Experiment (SAGA 2)
[PB89-159685] N89-27280
Pacific Coast hindcast phase 3 north wave information
[AD-A207189] N89-27323

PAINTS
Microwave hardening technology development program
[AD-A207535] N89-27076

PAIR PRODUCTION
Evidence for phonon-mediated coupling in superconducting Ba sub 0.6 K sub 0.4 BiO3
[DE89-014642] N89-27568

PANELS
Superplastic forming of aluminum, task C
[AD-A207282] N89-26962

PARABOLIC DIFFERENTIAL EQUATIONS
The h-p version of the finite element method parabolic equations. Part 2: The h-p version in time
[AD-A207575] N89-27429

PARALLEL PROCESSING (COMPUTERS)
Data traffic reduction schemes for Cholesky factorization on asynchronous multiprocessor systems
[NASA-CR-181863] N89-27349
A parallel version of the Boyer-Moore prover
[AD-A207190] N89-27351
Memory-reference characteristics of multiprocessor applications under MACH
[AD-A207318] N89-27352
Parallel implementation of OPS5 on the encore multiprocessor: Results and analysis
[AD-A207320] N89-27353
Programming parallel architectures: The BLAZE family of languages
[NASA-CR-185826] N89-27362
A theoretical investigation of a parallel genetic algorithm
[DE89-012508] N89-27384
Indirect addressing and load balancing for faster solution to Mandelbrot Set on SIMD architectures
[NASA-CR-181847] N89-27390
Portable parallel programming in a FORTRAN environment
[DE89-014670] N89-27399
Machines for lattice gauge theory
[DE89-014815] N89-27400
Automatic code vectorization of arithemetic expressions by bottom-up structure recognition
[MEMO-INF-88-48] N89-27414
Row-oriented direct solving of linear algebraic equations. Inverse projection method
[REPT-88-81] N89-27432

PARALLEL PROGRAMMING
Implementation indices (1975-1979), volume 1
[AD-A207609] N89-27354
Portable parallel programming in a FORTRAN environment
[DE89-014670] N89-27399
An overview of some methods for the high-level specification of synchronization
[MEMO-INF-88-50] N89-27403

PARAMETER IDENTIFICATION
Method for experimental determination of flutter speed by parameter identification
[NASA-TP-2923] N89-26844
Frequency-domain transient analysis of silicon solar cells
[DE89-010555] N89-27243
Study of dispersion and penetration of tracer and pollutants in porous media and fractured rocks
[ETN-89-94806] N89-27277
Determination of the kinetic parameters of the thermoluminescent CaF2 (Tm) crystal
[NOTA-INTERNA-915] N89-27569

PARAMETERIZATION
Model-based parameter estimation in electromagnetic computer modeling
[AD-A207399] N89-27052

PARSING ALGORITHMS
Northeast Artificial Intelligence Consortium annual report 1987. Volume 2, part b: Discussing, using, and recognizing plans
[AD-A208378] N89-27418

PARTIAL DIFFERENTIAL EQUATIONS
Control of flexible structures
[AD-A207520] N89-26883
Use of the Fox derivatives in the solution of the word problem for groups
[DE88-705978] N89-27421

PARTICLE ACCELERATORS
Multiple-electron processes in fast ion-atom collisions
[DE89-012982] N89-27475

PARTICLE BEAMS
Beam-gas background rejection in L3 first level energy transfer
[NOTA-INTERNA-919] N89-27496

PARTICLE COLLISIONS
Influence of particle collisions on the characteristics of H-like ion emission due to charge exchange reactions with fast atoms
[IPP-III/142] N89-27480
Search for the inclusive production of J/psi in e(+)e(-) collisions using PLUTO data
[NOTA-INTERNA-923] N89-27484
Multiparticle dynamics at the Sp(-)p collider
[NOTA-INTERNA-929] N89-27490
Collision processes of interest in MFE plasma research
[DE89-013681] N89-27524

PARTICLE INTERACTIONS
Momentum distributions: An overview
[DE89-012617] N89-27453
Physics with ETA mesons
[DE89-012582] N89-27478

PARTICLE PRECIPITATION
Airborne measurements of the electric field and the charge precipitation particles in convective clouds: Lower positive charge centers
[ONERA-NT-1988-1] N89-27319

PARTICLE PRODUCTION
Method for refining microstructures of blended elemental titanium powder compacts
[AD-D014067] N89-26961

PARTICULATES
Cloud and precipitation scavenging process in the South Coast Air Basin
[PB89-181788] N89-27313

PASSENGERS
Injuries to seat occupants of light airplanes
[AD-A207579] N89-26830

PATTERN RECOGNITION
An expert system for correlation of radar and passive sensor signals
[DE89-011575] N89-27056
Applications of holography to pattern recognition and optical memories
[PB89-174668] N89-27146
Categorization in neural networks and prosopagnosia
[PREPRINT-608] N89-27327
The effect of synapses destruction on categorization by neural networks
[PREPRINT-609] N89-27328
High efficiency pattern recognition
[AD-A207210] N89-27368
Image algebra synthesis
[AD-A207257] N89-27425
Research in knowledge delivery
[AD-A208327] N89-27599

PENDULUMS
On-line computer utilization to understand some physical processes (example: Pendulum motion)
[NOTA-INTERNA-927] N89-27360
PENETRATION
Pulsed lower-hybrid wave penetration in reactor plasmas
[DE89-013260] N89-27521
PERFLUORO COMPOUNDS
Comparison of modelled and measured tracer gas concentrations during the Across North America Tracer Experiment (ANATEX)
[PB89-136709] N89-27260
PERFORMANCE PREDICTION
Technical Status Review on Drag Prediction and Analysis from Computational Fluid Dynamics: State of the Art
[AGARD-AR-256] N89-26817
Drag prediction and analysis from computational fluid dynamics, state-of-the-art in France N89-26818
Drag prediction and analysis from CFD state-of-the-art in Germany N89-26819
Some results on flow calculations involving drag prediction N89-26820
State-of-the-art of aircraft drag prediction in Italy by means of theoretical methods N89-26821
Aircraft drag prediction for transonic potential flow N89-26822
CFD methods for drag prediction and analysis currently in use in UK N89-26823
CFD drag prediction for aerodynamic design N89-26825
PERFORMANCE TESTS
Hose reel monitor for inflight refueling system
[AD-D014054] N89-26836
Evaluation of an updated design of an internally lighted wind cone
[DOT/FAA/CT-TN89/45] N89-26868
Automatic oxygen measuring system
[AD-D014003] N89-26931
Effect of heating rate to test temperature on superplastic response in an Al-8 percent Mg-1 percent Li-0.2 percent Zr alloy
[AD-A208462] N89-26990
Evaluation of low data rate voice CODECS for air traffic control applications
[DOT/FAA/CT-TN89/13] N89-27047
Performance comparison among several filters for the reducton of speckle noise in radar imagery
[INPE-4768-PRE/1437] N89-27055
Millimeter-wave propagation characteristics and channel performance for urban-suburban environments
[PB89-180251] N89-27058
Evaluation of a FTIR (Fourier Transform Infrared Spectrometer) mobile source measurement system
[PB89-180822] N89-27147
High performance intercooled and recuperated gas turbine
[PB89-152284] N89-27178
Performance analysis of data-driven networks
[PB89-170906] N89-27412
PERMEABILITY
Molecular sieve films from zeolited-silica microcomposites
[DE89-009831] N89-26921
Gas separations using inorganic membranes
[DE89-013010] N89-26948
Study of dispersion and penetration of tracer and pollutants in porous media and fractured rocks
[ETN-89-94806] N89-27277
PERMITTIVITY
Measurements of complex permittivity of microwave substrates in the 20 to 300 K temperature range from 26.5 to 40.0 GHz
[NASA-TM-102123] N89-27038
Solutions of differential equations with regular coefficients by the methods of Richmond and Runge-Kutta
[NASA-TM-101609] N89-27060
PERTURBATION THEORY
Theoretical studies in elementary particle physics
[DE89-012701] N89-27473
PHASE CONTRAST
Theory of X-ray holography including phase and amplitude contrast and finite transfer functions
[DE89-012835] N89-27148
PHASE DIAGRAMS
Local density theory of heats of formation and short-range order parameters in substitutionally disordered alloys
[DE89-014696] N89-26986
Evidence for phonon-mediated coupling in superconducting Ba sub 0.6 K sub 0.4 BiO3
[DE89-014642] N89-27568
PHASE LOCKED SYSTEMS
Compressor blade clearance measurement system
[AD-D014073] N89-26850
Optical couplers for coherent optical phase diversity systems
[EUT-88-E-190] N89-27498
PHASE SHIFT
Theory of X-ray holography including phase and amplitude contrast and finite transfer functions
[DE89-012835] N89-27148
PHASE SHIFT CIRCUITS
Radio frequency plasma generator
[AD-D013990] N89-27514
PHASE SHIFT KEYING
Programmable rate modem utilizing digital signal processing techniques
[NASA-CR-185124] N89-26879
PHASE TRANSFORMATIONS
Fracture behavior of a pressure vessel steel in the ductile-to-brittle transition region
[PB89-189195] N89-26977
High energy laser target plate
[AD-D014053] N89-27164
High temperature solar electrothermal processing
[AD-A207555] N89-27246
Quantum and thermodynamic fluctuations in the degenerate schematic model of the finite temperature random phase approximation
[DE88-706310] N89-27580
PHENOLS
Thermal stability of jet fuel
[DE89-013516] N89-27032
PHENYLS
Optical detection and spectroscopy of single molecules in a solid
[AD-A207594] N89-26940
PHOSPHATES
Passive optical losses in laser glass
[DE89-013784] N89-27172
PHOSPHAZENE
Synthesis, characterization and physical properties of polyphosphazenes
[AD-A208296] N89-27013
PHOSPHONIUM COMPOUNDS
Synthesis of novel fluorinated phosphonic and phosphinic acid electrolytes for phosphoric acid fuel cells
[PB89-194120] N89-27086
PHOSPHORIC ACID FUEL CELLS
Development of ternary alloy cathode catalysts for phosphoric acid fuel cells
[DE89-000926] N89-27250
Electrochemical evaluation of new fluorosulfonic and fluorophosphonic acids as fuel cell electrolytes
[DE89-012840] N89-27254
PHOTOABSORPTION
A preliminary report on X-ray photoabsorption coefficients and atomic scattering factors for 92 elements in the 10-10,000 eV region
[DE89-013392] N89-26950
PHOTOACOUSTIC SPECTROSCOPY
The photoacoustic effect, refined and applied to biological problems
[PB89-153597] N89-27263
PHOTOCHEMICAL OXIDANTS
Concentrations and patterns of photochemical oxidants in the United States
[PB89-136683] N89-27258
PHOTOCHEMICAL REACTIONS
Technical activities 1986-1988, Molecular Spectroscopy Div.
[PB89-175418] N89-26942
Laser dyes derived from bimanes
[AD-D013994] N89-27160
PHOTOCONDUCTIVITY
Photoconductive semiconductor switch (PCSS) recovery
[DE89-012657] N89-27080
Photoelectronic properties of low temperature GaAs grown on silicon and GaAs substrates by MBE
[DE89-013148] N89-27557
PHOTOCONDUCTORS
Photoconductive semiconductor switch (PCSS) recovery
[DE89-012657] N89-27080
Closing photoconductive semiconductor switches
[DE89-013073] N89-27082
PHOTODECOMPOSITION
Photodegradation of polyimides 2. Thermal property changes of polyimides based on a perfluorinated dianhydride
[AD-A208447] N89-27018
PHOTODISSOCIATION
Primary dissociation processes of energetic compounds
[AD-A208312] N89-27033
PHOTOELECTRICITY
New strategies for display devices based on 2-6 materials
[AD-A208288] N89-27573
PHOTOGRAPHIC MEASUREMENT
Sensor development programs at NASA Ames Research Center
[NASA-TM-102217] N89-26808
PHOTOGRAPHY
Film annotation system for a space experiment
[NASA-CR-185114] N89-27152
PHOTOINTERPRETATION
Satellite image processing using symbolic structures of reduced vision conditions
[INPE-4638-TDL/337] N89-27367
Northeast Artificial Intelligence Consortium annual report 1987. Volume 2, part b: Discussing, using, and recognizing plans
[AD-A208378] N89-27418
Northeast Artificial Intelligence Consortium annual report 1987. Volume 3: Distributed artificial intelligence for communications network management
[AD-A208379] N89-27419
PHOTOIONIZATION
Computer code prediction of picosecond voltage switching and TEM wave generation in air gas avalanche switches
[DE89-013778] N89-27084
Molecules in intense laser fields
[DE89-013807] N89-27479
Two-dimensional effects in hollow core z-pinches
[DE89-014188] N89-27531
PHOTOLUMINESCENCE
New strategies for display devices based on 2-6 materials
[AD-A208288] N89-27573
PHOTOLYSIS
Laser spectroscopy and dynamics of combustion intermediates
[DE89-014498] N89-26956
Photodegradation of polyimides 2. Thermal property changes of polyimides based on a perfluorinated dianhydride
[AD-A208447] N89-27018
PHOTOMETERS
Optical couplers for coherent optical phase diversity systems
[EUT-88-E-190] N89-27498
A fiber optic test system for quantum efficiency measurements
[DE89-012823] N89-27505
PHOTOMETRY
Development of a second-generation, video-based luminance mapper for daylighting research
[DE89-000850] N89-27143
PHOTONS
Relativistic corrections to photon scattering polarizabilities
[NOTA-INTERNA-916] N89-27487
Dynamics of an M-level atom interacting with gravity fields. 1: Effects of the level number on quantum collapse and revival
[AD-A207278] N89-27579
PHOTORECEPTORS
Meridian variations in spectral dark adaptation
[AD-A207248] N89-27331
PHOTOSENSITIVITY
Synthesis and structural characterization of Pt-Si dimers with unusually short cross-ring silicon-silicon interactions
[AD-A208310] N89-27014
PHOTOVOLTAIC EFFECT
Photovoltaic module on-orbit assembly for Space Station Freedom
[NASA-TM-102297] N89-26887
PHTHALOCYANIN
Magnetic and electrical properties of sandwich-like lanthanide phthalocyanines
[AD-A208411] N89-26958
PHYSICAL EXERCISE
Development of advanced methods based on stable isotope technology for studies of exercise in heat
[AD-A208758] N89-27329
Endogenous hormonal and growth factor responses to heavy resistance exercise protocols
[AD-A208375] N89-27336
PHYSICAL FITNESS
Annual historical report - AMEDD activities
[AD-A208301] N89-27333
PHYSIOLOGICAL ACCELERATION
Full coverage anti-G-suit and balanced pressure breathing
[PB89-174635] N89-27343
PHYSIOLOGICAL EFFECTS
Altitude symptomatology and mood states during a climb to 3830 m
[AD-A208261] N89-27332

Submarine air quality: Monitoring the air in submarines. Health effects in divers of breathing submarine air under hyperbaric conditions
[PB89-174213] N89-27345

PHYSIOLOGICAL RESPONSES
Thermoregulatory responses in the cold-effect of an Extended Cold Weather Clothing System (ECWCS)
[AD-A206314] N89-27334
Endogenous hormonal and growth factor responses to heavy resistance exercise protocols
[AD-A208375] N89-27336

PICKLING (METALLURGY)
Effect of oxidation, sandblasting and pickling on weldability
[DE89-013795] N89-26975

PIEZOELECTRIC TRANSDUCERS
Polarization matrices of lithium tantalate
[AD-A206349] N89-27097

PIEZOELECTRICITY
Standardized piezoelectric polymer (PVDF) gauge for detonator response measurement
[DE89-010437] N89-27144
Sensors for in situ monitoring of elastic properties
[DE89-012795] N89-27145
Polarization matrices of lithium niobate
[AD-A207231] N89-27462

PILOT PERFORMANCE
F-15E EADI (Electronic Attitude Director Indicator) evaluation: A comparison of three formats
[AD-A206809] N89-26846
Design considerations of manipulator and feel system characteristics in roll tracking
[NASA-CR-4111] N89-26860

PINCH EFFECT
Equilibrium of a plasma in the fluid- and Vlasov-Maxwell systems
[DE89-013315] N89-27518

PINHOLE CAMERAS
Advanced Solar Observatory (ASO) accommodations requirements study
[NASA-CR-183718] N89-26885
A one-dimensional scintillator camera for the SATURN X-ray simulation accelerator
[DE89-009327] N89-27492

PINS
Dual load path pin clevis joint
[AD-D014081] N89-27188

PIPELINING (COMPUTERS)
Row-oriented direct solving of linear algebraic equations. Inverse projection method
[REPT-88-81] N89-27432

PISTON ENGINES
Advanced ceramics: A critical assessment of wear and lubrication
[PB89-188569] N89-27005

PITCH (INCLINATION)
Reduction of blade-vortex interaction noise using higher harmonic pitch control
[NASA-TM-101624] N89-27465

PIVOTS
OH-58 energy attenuating crew seat feasibility study
[AD-A207506] N89-26829
Dual load path pin clevis joint
[AD-D014081] N89-27188

PLANAR STRUCTURES
Dynamic analysis of flexible mechanisms by a combined transfer matrix finite element method
[PB89-160865] N89-27181

PLANE WAVES
Solutions of differential equations with regular coefficients by the methods of Richmond and Runge-Kutta
[NASA-TM-101609] N89-27060

PLANETARY COMPOSITION
Mercury's magnetic field: Implications on the inner composition of the planet
[NOTA-INTERNA-926] N89-27620

PLANETARY CORES
Mercury's magnetic field: Implications on the inner composition of the planet
[NOTA-INTERNA-926] N89-27620

PLANETARY EVOLUTION
Dynamics of the solar system: Proceedings, volume 3
[DE89-609826] N89-27615

PLANETARY MAGNETIC FIELDS
Mercury's magnetic field: Implications on the inner composition of the planet
[NOTA-INTERNA-926] N89-27620

PLANETARY ORBITS
Relativistic explanation of the inclination of planetary orbits
[PB89-170005] N89-27611

PLANETARY STRUCTURE
Mercury's magnetic field: Implications on the inner composition of the planet
[NOTA-INTERNA-926] N89-27620

PLANTS (BOTANY)
The photoacoustic effect, refined and applied to biological problems
[PB89-153597] N89-27263

PLASMA ACCELERATION
Ionospheric plasma escape by high-altitude electric fields: Magnetic moment pumping
[IRF-PREPRINT-111] N89-27542

PLASMA COMPRESSION
Radiative collapse of a Bennett-relaxed z-pinch
[DE89-014290] N89-27533

PLASMA CONTROL
Limiter H-modes in the JIPP T-IIU tokamak
[IPPJ-898] N89-27511
TORE SUPRA graphite inner first wall --- tokamak devices
[DE89-009325] N89-27512
Application of modern mathematical concepts to plasma confinement
[DE89-012952] N89-27517
Pacing the US magnetic fusion program
[DE89-012959] N89-27519
Improved confinement regimes in JIPP T-IIU
[IPPJ-909] N89-27527

PLASMA CURRENTS
On bootstrap currents in toroidal systems
[IPP-2/297] N89-27536

PLASMA DENSITY
Equilibrium of a plasma in the fluid- and Vlasov-Maxwell systems
[DE89-013315] N89-27518
Radiative collapse of a Bennett-relaxed z-pinch
[DE89-014290] N89-27533
Two-dimensional effects in imploding plasma liners
[DE89-014482] N89-27534

PLASMA DIAGNOSTICS
Collision processes of interest in MFE plasma research
[DE89-013681] N89-27524
Integral constitutive relation for the investigation of ion Bernstein waves in non-homogeneous plasmas
[IPP-5/27] N89-27538

PLASMA ELECTRODES
Two-dimensional effects in imploding plasma liners
[DE89-014482] N89-27534

PLASMA EQUILIBRIUM
Equilibrium of a plasma in the fluid- and Vlasov-Maxwell systems
[DE89-013315] N89-27518

PLASMA FOCUS
Study of atomic physics and population inversions with plasma focus
[DE89-014282] N89-27532

PLASMA GENERATORS
Radio frequency plasma generator
[AD-D013990] N89-27514

PLASMA HEATING
Improved confinement regimes in JIPP T-IIU
[IPPJ-909] N89-27527
Stochasticity and symmetry of the standard map
[IPPJ-910] N89-27528
A new version of the full-wave ICRH code FISIC for plasmas with noncircular flux surfaces
[IPP-5/25] N89-27537
Radio frequency plasma heating and current drive
[IPP-6/278] N89-27540

PLASMA PHYSICS
Collision processes of interest in MFE plasma research
[DE89-013681] N89-27524

PLASMA PINCH
Experimental measurement of nonlinear plasma wake-fields
[DE89-014636] N89-27525

PLASMA TURBULENCE
Limiter H-modes in the JIPP T-IIU tokamak
[IPPJ-898] N89-27511

PLASMA WAVES
Waves and instabilities in nonneutral plasmas
[DE89-012403] N89-27515
Experimental measurement of nonlinear plasma wake-fields
[DE89-014636] N89-27525
Integral constitutive relation for the investigation of ion Bernstein waves in non-homogeneous plasmas
[IPP-5/27] N89-27538

PLASMAS (PHYSICS)
Development of a high power microwave thruster, with a magnetic nozzle, for space applications
[NASA-TM-102321] N89-26904
Solutions of differential equations with regular coefficients by the methods of Richmond and Runge-Kutta
[NASA-TM-101609] N89-27060
Waves and instabilities in nonneutral plasmas
[DE89-012403] N89-27515
Equilibrium of a plasma in the fluid- and Vlasov-Maxwell systems
[DE89-013315] N89-27518
Pulsed lower-hybrid wave penetration in reactor plasmas
[DE89-013260] N89-27521
Experimental measurement of nonlinear plasma wake-fields
[DE89-014636] N89-27525
The magnetic topology of the plasmoid flux rope in a MHD simulation of magnetotail reconnection
[DE89-012621] N89-27529
Two-dimensional effects in hollow core z-pinches
[DE89-014188] N89-27531
Radiative collapse of a Bennett-relaxed z-pinch
[DE89-014290] N89-27533
Two-dimensional effects in imploding plasma liners
[DE89-014482] N89-27534
MHD calculations of anode plasmas
[DE89-014485] N89-27535

PLASMONS
Surface plasmon study of monolayer-bilayer transition in poly-4-BCMU and poly-3-BCMU polydiacetylene Langmuir-Blodgett films
[AD-A207404] N89-26938

PLASTIC DEFORMATION
Dynamic plastic buckling of spherical shells during collapse
[DE89-006543] N89-27217
Residual stress changes in fatigue. Volume 1: Residual stress measurements by X-ray diffraction in notched test specimens
[AD-A208345] N89-27225

PLASTIC PROPERTIES
Polycrystal plasticity as applied to the problem of in-plane anisotropy in rolled cubic metals
[DE89-011181] N89-26983
Thermomechanical processing of aluminum alloy 2090 for superplasticity
[AD-A208764] N89-26992
Atomic simulation of crystalline defects in ordered structures
[ETN-89-94807] N89-27571

PLASTICIZERS
Development of magnetic resonance imaging technology for imaging binder distribution in ceramics
[DE89-013185] N89-27003
The 15N NMR powder spectra of semicrystalline nylon 6
[AD-A208502] N89-27577

PLASTICS
Automated immersion testing robotic system: Hardware and software design
[AD-A208755] N89-27201

PLATE THEORY
On the multiplicity and symmetries of the bifurcation branching point in the square clamped plate
[PREPRINT-604] N89-27224

PLATES (STRUCTURAL MEMBERS)
A three-node C deg element for analysis of laminated composite sandwich shells
[NASA-TM-4125] N89-27213

PLATINUM
Catalytic combustion of methane
[PB89-188874] N89-26946

PLATINUM COMPOUNDS
Synthesis and structural characterization of Pt-Si dimers with unusually short cross-ring silicon-silicon interactions
[AD-A208310] N89-27014

PLOTTERS
A graphics package for meteorological data, version 1.5
[NASA-TM-100742] N89-27314

PLOTTING
A graphics package for meteorological data, version 1.5
[NASA-TM-100742] N89-27314

PLUMES
Flow fields of low pressure vent exhausts
[NASA-TM-100738] N89-26902
Mechanisms that control the geometry of pulsed Nd:YAG laser welds
[DE89-014490] N89-27200
Comparison of modelled and measured tracer gas concentrations during the Across North America Tracer Experiment (ANATEX)
[PB89-136709] N89-27260
Aerial smoke plume observations and surface layer turbulence measurements. Part 1: Project WIND. Phase 4: Dispersion study
[AD-A207370] N89-27305

PLUTONIUM
History of the application of the generalized Lewis acid-base theory to metals
[DE89-012992] N89-26984

POINT DEFECTS
Theory of aggregate defects in silicon
[AD-A207273] N89-26999
Composition of superconducting La2CuO4+delta: A superconductor doped by excess oxygen defects
[DE89-013299] N89-27555
POISSON DENSITY FUNCTIONS
Capacity of the Poisson channel with time-varying noise intensity and jamming
[AD-A207225] N89-27446
Capacity of the poisson channel with random noise intensity
[AD-A207226] N89-27447
POISSON EQUATION
A dual potential formulation of the Navier-Stokes equations
[NASA-CR-185098] N89-27111
POLAR GASES
Supercritical fluid chromatography of polar organic compounds in combustion particulates
[PB89-152441] N89-26930
POLARIZATION (SPIN ALIGNMENT)
Relativistic corrections to photon scattering polarizabilities
[NOTA-INTERNA-916] N89-27487
POLARIZATION (WAVES)
Complex vectors and dyadics for electromagnetists
[PB89-146443] N89-27045
Polarization matrices of lithium tantalate
[AD-A208349] N89-27097
POLES (SUPPORTS)
A qualitative way of solving the pole balancing problem
[MEMO-INF-88-44] N89-27439
POLICIES
A parallel version of the Boyer-Moore prover
[AD-A207190] N89-27351
Science and technology advice in the White House: Recommendations for President-Elect George Bush
[PB89-166817] N89-27600
POLISHING
Evaluation of mechanical properties of TiN films by ultra-low load indentation
[DE89-009618] N89-26969
Passive optical losses in laser glass
[DE89-013784] N89-27172
Design, development and evaluation of a doubly rotated AK-cut quartz crystal
[AD-A207209] N89-27549
POLLUTION MONITORING
Concentrations and patterns of photochemical oxidants in the United States
[PB89-136683] N89-27258
Assessing the sensitivity of high altitude New Mexican wilderness lakes to acidic precipitation and trace metal contamination
[PB89-148456] N89-27262
Analytical procedures for environmental quality control, volume 1
[PB89-158604] N89-27266
Cloud and precipitation scavenging process in the South Coast Air Basin
[PB89-181788] N89-27313
POLLUTION TRANSPORT
Comparison of modelled and measured tracer gas concentrations during the Across North America Tracer Experiment (ANATEX)
[PB89-136709] N89-27260
Field studies for determining the characteristics and dynamics of local circulations
[DE89-013639] N89-27275
POLYAMIDE RESINS
Natural abundance 15N CP/MAS NMR of solid polyamides: A sensitive technique for examining crystalline composition and conformation in the solid state
[AD-A208563] N89-27019
Synthesis and optical properties of a new class of polyamides containing reactive diacetylene groups
[AD-A208752] N89-27021
POLYATOMIC MOLECULES
Primary dissociation processes of energetic compounds
[AD-A208312] N89-27033
POLYCARBONATES
Dynamic mechanical investigations of LLDPE/PC blends
[NPL-DMA(A)-177] N89-27010
POLYCRYSTALS
Magnetic and electrical properties of sandwich-like lanthanide phthalocyanines
[AD-A208411] N89-26958
Polycrystal plasticity as applied to the problem of in-plane anisotropy in rolled cubic metals
[DE89-011181] N89-26983
The study of structure-processing-property relations in copper oxide-based high T sub c superconductors
[DE89-012764] N89-27554
Thin film preparation and single film device fabrication in the Tl-Ca-Ba-Cu-O HTS system
[DE89-013560] N89-27561
The response of single crystal and polycrystal nickel to quasistatic and shock deformation
[DE89-011168] N89-27564
POLYETHYLENES
Dynamic mechanical investigations of LLDPE/PC blends
[NPL-DMA(A)-177] N89-27010
POLYIMIDES
Flexible backbone aromatic polyimide adhesives
[NASA-TM-100631] N89-27001
Photodegradation of polyimides 2. Thermal property changes of polyimides based on a perfluorinated dianhydride
[AD-A208447] N89-27018
POLYMER CHEMISTRY
Institute for Materials Science and Engineering, Polymers: Technical activities 1988
[PB89-166094] N89-26993
POLYMER MATRIX COMPOSITES
Tailoring of composite links for optimal damped elasto-dynamic performance
[NASA-TM-102094] N89-26912
Composites databases for the 1990's
[PB89-180376] N89-26914
On processing development for fabrication of fiber reinforced composite, part 2
[NASA-CR-181866] N89-26917
Statistical strength comparison of metal-matrix and polymeric-matrix composites
[AD-A208316] N89-26925
POLYMERIZATION
Synthesis and optical properties of a new class of polyamides containing reactive diacetylene groups
[AD-A208752] N89-27021
Standardized piezoelectric polymer (PVDF) gauge for detonator response measurement
[DE89-010437] N89-27144
Nitrogen 15 T1 measurements of semicrystalline nylon 6
[AD-A208481] N89-27575
The 15N NMR powder spectra of semicrystalline nylon 6
[AD-A208502] N89-27577
POLYNOMIALS
A MACSYMA package for the generation and manipulation of Chebyshev series
[DE89-011404] N89-27436
POLYPHENYLS
Thermodynamic equilibria in the biphenyl/hydrogen system (the power and limitations of group additivity estimations)
[DE89-000754] N89-26954
POLYTOPES
Heuristic algorithms for stability testing polytopes of matrices
[PB89-160840] N89-27365
POLYURETHANE RESINS
Thermal and mechanical properties of polyurethane-diacetylene segmented copolymers. Part 1: Molecular weight and annealing effects
[AD-A208753] N89-27022
Thermal and mechanical properties of polyurethane-diacetylene segmented copolymers. Part 2: Effects of diacetylene cross-polymerization
[AD-A208754] N89-27023
POPULATION INVERSION
Study of atomic physics and population inversions with plasma focus
[DE89-014282] N89-27532
POROSITY
Gas separations using inorganic membranes
[DE89-013010] N89-26948
POROUS MATERIALS
Molecular sieve films from zeolited-silica microcomposites
[DE89-009831] N89-26921
Study of dispersion and penetration of tracer and pollutants in porous media and fractured rocks
[ETN-89-94806] N89-27277
PORTABLE EQUIPMENT
Millimeter-wave propagation characteristics and channel performance for urban-suburban environments
[PB89-180251] N89-27058
POSITIONING DEVICES (MACHINERY)
Antenna shaft positioning device
[AD-D014120] N89-27191
POTASSIUM
Development of advanced methods based on stable isotope technology for studies of exercise in heat
[AD-A208758] N89-27329
POTENTIAL FLOW
Aircraft drag prediction for transonic potential flow
N89-26822
A nonlinear multigrid method for three-dimensional transonic potential flow
[ETN-89-94802] N89-26827
POWDER (PARTICLES)
Non-polymeric binders for ceramic powders: Utilization of neutral and ionic species derived from decaborane(14)
[AD-A208338] N89-27015
Combustion characteristics of dry coal-powder-fueled adiabatic diesel engine
[DE89-000978] N89-27197
POWDER METALLURGY
Method for refining microstructures of blended elemental titanium powder compacts
[AD-D014067] N89-26961
Bearings fabricated from rapidly solidified powder and method
[AD-D014072] N89-27185
POWER EFFICIENCY
Compact, lightweight CO2 lasers for SDIO applications
[AD-A207052] N89-27162
PREBURNERS
Investigation of the transient fuel preburner manifold and combustor
[NASA-CR-183715] N89-26900
PRECESSION
Geodetic precession or dragging of inertial frames
[NASA-TM-100744] N89-27456
PRECIPITATION (METEOROLOGY)
Climatology of temperature and precipitation variability in the United States
[PB89-165930] N89-27299
Cloud and precipitation scavenging process in the South Coast Air Basin
[PB89-181788] N89-27313
Tropical circulation and the associated precipitation anomalies in two years of contrast
[INPE-4715-PRE/1395] N89-27315
PREDICTION ANALYSIS TECHNIQUES
Advanced durability analysis. Volume 2: Analytical predictions, test results and analytical correlations
[AD-A207215] N89-26838
Noise produced by turbulent flow into a rotor: Theory manual for atmospheric turbulence prediction and mean flow and turbulence contraction prediction
[NASA-CR-181789] N89-27466
PREDICTIONS
Inelastic buckling of channel columns in the distortional mode
[PB89-156053] N89-27207
Intense heat checklist based on the 1980 heat wave
[PB89-181200] N89-27312
PRESSURE
Variable nozzle area turbine vane cooling
[AD-D014071] N89-26849
PRESSURE DISTRIBUTION
Wind-tunnel investigation of aerodynamic characteristics and wing pressure distributions of an airplane with variable-sweep wings modified for laminar flow
[NASA-TM-4124] N89-26810
PRESSURE EFFECTS
An experimental investigation of the ground vortex created by a moving jet
[NASA-CR-181841] N89-26815
PRESSURE MEASUREMENT
Standardized piezoelectric polymer (PVDF) gauge for detonator response measurement
[DE89-010437] N89-27144
Thermal enclosures for electronically scanned pressure modules operating in cryogenic environments
[NASA-TM-101635] N89-27151
PRESSURE REDUCTION
Measurement of wall shear and wall pressure downstream of a honeycomb boundary layer manipulator
[AD-A208297] N89-27132
PRESSURE SENSORS
Solid state gas pressure sensor
[AD-D014105] N89-27139
PRESSURE SUITS
Research and development of anti-G life support systems. Part 4: Engineering test and evaluation of six anti-G valves
[AD-A206996] N89-27341
Full coverage anti-G-suit and balanced pressure breathing
[PB89-174635] N89-27343
PRESSURE VESSELS
Development of a thin wall graphite/polyimide composite pressure vessel with a large aspect ratio
[DE89-002536] N89-26920
Structural integrity evaluation based on an innovative field indentation microprobe
[DE89-010840] N89-27156

Dynamic plastic buckling of spherical shells during collapse
[DE89-006543] N89-27217
Strain to failure of pressurized thick wall cylinders
[DE89-009969] N89-27219
Estimating fracture toughness using tension or ball indentation tests and a modified critical strain model
[DE89-010324] N89-27220

PROBABILITY DENSITY FUNCTIONS
Lognormal distribution maximum-likelihood parameter estimation algorithms
[AD-A207586] N89-27378

PROBABILITY DISTRIBUTION FUNCTIONS
Some results on nonGaussian signal detection
[AD-A207255] N89-27050
On estimating the dependence between two point processes
[AD-A208311] N89-27445
Sampling based approaches to calculating marginal densities
[AD-A208388] N89-27451

PROBABILITY THEORY
Analysis of human-error sequences with fault trees
[PB89-147631] N89-27422
Safety in numbers: The boundless errors of numerical computation
[DE89-014813] N89-27438
Dynamics of an M-level atom interacting with gravity fields. 1: Effects of the level number on quantum collapse and revival
[AD-A207278] N89-27579

PROBLEM SOLVING
Solutions of differential equations with regular coefficients by the methods of Richmond and Runge-Kutta
[NASA-TM-101609] N89-27060
On the feasibility of a generalized linear program
[AD-A207402] N89-27373
Rapidly convergent algorithms for nonsmooth optimization
[AD-A207629] N89-27379
Autonomous discovery and learning by a mobile robot in unstructured environments
[DE89-001525] N89-27415
Multigrid method for stability problems
[NASA-CR-185825] N89-27420
Use of the Fox derivatives in the solution of the word problem for groups
[DE88-705978] N89-27421
The h-p version of the finite element method parabolic equations. Part 2: The h-p version in time
[AD-A207575] N89-27429
A qualitative way of solving the pole balancing problem
[MEMO-INF-88-44] N89-27439

PROCEDURES
Novel applications of the field ion microscope and atom-probe
[DE89-008684] N89-27154
Procedures for the preparation of emission inventories for precursors of ozone, volume 1, third edition
[PB89-154209] N89-27264

PROCESS CONTROL (INDUSTRY)
SiC-MoSi composites
[DE89-013656] N89-26923
Institute for Materials Science and Engineering, Polymers: Technical activities 1988
[PB89-166094] N89-26993
Quality in automation project for FY 88
[PB89-193296] N89-27040
Optimum interface properties for metal matrix composites
[NASA-TM-102295] N89-27223
Recent improvements in bulk properties of ceramic superconductors
[DE89-013626] N89-27562

PROCUREMENT
Estimating and explaining the production cost of high-technology systems: The case of military aircraft
[AD-A208391] N89-26809

PRODUCTION COSTS
Estimating and explaining the production cost of high-technology systems: The case of military aircraft
[AD-A208391] N89-26809
Superplastic forming of aluminum, task C
[AD-A207282] N89-26962

PRODUCTION ENGINEERING
A dynamic scheduler for a computer aided prototyping system
[AD-A208389] N89-27407

PRODUCTIVITY
Efficiency of N use by wheat as a function of influx and efflux of NO sub 3
[NASA-CR-177534] N89-27346
New Frontier: Environments for Innovation --- sick building syndrome
[PB89-151054] N89-27601

PROGRAM VERIFICATION (COMPUTERS)
Experimental program for real gas flow code validation at NASA Ames Research Center
[NASA-TM-100093] N89-26816
Validation of computational fluid dynamics
[AGARD-AR-257] N89-27104

PROGRAMMING LANGUAGES
Human Operator Simulator (HOS) 4 programmer's guide
[AD-A207241] N89-27342
Implementation indices (1975-1979), volume 1
[AD-A207609] N89-27354
Programming parallel architectures: The BLAZE family of languages
[NASA-CR-185826] N89-27362
The HERMOD behavioral synthesis system
[AD-A207319] N89-27371
XCL: A family of programming language-based shell s
[DE89-013442] N89-27388

PROJECT MANAGEMENT
NASA's Chemical Transfer Propulsion Program for Pathfinder
[NASA-TM-102298] N89-26876
Software management indicators: Managing the risk of project management
[AD-A208443] N89-27408
Estimation of the relationship between project attributes and the implementation of engineering tools
[PB89-149470] N89-27588

PROJECT PLANNING
Emerging technologies in electronics and their measurement needs
[PB89-189245] N89-27078

PROPAGATION MODES
System for measuring optical waveguide intensity profiles
[PB89-188593] N89-27507

PROPELLANT COMBUSTION
Detonability of hydrocarbon fuels in air
[DE89-008801] N89-26926
Process for assessing the effect of propellant strain on propellant burn rate
[AD-D014119] N89-27026

PROPELLANTS
Development of a high power microwave thruster, with a magnetic nozzle, for space applications
[NASA-TM-102321] N89-26904
Nonlinear dynamic response of pressurized composite bottles subjected to shock loading
[DE89-010553] N89-26922

PROPELLER NOISE
Reduction of blade-vortex interaction noise using higher harmonic pitch control
[NASA-TM-101624] N89-27465
Noise produced by turbulent flow into a rotor: Theory manual for atmospheric turbulence prediction and mean flow and turbulence contraction prediction
[NASA-CR-181789] N89-27466
Experimental assessment of helicopter rotor turbulence ingestion noise in hover
[NASA-CR-181792] N89-27468

PROPULSION SYSTEM PERFORMANCE
Measurement uncertainty within the Uniform Engine Test Programme
[AGARD-AG-307] N89-26854
The NASA low thrust propulsion program
[NASA-TM-102065] N89-26895
Electric propulsion options for 10 kW class earth space missions
[NASA-TM-102337] N89-26906

PROTECTIVE CLOTHING
Thermoregulatory responses in the cold-effect of an Extended Cold Weather Clothing System (ECWCS)
[AD-A208314] N89-27334

PROTECTIVE COATINGS
Diamondlike carbon protective coatings for optical windows
[NASA-TM-102111] N89-27506
Development of elements of a high Tc superconducting cable
[AD-A208370] N89-27574

PROTEINS
Large protein crystallization facility, phase A. Executive summary
[AQ-ES-175/88] N89-27035

PROTONS
Multiparticle dynamics at the Sp(-)p collider
[NOTA-INTERNA-929] N89-27490

PROTOTYPES
Evaluation of a FTIR (Fourier Transform Infrared Spectrometer) mobile source measurement system
[PB89-180822] N89-27147
A language translator for a computer aided rapid prototyping system
[AD-A208358] N89-27406

PSYCHOLOGICAL EFFECTS
Altitude symptomatology and mood states during a climb to 3630 m
[AD-A208261] N89-27332

PSYCHOLOGICAL FACTORS
Psychological attributes, coping strategies and other factors associated with ultramarathon performance
[AD-A208300] N89-27340

PSYCHOLOGICAL TESTS
Human performance assessment methods
[AGARD-AG-308] N89-27338

PSYCHOMETRICS
Human performance assessment methods
[AGARD-AG-308] N89-27338

PULMONARY CIRCULATION
Short course on cardiopulmonary aspects of aerospace medicine
[AGARD-R-758-ADD] N89-27330

PULMONARY FUNCTIONS
Short course on cardiopulmonary aspects of aerospace medicine
[AGARD-R-758-ADD] N89-27330

PULSARS
Detection of very high energy gamma-rays from the Crab nebula
[DE89-011840] N89-27627
Spectra of crab-like pulsars: A GRO perspective
[DE89-013461] N89-27628

PULSE GENERATORS
Proceedings of the Switched Power Workshop: Power Supply Working Group
[DE89-012293] N89-27077

PULSE HEATING
System for boundary layer control through pulsed heating of a strip heater
[AD-D013999] N89-27101

PULSED LASERS
Electron-impact ionization time-of-flight mass spectrometer for molecular beams
[AD-A207585] N89-27141
Free electron lasers with small period wigglers
[DE89-014715] N89-27173
Mechanisms that control the geometry of pulsed Nd:YAG laser welds
[DE89-014490] N89-27200
Measurement of the time-dependent distribution of ionization states in an argon plasma from a Mach-10 jet
[DE89-014699] N89-27526

PULSES
Mixing and combustion of pulsed gas jets
[PB89-155550] N89-26929
Investigations of dielectric properties of some frozen materials using cross-borehole radiowave pulse transmissions
[AD-A207302] N89-27285
Cepstral method for the measurement of ultrasonic pulse transmission time variations
[AD-A207410] N89-27463

PUMP IMPELLERS
Space Shuttle Main Engine structural analysis and data reduction/evaluation. Volume 7: High pressure fuel turbo-pump third stage impeller analysis
[NASA-CR-183670] N89-26894

PYRIDINES
Blends of poly(enaminonitriles)
[AD-A208441] N89-27017

PYROLYSIS
Analysis of low-pressure gas-phase pyrolytic reactions by mass spectrometric techniques
[AD-A207457] N89-26939
Micropyrolyzer design for infrared spectroscopy applications
[DE89-013329] N89-26949
Laser spectroscopy and dynamics of combustion intermediates
[DE89-014498] N89-26956
Non-polymeric binders for ceramic powders: Utilization of neutral and ionic species derived from decaborane(14)
[AD-A208338] N89-27015

PYROTECHNICS
SPOT 1-2-3 Pyrotechnics System: Definition repo rt
[CNES-CT/DRT/TVE/IL-89-035] N89-26889

Q

QUADRATIC EQUATIONS
Linearization of nonlinear systems
[AD-A206073] N89-27423

QUADRATIC PROGRAMMING
Semi-infinite programming
[AD-A207403] N89-27374

Rapidly convergent algorithms for nonsmooth optimization
[AD-A207629] N89-27379

QUADRATURES
The Burgers equation on the semi-finite and finite intervals
[PREPRINT-602] N89-27441

QUALITY CONTROL
Quality in automation project for FY 88
[PB89-193296] N89-27040
Cost of quality evaluation methodologies handbook
[AD-A206935] N89-27202
Analytical procedures for environmental quality control, volume 1
[PB89-156604] N89-27266

QUANTUM AMPLIFIERS
BAE measurement schemes and optimal sensitivity for generalized parametric devices
[PREPRINT-641] N89-27586

QUANTUM CHEMISTRY
Technical activities 1986-1988, Molecular Spectroscopy Div.
[PB89-175418] N89-26942

QUANTUM CHROMODYNAMICS
Theoretical studies in elementary particle physics
[DE89-012701] N89-27473
First results for the delta I = 1/2 amplitude in K decays, with quenched lattice QCD and Wilson fermions
[PREPRINT-599] N89-27485

QUANTUM EFFICIENCY
High-efficiency, large-area CdTe panels
[DE89-000891] N89-27242
A fiber optic test system for quantum efficiency measurements
[DE89-012823] N89-27505

QUANTUM MECHANICS
Differential stochastic equations
[PREPRINT-635] N89-27449
Momentum distributions: An overview
[DE89-012617] N89-27453
The sl (1/1;R)-cohomologies in BRST-Gupta-Bleuler quantization
[NIKHEF-H/88-17] N89-27578
Stochastic mechanics
[PREPRINT-634] N89-27582
Knot theory and quantum gravity
[PREPRINT-607] N89-27585

QUANTUM THEORY
Activities of the Werner-Heisenberg Institute of Physics
[ISSN-0173-6256] N89-27481
Effective action for quantum gravity in two dimensions
[PREPRINT-600] N89-27583
Knot theory and quantum gravity
[PREPRINT-607] N89-27585

QUANTUM WELLS
High power semiconductor laser sources
[AD-A207569] N89-27167

QUARK MODELS
Covariance properties of the multiquark Hamiltonian in the constituent quark model
[NOTA-INTERNA-920] N89-27489

QUARKS
Search for the inclusive production of J/psi in e(+)e(-) collisions using PLUTO data
[NOTA-INTERNA-923] N89-27484

QUARTZ CRYSTALS
Design, development and evaluation of a doubly rotated AK-cut quartz crystal
[AD-A207209] N89-27549

QUEUEING THEORY
Indirect addressing and load balancing for faster solution to Mandelbrot Set on SIMD architectures
[NASA-CR-181847] N89-27390
Computation and theory in nonlinear optimization
[AD-A207610] N89-27430

R

RADAR
Low loss radar window for reentry vehicle
[AD-D014045] N89-26882

RADAR CROSS SECTIONS
Radar cross section studies/compact range research
[NASA-CR-185848] N89-27064

RADAR DATA
Alaska collection SAR (Synthetic Aperture Radar) data summary
[AD-A208530] N89-27067

RADAR DETECTION
Earth sciences
[DE89-013344] N89-27228

RADAR IMAGERY
Performance comparison among several filters for the reducton of speckle noise in radar imagery
[INPE-4788-PRE/1437] N89-27055
Alaska collection SAR (Synthetic Aperture Radar) data summary
[AD-A208530] N89-27067
Implementation of an order filter and its applications in radar imagery (SAR)
[INPE-4749-PRE/1422] N89-27385

RADAR SCATTERING
Radar cross section studies/compact range research
[NASA-CR-185848] N89-27064

RADAR TARGETS
Radar cross section studies/compact range research
[NASA-CR-185848] N89-27064

RADAR TRANSMITTERS
Miniature high voltage solid state relay
[AD-D013979] N89-27070

RADIANCE
Attitude angle effects on Nimbus-7 Scanning Multichannel Microwave Radiometer radiances and geophysical parameter retrievals
[NASA-TM-4132] N89-27289

RADIATION ABSORPTION
Frequency-domain transient analysis of silicon solar cells
[DE89-010555] N89-27243

RADIATION BELTS
The space particle environment
[AD-A207547] N89-27287

RADIATION COUNTERS
Vertex detectors at e(+) e(-) B meson factories
[NOTA-INTERNA-914] N89-27486
Correlation and analysis between the Kamioka neutrino detector data and the Maryland and Rome gravitational antenna data
[NOTA-INTERNA-918] N89-27488

RADIATION DAMAGE
A radiation-hardened 16/32-bit microprocessor
[DE89-008111] N89-27357
Shield optimization program. Part 1: Executive summary
[DE89-013335] N89-27476

RADIATION DISTRIBUTION
Transverse pumping with diode lasers
[AD-A207261] N89-27165

RADIATION EFFECTS
Total-dose hardness assurance for space applications of commercial CMOS devices
[DE89-006765] N89-27089

RADIATION HARDENING
Microwave hardening technology development program
[AD-A207535] N89-27076
Total-dose hardness assurance for space applications of commercial CMOS devices
[DE89-006765] N89-27089
The 1/f noise: A nondestructive technique to predict MOS radiation hardness
[DE89-007419] N89-27205
A radiation-hardened 16/32-bit microprocessor
[DE89-008111] N89-27357

RADIATION MEASUREMENT
Solar radiation on Mars
[NASA-TM-102299] N89-27623

RADIATION PROTECTION
Computational techniques in gamma-ray Skyshine analysis
[DE89-010156] N89-27282

RADIATION PYROMETERS
Infrared temperature measurement with self regulating emission ratio
[ETN-89-94654] N89-27157

RADIATION SHIELDING
Shield optimization program. Part 1: Executive summary
[DE89-013335] N89-27476

RADIATION TOLERANCE
Radiation evaluation of several complex very large scale integration circuits
[DE89-007985] N89-27090

RADIATION TRAPPING
The space particle environment
[AD-A207547] N89-27287

RADIO BURSTS
Statistical study of the correlation of hard X-ray and type 3 radio bursts in solar flares
[NASA-CR-185833] N89-27629

RADIO EMISSION
Space Shuttle Main Engine radio frequency emissions
[NASA-CR-184707] N89-26896

RADIO FREQUENCIES
Space Shuttle Main Engine radio frequency emissions
[NASA-CR-184707] N89-26896
Dual frequency microstrip antenna
[AD-D014019] N89-27046

RADIO FREQUENCY HEATING
Radio frequency plasma heating and current drive
[IPP-6/278] N89-27540

RADIO METEOROLOGY
Observations of atmospheric emission and attenuation at 20.6, 31.65 and 90 GHz by a ground-based radiometer
[NASA-CR-185719] N89-27257

RADIO TELESCOPES
The Swedish-ESO Submillimeter Telescope (SEST)
[PB89-154892] N89-27605

RADIO WAVES
Investigations of dielectric properties of some frozen materials using cross-borehole radiowave pulse transmissions
[AD-A207302] N89-27285

RADIOACTIVE CONTAMINANTS
Analysis of the wind data and estimation of the resultant air concentration rates
[DE88-705980] N89-27296

RADIOACTIVE ISOTOPES
Safety testing program for the Galileo mission radioisotope thermoelectric generator
[DE89-011192] N89-27494

RADIOACTIVE WASTES
Earth sciences
[DE89-013344] N89-27228

RADIOACTIVITY
Analysis of the wind data and estimation of the resultant air concentration rates
[DE88-705980] N89-27296

RADIOMETERS
Observations of atmospheric emission and attenuation at 20.6, 31.65 and 90 GHz by a ground-based radiometer
[NASA-CR-185719] N89-27257

RADIOSONDES
Observations of atmospheric emission and attenuation at 20.6, 31.65 and 90 GHz by a ground-based radiometer
[NASA-CR-185719] N89-27257

RAIL TRANSPORTATION
Attractive levitation for high-speed ground transport with large guideway clearance and alternating-gradient stabilization
[DE89-013640] N89-27195

RAIN
Field joint protection system rain qualification test report
[NASA-CR-183702] N89-26901

RAIN FORESTS
Amazon Forest wind and temperature profiles
[INPE-4724-PRE/1401] N89-27301

RAINDROPS
Procedural guide for the retrieval of dropsize distributions in water clouds from ground-based clear-air-sensing Doppler radar observations
[PB89-152474] N89-27300

RAMAN SPECTRA
Study of nanophase TiO2 grain boundaries by Raman spectroscopy
[DE89-012416] N89-27553

RAMAN SPECTROSCOPY
Study of nanophase TiO2 grain boundaries by Raman spectroscopy
[DE89-012416] N89-27553

RAMJET ENGINES
Investigation of the transient fuel preburner manifold and combustor
[NASA-CR-183715] N89-26900

RANDOM ACCESS
Detection, acquisition and signal demodulation in a communication system with random access
[INPE-4779-RPE/581] N89-27061

RANDOM NOISE
Some results on nonGaussian signal detection
[AD-A207255] N89-27050
Information capacity of additive Gaussian channels with jamming
[AD-A207256] N89-27051
Capacity of the poisson channel with random noise intensity
[AD-A207226] N89-27447

RANDOM PROCESSES
Constant access systems: A general framework for greedy optimization on stochastic networks
[AD-A207525] N89-27448

RANGE FINDERS
Multiple sensor fusion for detecting targets in FLIR (Forward-Looking Infrared) and range images
[AD-A207577] N89-27502

RAPID TRANSIT SYSTEMS
Attractive levitation for high-speed ground transport with large guideway clearance and alternating-gradient stabilization
[DE89-013640] N89-27195
RATS
Development of advanced methods based on stable isotope technology for studies of exercise in heat
[AD-A208758] N89-27329
RAY TRACING
EIGEN: A program to compute eigenrays from HARPA (Hamiltonian Acoustic Ray-Tracing Program for the Atmosphere)/HARPO (Hamiltonian Acoustic Ray-Tracing Program for the Ocean) raysets
[PB89-165781] N89-27460
Improved confinement regimes in JIPP T-IIU
[IPPJ-909] N89-27527
REACTION KINETICS
Studies of the fundamental nature of catalytic acidity, sites and intermediates
[DE89-012946] N89-26947
Vertex detectors at e(+) e(-) B meson factories
[NOTA-INTERNA-914] N89-27486
Multiparticle dynamics at the Sp(-)p collider
[NOTA-INTERNA-929] N89-27490
Determination of the kinetic parameters of the thermoluminescent CaF2 (Tm) crystal
[NOTA-INTERNA-915] N89-27569
REACTION TIME
A model of human reaction time to dangerous robot arm movements
[PB89-186522] N89-27339
REACTIVITY
The structure and reactivity of alkylsiloxane monolayers formed by reaction of alkyltrichlorosilanes on silicon substrates
[AD-A208267] N89-27011
REACTOR DESIGN
TORE SUPRA graphite inner first wall --- tokamak devices
[DE89-009325] N89-27512
REACTOR MATERIALS
High-temperature flaw assessment procedure: A state-of-the-art survey
[DE89-012740] N89-27210
REAL GASES
Experimental program for real gas flow code validation at NASA Ames Research Center
[NASA-TM-100093] N89-26816
Hypervelocity atmospheric flight: Real gas flow fields
[NASA-TM-101055] N89-27117
REAL TIME OPERATION
A center for commercial development of space: Real-time satellite mapping. Remote sensing-based agricultural information expert system
[NASA-CR-185473] N89-27235
RECEIVERS
Development of a DFS (Deutsche Femmeldesatellit) reception converter
[ETN-89-94629] N89-27065
RECOMMENDATIONS
Science and technology advice in the White House: Recommendations for President-Elect George Bush
[PB89-169817] N89-27600
RECONNAISSANCE
Tropical cyclone report, 1988
[AD-A207206] N89-27303
RECONSTRUCTION
A new state reconstructor for digital controls systems using weighted-average measurements
[NASA-TP-2936] N89-27039
RECORDING
Automated immersion testing robotic system: Hardware and software design
[AD-A208755] N89-27201
RECREATION
The effects of arms and countermovement on vertical jumping
[AD-A208298] N89-27347
RECRYSTALLIZATION
The recrystallization and respheroidization of tungsten grains in a tungsten-heavy alloy
[AD-A207647] N89-26964
REDUCED GRAVITY
Industrial applications of the microgravity environment
[NASA-CR-181516] N89-27034
REDUCTION (CHEMISTRY)
Catalytic reduction of carbon dioxide by metal centers
[AD-A207227] N89-26934
REDUNDANCY
Control surface dual redundant servomechanism
[AD-D014058] N89-26857
REELS
Hose reel monitor for inflight refueling system
[AD-D014054] N89-26836
REENTRY VEHICLES
Low loss radar window for reentry vehicle
[AD-D014045] N89-26882
REFINING
Method for refining microstructures of blended elemental titanium powder compacts
[AD-D014067] N89-26961
REFLECTANCE
The structure of self-assembled monolayers of alkylsiloxanes on silicon: A comparison of results from ellipsometry and low-angle X-ray reflectivity
[AD-A208341] N89-27016
Modeling of the angular reflectance of an artificial plant canopy near the retroreflection peak in the optical regime
[DE89-011174] N89-27239
REFLECTING TELESCOPES
The Swedish-ESO Submillimeter Telescope (SEST)
[PB89-154892] N89-27605
REFLECTOMETERS
Group index and time delay measurements of a standard reference fiber
[PB89-189179] N89-27457
REFLECTORS
Rotation of images by scan mirrors
[NASA-TM-101628] N89-27504
REFRACTORY MATERIALS
Structural ceramics in the advanced materials world
[DE89-013046] N89-27008
REFRIGERANTS
Refrigerator-freezer energy testing with alternative refrigerants
[DE89-013543] N89-27037
REGENERATORS
Compact ceramic heat exchangers
[PB89-173603] N89-26997
REGRESSION ANALYSIS
Estimating and explaining the production cost of high-technology systems: The case of military aircraft
[AD-A208391] N89-26809
Estimation of the relationship between project attributes and the implementation of engineering tools
[PB89-149470] N89-27588
REGULATIONS
National Engineering Laboratory's 1989 report to the National Research Council's Board on Assessment of NIST (National Institute of Standards and Technology) programs
[PB89-189294] N89-27602
REINFORCING FIBERS
Unified micromechanics of damping for unidirectional fiber reinforced composites
[NASA-TM-102107] N89-26919
RELATIVISTIC EFFECTS
Relativistic corrections to photon scattering polarizabilities
[NOTA-INTERNA-916] N89-27487
Relativistic explanation of the inclination of planetary orbits
[PB89-170005] N89-27611
RELATIVISTIC PARTICLES
Nuclear fragmentation energy and momentum transfer distributions in relativistic heavy-ion collisions
[NASA-CR-185501] N89-27477
RELATIVITY
Geodetic precession or dragging of inertial frames
[NASA-TM-100744] N89-27456
Knot theory and quantum gravity
[PREPRINT-607] N89-27585
RELAXATION (MECHANICS)
Nuclear relaxation rates at copper and oxygen sites in YBa2Cu3O7
[DE89-014308] N89-27567
RELIABILITY
System-based component test plans and operating characteristics: Introduction and overview
[DE89-012255] N89-27203
RELIABILITY ENGINEERING
MM and T for linear resonant cooler, volume 2
[AD-A207236] N89-27073
RELOCATION
Satellite relocation by tether deployment
[NASA-TM-101992] N89-26877
REMOTE MANIPULATOR SYSTEM
Photovoltaic module on-orbit assembly for Space Station Freedom
[NASA-TM-102297] N89-26887
REMOTE SENSING
Study for advanced civil earth remote sensing system: Focused finance study. Volume 1: Executive summary
[PB89-163224] N89-27230
Study for an advanced civil earth remote sensing system. Volume 1: Executive summary
[PB89-163257] N89-27231
Study for an advanced civil earth remote sensing system. Volume 2: Market and financial assessment
[PB89-163265] N89-27232
An assessment of information demands for remote sensing and Geographic Information System technologies
[PB89-159313] N89-27233
Procedural guide for the retrieval of dropsize distributions in water clouds from ground-based clear-air-sensing Doppler radar observations
[PB89-152474] N89-27300
Satellite image processing using symbolic structures of reduced vision conditions
[INPE-4638-TDL/337] N89-27367
Activities report in space activities
[ISSN-0284-169X] N89-27458
Rotation of images by scan mirrors
[NASA-TM-101628] N89-27504
REMOTE SENSORS
Integrated silicon color sensors
[ETN-89-94800] N89-27509
REQUIREMENTS
Cost-optimal state feedback controller for all-attitude gimbal system
[AD-D013972] N89-26845
Deep space LADAR, phase 1
[AD-A207454] N89-27166
Software deficiency issues confronting the utilization of non-Von Neumann architectures
[AD-A207268] N89-27369
RESEARCH AND DEVELOPMENT
Ocean Energy Program summary. Volume 2: Research summaries, fiscal year 1988
[DE89-000859] N89-27248
RESEARCH FACILITIES
Institute for Materials Science and Engineering, Polymers: Technical activities 1988
[PB89-166094] N89-26993
RESEARCH MANAGEMENT
Wind power: Today's energy option
[DE89-000876] N89-27253
RESEARCH VEHICLES
Research in knowledge-based vision techniques for the autonomous land vehicle program
[AD-A208545] N89-26834
RESIDENTIAL ENERGY
Refrigerator-freezer energy testing with alternative refrigerants
[DE89-013543] N89-27037
User guide for the Data Analysis, Retrieval, and Tabulation System (DARTS): A mainframe computer code for generating cross-tabulation reports
[DE89-012930] N89-27592
RESIDUAL STRESS
Optimum interface properties for metal matrix composites
[NASA-TM-102295] N89-27223
Residual stress changes in fatigue. Volume 1: Residual stress measurements by X-ray diffraction in notched test specimens
[AD-A208345] N89-27225
Residual stress changes in fatigue. Volume 2: A simulation model for stress measurements in notched test specimens by X-ray diffraction
[AD-A208346] N89-27226
RESISTANCE HEATING
MHD calculations of anode plasmas
[DE89-014485] N89-27535
RESISTANCE THERMOMETERS
Method for calibrating a heat flux gauge
[AD-D013974] N89-27138
RESISTOJET ENGINES
The NASA low thrust propulsion program
[NASA-TM-102065] N89-26895
RESISTORS
Solid state gas pressure sensor
[AD-D014105] N89-27139
RESONANCE
Surface plasmon study of monolayer-bilayer transition in poly-4-BCMU and poly-3-BCMU polydiacetylene Langmuir-Blodgett films
[AD-A207404] N89-26938
RESONANT FREQUENCIES
Sensors for in situ monitoring of elastic properties
[DE89-012795] N89-27145
RESONANT VIBRATION
KC-135R rumble investigation
[AD-A207532] N89-27464
RESONATORS
Polarization matrices of lithium tantalate
[AD-A208349] N89-27097
Design, development and evaluation of a doubly rotated AK-cut quartz crystal
[AD-A207209] N89-27549

RESPIRATORY SYSTEM
Altitude symptomatology and mood states during a climb to 3630 m
[AD-A206261] N89-27332
RETINA
Meridian variations in spectral dark adaptation
[AD-A207248] N89-27331
RETROREFLECTION
Modeling of the angular reflectance of an artificial plant canopy near the retroreflection peak in the optical regime
[DE89-011174] N89-27239
REUSABLE SPACECRAFT
Two-stage reusable launch system utilizing a winged core vehicle and glideback boosters
[NASA-TM-101513] N89-26878
REYNOLDS STRESS
Calculation of turbulence-driven secondary motion in ducts with arbitrary cross section
[NASA-TM-102142] N89-27115
RHENIUM ALLOYS
Local density theory of heats of formation and short-range order parameters in substitutionally disordered alloys
[DE89-014896] N89-26986
RHODIUM
Modifiers in rhodium catalysts for carbon monoxide hydrogenation: Structure-activity relationships
[DE89-013802] N89-27026
RIEMANN MANIFOLD
On a computational method for the second fundamental tensor and its application to bifurcation problems
[AD-A207517] N89-27377
RIGID STRUCTURES
Stability of a rigid rotor supported on oil-film journal bearings under dynamic load
[NASA-TM-102309] N89-27114
RISK
Risk assessment of compressed natural gas-fueled vehicle operations, phase 1
[PB89-188641] N89-27196
Study for advanced civil earth remote sensing system: Focused finance study. Volume 1: Executive summary
[PB89-163224] N89-27230
Software management indicators: Managing the risk of project management
[AD-A206443] N89-27408
ROBOTICS
Autonomous underwater systems for survey operations
[PB89-187397] N89-27041
Interactions between the National Institute of Standards and Technology and the American Society of Mechanical Engineers
[PB89-172563] N89-27182
Six degrees of freedom micromanipulator
[AD-D014113] N89-27190
Research in autonomous robotics at ORNL using HERMIES-3
[DE89-004933] N89-27198
Automated immersion testing robotic system: Hardware and software design
[AD-A208755] N89-27201
A model of human reaction time to dangerous robot arm movements
[PB89-186522] N89-27339
An efficient exact algorithm for the least squares image registration problems
[DE89-013116] N89-27387
ROBOTS
Autonomous land navigation: A demonstration of retrotraverse
[DE89-011881] N89-26855
Research in autonomous robotics at ORNL using HERMIES-3
[DE89-004933] N89-27198
Autonomous discovery and learning by a mobile robot in unstructured environments
[DE89-001525] N89-27415
ROBUSTNESS (MATHEMATICS)
Heuristic algorithms for stability testing polytopes of matrices
[PB89-160840] N89-27365
ROCKET ENGINE CASES
Contemporary composite polar boss
[AD-D014074] N89-26897
ROCKET ENGINE DESIGN
NASA's Chemical Transfer Propulsion Program for Pathfinder
[NASA-TM-102296] N89-26878
ROCKET ENGINES
Development of a high power microwave thruster, with a magnetic nozzle, for space applications
[NASA-TM-102321] N89-26904
Space station hydrogen/oxygen thruster technology
[NASA-CR-182280] N89-26905
ROCKET NOZZLES
Development of a high power microwave thruster, with a magnetic nozzle, for space applications
[NASA-TM-102321] N89-26904
Space station hydrogen/oxygen thruster technology
[NASA-CR-182280] N89-26905
ROCKS
Comparison of spectral data gathered from a laboratory spectrometer and TM images with and without shadow correction
[DE89-010877] N89-27237
Mafic and ultramafic xenoliths from volcanic rocks of the western United States
[PB89-124127] N89-27278
ROLL
Design considerations of manipulator and feel system characteristics in roll tracking
[NASA-CR-4111] N89-26860
ROLL FORMING
Thermomechanical processing of aluminum alloy 2090 for superplasticity
[AD-A206764] N89-26992
ROOM TEMPERATURE
Rate-sensitivity and short term relaxation behavior of AISI Type 304 stainless steel at room temperature and at 650 C; influence of prior aging
[DE89-007823] N89-26978
ROTARY ENGINES
Advanced ceramics: A critical assessment of wear and lubrication
[PB89-188569] N89-27005
ROTARY WINGS
Design of an active helicopter control experiment at the Princeton Rotorcraft Dynamics Laboratory
[NASA-CR-185490] N89-26859
ROTATING SHAFTS
OTVE turbopump condition monitoring, task E.5
[NASA-CR-182274] N89-27204
ROTATION
Anti-rotation guide bushing
[AD-D014079] N89-27186
Electromagnetic pulse rotary seal
[AD-D014080] N89-27187
ROTATIONAL SPECTRA
Temporal variability of water masers in the Southern Hemisphere
[INPE-4646-TDL/338] N89-27609
ROTOR BLADES (TURBOMACHINERY)
Experimental assessment of helicopter rotor turbulence ingestion noise in hover
[NASA-CR-181792] N89-27468
ROTORS
Statistics on aircraft gas turbine engine rotor failures that occurred in US commercial aviation during 1983
[AD-A207592] N89-26851
Verification analysis of the Toroidal Accelerator Rotor Platform wind energy conversion system
[PB89-162069] N89-27241
RULES
Rule-based air combat simulation
[NASA-CR-4160] N89-27393
RUN TIME (COMPUTERS)
Model-based parameter estimation in electromagnetic computer modeling
[AD-A207399] N89-27052
RUNGE-KUTTA METHOD
Solutions of differential equations with regular coefficients by the methods of Richmond and Runge-Kutta
[NASA-TM-101609] N89-27060
RUNWAYS
Acta Aeronautica et Astronautica Sinica, Volume 8, Number 12, December 1987 (selected articles)
[AD-A206782] N89-26807
Evaluation of barrier cable impact pad materials
[AD-A207554] N89-26864

S

SAFETY
Risk assessment of compressed natural gas-fueled vehicle operations, phase 1
[PB89-188641] N89-27196
Safety testing program for the Galileo mission radioisotope thermoelectric generator
[DE89-011192] N89-27494
SALT SPRAY TESTS
Stress corrosion study of PH13-8Mo stainless steel using the Slow Strain Rate Technique
[NASA-TP-2934] N89-26976
SAMPLING
Sampling based approaches to calculating marginal densities
[AD-A208368] N89-27451
SAN ANDREAS FAULT
Geodetic measurement of deformation in California
[NASA-TM-100732] N89-27279
SATELLITE ALTIMETRY
Altimetric system: Earth observing system. Volume 2h: Panel report
[NASA-TM-89722] N89-27229
GEOSAT altimeter sea-ice mapping
[AD-A207391] N89-27234
SATELLITE ATTITUDE CONTROL
Satellite attitude control analysis and design using linearizing transformations
[INPE-4772-PRE/1441] N89-26886
Spin stabilization of the ORION satellite using a thruster attitude control system with optimal control considerations
[AD-A208484] N89-26892
SATELLITE COMMUNICATION
Programmable rate modem utilizing digital signal processing techniques
[NASA-CR-185124] N89-26879
Evaluation of low data rate voice CODECS for air traffic control applications
[DOT/FAA/CT-TN89/13] N89-27047
SATELLITE IMAGERY
SP-ATUS: An expert system for specifications of satellite imagery
[INPE-4754-PRE/1426] N89-27236
Rotation of images by scan mirrors
[NASA-TM-101628] N89-27504
SATELLITE OBSERVATION
A center for commercial development of space: Real-time satellite mapping. Remote sensing-based agricultural information expert system
[NASA-CR-185473] N89-27235
SATELLITE ORBITS
Satellite relocation by tether deployment
[NASA-TM-101992] N89-26877
SATELLITE PERTURBATION
Satellite relocation by tether deployment
[NASA-TM-101992] N89-26877
SATELLITE ROTATION
Study of jitter on the attitude motion of a spin stabilized satellite with two flexible solar panels
[INPE-4744-PRE/1418] N89-26884
SATELLITE SOUNDING
The international TOVS (Tiros Operational Vertical Sounder) processing package: An evaluation
[AD-A207548] N89-27306
Activities report in space activities
[ISSN-0284-169X] N89-27458
SATELLITE TRANSMISSION
Development of a DFS (Deutsche Fernmeldesatellit) reception converter
[ETN-89-94629] N89-27065
SATELLITE-BORNE INSTRUMENTS
Space Environment Laboratory
[PB89-159602] N89-27607
SATURABLE REACTORS
Improved core insulation schemes for multi-terawatt magnetic switches
[DE89-013814] N89-27093
SCALE (CORROSION)
Breakdown mechanisms of Al2O3, Cr2O3 and SiO2 scales in H2/H2O/H2S environments, volume 1
[DE89-014789] N89-26988
SCALING LAWS
Scaling effects in the static large deflection response of graphite-epoxy composite beams
[NASA-TM-101619] N89-26843
A compound scaling algorithm for mathematical optimization
[AD-A208446] N89-27409
SCATTERING
Synthesis of resistive tapers to control scattering patterns of strips
[AD-A207211] N89-27049
Computational techniques in gamma-ray Skyshine analysis
[DE89-010156] N89-27282
Relativistic corrections to photon scattering polarizabilities
[NOTA-INTERNA-916] N89-27487
SCATTERING CROSS SECTIONS
A preliminary report on X-ray photoabsorption coefficients and atomic scattering factors for 92 elements in the 10-10,000 eV region
[DE89-013392] N89-26950
Theory of X-ray holography including phase and amplitude contrast and finite transfer functions
[DE89-012835] N89-27148
Collision processes of interest in MFE plasma research
[DE89-013681] N89-27524

SCINTILLATION COUNTERS
The diagonal strip system in the Macro experiment [NOTA-INTERNA-924] N89-27159
A one-dimensional scintillator camera for the SATURN X-ray simulation accelerator [DE89-009327] N89-27492
SEA ICE
Alaska collection SAR (Synthetic Aperture Radar) data summary [AD-A208530] N89-27067
GEOSAT altimeter sea-ice mapping [AD-A207391] N89-27234
SEA SURFACE TEMPERATURE
Attitude angle effects on Nimbus-7 Scanning Multichannel Microwave Radiometer radiances and geophysical parameter retrievals [NASA-TM-4132] N89-27289
SEALING
Vane platform sealing and retention means [AD-D013980] N89-27180
SEALS (STOPPERS)
Nozzle flange attachment and sealing arrangement [AD-D014123] N89-26853
Self-locking outer air seal with full backside cooling [AD-D013975] N89-27179
Vane platform sealing and retention means [AD-D013980] N89-27180
Electromagnetic pulse rotary seal [AD-D014080] N89-27187
Bimetallic air seal for exhaust nozzles [AD-D014106] N89-27189
SEAMS (JOINTS)
Field joint protection system rain qualification test report [NASA-CR-183702] N89-26901
SEATS
OH-58 energy attenuating crew seat feasibility study [AD-A207506] N89-26829
Injuries to seat occupants of light airplanes [AD-A207579] N89-26830
SEEBECK EFFECT
Thermoelectric terminology in metrology and standards [DE89-011512] N89-27079
SEISMIC WAVES
Investigations on local seismic phases and evaluation of body waves magnitude [AD-A206633] N89-27283
Application of the theory of wave propagation through random media to phase and amplitude fluctuations of seismic P-waves [AD-A207207] N89-27284
SEISMOGRAMS
Investigations on local seismic phases and evaluation of body waves magnitude [AD-A206633] N89-27283
SEISMOLOGY
Earth sciences [DE89-013344] N89-27228
Investigations on local seismic phases and evaluation of body waves magnitude [AD-A206633] N89-27283
Application of the theory of wave propagation through random media to phase and amplitude fluctuations of seismic P-waves [AD-A207207] N89-27284
Computer simulations of explosive volcanic eruptions [DE89-014024] N89-27290
SELENIDES
New strategies for display devices based on 2-6 materials [AD-A208288] N89-27573
SELENIUM ALLOYS
New strategies for display devices based on 2-6 materials [AD-A208288] N89-27573
SEMANTICS
Northeast Artificial Intelligence Consortium annual report 1987. Volume 2, part b: Discussing, using, and recognizing plans [AD-A208378] N89-27418
SEMICONDUCTOR DEVICES
Dual-transistor method to determine delta V sub ot and delta V sub it for MOS devices [DE89-006725] N89-27088
SEMICONDUCTOR LASERS
Evaluation of an optical correlator and matched filter maker [AD-A207556] N89-27054
Transverse pumping with diode lasers [AD-A207261] N89-27165
High power semiconductor laser sources [AD-A207569] N89-27167
SEMICONDUCTOR PLASMAS
Depth profiles and bulk analysis of semiconductor materials using ICP mass spectroscopy with electrothermal atomization [AD-A206974] N89-27548
SEMICONDUCTORS (MATERIALS)
Magnetic and electrical properties of sandwich-like lanthanide phthalocyanines [AD-A208411] N89-26958
Photoconductive semiconductor switch (PCSS) recovery [DE89-012657] N89-27080
Closing photoconductive semiconductor switches [DE89-013073] N89-27082
Frequency-domain transient analysis of silicon solar cells [DE89-010555] N89-27243
Model for hot electron phenomena: Theory and general results [DE88-705986] N89-27544
Depth profiles and bulk analysis of semiconductor materials using ICP mass spectroscopy with electrothermal atomization [AD-A206974] N89-27548
SENSITIVITY
BAE measurement schemes and optimal sensitivity for generalized parametric devices [PREPRINT-641] N89-27586
SENSORIMOTOR PERFORMANCE
Design considerations of manipulator and feel system characteristics in roll tracking [NASA-CR-4111] N89-26860
SEPARATED FLOW
Numerical study of three-dimensional separation and flow control at a wing/body junction [NASA-CR-185819] N89-26826
A review of high-speed, convective, heat-transfer computation methods [NASA-TP-2914] N89-27116
SEPARATION
Loss of grain boundary segregant during ion milling [DE89-007835] N89-26979
SEPARATORS
Gas separations using inorganic membranes [DE89-013010] N89-26948
SEQUENCING
Window generator [AD-D014068] N89-27048
An overview of some methods for the high-level specification of synchronization [MEMO-INF-88-50] N89-27403
SEQUENTIAL COMPUTERS
Easily testable PLA-based finite state machines [AD-A208371] N89-27098
SERIES EXPANSION
A MACSYMA package for the generation and manipulation of Chebyshev series [DE89-011404] N89-27436
SERUMS
Endogenous hormonal and growth factor responses to heavy resistance exercise protocols [AD-A208375] N89-27336
SERVOMECHANISMS
Control surface dual redundant servomechanism [AD-D014058] N89-26857
SHADOWGRAPH PHOTOGRAPHY
An investigation into the use of an existing shock tube as a driver for a hypersonic shock tunnel [AD-A208483] N89-26872
SHADOWS
Comparison of spectral data gathered from a laboratory spectrometer and TM images with and without shadow correction [DE89-010877] N89-27237
SHAFTS (MACHINE ELEMENTS)
Antenna shaft positioning device [AD-D014120] N89-27191
SHEAR FLOW
Inviscid spatial stability of a compressible mixing layer. Part 3: Effect of thermodynamics [NASA-CR-181855] N89-27112
SHEAR LAYERS
Design and calibration of the mixing layer and wind tunnel [NASA-CR-185472] N89-26866
SHEAR PROPERTIES
Measurement of wall shear and wall pressure downstream of a honeycomb boundary layer manipulator [AD-A208297] N89-27132
Measured damping and modulus of composite cylinders [DE89-010369] N89-27209
A three-node C deg element for analysis of laminated composite sandwich shells [NASA-TM-4125] N89-27213
Fate and effects of PAHs in the terrestrial environment: An overview [DE89-010319] N89-27267
SHELLS (STRUCTURAL FORMS)
A three-node C deg element for analysis of laminated composite sandwich shells [NASA-TM-4125] N89-27213
SHOCK HEATING
A review of high-speed, convective, heat-transfer computation methods [NASA-TP-2914] N89-27116
SHOCK LOADS
MM and T for linear resonant cooler, volume 2 [AD-A207236] N89-27073
SHOCK SIMULATORS
A multidriver shock tube model of a large blast simulator [AD-A208324] N89-26871
SHOCK TUBES
A multidriver shock tube model of a large blast simulator [AD-A208324] N89-26871
SHOCK TUNNELS
An investigation into the use of an existing shock tube as a driver for a hypersonic shock tunnel [AD-A208483] N89-26872
SHOCK WAVE INTERACTION
Numerical simulation of a turbulent flow through a shock wave [AD-A207581] N89-27107
Numerical studies of shock wave structure sensitivity to interactions with turbulent fields [DE89-012288] N89-27110
The structure of Normal-Shock/Turbulent-Boundary-Layer interactions modified by mass removal [AD-A208402] N89-27134
SHOCK WAVE PROPAGATION
The behavior of flux difference splitting schemes near slowly moving shock waves [FFA-TN-1988-58] N89-27130
SHOCK WAVES
A multidriver shock tube model of a large blast simulator [AD-A208324] N89-26871
Application of crystal lattice disintegration criteria to compute minimum shock induced reactive conditions in solid explosives and inert materials [AD-A207557] N89-27025
Thin pulse shock initiation characterization of extrusion-cast explosives: Revision [DE89-008029] N89-27027
Characterization of Morton-Thiokol booster-rocket propellant TP-H1207C and its simulant H-19 [DE89-013347] N89-27031
Numerical simulation of a turbulent flow through a shock wave [AD-A207581] N89-27107
Numerical studies of shock wave structure sensitivity to interactions with turbulent fields [DE89-012288] N89-27110
Computer simulations of explosive volcanic eruptions [DE89-014024] N89-27290
SHORT CIRCUITS
The short-circuited fluxgate output current [ISSN-0109-6605] N89-27069
SIDELOBES
Synthesis of resistive tapers to control scattering patterns of strips [AD-A207211] N89-27049
SIEVES
Molecular sieve films from zeolited-silica microcomposites [DE89-009831] N89-26921
SIGNAL DETECTION
Some results on nonGaussian signal detection [AD-A207255] N89-27050
Detection, acquisition and signal demodulation in a communication system with random access [INPE-4779-RPE/581] N89-27061
SIGNAL DETECTORS
Development of a system model and Least Mean Square (LMS) filter for the Naval Postgraduate School (NPS) Infrared Search and Target Designation System (IRSTD) [AD-A208536] N89-27068
System for measuring optical waveguide intensity profiles [PB89-188593] N89-27507
SIGNAL DISTORTION
Efficient dynamic phasefront modulation system for free-space optical communications [AD-D014128] N89-27503
SIGNAL MEASUREMENT
Loran C coverage in Alaska after dual rating Port Clarence [AD-A196032] N89-26831

Wideband electromagnetic damping of vibrating structures
[AD-D014069] N89-27206

SIGNAL MIXING
Theoretical analysis of microwave and millimeter wave integrated circuits based on magnetic films
[AD-A207508] N89-27074

SIGNAL PROCESSING
Programmable rate modem utilizing digital signal processing techniques
[NASA-CR-185124] N89-26879
Detection, acquisition and signal demodulation in a communication system with random access
[INPE-4779-RPE/581] N89-27061
Polarization matrices of lithium tantalate
[AD-A208349] N89-27097
Infrared temperature measurement with self regulating emission ratio
[ETN-89-94654] N89-27157
Joint CGS-AOML (Charting and Geodetic Service-Atlantic Oceanographic and Meteorological Laboratory) acoustical bottom echo-formation research. 2: Field experiment results and recommendations for echo-sounder design
[PB89-152417] N89-27322
DFT algorithms for bit-serial GaAs array processor architectures
[NASA-CR-183436] N89-27361
High efficiency pattern recognition
[AD-A207210] N89-27366
Polarization matrices of lithium niobate
[AD-A207231] N89-27462

SIGNAL RECEPTION
Millimeter-wave propagation characteristics and channel performance for urban-suburban environments
[PB89-180251] N89-27058
On capture effect of FM demodulators
[AD-A208479] N89-27066

SIGNAL TO NOISE RATIOS
Development of a system model and Least Mean Square (LMS) filter for the Naval Postgraduate School (NPS) Infrared Search and Target Designation System (IRSTD)
[AD-A208536] N89-27068
Low-noise cable for diagnostics, control and instrumentation of the ASDEX tokamak fusion experiment
[IPP-III/87] N89-27094

SIGNATURES
Issues and approaches for electronic document approval and transmittal using digital signatures and text authentication
[DE89-013102] N89-27596

SIGNS AND SYMPTOMS
Altitude symptomatology and mood states during a climb to 3630 m
[AD-A208261] N89-27332

SILANES
The structure and reactivity of alkylsiloxane monolayers formed by reaction of alkyltrichlorosilanes on silicon substrates
[AD-A208267] N89-27011
Chemical vapor deposition of silicon carbide using a novel organometallic precursor
[AD-A208273] N89-27012
Synthesis and structural characterization of Pt-Si dimers with unusually short cross-ring silicon-silicon interactions
[AD-A208310] N89-27014
Dynamics of surface bound polymers and coupling agents
[AD-A208747] N89-27020

SILICON
Theory of aggregate defects in silicon
[AD-A207273] N89-26999
Proposed thin film electronics for a-Si:H PIXEL detector
[DE89-013410] N89-27083
Integrated silicon color sensors
[ETN-89-94800] N89-27509
Photoelectronic properties of low temperature GaAs grown on silicon and GaAs substrates by MBE
[DE89-013148] N89-27557

SILICON CARBIDES
Erosion of Al and Al/SiC
[DE89-013623] N89-26913
Fracture toughness of SiC/Al metal matrix composite
[NASA-TM-100745] N89-26918
SiC-MoSi composites
[DE89-013656] N89-26923
Fatigue crack growth study of SCS6/Ti-15-3 composite
[NASA-TM-102332] N89-26989
Structural reliability and damage tolerance of ceramic composites for high-temperature applications
[PB89-156350] N89-26994
Structural reliability and damage tolerance of ceramic composites for high-temperature applications
[PB89-156368] N89-26995
Toughening mechanisms in ceramic composites
[PB89-162606] N89-26996
Chemical vapor deposition of silicon carbide using a novel organometallic precursor
[AD-A208273] N89-27012

SILICON COMPOUNDS
Synthesis and structural characterization of Pt-Si dimers with unusually short cross-ring silicon-silicon interactions
[AD-A208310] N89-27014

SILICON DIOXIDE
Molecular sieve films from zeolited-silica microcomposites
[DE89-009831] N89-26921
Breakdown mechanisms of Al2O3, Cr2O3 and SiO2 scales in H2/H2O/H2S environments, volume 1
[DE89-014789] N89-26988
The structure of self-assembled monolayers of alkylsiloxanes on silicon: A comparison of results from ellipsometry and low-angle X-ray reflectivity
[AD-A208341] N89-27016
Electrochemical reactions in submerged arc welding with SiO2-CaO-CaF2 fluxes with high and low silica contents
[DE89-012421] N89-27194

SILICON FILMS
The structure and reactivity of alkylsiloxane monolayers formed by reaction of alkyltrichlorosilanes on silicon substrates
[AD-A208267] N89-27011
Chemical vapor deposition of silicon carbide using a novel organometallic precursor
[AD-A208273] N89-27012

SILICON NITRIDES
Development of magnetic resonance imaging technology for imaging binder distribution in ceramics
[DE89-013185] N89-27003
Fractographic study of a silicon nitride ceramic
[DE89-013012] N89-27006

SILOXANES
The structure and reactivity of alkylsiloxane monolayers formed by reaction of alkyltrichlorosilanes on silicon substrates
[AD-A208267] N89-27011
The structure of self-assembled monolayers of alkylsiloxanes on silicon: A comparison of results from ellipsometry and low-angle X-ray reflectivity
[AD-A208341] N89-27016

SILVER
Oxygen transfer to ethylene catalyzed by the Ag(110) surface
[AD-A207325] N89-26936
Study of the microstructure of silver films deposited by ion assisted deposition onto aluminum oxide substrates
[DE89-014665] N89-27563

SIMULATION
Hose reel monitor for inflight refueling system
[AD-D014054] N89-26836
Field joint protection system rain qualification test report
[NASA-CR-183702] N89-26901
Development of a system model and Least Mean Square (LMS) filter for the Naval Postgraduate School (NPS) Infrared Search and Target Designation System (IRSTD)
[AD-A208536] N89-27068
Numerical simulation of a turbulent flow through a shock wave
[AD-A207581] N89-27107
High efficiency pattern recognition
[AD-A207210] N89-27366
A one-dimensional scintillator camera for the SATURN X-ray simulation accelerator
[DE89-009327] N89-27492

SIMULATORS
Human Operator Simulator (HOS) 4 programmer's guide
[AD-A207241] N89-27342

SINGLE CRYSTALS
Magnetic and electrical properties of sandwich-like lanthanide phthalocyanines
[AD-A208411] N89-26958
Analysis of microstructural development in single crystal welds
[DE89-013537] N89-26973
Large protein crystallization facility, phase A. Executive summary
[AQ-ES-175/88] N89-27035
Hybrid single crystal optic fibers by embedding
[AD-D013986] N89-27545
The response of single crystal and polycrystal nickel to quasistatic and shock deformation
[DE89-011168] N89-27564

SINTERING
The study of structure-processing-property relations in copper oxide-based high T sub c superconductors
[DE89-012764] N89-27554
Thin film preparation and single film device fabrication in the Tl-Ca-Ba-Cu-O HTS system
[DE89-013560] N89-27561
Recent improvements in bulk properties of ceramic superconductors
[DE89-013626] N89-27562

SITE SELECTION
The impact of solar radiation resources on the siting of solar thermal power plants
[DE89-000839] N89-27252

SKIN (STRUCTURAL MEMBER)
Composite transport wing technology development
[NASA-CR-178409] N89-26842

SKIN TEMPERATURE (BIOLOGY)
Thermoregulatory responses in the cold-effect of an Extended Cold Weather Clothing System (ECWCS)
[AD-A208314] N89-27334

SLEEVES
Anti-rotation guide bushing
[AD-D014079] N89-27186

SLIDING FRICTION
Wear and friction of thin film high temperature oxide superconductors
[DE89-009397] N89-27543

SLOTS
Vane platform sealing and retention means
[AD-D013980] N89-27180

SMOG
Regional ozone modeling in the northeastern US: Selection of meteorological episodes
[PB89-136691] N89-27259

SMOKE
Aerial smoke plume observations and surface layer turbulence measurements. Part 1: Project WIND. Phase 4: Dispersion study
[AD-A207370] N89-27305

SODIUM
Modifiers in rhodium catalysts for carbon monoxide hydrogenation: Structure-activity relationships
[DE89-013802] N89-27028

SOFTWARE ENGINEERING
Automated immersion testing robotic system: Hardware and software design
[AD-A208755] N89-27201
Software deficiency issues confronting the utilization of non-Von Neumann architectures
[AD-A207268] N89-27369
Kernel user's manual version 1.0
[AD-A207414] N89-27375
Abstract data types in computer graphics and image processing
[INPE-4745-PRE/1419] N89-27381
Small Computer System Interface (SCSI) command system: Software support for control of small computer system interface devices
[PB89-151815] N89-27389
Portable parallel programming in a FORTRAN environment
[DE89-014670] N89-27399

SOFTWARE TOOLS
Natural language processing
[INPE-4449-TDL/314] N89-27366
Software deficiency issues confronting the utilization of non-Von Neumann architectures
[AD-A207268] N89-27369

SOILS
Investigations of dielectric properties of some frozen materials using cross-borehole radiowave pulse transmissions
[AD-A207302] N89-27285

SOLAR ACTIVITY
Solar microwave radiation maps measured at Metsaehovi Radio Research Station in 1982 - 1983
[PB89-154876] N89-27621
Solar-geophysical data number 535, part 1. Data for February, January 1989, and late data
[PB89-185987] N89-27624
Berne solar observations for January-December 1988
[REPT-54] N89-27626

SOLAR ARRAYS
Photovoltaic module on-orbit assembly for Space Station Freedom
[NASA-TM-102297] N89-26887

SOLAR AUXILIARY POWER UNITS
LH sub 2/LO sub 2 rocket engine with solar energy
[NAL-TR-992] N89-26893

SOLAR CELLS
Study of jitter on the attitude motion of a spin stabilized satellite with two flexible solar panels
[INPE-4744-PRE/1418] N89-26884
LH sub 2/LO sub 2 rocket engine with solar energy
[NAL-TR-992] N89-26893

High-efficiency, large-area CdTe panels
[DE89-000891] N89-27242
Frequency-domain transient analysis of silicon solar cells
[DE89-010555] N89-27243
Lunar production of solar cells
[NASA-TM-102102] N89-27619

SOLAR COLLECTORS
Dynamic simulation of a molten-salt solar receiver
[DE89-010556] N89-27244

SOLAR COOLING
Sun synchronous solar refrigeration
[DE89-011375] N89-27245

SOLAR CORONA
Equilibrium of solar coronal arcades
[AD-A207311] N89-27622

SOLAR DYNAMIC POWER SYSTEMS
Alternate space station freedom configuration considerations to accommodate solar dynamic power
[NASA-TM-101603] N89-26888
Performance estimates for the Space Station power system Brayton Cycle compressor and turbine
[NASA-CR-182263] N89-26903
Thermal evaluation of advanced solar dynamic heat receiver performance
[NASA-CR-185117] N89-27256

SOLAR ENERGY
Alternate space station freedom configuration considerations to accommodate solar dynamic power
[NASA-TM-101603] N89-26888
LH sub 2/LO sub 2 rocket engine with solar energy
[NAL-TR-992] N89-26893
Dynamic simulation of a molten-salt solar receiver
[DE89-010556] N89-27244
Proceedings of the Annual Solar Thermal Technology Research and Development Conference
[DE89-010538] N89-27251
The impact of solar radiation resources on the siting of solar thermal power plants
[DE89-000839] N89-27252
Thermal evaluation of advanced solar dynamic heat receiver performance
[NASA-CR-185117] N89-27256
Solar radiation on Mars
[NASA-TM-102299] N89-27623

SOLAR FLARES
Solar-geophysical data number 535, part 2. Data for September 1988, and miscellaneous
[PB89-185995] N89-27625
Statistical study of the correlation of hard X-ray and type 3 radio bursts in solar flares
[NASA-CR-185833] N89-27629

SOLAR FURNACES
High temperature solar electrothermal processing
[AD-A207555] N89-27246

SOLAR OBSERVATORIES
Advanced Solar Observatory (ASO) accommodations requirements study
[NASA-CR-183718] N89-26885
Berne solar observations for January-December 1988
[REPT-54] N89-27626

SOLAR OSCILLATIONS
Solar microwave radiation maps measured at Metsaehovi Radio Research Station in 1982 - 1983
[PB89-154876] N89-27621

SOLAR PHYSICS
Space research in the Federal Republic of Germany (FRG), 1986 and 1987
[ETN-89-94427] N89-26874
Space Environment Laboratory
[PB89-159602] N89-27607
Solar-geophysical data number 535, part 1. Data for February, January 1989, and late data
[PB89-185987] N89-27624
Solar-geophysical data number 535, part 2. Data for September 1988, and miscellaneous
[PB89-185995] N89-27625

SOLAR PROMINENCES
Solar-geophysical data number 535, part 2. Data for September 1988, and miscellaneous
[PB89-185995] N89-27625

SOLAR RADIATION
The impact of solar radiation resources on the siting of solar thermal power plants
[DE89-000839] N89-27252
Global environmental effects of impact-generated aerosols: Results from a general circulation model, revision 1
[DE89-014179] N89-27276
Solar microwave radiation maps measured at Metsaehovi Radio Research Station in 1982 - 1983
[PB89-154876] N89-27621
Solar radiation on Mars
[NASA-TM-102299] N89-27623

SOLAR RADIO BURSTS
Solar-geophysical data number 535, part 2. Data for September 1988, and miscellaneous
[PB89-185995] N89-27625

SOLAR RADIO EMISSION
Solar microwave radiation maps measured at Metsaehovi Radio Research Station in 1982 - 1983
[PB89-154876] N89-27621
Solar-geophysical data number 535, part 1. Data for February, January 1989, and late data
[PB89-185987] N89-27624

SOLAR ROTATION
Relativistic explanation of the inclination of planetary orbits
[PB89-170005] N89-27611

SOLAR SYSTEM
Dynamics of the solar system: Proceedings, volume 3
[DE89-609828] N89-27615

SOLAR THERMAL ELECTRIC POWER PLANTS
Proceedings of the Annual Solar Thermal Technology Research and Development Conference
[DE89-010538] N89-27251
The impact of solar radiation resources on the siting of solar thermal power plants
[DE89-000839] N89-27252

SOLAR THERMAL PROPULSION
LH sub 2/LO sub 2 rocket engine with solar energy
[NAL-TR-992] N89-26893

SOLAR WIND
Space research in the Federal Republic of Germany (FRG), 1986 and 1987
[ETN-89-94427] N89-26874

SOLAR X-RAYS
Solar-geophysical data number 535, part 2. Data for September 1988, and miscellaneous
[PB89-185995] N89-27625

SOLDERED JOINTS
Observations on the mechanisms of fatigue in eutectic Pb-Sn solder joints
[DE89-000553] N89-26968

SOLDERS
Observations on the mechanisms of fatigue in eutectic Pb-Sn solder joints
[DE89-000553] N89-26968

SOLID ELECTROLYTES
Supersonics
[AD-A207394] N89-26814

SOLID MECHANICS
Computational methods for nonlinear dynamic problems in solid and structural mechanics: Progress in the theory and modeling of friction and in the control of dynamical systems with frictional forces
[AD-A208763] N89-27227

SOLID PROPELLANT COMBUSTION
Numerical computation of bifurcation phenomena and pattern formation in combustion
[DE89-013628] N89-26941

SOLID PROPELLANT IGNITION
Characterization of Morton-Thiokol booster-rocket propellant TP-H1207C and its simulant H-19
[DE89-013347] N89-27031

SOLID ROCKET PROPELLANTS
Process for assessing the effect of propellant strain on propellant burn rate
[AD-D014119] N89-27026

SOLID STATE
Miniature high voltage solid state relay
[AD-D013979] N89-27070
Solid state gas pressure sensor
[AD-D014105] N89-27139

SOLID STATE LASERS
Bibliography of Soviet laser developments, No. 92, November - December 1987
[AD-A207794] N89-27177

SOLID SURFACES
Dynamics of surface bound polymers and coupling agents
[AD-A208747] N89-27020

SOLIDIFICATION
Method to produce metal matrix composite articles from rich metastable-beta titanium alloys
[AD-D014064] N89-26907
Method to produce metal matrix composite articles from lean metastable beta titanium alloys
[AD-D014065] N89-26908
Dispersion strengthened aluminum-base alloy
[AD-D014044] N89-26959
The solidification metallurgy of Alloy 718 and other Nb-containing superalloys
[DE89-008196] N89-26966
Bearings fabricated from rapidly solidified powder and method
[AD-D014072] N89-27185

SOLIDS
The role of X-ray absorption spectroscopy in electronic structure studies
[DE89-014677] N89-26952
DYNA3D user's manual: (Nonlinear Dynamic Analysis of Structures in Three Dimensions), revision 5
[DE89-014304] N89-27222

SOLITARY WAVES
Statistics of an integrable discrete Sine Gordon system
[PREPRINT-638] N89-27128
Cosmic evolution of non-topological solitons, paper 1
[NASA-CR-185353] N89-27608

SOLVENTS
Laser dyes derived from bimanes
[AD-D013994] N89-27160

SORPTION
Automated immersion testing robotic system: Hardware and software design
[AD-A208755] N89-27201

SOUND FIXING AND RANGING
Propagating solutions and far-field patterns for acoustic harmonic waves in a finite depth ocean
[PB89-180715] N89-27325

SOUND PROPAGATION
Low-frequency sound propagation modeling over a locally-reacting boundary using the parabolic approximation
[NASA-CR-185864] N89-27469

SOUND TRANSMISSION
Measurement of the bending wave power flow by the structural intensity technique
[VTT-583] N89-27129
Cepstral method for the measurement of ultrasonic pulse transmission time variations
[AD-A207410] N89-27463

SOUND WAVES
Dynamics of double stimulated Brillouin scattering
[PB89-146369] N89-27513

SOUTHERN HEMISPHERE
Temporal variability of water masers in the Southern Hemisphere
[INPE-4646-TDL/338] N89-27609

SPACE BASED RADAR
Deep space LADAR, phase 1
[AD-A207454] N89-27166

SPACE COMMERCIALIZATION
Big dumb boosters: A low-cost space transportation option. An OTA (Office of Technology and Assessment) background paper
[PB89-155196] N89-26881
Industrial applications of the microgravity environment
[NASA-CR-181516] N89-27034

SPACE COMMUNICATION
Atmospheric propagation issues relevant to optical communications
[NASA-CR-185718] N89-27261

SPACE EXPLORATION
NASA's Chemical Transfer Propulsion Program for Pathfinder
[NASA-TM-102298] N89-26876

SPACE INDUSTRIALIZATION
Industrial applications of the microgravity environment
[NASA-CR-181516] N89-27034

SPACE LOGISTICS
Columbus Logistics Program
[MBB-UO-0039/88-PUB] N89-26890

SPACE MANUFACTURING
Lunar production of solar cells
[NASA-TM-102102] N89-27619

SPACE MISSIONS
The best we can be
[NASA-TM-101781] N89-26873

SPACE OBSERVATIONS (FROM EARTH)
Berne solar observations for January-December 1988
[REPT-54] N89-27626

SPACE PERCEPTION
Research in knowledge-based vision techniques for the autonomous land vehicle program
[AD-A206546] N89-26834

SPACE PLASMAS
Activities report in space activities
[ISSN-0284-169X] N89-27458
Ionospheric plasma escape by high-altitude electric fields: Magnetic moment pumping
[IRF-PREPRINT-111] N89-27542

SPACE PLATFORMS
SDS software measurement requirements
[AD-A207449] N89-27376
Shield optimization program. Part 1: Executive summary
[DE89-013335] N89-27478

SPACE PROCESSING
Space research in the Federal Republic of Germany (FRG), 1986 and 1987
[ETN-89-94427] N89-26874

SPACE PROGRAMS
NASA's Chemical Transfer Propulsion Program for Pathfinder
[NASA-TM-102298] N89-26876
SPACE SHUTTLE BOOSTERS
Field joint protection system rain qualification test report
[NASA-CR-183702] N89-26901
SPACE SHUTTLE MAIN ENGINE
Space Shuttle Main Engine structural analysis and data reduction/evaluation. Volume 7: High pressure fuel turbo-pump third stage impeller analysis
[NASA-CR-183670] N89-26894
Space Shuttle Main Engine radio frequency emissions
[NASA-CR-184707] N89-26896
SPACE SHUTTLES
Atmospheric environment for Space Shuttle (STS-27) launch
[NASA-TM-100370] N89-27316
SPACE STATION POWER SUPPLIES
Alternate space station freedom configuration considerations to accommodate solar dynamic power
[NASA-TM-101603] N89-26888
Performance estimates for the Space Station power system Brayton Cycle compressor and turbine
[NASA-CR-182263] N89-26903
SPACE STATIONS
Advanced Solar Observatory (ASO) accommodations requirements study
[NASA-CR-183718] N89-26885
Photovoltaic module on-orbit assembly for Space Station Freedom
[NASA-TM-102297] N89-26887
Alternate space station freedom configuration considerations to accommodate solar dynamic power
[NASA-TM-101603] N89-26888
Space station hydrogen/oxygen thruster technology
[NASA-CR-182280] N89-26905
SPACE WEAPONS
Directed energy weapons/en dash/lasers: Ground- and space-based systems
[DE89-012804] N89-27452
Shield optimization program. Part 1: Executive summary
[DE89-013335] N89-27476
SPACE-TIME FUNCTIONS
On the integrability of the Ernst equation
[PREPRINT-606] N89-27584
SPACEBORNE ASTRONOMY
Space research in the Federal Republic of Germany (FRG), 1986 and 1987
[ETN-89-94427] N89-26874
SPACEBORNE TELESCOPES
Advanced Solar Observatory (ASO) accommodations requirements study
[NASA-CR-183718] N89-26885
SPACECRAFT CONFIGURATIONS
Alternate space station freedom configuration considerations to accommodate solar dynamic power
[NASA-TM-101603] N89-26888
SPACECRAFT CONSTRUCTION MATERIALS
Fatigue crack growth study of SCS6/Ti-15-3 composite
[NASA-TM-102332] N89-26989
SPACECRAFT DESIGN
Alternate space station freedom configuration considerations to accommodate solar dynamic power
[NASA-TM-101603] N89-26888
SPOT 1-2-3 Pyrotechnics System: Definition repo rt
[CNES-CT/DRT/TVE/IL-89-035] N89-26889
SPACECRAFT EQUIPMENT
Total-dose hardness assurance for space applications of commercial CMOS devices
[DE89-006765] N89-27089
SPACECRAFT LAUNCHING
Atmospheric environment for Space Shuttle (STS-27) launch
[NASA-TM-100370] N89-27316
SPACECRAFT MODELS
Modeling of liquid sloshing effects in multi body systems
[MBB-UK-0024/88-PUB] N89-26891
SPACECRAFT PROPULSION
NASA's Chemical Transfer Propulsion Program for Pathfinder
[NASA-TM-102298] N89-26876
The NASA low thrust propulsion program
[NASA-TM-102065] N89-26895
Hybrid electric chemical propulsion
[AD-A207584] N89-26898
Development of a high power microwave thruster, with a magnetic nozzle, for space applications
[NASA-TM-102321] N89-26904
Space station hydrogen/oxygen thruster technology
[NASA-CR-182280] N89-26905
Electric propulsion options for 10 kW class earth space missions
[NASA-TM-102337] N89-26906
SPACELAB PAYLOADS
Large protein crystallization facility, phase A. Executive summary
[AQ-ES-175/88] N89-27035
SPARK IGNITION
Lean-burn gas engine ignition processes
[PB89-181119] N89-26943
SPATIAL DISTRIBUTION
Distribution of auroral arcs during quiet geomagnetic conditions
[DMI-GEOPHYS-PAPERS-R-78] N89-27292
SPECIFICATIONS
SPOT 1-2-3 Pyrotechnics System: Definition repo rt
[CNES-CT/DRT/TVE/IL-89-035] N89-26889
Hardware C - A language for hardware design
[AD-A207317] N89-27370
The HERMOD behavioral synthesis system
[AD-A207319] N89-27371
SPECKLE PATTERNS
Performance comparison among several filters for the reducton of speckle noise in radar imagery
[INPE-4768-PRE/1437] N89-27055
Implementation of an order filter and its applications in radar imagery (SAR)
[INPE-4749-PRE/1422] N89-27385
SPECTRA
Micropyrolyzer design for infrared spectroscopy applications
[DE89-013329] N89-26949
Dynamics of surface bound polymers and coupling agents
[AD-A208747] N89-27020
Spectra of surface waves
[AD-A208462] N89-27326
SPECTRAL CORRELATION
Evaluation of an optical correlator and matched filter maker
[AD-A207556] N89-27054
SPECTRAL LINE WIDTH
Anomalous temperature dependence of Cu NMR line width and magnetization in YBa2Cu3O(7-delta)
[DE89-014291] N89-27565
SPECTRAL METHODS
Solution of compressible time-dependent Navier-Stokes equations by Chebychev spectral methods
[ONERA-NT-1987-1] N89-27126
Nonlinear wave equations solvable by the spectral transform
[PREPRINT-957] N89-27443
SPECTROMETERS
An instantaneous CCN (Cloud Condensation Nucleus) spectrometer
[DE89-014807] N89-27150
Comparison of spectral data gathered from a laboratory spectrometer and TM images with and without shadow correction
[DE89-010877] N89-27237
SPECTROSCOPIC ANALYSIS
Micropyrolyzer design for infrared spectroscopy applications
[DE89-013329] N89-26949
An Auger sputter profiling study of nitrogen and oxygen ion implantation in two titanium alloys
[DE89-014734] N89-26957
SPECTROSCOPY
Surface plasmon study of monolayer-bilayer transition in poly-4-BCMU and poly-3-BCMU polydiacetylene Langmuir-Blodgett films
[AD-A207404] N89-26936
Materials analysis with nuclear microprobes: Superconductors and buried conductors
[DE89-006580] N89-27206
Nitrogen 15 T1 measurements of semicrystalline nylon 6
[AD-A208481] N89-27575
SPHERICAL SHELLS
Dynamic plastic buckling of spherical shells during collapse
[DE89-006543] N89-27217
SPIN DYNAMICS
Spin stabilization of the ORION satellite using a thruster attitude control system with optimal control considerations
[AD-A208484] N89-26892
Dynamics of surface bound polymers and coupling agents
[AD-A208747] N89-27020
SPIN STABILIZATION
Study of jitter on the attitude motion of a spin stabilized satellite with two flexible solar panels
[INPE-4744-PRE/1418] N89-26884
Spin stabilization of the ORION satellite using a thruster attitude control system with optimal control considerations
[AD-A208484] N89-26892
SPIN-SPIN COUPLING
Dynamics of surface bound polymers and coupling agents
[AD-A208747] N89-27020
SPIRAL GALAXIES
The molecular cloud content of early type galaxies. 1: Detections and global properties
[PB89-184949] N89-27613
SPOT (FRENCH SATELLITE)
SPOT 1-2-3 Pyrotechnics System: Definition repo rt
[CNES-CT/DRT/TVE/IL-89-035] N89-26889
SPUTTERING
Technical activities 1988, Surface Science Division
[PB89-161889] N89-26928
An Auger sputter profiling study of nitrogen and oxygen ion implantation in two titanium alloys
[DE89-014734] N89-26957
Sputtering of high-temperature superconductors: A bibliography
[DE89-013374] N89-27558
STABILITY
Inviscid spatial stability of a compressible mixing layer. Part 3: Effect of thermodynamics
[NASA-CR-181855] N89-27112
Stability of a rigid rotor supported on oil-film journal bearings under dynamic load
[NASA-TM-102309] N89-27114
Waves and instabilities in nonneutral plasmas
[DE89-012403] N89-27515
STAINLESS STEELS
The effect of aging at 343 deg C on type 308 stainless steel welds
[DE89-013545] N89-26974
Stress corrosion study of PH13-8Mo stainless steel using the Slow Strain Rate Technique
[NASA-TP-2934] N89-26976
An experimental study of the effect of stainless steel cladding on the structural integrity of flawed steel plates in bending
[DE89-008735] N89-26980
STANDARDIZATION
Automatic oxygen measuring system
[AD-D014003] N89-26931
STANDARDS
Compositas databases for the 1990's
[PB89-180376] N89-26914
Technical activities 1988, Surface Science Division
[PB89-161889] N89-26928
Thermoelectric terminology in metrology and standards
[DE89-011512] N89-27079
Center for Electronics and Electrical Engineering Technical Progress Bulletin covering center programs, October to December 1988 with 1989 CEEE events calender
[PB89-193270] N89-27087
Interactions between the National Institute of Standards and Technology and the American Society of Mechanical Engineers
[PB89-172563] N89-27182
Group index and time delay measurements of a standard reference fiber
[PB89-189179] N89-27457
National Engineering Laboratory's 1989 report to the National Research Council's Board on Assessment of NIST (National Institute of Standards and Technology) programs
[PB89-189294] N89-27602
STAR FORMATION
Temporal variability of water masers in the Southern Hemisphere
[INPE-4646-TDL/338] N89-27609
Evolution of Galaxies. Proceedings, volume 4
[DE89-609650] N89-27616
STATE ESTIMATION
A new state reconstructor for digital controls systems using weighted-average measurements
[NASA-TP-2936] N89-27039
STATIC TESTS
Space Shuttle Main Engine structural analysis and data reduction/evaluation. Volume 7: High pressure fuel turbo-pump third stage impeller analysis
[NASA-CR-183670] N89-26894
Superplastic forming of aluminum, task C
[AD-A207282] N89-26962
STATICS
Static periodic field device for free electron laser
[AD-D014125] N89-27168
STATISTICAL ANALYSIS
Expendable air vehicles/high altitude balloon technology
[AD-A206972] N89-26813

Statistics on aircraft gas turbine engine rotor failures that occurred in US commercial aviation during 1983
[AD-A207592] N89-26851
GEO-EAS (Geostatistical Environmental Assessment Software) user's guide
[PB89-151252] N89-27261
Application of the theory of wave propagation through random media to phase and amplitude fluctuations of seismic P-waves
[AD-A207207] N89-27284
Solution of deterministic differential games: The approximate strategy method
[ONERA-NT-1987-6] N89-27450
Stochasticity and symmetry of the standard map
[IPPJ-910] N89-27528
User guide for the Data Analysis, Retrieval, and Tabulation System (DARTS): A mainframe computer code for generating cross-tabulation reports
[DE89-012930] N89-27592
Statistical study of the correlation of hard X-ray and type 3 radio bursts in solar flares
[NASA-CR-185833] N89-27629

STATISTICAL CORRELATION
Correlation and analysis between the Kamioka neutrino detector data and the Maryland and Rome gravitational antenna data
[NOTA-INTERNA-918] N89-27488

STATISTICAL DECISION THEORY
Solution of deterministic differential games: The approximate strategy method
[ONERA-NT-1987-6] N89-27450

STEADY STATE
Multigrid method for stability problems
[NASA-CR-185825] N89-27420

STEAM TURBINES
Advanced coal-fueled gas turbine systems, volume 2
[DE89-000954] N89-27183

STEEL STRUCTURES
An experimental study of the effect of stainless steel cladding on the structural integrity of flawed steel plates in bending
[DE89-008735] N89-26980

STEELS
Fracture behavior of a pressure vessel steel in the ductile-to-brittle transition region
[PB89-189195] N89-26977
Relaxation response of A533B steel from 25 to 600 C
[DE89-010179] N89-26982
Strength tests and design methods for cold-formed channel columns undergoing distortional buckling
[PB89-183958] N89-27216

STELLAR ATMOSPHERES
Commentary on interstellar matter associated with 18 open clusters
[NASA-RP-1229] N89-27612
Spectra of crab-like pulsars: A GRO perspective
[DE89-013461] N89-27628

STELLAR MASS EJECTION
Solar-geophysical data number 535, part 2. Data for September 1988, and miscellaneous
[PB89-185995] N89-27625

STELLAR SPECTRA
Spectra of crab-like pulsars: A GRO perspective
[DE89-013461] N89-27628

STELLARATORS
On bootstrap currents in toroidal systems
[IPP-2/297] N89-27536

STIFFENING
Stability and dynamic analysis of a slender column with curved longitudinal stiffeners
[NASA-TM-101636] N89-27215

STIFFNESS
Tailoring of composite links for optimal damped elasto-dynamic performance
[NASA-TM-102094] N89-26912

STIRLING CYCLE
Thermal evaluation of advanced solar dynamic heat receiver performance
[NASA-CR-185117] N89-27256

STOCHASTIC PROCESSES
Advanced durability analysis. Volume 2: Analytical predictions, test results and analytical correlations
[AD-A207215] N89-26838
Differential stochastic equations
[PREPRINT-635] N89-27449
Sampling based approaches to calculating marginal densities
[AD-A208388] N89-27451
Stochasticity and symmetry of the standard map
[IPPJ-910] N89-27528
Stochastic mechanics
[PREPRINT-634] N89-27582

STORAGE BATTERIES
Advanced calcium-thionyl chloride high-power battery
[AD-A207612] N89-27247

STORAGE RINGS (PARTICLE ACCELERATORS)
Precision measurements without polarization at LEP --- LEP storage ring
[NOTA-INTERNA-921] N89-27483
A method to calibrate the light response of a high resolution electromagnetic calorimeter with cosmic rays
[NOTA-INTERNA-925] N89-27631

STRAIN GAGE BALANCES
On internal bending-beam strain-gage wind tunnel balances
[RR-070] N89-26870

STRAIN GAGES
Interferometric load sensor and strain gage
[AD-D014122] N89-27142

STRAIN HARDENING
Weld stresses beyond elastic limit: Materials discontinuity
[NASA-TP-2935] N89-27214
Strain to failure of pressurized thick wall cylinders
[DE89-009969] N89-27219
The response of single crystal and polycrystal nickel to quasistatic and shock deformation
[DE89-011168] N89-27564

STRAIN RATE
Stress corrosion study of PH13-8Mo stainless steel using the Slow Strain Rate Technique
[NASA-TP-2934] N89-26976
Rate-sensitivity and short term relaxation behavior of AISI Type 304 stainless steel at room temperature and at 650 C; influence of prior aging
[DE89-007823] N89-26978
Relaxation response of A533B steel from 25 to 600 C
[DE89-010179] N89-26982
Process for assessing the effect of propellant strain on propellant burn rate
[AD-D014119] N89-27026

STRATEGY
Reconfiguration strategies in VLSI (Very Large Scale Integration) arrays and trees
[PB89-165468] N89-27071

STRATOSPHERE
Preventing depletion of stratospheric ozone: Implications on future aircraft emissions, revision 1
[DE89-013779] N89-27273

STRESS (PHYSIOLOGY)
Development of advanced methods based on stable isotope technology for studies of exercise in heat
[AD-A208758] N89-27329
Annual historical report - AMEDD activities
[AD-A208301] N89-27333
Considerations for replacement beverages: Fluid-electrolyte balance and heat illness
[AD-A208342] N89-27335
Effectiveness and acceptability of nutrient solutions in enhancing fluid intake in the heat
[AD-A208428] N89-27337

STRESS (PSYCHOLOGY)
Human performance assessment methods
[AGARD-AG-308] N89-27338
Psychological attributes, coping strategies and other factors associated with ultramarathon performance
[AD-A208300] N89-27340

STRESS ANALYSIS
On internal bending-beam strain-gage wind tunnel balances
[RR-070] N89-26870
Space Shuttle Main Engine structural analysis and data reduction/evaluation. Volume 7: High pressure fuel turbo-pump third stage impeller analysis
[NASA-CR-183670] N89-26894
Strain to failure of pressurized thick wall cylinders
[DE89-009969] N89-27219
Creep-fatigue assessment methods using elastic analysis results and adjustments
[DE89-011858] N89-27221
Residual stress changes in fatigue. Volume 2: A simulation model for stress measurements in notched test specimens by X-ray diffraction
[AD-A208346] N89-27226
The response of single crystal and polycrystal nickel to quasistatic and shock deformation
[DE89-011168] N89-27564

STRESS CONCENTRATION
Compressive properties of high performance polymeric fibers
[AD-A207271] N89-26998
Weld stresses beyond elastic limit: Materials discontinuity
[NASA-TP-2935] N89-27214
Residual stress changes in fatigue. Volume 2: A simulation model for stress measurements in notched test specimens by X-ray diffraction
[AD-A208346] N89-27226

STRESS CORROSION CRACKING
Stress corrosion study of PH13-8Mo stainless steel using the Slow Strain Rate Technique
[NASA-TP-2934] N89-26976

STRESS MEASUREMENT
Residual stress changes in fatigue. Volume 2: A simulation model for stress measurements in notched test specimens by X-ray diffraction
[AD-A208346] N89-27226

STRESS RELAXATION
Rate-sensitivity and short term relaxation behavior of AISI Type 304 stainless steel at room temperature and at 650 C; influence of prior aging
[DE89-007823] N89-26978
Relaxation response of A533B steel from 25 to 600 C
[DE89-010179] N89-26982
Creep-fatigue assessment methods using elastic analysis results and adjustments
[DE89-011858] N89-27221

STRESS TENSORS
Effective action for quantum gravity in two dimensions
[PREPRINT-600] N89-27583

STRESS-STRAIN RELATIONSHIPS
Metal matrix composite micromechanics: In-situ behavior influence on composite properties
[NASA-TM-102302] N89-26924

STRESSES
Thermal and mechanical properties of polyurethane-diacetylene segmented copolymers. Part 2: Effects of diacetylene cross-polymerization
[AD-A208754] N89-27023
Structural integrity evaluation based on an innovative field indentation microprobe
[DE89-010840] N89-27156
Structural analysis of a thermal insulation retainer assembly
[NASA-TM-101580] N89-27212
Weld stresses beyond elastic limit: Materials discontinuity
[NASA-TP-2935] N89-27214
Strain to failure of pressurized thick wall cylinders
[DE89-009969] N89-27219
ASR4: A computer code for fitting and processing 4-gage anelastic strain recovery data
[DE89-012239] N89-27395

STRING THEORY
Theoretical studies in elementary particle physics
[DE89-012701] N89-27473
Note on multiloop calculations for superstrings in the NSR formalism
[PREPRINT-601] N89-27581

STRIP TRANSMISSION LINES
Dual frequency microstrip antenna
[AD-D014019] N89-27046

STRONG INTERACTIONS (FIELD THEORY)
Machines for lattice gauge theory
[DE89-014815] N89-27400

STRONGLY COUPLED PLASMAS
Depth profiles and bulk analysis of semiconductor materials using ICP mass spectroscopy with electrothermal atomization
[AD-A206974] N89-27548

STRONTIUM COMPOUNDS
Composition of superconducting La2CuO4+delta: A superconductor doped by excess oxygen defects
[DE89-013299] N89-27555

STRUCTURAL ANALYSIS
Advanced durability analysis. Volume 2: Analytical predictions, test results and analytical correlations
[AD-A207215] N89-26838
Composite transport wing technology development
[NASA-CR-178409] N89-26842
Space Shuttle Main Engine structural analysis and data reduction/evaluation. Volume 7: High pressure fuel turbo-pump third stage impeller analysis
[NASA-CR-183670] N89-26894
Structural reliability and damage tolerance of ceramic composites for high-temperature applications
[PB89-156350] N89-26994
Structural reliability and damage tolerance of ceramic composites for high-temperature applications
[PB89-156368] N89-26995
Structural analysis of a thermal insulation retainer assembly
[NASA-TM-101580] N89-27212
A three-node C deg element for analysis of laminated composite sandwich shells
[NASA-TM-4125] N89-27213
Strength tests and design methods for cold-formed channel columns undergoing distortional buckling
[PB89-183958] N89-27216
Computational methods for nonlinear dynamic problems in solid and structural mechanics: Progress in the theory and modeling of friction and in the control of dynamical systems with frictional forces
[AD-A208763] N89-27227

Quantitative three-dimensional structural techniques [DE89-010879] N89-27238
The HERMOD behavioral synthesis system [AD-A207319] N89-27371
ASR4: A computer code for fitting and processing 4-gage anelastic strain recovery data [DE89-012239] N89-27395
Transactions of the 6th Army Conference on Applied Mathematics and Computing held in Boulder, Colorado on 31 May - 3 June 1988 [AD-A207252] N89-27424
MeV implantation studies in LPE-grown GaAs and InP [AD-A207220] N89-27550

STRUCTURAL DESIGN
Two-stage reusable launch system utilizing a winged core vehicle and glideback boosters [NASA-TM-101513] N89-26878
The HERMOD behavioral synthesis system [AD-A207319] N89-27371

STRUCTURAL ENGINEERING
Computational methods for nonlinear dynamic problems in solid and structural mechanics: Progress in the theory and modeling of friction and in the control of dynamical systems with frictional forces [AD-A208763] N89-27227
Transactions of the 6th Army Conference on Applied Mathematics and Computing held in Boulder, Colorado on 31 May - 3 June 1988 [AD-A207252] N89-27424
Estimation of the relationship between project attributes and the implementation of engineering tools [PB89-149470] N89-27588
National Engineering Laboratory's 1989 report to the National Research Council's Board on Assessment of NIST (National Institute of Standards and Technology) programs [PB89-189294] N89-27602

STRUCTURAL FAILURE
An experimental study of the effect of stainless steel cladding on the structural integrity of flawed steel plates in bending [DE89-006735] N89-26980
Structural integrity evaluation based on an innovative field indentation microprobe [DE89-010840] N89-27156

STRUCTURAL MEMBERS
Dual load path pin clevis joint [AD-D014081] N89-27188
Structural analysis of a thermal insulation retainer assembly [NASA-TM-101580] N89-27212

STRUCTURAL RELIABILITY
Structural reliability and damage tolerance of ceramic composites for high-temperature applications [PB89-156350] N89-26994
Structural reliability and damage tolerance of ceramic composites for high-temperature applications [PB89-156368] N89-26995

STRUCTURAL STABILITY
Stability and dynamic analysis of a slender column with curved longitudinal stiffeners [NASA-TM-101636] N89-27215

STRUCTURAL STRAIN
The quantitative dependence of transmissivity on flexural strain for multimode optical fiber [AD-A207522] N89-27501

STRUCTURAL VIBRATION
Design of an active helicopter control experiment at the Princeton Rotorcraft Dynamics Laboratory [NASA-CR-185490] N89-26859
Unified micromechanics of damping for unidirectional fiber reinforced composites [NASA-TM-102107] N89-26919

SUBMARINES
Submarine air quality: Monitoring the air in submarines. Health effects in divers of breathing submarine air under hyperbaric conditions [PB89-174213] N89-27345

SUBMILLIMETER WAVES
The Swedish-ESO Submillimeter Telescope (SEST) [PB89-154892] N89-27605

SUBSTRATES
Measurements of complex permittivity of microwave substrates in the 20 to 300 K temperature range from 26.5 to 40.0 GHz [NASA-TM-102123] N89-27038
Magneto-optical properties of ultrathin ferromagnetic films [DE89-014640] N89-27508
Photoelectronic properties of low temperature GaAs grown on silicon and GaAs substrates by MBE [DE89-013148] N89-27557

SUCTION
Combination boundary layer control system for high altitude aircraft [AD-D014075] N89-26837

SULFIDES
Degradation of Fe-25Cr, Fe-25Cr-20Ni and Fe-25Cr-6Al alloys in H2/H2O/H2S environments at 700 C [DE89-011673] N89-26967

SULFONIC ACID
Electrochemical evaluation of new fluorosulfonic and fluorophosphonic acids as fuel cell electrolytes [DE89-012840] N89-27254
Electrochemical evaluation of new fluorosulfonic and fluorophosphonic acids as fuel cell electrolytes [DE89-013391] N89-27255

SULFUR CHLORIDES
Advanced calcium-thionyl chloride high-power battery [AD-A207612] N89-27247

SUN
Solar microwave radiation maps measured at Metsaehovi Radio Research Station in 1982 - 1983 [PB89-154876] N89-27621

SUNLIGHT
High temperature solar electrothermal processing [AD-A207555] N89-27246
Global environmental effects of impact-generated aerosols: Results from a general circulation model, revision 1 [DE89-014179] N89-27276

SUPERCOMPUTERS
Machines for lattice gauge theory [DE89-014815] N89-27400

SUPERCONDUCTING FILMS
Measurements of complex permittivity of microwave substrates in the 20 to 300 K temperature range from 26.5 to 40.0 GHz [NASA-TM-102123] N89-27038

SUPERCONDUCTING MAGNETS
Development of a high power microwave thruster, with a magnetic nozzle, for space applications [NASA-TM-102321] N89-26904
Cryogenic techniques for large superconducting magnets in space [DE89-013431] N89-27455
Passive superconductor: A viable method of controlling magnetization multipoles in the SSC dipole [DE89-013432] N89-27559

SUPERCONDUCTING SUPER COLLIDER
Passive superconductor: A viable method of controlling magnetization multipoles in the SSC dipole [DE89-013432] N89-27559

SUPERCONDUCTIVITY
Diffusion in high-T sub c superconductors [DE89-009792] N89-27546
Composition of superconducting La2CuO4+delta: A superconductor doped by excess oxygen defects [DE89-013299] N89-27555
Anomalous temperature dependence of Cu NMR line width and magnetization in YBa2Cu3O(7-delta) [DE89-014291] N89-27565
O-17 NMR study of YBa2Cu3O(7-delta) [DE89-014292] N89-27566
Nuclear relaxation rates at copper and oxygen sites in YBa2Cu3O7 [DE89-014308] N89-27567
Superconductivity and magnetism in layered materials [AD-A208487] N89-27576

SUPERCONDUCTORS
JTECH (Japanese Technology Evaluation Program) panel report on advanced sensors in Japan [PB89-158760] N89-27136
Materials analysis with nuclear microprobes: Superconductors and buried conductors [DE89-008580] N89-27206
Optical mirror coated with organic superconducting material [AD-D014047] N89-27499
The study of structure-processing-property relations in copper oxide-based high T sub c superconductors [DE89-012764] N89-27554
Composition of superconducting La2CuO4+delta: A superconductor doped by excess oxygen defects [DE89-013299] N89-27555
A method for generating the J sub c, B, T surface for niobium-alloy superconductors [DE89-012977] N89-27556
Passive superconductor: A viable method of controlling magnetization multipoles in the SSC dipole [DE89-013432] N89-27559
High-frequency cavity applications and measurements of high-temperature superconductors [DE89-013467] N89-27560
Recent improvements in bulk properties of ceramic superconductors [DE89-013626] N89-27562
Superconductivity and magnetism in layered materials [AD-A208487] N89-27576

SUPERFLUIDITY
Momentum distributions in liquid helium [DE89-014679] N89-26953
Transient heat transfer into superfluid helium under confined conditions [DE88-706312] N89-27109
Momentum distributions: An overview [DE89-012617] N89-27453
Quantum and thermodynamic fluctuations in the degenerate schematic model of the finite temperature random phase approximation [DE88-706310] N89-27580

SUPERLATTICES
Advanced electron beam evaporation [ETN-89-94799] N89-27495
Artificial superlattices [ETN-89-94889] N89-27551

SUPERNOVA 1987A
Resonant helicity flip of electron neutrino due to magnetic moment and dynamics of supernova [PREPRINT-598] N89-27617

SUPERPLASTICITY
Superplastic forming of aluminum, task C [AD-A207282] N89-26962
Effect of heating rate to test temperature on superplastic response in an Al-8 percent Mg-1 percent Li-0.2 percent Zr alloy [AD-A208462] N89-26990
Thermomechanical processing of aluminum alloy 2090 for superplasticity [AD-A208764] N89-26992

SUPERPRESSURE BALLOONS
Expendable air vehicles/high altitude balloon technology [AD-A206972] N89-26813

SUPERSATURATION
An instantaneous CCN (Cloud Condensation Nucleus) spectrometer [DE89-014807] N89-27150

SUPERSONIC AIRCRAFT
Feasibility and benefits of laminar flow control on supersonic cruise airplanes [NASA-CR-181817] N89-26841

SUPERSONIC COMBUSTION RAMJET ENGINES
Demonstration of oblique detonation wave for hypersonic propulsion [AD-A208266] N89-26856

SUPERSONIC COMMERCIAL AIR TRANSPORT
Preventing depletion of stratospheric ozone: Implications on future aircraft emissions, revision 1 [DE89-013779] N89-27273

SUPERSONIC CRUISE AIRCRAFT RESEARCH
Feasibility and benefits of laminar flow control on supersonic cruise airplanes [NASA-CR-181817] N89-26841

SUPERSONIC FLOW
The structure of Normal-Shock/Turbulent-Boundary-Layer interactions modified by mass removal [AD-A208402] N89-27134

SUPERSONIC TRANSPORTS
Feasibility and benefits of laminar flow control on supersonic cruise airplanes [NASA-CR-181817] N89-26841

SUPPORTS
Dual load path pin clevis joint [AD-D014081] N89-27188

SUPPRESSORS
Design, development and evaluation of a doubly rotated AK-cut quartz crystal [AD-A207209] N89-27549

SURFACE COOLING
Surface cooling system [AD-D014057] N89-27106

SURFACE LAYERS
Oxygen transfer to ethylene catalyzed by the Ag(110) surface [AD-A207325] N89-26936

SURFACE NAVIGATION
Autonomous land navigation: A demonstration of retrotraverse [DE89-011881] N89-26855

SURFACE PROPERTIES
Technical activities 1988, Surface Science Division [PB89-161889] N89-26928
Radiation from waves guided by nonuniform active surfaces [DE89-012286] N89-27057
Arcjet cathode phenomena [NASA-TM-102099] N89-27121
A method for generating the J sub c, B, T surface for niobium-alloy superconductors [DE89-012977] N89-27556
High-frequency cavity applications and measurements of high-temperature superconductors [DE89-013467] N89-27560

SURFACE REACTIONS
Technical activities 1988, Surface Science Division [PB89-161889] N89-26928

The structure and reactivity of alkylsiloxane monolayers formed by reaction of alkyltrichlorosilanes on silicon substrates
[AD-A208267] N89-27011

SURFACE ROUGHNESS
An experimental investigation of the ground vortex created by a moving jet
[NASA-CR-181841] N89-26815
Joint CGS-AOML (Charting and Geodetic Service-Atlantic Oceanographic and Meteorological Laboratory) acoustical bottom echo-formation research. 2: Field experiment results and recommendations for echo-sounder design
[PB89-152417] N89-27322

SURFACE TEMPERATURE
Combination boundary layer control system for high altitude aircraft
[AD-D014075] N89-26837

SURFACE VEHICLES
Research in knowledge-based vision techniques for the autonomous land vehicle program
[AD-A208546] N89-26834

SURFACE WATER
Trace gases in and over the West Pacific and East Indian Oceans during the El Nino-southern oscillation event of 1987: A report of GMCC (Geophysical Monitoring for Climatic Change) data collected on the second Soviet-American Gas and Aerosol Experiment (SAGA 2)
[PB89-159685] N89-27280

SURFACE WAVES
A procedure for computing surface wave trajectories on an inhomogeneous surface
[NASA-TP-2929] N89-26811
Spectra of surface waves
[AD-A208482] N89-27326

SURGES
The effects of steep-front, short-duration impulses on power distribution components
[DE89-012338] N89-27091

SWEDISH SPACE PROGRAM
Activities report in space activities
[ISSN-0284-169X] N89-27458

SWINE
Development of advanced methods based on stable isotope technology for studies of exercise in heat
[AD-A208758] N89-27329

SWITCHES
Photoconductive semiconductor switch (PCSS) recovery
[DE89-012657] N89-27080
Closing photoconductive semiconductor switches
[DE89-013073] N89-27082
Computer code prediction of picosecond voltage switching and TEM wave generation in air gas avalanche switches
[DE89-013778] N89-27084
Improved core insulation schemes for multi-terawatt magnetic switches
[DE89-013814] N89-27093
Fiber optic rotary switching device
[AD-D013978] N89-27497

SWITCHING
Computer code prediction of picosecond voltage switching and TEM wave generation in air gas avalanche switches
[DE89-013778] N89-27084
Fiber optic rotary switching device
[AD-D013978] N89-27497

SWITCHING CIRCUITS
The effects of steep-front, short-duration impulses on power distribution components
[DE89-012338] N89-27091

SYMBOLS
An algorithm for symbolic dimensional analysis
[DE89-010409] N89-27363

SYMMETRY
Theory of aggregate defects in silicon
[AD-A207273] N89-26999
On the multiplicity and symmetries of the bifurcation branching point in the square clamped plate
[PREPRINT-604] N89-27224
Stochasticity and symmetry of the standard map
[IPPJ-910] N89-27528

SYMPTOMOLOGY
Altitude symptomatology and mood states during a climb to 3630 m
[AD-A208261] N89-27332

SYNAPSES
The effect of synapses destruction on categorization by neural networks
[PREPRINT-609] N89-27328

SYNCHRONISM
An overview of some methods for the high-level specification of synchronization
[MEMO-INF-88-50] N89-27403

SYNCHROTRON RADIATION
X-ray microscopy using synchrotron radiation
[NASA-CR-184800] N89-27155

SYNCODERS
Categorization in neural networks and prosopagnosia
[PREPRINT-608] N89-27327

SYNOPTIC METEOROLOGY
Atmospheric environment for Space Shuttle (STS-27) launch
[NASA-TM-100370] N89-27316
Synoptic forcing of East Asian cold surges
[AD-A208765] N89-27321

SYNTHESIS (CHEMISTRY)
Synthesis and characterization of Group 4 organometal oxide complexes
[DE89-010944] N89-26932
Synthesis, characterization and physical properties of polyphosphazenes
[AD-A208296] N89-27013
Synthesis and structural characterization of Pt-Si dimers with unusually short cross-ring silicon-silicon interactions
[AD-A208310] N89-27014
Synthesis and optical properties of a new class of polyamides containing reactive diacetylene groups
[AD-A208752] N89-27021
Synthesis of novel fluorinated phosphonic and phosphinic acid electrolytes for phosphoric acid fuel cells
[PB89-194120] N89-27086

SYNTHETIC APERTURE RADAR
Alaska collection SAR (Synthetic Aperture Radar) data summary
[AD-A208530] N89-27067

SYSTEM EFFECTIVENESS
Gas engine heat pump system and component efficiency and reliability improvement, phase 2
[PB89-173645] N89-27184
Small Computer System Interface (SCSI) command system: Software support for control of small computer system interface devices
[PB89-151815] N89-27389
A fiber optic test system for quantum efficiency measurements
[DE89-012823] N89-27505

SYSTEMS ANALYSIS
An expert system for fault diagnosis in digital circuits
[INPE-4743-PRE/1417] N89-27085

SYSTEMS ENGINEERING
Elements of a realistic 17 GHz FEL/TBA design
[DE89-013427] N89-27169
Narrow-angle laser scanning microscope system for linewidth measurements on wafers
[PB89-189344] N89-27174
Automated immersion testing robotic system: Hardware and software design
[AD-A208755] N89-27201
Kernel user's manual version 1.0
[AD-A207414] N89-27375
Time-sequential optical data processing
[AD-A207514] N89-27500

SYSTEMS SIMULATION
On transformer modeling. A physically based three-phase transformer model for the study of low frequency phenomena in electrical power systems
[ETN-89-94801] N89-27095

SYSTOLIC ARRAYS
A virtual zero-time, monolithic systolic sorting array
[DE89-007515] N89-27394

T

TABLES (DATA)
User guide for the Data Analysis, Retrieval, and Tabulation System (DARTS): A mainframe computer code for generating cross-tabulation reports
[DE89-012930] N89-27592

TAKEOFF
The effects of arms and countermovement on vertical jumping
[AD-A208298] N89-27347

TANTALUM COMPOUNDS
Polarization matrices of lithium tantalate
[AD-A208349] N89-27097

TARGET RECOGNITION
Research in knowledge-based vision techniques for the autonomous land vehicle program
[AD-A208546] N89-26834
Window generator
[AD-D014068] N89-27048
Development of a system model and Least Mean Square (LMS) filter for the Naval Postgraduate School (NPS) Infrared Search and Target Designation System (IRSTD)
[AD-A208536] N89-27068
Image algebra synthesis
[AD-A207257] N89-27425
Time-sequential optical data processing
[AD-A207514] N89-27500
Multiple sensor fusion for detecting targets in FLIR (Forward-Looking Infrared) and range images
[AD-A207577] N89-27502

TARGETS
Time-sequential optical data processing
[AD-A207514] N89-27500
Multiple sensor fusion for detecting targets in FLIR (Forward-Looking Infrared) and range images
[AD-A207577] N89-27502

TASKS
A parallel version of the Boyer-Moore prover
[AD-A207190] N89-27351

TAXIING
Acta Aeronautica et Astronautica Sinica, Volume 8, Number 12, December 1987 (selected articles)
[AD-A206782] N89-26807

TEARING
Collisionless tearing instability of a bi-Maxwellian neutral sheet with exact particle orbits
[AD-A207310] N89-27286

TECHNOLOGICAL FORECASTING
Emerging technologies in electronics and their measurement needs
[PB89-189245] N89-27078
Report to the Congress --- Fiscal Year 1988
[PB89-195408] N89-27603

TECHNOLOGIES
Science and technology advice in the White House: Recommendations for President-Elect George Bush
[PB89-169817] N89-27600

TECHNOLOGY ASSESSMENT
Technical Status Review on Drag Prediction and Analysis from Computational Fluid Dynamics: State of the Art
[AGARD-AR-258] N89-26817
State-of-the-art of aircraft drag prediction in Italy by means of theoretical methods N89-26821
Emerging technologies in electronics and their measurement needs
[PB89-189245] N89-27078
JTECH (Japanese Technology Evaluation Program) panel report on advanced sensors in Japan
[PB89-158760] N89-27136
Study for advanced civil earth remote sensing system: Focused finance study. Volume 1: Executive summary
[PB89-163224] N89-27230
Software deficiency issues confronting the utilization of non-Von Neumann architectures
[AD-A207268] N89-27369
Report to the Congress --- Fiscal Year 1988
[PB89-195408] N89-27603

TECHNOLOGY TRANSFER
Interactions between the National Institute of Standards and Technology and the American Society of Mechanical Engineers
[PB89-172563] N89-27182

TECTONICS
Geodetic measurement of deformation in California
[NASA-TM-100732] N89-27279

TELECOMMUNICATION
Information capacity of additive Gaussian channels with jamming
[AD-A207256] N89-27051

TELEVISION SYSTEMS
Window generator
[AD-D014068] N89-27048

TEMPERATURE
Contemporary composite polar boss
[AD-D014074] N89-26897
Climatology of temperature and precipitation variability in the United States
[PB89-165930] N89-27299

TEMPERATURE DEPENDENCE
Anomalous temperature dependence of Cu NMR line width and magnetization in YBa2Cu3O(7-delta)
[DE89-014291] N89-27565

TEMPERATURE EFFECTS
Thermodynamic equilibria in the biphenyl/hydrogen system (the power and limitations of group additivity estimations)
[DE89-000754] N89-26954
Effect of heating rate to test temperature on superplastic response in an Al-8 percent Mg-1 percent Li-0.2 percent Zr alloy
[AD-A208462] N89-26990
Corrosion of Ceramic Materials Workshop held November 12-13, 1987, Pennsylvania State University, University Park, Pennsylvania
[PB89-175343] N89-27004

TEMPERATURE MEASURING INSTRUMENTS
Automatic oxygen measuring system
[AD-D014003] N89-26931

TEMPERATURE PROFILES
High energy laser target plate
[AD-D014053] N89-27164
Amazon Forest wind and temperature profiles
[INPE-4724-PRE/1401] N89-27301
TEMPORAL DISTRIBUTION
Distribution of auroral arcs during quiet geomagnetic conditions
[DMI-GEOPHYS-PAPERS-R-78] N89-27292
Temporal variability of water masers in the Southern Hemisphere
[INPE-4646-TDL/338] N89-27609
TENSILE CREEP
Evaluation of weldment creep and fatigue strength-reduction factors for elevated-temperature design
[DE89-008242] N89-27218
TENSILE DEFORMATION
Thermal and mechanical properties of polyurethane-diacetylene segmented copolymers. Part 1: Molecular weight and annealing effects
[AD-A208753] N89-27022
TENSILE PROPERTIES
Cryogenic tensile properties of AA 2090 weldments
[DE89-012979] N89-26971
Dynamic mechanical investigations of LLDPE/PC blends
[NPL-DMA(A)-177] N89-27010
Structural integrity evaluation based on an innovative field indentation microprobe
[DE89-010840] N89-27156
Micromechanical characterization of near-surface layers
[DE89-008710] N89-27199
Strain to failure of pressurized thick wall cylinders
[DE89-009969] N89-27219
TENSILE STRENGTH
Examination of the tensile strength of graphite fibers
[AD-A207277] N89-26909
Thermal and mechanical properties of polyurethane-diacetylene segmented copolymers. Part 2: Effects of diacetylene cross-polymerization
[AD-A208754] N89-27023
TENSORS
On a computational method for the second fundamental tensor and its application to bifurcation problems
[AD-A207517] N89-27377
TERMINOLOGY
Thermoelectric terminology in metrology and standards
[DE89-011512] N89-27079
TERNARY ALLOYS
Development of ternary alloy cathode catalysts for phosphoric acid fuel cells
[DE89-000926] N89-27250
TEST FACILITIES
High-speed data acquisition for the Princeton University Dynamic Model Track
[NASA-CR-185491] N89-26865
TETHERED BALLOONS
Navy tethered balloon measurements made during the Fire marine stratocu IFO (Intensive Field Operation)
[AD-A207312] N89-27304
TETHERLINES
Satellite relocation by tether deployment
[NASA-TM-101992] N89-26877
TETRYL
Application of crystal lattice disintegration criteria to compute minimum shock induced reactive conditions in solid explosives and inert materials
[AD-A207557] N89-27025
TEXTS
Issues and approaches for electronic document approval and transmittal using digital signatures and text authentication
[DE89-013102] N89-27596
TEXTURES
Polycrystal plasticity as applied to the problem of in-plane anisotropy in rolled cubic metals
[DE89-011181] N89-26983
THEMATIC MAPPING
Comparison of spectral data gathered from a laboratory spectrometer and TM images with and without shadow correction
[DE89-010877] N89-27237
THEOREM PROVING
A parallel version of the Boyer-Moore prover
[AD-A207190] N89-27351
THEORETICAL PHYSICS
On-line computer utilization to understand some physical processes (example: Pendulum motion)
[NOTA-INTERNA-927] N89-27360
Differential stochastic equations
[PREPRINT-635] N89-27449
Theoretical studies in elementary particle physics
[DE89-012701] N89-27473
Some considerations on the birth of molecular physics in the first half of the 19th century
[NOTA-INTERNA-917] N89-27482
Stochastic mechanics
[PREPRINT-634] N89-27582
THERMAL ANALYSIS
Synthesis and optical properties of a new class of polyamides containing reactive diacetylene groups
[AD-A208752] N89-27021
Thermal and mechanical properties of polyurethane-diacetylene segmented copolymers. Part 1: Molecular weight and annealing effects
[AD-A208753] N89-27022
Thermal evaluation of advanced solar dynamic heat receiver performance
[NASA-CR-185117] N89-27256
THERMAL BARRIERS (PLASMA CONTROL)
TORE SUPRA graphite inner first wall --- tokamak devices
[DE89-009325] N89-27512
THERMAL CYCLING TESTS
Synthesis and optical properties of a new class of polyamides containing reactive diacetylene groups
[AD-A208752] N89-27021
THERMAL DEGRADATION
Photodegradation of polyimides 2. Thermal property changes of polyimides based on a perfluorinated dianhydride
[AD-A208447] N89-27018
Arcjet cathode phenomena
[NASA-TM-102099] N89-27121
THERMAL EMISSION
Infrared temperature measurement with self regulating emission ratio
[ETN-89-94654] N89-27157
THERMAL ENVIRONMENTS
Feasibility demonstration of the Thermal Ignition Combustion System (TICS) for high pressure natural gas injected engine
[PB89-178792] N89-26944
Thermal enclosures for electronically scanned pressure modules operating in cryogenic environments
[NASA-TM-101635] N89-27151
Annual historical report - AMEDD activities
[AD-A208301] N89-27333
THERMAL EXPANSION
Optimum interface properties for metal matrix composites
[NASA-TM-102295] N89-27223
THERMAL FATIGUE
Observations on the mechanisms of fatigue in eutectic Pb-Sn solder joints
[DE89-000553] N89-26968
THERMAL INSULATION
Development of compressed multifoil insulation for high-temperature batteries and other applications
[DE89-012877] N89-27092
Thermal enclosures for electronically scanned pressure modules operating in cryogenic environments
[NASA-TM-101635] N89-27151
Structural analysis of a thermal insulation retainer assembly
[NASA-TM-101580] N89-27212
Thermoregulatory responses in the cold-effect of an Extended Cold Weather Clothing System (ECWCS)
[AD-A208314] N89-27334
THERMAL STABILITY
Thermal stability of jet fuel
[DE89-013516] N89-27032
THERMIONIC DIODES
MHD calculations of anode plasmas
[DE89-014485] N89-27535
THERMIONIC EMISSION
Supercritical fluid chromatography of polar organic compounds in combustion particulates
[PB89-152441] N89-26930
THERMOCHEMISTRY
Synthesis and optical properties of a new class of polyamides containing reactive diacetylene groups
[AD-A208752] N89-27021
Primary dissociation processes of energetic compounds
[AD-A208312] N89-27033
High energy laser target plate
[AD-D014053] N89-27164
THERMOCHROMATIC MATERIALS
Synthesis and optical properties of a new class of polyamides containing reactive diacetylene groups
[AD-A208752] N89-27021
THERMODYNAMIC EQUILIBRIUM
Thermodynamic equilibria in the biphenyl/hydrogen system (the power and limitations of group additivity estimations)
[DE89-000754] N89-26954
THERMODYNAMIC PROPERTIES
Effects of high thermal and high fast fluences on the mechanical properties of type 6061 aluminum in the HFBR
[DE89-012636] N89-26970
Thermal and mechanical properties of polyurethane-diacetylene segmented copolymers. Part 1: Molecular weight and annealing effects
[AD-A208753] N89-27022
Thermal and mechanical properties of polyurethane-diacetylene segmented copolymers. Part 2: Effects of diacetylene cross-polymerization
[AD-A208754] N89-27023
Variable area manifolds for ring mirror heat exchangers
[AD-D014050] N89-27163
Two-photon absorption characterization of HgCdTe
[AD-A207198] N89-27471
THERMODYNAMICS
Hybrid electric chemical propulsion
[AD-A207584] N89-26898
Thermodynamics and high temperature chemistry of the chemical vapor deposition of diamond films
[DE89-013574] N89-26951
Effect of heating rate to test temperature on superplastic response in an Al-8 percent Mg-1 percent Li-0.2 percent Zr alloy
[AD-A208462] N89-26990
Thermomechanical processing of aluminum alloy 2090 for superplasticity
[AD-A208764] N89-26992
Inviscid spatial stability of a compressible mixing layer. Part 3: Effect of thermodynamics
[NASA-CR-181855] N89-27112
Optimum interface properties for metal matrix composites
[NASA-TM-102295] N89-27223
Differential forms of Euler's turbo-machinery equation
[AD-A207279] N89-27426
Quantum and thermodynamic fluctuations in the degenerate schematic model of the finite temperature random phase approximation
[DE88-706310] N89-27580
THERMOELECTRIC GENERATORS
Safety testing program for the Galileo mission radioisotope thermoelectric generator
[DE89-011192] N89-27494
THERMOELECTRICITY
Thermoelectric terminology in metrology and standards
[DE89-011512] N89-27079
Depth profiles and bulk analysis of semiconductor materials using ICP mass spectroscopy with electrothermal atomization
[AD-A206974] N89-27548
THERMOLUMINESCENCE
Determination of the kinetic parameters of the thermoluminescent CaF2 (Tm) crystal
[NOTA-INTERNA-915] N89-27569
THERMONUCLEAR REACTIONS
Recent progress in the Los Alamos KrF Program
[DE88-016235] N89-27493
THERMOPHYSICAL PROPERTIES
Thermophysical properties of advanced carbon materials for Tokamak limiters
[DE89-012799] N89-27516
THERMOPLASTIC RESINS
Interface modified glass fiber/thermoplastic matrix composites
[AD-A207308] N89-26910
Measured damping and modulus of composite cylinders
[DE89-010369] N89-27209
Fate and effects of PAHs in the terrestrial environment: An overview
[DE89-010319] N89-27267
THERMOREGULATION
Thermoregulatory responses in the cold-effect of an Extended Cold Weather Clothing System (ECWCS)
[AD-A208314] N89-27334
THERMOSETTING RESINS
Measured damping and modulus of composite cylinders
[DE89-010369] N89-27209
Fate and effects of PAHs in the terrestrial environment: An overview
[DE89-010319] N89-27267
THICK WALLS
Strain to failure of pressurized thick wall cylinders
[DE89-009969] N89-27219
THICKNESS
OTVE combustor wall condition monitoring
[NASA-CR-182275] N89-26899

The structure of self-assembled monolayers of alkylsiloxanes on silicon: A comparison of results from ellipsometry and low-angle X-ray reflectivity
[AD-A208341] N89-27016
ELLIPSE user's manual and program reference
[DE89-014575] N89-27398

THIN FILMS
Surface plasmon study of monolayer-bilayer transition in poly-4-BCMU and poly-3-BCMU polydiacetylene Langmuir-Blodgett films
[AD-A207404] N89-26938
Thermodynamics and high temperature chemistry of the chemical vapor deposition of diamond films
[DE89-013574] N89-26951
Evaluation of mechanical properties of TiN films by ultra-low load indentation
[DE89-009618] N89-26969
Quantitative thin film X-ray microanalysis of Nb modified Ti3Al
[DE89-009946] N89-26981
Cross-sectional TEM (Transmission Electron Microscopy) studies of Cr films deposited by ion-assisted deposition and physical vapor deposition
[DE89-014643] N89-26985
An Auger sputter profiling study of nitrogen and oxygen ion implantation in two titanium alloys
[DE89-014734] N89-26987
The structure and reactivity of alkylsiloxane monolayers formed by reaction of alkyltrichlorosilanes on silicon substrates
[AD-A208267] N89-27011
Proposed thin film electronics for a-Si:H PIXEL detector
[DE89-013410] N89-27063
Improved core insulation schemes for multi-terawatt magnetic switches
[DE89-013814] N89-27093
Micromechanical characterization of near-surface layers
[DE89-008710] N89-27199
High-efficiency, large-area CdTe panels
[DE89-000891] N89-27242
ELLIPSE user's manual and program reference
[DE89-014575] N89-27398
Diamondlike carbon protective coatings for optical windows
[NASA-TM-102111] N89-27506
Magneto-optical properties of ultrathin ferromagnetic films
[DE89-014640] N89-27508
Wear and friction of thin film high temperature oxide superconductors
[DE89-009397] N89-27543
Magnetic multilayers
[ETN-89-94294] N89-27547
Sputtering of high-temperature superconductors: A bibliography
[DE89-013374] N89-27558
High-frequency cavity applications and measurements of high-temperature superconductors
[DE89-013467] N89-27560
Thin film preparation and single film device fabrication in the Tl-Ca-Ba-Cu-O HTS system
[DE89-013560] N89-27561
Study of the microstructure of silver films deposited by ion assisted deposition onto aluminum oxide substrates
[DE89-014665] N89-27563

THIN WALLS
Development of a thin wall graphite/polyimide composite pressure vessel with a large aspect ratio
[DE89-002536] N89-26920

THREE DIMENSIONAL FLOW
A nonlinear multigrid method for three-dimensional transonic potential flow
[ETN-89-94802] N89-26827
A model for transition by attachment-line contamination and an examination of cross-flow instability in 3-D boundary layers
[AERO-REPT-8804] N89-27108
A dual potential formulation of the Navier-Stokes equations
[NASA-CR-185098] N89-27111
Numerical solution of the Navier-Stokes equations for three-dimensional incompressible flows with open boundaries
[DE89-009333] N89-27119

THREE DIMENSIONAL MOTION
Wideband electromagnetic damping of vibrating structures
[AD-D014069] N89-27208

THRUST CONTROL
Back-up control system for f101 engine and its derivatives
[AD-D014051] N89-26848

THUNDERSTORMS
An investigation into the gravity current aspects of a cold air outbreak using variational analysis techniques
[AD-A208464] N89-27295
Verification of severe local storm forecasts issued by the National Severe Storms Forecast Center, 1987
[PB89-159719] N89-27297

TIME
Formulation of numerical orbit propagation and time error correction
[INPE-4774-PRE/1443] N89-26875
NIST (National Institute of Standards and Technology) research reports, March 1989
[PB89-189310] N89-27594

TIME DEPENDENCE
Measurement of the time-dependent distribution of ionization states in an argon plasma from a Mach-10 jet
[DE89-014699] N89-27526

TIME LAG
Group index and time delay measurements of a standard reference fiber
[PB89-189179] N89-27457
Correlation and analysis between the Kamioka neutrino detector data and the Maryland and Rome gravitational antenna data
[NOTA-INTERNA-018] N89-27488

TIME MEASURING INSTRUMENTS
Automatic oxygen measuring system
[AD-D014003] N89-26931

TIME OF FLIGHT SPECTROMETERS
Electron-impact ionization time-of-flight mass spectrometer for molecular beams
[AD-A207585] N89-27141

TIME SERIES ANALYSIS
Aerial smoke plume observations and surface layer turbulence measurements. Part 1: Project WIND. Phase 4: Dispersion study
[AD-A207370] N89-27305
Brief instructions for SIMBAT, a computer package for unconditional and conditional simulation of ocean wave kinematics
[AD-A207627] N89-27324

TIME SHARING
Competitive management of distributed shared memory
[AD-A207322] N89-27372

TITANATES
Compact ceramic heat exchangers
[PB89-173603] N89-26997

TITANIUM
Method to produce titanium metal matrix composites with improved fracture and creep resistance
[AD-D014111] N89-26911
Fatigue crack growth study of SCS6/Ti-15-3 composite
[NASA-TM-102332] N89-26989

TITANIUM ALLOYS
Method to produce metal matrix composite articles from rich metastable-beta titanium alloys
[AD-D014064] N89-26907
Method to produce metal matrix composite articles from lean metastable beta titanium alloys
[AD-D014065] N89-26908
Method for making an integral titanium alloy article having at least two distinct microstructural regions
[AD-D014066] N89-26960
Method for developing ultrafine microstructures in titanium alloy castings
[AD-D014115] N89-26965
Residual stress changes in fatigue. Volume 1: Residual stress measurements by X-ray diffraction in notched test specimens
[AD-A208345] N89-27225

TITANIUM NITRIDES
Evaluation of mechanical properties of TiN films by ultra-low load indentation
[DE89-009618] N89-26969

TITANIUM OXIDES
Study of nanophase TiO2 grain boundaries by Raman spectroscopy
[DE89-012416] N89-27553

TOKAMAK DEVICES
Low-noise cable for diagnostics, control and instrumentation of the ASDEX tokamak fusion experiment
[IPP-III/67] N89-27094
Limiter H-modes in the JIPP T-IIU tokamak
[IPPJ-898] N89-27511
TORE SUPRA graphite inner first wall --- tokamak devices
[DE89-009325] N89-27512
Thermophysical properties of advanced carbon materials for Tokamak limiters
[DE89-012799] N89-27516
Application of modern mathematical concepts to plasma confinement
[DE89-012952] N89-27517
Equilibrium of a plasma in the fluid- and Vlasov-Maxwell systems
[DE89-013315] N89-27518
Pacing the US magnetic fusion program
[DE89-012959] N89-27519
Pulsed lower-hybrid wave penetration in reactor plasmas
[DE89-013260] N89-27521
Modeling of LH current drive in self-consistent elongated tokamak MHD equilibria
[DE89-013263] N89-27522
On bootstrap currents in toroidal systems
[IPP-2/297] N89-27536
On the economic prospects of nuclear fusion with tokamaks
[IPP-6/271] N89-27539

TOLERANCES (MECHANICS)
Structural reliability and damage tolerance of ceramic composites for high-temperature applications
[PB89-156350] N89-26994
Structural reliability and damage tolerance of ceramic composites for high-temperature applications
[PB89-156368] N89-26995

TOLERANCES (PHYSIOLOGY)
OH-58 energy attenuating crew seat feasibility study
[AD-A207506] N89-26829

TOLLMIEN-SCHLICHTING WAVES
Interaction between Tollmien-Schlichting waves and free-stream disturbances in boundary-layer flows
[NASA-CR-185847] N89-27118

TOPOGRAPHY
Comparison of spectral data gathered from a laboratory spectrometer and TM images with and without shadow correction
[DE89-010877] N89-27237
The impact of solar radiation resources on the siting of solar thermal power plants
[DE89-000839] N89-27252
Investigations on local seismic phases and evaluation of body waves magnitude
[AD-A206633] N89-27283

TOPOLOGY
A symbolic generator of state equations for modeling of dynamic systems based on the electrical network analog paradigm
[DE89-013763] N89-27397

TORNADOES
Verification of severe local storm forecasts issued by the National Severe Storms Forecast Center, 1987
[PB89-159719] N89-27297

TOROIDAL PLASMAS
Improved confinement regimes in JIPP T-IIU
[IPPJ-909] N89-27527
On bootstrap currents in toroidal systems
[IPP-2/297] N89-27536

TOROIDS
Verification analysis of the Toroidal Accelerator Rotor Platform wind energy conversion system
[PB89-162069] N89-27241

TOTAL OZONE MAPPING SPECTROMETER
The 1989 Airborne Arctic Stratospheric Expedition Nimbus-7 TOMS data atlas
[NASA-RP-1227] N89-27302

TOUCH
Design considerations of manipulator and feel system characteristics in roll tracking
[NASA-CR-4111] N89-26880

TOWERS
A test of Newton's Law of Gravity using the BREN Tower, Nevada
[DE89-013262] N89-27454

TRACE CONTAMINANTS
Comparison of modelled and measured tracer gas concentrations during the Across North America Tracer Experiment (ANATEX)
[PB89-136709] N89-27260
Assessing the sensitivity of high altitude New Mexican wilderness lakes to acidic precipitation and trace metal contamination
[PB89-148456] N89-27262
Study of dispersion and penetration of tracer and pollutants in porous media and fractured rocks
[ETN-89-94806] N89-27277
Trace gases in and over the West Pacific and East Indian Oceans during the El Nino-southern oscillation event of 1987: A report of GMCC (Geophysical Monitoring for Climatic Change) data collected on the second Soviet-American Gas and Aerosol Experiment (SAGA 2)
[PB89-159685] N89-27280
Cloud and precipitation scavenging process in the South Coast Air Basin
[PB89-181788] N89-27313

TRACKING (POSITION)
Research in knowledge-based vision techniques for the autonomous land vehicle program
[AD-A206546] N89-26834
Design considerations of manipulator and feel system characteristics in roll tracking
[NASA-CR-4111] N89-26860
Deep space LADAR, phase 1
[AD-A207454] N89-27166
Tropical cyclone report, 1988
[AD-A207206] N89-27303
Time-sequential optical data processing
[AD-A207514] N89-27500
TRAJECTORIES
An Apple-2 compatible program to draw maps containing oceanographic station positions buoy trajectories and the coastal margins of the Antarctic Peninsula and nearby islands
[INPE-4805-RPE/588] N89-27391
TRANSDUCERS
Cepstral method for the measurement of ultrasonic pulse transmission time variations
[AD-A207410] N89-27463
BAE measurement schemes and optimal sensitivity for generalized parametric devices
[PREPRINT-641] N89-27586
TRANSFERRING
Oxygen transfer to ethylene catalyzed by the Ag(110) surface
[AD-A207325] N89-26936
TRANSFORMATIONS (MATHEMATICS)
Formulation of numerical orbit propagation and time error correction
[INPE-4774-PRE/1443] N89-26875
Satellite attitude control analysis and design using linearizing transformations
[INPE-4772-PRE/1441] N89-26886
TRANSISTORS
Dual-transistor method to determine delta V sub ot and delta V sub it for MOS devices
[DE89-006725] N89-27088
The 1/f noise: A nondestructive technique to predict MOS radiation hardness
[DE89-007419] N89-27205
TRANSITION FLOW
Some results on flow calculations involving drag prediction N89-26820
TRANSITION METALS
Catalytic reduction of carbon dioxide by metal centers
[AD-A207227] N89-26934
TRANSITION TEMPERATURE
Diffusion in high-T sub c superconductors
[DE89-009792] N89-27546
TRANSLATING
A language translator for a computer aided rapid prototyping system
[AD-A208358] N89-27406
TRANSMISSION LINES
Low-noise cable for diagnostics, control and instrumentation of the ASDEX tokamak fusion experiment
[IPP-III/87] N89-27094
TRANSMISSION LOSS
The quantitative dependence of transmissivity on flexural strain for multimode optical fiber
[AD-A207522] N89-27501
TRANSMISSIVITY
The quantitative dependence of transmissivity on flexural strain for multimode optical fiber
[AD-A207522] N89-27501
TRANSMITTANCE
Nanostructure and defect chemistry of relaxor ferro electrics
[AD-A207217] N89-26933
Cepstral method for the measurement of ultrasonic pulse transmission time variations
[AD-A207410] N89-27463
TRANSONIC FLOW
Aircraft drag prediction for transonic potential flow N89-26822
Computational fluid dynamics drag prediction: Results from the Viscous Transonic Airfoil Workshop N89-26824
A nonlinear multigrid method for three-dimensional transonic potential flow
[ETN-89-94802] N89-26827
Numerical simulation of a turbulent flow through a shock wave
[AD-A207581] N89-27107
The structure of Normal-Shock/Turbulent-Boundary-Layer interactions modified by mass removal
[AD-A208402] N89-27134
TRANSONIC WIND TUNNELS
Structural analysis of a thermal insulation retainer assembly
[NASA-TM-101580] N89-27212
TRANSPORT AIRCRAFT
Composite transport wing technology development
[NASA-CR-178409] N89-26842
TRANSPORT PROPERTIES
Catalytic combustion of methane
[PB89-188874] N89-26946
Electrochemical transport of manganese between the flux and the weld metal in submerged arc welding
[DE89-012419] N89-27193
TRAPPED PARTICLES
The space particle environment
[AD-A207547] N89-27287
TRAVELING WAVE AMPLIFIERS
Development of theoretical and numerical techniques for achieving stability in gyrotron traveling-wave amplifiers
[AD-A207451] N89-27140
TREES (MATHEMATICS)
Reconfiguration strategies in VLSI (Very Large Scale Integration) arrays and trees
[PB89-165466] N89-27071
Hybrid structures for simple computer performance estimates
[PB89-189161] N89-27356
Attributed tree transformations with delayed and smart re-evaluation
[MEMO-INF-88-45] N89-27440
TRIANGULATION
Geodetic measurement of deformation in California
[NASA-TM-100732] N89-27279
TRIBOLOGY
Advanced ceramics: A critical assessment of wear and lubrication
[PB89-188569] N89-27005
Interactions between the National Institute of Standards and Technology and the American Society of Mechanical Engineers
[PB89-172563] N89-27182
TRIGGER CIRCUITS
Miniature high voltage solid state relay
[AD-D013979] N89-27070
TRINITROTOLUENE
Application of crystal lattice disintegration criteria to compute minimum shock induced reactive conditions in solid explosives and inert materials
[AD-A207557] N89-27025
TROPICAL REGIONS
Tropical circulation and the associated precipitation anomalies in two years of contrast
[INPE-4715-PRE/1395] N89-27315
TUNABLE LASERS
Selective nitrations: Laser-induced nitrations
[AD-A207406] N89-27024
Recent experiments with the free-electron laser at Los Alamos
[DE89-013469] N89-27171
TUNGSTEN ALLOYS
The recrystallization and respheroidization of tungsten grains in a tungsten-heavy alloy
[AD-A207647] N89-26964
TURBINE BLADES
Method for calibrating a heat flux gauge
[AD-D013974] N89-27138
TURBINE ENGINES
Advanced ceramics: A critical assessment of wear and lubrication
[PB89-188569] N89-27005
TURBINE PUMPS
Space Shuttle Main Engine structural analysis and data reduction/evaluation. Volume 7: High pressure fuel turbo-pump third stage impeller analysis
[NASA-CR-183670] N89-26894
OTVE turbopump condition monitoring, task E.5
[NASA-CR-182274] N89-27204
TURBOCOMPRESSORS
Performance estimates for the Space Station power system Brayton Cycle compressor and turbine
[NASA-CR-182263] N89-26903
TURBOFAN ENGINES
Back-up control system for f101 engine and its derivatives
[AD-D014051] N89-26848
TURBOMACHINERY
Differential forms of Euler's turbo-machinery equation
[AD-A207279] N89-27426
TURBULENCE
Fire propagation in concurrent flows
[PB89-188577] N89-26945
TURBULENCE MODELS
Calculation of turbulence-driven secondary motion in ducts with arbitrary cross section
[NASA-TM-102142] N89-27115
Lagrangian turbulence near walls: Structures and mixing in admissible model flows
[AD-A208466] N89-27135
TURBULENT BOUNDARY LAYER
A model for transition by attachment-line contamination and an examination of cross-flow instability in 3-D boundary layers
[AERO-REPT-8804] N89-27108
A review of high-speed, convective, heat-transfer computation methods
[NASA-TP-2914] N89-27116
Study of a turbulent boundary layer by laser plane visualization
[IMFL-88/33] N89-27124
Measurement of wall shear and wall pressure downstream of a honeycomb boundary layer manipulator
[AD-A208297] N89-27132
The structure of Normal-Shock/Turbulent-Boundary-Layer interactions modified by mass removal
[AD-A208402] N89-27134
TURBULENT FLOW
Lean-burn gas engine ignition processes
[PB89-181119] N89-26943
System for boundary layer control through pulsed heating of a strip heater
[AD-D013999] N89-27101
The 1st Scandinavian Conference on Viscous and T urbulent Flow in Hydraulic Machinery
[PB89-161327] N89-27102
Numerical simulation of a turbulent flow through a shock wave
[AD-A207581] N89-27107
Numerical studies of shock wave structure sensitivity to interactions with turbulent fields
[DE89-012288] N89-27110
Calculation of turbulence-driven secondary motion in ducts with arbitrary cross section
[NASA-TM-102142] N89-27115
Finite control volume modeling of laminar and turbulent flow of air in an enclosure
[DE89-009334] N89-27120
Study of subgrid models in incompressible turbulent flow, homogeneous or inhomogeneous
[ONERA-RSF-17/3619-AY-110-A] N89-27123
Base wakes from two dimensional jets in subsonic flow with injection
[IMFL-86/20] N89-27125
Lagrangian turbulence near walls: Structures and mixing in admissible model flows
[AD-A208466] N89-27135
Aerial smoke plume observations and surface layer turbulence measurements. Part 1: Project WIND. Phase 4: Dispersion study
[AD-A207370] N89-27305
Noise produced by turbulent flow into a rotor: Theory manual for atmospheric turbulence prediction and mean flow and turbulence contraction prediction
[NASA-CR-181789] N89-27466
Experimental assessment of helicopter rotor turbulence ingestion noise in hover
[NASA-CR-181792] N89-27468
TURBULENT HEAT TRANSFER
Transient heat transfer into superfluid helium under confined conditions
[DE88-706312] N89-27109
TWO DIMENSIONAL FLOW
Global flows with invariant (Gibbs) measures for Euler and Navier-Stokes two-dimensional fluids
[BIBOS-310/88] N89-27105
A dual potential formulation of the Navier-Stokes equations
[NASA-CR-185098] N89-27111
Ideal jet flow in two dimensions
[AD-A208275] N89-27131
Dynamics of decaying two-dimensional magnetohydrodynamic turbulence
[IPP-6/279] N89-27541
TYPHOONS
Tropical cyclone report, 1988
[AD-A207206] N89-27303

U

UH-60A HELICOPTER
Preliminary airworthiness evaluation of the UH-60A external fuel system
[AD-A207570] N89-26840
ULTRASONIC SPECTROSCOPY
Optical detection and spectroscopy of single molecules in a solid
[AD-A207594] N89-26940

ULTRASONIC WAVE TRANSDUCERS
Structural integrity evaluation based on an innovative field indentation microprobe
[DE89-010840] N89-27156
ULTRASONICS
Cepstral method for the measurement of ultrasonic pulse transmission time variations
[AD-A207410] N89-27463
ULTRAVIOLET ABSORPTION
Absorption cross-section of ozone in the 590 to 610 nm region at different temperatures
[NOTA-INTERNA-928] N89-27291
UNDERWATER ACOUSTICS
Propagating solutions and far-field patterns for acoustic harmonic waves in a finite depth ocean
[PB89-180715] N89-27325
UNDERWATER VEHICLES
Autonomous underwater systems for survey operations
[PB89-187397] N89-27041
UNITED STATES
Mafic and ultramafic xenoliths from volcanic rocks of the western United States
[PB89-124127] N89-27278
Climatology of temperature and precipitation variability in the United States
[PB89-165930] N89-27299
UNIVERSE
Cosmic evolution of non-topological solitons, paper 1
[NASA-CR-185353] N89-27608
Black holes in closed universes
[PB89-170039] N89-27610
UPPER ATMOSPHERE
Environmental Research Laboratories publication abstracts, FY 1988
[PB89-152656] N89-27589
URANIUM
A computer program for simulating the atmospheric dispersion of UF6 and other reactive gases having positive, neutral, or negative buoyancy
[DE89-012734] N89-27269
USER MANUALS (COMPUTER PROGRAMS)
DYNA3D user's manual: (Nonlinear Dynamic Analysis of Structures in Three Dimensions), revision 5
[DE89-014304] N89-27222
Human Operator Simulator (HOS) 4 programmer's guide
[AD-A207241] N89-27342
Kernel user's manual version 1.0
[AD-A207414] N89-27375
ORMONTE: An uncertainty analysis code for use with user-developed systems models on mainframe or personal computers. A user's guide
[DE89-013730] N89-27396
ELLIPSE user's manual and program reference
[DE89-014575] N89-27398
A new version of the full-wave ICRH code FISIC for plasmas with noncircular flux surfaces
[IPP-5/25] N89-27537
Technology Master List data base management system, user's manual
[PB89-177802] N89-27590
User guide for the Data Analysis, Retrieval, and Tabulation System (DARTS): A mainframe computer code for generating cross-tabulation reports
[DE89-012930] N89-27592
USER REQUIREMENTS
A parallel version of the Boyer-Moore prover
[AD-A207190] N89-27351
Northeast artificial intelligence consortium: Volume 2, part A: The Versatile Maintenance Expert System (VMES) research project
[AD-A208344] N89-27417

V

VACUUM DEPOSITION
Advanced electron beam evaporation
[ETN-89-94799] N89-27495
VALLEYS
Field studies for determining the characteristics and dynamics of local circulations
[DE89-013639] N89-27275
VALVES
Research and development of anti-G life support systems. Part 4: Engineering test and evaluation of six anti-G valves
[AD-A206996] N89-27341
VANADIUM ALLOYS
Local density theory of heats of formation and short-range order parameters in substitutionally disordered alloys
[DE89-014696] N89-26986
VAPOR DEPOSITION
Thermodynamics and high temperature chemistry of the chemical vapor deposition of diamond films
[DE89-013574] N89-26951
Cross-sectional TEM (Transmission Electron Microscopy) studies of Cr films deposited by ion-assisted deposition and physical vapor deposition
[DE89-014643] N89-26985
Chemical vapor deposition of silicon carbide using a novel organometallic precursor
[AD-A208273] N89-27012
VAPOR PHASES
Analysis of low-pressure gas-phase pyrolytic reactions by mass spectrometric techniques
[AD-A207457] N89-26939
VAPORS
Detonation of unconfined large scale fuel spray-air clouds
[DE89-006510] N89-26955
VARIABLE SWEEP WINGS
Wind-tunnel investigation of aerodynamic characteristics and wing pressure distributions of an airplane with variable-sweep wings modified for laminar flow
[NASA-TM-4124] N89-26810
VARIANCE (STATISTICS)
Statistical strength comparison of metal-matrix and polymeric-matrix composites
[AD-A208316] N89-26925
VARIATIONAL PRINCIPLES
Ideal jet flow in two dimensions
[AD-A208275] N89-27131
Stochastic mechanics
[PREPRINT-634] N89-27582
VARIATIONS
Natural abundance 15N CP/MAS NMR of solid polyamides: A sensitive technique for examining crystalline composition and conformation in the solid state
[AD-A208563] N89-27019
VARISTORS
Microwave hardening technology development program
[AD-A207535] N89-27076
VARNISHES
Tests of low resistivity electrodeless streamer tubes
[NOTA-INTERNA-922] N89-27158
VECTOR ANALYSIS
Implementation of a design for testability strategy using the Genesil silicon compiler
[AD-A208456] N89-27099
Time-sequential optical data processing
[AD-A207514] N89-27500
VECTORS (MATHEMATICS)
Complex vectors and dyadics for electromagnetists
[PB89-146443] N89-27045
Automatic code vectorization of arithemetic expressions by bottom-up structure recognition
[MEMO-INF-88-48] N89-27414
VEHICULAR TRACKS
High-speed data acquisition for the Princeton University Dynamic Model Track
[NASA-CR-185491] N89-26865
VELOCITY
The effects of arms and countermovement on vertical jumping
[AD-A208298] N89-27347
VELOCITY MEASUREMENT
Sensor development programs at NASA Ames Research Center
[NASA-TM-102217] N89-26808
The structure of Normal-Shock/Turbulent-Boundary-Layer interactions modified by mass removal
[AD-A208402] N89-27134
VENTS
Flow fields of low pressure vent exhausts
[NASA-TM-100738] N89-26902
VERTICAL ORIENTATION
The effects of arms and countermovement on vertical jumping
[AD-A208298] N89-27347
VERY LARGE SCALE INTEGRATION
Reconfiguration strategies in VLSI (Very Large Scale Integration) arrays and trees
[PB89-165468] N89-27071
Radiation evaluation of several complex very large scale integration circuits
[DE89-007985] N89-27090
Fault tolerant VLSI (Very Large-Scale Integration) design using error correcting codes
[AD-A208337] N89-27096
Processor control path synthesis: Literature survey and preliminary analysis
[MEMO-INF-88-46] N89-27401
VERY LONG BASE INTERFEROMETRY
Geodetic measurement of deformation in California
[NASA-TM-100732] N89-27279
VIBRATION
Study of jitter on the attitude motion of a spin stabilized satellite with two flexible solar panels
[INPE-4744-PRE/1418] N89-26884
MM and T for linear resonant cooler, volume 2
[AD-A207236] N89-27073
VIBRATION DAMPING
Design of an active helicopter control experiment at the Princeton Rotorcraft Dynamics Laboratory
[NASA-CR-185490] N89-26859
Tailoring of composite links for optimal damped elasto-dynamic performance
[NASA-TM-102094] N89-26912
Unified micromechanics of damping for unidirectional fiber reinforced composites
[NASA-TM-102107] N89-26919
A microstructural investigation of the shear distortions and energetics of motions observed in an aged high damping 53Cu-45Mn-2Al alloy
[AD-A208467] N89-26991
Low frequency structureborne vibration isolation mount
[AD-D014133] N89-27192
Wideband electromagnetic damping of vibrating structures
[AD-D014069] N89-27208
VIBRATION ISOLATORS
Low frequency structureborne vibration isolation mount
[AD-D014133] N89-27192
VIDEO EQUIPMENT
Window generator
[AD-D014068] N89-27048
Development of a second-generation, video-based luminance mapper for daylighting research
[DE89-000850] N89-27143
VIDEO SIGNALS
Window generator
[AD-D014068] N89-27048
Evaluation of an optical correlator and matched filter maker
[AD-A207556] N89-27054
VISCOELASTICITY
Modeling and computational algorithms for parameter estimation and optimal control of aeroelastic systems and large flexible structures
[AD-A208274] N89-27404
VISCOSITY
Aircraft drag prediction for transonic potential flow
N89-26822
VISCOUS FLOW
MHD forced and free convection boundary layer flow near the leading edge
[DE88-705974] N89-26812
Computational fluid dynamics drag prediction: Results from the Viscous Transonic Airfoil Workshop
N89-26824
The 1st Scandinavian Conference on Viscous and T urbulent Flow in Hydraulic Machinery
[PB89-161327] N89-27102
Numerical studies of shock wave structure sensitivity to interactions with turbulent fields
[DE89-012288] N89-27110
VISCOUS FLUIDS
Design and characterization of large-drop generators for viscous, Newtonian, and non-Newtonian liquids
[AD-A208330] N89-27133
VISUAL OBSERVATION
Atmospheric environment for Space Shuttle (STS-27) launch
[NASA-TM-100370] N89-27316
VLASOV EQUATIONS
Equilibrium of a plasma in the fluid- and Vlasov-Maxwell systems
[DE89-013315] N89-27518
Integral constitutive relation for the investigation of ion Bernstein waves in non-homogeneous plasmas
[IPP-5/27] N89-27538
VOIDS
Thin pulse shock initiation characterization of extrusion-cast explosives: Revision
[DE89-008029] N89-27027
Arcjet cathode phenomena
[NASA-TM-102099] N89-27121
VOLATILITY
Historic emissions of VOC (Volatile Organic Compounds) and NOx in the United States from 1900 to 1985
[PB89-173223] N89-27270
VOLCANOES
Mafic and ultramafic xenoliths from volcanic rocks of the western United States
[PB89-124127] N89-27278
VOLCANOLOGY
Computer simulations of explosive volcanic eruptions
[DE89-014024] N89-27290

VOLTAGE CONVERTERS (AC TO AC)
On transformer modeling. A physically based three-phase transformer model for the study of low frequency phenomena in electrical power systems
[ETN-89-94801] N89-27095
VORTICES
An experimental investigation of the ground vortex created by a moving jet
[NASA-CR-181841] N89-26815
Ideal jet flow in two dimensions
[AD-A208275] N89-27131
VORTICITY EQUATIONS
Construction of differential equations from experimental data of Karman vortex streets
[MPIS-11/1988] N89-27127

W

WAFERS
Narrow-angle laser scanning microscope system for linewidth measurements on wafers
[PB89-189344] N89-27174
WAKES
Base wakes from two dimensional jets in subsonic flow with injection
[IMFL-86/20] N89-27125
Experimental measurement of nonlinear plasma wake-fields
[DE89-014636] N89-27525
WALL PRESSURE
Development of a thin wall graphite/polyimide composite pressure vessel with a large aspect ratio
[DE89-002536] N89-26920
Measurement of wall shear and wall pressure downstream of a honeycomb boundary layer manipulator
[AD-A208297] N89-27132
WALLS
Combination boundary layer control system for high altitude aircraft
[AD-D014075] N89-26837
OTVE combustor wall condition monitoring
[NASA-CR-182275] N89-26899
TORE SUPRA graphite inner first wall --- tokamak devices
[DE89-009325] N89-27512
WARNING SYSTEMS
Tropical cyclone report, 1988
[AD-A207206] N89-27303
WATER BALANCE
Considerations for replacement beverages: Fluid-electrolyte balance and heat illness
[AD-A208342] N89-27335
Effectiveness and acceptability of nutrient solutions in enhancing fluid intake in the heat
[AD-A208428] N89-27337
WATER CONSUMPTION
Effectiveness and acceptability of nutrient solutions in enhancing fluid intake in the heat
[AD-A208428] N89-27337
WATER HAMMER
Generation of underwater sound pulses, cavitation and shear waves with hydraulic hammer
[MPIS-8/1988] N89-27122
WATER IMMERSION
Automated immersion testing robotic system: Hardware and software design
[AD-A208755] N89-27201
WATER MASERS
Temporal variability of water masers in the Southern Hemisphere
[INPE-4646-TDL/338] N89-27609
WATER POLLUTION
Assessing the sensitivity of high altitude New Mexican wilderness lakes to acidic precipitation and trace metal contamination
[PB89-148456] N89-27262
Chesapeake Bay nonpoint source programs
[PB89-152037] N89-27265
Trace gases in and over the West Pacific and East Indian Oceans during the El Nino-southern oscillation event of 1987: A report of GMCC (Geophysical Monitoring for Climatic Change) data collected on the second Soviet-American Gas and Aerosol Experiment (SAGA 2)
[PB89-159685] N89-27280
Environmental Research Laboratories publication abstracts, FY 1988
[PB89-152656] N89-27589
WATER RECLAMATION
Chesapeake Bay nonpoint source programs
[PB89-152037] N89-27265
WATER RESOURCES
Trace gases in and over the West Pacific and East Indian Oceans during the El Nino-southern oscillation event of 1987: A report of GMCC (Geophysical Monitoring for Climatic Change) data collected on the second Soviet-American Gas and Aerosol Experiment (SAGA 2)
[PB89-159685] N89-27280
WATER VAPOR
Dual-channel microwave radiometer for airborne meteorological applications
[PB89-159603] N89-27298
Low relative humidity in the atmosphere
[AD-A207558] N89-27307
WATER WAVES
Pacific Coast hindcast phase 3 north wave information
[AD-A207189] N89-27323
Brief instructions for SIMBAT, a computer package for unconditional and conditional simulation of ocean wave kinematics
[AD-A207627] N89-27324
Spectra of surface waves
[AD-A208482] N89-27326
WAVE DISPERSION
Modeling of LH current drive in self-consistent elongated tokamak MHD equilibria
[DE89-013263] N89-27522
WAVE EQUATIONS
Statistics of an integrable discrete Sine Gordon system
[PREPRINT-638] N89-27128
Universality and integrability of the nonlinear evolution PDEs describing N-wave interactions
[PREPRINT-603] N89-27442
Nonlinear wave equations solvable by the spectral transform
[PREPRINT-957] N89-27443
Fast wave current drive modeling for ITER and prospects for a near-term proof of principle experiment
[DE89-013049] N89-27520
WAVE FRONTS
Numerical computation of bifurcation phenomena and pattern formation in combustion
[DE89-013628] N89-26941
Efficient dynamic phasefront modulation system for free-space optical communications
[AD-D014128] N89-27503
WAVE FUNCTIONS
Physics with ETA mesons
[DE89-012582] N89-27478
WAVE GENERATION
On the production and detection of gravitational waves from artificial sources
[NOTA-INTERNA-912] N89-27587
WAVE INTERACTION
Interaction between Tollmien-Schlichting waves and free-stream disturbances in boundary-layer flows
[NASA-CR-185847] N89-27118
Synoptic forcing of East Asian cold surges
[AD-A208765] N89-27321
Universality and integrability of the nonlinear evolution PDEs describing N-wave interactions
[PREPRINT-603] N89-27442
WAVE PROPAGATION
Radiation from waves guided by nonuniform active surfaces
[DE89-012286] N89-27057
Millimeter-wave propagation characteristics and channel performance for urban-suburban environments
[PB89-180251] N89-27058
Application of the theory of wave propagation through random media to phase and amplitude fluctuations of seismic P-waves
[AD-A207207] N89-27284
Propagating solutions and far-field patterns for acoustic harmonic waves in a finite depth ocean
[PB89-180715] N89-27325
Waves and instabilities in nonneutral plasmas
[DE89-012403] N89-27515
Fast wave current drive modeling for ITER and prospects for a near-term proof of principle experiment
[DE89-013049] N89-27520
Pulsed lower-hybrid wave penetration in reactor plasmas
[DE89-013260] N89-27521
WAVE REFLECTION
Rotation of images by scan mirrors
[NASA-TM-101628] N89-27504
WAVE SCATTERING
Dynamics of double stimulated Brillouin scattering
[PB89-146369] N89-27513
WAVEFORMS
Accuracy increase in waveform Gauss Seidel
[DE89-014812] N89-27437
WAVEGUIDES
Radiation from waves guided by nonuniform active surfaces
[DE89-012286] N89-27057
WAVELENGTHS
Narrow-angle laser scanning microscope system for linewidth measurements on wafers
[PB89-189344] N89-27174
WEAK INTERACTIONS (FIELD THEORY)
First results for the delta I = 1/2 amplitude in K decays, with quenched lattice QCD and Wilson fermions
[PREPRINT-599] N89-27485
WEAR
OTVE combustor wall condition monitoring
[NASA-CR-182275] N89-26899
Advanced ceramics: A critical assessment of wear and lubrication
[PB89-188569] N89-27005
OTVE turbopump condition monitoring, task E.5
[NASA-CR-182274] N89-27204
Wear and friction of thin film high temperature oxide superconductors
[DE89-009397] N89-27543
WEATHER
Low relative humidity in the atmosphere
[AD-A207558] N89-27307
Environmental Research Laboratories publication abstracts, FY 1988
[PB89-152656] N89-27589
WEATHER FORECASTING
Verification of severe local storm forecasts issued by the National Severe Storms Forecast Center, 1987
[PB89-159719] N89-27297
Tropical cyclone report, 1988
[AD-A207206] N89-27303
Meteorological database and synthesis for the Gulf of Mexico
[PB89-178222] N89-27311
Intense heat checklist based on the 1980 heat wave
[PB89-181200] N89-27312
Weather predictions and surface radiation estimates for Project BUGGY 1
[DE89-014687] N89-27318
Development of Low-Level Turbulence (LLT) forecasting methodologies
[AD-A208457] N89-27320
WEIGHT REDUCTION
Contemporary composite polar boss
[AD-D014074] N89-26897
WEIGHTING FUNCTIONS
An investigation into the gravity current aspects of a cold air outbreak using variational analysis techniques
[AD-A208464] N89-27295
WELD STRENGTH
Evaluation of weldment creep and fatigue strength-reduction factors for elevated-temperature design
[DE89-008242] N89-27218
WELDABILITY
Effect of oxidation, sandblasting and pickling on weldability
[DE89-013795] N89-26975
WELDED JOINTS
Cryogenic tensile properties of AA 2090 weldments
[DE89-012979] N89-26971
Analysis of microstructural development in single crystal welds
[DE89-013537] N89-26973
The effect of aging at 343 deg C on type 308 stainless steel welds
[DE89-013545] N89-26974
Mechanisms that control the geometry of pulsed Nd:YAG laser welds
[DE89-014490] N89-27200
The use of field indentation microprobe in measuring mechanical properties of welds
[DE89-013548] N89-27211
Evaluation of weldment creep and fatigue strength-reduction factors for elevated-temperature design
[DE89-008242] N89-27218
WELDING
Analysis of microstructural development in single crystal welds
[DE89-013537] N89-26973
Weld stresses beyond elastic limit: Materials discontinuity
[NASA-TP-2935] N89-27214
WELLS
Drilling operations plan for the Magma Energy Exploratory Well
[DE89-010037] N89-27240
WHEAT
Efficiency of N use by wheat as a function of influx and efflux of NO sub 3
[NASA-CR-177534] N89-27346

WHISKER COMPOSITES
Erosion of Al and Al/SiC
[DE89-013623] N89-26913
SiC-MoSi composites
[DE89-013656] N89-26923
WHITE NOISE
High efficiency pattern recognition
[AD-A207210] N89-27368
WIGGLER MAGNETS
Recent experiments with the free-electron laser at Los Alamos
[DE89-013469] N89-27171
Free electron lasers with small period wigglers
[DE89-014715] N89-27173
Prospects for the FEL (Free Electron Laser)
[DE89-012998] N89-27175
WIND (METEOROLOGY)
Expendable air vehicles/high altitude balloon technology
[AD-A206972] N89-26813
Field studies for determining the characteristics and dynamics of local circulations
[DE89-013639] N89-27275
Analysis of the wind data and estimation of the resultant air concentration rates
[DE88-705980] N89-27296
Synoptic forcing of East Asian cold surges
[AD-A208765] N89-27321
Spectra of surface waves
[AD-A208482] N89-27326
WIND DIRECTION
Evaluation of an updated design of an internally lighted wind cone
[DOT/FAA/CT-TN89/45] N89-26868
WIND MEASUREMENT
Analysis of the wind data and estimation of the resultant air concentration rates
[DE88-705980] N89-27296
Aerial smoke plume observations and surface layer turbulence measurements. Part 1: Project WIND. Phase 4: Dispersion study
[AD-A207370] N89-27305
WIND PROFILES
Amazon Forest wind and temperature profiles
[INPE-4724-PRE/1401] N89-27301
WIND TUNNEL APPARATUS
Sensor development programs at NASA Ames Research Center
[NASA-TM-102217] N89-26808
Design and calibration of the mixing layer and wind tunnel
[NASA-CR-185472] N89-26866
On internal bending-beam strain-gage wind tunnel balances
[RR-070] N89-26870
WIND TUNNEL TESTS
Wind-tunnel investigation of aerodynamic characteristics and wing pressure distributions of an airplane with variable-sweep wings modified for laminar flow
[NASA-TM-4124] N89-26810
An experimental investigation of the ground vortex created by a moving jet
[NASA-CR-181841] N89-26815
Aerodynamic parameters of an advanced fighter aircraft estimated from flight data. Preliminary results
[NASA-TM-101631] N89-26861
Study of a turbulent boundary layer by laser plane visualization
[IMFL-88/33] N89-27124
Base wakes from two dimensional jets in subsonic flow with injection
[IMFL-86/20] N89-27125
WIND TUNNELS
Design and calibration of the mixing layer and wind tunnel
[NASA-CR-185472] N89-26866
WIND TURBINES
Yaw dynamics of horizontal axis wind turbines
[DE89-000868] N89-27249
Wind power: Today's energy option
[DE89-000876] N89-27253
Noise radiation characteristics of the Westinghouse WWG-0600 (600kW) wind turbine generator
[NASA-TM-101576] N89-27467
WIND VELOCITY
Evaluation of an updated design of an internally lighted wind cone
[DOT/FAA/CT-TN89/45] N89-26868
Aerial smoke plume observations and surface layer turbulence measurements. Part 1: Project WIND. Phase 4: Dispersion study
[AD-A207370] N89-27305
WINDOWS (APERTURES)
Diamondlike carbon protective coatings for optical windows
[NASA-TM-102111] N89-27506
WINDPOWER UTILIZATION
Verification analysis of the Toroidal Accelerator Rotor Platform wind energy conversion system
[PB89-162069] N89-27241
Wind power: Today's energy option
[DE89-000876] N89-27253
WINDPOWERED GENERATORS
Verification analysis of the Toroidal Accelerator Rotor Platform wind energy conversion system
[PB89-162069] N89-27241
WING LOADING
Wind-tunnel investigation of aerodynamic characteristics and wing pressure distributions of an airplane with variable-sweep wings modified for laminar flow
[NASA-TM-4124] N89-26810
WING PANELS
Composite transport wing technology development
[NASA-CR-178409] N89-26842
WING PROFILES
Drag prediction and analysis from computational fluid dynamics, state-of-the-art in France N89-26818
WINGS
Numerical study of three-dimensional separation and flow control at a wing/body junction
[NASA-CR-185819] N89-26826
Composite transport wing technology development
[NASA-CR-178409] N89-26842
WIRING
An expert system in C for computer-aided digital circuit design
[AD-A207518] N89-27075

X

X RAY ABSORPTION
The role of X-ray absorption spectroscopy in electronic structure studies
[DE89-014677] N89-26952
X RAY IMAGERY
An approach to accurate X-ray mask measurements in a scanning electron microscope
[PB89-172555] N89-27137
X RAY LASERS
Z-pinch experiments on Saturn at 30 TW
[DE89-013497] N89-27523
Study of atomic physics and population inversions with plasma focus
[DE89-014282] N89-27532
X RAY SCATTERING
A preliminary report on X-ray photoabsorption coefficients and atomic scattering factors for 92 elements in the 10-10,000 eV region
[DE89-013392] N89-26950
X RAY SPECTROSCOPY
The role of X-ray absorption spectroscopy in electronic structure studies
[DE89-014677] N89-26952
X RAY STRESS MEASUREMENT
Residual stress changes in fatigue. Volume 2: A simulation model for stress measurements in notched test specimens by X-ray diffraction
[AD-A208346] N89-27226
X RAYS
Quantitative thin film X-ray microanalysis of Nb modified Ti3Al
[DE89-009946] N89-26981
Natural abundance 15N CP/MAS NMR of solid polyamides: A sensitive technique for examining crystalline composition and conformation in the solid state
[AD-A208563] N89-27019
Theory of X-ray holography including phase and amplitude contrast and finite transfer functions
[DE89-012835] N89-27148
X-ray holography: A history
[DE89-012983] N89-27149
X-ray microscopy using synchrotron radiation
[NASA-CR-184800] N89-27155
A one-dimensional scintillator camera for the SATURN X-ray simulation accelerator
[DE89-009327] N89-27492
Statistical study of the correlation of hard X-ray and type 3 radio bursts in solar flares
[NASA-CR-185833] N89-27629
XENON
Z-pinch experiments on Saturn at 30 TW
[DE89-013497] N89-27523
XYLENE
Crystallization of paraxylene with scraped surface heat exchangers
[WTHD-189] N89-27570

Y

YAG LASERS
Mechanisms that control the geometry of pulsed Nd:YAG laser welds
[DE89-014490] N89-27200
YARNS
Low loss radar window for reentry vehicle
[AD-D014045] N89-26882
YAW
Yaw dynamics of horizontal axis wind turbines
[DE89-000868] N89-27249
YIELD STRENGTH
Statistical strength comparison of metal-matrix and polymeric-matrix composites
[AD-A208316] N89-26925
Dispersion strengthened aluminum-base alloy
[AD-D014044] N89-26959
Cryogenic tensile properties of AA 2090 weldments
[DE89-012979] N89-26971
The use of field indentation microprobe in measuring mechanical properties of welds
[DE89-013548] N89-27211
YTTRIUM COMPOUNDS
Anomalous temperature dependence of Cu NMR line width and magnetization in YBa2Cu3O(7-delta)
[DE89-014291] N89-27565
YTTRIUM OXIDES
O-17 NMR study of YBa2Cu3O(7-delta)
[DE89-014292] N89-27566
Nuclear relaxation rates at copper and oxygen sites in YBa2Cu3O7
[DE89-014308] N89-27567

Z

ZEOLITES
Molecular sieve films from zeolited-silica microcomposites
[DE89-009831] N89-26921
ZETA PINCH
Z-pinch experiments on Saturn at 30 TW
[DE89-013497] N89-27523
Two-dimensional effects in hollow core z-pinches
[DE89-014188] N89-27531
Radiative collapse of a Bennett-relaxed z-pinch
[DE89-014290] N89-27533
Two-dimensional effects in imploding plasma liners
[DE89-014482] N89-27534
ZINC SELENIDES
Diamondlike carbon protective coatings for optical windows
[NASA-TM-102111] N89-27506
ZINC SULFIDES
Diamondlike carbon protective coatings for optical windows
[NASA-TM-102111] N89-27506

Typical Personal Author Index Listing

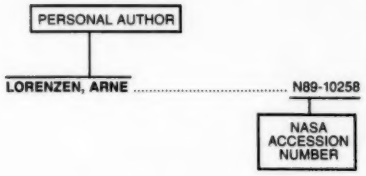

Listings in this index are arranged alphabetically by personal author. The NASA accession number denotes the number by which the citation is identified.

A

ACKERMAN, B. N89-27242
ACKERMAN, J. L. N89-27003
ADAM, COLIN M. N89-27185
ADAMS, CARL L. N89-27025
ADATI, K. N89-27511
N89-27527
AGARWAL, ANANT N89-27352
AGRAWAL, RENU N. N89-27022
N89-27023
AGRAWAL, S. N89-26841
AHERN, BRIAN S. N89-27168
AHMED, M. N89-26812
AINES, ROGER N89-27557
AKERLOF, C. N89-27627
AKIYAMA, R. N89-27511
N89-27527
ALBERTAZZI, E. N89-27288
ALBERTODEOLIVEIRA, CARLOS N89-27366
N89-27382
ALBEVERIO, SERGIO N89-27105
ALBLAS, HENK N89-27440
ALBRIGHT, S. P. N89-27242
ALCOCK, CHARLES N89-27608
ALEXANDER, D. J. N89-26974
N89-27211
ALEXANDER, K. B. N89-26974
ALGER, LINDA N89-27413
ALI, A. M. N89-27096
ALLAN, CRAIG R. N89-27133
ALLEGA, ARTURO MARCELLO N89-27224
ALLEN, COURT C. N89-27408
ALLEN, KENNETH C. N89-27058
ALLEN, STEPHEN B. N89-27295
ALMING, KURT N89-27102
ALP, E. ERCON N89-26952
AMALDI, E. N89-27488
AMIET, R. K. N89-27468
AMORUSO, A. N89-27291
ANDERSEN, K. HARBO N89-27069
ANDERSON, JOHN L. N89-27592
ANDO, A. N89-27511
N89-27527
ANDO, R. N89-27511
ANDRIULLI, J. B. N89-27209
ANGER, BERND N89-27065
ANTONSEN, T. M., JR. N89-27173
ANZURES, E. T. N89-27018
AOKI, T. N89-27511
APONSO, BIMAL L. N89-26860
APPELBAUM, JOSEPH N89-27623
ARCONE, STEVEN A. N89-27285
ARETI, H. N89-27355
ARMSTRONG, LAWRENCE E. N89-27335
N89-27337
ARNOLD, ALISON M. N89-27188
ARNOLD, J. A. N89-27604
ARRINGTON, JEFF E. N89-27140
ASH, DON N89-27240
ASH, ROBERT L. N89-26826
ASHBY, NEIL N89-27456
ASHILL, P. R. N89-26823
ASLAM, M. N89-27346
ATAC, R. N89-27355
ATTWOOD, MIKE C. N89-26890
AXE, J. D. N89-27016
AYMAR, R. N89-27512

B

BABCOCK, LAURA MAE N89-26932
BABUSKA, IVO N89-27427
N89-27428
N89-27429
BADER, S. D. N89-27508
BADGLEY, P. N89-26944
BAILEY, M. C. N89-27063
BAILEY, MICHAEL P. N89-27448
BAKER, C. R. N89-27050
N89-27051
BALACHANDRAN, U. N89-27562
BALAKRISHNA, S. N89-26869
BALLATO, ARTHUR N89-27097
N89-27462
BALLDIN, ULF N89-27343
BAMBERGER, JUDY N89-27375
BANON, GERALD JEAN FRANCIS N89-27055
BARAS, CHRISTIAN N89-26957
BARATTI, P. N89-27496
BARBOUR, J. C. N89-27206
BARE, CHRISTOPHER N89-27342
BARGER, RAYMOND L. N89-26811
BARKHOUDARIAN, S. N89-26899
BARNES, PAUL R. N89-27091
BARNETT, D. L. N89-27415
BARSOUM, M. N89-27007
BARTEL, J. J. N89-26920
BARTON, B. D. N89-26987
BATCHELOR, D. B. N89-27520
BATTLE, STANLEY D. N89-27070
N89-27497
BATTS, G. W. N89-27316
BAUER, F. N89-27144
BAUGHMAN, R. J. N89-27561
BAYLISS, A. N89-26941
BEAN, DENNIS L. N89-26864
BEAUCHAMP, P. N89-27571
BECKHAM, H. W. N89-27021
BEDARD, A. J., JR. N89-27298
BEESON, H. D. N89-26926
BEIN, T. N89-26921
BELKHALE, KRISHNA P. N89-27071
BELL, JAMES H. N89-26866
BENCIVENGA, VINCENT L. N89-26833
BENEDICK, W. B. N89-26955
BENNETT, GARY L. N89-26895
BENZ, F. J. N89-26926
BERDAHL, PAUL N89-27558
BERKOPEC, FRANK D. N89-26876
BERNARDINI, P. N89-27569
BEYER, J. B. N89-27561
BHARATHAN, D. N89-27248
BHASIN, KUL B. N89-27038
BHORE, NAZEER AHMED N89-27028
Bi, D. G. N89-27511
BIEDERMAN, R. T. N89-27604
BIEL, J. N89-27355
BILLINGSLEY, JAMES P. N89-27025
BINDSCHADLER, ROBERT A. N89-27229
BINI, C. N89-27569
BINI, DONATO N89-27584
BIRN, J. N89-27529
BISKAMP, DIETER N89-27541
BLACK, DAVID L. N89-27372
BLACKER, TED D. N89-27435
BLACKFIELD, D. T. N89-27522
BLAIR, D. S. N89-26949
BLANDER, M. N89-27193
N89-27194
BLANK, TOM N89-27371
BLAZEK, C. F. N89-27604
BLOOM, GEORGE N89-27027
BLOOM, I. N89-27562
BLOOM, S. G. N89-27269
BLUM, FRANK D. N89-27020
BLUZER, NATHAN N89-27139
BOATNER, L. A. N89-26973
BODONYI, R. J. N89-27118
BOGAR, T. J. N89-27134
BOHLIN, JOHN N89-27166
BOLDRIN, CLETE M. N89-26857
BOLING, M. E. N89-27596
BOLLING, E. N89-26982
BONADIES, GARY N. N89-27026
N89-27191
BONIFAZI, P. N89-27488
BONNER, GEORGE A. N89-27180
BONOLI, PAUL T. N89-27521
N89-27522
BOONER, GEORGE N89-27186
BOOSKE, J. H. N89-27173
BOOTH, EARL R., JR. N89-27465
BOOTH, R. S. N89-27605
BOPPE, CHARLES W. N89-26825
BOREL, CHRISTOPH C. N89-27239
BORGIA, B. N89-27631
BORGMAN, LEON E. N89-27324
BORN, GEORGE N89-27229
BORSI, M. N89-26821
BOULDIN, D. W. N89-27394
BOULOUMIE, JEAN-PIERRE N89-26889
BOURCIER, ROY J. N89-27199
BOYD, STEPHEN P. N89-27423
BOYER, JOSEPH H. N89-27160
BRADLEY, R. G., JR. N89-27104
BRAMBILLA, MARCO N89-27538
BRASKI, D. N. N89-27156
BREITMAIER, WILLIAM A. N89-26828
BRENEMAN, KEVEN P. N89-26861
BREWE, D. E. N89-27114
BREWER, GEORGE D. N89-26837
BREWER, L. N89-26984
BRILEY, G. L. N89-26905
BRINKER, C. J. N89-26921
BRITTON, C. L. N89-27394
BROOKS, THOMAS F. N89-27465
BROONER, WILLIAM G. N89-27233
BROWN, K. N89-26921
BROWN, V. N89-27184
BROWNE, W. R. N89-27152
BROWNING, J. S. N89-27090
BRUNSON, CHRISTINA M. N89-27280
BUBSHAIT, K. A. N89-27588
BUCCIANTINI, G. N89-26821
BUCHALTER, S. N89-27461
BUCKINGHAM, ALFRED C. N89-27110
BUCKIUS, RICHARD B. N89-27558
BUNYA, GEORGE K. N89-26879
BURGIN, G. H. N89-27393
BURKHART, G. R. N89-27286
BURKS, B. L. N89-27198
BURNS, JOHN A. N89-26883
N89-27404
BURNS, R. K. N89-26846
BURNSIDE, W. D. N89-27064
BURTON, DONALD J. N89-27086
BURTON, MARK W. N89-27320
BURZYNSKI, R. N89-26938
BUSSDESOUZA, RONALD N89-27391
BUTLER, JAMES H. N89-27280

C

CACCIANI, MARCO N89-27042
N89-27291
CAIRD, J. A. N89-27172
CALABRESE, O. JOSEPH N89-27331
CALDWELL, STEPHEN P. N89-27461
CALK, L. C. N89-27278
CALOGERO, F. N89-27441
N89-27442
CAMARANETO, GILBERTO N89-27381
CANAVAN, GREGORY H. N89-27452
CANCE, WILLIAM N89-27202
CANGELLARIS, ANDREAS C. N89-27059

CANNON, T. W. N89-27143
CANOBBIO, E. N89-27540
CARDELLO, ARMAND V. N89-27337
CARL, U. B. N89-26862
CARLON, HUGH R. N89-27133
CARLSEN, LARS N89-26939
CARR, M. J. N89-26981
N89-27544
CARRILLO, J. L. N89-27500
CARTER, DAVID H. N89-26923
CARTER, M. D. N89-27520
CARTWRIGHT, D. C. N89-27493
CARY, JOHN R. N89-27517
CASASENT, DAVID N89-27500
CASTELLARI, SUELI PISSARRA N89-27385
CERADINI, FILIPPO N89-27490
CHAMIS, C. C. N89-26912
N89-26919
N89-26924
CHAO, I. F. N89-27051
CHAPMAN, RANDALL A. N89-26904
CHAPPUIS, P. N89-27512
CHASE, ROBERT R. P. N89-27229
CHEN, JAMES N89-27286
N89-27622
CHEN, YEN-SEN N89-26900
CHENG, C. C. N89-26985
CHIAPPINI, M. N89-27620
CHILD, JOSEPH N89-27047
CHILENSKAS, A. A. N89-27092
CHIRICO, R. D. N89-26954
CHO, G. N89-27083
CHO, Y.-C. N89-26808
CHOU, SHUN-CHIN N89-26909
N89-26925
CHOUDHRY, MOHAMMAD B. N89-26992
CHRISTENSEN, CHARLES R. N89-27054
CHRISTMAS, STANLEY C. N89-27312
CHU, H. P. N89-26918
CHURNSIDE, JAMES H. N89-27261
CIESLAK, M. J. N89-26966
N89-26981
CLARK, D. N89-26887
CLARK, J. W. N89-27453
CLARK, T. L. N89-27260
CLARKE, THOMAS L. N89-27322
CLEMENTS, WILLIAM E. N89-27275
CLEVE, ROBERT N89-27047
CLIFF, EUGENE M. N89-26863
N89-27404
CLOUTHIER, DENNIS J. N89-26956
COCCIA, E. N89-27488
COCKRELL, C. R. N89-27060
CODDINGTON, TIM N89-27375
COFFEY, HELEN E. N89-27624
N89-27625
COGGESHALL, S. V. N89-27493
COHEN, RONALD B. N89-26898
N89-27141
COHEN, RONALD H. N89-27521
COHN, R. D. N89-27260
COIRIER, WILLIAM J. N89-27103
COLANGELO, EUGENE J. N89-26830
COLE, B. N89-27525
COLEMAN, PAUL T. N89-27204
COLLINS, J. J. N89-27204
COLLINS, JOHN CLEMENTS N89-27473
CONRY, SUSAN E. N89-27419
CONSTERDINE, IAN N89-27304
CONWAY, THOMAS J. N89-27280
COOK, A. N89-27355
COOK, M. N89-26901
COOKE, D. W. N89-27560
COPENHAVER, RONALD M. N89-27032
CORTINI, G. N89-27360
CORUM, J. M. N89-27218
COUBROUGH, LAWRENCE E. N89-26997
COUCH, W. A. N89-27251
COULTER, RICHARD L. N89-27275
COVEY, CURT N89-27276
COX, M. G. N89-27444
COYLE, T. W. N89-26994
N89-26995
COZZENS, ROBERT F. N89-27000
CRAIG, DOUGLAS F. N89-27008
CRANE, ROGER A. N89-27256
CRANMER, D. C. N89-27007
CRIPPS, DAVID B. N89-26839
CRISAFULLI, M. N89-27569
CRISSMAN, JOHN M. N89-26914
CROCI, R. N89-27540
CROESSMAN, C. N89-27512
CROWELL, CHARLES G. N89-26839
CROWLEY, R. D. N89-26880
CRUZ, J. N. N89-26888
CRUZEIRO, ANA-BELA N89-27105
CULL, THERESA A. N89-27494
CUMMINGS, ROBERT L. N89-26903
CUNNINGHAM, JANET L. N89-26892
CURRAN, FRANCIS M. N89-26906
N89-27121
CUSHMAN, ROBERT N89-27268
CUTTS, D. N89-27359
CZAJKOWSKI, CARL J. N89-26970
CZEKAJ, CORRINA N89-27012

D

DABROWSKI, B. N89-27555
N89-27568
DADKHAH, MAHYAR N89-26963
DAHLBACKA, G. N89-27526
DAHLBAECK, GUNNAR N89-27343
DAHM, THOMAS J. N89-26856
DAMICO, KATY N89-27076
DAMP, S. N89-27176
DANDRIDGE, A. N89-27510
DANG, DINH NGUYEN N89-27580
DANIELSEN, C. N89-27292
DANIELSON, B. L. N89-27457
DANUSSO, L. N89-27360
DAVID, S. A. N89-26973
DAVIDSON, F. E. N89-27503
DAVIDSON, JENNIFER L. N89-27425
DAVIDSON, JOHN C. N89-27099
DAVIDSON, RONALD C. N89-27515
DAVIS, DENNIS G. N89-27464
DAVIS, J. C. N89-26950
DAVIS, R. C. N89-26880
DEABREUSA, LEONARDO DEANE N89-27301
DEFREITASOLIVEIRA, JOAO RICARDO N89-27381
DEGASPERIS, A. N89-27443
DEGOEDE, R. N89-27570
DEIWERT, GEORGE S. N89-26816
DEKKER, E. N89-27432
DEKKER, L. N89-27432
DELANEY, ALLAN J. N89-27285
DELEO, GARY G. N89-26999
DELGADO, G. N89-27605
DELILLO, S. N89-27128
N89-27441
DELUCIA, R. A. N89-26851
DEMAREST, KENNETH R. N89-27052
DEMERS, ROSARIO N. N89-26850
DEMICHELI, GIOVANNI N89-27370
DEMKO, MICHAEL G. N89-26865
DEMUREN, A. O. N89-27115
DENNENG, HORST N89-27065
DEPAULASILVAFILHO, VICENTE N89-27301
DEPIANTE, EDUARDO V. N89-27397
DEPPE, J. N89-27355
DERMER, CHARLES D. N89-27630
DERYDER, L. J. N89-26888
DESANCTIS, M. N89-27487
N89-27489
DESAUSSURE, GERARD N89-27415
DESCHAMPS, P. N89-27512
DESHMUKH, U. V. N89-27007
DESJARLAIS, M. P. N89-27535
DESSE, J. M. N89-27125
DESTLER, W. W. N89-27173
DEUTSCH, STANLEY N89-27344
DEVADAS, SRINIVAS N89-27098
DEVICENZI, M. N89-27159
DEVOTO, R. S. N89-27522
DIAMBRINIPALAZZI, GIORDANO N89-27587
DIASVELASCO, FLAVIO ROBERTO N89-27236
N89-27381
DIAZ, CARLOS F. N89-27235
DIEGERT, KATHLEEN V. N89-27203
DIEMOZ, M. N89-27631
DIERKS, HEINRICH N89-27065
DIJK, HAROLD EDWIN N89-27095
DIMARCO, J. N89-27627
DIMARZO, M. N89-27100
DISARRA, ALCIDE N89-27042
N89-27291
DIXIT, S. N. N89-27479
DIXON, WILLIAM P. N89-27142
DOBOS, CHARLES J. N89-26997
DOELLING, NORMAN N89-27041
DOERR, T. P. N89-27205
DOIRON, SCOTT D. N89-27302
DOLGOV, A. D. N89-27614
DOLL, DENNIS C. N89-27259
DOMINEK, A. K. N89-27064
DONOHUE, M. L. N89-27228
DORRIS, S. E. N89-27562
DOSS, HANI N89-27445
DOWDING, ROBERT J. N89-26964
DOWLING, N. E. N89-27225
DOWNEY, DAVID A. N89-26839
DOYLE, B. L. N89-27206
DRAAISMA, HENRICUS JOHANNES GEORGE
N89-27547
DRAKE, MICHAEL L. N89-27464
DRAXLER, R. R. N89-27260
DRERUP, VINCENT M. N89-26853
DRESSELHAUS, G. N89-27576
DRESSELHAUS, M. S. N89-27576
DRISCOLL, MICHAEL M. N89-27072
DROTNING, W. D. N89-27516
DUCRUET, C. N89-27125
DUDEL, H. P. N89-27378
DUFFEY, THOMAS A. N89-27217
DUFFY, ROBERT E. N89-27241
DUGAN, D. W. N89-27031
DUGGAN, D. W. N89-27053
DUKART, R. J. N89-27523
DUNN, D. O. N89-27225
DUNN, SUZANNE G. N89-27201
DUQUETTE, MILES O. N89-26878
DUSEK, J. T. N89-27562
DUTRA, LUCIANO VIEIRA N89-27385
DZIADOS, JOSEPH E. N89-27336

E

EASTERLING, ROBERT G. N89-27203
EASTERLING, WILLIAM N89-27268
EATON, SUSAN L. N89-27407
EBERT, K. N89-26891
EBIHARA, BEN T. N89-27038
ECKELMANN, H. N89-27127
ECKMAN, R. M. N89-27305
EDEL, M. N89-27355
EDER, BRIAN K. N89-27299
EDMONDS, JAE N89-27268
EDWARDS, NELSON T. N89-27267
EGAN, B. Z. N89-26948
EGAN, KEITH B. N89-27280
EHRLICH, GAIL K. N89-27182
N89-27602
EINSTEIN, J. R. N89-27198
EINWOHNER, THEODORE H. N89-27436
ELCRAT, A. N89-27131
ELDREDGE, DONALD W. N89-26852
ELIASON, JAY R. N89-27237
N89-27238
ELIASSON, LARS N89-27458
ELKINS, JAMES W. N89-27280
ELLINGSON, W. A. N89-27003
ELLIS, ARTHUR B. N89-27573
ENDRUSICK, THOMAS L. N89-27334
ENG, ALBERT N89-27163
ENGELHART, PAUL M. N89-27369
ENGLUND, EVAN J. N89-27261
EPSTEIN, ALAN H. N89-27138
ERCK, R. A. N89-26985
N89-27563
ERICSON, M. N. N89-27394
ERIKSON, ROBERT H. N89-26831
ERTHAL, GUARACI JOSE N89-27392
ESER, SEMIH N89-27032
ESPELAND, RICHARD N89-27058
ETHERTON, JOHN N89-27339
EYLON, DANIEL N89-26907
N89-26908
N89-26911
N89-26960
N89-26961
N89-26965

F

FACKLER, O. N89-27454
FAIN, D. E. N89-26948
FALK, KENNETH W. N89-27312
FALLS, M. N89-27257
FANCONI, BRUNU M. N89-26993
FARKAS, DAVID M. N89-26991
FARMER, RICHARD C. N89-26900
FARSHCHI, MOHAMMAD N89-27107
FASANELLA, EDWIN L. N89-26843
FATEMAN, RICHARD J. N89-27436
FAULKNER, WILLIAM N89-27548
FAWAZ, SCOTT A. N89-26998
FAZI, VALENTINO N., JR. N89-27192
FEDOR, L. S. N89-27298
FEEZELL, R. R. N89-27198
FEHL, D. L. N89-27492
FELDMAN, DONALD W. N89-27171
FELGUEIRAS, CARLOS ALBERTO N89-27392
FELSKE, D. N89-27454
FENSKE, G. R. N89-26985
N89-27563

FENSTERMACHER, C. A. N89-27493
FENSTERMACHER, M. E. N89-27522
FERBER, M. K. N89-27006
FERNANDEZ-PELLO, A. C. N89-26945
FERRARI, VALERIA N89-27584
FERRAROTTO, F. N89-27158
N89-27484
FESTA, P. N89-27360
FEYNMAN, S. N89-27368
FIGUEIRA, J. F. N89-27493
FILBERT, P. C. N89-27526
FILIPPOV, YU. P. N89-27109
FINGER, JOHN T. N89-27240
FINKELSTEIN, PETER L. N89-27299
FINN, JOHN M. N89-27622
FIOCCO, G. N89-27291
FIRESTINE, M. W. N89-27271
FIRTH, ROBERT N89-27375
FISCHLER, M. N89-27355
FISHER, JAMES E. N89-27180
FISHER, T. R. N89-27526
FISK, ZACHARY N89-27565
N89-27566
N89-27567
FLATTE, STANLEY M. N89-27284
FLECK, STEVEN J. N89-27336
FLEETWOOD, D. M. N89-27088
N89-27089
N89-27205
FLETCHER, EDWARD A. N89-27246
FLOM, YURY N89-26918
FLOOD, DENNIS J. N89-27623
FOLLANSBEE, P. S. N89-27564
FOOTE, HARLAN P. N89-27238
FORD, JERRY N89-27311
FOREMAN, L. R. N89-27493
FORGY, CHARLES N89-27353
FORREST, STEPHANIE N89-27383
FORWARD, ROBERT L. N89-27208
FOUTCH, RICHARD N89-27332
FOWLER, W. B. N89-26999
FOX, ROY G. N89-26829
FRANCASENNE, EDSON LUIZ N89-27236
FRANCESCONI, RALPH P. N89-27337
FRANCISCOJUNIOR, ANTONIO N89-27236
FRANKE, MILTON E. N89-27101
FRANZEN, W. N89-26834
FRASCA, S. N89-27488
FREAR, D. R. N89-26968
FREEMAN, A. J. N89-26986
FREEMAN, B. L. N89-27532
FREIMAN, S. W. N89-27007
FREY, MICHAEL R. N89-27050
N89-27446
N89-27447
FREY, RANDY W. N89-27166
FRIEDMAN, DAVID M. N89-27196
FRIEMAN, JOSHUA A. N89-27608
FRISTEDT, KNUT N89-26870
FRITSCH, FREDERICK N. N89-27386
FROES, FRANCIS H. N89-26907
N89-26908
N89-26911
N89-26959
N89-26960
N89-26961
N89-26965
FRYKMAN, PETER N. N89-27336
N89-27347
FU, LEE-LUENG N89-27229
FUJIEDA, I. N89-27083
FUJITA, J. N89-27511
FULLER, E. R. N89-26995
N89-26996
FULLER, E. R., JR. N89-26994
N89-27007
FUNCHESS, ROBERT B. N89-27020

G

GABRIEL, M. N89-27512
GABRIEL, T. A. N89-27476
GABRIELSE, GERALD N89-27491
GAFFET, STEPHANE N89-27283
GAI, W. N89-27525
GAINES, I. N89-27355
GALLEGO, E. N89-27340
GAMBERINI, RUDY J. N89-27056
GANGULY, S. N89-27096
GANN, J. A. N89-26880
GATHMAN, S. G. N89-27304
GAUSE, EMILY M. N89-27341
GAVELA, M. B. N89-27485
GAZIT, S. N89-26834
GEAR, C. W. N89-27437
GEGG, S. G. N89-27111
GELFAND, ALAN E. N89-27451
GEORGE, DARIN L. N89-27282
GEORGE, THOMAS F. N89-27470
N89-27579
GEORGES, T. M. N89-27460
GERBER, H. N89-27304
GERICKE, OTTO R. N89-27463
GERNHARDT, JOACHIM N89-27094
GERSTL, S. A. W. N89-27239
GHAN, STEVEN J. N89-27276
GHOSN, LOUIS J. N89-27223
GIBBS, W. SCOTT N89-26923
GIDDINGS, A. E. N89-27357
GILBREATH, G. G. N89-27503
GILYARD, GLENN B. N89-26844
GINERIS, D. H. N89-27067
GINLEY, D. S. N89-27561
GION, EDMUND J. N89-26871
GLEASON, MICHAEL A. N89-26840
GLEISER, MARCELO N89-27608
GLISH, GARY L. N89-27029
GODBEY, S. E. N89-27024
GOEHLER, JUERGEN N89-27065
GOEKE, ELIZABETH C. N89-26909
GOLDFRANK, B. N89-27549
GOLDMAN, V. V. N89-27402
N89-27414
GOLDSTONE, P. D. N89-27493
GONDOT, PASCAL N89-27319
GONIS, A. N89-26986
GONZALEZ, RICHARD R. N89-27334
GORCZYCA, JOHN N89-27389
GORDON, B. M. N89-27155
GORDON, SCOTT E. N89-27336
GORDON, WILLIAM L. N89-27038
GORETTA, K. C. N89-26913
N89-27562
GOSSARD, E. E. N89-27300
GOWELL, ELIZABETH T. N89-27041
GOWENLOCK, L. N89-27340
GRABLE, MARK N89-27047
GRAHAM, R. A. N89-27144
GRANATSTEIN, V. L. N89-27173
GRANT, BARRY C. N89-27029
GRATTA, G. N89-27486
GRAY, CARL E., JR. N89-27212
GRAY, E. R. N89-27560
GRAY, G. T., III N89-27564
GRAY, G. W. N89-27330
GREEN, MICHAEL A. N89-27455
N89-27556
N89-27559
GREENE, WILLIAM H. N89-27212
GREENLEE, TERRY L. N89-27244
GRETHE, WOLFGANG N89-27065
GRETZ, D. N89-27488
GREVE, A. N89-27605
GRIBAUDO, MICHAEL L. N89-27068
GRIFFIN, WILLIAM S. N89-27208
GRILLI, M. N89-27482
GRIVAS, D. N89-26968
GROSCH, C. E. N89-27112
N89-27113
GRUNEWALD, WILLIAM J. N89-27202
GRZYBOWSKI, STANISLAW N89-27091
GSCHWANDTNER, GERHARD N89-27270
GUALTIEROTTI, A. F. N89-27050
GUCKEL, H. N89-27136
GUDIKSEN, PAUL N89-27275
GUENETTE, GERALD R. N89-27138
GUERRA, FRANCESCO N89-27449
N89-27582
GUIMARAES, PATRICIA T. N89-27302
GULLIKSON, E. M. N89-26950
GUPTA, ANOOP N89-27352
N89-27353
N89-27372
N89-27411
GUPTA, I. J. N89-27064
GUPTA, K. K. N89-27213

H

HAAG, THOMAS W. N89-27121
HAASE, DAVID G. N89-27554
HADIPRIONO, FABIAN C. N89-27235
HAGGAG, FAHMY M. N89-27156
N89-27211
N89-27220
HAGSTROEM, M. N89-27605
HALBACH, K. N89-27169
HALE, BARBARA S. N89-27332
HALL, BRAD D. N89-27280
HALL, C. E., JR. N89-27378
HALL, MATTHEW J. N89-26943
HALLER, E. N89-27136
HALLER, W. N89-27007
HALLISSY, JAMES B. N89-26810
HALLQUIST, JOHN O. N89-27222
HALVIS, JAMES N89-27139
HAMADA, Y. N89-27511
N89-27527
HAMIL, R. A. N89-27080
HAMILTON, BOB N89-27311
HAMILTON, RUSSELL J. N89-27629
HAMMEL, B. A. N89-27523
HAMMEL, CHRIS P. N89-27565
N89-27566
N89-27567
HAN, DAESOO N89-27289
HANCOCK, ERNEST O. N89-27192
HANCOCK, G. J. N89-27207
N89-27216
HANEY, RUSSEL E. N89-27243
HANNUM, NED P. N89-26876
HANSEL, HAROLD R. N89-26853
HANSEN, A. N89-27249
N89-27305
HANSON, A. L. N89-27155
HANSON, D. E. N89-27493
HANSON, D. L. N89-27523
HANSSON, B. N89-27605
HARDEE, J. L. N89-27596
HARJES, H. C. N89-27093
HARMAN, EVERETT A. N89-27336
N89-27347
HARMER, MARTIN P. N89-26933
HARREN, FRANSISCUS JOHANNES MARIA N89-27263
HARRIS, B. N89-27454
HARRIS, D. B. N89-27493
HARRIS, REGINA N89-27342
HARTMANN, C. R. N89-27096
HASBROUCK, R. T. N89-27308
HASEROTH, H. N89-27077
HASIEWICZ, Z. N89-27578
HASS, K. J. N89-27357
HATFIELD, WILLIAM E. N89-26958
HATORI, T. N89-27528
HAUER, A. A. N89-27493
HAUPT, RANDY L. N89-27049
HAWKINS, JEFFREY D. N89-27234
HAWKINS, ROBERT L. N89-26813
HAYNES, JAMES T. N89-27461
HEADLEY, T. J. N89-26966
N89-26981
HEATH, WILLIAM B. N89-27499
HECK, M. L. N89-26888
HEDEMANN, M. A. N89-27492
HEERENS, JUERGEN N89-26977
HEFFNER, ROBERT H. N89-27565
N89-27566
N89-27567
HEFFTER, J. L. N89-27260
HEGG, DEAN A. N89-27313
HEGYI, DENNIS J. N89-27606
HEHLGANS, JOERG N89-27065
HEIKEN, GRANT N89-27618
HEINEN, VERNON O. N89-27038
HELANDER, MARTIN G. N89-27339
HENDERSON, WILLIAM N89-27548
HENKE, B. L. N89-26950
HENKEL, CHRISTIAN N89-27613
HERBST, MICHAEL K. N89-26840
HESLINGA, G. N89-27422
HESSE, M. N89-27529
HEVRDEYS, GERALD E. N89-27294
HIDEKUMA, S. N89-27511
HIGGINS, BRIAN G. N89-26915
HIJALMARSON, H. P. N89-27080
HINKS, D. G. N89-27555
N89-27568
HIRVONEN, JUHA-PEKKA N89-27543
HJALMARSON, H. P. N89-27082
HO, CHENG N89-27628
HOBBS, PETER V. N89-27313
HODGDON, M. L. N89-27532
HOFFER, THOMAS E. N89-27133
HOFFMANN, MICHAEL R. N89-27317
HOFFMANN, ROALD N89-26935
N89-26936
HOFTUN, J. N89-27359
HOGAN, R. E. N89-27120
HOGG, D. C. N89-27298
HOHENWARTER, G. K. G. N89-27561
HOLMGREN, GUNNAR N89-27458
HOLOWACH, JOSEPH N89-27189
HOLST, TERRY L. N89-26824
HOLTKAMP, D. B. N89-27090
HONNELL, RICHARD E. N89-26923
HOPKINS, D. N89-27077

HOPKINS, D. A. N89-26924
HOPKINS, D. B. N89-27169
HOSANGADI, A. N89-26929
HOSKER, RAYFORD P., JR. N89-27275
HOSSAIN, M. A. N89-26812
HOU, GENE J. W. N89-26917
HOU, TAN-HUNG N89-26917
HOU, Y.-T. N89-27286
HOVY, EDUARD H. N89-27599
HOWE, JOHN T. N89-27117
HOWELLS, M. R. N89-27148
HOYER, E. H. N89-27169
HOYEZ, M. C. N89-27124
HOYLE, C. E. N89-27018
HRACH, FRANK J. N89-26877
HSIA, EDWARD S. N89-26849
HSIEH, YOU-LO N89-26915
HSING, W. W. N89-27523
HSU, S. M. N89-27005
HU, HUI N89-27373
N89-27374
HU, SHZE JER N89-27296
HUANG, X. N89-26936
HUBBARD, HARVEY H. N89-27467
HUBERTZ, JON M. N89-27323
HUDSON, C. R., II N89-27396
HUDSON, J. G. N89-27150
HUDSON, JOHN N89-27012
HUEBLER, A. N89-27127
HUFF, LLOYD C. N89-27322
HUFFAKER, R. C. N89-27346
HUGGINS, ROBERT A. N89-27081
HULL, JOHN R. N89-27195
HULTQVIST, BENGT N89-27542
HUNSTON, DONALD L. N89-26914
HUNT, CHARLES E. N89-27557
HUNTER, K. C. N89-27143
HUSBANDS, TONY B. N89-26864
HUSBY, D. N89-27355
HUSSEY, T. W. N89-27531
N89-27534
N89-27535
HUTTO, WALTER D., JR. N89-26848
HWANG, SUN Y. N89-27371

I

IACABUCCI, R. S. N89-26905
ICHIKAWA, Y. H. N89-27528
II, SILVIA SHIZUE N89-27055
IKEZI, H. N89-27077
INDACOCHEA, J. E. N89-27193
N89-27194
INTERRANTE, LEONARD V. N89-27012
ISELY, M. N89-27355
ISKANDER, S. K. N89-26980

J

JACKSON, KAREN E. N89-26843
JACKSON, T. L. N89-27112
N89-27113
JACOB, JONAH N89-27162
JACOBI, GERALD Z. N89-27262
JACOBSEN, CHRIS N89-27149
JACOBSON, M. D. N89-27296
JACOBSON, M. J. N89-27469
JAEGER, E. F. N89-27520
JAKOB, FRANK E. N89-27184
JAMES, JEFFREY E. N89-27304
JANGHORBANI, MORTEZA N89-27329
JANIK, TADEUSZ N89-27429
JANSEN, SUSAN A. N89-26935
JASPER, G. L. N89-27316
JELLISON, J. L. N89-27200
JENKINS, M. W. N89-27505
JENSEN, ROBERT E. N89-27323
JOHANSSON, L. E. B. N89-27605
JOHNSON, A. M. N89-26937
JOHNSON, D. L. N89-27316
JOHNSON, S. S. N89-27152
JOHNSON, WILLIAM K. N89-27048
JOHNSTON, DONALD E. N89-26860
JOLLY, J. RALPH, JR. N89-27465
JONAS, JIRI N89-26927
JONES, K. W. N89-27155
JONES, R. M. N89-27460
JORGENSEN, J. D. N89-27555
N89-27568
JORGENSEN, KARL ANKER N89-26936
JUANG, F. N89-27437
JUST, R. A. N89-27269

K

KAAE, J. L. N89-27053
KADOR, L. N89-26940
KAKWANI, R. M. N89-27197
KALLMEYER, PETER N89-27065
KALP, DIRK N89-27353
KALWANI, R. M. N89-26944
KALWEIT, HARVEY N89-27573
KAMIMURA, T. N89-27528
KAMMERAAD, J. N89-27454
KAMO, R. N89-26944
N89-27197
KANADE, T. N89-27136
KANDA, TAKESHI N89-26893
KANEKO, O. N89-27527
KANMURI, AKIO N89-26893
KANTZOS, PETER N89-26989
KAPLAN, JONATHAN N89-27342
KAPLAN, S. N. N89-27063
KARWAN, MARK H. N89-27339
KASAMEYER, P. N89-27454
KASISCHKE, E. S. N89-27067
KASKEY, JEFFREY A. N89-27552
KATAGIRI, HIROSHI N89-27296
KATZ, ERIC S. N89-26868
KATZBERG, STEPHEN J. N89-27504
KAUFMANN, MATT N89-27351
KAVOOSI, F. N89-27100
KAWABATA, CURT M. N89-26897
KAWAHATA, K. N89-27527
KAYANO, MARY TOSHIE N89-27315
KEERY, WILLIAM J. N89-27137
KELLEY, H. J. N89-26883
KELLOGG, G. L. N89-27154
KENIK, E. A. N89-26979
KENNEDY, B. K. N89-27004
KENNEDY, C. R. N89-26916
KERSEY, A. D. N89-27510
KERSTETER, SHARON L. N89-27264
KETTLEBOROUGH, C. F. N89-27120
KHALIL, M. N89-27431
KHAN, FERDOUS N89-27477
KHANDELWAL, GOVIND S. N89-27477
KIDD, G. J. N89-26948
KIDD, JAMES A., JR. N89-27501
KILGORE, W. ALLEN N89-26869
KILLOUGH, S. M. N89-27415
KIM, GIL M. N89-26988
KIM, JI-HEUNG N89-27017
KIM, RAYMOND K. N89-27153
KIM, S. Y. N89-27528
KINCAID, J. PETER N89-27350
KING, R. J. N89-27057
KINGON, ANGUS I. N89-27554
KINNISON, DOUGLAS E. N89-27273
KINTER, J. L., III N89-27288
KIRBIE, H. C. N89-27077
KIRCHOFF, SUSAN D. N89-26959
KISLING, DOUGLAS L. N89-27186
KITIS, LEVENT N89-27181
KLARER, P. R. N89-26855
KLASSEN, M. N89-27100
KLEIN, A. J. N89-27596
KLEIN, DANIEL N89-27375
KLEIN, VLADISLAV N89-26861
KLEINER, RICHARD N. N89-26997
KNOROVSKY, G. A. N89-26966
KNOX, JOHN B. N89-27272
KNYSTAUTAS, R. N89-26955
KO, W. N89-27136
KOBAYASHI, ALBERT S. N89-26963
KOBAYASHI, HIDEO N89-27296
KOCH, CARL C. N89-27554
KOCH, MARTIN N89-27065
KOCKS, U. FRED N89-26983
KOCZAK, M. J. N89-27007
KOFFEL, WILLIAM K. N89-26849
KOHLER, D. N89-27526
KOITIKUGA, HELIO N89-26875
KOLB, GREGORY J. N89-27244
KONECNY, R. N89-27525
KONG, JIN AU N89-27074
KOROTKOV, A. A. N89-27480
KOTOWSKI, MARIE N89-27591
KOVAR, ROBERT F. N89-26910
KOWALSKI-GLIKMAN, J. N89-27578
KRAEMER, WILLIAM J. N89-27336
KRAUSE, R. F. N89-26995
N89-26996
KRAUSE, R. F., JR. N89-26994
KRAWETZ, ARTHUR A. N89-26931
KREBS-JESPERSEN, MARGARET L. N89-27593
KREMPL, ERHARD N89-26978
KROEMER, KARL H. E. N89-27344
KRONER, WALTER M. N89-27601
KROUTIL, J. C. N89-27134
KRUECKEN, T. N89-27537
KRUEGER, ARLIN J. N89-27302
KRUEGER, ARNOLD G. N89-27341
KRUTZ, ROBERT W. N89-27341
KU, DAVID C. N89-27370
KUDELKA, LAWRENCE N89-27101
KUHN, GARY D. N89-27107
KULIKOWSKI, CASIMIR A. N89-27598
KUMAZAWA, R. N89-27527
KWAK, J. F. N89-27561

L

LAAKE, A. N89-27122
LACEY, T. R. N89-26841
LAHTI, TAPIO N89-27129
LAJEUNESSE, C. A. N89-26920
LAKE, JOHN A. N89-27499
LAKE, MARK S. N89-27215
LAKSHMANAN, BALAKRISHNAN N89-26826
LALA, P. K. N89-27096
LAMAR, CHARLES R. N89-27164
LANAGAN, M. T. N89-27562
LANDIS, GEOFFREY A. N89-26877
N89-27619
LARKO, DAVID E. N89-27302
LARRABEE, ROBERT D. N89-27137
LARSEN, ROBERT P. N89-27002
LARSON, DONALD R. N89-27507
LARSON, LEE E. N89-27507
LARSSON, LARS-ERIK N89-27343
LASSEN, K. N89-27292
LAU, S. C. W. N89-27207
N89-27216
LAURO, GEORGE L. N89-26845
LAVECCHIA, HELENE N89-27342
LAY, KENNETH W. N89-27574
LEBLANC, RICHARD J. N89-27405
LEE, GEORGE D. N89-27189
LEE, J. H. S. N89-26926
N89-26955
LEE, J. R. N89-27492
LEE, L. M. N89-27144
LEE, MILTON L. N89-26930
LEE, ROBERT N89-27059
LEE, RONALD N89-27027
LEE, S. H. N89-27368
LEE, WEI N89-27012
LEE, WEN-CHAU N89-27309
LEE, YUAN T. N89-27033
LEEHEY, PATRICK N89-27132
LEEPER, R. J. N89-27492
LEFEVRE, RANDY J. N89-27321
LEHNIGK, S. H. N89-27378
LEINONEN, JOUKO N89-26975
LEISAWITZ, DAVID N89-27612
LEISHMAN, NANCY L. N89-27597
LENZ, KLAUS N89-27012
LERCH, BRADLEY A. N89-27223
LESTER, LAURIE S. N89-27337
LESTER, PETER F. N89-27320
LEU, H. J. N89-27562
LEUBKER, ELIZABETH R. N89-27573
LEUZE, MICHAEL R. N89-27384
LEVI, D. N89-27128
LEVY, H. N89-27627
LI, FU-LI N89-27579
LI, WANN-QUAN N89-27518
LI, XIAO-SHEN N89-27470
N89-27579
LIANG, GEORGE N89-27179
LIEPA, VALDIS V. N89-27049
LIN, D. L. N89-27470
N89-27579
LIN, SHU N89-27062
LINCKE, E. N89-27077
LINDELL, ISMO V. N89-27044
N89-27045
LINDHOLM, FREDRIK A. N89-27243
LINDSTROEM, C. O. N89-27605
LINJAMA, JUKKA N89-27129
LIPARI, P. N89-27159
LIU, C. N89-27508
LIU, LON-CHANG N89-27478
LIU, ZHEN-DONG N89-27470
LIVESAY, BILL J. N89-27240
LO, YUEN T. N89-27046
LOEHLE, C. S. N89-27363
LOISEL, PATRICE N89-27126
LONGO, E. N89-27483
LOSIER, PAUL N89-26840
LOUBRIEL, G. M. N89-27080
N89-27082

LOVE, PAUL E. N89-27341
LOVELY, R. N89-26887
LOVERING, P. B. N89-26846
LOVETT, C. D. N89-27040
LOVETT, J. A. N89-26929
LUCAS, MICHAEL J. N89-27459
LUKIERSKI, J. N89-27578
LUNDIN, RICHARD N89-27542
LUNG, S. F. N89-27213
LUSIGNEA, RICHARD W. N89-26910
LUTSKO, J. F. N89-27474
LUTZE, F. H. N89-26883
LUURSEMA, J. J. N89-27403
LUX, ANDRE E. N89-27091
LYBANON, MATTHEW N89-27234
LYDEN, J. D. N89-27067
LYLE, JOSEPH A. N89-26839
LYNCH, THOMAS R. N89-27262
LYON, GORDON E. N89-27356

M

MA, HI-KEUNG TONY N89-27098
MACCALLUM, C. N89-27627
MACCONOCHIE, IAN O. N89-26878
MACKENZIE, PAUL B. N89-27400
MACMILLAN, DANIEL S. N89-27289
MADAN, RAM C. N89-26842
MADDEN, WILLIAM M. N89-26847
MAGILL, J. H. N89-27013
MAHAJAN, SWADESH M. N89-27518
MAHAJAN, YASHWANT R. N89-26959
MAIANI, L. N89-27485
MAJUMDAR, B. C. N89-27114
MAJUMDAR, SUBRATA N89-27421
MAKAROVIC, A. N89-27439
MALECHA, R. F. N89-27092
MALEY, MARTIN N89-27565
MALONE, THOMAS N89-27268
MANGES, W. W. N89-27198
MANN, G. A. N89-27093
MANN, WILLIAM C. N89-27599
MANNING, S. D. N89-26838
MANZI, ANTONIO OCIMAR N89-27301
MARCHAL, C. N89-27450
MARCHITELLI, LOUIS N89-27336
MARIELLA, RAYMOND P. N89-27557
MARION, J. E. N89-27172
MARONI, V. A. N89-27553
N89-27562
MARRAFFA, ANDREW M. N89-26859
MARSHALL, DAVID P. N89-26837
MARTELLOTTI, G. N89-27159
MARTIN, C. WAYNE N89-27213
MARTIN, JAMES A. N89-26878
MARTINELLI, G. N89-27485
MARTINS, J. A. N89-27227
MARTINS, J. S. N89-27561
MASOTTO, TOM N89-27413
MASSINON, BERNARD N89-27283
MATHIAS, LON J. N89-27019
N89-27575
N89-27577
MATKOWSKY, B. J. N89-26941
MATTHEW, WILLIAM N89-27337
MATZEN, M. K. N89-27523
MAUGHAN, PAUL M. N89-27233
MAXWELL, E. L. N89-27252
MAY, EDWARD N. N89-27399
MAY, ROGER A. N89-27048
MAYERGOYZ, I. D. N89-27173
MAYHALL, D. J. N89-27084
MAZUMDAR, MAINAK N89-27203
MCARVER, ALEX N89-27147
MCCLENAGAN, R. D. N89-26926
MCCORKLE, RICHARD D. N89-26857
MCCURRY, DINI N89-27336
MCDONALD, T. E. N89-27493
MCGARRY, E. C. N89-27510
MCGREADY, JOHN W. N89-27192
MCKENZIE, B. B. N89-27080
MCKILLIP, R. M., JR. N89-26859
N89-26865
MCKOY, V. N89-27479
MCLUCKEY, SCOTT A. N89-27029
MCMENEMY, D. J. N89-27340
MCMILLAN, GARY B. N89-27361
MCMORROW, DANIEL J. N89-27303
MCNULTY, D. N89-26944
MEADOWS, SUSAN K. N89-27344
MECHLER, PIERRE N89-27283
MEDIONI, G. N89-26834
MEEKER, LARRY J. N89-27341
MEEKS, S. A. N89-27258
MEESIRI, WIRIYA N89-27020
MEHROTRA, PIYUSH N89-27362
MEHTA, RABINDRA D. N89-26866
MEIER, G. E. A. N89-27122
MEIER, GERALD H. N89-26988
MELENDRES, C. A. N89-27553
MELLO, ROBERT N89-27336
MENDES, CELSO LUIZ N89-27380
MENON, P. K. A. N89-27416
MERKLE, C. L. N89-26929
MERRITT, EARL S. N89-27235
MEYER, C. E. N89-27278
MEYER, D. N89-27627
MEYER, F. J. N89-27092
MEYER, ROBERT A. N89-27419
MEYERS, S. N89-27274
MICHAL, G. M. N89-26967
MIFFLIN, ROBERT N89-27379
MIGNANI, R. N89-27489
MIKKELSEN, TORBEN N89-27305
MIKLYAEV, V. M. N89-27109
MILAGREDAFONSECA, IJAR N89-26884
MILAM, BILLY R. N89-26852
MILANOVICH, F. P. N89-27172
MILLER, DAVID B. N89-27091
MILLER, G. L. N89-27136
MILLER, JOHN H. N89-27383
MILLER, R. E. N89-26883
MILLER, W. A. N89-27037
MILLETT, M. N89-27454
MILMAN, A. S. N89-27067
MINKOFF, M. N89-26941
MIRANDA, FELIX A. N89-27038
MIRTICH, MICHAEL J. N89-27506
MISIAKOS, KONSTANTINO N89-27243
MISSIQ, J. R. N89-27092
MITCHELL, MICHAEL N89-27151
MIYASATO, S. N89-26972
MOBLEY, J. DAVID N89-27270
MODESTODESOUZA, RICARDO CARTAXO N89-27381
MOERNER, W. E. N89-26940
MOFFITT, CHARLIE ROBERT, II N89-27406
MOLLER, JAMES CHRISTIAN N89-27132
MONTGOMERY, SUZANNE N89-26916
MOOG, E. R. N89-27508
MOORE, J. A. N89-27017
MOORE, JOHANNA D. N89-27364
MOORE, L. M. N89-27144
MOORTHI, SHRINIVAS N89-27314
MORALDI, D. N89-27569
MORGAN, F. A. N89-27093
MORGAN, R. C. N89-27427
N89-27428
MORGANTI, S. N89-27631
MOROSIN, B. N89-27561
MOROZOV, A. YU. N89-27581
MORRIS, J. W., JR. N89-26968
N89-26971
MORRIS, M. J. N89-27134
MORSE, JEFFREY D. N89-27557
MOSES, O. DOUGLAS N89-26809
MOSS, M. N89-27516
MOSTOVOY, S. N89-26913
MOUGINIS-MARK, PETER N89-27229
MOUSSA, N. ALBERT N89-26937
MUGGE, M. N89-27454
MUNRO, R. G. N89-27005
MURDOCK, RONALD G. N89-27192
MURPHY, D. C. N89-27605
MURRELL, REGINALD C. N89-26840
MURTHY, P. L. N. N89-26924

N

NAIK, VIJAY K. N89-27349
NAKAMURA, TAKASHI N89-26856
NAKATA, J. K. N89-27278
NAMIKAWA, LAERCIO MASSARU N89-27085
NANSTAD, RANDY K. N89-26974
N89-26980
N89-27156
N89-27211
N89-27220
NARAYAN, R. N89-27073
NARAYANASAMY, A. N89-27553
NASTASI, MICHAEL N89-27543
NEARY, DOUGLAS N89-27244
NEAU, E. L. N89-27093
NEFF, WILLIAM D. N89-27275
NEHER, CLARENCE W. N89-27187
NELSON, ROBERT S. N89-26899
NETO, ANTONIO FELIX MARTINS N89-26886
NEUGROSCHEL, ARNOST N89-27243
NEVATIA, R. N89-26834
NEWELL, ALLEN N89-27353
NEWELL, ALLEN C. N89-27043
NEWMAN, E. H. N89-27064
NEWTON, A. RICHARD N89-27098
NIELSEN, N. D. N89-27172
NIELSON, J. E. N89-27278
NISHIYAMA, R. T. N89-27298
NISSIM, E. N89-26844
NIXON, DAVID N89-27107
NORDMAN, J. E. N89-27561
NOREM, J. N89-27525
NORTON, ROBERT J. N89-27138
NYYSSONEN, DIANE N89-27174

O

OBORNY, M. C. N89-26949
OCKO, B. M. N89-27016
OCLAIR, MARK N89-27026
N89-27191
ODANI, MASAYASU N89-27371
ODEN, J. T. N89-27227
OHERN, MICHAEL E. N89-26969
OKA, Y. N89-27527
OLAND, C. B. N89-26980
OLBERG, M. N89-27605
OLIN, C. N89-27069
OLINTO, ANGELA V. N89-27608
OLIVER, WARREN C. N89-26969
OLNESS, D. N89-27145
OLOUGHLIN, JAMES P. N89-27514
OLSDER, GEERT JAN N89-27412
OMALLEY, M. W. N89-27082
OMALLEY, W. M. N89-27080
OMARA, DUNCAN N89-26990
ONOFIO, R. N89-27586
OONA, H. N89-27532
ORLANDO, S. N89-27569
OTT, E. N89-27173
OTT, KEVIN C. N89-27566
N89-27567
OTTINO, J. M. N89-27135
OTTO, KAREN LORRAINE N89-27365
OUDIN, LOUIS-REMY N89-26957
OWENS, MARLENE J. N89-27590

P

PACOLASOBRINHO, LUIZ CARLOS N89-27061
PADILLA, JUAN N89-26958
PAETTIKANGAS, T. J. H. N89-27513
PALAMIDES, T. R. N89-26995
N89-26996
N89-27007
PALAZOTTO, ANTHONY N. N89-26998
PALLOTINO, G. V. N89-27488
PALOUS, JAN N89-27616
PAOLIN, I. N89-26834
PAPADOPOULOS, GREGORY MICHAEL N89-27354
PAPAILIOU, K. D. N89-26820
PARK, CHUL N89-26816
PARK, Y. S. N89-27550
PARKER, B. H. N89-26918
PARRISH, ROBERT H. N89-26969
PARRY, DAVID W. N89-27026
N89-27191
PARSONS, CHESTER N89-27229
PARTRIDGE, R. N89-27359
PASTOR, RICARDO C. N89-27545
PATHAK, P. H. N89-27064
PATRICK, MERRELL L. N89-27349
PATTERSON, M. J. N89-26906
PAVLOPOULOS, THEODORE G. N89-27160
PAYNE, JANE B. N89-27323
PEASE, R. L. N89-27089
PEEBLES, H. C. N89-27200
PEI, SHIYOU N89-27568
PELED, EMANUEL N89-27247
PELLIZZONI, G. N89-27159
PENE, O. N89-27485
PENG, S. N89-26834
PENN, LANNING M. N89-27302
PERELOMOV, A. M. N89-27581
PERERA, R. C. C. N89-26950
PEREZ-MENDEZ, V. N89-27083
PEREZ, J. D. N89-27526
PERINO, MARIA ANTONIETTA N89-27619
PERISON, JANICE N89-27032
PERSHAN, PETER S. N89-27016
PERTICA, A. J. N89-27172
PETERS, L., JR. N89-27064
PETERSEN, J. R. N89-27069
PETERSON, S. J. N89-27228
PETRARCA, S. N89-27485
PETROSIAN, VAHE N89-27629
PETROVIC, JOHN J. N89-26923

PETTEY, CHRISILA C. N89-27384
PFEFFERLE, L. D. N89-26946
PFEIFER, K. B. N89-27505
PFIRSCH, D. N89-27539
PHELAN, ROBERT J., JR. N89-27507
PHILLIPS, BILL N89-27314
PHILLIPS, PAMELA S. N89-26810
PHILLPOT, S. R. N89-27474
PICCIOLA, J. J. N89-27562
PIERCE, THOMAS E. N89-27259
PIN, FRANCOIS G. N89-27415
PINHEIROGOMES, SEBASTIAO CICERO N89-26875
PITTER, RICHARD L. N89-27133
PITZ, W. J. N89-26926
PIZZELLA, G. N89-27488
PLACE, THOMAS M., JR. N89-26882
PLANTE, ROBERT J. N89-27303
PLETCHER, R. H. N89-27111
PLOTKIN, KENNETH J. N89-27459
POEPPEL, R. B. N89-27562
POHJOLAINEN, SILJA N89-27621
POLAR, A. N89-27193
N89-27194
POLITES, MICHAEL E. N89-27039
POLL, D. I. A. N89-27108
POLLARD, JAMES E. N89-26896
N89-27141
POLLINGER, J. P. N89-27003
POOL, KIRBY V. N89-26894
POPE, L. E. N89-26967
POPP, CARL J. N89-27262
POPPER, RICHARD D. N89-27337
PORKOLAB, MIKLOS N89-27521
N89-27522
PORTER, J. L. N89-27523
POSSIEL, NORMAN C. N89-27259
POSTEK, MICHAEL T. N89-27137
POUNDS, J. G. N89-27155
POWELL, A. G. N89-26841
POWELL, C. J. N89-26928
POWELL, DOUGLAS G. N89-27019
N89-27575
N89-27577
POWELL, H. T. N89-27172
POWELL, ROBERT L. N89-26915
POWER, JOHN L. N89-26904
POWERS, B. J. N89-27239
PRASAD, P. N. N89-26938
PRATT, DAVID T. N89-26856
PREGENZER, ARIAN L. N89-27530
PRIATKO, GORDON J. N89-27552
PRICE, K. N89-26834
PRIDDY, THOMAS G. N89-27219
PRIMDAHL, F. N89-27069
PROGAR, DONALD J. N89-27001
PRONI, JOHN R. N89-27322
PROSPERI, D. N89-27489
PRUVOST, J. N89-27124
PURSEL, ROBERT H. N89-26833

Q

QADIR, ASGHAR N89-27610
N89-27611
QURESHI, S. N89-27083

R

RABIER, PATRICK J. N89-27377
RADEKA, V. N89-27136
RADUSEWICZ, P. N89-27627
RAND, STEPHEN C. N89-27545
RANDALL, D. A. N89-27288
RANDALL, DONALD S. N89-26856
RANGANATHAN, K. N89-27226
RAPAGNAGNI, P. N89-27488
RAPPAZ, M. N89-26973
RAQUET, JOHN F. N89-27121
RATVASKY, THOMAS P. N89-26861
RAUCH, T. M. N89-27340
RAUCH, TERRY M. N89-27332
RAWLINS, GREG N89-27166
READ, B. E. N89-27010
READ, D. T. N89-26977
REED, R. P. N89-27079
N89-27144
REED, RONALD G. N89-27188
REES, WILLIAM S., JR. N89-27015
REHMAN, SHAKIL-UR N89-27146
REIN, M. N89-27122
RENEKER, DARRELL H. N89-26914
RENSHAW, THEODORE N89-26962
REQUA, JOE N89-27358
RESTER, A. W. N89-26896
REYNOLDS, HUGH M. N89-26897
RHEINBOLDT, WERNER C. N89-27377
RICCI, F. N89-27488
RICE, JIMMY W. N89-26857
RICH, THOMAS H. N89-27410
RICHARDS, D. R. N89-27555
N89-27568
RICKEL, D. G. N89-27532
RILEY, J. P. N89-27460
RIMPO, JEANNE YATES N89-27590
RINGHAM, MICHAEL R. N89-27244
RITTER, G. X. N89-27425
RIVERS, M. L. N89-27155
RIVIERE, FLORENCE N89-27283
RIZVI, H. A. N89-27611
ROACH, DENNIS P. N89-27219
ROBBINS, C. L. N89-27143
ROBERTS, THOMAS W. N89-27130
ROBERTSON, B. P. N89-26888
ROBERTSON, J. S. N89-27469
ROBERTSON, JAMES N89-27262
ROBINSON, G. C. N89-26980
ROBINSON, STEPHEN M. N89-27430
RODERICK, N. F. N89-27531
N89-27534
RODRIGUEZ, MILO R. N89-27186
RODRIGUEZ, O. N89-27125
RODRIGUEZ, M. A. N89-27544
ROE, J. N. N89-27172
ROESCH, E. N89-27127
ROESCH, J. F. N89-26880
ROESKE, S. B. N89-27090
ROETTGER, G. E. N89-26948
ROGERS, MICHAEL N89-27548
ROGGEMANN, MICHAEL C. N89-27502
ROGNLIEN, THOMAS D. N89-27521
ROHATGI, P. K. N89-26913
ROKICKI, TOM N89-27371
ROLLETT, ANTHONY D. N89-26983
ROMIG, A. D., JR. N89-26966
N89-26981
ROSCHKE, MARK A. N89-27388
ROSE, MADELEINE S. N89-27337
ROSENBERG, NORMAN N89-27268
ROSENSTEIN, MICHAEL T. N89-27347
ROSENSTEIN, RICHARD N89-27347
ROSENZWEIG, J. B. N89-27525
ROSS, LORNA N89-27342
ROSS, P. N. N89-27254
N89-27255
ROTH, A. J. N89-26937
ROTH, E. P. N89-27516
ROTHMAN, S. J. N89-27546
ROUTBORT, J. L. N89-26913
N89-27546
ROVELLI, CARLO N89-27585
ROYER, HENRI N89-26957
RUBNER, M. F. N89-27021
N89-27022
N89-27023
RUGGLES, MARINA B. N89-26978
N89-27210
RUSSELL, JULIE C. N89-26830
RUSSO, A. J. N89-27200
RUSTIK, JAMES J. N89-26857
RYMES, M. D. N89-27252

S

SACHER, P. W. N89-27104
SACHER, PETER N89-26819
SAFFARIAN, M. H. N89-27254
N89-27255
SAJBEN, M. N89-27134
SALOMAA, R. R. E. N89-27513
SALVINO, J. T. N89-26851
SAMIRANT, MICHEL N89-26957
SAMPSON, CHARLES R. N89-27306
SAND, J. R. N89-27037
SANG, PARK S. N89-27066
SANTANNABINS, LEONARDO N89-27236
SANTEE, WILLIAM L. N89-27334
SANTORO, R. T. N89-27476
SANTOS, JORGE S. N89-27075
SARAVANOS, D. A. N89-26912
N89-26919
SATO, N. N89-27288
SAUBER, JEANNE N89-27279
SCALZO, F. N89-27360
SCHANWALD, L. P. N89-27080
SCHELLINGERHOUT, ABRAHAM JACOB GUILLAUME
N89-27495
SCHEMM, JAE-KYUNG N89-27314
SCHIDLOVSKY, GEORGE N89-27155
SCHLACHTER, A. S. N89-27475
SCHLINKER, R. H. N89-27468
SCHMIDT, W. N89-27104
SCHMIDT, WOLFGANG N89-26819
SCHMITTER, K. H. N89-27539
SCHNEIDER, E. K. N89-27288
SCHOBERT, HAROLD H. N89-27032
SCHOESSOW, P. N89-27525
SCHROEDL, HEINO N89-27065
SCHUBERT, SIEGFRIED N89-27314
SCHUH, MICHAEL J. N89-26856
SCHURMAN, DONALD L. N89-27350
SCHUTT, J. A. N89-27119
SCHWANK, J. R. N89-27088
SCHWARZ, A. S. N89-27486
SCHWARZMAN, E. C. N89-27278
SCIALDONE, JOHN J. N89-26902
SCOFIELD, JOHN H. N89-27205
SCOTT, MICHAEL N89-27268
SEALEY, BRADLEY S. N89-27151
SEBASTIANI, F. N89-27482
SEILER, DAVID G. N89-27471
SEILKOP, S. K. N89-27260
SEKI, RYCICHI N89-27434
SELEN, W. J. N89-27588
SELLERS, P. J. N89-27288
SENTERFITT, DONALD R. N89-27163
SERGEEV, I. A. N89-27109
SESSLER, A. M. N89-27169
SESSLER, ANDREW M. N89-27175
SESTOKASFILHO, BRUNO N89-27609
SEVERUD, L. K. N89-27221
SEXTON, F. W. N89-27088
SEYFERTH, DIETMAR N89-27015
SHAHID-SALESS, BAHMAN N89-27456
SHAIK, KAMRAN N89-27281
SHAPIRO, STUART C. N89-27417
N89-27418
SHARMA, SURENDRA P. N89-26816
SHEEN, JEEN S. N89-26917
SHELEF, GAD N89-27190
SHEPHERD, KEVIN P. N89-27467
SHERMAN, MICHAEL H. N89-26872
SHERVAIS, J. W. N89-27278
SHISKOWSKI, ROBERT N89-27139
SHUCHMAN, R. A. N89-27067
SHUKITT, B. L. N89-27340
SHUKLA, J. N89-27288
SIDLICHOVSKY, MILOS N89-27615
SIDOR, L. B. N89-27393
SIEGEL, R. W. N89-27553
SIEGMAN, W. L. N89-27469
SIGSBY, JOHN E., JR. N89-27147
SIHVOLA, ARI H. N89-27044
SIKES, ALLISON M. N89-27019
SILS, INGRID N89-27337
SILVER, R. N. N89-27453
N89-27472
SILVESTRO, J. N89-27073
SIMON, ROBERT N89-27202
SIMONICH, J. C. N89-27466
N89-27468
SIMPSON, J. N89-27525
SINGH, S. P. N. N89-26948
SINGH, V. P. N89-27242
SIUZDAK, J. N89-27498
SKEEL, ROBERT D. N89-27438
SLUTZ, S. A. N89-27535
SMEETS, GUENTER N89-26957
SMITH, ADRIAN F. M. N89-27451
SMITH, CHRISTOPHER C. N89-27076
SMITH, D. ROBERT N89-27076
SMITH, F. W. N89-26951
SMITH, J. V. N89-27155
SMITH, KIMBERLY K. N89-26863
SMITH, L. R. N89-26896
SMITH, LESLIE E. N89-26993
SMITH, MIKE N89-27304
SMOLIN, LEE N89-27585
SMOOKE, M. D. N89-26946
SMYTH, DONALD M. N89-26933
SNIDER, J. B. N89-27257
SNOOK, STOVER H. N89-27344
SNOW, RICHARD N89-27147
SNOW, W. M. N89-26953
N89-27472
SOKOL, P. E. N89-26953
N89-27453
N89-27472
SOMMER, M. N89-26951
SOSNICK, T. R. N89-26953
N89-27472
SOURS, THOMAS N89-26887
SPAETH, CHARLES E. N89-26847
SPANNE, PER N89-27155
SPARKS, ALLEN R. N89-27261
SPELT, PHILIP F. N89-27415

SPENCER, FLOYD W. N89-27203
SPIELMAN, R. B. N89-27523
SPINGARN, J. R. N89-26920
SPRAGGINS, S. A. N89-27090
SRIHARI, SARGUR N. N89-27417
ST.CLAIR, TERRY L. N89-27001
STANISLAS, M. N89-27124
STANLEY, A. E. N89-27024
STARKWEATHER, JOHN H. N89-26849
START, G. EUGENE N89-27275
STAUDT, JAMES E. N89-27178
STEELE, W. V. N89-26954
STEGER, J. L. N89-27111
STELLA, B. N89-27158
STENSBY, JOHN L. N89-27054
STEPHENSON, MICHAEL B. N89-27435
STERNBACH, E. J. N89-27169
STEVENSON, MERRITT R. N89-27391
STEWART, DORATHY A. N89-27307
STEWART, I. R. N89-27108
STEWART, JAMES M. N89-27572
STEWART, V. R. N89-26815
STINCHCOMB, DAVID N89-27375
STOCKTON, WILLIAM W. N89-26848
STOGNER, CLAUDE R. N89-26847
STOKES, GEROLD N89-27268
STONE, JAMES R. N89-26895
STOUT, MICHAEL G. N89-26983
STRAUCH, R. G. N89-27300
STRAWA, ANTHONY W. N89-26816
STREET, R. A. N89-27083
STREETMAN, K. D. N89-27596
STUEMPFLE, ARTHUR K. N89-27133
STWALLEY, WILLIAM C. N89-27161
STYGAR, W. A. N89-27492
SUAREZ, MAX N89-27314
SUNWOO, A. J. N89-26971
SUTTON, S. R. N89-27155
SWAIN, D. W. N89-27520
SWARTOUT, WILLIAM R. N89-27364
SWEC, DIANE M. N89-27506
SWINDEMAN, R. W. N89-26982
SZEMENYEI, BRIAN N89-26899
SZLYK, PATRICA C. N89-27337

T

TAASAN, SHLOMO N89-27420
TAKAHASHI, Y. N89-27210
TAKIGAWA, MASASHI N89-27565
N89-27566
N89-27567
TAMBE, MILIND N89-27353
N89-27411
TANK, V. N89-27157
TAO, YU-TAI N89-27011
TAPLEY, BYRON N89-27229
TARDY, HERBERT L. N89-27398
TAUBER, MICHAEL E. N89-27116
TEISSEDRE, C. N89-27123
TELESMAN, JACK N89-26989
TENBERG, A. J. W. M. N89-27401
TENNERY, V. J. N89-27006
TERAESRANTA, HARRI N89-27621
TERRY, A. L. N89-27340
TESSIER-YOUNGS, CLAIRE A. N89-27014
THARION, W. J. N89-27340
THIBAULT, DAVID A. N89-27233
THIBERT, J. J. N89-26818
THIESSEN, RICHARD L. N89-27237
N89-27238
THOMAS, G. N89-26972
THOMAS, GLENN N89-27337
THOMAS, J. N89-27454
THOMPSON, BARRY L. N89-27552
THOMPSON, D. H. N89-27198
THOMPSON, JOE D. N89-27565
N89-27566
THOMPSON, THAYNE M. N89-27280
THYKIER-NIELSEN, S. N89-27305
TICHLER, PAUL R. N89-26970
TIDSWELL, I. M. N89-27016
TILTON, B. E. N89-27258
TISCHLER, VICTORIA A. N89-27409
TOI, K. N89-27511
N89-27527
TOIVANEN, RISTO O. N89-27543
TOMBOULIAN, SHERRYL N89-27390
TORRES, PABLO D. N89-26976
TORUNSKY, EBERHARD N89-27065
TOVROG, THEODORE N89-26931
TOWNSEND, JOHN N89-26832
TREACY, E. B. N89-27165
TREECE, R. K. N89-27357
TRIBULA, D. N89-26968
TRINH, K. V. N89-26920
N89-26922
TROUTMAN, P. A. N89-26888
TRUPPI, LAWRENCE E. N89-27299
TSCHIRHART, R. N89-27627
TUMMILLO, A. F. N89-27092
TURNER, LEAF N89-27533
TURNS, S. R. N89-26929
TVETEN, A. B. N89-27510
TWORZYDLO, W. W. N89-27227

U

UNDERWOOD, DONALD L. N89-26839
URBACH, HERMAN B. N89-27426
URPO, SEPPO N89-27621

V

VALENTI, E. L. N89-26896
VALENTINE, GREG A. N89-27290
VAMPOLA, ALFRED L. N89-27287
VANDELEUR, ROLAND HENRI MARIE N89-27551
VANDENHEUVEL, P. N89-27402
VANDERVOOREN, J. N89-26822
VANDERWEES, A. J. N89-26827
VANHOLTEN, J. W. N89-27578
VANHULZEN, J. A. N89-27402
N89-27414
VANIMAN, DAVID T. N89-27618
VANPATTEN, ROBERT E. N89-26858
VANSCIVER, S. W. N89-26867
N89-27036
VANSCOY, ROGER N89-27375
VASKA, LAURI N89-26934
VASSENDEN, J. N89-27102
VAUDIN, M. D. N89-26996
VEDULA, K. N89-26967
VELASCO, FLAVIO ROBERTO DIAS N89-27085
VENKAYYA, VIPPERLA B. N89-27409
VENTURINI, E. L. N89-27561
VERDERAIME, V. N89-27214
VEYSSIERE, P. N89-27571
VIEIRAMONTEIRO, ANTONIO MIGUEL N89-27236
N89-27367
VILLA, F. N89-27084
VINEYARD, E. A. N89-27037
VIOLETTE, EDMOND N89-27058
VIRASORO, M. A. N89-27327
N89-27328
VISWANADHAM, Y. N89-27301
VISWESWARAN, G. S. N89-27096
VITEK, J. M. N89-26973
VLEGHERT, J. P. K. N89-26854
VOLOSHIN, M. B. N89-27617
VONHOLLE, WILLIAM N89-27027
VUCKOVIC, DRAGAN LJ. N89-26935

W

WADDELL, EVANS N89-27311
WAKAMATSU, YOSHIO N89-26893
WALKER, R. A. N89-27416
WALLACE, ROBERT L. N89-26879
WALLIS, R. F. N89-26814
WALTERS, E. JANE N89-27087
WALTON, JOHN J. N89-27276
WALTON, R. A. N89-27526
WANG, BOA F. N89-27046
WANG, CHYI-SHAN N89-26998
WANG, LAWRENCE K. N89-27266
WANG, MU HAO SUNG N89-27266
WANG, TEN-SEE N89-26900
WARD, M. R. N89-27346
WARPINSKI, N. R. N89-27395
WARREN, ROGER W. N89-27171
WARREN, T. W. N89-27144
WASSERMAN, STEPHEN R. N89-27011
N89-27016
WATARI, T. N89-27527
WATSON, K. N89-27326
WATSON, R. D. N89-27516
WAYLAND, ROBERT N89-27311
WEAVER, N. L. N89-27143
WEBER, A. N89-26942
WEBER, J. N89-27488
WEBER, WOLF-DIETRICH N89-27372
WEEKS, JOHN R. N89-26970
WEICKMANN, A. M. N89-27460
WEINGARTEN, L. I. N89-26922
WEIRICK, L. J. N89-27031
WEISBIN, C. R. N89-27198
N89-27415
WEISS, SHOLOM M. N89-27598
WEISSMAN, PAUL R. N89-27276
WELTER, HELMUT N89-27541
WERNLUND, J. V. N89-26880
WESTBROOK, C. K. N89-26926
WESTWATER, E. R. N89-27257
N89-27298
WHIRLEY, ROBERT G. N89-27222
WHITE, D. E. N89-26948
WHITEMAN, C. DAVID N89-27275
WHITESIDES, GEORGE M. N89-27011
N89-27016
WHITTENBERG, C. D. N89-27457
WHYBORN, N. D. N89-27605
WIESEND, J. G., II N89-26867
WIKLIND, TOMMY N89-27613
WIKSTROM, DONOVAN C. N89-27202
WILBUR, MATTHEW L. N89-27485
WILDING, MATT N89-27351
WILLIAMS, K. A. N89-27396
WILLIAMS, LAIRD C. N89-27056
WILLIAMS, W. R. N89-27269
WILLIAMSON, R. L. N89-27200
WILSHIRE, H. G. N89-27278
WILSON, JOSEPH N. N89-27425
WILSON, M. N89-27077
WINOKUR, P. S. N89-27089
WITTBERG, T. N. N89-26987
WOBIG, HORST N89-27536
WOHLETZ, KENNETH H. N89-27290
WOLF, D. N89-27474
WOLFFENBUTTEL, REINOUD FELIX N89-27509
WONG, H. N89-27211
WONG, P. S. N89-27003
WOOD, JAMES S. N89-26878
WOOLF, BEVERLY N89-27418
WRIGHT, T. N89-26880
WU, EDWARD M. N89-26925
WU, W. N89-26913
WUEBBLES, DONALD J. N89-27273

X

XU, YONGZHI N89-27325
XUDONG, C. N89-27249

Y

YAMA, Z. N89-27627
YAMAGUCHI, FERNANDO YTAKA N89-27381
YAMAKAWA, GEORGE M. N89-26839
YAMAMOTO, TSUTOMU N89-26836
YANG, J. N. N89-26838
YARIV, AMNON N89-27167
YARROW, MAURICE N89-27433
YEAGER, WILLIAM T., JR. N89-27465
YEE, J. H. N89-27084
YEH, H. C. N89-27003
YELTON, W. GRAHAM N89-27009
YOLTON, CHARLES F. N89-26965
YOSHIDA, K. N89-27583
YOUNGS, WILEY J. N89-27014
YOUNKER, L. W. N89-27228
YUGO, J. N89-27522
YUREK, A. M. N89-27510

Z

ZACCARDELLI, C. N89-27486
ZAK, J. N89-27508
ZARATE, EUGENE A. N89-27014
ZASADZINSKI, J. F. N89-27568
ZEPKIN, NEIL N89-27166
ZIKAN, KAREL N89-27387
ZIMMERMAN, ANTHONY M. N89-27106
ZINGG, DAVID W. N89-27433
ZUBER, LAURA C. N89-27196
ZURAWSKI, ROBERT L. N89-26876
ZUTAVERN, F. J. N89-27080
N89-27082
ZWICK, HARRY N89-27331

Typical Corporate Source Index Listing

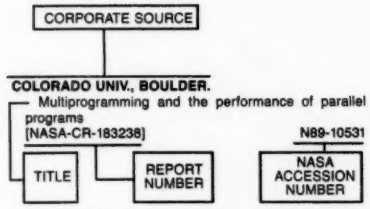

Listings in this index are arranged alphabetically by corporate source. The title of the document provides the user with a brief description of the subject matter. The report number helps to indicate the type of document cited (e.g., NASA report, translation, NASA contractor report). The NASA accession number denotes the number by which the citation is identified. The titles are arranged under each corporate source in ascending accession number order.

A

AARHUS UNIV. (DENMARK).
Oxygen transfer to ethylene catalyzed by the Ag(110) surface
[AD-A207325] N89-26936

ACADEMIA SINICA, SHANGHAI (CHINA).
Nonresonant interaction of a three-level atom with cavity fields. Part 4: Atomic dipole moment and squeezing effects
[AD-A206788] N89-27470

ACADEMY OF SCIENCES (USSR), MOSCOW.
Resonant helicity flip of electron neutrino due to magnetic moment and dynamics of supernova
[PREPRINT-598] N89-27617

ADIABATICS, INC., COLUMBUS, IN.
Feasibility demonstration of the Thermal Ignition Combustion System (TICS) for high pressure natural gas injected engine
[PB89-178792] N89-26944
Combustion characteristics of dry coal-powder-fueled adiabatic diesel engine
[DE89-000978] N89-27197

ADVISORY GROUP FOR AEROSPACE RESEARCH AND DEVELOPMENT, NEUILLY-SUR-SEINE (FRANCE).
Technical Status Review on Drag Prediction and Analysis from Computational Fluid Dynamics: State of the Art
[AGARD-AR-256] N89-26817
Measurement uncertainty within the Uniform Engine Test Programme
[AGARD-AG-307] N89-26854
Validation of computational fluid dynamics
[AGARD-AR-257] N89-27104
Short course on cardiopulmonary aspects of aerospace medicine
[AGARD-R-758-ADD] N89-27330
Human performance assessment methods
[AGARD-AG-308] N89-27338

AERITALIA S.P.A., TURIN (ITALY).
State-of-the-art of aircraft drag prediction in Italy by means of theoretical methods N89-26821

AERONAUTICAL RESEARCH INST. OF SWEDEN, STOCKHOLM.
The behavior of flux difference splitting schemes near slowly moving shock waves
[FFA-TN-1988-58] N89-27130

AERONAUTICAL SYSTEMS DIV., WRIGHT-PATTERSON AFB, OH.
F-15E EADI (Electronic Attitude Director Indicator) evaluation: A comparison of three formats
[AD-A206809] N89-26846

AEROSPACE CORP., EL SEGUNDO, CA.
Hybrid electric chemical propulsion
[AD-A207584] N89-26898
Electron-impact ionization time-of-flight mass spectrometer for molecular beams
[AD-A207585] N89-27141
The space particle environment
[AD-A207547] N89-27287

AEROSPATIALE AQUITAINE, SAINT-MEDARD EN JALLES (FRANCE).
Large protein crystallization facility, phase A. Executive summary
[AQ-ES-175/88] N89-27035

AIR FORCE FLIGHT DYNAMICS LAB., WRIGHT-PATTERSON AFB, OH.
A compound scaling algorithm for mathematical optimization
[AD-A208446] N89-27409

AIR FORCE INST. OF TECH., WRIGHT-PATTERSON AFB, OH.
An expert system in C for computer-aided digital circuit design
[AD-A207518] N89-27075
An objective comparison of vertical motions from the kinematic method and three forms of the omega equation
[AD-A208451] N89-27294
An investigation into the gravity current aspects of a cold air outbreak using variational analysis techniques
[AD-A208464] N89-27295
Software management indicators: Managing the risk of project management
[AD-A208443] N89-27408
Multiple sensor fusion for detecting targets in FLIR (Forward-Looking Infrared) and range images
[AD-A207577] N89-27502

AIR FORCE SYSTEMS COMMAND, WRIGHT-PATTERSON AFB, OH.
Acta Aeronautica et Astronautica Sinica, Volume 8, Number 12, December 1987 (selected articles)
[AD-A206782] N89-26807

AKTIEBOLAGET ROLLAB, STOCKHOLM (SWEDEN).
On internal bending-beam strain-gage wind tunnel balances
[RR-070] N89-26870

ALLIANCE TECHNOLOGIES CORP., CHAPEL HILL, NC.
Procedures for the preparation of emission inventories for precursors of ozone, volume 1, third edition
[PB89-154209] N89-27264

ANALYTIC SCIENCES CORP., ARLINGTON, VA.
SDS software measurement requirements
[AD-A207449] N89-27376

ANALYTICS, INC., WILLOW GROVE, PA.
Human Operator Simulator (HOS) 4 programmer's guide
[AD-A207241] N89-27342

ARGONNE NATIONAL LAB., IL.
Erosion of Al and Al/SiC
[DE89-013623] N89-26913
Numerical computation of bifurcation phenomena and pattern formation in combustion
[DE89-013628] N89-26941
The role of X-ray absorption spectroscopy in electronic structure studies
[DE89-014677] N89-26952
Momentum distributions in liquid helium
[DE89-014679] N89-26953
Cross-sectional TEM (Transmission Electron Microscopy) studies of Cr films deposited by ion-assisted deposition and physical vapor deposition
[DE89-014643] N89-26985
Future applications of engine ceramics: Factors influencing market opportunities, timing, and growth
[DE89-012426] N89-27002
Development of magnetic resonance imaging technology for imaging binder distribution in ceramics
[DE89-013185] N89-27003
Development of compressed multifoil insulation for high-temperature batteries and other applications
[DE89-012877] N89-27092
Attractive levitation for high-speed ground transport with large guideway clearance and alternating-gradient stabilization
[DE89-013640] N89-27195
Field studies for determining the characteristics and dynamics of local circulations
[DE89-013639] N89-27275
Portable parallel programming in a FORTRAN environment
[DE89-014670] N89-27399
High-temperature behavior of grain boundaries from embedded atom method molecular dynamics simulation
[DE89-013641] N89-27474
Magneto-optical properties of ultrathin ferromagnetic films
[DE89-014640] N89-27508
Experimental measurement of nonlinear plasma wake-fields
[DE89-014636] N89-27525
Diffusion in high-T sub c superconductors
[DE89-009792] N89-27546
Study of nanophase TiO2 grain boundaries by Raman spectroscopy
[DE89-012416] N89-27553
Composition of superconducting La2CuO4+delta: A superconductor doped by excess oxygen defects
[DE89-013299] N89-27555
Recent improvements in bulk properties of ceramic superconductors
[DE89-013626] N89-27562
Study of the microstructure of silver films deposited by ion assisted deposition onto aluminum oxide substrates
[DE89-014665] N89-27563
Evidence for phonon-mediated coupling in superconducting Ba sub 0.6 K sub 0.4 BiO3
[DE89-014642] N89-27568
User guide for the Data Analysis, Retrieval, and Tabulation System (DARTS): A mainframe computer code for generating cross-tabulation reports
[DE89-012930] N89-27592

ARIZONA UNIV., TUCSON.
A finite element method for solving electromagnetic scattering problems
[DE89-013496] N89-27059

ARMY AEROSTRUCTURES DIRECTORATE, HAMPTON, VA.
Scaling effects in the static large deflection response of graphite-epoxy composite beams
[NASA-TM-101619] N89-26843

ARMY AVIATION ENGINEERING FLIGHT ACTIVITY, EDWARDS AFB, CA.
Airworthiness and flight characteristics evaluation of the EH-60A (Quick Fix) helicopter
[AD-A207417] N89-26839
Preliminary airworthiness evaluation of the UH-60A external fuel system
[AD-A207570] N89-26840

ARMY COLD REGIONS RESEARCH AND ENGINEERING LAB., HANOVER, NH.
Investigations of dielectric properties of some frozen materials using cross-borehole radiowave pulse transmissions
[AD-A207302] N89-27285

ARMY ENGINEER TOPOGRAPHIC LABS., FORT BELVOIR, VA.
Research in knowledge-based vision techniques for the autonomous land vehicle program
[AD-A208546] N89-26834

ARMY LAB. COMMAND, FORT MONMOUTH, NJ.
Polarization matrices of lithium tantalate
[AD-A208349] N89-27097
Polarization matrices of lithium niobate
[AD-A207231] N89-27462

ARMY LAB. COMMAND, WATERTOWN, MA.
Examination of the tensile strength of graphite fibers
[AD-A207277] N89-26909
The recrystallization and respheroidization of tungsten grains in a tungsten-heavy alloy
[AD-A207647] N89-26964
Automated immersion testing robotic system: Hardware and software design
[AD-A208755] N89-27201
Cepstral method for the measurement of ultrasonic pulse transmission time variations
[AD-A207410] N89-27463

The quantitative dependence of transmissivity on flexural strain for multimode optical fiber
[AD-A207522] N89-27501
ARMY MATERIALS TECHNOLOGY LAB., WATERTOWN, MA.
Statistical strength comparison of metal-matrix and polymeric-matrix composites
[AD-A208316] N89-26925
ARMY MISSILE COMMAND, REDSTONE ARSENAL, AL.
Selective nitrations: Laser-induced nitrations
[AD-A207406] N89-27024
Application of crystal lattice disintegration criteria to compute minimum shock induced reactive conditions in solid explosives and inert materials
[AD-A207557] N89-27025
Evaluation of an optical correlator and matched filter maker
[AD-A207556] N89-27054
Low relative humidity in the atmosphere
[AD-A207558] N89-27307
Lognormal distribution maximum-likelihood parameter estimation algorithms
[AD-A207586] N89-27378
ARMY RESEARCH INST. OF ENVIRONMENTAL MEDICINE, NATICK, MA.
Altitude symptomatology and mood states during a climb to 3630 m
[AD-A208261] N89-27332
Annual historical report - AMEDD activities
[AD-A208301] N89-27333
Thermoregulatory responses in the cold-effect of an Extended Cold Weather Clothing System (ECWCS)
[AD-A208314] N89-27334
Considerations for replacement beverages: Fluid-electrolyte balance and heat illness
[AD-A208342] N89-27335
Endogenous hormonal and growth factor responses to heavy resistance exercise protocols
[AD-A208375] N89-27336
Effectiveness and acceptability of nutrient solutions in enhancing fluid intake in the heat
[AD-A208428] N89-27337
Psychological attributes, coping strategies and other factors associated with ultramarathon performance
[AD-A208300] N89-27340
The effects of arms and countermovement on vertical jumping
[AD-A208298] N89-27347
ARMY RESEARCH OFFICE, RESEARCH TRIANGLE PARK, NC.
Transactions of the 6th Army Conference on Applied Mathematics and Computing held in Boulder, Colorado on 31 May - 3 June 1988
[AD-A207252] N89-27424
ASTRON RESEARCH AND ENGINEERING, SUNNYVALE, CA.
Demonstration of oblique detonation wave for hypersonic propulsion
[AD-A208268] N89-26856
AUTONOMOUS TECHNOLOGIES, ORLANDO, FL.
Deep space LADAR, phase 1
[AD-A207454] N89-27166

B

BABCOCK AND WILCOX CO., ALLIANCE, OH.
Fundamental studies of the cavity flowmeter
[PB89-188825] N89-27153
BALLISTIC RESEARCH LABS., ABERDEEN PROVING GROUND, MD.
A multidriver shock tube model of a large blast simulator
[AD-A208324] N89-26871
BATTELLE COLUMBUS LABS., OH.
Gas engine heat pump system and component efficiency and reliability improvement, phase 2
[PB89-173645] N89-27184
BATTELLE MEMORIAL INST., RESEARCH TRIANGLE PARK, NC.
Development of Low-Level Turbulence (LLT) forecasting methodologies
[AD-A208457] N89-27320
BERN UNIV. (SWITZERLAND).
Berne solar observations for January-December 1988
[REPT-54] N89-27626
BIELEFELD UNIV. (GERMANY, F.R.).
Global flows with invariant (Gibbs) measures for Euler and Navier-Stokes two-dimensional fluids
[BIBOS-310/88] N89-27105
BOEING ADVANCED SYSTEMS CO., SEATTLE, WA.
Hot surface ignition tests of aircraft fluids
[AD-A207372] N89-26937
BOOZ-ALLEN AND HAMILTON, INC., NEW YORK, NY.
Microwave hardening technology development program
[AD-A207535] N89-27076
BORGMAN (LEON E.), INC., LARAMIE, WY.
Brief instructions for SIMBAT, a computer package for unconditional and conditional simulation of ocean wave kinematics
[AD-A207627] N89-27324
BRIGHAM YOUNG UNIV., PROVO, UT.
Supercritical fluid chromatography of polar organic compounds in combustion particulates
[PB89-152441] N89-26930
BROOKHAVEN NATIONAL LAB., UPTON, NY.
Effects of high thermal and high fast fluences on the mechanical properties of type 6061 aluminum in the HFBR
[DE89-012636] N89-26970
X-ray microscopy using synchrotron radiation
[NASA-CR-184800] N89-27155
BROWN UNIV., PROVIDENCE, RI.
Offline computing farms
[DE89-013958] N89-27359

C

CALIFORNIA INST. OF TECH., PASADENA.
High power semiconductor laser sources
[AD-A207569] N89-27167
Fog, cloud, and dew chemistry
[PB89-187314] N89-27317
CALIFORNIA STATE UNIV., NORTHRIDGE.
Efficient grid generation
[NASA-CR-185034] N89-27434
CALIFORNIA UNIV., BERKELEY.
Fire propagation in concurrent flows
[PB89-188577] N89-26945
Observations on the mechanisms of fatigue in eutectic Pb-Sn solder joints
[DE89-000553] N89-26966
Cryogenic tensile properties of AA 2090 weldments
[DE89-012979] N89-26971
History of the application of the generalized Lewis acid-base theory to metals
[DE89-012992] N89-26984
Primary dissociation processes of energetic compounds
[AD-A208312] N89-27033
CALIFORNIA UNIV., BERKELEY. LAWRENCE BERKELEY LAB.
A preliminary report on X-ray photoabsorption coefficients and atomic scattering factors for 92 elements in the 10-10,000 eV region
[DE89-013392] N89-26950
Observations on the mechanisms of fatigue in eutectic Pb-Sn solder joints
[DE89-000553] N89-26966
Cryogenic tensile properties of AA 2090 weldments
[DE89-012979] N89-26971
Microstructural evolution of Al-Li and Al-Li-Cu-Mg alloys
[DE89-012981] N89-26972
History of the application of the generalized Lewis acid-base theory to metals
[DE89-012992] N89-26984
Proposed thin film electronics for a-Si:H PIXEL detector
[DE89-013410] N89-27083
Theory of X-ray holography including phase and amplitude contrast and finite transfer functions
[DE89-012835] N89-27148
X-ray holography: A history
[DE89-012983] N89-27149
Elements of a realistic 17 GHz FEL/TBA design
[DE89-013427] N89-27169
Report of the Workshop on Scientific Opportunities for Infrared Free-Electron Lasers, volume 1
[DE89-012836] N89-27170
Prospects for the FEL (Free Electron Laser)
[DE89-012998] N89-27175
Electrochemical evaluation of new fluorosulfonic and fluorophosphonic acids as fuel cell electrolytes
[DE89-012840] N89-27254
Electrochemical evaluation of new fluorosulfonic and fluorophosphonic acids as fuel cell electrolytes
[DE89-013391] N89-27255
Proceedings of the Energy Efficiency and Structural Change: Implications for the Greenhouse Problem Workshop
[DE89-012852] N89-27274
Cryogenic techniques for large superconducting magnets in space
[DE89-013431] N89-27455
Multiple-electron processes in fast ion-atom collisions
[DE89-012982] N89-27475
A method for generating the J sub c, B, T surface for niobium-alloy superconductors
[DE89-012977] N89-27556
Sputtering of high-temperature superconductors: A bibliography
[DE89-013374] N89-27558
Passive superconductor: A viable method of controlling magnetization multipoles in the SSC dipole
[DE89-013432] N89-27559
CALIFORNIA UNIV., DAVIS.
Processing of continuous fiber composites
[DE89-012608] N89-26915
Efficiency of N use by wheat as a function of influx and efflux of NO sub 3
[NASA-CR-177534] N89-27346
CALIFORNIA UNIV., IRVINE.
Supersonics
[AD-A207394] N89-26814
CALIFORNIA UNIV., LOS ANGELES.
Evolution and structure of the bow echo/microburst events
[PB89-174767] N89-27309
CALIFORNIA UNIV., MARINA DEL REY.
Research in knowledge delivery
[AD-A208327] N89-27599
CALIFORNIA UNIV., SAN DIEGO, LA JOLLA.
High efficiency pattern recognition
[AD-A207210] N89-27368
CALIFORNIA UNIV., SANTA CRUZ.
Application of the theory of wave propagation through random media to phase and amplitude fluctuations of seismic P-waves
[AD-A207207] N89-27284
CARNEGIE-MELLON UNIV., PITTSBURGH, PA.
Competitive management of distributed shared memory
[AD-A207322] N89-27372
Kernel user's manual version 1.0
[AD-A207414] N89-27375
Time-sequential optical data processing
[AD-A207514] N89-27500
CASE WESTERN RESERVE UNIV., CLEVELAND, OH.
Synthesis and structural characterization of Pt-Si dimers with unusually short cross-ring silicon-silicon interactions
[AD-A208310] N89-27014
CD METROLOGY, INC., GERMANTOWN, MD.
Narrow-angle laser scanning microscope system for linewidth measurements on wafers
[PB89-189344] N89-27174
CENTRE NATIONAL D'ETUDES SPATIALES, TOULOUSE (FRANCE).
SPOT 1-2-3 Pyrotechnics System: Definition repo rt
[CNES-CT/DRT/TVE/IL-89-035] N89-26889
CESKOSLOVENSKA AKADEMIE VED, ONDREJOV.
Dynamics of the solar system: Proceedings, volume 3
[DE89-609828] N89-27615
Evolution of Galaxies. Proceedings, volume 4
[DE89-609850] N89-27616
CHEMICAL RESEARCH AND DEVELOPMENT CENTER, ABERDEEN PROVING GROUND, MD.
Design and characterization of large-drop generators for viscous, Newtonian, and non-Newtonian liquids
[AD-A208330] N89-27133
CHICAGO UNIV., IL.
Development of advanced methods based on stable isotope technology for studies of exercise in heat
[AD-A208758] N89-27329
CITY COLL. OF THE CITY UNIV. OF NEW YORK, NY.
Thermodynamics and high temperature chemistry of the chemical vapor deposition of diamond films
[DE89-013574] N89-26951
CLARKSON UNIV., POTSDAM, NY.
Catalytic reduction of carbon dioxide by metal centers
[AD-A207227] N89-26934
COASTAL ENGINEERING RESEARCH CENTER, VICKSBURG, MS.
Pacific Coast hindcast phase 3 north wave information
[AD-A207189] N89-27323
COLEMAN RESEARCH CORP., HUNTSVILLE, AL.
Expendable air vehicles/high altitude balloon technology
[AD-A206972] N89-26813
COLORADO UNIV., BOULDER.
Application of modern mathematical concepts to plasma confinement
[DE89-012952] N89-27517
COMMISSARIAT A L'ENERGIE ATOMIQUE, SAINT-PAUL-LES-DURANCE (FRANCE).
TORE SUPRA graphite inner first wall
[DE89-009325] N89-27512
COMPUTATIONAL LOGIC, INC., AUSTIN, TX.
A parallel version of the Boyer-Moore prover
[AD-A207190] N89-27351

COMPUTATIONAL MECHANICS CO., AUSTIN, TX.
Computational methods for nonlinear dynamic problems in solid and structural mechanics: Progress in the theory and modeling of friction and in the control of dynamical systems with frictional forces
[AD-A208763] N89-27227
COMPUTER TECHNOLOGY ASSOCIATES, INC., MCLEAN, VA.
Evaluation of low data rate voice CODECS for air traffic control applications
[DOT/FAA/CT-TN89/13] N89-27047
CONCRETE TECHNOLOGY INFORMATION ANALYSIS CENTER, VICKSBURG, MS.
Evaluation of barrier cable impact pad materials
[AD-A207554] N89-26864
CONNECTICUT UNIV., STORRS.
Endogenous hormonal and growth factor responses to heavy resistance exercise protocols
[AD-A208375] N89-27336
COORS PORCELAIN CO., GOLDEN, CO.
Compact ceramic heat exchangers
[PB89-173603] N89-26997
CORNELL UNIV., ITHACA, NY.
Adsorption and coadsorption of CO and NO on the Rh(100) surface: A theoretical analysis
[AD-A207323] N89-26835
CUMMINGS (ROBERT L.), LITCHFIELD, OH.
Performance estimates for the Space Station power system Brayton Cycle compressor and turbine
[NASA-CR-182263] N89-26903

D

DANISH METEOROLOGICAL INST., COPENHAGEN.
Distribution of auroral arcs during quiet geomagnetic conditions
[DMI-GEOPHYS-PAPERS-R-78] N89-27292
Brorfelde Geomagnetic Observatory: Magnetic results, 1986
[ISBN-87-7478-287-8] N89-27293
DANISH SPACE RESEARCH INST., LYNGBY.
The short-circuited fluxgate output current
[ISSN-0109-6605] N89-27069
DAYTON UNIV., OH.
Compressive properties of high performance polymeric fibers
[AD-A207271] N89-26998
KC-135R rumble investigation
[AD-A207532] N89-27464
DEFENSE ADVANCED RESEARCH PROJECTS AGENCY, ARLINGTON, VA.
Research in knowledge-based vision techniques for the autonomous land vehicle program
[AD-A208546] N89-26834
The structure of self-assembled monolayers of alkylsiloxanes on silicon: A comparison of results from ellipsometry and low-angle X-ray reflectivity
[AD-A208341] N89-27016
DEFENSE INTELLIGENCE AGENCY, WASHINGTON, DC.
Bibliography of Soviet laser developments, No. 92, November - December 1987
[AD-A207794] N89-27177
DELAWARE UNIV., NEWARK.
Modifiers in rhodium catalysts for carbon monoxide hydrogenation: Structure-activity relationships
[DE89-013802] N89-27028
Propagating solutions and far-field patterns for acoustic harmonic waves in a finite depth ocean
[PB89-180715] N89-27325
DEPARTMENT OF ENERGY, WASHINGTON, DC.
Quality in automation project for FY 88
[PB89-193296] N89-27040
Atmospheric carbon dioxide and the greenhouse effect
[DE89-012869] N89-27271
DEPARTMENT OF THE AIR FORCE, WASHINGTON, DC.
Hose reel monitor for inflight refueling system
[AD-D014054] N89-26836
Combination boundary layer control system for high altitude aircraft
[AD-D014075] N89-26837
Nozzle flap hinge joint
[AD-D014002] N89-26847
Back-up control system for f101 engine and its derivatives
[AD-D014051] N89-26848
Variable nozzle area turbine vane cooling
[AD-D014071] N89-26849
Compressor blade clearance measurement system
[AD-D014073] N89-26850
Afterburner flameholder construction
[AD-D014116] N89-26852
Nozzle flange attachment and sealing arrangement
[AD-D014123] N89-26853
Control surface dual redundant servomechanism
[AD-D014058] N89-26857
Brain o2 reserve limiter for high performance aircraft
[AD-D014137] N89-26858
Low loss radar window for reentry vehicle
[AD-D014045] N89-26882
Contemporary composite polar boss
[AD-D014074] N89-26897
Method to produce metal matrix composite articles from rich metastable-beta titanium alloys
[AD-D014064] N89-26907
Method to produce metal matrix composite articles from lean metastable beta titanium alloys
[AD-D014065] N89-26908
Method to produce titanium metal matrix composites with improved fracture and creep resistance
[AD-D014111] N89-26911
Automatic oxygen measuring system
[AD-D014003] N89-26931
Dispersion strengthened aluminum-base alloy
[AD-D014044] N89-26959
Method for making an integral titanium alloy article having at least two distinct microstructural regions
[AD-D014066] N89-26960
Method for refining microstructures of blended elemental titanium powder compacts
[AD-D014067] N89-26961
Method for developing ultrafine microstructures in titanium alloy castings
[AD-D014115] N89-26965
Process for assessing the effect of propellant strain on propellant burn rate
[AD-D014119] N89-27026
Dual frequency microstrip antenna
[AD-D014019] N89-27046
Window generator
[AD-D014068] N89-27048
Miniature high voltage solid state relay
[AD-D013979] N89-27070
Low noise crystal controlled oscillator
[AD-D014070] N89-27072
System for boundary layer control through pulsed heating of a strip heater
[AD-D013999] N89-27101
Surface cooling system
[AD-D014057] N89-27106
Solid state gas pressure sensor
[AD-D014105] N89-27139
Interferometric load sensor and strain gage
[AD-D014122] N89-27142
Variable area manifolds for ring mirror heat exchangers
[AD-D014050] N89-27163
High energy laser target plate
[AD-D014053] N89-27164
Static periodic field device for free electron laser
[AD-D014125] N89-27168
Self-locking outer air seal with full backside cooling
[AD-D013975] N89-27179
Vane platform sealing and retention means
[AD-D013980] N89-27180
Bearings fabricated from rapidly solidified powder and method
[AD-D014072] N89-27185
Anti-rotation guide bushing
[AD-D014079] N89-27186
Electromagnetic pulse rotary seal
[AD-D014080] N89-27187
Dual load path pin clevis joint
[AD-D014081] N89-27188
Bimetallic air seal for exhaust nozzles
[AD-D014106] N89-27189
Six degrees of freedom micromanipulator
[AD-D014113] N89-27190
Antenna shaft positioning device
[AD-D014120] N89-27191
Wideband electromagnetic damping of vibrating structures
[AD-D014069] N89-27208
Multichannel phase noise measurement system
[AD-D014056] N89-27461
Fiber optic rotary switching device
[AD-D013978] N89-27497
Optical mirror coated with organic superconducting material
[AD-D014047] N89-27499
Radio frequency plasma generator
[AD-D013990] N89-27514
Hybrid single crystal optic fibers by embedding
[AD-D013986] N89-27545
DEPARTMENT OF THE NAVY, ARLINGTON, VA.
The structure of self-assembled monolayers of alkylsiloxanes on silicon: A comparison of results from ellipsometry and low-angle X-ray reflectivity
[AD-A208341] N89-27016
DEPARTMENT OF THE NAVY, WASHINGTON, DC.
Cost-optimal state feedback controller for all-attitude gimbal system
[AD-D013972] N89-26845
Quality in automation project for FY 88
[PB89-193296] N89-27040
Method for calibrating a heat flux gauge
[AD-D013974] N89-27138
Laser dyes derived from bimanes
[AD-D013994] N89-27160
Low frequency structureborne vibration isolation mount
[AD-D014133] N89-27192
Efficient dynamic phasefront modulation system for free-space optical communications
[AD-D014128] N89-27503
DEUTSCHE FORSCHUNGSGEMEINSCHAFT, BONN (GERMANY, F.R.).
Space research in the Federal Republic of Germany (FRG), 1986 and 1987
[ETN-89-94427] N89-26874
DIRECTION DES RECHERCHES, ETUDES ET TECHNIQUES, PARIS (FRANCE).
Study of dispersion and penetration of tracer and pollutants in porous media and fractured rocks
[ETN-89-94806] N89-27277
DORNIER-WERKE G.M.B.H., FRIEDRICHSHAFEN (GERMANY, F.R.).
Drag prediction and analysis from CFD state-of-the-art in Germany N89-26819
DOUGLAS AIRCRAFT CO., INC., LONG BEACH, CA.
Composite transport wing technology development
[NASA-CR-178409] N89-26842
DRAPER (CHARLES STARK) LAB., INC., CAMBRIDGE, MA.
Advanced information processing system: Input/output system services
[NASA-CR-181874] N89-27413
DU PONT DE NEMOURS (E. I.) AND CO., AIKEN, SC.
An algorithm for symbolic dimensional analysis
[DE89-010409] N89-27363

E

EARTH SATELLITE CORP., CHEVY CHASE, MD.
An assessment of information demands for remote sensing and Geographic Information System technologies
[PB89-159313] N89-27233
ECONOMIC SYSTEMS ANALYSIS, INC., OAK RIDGE, TN.
Technology Master List data base management system, user's manual
[PB89-177802] N89-27590
EDGERTON, GERMESHAUSEN AND GRIER, INC., IDAHO FALLS, ID.
Electronic information delivery at the job site
[DE89-009726] N89-27350
EG AND G MOUND APPLIED TECHNOLOGIES, MIAMISBURG, OH.
An Auger sputter profiling study of nitrogen and oxygen ion implantation in two titanium alloys
[DE89-014734] N89-26987
EGAN GROUP, WASHINGTON, DC.
Study for advanced civil earth remote sensing system: Focused finance study. Volume 1: Executive summary
[PB89-163224] N89-27230
ENVIRONMENTAL PROTECTION AGENCY, ANNAPOLIS, MD.
Chesapeake Bay nonpoint source programs
[PB89-152037] N89-27265
ENVIRONMENTAL PROTECTION AGENCY, LAS VEGAS, NV.
GEO-EAS (Geostatistical Environmental Assessment Software) user's guide
[PB89-151252] N89-27261
ENVIRONMENTAL PROTECTION AGENCY, RESEARCH TRIANGLE PARK, NC.
Evaluation of a FTIR (Fourier Transform Infrared Spectrometer) mobile source measurement system
[PB89-180822] N89-27147
Concentrations and patterns of photochemical oxidants in the United States
[PB89-136683] N89-27258
Regional ozone modeling in the northeastern US: Selection of meteorological episodes
[PB89-136691] N89-27259
Comparison of modelled and measured tracer gas concentrations during the Across North America Tracer Experiment (ANATEX)
[PB89-136709] N89-27260
Climatology of temperature and precipitation variability in the United States
[PB89-165930] N89-27299

ENVIRONMENTAL PROTECTION AGENCY, WASHINGTON, DC.
Analytical procedures for environmental quality control, volume 1
[PB89-158604] N89-27266
ENVIRONMENTAL RESEARCH INST. OF MICHIGAN, ANN ARBOR.
Alaska collection SAR (Synthetic Aperture Radar) data summary
[AD-A208530] N89-27067
ESSCOR CORP., SOLANA BEACH, CA.
Dynamic simulation of a molten-salt solar receiver
[DE89-010556] N89-27244

F

FAIRCHILD REPUBLIC DIV., FARMINGDALE, NY.
Superplastic forming of aluminum, task C
[AD-A207282] N89-26962
FEDERAL AVIATION ADMINISTRATION, ATLANTIC CITY, NJ.
Loran C coverage in Alaska after dual rating Port Clarence
[AD-A196032] N89-26831
ILS/MLS collocation tests at Miami/Tamiami, Florida Airport
[NASA-CR-185715] N89-26832
An operational demonstration and flight test of the Microwave Landing System (MLS) at the Miami/Tamiami, Florida Airport
[DOT/FAA/CT-TN89/37] N89-26833
Evaluation of an updated design of an internally lighted wind cone
[DOT/FAA/CT-TN89/45] N89-26868
FEDERAL AVIATION ADMINISTRATION, WASHINGTON, DC.
Injuries to seat occupants of light airplanes
[AD-A207579] N89-26830
FEDERAL COMMUNICATIONS COMMISSION, WASHINGTON, DC.
Common carrier earth station database documentation
[PB89-186050] N89-27595
FERMI NATIONAL ACCELERATOR LAB., BATAVIA, IL.
ACP/R3000 processors in data acquisition systems
[DE89-014811] N89-27355
Machines for lattice gauge theory
[DE89-014815] N89-27400
Cosmic evolution of non-topological solitons, paper 1
[NASA-CR-185353] N89-27608
The cosmological constant problem
[DE89-013150] N89-27614
FLORIDA AGRICULTURAL AND MECHANICAL UNIV., TALLAHASSEE.
Meteorological database and synthesis for the Gulf of Mexico
[PB89-178222] N89-27311
FLORIDA UNIV., GAINESVILLE.
Frequency-domain transient analysis of silicon solar cells
[DE89-010555] N89-27243
Image algebra synthesis
[AD-A207257] N89-27425
FOERSVARETS FORSKINGSANSTALT, STOCKHOLM (SWEDEN).
Full coverage anti-G-suit and balanced pressure breathing
[PB89-174635] N89-27343
FOSTER-MILLER ASSOCIATES, INC., WALTHAM, MA.
Interface modified glass fiber/thermoplastic matrix composites
[AD-A207308] N89-26910
FREQUENCY ELECTRONICS, INC., MITCHEL AFB, NY.
Design, development and evaluation of a doubly rotated AK-cut quartz crystal
[AD-A207209] N89-27549
FUBA HANS KOLBE UND CO., BAD SALZDETFURTH (GERMANY, F.R.).
Development of a DFS (Deutsche Fernmeldesatellit) reception converter
[ETN-89-94629] N89-27065

G

GENERAL ATOMICS TECHNOLOGIES CORP., SAN DIEGO, CA.
Dispersed and periodic microstructures for magnetic and infrared absorbers
[AD-A207428] N89-27053
GENERAL DYNAMICS CORP., FORT WORTH, TX.
Advanced durability analysis. Volume 2: Analytical predictions, test results and analytical correlations
[AD-A207215] N89-26838
GENERAL ELECTRIC CO., SCHENECTADY, NY.
Development of elements of a high Tc superconducting cable
[AD-A208370] N89-27574
GEOCHEMICAL SERVICES, INC., TORRANCE, CA.
Depth profiles and bulk analysis of semiconductor materials using ICP mass spectroscopy with electrothermal atomization
[AD-A206974] N89-27548
GEOLOGICAL SURVEY, RESTON, VA.
Mafic and ultramafic xenoliths from volcanic rocks of the western United States
[PB89-124127] N89-27278
GEORGE MASON UNIV., FAIRFAX, VA.
Analysis and evaluation of technical data on the photochromic and non-linear optical properties of materials
[AD-A207275] N89-27000
GEORGIA INST. OF TECH., ATLANTA.
Fault tolerant software technology for distributed computer systems
[AD-A208329] N89-27405
GINER, INC., WALTHAM, MA.
Development of ternary alloy cathode catalysts for phosphoric acid fuel cells
[DE89-000926] N89-27250
GRUMMAN AEROSPACE CORP., BETHPAGE, NY.
CFD drag prediction for aerodynamic design
N89-26825

H

HARRIS CORP., MELBOURNE, FL.
Advanced modulation technology development for earth station demodulator applications
[NASA-CR-185126] N89-26880
HARVARD UNIV., CAMBRIDGE, MA.
The structure and reactivity of alkylsiloxane monolayers formed by reaction of alkyltrichlorosilanes on silicon substrates
[AD-A208267] N89-27011
The structure of self-assembled monolayers of alkylsiloxanes on silicon: A comparison of results from ellipsometry and low-angle X-ray reflectivity
[AD-A208341] N89-27016
HAWAII UNIV., HONOLULU.
Bandwidth efficient coding for error control
[NASA-CR-185836] N89-27062
HELSINKI UNIV. OF TECHNOLOGY, ESPOO (FINLAND).
The 14th Convention on Radio Science, Finnish National Committee of URSI held in Otaniemi (Finland) on October 17-18, 1988: Abstracts of papers
[PB89-145767] N89-27044
Complex vectors and dyadics for electromagnetists
[PB89-146443] N89-27045
Dynamics of double stimulated Brillouin scattering
[PB89-146369] N89-27513
HELSINKI UNIV. OF TECHNOLOGY, KYLMAELAE (FINLAND).
Solar microwave radiation maps measured at Metsaehovi Radio Research Station in 1982 - 1983
[PB89-154876] N89-27621

I

IIT RESEARCH INST., BARTLESVILLE, OK.
Thermodynamic equilibria in the biphenyl/hydrogen system (the power and limitations of group additivity estimations)
[DE89-000754] N89-26954
ILLINOIS INST. OF TECH., CHICAGO.
Theoretical studies in elementary particle physics
[DE89-012701] N89-27473
ILLINOIS UNIV., CHICAGO.
Electrochemical transport of manganese between the flux and the weld metal in submerged arc welding
[DE89-012419] N89-27193
Electrochemical reactions in submerged arc welding with SiO2-CaO-CaF2 fluxes with high and low silica contents
[DE89-012421] N89-27194
ILLINOIS UNIV., URBANA.
Fluids, gels and glasses under extreme conditions of pressure and temperature
[AD-A205292] N89-26927
Accuracy increase in waveform Gauss Seidel
[DE89-014812] N89-27437
Safety in numbers: The boundless errors of numerical computation
[DE89-014813] N89-27438
ILLINOIS UNIV., URBANA-CHAMPAIGN.
Synthesis and characterization of Group 4 organometal oxide complexes
[DE89-010944] N89-26932
Reconfiguration strategies in VLSI (Very Large Scale Integration) arrays and trees
[PB89-165468] N89-27071
Heuristic algorithms for stability testing polytopes of matrices
[PB89-160840] N89-27365
INSTITUT DE MECANIQUE DES FLUIDES DE LILLE (FRANCE).
Study of a turbulent boundary layer by laser plane visualization
[IMFL-88/33] N89-27124
Base wakes from two dimensional jets in subsonic flow with injection
[IMFL-86/20] N89-27125
INSTITUT FRANCO-ALLEMAND DE RECHERCHES, SAINT-LOUIS (FRANCE).
Dynamic measurements in combustible and detonable aerosols
[ISL-PU-306/86] N89-26957
Battery-driven miniature LDA system with semiconductor laser diode
[ISL-CO-214/88] N89-27176
INSTITUTE FOR COMPUTER APPLICATIONS IN SCIENCE AND ENGINEERING, HAMPTON, VA.
Inviscid spatial stability of a compressible mixing layer. Part 3: Effect of thermodynamics
[NASA-CR-181855] N89-27112
Absolute/convective instabilities and the convective Mach number in a compressible mixing layer
[NASA-CR-181861] N89-27113
Summary of research conducted at the Institute for Computer Applications in Science and Engineering in applied mathematics, numerical analysis and computer science
[NASA-CR-181858] N89-27348
Data traffic reduction schemes for Cholesky factorization on asynchronous multiprocessor systems
[NASA-CR-181863] N89-27349
Programming parallel architectures: The BLAZE family of languages
[NASA-CR-185826] N89-27362
Indirect addressing and load balancing for faster solution to Mandelbrot Set on SIMD architectures
[NASA-CR-181847] N89-27390
Multigrid method for stability problems
[NASA-CR-185825] N89-27420
INSTITUTE OF GAS TECHNOLOGY, CHICAGO, IL.
Dedicated low-pressure natural gas-fueled vehicle baseline assessment. Task 3 topical report on light-duty vehicles
[PB89-195820] N89-27604
INSTITUTO DE PESQUISAS ESPACIAIS, ITAJUBA (BRAZIL).
Formulation of numerical orbit propagation and time error correction
[INPE-4774-PRE/1443] N89-26875
Tropical circulation and the associated precipitation anomalies in two years of contrast
[INPE-4715-PRE/1395] N89-27315
An Apple-2 compatible program to draw maps containing oceanographic station positions buoy trajectories and the coastal margins of the Antarctic Peninsula and nearby islands
[INPE-4805-RPE/588] N89-27391
INSTITUTO DE PESQUISAS ESPACIAIS, SAO JOSE DOS CAMPOS (BRAZIL).
Study of jitter on the attitude motion of a spin stabilized satellite with two flexible solar panels
[INPE-4744-PRE/1418] N89-26884
Satellite attitude control analysis and design using linearizing transformations
[INPE-4772-PRE/1441] N89-26886
Performance comparison among several filters for the reducton of speckle noise in radar imagery
[INPE-4768-PRE/1437] N89-27055
Detection, acquisition and signal demodulation in a communication system with random access
[INPE-4779-RPE/581] N89-27061
SP-ATUS: An expert system for specifications of satellite imagery
[INPE-4754-PRE/1426] N89-27236
Amazon Forest wind and temperature profiles
[INPE-4724-PRE/1401] N89-27301
Natural language processing
[INPE-4449-TDL/314] N89-27366
Satellite image processing using symbolic structures of reduced vision conditions
[INPE-4638-TDL/337] N89-27367
Abstract data types in computer graphics and image processing
[INPE-4745-PRE/1419] N89-27381
Automatic treatment of natural language in processes in the acquistion of knowledge
[INPE-4737-PRE/1412] N89-27382

Temporal variability of water masers in the Southern Hemisphere
[INPE-4646-TDL/338] N89-27609

INSTITUTO DE PESQUISAS ESPACIAIS, SAO PAULO (BRAZIL).
An expert system for fault diagnosis in digital circuits
[INPE-4743-PRE/1417] N89-27085

Classification by maximum likelihood method of the massively parallel environment
[INPE-4765-PRE/1434] N89-27380

Implementation of an order filter and its applications in radar imagery (SAR)
[INPE-4749-PRE/1422] N89-27385

Applications of numerical models for elevation and integration with digital images
[INPE-4776-PRE/1445] N89-27392

INTEGRATED SYSTEMS, INC., PALO ALTO, CA.
Aircraft flight test trajectory control
[NASA-CR-4161] N89-27416

INTERNATIONAL BUSINESS MACHINES CORP., SAN JOSE, CA.
Optical detection and spectroscopy of single molecules in a solid
[AD-A207594] N89-26940

INTERNATIONAL CENTRE FOR THEORETICAL PHYSICS, TRIESTE (ITALY).
MHD forced and free convection boundary layer flow near the leading edge
[DE88-705974] N89-26812

Analysis of the wind data and estimation of the resultant air concentration rates
[DE88-705980] N89-27296

Use of the Fox derivatives in the solution of the word problem for groups
[DE88-705978] N89-27421

Model for hot electron phenomena: Theory and general results
[DE88-705986] N89-27544

Black holes in closed universes
[PB89-170039] N89-27610

IOWA STATE UNIV. OF SCIENCE AND TECHNOLOGY, AMES.
A dual potential formulation of the Navier-Stokes equations
[NASA-CR-185098] N89-27111

Partial support of the 3rd International Laser Science Conference held in Atlantic City, New Jersey on 1-4 November 1987
[AD-A206812] N89-27161

IOWA UNIV., IOWA CITY.
Synthesis of novel fluorinated phosphonic and phosphinic acid electrolytes for phosphoric acid fuel cells
[PB89-194120] N89-27086

ISTITUTO NAZIONALE DI FISICA NUCLEARE, ROME (ITALY).
On the multiplicity and symmetries of the bifurcation branching point in the square clamped plate
[PREPRINT-604] N89-27224

Covariance properties of the multiquark Hamiltonian in the constituent quark model
[NOTA-INTERNA-920] N89-27489

J

JAPAN METEOROLOGICAL AGENCY, TOKYO.
Implementing the Simple Biosphere Model (SiB) in a general circulation model: Methodologies and results
[NASA-CR-185509] N89-27288

JET PROPULSION LAB., CALIFORNIA INST. OF TECH., PASADENA.
Atmospheric propagation issues relevant to optical communications
[NASA-CR-185718] N89-27281

JIANGXI NORMAL UNIV., NANCHANG (CHINA).
Nonresonant interaction of a three-level atom with cavity fields. Part 4: Atomic dipole moment and squeezing effects
[AD-A206788] N89-27470

JOINT INST. FOR NUCLEAR RESEARCH, DUBNA (USSR).
Transient heat transfer into superfluid helium under confined conditions
[DE88-706312] N89-27109

Quantum and thermodynamic fluctuations in the degenerate schematic model of the finite temperature random phase approximation
[DE88-706310] N89-27580

K

KAMAN SCIENCES CORP., COLORADO SPRINGS, CO.
Microwave hardening technology development program
[AD-A207535] N89-27076

KANSAS STATE UNIV., MANHATTAN.
Computational techniques in gamma-ray Skyshine analysis
[DE89-010156] N89-27282

KANSAS UNIV. CENTER FOR RESEARCH, INC., LAWRENCE.
Model-based parameter estimation in electromagnetic computer modeling
[AD-A207399] N89-27052

KATHOLIEKE UNIVERSITEIT, NIJMEGEN (NETHERLANDS).
The photoacoustic effect, refined and applied to biological problems
[PB89-153597] N89-27263

KENTUCKY UNIV., LEXINGTON.
Laser spectroscopy and dynamics of combustion intermediates
[DE89-014498] N89-26956

KEURING VAN ELECTROTECHNISCHE MATERIALEN N.V., ARNHEM (NETHERLANDS).
Analysis of human-error sequences with fault trees
[PB89-147631] N89-27422

KRS REMOTE SENSING, LANDOVER, MD.
Study for an advanced civil earth remote sensing system. Volume 1: Executive summary
[PB89-163257] N89-27231

Study for an advanced civil earth remote sensing system. Volume 2: Market and financial assessment
[PB89-163265] N89-27232

L

LAWRENCE LIVERMORE NATIONAL LAB., CA.
Detonability of hydrocarbon fuels in air
[DE89-008801] N89-26926

Thin pulse shock initiation characterization of extrusion-cast explosives: Revision
[DE89-008029] N89-27027

Radiation from waves guided by nonuniform active surfaces
[DE89-012286] N89-27057

Proceedings of the Switched Power Workshop: Power Supply Working Group
[DE89-012293] N89-27077

Computer code prediction of picosecond voltage switching and TEM wave generation in air gas avalanche switches
[DE89-013778] N89-27084

Numerical studies of shock wave structure sensitivity to interactions with turbulent fields
[DE89-012288] N89-27110

Sensors for in situ monitoring of elastic properties
[DE89-012795] N89-27145

An instantaneous CCN (Cloud Condensation Nucleus) spectrometer
[DE89-014807] N89-27150

Passive optical losses in laser glass
[DE89-013784] N89-27172

DYNA3D user's manual: (Nonlinear Dynamic Analysis of Structures in Three Dimensions), revision 5
[DE89-014304] N89-27222

Earth sciences
[DE89-013344] N89-27228

Introduction to background materials for Workshop No. 1: Global climate change and its effects on California
[DE89-013381] N89-27272

Preventing depletion of stratospheric ozone: Implications on future aircraft emissions, revision 1
[DE89-013779] N89-27273

Global environmental effects of impact-generated aerosols: Results from a general circulation model, revision 1
[DE89-014179] N89-27276

Lightning: Understanding it and protecting systems from its effects
[DE89-012796] N89-27308

Cray-to-sun prototype
[DE89-013087] N89-27358

Monotone piecewise cubic data fitting
[DE89-006742] N89-27386

A MACSYMA package for the generation and manipulation of Chebyshev series
[DE89-011404] N89-27436

A test of Newton's Law of Gravity using the BREN Tower, Nevada
[DE89-013262] N89-27454

Molecules in intense laser fields
[DE89-013807] N89-27479

Pulsed lower-hybrid wave penetration in reactor plasmas
[DE89-013260] N89-27521

Modeling of LH current drive in self-consistent elongated tokamak MHD equilibria
[DE89-013263] N89-27522

A hydrid 3 Gs/s, 6-bit digital to analog converter
[DE89-012302] N89-27552

Photoelectronic properties of low temperature GaAs grown on silicon and GaAs substrates by MBE
[DE89-013148] N89-27557

Technical Abstracts, 1988
[DE89-012811] N89-27591

Use of the EGRET (Energetic Gamma-Ray Experiment Telescope) in studies of the origin of the cosmic radiation
[DE89-013785] N89-27630

LEHIGH UNIV., BETHLEHEM, PA.
Nanostructure and defect chemistry of relaxor ferro electrics
[AD-A207217] N89-26933

Theory of aggregate defects in silicon
[AD-A207273] N89-26999

LETTERMAN ARMY INST. OF RESEARCH, SAN FRANCISCO, CA.
Meridian variations in spectral dark adaptation
[AD-A207248] N89-27331

LOCKHEED MISSILES AND SPACE CO., HUNTSVILLE, AL.
Space Shuttle Main Engine structural analysis and data reduction/evaluation. Volume 7: High pressure fuel turbo-pump third stage impeller analysis
[NASA-CR-183670] N89-26894

LOCKHEED MISSILES AND SPACE CO., PALO ALTO, CA.
Measurement of the time-dependent distribution of ionization states in an argon plasma from a Mach-10 jet
[DE89-014699] N89-27526

LOS ALAMOS NATIONAL LAB., NM.
SiC-MoSi composites
[DE89-013656] N89-26923

Polycrystal plastic, as applied to the problem of in-plane anisotropy in rolled cubic metals
[DE89-011181] N89-26983

Radiation evaluation of several complex very large scale integration circuits
[DE89-007985] N89-27090

Recent experiments with the free-electron laser at Los Alamos
[DE89-013469] N89-27171

Dynamic plastic buckling of spherical shells during collapse
[DE89-006543] N89-27217

Modeling of the angular reflectance of an artificial plant canopy near the retroreflection peak in the optical regime
[DE89-011174] N89-27239

Computer simulations of explosive volcanic eruptions
[DE89-014024] N89-27290

The dynamical behavior of classifier systems
[DE89-009407] N89-27383

XCL: A family of programming lanquage-based shell s
[DE89-013442] N89-27388

Directed energy weapons/en dash/lasers: Ground- and space-based systems
[DE89-012804] N89-27452

Momentum distributions: An overview
[DE89-012617] N89-27453

Final state effects in liquid He4: An experimental test
[DE89-012615] N89-27472

Physics with ETA mesons
[DE89-012582] N89-27478

Recent progress in the Los Alamos KrF Program
[DE88-016235] N89-27493

Safety testing program for the Galileo mission radioisotope thermoelectric generator
[DE89-011192] N89-27494

The magnetic topology of the plasmoid flux rope in a MHD simulation of magnetotail reconnection
[DE89-012621] N89-27529

Study of atomic physics and population inversions with plasma focus
[DE89-014282] N89-27532

Radiative collapse of a Bennett-relaxed z-pinch
[DE89-014290] N89-27533

Wear and friction of thin film high temperature oxide superconductors
[DE89-009397] N89-27543

High-frequency cavity applications and measurements of high-temperature superconductors
[DE89-013467] N89-27560

The response of single crystal and polycrystal nickel to quasistatic and shock deformation
[DE89-011168] N89-27564

Anomalous temperature dependence of Cu NMR line width and magnetization in YBa2Cu3O(7-delta)
[DE89-014291] N89-27565
O-17 NMR study of YBa2Cu3O(7-delta)
[DE89-014292] N89-27566
Nuclear relaxation rates at copper and oxygen sites in YBa2Cu3O7
[DE89-014308] N89-27567
Characterization of lunar ilmenite resources
[DE89-013455] N89-27618
Spectra of crab-like pulsars: A GRO perspective
[DE89-013461] N89-27628

M

MAGNAVOX GOVERNMENT AND INDUSTRIAL ELECTRONICS CO., MAHWAH, NJ.
MM and T for linear resonant cooler, volume 2
[AD-A207236] N89-27073
MANCHESTER UNIV. (ENGLAND).
A model for transition by attachment-line contamination and an examination of cross-flow instability in 3-D boundary layers
[AERO-REPT-8804] N89-27108
MARYLAND UNIV., COLLEGE PARK.
Transient cooling of a hot surface by droplets evaporation
[PB89-161897] N89-27100
Free electron lasers with small period wigglers
[DE89-014715] N89-27173
An approach for constructing families of homogenized equations for periodic media. 1: An integral representation and its consequences
[AD-A207572] N89-27427
An approach for constructing families of homogenized equations for periodic media. 2: Properties of the kernel
[AD-A207573] N89-27428
The h-p version of the finite element method parabolic equations. Part 2: The h-p version in time
[AD-A207575] N89-27429
Macromolecular calculations for the XTAL system of crystallographic programs
[AD-A208272] N89-27572
Equilibrium of solar coronal arcades
[AD-A207311] N89-27622
MASSACHUSETTS INST. OF TECH., CAMBRIDGE.
Non-polymeric binders for ceramic powders: Utilization of neutral and ionic species derived from decaborane(14)
[AD-A208338] N89-27015
Synthesis and optical properties of a new class of polyamides containing reactive diacetylene groups
[AD-A208752] N89-27021
Thermal and mechanical properties of polyurethane-diacetylene segmented copolymers. Part 1: Molecular weight and annealing effects
[AD-A208753] N89-27022
Thermal and mechanical properties of polyurethane-diacetylene segmented copolymers. Part 2: Effects of diacetylene cross-polymerization
[AD-A208754] N89-27023
Autonomous underwater systems for survey operations
[PB89-187397] N89-27041
Theoretical analysis of microwave and millimeter wave integrated circuits based on magnetic films
[AD-A207508] N89-27074
Easily testable PLA-based finite state machines
[AD-A208371] N89-27098
Measurement of wall shear and wall pressure downstream of a honeycomb boundary layer manipulator
[AD-A208297] N89-27132
Implementation indices (1975-1979), volume 1
[AD-A207609] N89-27354
Waves and instabilities in nonneutral plasmas
[DE89-012403] N89-27515
Superconductivity and magnetism in layered materials
[AD-A208487] N89-27576
MASSACHUSETTS UNIV., AMHERST.
Lagrangian turbulence near walls: Structures and mixing in admissible model flows
[AD-A208466] N89-27135
MAX-PLANCK-INST. FUER PHYSIK UND ASTROPHYSIK, MUNICH (GERMANY, F.R.).
Activities of the Werner-Heisenberg Institute of Physics
[ISSN-0173-6256] N89-27481
MAX-PLANCK-INST. FUER PLASMAPHYSIK, GARCHING (GERMANY, F.R.).
Low-noise cable for diagnostics, control and instrumentation of the ASDEX tokamak fusion experiment
[IPP-III/67] N89-27094
Influence of particle collisions on the characteristics of H-like ion emission due to charge exchange reactions with fast atoms
[IPP-III/142] N89-27480
On bootstrap currents in toroidal systems
[IPP-2/297] N89-27536
A new version of the full-wave ICRH code FISIC for plasmas with noncircular flux surfaces
[IPP-5/25] N89-27537
Integral constitutive relation for the investigation of ion Bernstein waves in non-homogeneous plasmas
[IPP-5/27] N89-27538
On the economic prospects of nuclear fusion with tokamaks
[IPP-6/271] N89-27539
Radio frequency plasma heating and current drive
[IPP-6/278] N89-27540
Dynamics of decaying two-dimensional magnetohydrodynamic turbulence
[IPP-6/279] N89-27541
MAX-PLANCK-INSTITUT FUER STROEMUNGSFORSCHUNG, GOETTINGEN (GERMANY, F.R.).
Generation of underwater sound pulses, cavitation and shear waves with hydraulic hammer
[MPIS-8/1988] N89-27122
Construction of differential equations from experimental data of Karman vortex streets
[MPIS-11/1988] N89-27127
MCDONNELL AIRCRAFT CO., SAINT LOUIS, MO.
Feasibility and benefits of laminar flow control on supersonic cruise airplanes
[NASA-CR-181817] N89-26841
MCDONNELL-DOUGLAS CORP., LONG BEACH, CA.
Feasibility and benefits of laminar flow control on supersonic cruise airplanes
[NASA-CR-181817] N89-26841
MCDONNELL-DOUGLAS RESEARCH LABS., SAINT LOUIS, MO.
The structure of Normal-Shock/Turbulent-Boundary-Layer interactions modified by mass removal
[AD-A208402] N89-27134
MESSERSCHMITT-BOELKOW-BLOHM G.M.B.H., BREMEN (GERMANY, F.R.).
Electrical primary flight control system (fly by wire). Flight control systems of new technology
[MBB-UT-122/88] N89-26862
Columbus Logistics Program
[MBB-UO-0039/88-PUB] N89-26890
MESSERSCHMITT-BOELKOW-BLOHM G.M.B.H., OTTOBRUNN (GERMANY, F.R.).
Modeling of liquid sloshing effects in multi body systems
[MBB-UK-0024/88-PUB] N89-26891
MICHIGAN UNIV., ANN ARBOR.
Synthesis of resistive tapers to control scattering patterns of strips
[AD-A207211] N89-27049
Observing primeval galaxies and dark matter with LAIRTS
[AD-A208285] N89-27606
Detection of very high energy gamma-rays from the Crab nebula
[DE89-011840] N89-27627
MIDWEST RESEARCH INST., GOLDEN, CO.
Development of a second-generation, video-based luminance mapper for daylighting research
[DE89-000850] N89-27143
High-efficiency, large-area CdTe panels
[DE89-000891] N89-27242
Ocean Energy Program summary. Volume 2: Research summaries, fiscal year 1988
[DE89-000859] N89-27248
Yaw dynamics of horizontal axis wind turbines
[DE89-000886] N89-27249
The impact of solar radiation resources on the siting of solar thermal power plants
[DE89-000839] N89-27252
Wind power: Today's energy option
[DE89-000876] N89-27253
MILETUS ASSOCIATES, INC., ALBUQUERQUE, NM.
Film annotation system for a space experiment
[NASA-CR-185114] N89-27152
MINNESOTA UNIV., MINNEAPOLIS.
High temperature solar electrothermal processing
[AD-A207555] N89-27246
MISSOURI UNIV., ROLLA.
Dynamics of surface bound polymers and coupling agents
[AD-A208747] N89-27020
Collision processes of interest in MFE plasma research
[DE89-013681] N89-27524
MITRE CORP., MCLEAN, VA.
Spectra of surface waves
[AD-A208482] N89-27326
MORTON THIOKOL, BRIGHAM CITY, UT.
Field joint protection system rain qualification test report
[NASA-CR-183702] N89-26901
MULTIPOINT COMMUNICATIONS CORP., SUNNYVALE, CA.
Programmable rate modem utilizing digital signal processing techniques
[NASA-CR-185124] N89-26879

N

NAGOYA UNIV. (JAPAN).
Limiter H-modes in the JIPP T-IIU tokamak
[IPPJ-898] N89-27511
Improved confinement regimes in JIPP T-IIU
[IPPJ-909] N89-27527
Stochasticity and symmetry of the standard map
[IPPJ-910] N89-27528
NATIONAAL INST. VOOR KERNFYSICA EN HOGE ENERGIEFYSICA, AMSTERDAM (NETHERLANDS).
The sl (1/1;R)-cohomologies in BRST-Gupta-Bleuler quantization
[NIKHEF-H/88-17] N89-27578
NATIONAL ACADEMY OF SCIENCES - NATIONAL RESEARCH COUNCIL, WASHINGTON, DC.
Industrial applications of the microgravity environment
[NASA-CR-181516] N89-27034
Ergonomic Models of Anthropometry, Human Biomechanics and Operator-Equipment Interfaces
[NASA-CR-185720] N89-27344
Submarine air quality: Monitoring the air in submarines. Health effects in divers of breathing submarine air under hyperbaric conditions
[PB89-174213] N89-27345
Pacing the US magnetic fusion program
[DE89-012959] N89-27519
Science and technology advice in the White House: Recommendations for President-Elect George Bush
[PB89-169817] N89-27600
NATIONAL AERONAUTICS AND SPACE ADMINISTRATION, WASHINGTON, DC.
The best we can be
[NASA-TM-101781] N89-26873
The NASA low thrust propulsion program
[NASA-TM-102065] N89-26895
NATIONAL AERONAUTICS AND SPACE ADMINISTRATION. AMES RESEARCH CENTER, MOFFETT FIELD, CA.
Sensor development programs at NASA Ames Research Center
[NASA-TM-102217] N89-26808
Experimental program for real gas flow code validation at NASA Ames Research Center
[NASA-TM-100093] N89-26816
Computational fluid dynamics drag prediction: Results from the Viscous Transonic Airfoil Workshop
N89-26824
Method for experimental determination of flutter speed by parameter identification
[NASA-TP-2923] N89-26844
A review of high-speed, convective, heat-transfer computation methods
[NASA-TP-2914] N89-27116
Hypervelocity atmospheric flight: Real gas flow fields
[NASA-TM-101055] N89-27117
A three-node C deg element for analysis of laminated composite sandwich shells
[NASA-TM-4125] N89-27213
A direct procedure for interpolation on a structured curvilinear two-dimensional grid
[NASA-TM-102213] N89-27433
NATIONAL AERONAUTICS AND SPACE ADMINISTRATION. GODDARD SPACE FLIGHT CENTER, GREENBELT, MD.
Flow fields of low pressure vent exhausts
[NASA-TM-100738] N89-26902
Fracture toughness of SiC/Al metal matrix composite
[NASA-TM-100745] N89-26918
Altimetric system: Earth observing system. Volume 2h: Panel report
[NASA-TM-89722] N89-27229
Geodetic measurement of deformation in California
[NASA-TM-100732] N89-27279
Attitude angle effects on Nimbus-7 Scanning Multichannel Microwave Radiometer radiances and geophysical parameter retrievals
[NASA-TM-4132] N89-27289
The 1989 Airborne Arctic Stratospheric Expedition Nimbus-7 TOMS data atlas
[NASA-RP-1227] N89-27302

A graphics package for meteorological data, version 1.5
[NASA-TM-100742] N89-27314
Geodetic precession or dragging of inertial frames
[NASA-TM-100744] N89-27456
Commentary on interstellar matter associated with 18 open clusters
[NASA-RP-1229] N89-27612

NATIONAL AERONAUTICS AND SPACE ADMINISTRATION. LANGLEY RESEARCH CENTER, HAMPTON, VA.

Wind-tunnel investigation of aerodynamic characteristics and wing pressure distributions of an airplane with variable-sweep wings modified for laminar flow
[NASA-TM-4124] N89-26810
A procedure for computing surface wave trajectories on an inhomogeneous surface
[NASA-TP-2929] N89-26811
Aerodynamic parameters of an advanced fighter aircraft estimated from flight data. Preliminary results
[NASA-TM-101631] N89-26861
Two-stage reusable launch system utilizing a winged core vehicle and glideback boosters
[NASA-TM-101513] N89-26878
Alternate space station freedom configuration considerations to accommodate solar dynamic power
[NASA-TM-101603] N89-26888
Flexible backbone aromatic polyimide adhesives
[NASA-TM-100631] N89-27001
Solutions of differential equations with regular coefficients by the methods of Richmond and Runge-Kutta
[NASA-TM-101609] N89-27060
CWG: A FORTRAN program for mutual coupling in a planar array of circular waveguide-fed apertures
[NASA-TM-101614] N89-27063
Thermal enclosures for electronically scanned pressure modules operating in cryogenic environments
[NASA-TM-101635] N89-27151
Structural analysis of a thermal insulation retainer assembly
[NASA-TM-101580] N89-27212
Stability and dynamic analysis of a slender column with curved longitudinal stiffeners
[NASA-TM-101636] N89-27215
Reduction of blade-vortex interaction noise using higher harmonic pitch control
[NASA-TM-101624] N89-27465
Noise radiation characteristics of the Westinghouse WWG-0600 (600kW) wind turbine generator
[NASA-TM-101576] N89-27467
Rotation of images by scan mirrors
[NASA-TM-101628] N89-27504

NATIONAL AERONAUTICS AND SPACE ADMINISTRATION. LEWIS RESEARCH CENTER, CLEVELAND, OH.

NASA's Chemical Transfer Propulsion Program for Pathfinder
[NASA-TM-102298] N89-26876
Satellite relocation by tether deployment
[NASA-TM-101992] N89-26877
Photovoltaic module on-orbit assembly for Space Station Freedom
[NASA-TM-102297] N89-26887
Development of a high power microwave thruster, with a magnetic nozzle, for space applications
[NASA-TM-102321] N89-26904
Electric propulsion options for 10 kW class earth space missions
[NASA-TM-102337] N89-26906
Tailoring of composite links for optimal damped elasto-dynamic performance
[NASA-TM-102094] N89-26912
Unified micromechanics of damping for unidirectional fiber reinforced composites
[NASA-TM-102107] N89-26919
Metal matrix composite micromechanics: In-situ behavior influence on composite properties
[NASA-TM-102302] N89-26924
Fatigue crack growth study of SCS6/Ti-15-3 composite
[NASA-TM-102332] N89-26989
Measurements of complex permittivity of microwave substrates in the 20 to 300 K temperature range from 26.5 to 40.0 GHz
[NASA-TM-102123] N89-27038
High speed corner and gap-seal computations using an LU-SGS scheme
[NASA-TM-102138] N89-27103
Stability of a rigid rotor supported on oil-film journal bearings under dynamic load
[NASA-TM-102309] N89-27114
Calculation of turbulence-driven secondary motion in ducts with arbitrary cross section
[NASA-TM-102142] N89-27115
Arcjet cathode phenomena
[NASA-TM-102099] N89-27121
Optimum interface properties for metal matrix composites
[NASA-TM-102295] N89-27223
Diamondlike carbon protective coatings for optical windows
[NASA-TM-102111] N89-27506
Lunar production of solar cells
[NASA-TM-102102] N89-27619
Solar radiation on Mars
[NASA-TM-102299] N89-27623

NATIONAL AERONAUTICS AND SPACE ADMINISTRATION. MARSHALL SPACE FLIGHT CENTER, HUNTSVILLE, AL.

Stress corrosion study of PH13-8Mo stainless steel using the Slow Strain Rate Technique
[NASA-TP-2934] N89-26976
A new state reconstructor for digital controls systems using weighted-average measurements
[NASA-TP-2936] N89-27039
Weld stresses beyond elastic limit: Materials discontinuity
[NASA-TP-2935] N89-27214
Atmospheric environment for Space Shuttle (STS-27) launch
[NASA-TM-100370] N89-27316

NATIONAL AEROSPACE LAB., AMSTERDAM (NETHERLANDS).

Aircraft drag prediction for transonic potential flow
N89-26822

NATIONAL AEROSPACE LAB., TOKYO (JAPAN).

The conceptional design study of USB powered lift aircrafts in FY 1986
[NAL-TR-958] N89-26835
LH sub 2/LO sub 2 rocket engine with solar energy
[NAL-TR-992] N89-26893

NATIONAL BUREAU OF STANDARDS, BOULDER, CO.

Development of near-field test procedures for communication satellite antennas, phase 1, part 2
[PB89-156152] N89-27043
Group index and time delay measurements of a standard reference fiber
[PB89-189179] N89-27457
System for measuring optical waveguide intensity profiles
[PB89-188593] N89-27507

NATIONAL BUREAU OF STANDARDS, GAITHERSBURG, MD.

Structural reliability and damage tolerance of ceramic composites for high-temperature applications
[PB89-156350] N89-26994

NATIONAL CENTER FOR ATMOSPHERIC RESEARCH, BOULDER, CO.

Evolution and structure of the bow echo/microburst events
[PB89-174767] N89-27309

NATIONAL CHENG KUNG UNIV., TAINAN (TAIWAN).

Analytical procedures for environmental quality control, volume 1
[PB89-158604] N89-27266

NATIONAL GEOPHYSICAL DATA CENTER, BOULDER, CO.

Solar-geophysical data number 535, part 1. Data for February, January 1989, and late data
[PB89-185987] N89-27624
Solar-geophysical data number 535, part 2. Data for September 1988, and miscellaneous
[PB89-185995] N89-27625

NATIONAL INST. FOR OCCUPATIONAL SAFETY AND HEALTH, MORGANTOWN, WV.

A model of human reaction time to dangerous robot arm movements
[PB89-186522] N89-27339

NATIONAL INST. OF STANDARDS AND TECHNOLOGY, BOULDER, CO.

Fracture behavior of a pressure vessel steel in the ductile-to-brittle transition region
[PB89-189195] N89-26977

NATIONAL INST. OF STANDARDS AND TECHNOLOGY, GAITHERSBURG, MD.

Composites databases for the 1990's
[PB89-180376] N89-26914
Technical activities 1988, Surface Science Division
[PB89-161889] N89-26928
Technical activities 1986-1988, Molecular Spectroscopy Div.
[PB89-175418] N89-26942
Institute for Materials Science and Engineering, Polymers: Technical activities 1988
[PB89-166094] N89-26993
Structural reliability and damage tolerance of ceramic composites for high-temperature applications
[PB89-156368] N89-26995
Toughening mechanisms in ceramic composites
[PB89-162606] N89-26996
Advanced ceramics: A critical assessment of wear and lubrication
[PB89-188569] N89-27005
Mechanical property enhancement in ceramic matrix composites
[PB89-189138] N89-27007
Quality in automation project for FY 88
[PB89-193296] N89-27040
Emerging technologies in electronics and their measurement needs
[PB89-189245] N89-27078
Center for Electronics and Electrical Engineering Technical Progress Bulletin covering center programs, October to December 1988 with 1989 CEEE events calender
[PB89-193270] N89-27087
An approach to accurate X-ray mask measurements in a scanning electron microscope
[PB89-172555] N89-27137
Interactions between the National Institute of Standards and Technology and the American Society of Mechanical Engineers
[PB89-172563] N89-27182
Hybrid structures for simple computer performance estimates
[PB89-189161] N89-27356
Small Computer System Interface (SCSI) command system: Software support for control of small computer system interface devices
[PB89-151815] N89-27389
NIST (National Institute of Standards and Technology) research reports, March 1989
[PB89-189310] N89-27594
National Engineering Laboratory's 1989 report to the National Research Council's Board on Assessment of NIST (National Institute of Standards and Technology) programs
[PB89-189294] N89-27602

NATIONAL OCEANIC AND ATMOSPHERIC ADMINISTRATION, BOULDER, CO.

Observations of atmospheric emission and attenuation at 20.6, 31.65 and 90 GHz by a ground-based radiometer
[NASA-CR-185719] N89-27257
Trace gases in and over the West Pacific and East Indian Oceans during the El Nino-southern oscillation event of 1987: A report of GMCC (Geophysical Monitoring for Climatic Change) data collected on the second Soviet-American Gas and Aerosol Experiment (SAGA 2)
[PB89-159685] N89-27280
Dual-channel microwave radiometer for airborne meteorological applications
[PB89-159693] N89-27298
Procedural guide for the retrieval of dropsize distributions in water clouds from ground-based clear-air-sensing Doppler radar observations
[PB89-152474] N89-27300
EIGEN: A program to compute eigenrays from HARPA (Hamiltonian Acoustic Ray-Tracing Program for the Atmosphere)/HARPO (Hamiltonian Acoustic Ray-Tracing Program for the Ocean) raysets
[PB89-165781] N89-27460
Environmental Research Laboratories publication abstracts, FY 1988
[PB89-152656] N89-27589
Space Environment Laboratory
[PB89-159602] N89-27607

NATIONAL OCEANIC AND ATMOSPHERIC ADMINISTRATION, LAS VEGAS, NV.

Weather predictions and surface radiation estimates for Project BUGGY 1
[DE89-014687] N89-27318

NATIONAL OCEANIC AND ATMOSPHERIC ADMINISTRATION, MIAMI, FL.

Joint CGS-AOML (Charting and Geodetic Service-Atlantic Oceanographic and Meteorological Laboratory) acoustical bottom echo-formation research. 2: Field experiment results and recommendations for echo-sounder design
[PB89-152417] N89-27322

NATIONAL PHYSICAL LAB., TEDDINGTON (ENGLAND).

Dynamic mechanical investigations of LLDPE/PC blends
[NPL-DMA(A)-177] N89-27010
The least squares solution of linear equations with block-angular observation matrix
[NPL-DITC-139/89] N89-27444

NATIONAL SEVERE STORMS FORECAST CENTER, KANSAS CITY, MO.

Verification of severe local storm forecasts issued by the National Severe Storms Forecast Center, 1987
[PB89-159719] N89-27297

NATIONAL TECHNICAL UNIV., ATHENS (GREECE).

Some results on flow calculations involving drag prediction
N89-26820

NATIONAL TELECOMMUNICATIONS AND INFORMATION ADMINISTRATION, BOULDER, CO.
Millimeter-wave propagation characteristics and channel performance for urban-suburban environments
[PB89-180251] N89-27058
NATIONAL WEATHER SERVICE, FORT WORTH, TX.
Intense heat checklist based on the 1980 heat wave
[PB89-181200] N89-27312
NATIONAL WEATHER SERVICE, WASHINGTON, DC.
Proceedings of the 13th Annual Climate Diagnostics Workshop held at Cambridge, Massachusetts on October 31 - November 4, 1988
[PB89-178115] N89-27310
NAVAL AIR DEVELOPMENT CENTER, WARMINSTER, PA.
Aircraft color displays: Chromaticity and luminance requirements
[AD-A206786] N89-26828
NAVAL AIR PROPULSION TEST CENTER, TRENTON, NJ.
Statistics on aircraft gas turbine engine rotor failures that occurred in US commercial aviation during 1983
[AD-A207592] N89-26851
NAVAL ENVIRONMENTAL PREDICTION RESEARCH FACILITY, MONTEREY, CA.
The international TOVS (Tiros Operational Vertical Sounder) processing package: An evaluation
[AD-A207548] N89-27306
NAVAL OCEAN RESEARCH AND DEVELOPMENT ACTIVITY, BAY SAINT LOUIS, MS.
GEOSAT altimeter sea-ice mapping
[AD-A207391] N89-27234
NAVAL OCEANOGRAPHY COMMAND CENTER/JOINT TYPHOON WARNING CENTER, FPO SAN FRANCISCO, CA.
Tropical cyclone report, 1988
[AD-A207206] N89-27303
NAVAL POSTGRADUATE SCHOOL, MONTEREY, CA.
Estimating and explaining the production cost of high-technology systems: The case of military aircraft
[AD-A208391] N89-26809
Feasibility study for enhanced lateral control of the P-3C aircraft
[AD-A208461] N89-26863
An investigation into the use of an existing shock tube as a driver for a hypersonic shock tunnel
[AD-A208483] N89-26872
Spin stabilization of the ORION satellite using a thruster attitude control system with optimal control considerations
[AD-A208484] N89-26892
Effect of heating rate to test temperature on superplastic response in an Al-8 percent Mg-1 percent Li-0.2 percent Zr alloy
[AD-A208462] N89-26990
A microstructural investigation of the shear distortions and energetics of motions observed in an aged high damping 53Cu-45Mn-2Al alloy
[AD-A208467] N89-26991
Thermomechanical processing of aluminum alloy 2090 for superplasticity
[AD-A208764] N89-26992
On capture effect of FM demodulators
[AD-A208479] N89-27066
Development of a system model and Least Mean Square (LMS) filter for the Naval Postgraduate School (NPS) Infrared Search and Target Designation System (IRSTD)
[AD-A208536] N89-27068
Implementation of a design for testability strategy using the Genesil silicon compiler
[AD-A208458] N89-27099
Synoptic forcing of East Asian cold surges
[AD-A208765] N89-27321
A language translator for a computer aided rapid prototyping system
[AD-A208358] N89-27406
A dynamic scheduler for a computer aided prototyping system
[AD-A206389] N89-27407
Algorithms for computer aided design of digital filters
[AD-A208485] N89-27410
Constant access systems: A general framework for greedy optimization on stochastic networks
[AD-A207525] N89-27448
NAVAL RESEARCH LAB., WASHINGTON, DC.
Collisionless tearing instability of a bi-Maxwellian neutral sheet with exact particle orbits
[AD-A207310] N89-27286
Navy tethered balloon measurements made during the Fire marine stratocu IFO (Intensive Field Operation)
[AD-A207312] N89-27304
Frequency division multiplexing of interferometric sensor arrays
[AD-A208448] N89-27510
Equilibrium of solar coronal arcades
[AD-A207311] N89-27622
NAVAL SHIP RESEARCH AND DEVELOPMENT CENTER, BETHESDA, MD.
Differential forms of Euler's turbo-machinery equation
[AD-A207279] N89-27426
NEVADA UNIV., RENO.
Design and characterization of large-drop generators for viscous, Newtonian, and non-Newtonian liquids
[AD-A208330] N89-27133
NEW MEXICO INST. OF MINING AND TECHNOLOGY, SOCORRO.
Assessing the sensitivity of high altitude New Mexican wilderness lakes to acidic precipitation and trace metal contamination
[PB89-148456] N89-27262
NIELSEN ENGINEERING AND RESEARCH, INC., MOUNTAIN VIEW, CA.
Numerical simulation of a turbulent flow through a shock wave
[AD-A207581] N89-27107
NORTH CAROLINA STATE UNIV., RALEIGH.
The study of structure-processing-property relations in copper oxide-based high T sub c superconductors
[DE89-012764] N89-27554
NORTH CAROLINA UNIV., CHAPEL HILL.
Magnetic and electrical properties of sandwich-like lanthanide phthalocyanines
[AD-A208411] N89-26958
Some results on nonGaussian signal detection
[AD-A207255] N89-27050
Information capacity of additive Gaussian channels with jamming
[AD-A207256] N89-27051
Capacity of the Poisson channel with time-varying noise intensity and jamming
[AD-A207225] N89-27446
Capacity of the poisson channel with random noise intensity
[AD-A207226] N89-27447
NORTH TEXAS STATE UNIV., DENTON.
Two-photon absorption characterization of HgCdTe
[AD-A207198] N89-27471
NORTHEAST ARTIFICIAL INTELLIGENCE CONSORTIUM, SYRACUSE, NY.
Northeast Artificial Intelligence Consortium annual report 1987. Volume 2, part b: Discussing, using, and recognizing plans
[AD-A208378] N89-27418
Northeast Artificial Intelligence Consortium annual report 1987. Volume 3: Distributed artificial intelligence for communications network management
[AD-A208379] N89-27419
NORTHERN RESEARCH AND ENGINEERING CORP., WOBURN, MA.
High performance intercooled and recuperated gas turbine
[PB89-152284] N89-27178
NORTHWESTERN UNIV., EVANSTON, IL.
Local density theory of heats of formation and short-range order parameters in substitutionally disordered alloys
[DE89-014696] N89-26986

O

OAK RIDGE GASEOUS DIFFUSION PLANT, TN.
A computer program for simulating the atmospheric dispersion of UF6 and other reactive gases having positive, neutral, or negative buoyancy
[DE89-012734] N89-27269
Issues and approaches for electronic document approval and transmittal using digital signatures and text authentication
[DE89-013102] N89-27596
OAK RIDGE NATIONAL LAB., TN.
Statistics of fracture in two grades of isotropic graphite
[DE89-013703] N89-26916
Gas separations using inorganic membranes
[DE89-013010] N89-26948
Degradation of Fe-25Cr, Fe-25Cr-20Ni and Fe-25Cr-6Al alloys in H2/H2O/H2S environments at 700 C
[DE89-011873] N89-26967
Evaluation of mechanical properties of TiN films by ultra-low load indentation
[DE89-009618] N89-26969
Analysis of microstructural development in single crystal welds
[DE89-013537] N89-26973
The effect of aging at 343 deg C on type 308 stainless steel welds
[DE89-013545] N89-26974
Rate-sensitivity and short term relaxation behavior of AISi Type 304 stainless steel at room temperature and at 650 C; influence of prior aging
[DE89-007823] N89-26978
Loss of grain boundary segregant during ion milling
[DE89-007835] N89-26979
An experimental study of the effect of stainless steel cladding on the structural integrity of flawed steel plates in bending
[DE89-008735] N89-26980
Relaxation response of A533B steel from 25 to 600 C
[DE89-010179] N89-26982
Breakdown mechanisms of Al2O3, Cr2O3 and SiO2 scales in H2/H2O/H2S environments, volume 1
[DE89-014789] N89-26988
Fractographic study of a silicon nitride ceramic
[DE89-013012] N89-27006
Structural ceramics in the advanced materials world
[DE89-013046] N89-27008
Explosives detection with an ion trap mass spectrometer
[DE89-012510] N89-27029
Refrigerator-freezer energy testing with alternative refrigerants
[DE89-013543] N89-27037
An expert system for correlation of radar and passive sensor signals
[DE89-011575] N89-27056
The effects of steep-front, short-duration impulses on power distribution components
[DE89-012338] N89-27091
Structural integrity evaluation based on an innovative field indentation microprobe
[DE89-010840] N89-27156
Research in autonomous robotics at ORNL using HERMIES-3
[DE89-004933] N89-27198
Measured damping and modulus of composite cylinders
[DE89-010369] N89-27209
High-temperature flaw assessment procedure: A state-of-the-art survey
[DE89-012740] N89-27210
The use of field indentation microprobe in measuring mechanical properties of welds
[DE89-013548] N89-27211
Evaluation of weldment creep and fatigue strength-reduction factors for elevated-temperature design
[DE89-006242] N89-27218
Estimating fracture toughness using tension or ball indentation tests and a modified critical strain model
[DE89-010324] N89-27220
Fate and effects of PAHs in the terrestrial environment: An overview
[DE89-010319] N89-27267
Criteria for selecting a CO2/climate change region of study
[DE89-011233] N89-27268
A theoretical investigation of a parallel genetic algorithm
[DE89-012508] N89-27384
A virtual zero-time, monolithic systolic sorting array
[DE89-007515] N89-27394
ORMONTE: An uncertainty analysis code for use with user-developed systems models on mainframe or personal computers. A user's guide
[DE89-013730] N89-27396
A symbolic generator of state equations for modeling of dynamic systems based on the electrical network analog paradigm
[DE89-013763] N89-27397
Autonomous discovery and learning by a mobile robot in unstructured environments
[DE89-001525] N89-27415
Shield optimization program. Part 1: Executive summary
[DE89-013335] N89-27476
Fast wave current drive modeling for ITER and prospects for a near-term proof of principle experiment
[DE89-013049] N89-27520
OFFICE NATIONAL D'ETUDES ET DE RECHERCHES AEROSPATIALES, PARIS (FRANCE).
Drag prediction and analysis from computational fluid dynamics, state-of-the-art in France N89-26818
Study of subgrid models in incompressible turbulent flow, homogeneous or inhomogeneous
[ONERA-RSF-17/3619-AY-110-A] N89-27123
Solution of compressible time-dependent Navier-Stokes equations by Chebychev spectral methods
[ONERA-NT-1987-1] N89-27126
Airborne measurements of the electric field and the charge precipitation particles in convective clouds: Lower positive charge centers
[ONERA-NT-1988-1] N89-27319
Solution of deterministic differential games: The approximate strategy method
[ONERA-NT-1987-6] N89-27450

OFFICE OF TECHNOLOGY ASSESSMENT, WASHINGTON, DC.
Big dumb boosters: A low-cost space transportation option. An OTA (Office of Technology and Assessment) background paper
[PB89-155196] N89-26881
Report to the Congress
[PB89-195408] N89-27603
OHIO STATE UNIV., COLUMBUS.
Radar cross section studies/compact range research
[NASA-CR-185848] N89-27064
Interaction between Tollmien-Schlichting waves and free-stream disturbances in boundary-layer flows
[NASA-CR-185847] N89-27118
A center for commercial development of space: Real-time satellite mapping. Remote sensing-based agricultural information expert system
[NASA-CR-185473] N89-27235
OLD DOMINION UNIV., NORFOLK, VA.
Numerical study of three-dimensional separation and flow control at a wing/body junction
[NASA-CR-185819] N89-26826
Nuclear fragmentation energy and momentum transfer distributions in relativistic heavy-ion collisions
[NASA-CR-185501] N89-27477
ONSALA SPACE OBSERVATORY (SWEDEN).
The Swedish-ESO Submillimeter Telescope (SEST)
[PB89-154892] N89-27605
The molecular cloud content of early type galaxies. 1: Detections and global properties
[PB89-184949] N89-27613
OPTIMIZATION, INC., BLACKSBURG, VA.
Control of flexible structures
[AD-A207520] N89-26883

P

PECHAN (E. H.) AND ASSOCIATES, INC., DURHAM, NC.
Historic emissions of VOC (Volatile Organic Compounds) and NOx in the United States from 1900 to 1985
[PB89-173223] N89-27270
PENNSYLVANIA STATE UNIV., UNIVERSITY PARK.
Mixing and combustion of pulsed gas jets
[PB89-155550] N89-26929
Corrosion of Ceramic Materials Workshop held November 12-13, 1987, Pennsylvania State University, University Park, Pennsylvania
[PB89-175343] N89-27004
Thermal stability of jet fuel
[DE89-013516] N89-27032
PHILIPS GLOEILAMPENFABRIEKEN N. V., EINDHOVEN (NETHERLANDS).
Magnetic multilayers
[ETN-89-94294] N89-27547
PHOTON ENERGY, INC., EL PASO, TX.
High-efficiency, large-area CdTe panels
[DE89-000891] N89-27242
PITTSBURGH UNIV., PA.
Studies of the fundamental nature of catalytic acidity, sites and intermediates
[DE89-012946] N89-26947
Breakdown mechanisms of Al2O3, Cr2O3 and SiO2 scales in H2/H2O/H2S environments, volume 1
[DE89-014789] N89-26988
Synthesis, characterization and physical properties of polyphosphazenes
[AD-A208296] N89-27013
On a computational method for the second fundamental tensor and its application to bifurcation problems
[AD-A207517] N89-27377
PLANNING RESEARCH CORP., HAMPTON, VA.
On processing development for fabrication of fiber reinforced composite, part 2
[NASA-CR-181866] N89-26917
POITIERS UNIV. (FRANCE).
Atomic simulation of crystalline defects in ordered structures
[ETN-89-94807] N89-27571
POLAR PRODUCTS, TORRANCE, CA.
Sun synchronous solar refrigeration
[DE89-011375] N89-27245
PRINCETON UNIV., NJ.
Design of an active helicopter control experiment at the Princeton Rotorcraft Dynamics Laboratory
[NASA-CR-185490] N89-26859
High-speed data acquisition for the Princeton University Dynamic Model Track
[NASA-CR-185491] N89-26865

Q

QUAID-I-AZAM UNIV., ISLAMABAD (PAKISTAN).
Applications of holography to pattern recognition and optical memories
[PB89-174668] N89-27146
Black holes in closed universes
[PB89-170039] N89-27610
Relativistic explanation of the inclination of planetary orbits
[PB89-170005] N89-27611

R

RADIOMANA, PARIS (FRANCE).
Investigations on local seismic phases and evaluation of body waves magnitude
[AD-A206633] N89-27283
RENSSELAER POLYTECHNIC INST., TROY, NY.
Chemical vapor deposition of silicon carbide using a novel organometallic precursor
[AD-A208273] N89-27012
Blends of poly(enaminonitriles)
[AD-A208441] N89-27017
Verification analysis of the Toroidal Accelerator Rotor Platform wind energy conversion system
[PB89-162069] N89-27241
Analytical procedures for environmental quality control, volume 1
[PB89-158604] N89-27266
Low-frequency sound propagation modeling over a locally-reacting boundary using the parabolic approximation
[NASA-CR-185864] N89-27469
New Frontier: Environments for Innovation
[PB89-151054] N89-27601
RISOE NATIONAL LAB., ROSKILDE (DENMARK).
Analysis of low-pressure gas-phase pyrolytic reactions by mass spectrometric techniques
[AD-A207457] N89-26939
Aerial smoke plume observations and surface layer turbulence measurements. Part 1: Project WIND. Phase 4: Dispersion study
[AD-A207370] N89-27305
ROCKWELL INTERNATIONAL CORP., CANOGA PARK, CA.
OTVE combustor wall condition monitoring
[NASA-CR-182275] N89-26899
Space station hydrogen/oxygen thruster technology
[NASA-CR-182280] N89-26905
OTVE turbopump condition monitoring, task E.5
[NASA-CR-182274] N89-27204
ROCKWELL INTERNATIONAL CORP., GOLDEN, CO.
Effect of oxidation, sandblasting and pickling on weldability
[DE89-013795] N89-26975
ROME AIR DEVELOPMENT CENTER, GRIFFISS AFB, NY.
Software deficiency issues confronting the utilization of non-Von Neumann architectures
[AD-A207268] N89-27369
ROME UNIV. (ITALY).
Production of pure ozone by means of electric discharges for measuring absorption coefficients
[NOTA-INTERNA-913] N89-27042
Statistics of an integrable discrete Sine Gordon system
[PREPRINT-638] N89-27128
Tests of low resistivity electrodeless streamer tubes
[NOTA-INTERNA-922] N89-27158
The diagonal strip system in the Macro experiment
[NOTA-INTERNA-924] N89-27159
On the multiplicity and symmetries of the bifurcation branching point in the square clamped plate
[PREPRINT-604] N89-27224
Absorption cross-section of ozone in the 590 to 610 nm region at different temperatures
[NOTA-INTERNA-928] N89-27291
Categorization in neural networks and prosopagnosia
[PREPRINT-608] N89-27327
The effect of synapses destruction on categorization by neural networks
[PREPRINT-609] N89-27328
On-line computer utilization to understand some physical processes (example: Pendulum motion)
[NOTA-INTERNA-927] N89-27360
The Burgers equation on the semi-finite and finite intervals
[PREPRINT-602] N89-27441
Universality and integrability of the nonlinear evolution PDEs describing N-wave interactions
[PREPRINT-603] N89-27442

Nonlinear wave equations solvable by the spectral transform
[PREPRINT-957] N89-27443
Differential stochastic equations
[PREPRINT-635] N89-27449
Some considerations on the birth of molecular physics in the first half of the 19th century
[NOTA-INTERNA-917] N89-27482
Precision measurements without polarization at LEP
[NOTA-INTERNA-921] N89-27483
Search for the inclusive production of J/psi in e(+)e(-) collisions using PLUTO data
[NOTA-INTERNA-923] N89-27484
First results for the delta I = 1/2 amplitude in K decays, with quenched lattice QCD and Wilson fermions
[PREPRINT-599] N89-27485
Vertex detectors at e(+) e(-) B meson factories
[NOTA-INTERNA-914] N89-27486
Relativistic corrections to photon scattering polarizabilities
[NOTA-INTERNA-916] N89-27487
Correlation and analysis between the Kamioka neutrino detector data and the Maryland and Rome gravitational antenna data
[NOTA-INTERNA-918] N89-27488
Covariance properties of the multiquark Hamiltonian in the constituent quark model
[NOTA-INTERNA-920] N89-27489
Multiparticle dynamics at the Sp(-)p collider
[NOTA-INTERNA-929] N89-27490
Beam-gas background rejection in L3 first level energy transfer
[NOTA-INTERNA-919] N89-27496
Determination of the kinetic parameters of the thermoluminescent CaF2 (Tm) crystal
[NOTA-INTERNA-915] N89-27569
Note on multiloop calculations for superstrings in the NSR formalism
[PREPRINT-601] N89-27581
Stochastic mechanics
[PREPRINT-634] N89-27582
Effective action for quantum gravity in two dimensions
[PREPRINT-600] N89-27583
On the integrability of the Ernst equation
[PREPRINT-606] N89-27584
Knot theory and quantum gravity
[PREPRINT-607] N89-27585
BAE measurement schemes and optimal sensitivity for generalized parametric devices
[PREPRINT-641] N89-27586
On the production and detection of gravitational waves from artificial sources
[NOTA-INTERNA-912] N89-27587
Resonant helicity flip of electron neutrino due to magnetic moment and dynamics of supernova
[PREPRINT-598] N89-27617
Mercury's magnetic field: Implications on the inner composition of the planet
[NOTA-INTERNA-926] N89-27620
A method to calibrate the light response of a high resolution electromagnetic calorimeter with cosmic rays
[NOTA-INTERNA-925] N89-27631
ROYAL AIRCRAFT ESTABLISHMENT, BEDFORD (ENGLAND).
CFD methods for drag prediction and analysis currently in use in UK N89-26823
RUTGERS - THE STATE UNIV., NEW BRUNSWICK, NJ.
Empirical analysis and refinement of expert system knowledge bases
[AD-A208294] N89-27598

S

SAN JOSE STATE UNIV., CA.
Development of Low-Level Turbulence (LLT) forecasting methodologies
[AD-A208457] N89-27320
SANDIA NATIONAL LABS., ALBUQUERQUE, NM.
Autonomous land navigation: A demonstration of retrotraverse
[DE89-011681] N89-26855
Molecular sieve films from zeolited-silica microcomposites
[DE89-009831] N89-26921
Lean-burn gas engine ignition processes
[PB89-181119] N89-26943
Micropyrolyzer design for infrared spectroscopy applications
[DE89-013329] N89-26949
Detonation of unconfined large scale fuel spray-air clouds
[DE89-006510] N89-26955
The solidification metallurgy of Alloy 718 and other Nb-containing superalloys
[DE89-008196] N89-26966

Quantitative thin film X-ray microanalysis of Nb modified Ti3Al
[DE89-009946] N89-26981
A method of removing oxides from the surface of Fe-Ni-Co alloy particles by chemical etching
[DE89-014597] N89-27009
Techniques for the detection of explosives
[DE89-012570] N89-27030
Characterization of Morton-Thiokol booster-rocket propellant TP-H1207C and its simulant H-19
[DE89-013347] N89-27031
A finite element method for solving electromagnetic scattering problems
[DE89-013496] N89-27059
Thermoelectric terminology in metrology and standards
[DE89-011512] N89-27079
Photoconductive semiconductor switch (PCSS) recovery
[DE89-012657] N89-27080
Closing photoconductive semiconductor switches
[DE89-013073] N89-27082
Dual-transistor method to determine delta V sub ot and delta V sub it for MOS devices
[DE89-006725] N89-27088
Total-dose hardness assurance for space applications of commercial CMOS devices
[DE89-006765] N89-27089
Improved core insulation schemes for multi-terawatt magnetic switches
[DE89-013814] N89-27093
Numerical solution of the Navier-Stokes equations for three-dimensional incompressible flows with open boundaries
[DE89-009333] N89-27119
Finite control volume modeling of laminar and turbulent flow of air in an enclosure
[DE89-009334] N89-27120
Standardized piezoelectric polymer (PVDF) gauge for detonator response measurement
[DE89-010437] N89-27144
Novel applications of the field ion microscope and atom-probe
[DE89-008684] N89-27154
Micromechanical characterization of near-surface layers
[DE89-008710] N89-27199
Mechanisms that control the geometry of pulsed Nd:YAG laser welds
[DE89-014490] N89-27200
System-based component test plans and operating characteristics: Introduction and overview
[DE89-012255] N89-27203
The 1/f noise: A nondestructive technique to predict MOS radiation hardness
[DE89-007419] N89-27205
Materials analysis with nuclear microprobes: Superconductors and buried conductors
[DE89-008580] N89-27206
Strain to failure of pressurized thick wall cylinders
[DE89-009969] N89-27219
Drilling operations plan for the Magma Energy Exploratory Well
[DE89-010037] N89-27240
Dynamic simulation of a molten-salt solar receiver
[DE89-010556] N89-27244
Proceedings of the Annual Solar Thermal Technology Research and Development Conference
[DE89-010538] N89-27251
A radiation-hardened 16/32-bit microprocessor
[DE89-008111] N89-27357
ASR4: A computer code for fitting and processing 4-gage anelastic strain recovery data
[DE89-012239] N89-27395
ELLIPSE user's manual and program reference
[DE89-014575] N89-27398
Using conjoint meshing primitives to generate quadrilateral and hexahedral elements in irregular regions
[DE89-005918] N89-27435
A one-dimensional scintillator camera for the SATURN X-ray simulation accelerator
[DE89-009327] N89-27492
A fiber optic test system for quantum efficiency measurements
[DE89-012823] N89-27505
Thermophysical properties of advanced carbon materials for Tokamak limiters
[DE89-012799] N89-27516
Z-pinch experiments on Saturn at 30 TW
[DE89-013497] N89-27523
Electrohydrodynamically driven, large-area liquid metal ion source for inertial confinement fusion
[DE89-012665] N89-27530
Two-dimensional effects in hollow core z-pinches
[DE89-014188] N89-27531
Two-dimensional effects in imploding plasma liners
[DE89-014482] N89-27534
MHD calculations of anode plasmas
[DE89-014485] N89-27535
Thin film preparation and single film device fabrication in the Tl-Ca-Ba-Cu-O HTS system
[DE89-013560] N89-27561
Developing a geologic and engineering properties data base with INGRES
[DE89-013520] N89-27593
Management Information Database System
[DE89-014595] N89-27597
Detection of very high energy gamma-rays from the Crab nebula
[DE89-011840] N89-27627

SANDIA NATIONAL LABS., LIVERMORE, CA.
Development of a thin wall graphite/polyimide composite pressure vessel with a large aspect ratio
[DE89-002536] N89-26920
Nonlinear dynamic response of pressurized composite bottles subjected to shock loading
[DE89-010553] N89-26922

SCIENCE APPLICATIONS INTERNATIONAL CORP., MCLEAN, VA.
JTECH (Japanese Technology Evaluation Program) panel report on advanced sensors in Japan
[PB89-158760] N89-27136
Risk assessment of compressed natural gas-fueled vehicle operations, phase 1
[PB89-188841] N89-27196

SCIENCE RESEARCH CORP., SOMERVILLE, MA.
Compact, lightweight CO2 lasers for SDIO applications
[AD-A207052] N89-27162

SECA, INC., HUNTSVILLE, AL.
Investigation of the transient fuel preburner manifold and combustor
[NASA-CR-183715] N89-26900

SELSKAPET FOR INDUSTRIELL OG TEKNISK FORSKNING, TRONDHEIM (NORWAY).
The 1st Scandinavian Conference on Viscous and T urbulent Flow in Hydraulic Machinery
[PB89-161327] N89-27102

SPARTA, INC., HUNTSVILLE, AL.
SDS software measurement requirements
[AD-A207449] N89-27376

STANFORD UNIV., CA.
Design and calibration of the mixing layer and wind tunnel
[NASA-CR-185472] N89-26886
New battery materials
[DE89-012845] N89-27081
Memory-reference characteristics of multiprocessor applications under MACH
[AD-A207318] N89-27352
Parallel implementation of OPS5 on the encore multiprocessor: Results and analysis
[AD-A207320] N89-27353
Hardware C - A language for hardware design
[AD-A207317] N89-27370
The HERMOD behavioral synthesis system
[AD-A207319] N89-27371
On the feasibility of a generalized linear program
[AD-A207402] N89-27373
Semi-infinite programming
[AD-A207403] N89-27374
An efficient exact algorithm for the least squares image registration problems
[DE89-013116] N89-27387
Suitability of message passing computers for implementing production systems
[AD-A207321] N89-27411
Linearization of nonlinear systems
[AD-A206073] N89-27423
On estimating the dependence between two point processes
[AD-A208311] N89-27445
Sampling based approaches to calculating marginal densities
[AD-A208388] N89-27451
Statistical study of the correlation of hard X-ray and type 3 radio bursts in solar flares
[NASA-CR-185833] N89-27629

STATE UNIV. OF NEW YORK, BUFFALO.
Surface plasmon study of monolayer-bilayer transition in poly-4-BCMU and poly-3-BCMU polydiacetylene Langmuir-Blodgett films
[AD-A207404] N89-26938
Nonresonant interaction of a three-level atom with cavity fields. Part 4: Atomic dipole moment and squeezing effects
[AD-A206788] N89-27470
MeV implantation studies in LPE-grown GaAs and InP
[AD-A207220] N89-27550
Dynamics of an M-level atom interacting with gravity fields. 1: Effects of the level number on quantum collapse and revival
[AD-A207278] N89-27579

STEVENS INST. OF TECH., HOBOKEN, NJ.
Analytical procedures for environmental quality control, volume 1
[PB89-158804] N89-27266

STEWART (V. R.), COLUMBUS, OH.
An experimental investigation of the ground vortex created by a moving jet
[NASA-CR-181841] N89-26815

SVERDRUP TECHNOLOGY, INC., BAY SAINT LOUIS, MS.
Space Shuttle Main Engine radio frequency emissions
[NASA-CR-184707] N89-26896

SWEDISH INST. OF SPACE PHYSICS, KIRUNA.
Activities report in space activities
[ISSN-0284-169X] N89-27458
Ionospheric plasma escape by high-altitude electric fields: Magnetic moment pumping
[IRF-PREPRINT-111] N89-27542

SYDNEY UNIV. (AUSTRALIA).
Inelastic buckling of channel columns in the distortional mode
[PB89-156053] N89-27207
Strength tests and design methods for cold-formed channel columns undergoing distortional buckling
[PB89-183958] N89-27216

SYRACUSE UNIV., NY.
Fault tolerant VLSI (Very Large-Scale Integration) design using error correcting codes
[AD-A208337] N89-27096
Northeast artificial intelligence consortium: Volume 2, part A: The Versatile Maintenance Expert System (VMES) research project
[AD-A208344] N89-27417

SYSTEMS AND PROCESSES ENGINEERING CORP., AUSTIN, TX.
DFT algorithms for bit-serial GaAs array processor architectures
[NASA-CR-183436] N89-27361

SYSTEMS TECHNOLOGY, INC., HAWTHORNE, CA.
Design considerations of manipulator and feel system characteristics in roll tracking
[NASA-CR-4111] N89-26860

T

TECHNICAL RESEARCH CENTRE OF FINLAND, ESPOO.
Measurement of the bending wave power flow by the structural intensity technique
[VTT-583] N89-27129

TECHNISCHE HOGESCHOOL, DELFT (NETHERLANDS).
Performance analysis of data-driven networks
[PB89-170906] N89-27412

TECHNISCHE UNIV., DELFT (NETHERLANDS).
A nonlinear multigrid method for three-dimensional transonic potential flow
[ETN-89-94802] N89-26827
On transformer modeling. A physically based three-phase transformer model for the study of low frequency phenomena in electrical power systems
[ETN-89-94801] N89-27095
Local mode smoothing analysis of various two-dimensional incomplete factorization iterative methods
[REPT-88-67] N89-27431
Row-oriented direct solving of linear algebraic equations. Inverse projection method
[REPT-88-81] N89-27432
Advanced electron beam evaporation
[ETN-89-94799] N89-27495
Integrated silicon color sensors
[ETN-89-94800] N89-27509
Artificial superlattices
[ETN-89-94889] N89-27551
Crystallization of paraxylene with scraped surface heat exchangers
[WTHD-189] N89-27570

TECHNISCHE UNIV., EINDHOVEN (NETHERLANDS).
Optical couplers for coherent optical phase diversity systems
[EUT-88-E-190] N89-27498
Magnetic multilayers
[ETN-89-94294] N89-27547

TECHNISCHE UNIV., MUNICH (GERMANY, F.R.).
Infrared temperature measurement with self regulating emission ratio
[ETN-89-94654] N89-27157

TECHNOLOGY, INC., SAN ANTONIO, TX.
Research and development of anti-G life support systems. Part 4: Engineering test and evaluation of six anti-G valves
[AD-A206996] N89-27341
TEL-AVIV UNIV. (ISRAEL).
Advanced calcium-thionyl chloride high-power battery
[AD-A207612] N89-27247
Solar radiation on Mars
[NASA-TM-102299] N89-27623
TELEDYNE BROWN ENGINEERING, HUNTSVILLE, AL.
Advanced Solar Observatory (ASO) accommodations requirements study
[NASA-CR-183718] N89-26885
SDS software measurement requirements
[AD-A207449] N89-27376
TEXAS UNIV., AUSTIN.
Equilibrium of a plasma in the fluid- and Vlasov-Maxwell systems
[DE89-013315] N89-27518
TEXTRON BELL HELICOPTER, FORT WORTH, TX.
OH-58 energy attenuating crew seat feasibility study
[AD-A207506] N89-26829
THERMO ELECTRON TECHNOLOGIES CORP., SAN DIEGO, CA.
Transverse pumping with diode lasers
[AD-A207261] N89-27165
TILBURG UNIV. (NETHERLANDS).
Estimation of the relationship between project attributes and the implementation of engineering tools
[PB89-149470] N89-27588
TITAN SYSTEMS, INC., LA JOLLA, CA.
Rule-based air combat simulation
[NASA-CR-4160] N89-27393

U

UNITED TECHNOLOGIES RESEARCH CENTER, EAST HARTFORD, CT.
Noise produced by turbulent flow into a rotor: Theory manual for atmospheric turbulence prediction and mean flow and turbulence contraction prediction
[NASA-CR-181789] N89-27466
Experimental assessment of helicopter rotor turbulence ingestion noise in hover
[NASA-CR-181792] N89-27468
UNIVERSITEIT TWENTE, ENSCHEDE (NETHERLANDS).
Processor control path synthesis: Literature survey and preliminary analysis
[MEMO-INF-88-46] N89-27401
Automatic generation of FORTRAN-coded Jacobians and Hessians
[MEMO-INF-88-47] N89-27402
An overview of some methods for the high-level specification of synchronization
[MEMO-INF-88-50] N89-27403
Automatic code vectorization of arithemetic expressions by bottom-up structure recognition
[MEMO-INF-88-48] N89-27414
A qualitative way of solving the pole balancing problem
[MEMO-INF-88-44] N89-27439
Attributed tree transformations with delayed and smart re-evaluation
[MEMO-INF-88-45] N89-27440
UNIVERSITY OF CENTRAL FLORIDA, ORLANDO.
Dynamic analysis of flexible mechanisms by a combined transfer matrix finite element method
[PB89-160865] N89-27181
UNIVERSITY OF SOUTH FLORIDA, TAMPA.
Thermal evaluation of advanced solar dynamic heat receiver performance
[NASA-CR-185117] N89-27256
UNIVERSITY OF SOUTHERN CALIFORNIA, LOS ANGELES.
Research in knowledge-based vision techniques for the autonomous land vehicle program
[AD-A208546] N89-26834
UNIVERSITY OF SOUTHERN CALIFORNIA, MARINA DEL REY.
Explanation in expert systems: A survey
[NASA-CR-185335] N89-27364
UNIVERSITY OF SOUTHERN MISSISSIPPI, HATTIESBURG.
Photodegradation of polyimides 2. Thermal property changes of polyimides based on a perfluorinated dianhydride
[AD-A208447] N89-27018
Natural abundance 15N CP/MAS NMR of solid polyamides: A sensitive technique for examining crystalline composition and conformation in the solid state
[AD-A208563] N89-27019
Nitrogen 15 T1 measurements of semicrystalline nylon 6
[AD-A208481] N89-27575
The 15N NMR powder spectra of semicrystalline nylon 6
[AD-A208502] N89-27577
US OLYMPIC COMMITTEE, COLORADO SPRINGS, CO.
Endogenous hormonal and growth factor responses to heavy resistance exercise protocols
[AD-A208375] N89-27336
UTAH UNIV., SALT LAKE CITY.
Development of theoretical and numerical techniques for achieving stability in gyrotron traveling-wave amplifiers
[AD-A207451] N89-27140

V

VIGYAN RESEARCH ASSOCIATES, INC., HAMPTON, VA.
The NASA Langley Research Center 0.3-meter transonic cryogenic tunnel T-P/Re-M controller manual
[NASA-CR-181868] N89-26869
VIRGINIA POLYTECHNIC INST. AND STATE UNIV., BLACKSBURG.
Residual stress changes in fatigue. Volume 1: Residual stress measurements by X-ray diffraction in notched test specimens
[AD-A206345] N89-27225
Residual stress changes in fatigue. Volume 2: A simulation model for stress measurements in notched test specimens by X-ray diffraction
[AD-A206346] N89-27226
Modeling and computational algorithms for parameter estimation and optimal control of aeroelastic systems and large flexible structures
[AD-A208274] N89-27404

W

WALLACE AND CO., FAIRBORN, OH.
Cost of quality evaluation methodologies handbook
[AD-A206935] N89-27202
WASHINGTON STATE UNIV., PULLMAN.
Comparison of spectral data gathered from a laboratory spectrometer and TM images with and without shadow correction
[DE89-010877] N89-27237
Quantitative three-dimensional structural techniques
[DE89-010879] N89-27238
Rapidly convergent algorithms for nonsmooth optimization
[AD-A207629] N89-27379
WASHINGTON UNIV., SEATTLE.
HRR field in an aluminum SEN specimen
[AD-A207578] N89-26963
Cloud and precipitation scavenging process in the South Coast Air Basin
[PB89-181788] N89-27313
Antiproton and millimeter wave research
[AD-A208363] N89-27491
WESTINGHOUSE ELECTRIC CORP., ORLANDO, FL.
Advanced coal-fueled gas turbine systems, volume 2
[DE89-000954] N89-27183
WESTINGHOUSE HANFORD CO., RICHLAND, WA.
Creep-fatigue assessment methods using elastic analysis results and adjustments
[DE89-011858] N89-27221
WICHITA STATE UNIV., KS.
Ideal jet flow in two dimensions
[AD-A208275] N89-27131
WISCONSIN UNIV., MADISON.
Design and operation of a horizontal liquid helium flow facility
[DE89-013482] N89-26867
Liquid helium fluid dynamics studies
[DE89-013124] N89-27036
Computation and theory in nonlinear optimization
[AD-A207610] N89-27430
Thin film preparation and single film device fabrication in the Tl-Ca-Ba-Cu-O HTS system
[DE89-013560] N89-27561
New strategies for display devices based on 2-6 materials
[AD-A208288] N89-27573
WYLE LABS., INC., ARLINGTON, VA.
ROUTEMAP model for predicting noise exposure from aircraft operations on Military Training Routes
[AD-A203849] N89-27459

Y

YALE UNIV., NEW HAVEN, CT.
Catalytic combustion of methane
[PB89-188874] N89-26946

Typical Contract Number Index Listing

Listings in this index are arranged alphanumerically by contract number. Under each contract number the NASA accession numbers denoting documents that have been produced as a result of research done under that contract are arranged in ascending order. The NASA accession number denotes the number by which the citation is identified.

AF PROJ. 7A10 ..... N89-27283
AF PROJ. 2155 ..... N89-27419
AF PROJ. 2301 ..... N89-27161
AF PROJ. 2302 ..... N89-27227
AF PROJ. 2303 ..... N89-26927
AF PROJ. 2304 ..... N89-27131
N89-27379
N89-27404
N89-27598
AF PROJ. 2306 ..... N89-27576
AF PROJ. 2307 ..... N89-27134
N89-27135
AF PROJ. 2311 ..... N89-27606
AF PROJ. 2338 ..... N89-27096
AF PROJ. 2917 ..... N89-27491
AF PROJ. 5581 ..... N89-27405
N89-27418
AF PROJ. 7231 ..... N89-27459
AF-AFOSR-0021-88 ..... N89-27576
AF-AFOSR-0090-88 ..... N89-27430
AF-AFOSR-0117-88 ..... N89-27349
AF-AFOSR-0120-85 ..... N89-27606
AF-AFOSR-0127-86 ..... N89-27420
AF-AFOSR-0210-83 ..... N89-27379
AF-AFOSR-0250-86 ..... N89-27491
AF-AFOSR-0276-86 ..... N89-27131
AF-AFOSR-0287-85 ..... N89-27404
AF-AFOSR-0319-87 ..... N89-27161
AF-AFOSR-0331-87 ..... N89-27283
AF-AFOSR-0345-85 ..... N89-26927
AF-AFOSR-0385-87 ..... N89-27135
AID/PDC-1406-I-00-7070-00 ..... N89-27233
ARB-A4-075-32 ..... N89-27317
ARPA ORDER 4864 ..... N89-27353
ARPA ORDER 4976 ..... N89-27411
ARPA ORDER 5520 ..... N89-27356
ARPA ORDER 5916 ..... N89-26813
ARPA ORDER 6631 ..... N89-27000
BMFT-LFL-8360-7 ..... N89-26862
BMFT-01-YH-86-138 ..... N89-27065
DA PROJ. 1L1-61102-A-31-B N89-27471
DA PROJ. 1L1-61102-BH-57 ..... N89-27305
DA PROJ. 1L1-62705-H-94 ..... N89-27097
DA PROJ. 3A1-61101-A-91C N89-27340
DA PROJ. 3E1-62777-A-878 ..... N89-26829
DA PROJ. 3E1-62787-A-878 ..... N89-27334
DA PROJ. 3M1-61102-AS-15 ..... N89-27329
DAAB07-87-C-F094 ..... N89-27471
DAAB07-89-C-F404 ..... N89-27000
DAAH01-88-C-0581 ..... N89-26813
DAAK20-84-C-0440 ..... N89-27073
DAAL02-86-D-0042 ..... N89-27076
DAAL03-86-D-0001 ..... N89-27320
DAAL03-86-G-0022 ..... N89-27446
DACA76-85-C-0009 ..... N89-26834
DAJA45-87-M-0475 ..... N89-27305
DAJA45-88-C-0012 ..... N89-27247
DAMD17-86-C-6151 ..... N89-27345
DAMD17-87-C-7032 ..... N89-26829
DAMD17-87-C-7235 ..... N89-27329
DARPA ORDER 5299 ..... N89-27283
DASG60-88-C-0076 ..... N89-27166
DE-AC02-76CH-00016 ..... N89-26970
N89-27155
N89-27170
DE-AC02-76CH-03000 ..... N89-27355
N89-27400
N89-27614
DE-AC02-76ER-01112 ..... N89-27627
DE-AC02-76ER-01198 ..... N89-26932
DE-AC02-76ER-03130 ..... N89-27359
DE-AC02-83CH-10093 ..... N89-27143
N89-27242
N89-27248
N89-27249
N89-27252
N89-27253
DE-AC02-86ER-40306 ..... N89-26867
N89-27036
DE-AC03-76SF-00098 ..... N89-26950
N89-26968
N89-26971
N89-26972
N89-26984
N89-27081
N89-27083
N89-27148
N89-27149
N89-27169
N89-27170
N89-27175
N89-27254
N89-27255
N89-27274
N89-27455
N89-27475
N89-27556
N89-27558
N89-27559
DE-AC03-81ER-40050 ..... N89-27454
DE-AC04-76DP-00789 ..... N89-26855
N89-26921
N89-26949
N89-26955
N89-26966
N89-26981
N89-27009
N89-27030
N89-27031
N89-27059
N89-27079
N89-27080
N89-27082
N89-27088
N89-27089
N89-27093
N89-27119
N89-27120
N89-27144
N89-27154
N89-27199
N89-27200
N89-27203
N89-27205
N89-27206
N89-27219
N89-27240
N89-27243
N89-27244
N89-27251
N89-27357
N89-27395
N89-27398
N89-27435
N89-27492
N89-27505
N89-27512
N89-27516
N89-27523
N89-27530
N89-27531
N89-27534
N89-27535
N89-27561
N89-27593
N89-27597
N89-27627
DE-AC04-76DP-03533 ..... N89-26975
DE-AC04-76DR-00789 ..... N89-26920
N89-26922
DE-AC04-88DP-43495 ..... N89-26987
DE-AC05-76OR-00033 ..... N89-27282
DE-AC05-84OR-21400 ..... N89-26916
N89-26948
N89-26967
N89-26969
N89-26973
N89-26974
N89-26978
N89-26979
N89-26980
N89-26982
N89-26988
N89-27006
N89-27008
N89-27029
N89-27037
N89-27056
N89-27091
N89-27156
N89-27198
N89-27209
N89-27210
N89-27211
N89-27218
N89-27220
N89-27267
N89-27268
N89-27384
N89-27394
N89-27396
N89-27397
N89-27415
N89-27476
N89-27520
DE-AC05-84OT-21400 ..... N89-27269
N89-27596
DE-AC06-76RL-01830 ..... N89-27268
DE-AC06-87RL-10930 ..... N89-27221
DE-AC07-76ID-01570 ..... N89-27350
DE-AC08-86NV-10571 ..... N89-27526
DE-AC09-76SR-00001 ..... N89-27363
DE-AC21-82MC-24261 ..... N89-27250
DE-AC21-86MC-23167 ..... N89-27183
DE-AC21-86MC-23258 ..... N89-27197
DE-AC22-88PC-88827 ..... N89-27032
DE-AI05-87ER-25046 ..... N89-27356
DE-AI08-87NV-10566 ..... N89-27318
DE-FC22-83FE-60149 ..... N89-26954
DE-FG01-85CE-15219 ..... N89-27245
DE-FG02-84ER-45080 ..... N89-26986
DE-FG02-84ER-53175 ..... N89-27524
DE-FG02-85ER-40235 ..... N89-27473
DE-FG02-85ER-53207 ..... N89-27517
DE-FG02-87ER-13774 ..... N89-26947
DE-FG02-87ER-25026 ..... N89-27437
N89-27438
DE-FG02-87ER-25027 ..... N89-26941
DE-FG02-87ER-45317 ..... N89-26951
DE-FG02-88ER-40465 ..... N89-27515
DE-FG03-87ER-25028 ..... N89-27387
DE-FG05-80ET-53088 ..... N89-27518
DE-FG05-86ER-13544 ..... N89-26956
DE-FG05-87ER-13758 ..... N89-26954
DE-FG05-87ER-52147 ..... N89-27173
DE-FG05-87ER-54034 ..... N89-27519
DE-FG05-88ER-45359 ..... N89-27554
DE-FG06-87ER-13796 ..... N89-27237
N89-27238
DE-FG22-84PC-70780 ..... N89-27028
DI-14-08-0001-G-1505 ..... N89-27262
DI-14-12-0001-30191 ..... N89-27311
DOT-FA71NAA-P98 ..... N89-26851
DRET-84-003 ..... N89-27125
DRET-85-172 ..... N89-27277
DRET-86-003/05 ..... N89-27124
DRET-87-003/05 ..... N89-27124

DTFA-03-86-C-00018 ..... N89-27047
EPA-68-01-7325 ..... N89-27261
EPA-68-02-4271 ..... N89-27270
EPA-68-02-4396 ..... N89-27264
EPA-68-02-4443 ..... N89-27147
EPRI PROJ. 2658-21 ..... N89-27210
ERS-86/1468/DRET/DS/SR N89-27571
ESA-7004/86/F/FL(SC) N89-27035
FAA-T0702-N N89-26831
F04611-86-C-0008 ..... N89-26883
F04701-85-C-0086 ..... N89-26898
N89-27141
N89-27267
F08635-84-C-0295 ..... N89-27425
F19628-84-C-0074 ..... N89-27549
F19628-85-C-0003 ..... N89-27375
F19628-85-K-0039 ..... N89-27368
F19628-86-C-0122 ..... N89-27548
F19628-86-K-0014 ..... N89-27284
F30602-81-C-0169 ..... N89-27096
F30602-81-C-0206 ..... N89-27049
F30602-84-C-0153 ..... N89-27140
F30602-85-C-0008 ..... N89-27417
N89-27418
N89-27419
F30602-86-C-0032 ..... N89-27405
F33615-81-C-0600 ..... N89-27341
F33615-83-C-3208 ..... N89-26962
F33615-84-C-2431 ..... N89-26937
F33615-84-C-3208 ..... N89-26838
F33615-85-C-0534 ..... N89-27459
F33615-85-C-5040 ..... N89-27464
F33615-85-K-2501 ..... N89-26814
F33615-86-C-0019 ..... N89-27342
F33615-87-C-5241 ..... N89-26998
F33657-86-D-0094 ..... N89-27202
F49620-86-C-0051 ..... N89-27227
F49620-86-C-0063 ..... N89-27134
F49620-87-C-0005 ..... N89-27599
F49620-87-C-0042 ..... N89-26938
F49620-88-C-0130 ..... N89-26856
GRI-5082-232-0696 ..... N89-26997
GRI-5084-223-1048 ..... N89-26944
GRI-5084-238-1302 ..... N89-27004
N89-27005
GRI-5084-242-1118 ..... N89-27184
GRI-5084-260-1081 ..... N89-27086
GRI-5086-233-1436 ..... N89-27178
GRI-5086-260-1229 ..... N89-27254
GRI-5086-260-1249 ..... N89-26946
GRI-5086-260-1296 ..... N89-27153
GRI-5086-260-1308 ..... N89-26929
GRI-5086-260-1458 ..... N89-26943
GRI-5086-530-1365 ..... N89-27604
GRI-5087-254-1621 ..... N89-27196
GRI-5088-450-1667 ..... N89-27590
IGT PROJ. 32001-03 ..... N89-27604
ITA-87-PAY-226-B N89-27356
MANE-8-00001 ..... N89-27231
N89-27232
MANE-8-00003 ..... N89-27230
MDA903-83-C-0335 ..... N89-27352
NAGW-492 ..... N89-27288
NAGW-557 ..... N89-27288
NAGW-973 ..... N89-27235
NAGW-1340 ..... N89-27608
NAG1-530 ..... N89-26826
NAG1-561 ..... N89-26917
NAG1-929 ..... N89-27469
NAG2-415 ..... N89-26859
N89-26865
NAG3-743 ..... N89-27118
NAG3-851 ..... N89-27256
NAG5-459 ..... N89-27279
NAG5-814 ..... N89-27279
NAG5-931 ..... N89-27062
NAG9-109 ..... N89-27155
NASA ORDER C-22187-M N89-26903
NASA ORDER C-99066-G N89-27115
NASA ORDER L-29341-C N89-26815
NASA ORDER T-0604-L N89-26832
NASW-4154 ..... N89-27034
NAS1-17763 ..... N89-27466
N89-27468
NAS1-17919 ..... N89-26869
NAS1-17970 ..... N89-26842
NAS1-18000 ..... N89-26917
NAS1-18037 ..... N89-26841
NAS1-18107 ..... N89-27348
N89-27349
N89-27362
N89-27420
NAS1-18565 ..... N89-27413
NAS1-18605 ..... N89-27112
N89-27113
N89-27348
N89-27349
N89-27390
N89-27420
NAS2-11877 ..... N89-27416
NAS2-11990 ..... N89-27393
NAS2-12221 ..... N89-26860
NAS3-23773 ..... N89-26899
N89-27204
NAS3-24881 ..... N89-26880
NAS3-25055 ..... N89-27152
NAS3-25142 ..... N89-26905
NAS3-25336 ..... N89-26879
NAS5-29373 ..... N89-27302
NAS5-29386 ..... N89-27289
NAS5-30291 ..... N89-27361
NAS5-30506 ..... N89-27314
NAS8-30490 ..... N89-26901
NAS8-37128 ..... N89-26885
NAS8-37282 ..... N89-26894
NAS8-37461 ..... N89-26900
NA86AA-D-SG040 ..... N89-27325
NCA2-174 ..... N89-27111
NCC1-42 ..... N89-27477
NCC2-55 ..... N89-26866
NCC2-99 ..... N89-27346
NCC2-515 ..... N89-27434
NCC2-520 ..... N89-27364
NGT-50103 ..... N89-27279
NI PROJ. P87035 ..... N89-27102
NIH-P41RR01838 ..... N89-27155
NIST-60NANB7D0737 ..... N89-26945
NIST-70NANB5H0525 ..... N89-27100
NOAA-NA86AA-D-SG089 ..... N89-27041
NR PROJ. 042-267 ..... N89-27445
N89-27451
NR PROJ. 356-856 ..... N89-27011
NSF AST-81-6403 ..... N89-27612
NSF AST-83-12332 ..... N89-27612
NSF ATM-87-05084 ..... N89-27629
NSF ATM-87-09659 ..... N89-27309
NSF DCR-83-09926 ..... N89-27377
NSF DMR-84-03987 ..... N89-26938
NSF DMR-87-06167 ..... N89-26921
NSF DMS-85-16191 ..... N89-27429
NSF DMS-87-01543 ..... N89-26941
NSF DMS-88-00589 ..... N89-27373
N89-27374
NSF EAR-86-18346 ..... N89-27155
NSF ECS-87-09265 ..... N89-27365
NSF MEA-84-21249 ..... N89-27181
NSF MID-87-14646 ..... N89-27071
NSF MSM-86-13483 ..... N89-27601
NSF NCR-87-13726 ..... N89-27051
NSF PHY-82-17853 ..... N89-27608
NSG-1613 ..... N89-27064
NSG-7092 ..... N89-27629
N00014-80-C-9455 ..... N89-27377
N00014-82-K-0190 ..... N89-26933
N00014-82-K-0322 ..... N89-27015
N00014-82-K-0523 ..... N89-27246
N00014-82-K-0576 ..... N89-26935
N89-26936
N00014-83-K-0069 ..... N89-27033
N00014-84-C-0708 ..... N89-26940
N00014-84-K-0099 ..... N89-27354
N00014-84-K-0658 ..... N89-26934
N00014-85-G-0093 ..... N89-27344
N00014-85-K-0169 ..... N89-27427
N89-27428
N89-27429
N00014-85-K-0211 ..... N89-27167
N00014-85-K-0358 ..... N89-27013
N00014-85-K-0460 ..... N89-26999
N00014-85-K-0631 ..... N89-27573
N00014-85-K-0632 ..... N89-27012
N89-27017
N00014-85-K-0898 ..... N89-27011
N89-27016
N00014-86-F-0096 ..... N89-27007
N00014-86-K-0039 ..... N89-27050
N89-27051
N89-27446
N89-27447
N00014-86-K-0043 ..... N89-27470
N89-27579
N00014-86-K-0112 ..... N89-27423
N00014-86-K-0156 ..... N89-27445
N89-27451
N00014-86-K-0183 ..... N89-27132
N00014-86-K-0326 ..... N89-27052
N00014-86-K-0599 ..... N89-27500
N00014-86-K-0640 ..... N89-27014
N00014-87-C-0483 ..... N89-27107
N00014-87-C-0726 ..... N89-27087
N00014-87-C-2412 ..... N89-27165
N00014-87-K-0398 ..... N89-27598
N00014-87-K-0799 ..... N89-27550
N00014-87-K-0825 ..... N89-27098
N00014-87-K-0828 ..... N89-27353
N89-27370
N89-27371
N89-27372
N89-27411
N00014-88-C-0165 ..... N89-27053
N00014-88-C-0454 ..... N89-27351
N00014-88-C-0681 ..... N89-27574
N00014-88-C-0725 ..... N89-26910
N00014-88-C-0727 ..... N89-27162
N00014-88-K-0109 ..... N89-27020
N00014-88-K-0144 ..... N89-27021
N89-27022
N89-27023
N00014-88-K-0323 ..... N89-27572
N00014-89-J-1019 ..... N89-27074
N00014-89-J-1028 ..... N89-27018
N00014-89-J-1175 ..... N89-27050
N89-27447
N00014-89-J-1225 ..... N89-27019
N89-27575
N89-27577
N00014-89-J-1276 ..... N89-26963
N00014-89-J-1659 ..... N89-27373
N89-27374
N00014-89-J-1734 ..... N89-26958
N00173-88-WR-80360 ..... N89-27137
N62269-85-C-0256 ..... N89-27225
N89-27226
PROJ. MEDICA-9571 ..... N89-27391
RR02303 ..... N89-27226
R033-87 ..... N89-27612
SDIO84-88-C-0018 ..... N89-27376
SRC-87-DP-109 ..... N89-27071
STU(F)-87-00415P N89-27130
W-31-109-ENG-38 ..... N89-26913
N89-26941
N89-26952
N89-26953
N89-26985
N89-27002
N89-27003
N89-27092
N89-27193
N89-27194
N89-27195
N89-27275
N89-27399
N89-27453
N89-27474
N89-27508
N89-27525
N89-27546
N89-27553
N89-27555
N89-27562
N89-27563
N89-27568
N89-27592
N89-27628
W-7405-ENG-36 ..... N89-26923
N89-26983
N89-27090
N89-27171
N89-27217
N89-27239
N89-27290
N89-27383
N89-27388
N89-27452
N89-27453
N89-27472
N89-27478
N89-27493
N89-27494
N89-27529
N89-27532
N89-27533
N89-27543
N89-27560
N89-27564
N89-27565
N89-27566
N89-27567
N89-27618
W-7405-ENG-48 ..... N89-26915
N89-26926
N89-27027
N89-27057
N89-27077
N89-27084
N89-27110
N89-27145
N89-27150

N89-27172
N89-27222
N89-27228
N89-27272
N89-27273
N89-27276
N89-27308
N89-27358
N89-27386
N89-27436
N89-27454
N89-27479
N89-27521
N89-27522
N89-27552
N89-27557
N89-27591
N89-27608
N89-27630
199-61-12 ..... N89-27346
324-01-00 ..... N89-26879
474-18-10 ..... N89-26887
474-52-10 ..... N89-26903
476-50-02-02 ..... N89-26888
481-01-02 ..... N89-26905
488-80-07-01 ..... N89-27504
505-60-01-02 ..... N89-26811
505-60-21-02 ..... N89-26810
505-60-41-01 ..... N89-26841
505-61-01 ..... N89-26808
505-61-01-05 ..... N89-27151
505-61-01-09 ..... N89-26869
505-61-71-02 ..... N89-26815
505-63-01 ..... N89-26917
505-63-01-01 ..... N89-27001
505-63-01-09 ..... N89-26842
505-63-01-11 ..... N89-26843
505-63-11 ..... N89-26912
N89-26919
N89-26924
505-63-51 ..... N89-27466
N89-27468
505-63-51-06 ..... N89-27465
505-63-81 ..... N89-27114
505-66-01-02 ..... N89-26861
505-66-11 ..... N89-27393
N89-27416
505-66-71 ..... N89-26844
505-67-01 ..... N89-26860
505-80-21 ..... N89-27103
505-90-21-01 ..... N89-27112
N89-27113
N89-27348
N89-27349
N89-27362
N89-27390
N89-27420
506-40-11 ..... N89-27116
506-40-91 ..... N89-26816
N89-27117
506-41-11 ..... N89-26877
N89-27619
506-41-31 ..... N89-27256
506-41-41 ..... N89-27506
506-42-21 ..... N89-27204
506-42-31 ..... N89-26895
N89-26904
N89-26906
N89-27121
506-43-31-02 ..... N89-27215
506-43-41-02 ..... N89-27212
506-44-20 ..... N89-27038
506-44-21-03 ..... N89-27063
506-46-21-05 ..... N89-27413
506-49-11-01 ..... N89-26878
506-62-21 ..... N89-27115
510-01-0A N89-27223
510-01-01 ..... N89-26989
533-02-51 ..... N89-27213
535-03-11-03 ..... N89-27467
583-01-11-12 ..... N89-27060
591-41-21 ..... N89-26876
650-60-21 ..... N89-26880

Typical Report Number Index Listing

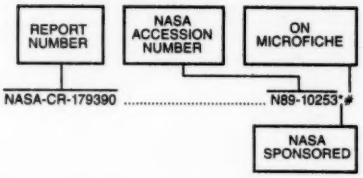

Listings in this index are arranged alphanumerically by report number. The NASA accession number denotes the number by which the citation is identified. An asterisk (*) indicates that the itemis a NASA report. A pound sign (#) indicates that the item is available on microfiche.

A-88135 ..... N89-26816* #
A-89011 ..... N89-27117* #
A-89042 ..... N89-27116* #
A-89167 ..... N89-26808* #
A-89210 ..... N89-27433* #

A/V-97457-3 ..... N89-27132 #

AAMRL-TR-88-060 ..... N89-27459 #

AD-A196032 ..... N89-26831 #
AD-A203849 ..... N89-27459 #
AD-A205292 ..... N89-26927 #
AD-A206073 ..... N89-27423 #
AD-A206633 ..... N89-27283 #
AD-A206782 ..... N89-26807 #
AD-A206786 ..... N89-26828 #
AD-A206788 ..... N89-27470 #
AD-A206809 ..... N89-26846 #
AD-A206812 ..... N89-27161 #
AD-A206935 ..... N89-27202 #
AD-A206972 ..... N89-26813 #
AD-A206974 ..... N89-27548 #
AD-A206996 ..... N89-27341 #
AD-A207052 ..... N89-27162 #
AD-A207189 ..... N89-27323 #
AD-A207190 ..... N89-27351 #
AD-A207198 ..... N89-27471 #
AD-A207206 ..... N89-27303 #
AD-A207207 ..... N89-27284 #
AD-A207209 ..... N89-27549 #
AD-A207210 ..... N89-27368 #
AD-A207211 ..... N89-27049 #
AD-A207215 ..... N89-26838 #
AD-A207217 ..... N89-26933 #
AD-A207220 ..... N89-27550 #
AD-A207225 ..... N89-27446 #
AD-A207226 ..... N89-27447 #
AD-A207227 ..... N89-26934 #
AD-A207231 ..... N89-27462 #
AD-A207236 ..... N89-27073 #
AD-A207241 ..... N89-27342 #
AD-A207248 ..... N89-27331 #
AD-A207252 ..... N89-27424 #
AD-A207255 ..... N89-27050 #
AD-A207256 ..... N89-27051 #
AD-A207257 ..... N89-27425 #
AD-A207261 ..... N89-27165 #
AD-A207268 ..... N89-27369 #
AD-A207271 ..... N89-26998 #
AD-A207273 ..... N89-26999 #
AD-A207275 ..... N89-27000 #
AD-A207277 ..... N89-26909 #
AD-A207278 ..... N89-27579 #
AD-A207279 ..... N89-27426 #
AD-A207282 ..... N89-26962 #
AD-A207302 ..... N89-27285 #
AD-A207308 ..... N89-26910 #
AD-A207310 ..... N89-27286 #
AD-A207311 ..... N89-27622 #
AD-A207312 ..... N89-27304 #
AD-A207317 ..... N89-27370 #
AD-A207318 ..... N89-27352 #
AD-A207319 ..... N89-27371 #
AD-A207320 ..... N89-27353 #
AD-A207321 ..... N89-27411 #
AD-A207322 ..... N89-27372 #
AD-A207323 ..... N89-26935 #
AD-A207325 ..... N89-26936 #
AD-A207370 ..... N89-27305 #
AD-A207372 ..... N89-26937 #
AD-A207391 ..... N89-27234 #
AD-A207394 ..... N89-26814 #
AD-A207399 ..... N89-27052 #
AD-A207402 ..... N89-27373 #
AD-A207403 ..... N89-27374 #
AD-A207404 ..... N89-26938 #
AD-A207406 ..... N89-27024 #
AD-A207410 ..... N89-27463 #
AD-A207414 ..... N89-27375 #
AD-A207417 ..... N89-26839 #
AD-A207428 ..... N89-27053 #
AD-A207449 ..... N89-27376 #
AD-A207451 ..... N89-27140 #
AD-A207454 ..... N89-27166 #
AD-A207457 ..... N89-26939 #
AD-A207506 ..... N89-26829 #
AD-A207508 ..... N89-27074 #
AD-A207514 ..... N89-27500 #
AD-A207517 ..... N89-27377 #
AD-A207518 ..... N89-27075 #
AD-A207520 ..... N89-26883 #
AD-A207522 ..... N89-27501 #
AD-A207525 ..... N89-27448 #
AD-A207532 ..... N89-27464 #
AD-A207535 ..... N89-27076 #
AD-A207547 ..... N89-27287 #
AD-A207548 ..... N89-27306 #
AD-A207554 ..... N89-26864 #
AD-A207555 ..... N89-27246 #
AD-A207556 ..... N89-27054 #
AD-A207557 ..... N89-27025 #
AD-A207558 ..... N89-27307 #
AD-A207569 ..... N89-27167 #
AD-A207570 ..... N89-26840 #
AD-A207572 ..... N89-27427 #
AD-A207573 ..... N89-27428 #
AD-A207575 ..... N89-27429 #
AD-A207577 ..... N89-27502 #
AD-A207578 ..... N89-26963 #
AD-A207579 ..... N89-26830 #
AD-A207581 ..... N89-27107 #
AD-A207584 ..... N89-26898 #
AD-A207585 ..... N89-27141 #
AD-A207586 ..... N89-27378 #
AD-A207592 ..... N89-26851 #
AD-A207594 ..... N89-26940 #
AD-A207609 ..... N89-27354 #
AD-A207610 ..... N89-27430 #
AD-A207612 ..... N89-27247 #
AD-A207627 ..... N89-27324 #
AD-A207629 ..... N89-27379 #
AD-A207647 ..... N89-26964 #
AD-A207784 ..... N89-27177 #
AD-A208261 ..... N89-27332 #
AD-A208267 ..... N89-27011 #
AD-A208268 ..... N89-26856 #
AD-A208272 ..... N89-27572 #
AD-A208273 ..... N89-27012 #
AD-A208274 ..... N89-27404 #
AD-A208275 ..... N89-27131 #
AD-A208286 ..... N89-27606 #
AD-A208288 ..... N89-27573 #
AD-A208294 ..... N89-27598 #
AD-A208296 ..... N89-27013 #
AD-A208297 ..... N89-27132 #
AD-A208298 ..... N89-27347 #
AD-A208300 ..... N89-27340 #
AD-A208301 ..... N89-27333 #
AD-A208310 ..... N89-27014 #
AD-A208311 ..... N89-27445 #
AD-A208312 ..... N89-27033 #
AD-A208314 ..... N89-27334 #
AD-A208316 ..... N89-26925 #
AD-A208324 ..... N89-26871 #
AD-A208327 ..... N89-27599 #
AD-A208329 ..... N89-27405 #
AD-A208330 ..... N89-27133 #
AD-A208337 ..... N89-27096 #
AD-A208338 ..... N89-27015 #
AD-A208341 ..... N89-27016 #
AD-A208342 ..... N89-27335 #
AD-A208344 ..... N89-27417 #
AD-A208345 ..... N89-27225 #
AD-A208346 ..... N89-27226 #
AD-A208349 ..... N89-27097 #
AD-A208358 ..... N89-27406 #
AD-A208363 ..... N89-27491 #
AD-A208370 ..... N89-27574 #
AD-A208371 ..... N89-27098 #
AD-A208375 ..... N89-27336 #
AD-A208378 ..... N89-27418 #
AD-A208379 ..... N89-27419 #
AD-A208388 ..... N89-27451 #
AD-A208389 ..... N89-27407 #
AD-A208391 ..... N89-26809 #
AD-A208402 ..... N89-27134 #
AD-A208411 ..... N89-26958 #
AD-A208428 ..... N89-27337 #
AD-A208441 ..... N89-27017 #
AD-A208443 ..... N89-27408 #
AD-A208446 ..... N89-27409 #
AD-A208447 ..... N89-27018 #
AD-A208448 ..... N89-27510 #
AD-A208451 ..... N89-27294 #
AD-A208457 ..... N89-27320 #
AD-A208458 ..... N89-27099 #
AD-A208461 ..... N89-26863 #
AD-A208462 ..... N89-26990 #
AD-A208464 ..... N89-27295 #
AD-A208466 ..... N89-27135 #
AD-A208467 ..... N89-26991 #
AD-A208479 ..... N89-27066 #
AD-A208481 ..... N89-27575 #
AD-A208482 ..... N89-27326 #
AD-A208483 ..... N89-26872 #
AD-A208484 ..... N89-26892 #
AD-A208485 ..... N89-27410 #
AD-A208487 ..... N89-27576 #
AD-A208502 ..... N89-27577 #
AD-A208530 ..... N89-27067 #
AD-A208536 ..... N89-27068 #
AD-A208546 ..... N89-26834 #
AD-A208563 ..... N89-27019 #
AD-A208747 ..... N89-27020 #
AD-A208752 ..... N89-27021 #
AD-A208753 ..... N89-27022 #
AD-A208754 ..... N89-27023 #
AD-A208755 ..... N89-27201 #
AD-A208758 ..... N89-27329 #
AD-A208763 ..... N89-27227 #
AD-A208764 ..... N89-26992 #
AD-A208785 ..... N89-27321 #

AD-D013972 ..... N89-26845
AD-D013974 ..... N89-27138
AD-D013975 ..... N89-27179
AD-D013978 ..... N89-27497
AD-D013979 ..... N89-27070
AD-D013980 ..... N89-27180
AD-D013986 ..... N89-27545
AD-D013990 ..... N89-27514
AD-D013994 ..... N89-27160
AD-D013999 ..... N89-27101
AD-D014002 ..... N89-26847
AD-D014003 ..... N89-26931
AD-D014019 ..... N89-27046
AD-D014044 ..... N89-26959
AD-D014045 ..... N89-26882
AD-D014047 ..... N89-27499
AD-D014050 ..... N89-27163
AD-D014051 ..... N89-26848
AD-D014053 ..... N89-27164
AD-D014054 ..... N89-26836
AD-D014056 ..... N89-27461
AD-D014057 ..... N89-27106
AD-D014058 ..... N89-26857

AD-D014064 ..... N89-26907
AD-D014065 ..... N89-26908
AD-D014066 ..... N89-26960
AD-D014067 ..... N89-26961
AD-D014068 ..... N89-27048
AD-D014069 ..... N89-27208
AD-D014070 ..... N89-27072
AD-D014071 ..... N89-26849
AD-D014072 ..... N89-27185
AD-D014073 ..... N89-26850
AD-D014074 ..... N89-26897
AD-D014075 ..... N89-26837
AD-D014079 ..... N89-27186
AD-D014080 ..... N89-27187
AD-D014081 ..... N89-27188
AD-D014105 ..... N89-27139
AD-D014106 ..... N89-27189
AD-D014111 ..... N89-26911
AD-D014113 ..... N89-27190
AD-D014115 ..... N89-26965
AD-D014116 ..... N89-26852
AD-D014119 ..... N89-27026
AD-D014120 ..... N89-27191
AD-D014122 ..... N89-27142
AD-D014123 ..... N89-26853
AD-D014125 ..... N89-27168 #
AD-D014126 ..... N89-27503 #
AD-D014133 ..... N89-27192
AD-D014137 ..... N89-26858

AD-E801886 ..... N89-27050 #
AD-E801886 ..... N89-27051 #
AD-E801886 ..... N89-27331 #
AD-E801886 ..... N89-27424 #
AD-E801886 ..... N89-27425 #
AD-E951322 ..... N89-27024 #
AD-E951328 ..... N89-27307 #
AD-E951331 ..... N89-27054 #
AD-E951331 ..... N89-27246 #
AD-E951334 ..... N89-27025 #
AD-E951337 ..... N89-27378 #

AERO-REPT-8804 ..... N89-27106 #

AFATL-TR-88-155 ..... N89-27425 #

AFGL-TR-88-0315 ..... N89-27284 #
AFGL-TR-88-0334 ..... N89-27283 #

AFIT/CI/CIA-88-202 ..... N89-27294 #
AFIT/CI/CIA-88-214 ..... N89-27295 #
AFIT/CI/CIA-88-216 ..... N89-27406 #

AFIT/DS/ENP/89-1 ..... N89-27502 #

AFIT/GCS/ENG/89J-1 ..... N89-27075 #

AFOSR-89-0263TR ..... N89-26927 #
AFOSR-89-0411TR ..... N89-27131 #
AFOSR-89-0413TR ..... N89-27161 #
AFOSR-89-0471TR ..... N89-26938 #
AFOSR-89-0534TR ..... N89-27430 #
AFOSR-89-0575TR ..... N89-27606 #
AFOSR-89-0592TR ..... N89-27379 #
AFOSR-89-0600TR ..... N89-27404 #
AFOSR-89-0609TR ..... N89-27599 #
AFOSR-89-0627TR ..... N89-27227 #
AFOSR-89-0650TR ..... N89-27134 #
AFOSR-89-0657TR ..... N89-27491 #
AFOSR-89-0659TR ..... N89-26856 #
AFOSR-89-0719TR ..... N89-27578 #
AFOSR-89-0733TR ..... N89-27135 #

AFWAL-TR-88-3017-VOL-2 ..... N89-26838 #
AFWAL-TR-88-2101 ..... N89-26937 #
AFWAL-TR-88-2141 ..... N89-26814 #
AFWAL-TR-88-4260 ..... N89-27464 #
AFWAL-TR-88-4262 ..... N89-26998 #

AGARD-AG-307 ..... N89-26854 #
AGARD-AG-308 ..... N89-27338 #

AGARD-AR-256 ..... N89-26817 #
AGARD-AR-257 ..... N89-27104 #

AGARD-R-758-ADD ..... N89-27330 #

AI-84-15-1 ..... N89-26944 #

AIAA-87-0751-CP ..... N89-26917* #
AIAA-89-2296 ..... N89-26876* #
AIAA-89-2492 ..... N89-26895* #
AIAA-89-2669 ..... N89-27103* #

AID-PN-AAZ-554 ..... N89-27233 #

AL-TR-89-001 ..... N89-26883 #

AMSMI/TR-RD-RE-88-6 ..... N89-27024 #
AMSMI/TR-RD-RE-89-1 ..... N89-27378 #
AMSMI/TR-RD-RE-89-3 ..... N89-27307 #
AMSMI/TR-RD-RE-89-4 ..... N89-27054 #

AMSMI/TR-RD-SS-88-10 ..... N89-27025 #

ANL-HEP-CP-89-50 ..... N89-27399 #

ANL-HEP-PR-89-45 ..... N89-27525 #

ANL-89/4 ..... N89-27092 #

ANL/EES-TM-371 ..... N89-27592 #

AQ-ES-175/88 ..... N89-27035 #

ARB-R-89/386 ..... N89-27313 #
ARB-R-89/390 ..... N89-27317 #

ARI-RP-89-06 ..... N89-27342 #

ARO-TCN-87-597 ..... N89-27320 #

ARO-89-1 ..... N89-27424 #

ASD-TR-88-5030 ..... N89-26848 #

ASTRON-7151-001 ..... N89-26856 #

AVSCOM-TM-89-B-005 ..... N89-27465* #
AVSCOM-TM-89-B-006 ..... N89-26843* #

AVSCOM-TR-87-C-26 ..... N89-27114* #

BHTI-699-099-286 ..... N89-26829 #

BIBOS-310/88 ..... N89-27105 #

BN-1093-PT-2 ..... N89-27429 #
BN-1094-1 ..... N89-27427 #
BN-1095-2 ..... N89-27428 #

BNL-42582 ..... N89-27155* #
BNL-42692 ..... N89-26970 #

BRL-MR-3757 ..... N89-26871 #

CAM-8809 ..... N89-27004 #
CAM-8901 ..... N89-27005 #

CDRL-0001AB ..... N89-26910 #

CERC-WIS-17 ..... N89-27323 #

CFD-21 ..... N89-27111* #

CHR/89-1909 ..... N89-26813 #

CMU/SEI-89-UG-1 ..... N89-27375 #

CNES-CT/DRT/TVE/IL-89-035 ..... N89-26889 #

CONF-861109-9 ..... N89-27143 #
CONF-880613-32 ..... N89-26970 #
CONF-880736-6 ..... N89-26867 #
CONF-880929-11 ..... N89-27512 #
CONF-881015-7 ..... N89-27493 #
CONF-881120-10 ..... N89-26968 #
CONF-890108-1 ..... N89-27002 #
CONF-890197-9 ..... N89-27169 #
CONF-890199-5 ..... N89-27454 #
CONF-890216-2 ..... N89-27582 #
CONF-890270-16 ..... N89-27559 #
CONF-890277-1 ..... N89-27209 #
CONF-890306-4 ..... N89-26913 #
CONF-890309-1 ..... N89-27195 #
CONF-890335-183 ..... N89-27171 #
CONF-890335-210 ..... N89-27525 #
CONF-890352-4 ..... N89-27240 #
CONF-890367-6 ..... N89-27475 #
CONF-890415-3 ..... N89-27399 #
CONF-890415-5 ..... N89-27400 #
CONF-890423-10 ..... N89-27172 #
CONF-890426-11 ..... N89-27555 #
CONF-890426-12 ..... N89-27553 #
CONF-890426-17 ..... N89-27557 #
CONF-890426-20 ..... N89-27508 #
CONF-890426-21 ..... N89-27568 #
CONF-890435-3 ..... N89-26951 #
CONF-890468-1 ..... N89-27543 #
CONF-890468-2 ..... N89-26969 #
CONF-890468-9 ..... N89-27563 #
CONF-890468-11 ..... N89-26985 #

CONF-890522-2 ..... N89-27415 #
CONF-890541-1 ..... N89-27008 #
CONF-890545-3 ..... N89-27355 #
CONF-890589-2 ..... N89-27308 #
CONF-890609-4 ..... N89-27037 #
CONF-890627-1 ..... N89-26916 #
CONF-890646-1 ..... N89-26966 #
CONF-890653-1 ..... N89-27006 #
CONF-890660-7 ..... N89-27057 #
CONF-890660-8 ..... N89-27059 #
CONF-890661-6-REV ..... N89-27027 #
CONF-890663-1 ..... N89-27561 #
CONF-890665-2 ..... N89-27080 #
CONF-890665-10 ..... N89-27082 #
CONF-890665-15 ..... N89-27084 #
CONF-890665-21 ..... N89-27093 #
CONF-890665-23 ..... N89-27535 #
CONF-890666-1 ..... N89-26948 #
CONF-890692-4-REV-1 ..... N89-27273 #
CONF-890692-5 ..... N89-27267 #
CONF-890692-6 ..... N89-27268 #
CONF-890693-1 ..... N89-27383 #
CONF-890693-2 ..... N89-27384 #
CONF-890694-1 ..... N89-27492 #
CONF-890702-3 ..... N89-27290 #
CONF-890703-2 ..... N89-27530 #
CONF-890705-2 ..... N89-26921 #
CONF-890710-1 ..... N89-27534 #
CONF-890710-14 ..... N89-27532 #
CONF-890716-3 ..... N89-27566 #
CONF-890716-4 ..... N89-27565 #
CONF-890716-5 ..... N89-27567 #
CONF-890721-1 ..... N89-26920 #
CONF-890721-5 ..... N89-27198 #
CONF-890721-8 ..... N89-27217 #
CONF-890721-9 ..... N89-26978 #
CONF-890721-11 ..... N89-26980 #
CONF-890721-12 ..... N89-27218 #
CONF-890721-20 ..... N89-27219 #
CONF-890721-22 ..... N89-26982 #
CONF-890721-24 ..... N89-27220 #
CONF-890721-25 ..... N89-27156 #
CONF-890721-26 ..... N89-26922 #
CONF-890721-30 ..... N89-27221 #
CONF-890723-1 ..... N89-27088 #
CONF-890723-2 ..... N89-27089 #
CONF-890723-3 ..... N89-27205 #
CONF-890723-4 ..... N89-27090 #
CONF-890723-5 ..... N89-27357 #
CONF-890739-1 ..... N89-26955 #
CONF-890741-1 ..... N89-27435 #
CONF-890742-1 ..... N89-27386 #
CONF-890744-2 ..... N89-27394 #
CONF-890748-3 ..... N89-26979 #
CONF-890748-4 ..... N89-27154 #
CONF-890748-5 ..... N89-27206 #
CONF-890748-6 ..... N89-27199 #
CONF-890748-7 ..... N89-26981 #
CONF-890748-9 ..... N89-27155* #
CONF-890752-1 ..... N89-27119 #
CONF-890752-2 ..... N89-27120 #
CONF-890752-3 ..... N89-27110 #
CONF-890768-1 ..... N89-27237 #
CONF-890768-3 ..... N89-27239 #
CONF-890769-2 ..... N89-27029 #
CONF-890769-3 ..... N89-27030 #
CONF-890772-1 ..... N89-26983 #
CONF-890772-2 ..... N89-27564 #
CONF-890773-1 ..... N89-27079 #
CONF-890779-1 ..... N89-27436 #
CONF-890780-1 ..... N89-27494 #
CONF-890781-2 ..... N89-27091 #
CONF-890783-1 ..... N89-26855 #
CONF-890784 ..... N89-27238 #
CONF-8708269-VOL-3 ..... N89-27615 #
CONF-8708269-VOL-4 ..... N89-27616 #
CONF-8803133-1 ..... N89-27515 #
CONF-8805294-SUMM ..... N89-27274 #
CONF-8807123-2 ..... N89-27455 #
CONF-8807160-1 ..... N89-26926 #
CONF-8808208-1 ..... N89-27350 #
CONF-8808233-1 ..... N89-27149 #
CONF-8809360-1 ..... N89-26984 #
CONF-8810117-2 ..... N89-26952 #
CONF-8810118-7 ..... N89-27453 #
CONF-8810118-8 ..... N89-27472 #
CONF-8810118-9 ..... N89-26953 #
CONF-8810126-VOL-1 ..... N89-27170 #
CONF-8810135-4 ..... N89-27077 #
CONF-8810176-5 ..... N89-27200 #
CONF-8810290-2 ..... N89-27003 #
CONF-8810341-2-REV-1 ..... N89-27276 #
CONF-8810376-1 ..... N89-27479 #
CONF-8811147-3 ..... N89-27474 #
CONF-8902100-2 ..... N89-27556 #
CONF-8903102-2 ..... N89-27546 #

CONF-8903109-4 ..... N89-26971 #
CONF-8903109-5 ..... N89-26972 #
CONF-8903111-3 ..... N89-27618 #
CONF-8903117-VUGRAPHS ..... N89-27251 #
CONF-8903131-2 ..... N89-27529 #
CONF-8903132-2 ..... N89-27614 #
CONF-8904107-3 ..... N89-27523 #
CONF-8904107-4 ..... N89-27531 #
CONF-8904107-5 ..... N89-27533 #
CONF-8904194-3 ..... N89-27593 #
CONF-8904210-5 ..... N89-27388 #
CONF-8904210-6 ..... N89-27358 #
CONF-8904216-1 ..... N89-27627 #
CONF-8904216-2 ..... N89-27628 #
CONF-8904216-4 ..... N89-27630 #
CONF-8904228-1 ..... N89-27175 #
CONF-8904233-1 ..... N89-27478 #
CONF-8905105-2 ..... N89-26941 #
CONF-8905118-8 ..... N89-27194 #
CONF-8905118-9 ..... N89-27193 #
CONF-8905118-10 ..... N89-26973 #
CONF-8905118-11 ..... N89-27211 #
CONF-8905118-12 ..... N89-26974 #
CONF-8905120-13 ..... N89-27521 #
CONF-8905120-14 ..... N89-27522 #
CONF-8905120-16 ..... N89-27520 #
CONF-8905133-2 ..... N89-27560 #
CONF-8905135-1 ..... N89-27056 #
CONF-8905148-1 ..... N89-27275 #
CONF-8905167-1 ..... N89-26967 #
CONF-8906118-1 ..... N89-27144 #
CONF-8906127-1 ..... N89-27552 #

CRC-APRAC-CAPE-30-81-07A ..... N89-26930 #

CRDEC-TR-050 ..... N89-27133 #

CRREL-89-4 ..... N89-27285 #

CSG-93 ..... N89-27071 #

CSL-TR-88-362 ..... N89-27370 #

CSSA-ASTRO-89-03 ..... N89-27629* #

CTIAC-84 ..... N89-26864 #

DC-106 ..... N89-27365 #

DEL-SG-07-89 ..... N89-27325 #

DE88-016235 ..... N89-27493 #
DE88-705974 ..... N89-26812 #
DE88-705978 ..... N89-27421 #
DE88-705980 ..... N89-27296 #
DE88-705986 ..... N89-27544 #
DE88-706310 ..... N89-27580 #
DE88-706312 ..... N89-27109 #
DE89-000553 ..... N89-26968 #
DE89-000754 ..... N89-26954 #
DE89-000839 ..... N89-27252 #
DE89-000850 ..... N89-27143 #
DE89-000859 ..... N89-27248 #
DE89-000876 ..... N89-27253 #
DE89-000888 ..... N89-27249 #
DE89-000891 ..... N89-27242 #
DE89-000926 ..... N89-27250 #
DE89-000954 ..... N89-27183 #
DE89-000978 ..... N89-27197 #
DE89-001525 ..... N89-27415 #
DE89-002536 ..... N89-26920 #
DE89-004933 ..... N89-27198 #
DE89-005918 ..... N89-27435 #
DE89-006510 ..... N89-26955 #
DE89-006543 ..... N89-27217 #
DE89-006725 ..... N89-27088 #
DE89-006742 ..... N89-27386 #
DE89-006765 ..... N89-27089 #
DE89-007419 ..... N89-27205 #
DE89-007515 ..... N89-27394 #
DE89-007823 ..... N89-26978 #
DE89-007835 ..... N89-26979 #
DE89-007985 ..... N89-27090 #
DE89-008029 ..... N89-27027 #
DE89-008111 ..... N89-27357 #
DE89-008196 ..... N89-26966 #
DE89-008242 ..... N89-27218 #
DE89-008580 ..... N89-27206 #
DE89-008684 ..... N89-27154 #
DE89-008710 ..... N89-27199 #
DE89-008735 ..... N89-26980 #
DE89-008801 ..... N89-26926 #
DE89-009325 ..... N89-27512 #
DE89-009327 ..... N89-27492 #
DE89-009333 ..... N89-27119 #
DE89-009334 ..... N89-27120 #
DE89-009397 ..... N89-27543 #
DE89-009407 ..... N89-27383 #
DE89-009618 ..... N89-26969 #
DE89-009726 ..... N89-27350 #
DE89-009792 ..... N89-27546 #
DE89-009831 ..... N89-26921 #
DE89-009946 ..... N89-26981 #
DE89-009969 ..... N89-27219 #
DE89-010037 ..... N89-27240 #
DE89-010156 ..... N89-27282 #
DE89-010179 ..... N89-26982 #
DE89-010319 ..... N89-27267 #
DE89-010324 ..... N89-27220 #
DE89-010369 ..... N89-27209 #
DE89-010409 ..... N89-27363 #
DE89-010437 ..... N89-27144 #
DE89-010538 ..... N89-27251 #
DE89-010553 ..... N89-26922 #
DE89-010555 ..... N89-27243 #
DE89-010556 ..... N89-27244 #
DE89-010569 ..... N89-27155* #
DE89-010640 ..... N89-27156 #
DE89-010677 ..... N89-27237 #
DE89-010679 ..... N89-27238 #
DE89-010944 ..... N89-26932 #
DE89-011168 ..... N89-27564 #
DE89-011174 ..... N89-27239 #
DE89-011181 ..... N89-26983 #
DE89-011192 ..... N89-27494 #
DE89-011233 ..... N89-27268 #
DE89-011375 ..... N89-27245 #
DE89-011404 ..... N89-27436 #
DE89-011512 ..... N89-27079 #
DE89-011575 ..... N89-27056 #
DE89-011840 ..... N89-27627 #
DE89-011858 ..... N89-27221 #
DE89-011873 ..... N89-26967 #
DE89-011881 ..... N89-26855 #
DE89-012239 ..... N89-27395 #
DE89-012255 ..... N89-27203 #
DE89-012286 ..... N89-27057 #
DE89-012288 ..... N89-27110 #
DE89-012293 ..... N89-27077 #
DE89-012302 ..... N89-27552 #
DE89-012338 ..... N89-27091 #
DE89-012403 ..... N89-27515 #
DE89-012416 ..... N89-27553 #
DE89-012419 ..... N89-27193 #
DE89-012421 ..... N89-27194 #
DE89-012426 ..... N89-27002 #
DE89-012508 ..... N89-27384 #
DE89-012510 ..... N89-27029 #
DE89-012570 ..... N89-27030 #
DE89-012582 ..... N89-27478 #
DE89-012608 ..... N89-26915 #
DE89-012615 ..... N89-27472 #
DE89-012617 ..... N89-27453 #
DE89-012621 ..... N89-27529 #
DE89-012636 ..... N89-26970 #
DE89-012657 ..... N89-27080 #
DE89-012665 ..... N89-27530 #
DE89-012701 ..... N89-27473 #
DE89-012734 ..... N89-27269 #
DE89-012740 ..... N89-27210 #
DE89-012764 ..... N89-27554 #
DE89-012795 ..... N89-27145 #
DE89-012796 ..... N89-27308 #
DE89-012799 ..... N89-27516 #
DE89-012804 ..... N89-27452 #
DE89-012811 ..... N89-27591 #
DE89-012823 ..... N89-27505 #
DE89-012835 ..... N89-27148 #
DE89-012836 ..... N89-27170 #
DE89-012840 ..... N89-27254 #
DE89-012845 ..... N89-27081 #
DE89-012852 ..... N89-27274 #
DE89-012869 ..... N89-27271 #
DE89-012877 ..... N89-27092 #
DE89-012930 ..... N89-27592 #
DE89-012946 ..... N89-26947 #
DE89-012952 ..... N89-27517 #
DE89-012959 ..... N89-27519 #
DE89-012977 ..... N89-27556 #
DE89-012979 ..... N89-26971 #
DE89-012981 ..... N89-26972 #
DE89-012982 ..... N89-27475 #
DE89-012983 ..... N89-27149 #
DE89-012992 ..... N89-26984 #
DE89-012998 ..... N89-27175 #
DE89-013010 ..... N89-26948 #
DE89-013012 ..... N89-27006 #
DE89-013046 ..... N89-27008 #
DE89-013049 ..... N89-27520 #
DE89-013073 ..... N89-27082 #
DE89-013087 ..... N89-27358 #
DE89-013102 ..... N89-27596 #
DE89-013116 ..... N89-27387 #
DE89-013124 ..... N89-27036 #
DE89-013148 ..... N89-27557 #
DE89-013150 ..... N89-27614 #
DE89-013185 ..... N89-27003 #
DE89-013260 ..... N89-27521 #
DE89-013262 ..... N89-27454 #
DE89-013263 ..... N89-27522 #
DE89-013299 ..... N89-27555 #
DE89-013315 ..... N89-27518 #
DE89-013329 ..... N89-26949 #
DE89-013335 ..... N89-27476 #
DE89-013344 ..... N89-27228 #
DE89-013347 ..... N89-27031 #
DE89-013374 ..... N89-27558 #
DE89-013381 ..... N89-27272 #
DE89-013391 ..... N89-27255 #
DE89-013392 ..... N89-26950 #
DE89-013410 ..... N89-27083 #
DE89-013427 ..... N89-27169 #
DE89-013431 ..... N89-27455 #
DE89-013432 ..... N89-27559 #
DE89-013442 ..... N89-27388 #
DE89-013455 ..... N89-27618 #
DE89-013461 ..... N89-27628 #
DE89-013467 ..... N89-27560 #
DE89-013469 ..... N89-27171 #
DE89-013482 ..... N89-26867 #
DE89-013496 ..... N89-27059 #
DE89-013497 ..... N89-27523 #
DE89-013516 ..... N89-27032 #
DE89-013520 ..... N89-27593 #
DE89-013537 ..... N89-26973 #
DE89-013543 ..... N89-27037 #
DE89-013545 ..... N89-26974 #
DE89-013548 ..... N89-27211 #
DE89-013560 ..... N89-27561 #
DE89-013574 ..... N89-26951 #
DE89-013623 ..... N89-26913 #
DE89-013626 ..... N89-27562 #
DE89-013628 ..... N89-26941 #
DE89-013639 ..... N89-27275 #
DE89-013640 ..... N89-27195 #
DE89-013641 ..... N89-27474 #
DE89-013656 ..... N89-26923 #
DE89-013681 ..... N89-27524 #
DE89-013703 ..... N89-26916 #
DE89-013730 ..... N89-27396 #
DE89-013763 ..... N89-27397 #
DE89-013778 ..... N89-27084 #
DE89-013779 ..... N89-27273 #
DE89-013784 ..... N89-27172 #
DE89-013785 ..... N89-27630 #
DE89-013795 ..... N89-26975 #
DE89-013802 ..... N89-27028 #
DE89-013807 ..... N89-27479 #
DE89-013814 ..... N89-27093 #
DE89-013958 ..... N89-27359 #
DE89-014024 ..... N89-27290 #
DE89-014179 ..... N89-27276 #
DE89-014188 ..... N89-27531 #
DE89-014282 ..... N89-27532 #
DE89-014290 ..... N89-27533 #
DE89-014291 ..... N89-27565 #
DE89-014292 ..... N89-27566 #
DE89-014304 ..... N89-27222 #
DE89-014308 ..... N89-27567 #
DE89-014482 ..... N89-27534 #
DE89-014485 ..... N89-27535 #
DE89-014490 ..... N89-27200 #
DE89-014498 ..... N89-26956 #
DE89-014575 ..... N89-27398 #
DE89-014595 ..... N89-27597 #
DE89-014597 ..... N89-27009 #
DE89-014636 ..... N89-27525 #
DE89-014640 ..... N89-27508 #
DE89-014642 ..... N89-27568 #
DE89-014643 ..... N89-26985 #
DE89-014665 ..... N89-27563 #
DE89-014670 ..... N89-27399 #
DE89-014677 ..... N89-26952 #
DE89-014679 ..... N89-26953 #
DE89-014687 ..... N89-27318 #
DE89-014696 ..... N89-26986 #
DE89-014699 ..... N89-27526 #
DE89-014715 ..... N89-27173 #
DE89-014734 ..... N89-26987 #
DE89-014789 ..... N89-26988 #
DE89-014807 ..... N89-27150 #
DE89-014811 ..... N89-27355 #
DE89-014812 ..... N89-27437 #
DE89-014813 ..... N89-27438 #
DE89-014815 ..... N89-27400 #
DE89-609828 ..... N89-27615 #
DE89-609850 ..... N89-27616 #

DIA-DST-2700Z-006-88 ..... N89-27177 #

DMI-GEOPHYS-PAPERS-R-78 ..... N89-27292 #

DOE/CE-15219/T4 ..... N89-27245 #

DOE/CH-10093/44 ..... N89-27248 #

DOE/ER-0411 ..... N89-27271 #
DOE/ER-01198/T34 ..... N89-26932 #
DOE/ER-03130/48C ..... N89-27359 #
DOE/ER-13544/T2 ..... N89-26956 #
DOE/ER-13774/T1 ..... N89-26947 #
DOE/ER-13796/3 ..... N89-27237 #
DOE/ER-13796/6 ..... N89-27238 #
DOE/ER-25026/29 ..... N89-27437 #
DOE/ER-25026/30 ..... N89-27438 #
DOE/ER-40235/T5 ..... N89-27473 #
DOE/ER-40306/1 ..... N89-27036 #
DOE/ER-40465/T1 ..... N89-27515 #
DOE/ER-45080/T3 ..... N89-26986 #
DOE/ER-45359/1 ..... N89-27554 #
DOE/ER-52147/2 ..... N89-27173 #
DOE/ER-53175/T1 ..... N89-27524 #
DOE/ER-53207/4 ..... N89-27517 #

DOE/ET-53088/372 ..... N89-27518 #

DOE/MC-23167/2678-VOL-2 ..... N89-27183 #
DOE/MC-23258/2693 ..... N89-27197 #
DOE/MC-24261/2672 ..... N89-27250 #

DOE/NV-10571/T2 ..... N89-27526 #

DOE/OR-00033/T417 ..... N89-27262 #

DOE/PC-70780/T10 ..... N89-27028 #
DOE/PC-88827/T2 ..... N89-27032 #

DOT/FAA/AM-89/3 ..... N89-26830 #

DOT/FAA/CT-TN88/22 ..... N89-26831 #
DOT/FAA/CT-TN89/13 ..... N89-27047 #
DOT/FAA/CT-TN89/37 ..... N89-26833 #
DOT/FAA/CT-TN89/38 ..... N89-26832* #
DOT/FAA/CT-TN89/45 ..... N89-26868 #

DOT/FAA/CT-89/5 ..... N89-26851 #

DP-MS-88-240 ..... N89-27363 #

DTRC/TM-27-88-56 ..... N89-27426 #

E-3727 ..... N89-27114* #
E-4657 ..... N89-26903* #
E-4696 ..... N89-26877* #
E-4822 ..... N89-26895* #
E-4841 ..... N89-27121* #
E-4865 ..... N89-27623* #
E-4866 ..... N89-27619* #
E-4874 ..... N89-26919* #
E-4875 ..... N89-26912* #
E-4881 ..... N89-27506* #
E-4903 ..... N89-27038* #
E-4936 ..... N89-27103* #
E-4941 ..... N89-27115* #
E-4964 ..... N89-27223* #
E-4973 ..... N89-26887* #
E-4976 ..... N89-26876* #
E-4982 ..... N89-26924* #
E-5017 ..... N89-26904* #
E-5041 ..... N89-26889* #
E-5046 ..... N89-26906* #

ECAO-R-0223 ..... N89-27258 #

ECS-SS1323 ..... N89-26901* #

EGG-M-20887 ..... N89-27350 #

EOSR-1608-VOL-2 ..... N89-27073 #

EPA/SW/DK-89/019A ..... N89-27261 #

EPA/450/4-88/021-VOL-1 ..... N89-27264 #
EPA/600/D-88/239 ..... N89-27258 #
EPA/600/D-88/273 ..... N89-27259 #
EPA/600/D-88/274 ..... N89-27260 #
EPA/600/D-89/012 ..... N89-27270 #
EPA/600/3-89/025 ..... N89-27299 #
EPA/600/3-89/036 ..... N89-27147 #
EPA/600/4-88/033A ..... N89-27261 #

ERIM-202-800-1-T ..... N89-27067 #

ESA-CR(P)-2714 ..... N89-27035 #

ESD-TR-89-15 ..... N89-27375 #

ETL-0522 ..... N89-26834 #

ETN-89-94256 ..... N89-27578 #
ETN-89-94294 ..... N89-27547 #
ETN-89-94385 ..... N89-27122 #
ETN-89-94403 ..... N89-27105 #
ETN-89-94427 ..... N89-26874 #
ETN-89-94451 ..... N89-27035 #
ETN-89-94566 ..... N89-27127 #
ETN-89-94571 ..... N89-27536
ETN-89-94573 ..... N89-27094
ETN-89-94574 ..... N89-27480
ETN-89-94575 ..... N89-27537
ETN-89-94576 ..... N89-27538
ETN-89-94577 ..... N89-27539
ETN-89-94578 ..... N89-27540
ETN-89-94579 ..... N89-27541
ETN-89-94607 ..... N89-27481 #
ETN-89-94615 ..... N89-26862 #
ETN-89-94617 ..... N89-26890 #
ETN-89-94618 ..... N89-26891 #
ETN-89-94629 ..... N89-27065 #
ETN-89-94654 ..... N89-27157 #
ETN-89-94687 ..... N89-27617 #
ETN-89-94688 ..... N89-27485 #
ETN-89-94689 ..... N89-27583 #
ETN-89-94690 ..... N89-27581 #
ETN-89-94691 ..... N89-27441 #
ETN-89-94692 ..... N89-27442 #
ETN-89-94693 ..... N89-27224 #
ETN-89-94694 ..... N89-27584 #
ETN-89-94695 ..... N89-27585 #
ETN-89-94696 ..... N89-27327 #
ETN-89-94697 ..... N89-27326 #
ETN-89-94714 ..... N89-27582 #
ETN-89-94715 ..... N89-27449 #
ETN-89-94718 ..... N89-27126 #
ETN-89-94719 ..... N89-27586 #
ETN-89-94730 ..... N89-27443 #
ETN-89-94731 ..... N89-27587 #
ETN-89-94732 ..... N89-27042 #
ETN-89-94733 ..... N89-27486 #
ETN-89-94734 ..... N89-27569 #
ETN-89-94735 ..... N89-27487 #
ETN-89-94736 ..... N89-27482 #
ETN-89-94737 ..... N89-27488 #
ETN-89-94738 ..... N89-27496 #
ETN-89-94739 ..... N89-27489 #
ETN-89-94740 ..... N89-27483 #
ETN-89-94741 ..... N89-27158 #
ETN-89-94742 ..... N89-27484 #
ETN-89-94743 ..... N89-27159 #
ETN-89-94744 ..... N89-27631 #
ETN-89-94745 ..... N89-27620 #
ETN-89-94746 ..... N89-27360 #
ETN-89-94747 ..... N89-27291 #
ETN-89-94748 ..... N89-27490 #
ETN-89-94762 ..... N89-27439 #
ETN-89-94763 ..... N89-27440 #
ETN-89-94764 ..... N89-27401 #
ETN-89-94765 ..... N89-27402 #
ETN-89-94766 ..... N89-27414 #
ETN-89-94768 ..... N89-27403 #
ETN-89-94778 ..... N89-27498 #
ETN-89-94799 ..... N89-27495 #
ETN-89-94800 ..... N89-27509 #
ETN-89-94801 ..... N89-27095 #
ETN-89-94802 ..... N89-26827 #
ETN-89-94803 ..... N89-27570
ETN-89-94806 ..... N89-27277 #
ETN-89-94807 ..... N89-27571 #
ETN-89-94808 ..... N89-26889 #
ETN-89-94809 ..... N89-27123 #
ETN-89-94810 ..... N89-27124 #
ETN-89-94811 ..... N89-27125 #
ETN-89-94812 ..... N89-27450 #
ETN-89-94813 ..... N89-27126 #
ETN-89-94814 ..... N89-27319 #
ETN-89-94852 ..... N89-27176 #
ETN-89-94859 ..... N89-26957 #
ETN-89-94889 ..... N89-27551 #
ETN-89-94896 ..... N89-27431 #
ETN-89-94910 ..... N89-27432 #
ETN-89-94922 ..... N89-27129 #
ETN-89-94924 ..... N89-27292 #
ETN-89-94925 ..... N89-27293 #
ETN-89-94926 ..... N89-27626 #
ETN-89-94940 ..... N89-26870 #
ETN-89-94941 ..... N89-27542 #
ETN-89-94942 ..... N89-27458 #
ETN-89-94945 ..... N89-27130 #
ETN-89-94955 ..... N89-27108 #
ETN-89-94964 ..... N89-27444
ETN-89-94965 ..... N89-27010

EUT-88-E-190 ..... N89-27498 #

FCC/DF/MT-89/005A ..... N89-27595 #

FERMILAB-PUB-89/126-A-PAPER-1 ..... N89-27608* #

FEW-350 ..... N89-27588 #

FFA-TN-1988-58 ..... N89-27130 #

FNAL/C-89/112-A ..... N89-27614 #
FNAL/C-89/118 ..... N89-27355 #
FNAL/C-89/125-T ..... N89-27400 #

FOA-C-50065-5.1 ..... N89-27343 #

FTD-ID(RS)T-0942-88 ..... N89-26807 #

GA-C19612 ..... N89-27053 #

GRI-88/0160 ..... N89-27255 #
GRI-88/0172 ..... N89-26997 #
GRI-88/0249 ..... N89-27590 #
GRI-88/0274 ..... N89-27178 #
GRI-88/0284 ..... N89-26946 #
GRI-88/0290 ..... N89-27005 #
GRI-88/0297 ..... N89-26929 #
GRI-88/0331 ..... N89-27184 #
GRI-88/0356 ..... N89-27004 #
GRI-89/0007 ..... N89-26943 #
GRI-89/0037 ..... N89-27196 #
GRI-89/0056 ..... N89-26944 #
GRI-89/0060 ..... N89-27254 #
GRI-89/0061 ..... N89-27086 #
GRI-89/0064 ..... N89-27153 #
GRI-89/0122 ..... N89-27604 #

H-1436 ..... N89-26860* #
H-1479 ..... N89-27213* #
H-1497 ..... N89-27416* #
H-1501 ..... N89-27393* #
H-1510 ..... N89-26844* #

HDL-CR-88-042-1 ..... N89-27076 #

HTL-51 ..... N89-27111* #

IAEA-CN-50/B272 ..... N89-27493 #

IC-88/140 ..... N89-26812 #
IC-88/242 ..... N89-27421 #
IC-88/294 ..... N89-27296 #
IC-88/336 ..... N89-27544 #

ICASE-88-21 ..... N89-27362* #
ICASE-88-50 ..... N89-27420* #
ICASE-89-32-PT-3 ..... N89-27112* #
ICASE-89-33 ..... N89-27390* #
ICASE-89-38 ..... N89-27113* #
ICASE-89-40 ..... N89-27349* #

ICMA-89-131 ..... N89-27377 #

ICOMP-89-16 ..... N89-27115* #

IFSR-372 ..... N89-27518 #

IMFL-86/20 ..... N89-27125 #
IMFL-88/33 ..... N89-27124 #
IMFL-4107 ..... N89-27125 #

INIS-MF-11400-VOL-3 ..... N89-27615 #
INIS-MF-11401-VOL-4 ..... N89-27616 #

INPE-4449-TDL/314 ..... N89-27366 #
INPE-4638-TDL/337 ..... N89-27367 #
INPE-4648-TDL/338 ..... N89-27609 #
INPE-4715-PRE/1395 ..... N89-27315 #
INPE-4724-PRE/1401 ..... N89-27301 #
INPE-4737-PRE/1412 ..... N89-27382 #
INPE-4743-PRE/1417 ..... N89-27085 #
INPE-4744-PRE/1418 ..... N89-26884 #
INPE-4745-PRE/1419 ..... N89-27381 #
INPE-4749-PRE/1422 ..... N89-27385 #
INPE-4754-PRE/1426 ..... N89-27236 #
INPE-4765-PRE/1434 ..... N89-27380 #
INPE-4768-PRE/1437 ..... N89-27055 #
INPE-4772-PRE/1441 ..... N89-26886 #
INPE-4774-PRE/1443 ..... N89-26875 #
INPE-4776-PRE/1445 ..... N89-27392 #
INPE-4779-RPE/581 ..... N89-27061 #
INPE-4805-RPE/588 ..... N89-27391 #

IPP-III/67 ..... N89-27094
IPP-III/142 ..... N89-27480

IPP-2/297 N89-27536
IPP-5/25 N89-27537
IPP-5/27 N89-27538
IPP-6/271 N89-27539
IPP-6/278 N89-27540
IPP-6/279 N89-27541

IPPJ-898 N89-27511 #
IPPJ-909 N89-27527 #
IPPJ-910 N89-27528 #

IRF-PREPRINT-111 N89-27542 #

IRIS-248 N89-26834 #

ISBN-82-595-5290-6 N89-27102 #
ISBN-87-550-1431-3 N89-27305 #
ISBN-87-7478-285-1 N89-27292 #
ISBN-87-7478-287-8 N89-27293 #
ISBN-90-353-0070-X N89-27422 #
ISBN-90-365-0216-0 N89-27401 #
ISBN-90-365-0220-9 N89-27439 #
ISBN-90-365-0223-3 N89-27403 #
ISBN-90-370-0018-5 N89-27570
ISBN-90-6144-190-0 N89-27498 #
ISBN-92-835-0497-6 N89-27330 #
ISBN-92-835-0504-2 N89-27104 #
ISBN-92-835-0508-5 N89-26854 #
ISBN-92-835-0510-7 N89-27338 #
ISBN-92-835-0516-6 N89-26817 #
ISBN-951-38-3351-8 N89-27129 #
ISBN-951-42-0965-6 N89-26975 #
ISBN-951-754-628-0 N89-27044 #
ISBN-951-754-677-7 N89-27621 #
ISBN-951-754-704-8 N89-27513 #
ISBN-951-754-706-4 N89-27045 #

ISI/RR-88-228 N89-27364* #

ISL-CO-214/88 N89-27176 #

ISL-PU-306/88 N89-26957 #

ISSN-0038-0911 N89-27624 #
ISSN-0038-0911 N89-27625 #
ISSN-0078-3781 N89-27126 #
ISSN-0078-3781 N89-27319 #
ISSN-0078-3781 N89-27450 #
ISSN-0109-6605 N89-27069 #
ISSN-0143-7313 N89-27010
ISSN-0167-8590 N89-27422 #
ISSN-0167-9708 N89-27496 #
ISSN-0173-6256 N89-27481 #
ISSN-0262-5369 N89-27444
ISSN-0284-169X N89-27458 #
ISSN-0347-7665 N89-27343 #
ISSN-0356-5077 N89-27129 #
ISSN-0389-4010 N89-26835 #
ISSN-0389-4010 N89-26893 #
ISSN-0418-6435 N89-27305 #
ISSN-0436-1199 N89-27122 #
ISSN-0436-1199 N89-27127 #
ISSN-0469-4732 N89-27511 #
ISSN-0783-8751 N89-27621 #
ISSN-0784-848X N89-27045 #
ISSN-0922-5641 N89-27431 #
ISSN-0922-5641 N89-27432 #

ISU-ERI-AMES-90030 N89-27111* #

JIAA-TR-89 N89-26866* #

JINR-E-4-88-40 N89-27580 #
JINR-E-8-88-361 N89-27109 #

JSR-88-130 N89-27326 #

K/D-5694 N89-27269 #

K/DSRD-96 N89-27596 #

K511-3 N89-26883 #

L-16493 N89-26810* #
L-16558 N89-26811* #

LA-UR-88-2743 N89-27493 #
LA-UR-89-5 N89-27217 #
LA-UR-89-490 N89-27090 #
LA-UR-89-760 N89-27383 #
LA-UR-89-825 N89-27543 #
LA-UR-89-1178 N89-27494 #
LA-UR-89-1241 N89-26983 #
LA-UR-89-1305 N89-27239 #
LA-UR-89-1423 N89-27564 #
LA-UR-89-1593 N89-27529 #
LA-UR-89-1604 N89-27453 #
LA-UR-89-1607 N89-27472 #
LA-UR-89-1693 N89-27388 #
LA-UR-89-1751 N89-27478 #
LA-UR-89-1760 N89-27628 #
LA-UR-89-1793 N89-27618 #
LA-UR-89-1836 N89-27171 #
LA-UR-89-1852 N89-27560 #
LA-UR-89-1928 N89-27290 #
LA-UR-89-2059 N89-27567 #
LA-UR-89-2141 N89-27566 #
LA-UR-89-2142 N89-27565 #
LA-UR-89-2144 N89-27533 #
LA-UR-89-2164 N89-27532 #

LA-11557-MS N89-27452 #
LA-11577-MS N89-26923 #

LAIR-372 N89-27331 #

LBL-25492 N89-27255 #
LBL-25716 N89-27274 #
LBL-25722 N89-27558 #
LBL-25735 N89-27455 #
LBL-25831 N89-26968 #
LBL-26166 N89-26972 #
LBL-26254 N89-27083 #
LBL-26259 N89-26950 #
LBL-26651 N89-26971 #
LBL-26783-VOL-1 N89-27170 #
LBL-26900 N89-27475 #
LBL-26923 N89-27081 #
LBL-26942 N89-26984 #
LBL-26953 N89-27148 #
LBL-27025 N89-27254 #
LBL-27034 N89-27175 #
LBL-27040 N89-27149 #
LBL-27059 N89-27169 #
LBL-27062 N89-27559 #
LBL-27064 N89-27556 #

LC-79-640375 N89-27624 #
LC-79-640375 N89-27625 #
LC-88-600047 N89-27278 #
LC-89-060510 N89-27601 #

LIR/1-89/331-VOL-1 N89-27266 #

LISS-25 N89-27446 #
LISS-31 N89-27050 #
LISS-32 N89-27051 #
LISS-33 N89-27447 #

LMSC-HEC-TR-F268584-VOL-7 N89-26894* #

M-815 N89-27039* #

MBB-UK-0024/88-PUB N89-26891 #

MBB-UO-0039/88-PUB N89-26890 #

MBB-UT-122/88 N89-26862 #

MDC-QA026 N89-27134 #

MD89-04-IB-TJ-PT-2 N89-27429 #
MD89-09-RCM-IB-1 N89-27427 #
MD89-10-RCM-IB-2 N89-27426 #

MEMO-INF-87-4 N89-27402 #
MEMO-INF-88-44 N89-27439 #
MEMO-INF-88-45 N89-27440 #
MEMO-INF-88-46 N89-27401 #
MEMO-INF-88-47 N89-27402 #
MEMO-INF-88-48 N89-27414 #
MEMO-INF-88-50 N89-27403 #

MIT/LCS/TR-432-VOL-1 N89-27354 #

MITSG-89-4 N89-27041 #

MLM-3951(OP) N89-26987 #

MMS/GM-88/0064 N89-27311 #

MPIS-8/1988 N89-27122 #
MPIS-11/1988 N89-27127 #

MTL-TR-89-14 N89-27501 #
MTL-TR-89-16 N89-26909 #
MTL-TR-89-25 N89-27463 #
MTL-TR-89-30 N89-26925 #
MTL-TR-89-31 N89-26964 #
MTL-TR-89-36 N89-27201 #

NADC-88105-60 N89-26828 #
NADC-88141-60-VOL-1 N89-27225 #
NADC-88141-60-VOL-2 N89-27226 #

NAL-TR-958 N89-26835 #
NAL-TR-992 N89-26893 #

NAPC-PE-184 N89-26851 #

NAS 1.15:4124 N89-26810* #
NAS 1.15:4125 N89-27213* #
NAS 1.15:4132 N89-27269* #
NAS 1.15:89722 N89-27229* #
NAS 1.15:100093 N89-26816* #
NAS 1.15:100370 N89-27316* #
NAS 1.15:100631 N89-27001* #
NAS 1.15:100732 N89-27279* #
NAS 1.15:100738 N89-26902* #
NAS 1.15:100742 N89-27314* #
NAS 1.15:100744 N89-27456* #
NAS 1.15:100745 N89-26918* #
NAS 1.15:101055 N89-27117* #
NAS 1.15:101513 N89-26878* #
NAS 1.15:101576 N89-27467* #
NAS 1.15:101580 N89-27212* #
NAS 1.15:101603 N89-26888* #
NAS 1.15:101609 N89-27060* #
NAS 1.15:101614 N89-27063* #
NAS 1.15:101619 N89-26843* #
NAS 1.15:101624 N89-27465* #
NAS 1.15:101628 N89-27504* #
NAS 1.15:101631 N89-26861* #
NAS 1.15:101635 N89-27151* #
NAS 1.15:101636 N89-27215* #
NAS 1.15:101781 N89-26873* #
NAS 1.15:101992 N89-26877* #
NAS 1.15:102065 N89-26895* #
NAS 1.15:102084 N89-26912* #
NAS 1.15:102099 N89-27121* #
NAS 1.15:102102 N89-27619* #
NAS 1.15:102107 N89-26919* #
NAS 1.15:102111 N89-27506* #
NAS 1.15:102123 N89-27038* #
NAS 1.15:102138 N89-27103* #
NAS 1.15:102142 N89-27115* #
NAS 1.15:102213 N89-27433* #
NAS 1.15:102217 N89-26808* #
NAS 1.15:102295 N89-27223* #
NAS 1.15:102297 N89-26887* #
NAS 1.15:102298 N89-26876* #
NAS 1.15:102299 N89-27623* #
NAS 1.15:102302 N89-26924* #
NAS 1.15:102309 N89-27114* #
NAS 1.15:102321 N89-26904* #
NAS 1.15:102332 N89-26909* #
NAS 1.15:102337 N89-26906* #
NAS 1.26:4111 N89-26860* #
NAS 1.26:4160 N89-27393* #
NAS 1.26:4161 N89-27416* #
NAS 1.26:177534 N89-27346* #
NAS 1.26:178409 N89-26842* #
NAS 1.26:181516 N89-27034* #
NAS 1.26:181789 N89-27466* #
NAS 1.26:181792 N89-27468* #
NAS 1.26:181817 N89-26841* #
NAS 1.26:181841 N89-26815* #
NAS 1.26:181847 N89-27390* #
NAS 1.26:181855 N89-27112* #
NAS 1.26:181858 N89-27348* #
NAS 1.26:181861 N89-27113* #
NAS 1.26:181863 N89-27349* #
NAS 1.26:181866 N89-26917* #
NAS 1.26:181868 N89-26869* #
NAS 1.26:181874 N89-27413* #
NAS 1.26:182263 N89-26903* #
NAS 1.26:182274 N89-27204* #
NAS 1.26:182275 N89-26899* #
NAS 1.26:182280 N89-26905*
NAS 1.26:183436 N89-27361* #
NAS 1.26:183670 N89-26894* #
NAS 1.26:183702 N89-26901* #
NAS 1.26:183715 N89-26900* #
NAS 1.26:183718 N89-26885* #
NAS 1.26:184707 N89-26896* #
NAS 1.26:184800 N89-27155* #
NAS 1.26:185034 N89-27434* #
NAS 1.26:185098 N89-27111* #
NAS 1.26:185114 N89-27152* #
NAS 1.26:185117 N89-27256* #
NAS 1.26:185124 N89-26879* #
NAS 1.26:185126 N89-26880* #
NAS 1.26:185335 N89-27364* #
NAS 1.26:185353 N89-27608* #
NAS 1.26:185472 N89-26866* #
NAS 1.26:185473 N89-27235* #
NAS 1.26:185490 N89-26859* #
NAS 1.26:185491 N89-26885* #

NAS 1.26:185501 ..... N89-27477* #
NAS 1.26:185509 ..... N89-27288* #
NAS 1.26:185715 ..... N89-26832* #
NAS 1.26:185718 ..... N89-27281* #
NAS 1.26:185719 ..... N89-27257* #
NAS 1.26:185720 ..... N89-27344* #
NAS 1.26:185819 ..... N89-26826* #
NAS 1.26:185825 ..... N89-27420* #
NAS 1.26:185826 ..... N89-27362* #
NAS 1.26:185833 ..... N89-27629* #
NAS 1.26:185836 ..... N89-27062* #
NAS 1.26:185847 ..... N89-27118* #
NAS 1.26:185848 ..... N89-27064* #
NAS 1.26:185864 ..... N89-27469* #
NAS 1.60:2914 ..... N89-27116* #
NAS 1.60:2923 ..... N89-26844* #
NAS 1.60:2929 ..... N89-26811* #
NAS 1.60:2934 ..... N89-26976* #
NAS 1.60:2935 ..... N89-27214* #
NAS 1.60:2936 ..... N89-27039* #
NAS 1.61:1227 ..... N89-27302* #
NAS 1.61:1229 ..... N89-27612* #

NASA-CR-4111 ..... N89-26860* #
NASA-CR-4160 ..... N89-27393* #
NASA-CR-4161 ..... N89-27416* #
NASA-CR-177534 ..... N89-27346* #
NASA-CR-178409 ..... N89-26842* #
NASA-CR-181516 ..... N89-27034* #
NASA-CR-181789 ..... N89-27466* #
NASA-CR-181792 ..... N89-27468* #
NASA-CR-181817 ..... N89-26841* #
NASA-CR-181841 ..... N89-26815* #
NASA-CR-181847 ..... N89-27390* #
NASA-CR-181855 ..... N89-27112* #
NASA-CR-181858 ..... N89-27348* #
NASA-CR-181861 ..... N89-27113* #
NASA-CR-181863 ..... N89-27349* #
NASA-CR-181866 ..... N89-26917* #
NASA-CR-181868 ..... N89-26869* #
NASA-CR-181874 ..... N89-27413* #
NASA-CR-182263 ..... N89-26903* #
NASA-CR-182274 ..... N89-27204* #
NASA-CR-182275 ..... N89-26899* #
NASA-CR-182280 ..... N89-26905*
NASA-CR-183436 ..... N89-27361* #
NASA-CR-183670 ..... N89-26894* #
NASA-CR-183702 ..... N89-26901* #
NASA-CR-183715 ..... N89-26900* #
NASA-CR-183718 ..... N89-26885* #
NASA-CR-184707 ..... N89-26896* #
NASA-CR-184800 ..... N89-27155* #
NASA-CR-185034 ..... N89-27434* #
NASA-CR-185098 ..... N89-27111* #
NASA-CR-185114 ..... N89-27152* #
NASA-CR-185117 ..... N89-27256* #
NASA-CR-185124 ..... N89-26879* #
NASA-CR-185126 ..... N89-26880* #
NASA-CR-185335 ..... N89-27364* #
NASA-CR-185353 ..... N89-27608* #
NASA-CR-185472 ..... N89-26866* #
NASA-CR-185473 ..... N89-27235* #
NASA-CR-185490 ..... N89-26859* #
NASA-CR-185491 ..... N89-26865* #
NASA-CR-185501 ..... N89-27477* #
NASA-CR-185509 ..... N89-27288* #
NASA-CR-185715 ..... N89-26832* #
NASA-CR-185718 ..... N89-27281* #
NASA-CR-185719 ..... N89-27257* #
NASA-CR-185720 ..... N89-27344* #
NASA-CR-185819 ..... N89-26826* #
NASA-CR-185825 ..... N89-27420* #
NASA-CR-185826 ..... N89-27362* #
NASA-CR-185833 ..... N89-27629* #
NASA-CR-185836 ..... N89-27062* #
NASA-CR-185847 ..... N89-27118* #
NASA-CR-185848 ..... N89-27064* #
NASA-CR-185864 ..... N89-27469* #

NASA-RP-1227 ..... N89-27302* #
NASA-RP-1229 ..... N89-27612* #

NASA-TM-4124 ..... N89-26810* #
NASA-TM-4125 ..... N89-27213* #
NASA-TM-4132 ..... N89-27289* #
NASA-TM-89722 ..... N89-27229* #
NASA-TM-100093 ..... N89-26816* #
NASA-TM-100370 ..... N89-27316* #
NASA-TM-100631 ..... N89-27001* #
NASA-TM-100732 ..... N89-27279* #
NASA-TM-100738 ..... N89-26902* #
NASA-TM-100742 ..... N89-27314* #
NASA-TM-100744 ..... N89-27456* #
NASA-TM-100745 ..... N89-26918* #
NASA-TM-101055 ..... N89-27117* #
NASA-TM-101513 ..... N89-26878* #
NASA-TM-101576 ..... N89-27467* #
NASA-TM-101580 ..... N89-27212* #
NASA-TM-101603 ..... N89-26888* #
NASA-TM-101609 ..... N89-27060* #
NASA-TM-101614 ..... N89-27063* #
NASA-TM-101619 ..... N89-26843* #
NASA-TM-101624 ..... N89-27465* #
NASA-TM-101628 ..... N89-27504* #
NASA-TM-101631 ..... N89-26861* #
NASA-TM-101635 ..... N89-27151* #
NASA-TM-101636 ..... N89-27215* #
NASA-TM-101781 ..... N89-26873* #
NASA-TM-101992 ..... N89-26877* #
NASA-TM-102065 ..... N89-26895* #
NASA-TM-102094 ..... N89-26912* #
NASA-TM-102099 ..... N89-27121* #
NASA-TM-102102 ..... N89-27619* #
NASA-TM-102107 ..... N89-26919* #
NASA-TM-102111 ..... N89-27506* #
NASA-TM-102123 ..... N89-27038* #
NASA-TM-102138 ..... N89-27103* #
NASA-TM-102142 ..... N89-27115* #
NASA-TM-102213 ..... N89-27433* #
NASA-TM-102217 ..... N89-26808* #
NASA-TM-102295 ..... N89-27223* #
NASA-TM-102297 ..... N89-26887* #
NASA-TM-102298 ..... N89-26876* #
NASA-TM-102299 ..... N89-27623* #
NASA-TM-102302 ..... N89-26924* #
NASA-TM-102309 ..... N89-27114* #
NASA-TM-102321 ..... N89-26904* #
NASA-TM-102332 ..... N89-26889* #
NASA-TM-102337 ..... N89-26906* #

NASA-TP-2914 ..... N89-27116* #
NASA-TP-2923 ..... N89-26844* #
NASA-TP-2929 ..... N89-26811* #
NASA-TP-2934 ..... N89-26976* #
NASA-TP-2935 ..... N89-27214* #
NASA-TP-2936 ..... N89-27039* #

NASA-89-001 ..... N89-27062* #

NAV-0125-FM-8945-182 ..... N89-26910 #

NBSIR-87/3081-PT-2 ..... N89-27043 #
NBSIR-88/3091 ..... N89-27457 #
NBSIR-88/3092 ..... N89-27507 #
NBSIR-88/3710 ..... N89-26994 #

NCAR/CT-117 ..... N89-27309 #

NCEL-CR-89.007 ..... N89-27324 #

NCG-89-3 ..... N89-27438 #

NEAR-TR-402 ..... N89-27107 #

NEPRF-TR-89-05 ..... N89-27306 #

NIKHEF-H/88-17 ..... N89-27578 #

NIPER-403 ..... N89-26954 #

NIST/GCR-89/559 ..... N89-27100 #
NIST/GCR-89/560 ..... N89-26945 #

NIST/SP-761 ..... N89-27594 #

NISTIR-88/3099 ..... N89-26977 #
NISTIR-88/3722 ..... N89-27005 #
NISTIR-88/3808 ..... N89-27174 #
NISTIR-88/3817 ..... N89-26995 #
NISTIR-88/3842 ..... N89-26993 #
NISTIR-88/4016 ..... N89-26914 #
NISTIR-88/4018 ..... N89-26996 #
NISTIR-89/4023 ..... N89-27389 #
NISTIR-89/4025 ..... N89-26928 #
NISTIR-89/4038 ..... N89-27182 #
NISTIR-89/4045 ..... N89-27040 #
NISTIR-89/4047 ..... N89-27137 #
NISTIR-89/4051 ..... N89-26942 #
NISTIR-89/4057 ..... N89-27078 #
NISTIR-89/4060 ..... N89-27602 #
NISTIR-89/4063 ..... N89-27356 #
NISTIR-89/4073 ..... N89-27007 #
NISTIR-89/4076 ..... N89-27087 #

NOAA-DR-ERL-ARL-16 ..... N89-27280 #

NOAA-NERDIS-89/05-VOL-1 ..... N89-27231 #

NOAA-NESDIS-89/03-VOL-1 ..... N89-27230 #
NOAA-NESDIS-89/05-VOL-2 ..... N89-27232 #

NOAA-TM-ERL-AOML-67 ..... N89-27322 #

NOAA-TM-ERL-WPL-156 ..... N89-27257* #
NOAA-TM-ERL-WPL-157 ..... N89-27298 #
NOAA-TM-ERL-WPL-159 ..... N89-27261* #
NOAA-TM-ERL-WPL-160 ..... N89-27460 #

NOAA-TM-NWS-NSSFC-21 ..... N89-27297 #

NOAA-TM-NWS-SR-124 ..... N89-27312 #

NORDA-JA-321-061-88 ..... N89-27234 #

NOTA-INTERNA-912 ..... N89-27587 #
NOTA-INTERNA-913 ..... N89-27042 #
NOTA-INTERNA-914 ..... N89-27486 #
NOTA-INTERNA-915 ..... N89-27569 #
NOTA-INTERNA-916 ..... N89-27487 #
NOTA-INTERNA-917 ..... N89-27482 #
NOTA-INTERNA-918 ..... N89-27488 #
NOTA-INTERNA-919 ..... N89-27496 #
NOTA-INTERNA-920 ..... N89-27489 #
NOTA-INTERNA-921 ..... N89-27483 #
NOTA-INTERNA-922 ..... N89-27158 #
NOTA-INTERNA-923 ..... N89-27484 #
NOTA-INTERNA-924 ..... N89-27159 #
NOTA-INTERNA-925 ..... N89-27631 #
NOTA-INTERNA-926 ..... N89-27620 #
NOTA-INTERNA-927 ..... N89-27360 #
NOTA-INTERNA-928 ..... N89-27291 #
NOTA-INTERNA-929 ..... N89-27490 #

NPL-DITC-139/89 ..... N89-27444

NPL-DMA(A)-177 ..... N89-27010

NPS52-88-019 ..... N89-27407 #
NPS52-88-021 ..... N89-27406 #
NPS54-89-07 ..... N89-26809 #
NPS55-89-02 ..... N89-27448 #

NRC-9012959 ..... N89-27519 #

NREC-1626 ..... N89-27178 #

NRL-MR-6402 ..... N89-27622 #
NRL-MR-6405 ..... N89-27286 #
NRL-MR-6445 ..... N89-27304 #
NRL-MR-6457 ..... N89-27510 #

NSF-ITP-89-87-PAPER-1 ..... N89-27608* #

NSF/ENG-88026 ..... N89-27181 #

NTIA-88-239 ..... N89-27058 #

NVO-332 ..... N89-27318 #

NYSERDA-88-5 ..... N89-27241 #

N4577-2501 ..... N89-27184 #

ONERA-NT-1987-1 ..... N89-27126 #
ONERA-NT-1987-6 ..... N89-27450 #
ONERA-NT-1988-1 ..... N89-27319 #

ONERA-RSF-17/3619-AY-110-A ..... N89-27123 #

ORNL-6546 ..... N89-27210 #

ORNL/SUB-83-43346/02-VOL-1 ..... N89-26988 #
ORNL/SUB-86-95900/01 ..... N89-26967 #

ORNL/TM-10714 ..... N89-27396 #
ORNL/TM-10979 ..... N89-27397 #
ORNL/TM-11143-PT-1 ..... N89-27476 #

OSU-719493-7 ..... N89-27064* #

OTA-A-411 ..... N89-27603 #

OU-REPT-28 ..... N89-26975 #

PB89-124127 ..... N89-27278 #
PB89-136683 ..... N89-27258 #
PB89-136691 ..... N89-27259 #
PB89-136709 ..... N89-27260 #
PB89-145767 ..... N89-27044 #
PB89-146389 ..... N89-27513 #
PB89-146443 ..... N89-27045 #
PB89-147631 ..... N89-27422 #
PB89-148456 ..... N89-27262 #
PB89-149470 ..... N89-27588 #
PB89-151054 ..... N89-27601 #
PB89-151252 ..... N89-27261 #
PB89-151815 ..... N89-27389 #
PB89-152037 ..... N89-27265 #
PB89-152284 ..... N89-27178 #

PB89-152417 ..... N89-27322 #
PB89-152441 ..... N89-26930 #
PB89-152466 ..... N89-27257* #
PB89-152474 ..... N89-27300 #
PB89-152656 ..... N89-27589 #
PB89-153597 ..... N89-27263 #
PB89-154209 ..... N89-27264 #
PB89-154876 ..... N89-27621 #
PB89-154892 ..... N89-27605 #
PB89-155196 ..... N89-26881 #
PB89-155550 ..... N89-26929 #
PB89-156053 ..... N89-27207 #
PB89-156152 ..... N89-27043 #
PB89-156350 ..... N89-26994 #
PB89-156368 ..... N89-26995 #
PB89-158604 ..... N89-27266 #
PB89-158760 ..... N89-27136 #
PB89-159313 ..... N89-27233 #
PB89-159602 ..... N89-27607 #
PB89-159685 ..... N89-27280 #
PB89-159693 ..... N89-27298 #
PB89-159701 ..... N89-27281* #
PB89-159719 ..... N89-27297 #
PB89-160840 ..... N89-27365 #
PB89-160865 ..... N89-27181 #
PB89-161327 ..... N89-27102 #
PB89-161889 ..... N89-26928 #
PB89-161897 ..... N89-27100 #
PB89-162069 ..... N89-27241 #
PB89-162606 ..... N89-26996 #
PB89-163224 ..... N89-27230 #
PB89-163257 ..... N89-27231 #
PB89-163265 ..... N89-27232 #
PB89-165468 ..... N89-27071 #
PB89-165781 ..... N89-27460 #
PB89-165930 ..... N89-27299 #
PB89-166094 ..... N89-26993 #
PB89-169817 ..... N89-27600 #
PB89-170005 ..... N89-27611 #
PB89-170039 ..... N89-27610 #
PB89-170559 ..... N89-27034* #
PB89-170906 ..... N89-27412 #
PB89-172555 ..... N89-27137 #
PB89-172563 ..... N89-27182 #
PB89-173223 ..... N89-27270 #
PB89-173603 ..... N89-26997 #
PB89-173645 ..... N89-27184 #
PB89-174213 ..... N89-27345 #
PB89-174635 ..... N89-27343 #
PB89-174668 ..... N89-27146 #
PB89-174767 ..... N89-27309 #
PB89-175343 ..... N89-27004 #
PB89-175418 ..... N89-26942 #
PB89-175491 ..... N89-27344* #
PB89-177802 ..... N89-27590 #
PB89-178115 ..... N89-27310 #
PB89-178222 ..... N89-27311 #
PB89-178792 ..... N89-26944 #
PB89-180251 ..... N89-27058 #
PB89-180376 ..... N89-26914 #
PB89-180715 ..... N89-27325 #
PB89-180822 ..... N89-27147 #
PB89-181119 ..... N89-26943 #
PB89-181200 ..... N89-27312 #
PB89-181788 ..... N89-27313 #
PB89-183958 ..... N89-27216 #
PB89-184949 ..... N89-27613 #
PB89-185987 ..... N89-27624 #
PB89-185995 ..... N89-27625 #
PB89-186050 ..... N89-27595 #
PB89-186522 ..... N89-27339 #
PB89-187314 ..... N89-27317 #
PB89-187397 ..... N89-27041 #
PB89-188569 ..... N89-27005 #
PB89-188577 ..... N89-26945 #
PB89-188593 ..... N89-27507 #
PB89-188825 ..... N89-27153 #
PB89-188841 ..... N89-27196 #
PB89-188874 ..... N89-26946 #
PB89-189138 ..... N89-27007 #
PB89-189161 ..... N89-27356 #
PB89-189179 ..... N89-27457 #
PB89-189195 ..... N89-26977 #
PB89-189245 ..... N89-27078 #
PB89-189294 ..... N89-27602 #
PB89-189310 ..... N89-27594 #
PB89-189344 ..... N89-27174 #
PB89-193270 ..... N89-27087 #
PB89-193296 ..... N89-27040 #
PB89-194120 ..... N89-27086 #
PB89-195408 ..... N89-27603 #
PB89-195820 ..... N89-27604 #

PNE-328 ..... N89-27318 #

PP-1443 ..... N89-27278 #

PREPRINT-598 ..... N89-27617 #
PREPRINT-599 ..... N89-27485 #
PREPRINT-600 ..... N89-27583 #
PREPRINT-601 ..... N89-27581 #
PREPRINT-602 ..... N89-27441 #
PREPRINT-603 ..... N89-27442 #
PREPRINT-604 ..... N89-27224 #
PREPRINT-606 ..... N89-27584 #
PREPRINT-607 ..... N89-27585 #
PREPRINT-608 ..... N89-27327 #
PREPRINT-609 ..... N89-27328 #
PREPRINT-634 ..... N89-27582 #
PREPRINT-635 ..... N89-27449 #
PREPRINT-638 ..... N89-27126 #
PREPRINT-641 ..... N89-27586 #
PREPRINT-957 ..... N89-27443 #

PSU-ME-R-0053-87/88 ..... N89-26929 #

PUBL-68-VOL-3 ..... N89-27615 #
PUBL-69-VOL-4 ..... N89-27616 #

QAUM-88/35 ..... N89-27611 #
QAUM-88/36 ..... N89-27610 #

R-578 ..... N89-27207 #
R-579 ..... N89-27216 #

R/D-5898-EN-01-PT-1 ..... N89-27305 #
R/D-5899-CH-01 ..... N89-27247 #

RADC-TR-88-198 ..... N89-27049 #
RADC-TR-88-218 ..... N89-27548 #
RADC-TR-88-263 ..... N89-27549 #
RADC-TR-88-285 ..... N89-27368 #
RADC-TR-88-296 ..... N89-27405 #
RADC-TR-88-298 ..... N89-27140 #
RADC-TR-88-319 ..... N89-27369 #
RADC-TR-88-321 ..... N89-27096 #
RADC-TR-88-324-VOL-2-PT-A ..... N89-27417 #
RADC-TR-88-324-VOL-2-PT-B ..... N89-27418 #
RADC-TR-88-324-VOL-3 ..... N89-27419 #

RCS-MED-41(R4) ..... N89-27333 #

RDD:88:4744-24-01:01 ..... N89-27153 #

REPT-32 ..... N89-27044 #
REPT-36 ..... N89-27045 #
REPT-54 ..... N89-27626 #
REPT-88-3 ..... N89-27100 #
REPT-88-67 ..... N89-27431 #
REPT-88-81 ..... N89-27432 #
REPT-88-84 ..... N89-27412 #
REPT-88/31 ..... N89-27605 #
REPT-89/01 ..... N89-27613 #
REPT-89B00124 ..... N89-27279* #
REPT-89B00151 ..... N89-26902* #
REPT-89B00188 ..... N89-27302* #
REPT-89B00215 ..... N89-26918* #
REPT-89B00216 ..... N89-27314* #
REPT-89B00237 ..... N89-27289* #
REPT-89B00238 ..... N89-27612* #
REPT-89B00267 ..... N89-27456* #
REPT-204 ..... N89-27282 #
REPT-431-ET-RER-82 ..... N89-27241 #

RFP-TRANS-499 ..... N89-26975 #

RI/RD88-256 ..... N89-26905*
RI/RD89-212 ..... N89-26899* #
RI/RD89-214-TASK-E.5 ..... N89-27204* #

RISOE-M-2718-PT-1 ..... N89-27305 #

RISOE-R-545 ..... N89-26939 #

RPI-MATH-175 ..... N89-27489* #

RPI/DC-TR-5 ..... N89-27012 #

RR-070 ..... N89-26870 #

RSL-TR-7360-5 ..... N89-27052 #

SAND-87-1249 ..... N89-27009 #
SAND-88-0173 ..... N89-27203 #
SAND-88-0930 ..... N89-27031 #
SAND-88-0973C ..... N89-27200 #
SAND-88-2057 ..... N89-27516 #
SAND-88-2098C ..... N89-27144 #
SAND-88-2895 ..... N89-27244 #
SAND-88-3089C ..... N89-27435 #
SAND-88-3311C ..... N89-27534 #
SAND-88-3356C ..... N89-27080 #
SAND-88-3399C ..... N89-27082 #

SAND-88-3408C ..... N89-27079 #
SAND-88-3439 ..... N89-27597 #
SAND-88-7039 ..... N89-27243 #
SAND-88-8934 ..... N89-26920 #
SAND-88-8935 ..... N89-26922 #
SAND-89-0008 ..... N89-27398 #
SAND-89-0025C ..... N89-27535 #
SAND-89-0046C ..... N89-27119 #
SAND-89-0090C ..... N89-26955 #
SAND-89-0091C ..... N89-27093 #
SAND-89-0181C ..... N89-27089 #
SAND-89-0188C ..... N89-27492 #
SAND-89-0218C ..... N89-27088 #
SAND-89-0264C ..... N89-26966 #
SAND-89-0289C ..... N89-27523 #
SAND-89-0334C ..... N89-27357 #
SAND-89-0343C ..... N89-27219 #
SAND-89-0379C ..... N89-27205 #
SAND-89-0393C ..... N89-26855 #
SAND-89-0440C ..... N89-27240 #
SAND-89-0443C ..... N89-27531 #
SAND-89-0463 ..... N89-27251 #
SAND-89-0484 ..... N89-27395 #
SAND-89-0490C ..... N89-27199 #
SAND-89-0589C ..... N89-27154 #
SAND-89-0593 ..... N89-27505 #
SAND-89-0633C ..... N89-27206 #
SAND-89-0664C ..... N89-26921 #
SAND-89-0670C ..... N89-27512 #
SAND-89-0677C ..... N89-27030 #
SAND-89-0683C ..... N89-26981 #
SAND-89-0780C ..... N89-27120 #
SAND-89-0838C ..... N89-27593 #
SAND-89-0842 ..... N89-26949 #
SAND-89-1234C ..... N89-27627 #
SAND-89-1300C ..... N89-27561 #
SAND-89-1390C ..... N89-27530 #
SAND-89-7082C ..... N89-27059 #

SCIPP-88/04 ..... N89-27486 #

SD-TR-89-24 ..... N89-26898 #
SD-TR-89-25 ..... N89-27141 #
SD-TR-89-30 ..... N89-27287 #

SECA-89-10 ..... N89-26900* #

SER-A-3 ..... N89-27621 #

SERI/SP-220-3486 ..... N89-27253 #

SERI/STR-211-3450 ..... N89-27242 #
SERI/STR-217-3476 ..... N89-27249 #

SERI/TP-254-3049 ..... N89-27143 #

SERI/TR-215-3323 ..... N89-27252 #

SFB-PREPRINT-10 ..... N89-27105 #

SGD-535-PT-1 ..... N89-27624 #
SGD-535-PT-2 ..... N89-27625 #

SLCET-TR-89-1 ..... N89-27462 #
SLCET-TR-89-2 ..... N89-27097 #

SP89-MSFC-3225 ..... N89-26885* #

SRL-07-F-1989 ..... N89-27162 #

STF67-A88031 ..... N89-27102 #

SU-SOL-TR-89-1 ..... N89-27373 #
SU-SOL-TR-89-2 ..... N89-27374 #

SU-SOL-89-5 ..... N89-27387 #

SU-TR-415 ..... N89-27451 #
SU-TR-417 ..... N89-27445 #

TASC-TR-9033-1 ..... N89-27376 #

TKK-F-A638 ..... N89-27513 #

TR-15 ..... N89-27016 #
TR-16 ..... N89-27017 #
TR-17 ..... N89-26940 #
TR-17 ..... N89-27011 #
TR-24 ..... N89-27019 #
TR-30 ..... N89-27015 #
TR-34 ..... N89-26958 #
TR-39 ..... N89-27351 #
TR-41 ..... N89-26935 #
TR-43 ..... N89-26936 #
TR-89-05 ..... N89-27227 #
TR-0086(6908)-1 ..... N89-27141 #

TR-0086(6930-03)-1 ..... N89-26898 #
TR-0086(3940-05)-8 ..... N89-27287 #

TR89-04-PT-2 ..... N89-27429 #
TR89-09-1 ..... N89-27427 #
TR89-10-2 ..... N89-27428 #

TTC-1529-R ..... N89-27165 #

TWR-18076 ..... N89-26901* #

UBUFFALO/DC/89/TR-97 ..... N89-27470 #
UBUFFALO/DC/89/TR-99-1 ..... N89-27579 #

UCID-19592-REV-5 ..... N89-27222 #
UCID-21631 ..... N89-27272 #
UCID-21646 ..... N89-27591 #

UCRL-21154 ..... N89-27150 #
UCRL-21206 ..... N89-26915 #
UCRL-53615-87 ..... N89-27226 #
UCRL-53924 ..... N89-27145 #
UCRL-53925 ..... N89-27306 #
UCRL-98149 ..... N89-27386 #
UCRL-98864-REV ..... N89-27027 #
UCRL-98894-REV-1 ..... N89-27276 #
UCRL-99832 ..... N89-27557 #
UCRL-99926-REV-1 ..... N89-27273 #
UCRL-100012 ..... N89-27172 #
UCRL-100122 ..... N89-27084 #
UCRL-100203 ..... N89-27110 #
UCRL-100490 ..... N89-26926 #
UCRL-100574 ..... N89-27521 #
UCRL-100591 ..... N89-27522 #
UCRL-100861 ..... N89-27552 #
UCRL-100883 ..... N89-27057 #
UCRL-100911 ..... N89-27077 #
UCRL-100959 ..... N89-27436 #
UCRL-101001 ..... N89-27454 #
UCRL-101034 ..... N89-27358 #
UCRL-101129 ..... N89-27630 #
UCRL-101134 ..... N89-27479 #

UDR-TR-88-04 ..... N89-27464 #

UILU-ENG-88-2239 ..... N89-27365 #
UILU-ENG-88-2260 ..... N89-27071 #
UILU-ENG-89-1737 ..... N89-27437 #

UIUCDCS-R-89-1518 ..... N89-27437 #

UM-HE-89-11 ..... N89-27627 #

UMR-FDB-5 ..... N89-27020 #

US-PATENT-APPL-SN-018118 ..... N89-26847
US-PATENT-APPL-SN-024490 ..... N89-26850
US-PATENT-APPL-SN-035425 ..... N89-26858
US-PATENT-APPL-SN-036225 ..... N89-26845
US-PATENT-APPL-SN-045970 ..... N89-26959
US-PATENT-APPL-SN-049351 ..... N89-26848
US-PATENT-APPL-SN-049356 ..... N89-27206
US-PATENT-APPL-SN-049363 ..... N89-27139
US-PATENT-APPL-SN-055092 ..... N89-27164
US-PATENT-APPL-SN-057461 ..... N89-27072
US-PATENT-APPL-SN-058004 ..... N89-27186
US-PATENT-APPL-SN-060881 ..... N89-27514
US-PATENT-APPL-SN-066154 ..... N89-26852
US-PATENT-APPL-SN-069999 ..... N89-27187
US-PATENT-APPL-SN-084341 ..... N89-26837
US-PATENT-APPL-SN-095062 ..... N89-26882
US-PATENT-APPL-SN-107184 ..... N89-27026
US-PATENT-APPL-SN-109557 ..... N89-26897
US-PATENT-APPL-SN-110918 ..... N89-27048
US-PATENT-APPL-SN-111846 ..... N89-27138
US-PATENT-APPL-SN-121493 ..... N89-27190
US-PATENT-APPL-SN-122153 ..... N89-26853
US-PATENT-APPL-SN-124805 ..... N89-27185
US-PATENT-APPL-SN-125646 ..... N89-27160
US-PATENT-APPL-SN-128839 ..... N89-26965
US-PATENT-APPL-SN-128840 ..... N89-26961
US-PATENT-APPL-SN-137558 ..... N89-27192
US-PATENT-APPL-SN-144885 ..... N89-26836
US-PATENT-APPL-SN-149814 ..... N89-27101
US-PATENT-APPL-SN-150677 ..... N89-26911
US-PATENT-APPL-SN-198800 ..... N89-26960
US-PATENT-APPL-SN-242678 ..... N89-27503 #
US-PATENT-APPL-SN-280807 ..... N89-27168 #
US-PATENT-APPL-SN-680674 ..... N89-26857
US-PATENT-APPL-SN-705950 ..... N89-26931
US-PATENT-APPL-SN-771529 ..... N89-27046
US-PATENT-APPL-SN-795572 ..... N89-27545
US-PATENT-APPL-SN-818922 ..... N89-27070
US-PATENT-APPL-SN-818922 ..... N89-27497
US-PATENT-APPL-SN-853827 ..... N89-27461
US-PATENT-APPL-SN-861905 ..... N89-27180
US-PATENT-APPL-SN-861908 ..... N89-27179
US-PATENT-APPL-SN-881741 ..... N89-27186
US-PATENT-APPL-SN-882059 ..... N89-27142
US-PATENT-APPL-SN-895016 ..... N89-26849
US-PATENT-APPL-SN-917933 ..... N89-27163
US-PATENT-APPL-SN-922642 ..... N89-27191
US-PATENT-APPL-SN-925959 ..... N89-27499
US-PATENT-APPL-SN-935362 ..... N89-26908
US-PATENT-APPL-SN-935363 ..... N89-26907
US-PATENT-APPL-SN-939999 ..... N89-27189
US-PATENT-APPL-SN-946541 ..... N89-27106

US-PATENT-CLASS-60-39-281 ..... N89-26848
US-PATENT-CLASS-60-264 ..... N89-27106
US-PATENT-CLASS-73-35 ..... N89-27026
US-PATENT-CLASS-74-573 ..... N89-27192
US-PATENT-CLASS-102-347 ..... N89-26897
US-PATENT-CLASS-148-20.3 ..... N89-26961
US-PATENT-CLASS-148-133 ..... N89-26960
US-PATENT-CLASS-156-621 ..... N89-27545
US-PATENT-CLASS-162-23 ..... N89-26847
US-PATENT-CLASS-228-194 ..... N89-26907
US-PATENT-CLASS-239-265.37 ..... N89-27189
US-PATENT-CLASS-244-76R N89-26858
US-PATENT-CLASS-244-117 ..... N89-26837
US-PATENT-CLASS-244-135 ..... N89-26836
US-PATENT-CLASS-244-204 ..... N89-27101
US-PATENT-CLASS-248-550 ..... N89-27208
US-PATENT-CLASS-250-336.1 ..... N89-27164
US-PATENT-CLASS-277-80 ..... N89-27187
US-PATENT-CLASS-288-190 ..... N89-26908
US-PATENT-CLASS-324-61 ..... N89-26850
US-PATENT-CLASS-331-158 ..... N89-27072
US-PATENT-CLASS-338-4 ..... N89-27139
US-PATENT-CLASS-350-610 ..... N89-27163
US-PATENT-CLASS-356-358 ..... N89-27142
US-PATENT-CLASS-356-183 ..... N89-27048
US-PATENT-CLASS-372-53 ..... N89-27160
US-PATENT-CLASS-374-1 ..... N89-27138
US-PATENT-CLASS-403-157 ..... N89-27188
US-PATENT-CLASS-415-115 ..... N89-26849
US-PATENT-CLASS-415-160 ..... N89-27186
US-PATENT-CLASS-415-189 ..... N89-26853
US-PATENT-CLASS-422-92 ..... N89-26931
US-PATENT-CLASS-602-610 ..... N89-26852

US-PATENT-4,743,104 ..... N89-27163
US-PATENT-4,748,399 ..... N89-27461
US-PATENT-4,749,333 ..... N89-27180
US-PATENT-4,752,184 ..... N89-27179
US-PATENT-4,753,501 ..... N89-27497
US-PATENT-4,754,176 ..... N89-27070
US-PATENT-4,756,053 ..... N89-26847
US-PATENT-4,758,408 ..... N89-26931
US-PATENT-4,764,003 ..... N89-27499
US-PATENT-4,771,291 ..... N89-27046
US-PATENT-4,784,716 ..... N89-27545
US-PATENT-4,786,020 ..... N89-27101
US-PATENT-4,786,548 ..... N89-26882
US-PATENT-4,787,943 ..... N89-26959
US-PATENT-4,792,732 ..... N89-27514
US-PATENT-4,794,755 ..... N89-26848
US-PATENT-4,795,123 ..... N89-27206
US-PATENT-4,796,838 ..... N89-26836
US-PATENT-4,797,555 ..... N89-27164
US-PATENT-4,797,639 ..... N89-27072
US-PATENT-4,798,515 ..... N89-26849
US-PATENT-4,799,230 ..... N89-27160
US-PATENT-4,800,718 ..... N89-27106
US-PATENT-4,800,798 ..... N89-26857
US-PATENT-4,806,846 ..... N89-26850
US-PATENT-4,807,531 ..... N89-26897
US-PATENT-4,807,798 ..... N89-26908
US-PATENT-4,807,831 ..... N89-26837
US-PATENT-4,807,891 ..... N89-27187
US-PATENT-4,808,023 ..... N89-27188
US-PATENT-4,808,226 ..... N89-27185
US-PATENT-4,808,249 ..... N89-26960
US-PATENT-4,808,250 ..... N89-26961
US-PATENT-4,809,903 ..... N89-26907
US-PATENT-4,811,233 ..... N89-26845
US-PATENT-4,812,050 ..... N89-27138
US-PATENT-4,812,801 ..... N89-27139
US-PATENT-4,813,608 ..... N89-27189
US-PATENT-4,814,684 ..... N89-27048
US-PATENT-4,815,283 ..... N89-26852
US-PATENT-4,815,315 ..... N89-27026
US-PATENT-4,815,339 ..... N89-27191
US-PATENT-4,815,855 ..... N89-27142
US-PATENT-4,815,933 ..... N89-26853
US-PATENT-4,819,496 ..... N89-27190
US-PATENT-4,819,503 ..... N89-27192
US-PATENT-4,820,360 ..... N89-26965
US-PATENT-4,821,982 ..... N89-26858
US-PATENT-4,822,432 ..... N89-26911

USAAEFA-87-04 ..... N89-26840 #
USAAEFA-87-07 ..... N89-26839 #

USAFSAM-TR-86-36-PT-4 ..... N89-27341 #

USARIEM-M32-89 ..... N89-27335 #
USARIEM-M41-89 ..... N89-27332 #
USARIEM-M42-89 ..... N89-27334 #

USARIEM-T-8/89 ..... N89-27340 #
USARIEM-T-10/89 ..... N89-27337 #

UT-KBS-88-03 ..... N89-27439 #

UTEC-MD-88-072 ..... N89-27140 #

UWA/DME/TR-89/63 ..... N89-26963 #

UWIS/DC/TR-89/2 ..... N89-27573 #

VLSI-MEMO-89-514 ..... N89-27098 #

VS-1-88 ..... N89-26815* #

VTT-583 ..... N89-27129 #

WBS-4B102-10-03 ..... N89-26901* #

WES/TR/SL-87-33 ..... N89-26864 #
WES/TR/SL-89-5 ..... N89-26864 #

WHC-SA-0536 ..... N89-27221 #

WR-88-15 ..... N89-27459 #

WRDC-TR-89-3027 ..... N89-26962 #
WRDC-TR-89-3040 ..... N89-27409 #

WTHD-189 ..... N89-27570

☆ U.S. GOVERNMENT PRINTING OFFICE: 1989—261 -275 / 00112

FEDERAL REGIONAL DEPOSITORY LIBRARIES

ALABAMA

AUBURN UNIV. AT MONTGOMERY LIBRARY
Documents Department
Montgomery, AL 36193
(205) 271-9650

UNIV. OF ALABAMA LIBRARY
Documents Dept.-Box S
University, AL 35486
(205) 348-6046

ARIZONA

DEPT. OF LIBRARY, ARCHIVES AND PUBLIC RECORDS
Third Floor—State Cap.
1700 West Washington
Phoenix, AZ 85007
(602) 255-4121

UNIVERSITY OF ARIZONA LIB.
Government Documents Dept.
Tucson, AZ 85721
(602) 621-6433

ARKANSAS

ARKANSAS STATE LIBRARY
One Capitol Mall
Little Rock, AR 72201
(501) 371-2326

CALIFORNIA

CALIFORNIA STATE LIBRARY
Govt. Publications Section
P.O. Box 2037
Sacramento, CA 95809
(916) 324-4863

COLORADO

UNIV OF COLORADO LIB.
Government Pub. Division
Campus Box 184
Boulder, CO 80309
(303) 492-8834

DENVER PUBLIC LIBRARY
Govt. Pub. Department
1357 Broadway
Denver, CO 80203
(303) 571-2131

CONNECTICUT

CONNECTICUT STATE LIBRARY
Government Documents Unit
231 Capitol Avenue
Hartford, CT 06106
(203) 566-7029

FLORIDA

UNIV. OF FLORIDA LIBRARIES
Library West
Documents Department
Gainesville, FL 32611
(904) 392-0367

GEORGIA

UNIV. OF GEORGIA LIBRARIES
Government Reference Dept.
Athens, GA 30602
(404) 542-8949

HAWAII

UNIV. OF HAWAII LIBRARY
Govt. Documents Collection
2550 The Mall
Honolulu, HI 96822
(808) 948-8230

IDAHO

UNIV. OF IDAHO LIBRARY
Documents Section
Moscow, ID 83843
(208) 885-6344

ILLINOIS

ILLINOIS STATE LIBRARY
Information Services Branch
Centennial Building
Springfield, IL 62756
(217) 782-5185

INDIANA

INDIANA STATE LIBRARY
Serials Documents Section
140 North Senate Avenue
Indianapolis, IN 46204
(317) 232-3686

IOWA

UNIV. OF IOWA LIBRARIES
Govt. Documents Department
Iowa City, IA 52242
(319) 353-3318

KANSAS

UNIVERSITY OF KANSAS
Doc. Collect—Spencer Lib.
Lawrence, KS 66045-2800
(913) 864-4662

KENTUCKY

UNIV. OF KENTUCKY LIBRARIES
Govt. Pub. Department
Lexington, KY 40506-0039
(606) 257-3139

LOUISIANA

LOUISIANA STATE UNIVERSITY
Middleton Library
Govt. Docs. Dept.
Baton Rouge, LA 70803
(504) 388-2570

LOUISIANA TECHNICAL UNIV. LIBRARY
Documents Department
Ruston, LA 71272-0046
(318) 257-4962

MAINE

UNIVERSITY OF MAINE
Raymond H. Fogler Library
Tri-State Regional Documents Depository
Orono, ME 04469
(207) 581-1680

MARYLAND

UNIVERSITY OF MARYLAND
McKeldin Lib.—Doc. Div.
College Park, MD 20742
(301) 454-3034

MASSACHUSETTS

BOSTON PUBLIC LIBRARY
Government Docs. Dept.
Boston, MA 02117
(617) 536-5400 ext.226

MICHIGAN

DETROIT PUBLIC LIBRARY
Sociology Department
5201 Woodward Avenue
Detroit, MI 48202-4093
(313) 833-1409

MICHIGAN STATE LIBRARY
P.O. Box 30007
Lansing, MI 48909
(517) 373-1593

MINNESOTA

UNIVERSITY OF MINNESOTA
Government Pubs. Division
409 Wilson Library
309 19th Avenue South
Minneapolis, MN 55455
(612) 373-7870

MISSISSIPPI

UNIV. OF MISSISSIPPI LIB.
Documents Department
University, MS 38677
(601) 232-5857

MONTANA

UNIV. OF MONTANA
Mansfield Library
Documents Division
Missoula, MT 59812
(406) 243-6700

NEBRASKA

UNIVERSITY OF NEBRASKA - LINCOLN
Love Library
Documents Department
Lincoln, NE 68588-0410
(402) 472-2562

NEVADA

UNIVERSITY OF NEVADA LIB.
Govt. Pub. Department
Reno, NV 89557-0044
(702) 784-6579

NEW JERSEY

NEWARK PUBLIC LIBRARY
5 Washington Street
Newark, NJ 07101-0630
(201) 733-7812

NEW MEXICO

UNIVERSITY OF NEW MEXICO
Zimmerman Library
Government Pub. Dept.
Albuquerque, NM 87131
(505) 277-5441

NEW MEXICO STATE LIBRARY
Reference Department
325 Don Gaspar Avenue
Santa Fe, NM 87503
(505) 827-3826

NEW YORK

NEW YORK STATE LIBRARY
Empire State Plaza
Albany, NY 12230
(518) 474-5563

NORTH CAROLINA

UNIVERSITY OF NORTH CAROLINA AT CHAPEL HILL
Davis Library
BA/SS Documents Division
Chapel Hill, NC 27515
(919) 962-1151

NORTH DAKOTA

UNIVERSITY OF NORTH DAKOTA
Chester Fritz Library
Documents Department
Grand Forks, ND 58202
(701) 777-4629
In cooperation with North Dakota State Univ. Library

OHIO

STATE LIBRARY OF OHIO
Documents Department
65 South Front Street
Columbus, OH 43266-0334
(614) 462-7051

OKLAHOMA

OKLAHOMA DEPT. OF LIB.
Government Documents
200 NE 18th Street
Oklahoma City, OK 73105
(405) 521-2502, ext. 252

OKLAHOMA STATE UNIV. LIB.
Documents Department
Stillwater, OK 74078
(405) 624-6546

OREGON

PORTLAND STATE UNIV. LIB.
Documents Department
P.O. Box 1151
Portland, OR 97207
(503) 229-3673

PENNSYLVANIA

STATE LIBRARY OF PENN.
Government Pub. Section
P.O. Box 1601
Harrisburg, PA 17105
(717) 787-3752

TEXAS

TEXAS STATE LIBRARY
Public Services Department
P.O. Box 12927—Cap. Sta.
Austin, TX 78711
(512) 475-2996

TEXAS TECH. UNIV. LIBRARY
Govt. Documents Department
Lubbock, TX 79409
(806) 742-2268

UTAH

UTAH STATE UNIVERSITY
Merrill Library, U.M.C. 30
Logan, UT 84322
(801) 750-2682

VIRGINIA

UNIVERSITY OF VIRGINIA
Alderman Lib.—Public Doc.
Charlottesville, VA 22903-2498
(804) 924-3133

WASHINGTON

WASHINGTON STATE LIBRARY
Documents Section
Olympia, WA 98504
(206) 753-4027

WEST VIRGINIA

WEST VIRGINIA UNIV. LIB.
Documents Department
Morgantown, WV 26506-6069
(304) 293-3640

WISCONSIN

MILWAUKEE PUBLIC LIBRARY
814 West Wisconsin Avenue
Milwaukee, WI 53233
(414) 278-3065

ST. HIST LIB. OF WISCONSIN
Government Pub. Section
816 State Street
Madison, WI 53706
(608) 262-4347

WYOMING

WYOMING STATE LIBRARY
Supreme Ct. & Library Bld.
Cheyenne, WY 82002
(307) 777-5919

National Aeronautics and
Space Administration
Code NTT-4
Washington, D.C.
20546

Official Business

Penalty for Private Use, $300

SPECIAL FOURTH-CLASS RATE
POSTAGE & FEES PAID
NASA
PERMIT No. G 27

POSTMASTER If Undeliverable (Section 158
Postal Manual) Do Not Return